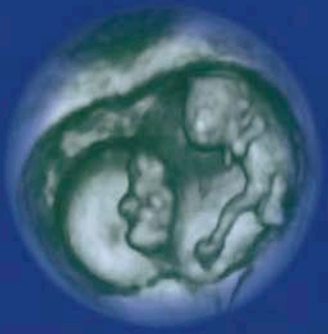

Donald School

Textbook of Ultrasound in Obstetrics & Gynecology

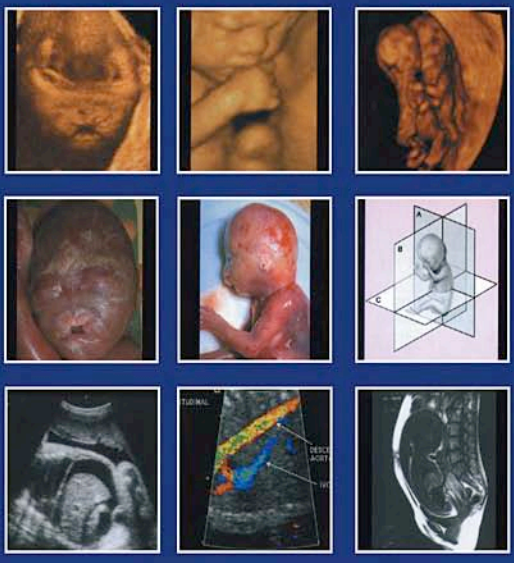

PARTHENON PUBLISHING

Editors
Asim Kurjak
Frank A Chervenak

Also available as a printed book
see title verso for ISBN details

Donald School Textbook of Ultrasound in Obstetrics and Gynecology

Editors

Asim Kurjak MD PhD
Professor and Chairman
Department of Obstetrics and Gynecology
Medical School University of Zagreb
Sveti Duh Hospital, Zagreb, Croatia

Frank A Chervenak MD PhD
Professor and Chairman
Department of Obstetrics Ultrasound and Ethics
The New York Hospital-Cornell Medical Center
New York, USA

Published in association with

JAYPEE BROTHERS

MEDICAL PUBLISHERS (P) LTD
New Delhi

By

The Parthenon Publishing Group
International Publishers in Medicine, Science & Technology
A CRC PRESS COMPANY
BOCA RATON LONDON NEW YORK WASHINGTON, D.C.

First published in 2003 by Jaypee Brothers Medical Publishers (P) Ltd, EMCA House, 23/23B Ansari Road, Daryaganj, New Delhi 110 002, India
First published in the United Kingdom in 2004 by The Parthenon Publishing Group, an imprint of the Taylor & Francis Group plc, 11 New Fetter Lane, London EC4P 4EE. Exclusively distributed worldwide (excluding the Indian subcontinent) by The Parthenon Publishing Group, an imprint of the Taylor & Francis Group pic. Website: http://www.crcpress.com/
This edition published in the Taylor & Francis e-Library, 2006.

A CIP record for this book is available from the British Library.

ISBN 0-203-64059-4 Master e-book ISBN

ISBN 0-203-69028-1 (Adobe e-Reader Format)
ISBN 1 84214 257 7 (Print Edition)

Distributed in the USA by Fulfilment Center Taylor & Francis 10650 Toebben Drive Independence, KY 41051, USA Toll Free Tel.: +1 800 634 7064 E-mail: taylorandfrancis@thomsonlearning.com
Distributed in Canada by Taylor & Francis 74 Rolark Drive Scarborough, Ontario M1R 4G2, Canada Toll Free Tel.: +1 877 226 2237 E-mail: tal_fran@istar.ca
Distributed in the rest of the world by Thomson Publishing Services Cheriton House, North Way Andover, Hampshire SP10 5BE, UK Tel.: +44 (0)1264 332424 E-mail: salesorder.tandf@thomsonpublishingservices.co.uk

To

Ian Donald—Teacher and Friend Editors

Contributors

Alenka Aksamija
Department of Obstetrics and Gynecology
Medical School University of Zagreb
Sveti Duh Hospital
Zagreb, Croatia
aalenka75@hotmail.com

Aris J.Antsaklis
1st Department of Obstetrics and Gynecology
Hospital “Alexandria”
Athens, Greece
arisants@otenet.gr

Kazunori Baba
Division of Maternal and Fetal Medicine
Center for Maternal, Fetal and Neonatal Medicine
Saitama Medical Center, Saitama Medical School
Saitama, Japan
baba-tokyo@umin.ac.jp

Zoltán Bán
1st Department of Obstetrics and Gynecology
Semmelweis University
Budapest, Hungary
pz@noil.sote.hu

Renato Bauman
Department of Obstetrics and Gynecology
Medical School University of Zagreb
Sveti Duh Hospital, Zagreb, Croatia
renato.bauman@zg.hinet.hr

Ivanka Bekavac
Department of Obstetrics and Gynecology
Medical School University of Zagreb
Sveti Duh Hospital
Zagreb, Croatia
bekavacdr@hotmail.com

Bernard Benoit
Nice, France
dr.bernard.benoit@wanadoo.fr

Drazena Bjelos
Department of Obstetrics and Gynecology
Medical School University of Zagreb

Sveti Duh Hospital, Zagreb, Croatia
drazena.bjelos@zg.hinet.hr

Fernando Bonilla-Musoles
Chairman
Department of Obstetrics and Gynecology
Valencia School of Medicine, Valencia, Spain
bonilla_fer@gva.es

Branko Breyer
Laboratory “Breyer”
Zagreb, Croatia
branko.breyer@lab-breyer.hr

Boris Brkljacic
Head, Department of Radiology
Clinical Hospital Dubrava, Zagreb, Croatia
boris.brkljacic@zg.tel.hr

Jose Maria Carrera
Head, Fetal Medicine Service
Department of Obstetrics and Gynecology
University Institute “Dexeus”
Barcelona, Spain
silnun@iudexeus.uab.es

Stephen T.Chasen
Department of Obstetrics and Gynecology
Cornell Medical Center
New York, USA
stchasen@med.cornell.edu

Frank A.Chervenak
Given Foundation Professor and Chairman
Department of Obstetrics and Gynecology
New York Weill Cornell Medical Center
New York, USA
fac2001@med.cornell.edu

Matilde T.Clavijo Rodriguez
Division of US and Fetal Medicine
Department of Obstetrics and Gynecology
University Hospital of the Canary Islands
Tenerife, Spain
mclavijor@sego.es

Giancarlo Conoscenti
Divisione Ostetricia e Ginecologia
Burlo Garofolo, Trieste, Italy
gconoscenti@tin.it

Vincenzo D’Addario
Department of Obstetrics and Gynecology
University Medical School of Bari

Bari, Italy
v.daddario@gynecology4.uniba.it
Luca Di Cagno
Department of Obstetrics and Gynecology
University Medical School of Bari
Bari, Italy
v.daddario@gynecology4.uniba.it
Edoardo Di Naro
Department of Obstetrics and Gynecology
University Medical School of Bari
Bari, Italy
v.daddario@gynecology4.uniba.it
A Kubilay Ertan
Prenatal Diagnosis and Therapy
Department of Obstetrics and Gynecology
University of Saarland
Homburg/Saar, Germany
ertan@uniklinik-saarland.de
Kotaro Fukushima
Maternity and Perinatal Care Unit
Department of Obstetrics and Gynecology
Graduate School of Medical Sciences
Kyushu University Hospital
Kyushu University, Fukuoka, Japan
kfuku@gynob.med.kyushu-u.ac.jp
Biserka Funduk-Kurjak MD PhD
Modern Medical Center
Zagreb, Croatia
Srecko Gajovic
Department of Histology and Embryology
Medical School University of Zagreb
Zagreb, Croatia
sgajovi@mef.hr
Mattia Gentile
Department of Medical Genetics
I.R.C.C.S. “Saverio de Bellis”
Castellana Grotte (BA), Italy
mattiagentile@libero.i
Ozren Grgic
Department of Obstetrics and Gynecology
Medical School University of Zagreb
Sveti Duh Hospital, Zagreb, Croatia
ozreng@net.hr
Tomislav Hafner
Department of Obstetrics and Gynecology
Medical School University of Zagreb Sveti Duh Hospital, Zagreb, Croatia

Toshiyuki Hata
Professor and Chairman
Department of Perinatology
Kagawa Medical University
Kagawa, Japan
toshi28@kms.ac.jp
Radoslav Herman
Department of Obstetrics and Gynecology
Clinical Hospital “Sestre milosrdnice”
Zagreb, Croatia
radoslav.herman@zg.htnet.hr
Shigenori Iwagaki
Department of Obstetrics and Gynecology
Gifu University School of Medicine
Gifu, Japan
Robin B. Kalish
Department of Obstetrics and Gynecology
Cornell Medical Center, New York, USA
rbk9001@med.cornell.edu
ROBINKAL@aol.com
Nika Kalogjera MD
Ultrasonic Unit
Department of Obstetrics and Gynecology
University of Zagreb
Sveti Duh Hospital
Sveti Duh 64
10 000 Zagreb, Croatia
nika.kalogjera@lycos.com
Ichiro Kawabata
Department of Obstetrics and Gynecology
Gifu University School of Medicine
Gifu, Japan
kawabata@cc.gifu-u.ac.jp
Milan Kos
Department of Obstetrics and Gynecology
Medical School University of Zagreb
Sveti Duh Hospital, Zagreb, Croatia
dr_marina_kos@yahoo.com
Ljiljana Kostovic-Knezevic
Department of Histology and Embryology
Medical School University of Zagreb
Zagreb, Croatia
lili@mef.hr
Sanja Kupesic
Department of Obstetrics and Gynecology
Medical School University of Zagreb

Zagreb, Croatia
sanja.kupesic@zg.tel.hr
Asim Kurjak
Department of Obstetrics and Gynecology
Medical School University of Zagreb
Zagreb, Croatia
asim.kurjak@public.srce.hr
Keith B. Lescale
Department of Obstetrics and Gynecology
Cornell Medical Center,
New York, USA
kbl9001@nyp.org
Luiz Eduardo Machado
Department of Obstetrics and Gynecology
INTRO, Salvador, Brazil
Le_machado@uol.com
Kazuo Maeda
Yonago, Japan
maedak@mocha.ocn.ne.jp
Jaideep Malhotra
Malhotra Nursing and Maternity Home Pvt. Ltd.
and Malhotra Test Tube Baby Centre
Agra, India
mnmhagra@sancharnet.in
Narendra Malhotra
Malhotra Nursing and Maternity Home Pvt. Ltd.
and Malhotra Test Tube Baby Centre
Agra, India
mnmhagra@sancharnet.in
Giampaolo Mandruzzato
Divisione Ostetricia e Ginecologia
Burlo Garofolo, Trieste, Italy
mandruzzatogiampaolo@tin.it
Tamás Marton
1st Department of Obstetrics and Gynecology
Semmelweis University
Budapest, Hungary
pz@noil.sote.hu
Gianpaolo Maso
Divisione Ostetricia e Ginecologia
Burlo Garofolo
Trieste, Italy
maso@burlo.trieste.it
Ratko Matijevic
Department of Obstetrics and Gynecology
Medical School University of Zagreb

Sveti Duh Hospital
Zagreb, Croatia
ratko.matijevic@zg.tel.hr

Yoram Jacob Meir
Divisione Ostetricia e Ginecologia
Burlo Garofolo
Trieste, Italy
y.meir@tin.it

Luis T.Mercé
Unit of Assisted Reproduction
International Ruber Hospital
Madrid, Spain
ltmerce@meditex.es

Giovanni Monni
Head
Prenatal and Preimplantation Genetic Diagnosis
Fetal Therapy
Department of Obstetrics and Gynecology
Ospedale Regionale Microcitemico
Cagliari, Italy
prenatalmonni@tiscalinet.it

Ajlana Mulic-Lutvica
Department of Obstetrics and Gynecology
Uppsala University Hospital, Uppsala, Sweden
ajli_ml@hotmail.com

Hitoo Nakano
Chairman
Department of Obstetrics and Gynecology
Maternity and Perinatal Care Unit
Graduate School of Medical Sciences
Kyushu University Hospital
Kyushu University, Fukuoka, Japan
midori@med.kyushu-u.ac.jp

Zoltán Papp
1st Department of Obstetrics and Gynecology
Semmelweis University, Budapest, Hungary
pz@noil.sote.hu

Ladislav Pavic
Department of Radiology
Clinical Hospital Dubrava
Zagreb, Croatia
ladislav.pavic@zg.hinet.hr

Sriram C.Perni
Department of Obstetrics and Gynecology
New York Weill Cornell Medical Center

New York, USA
scperni@yahoo.com
M.Piccoli
Divisione Ostetricia e Ginecologia
Burlo Garofolo, Trieste, Italy
Vincenzo Pinto
Department of Obstetrics and Gynecology
University Medical School of Bari
Bari, Italy
v.pinto@gynecology4.uniba.it
Kyong H Pooh
Department of Neurosurgery
National Kagawa Children's Hospital
Zentsuji, Japan
kpooh@kagawasyoni.hosp.go.jp
Ritsuko K.Pooh
Department of Obstetrics and Maternal Fetal
Medicine, National Kagawa Children's Hospital
Zentsuji, Japan
rkpooh@guitar.ocn.ne.jp
Matija Prka
Department of Obstetrics and Gynecology
Medical School University of Zagreb
Sveti Duh Hospital, Zagreb, Croatia
mprka@mef.hr
Francisco Raga
Department of Obstetrics and Gynecology
Valencia School of Medicine, Valencia, Spain
Cegiob@interbook.net
Luigi Raio
Department of Obstetrics and Gynecology
University Medical School of Bern
Bern, Switzerland
luigi.raio@insel.ch
Maria Angela Rustico
Divisione Ostetricia e Ginecologia
Burlo Garofolo, Trieste, Italy
cast@interware.it
Maher G.Sarraf
Al-Amal Hospital
Maternity Hospital, Amman, Jordan
sarraf@go.com.jo
Shoji Satoh
Maternity and Perinatal Care Unit
Department of Obstetrics and Gynecology
Graduate School of Medical Sciences

Kyushu University Hospital
Kyushu University, Fukuoka, Japan
satoh@gynob.med.kyushu-u.ac.jp

Werner Schmidt
Chief of Department of Obstetrics and Gynecology
Saarland University Medical School
Homburg/SAAR, Germany
ufk@med-fr.uni-sb.de

Cihat Sen
Department of Perinatology, Obstetrics and Gynecology
Cerrahpasa Medical School
University of Istanbul, Istanbul, Turkey
csen@obusg.org.tr

Geeta Sharma
Department of Obstetrics and Gynecology
Cornell Medical Center, New York, USA
gsharma@med.cornell.edu

Kuldeep Singh
Dr. Kuldeep's Ultrasound and Color Doppler Clinic
New Delhi, India
singhdrkuldeep@rediffmail.com

Daniel W.Skupski
Division of Maternal-Fetal Medicine
Department of Obstetrics and Gynecology
Cornell Medical Center
New York, USA
dwskupsk@mail.med.cornell.edu

Vladimir Sparac MD
Department of Obstetrics and Gynecology
Medical School University of Zagreb
Sveti Duh Hospital
Zagreb, Croatia
vladimir.sparac@zg.hinet.hr

Yuichiro Takahashi
Department of Obstetrics and Gynecology
Gifu University School of Medicine
Gifu, Japan
y-taka@cc.gifu-u.ac.jp

Riccardo Tamburro
Department of Obstetrics and Gynecology
University Medical School of Bari
Bari, Italy
v.daddario@gynecology4.uniba.it

H.Alper Tanriverdi
Department of Obstetrics and Gynecology

Karaelmas University Medical School
Kozlu-Zonguldak
Turkey
tanriverdi@artemisonline.net

Ana Tripalo
Department of Obstetrics and Gynecology
Medical School University of Zagreb
Sveti Duh Hospital
Zagreb, Croatia
ana.tripalo@zg.hinet.hr

Juan M.Troyano Luque
Head
Division of US and Fetal Medicine
Department of Obstetrics and Gynecology
University Hospital of the Canary Islands
Tenerife, Spain
uecografia@sego.es
jtroyanol@meditex.es

Boris Ujevic
Department of Obstetrics and Gynecology
Medical School University of Zagreb
Sveti Duh Hospital
Zagreb, Croatia
boris.ujevic@zg.tel.hr

Paolo Volpe
Department of Obstetrics and Gynecology
Hospital Di Venere, Bari, Italy
paolo-volpe@libero.it

Mira Wankelmuth
Department of Obstetrics and Gynecology
University Medical School of Bari
Bari, Italy
v.daddario@gynecology4.uniba.it

Ivica Zalud
Division of Maternal Fetal Medicine
Fetal Diagnostic Center
Kapiolani Medical Center for Women and
Children
Honolulu, Hawaii
zaludi001@hawaii.rr.com

Maria Angelica Zoppi
Prenatal and Preimplantation Genetic Diagnosis
Fetal Therapy

Department of Obstetrics and Gynecology
Ospedale Regionale Microcitemico
Cagliari, Italy
prenatalmonni@tiscalinet.it

Preface

Ultrasound is the backbone of modern obstetric and gynecology practice. For those of us old enough to remember the dark ages of clinical practice prior to ultrasound, this is not an overstatement. Younger physicians may find it hard to imagine the clinical realities of doctors who delivered undiagnosed twins presenting at delivery, who performed unnecessary surgeries for the clinical suspicion of a pelvic mass that was not present, and who consoled anguished parents when an anomalous infant was born unexpectedly. Recent technological breakthroughs in diagnostic ultrasound, including the advent of color Doppler, power Doppler, three-dimensional and four-dimensional imaging, have led ultrasound to surpass the expectations of Ian Donald, its visionary father.

The Ian Donald School was founded in 1981 and is devoted to international education and research cooperation concerning also aspects of diagnostic ultrasound. The first chapter was founded in Dubrovnik at that time and has now expanded to 7 additional national branches.

To facilitate the educational efforts of the Ian Donald School we believed a textbook would be of value. The text is divided into three parts: general aspects, obstetrics, and gynecology. All contributors are either present or former teachers in the 8 branches of the Ian Donald School. We believe this comprehensive text with state-of-the-art images will be of value to both new learners and experienced practitioners.

We are grateful to all of the teachers in the school and especially to all of the contributors to this textbook for their tireless efforts to enhance the quality of ultrasound practice throughout the world.

Asim Kurjak
Frank A Chervenak

Contents

Section 1 General Aspects

1. **Understanding Technology—Key to Correct Diagnostics** **2**
   Branko Breyer
2. **Proposals on the Safe Fetal Exposure Time to Doppler Ultrasound** **27**
   Kazuo Maeda
3. **Development of 3D Ultrasound** **34**
   Kazunori Baba
4. **Artifacts, Pitfalls and Normal Variants** **57**
   Ivica Zauld
5. **Screening by Ultrasound** **70**
   Glampaolo Mandruzzato, Gianpaolo Maso, Glanclarlo Conosscenti
6. **Routine Use of Obstetric Ultrasound** **74**
   Geeta Sharmo, Stephen T Chasen, Frank A Chervenak
7. **Legal Concerns in the Use of Ultrasound in Obstetrics and Gynecology** **105**
   Keith B Lescale, Frank A Chervenak
8. **Ultrasound in Developing Countries** **113**
   Narendra Malhotra, Kuldeep Singh, Jaideep Malhotra

Section 2 Obstetrics

9. **Development of Human Embryo** **142**
   Ljiljana Kostovic-Knezevic, Srecko Gajovic
10. **Ultrasound Evaluation during the First Trimester of Normal Pregnancy** **156**
    Maher G Sarraf
11. **Sonographic Determination of Gestational Age** **178**
    Robin B Kalish
12. **Ultrasound Markers of Chromosomal Anomalies in First Trimester** **191**
    Giovanni Monni, Maria Angelica Zoppi
13. **Ultrasound Evaluation of Abnormal Early Pregnancy** **202**
    Asim Kurjak, Sanja Kupesic, Ana Tripalo
14. **Ectopic Pregnancy** **236**
    Sanja Kupesic, Alenka Aksamija, Asim Kurjak

15. Trophoblastic Disease **259**
Kazuo Maeda
16. Normal Fetal Anatomy **286**
Vincenzo D'Addario, Edoardo Di Naro, Luca Di Cagno
17. Fetal Growth and Biometry **301**
Toshiyuki Hata
18. Ultrasonographic Diagnosis of Intrauterine Growth Restriction **318**
Jose Maria Carrera
19. Fetal Central Nervous System **353**
Ritsuko K Pooh, Kyong H Pooh
20. Ultrasound Examination of the Fetal Thorax **383**
Zoltan Papp
21. Ultrasound Evaluation of the Fetal Heart **395**
Paolo Volpe, Maria Angela Rustico, Mattia Gentile
22. Malformations of the Gastrointestinal System **411**
Vincenzo D'Addario, Luca Di Cagno, Riccardo Tamburro
23. Fetal Genitourinary Tract: Prenatal Diagnosis and Assessment of Nephrouropathies **425**
Juan M Troyano Luque, Matilde T Clavijo Rodriguez
24. The Umbilical Cord: Sonographic Assessment **459**
Edoardo Di Naro, Luigi Raio, Vincenzo D'Addario
25. The Placenta **468**
Ratko Matijevic
26. Ultrasound Based Diagnosis of Cervical Insufficiency and Evidence to Support the Intervention **489**
Ratko Matijevic, Asim Kurjak, Ozren Grgic
27. Ultrasound Evaluation of the Multifetal Gestation **501**
Sriram C Perni
28. General Aspects on Ultrasound Screening of Congenital Anomalies **522**
Vincenzo Pinto, Mira Wankelmuth, Vincenzo D'Addario
29. Fetal Hydrops **531**
Ratko Matijevic
30. Ultrasound in the Management of the Alloimmunized Pregnancy **542**
Daniel W Skupski
31. Post-termination Fetopathology **551**
Tamas Marion, Zoltan Ban, Zoltan Papp
32. Doppler Sonography in Obstetrics **567**
A Kubilay Ertan, H Alper Tanriverdi, Werner Schmidt
33. Doppler Study of Fetal Arterial Circulation **606**
Giampaolo Mandruzzato, Gianpaolo Maso, Yoram Jacob Meir
34. Doppler Study of Fetal Venous System **612**
Gianpaolo Maso, Giancarlo Conoscenti, M Piccoli
35. Postpartum Ultrasound **631**
Ajlana Mulic-Lutvica

36. **Three-Dimensional Sonoembryology** **646**
Bernard Benoit, Tomislav Hafner, Asim Kurjak
37. **Three-Dimensional (3D) Ultrasound in Obstetrics** **662**
Asim Kurjak, Milan Kos, Nika Kalogjera
38. **Three-Dimensional Visualization of Fetal Malformations** **686**
Fernando Bonilla-Musoles, Luiz Eduardo Machado, Francisco Raga
39. **Fetal Behavior: Ontogenesis and Clinical Applications** **713**
Kotaro Fukushima, Shoji Satoh, Hitoo Nakano
40. **Ultrasound-Guided Fetal Invasive Procedures: Current Status** **751**
Juan M Troyano Luque, Matilde T Clavijo Rodriguez
41. **Chorionic Villus Sampling** **773**
CihatSen
42. **Amniocentesis and Fetal Blood Sampling for Prenatal Diagnosis** **783**
Aris J Antsaklis
43. **Invasive Genetic Studies in Multiple Pregnancy** **798**
Aris J Antsaklis
44. **MRI: How to Use it during Pregnancy** **807**
Ichiro Kawabata, Yuichiro Takahashi, Shigenori Iwagaki

Section 3 Gynecology

45. **Normal Pelvic Anatomy Assessed by Ultrasound Methods** **828**
Sanja Kupesic, Asim Kurjak, Ana Tripalo
46. **Ultrasound of the Uterus** **846**
Sania Kupesic, Asim Kurjak, Drazena Bjelos
47. **Ovarian Sonography** **870**
Asim Kurjak, Matija Prka
48. **Fallopian Tube** **896**
Asim Kurjak, Sanja Kupesic, Drazena Bjelos
49. **Color Doppler in Adnexal Masses** **913**
Asim Kurjak, Ivanka Bekavac, Sanja Kupesic
50. **Sonographic Imaging in Infertility** **940**
Sanja Kupesic, Asim Kurjak, Drazen a Bjel
51. **Ultrasound Markers of Implantation** **985**
Luis T Mercé
52. **Sonohysterography and Sonohysterosalpingography: A Text-atlas of Normal and Abnormal Findings** **999**
Sanja Kupesic, Asim Kurjak, Drazena Bjelos
53. **Guided Procedures using Transvaginal Sonography** **1019**
Sanja Kupesic, Asim Kurjak, Drazen a Bjel
54. **Ultrasound in the Postmenopause** **1033**
Boris Ujevic, Biserka Funduk-Kurjak, Asim Kurjak

55. Sonographic Evaluation of Acute Pelvic Pain **1059**
Sanja Kupesic, Alenka Aksamija, Asim K
56. Gynecologic Ultrasound in Emergency Room **1083**
Vladimir Sparac, Asim Kurjak
57. Ultrasound in Gynecological Urology **1088**
Ivanka Bekavac, Renato Bauman, Radoslav Herman
58. Ultrasound of the Breast 1094
Boris Brkljacic, Ladislav Pavic

Index 1129

Introduction

The History of the Ian Donald School

In 1981, during the 4th European Congress on Ultrasound in Medicine and Biology held in Dubrovnik, a rnultidisciplinary group of enthusiasts met at the Inter-University Center for Postgraduate Studies (IUC) and established an advanced course which was named after Ian Donald and planned to have annual meetings within this unique institution. The IUC is an international, non-governmental, nonprofit organization located in Dubrovnik, Croatia, devoted to the purpose of furthering teaching and research cooperation between institutions throughout the world on themes of international importance. The IUC was established at the initiative of the Zagreb University in 1972 and united 240 universities and scientific institutions from 50 countries. Over the years, the IUC has become one of the world's leading centers of high education and scientific communication.

The first Ian Donald course was held in 1982, co-organized by Asim Kurjak and George Kossoff, attended by 152 participants from 42 countries. Ian Donald and his wife Alix attended the first 12 courses held at the School. Since its foundation, the School has organized 32 advanced courses in Dubrovnik and throughout the world and has been attended by 2520 students from 63 countries. It is now an integral part of the University of Zagreb. In 2002 the School celebrated its 20th year of existence by organizing a special course at the end of May attended by all School Directors and many of the previous lecturers. After George Kossoff's retirement, Frank Chervenak was named co-director.

One of our many guests, Professor Tommy Thompson, former president of The World Federation for Ultrasound in Medicine and Biology, wrote:

"Recently, I had the opportunity of taking part in a rather unique and outstanding ultrasound conference held in Dubrovnik, organized by the Ultrasonic Institute, Medical School University of Zagreb. The Ian Donald course was outstanding in that it presented the most up-to-date, state-of-the-art information on ultrasound that is available today. The faculty was exceptional in that the world leaders were brought together from more than a dozen different countries. The subjects covered included prenatal diagnosis and therapy of congenital fetal abnormalities, ultrasonic-guided puncture techniques, ultrasound in the management of female infertility, fetal, uterine, and ovarian blood flow determinations and application, and a round-table on controversies in obstetric ultrasonography. There was a free flow of information and an unusual amount of participation by the audience, most of whom were authorities on many of these subjects in their own rights. This was an intense 5-day meeting dedicated to the higher levels of ultrasound knowledge and thinking in the world and it took place in a unique and beautiful setting on the Adriatic coast. It was by all standards a superb conference geared to the leading edge of present-day ultrasound knowledge. The Ultrasonic Institute from Zagreb should be congratulated

for having developed most timely, informative, and well-presented international ultrasound school."

The School has evolved to have seven international Chapters. This permits the dissemination of knowledge throughout the world. Each Ian Donald Chapter has developed according to the character of the respective country and culture. This structure permits an international cross-fertilization of ideas while remaining sensitive to the uniqueness of each participating country throughout the world.

The first Chapter was organized in Trieste, Italy by Giampaolo Mandruzzato who coordinated three successful courses. Professor Vincenzo D'Addario, Head of the Department of Obstetrics and Gynecology, University of Bari is the new director of the Italian branch. Professor D'Addario taught at the first Ian Donald School in Dubrovnik and has coordinated basic ultrasound courses in Bari. This program will be complemented by advances of ultrasound in Obstetrics and Gynecology under the Ian Donald School. The first Ian Donald advanced course was held in Bari in June 2003.

In 1992, the first Ian Donald course was established in Granada, Spain with Professor Gonzalez-Gomez as the course director. The program of the School was soon recognized as an integral part of the postgraduate curriculum at the Medical School, University of Granada. Three successful courses have been organized in Granada. In 2002, the decision was made to continue the Spanish Ian Donald courses in Barcelona under the leadership of Professor Jose Maria Carrera. The Ian Donald School in Barcelona was held on November 25, 2002.

In 1984, we were invited by Professor Cihat Sen to organize the first Ian Donald course in Istanbul, Turkey. Since then, the Turkish branch has been extremely active. Four courses have been held in Turkey under the organization of Professor Sen as the Course Director. There have been two courses in Istanbul and two courses in Antalya. Last year in Antalya, there were more than 600 participants.

Ian Donald courses started in Japan where Professor Kazuo Maeda organized the first course in Fukuoka in July, 1998. The second school was held from 17–18 June 2000 in Tokyo with Professors Hisaya Takeuchi and Asim Kurjak as Directors, while the third one took place in Echigo-Yuzawa in April 2001. All three meetings were very well attended not only by physicians but also by enthusiastic nurses and midwives. The fourth Ian Donald School was held in October 2002 in Nagoya. The coordinator was Professor Ichiro Kawabata. The next one will be in November 2003, organized by Professor Kunihiro Okamura.

In 2000, Professor Sarraf from Al-Amal Hospital, Amman, Jordan established a Center for postgraduate teaching in ultrasound, joining the Ian Donald School. The new center in Amman, now in its third round of training, stands as a great opportunity for physicians to learn their skills in the field of ultrasound. The Amman Center for the Middle East initiated its first training course in 2001. Despite the fact that the idea of such a center was novel in the region, the interest and the participation of physicians who readily enrolled on the course were overwhelming. The positive response of the participants demonstrated the success and the welcoming of such courses.

It is important to note that the Amman Center is publishing a quarterly journal Sonanews, edited by Maher G.Sarraf, containing many useful scientific and organizational information and distribute all over the Middle East region.

There is a long-standing tradition of organizing annual advanced national courses in Athens by Professor Aris Antsaklis. One year ago, our Greek colleagues joined the Ian Donald School, becoming the Greek branch with Aris Antsaklis as the course director. The first course sponsored by the Ian Donald School was held from 22–23 February 2003 in Athens and was attended by 300 participants.

We now welcome the 7th branch of our School—the Indian Ian Donald course, organized this year in Agra. Professor N.Malhotra is a very well-known ultrasonic expert in India and was organizer of several advanced courses under the title "Agra Update—Obstetrics and Gynecology Ultrasound Course". In 2003, he will continue his courses under the direction of the Ian Donald School, where he expects 600–700 participants.

The newest branch of the Ian Donald School is planned for Hungary. This branch will be directed by Professor Zoltan Papp. The course is scheduled for November 2003.

We believe that the Ian Donald School in its 21st year of existence has had a remarkable past and we look forward to a remarkable future. It is most appropriate to finish this review by quoting some parts of Professor Ian Donald's speech at the opening of his School in Dubrovnik in 1982.

"Looking back over what has been a long story of trial and even more of error, I cannot help feel a sense of surprise at all the lucky strikes which have been made over the years and the associated spin-offs. Who, for example, would have thought that our crude early work would have made possible the correct diagnosis of hydatidiform mole within a matter of minutes or that we would ultimately, following upon this, have refined the technique to the demonstration of the placenta, both as to site and nature? Here I must acknowledge our co-operation with our friend in Denver, Colorado with whom we have maintained a happy liaison over the years. Our experiments in 1961 in measuring the biparietal diameter proved to be the start of all the present sophisticated forms of fetal biometry.

To newcomers to the field of ultrasound, there must be some bewilderment as to what sort of apparatus to start off with. There are many manufacturers and I have noticed a steadily increasing convergence as to quality of performance as well as price, so that you get roughly what you pay for. Cheap apparatus, cheap results. Expensive apparatus which may yield results beyond your clinical needs. So you should think well before choosing.

When a pupil can teach his teacher, as I now recognize, then it is not only time to stop but also to rejoice at the newly found success of his one-time discipline. For myself, I do not think that I deserve more acknowledgment than a man who happens to win a football pool. Nevertheless, I trust that I may be forgiven for feeling proud of so many of you, proud of who and what you are and proud of what I know you will achieve."

Zoltan Papp
Maher Sarraf
Cihat Sen

Section 1
General Aspects

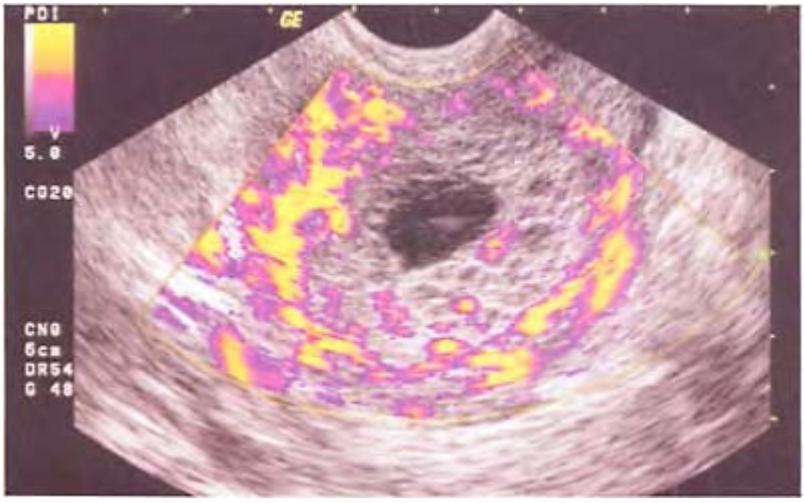

Chapter 1
Understanding Technology—Key to Correct Diagnostics

Branko Breyer

THE NATURE OF ULTRASOUND

Ultrasound Waves and Their Interaction with Tissues

Ultrasound is sound of a frequency higher than humans can hear (above 20 kHz). In medical diagnostics one uses frequencies between 2 and 20 MHz (1 MHz=1 million cycles per second). Only the longitudinal mode of ultrasound vibration is used in soft tissues. The waves propagate in soft tissues at an average speed of 1540 m/s. The wavelength is the distance between two adjacent pressure maxima in space and it is inversely proportional to the frequency.

$v = f\lambda$

At 1.5 MHz the wavelength is 1 mm, at 3 MHz it is 0.5 mm, at 6 MHz it is 0.25 mm, etc. The shorter the wavelength the better the resolution of an ultrasound scanner. The intensity of ultrasound waves is measured in watts per square centimeter (W/cm^2).

The practical consequence of this is that, in order to get the best resolution, one ought to work with the highest practical frequency in any particular case.

There are densifications and the rarefactions of the medium as ultrasound passes through it.

As ultrasound encounters a boundary between two media of different characteristic acoustic impedances and different propagation speeds it can be reflected and refracted while crossing the boundary.

The ratio of the reflected wave intensity to the incident intensity depends on the difference of the characteristic acoustic impedances of the two media, the angle of incidence and on the propagation speed ratio. At perpendicular incidence the reflection does not depend on the propagation speeds.

$$\frac{p_r}{p_u} = \frac{Z_2 - Z_1}{Z_2 + Z_1}$$

Where p_r is the pressure amplitude of the reflected wave and p_u is the pressure amplitude of the incident wave.

The larger the difference of the acoustic impedances (Z_1 and Z_2)-the larger the fraction of ultrasound reflected.

The reflection laws (Fig. 1.1A) are valid if the boundary is much larger than the wavelength (fetal skull gallbladder, urinary bladder wall are examples of specular reflectors). If the reflecting entities are smaller than the wavelength they scatter (Fig. 1.1B) ultrasound in all directions and only a small fraction goes back towards the transmitter. This means that we can obtain ultrasound echoes from a scattering tissue from all directions, which is not the case with the larger specular reflectors. The echoes are, however, smaller and the position information is, unlike with the specular reflectors, lost in the case of scatterers, but the pattern obtained can still bear useful information. Liver, spleen, brain are examples of such scattering media,

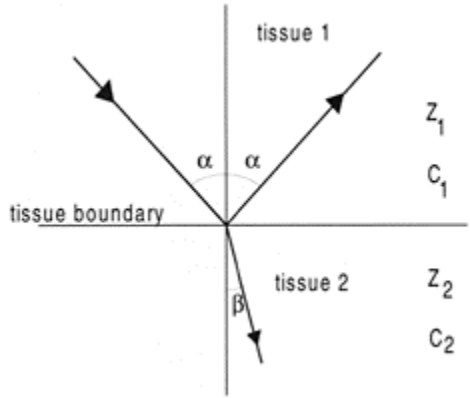

Figure 1.1A: Reflection and refraction

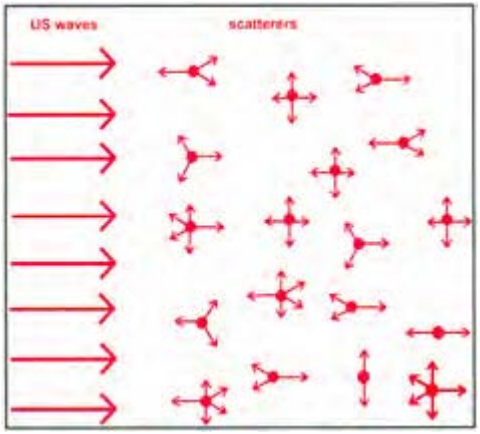

Figure 1.1B: Scattering

When crossing through a medium, ultrasound waves are attenuated, i.e. the energy in the beam decreases due to absorption, scattering and reflection. Attenuation is proportional to frequency—the higher the frequency the less penetrating the ultrasound waves. The law of attenuation is exponential, and the coefficient of the exponential in Nepers/cm or Decibels/cm is quoted in tissue property tables.

Soft human tissues, bones and gases have distinctly different ultrasound propagation properties.

Characteristic acoustic impedance is about five thousand times smaller in gases than in soft tissues, and is two to three times higher in calcified bones than in soft tissues.

Speed of ultrasound is about 340 m/s in gases, it is on the average 1540 m/s in soft tissues and is between 3000 and 4000 m/s in bones.

Attenuation in gases and bones is 10 to 30 times higher in bones and gases than in human soft tissues.

The difference between these parameters among the soft tissues is of the order of 5 15%. Blood is an exception in that it has a low attenuation coefficient.

Summary
Ultrasound waves are mechanical waves, which can propagate, in human tissues. The waves reflect and refract at tissue interfaces much larger than ultrasound wavelength and scatter at scatterers smaller than the wavelength. Ultrasound waves attenuate when crossing through tissues. Bones and gases reflect ultrasound much more than different soft tissues. Average ultrasound speed in soft tissues is 1540m/s, Speed in gases is much smaller and in bones much larger than in soft tissues.

THE ULTRASOUND SCANNER

An echoscope or an ultrasound scanner is a device, which makes section images of the interior of the body using the information obtained from the echoes of ultrasound pulses transmitted into the body. An echoscope transmits short pulses of high frequency ultrasound (less than 1 microsecond long, frequency between 2 MHz and 10 MHz, about 1000 times per second) into the body via a probe. The system then waits for the echoes to return, and picks them up by the same probe. The direction of transmission-reception is known, because the probe scans in a predetermined way and the round-trip time for the echoes is measured in the echoscope and so all the data to form a two-dimensional (2D) image are there.

An echoscope (sonar, echograph, US, scanner) consists of the following parts:

- A probe which contains piezoelectric transducers to generate and detect ultrasound and some scanning means to direct ultrasound in desired directions.
- A microprocessor controlled electronic system which generates electrical pulses for the probe activation, directs the pulses into the probe for focusing and steering, amplifies the signals obtained from the echoes, and stores the data and displays them on a TV monitor. The amplifier amplifies the echoes that come later (from deeper structures) more than those coming from shallower structures in order to compensate for attenuation of ultrasound.

• The signals, which represent ultrasound echoes, are, as said, processed. Processing before storage in the computer memory is called preprocessing. This includes the TGC and other gain and focusing processing. After the data are stored in the memory they can again be processed in order to show them with different shades of gray and different relations of echo intensity to brightness on the screen. This is called postprocessing.

The echoes from the body can be displayed in three basic ways: the A mode, the B mode and the M mode.

In the A mode display (amplitude mode) the echoes from the axis of the beam in front of the probe are shown as peaks proportional to the echo amplitude positioned at their respective distances along the line-of-sight (Fig. 1.2A). This is a one-dimensional display. It is used in ophthalmology and sinuses examination, and sometimes in neurology.

In the B mode display (brightness mode) the echoes are shown as bright dots with brightness proportional to the echo amplitudes (Fig. 1.2B). This mode is normally used as 2D scan, in that the interior of the body is scanned with the beam so that the bright dots merge into tomographic contours.

Since the image is formed by using ultrasound beams of varying diameter, they result in sections (tomographic slices) of definite thickness. This thickness cannot be seen on the screen of a TV monitor, but results in reduction of resolution of the B mode image.

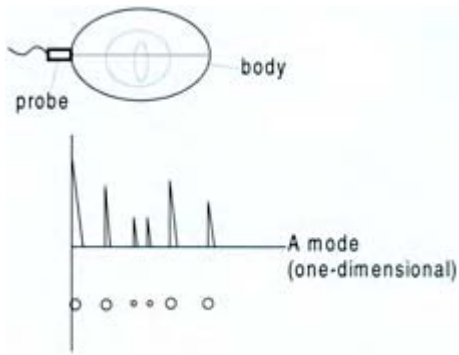

Figure 1.2A: A mode

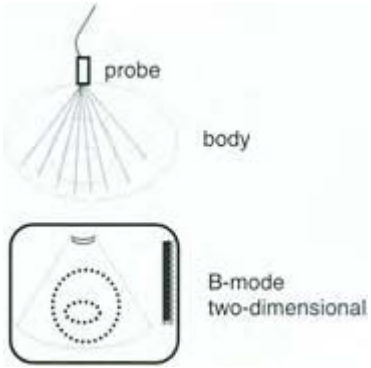

Figure 1.2B: B mode

The M mode display (motion mode) serves to present the movement of structures in the body (usually cardiac). The ordinate is the depth from the skin and the abscissa is the running time (Fig. 1.3). A reflector at rest is shown as a straight line, while the moving reflectors leave a wavy trace, which is the time function of their movement.

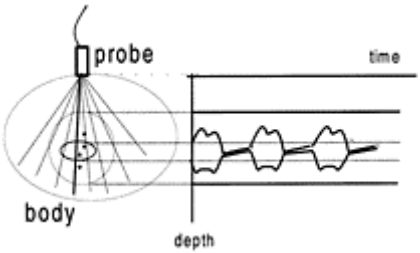

Figure 1.3: M mode

So far we have explained the method of echography with no details, but for operating the machine or in order to purchase one, some of the details must be known in more specifically. These include the TGC amplifier and the probes.

The Time Gain Compensation (TGC)

Ultrasound pulses are attenuated as they travel through the body and therefore the echoes from deeper structures are weaker (have less intensity) than those from shallower reflectors. Since we want to show equal tissue interfaces equally on the screen, the attenuation must be compensated for by more amplifying the echoes which come later (from deeper) than the earlier echoes. This TGC system is accessible from the front panel of a scanner and must be used to obtain balanced images. It always contains controls for separately controlling the near gain, the far gain, the slope between the two and the overall gain. The overall gain equally changes the gain for the echoes from all depths (in practice this means changing the number of details in the whole image). By adjusting the

near and the far gain and the slope between them we balance the image so that the deep and the shallow parts are of approximately equal intensity on the TV monitor. There exist many different ways to achieve this balancing, but if the basic idea is understood the knobs can soundly be used after reading the manual accompanying the scanner.

Summary
An echoscope makes section (thomographic) images by registration of echoes of short ultrasound pulses transmitted into the body. In practice one uses frequencies of 3 to 7 MHz, lower frequencies for deeper and higher for shallower scanning. Echoes returning from deeper structures are amplified more in order to compensate attenuation of waves in the body. The echoes returned are shown as bright dots on a TV monitor. The imaged section has a thickness, which depends on focusing and nature of reflectors (2 to 8 mm).

Ultrasound Beam from a Piezoelectric Transducer

A piezoelectric transducer converts electrical pulses into ultrasound vibrations and vice versa. The piezoelectric material in medical uses is a thin plate of synthetic ceramics or a foil of piezoelectric plastics. An ultrasound probe contains one or more piezoelectric transducers. The radiating and receiving face of the transducer must be much larger than the wavelength used (e.g. 20 times). The part of the medium occupied by ultrasound in front of the transducer is the beam that could be for example measured in water.

The beam is not sharply cut off, but the intensity decreases gradually towards the sides. We can represent it as a collection of isointensity lines. The beam narrows in the focal zone.

A probe that operates at higher frequency is smaller, has a better resolution and less penetration.

The tomographic section (slice) has the thickness of the effective beam. Therefore its thickness is not equal at all depths.

It is irregular in the near field (i.e. the field near to the transducer). This irregularity is a consequence of interference of waves from different parts of the transducer face and can introduce problems when scanning shallow organs such as the breast, eye or thyroid. To scan these organs we introduce a layer of water or gel between the probe and the body. Further away from the transducer the ultrasound field decreases monotonically and is called the far field.

Focusing

A narrower beam yields better images. In order to narrow a beam, one focuses it. The beam can be focused with lenses and mirrors as well as electronically with composite transducers (Fig. 1.4). Ultrasonic lenses act in the same way as optical lenses. They can be focused at different distances. However, when choosing a particular probe, the focus must be chosen at the depth of interest. Electronic focusing is based on using composite transducers, i.e. densely-packed sets of narrow transducers of annular-or strip-shaped

arrays. These transducers are activated with delays chosen such that the waves from each of the transducers reach the intended focus position at the same time. This type of focusing is flexible; i.e. the focus can be set at the desired position. Both fixed and electronic focusing are used in real probes.

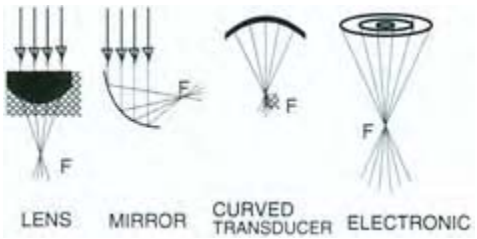

Figure 1.4: Focusing methods

Scanner Probes

Figure 1.5 illustrates the most common types of probes in use today.

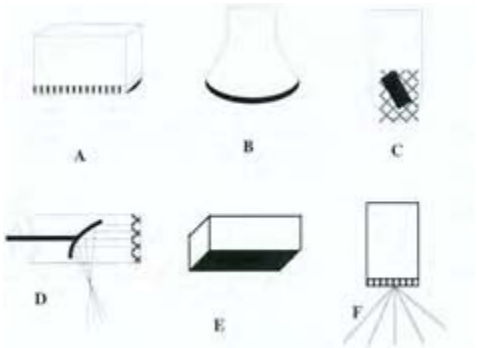

Figure 1.5: Probes

The probes contain one or more piezoelectric transducers. They can basically be divided into sector and linear probes. Sector probes look into the body through a small acoustic "window" (1×1 to 2×2 cm), have acoustic lines-of-sight fanning out and yield a nearly triangular (sector) image. The linear probe has a longer front face in contact with the patient's body (5–12 cm), parallel or nearly parallel lines-of-sight and yield a rectangular image.

The probe in Figure 1.5A is the linear array consisting of about 60 to 200 strip transducers arrayed side-by-side and each connected to the scanner electronics via a separate wire. Groups of about ten to 32 transducers are activated at a time yielding a composite transducer ten strip transducers wide. This is then shifted in a fast sequence to the end of the probe. This operation achieves the same effect as though we had moved a 32 strip wide single transducer along the probe length and thereby scanned whatever was

in front of the probe. Since we, at each instance, activate a group of transducers there is the possibility to electronically focus the beam by first firing the outermost members of the group and then with small delays the others towards the center. Depending on the delays the ultrasound pulses from the different transducers will meet at the same time at a point—the focus point. This applies to one plane, in the other plane the focus is fixed with a lens. The resulting image consists of parallel lines and is of a square format. This kind of probe is the least expensive, and is suitable for obstetric, breast and thyroid scanning. This probe can have a flexible focus in one plane but it has a fixed focus in the plane perpendicular to the scanning plane.

A rocking annular array mechanical sector probe is shown in Figure 1.5C. The transducer consists of a number of concentric annular transducers, which can be activated with delays, yielding a flexible circular focus. The sector probes are suitable for upper abdomen, gynecology, cardiology and neonatal head scanning.

Figure 1.5B shows the convex or curvilinear probe which functions very much like the linear array (Fig. 1.5A) only the transducers are mounted on a curved surface so that the lines-of-sight fan out, making it suitable for upper abdomen and gynecological applications. The curvilinear probe is a good compromise between parallel and sector scanning. This probe can have a flexible focus in one plane but it has a fixed focus in the plane perpendicular to the scanning plane.

Figure 1.5E shows a matrix array probe that can steer and focus the ultrasound beam in two planes. Unlike the probes in Figures 1.5A and 1.5B, the probe in Figure 1.5E can have focusing in both planes adjustable or dynamic.

The phased array sector probe (Fig. 1.5F) is built like the linear array but is much shorter (1.5 to 2 cm) and uses delays for both steering and focusing of the beam. It has no moving parts, is very popular in echocardiography and is usually somewhat higher priced than the simpler types of probes.

Summary

Scanning probes can be divided into sector, linear and curvilinear (convex). Sector probes yield a triangular (sector) image and look into the body through a small acoustic window. They are suitable for imaging of the upper abdomen, in gynecology and in cardiology. Linear probes yield a rectangular image and are best suited for obstetrics, breast and thyroid scanning. Convex probes are a compromise between the sector and linear type and can be used in the majority of body areas. For different areas different curvatures of the probes can be chosen. All probes are normally focused and when choosing them one must take the focus at the depth of interest. Approx. 3 MHz probes are used for adult deep scanning. 5 MHz probes are used for child and superficial scanning. Higher frequency yields a better resolution, but a poorer penetration

PRACTICAL ASPECTS

Use of the Probes

Different probes are optimal for different examinations. Probes of lower frequencies are better suited for deeper scanning. Frequency of about 3 MHz are suitable for adult upper abdomen, heart and gynecologic scanning. Frequencies of about 5 MHz are suitable for child, slim adult, breast and limb scanning. Frequency of 7 MHz is suitable for some of the child examinations, for thyroid and eye scanning. The basic rule is to use as high a frequency as possible for the particular depth.

Focusing is of great importance for quality of the scanning. Therefore one must choose the probes which can focus at the depth of interest. For annular arrays and matrix probes the focus is truly adjustable. For all other presently available types the focus is either fixed or adjustable in one plane, but fixed in the other. Therefore it is not sufficient to choose only the frequency but the focus must be decided too.

The type of scanning to use depends on the body area to be examined.

Linear arrays are suitable for obstetrics, breast, thyroid and neonatal hip examination.

Sector probes are suitable for upper abdomen, gynecology, neonatal head, sinus cavities and the only type for heart scanning.

Convex (curvilinear) probes are a good compromise. They are suitable, depending on the curvature, for all areas (although a true sector probe is better for echocardiography).

There exist many variations of the described types of probes. Probes have been designed for intracavitary applications (vaginal, rectal, vesical, esophageal), for intraoperative applications, for puncture guidance (with appropriate guiding holes) etc. The only way to chose among them is to well understand the outlined basic principles and then to see the special variation.

The probe is the most sensitive, the most exposed and the most expensive single part of a scanner. It must be handled with care at all times. The most usual cause of malfunction is dropping the probe. The other critical part is the probe cable that tends to break at the probe end due to mechanical stress and aggressive oils. Probes should not be changed during the scanner operation unless specifically allowed by the manufacturers. Some of the probe materials can not stand some contact oils (this generally applies to the cable sheath). This must be learned from the manufacturer before purchase. In mechanical sector probes occasional service of the bearing might be needed. If the probe becomes noisy, it is likely to perform poorly.

Resolution

The ability of an imaging system to separately show adjacent reflectors is called resolution. Resolution across the ultrasound beam is called the lateral resolution and resolution along the beam is the axial resolution. In virtually all the present scanners is the axial resolution better than the lateral. Therefore shall we consider mainly the lateral resolving power. The lateral resolution depends mainly on the effective width of ultrasound beam. In the focus zone of a transducer is the beam narrower and the

resolution in that part of the image is better. A long synthetic focus yields a good resolution in larger parts of ultrasound images than if the focus is fixed within a short area. If two reflectors are side-by-side within the beam width they can not be resolved. As shown previously the intensity of ultrasound gradually falls off as we move to the side of the beam. If a small reflector is faint, only the central, intensive, part of the beam yields echoes strong enough to be detected. A strong reflector will be recorded during the scanning process across a much larger width than a faint reflector. As a consequence, the resolution of fainter reflectors in an image is better than that of stronger reflectors, as long as they can be seen at the same time in the same image. The ratio of the most intensive to the least intensive echo in an image is called the dynamic range. If the dynamic range is large we can see a broad range of different echo intensities in the same image and the image is “soft”.

A word of warning: The contrast (image dynamic range) can be changed with the contrast and brightness controls on the monitor. These must be adjusted so that the electronically generated gray wedge is best seen. Once this is adjusted—do not change the setting! Adjust the image quality using other scanner controls. The effective imaging dynamic range changes when we change the overall sensitivity but it can be changed with specific controls for dynamic range and suppressor level as well.

Bones are strong reflectors broadened due to the large effective beam width. Other reflectors are shown with better resolution. If we reduce overall sensitivity the faint reflectors disappear from the image, but the strong reflectors are shown accurately. In practice this means that one should use broad dynamics and fairly large sensitivity for orientation and general information and then, if stronger reflectors must be measured, the sensitivity must be reduced to obtain good resolution and accurate measurements. This procedure is of importance in obstetric scanning for obtaining accurate measurements of fetal bones. Sometimes one can intentionally use the axial resolution, for example; in order to image a narrow blood vessel we should orient the probe in such a way that the diameter of the blood vessel is along the beam, i.e. the vessel runs across the screen approximately horizontally.

Measurement

Lengths can be measured on the monitor screen using electronic calipers. This is done by moving marks on the screen using a joystick, a trackball or some keys. Two marks are put at two ends of the structure to be measured and the distance is read off on the screen. Exact physical measurements imply the knowledge of the speed of ultrasound in the particular area and other special knowledge about the instrument. Fortunately, normal routine measurements are, in fact, a comparison of the normal measured data and the particular result and so the detailed knowledge is not needed as long as one measures in the same way in which the normal data have been obtained.

Summary

Linear probes are used in obstetric, breast and thyroid scanning. Sector probes are used in the upper abdomen, gynecology, and cardiac work. Convex probes can be used for

everything, depending on their curvature. Frequency of approx. 3 MHz is used in general work. Frequency of approx. 5 MHz is used in

child and shallow scanning. Focus must be chosen according to the depth of interest. Skin must be oiled or pasted with gel before scanning, Depth (axial) resolution is better than the sideways (lateral) resolution. The scanning should be started with large dynamics and sensitivity of the scanner to gain a general overview of the situation and then reduced if bones or prominent contours are to be measured.

Artifacts

An artifact in an echographic image is everything that does not conform to the idealized section image described so far. Recognition of such artifacts is important because they sometimes mislead and sometimes yield additional data about the character of the imaged structures.

- A cyst appears as an echo free area and an echo enhancement behind it. Sometimes shadows appear laterally behind the cyst. The absence of echoes is due to absence of impedance interfaces within the liquid. The posterior enhancement is due to lower absorption of ultrasound in the liquid so that the posterior echoes are overcompensated by the TGC. Lateral shadowing is due to reflection, refraction and absorption of waves in the walls.
- Bones cast shadows and obscure tissues behind them. This means that one must look into the body through acoustic windows avoiding the bones, e.g. ribs in the upper abdomen and echocardiography. The bones themselves can not be correctly imaged with the present echoscope.
- Gas causes strong reflection of ultrasound and obscures the tissues behind it by reverberation and shadowing. Intestinal gas causes problems in scanning the liver, pancreas, paraaortic lymph nodes, uterus and ovaries. Uterus and ovaries can be exposed to ultrasound by filling the urinary bladder, thereby pushing the bowel out of the viewing field.
- Fetal bones are the strongest reflectors in the fetus. When the scanner setting is such that all the fetal organs can be seen—the bones are shown with poor resolution, i.e. they are shown broadened. To measure a bony structure the overall sensitivity of the scanner must be decreased by about 10–15 dB.
- Subcutaneous fat can scatter ultrasound and blur the image.
- Reverberation appears behind parallel structures and strong reflectors. Reverberation often shows in liquid filled areas, but exists elsewhere as well, only cannot be seen so well. Structure behind the diaphragm is normally a repeated image of the liver. When using a delay bath (in breast, thyroid) multiple images appear due to reverberation.

Puncture Guiding with Ultrasound

Ultrasound can be used for aiming and guiding puncture. The steel needle reflects ultrasound and can be followed when penetrating the body. However, this must be done with due caution, because the needle shows poorly if hit by the ultrasound beam under an

acute angle and because only the part of the needle which is within the scanning plane is actually imaged. If the needle bends and leaves the scanning plane, the apparent tip is just the position where the needle leaves the plane. In such a case the puncture will be missed.

The basic method to avoid this is to use a needle holder for puncture guidance, which keeps the needle in the plane. The most common type is a device fixed to the probe with a calibrated hole to guide the needle. The holder can be opened and detached from the probe so that the needle or a cannula can be left indwelled after finishing the scanning.

Puncturing is always easier to guide in liquid filled spaces, e.g. amniotic fluid or ascites. In solid tissue the needle visibility is not always good and sometimes the tip is seen as a slightly brighter dot which moves in coordination with the operators hand movement and can thus be recognized only during the procedure but not on a frozen image.

Recently a number of systems have been devised to visualize the puncture needle or indwelled catheters. These operate by making the needle or catheter tip ultrasonically different to the surrounding. The majority of routine punctures are still done with serial fine needles up to a diameter of 0.9 mm.

Physical Principles of the Doppler Effect and its Application in Medicine

Doppler technique has been used in medicine for many years but only in the last decade this diagnostic modality has gained importance in obstetrics and gynecology. B-mode ultrasound gives information about morphology. Doppler ultrasound gives information about blood flow.

Potentials for Doppler ultrasound application in gynecology are still not very well explored. However, despite tremendous effort and research interest from all around the world, promising results from Doppler research are still far from practical and routine clinical application. There are many objective and subjective reasons for that situation such as: low results reliability and reproducibility, high technique complexity, inadequate education and knowledge of pelvic hemodynamics, lack of standardization in Doppler measurements, cost-benefits issues (Doppler machines are usually very expensive), question whether Doppler should be used as a screening tool or as a secondary or even tertiary test, interpretation of results, time consuming procedure, question of safety in early pregnancy, etc.

For intelligent and successful application of the technique to medical diagnosis, an understanding of Doppler physics, its possibilities and limitations is necessary. Flow can be detected even in vessels that are too small to image. Doppler ultrasound can determine the presence or absence of flow, flow direction, and flow character. One of the fundamental limitations of flow information provided by the Doppler effects is that it is angle dependent. Furthermore, artifacts in Doppler ultrasound can be confusing and lead to misinter-pretation of flow information. These problems will be addressed in this chapter.

The Doppler Effect

The basic principle of the Doppler effect for the case when the waves reflect from a reflector is illustrated in Figure 1.6. If the reflector does not move (case a) the frequency of the reflected wave f_1 is equal to the transmitted frequency f_0. If the reflector moves towards the transceiver, the reflected frequency will be higher than the transmitted (case b), while in case that the reflector moves away (case c) from the transceiver the received frequency f_1 will be lower than the transmitted f_0. This frequency change Δf (called the Doppler shift) is proportional to the velocity v of the reflector movement.

In practice this means that we need an apparatus that transmits ultrasound waves into the body and receives their reflections from the body. The apparatus must then measure the difference between the transmitted and received frequency. The frequency difference (Doppler shift expressed in Hz) is proportional to the velocity of the movement along the line that connects the wave transceiver and the moving reflector.

In Doppler systems we measure just one component of the movement. The relation of this component to the total velocity depends on the angle.

In medical applications the Doppler effect is usually used by insonating the moving blood and assessment of the Doppler shift of ultrasound scattered on erythrocytes (see Figure 1.1B). Single erythrocytes reflect (retransmit) ultrasound in various directions, but the back-scattered energy is sufficient for velocity assessment.

The general method of measurement consists of transmission of bundled ultrasound into the body at a general angle a to the flow (Fig. 1.7). In this case the following equation of Doppler shift is valid to sufficient approximation.

$$\Delta f = \frac{2 f_0 \, V}{C} \cos(\alpha)$$

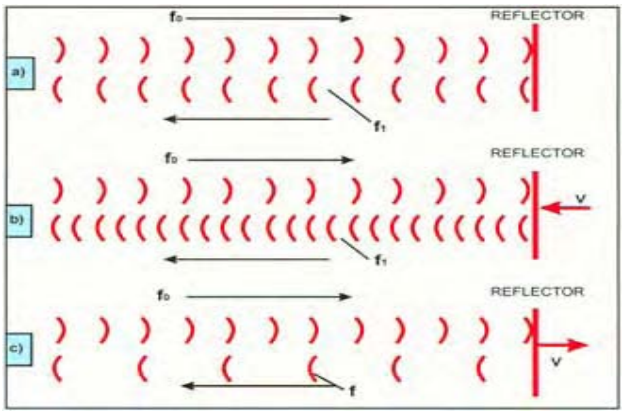

Figure 1.6: Illustration of the Doppler effect: change of frequency due to the movement of the reflector

It is important to note that in this approximation the Doppler shift for α=90° equals zero.

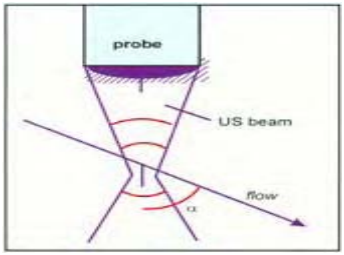

Figure 1.7: Relation between ultrasound beam and the flow

A more detailed theory shows that for wave beams the Doppler shift is not exactly zero at α=90°, but the shift is small and not used in the present commercial instrumentation. Thus the plane wave approximation from the above equation is valid for the normal practice.

From the above Doppler shift formula we can calculate the velocity v by equation:

$$V = \frac{\Delta f \bullet c}{2\, f_0 \cos \alpha} \text{ (m/s)}$$

With c=ultrasound propagation speed, Δf= Doppler shift, f_0=transmitted wave frequency, and a is the angle among the ultrasound beam and flow direction.

The flow in blood vessels depends on the quality of their walls and vessel dimensions. If the flow is laminar (when the walls are even and blood vessel is large enough) the flow profile is parabolic, that is, the velocity in the center is the fastest and slows down as we approach the walls. The law by which this change is approximately a parabola. (Fig. 1.8). If there is an obstacle in the blood vessel (a plaque, a branching, etc.) the profile deviates from parabolic and can become turbulent. In any case, at any instance at any cross

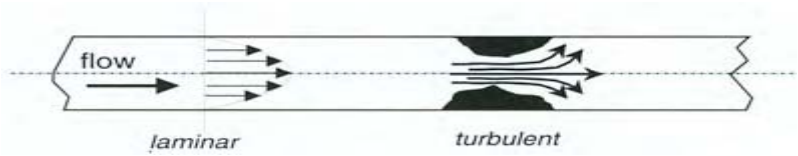

Figure 1.8: Real-time Doppler spectrum. Ordinate is the Doppler shift; abscissa is the real time

section the blood flows at many different velocities at the same time, i.e. there is a full spectrum of flow velocities.

The results are usually shown as Doppler shift spectra in real-time according as in Figure 1.9. The ordinate is the Doppler shift (Fig. 1.9) and the abscissa is the running time. Doppler shift measured in Hz is proportional to flow velocity and if the angle α is known, one can put velocities onto the ordinate by using the equation for velocity calculation.

The upper spectrum (ART) has the typical shape of an arterial spectrum. It is pulsatile. The venous spectrum of a peripheral vein (VEN) in the lower part of Figure 1.9 is not pulsatile. Venous flow is not pulsatile in peripheral blood vessels but can be very pulsatile as they approach the heart. Since the blood flows at each instance at different velocities, the spectra are generally filled-in. The lowest frequencies are cut off with special high-pass filters, the so-called, wall filters (wf). The filter was originally designed to eliminate the artifacts from moving blood vessel walls.

Apart from absolute velocity measurement, one can define relative indices, which are particularly useful for flow evaluation without known angle between the flow and ultrasound beam.

Summary
The Doppler effect consists of a change in frequency of waves that reflect from moving reflectors. The amount of the change of frequency is called Doppler shift and is measured in Hz. Velocity of the movement can be calculated if the angle between ultrasound beam and the movement, e.g. blood flow.

Doppler Indices

Because of inherent difficulties in quantitatively evaluating blood flow the blood flow velocity

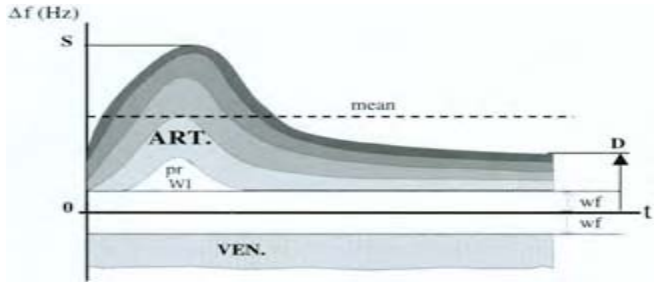

Figure 1.9: Illustrative arterial (ART) and venous (VEN) flow Doppler spectra

waveform has commonly been interpreted to distinguish patterns associated with high and low resistance in the distal vascular tree (Fig. 1.9). Three indices are in common use,

the systolic/ diastolic ratio (S/D ratio), the pulsatility index (PI, also called the impedance index), and the resistance index (RI, also called the Pourcelot ratio).

The S/D ratio is the simplest but it is irrelevant when diastolic velocities are absent, and the ratio becomes infinite. Values above 8.0 are considered “extremely high”.

Definitions of RI and PI are as follows:

$$\text{Resistance index } RI = \frac{S-D}{S}$$

$$\text{Pulsatility index } PI = \frac{S-D}{(mean)}$$

The RI is moderately complicated but has the appeal of approaching 1.0 when diastolic velocities are abnormally low and does, therefore, reflect the relative impairment of flow by high resistance. These indices are ratios, independent of the angle between the ultrasound beam and the insonated blood vessel, and therefore not dependent on absolute measurement of true velocity.

The PI requires computer-assisted calculation of mean velocity, which still may be subject to very large experimental error. In a normal pregnancy, neither the S/D ratio nor PI is normally distributed across all gestational ages.

L.Pourcelot and R.Gossling initially derived the indices for their statistically demonstrated association with adverse clinical findings. However, the RI must not be considered independent of changes in physiologic variables such as heart rate, cardiac contractility, blood pressure, and the many other determinants of flow. This information does not depend on the measurement angle since all the parts of the spectrum change proportionally when angle α changes. However, as the angle approaches 90° the measurement error increases rapidly. In practice is the best compromise between the resolution of B mode image resolution and accuracy of Doppler spectroscopy is obtained at angles between 30° and 60°

The three indices are highly correlated.[3,4] There are intrinsic errors in all that have been quantified and lie between 10 and 20%. There may be advantages to the RI or PI where flow is markedly abnormal or in early pregnancy, when a very low end-diastolic velocity can be a normal finding.

One should bear in mind that the RI depends on the peak systolic and end diastolic values only, so it is not sensitive to the rest of the waveform while the PI is, to some degree, sensitive to the shape of the spectrum.

INSTRUMENTATION FOR DOPPLER MEASUREMENTS

There are two basic technological methods for application of the Doppler effect in medicine (Fig. 1.10). It is possible to transmit and receive ultrasound waves continuously with a probe that contains a transmission transducer and a reception transducer (CW in Fig. 1.10). Another possibility is to transmit in the form of pulses whose Doppler shift is measured after the time necessary for ultrasound to reach a defined depth in the body (PW in Fig. 1.10).

These two systems have different properties. The CW system has no depth resolution so that the measurement results of all flows along the line-of-sight add together and mix. On the other hand, this system measures well all (fast and slow) velocities. If there is only one blood vessel along the line-of-sight or one flow is dominant, the CW system is very good for practice.

If, however, one must measure the flow in a single blood vessel, the PW system can measure within a well-defined sensitive volume. The sensitive volume has a length that depends on the pulse length (in time) and a width that depends on the beam width (and focusing) (shown as sens, vol. in Fig. 1.12). The disadvantage of such a pulse Doppler system is that it can not measure high

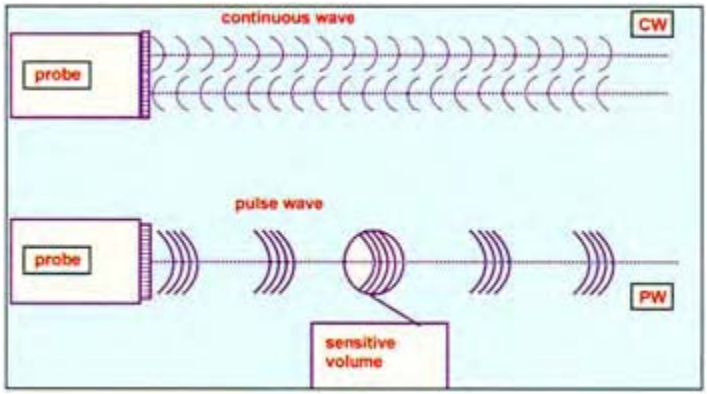

Figure 1.10: Continuous wave (CW) and pulse wave (PW) Doppler

velocities deep in the body. The reason for this is that a PW system only occasionally looks at the flow so that it can not convey all the information at an enough high throughput. The phenomenon can mathematically be described by the sampling theorem, which results in the so-called aliasing, i.e. reverse indication of flow that is too fast. The resulting artifact is shown in Figure 1.11. The top of the pulsatile spectrum (highest velocities) are shown as negative (reverse flow). If the spectrum is simple like in Figure 1.11, the recognition of the aliasing artifact is easy. In complex spectra this can be hard. In such cases it may be useful to have a combined PW and CW system or a HPRF system. The HPRF system has such a pulse rate that it violates the sampling theorem and thus yields mathematically ambiguous results. In the screen this is usually shown as multiple sampling volumes (spots, cursors). Such a system measures at multiple spots at a time. If the operator can recognize the spots with dominant flow or positions the cursors in such a way that only one of them hits flow, the system achieves a better performance for high velocity flow measurement.

Flow vs Velocity

The actually measured quantity is the Doppler shift in Hz. The actual display is Doppler shift versus time. If the angle between the ultrasound beam and the flow is known, one can calculate and display velocity versus time. The actual measurement of the Doppler angle is often difficult. In some disciplines the practice is to ignore the angle and speak about "velocities" (TCD, sometimes fetal echocardiography). The nature of the flow (pulsatile or steady, regular or turbulent, single or branching, parabolic or plug), impacts significantly on the frequencies returned. Thus, although volume blood flow can be calculated as the product of mean blood flow velocity and vessel area, this is fraught with variation in practical terms.

The cross-sectional area of the vessel measured from the gray scale image is very susceptible to error. Additionally the volume flow depends on the fourth power of the vessel diameter so that any measurement error is grossly amplified.[1,2,15] Even the thickness of the distance measurement cursor plays a major role in measurement accuracy in blood vessels of a few millimeters in diameter.

Another major problem in measuring flow is the variation of blood velocity across the vessel cross section. Because the overall flow rate is the sum of the contributions made by the blood at every point on the cross section, it is necessary to average the velocity profile (mean blood flow velocity). Various approaches to this have been described. The calculation is different when the velocity profile is measured (with multigated pulsed Doppler) and averaged or if it is averaged using a large sample volume to encompass the whole vessel. Volume blood flow has been expressed as milliliters per minute. In fetal applications the result may be normalized to the fetal weight. Estimating the fetal weight by ultrasound measurement formulas is also error-prone. It is clear, to allow accurate or even vaguely useful volume flow measurement, that Doppler interrogation must be limited to large vessels, with meticulous attention to methodology.

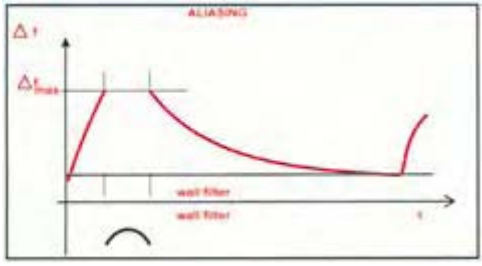

Figure 1.11: Aliasing

Figure 1.11 is an illustration of the aliasing effect on an arterial spectrum where the peak velocities have been too fast to measure with the particular pulse repetition frequency (PRF) of a pulsed Doppler system.

Two Dimensional Flow Measurements

2D COLOR DOPPLER DISPLAY

The flow can be shown in two dimensions (2D). In principle, comparison or subtraction of successive two-dimensional images can achieve this. Only echoes from moving structures stay in such images. The final result is a two-dimensional display of moving structures, mainly blood flowing through blood vessels.

The directions and speeds are color coded. Movements towards the probe are shown in different shades of one color, e.g. red, and away from the probe in shades of another color, e.g. blue. The different shades signify relative velocity. One must always bear in mind that this system shows the component of velocity projected onto the probing ultrasound beam. This makes the display semiquantitative. One can display the multiple Doppler shift measurement variance. In the red-blue combination code, the variance is usually shown in green. The larger the measurement variance—the more green. This gives an indication of turbulence. Flow at 90° to the ultrasound beam is not shown (in the image they are shown black, i.e. as if it were not there). The color code is arbitrary and in the majority of machines can be chosen from a number of different possibilities. Since the 2D, color Doppler is semiquantitative it is as a rule combined with a PW Doppler spectrometer. The 2D display helps in fast finding of the points where we wish to analyze the flow by spectrometry. In this way the 2D system reduces the duration of Doppler examinations. Sometimes, however, the 2D map is characteristic enough to help with the diagnosis. The limitations of the method are equal to the pulse Doppler technique and so we got the, now ubiquitous “Color Doppler”. As with any new method, the first amazement yielded its place to systematic and often controversial, but always tedious evaluation in clinical medicine. Since many of the most feared illnesses develop on a

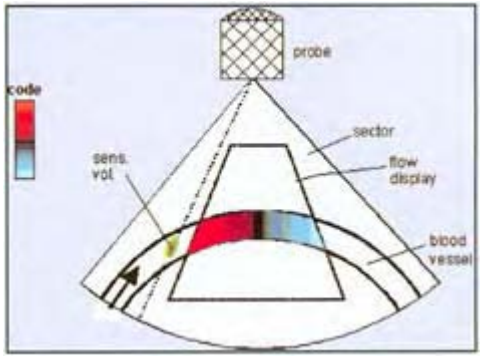

Figure 1.12: 2D flow mapping

long time scale, the method is still under scrutiny but is already accepted as a useful tool.

A particular form of 2D-flow mapping is the, so-called, Power Doppler (Fig. 1.13).

POWER DOPPLER ULTRASOUND

The shortcomings of the two dimensional directional Doppler ("color Doppler") are many. Above all, the sensitivity to direction is a mixed blessing. It does give the much-valued information about the direction of flow, but suffers from not-very-high sensitivity and direction artifacts. Now, in many cases the directional information if very valuable, like in echocardiography. However, there are many instances when the only relevant question is "Where are the blood vessels?" or "How many blood vessels are there?" or "What is the perfusion of this area?" The direction may be of little importance or determinable with a built-in Doppler spectrometer. Basically color Doppler yields that information. However, it is not uncommon to find a clear Doppler spectrum signal from an area that is completely without any color signal or where (if we are lucky) the color appears occasionally. The reason for this is that the directional information is evaluated from a number of subsequent frames and ambiguous and low signals average out to zero.

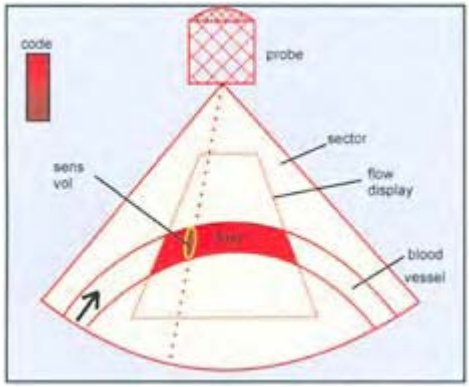

Figure 1.13: Doppler angiography or power Doppler

All these considerations led the instrumentation researchers to take a step backward and develop a two dimensional system which just detects and displays movement; any movement, in two dimensions. The result is an instrument, which displays areas with moving structures in color. The color means that there is flow in the area and the brightness of the color qualitatively indicates the quantity of moving erythrocytes.[14]

Every normal color Doppler system has the basic capability for "power Doppler" or "Doppler Anglo". Actually the power Doppler is a mode of operation in which any signal which shows a Doppler shift (change in frequency) is tagged with color. So the direction becomes irrelevant. Unlike color Doppler where a symmetrical turbulence shows a poor signal, in power Doppler the signal will be strong in this case too. The reason for this is that when directional information is displayed, the zero mean velocity is not displayed, while in the case when the total reflection from any moving structure is displayed a turbulent flow is as indicative as any.

The decision as to what is flow and what is not taken by looking at the frequency spectra and high enough frequency shifts are considered to represent blood flow. The

color-coding is made proportional in brightness to the total power of reflected ultrasound from moving structures. Structures that do not move, or move slowly are not color-coded.

The displayed color indicates the quantity of moving blood, but not the volume flow of blood per unit time. Actually the virtue of this display mode is that it shows about equally fast and slow flow so that we can get a feeling of the general blood perfusion in some area. However, if actual blood velocity or volume per unit time is of any interest, we must revert to other display and measurement modes.

The returned signal depends, in addition, on the attenuation of ultrasound in the intervening tissue. This means that the flow in deeper blood vessels or the flow in the same blood vessel that changes the depth will be shown with different brightness, depending on the depth. The density of the moving blood cells depends on the concentration of blood cells and local flow situation. The sampling volume depends on the length of ultrasound pulse and beam width. If the sampling volume is larger than the blood vessel, the average number of red blood cells in it will be smaller and the returned signal will be thus relatively weaker, showing a dimmer color on the display.

Summary
2D Doppler imaging uses color coding to indicate the direction of flow and different shades of the colors to qualitatively indicate the amount of Doppler shift. This modality is useful in orientation among tangled blood vessels and can be used to guide the positioning of quantitative Doppler measurement.

BASIC LIMITATIONS OF DOPPLER EXAMINATIONS

In Doppler measurements one encounters problems **of accuracy, precision and artifacts** like in any measurement and imaging method. It is important to clearly differentiate among the three concepts:

Accuracy

• Doppler spectrometry operates adequately for angles between ultrasound beam and flow less than 60°. The theoretical measurement error tends asymptomatically towards infinity when the angle approaches 90°. The raw result of the measurement is a spectrum that illustrates well the general behavior, but has the data on velocity hidden by an additional unknown factor—the angle. However, even with the angle α known, data like mean velocity can be calculated only by way of a fairly complicated numerical integral of the weighted spectrum. The automaton, which picks up the respective weights of single velocities within the spectrum at each instant operates fairly autonomously, usually without intervention of the operator. The intervention by way of changing measurement sensitivity can change the result of the calculation. One must continuously bear in mind that we measure Doppler shift only, while the rest of the data is derived from it. The accuracy of assessment of the Doppler shift really depends on the knowledge and control of the frequency content of the ultrasound

pulses. This is often not well controlled. An exception is operation with CW Doppler systems where the measurement can be made more accurate.
- Color Doppler itself is not designed as an accurate measurement method, but mainly a semiquantitative guiding method for Doppler shift spectroscopy. In spite of this, the significance of different colors must be known, and in particular one must carefully adjust the base-line shift since this can essentially change the velocity-color map.

There exists, however, a possibility to extract the accurate data on the Doppler shift by using a cursor, which helps in reading the frequency shift from the computer memory.

Fourier power spectra, where available, give quantitative data but are often not well understood. This spectrum is not a real-time spectrum but a graph with Doppler shift on the abscissa and the energy in frequency range on the ordinate. Its width and symmetry properties contain ample information about the nature of the flow (which is harder to read from a usual realtime spectrum). One should not confuse this power spectrum with the "Power Doppler".

Power Doppler display method has a slightly better geometrical accuracy in showing the blood vessel lumen than the normal "color Doppler". This happens at the cost of image repetition rate.

Precision

- The quantitative functional dependence of the velocity measurement error on the knowledge of the angle α is known. However, the usual method of measurement of the angle is very crude and thus one should try to avoid using absolute values whenever possible.
- Since the color map scale is virtually continuous there is only marginal accuracy in the judgment of the velocity by way of color assessment. The Fourier power spectra capability enables a precise variance calculation and the Power Doppler modality increases observation sensitivity at the cost of loosing directional information.

Artifacts

Several artifacts are encountered in Doppler ultrasound.[5–10] These are incorrect presentation of Doppler flow information. The most common of these is aliasing. However, others occur, including range ambiguity, spectrum mirror image, location mirror image, speckle, and electromagnetic interference.

Aliasing

Aliasing is the most common artifact encountered in Doppler ultrasound (Fig. 1.7).

There is an upper limit to Doppler shift that can be detected by pulsed instruments. If the Doppler shift frequency exceeds one half the pulse repetition frequency, aliasing occurs and improper Doppler shift information (wrong direction and wrong value) results. An analogous optical form of aliasing occurs in motion pictures when wagon wheels appear to rotate in reverse direction (This happens here because the number of pictures per second is insufficient to correctly show the rotation speed). Higher pulse

repetition frequencies permit higher Doppler shifts to be detected but also increase the chance of the range ambiguity artifact. Continuous-wave Doppler instruments do not have this limitation but neither do they provide depth resolution.

Aliasing can be eliminated by increasing pulse repetition frequency, increasing Doppler angle (which decreases the Doppler shift for a given flow), or by baseline shifting. The latter is an electronic “cut and paste” technique that moves the misplaced aliasing peaks over to their proper location. It is a successful technique as long as there are no legitimate Doppler shifts in the region of the aliasing. If there are, they will get moved over to an inappropriate location along with the aliasing peaks. Other approaches to eliminating aliasing include changing to a lower frequency Doppler transducer or changing to a continuous-wave instrument, which is often built-in into specialized cardiologic units. Aliasing can occur in a pulse system since it is a sampling system, which can not yield a correct result unless it samples often enough, that is, twice the highest Doppler shift frequency. This is called the Nyquist limit (of the sampling theorem).

Increasing the pulse repetition frequency can reduce the aliasing problem. However, this can cause localization ambiguity. This occurs when a

Table 1.1: Comparison of different Doppler instruments

Type	*Advantage*	*Disadvantage*	*Other*
SPECTROMETERS			
Pulsed wave (PW)	Has depth resolution	Poorly measures high velocities deep in the body	Higher price
HPRF (High pulse rate frequency) system	PW system which can measure fast flows	Ambiguous measurement (multiple sens, volumes)	Requires more caution from operator
Continuous wave (CW)	Measures all velocities	Has no depth resolution—mixes flows along the US beam	Lower price

pulse is emitted before all the echoes from the previous pulse have returned. When this happens, early echoes from the last pulse are simultaneously received with late echoes from the previous pulse. This causes difficulty with the ranging process. In effect, multiple gates or sample volumes are operating at different depths. Multiple sample gates are shown on the display to indicate this condition. Range ambiguity in color-flow Doppler, as in sonography, places echoes (color Doppler shifts in this case) that have come from deep locations after a subsequent pulse was emitted in shallow locations where they do not belong. As already said, the HPRF systems intentionally introduce this ambiguity for spectrometry, requiring sound judgment by the operator as to whether the results are correct or not.

The mirror image artifact can also occur with Doppler systems.

This means that an image of a vessel and a source of Doppler shifted echoes can be duplicated on the opposite side of a strong reflector (such as a bone). The duplicated

vessel containing flow could be misinterpreted as an additional vessel. It will have a spectrum similar to that for the real vessel. A mirror image of a Doppler spectrum can appear on the opposite side of the baseline when, indeed, flow is unidirectional and should appear only on one side of the baseline. This is an electronic duplication of the spectral information. It can occur when receiver gain is set too high (causing overloading in the receiver and cross talk between the two flow channels) or with low gain (where the receiver has difficulty determining the sign of the Doppler shift). It can also occur when Doppler angle is near 90 degrees. Here the duplication is usually legitimate. This is because beams are focused and not cylindrical in shape. Thus, portions of the beam can experience flow toward while other portions can experience flow away. An additional possibility is to fit a bend of a small blood vessel in the same sample volume, which then yields opposite flows in the two parts of the "hook" as opposite, nearly symmetrical 20 spectra.

Turbulent flow measured with a small sample volume can yield a symmetrical spectrum as well.

Electromagnetic interference from power lines and nearby equipment can also cloud the spectral display with lines or "snow". Improper pulse repetition frequency (PRF) settings can ultimately cause erroneous diagnosis of an absent diastolic blood flow.

In Figure 1.9 "WI" indicates the **"window"**—an empty space in the real-time spectrum. Strictly speaking, this space ought never be empty, but in the case of parabolic flow and somewhat reduced sensitivity the space will not fill in with measurement results. This logic applies if the sensitive volume takes up the whole blood vessel cross section. However, if we reduce the sensitive volume so as to take up only a small part of the blood vessel, a "window" will appear even at fairly irregular flows. This does not influence much the assessment of RI and PI, but disturbs our assessment of the turbulence. Very turbulent flow will show at the same time positive (towards probe) and negative (away from probe) flow spectrum. However, a similar spectrum appearance can be expected if we put the measurement angle near 90°. Therefore we must always interpret the cause of the apparent synchronous flow in opposite directions.

Inadvertent change of the wall filter can cut off the diastolic part of arterial Doppler spectrum and lead to wrong clinical diagnosis.

- *Use the sensitivity with caution (use as low a sensitivity as practical).*
- *Start examination with the standard symmetrical color map and then gradually change it to non-symmetrical types if needed.*
- *Be aware of the depth and increased aliasing probability at deeper structures and higher velocities.*
- *Use all the three modes (B mode, spectrum, and color) for survey, but use single modality to obtain the best quality of each of them.*

ACKNOWLEDGEMENT

In writing this chapter materials provided by Ivica Zalud, M.D., Ph.D. have extensively been used and this is kindly acknowledged.

REFERENCES

1. Mitchell DG. Color Doppler imaging: principles, limitations, and artifacts. Radiology 1990; 177: 1–1
2. Kremkau FW. Doppler color imaging: Principles and instrumentation. Clin Diagn Ultrasound 1992; 27 7–60.
3. Burns PN. Principles of Doppler and color flow. Radiol Med 1993; 85:3–16
4. Taylor KJW, Holland S. Doppler ultrasound. Part I: Basic principles, instrumentation, and pitfalls. Radiology 1990; 174:297–307
5. Zalud I, Kurjak A. Artifacts and pitfalls. In: Kurjak A: Transvaginal color Doppler. Parthenon Publishing, London-New York, Second ed., 1994; 353–58
6. Derchi LE, Giannoni M, Crespi G, Pretolesi F, Oliva L. Artifacts in echo-Doppler and color-Doppler. Radiol Medica 1992; 83:340–52
7. Jaffe R. Color Doppler imaging: A new interpretation of the Doppler effect. In: Jaffe R, Warsof SL (Eds): Color Doppler Imaging in Obstetrics and Gynecology. McGraw-Hill, New York, 1992; 17–3
8. Winkler P, Helmke K, Mahl M. Major pitfalls in Doppler investigations. Part II: Low flow velocity and colour Doppler application. Ped Radiology 1990; 20:304–10
9. Suchet IB. Colour-flow Doppler artifacts in anechoic soft-tissue masses of infants. Can Assoc Radiol J 1994; 45:201–03
10. Pozniak MA, Zagzebski JA, Scanlan KA. Spectral and color Doppler artifacts. Radiographics 1992; 12:35–44.
11. Maulik D. Biosafety of diagnostic Doppler ultrasonography. In: Maulik D: Doppler Ultrasound in Obstet¬ rics and Gynecology. Springer, New York, 1997; 88–106.
12. Duck F, Zauhar G. Report on experiments by Starrit H, Zauhar G, Duck F in Bath, autumn 1996.
13. Censor D, Newhouse VL, Ortega HV: Theory of ultrasound Doppler spectra velocimetry for arbitrary beam and flow configurations, IEEE Trans. on Biomed Eng, 1988; 35:740
14. Chen JF, Fowlkes JB, Carson PL, Rubin JM, Adler RS. Autocorrelation of integrated power Doppler signals and its application, Ultrasound in Medicine and Biology 1996; 22:1053–57
15. Lobkowicz F, Melissinos AC. Physics for Scientists and Engineers, WB Saunders Co., Philadelphia, 1975.

Chapter 2
Proposals on the Safe Fetal Exposure Time to Doppler Ultrasound

Kazuo Maeda

ABSTRACT

The principle for the safety of diagnostic ultrasound based on the thermal effect is to reduce output intensity and shorten exposure time when the thermal index is above one according to the ALARA principle. Research work and pregnancy screening should adhere the rule. Moderately higher TI than one is, however, allowed in clinical examination for more improved image, where the user should keep the preset exposure time by own responsibility. Temperature rise is estimated from the TI, and the exposure time to the high temperature reported by NCRP is reduced by the safety factor of 3 to 100. Although the factor depends on user's decision, 50 is probably appropriate, and actual exposure time is 5 or less min when TI is 2. It is one min when TI is 3, and higher TI than 3 is inadvisable to the user.

INTRODUCTION

Although no adverse effect of ultrasound diagnosis has been reported, ultrasound bio-effect and its safety have been discussed by the world federation of ultrasound in medicine and biology (WFUMB), European federation of the societies of ultrasound in medicine and biology (EFSUMB), National council for the radiation protection and measurement (NCRP), American institute of ultrasound in medicine (AIUM)/National electrical manufactures association (NEMA), Australian society of ultrasound in medicine (ASUM), British medical ultrasound society (BMUS), International society of ultrasound in obstetrics and gynecology (ISUOG), Japan society of ultrasonics in medicine (JSUM), and others. International electrotechnical commission (IEC) is also discussing classification of ultrasound devices. It is emphasized in the safety that ultrasonic examination is used only by medical indications. It is emphasized that young biological tissues of developing embryos and fetuses can be damaged by intense ultrasound. Main biological effect is the thermal effect due to temperature rise induced by ultrasound absorption, and non-thermal effects are the cavitation and other mechanical phenomena. Thermal effect has been particular concern of ultrasonic safety studies

because biological researches reported the teratogenesis of direct heating to animal fetuses or embryos.

Diagnostic ultrasound users are requested to know ultrasonic intensity of their devices, the mechanisms of ultrasound bio-effect, and the prudent use of the devices. No hazardous thermal effect is expected when the temperature rise of exposed tissue is less than 1.5°C, i.e. local temperature is lower than 38.5°C.[1] Five min' duration of 41°C temperature can be hazardous to the tissue. No hazardous thermal effect is suspected in common B-mode imaging device because of minimum heat production due to low ultrasound intensity. WFUMB[1] concluded that the use of simple imaging equipment is not contraindicated on thermal grounds. Non-thermal effects are discussed separately from the thermal effect with the mechanical index (MI). Recent issue in the ultrasound safety is, however, the safe use of Doppler ultrasound due to its high intensity. Practical discussion on the exposure time to Doppler ultrasound, particularly from the users' point of view, is the objectives of this paper.

THE INTENSITY OF DOPPLER ULTRASOUND

Thermal effect of Doppler devices should be carefully studied because of its heat producing ability due to high temporal average intensity. Maximum intensity of commercial Doppler devices is higher than the B-mode, reaching the level of therapeutic ultrasound physiotherapy for the tissue heating. The difference of the two devices is the exposure duration, i.e. it is short in Doppler measurement and long in the therapeutic ultrasound. Temperature rises not only at the sampling volume but also in all tissues passed by the ultrasound beam. Exposure duration is the concern for the safety of Doppler examination.

HAZARDOUS EXPOSURE TO HIGH TEMPERATURE

According to the NCRP report,[2] there is inverse relation between the hazardous intensity level and exposure time, i.e. exposure duration of no injury is long when the temperature is low, but it is short in high temperature. Moderate temperature and short exposure time should be safe even in the case of human fetus. Revised safety statement of AIUM[5] stated that equal or less than 2°C temperature rise above 37°C showed no adverse biological effects with exposure duration up to 50 hours, and that the upper limit of safe exposure duration was 16 min at 4°C rise and 1 min at 6°C rise above normal, respectively. The opinion of AIUM on the effect of high temperature is similar to NCRP,[2] and the safety statement is acceptable, if the temperature rise is accurately determined by the thermal index (TI), i.e. only the TI indicates tissue temperature elevation under ultrasound exposure in clinical study. In my opinion, however, fetal exposure to the temperature rise for 4 to 6°C, where absolute temperature is 41 to 43°C, are controversial. Since the safe level of high temperature is close to the level to develop hazard,[2] proposed exposure time at the high temperature is critically short in the NCRP report[2] and AIUM statement.[5] Although temperature rise is estimated from the TI displayed on the screen of ultrasound machine, e.g. TI 2 indicates 2°C temperature rise, accurate focus temperature may be

hardly confirmed in practical study. Since excess heating and/or prolonged exposure may not be completely avoided in clinical study, it is hard to keep the safety with strict exposure time when the temperature is as high as 41 to 43°C. Our aim in this report is, therefore, to propose practically applicable appropriate exposure time of ultrasound.

TWO MODES IN THE EXPOSURE TIME TO ULTRASOUND

Two modes are recommended in the use of Doppler ultrasound. The use of TI lower than one (AIUM), or the temperature rise below 1.5°C (WFUMB) after temperature equilibrium can be adopted for the infinite exposure. Therefore, the mode is suitable for research work of which exposure duration is hardly expected before the study. TI may also be lower than one in the screening for the fetal abnormality during pregnancy.

In common diagnostic Doppler studies, however, the exposure duration can be estimated and decided prior to the examination, i.e. the exposure time is preset before the study. Any arterial velocity wave-form recording in clinical study, for instance, may not be very long after the setting of sampling volume on the blood flow, and one minute or two may be sufficient for the purpose. Doppler study with moderate temperature rise for one to 3°C expressed by one to 3 of TI is the main field of this paper.

METHODS OF EXPOSURE TIME SETTING

The method is applied by the user's responsibility for the Doppler examination where the TI is mildly higher than one with the purpose of clear Doppler flow imaging. The method is similar to our past strategy for the safety, which was the ultrasound output limitation that was indicated in Japanese Industrial Standards for the ultrasound devices. Since the hazardous SPTA intensity of continuous wave ultrasound was 1.0 mW/cm2 or more in our group study and in the statement of JSUM, the output intensity was below SPTA 10 mW/cm^2 in common Doppler fetal heart detector, fetal monitor and B-mode devices,[8,9] i.e. safe output level was set at 1/100 of hazardous intensity. The safety reserve was so wide in the standards that we have had no safety issue for the diagnostic ultrasound safety in Japan, but now we need new strategy for the safety in the Doppler ultrasound. To keep both TI and MI lower than one has been global standard, and the user was requested to reduce the intensity and exposure time under the "as low as reasonably achievable (ALARA)" principle, if the indices are higher than one. In my experience, however, moderately higher TI than one has been shown in clinical trials where the safety was explained by the short exposure. My idea moved further to clearly set the exposure time in clinical Doppler studies according to some known evidences.

As for the thermal mechanism of ultrasonic bioeffect, only TI is useful in the estimation of heating, because TI represents the temperature rise above 37°C. In my opinion, exposure duration is preset according to the TI and non-hazardous exposure time in NCRP report.[2] The exposure time is reduced by the "safety factor" that expands from 3 to 100 by which exposure time to high temperature in the NCRP report[2] is divided and actual exposure time is obtained. Although the user can voluntarily select safety factor, appropriate level of the factor is proposed in this paper. As ultrasound intensity may

increase in the presence of influencing factors, e.g. it increases for about 3 times in case of standing wave formation, 3 is the lowest safety factor. Distortion of the shape of ultrasound wave, which expressed by A/B, may also increase the intensity.

Accumulation of the influences may form reasonable basis of large safety factor.

In the calculation of exposure time to Doppler ultrasound, for example, exposure time to high temperature is 256 min at 39°C in NCRP report,[2] where the temperature rise is 2°C and corresponding TI is 2. The 256 min are divided by the safety factor that is tentatively 50, and the safe exposure time is 5 min. Suppose +100% estimation error exists in the TI 2, then more 2°C is added to 39°C, and the temperature can be 41°C where NCRP[2] exposure time is 16 min. Exposure time to 41 °C is now approx. 5 min when the safety factor is 3 (Table 2.1). Therefore, if the safety factor is 50, 5 min' exposure time and TI 2 are reasonable combination. By using the same procedure, 1 min' exposure time is preset when TI is 3 (Table 2.1). The safety factor of 100 may be too conservative. Mildly longer exposure than the preset level may be safe due to the absorption of the over exposure to the wide safety reserve.

OTHER THERMAL ISSUES

Ultrasonic thermal effect has been mainly discussed in the relation to teratogenicity in the first trimester, however in other aspect, animal fetal skull or the brain surface was heated and the temperature elevation was more than 4°C by the exposure to intense ultrasound.[6] Hence, thermal damage of the brain surface can be not completely denied in this case. From the point of view, the use of maximum intensity level Doppler ultrasound is inadvisable in the flow study even in late pregnancy.

Caution should be paid for the temperature of the tissue exposed to Doppler ultrasound in febrile patients. Intracavitary scan users should be careful to on the screen displayed transducer temperature, because of possible hazard of attached sensitive tissue to the 41°C or higher temperature of the transducer. Every study should record the exposure duration and TI. The safety indices including TI and MI are recommended to appear in the "Methods" of the reports of Doppler ultrasound studies on human subjects.

DISCUSSION

Since the temperature rise is the indicator for the bioeffect of the temporal average ultrasound intensity, the usage of a Doppler device is precisely controlled, if the tissue temperature is directly measured. Actual temperature of clinical subject is, however, hardly measured by a thermometer, and therefore, TI is useful alternative to estimate the temperature elevation above 37°C. One degree C temperature rise is estimated when the TI is one. Continuously prolonged exposure to ultrasound is allowed when the temperature rise is lower than 1.5°C according to the WFUMB statement. However, further prudent use is required under the ALARA principle, when on the screen displayed TI is higher than one.

Although the temperature rise due to ultrasound exposure is determined in the TI with the standard tissue model, there may be any error in estimating the temperature from TI

in clinical ultrasound exposure to various tissue arrangements. Since the error can be nearly 100% according to BMUS,[11] higher temperature than expected from TI should be taken into account in clinical Doppler studies. For instance, in the case where TI is 2, theoretical temperature rise is 2°C over 37°C, while the safety may be complete by the addition of more 2°C that can be the maximum estimation error from TI. If the temperature rises for 4°C, 16 minutes is the safe exposure time in the NCRP report, and one-third of the time is approx. 5 min, that is the same as the value obtained by the 50 of safety factor in the 2°C temperature rise, of which TI is 2 (Table 2.1).

Table 2.1: Thermal index (TI), tissue temperature, exposure time in the NCRP report,[2] the safety factors and exposure time to ultrasound are listed. Although the user can voluntarily set the safety factor and exposure time, it may be appropriate to choose the safety factor at 50 and exposure time at 5 min when TI is 2

TI	*Absolute temperature (°C)*	*Exposure time to high temperature in NCRP report*[2]	*Exposure time (min) obtained from the exposure time of NCRP report*[2] *divided by various safety factors*			
			Safety	*Factor*		
			3	*10*	*50*	*100*
6	43	1	0.3	0.1	0.02	0.01
4	41	16	5	0.2	0.03	0.02
3	40	64	21	6	1	0.6
2	39	256	85	25	5	2.5

Since the exposure duration tends to prolong in research works or pregnancy screening, smaller TI than one is recommended. As almost all clinical Doppler examinations are done within 5 min, TI can be determined from the examination time, e.g. TI is set at 2, if the exposure time is 5 min and the safety factor is 50. Examination time is 2.6 min under the same TI, when the safety factor is 100 (Table 2.1). The user can voluntarily change the safety factor and prolong the exposure time or increase TI if the user wishes improved images, where he/she should be responsible for the increased risk at the same time. Possibly 50 is appropriate safety factor, and the exposure time is 5 min and the TI is 2. The setting is close to the BMUS safety statement[11] where the exposure time is 4 min when the TI is 2.

Although ISUOG safety statement[7] reported that there is no reason to withhold the use of scanners that have received current FDA clearance in the absence of gas bodies, AIUM[5] stated that for the current FDA regulatory limit of 720 mW/ cm^2 for ISPTA and lesser intensities, the best available estimate of the maximum temperature increase can exceed 2°C. In our studies[10] on the growth curves of cultured cells *in vitro,* threshold pulsed ultrasound intensity to suppress cell-growth curve was 240 mW/cm^2. The clearance of FDA regulation may be controversial from the opinions and reports.

The non-thermal bio-effect exhibits different influences on living tissue, and therefore, unique thermal effect of ultrasound on the embryo and fetus is the main topics in this paper. The MI is the index for the non-thermal bio-effect in the tissue particularly by the cavitation and the sound pressure. Roughly speaking, the exposure of ultrasound of higher MI than one is controversial due to cavitation in the presence of gas body, e.g. in the use of contrasted ultrasound, in air-containing neonatal lung, or free radical formation in gas-filled fluid. The effects of sound pressure are the stasis of capillary blood flow due to standing wave, microstreaming, direct mechanical effect, and so on.

CONCLUSION

The principle for the safe use of diagnostic ultrasound at present is the reduction of ultrasonic intensity and exposure time by the ALARA rule when displayed TI is above one. Basic research work and the screening of pregnancy adhere the principle. The TI may be allowed to be higher than one in clinical study when the user wish to get more improved image by increased intensity, where short exposure time is prescribed and the users should keep the preset time by their own responsibility. The exposure time to high temperature reported by NCRP is divided by the safety factor, and obtained exposure time is preset when TI is 2 or 3. Ultrasound exposure may be appropriate, if the safety factor is 50, where the exposure time is 5 min if TI is 2, and 1 min if TI is 3. Higher TI or longer exposure can be voluntarily selected by user's opinion, by reducing the safety factor to the lower level, where the user should be responsible to the increased risk. The author, however, does not wish to eternally warn the users their responsibility, but instead, do hope the engineers to provide clinical ultrasound tools of low intensity definitely below hazardous threshold in the future.

REFERENCES

1. Barnett SB, Kossoff G. WFUMB symposium on safety and standardisation in medical ultrasound: Issues and recommendations regarding thermal mechanisms for biological effects of ultrasound. Hornbick, 1991, Ultrasound in Med & Biol 1992; 18:v-xix, 731–814
2. National Council on Radiation Protection and Measurements; Exposure Criteria for Medical Diagnostic Ultrasound: I. Criteria Based on Thermal Mechanisms. NCRP Report No.113, 1992.
3. American Institute of Ultrasound in Medicine/National Electrical Manufacturers Association; Standard for Real Time Display of Thermal and Mechanical Acoustic Output Indices on Diagnostic Ultrasound Equipment, 1992.
4. Barnett SA, Ter Haar GA, Ziskin MC, Nyborg WL, Maeda K, Bang J. Current status of research on biophysical effects of ultrasound. Ultrasound in Med & Biol 1994; 20:205–18
5. AIUM Official Statement Changes; Revised statements; Clinical safety, AIUM Reporter 1998; 154, Issue 1, 6–7.
6. Barnett SB, Rott HD, Ter Haar GR, Ziskin MC, Maeda K. The sensitivity of biological tissue to ultrasound. Ultrasound in Med & Biol 1997; 23:805–12
7. ISUOG Bioeffects and Safety Committee; Safety statement, 2000 (reconfirmed 2002). Ultrasound Obstet Gynecol 2002; 19:105.
8. Ide, M; Japanese policy and status of standardisation. Ultrasound in Med & Biol 1986; 12:705–08

9. Maeda K, Ide M. The limitation of the ultrasound intensity for diagnostic devices in the Japanese Industrial standards. IEEE Trans Ultrasonics, Ferroelectrics and Frequency Control, 1986; UFFC 33:241–44.
10. Maeda K, Murao F, Yoshiga T, Yamauchi C, Tsuzaki T. Experimental studies on the suppression of cultured cell growth curves after irradiation with CW and pulsed ultrasound. IEEE Trans Ultrasonics, Ferroelectrics and Frequency Control, 1986; UFFC-33:186–93.
11. The Safety Group of the British Medical Ultrasound Society; Guidelines for the safe use of diagnostic ultrasound equipment. BMUS Bulletin 2000; 3:29 33.

Chapter 3
Development of 3D Ultrasound

Kazunori Baba

Szilard developed a mechanical three-dimensional (3D) display system to see a fetus three-dimensionally in 1974.[1] Brinkley and colleagues developed a 3D position sensor for a probe. They acquired many tomographic images of a stillbirth-baby under water, traced its outline manually and showed its wire-framed 3D image in 1982.[2] A modern 3D ultrasound system was first developed by Baba and colleagues in 1986 and a live fetus *in utero* was depicted three-dimensionally.[3] The system was comprised of an ultrasound scanner, position sensor and computer. An imaging technology named surface rendering was used for 3D image construction. This system was also applied to placental blood flows and breast ducts and tumors.[4]

A 3D probe and an ultrasound scanner, that displayed three orthogonal planes on a screen, were developed and became commercially available. In the early 1990s, clinical applications of the 3-orthogonal-plane display in obstetrics were reported.[5,6] Sohn reported translucent display by using volume rendering in 1991.[7] Since 1994, the number of reports on a 3D image of the fetus increased rapidly because a 3D ultrasound scanner, that could construct and display a 3D image as well as 3 orthogonal planes, became commercially available.

Two unique 3D ultrasound technologies were also developed. One was defocusing lens method[8,9] and the other was real time ultrasonic beam tracing.[10] Only a probe with a defocusing lens was used in the former method and a fetal volume image was obtained. In the latter, construction of a 3D image and 3D scanning were performed simultaneously and a complete 3D image could be obtained just when the 3D scanning was completed without any delay.

Three-dimensional ultrasound has been developed rapidly and several 3D ultrasound scanners are commercially available now.

What can 3D Ultrasound do?

Three-dimensional ultrasound handles 3D data, whereas conventional 2D ultrasound can handle only 2D data. These are some functions that 3D ultrasound can do but 2D ultrasound cannot:

1. Display of a 3D image
2. Display of an arbitrary section

3. Measurement in 3D space (including volume measurement)
4. Display of a 3D blood flow image
5. Keeping, copying and transmission of all information in 3D space
6. Reexamination with a saved 3D data set, without the patient.

TECHNICAL ASPECTS OF 3D ULTRASOUND

Various images are obtained through the following processes in 3D ultrasound.

1. Acquisition of 3D data (3D scanning)
2. Construction of a 3D data set
3. Volume visualization.

Acquisition of 3D Data

Three-dimensional data are usually acquired as a large number of consecutive tomographic

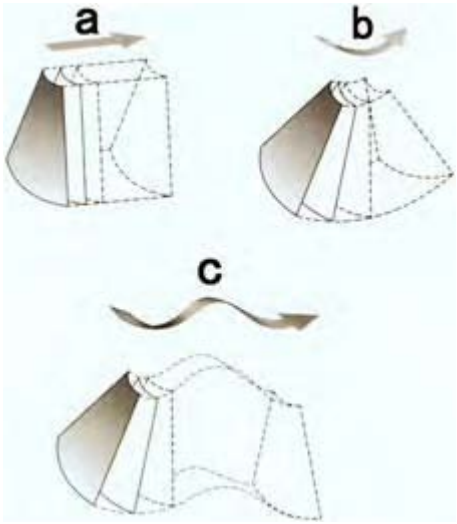

Figure 3.1: 3D scanning methods, a, parallel scanning; b, fan-like scanning; c, free surface scanning[11]

images through movements of an ultrasound transducer array (conventional 2D ultrasound probe). There are some 3D scanning methods, some of which are illustrated in Figure 3.1. Each tomographic image should be acquired with its positional information for the following process, construction of a 3D data set. Accurate positional information

can be obtained through an electromagnetic position sensor or an electric gyro attached to the probe as shown in Figure 3.2.

Several 3D probes are commercially available now. The scanning area by a 3D probe is not large enough in some cases, but 3D probes have been widely used because of its easiness to use. A 3D probe has a built-in transducer array (2D ultrasound probe) which tilts in the 3D probe and 3D data are obtained automatically (Fig. 3.3). Ultrasound travels in a soft tissue at an average speed of 1540 m/s. This speed limits 3D scanning speed. Parallel receiving technique (Fig. 3.4) is a method to overcome the limitation. In this technique, one broad ultrasonic beam is transmitted and its echoes are received as plural ultrasonic beams. In a 2D array probe (Fig. 3.5), a high degree of parallel receiving (at least 1:16) is used and high speed 3D scanning is possible.[13,14]

Construction of a 3D Data Set

A number of tomographic images obtained through 3D scanning must be constructed three-dimensionally into a 3D data set for further computer processing (Fig. 3.6). This construction process involves interpolation and improvement

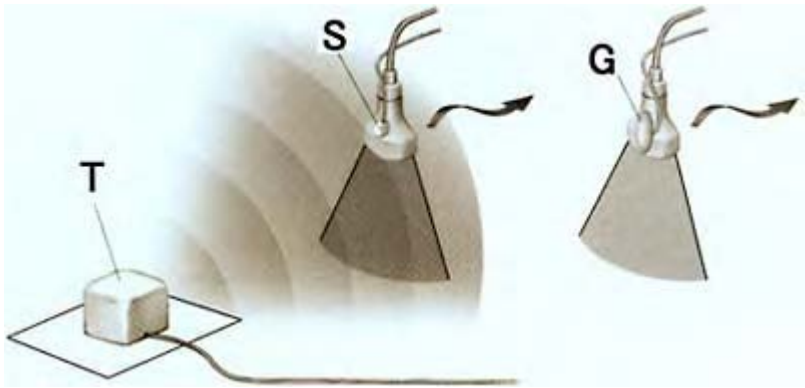

Figure 3.2: A position sensor or an electric gyro attached to a probe detects a relative position of the probe. T—transmitter; S—electromagnetic sensor; G—electric gyro[12]

Figure 3.3: 3D scanning by a 3D probe[12]

of data quality by filtering.[11] A 3D data set is composed of a set of voxels (volume elements). Each voxel has a gray value.

In scanning of the heart, gated technique is applied.[15,16] Tomographic images are rearranged according to the phase of the heart beat and a 3D data set is constructed with only tomographic images at the same phase of the heart beat. Many 3D data sets in a single cycle should be constructed to display the heart beating three-dimensionally.

Volume Visualization

A 3D data set should be processed by a computer to be displayed on a 2D screen. This process is called volume visualization. These three methods have been usually used for volume visualization in 3D ultrasound:

1. Section reconstruction
2. Surface rendering
3. Volume rendering

Section Reconstruction

A sectional image can be obtained by cutting a 3D data set. An arbitrary section can be selected and displayed through translation and rotation of the 3D data set (Fig. 3.7). Usually three orthogonal sections are displayed on a screen simultaneously for better understanding of the position and orientation of each section in 3D space (Fig. 3.8). Although a displayed image by section reconstruction is a sectional image, it is sometimes very

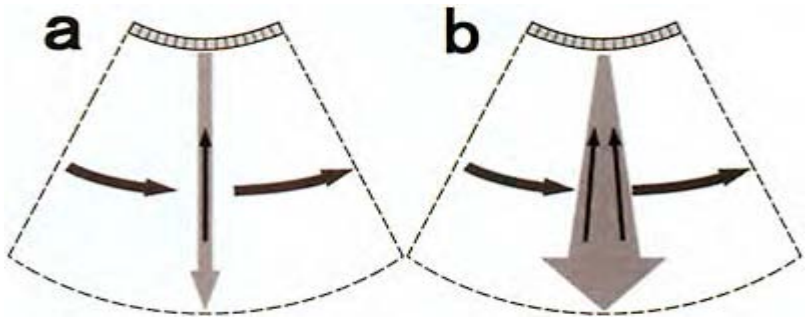

Figure 3.4: Electrical scanning, a, conventional 1:1 (transmission and reception) scanning; b, scanning time can be reduced to a half of conventional scanning by 1:2 parallel receiving[12]

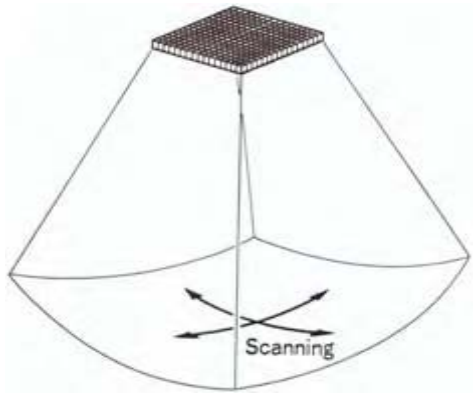

Figure 3.5: A 2D array probe. Transducers are arranged two dimensionally and 3D scanning is performed electrically[11]

useful for diagnosis. Because some of them cannot be obtained by conventional 2D ultrasound. Three orthogonal sections may also be allocated three-dimensionally (Fig. 3.9).

Surface Rendering

A 3D surface image of the object is obtained in surface rendering. A smaller 3D data set for rendering (3D image generation) is extracted from the original 3D data set to eliminate unnecessary parts around the object as much as possible (Fig. 3.10). Figure 3.11 illustrates the principle of surface rendering. The object is extracted from the 3D data set, transformed to a set of intermediate geometrical data and projected on a 2D plane. Extraction of the object is performed either by setting a appropriate threshold (Fig. 3.12) or by manual tracing. Intermediate geometrical data are composed of small cubes or small polygons (Fig. 3.13). There are two projection methods, parallel and perspective projections (Fig. 3.14). In the latter, the size of the projected object varies according to the distance from the object and the projection plane. Shading is necessary for the projected image to be seen as a 3D image. Figure 3.15 illustrates some examples of shading methods.[11]

A intermediate geometrical data can be easily used for the calculation of the object's volume (Fig. 3.16).

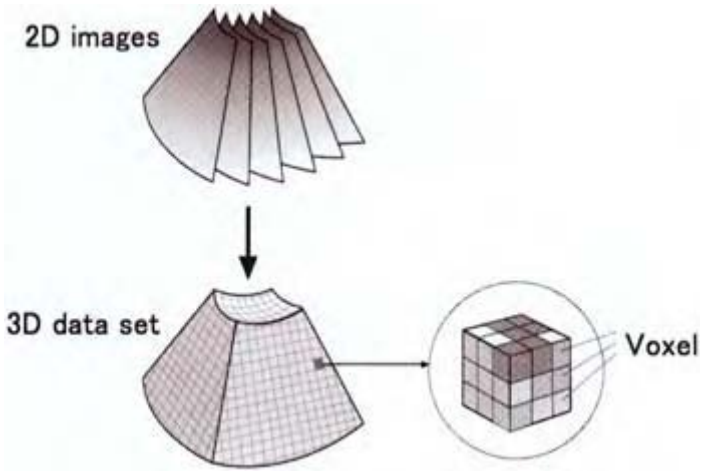

Figure 3.6: Construction of a 3D data set[12]

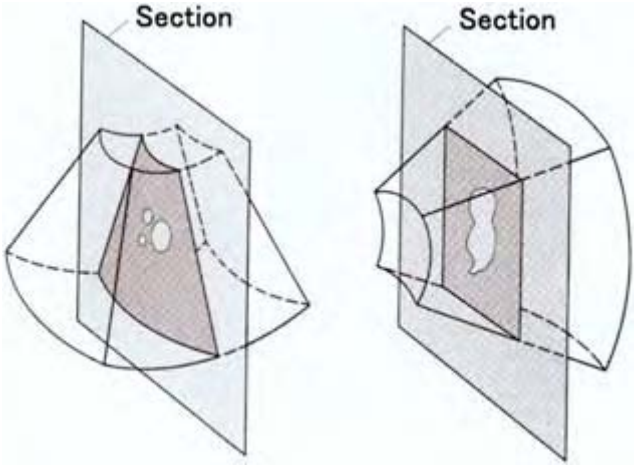

Figure 3.7: Arbitrary section display[12]

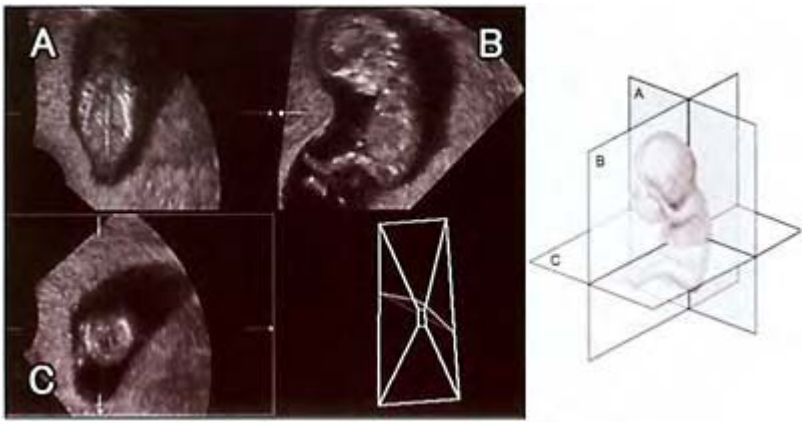

Figure 3.8: Three-orthogonal-plane display of a fetus. Orthogonal triple sections of a fetus are displayed simultaneously[12]

Volume Rendering

A 3D data set for rendering (Fig. 3.10) is projected directly on a projection plane (Fig. 3.17) not through intermediate geometrical data set. Rays are assumed from each pixel on the projection plane into the 3D data set. Brightness of each pixel is determined based on gray values of voxels on each corresponding ray. Figure 3.18 illustrates how gray values of voxels are calculated in the original volume rendering.[17] A fetal surface images (Fig. 3.19) can be obtained through this calculation.

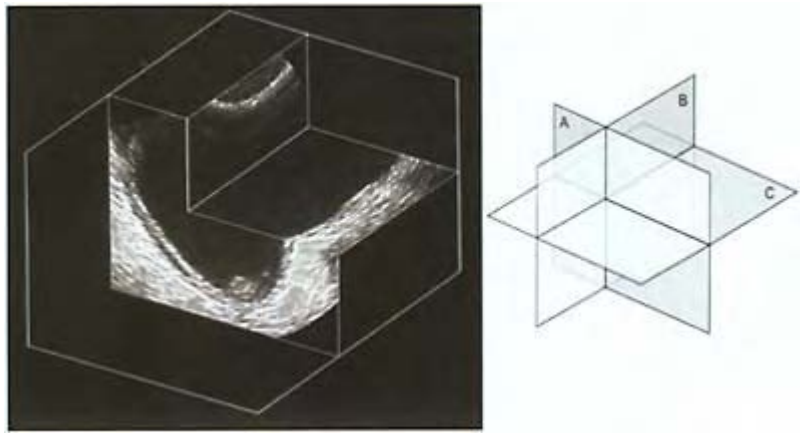

Figure 3.9: An ovarian cyst depicted with three orthogonal sections[12]

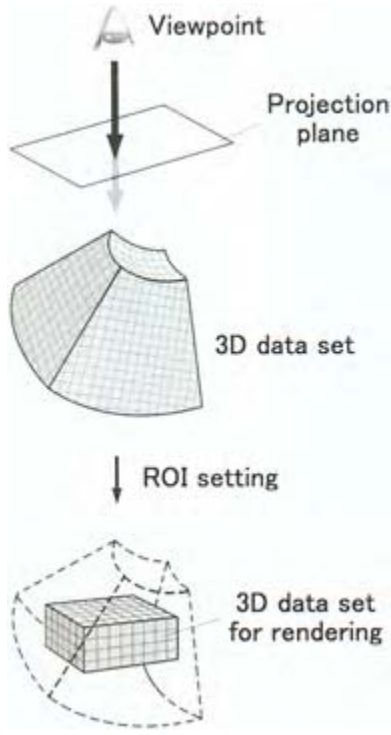

Figure 3.10: Settings of a viewpoint and ROI for a 3D data set for rendering[12]

In surface rendering, boundaries of the object should be outlined strictly, because even low level noises around the object affect a 3D image much. But in volume rendering, boundaries of the object does not need to be outlined strictly, because low level noises around the object become transparent and don't affect the final 3D image much. Speckle noises are accumulated in volume rendering and a higher contrast and clearer image than sectional image can be obtained in some cases (Fig. 3.20).

There are some other ways of volume rendering. When only the maximal gray values on each ray are displayed on the projection plane, the fetal skeleton can be seen (Fig. 3.21). When only the minimal gray values on each ray are displayed on the projection plane, a 3D image of cystic parts is obtained (Fig. 3.22). Volume rendering is a good rendering method for observation but not for volume measurement.

Real Time Ultrasonic Beam Tracing

In this method, each ultrasonic beam is regarded as a ray in volume rendering. Calculation for each ultrasonic beam is performed immediately after the beam is received (Fig. 3.23). This means that 3D scanning and volume rendering are performed simultaneously. This method does not require construction of a 3D data set nor a high

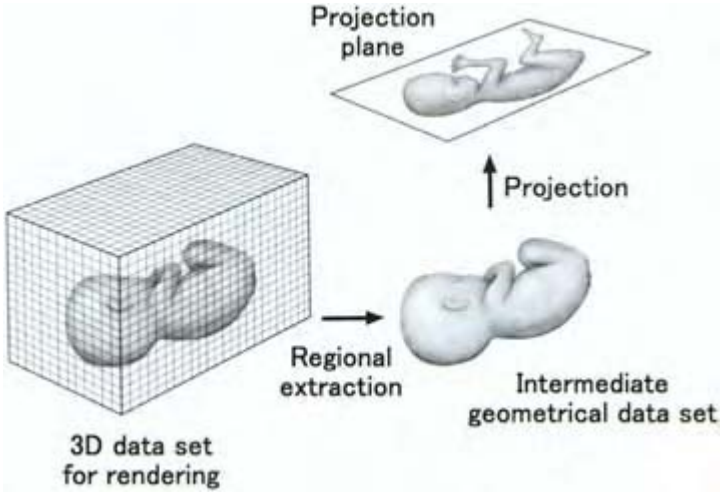

Figure 3.11: Surface rendering[12]

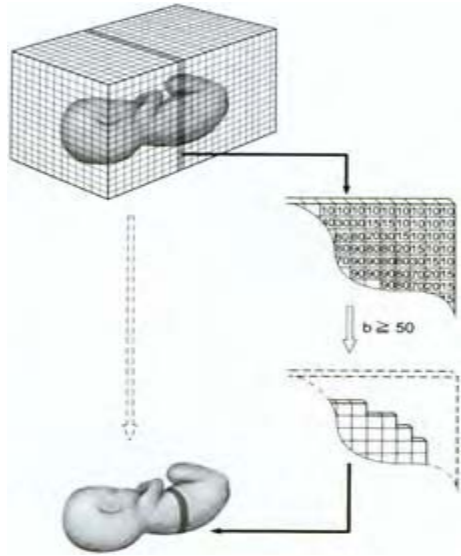

Figure 3.12: Extraction of the object (segmentation) can be performed by setting a threshold properly[12]

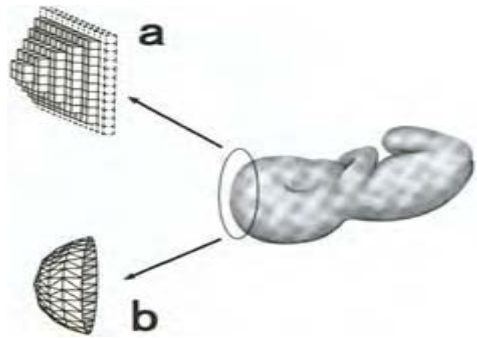

Figure 3.13: Intermediate geometrical data set composed of small cubes (a) or small polygons (b)[12]

performance computer. But a 3D image is always displayed as seen from the probe.

Defocusing Method

This method is referred to as volume imaging or thick slice 3D imaging. A thick slice by defocusing lens attached to the surface of a conventional

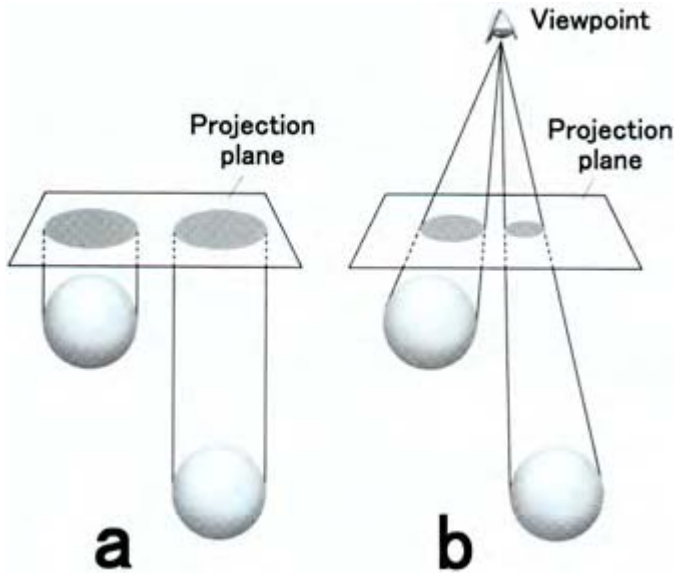

Figure 3.14: Projection of 3D data on a 2D plane. a, parallel projection; b, perspective projection[12]

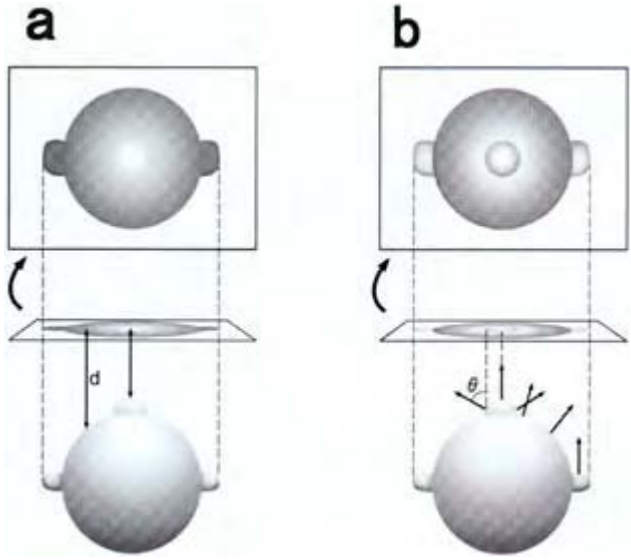

Figure 3.15: Shading makes a 3D image more realistic. a, depth-only

shading; b, shading by the orientation of the object surface[12]

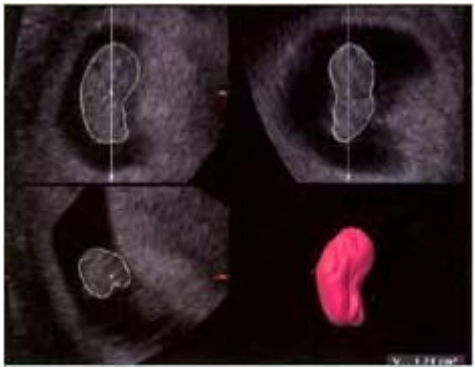

Figure 3.16: Measurement of the volume of a fetus at 7 weeks of gestation. The outlines of the fetus were traced on some sectional images. A 3D image by surface rendering is displayed (lower right) and its volume is calculated automatically.

probe captures a object three-dimensionally (Fig. 3.24). Real time observation is possible, but the clinical application of this method is very limited.

PRACTICAL TIPS

3D Scanning

Figure 3.25 illustrates the relation between a 3D probe and initial three orthogonal planes. The first point is to find a proper probe position and orientation for 3D scanning before 3D scanning. For a fetal surface image, it needs to find a position and orientation where a sufficient amount of amniotic fluid is seen around the fetus.

The second point is to consider the direction of 3D scanning. An ultrasonic beam is converged electrically in the direction of transducer array. In

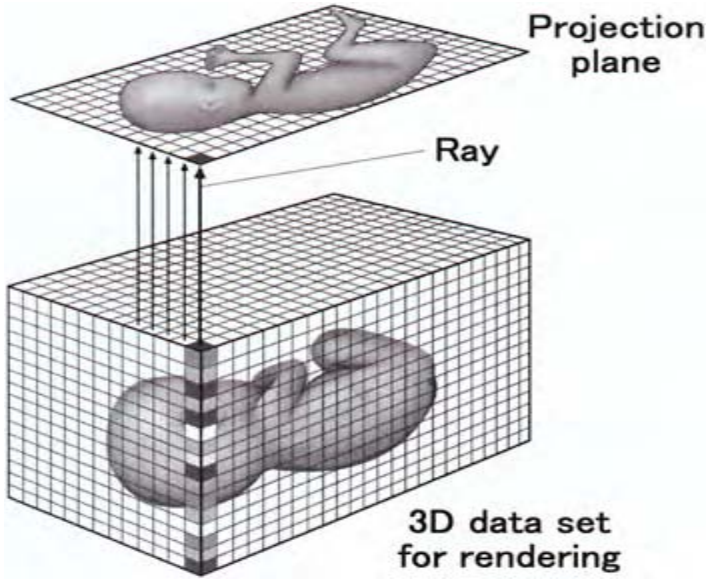

Figure 3.17: Volume rendering[12]

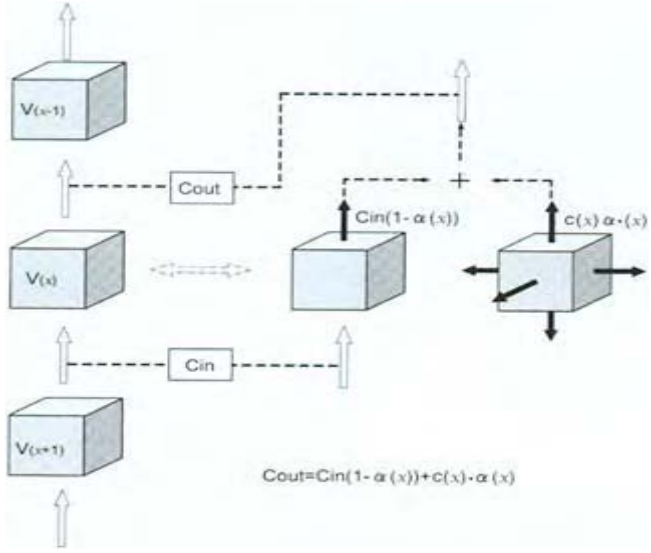

Figure 3.18: The original method of calculation in volume rendering[12]

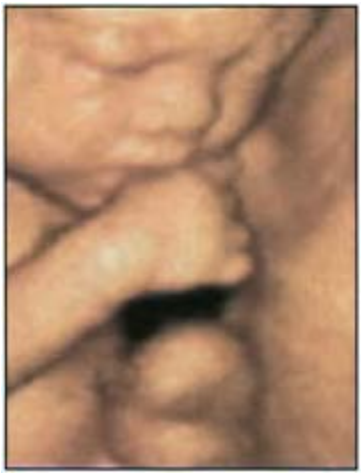

Figure 3.19: A surface-rendered image of a fetus by volume rendering

the direction perpendicular to the tomogram (the direction of slice width), only an acoustic lens is used for this purpose (Fig. 3.26). But convergence by an acoustic lens is not good enough and the object in the 3D data set tends to be expanded in the direction of slice width or in the direction of 3D scanning (Fig. 3.27). Consequently, the width of the object on a 3D image varies on the direction of 3D scanning (Fig. 3.28) and resolution of a 3D image varies on the direction.

Region of Interest

Figure 3.29 illustrates the relation between three orthogonal planes and a 3D image. A 3D data set for rendering is extracted by setting a ROI (region of interest) on the three orthogonal planes. The point is to fit the ROI to the object as much

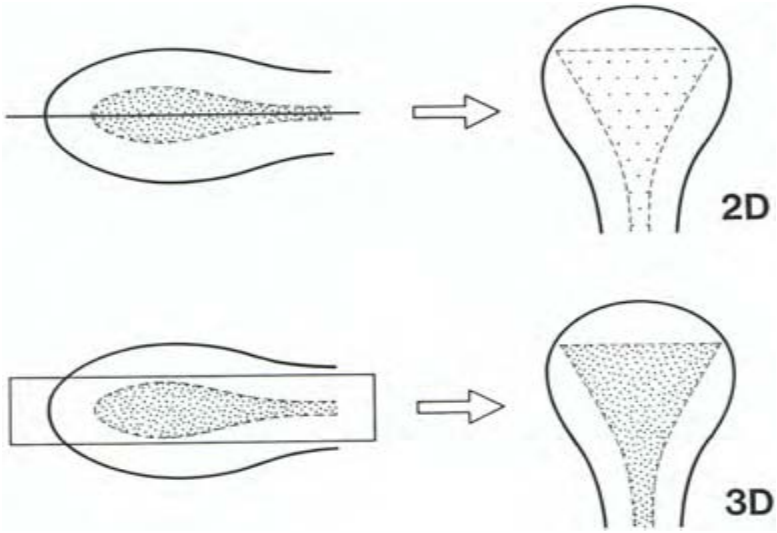

Figure 3.20: A plane image of a coronal section of the uterus (upper right) and a 3D image (lower right). A higher contrast image can be obtained by volume rendering

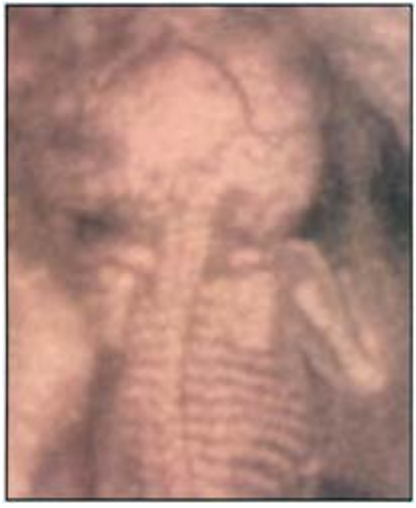

Figure 3.21: A 3D image of the fetal skeleton by maximum intensity projection

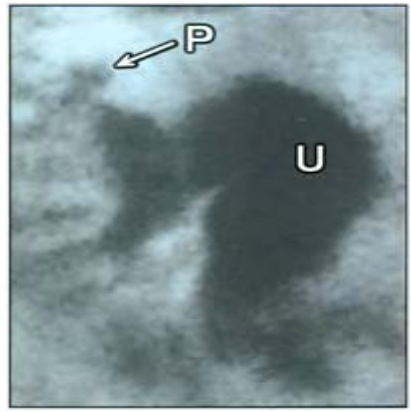

Figure 3.22: A 3D image of a fetal megaloureter by minimum intensity projection. P—pelvis; U—megaloureter[18]

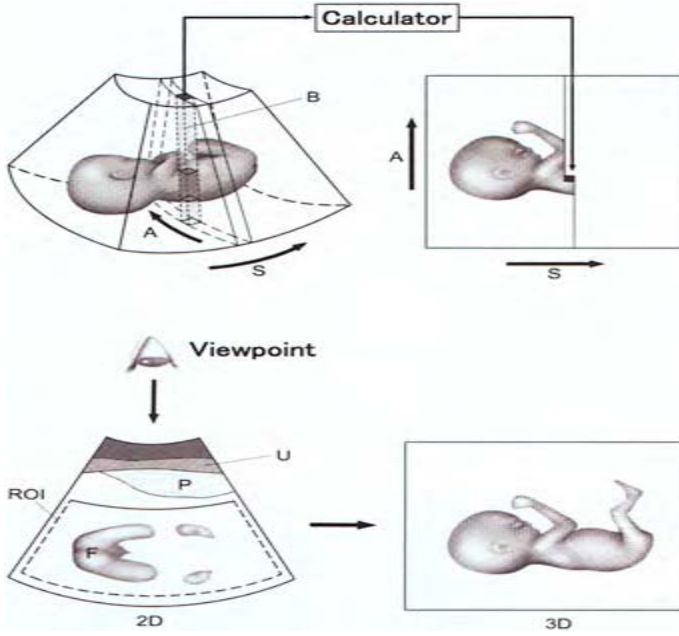

Figure 3.23: 3D image generation by real time ultrasonic beam tracing[12]

as possible, by translating and rotating the original 3D data set and by selecting ROI size.

Threshold

Setting the threshold properly is also very important to obtain a good 3D image as shown in Figure 3.30. By setting the threshold properly, unnecessary weak noises around the object can be removed and a clear 3D image can be obtained. When the threshold is too low, weak noises around the object hide the object. When the threshold is too high, the object itself is eliminated.

Electrical Scalpel

When unfavorable images remain around a 3D image of the object after proper settings of ROI and threshold, unnecessary parts in the 3D data

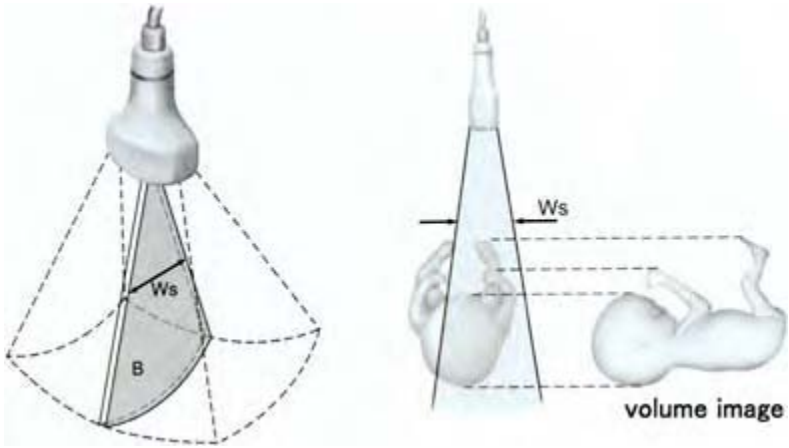

Figure 3.24: Volume imaging. Slice width (Ws) is widened by a defocusing lens attached to the surface of a conventional probe[12]

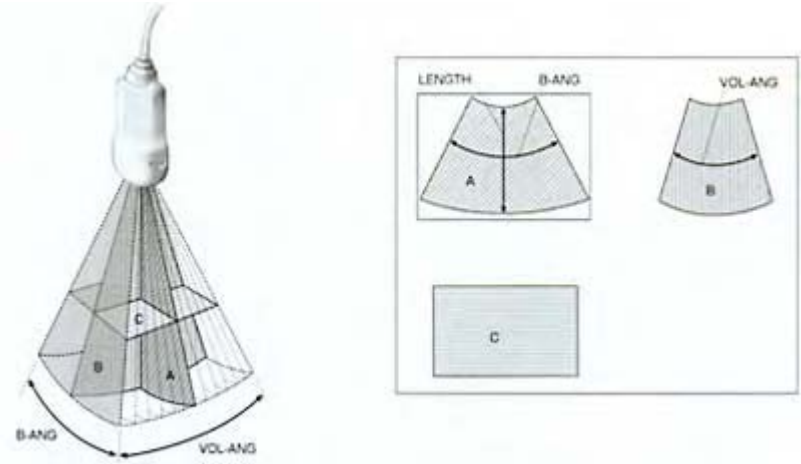

Figure 3.25: Relation between a 3D probe and initial three orthogonal planes on the screen[18]

set can be removed manually and unfavorable images can be eliminated. This function is called electrical scalpel or 3D cutting. Even a separated fetal bone can be displayed by this function (see Fig. 3.28).

CONCLUSION

Three-dimensional ultrasound has many functions and possibilities that are not involved in conventional 2D ultrasound. Both surface rendering and volume rendering give a 3D image. In the former,

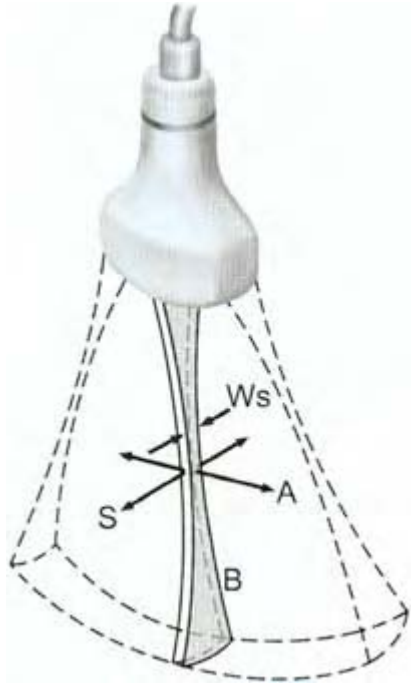

Figure 3.26: Widths of an ultrasonic beam (B). The width (Ws) in the direction of slice width (S) is much wider than the width in the direction of transducer array (A)[12]

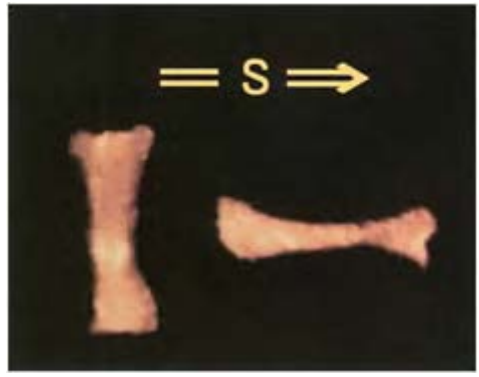

Figure 3.28: An example of influence of slice width on a 3D image. The

same fetal femur was scanned in different directions. Its thickness is displayed differently. S—direction of slice width

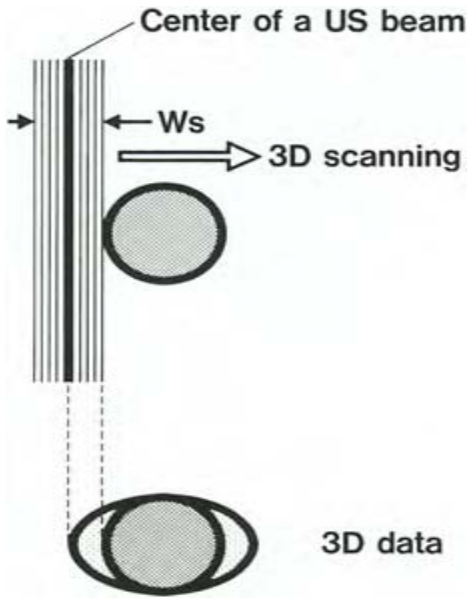

Figure 3.27: Influence of slice width (Ws) on 3D data

the intermediate geometrical 3D data set can be easily used for volume measurement of the object as well as 3D image generation. Volume rendering provides with various kinds of 3D images as well as a surface-rendered image. Some considerations are required in 3D scanning, ROI setting and threshold setting to obtain a good 3D image.

REFERENCES

1. Szilard J. An improved three-dimensional display system. Ultrasonics 1974; 76:273–76.
2. Brinkley JF, McCallum WD, Muramatsu SK et al. Fetal weight estimation from ultrasonic three-dimensional head and trunk reconstructions: evaluation in vitro. Am J Obstet Gynecol 1982; 144:715–21.

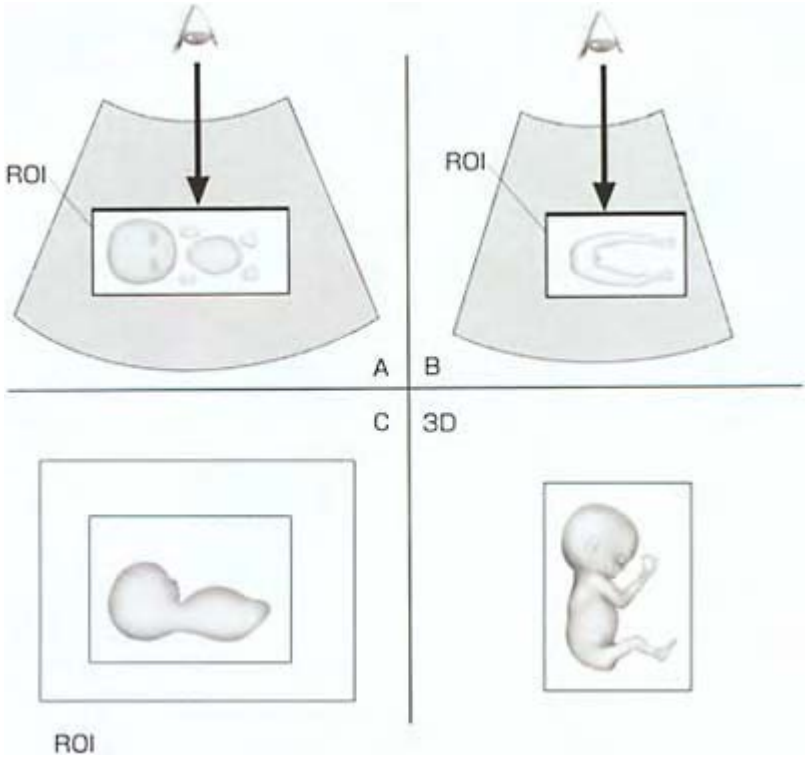

Figure 3.29: Relation between three orthogonal planes and a 3D image (lower right)[18]

3. Baba K, Satoh K. Development of the system for ultrasonic fetal three-dimensional reconstruction. Acta Obst Gynaec Jpn 1986; 38:1385
4. Baba K. Leaps of Obstetrics and Gynecology by ultrasonography. Osaka, Japan: Nagai Shoten, 1992.
5. Merz E, Macchiella D, Bahlmann F et al. Fetale Fehlbildungsdiagnostik mit Hilfe der 3D-Sonographie. Ultraschall Klin Prax 1991; 6:147
6. Kuo HC, Chang FM, Wu CH et al. The primary application of three-dimensional ultrasonography in obstetrics. Am J Obstet Gynecol 1992; 166:880–86.
7. Sohn C, Stolz W, Nuber B et al. Three-dimensional ultrasound diagnostics in gynaecology and obstetrics. Geburtsh u Frauenheilk 1991; 51:335–40
8. Chiba Y, Yamazaki S, Takamizawa K et al. Real-time three-dimensional effect using acoustic wide-angle lens for the view of fetuses. Jpn J Med Ultrasonics 1993; 20(supp 1):611–1
9. Kossoff G, Griffiths KA, Warren PS. Real-time quasi-three-dimensional viewing in sonography, with conventional gray-scale volume imaging. Ultrasound Obstet Gynecol 1994; 4:211–16.
10. Baba K, Okai T, Kozuma S. Real-time processable three-dimensional fetal ultrasound. Lancet 1996; 348: 1307.

11. Baba K, Okai T Basis and principles of three-dimensional ultrasound. In Baba K, Jurkovic D (Eds). Three-dimensional Ultrasound in Obstetrics and Gynecology. Parthenon Publishing, 1997; 1–19.

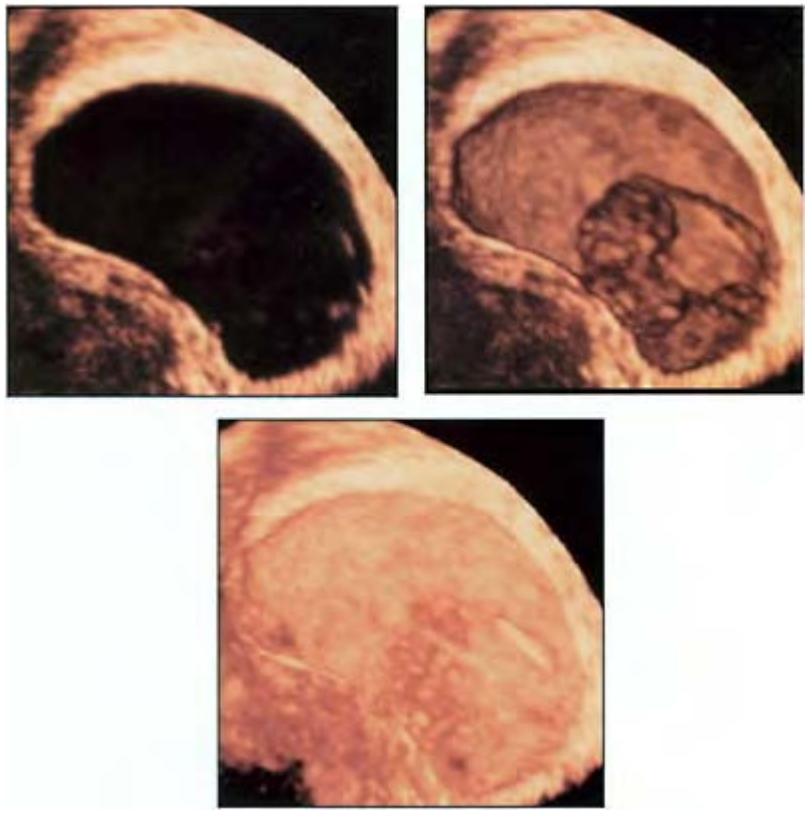

Figure 3.30: Three-dimensional images of a fetus at 7 weeks, a, the fetus cannot be seen in the gestational sac when the threshold is set too low; **b**, the fetus, amniotic membrane and umbilical cord can be seen when the threshold is set appropriately; **c**, the fetal image is eliminated when the threshold is set too high

12. Baba K. Basis and principles of three-dimensional ultrasound. In Takeuchi H, Baba K (Eds). Master three-dimensional ultrasound. Medical View, 2001; 12–29.
13. Smith SW, Trahey GE, vonRamm OT. Two dimensional array ultrasound transducers. J Ultrasound Med 1992; 11(suppl): S43

14. von Ramm OT, Smith SW, Carroll BA. Advanced realtime volumetric ultrasound scanning. J Ultrasound Med 1995; 14(suppl): S3
15. Nelson TR, Pretorius DH, Hagan-Ansert S. Fetal heart assessment using three-dimensional ultrasound. J Ultrasound Med 1995; 14(suppl):S30
16. Deng J, Gardener JE, Rodeck CH et al. Fetal echocardiography in three and four dimensions. Ultrasound Med Biol 1996; 22:979–86.
17. Levoy M. Display of surfaces from volume data. IEEE Computer Graphics and Applications 1988; 8:29–37.
18. Baba K, IO Y. Three-dimensional ultrasound in obstetrics and gynecology. Tokyo, Japan; Medical view, 2000.

Chapter 4
Artifacts, Pitfalls and Normal Variants

Ivica Zalud

Artifacts in ultrasound are common problem in everyday clinical practice. Differentiating real findings and deceptive artifacts is very important. A good understanding of the physical principles of ultrasound waves, equipment, and their interaction with anatomy being examined is essential in distinguishing reality, normal variants and artifacts.

What is the Problem?

• What gives the multiple appearance of an intrauterine contraceptive device?
Answer: reverberation.

• Why does an early single intrauterine pregnancy sometimes look like a twin gestation?
Answer: duplication artifact.

• Why is a large cyst-like structure occasionally seen in the pelvis when it does not exist?
Answer: mirror image artifact.

• Why does a simple cyst sometimes appear to contain a sludge-like layer?
Answer: slice thickness artifact.

• Why are dermoids, even large ones, sometimes not detectable sonographically?
Answer: shadowing (tip of the iceberg phenomenon).

• What does it all mean?

In this chapter, these intriguing artifacts are described and explained. Advice on how to recognize and, in some cases, how to minimize them is also given. On the other hand, the presence of artifacts can sometimes even be helpful in clinical practice and give additional information.

Definition

Artifacts in ultrasound imaging occur as structures that are one of the following:

- Not real
- Missing
- Of improper brightness
- Of improper shape
- Of improper size

Some artifacts are produced by improper equipment operation (e.g. improper transducer location and orientation information sent to the display) or settings (e.g. incorrect receiver compensation settings). Some are caused by improper scanning technique (e.g. allowing patient or organ movement during scanning). Other as inherent in the ultrasound diagnostic method and can occur even with proper equipment and technique.

Mechanism

Artifacts are merely errors in presentation that result from the following assumptions: Echoes come from interfaces that are

1. Directly in front of the transducer.
2. At a depth equal to half the time of flight of the sound pulse multiplied by a constant velocity (1,540 m/s).

In other words, if the pulse is reflected, refracted, or otherwise affected in the body, the ultrasound machine has no way of knowing that. A blip that does not correspond to an actual interface at a corresponding point in the body may appear on the screen. The blip always appears on the screen at a point corresponding to the time since the production of the pulse, and from the direction that the transducer was pointing.

Classification

Commonly encountered artifacts include:

- Reverberation and ring-down (comet tail)
- Shadowing
- Enhancement
- Mirror (multipath) artifacts
- Refraction and side lobes
- Curved and oblique reflector
- Propagation speed error
- Resolution
- Doppler artifacts

These artifacts are seen daily. Although some of these artifacts are more pronounced in the upper abdomen, chest, or neck, the examples chosen are mainly those encountered in obstetric and gynecologic ultrasound examinations.

Reverberation

Reverberation results in reflectors that are not real being placed on the image. They will be placed behind the second real reflector at separation intervals equal to the separation between the first and second real reflectors. Each subsequent reflection will be weaker than prior ones. This can occur from the anterior wall of the urinary bladder, especially in an obese person (Fig. 4.1). The sound pulse is reflected back from the anterior

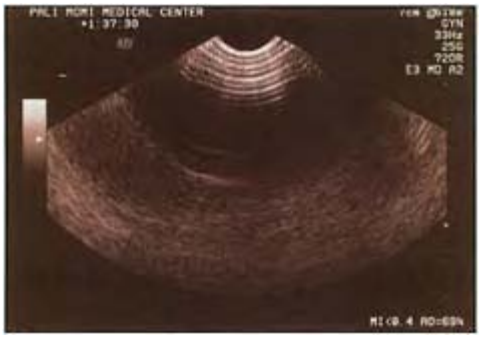

Figure 4.1: Reverberation. Anterior wall of the urinary bladder in an obese person

wall of the bladder to the transducer face. The transducer to produce the true echo absorbs some of the pulse. However, some of that sound is reflected from the transducer-skin interface back into the body. It again hits the anterior bladder interface and is reflected back a second time to the transducer. This produces a first reverberation artifact on the image. The ultrasound equipment assumes (incorrectly) that the signal has returned from a point in the body that is twice the distance from the transducer, as it is aware only of the time taken for the signal to return and not of the path actually traveled. This artifact is seen as a blip on the screen at twice the depth of the true echo. This is because the time taken for the first reverberation artifact is the same time taken for the pulse to travel the original distance and back. This same reverberation can occur a second and third time to give the second or third reverberation artifact. This is commonly known as “near-field” artifact, especially in obese patients. The echoes may be more diffuse and fuzzy if they bounce around in various directions in the subcutaneous fat before returning to the transducer.[1] Occasionally, care must be taken not to confuse this artifact for an anterior placenta.

Ring-down is another type of reverberation artifact. It occurs when the sound hits a metallic structure, such as a metallic surgical clip, or a group of small gas bubbles. In this situation, the sound bounces back and forth numerous times within the structure, each time sending some of the sound back to the transducer. This, therefore, appears on the screen as numerous tiny parallel echoes deep to the structure. This artifact has also been called a “comet tail”. There are also certain situations where there are only one or two

reverberations deep to a structure. This can occur with intrauterine device (IUD) in the uterus.

Since reverberation artifacts are produced by sound bouncing back and forth within the body, it is virtually impossible to adjust the machine to get rid of them. Although one can turn down the near gain, the real echoes will be lost along with the artifactual ones. The presence of a ring-down artifact enables the identification of gas. When this is found in an abnormal, extraluminal location, it may indicate that the patient has an abscess. In other situations, a ring-down artifact indicates that there is gas and therefore, the "mass" seen deep to it is likely to be an artifact. When needle biopsies are done under ultrasound guidance, the needle also produces a ring-down artifact, which is particularly helpful in identifying the location of the needle on the image.

Shadowing

Shadowing is the reduction in reflection amplitude from reflectors that lie behind a strongly reflecting or attenuating structure. Shadows in ultrasound may be due to reflection, absorption, or refraction. The reflective or absorptive shadows are entirely analogous to the shadow cast by a tree in the sun. All of the light is reflected and/or absorbed by the tree trunk so that there is a relative shadow on the tar side. With ultrasound, all of the sound beam must be blocked by a calcification to produce a shadow (Fig. 4.2). There should be an echo from the near side of the structure as well. It is possible to produce an echo without a shadow if the structure only impinges on part of the sound beam without being large enough to block it completely. It is therefore possible to have small clumps of calcification that do not produce a shadow. One cannot change the size of the calcified structure. However, one can choose the correct transducer

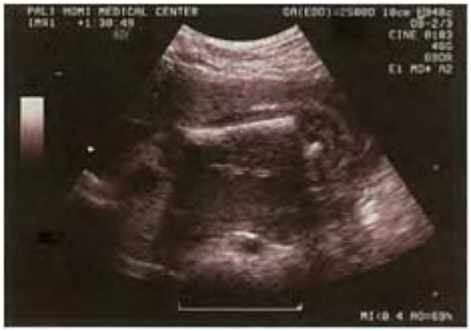

Figure 4.2: Shadowing. The ultrasound beam is blocked by a fetal femur to produce a shadow

or the correct focal level to maximize the chance of identifying the shadow. The narrowest beam and narrowest portion of the beam are necessary to identify a shadow. If the focal depth of a transducer is adjusted either too close or too far, the echoes may be

identified but not the shadows. If shadowing is not present, the calcified nature of a lesion or structure may be missed.

Air can also cause shadowing. Most of the time, this causes great interference on the ultrasound examination by obscuring the deeper structures. For this reason, patients have to be examined with a full bladder to displace the air-containing bowel from the pelvis (Fig. 4.3). The shadow deep to gas is different from the shadow deep to a calcified structure. With the latter, although some of the sound is reflected, much of it is absorbed. With gas, the acoustic mismatch is so great that virtually all of the sound is reflected. This sound bounces around in the tissues between the transducer and the gas, and can cause numerous reverberations and other mirror image artifacts, which on the image appear deep to the echo from the gas interface. This has been called a “dirty” shadow as opposed to the “clean” shadow deep to bone or other calcified (sound-absorbing) structures. This distinction does not always hold true but most of the shadows due to gas are easily differentiated from shadows due to hard and/or calcified structures. As previously mentioned, the presence of ring-down is of further value in recognizing gas. Another type of shadowing is associated

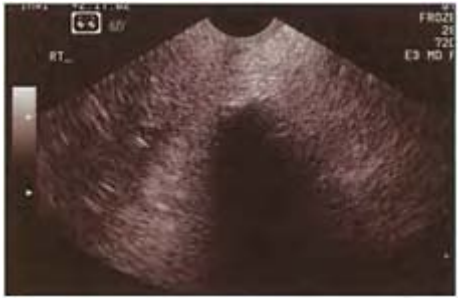

Figure 4.3: Shadowing. Air can also cause shadowing. Bowels seen with an empty urinary bladder

particularly with dermoid cysts. This is a peculiar situation in which there is a strong “dirty” shadow that is likely due to the inhomogeneous structures within a dermoid. These include hair, cartilage, fat, and so on. This appearance of strong shadowing can cause a difficulty in diagnosing dermoids because they can look very similar to gas and stool in the bowel, in both transverse and longitudinal scans. This is the so-called tip of the iceberg sign.[2] The stool-filled rectum can mimic a dermoid or a dermoid can be overlooked by assuming it is the rectum. When there is a clinical suspicion, a digital examination or water enema during ultrasound visualization may help differentiate between the two.

Another kind of shadow occurs at the edge of structures when the sound beam passes through an oblique interface. When the sound beam passes through a curved or oblique interface, some of the sound beam can be refracted away from the central line. This can result in a defocusing of the sound beam deep to the oblique interface and can be seen at the edge of the fetal skull, especially when the beam passes through the placenta.

Occasionally, these can be at the edges of cysts in the ovaries. Refractive shadowing can also cause a dropout of echoes deep to the bladder in the lower uterine segment or in the region of the cervix. This is especially true in patients with leiomyomas.

Enhancement

Enhancement is the opposite of shadowing. It is the increase in reflection amplitude from reflectors that lie behind a weakly attenuating structure. Shadowing and enhancement result in reflectors being placed on the image with amplitudes that are too low and too high, respectively. In this situation, the echoes returning from structures deep to cysts appear more intense than if the cyst were not interposed (Figs 4.4 and 4.5). There are two explanations for this phenomenon. One is that the fluid replaces normal soft tissue in the intervening space, decreasing its attenuation.[3] The time gain compensation (TGC) is set to expect tissue

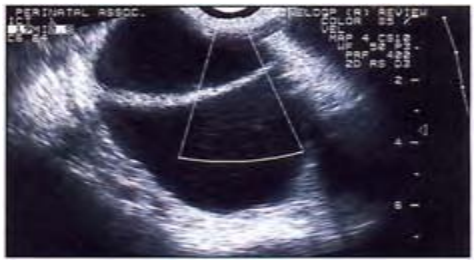

Figure 4.4: Enhancement. The echoes returning from structures deep to cysts appear more intense than if the ovarian cyst was not interposed

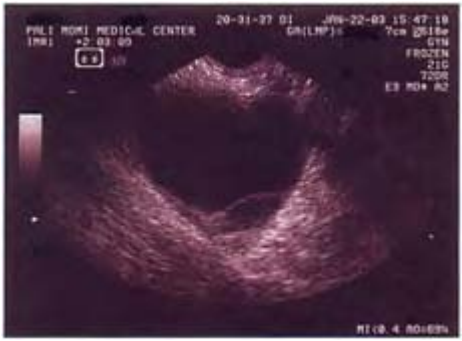

Figure 4.5: Another example of enhancement due to ovarian cysts.

between the transducer and the deepest echoes. If there is fluid instead, especially if the fluid occupies only the central portion of the image, the echoes returning from deep to the fluid collection will be more intense than expected.[3] This appears as a posterior enhancement of the beam, and this finding indicates that a lesion is truly cystic, even if there are internal echoes within the cyst. Occasionally, enhancement will be noted deep to a very small cystic structure, more than what can be explained by a lack of attenuation. The small cyst acting as a lens and refocusing the sound beam may cause this enhancement.[4] This is the opposite of refractive shadowing where the oblique interface defocusses the beam. Often the two coexist.

Mirror Artifacts

The term mirror or multipath artifact describes the situation in which the paths to and from a reflector are different. This artifact results in improper reflector image positioning. If separation is not sufficient, two reflectors are seen as one (missing-reflector artifact). Whereas reverberations and ring-downs are reflections that occur back and forth within the direction of the original sound beam, a mirror image artifact is one in which the sound beam is deflected away from the transducer. The reflected sound may hit a strong interface, be bounced back to the "mirror," and then back to the transducer. The machine will therefore receive an echo and display a blip on the screen in the direction that the transducer was pointing and at a distance corresponding to the time taken. However, this will be a phantom echo since there is no interface in that position. It can also cause significant trouble when it produces a mirror image of the bladder deep to the rectum or sigmoid colon. In this situation, the phantom can closely resemble a cyst, ovarian tumor, or leiomyoma.[1] This kind of artifact can fool even the most experienced sonologists. Differentiating between a true lesion and a mirror image artifact can be difficult. However, the phantom cyst frequently has an unusual, somewhat triangular shape on the longitudinal scan. The back wall is often very ill defined, whereas true cystic lesions invariably have a good, clear posterior wall. It is important to *realize* that this artifact is seen on both transverse and longitudinal scans. One can have the patient partially empty the bladder. This will cause the phantom mass to become proportionately smaller. It is, however, important that the patient does not empty the bladder completely as real lesions can then be missed. Transvaginal scanning can be very useful in difficult cases.

Refraction (Duplication) and Side Lobes

This most interesting artifact occurs uniquely when the transducer is held in a transverse plane over the linea alba. The sound is refracted toward the midline when the transducer is pointing to the medial edge of the rectal muscle on either side. This makes small midline structures appear duplicated on the screen. This phenomenon can cause an erroneous appearance of early twins due to duplication of a single small gestational sac. In addition, intrauterine device can appear duplicated. One could similarly diagnose a bicornuate uterus erroneously. This artifact does not occur in a sagittal or transverse section once the transducer is moved to either side of the midline.[5,6] Not only is the beam not as narrow as anticipated, but also there is a phenomenon called "side lobes." Due to refraction, there are relatively strong beams of sound outside the main beam. If one of

these “side lobes” strikes an interface, and especially if that interface is concave toward the transducer, an echo is received by the transducer. Once again, the transducer and machine have no way of knowing that this came from outside the main beam and it will be displayed as though it were an interface directly in front of the transducer. These artifacts generally appear as curved lines that can be followed back to their origin. They are commonly seen in the bladder, coming off the concave surface anterior to the fundus of the uterus. Occasionally, they come from a loop of bowel that indents the bladder slightly. Refraction can cause a reflector to be improperly positioned on the display. A similar occurrence can be caused by reflections from side lobes. Refraction and propagation speed error can also cause a structure to be displayed with incorrect shape.

Others Artifacts

A curved reflector can produce a reflection low in amplitude because some of the reflection is missed by the transducer. Oblique reflection can produce a reflection low in amplitude, or the reflection may be completely missed by the transducer. Resolution also increases the apparent size of a reflector on a display. Propagation speed error occurs when the assumed value for propagation speed in the range equation is incorrect. Diagnostic instrumentation assumes a speed of 1,540 m/s. If the propagation speed that exists over a path traveled is greater than 1,540 m/s, the calculated distance to the reflector is too small, and the display will, place the reflector too close to the transducer. If the actual speed is less than 1,540 m/s, the reflector will be displayed too far from the transducer. The minimum displayed lateral and longitudinal dimensions will be the beam diameter and one-half the spatial pulse length, respectively.

DOPPLER ULTRASOUND ARTIFACTS

Aliasing

Aliasing is the most common artifact encountered in Doppler ultrasound.[7] There is an upper limit to Doppler shift that can be detected by pulsed instruments. If the Doppler shift frequency exceeds one half the pulse repetition frequency (normally in the 1 to 30 kHz range), aliasing occurs and improper Doppler shift information (improper direction and improper value) results. Higher pulse repetition frequencies permit higher Doppler shifts to be detected but also increase the chance of the range ambiguity artifact (Figs 4.6 and 4.7). Aliasing in a color flow system is exposed in a spatial two-dimensional plane in which the aliased flow is shown in reversed color surrounded by

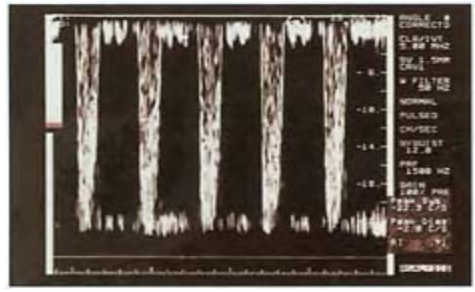

Figure 4.6: Aliasing. Higher pulse repetition frequecies permit higher Doppler shifts to be detected but also increase the chance of the range ambiguity artifact

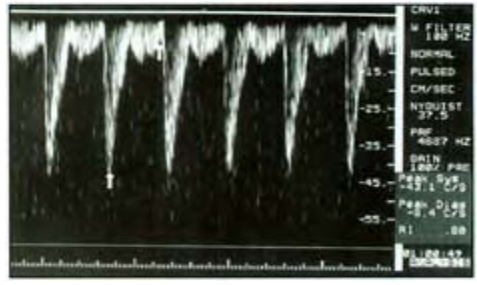

Figure 4.7: Appropriate PRF setting to avoid aliasing in pulsed Doppler waveform analysis

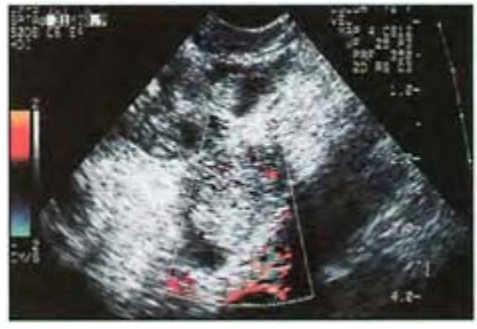

Figure 4.8: Aliasing. Color Doppler ultrasound of the internal iliac artery

nonaliased flow (Fig. 4.8). This pattern mimics the color flow appearance of separate streams in differing directions. The two patterns are, however, clearly distinguishable. In an aliased flow, the higher velocity generates a higher Doppler shifted frequency that is depicted with greater brightness. The higher the frequency shifts, the brighter the color. The brightest level in the color calibration bar (the uppermost for the flow toward the transducer and lowermost for the flow away from the transducer) represents the Nyquist limit. As the velocity and, therefore, the frequency shift exceeds this limit, the color wraps around the calibration bar and appears at the other end as the most luminous color of the opposite direction. For example, a flow toward the transducer with an increasing velocity is depicted with an increasingly bright red color changing to yellow. As the Nyquist limit is reached, the color flow shows brightest yellow in the color bar and as the limit is exceeded, flow is shown in the brightest blue. Thus in an aliased flow, bright or pale color of one direction is juxtaposed against bright color of the opposite direction. In contrast, in genuine flow separation the distinct flow streams are depicted in the directionally appropriate colors that are separated by a dark margin. It should be noted that the hue that demarcates an aliased flow would depend on the choice of the color-mapping scheme.

Aliasing can be eliminated by increasing pulse repetition frequency, increasing Doppler angle (which decreases the Doppler shift for a given flow), or by baseline shifting. The latter is an electronic “cut and paste” technique that moves the misplaced aliasing peaks over to their proper location. It is a successful technique as long as there is no legitimate Doppler shifts in the region of the aliasing. If there are, they will get moved over to an inappropriate location along with the aliasing peaks. Other approaches to eliminating aliasing include changing to a lower frequency Doppler transducer or changing to a continuous-wave instrument. Aliasing occurs with the pulsed system because it is a sampling system.[8] If samples are taken often enough, the correct result is achieved. Sufficient sampling yields the correct result. Insufficient sampling yields an incorrect result.

Range Ambiguity

In an attempt to solve the aliasing problem by increasing pulse repetition frequency, the range ambiguity problem can be encountered.[9] This occurs when a pulse is emitted before all the echoes from the previous pulse have been received. When this happens, early echoes from the last pulse are simultaneously received with late echoes from the previous pulse. This causes difficulty with the ranging process. The instrument is unable to determine whether an echo is an early one (superficial) from the last pulse or a late one (deep) from the previous pulse. To avoid this difficulty it simply assumes that all echoes are derived from the last pulse and that these echoes have originated from some depth. As long as all echoes are received before the next pulse is sent out, this will be true. However, with high pulse repetition frequencies, this may not be the case. Doppler flow information may, therefore, come from locations other than the assumed one (the gate location). In effect, multiple gates or sample volumes are operating at different depths. Instruments often increase pulse repetition frequency (to avoid aliasing) into the range where range ambiguity occurs. Multiple sample gates are shown on the display to indicate this condition. Range ambiguity in color-flow Doppler, as in sonography, places

echoes (color Doppler shifts in this case) that have come from deep locations after a subsequent pulse was emitted in shallow locations where they do not belong. In practice, however, most Doppler color flow devices prevent this problem by automatically reducing the depth when the pulse repetition frequency is increased to the threshold of range ambiguity.

Temporal Ambiguity

Temporal ambiguity occurs when Doppler color flow mapping fails to depict hemodynamic events with temporal accuracy. Specifically, such a situation arises when the frame rate for color flow is too slow relative to the circulatory dynamics. As discussed earlier, the basic unit of color flow depiction is a single frame which when completed shows the average mean frequency shifts color coded and superimposed on the gray scale tissue image. The flow dynamics are, therefore, summarized for the duration of one frame. As we have noted above, the frame rate is inversely proportional to the number of scan lines and the number of samples per scan line. The slower the frame rates the better the color image quality in terms of both spatial resolution and Doppler sensitivity. Herein lies the paradox as a slower rate means longer duration of a frame. As the frame duration increases, there is a progressive loss of the ability to recognize discrete hemo-dynamic events.

Angle of Insonation

Angle dependency of the Doppler shifted frequencies is also a critical factor in blood flow analysis. In sector scanning, multiple scan lines spread out from the transducer in a fan-like manner. When the sector scanner is used to inter-rogate a circulatory system in which the direction of flow is across these scan lines in a color window, the angle of insonation between the flow axis and the ultrasound beam changes. The angle is smallest when the flow stream enters in the sector field and progressively rises to 90° as the flow approaches the center of the field. Concurrently, the Doppler shifted frequencies progressively decline and may become undetectable at the center of the color field. A sector scanner may also create apparently contradictory directional information in a vessel traversing across the color field. As the flow approaches the midline of the field, the flow is depicted in color encoding for flow toward the transducer which usually is red; as the flow moves away, it will be encoded blue. Thus, the same vessel will show bi-directional flow. This paradox actually highlights the basic concept of representation of flow directionality by any Doppler system.

Doppler Mirror Artifact

The mirror image artifact can also occur with Doppler systems. This means that an image of a vessel and a source of Doppler shifted echoes can be duplicated on the opposite side of a strong reflector (such as a bone). The duplicated vessel containing flow could be misinterpreted as an additional vessel. It will have a spectrum similar to that for the real vessel. A mirror image of a Doppler spectrum can appear on the opposite side of the baseline when, indeed, flow is unidirectional and should appear only on one side of the

baseline.[10] This is an electronic duplication of the spectral information (Fig. 4.9). It can occur when 50 receiver gain is set too high (causing overloading

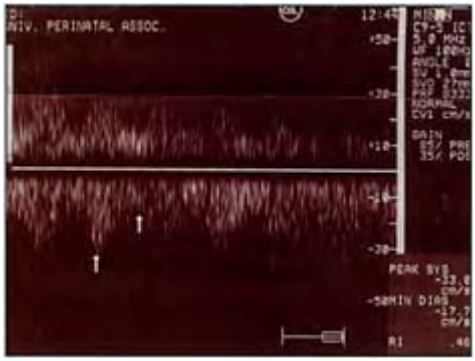

Figure 4.9: Mirror effect. A mirror image of a Doppler spectrum appeared on the opposite side of the baseline when blood flow was unidirectional and should appear only on one side of the baseline

in the receiver and cross talk between the two flow channels) or with low gain (where the receiver has difficulty determining the sign of the Doppler shift). It can also occur when Doppler angle is near 90°. Here the duplication is usually legitimate and this is because beams are focused and not cylindrical in shape. Thus, portions of the beam can experience flow toward while other portions can experience flow away.

CONCLUSIONS

A prerequisite for optimal utilization of ultrasound in obstetrics and gynecology is an in depth knowledge of the principles and limitations of this dynamic technique. It is important to appreciate that the appearance of Doppler images is influenced by the operational setting of the equipment that must be taken into account for any reliable interpretation. Only persons with sufficient training and education should perform diagnostic ultrasound. One of the major reasons for so many conflicting and controversial results in the ultrasound literature originates from technique complexity and rather limited education in physics and technique. With all artifacts, but especially with mirror image artifacts, it is important not to let a superficial knowledge cause trouble. Once the cause and nature of an artifact are understood, it is important not to misinterpret a real lesion as an artifact and miss the true pathology. This can happen, particularly with pelvic masses such as leiomyomas with poor throughtransmission in which the deep wall is not well seen. If there is also an artifact situated near where the deep wall would be, the

actual mass might be dismissed as simply an artifact. One must pay attention at all times not only to identify artifacts, but also not to let them interfere with the identification of true lesions. While the more common artifacts seen on ultrasound images frequently are ignored and appreciated as such, it is certainly interesting to know why they occur. On the other hand, the usefulness of artifacts cannot be underestimated. Occasionally, the identification of an artifact may prevent the novice from making an important error in diagnosis or management. An appreciation and understanding of how to avoid artifacts can help even the more experienced practitioner decide whether a structure is real. It is also important not to ignore real pathology under the assumption that it is caused by an artifact.

REFERENCES

1. Laing FC, Brown DL, DiSalvo DN. Gynecologic ultrasound. Radiol Clin North Am 2001; 39:523
2. Guttman PH. In search of the elusive benign cystic ovarian teratoma: Application of the ultrasound “tip of the iceberg” sign. J Clin Ultrasound 1977; 5:403–07
3. Filly RA, Sommer FG, Minton MJ. Characterization of biological fluids by ultrasonic computed tomography. Radiology 1980; 134:167–71
4. Robinson DE, Wilson LS, Kossoff G. Shadowing and enhancement in ultrasonic echograms by reflection and refraction. J Clin Ultrasound 1981; 9:181–86.
5. Buttery B, Davison G. The ghost artifact. J Ultrasound Med 1984; 3:49–52
6. Sauerbrei EE. The split image artifact in pelvic ultrasonography: The anatomy and physics. J Ultrasound Med 1985; 4:29–33
7. Zalud I, Kurjak A, Maulik D, Collea J: Transvaginal Doppler: measurements and errors. In: Kurjak A, Kupesic S: An Atlas of transvaginal color Doppler. New York-London: Parthenon Publishing, 2000; 255–62.
8. Mitchell DG. Color Doppler imaging: principles, limitations, and artifacts. Radiology 1990; 177:1–10
9. Kremkau FW. Doppler color imaging: Principles and instrumentation. Clin Diagn Ultrasound 1992; 27:7 60.
10. Burns PN. Principles of Doppler and color flow. Radiol Med 1993; 85:3–16

Chapter 5
Screening by Ultrasound

Giampaolo Mandruzzato, Gianpaolo Maso, Giancarlo Conoscenti

Screening is a procedure aimed to identify in a population believed to be free of a disease or a condition the subjects that have the disease or are carrying an increased risk to develop it. It is wise to remember that a positive screening test is non always a diagnosis. When applied to the fetus this concept we must take into consideration the fact that the fetus and his structures, organs and functions undergo a progressive and continuous development along the gestation. Due to the capacity of obstetrical ultrasound to offer images of the anatomical features of the fetus and of his adnexa and also to inform us about some functions like patterns of movements and hemo-dynamic changes, it is necessary to examine the screening and diagnostic capacities according to the gestational age in which the procedure is applied or to the condition or disease we are screening for.

First of all it is necessary to remember at least some of the conditions for which a screening procedure can be advisable and the criteria that a screening test must have in order to be considered as advisable.

As far as the first point is considered the condition or disease must be: severe enough to be a concern for public health; must have a known spectrum of symptoms; must be prevalent enough; a treatment must be available and must be subject to improvement of outcome if detected before the usual time of diagnosis. The screening test must have enough sensitivity and specificity, should be easy to perform and must not provoque discomfort.

Moreover a screening procedure can be applied to a general population (mass screening) or to a subgroup that already carries and increased risk (selective screening).

Taking into consideration the period of the gestation in which the procedure is performed (first, second or third trimester) the target of the procedure is obviously different.

Even if it is recognized and accepted that the best and possibly the only available technique to study precisely the fetus and his milieu is represented by ultrasound scanning surprisingly there is no agreement about the fact that a mass screening by ultrasound is advisable.

The Cochrane Library has addressed this issue in two reviews dividing the gestation into two groups: Early pregnancy (up to 24 weeks)[1] and late pregnancy (after 24 weeks).[2]

From that reviews it appears that routine ultrasound in early pregnancy enables better assessment of the gestational age, earlier detection of multiple pregnancies and of

unsuspected fetal malformations while routine ultrasound in unselected population after 24 weeks does not confer any benefit to mother or fetus.

This negative conclusion of the reviewers is based on the fact that evidence of a positive effect is lacking after evaluation of published randomized clinical trials. But examining carefully the evaluated studies it is easy to observe that the majority of them have been published more than 13 years ago, in many cases the endpoint was unclear, a protocol of management was not described and in some the quality of the operators was clearly insufficient.

As a consequence the conclusions have been negative. In our opinion evidence of benefit is lacking because properly designed and well conducted studies offering a high quality of the examination are not always available.

Remembering the characteristics that a screening test must have it is of paramount importance the level of sensitivity and specificity. As in the case of obstetric ultrasound they are strongly dependent by the quality of the used equipment but even more by the preparation and capacity of the operators it is necessary to evaluate with criticism this aspect. Just to give an example in one considered study[3] regarding the recognition of major malformations the detection rate was reported as low as 17%. In the same period in large studies conducted in Europe and US the sensitivity of ultrasound scanning for major malformations has been reported to be 75% or more.[4–6]

Therefore completely different conclusions can be drawn also if apparently the study is well designed.

The logical consequence is that before using ultrasound as a screening procedure and evaluating its efficacy the major problem is represented by the education of the operators in order to get the best possible sensitivity and specificity from the test.

Moreover the end point must be clearly defined. As an example all the considered studies regarding the screening of intrauterine growth restriction (IUGR) have considered IUGR as synonimous of Small for Dates Infants (SFD). Thi definition is no more acceptable and practically these studies were not directed toward recognition of the IUGR but to the prediction of a birthweight inferior to the 10th percentile.

It is possible to offer other examples of the inherent bias of many of the considered studies that are the cause of the negative conclusions.

What is true is that there are few studies that respected all the prerequisites that a screening procedure and a test must have and presenting also a protocol of management enabling us to evaluate on an objective ground if the screening policy is advisable or not.

At the moment, due to the large use of obstetric ultrasound in clinical practice, it is necessary to consider if double blind randomised trials are ethically acceptable at least in developed countries.

But going back to logical evidence and common sense let us see what are the possible clinical conditions in pregnancy that can have a potential benefit of an early recognition if there are possible management and cannot otherwise recognized with accuracy but by ultrasound along gestation in first, second and third trimester in pregnancies that are believed to be normal.

1. First trimester

a. Precise assessment of gestational age: It reduces the number of induction for suspected postdatism, allows a better and quicker recognition of fetal growth deviations from the expected when scanning in 2nd and 3rd trimester.
b. Recognition of twins and by assessing chorionicity and amnionicity classify the risk:

    Dichorionic/diamniotic: risk
    Monochorionic/diamniotic: high risk
    Monochorionic/monoamniotic: very high risk

c. Recognition of some major malformations and some structural abnormalities potentially indicating kariotype aberrations where invasive diagnostic procedures can be offered.

2. Second trimester (20–21 weeks)

a. Assessment of the normality of the fetal anatomy and recognition of malformations if present.

3. Third trimester (28–30 weeks)

a. Assessment of the fetal growth (IUGR recognition).
b. Detection of some malformations that due to their natural history are not yet observable at the 20–21 weeks scan.
c. Placental localisation.

4. Third trimester (34–36 weeks).

a. Assessment of fetal growth (late onset IUGR recognition).
b. Fetal presentation (possibility to offer external cephalic version).

CONCLUSIONS

Due to the inherent power of obstetrical ultrasound, if properly used, to offer to the clinician informations of clinical relevance regarding the normality and the abnormalities as well of the fetal condition. As a consequence, the characteristics of the controls and management can be modulated in a more objective way. Now it is very difficult for both the clinician and the pregnant women, to renounce to the great informative support of this technology also when dealing with pregnancies considered as normal or carrying only a presumptive low risk. In fact the risk condition becomes only evident after ultrasound scanning because many conditions that can affect the fetus or the fetuses can be only suspected or even ignored by common clinical assessment.

Being the task of any screening policy to identify and assess the risk it is hard to believe that ultrasound screening is not beneficial. The lack of evidence, so called A I, is mainly due to the lack of properly conducted studies.

Most of the aforementioned conditions are harmful or even lifethreatening for the fetus and in many cases an effective treatment is available in condition to improve the outcome. Of course any kind of management can be applied only after the diagnosis has been carried out. As a consequence we believe that, if some fundamental conditions are

respected like availability of resources and adequate preparation and optimal capacity of the operators, routine ultrasound screening must be carried out both for clinical and ethical reasons.

Anyway it must be stressed that the most critical point, that can conditions the evaluation of the efficacy of any screening procedure, is represented by the sensitivity and specificity of the test, that in the case of obstetrical ultrasound is strongly dependent by the preparation of the operator.

As a consequence a proper training must be offered and the level of competence of the operators must be assessed objectively before a screening procedure is offered.

REFERENCES

1. Neilson JP. Ultrasound for foetal assessment in early pregnancy (Cochrane Review) The Cochrane Library, Issue 3, 2000. Oxford
2. Bricker L, Neilson JP. Routine ultrasound in late pregnancy (after 24 weeks gestation) (Cochran Review) The Cochrane Library, Issue 3, 2000. Oxf
3. Ewigman BG, Crane JP, Frigolet to FD and Co. Ef of prenatal ultrasound screening on perinatal outcome. N E J Med 1993; 329:821
4. Grandjean H, Larroque D, Levi S. The performance of routine ultrasonographic screening of pregnancies in the Eurofetus Study. Am J Obstet Gynaecol 1999; 181:446.
5. Skupski DW, Newman S, Edersheim T and Co. The impact of routine obstetric ultrasonographic screening in a low risk population. Am J Obstet Gynaecol 1996; 175:1142.
6. D'Ottavio G, Meir YJ, Rustico MA and Co. Screening for fetal anomalies by ultrasound at 14 and 21 weeks. Ultrasound Obstet Gynaecol 1997; 10:1.

Chapters 6
Routine Use of Obstetric Ultrasound

Geeta Sharma, Stephen T Chasen, Frank A Cherv

INTRODUCTION

Ultrasound examination of the fetus became integrated into prenatal care soon after its introduction in the late 1950's. The past four decades have seen further improvements in ultrasound technology and advances in its utility as well as promotion of respect for patient's autonomy and involvement in medical care. There is concomitant support for and opposition to the routine use of ultrasound in pregnancy. Questions remain regarding the benefits and harms of routine obstetric ultrasound. How often should a "routine" ultrasound be performed? When should the "routine" ultrasound be performed? Who should receive an ultrasound? Who should perform the ultrasound? How should the results be interpreted? Currently, many of these questions do not have a clear answer. These answers gain importance as ultrasound burgeons with the dynamic field of obstetrics and gynecology research unveils a multitude of applications for this remarkable tool.

BASIC ULTRASOUND

The real time obstetric ultrasound examination is usually performed with the pregnant patient in the supine position. A distended bladder aids in displacing bowel loops and can facilitate visualization with the transabdominal approach.[1] Sonogram gel is applied to the transabdominal or transvaginal transducer. The gel simulates a liquid interface that permits optimum travel of the sound waves.

Ultrasound consists of high frequency sound waves that encounter a tissue interface and are reflected, refracted, attenuated or absorbed. The mechanical vibration required for most obstetric imaging ranges between 3–7 megahertz (MHz), million cycles per second. A transducer or ultrasound probe contains piezoelectric material and a crystal that together generate ultrasound waves. The crystal resonates when electrical current traverses the piezoelectric ceramic.[2]

The ultrasound beam is emitted radially and transmits through tissue as a longitudinal wave influenced by the velocity of the ultrasound between interacting particles and density of particles encountered. Therefore, ultrasound penetration is dependant on the

tissue particles' elasticity and mass which both contribute to the tissue's acoustic impedance. The velocity of ultrasound in soft tissue is relatively constant, except in adipose tissue where the speed is reduced by approximately 20%. In most soft tissue, changes in acoustic impedance are dependant on changes in tissue density. When the ultrasound beam contacts large differences in tissue interfaces, reflection of the beam can occur. Only 2–10% reflection occurs between soft tissues, permitting most of the ultrasound waves to travel deeper to distant structures. However, interfaces such as air-tissue or bone/calculus-tissue allow 100% and 67% reflection of the incident ultrasound beam, respectively, creating a distal acoustic shadow.[2]

After processing the reflected beams received by the transducer, an image is constructed and displayed on a monitor. Most obstetric ultrasound imaging uses the pulse-echo method that measures the time delay between the insonant beam to the echo reflected by the tissue back to the transducer. An image is recreated from these echoes and reflected waves. Real-time ultrasound relies on a continual sweep of pulsed waves. With rapid repetition, the transducer sweeps the area being scanned approximately 30 times in one second.[3]

Other ultrasound wave behaviors include refraction, attenuation and absorption. In addition to reflecting the insonant beam, tissue can refract or scatter the normally coherent waves. Ultrasound energy is lost by refraction, resulting in diminished energy returned to the transducer. Thus, the received signal is attenuated. Further attenuation can occur from the conversion of acoustic energy to thermal energy by tissues and energy is absorbed. A larger degree of absorption is seen with tissue containing larger molecules, greater viscosity and with higher frequency ultrasound. Although higher frequency ultrasound, with its shorter wavelengths, allows for greater resolution, its transabdominal use can be limited due to absorption. Conversely, endovaginal ultrasound minimizes both the distance between the transducer and the area being scanned and contact with tissue with high acoustic impedence, i.e. bone. The frequencies employed in diagnostic ultrasound do not generate significant thermal energy as is possible and often desired with therapeutic ultrasound.[2]

Ultrasound intensity is a temporal measure of energy (watts) exposure over a surface (centimeters^2). The special peak temporal average intensity represents the peak intensity. Devices for fetal heart auscultation use continuous wave ultrasound with a special peak temporal average intensity ranging between 0.6 to 80 mW/cm^2. The range for pulse echo imaging is between 1 to 200 mW/cm^2. The fetal dose depends on both intensity and exposure time, which are influenced by maternal habitus and operator skill.[4,5] It is prudent to minimize the number and duration of ultrasound examinations in order to keep the in *utero* exposure as low as reasonably achievable, i.e. the ALARA principle.[5]

SAFETY

Diagnostic ultrasound of the developing fetus has largely been considered safe without apparent deleterious effects. Greater image resolution and pulsed Doppler mode are possible with greater acoustic output. With this technological innovation, the fetal intensity may be increased up to eight fold. The potential teratogenicity of sound energy conversion to thermal energy and mechanical bioeffects of cavitation have not been

proven or ascribed to diagnostic ultrasound.[6] These effects are associated with the higher intensities of continuous wave therapeutic ultrasound. Cavitation refers to the escape of dissolved gases in tissues due to localized low pressure created by very high intensity ultrasound.[2]

The American Institute of Ultrasound in Medicine (AIUM) 1998 conference on mechanical bioeffects encouraged continued research regarding ultrasound safety, especially in tissues with known gas bodies, i.e. lung and intestine. The conference did conclude "there is no known risk of lung or intestinal hemorrhage in the fluid-filled human fetal lung or intestine that is exposed to diagnostic ultrasound during a routine obstetrical examination."[7] In 2002, the AIUM stated "although there are no confirmed biological effects from ultrasound at the present time, the possibility exists that such biological effects may be identified in the future."[8]

In order to monitor the potential bioeffects, newer ultrasound equipment can display the acoustic output, measured by the thermal and mechanical indices. The thermal index measures the temperature absorption; a value below 1.0 is not considered concerning. The mechanical index measures the likelihood of cavitation by measuring the decompressive and compressive forces of ultrasound pulses. Some machines will display one index; the thermal index will be shown for Dopplerimaging and the mechanical index for imaging.[5]

Long term follow up of randomized controlled studies of routine versus selected ultrasound in Norway[9,10] and in Sweden[11,12] do not show a significant affect on subsequent childhood neurological development (Fig. 6.1). In addition, a meta-analysis of childhood malignancies and birth weight showed, overall, no significant negative effects from antenatal ultrasound.[13] An association has been described between left handedness in a retrospective cohort study of males enlisting in the military. Their exposure or non-exposure to ultrasound was assumed in accordance to local practices based on their place of birth.[14] However, follow-up in the aforementioned randomized controlled trials did not show an increase in non-right handedness in children randomized to routine ultrasound when subgroup gender analysis was not performed and intention to treat maintained.[15]

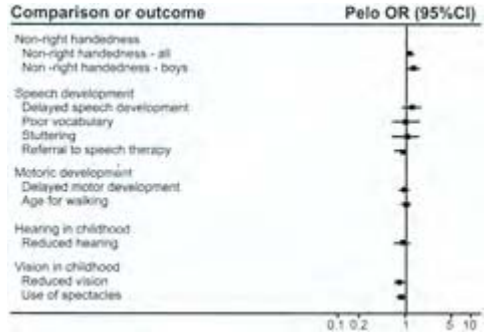

Figure 6.1: Meta-analysis of Nordic and Swedish studies on routine ultrasound during pregnancy and childhood neurological development.

Meta-analysis from Ultrasound during pregnancy and birthweight, childhood malignancies and neurological development. Ultrasound in Med & Biol 1999; 25(7):1028 Reproduced with permission

GUIDELINES FOR USE OF OBSTETRIC ULTRASOUND

The 1984 National Institutes of Health (NIH) Consensus Development Conference on Diagnostic Ultrasound Imaging in Pregnancy called for studies to evaluate the efficacy of antenatal ultrasound and its affect on perinatal morbidity and mortality.[16,17] The consensus statement suggested twenty-eight scenarios that may benefit from ultrasound evaluation (Box 6.1). However, "this document is no longer viewed by NIH as guidance for current medical practice."[16] In 1993 and 1997, the AIUM and Royal College of Obstetricians and Gynaecologists, respectively, set forth standards for the "antepartum obstetrical ultrasound examination" (Box 6.2 and Fig. 6.2).[18] Further detail for performing the anatomical survey is found in Table 6.1.[19] The AIUM has also delineated guidelines for ultrasound accreditation to ensure proper technique and expertise.[20] Responsible utilization of this technology obligates expert training in performance and interpretation of antenatal sonography to minimize false positive and false negative diagnoses.

Routine obstetric ultrasound has been implemented in the United Kingdom, Sweden (1976), Germany (1980), Denmark, Norway (1986), Iceland (1987), Austria (1988), Greece, France, Canada and Australia.[21–25] The rate of antenatal ultrasound performance in the United States by women with live births has steadily increased from 47.7% in 1989 to more than 67% in 2001. Since data was acquired from birth certificate information this percentage is underestimated, as it does not include spontaneous fetal losses and abortions.[26] The American College of Obstetrics and Gynecology (ACOG) does not support the use of routine ultrasound in pregnancy as stated in its 1997 practice pattern bulletin: "In a population of women with low-risk pregnancy, neither a reduction in perinatal morbidity and mortality nor a lower rate of unnecessary intervention can be expected from routine diagnostic ultrasound. Thus ultrasound should be performed for specific indications in low-risk pregnancy."[27] The US Preventive Services Task Force took an intermediate stance, concluding, "there is currently insufficient evidence to recommend for or against a single routine [screening] midtrimester ultrasound in low-risk pregnant women."[28]

Box 6.1: 1984 NIH Indications for Ultrasound Assesment *(No longer viewed by NIH as guidance for current medical practice*

1. **Estimation of gestational age for patients with uncertain clinical dates, or verification of dates for patients who are to undergo scheduled elective repeat cesarean delivery, indicated induction of labor, or other elective termination of pregnancy.** Ultrasonographic confirmation of dating permits proper timing of cesarean delivery or labor induction to avoid premature delivery.
2. **Evaluation of fetal growth** (e.g. when the patient has an identified etiology for uteroplacental insufficiency, such as severe pre-eclampsia, chronic hypertension, chronic renal disease, severe diabetes mellitus, or for other medical complications of pregnancy where fetal malnutrition, i.e. IUGR or macrosomia, is suspected). Following fetal growth permits assessment of the impact of a complicating condition on the fetus and guides pregnancy management.
3. **Vaginal bleeding of undetermined etiology in pregnancy.** Ultrasound often allows determination of the source of bleeding and status of the fetus.
4. **Determination of fetal presentation** when the presenting part cannot be adequately determined in labor for the fetal presentation is variable in late pregnancy. Accurate knowledge of presentation guides management of delivery.
5. **Suspected multiple gestation** based upon detection of more than one fetal heartbeat pattern, or fundal height larger than expected for dates, and/or prior use of fertility drugs. Pregnancy management may be altered in multiple gestations.
6. **Adjunct to amniocentesis.** Ultrasound permits guidance of the needle to avoid the placenta and fetus, to increase the chance of obtaining amniotic fluid, and to decrease the chance of fetal loss.
7. **Significant uterine size/dates discrepancy.** Ultrasound permits accurate dating and detection of such conditions as oligohydramnios and polyhydramnios, as well as multiple gestation, IUGR, and anomalies.
8. **Pelvic mass detected clinically.** Ultrasound can detect the location and nature of the mass and aid in diagnosis.
9. **Suspected hydatidiform mole** on the basis of clinical sign of hypertension, proteinuria, and/or the presence of ovarian cysts felt on pelvic examination or failure to detect fetal heart tones with a Doppler ultrasound device after 12 weeks. Ultrasound permits accurate diagnosis and differentiation of this neoplasm from fetal death.
10. **Adjunct to cervical cerclage placement.** Ultrasound aids in timing and proper placement of the cerclage for patients with incompetent cervix.
11. **Suspected ectopic pregnancy** or when pregnancy occurs after tuboplasty or prior ectopic gestation. Ultrasound is a valuable diagnostic aid for this complication.
12. **Adjunct to special procedures,** such as fetoscopy, intrauterine transfusion, shunt placement, *in vitro* fertilization, embryo transfer, or chorionic villi sampling. Ultrasound aids instrument guidance, which increases safety of these procedures.
13. **Suspected fetal death.** Rapid diagnosis enhances optimal management.

14 **Suspected uterine abnormality** (e.g. clinically significant leiomyomata, or congenital structural abnormalities, such as bicornuate uterus or uterus didelphys, etc.). Serial surveillance of fetal growth and state enhances fetal outcome.

15 **Intrauterine contraceptive device localization.** Ultrasound guidance facilitates removal, reducing chances of IUD-related complications.

16 **Ovarian follicle development surveillance.** This facilitates treatment of infertility.

17 **Biophysical evaluation for fetal well being** after 28 weeks of gestation. Assessment of amniotic fluid, fetal tone, body movements, breathing movements, and heart rate patterns assists in the management of high-risk pregnancies.

18 **Observation of intrapartum events** (e.g. version/extraction of second twin, manual removal of placenta, etc.). These procedures may be done more safely with the visualization provided by ultrasound.

19 **Suspected polyhydramnios or oligohydramnios.** Confirmation of the diagnosis is permitted, as well as identification of the cause of the condition in certain pregnancies.

20 **Suspected abruptio placentae.** Confirmation of the diagnosis and extent assists in clinical management.

21. **Adjunct to external version from breech to vertex presentation.** The visualization provided by ultrasound facilitates performance of this procedure.

22. **Estimation of fetal weight and/or presentation in premature rupture of membranes and/or premature labor.** Information provided by ultrasound guides management decisions on timing and method of delivery.

23. **Abnormal serum alpha-fetoprotein value** for clinical gestational age when drawn. Ultrasound provides an accurate assessment of gestational age for the AFP comparison standard and indicates several conditions (e.g. twins, anencephaly) that may cause elevated AFP values.

24. **Follow up observation of identified fetal anomaly.** Ultrasound assessment of progression of lack of change assists in clinical decision making.

25. **Follow up evaluation of placenta location for identified placenta previa.**

26. **History of previous congenital anomaly.** Detection of recurrence may be permitted, or psychological benefit to patients may result from reassurance of no recurrence.

27. **Serial evaluation of fetal growth in multiple gestation.** Ultrasound permits recognition of discordant growth, guiding patient management and timing of delivery.

28. **Evaluation of fetal condition in late registrants for prenatal care.** Accurate knowledge of gestational age assists in pregnancy management decisions for this group.

RANDOMIZED CONTROLLED TRIALS OF ROUTINE ULTRASOUND

The wide acceptance of antenatal ultrasound by physicians and patients precludes the fulfillment of a study that adequately and accurately evaluates the impact of ultrasound on prenatal care and perinatal outcomes. In addition, in the setting of uncertainty where benefits outweigh potential risks, respect for a patient's autonomy obligates the physician to offer obstetric ultrasound where available.[29]

Antecedent ultrasound studies randomized patients to routine versus selective antenatal sonography, but were of insufficient power to detect a reduction in perinatal mortality or morbidity. An early prospective randomized trial of routine obstetric ultrasound was performed by Bennet et al in London.[30] In this study, 1062 women underwent routine ultrasound at 16 weeks menstrual age. The fetal biparietal diameter (BPD) was measured and dates corrected in 25% of the patients, mostly due to an overestimation from the last menstrual period. Patients were then randomized to one of two groups, using the last digit of the patients' hospital number. In the study group, the BPD information was shared with the clinician while it was withheld in the control group. However, the authors conceded BPD results were revealed, due to ethical obligations, in 30% (161/ 531) of the patients in the control group in which there was a high degree of clinical concern. Intention to treat analysis between the two groups did not show a difference in fetal outcome (birth weight centile, Apgar score at 1 minute and perinatal mortality) or rate of labor induction. Subgroup analysis demonstrated a significantly greater labor induction rate for suspected growth retardation in the revealed control group, 34.8% (56/161) than in either the concealed control group, 13.8% (51/370), or the study group, 19.6% (104/531). The study did not look at differences in neonatal morbidity; therefore, the clinical significance of the ultrasound information could not be completely assessed. The authors concluded that accurate dating information was critical in assessment for growth retardation, and the ultrasound findings were of obstetric value in 25% of the patients. This study illustrates the difficulty of performing a randomized controlled trial of ultrasound utility, as concern surrounding the information generated from ultrasound obligated disclosure of the BPD in 15% of the population.

In another study designed to investigate early detection of growth restriction and perinatal outcome, Neilson et al[31] in Glasgow, Scotland,

Box 6.2: 1993 AIUM Standards (Reproduced from AIUM with permission)

Equipment: These studies should be conducted with real-time equipment, using an abdominal and/or vaginal approach. A transducer of appropriate frequency should be used. Fetal ultrasound should be performed only when there is a valid medical reason. The lowest possible ultrasonic exposure setting should be used to gain the necessary diagnostic information.

Documentation: Adequate documentation of the study is essential for quality patient care. This should include a permanent record of the ultrasound images, incorporating whenever possible the measurement parameters and anatomical findings proposed [herein]. Images should be appropriately labeled with the examination date, patient identification, and, if appropriate, image orientation. A report of the ultrasound findings should be included in the patient's medical record.

Retention of the ultrasound examination should be consistent both with clinical need and with relevant legal and local health care facility requirements.

Standards for first trimester sonography:

1. The uterus and adnexa should be evaluated for the presence of a gestational sac. If a gestational sac is seen, its location should be documented. The presence or absence of an embryo should be noted and the crown-rump length recorded.
2. Presence or absence of cardiac activity should be reported.
3. Fetal number should be documented.
4. Evaluation of the uterus, adnexal structures, and cul-de-sac should be performed.

Standards for second and third trimester sonography:

1. Fetal life, number, presentation, and activity should be documented.
2. An estimate of amniotic fluid volume (increased, decreased, normal) should be reported.
3. The placental location, appearance, and its relationship to the internal cervical os should be recorded. The umbilical cord should be imaged.
4. Assessment of gestational age should be accomplished at the time of the initial scan using a combination of cranial measurement such as biparietal diameter or head circumference, and limb measurement such as the femur length.

4A. The standard reference level for measurement of the biparietal diameter is an axial image that includes the thalamus.

4B. Head circumference is measured at the same level as the biparietal diameter, around the outer perimeter of the calvarium.

5. Fetal weight should be estimated in the late second and in the third trimesters and requires the measurement of abdominal diameter of circumference.

5A. Abdominal circumference should be determined on a true transverse view, preferably at the level of the junction of the left and right portal veins.

5B. If previous fetal biometric studies have been performed, an estimate of the appropriateness of interval growth should be given.

6. Evaluation of the uterus (including the cervix) and adnexal structures should be performed.
7. The study should include, but not necessarily be limited to, assessment of the following fetal anatomy: cerebral ventricles, posterior fossa (including cerebellar hemispheres and cisterna magna), four-chamber view of the heart (including its position within the thorax), spine, stomach, kidneys, urinary bladder, fetal umbilical cord insertion site and intactness of the anterior abdominal wall. While not considered part of the minimum required examination, when fetal position permits, it is desirable to examine other areas of the anatomy.

The *minimum standard* for a "20 week" anomaly scan:

Gestational age can be established by measurement of bi-parietal diameter, head circumference and femur length. The inclusion of abdominal circumference would be optional.

Fetal Normality

- Head shape+internal structures cavum pellucidum cerebellum ventricular size at atrium (<10 mm)
- Spine: longitudinal and transverse
- Abdominal shape and content at level of stomach
- Abdominal shape and content at level of kidneys and umbilicus
- Renal pelvis (<5 mm AP measurement)
- Longitudinal axis—abdominal-thoracic appearance (diaphragm/bladder)
- Thorax at level of 4 chamber cardiac view
- Arms—three bones and hand (not counting fingers)
- Legs—three bones and foot (not counting toes) The *optimal standard* for the "20 week" anomaly scan If resources allow, the following could be added to the features listed above:
- Cardiac outflow tracts

• Face and lips

Figure 6.2: Baseline examination views—20 week anomaly scan. (Reproduced with permission from: 2000: Routine Ultrasound Screening in Pregnancy—Protocol, Standards and Training Supplement to Ultrasound Screening for Fetal Abnormalities Report of the RCOG Working Party)

Table 6.1: Fetal measurements and anatomic features visualized on the routine scan between 18 and 22 weeks

1. Standard fetal measurements: Biparietal diameter Head circumference Abdominal circumference Femoral length
2. Fetal anatomic features and measurements: Brain
a. Ventricular section: anterior and posterior horns of the cerebral ventricles; measurement: anterior and posterior ventricle-hemisphere ratio
b. Posterior fossa section: cerebellum, vermis, cisterna magna, and nuchal skinfold; measurement: transcerebellar diameter and nuchal skinfold
Skull
Shape
Face
Orbits (and both lenses) measurement: interorbital, external orbital diameters Nose, lips, palate, and mandible
Spine
“Anterior” view of spinous processes down to tip of sacrum; clear view of skin margin throughout length of spine
Chest
Heart: 4-chamber view, aortic root and arch, pulmonary artery and ductus
Abdomen
Diaphragm Cord insertion Liver, stomach, and intestines Both kidneys for parenchyma and renal pelvis size

Bladder Genitalia
Limbs
Femur, tibia, fibula, foot, and toes (both limbs) Humerus, radius, ulna, hand, and fingers (both limbs)
Placenta
Morphology and site
Cord
Number of vessels
Amniotic Fluid
Volume assessment

Reproduced with permission from Campbell S. The obstetric ultrasound examination. In Chervenak FA, Isaacson GC, Campbell S, eds. Ultrasound in Obstetrics and Gynecology. Boston: Little Brown, 1993: p188.

conducted a practice-based randomized controlled trial between 1979 1981 of 877 (90%) low risk women without prior risk of growth restriction. All patients had gestational age confirmed by ultrasound prior to 24 weeks gestation and underwent crown-rump length and trunk area measurements at 34 to 36.5 weeks. Patients were randomized by hospital number to a study group or control group. The study group comprised 433 patients whose results were shared with the obstetricians, while the results of 455 patients in the control group were concealed with the exception of breech presentation (9 cases) or placenta previa (1 case). The control group information was made available by clinician request; no requests were made. The two-stage ultrasound approach was 94% sensitive and 90% specific for the detection of birth weight below the 5^{th} percentile. There were no differences noted between the two groups. The groups were compared with respect to many parameters, including number of labor inductions overall and for suspicion of growth restriction, number of emergency cesarean sections, unfavorable Apgar scores, mean gestational age at delivery, mean birth weight and number of small for dates neonates.

Bakketeig et al[32] investigated the use of a twostage ultrasound regimen in patients randomly selected for ultrasound examination compared to a control group of patients that did not undergo antenatal ultrasound. This randomized controlled practice-based trial was conducted between 1979 and 1980 in Trondheim, Norway. A total of 1009 patients were enrolled. The 510 women in the screened group underwent ultrasound examination at 18 weeks and 32 weeks gestation. When compared to the background rate of low birth weight, 4.2%, the rate in the study population, 3.9%, suggested that the study population was biased towards being more low risk and may not have accurately reflected the populace. A power analysis to assess perinatal mortality was not provided. There were no statistical differences between the screened and control groups, except for an unexplained greater number of antenatal admissions, mostly for pre-eclampsia, in the screened group.

There was a trend towards earlier detection of twin gestations, fewer post-date inductions and fewer low birth weight neonates in the screened group.

Another Norwegian trial was conducted from 1979–1980 in Ålesund. Eik-Nes et al reported preliminary results in 1984[33] and subsequently published a complete analysis in 2000.[34] This prospective randomized trial involved 1628 patients. Routine ultrasound screening at 18 and 32 weeks gestation was performed in the study group (n=825) and ultrasound examinations were performed upon clinician request in 34% of the control group (n=803). The screened group had significantly less post-term inductions, fewer neonates with 5 minute Apgar scores below 8, and fewer neonates that required positive pressure ventilation for more than one minute. Also, twins were detected earlier in the screened group, but there were no significant differences in twin outcome between the groups. The study lacked power to assess perinatal mortality, but did show a trend towards improved perinatal outcomes in the ultrasound screened group for both singleton and twin pregnancies.

In Copenhagen, Denmark, Secher et al[35] recruited patients between 1980 and 1983 and studied a low risk population that underwent ultrasound gestational age assessment before 22 weeks gestation and subsequently underwent third trimester screening for growth retardation. All patients were screened at 32 and 37 weeks gestation. An additional ultrasound was performed at 34 weeks if the estimated fetal weight was at or less than the 15th percentile at 32 weeks. There were 184 fetuses suspected to be at or less than the 15th percentile at one or more third trimester ultrasound examinations. These patients were randomized to a treatment (n=96) or control (n-88) group. The ultrasound results were withheld from the control group, but were revealed in 28 cases due to clinical concern. The treatment group was followed with weekly non-stress tests and serum estradiol and human placental lactogen. There were no differences between the two groups with respect to the number of neonates weighing <2500 grams, and maternal and neonatal complications. There were statistically more labor inductions in the treatment group, although the indications for induction were not detailed. There was suggestion of a marginal, not statistically significant, benefit of a reduced occurrence of neonatal hypoxia, measured by arterial cord pH <7.15, in the treatment group. The authors acknowledge there was insufficient power in the study and was further weakened by the 32% of the control group whose results were revealed.

The first randomized controlled trial in the United States included enrolled patients from 1984–1986. Ewigman et al[36] randomized 42% (915/2171) patients presenting for prenatal care to a study group that received an ultrasound at 10–12 weeks gestation or to a control group that received indicated ultrasonography; 23.9% of the control group underwent ultrasound scans. The strict inclusion and exclusion criteria of the study still did not ensure minimum control group exposure to ultrasound and the demographics of this study's population was not reflective of the general United States. Patient recruitment was practice-based, not population-based, with Caucasians representing over 90% of the patients. The power calculations permitted a 64% chance of detecting a 50% reduction in post-term inductions and a 70% chance of detecting a 50% reduction in adverse perinatal outcome. Adverse perinatal outcome was defined as perinatal death, NICU admission of 3 or more days or Apgar score at 5 minutes less than 6. The groups did not differ in the number of post-term inductions, total inductions or adverse perinatal outcomes.

Ultrasound was beneficial in both groups for adjustment of estimated date of confinement.

Waldenström et al[37] in Stockholm, Sweden randomized 4997 women without clinical indication for ultrasound into a screening group (n=2482) and a control group (n=2511). Patients were recruited between 1985 and 1987 from all local antenatal clinics. The screening group underwent an ultrasound at 15 weeks gestation. Subsequent ultrasound examinations were performed in either group at the request of the clinician. Excluding the initial screening ultrasound in the screening group, the 31.8% of unscreened group that underwent ultrasound, utilized more ultrasound examinations after 19 weeks than the screened group, 1279 and 736, p=0.039, respectively. Gestational age estimation by ultrasound prior to 19 weeks had been performed in 103 patients in the control group. Compared to the control group, the screening group had significantly fewer inductions for post-term pregnancy (9.1% versus 5.9% p<0.0001), greater average birth weight (3497±557, 3521±527 p=0.008) and fewer low birth weight neonates (4% versus 2.5% p=0.005). There were 48 sets of twins between the two groups. All 24 sets of twins in the screening group were identified by 24 weeks, and the 20 sets of twins in the control group were identified by 32 weeks. There were no significant differences in twin pregnancy outcomes, i.e. gestational age at delivery, birth weight, Apgar scores and perinatal death, between the two groups.

The largest European randomized controlled trial assessing routine versus selective antenatal ultrasound screening was also the first to compare systematically the detection of fetal abnormalities. The study took place in Helsinki, Finland and patients were recruited from 1986–1987. Saari-Kemppainen et al[38] randomized 9,310 patients into a study group (n=4691) that routinely underwent ultrasonography between 16 to 20 weeks, and a control group (n=4619) that selectively underwent ultrasonography. In the latter group, 77% of patients received an ultrasound during the course of the pregnancy, while most ultrasound examinations were performed prior to 20 weeks in the study group. The large number of controls exposed to ultrasound could account for the lack of significant difference in labor inductions and mean birth weights between the two groups. The study group utilized less antenatal care outpatient visits that the control group (2.3 versus 2.6, p<0.0001) and had improved detection of twins by 24 weeks (100% versus 76.3%). Most importantly, the perinatal mortality of singletons was reduced 49.2% in the study group (4.6/1000) as compared to the control group (9.0/1000). This difference was attributed to the detection of severe fetal abnormalities and the participants' acceptance of pregnancy termination. The rate of fetal abnormality detection varied according to ultrasound site. The detection rate at the City Hospital was less than that of the University Hospital, 36.0% versus 76.9%. The overall perinatal mortality rate was reduced, but the small number of twins restricted further analysis between the two groups; though it appeared that the perinatal mortality rate for twins was less in the study group than in the control group, 27.8/1000 versus 65.8/ 1000. The reduction in overall perinatal mortality rate was impressive as Finland already exhibited one of the lowest perinatal mortality rates in the world confirming the impact of congenital malformations on perinatal mortality.

Geerts et al[39] in South Africa, assessed the utility of a single screening ultrasound in a developing country. After randomization, 8% of patients were excluded; 909 patients remained with 457 in the routine ultrasound group and 452 in the selective ultrasound group. Patients were recruited from 1991 to 1992, and study patients received a screening

ultrasound between 18 and 24 weeks gestation. As seen in other similar studies, ultrasound examinations were performed in 25% of the control group. Compared to the study group, the control group had a greater degree of suspected post-dates pregnancies (9 versus 38, p=0.00002) and more ultrasounds (3 versus 23, p=0.0001) and inductions (1 versus 14, p=0.002) were performed for this indication. Five patient in the control group required confirmation of lung maturity by amniocentesis while no patients in the study group underwent fetal lung maturity testing, p=0.03. There were no differences seen in adverse pregnancy outcomes (perinatal mortality, NICU admission or long term morbidity) in singletons between the two groups. The routine group did have a greater proportion of low birth weight infants (p=0.007, OR 1.61; 95% CI 1.13–2.30), but the numbers were too small for statistical comparison of perinatal outcome. Similarly, as there were only a total of 6 sets of twins, perinatal outcomes for multiple gestations could not be compared. More major congenital anomalies were detected in the routine group (n=8) than in the control group (n=3). Within each group there were 2 pregnancy terminations due to these fetal abnormalities. The authors concluded that the selective use of ultrasound did not increase adverse pregnancy outcomes and that the results did not support the additional cost accrued by routine ultrasound.

In response to the 1984 NIH Consensus Conference, the Routine Antenatal Diagnostic Imaging with Ultrasound (RADIUS)[40] trial was created as the largest prospective randomized controlled trial of routine versus selective antenatal ultrasound. The RADIUS trial was a practice-based study that attempted to evaluate the effect of twostage routine ultrasound screening in a low risk population on perinatal morbidity and mortality. Patients were recruited from 1987 to 1991 from 109 private practices in 5 Midwestern states and 1 New England state. A total of 55,744 patients registered for prenatal care in the participating clinics. Ignoring patients that were lost to followup, 61% (32, 317/53, 36 7) of scree ned registr were deemed ineligible or were excluded. Another 26% were then lost to follow up or declined screening. The remaining 15,530 patients, representing 28% of the original registrants, were randomized. The study group (n=7,812) underwent sonography at 15–22 weeks and again at 31 to 35 weeks. Power calculations were performed but did not state the percent chance of detecting their primary goal of a 20% reduction in adverse perinatal outcomes (fetal or neonatal death, or moderate or severe neonatal morbidity). Secondary outcome measures included the incidence neonates born small for gestational age or post-term and rate of labor induction in presumed post-term pregnancies. Multiple gestations were analyzed separately according to birth weight and rate of premature births.

The RADIUS trial did not demonstrate significant differences between the routine and selective screening groups with respect to maternal and perinatal morbidity and perinatal mortality.[40] However, there were significant differences in the detection of fetal anomalies and multiple gestation, use of tocolysis and diagnosis of post-date pregnancy.[41,42] Prior to 24 weeks gestation, 4.9% (8/163) of fetal anomalies in the control group were detected, as opposed to the three fold increase in detection of fetal anomalies, 16.6% (31/187), seen in the routine screening group. Subgroup analysis revealed a 35% (19/54) detection rate of fetal anomalies at the tertiary centers while nontertiary centers detected 13% (8/ 64). Twin pregnancies were detected by 24 weeks in 98.5% (67/68) of patients in the study group. The one missed patient was noncompliant with the screening regimen. Conversely, 37% (23/61) of twin pregnancies were detected by 24 weeks in the

control group. Tocolysis was utilized by 3.4% (260/7617) patients in the study group versus 4.2% (318/7534) in the control group. The study group had significantly less pregnancies past 41 weeks and past 42 weeks than the control group, 19.1% versus 21.4%, p<0.001, and 3.2% and 4.6%, p<0.001, respectively.

CRITIQUE OF RADIUS TRIAL

Although the magnitude of the RADIUS trial is impressive, there are four important points to consider regarding its conclusions.[43]

Applicability of Results

An extremely low risk population was enrolled in the RADIUS trial. Selection bias commenced with enrollment in prenatal care and in private clinics. Most patients were white (93%), English speaking (100%), had ideal body weight (90%) had received college level education (70%)[44] and were indifferent to pregnancy termination. The stringent exclusion criteria removed 60% of patients at initial enrollment and 45% of the remaining 40% of patients considered low risk subsequently underwent ultrasonography.[45] Therefore, the conclusions of the trial are applicable to less than 40% of low risk private patients, who are deemed low risk after extensive scrutiny.[43]

Outcomes Emphasized

Although a power analysis was performed, the number of participants was insufficient to draw definitive conclusions on the lack of effect of a single technology, ultrasound, on perinatal morbidity and mortality. Therefore, the potential for improvement in perinatal morbidity and mortality cannot be dismissed. Published estimated power calculations show a minimum of 6250 patients in each group to demonstrate a 50% decrease in perinatal mortality (from 10/1000 to 5/1000).[46] Ultrasound screening could possibly predict approximately half of the congenital malformations or intrauterine growth restriction cases that lead to fetal or neonatal demise. Thus, a more realistic reduction from 10 to 8 per 1000 perinatal deaths would require 46,820 patients in each group.[47]

The RADIUS trial also ascribed therapeutic properties to ultrasound examination which serves purely a diagnostic role. Romero asserted it is unreasonable to expect ultrasound to reduce the rate of prematurity and small for gestational age neonates without the combination of an effective treatment modality.[48]

There were significant findings in the RADIUS trial that deserve emphasis. Routine ultrasound examination led to an increased detection of fetal anomalies, earlier diagnosis of twin pregnancies, fewer cases of tocolysis and induction of labor for post-dates.[49] With larger numbers, the benefits of these significant findings may have translated into improved perinatal morbidity and mortality.

Ultrasound Quality

The nonuniform detection rate of fetal anomalies between tertiary and nontertiary centers highlights a critical issue regarding the quality of the ultrasound examinations performed in the study. The detection rate prior to 24 weeks gestation of 16.6% was much lower than that seen in European studies. Romero compared the sensitivity of the RADIUS trial with a series of European trials for which a combined sensitivity was generated, 16.6% versus 50.9%, $p<0.00001$.[48] Proper and frequent ultrasound accreditation, training and auditing is required in any ultrasound setting to maximize the full potential of ultrasonography and to minimize harm.

Cost Analysis

According to the cost analysis proposed by the RADIUS trial, the additional 1.6 ultrasound scans at $200/scan would incur an increase cost of $500 million. However, DeVore illustrated that the cost per fetal anomaly detected in tertiary centers is 48% below the RADIUS trial's projected cost and also less than the cost of universal screening with maternal serum alpha-fetoprotein.[50] The RADIUS trial also did not address the financial cost of caring for infants with severe congenital anomalies.[49]

META-ANALYSES OF RANDOMIZED CONTROLLED TRIALS

Thacker summarized the first four randomized controlled trials of routine ultrasound in 1983.[30–33] The combined results did not show a significant difference in frequency of low Apgar score at one minute or in the rate of perinatal mortality between the pooled study and control groups. However, a significant reduction in labor induction for incorrectly presumed post-dates was seen.[46]

Bucher and Schmidt also analyzed four randomized control trials with a combined total of 15,935 pregnancies.[32,36–38] This meta-analysis demonstrated a significant reduction in perinatal mortality, largely due to the contribution of the Helsinki study. The Helsinki study achieved a reduction in perinatal mortality due to their reasonable early detection rate of fetal abnormalities that permitted the option of induced abortion.[51]

A recent Cochrane review concluded "routine ultrasound in early pregnancy appears to enable better gestational age assessment, earlier detection of multiple pregnancies and earlier detection of clinically unsuspected fetal malformation at a time when termination of pregnancy is possible. However, the benefits for other substantive outcomes (perinatal mortality) are less clear."[52] The use of routine ultrasound overall significantly improved detection of twin pregnancies by 20 and 24 weeks gestation, reduced the rate of post-term labor inductions and led to a greater proportion of pregnancy terminations. The meta-analysis did not show a difference in antenatal hospital admissions, Apgar score below 7 at 1 or 5 minutes, low birth weight or special care admissions for singletons or in perinatal mortality (twins and singletons). The follow up studies of ultrasound safety also did not show a difference between routine and unscreened groups in school related oral reading, reading comprehension, spelling, arithmetic, overall performance, dyslexia, reduced vision, reduced hearing, spectacle use, non-right-handedness, lefthandedness and ambidexterity.[52]

DIAGNOSTIC ABILITY OF ROUTINE ULTRASOUND

One of the pioneer programs integrating routine ultrasound in prenatal care began in Malmö, Sweden in 1973 in order to improve the diagnosis of twin pregnancies. A retrospective study of their screening program from 1973 to 1978 revealed most (94.4%) twin pregnancies were diagnosed by 19 to 20 weeks gestation. The benefit of early diagnosis of twins, compared to prior diagnosis by 27 weeks was seen in the reduction of premature births (from 33% to 10%) and perinatal mortality (from 6% to 0.6%).[53] In addition, placenta previa was better identified and greater accuracy of gestational age led to a reduction in post-term induction of labor from 8% to 2.6%. The authors estimated that the improved out¬ comes reduced the use of hospital care resources by 10%.[54]

Another early site for routine ultrasound, Barcelona, Spain, reported 22 years, 1970–1991, of ultrasound screening for fetal abnormalities in a mixed high and low risk population. As expected, the improving skill and technology led to better detection rates of major fetal abnormalities in the second decade of examination, 19.75% to 96.4%; detection rates prior to 22 weeks increased from 8.63% to 84.8%. The specificity remained 99%. Overall, 59.4% (598/1006) fetal anomalies were detected early in pregnancy. Termination of pregnancy procedures paralleled the increase in fetal anomaly detection and the perinatal mortality rate declined from 8.4/1000 in 1981–1985 to 5.5/1000 in 1986–1990. Although the population included many high risk referrals, the majority of fetal abnormalities, 85–90%, were detected in low risk patients.[25]

In Finland, Rosendahl and Kivinen[55] performed routine ultrasonography on 9012 patients between 1980 and 1988. For the first two years, a routine scan was completed at 18 weeks, subsequently; a second scan was added at 34 weeks. The additional third trimester survey increased the sensitivity of major malformations to 63.8% from 41.7%. The sensitivity of structural anomaly detection prior to 24 weeks was 39.4%. Fetal abnormality detection correlated with clinical suspicion of an abnormality in only 25.8% of cases; therefore, the authors "emphasized the necessity for ultrasound examination of all pregnancies."[55]

In Belgium, Levi et al[56] described a multicenter experience of ultrasonography performed in each trimester from 1984–1989. In this unselected population, a total of 16,361 fetuses were evaluated. Between 12 and 22 weeks, 62.1% (259/417) of fetal malformations were scanned with a 21% (59/259) sensitivity, 100% specificity and 100% positive predictive value. The sensitivity rose to a 40% (154/318) detection rate of abnormal fetuses with additional sonograms later in pregnancy. There were 66 false-negative and 8 false-positive cases. Anomaly detection was analyzed according to type, gestational age at detection, gestational age based probability of detection and severity. Eighty-five percent of lethal anomalies were correctly diagnosed antenatally. The authors evaluated the appropriateness of ultrasound as a screening test and found it to be suitable in their population.

In a similar analysis, Gonçalves et al[57] conducted a retrospective case-control study of congenital anomaly detection from 1987 to 1991. Participants were referred for indicated ultrasound examination. Infants and fetuses were selected based upon hospital discharge diagnoses. The study and control groups each contained 287 women. There were 152 true positives for 287 cases, yielding an overall sensitivity of 53%. Congenital anomalies were also analyzed according to diagnostic category and gestational age at detection.

Advanced gestational age, lethality of the anomaly and high risk categorization of the pregnancy all increased sensitivity. From 20 to 23 weeks the sensitivity was 59% while it reached 68% after 24 weeks. A high percentage, 89%, of lethal anomalies was detected. Sensitivity of detecting an anomaly was higher in high risk patients as compared to low or unknown risk patients, 71%, 36%, 46%, respectively. Since the study did not have a reference population and many false-negative cases may have been omitted.[58]

In another retrospective trial, Chitty et al[59] correctly identified 93 of 125 fetal anomalies in 8342 fetuses prior to 24 weeks gestation for a sensitivity of 4%. The study was conducted between 1988 and 1989. All patients who registered early for prenatal care underwent ultrasonography prior to 24 weeks gestation. There were 14 trisomies that were not included in the calculation of sensitivity; their inclusion would reduce the sensitivity to 63%. The authors were able to demonstrate the utility of ultrasonography for antenatal fetal anomaly detection in a low risk population. They also addressed problems encountered with routine ultrasonography in this population: 1. technical problems such as maternal obesity, fetal position and multiple gestations hindered diagnosis of some structural anomalies; 2. uncertain outcomes of recognizable anomalies such as mild ventriculomegaly; 3. late presentation of some findings such as duodenal atresia; 4. the abnormality may not be detectable, i.e. tracheo-esophageal fistula; 5. evolving data on minor markers such as choroid plexus cysts, mild pyelectasis; 6. late registration for prenatal care.

Shirley et al[60] performed a combined retrospective and prospective study in an unselected pregnant population. The study evaluated 6183 (96%) infants delivered from 1989–1990 who had been scanned in the second trimester. Of the 84 abnormal fetuses scanned prior to 22 weeks gestation, 51 had fetal anomalies detected yielding a sensitivity of 60.7%. The sensitivity for detecting lethal anomalies by 22 weeks gestation was 73% (41/56). There was one false-positive diagnosis of omphalocele that was a hemangioma at birth. The specificity was 99.98%. The authors supported a routine screening program that allowed patients the opportunity to adapt to or to consider termination of an abnormal fetus and acknowledged its potential to reduce perinatal mortality.

Papp et al[61] prospectively studied two-stage routine sonography in 51,675 women between 1988 and 1990. Of the 63,794 patients offered screening, 81% participated. Sensitivity of maternal serum alpha fetoprotein (MSAFP) was compared with the sensitivity of ultrasound scanning at 18–24 weeks and at 28 weeks. Of the 496 severe anomalies detected, 317 were detected by ultrasonography between 18–20 weeks. The sensitivity of ultrasound screening of major fetal anomalies was 63.9% and significantly exceeded that of MSAFP screening. The efficiency of prenatal detection in this study supports the contention of perinatal mortality reduction by offering patients the option of pregnancy termination.

Luck[62] examined the impact of routine ultrasonography at 19 weeks gestation in an unselected population. All pregnant women from 1988 to 1991 were offered to participate and 96% (8523/ 8849) accepted. There were 160 fetal anomalies of which 140 were detected at 19 weeks gestation.

The high prevalence and detection of minor renal anomalies inflated the study's sensitivity. According to Luck, the majority of anomalies occur in low risk pregnancies and thus routine screening of pregnant women by trained and skilled ultrasonographers is advocated. Additional benefits of early anomaly detection included appropriate and

timely tertiary care referrals and emotional preparation for parents with a fetal anomaly. A cost analysis demonstrated cost effectiveness of termination of pregnancy for lethal, crippling deformities detected with expert ultrasonography.

The Multicentric Eurofetus Study[63] investigated the sensitivity of fetal anomaly detection in a large unselected population involving 14 European countries. Routine ultrasound examination was performed between 18 and 22 weeks gestation from 1990 to 1993. Fetal abnormalities occurred in 3686 fetuses, 44% of all these cases were detected prior to 24 weeks whilst 55% of severe anomalies were identified. The information from this study supports the use of routine ultrasound performance and enhances physician-patient discussion regarding pregnancy options, limitations of ultrasonography (i.e. a negative test cannot provide absolute assurance) and areas to focus on to improve detection.

Routine obstetric ultrasonography in low risk patients was assessed by Skupski et al[64] from 1990 to 1994. A retrospective review of 860 fetuses revealed a 1.2% (10/860) incidence of major anomalies. Considering only diagnoses identifiable by ultrasound, a 75% (3/4) sensitivity for major anomaly detection was reported. As the incidence of major fetal anomalies detectable sonographi-cally was 0.5%, the authors analogize amniocentesis performance for a similar incidence of aneuploidy. With early prenatal diagnosis patients received non-directive counseling and 2 out of 3 patients with ultrasound detected major anomalies opted for pregnancy termination; thereby, availing themselves of autonomy enhancing facets of prenatal care.

Quisser-Luft et al[66] performed a retrospective case control analysis of patients with and without antenatally detected fetal anomalies. Cases from 1990–1994 were reviewed and 298 malformed cases were identified from 20,248 live births, stillbirths and abortuses; 30.3% (95/298) were identified antenatally. As per standard policy in Germany, each patient underwent a minimal of three ultrasounds. Specific detection rates for anomalies detectable with ultrasound were described. The detection rates improved during the course of the study and with increasing gestational age with 38% sensitivity for ultrasound examinations prior to 24 weeks gestation and 50% after 24 weeks. Anamnestic data was collected for the 298 cases and high risk criteria developed retrospectively to identify women with abnormal fetuses (Table 6.2).[66] Retrospective application of the risk factors identified 22% (4, 525/20, 24 8) the population as high risk of which 3.2% (145/ 4,525) newborns had detectable anomalies as opposed to 0.9% (142/15, 723) in the remainder of the population. However, the absolute number of detectable anomalies between the two groups remained the same, i.e. scanning for indications would potentially miss the opportunity to detect half of the anomalies.

In a six year retrospective analysis of antenatal fetal anomaly detection with ultrasound, Boyd et al[66] demonstrated an increase in sensitivity over time from 1991–1997. Cases (n=725) were selected from an ongoing birth and malformations registry (n=33,376) and matched with antenatal ultrasound data. In the first three years 42% of fetal anomalies were detected versus 68% in the latter half. However, there was a concomitant twelve fold increase in false positive diagnoses largely attributed to the incorporation of soft markers in screening. This study emphasized the cautious use of soft markers as isolated anomalies and respect for autonomy enhancing practices of non-directive counseling and offering of abortion. An estimated 23% reduction in congenital malformations occurred due to pregnancy termination.

Table 6.2: High risk characteristics identified from anamnestic data[$]

	Statistically significant increased odds ratios		
Risk Factors	*OR*	*CI*	*P value*
Anamnestic risk factors			
Sibling with malformation	4.6	1, 3–1	0.02
Mother/father with malformation	4.1	1.3–13	0.01
Consanguinity	3.1	1.4–6.6	0.004
Neonatal death/stillbirth	1,9	1, 1–3.	0.001
Alcohol abuse (mother)	2.4	1.1–6.3	0.04
Maternal age >35	1.3	1.1–1.7	0.007
Drug exposure (first trimester)	1.2	1.1–1.3	0.008
Clinical signs:			
Polyhydramnios*	13.5	9.5–19.0	0.001
Oligohydramnios*	8.7	5.2–14.0	0.001
Premature labor•	4.7	3.8–4.9	0.001
Placental insufficiency*	1.9	1.1–2.7	0.01
Growth retardation*	1.8	1.3–2.6	0.001
Vaginal bleeding*	1.5	1.2–1.8	0.001
Pre-eclampsia*	1.3	1.1–1.6	0.003

*(<32 weeks)
•(<28 weeks)
[$]Reproduced with permission from Queisser-Luft A, Stopfkuchen H, Stolz G et al. Prenatal diagnosis of major malformations: quality control of routine ultrasound examinations based on a five-year study of 20,2248 newborn fetuses and infants. Prenat Diag 1998; 18:p57

Sprigg et al[67] conducted a prospective trial from 1992 to 1994 comparing routine versus selective ultrasound practices for detection of fetal anomalies. The detection of fetal malformations from the year prior to establishing routine ultrasound surveillance was compared with the new policy. The incidence of major anomalies remained the same between the two scanning regimens. However, the routine scan permitted ultrasound detection of 29 anomalies of which 17 were true positives. There were 11 severe anomalies and 7 patients opted for pregnancy termination that led to a significant estimated cost savings. Weighing the benefit burden calculus of screening, the authors found the use of routine screening justified.

A large difference in detection of fetal anomalies between women screened routinely versus based on indication was seen in the prospective trial conducted by VanDorsten et al, 47.6% versus 75.0%, p=0.001.[68] From 1993 to 1996, 2031 patients enrolled for

prenatal care at a tertiary care center. The indicated scans were primarily performed at a maternal-fetal medicine unit whereas the screening ultrasounds took place in a primary care center. There were 15 anomalous fetuses that were not detected antenatally, 73% (11/15) were in the screening group. These false-negative diagnoses included eight missed cardiac anomalies, 5 ventricular septal defects, 1 atrial septal defect, 1 valvular incompetence and 1 atrioventricular canal defect. Detection rates of specific anomalies were analyzed. VanDorsten supported routine ultrasound as a screening test as it potentially can improve patients health care with respect to morbidity, mortality, disfigurement and anxiety. He acknowledged more experience and better equipment promotes antenatal ultrasound and that "low risk for adverse perinatal outcome does not confer low risk for anomalies."[68]

Routine prenatal ultrasound prior to 22 weeks for detection of congenital anomalies was strongly supported by the Euroscan study.[69] Included were 709,030 unselected pregnancies from 12 European countries. A total of 20 Congenital Malformation Registries participated from 1993 to 1996; 18 registries were population based and 16 collaborated with the EUROCAT program. Congenital malformations existed in 8,126 cases and 44.3% (3,601/8,126) were detected with antenatal ultrasound screening. All categories of major congenital anomalies capable of prenatal detection were detected less frequently in countries without a routine antenatal ultrasound policy and in Eastern Europe. These findings suggest that operator experience, equipment and gestational age at examination are important factors affecting the sensitivity of congenital anomaly detection. From the results of this largely population based trial, the authors recommend single stage routine ultrasound screening for fetal anomalies as the majority occur in pregnancies without ascertainable risks.[69,70]

A compilation of studies yielded a combined sensitivity of 50.9% for ultrasound detection of fetal anomalies before 24 weeks gestation (Table 6.3).[48] In this analysis, Romero proposed if prenatal care should encompass detection of fetal anomalies, then routine ultrasound screening by experts can achieve this goal. Clementi also supported the use of routine ultrasound as the detection of congenital anomalies continues to improve concomitant with experience and advances in ultrasound technology. In addition, congenital malformations impact heavily on perinatal morbidity and mortality and their detection can be amendable to secondary and tertiary prevention.[71]

In order to maximize visualization of fetal anatomy and minimize follow up ultrasound examinations, the ideal time to perform the second trimester ultrasound is between 20 to 22 weeks gestation. Schwärzler et al[24] determined this optimum gestational age by randomizing 1206 women who were available for follow up and had undergone normal first trimester ultrasonography. Three groups were established; group 1 was scanned between 18 weeks—18 weeks 6 days, group 2 was scanned between 20 weeks—20 weeks 6 days and group 3 was scanned between 22 weeks and 22 weeks and 6 days. The anatomy scan was more likely to be completed and within a shorter time period between 20 to 22 weeks than at 18 weeks, 88–90% versus 76%, p=0.001).

Table 6.3: Comparison of sensitivity of fetal anomaly detection*

Reference	*Period*	*n*	*Gestational age (weeks)*	*Prevalence of anomalies*	*Sensitivity*	*Specificity*	*PPV*	*NPV*
Saari-Kamppainen[38]	1986–87	4073	16–20	0.99%	40% (18/45)	99.8% (4636/4646)	64.3% (18/28)	99% (4636/4663)
Levi[56]	1984–89	16072	12–20	1.61%	20.8% (54/259)	100% (15972/15972)	100% (54/54)	98.7% (15972/16177)
Rosendahl[55]	1980–88	9012	<24	1.03	39.8% (37/93)	*	*	*
Shirley[60]	1989–91	6183	19	1.36%	60.7% (51/84)	99.9% (6098/6099)	98.1% (51/52)	99.5% (6098/6131)
Chitty[59]	1988–89	8432	<24	1.48%	74.4% (93/125)	99.9% (8305/8307)	97.9% (93/95)	99.6% (8305/8337)
Luck[62]	1988–91	8523	19	1.95%	84.3% (140/166)	99.9% (8355/8357)	98.6% (140/142)	99.7% (8355/8381)
Overall	**1980–91**	**52295**	**<24**		**52.9%** (393/772)	**99.9%** (43366/43381)	**95.9%** (356/371)	**99.26%** (43366/43689)

* Reproduced with permission from Romero R.Routine obstetric ultrasound. Ultrasound Obstet Gynecol 1993; p306.

FIRST TRIMESTER ULTRASONOGRAPHY

The benefits of antenatal ultrasound examination can proceed from assessment in the first trimester. Determination of fetal viability, accurate gestational age, multiple gestations and chorionicity and amnionicity,[71] and detection of fetal anomalies have been described with first trimester ultrasonography. Fetal nuchal translucency measurement has emerged as a valuable tool for aneuploidy screening and fetal nasal bone assessment is gaining importance.[72] Although the first trimester scan continually advances its ability to detect fetal anomalies, it does not currently substitute for the second trimester sonogram.[73,74]

Crowther et al[75] demonstrated the utility of first trimester sonography performed at the first prenatal visit. There were 648 eligible patients randomized to ultrasound versus no ultrasound prior to routine screening at 18 to 20 weeks, Patients presented for prenatal care at mean gestational ages of 10.7±2.7 and 10.6±2.6 weeks, respectively. The study

group who underwent early sonography had more accurate estimation of gestational age and expressed more positive feelings towards their pregnancy. There was a trend towards earlier detection of twins in the study group compared to the control group. Earlier diagnosis of twins and accurate gestational age determination are important factors in maternal biochemical screening.

Studies evaluating first trimester sonographic detection of structural anomalies demonstrate sensitivities similar to those reported for second trimester ultrasonography. Economides et al[75] assessed first trimester fetal anomaly detection in 1632 low risk pregnancies. The incidence of anomalous fetuses was 1% (17/1632) of which 64.7% (11/17) were detected in the first trimester. The routine second trimester ultrasound identified an additional 3 anomalous fetuses for a combined trimester sensitivity of 82.3% (14/17). The specificity at each screening ultrasound was greater than 99%. Analysis by time of detection and specific anomaly revealed similar disparities in detection rates of central nervous system and cardiac anomalies in first and second trimester ultrasound examinations in low risk populations. However, with nuchal translucency screening, the first trimester ultrasound can potentially identify those fetuses at increased risk of cardiac anomalies.[76,77] Whitlow et al[77] expanded the aforementioned study to include an additional 4811 viable pregnancies (n=6443). There were 92 abnormal fetuses yielding an incidence of 1.4%, that included 63 fetuses with prenatally detected structural anomalies of which 43 were aneuploid. There were 3 false-positive initial diagnoses of exophthalmos that were cancelled upon subsequent re-scanning. First trimester sensitivities for detection of structural anomalies and chromosomal abnormalities, were 59% (37/63) and 78% (31/40). Chromosomal abnormalities, except for 3 cases of Klinefelter's syndrome, were suspected by fetal structural anomalies and/or nuchal translucency greater than the 99th percentile for crown-rump length. Combining first and second trimester scans, increased the sensitivity for structural anomaly detection to 81% (51/63). The authors concluded that most structural and chromosomal abnormalities can be detected by fetal ultrasound examination between 11–14 weeks, ideally at 13 weeks, but should not replace second trimester ultrasound.

Carvalho et al[78] evaluated 2853 pregnancies with first trimester transabdominal and transvaginal ultrasound, median gestational age 12 weeks and 4 days. Patients enrolled in antenatal care at a tertiary referral center. There were a total of 130 fetal anomalies during the study period, 93 (71.5%) of which were detected with antenatal ultrasound. First trimester ultrasonography detected 29 out of 130 (22.3%) fetal anomalies representing 31.2% (29/93) of the prenatally detected fetal anomalies. Of the structural anomalies, 50.8% major anomalies (66/130) were noted and 78.8% (52/66) detected antenatally. The first trimester scan detected 37.8% (25/66) of all major anomalies.

With an increasing proportion of pregnant women of advanced maternal age, the incidence of trisomy 21 in the second trimester increased from 1/740 in 1974 to 1/504 in 1997.[73] Early detection of aneuploidy allows women to consider invasive diagnostic testing and termination of pregnancy in the first trimester or early second trimester. However, many of these aneuploid fetuses may result in spontaneous fetal demise. The advent of nuchal translucency screening in the first trimester has facilitated earlier detection of fetal aneuploidy. Nicolaides et al[79] in 1992 described an association between increased first trimester nuchal translucency thickness and aneuploidy and introduced first trimester nuchal translucency screening for abnormal karyotypes. He reported a

sensitivity of 64% for aneuploidy using a nuchal translucency cutoff of ≥3 mm. Snijders et al[80] in 1998 reported a detection rate of 82%, false-positive rate 8.3%, for trisomy 21 fetuses. This multicenter European trial involved 22 centers, 306 sonographers and 96, 127 fetuse Each fetus had a nuchal translucency measurement obtained from which a gestational age (by crown-rump length) related likelihood ratio was used to combine the maternal age and nuchal thickness related risks to estimate an adjusted risk. Nuchal translucency measurements vary normally with gestational age and a single cutoff should not be used to adjust risk since it will lead to a lower sensitivity than if nuchal translucency is treated as a continuous variable. Studies using nuchal translucency screening as a continuous, not dichotomous, variable, demonstrate similar detection rates for trisomy 21 and other abnormal karyotypes as reported by the Fetal Medicine Foundation.[81–84] After the introduction of a nuchal translucency screening protocol, Zoppi et al[85] compared the rate of declining an invasive diagnostic procedure in women of advanced maternal age. Prior to the initiation of such a screening program, the incidence of declined invasive procedures was 22% and detection of aneuploidy by transabdominal chorionic villi sampling was 31.5%. However, 30% of women who underwent nuchal translucency screening declined invasive procedures, yet the fewer number of chorionic villi samples revealed a higher rate, 65%, of chromosomal abnormalities. Therefore, nuchal translucency screening in this high risk population was able to influence a reduction in the number of invasive diagnostic procedures.

Nuchal translucency screening for aneuploidy has been used successfully in unselected populations. Economides et al[86] retrospectively investigated first trimester anatomy and nuchal translucency screening for detecting chromosomal abnormalities in 2281 consecutive, unselected gravidas. Of the 16 chromosomal abnormalities, 44% (7/16) were diagnosed between 11–14 weeks due to a nuchal translucency measurement at or greater than the 99th percentile for gestational age. Of the 8 cases of trisomy 21, 63% (5/8) were detected by nuchal translucency screening. The sensitivity of detection improved when combined with evaluation of first trimester anatomy. The combined sensitivities were 81% for all chromosome abnormalities and 75% for trisomy 21. Schwärzler et al[87] investigated the applicability of nuchal translucency screening in an unselected population of 4523 consecutive, viable fetuses. There were 230 patients (5.1%) that were screen positive for fetal aneuploidy. Patients were screen positive if the nuchal translucency measurement translated to an adjusted risk greater than 1:270. Chromosomal abnormalities were found in 23 (0.51%) cases. The sensitivity of nuchal translucency screening for detection of an abnormal karyotype was 78%, with a false-positive rate of 4.7%, specificity of 95.3%, positive and negative predictive values of 7.8% and 99.9%, respectively.

A preliminary analysis of the First Trimester Maternal Serum Biochemistry and Ultrasound Fetal Nuchal Translucency Screening Study (BUN)[88] found this test to be efficacious. In this prospective observational trial, the detection rate of trisomy 21 in 7668 patients based on maternal age and nuchal translucency measurement was 84.2% with a false-positive rate of 12.0%. With the same sensitivity, the false-positive rate was reduced to 9.4% with addition of first trimester maternal serum screening with pregnancy associated plasma protein A and free β-human chorionic gonadotropin. The BUN trial also assessed the feasibility of widespread implementation of nuchal translucency

screening. Quality sonographic images for assessment was possible with interventions such as diligent individual feedback and occasional equipment tuning.[90]

Large prospective trials assessing first and second trimester biochemical and sonographic screening for aneuploidy are underway. In North America, the FASTER (First And Second Trimester Evaluation of Risk for aneuploidy) trial and in the United Kingdom, the SURUSS (Serum Urine and Ultrasound Screening Study) trial will address comparisons between and among these screening modalities.[91]

ETHICAL DIMENSIONS

Controversy exists surrounding the practice of routine obstetric ultrasound with objections to its use inadequately addressing the central ethical principles of beneficence and respect for autonomy.

Beneficence

Beneficence, the oldest principle of medical ethics dating back to Hippocrates, obligates physicians to seek greater good than harm for patients. Using sound clinical judgment, physicians should seek clinical treatments that engender a greater balance toward good. Health-related interests should be promoted and protected rather than harmed. Therefore, the concept of nonmaleficence is subordinate to beneficence in obstetric ethics as avoiding harm for one patient in the mother-fetus unit, may portend worse harm for the other.[43] A beneficence based discussion regarding routine obstetric ultrasound centers on potential benefits and harms from application of this technique.[91] Arguments against ultrasound screening wrongly assume its benefits are diminutive with respect to its harms. The reported benefits include decreased postdatism, decreased labor induction and use of tocolytics and improved detection of multiple gestations.[52] Additional benefits of ultrasonography develop from continued research. In the case of multiple gestations, which are known to have an increased risk of anomalies, preventing the birth of an anomalous twin can be advantageous to decreased morbidity of the surviving co-twin. This tertiary prevention approach requires early detection of multiple gestations, an accurate determination of chorionicity and a thorough evaluation of fetal anatomy.[49] The putative harms involve the theoretical risk of fetal damage from ultrasound exposure and false-positive diagnoses yielding unnecessary interventions and maternal anxiety. No *in vivo* data exist to suggest that diagnostic two-dimensional ultrasound, performed adeptly and within reasonable time constraints is harmful.[6,21,52,92] It is the sonologist's integrity centered responsibility to ensure quality ultrasound performance. Expert quality ultrasonography can detect many lethal and disabling anomalies during a routine 18–20 week scan, even in low risk pregnancies. Quality of ultrasound performance underlies the wide range of rates of detection of anomalies.[93] Poor quality ultrasound can lead to a higher incidence of false-positive and false-negative diagnoses. These circumstances can lead to more harm than good incurring additional interventions such as invasive diagnostic testing with chorionic villi sampling, amniocentesis and cordocentesis and procedure related fetal loss.[94] Minor ultrasound markers of aneuploidy may cause maternal anxiety, especially in low risk populations.[94] However, one is unable to discern

with certainty for an individual whether a specific minor marker occurs as a normal variant or as a sign of aneuploidy. Careful scrutiny to reduce false-positive diagnoses is reasonable and achievable. In order to maximize the potential benefits of ultrasound and to minimize false-positive prenatal diagnoses, serial and composite screening modalities continue to evolve.[95–98] First trimester serum analyte testing coupled with nuchal translucency screening can reach 90% sensitivity and 5% false-positive rate for aneuploidy detection.[98] As seen with the introduction of nuchal translucency screening, improved sensitivity for aneuploidy with decreasing frequency of false-positive diagnoses can reduce both the number of invasive prenatal testing procedures and resulting fetal losses.[85] Nuchal translucency measurement also offers patients the ability to decline invasive prenatal testing or to decide whether to undergo chorionic villi sampling versus amniocentesis. The former may have slightly higher miscarriage and mosaicism rates, and does not permit simultaneous screening for neural tube defects with amniotic fluid α-fetoprotein determi-nation.[99] Since beneficence based clinical ment supports routine obstetric ultrasound practice, when quality ultrasound is available, patients should not be denied access to its use just as their autonomy should not be disrespected.[43,100]

Respect for Autonomy

The physician's role of patient advocate is supported by beneficence and autonomy based ethical principles. The physician's perspective on the patient's interests provides the basis for beneficence based obligations owed to her; the patient's perspective on those interests provides the basis for autonomy based obligations owed to her.[43] Respect for patient autonomy underlies medical, and therefore, obstetric ethics. Autonomy based practice warrants careful discussion with patients regarding the use of antenatal ultrasound as well as relevant antenatal diagnostic and therapeutic alternatives and acknowledgement by the physician of the patient's preferences and values. Eliciting a patient's views is integral in respecting one's autonomy since these views may influence management, barring any compelling constraints.[101] Chervenak et al[29] stated "the standard of care demands that prenatal informed consent for sonogram be accepted as an indication for the prudent use of obstetric ultrasonography performed by qualified personnel." Implementing autonomy based principles requires a three step process. 1. adequate information transfer regarding the patient's condition and management, 2. patient comprehension of the information and 3. voluntary action by the patient to either accept or decline clinical management.[43] Diagnostic and therapeutic alternatives should be discussed with the patient as a central component of prenatal care and autonomy enhancing practice. Nondisclosure of alternatives, such as not routinely offering obstetric ultrasound, impairs the patient's exercise of autonomy and may preclude options of diagno-sis of severe anomalies and pregnancy termination.

The fetus, prior to viability, does not directly possess autonomy. Therefore, autonomy based obligations to the fetus must be balanced with maternal autonomy and beneficence principles and practices.[43] Autonomy based obligation to the gravida seeking obstetric ultrasound is not diminished by controversy regarding lack of benefit or excess cost. Studies that did not show improvement in perinatal morbidity and mortality were limited by insufficient power[46–48,51] and exclusive definition of benefits. Beneficence based

clinical judgment would not condone ignoring outcomes that could reduce or prevent harm in a small but important subset of patients.[101] Regarding excessive cost, the argument to strip away autonomy due to financial concerns falls short of both cost-effective and cost-beneficial analysis. Cost-effectiveness of routine ultrasound was demonstrated by Devore[50] in California where the cost of anomaly detection with ultrasound was less than that detected by serum screening. Cost-benefit analysis incorporates long term emotional and financial benefits that are often ignored in discussions of implementation costs across a population. The costs to an individual and to society are harder to measure with regards to care of a child with severe malformation.

CONCLUSION

Routine midtrimester ultrasound is an effective diagnostic tool. Establishment of accurate gestational age, detection of fetal anomalies and multiple gestations, and reduction in postdate pregnancies and labor inductions are proven benefits of routine ultrasound. The benefit burden calculus of routine antenatal ultrasonography support its use and fulfillment of ethical principles of beneficence and respect for patient's autonomy.

REFERENCES

1. Fleischer AC. Ultrasound in obstetrics and gyne-cology. In Grainer & Allison's Diagnostic Radiology: A Textbook of Medical Imaging, 4th edition. Churchill Livingstone, 2001; 2177–85
2. Cosgrove DO. Ultrasound: general principles. In Grainer & Allison's Diagnostic Radiology: A Textbook of Medical Imaging, 4th edition. Churchill Livingstone, 2001; 43–57
3. Woo J. Obstetric Ultrasound: A comprehensive guide. Available at http://www.ob-ultrasound.net/. Accessed December 30, 2002.
4. NIH Consensus Conference. The use of diagnostic ultrasound imaging during pregnancy. JAMA 1984; 252(5): 669–72.
5. American College of Obstetricians and Gynecologists. New Ultrasound Output Display Standard. ACOG Committee Opinion No. 180. Washington, DC: ACOG, 1996.
6. Reece EA, Assimakopoulos E, Zheng XZ. The safety of obstetric ultrasonography: concern for the fetus. Obstet Gynecol 1990; 76:139–46
7. AIUM Bioeffects Report. Mechanical bioeffects from diagnostic ultrasound: AIUM consensus statements. J Ultrasound Med 2002; 29:73–76
8. AIUM News Release: AIUM opposes use of ultrasound for entertainment. Laurel, MD: November 5, 2002.
9. Salvesen KÅ, Bakketeig LS, Eik-Nes SH et al. Routine ultrasonography in utero and school performance at 8–9 years. Lancet 1992; 339:85–89
10. Salvesen KÅ. Routine ultrasonography in utero and development in childhood—a randomized controlled follow-up study. Acta Obstet Gynecol Scand 1995; 74:166–67.
11. Kieler H, Haglund B, Waldenström U et al. Routine ultrasound screening in pregnancy and the children's subsequent growth, vision and hearing. Br J Obstet and Gynaecol 1997; 104:1267–72
12. Kieler H, Ahlesten G, Haglund H et al. Routine ultrasound screening in pregnancy and the children's subsequent neurologic development. Obstet Gynecol 1998; 91:750–56
13. Salvesen KÅ, Eik-Nes SH. Meta-analysis of ultra-sound during pregnancy and birthweight, childhood malignancies and neurological development. Ultrasound in Med & Biol 1999; 25(7):1025–31

14. Kieler H, Cnattingius S, Halund B et al. Sinistrality—a side-effect of prenatal sonography: a comparative study of young men. Epidemiology 2001; 12:618–23
15. Salvesen KÅ, Eik-Nes SH. Ultrasound during preg-nancy and subsequent childhood non-right handedness: a meta-analysis. Ultrasound Obstet Gynecol 1999; 13:241–46.
16. National Institute Health Consensus Development Conference Consensus Statement 1984; 5(1):17p Available at http://hstat.nlm.nih.gov/hq/Hquest/%20screen/HquestHome/s/45672. Accessed December 30, 2002.
17. Ultrasound Screening: Implications of the RADIUS Study [draft summary]. NIH Technol Assess Statement Online 1993 Dec 3 [cited December 30, 2002]; 12:1–5
18. American Institute of Ultrasound In Medicine. Standards for Performance of the Antepartum Obstetrical Examination. J Ultrasound Med 1996; 29:185–87. Original publication available at http://www.aium.org/. Accessed December 30, 2002.
19. Campbell S. The obstetric ultrasound examination. In Chervenak FA, Isaacson GC, Campbell S, eds. Ultrasound in Obstetrics and Gynecology. Boston: Little Brown, 1993; 187–98.
20. American Institute of Ultrasound in Medicine. Standards and Guidelines for the Accreditation of Ultrasound Practices. March 2002. Available at www.aium.org/consumer/statement selected.asp? statement=27. Accessed December 30, 2002.
21. Marinac-Dabic D, Krulewitch CJ, Moore RM. The safety of prenatal ultrasound exposure in human studies. Epidemiology 2002; 13:S19-S22
22. Anderson G. Routine prenatal ultrasound screening. In: Canadian Task Force on the Periodic Health Examination. Canadian Guide to Clinical Preventive Health Care. Ottawa: Health Canada, 1994; 4–14.
23. Royal College of Obstetricians and Gynaecologists. Ultrasound Screening for Fetal Abnormalities Report of the RCOG Working Party. London, UK: RCOG; 1997.
24. Schwarzler R, Senat M-V, Holden D et al. Feasibility of the second-trimester ultrasound examination in an unselected population at 18, 20 or 22 weeks of pregnancy: a randomized controlled trial. Ultrasound Obstet Gynecol 1999; 14:92–97
25. Carrera JM, Torrents M, Mortera C et al. Routine prenatal ultrasound screening for fetal abnormalities: 22 years' experience Ultrasound Obstet Gynecol. 1995; 3:174–79
26. Martin JA, Hamilton BE, Ventura SJ et al. Births: Final data for 2001. National vital statistics reports; 51 (2) Hyattsville, MD: National Center for Health Statistics. 2002.
27. American College of Obstetricians and Gynecologists. Routine Ultrasound in Low-Risk Pregnancy. ACOG Practice Patterns No. 5. Washington, DC: ACOG, 1997.
28. U.S. Preventive Services Task Force. Chapter 36 Screening Ultrasonography in Pregnancy. In Guide to Clinical Preventive Services, 2nd Edition. Washington, DC: U.S. Department of Health and Human Services, Office of Disease Prevention and Health Promotion, 1996.
29. Chervenak FA, McCullough LB, Chervenak JL. Prenatal informed consent for sonogram: An indication for obstetric sonography. Am J Obstet Gynecol 1989; 161:857–60
30. Bennett MJ, Little G, Dewhurst J et al. Predictive value of ultrasound measurement in early pregnancy: a randomized controlled trial. British J Obstet Gynaecol 1982; 89:338–41
31. Neilson JP, Munjanja SP, Whitfield CR. Screening for small for dates fetuses: a controlled trial. Br Med J 1984; 289:1179–82
32. Bakketeig LS, Eik-Nes SH, Jacobsen G et al. Randomised controlled trial of ultrasonographic screening in pregnancy. Lancet 1984; 2(8396):207–11
33. Eik-Nes SH, Økland O, Aure JC et al. Ultrasound screening in pregnancy: a randomized controlled trial. Lancet 1984; 1(8390): 1347.
34. Eik-Nes SH, Salvesen KÅ, Økland O. Routine ultrasound fetal examination in pregnancy: the Ålesund' randomized controlled trial. Ultrasound Obstet Gynecol 2000; 15:473–78.
35. Secher NJ, Kern Hansen P, Lenstrup C. et al. A randomized study of fetal abdominal diameter and fetal weight estimation for detection of light-forgestation infants in low-risk pregnancies. Br J Obstet Gynaecol 1987; 94:105–09

36. Ewigman B, LeFevre M, Hesser J. A randomized trial of routine prenatal ultrasound. Obstet Gynecol 1990; 76:189–94.
37. Waldenström U, Axelsson O, Nilsson S et al. Effects of routine one-stage ultrasound screening in pregnancy: a randomized controlled trial. Lancet 1988; 2(8611):585–88
38. Saari-Kemppainen A, Karjalainen O, Ylöstalo P et al. Ultrasound screening and perinatal mortality: controlled trial of systemic one-stage screening in pregnancy. Lancet 1990; 336:387–91
39. Geerts L, Brand E, Theron G. Routine obstetric ultrasound examinations in South Africa: cost and effect on perinatal outcome—a prospective randomized controlled trial. Br J Obstet Gynaecol 1996; 103:501–07.
40. Ewigman BG, Crane JP, Frigoletto FD et al. Effect of prenatal ultrasound screening on perinatal outcome. N Engl J Med 1993; 329:821–27
41. LeFevre ML, Bain RP, Ewigman BG et al. A randomized trial of prenatal ultrasonographic screening: Impact on maternal management and outcome. Am J Obstet Gynecol 1993; 169:483–89.
42. Crane JP, LeFevre ML, Winborn RC et al. A randomized trial of prenatal ultrasonographic screening: Impact on the detection, management, and outcome of anomalous fetuses. Am J Obstet Gynecol 1994; 171:392–99
43. Skupski DW, Chervenak FA, McCullough LB. Is routine ultrasound screening for all patients? Clin Perinatol 1994; 21:707–22
44. Berkowitz RL. Should every pregnant woman undergo ultrasonography? New Eng J Med 1993; 329:874–75.
45. Gunderson EW. Cost of routine ultrasonography. Am J Obstet Gynecol 1994; 171:581–82
46. Thacker SB. Quality of controlled clinical trials. The case of imaging ultrasound in obstetrics: a review. Br J Obstet Gynaecol 1985; 92:437–44
47. Lilford RJ, Chard T. The routine use of ultrasound. Br J Obstet Gynaecol 1985; 92:434–36
48. Romero R. Routine obstetric ultrasound. Ultrasound Obstet Gynecol 1993; 3:303–07
49. Chasen ST, Chervenak FA. What is the relationship between the universal use of ultrasound, the rate of detection of twins and outcome differences? Clin Obstet Gynecol 1998; 41:67–77
50. DeVore GR. The routine antenatal diagnostic imaging with ultrasound study: another perspective. Obstet Gynecol 1994;84:622–26.
51. Bucher HC, Schmidt JG. Does routine ultrasound scanning improve outcome in pregnancy? Meta-analysis of various outcome measures. Br Med J 1993; 307:13–17.
52. Neilson JP. Ultrasound for fetal assessment in early pregnancy (Cochrane Review). In: The Cochrane Library, Issue 4, 2002. Oxford: Update Software.
53. Grennert L, Persson P-H, Gennser G. Benefits of ultrasonic screening of a pregnant population. Acta Obstet Gynecol Scand 1978; Suppl 78:5–1
54. Persson PH, Kullander S. Long-term experience of general ultrasound screening in pregnancy. Am J Obstet Gynecol 1983; 146:942–47.
55. Rosendahl H, Kivinen S. Antenatal Detection of Congenital Malformations by Routine Ultrasono-graphy. Obstet Gynecol 1989; 73:947–51
56. Levi S, Hyjazi Y, Schaaps JP et al. Sensitivity and specificity of routine antenatal screening for conge-nital anomalies by ultrasound: the Belgian multicentric study. Ultrasound Obstet Gynecol 1991; 1:102–10.
57. Gonçalves LF, Jeanty P, Piper JM. The accuracy of prenatal ultrasonography in detecting congenital anomalies. Am J Obstet Gynecol 1994; 171:1606–12
58. Boyle JG. The accuracy of prenatal ultrasonography in detecting congenital anomalies (letter). Am J Obstet Gynecol 1995; 173:667–68
59. Chitty LS, Hung GH, Moore J et al. Effectiveness of routine ultrasonography in detecting fetal structural abnormalities in a low risk population. BMJ 1991; 303:1165–69.

60. Shirley IM, Bottomley F, Robinson VP et al. Routine radiographer screening for fetal abnormalities by ultrasound in an unselected low risk population. British Journal of Radiology 1992; 65:564–69
61. Papp Z, Tóth-Pál E, Papp CS et al. Impact of prenatal mid-trimester screening on the prevalence of fetal structural anomalies: a prespective epidemiological study. Ultrasound Obstet Gynecol 1995; 6:320–26
62. Luck CA. Value of routine ultrasound scanning at 19 weeks: a four year study of 8849 deliveries. BMJ 1992; 304:1474–78
63. Grandjean H, Larroque D, Levi S et al. The performance of routine ultrasonographic screening of pregnancies in the Eurofetus Study. Am J Obstet Gynecol 1999; 181:446–54.
64. Skupski DW, Newman S, Edersheim T et al. The impact of routine obstetric ultrasonographic screening in a low-risk population. Am J Obstet Gynecol 1996; 175:1142–45.
65. Queisser-Luft A, Stopfkuchen H, Stolz G et al. Prenatal diagnosis of major malformations: quality control of routine ultrasound examinations based on a five-year study of 20,2248 newborn fetuses and infants. Prenat Diag 1998; 18:567–76.
66. Boyd PA, Chamberlain P, Hicks NR. 6-year experience of prenatal diagnosis in an unselected population in Oxford, UK. Lancet 1998; 352:1577–81.
67. Long G, Sprigg A. A comparative study of routine versus selective fetal anomaly ultrasound scanning. J Med Screen 1998; 5:6–10
68. VanDorsten JP, Hulsey TC, Newman RB et al. Fetal anomaly detection by second-trimester ultrasonography in a tertiary center. Am J Obstet Gynecol 1996; 178:742–49
69. Stoll C, Tenconi R, Clementi M et al. Detection of congenital anomalies by fetal ultrasonographic examination across Europe. Community Genet 2001; 4:225–32.
70. Clementi M, Stoll C. The Euroscan Study. Ultrasound Obstet Gynecol 2001; 18:297–300
71. Sepulveda W. Odibo A, Sebire NJ et al. The lambda sign at 10–14 weeks of gestation as a predictor of chorionicity in twin pregnancies. Ultrasound Obstet Gynecol 1996; 7:421–23
72. Cicero S, Curcio P, Papageorghiou A et al. Absence of nasal bone in fetuses with trisomy 21 at 11–14 weeks of gestation: an observational study. Lancet 2001; 358:1665–67
73. Souter VL, Nyberg DA. Sonographic screening for fetal aneuploidy first trimester. J Ultrasound Med 2001; 20:775–90
74. Economides DL, Braithwaite JM. First trimester ultrasonographic diagnosis of fetal structural abnormalities in a low risk population. Br J Obstet Gynaecol 1998; 105:53–57
75. Crowther CA, Kornman L, O'Callaghan S et al. Is ultrasound assessment of gestational age at the first antenatal visit of value? A randomized clinical trial. Br J Obstet Gynaecol 1999; 106:1273–79.
76. Hyett JA, Perdu M, Sharland GK et al. Using fetal nuchal translucency to screen for major congenital cardiac defects at 10–14 weeks of gestation: population based cohort study. Br Med J 1999; 318:81–85
77. Whitlow BJ, Chatzipapas IK, Lazanakis ML et al. The value of sonography in early pregnancy for the detection of fetal abnormalities in an unselected population. Br J Obstet Gynaecol 1999; 106:929–36
78. Carvalho MHB, Brizot ML, Lopes LM. Detection of fetal structural abnormalities at the 11–14 weeks ultrasound scan. Prenat Diagn 2002; 22:1–4
79. Nicolaides KH, Azar G, Byrne D, Mansur C, Marks K. Fetal nuchal translucency: ultrasound screening for chromosomal defects in first trimester of pregnancy. BMJ 1992; 304(6831):867–69
80. Snijders RJ, Noble P, Sebire N, Souka A, Nicolaides KH. UK multicentre project on assessment of risk of trisomy 21 by maternal age and fetal nuchal-translucency thickness at 10–14 weeks of gestation. Fetal Medicine Foundation First Trimester Screening Group. Lancet 1998; 352(9125):343–46

81. Fukada Y, Takizawa M, Amemiya A, Yoda H, Kohno K, Hoshi K. Detection of aneuploidy with fetal nuchal translucency and maternal serum markers in Japanese women. Acta Obstet Gynecol Scand 2000; 79(12):1124–25
82. Acacio GL, Barini R, Pinto Junior W, Ximenes RL, Pettersen H, Faria M. Nuchal translucency: an ultra-sound marker for fetal chromosomal abnormalities. Sao Paulo Med J 2001; 119(1):19–23
83. Comas C, Torrents M, Munoz A, Antolin E, Figueras F, Echevarria M. Measurement of nuchal translucency as a single strategy in trisomy 21 screening: should we use any other marker? Obstet Gynecol 2002; 100(4):648–54.
84. Sharma G, Chasen ST, Kalish RB et al. Aneuploidy screening with nuchal translucency: performance in a single institution. Am J Obstet Gynecol 2002; 187 part 2:S177.
85. Zoppi MA, Ibba RM, Putzolu M et al. Nuchal translucency and the acceptance of invasive prenatal chromosomal diagnosis in women aged 35 or older. Obstet Gynecol 2001; 97:916–20
86. Economides DL, Whitlow BJ, Kadir R et al. First trimester sonographic detection of chromosomal abnormalities in an unselected population. Br J Obstet Gynaecol 1998; 105:58–62.
87. Schwärzler P, Carvalho JS, Senat MV et al. Screening for fetal aneuploidies and fetal cardiac abnormalities by nuchal translucency thickness measurement at 10–14 weeks of gestation as part of routine antenatal care in an unselected population. Br J Obstet Gynaecol 1999; 106:1029–34
88. Wapner RJ et al. The BUN Study Group. First trimester aneuploid screening: Results of the NICHD multicenter study. Am J Obstet Gynecol 2001; 185 part 2:S70.
89. Snijders RJM, Thom EA, Zachary JM et al. The BUN Study Group. First trimester trisomy screening: nuchal translucency measurement training and quality assurance to correct and unify technique. Ultrasound Obstet Gynecol 2002; 19:353–59.
90. Malone FD, Berkowitz RL, Canick JA et al. First trimester screening for aneuploidy: research of standard of care? Am J Obstet Gynecol 2000;182: 490–96.
91. McCullough LB, Chervenak FA. Ethics in Obstetrics and Gynecology. New York, NY: Oxford University Press; 1994.
92. Salvesen KÅ. Ultrasound and left-handedness: a sinister association? Ultrasound Obstet Gynecol 2002; 19:217–21.
93. Chitty LS. Ultrasound screening for fetal abnormalities. Prenat Diag 1995; 15:1241–57
94. Smith-Bindman R, Hosmer W, Feldstein V et al. Second-trimester ultrasound to detect fetuses with Down syndrome. A meta-analysis. JAMA 2001; 285: 1044–55.
95. Nyberg DA, Luthy DA, Resta RG et al. Age-adjusted risk assessment for fetal Down's syndrome during the second trimester: description of the method and analysis of 142 cases. Ultrasound Obstet Gynecol 1998;12:8–14.
96. Wald NJ, Watt HC, Hackshaw AK. Integrated screening for Down's syndrome based on tests performed during the first and second trimesters. New Engl J Med 1999; 341:461–67
97. Spencer K. Accuracy of Down syndrome risks pro-duced in a first-trimester screening program incorpo-rating fetal nuchal translucency thickness and maternal serum biochemistry. Prenat Diag 2002; 22:244–46.
98. Bindra R, Heath V, Liao A et al. One-stop clinic for assessment of risk for trisomy 21 at 11–14 weeks: a prospective study of 15,030 pregnancies. Utrasound Obstet Gynecol 2002; 20:219–25
99. Chasen ST, Skupski DW, McCullough LB et al. Prenatal informed consent for sonogram—the time for first-trimester nuchal translucency has come. J Ultrasound Med 2001; 20:1147–52
100. Skupski DW, Chervenak FA, McCullough LB. A clinical and ethical evaluation of routine obstetric ultrasound. Curr Opin Obstet Gynecol 1994; 6:435–39
101. Chervenak FA, McCullough LB, Ledger WJ. Advocacy for routine obstetric ultrasound. ACOG Clinical Review 1996; 1;1–4

Chapter 7
Legal Concerns in the Use of Ultrasound in Obstetrics and Gynecology

Keith B Lescale, Frank A Chervenak

The frequency of malpractice litigation has continued to rise particularly in the United States, but throughout the world.[1] This epidemic of litigation is especially apparent in the field of Obstetrics and Gynecology. More obstetricians are sued than any other specialty group. Although ultrasound has revolutionized the practice of Obstetrics and Gynecology, it unfortunately has not been spared this crisis. In a survey conducted in the United States, 75% of medical malpractice cases related to ultrasound involved obstetric patients. The next highest area of litigation concerned gynecologic ultrasound (Table 7.1).[2]

Table 7.1: Legal cases related to ultrasound

	n	%
Obstetrical	318	75
Gynecologic	45	11
Abdominal	29	7
Neurological	1	0.2
Eye	4	1
Breast	2	0.5
Miscellaneous	28	6
Total	427	

From Sanders RC. Legal Problems Related to Obstetrical Ultrasound. Ann NY Acad Sci 1998 Jun 18; 847:330–3

A survey of Fellows and Junior Fellows of the American College of Obstetricians and Gynecologist (ACOG) conducted in 1981 by the American Institute of Ultrasound in Medicine and ACOG revealed that 32% of obstetricians had ultrasound nancies had at least one ultrasound examination.[3] At that time, amongst 2260 survey respondents 32 lawsuits related to ultrasonography were reported. Today, more than 75% of obstetricians have ultrasound equipment in their offices. And, although it is still not considered standard of care to perform an ultrasound examination on every pregnant woman in the

United States, more than 80% are offered at least one ultrasound examination during their pregnancy.[4] With the continued widespread use of ultrasound and the rapid advances in its' technology, greater demands and expectations of it's use have naturally lead to a rapid rise in malpractice litigation in this area.

Another reason litigation is so common in obstetrical ultrasound is because of the long life expectancy of the infant and awards are often expected to be very large. In addition, predictions about normality are being made *in utero,* and it is all too evident when the baby emerges if the predictions are wrong.[2] Finally, the increase of public awareness about imaging and medicolegal issues in general has had an impact the rising number of cases brought to litigation.[5]

In one of the earliest reports on legal liability of ultrasound by obstetricians in the obstetric literature in, Perone et al in 1983 reviewed the most likely causes of malpractice associated with office use of ultrasound.[6] They identified four areas of concern. First was the negligent use of ultrasound. This would be related to improper training and/or carelessness that would lead to the failure to diagnose a particular anomaly. Second was the use of ultrasound beyond the limits of equipment in their offices and that 34% of preg-one's skill and knowledge. A third malpractice risk arose from failure to use and obtain the diagnostic benefits of ultrasound where indicated. A fourth area of risk involved damage from ultrasound or an ultrasound guided procedure. The authors concluded by suggesting a need to establish certification of proficiency particularly for office ultrasound procedures.

According to standard legal teaching, there are four aspects to negligence which is the basis of almost all suits in obstetrical and gynecological ultrasound: (1) There should be negligence; (2) negligence should be the responsibility of the care provider; (3) negligence should have an assessable monetary value; and (4) negligence should be responsible for the problems the patient and/or fetus has.[2]

With regard to litigation in obstetrics ultrasound, claims can be made in the following areas: (1) wrongful pregnancy; (2) wrongful birth; (3) wrongful life and (4) wrongful death.

Claims of **wrongful pregnancy** arise most commonly after a failed sterilization procedure or unsuccessful abortion that has resulted in the birth of a normal child.[5] These claims are brought by the parent(s). An example of this would be an obstetric or gynecologic ultrasound in which a viable pregnancy is overlooked by a sonographer.

Wrongful birth clams are similar to those of wrongful pregnancy with one exception: the infant is born defective. Because the parents were not given the option to terminate the pregnancy, it is the birth itself that is wrongful.[5,6] The basic purpose of the fetal anatomic survey is to exclude fetal malformations. When such anomalies are diagnosable but overlooked on examinations, claims of wrongful birth may arise against the physician.[5]

Wrongful life claims are related to those of wrongful birth, but are brought by the defective child and not the parents. It's alleged that, if not for the negligence of the physician, the defective child would never have been born.[5,7] Again, the physician is not alleged to have caused the anomaly; it is the life itself that is construed as a burden.[5,8] A perplexing question is thus raised: Is an impaired existence better than none at all? Compensation for these claims is also difficult to assess. Therefore, in jurisdictions

permitting wrongful-life claims, damages usually are limited to the more tangible costs of pregnancy and extraordinary medical costs during infancy and childhood.[5]

Wrongful death claims are made when negligence has resulted in death. If an anomaly is erroneously diagnosed when in fact the fetus is normal, and the parents choose an elective abortion, a wrongful death claim may arise. Or, if a sonographically guided therapy is unsuccessful or leads to death of the fetus, the physician may be liable.[5]

Having reviewed the various types of claims which may arise as a result of presumed negligent obstetric ultrasound, six major categories will be used to illustrate cases over the last 20 years as carefully described by Roger Sanders comprehensive work.[2,9] Sanders collected legal cases related to ultrasound from a variety of different sources: two surveys of ACOG and AIUM members, contact with expert witnesses, from physicians being sued, or from a monthly review of settled cases.

The first category Sanders describes as **'invented lesions'**. As the technology of ultrasound has advanced this type of negligence is less common. Early examples include cases in which fetal death was diagnosed on ultrasound with subsequent induced delivery of a live infant. Another example includes a case of a diagnosis of ectopic pregnancy on ultrasound when in fact a ruptured corpus luteum was found at the time of surgery (Table 7.2).

The next category is **'misreported cases'.** These cases when reviewed retrospectively could have lead to a proper diagnosis. Misdating of the pregnancy makes of the majority of this category. However, 10 fetal anomaly cases are described; including a case of hydrocephalus which later revealed subtle ventriculomegaly at a 15 weeks' gestation ultrasound (Table 7.3).

Table 7.2: Type and number of invented lesions

Carcinoma of the pancreas	1
Intrauterine devices in the uterus	3
Fetal death	2
Anencephalic	3
Renal agenesis	2
Mole	2
Ectopic	2
Gallstones	4
IUGR	1
Amniotic bands	1
Hydrocephalus	2
Abnormal abdominal wall	1
Retained products	1

From Sanders RC. Legal Problems Related to Obstetrical Ultrasound. Ann NY Acad Sci 1998 Jun 18; 847:330–3

Table 7.3: Type and number of misreported cases

Misdated fetus	18
Fetal anomaly	10
Hydrocephalus	2
Posterior urethral valves	1
Decidual cast	9
Size underestimated	3
Early pregnancy called mole	1
Spina bifida	2
Intrauterine device not seen	1
Bladder called ovarian cyst	3
Bladder called mass in child; surgery and death	1
Miscalled ovarian cancer	6
Appendiceal abscess called bicornuate uterus	1
Buttock sarcoma called abscess	1
Wrong side of double uterus identified	1
Tampax called pelvic mass	1
From Sanders RC. Legal Problems Related to Obstetrical Ultrasound. Ann NY Acad Sci 1998 Jun 18; 847:330–3	

The third category is termed **'missed diagnosis'** and involves the largest number of cases. Of the 156 cases reported, cases involving the misdiagnosis of ectopic pregnancy, twins and placenta previa make up the majority. The failure to diagnose spina bifida is the most common fetal anomaly (Table 7.4)

Surprisingly a low number of reported malpractice cases fall into the next category: **"obstetrical procedures'.** Fourteen of the 19 cases listed in this category involve the misuse or the failure to use ultrasound at the time of amniocentesis (Table 7.5).

Table 7.4: Type and number of missed diagnoses

Ectopic pregnancy	45
Twins	22
Monoamniotic twins	1
Fetal anomalies	61
Spina bifida	23
Hydrocephalus	6

Missing limbs	12
Posterior urethral valves	1
Microcephaly	1
IUGR	4
Abruptio	2
Macrosomia	1
Hypoplastic heart	1
Rhythm problems	1
Trisomy 13	2
Trisomy 21—Nuchal thickening	1
Placenta previa	13
Placenta acreta	1
Abruptio—no images	2
Appendix abscess	2
Gallstones	2
Hepatic abscess	1
Ovarian cancer	3
Pancreatic abscess	1
Transplant tumor	1
Trophoblastic disease	1
From Sanders RC. Legal Problems Related to Obstetrical Ultrasound. Ann NY Acad Sci 1998 Jun 18; 847:330–3	

Table 7.5: Procedures

No sonogram for amniocentesis	6
Misperformed sonogram for amniocentesis	8
No sonogram for abscess drainage	1
Liver mass—bloody pleural effusion	1
Poor outcome for exchange transfusion for hydrops	3
From Sanders RC. Legal Problems Related to Obstetrical Ultrasound. Ann NY Acad Sci 1998 Jun 18; 847:330–3	

The **“failure to perform ultrasound’** for an accepted indication is an increasingly common category. Cases involving macrosomia, IUGR and twins were sited as the most

common in this category. In 1984 the National Institutes of Health consensus identified 26 accepted indications for obstetrical ultrasound (Table 7.6).

In a category Sanders classifies as **'miscellaneous',** he describes a minority cases in which alleged transducer pressure or the effects of the ultrasound examination were alleged to be the cause of spontaneous abortion or IUGR fetuses.

Table 7.6: Situations in which there was failure to perform ultrasound

For routine obstetrical care	2
Ultrasound unavailable for emergencies	4
Prior to second trimester abortion	1
Biophysical profile	1
Breast ultrasound	1
Neonatal intracranial	1
Uncertain dates	1
Twin—Failure to do biophysical profile	1
Large for dates	15
Multiple pregnancy	9
Macrosomia complications	4
Hydrocephalus	2
Breech vs. cephalic	1
Increased AFP	4
IUGR	7
In diabetes	1
Possible congenital heart defect	1
Oligohydramnios	1
Postmature	3
Premature	1
Previous anomaly	1
Previous ectopic	5
Failure to follow up previously diagnosed previa	1
Earlier scans raised question of anomaly	2
With ovarian cancer	1
With vaginal bleeding and abruptio	1
With pelvic mass—24 weeks twins	1

From Sanders RC. Legal Problems Related to Obstetrical Ultrasound. Ann NY Acad Sci 1998 Jun 18; 847:330–7

Sanders diligence in the collection and categorization of malpractice cases involving obstetric ultrasound over the last 2 decades is invaluable when trying to devise ways to make litigation less likely. Table 7.7 illustrates 19 possible ways in which litigation related to ultrasound can occur.

The damaging effects of the legal situation on the field of ultrasound are like those in other areas. There is undue caution in the performance of new and valuable procedures, needless procedures are performed merely to satisfy litigation worries, and the amount of new equipment introduced is limited because of insurance expenses.[2] A survey of a random sample of the American College of Obstetricians and Gynecologists' membership showed increased referrals to other physicians,

Table 7.7: Nineteen possible ways to get sued for ultrasound

1. Missing the sonographic finding
2. Misinterpretation of the sonographic finding
3. Failure to compare findings with previous ultrasound
4. Failure to properly communicate the sonographic report to the referring physician or the patient
5. Failure to personally examine the patient or take a proper history
6. Incorrect sonographic approach for a specific condition
7. Incomplete examination
8. Inadequate quality of films
9. Slip and fall injuries
10. Complications from puncture techniques under ultrasound control
11. Failure to obtain informed consent
12. Complications of ultrasound such as induced vaginal bleeding or abortion
13. Equipment complications (e.g., electric shocks)
14. Failure to recommend additional sonographic or radiologic studies or biopsy
15. Failure to order a sonographic examination
16. Inclusion of sonologist in a shotgun suit
17. Loss of films, inadequate filing system, misplacement of films or reports
18. Abuse of patient by sonologist or sonographer (sexual, physical, or mental)
19. Miscellaneous anxiety produced by misdiagnosis, invasion of privacy, etc.

From Sanders RC. The Effect of the Malpractice Crisis on Obstetrics and Gynecologic Ultrasound.

In *Ultrasound in Obstetrics and Gynecology*, ed. Frank A.Chervenak, Glenn C.Isaacson, Stuart Campbell, 263–276. Boston: Little, Brown and Company, 1993

increased consultation with other physicians, and the addition of more tests and diagnostic procedures in response to the respondents' professional liability claims experience.[10,11]

Clearly there are a number of ways to make litigation less likely. First, obtain adequate training within the guidelines issued by the AIUM, ACR, and ACOG for real-time ultrasound to avoid criticism for insufficient training. Continuing medical education is essential. Proper documentation of normal and abnormal images is required. The written report should be communicated to the referring doctor in a timely manner as well as verbal communication when necessary. If anatomy is not well visualized this should be clearly documented and a timely repeat ultrasound examination be performed when appropriated. Consultation with another sonologist should be offered when there is uncertainty of the findings. Lastly, accreditation by the American Institute of Ultrasound in Medicine is recommended as a minimal standard of quality control for American sonologists. Sonologists throughout the world are encouraged to cooperate with local accreditation procedures.

REFERENCES

1. Hecher K, Hackeloer BJ, Bock R. Legal Issues in Fetomaternal Medicine in Consideration of Ethical Quandaries—The German Perspective. Ultrasound Obstet Gynecol 2000; 15:347–49.
2. Sanders RC. Legal Problems Related to Obstetrical Ultrasound. Ann NY Acad Sci 1998 Jun 18; 847:330 37.
3. Horger III EO, Tsai CC. Ultrasound and the Prenatal Diagnosis of Congenital Anomalies: A Medicolegal Perspective. Obstet Gynecol 1989; 74:617–19
4. Vans H. Doctors Who Perform Fetal Sonograms Often Lack Sufficient Training and Skill. Wall Street Journal 1995; June 20.
5. Macones A, Lev-Toaff AS, Macones GA et al. Legal Aspects of Obstetrics Sonography. Am J Roentgenol 1989 Dec; 153(6):1255–57
6. Perone N, Carpenter RJ, Robertson JA. Legal Liability in the Use of Ultrasound by Office-based Obstetricians. Am J Obstet Gynecol 1984; 150:801–04.
7. Bundy AL, Jones TB. Guidelines for Obstetrical Scanning and Reporting the Legal Necessity. J Ultrasound Med 1985; 4:483–84
8. Botkin JR. The Legal Concept of Wrongful Life. JAMA 1988; 259(10):1541–45
9. Sanders RC. The Effect of the Malpractice Crisis on Obstetrics and Gynecologic Ultrasound. In *Ultrasound in Obstetrics and Gynecology*, ed. Frank A. Chervenak, Glenn C. Isaacson, Stuart Campbell, 263–76. Boston: Little, Brown and Company, 1993.
10. Baldwin L-M, Hart LG, Lloyd M et al. Defensive Medicine and Obstetrics. JAMA 1995; 274:1606–10.
11. ACOG. Professional Liability Insurance and Its Effect: Report of a Survey of ACOG's Membership. Washington D.C. American College of Obstetricians and Gynecologists; 1985.

Chapter 8
Ultrasound in Developing Countries

Narendra Malhotra, Kuldeep Singh, Jaideep Malhotra

The death of a woman in childbirth should be history with the improving health practice standards.[1] But maternal death still haunts the clinicians and obstetricians, as it is still common in many developing countries. This thus indicates the quality of health care system prevalent in that country.[2] The safety of the mother and neonate should be of utmost importance. A thorough monitoring of the Maternal and Perinatal Mortality[3] and also of equal importance Maternal and Perinatal Morbidity in the region should be regularly done. This will help us explain the deficiencies in the system and steps to be taken to improve them.[4]

This chapter is going to concentrate on the causes for Maternal and Perinatal Mortality and the role of ultrasound to enable timely action and termination of these pregnancies.[5]

MATERNAL MORTALITY AND MORBIDITY

Global Overview

According to the 1995 estimates, 515,000 maternal deaths occurred globally in 1995, 31% of them were in the WHO SEA Region. Most deaths (246,000) occurred in the WHO African Region. Twelve countries together contribute to nearly two-thirds of all maternal deaths in the world. *India, with an estimated 110,000 deaths, has the highest number of maternal deaths in the world.*

Official Govt. of India data, 1997 shows Maternal Mortality Rate as 408/100,000 live births.

In India 100,000 maternal deaths occur yearly and approximately 1 death every 5 minutes.

(Maternal Mortality Rate Surveys in India)

Dr. K.Baskar Rao, FOGSI, 1982 reported maternal death of 721/100,000 live births in 41 teaching hospitals in India.

Dr. N.Bedi, ICMR, New Delhi, 1994 reported maternal death of 582/100,000 live births in 31 teaching hospitals in India. Thus there was only 20% reduction in maternal mortality in India in 12 years.

Maternal Mortality in India is 50–100 times higher than in developed countries.

According to recent figures, in industrialized nations the risk of maternal death averages 30 per 100,000 births. However, there is an average of 450 maternal deaths per

100,000 live births in developing countries. The comparative risk of maternal death in a developing country may be 200 times than in industrialized nations.

Causes of Maternal Mortality

The commonest direct causes of maternal mortality in developing countries are Eclampsia, Post partum hemorrhage, Antepartum hemorrhage, Ectopic pregnancy, Spontaneous abortions, Sepsis and Operative complications.

Indeed, factors directly related to maternal death and disability problems, include lack of antepartum care, lack of well educated as well as well trained personnel's. In the developing world there is a chronic shortage of professionally qualified birth attendants including doctors and midwives, and this is most acute in rural areas. Furthermore, in many developing countries family planning services are not sufficiently introduced or inaccessible and effective contraceptives are financially beyond reach for many. Currently as many as 50% of pregnancies are unplanned, 25% are unwanted, and complications of unsafe abortions are responsible for a substantial proportion of maternal deaths.

The role of ultrasound and color Doppler in Eclampsia is going to be discussed in detail in Perinatal mortality.

Transvaginal ultrasound with color flow mapping, power angio studies and duplex Doppler plays a major role in diagnosing ectopic pregnancy, missed abortion, incomplete and complete abortion and extent of antepartum hemorrhage.

Normal physiological changes of vasculature, occurring before and after implantation are essential to study normal and pathological processes in the first trimester. Color and pulsed Doppler sonographies can trace the major branching of the uterine vasculature, from the main uterine arteries to the arcuate arteries, to the radial arteries, and ultimately to the spiral arteries deep in the endometrium. Spiral arteries undergo a structural alteration in early pregnancy resulting in a characteristic waveform that is termed peritrophoblastic flow. Peritrophoblastic flow is associated only with intrauterine pregnancy, whether normal or failing, and is found close to the gestational sac (if present) and within or just outside the endometrium.

Transvaginal ultrasound with color flow mapping, power angio studies and duplex Doppler in early pregnancy is to differentiate and diagnose normal and abnormal early pregnancy. It is used to diagnose:

1. Intrauterine or extrauterine pregnancy.
2. Intrauterine pregnancy failure and whether complete or incomplete.
3. Molar pregnancy and see extent of myometrial invasion.

With so much of overlap in 2D findings in ultrasound of very early normal and failed intrauterine pregnancy and of ectopic pregnancy often leads to a diagnostic dilemma requiring multiple laboratory tests even serial ultrasound examinations and sometimes also a surgical approach. All this leads to delayed diagnosis, and higher cost of care accompanied with invasive management. The management now of ectopic pregnancy, diagnostic and therapeutic, is now much less invasive. Transvaginal ultrasound with color flow mapping, power angio studies and duplex Doppler have played a significant roles for this change.

Ultrasound Features in Early Pregnancy

1. **Normal intrauterine gestation:** In a normal intrauterine pregnancy gestational sac, yolk sac (Fig. 8.1) and embryo (Fig. 8.2) with cardiac activity (Fig. 8.3) can be delineated depending on the stage (Fig. 8.4) of intra-uterine gestation.[6] Peritrophoblastic flow can be seen even before demonstration of a gestational sac, thus increasing the sensitivity to 99% and specificity to 90–99% for diagnosing intrauterine pregnancies.
2. **Incomplete spontaneous abortion:** Inhomogeneous echoes (Fig. 8.5) within the uterine cavity can be seen on 2D ultrasound.

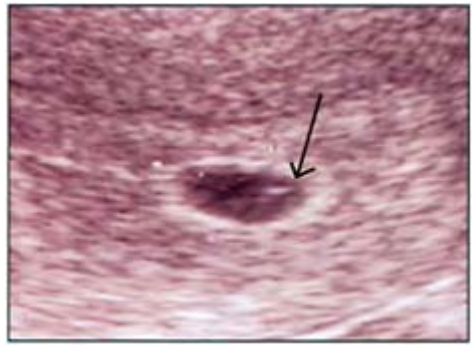

Figure 8.1: Transvaginal scan of a gestational sac of 05 weeks size also showing a small yolk sac (solid line)

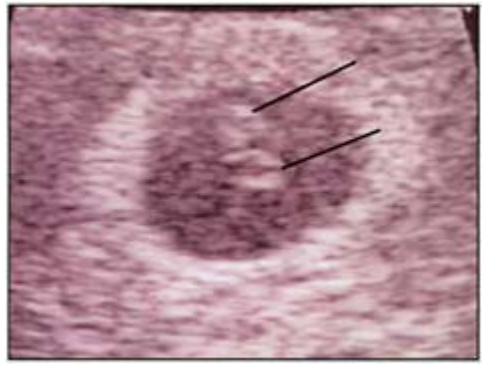

Figure 8.2: Pregnancy of 5 weeks and 6 days gestation showing a yolk sac (solid line) and an embryo (dotted line)

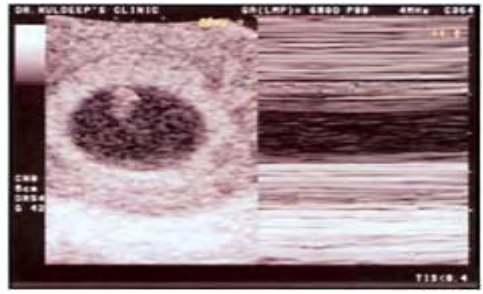

Figure 8.3: Embryonic cardiac activity with a heart rate of 134 beats per minute at 6 weeks and 4 days

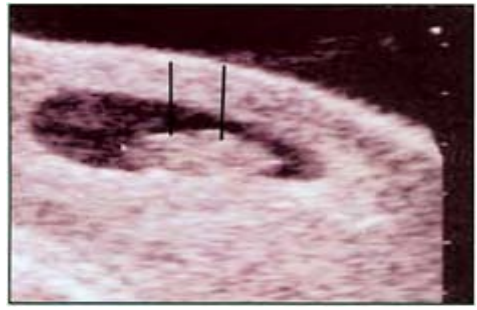

Figure 8.4: Longitudinal section of the embryo with an ovoid (solid line) and a triangle seen (dashed line)

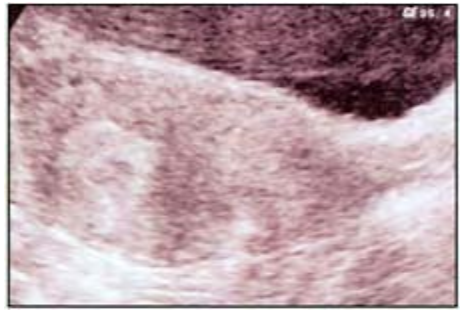

Figure 8.5: Inhomogeneous echoes within the uterine cavity seen on 2D Ultrasound in a case of amenorrhea 6 weeks with bleeding for 3 days

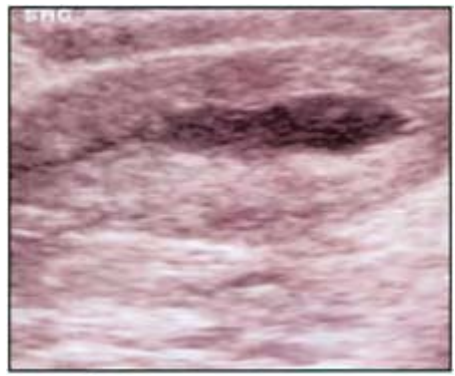

Figure 8.6: Thin-walled gestational sac in the uterine fundus with no embryo or yolk sac seen

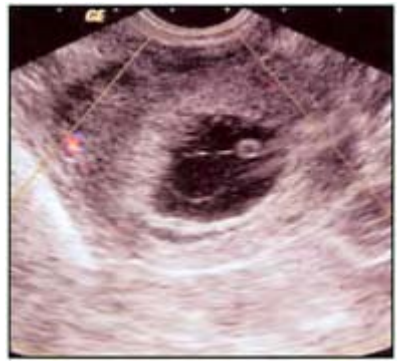

Figure 8.7: Seven weeks gestational sac showing a yolk sac but no embryo

SONOGRAPHIC FINDINGS OF AN EARLY PREGNANCY FAILURE

1. No embryonic cardiac activity with a CRL >5 mm.[7]
2. Gestational sac larger than 8 mm without a yolk sac (Fig. 8.6).[8]
3. Gestational sac larger than 16 mm without an embryo (Fig. 8.7).[9]
4. Abnormally large or floppy, amniotic sac.[10]

With color Doppler in incomplete spontaneous abortion, the overall uterine vascularity is increased over what would be seen in normal early pregnancy (Figs 8.8 and 8.9) (warm or hot vascularity). The peritrophoblastic arterial

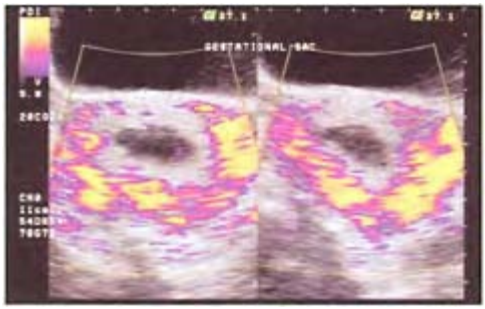

Figure 8.8: Serial evaluation shows no growth of the gestational sac and color flow mapping shows a hot uterine vascularity

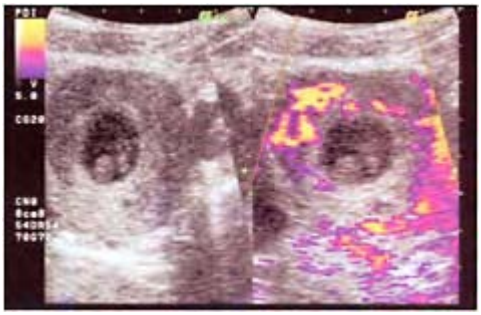

Figure 8.9: Case of missed abortion seen on 2D Ultrasound and on color Doppler, the overall uterine vascularity is increased (warm or hot vascularity)

flow is identified, with systolic velocities much above the normal range (Fig. 8.10) for intrauterine pregnancy. Increased periendometrial venous flow (Fig. 8.11) is also delineated. Corpus luteal flow is usually seen in one or both ovaries.

3. **Complete spontaneous abortion:** In complete spontaneous abortion the cavity echoes are very thin (Fig. 8.12), usually less than 04–05 mm. On color Doppler the uterine vascularity is cold (Fig. 8.13) or warm. Intrauterine peritrophoblastic flow is not seen and venous flow in the uterus is minimal (Fig. 8.14) or absent. Corpus luteal flow is often not seen.
4. **Ectopic pregnancy:** Ectopic pregnancies are seen as masses, which could measure from

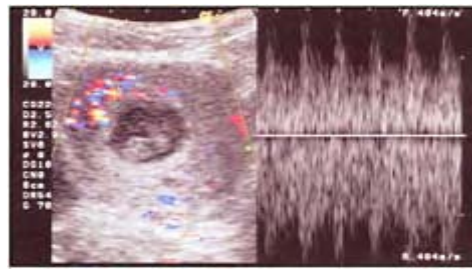

Figure 8.10: Same case on duplex Doppler evaluation the peritrophoblastic arterial flow is identified, with systolic velocities much above the normal range for intrauterine pregnancy

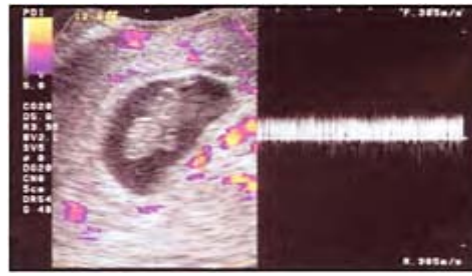

Figure 8.11: Case of missed abortion with increased periendometrial venous flow

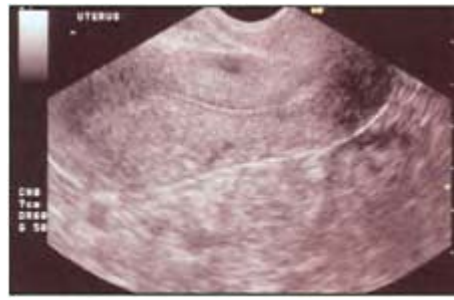

Figure 8.12: A case of complete spontaneous abortion with very thin cavity echoes, 03–04 mm

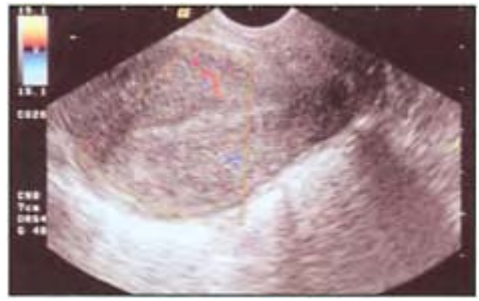

Figure 8.13: The uterine vascularity is usually cold in a case of complete spontaneous abortion

10 to 35 mm in size in the extrauterine areas. These masses could be seen as a central anechoic or hypoechoic area enveloped by a hyperechoic area (Fig. 8.18). The surest sign that you are diagnosing an ectopic pregnancy is to identify a gestational sac with a yolk sac or even an embryonic node with (Figs 8.15 and 8.17) or without cardiac activity. One can also identify the corpus luteum adjacent to the mass or even within the mass. Corpus luteum can be anechoic, hypoechoic or even hemorrhagic and is surrounded by ovarian tissue. On color Doppler in an ectopic pregnancy which is unruptured with viable trophoblasts a vascular ring can be delineated (Figs 8.16 and 8.19). The blood flow characteristically shows low-impedance, high-diastolic flow. The vascularity of ectopic pregnancies varies, probably

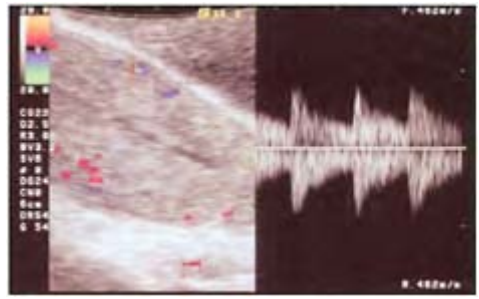

Figure 8.14: Intrauterine peritrophoblastic flow is not seen and only peripheral myometrial vascularity seen

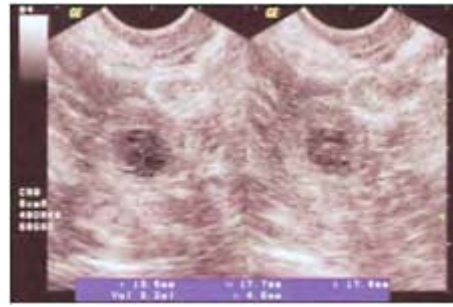

Figure 8.15: Live ectopic with a gestational sac, yolk sac and an embryo with cardiac activity

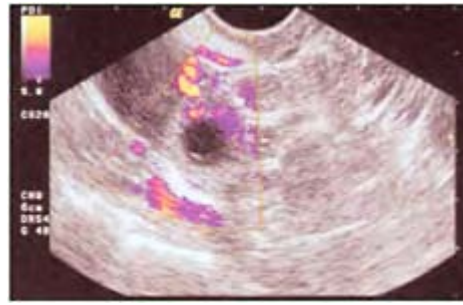

Figure 8.16: Same case with marked peritrophoblastic vascularity

depending on the viability of the trophoblasts as they invade the circular muscle of the tube (Fig. 8.20). The uterine vascularity is cold or warm. Intrauterine peritrophoblastic flow is not seen and periendometrial venous flow is also

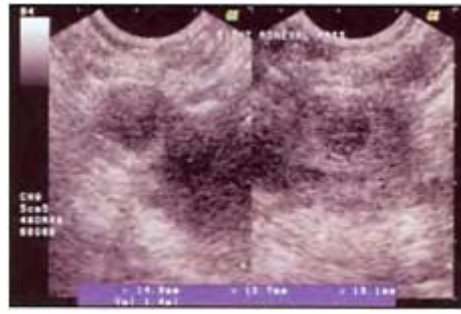

Figure 8.17: Right adnexal ectopic gestation with right ovary and corpus

luteum and a gestational sac with cardiac activity delineated

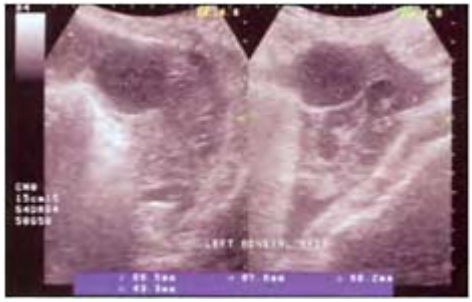

Figure 8.18: Left adnexal mass with corpus luteum in the left ovary with an adjacent inhomogeneous adnexal mass and peri-lesional fluid collection

very less. Corpus luteal flow is identified in one or both ovaries. When an adnexal ectopic mass is identified, typical peritrophoblastic flow is found within it in 79% of masses, no flow is seen in 6% of masses, and bizarre flow is found in 15% of masses.

5. **Molar pregnancy-** Characteristic cystic spaces packed in the uterine cavity are seen (Figs 8.21, 8.22 and 8.23). In uncomplicated cases only mild increase in peri-lesional vascularity is noted. In invasive moles very high velocity flow in areas of tumor invasion within the myometrium are seen (Fig. 8.24). Very low impedance flow with almost an arteriovenous shunt type waveform is also seen. This hypervascularity recedes with regression of the tumor.

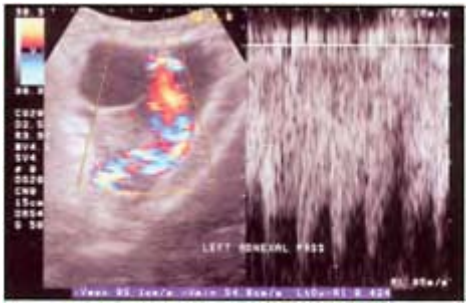

Figure 8.19: On color Doppler in an ectopic pregnancy which is unruptured with viable trophoblasts a vascular ring is delineated with the blood flow

characteristically showing low-impedance, high-diastolic flow

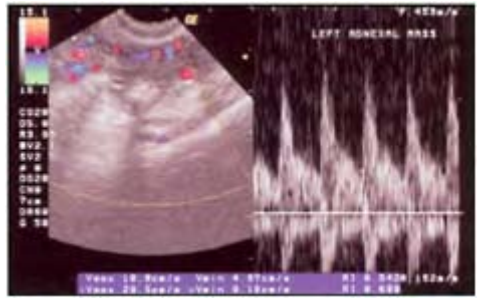

Figure 8.20: The vascularity of ectopic pregnancies varies, depending on the viability of the trophoblasts as they invade the circular muscle of the tube

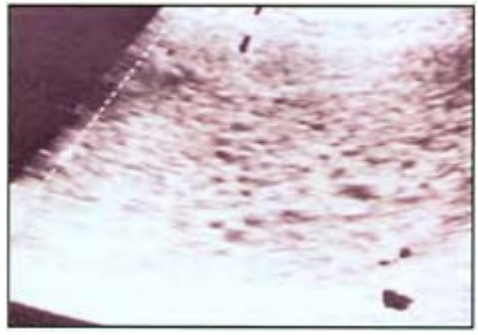

Figure 8.21: Characteristic cystic spaces packed in the uterine cavity are seen in this case of molar pregnancy

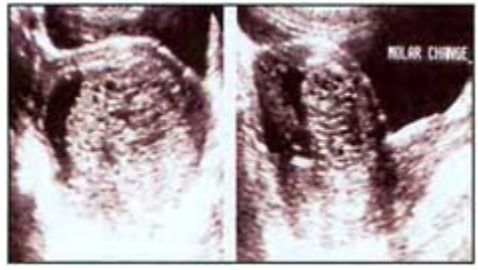

Figure 8.22: Another case of molar pregnancy with cystic spaces packed within the uterine cavity

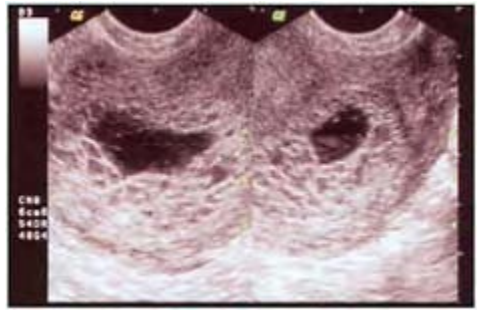

Figure 8.23: Non-viable gestational sac with thin-walled clear cystic spaces around the gestational sac

With transvaginal ultrasound with color Doppler being extensively used precious time is saved in diagnosing abnormal intrauterine pregnancy (complete or incomplete) or an extrauterine pregnancy leading to a marked decrease in time required and costs for management to the patient which is of utmost importance in developing countries. Unnecessary surgical intervention and proper mode of intervention help in the cost benefit aspect to the patients. Similarly in diagnosing early intrauterine pregnancy failures the cost of medical management is also saved.

It is noted that poor maternal health does not only affect the mother but the children as well. The factors responsible for an increase in maternal morbidity and mortality are responsible in contributing for stillbirths and neonatal deaths.

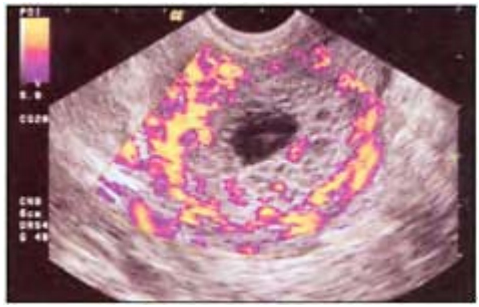

Figure 8.24: In molar pregnancy in uncomplicated cases only mild increase in peri-lesional vascularity is

noted. In invasive moles very high velocity flow in areas of tumor invasion within the myometrium are seen. Very low impedance flow with almost an arteriovenous shunt type waveform is also seen. This hypervascularity recedes with regression of the tumor

PERINATAL MORTALITY AND MORBIDITY

Deaths during the perinatal and neonatal periods are often been used as markers of health status in the region as they reflect the status of the country in terms of level of nutrition, obstetric and neonatology care.[11]

The number of perinatal deaths in the world in 1999 were estimated to be 6.9 million giving a rate of 52 deaths per 1,000 total births.[12] Neonatal deaths were estimated to be 4 million (neonatal death rate of 31 per 1,000 live births). Ninety eight percent of the perinatal and neonatal deaths occurred in less developed countries where 90% of the births took place. The highest death rates were in the WHO African Region (79 and 42 per 1,000 for perinatal and neonatal deaths respectively) while in the South East Asia Region, the corresponding rates were 67 and 42 per 1,000. The largest number of deaths however, took place in Asia where almost 60% of all births occurred.[13]

All India national Perinatal Mortality data on 1991 is 45/1000 total births (Govt. of India, CSSM Review 1994). This has slowly fallen in various states of India.

Contribution of stillbirth and first week death is almost 50:50.

CAUSES OF PERINATAL MORTALITY

The original classification by Professor Wiggles-worth for causes of Perinatal Mortality are as follows:

1. Congenital defect or malformation (lethal or severe)
2. Antepartum fetal death
3. Death from intrapartum asphyxia, anoxia or trauma
4. Immaturity
5. Infection
6. Other specific causes
7. Accident or non-intrapartum trauma
8. Sudden infant death, cause unknown
9. Unclassifiable (to be used as a last resort).

PRIME CAUSES OF PERINATAL MORTALITY IN INDIA

Precipitating causes of perinatal mortality are:

1.	Perinatal hypoxia (antepartum, labor, birth asphyxia), respiratory distress syndrome after birth.	40%
2.	Immaturity	20%
3.	Infection	20%
4.	Congenital malformations	10%
5.	Birth injury	5%
6.	Others (hemolytic disease, metabolic convulsion)	5%

Thus 41% of the total deaths up to the end of the first month of life were due to antepartum fetal death, 22% to immaturity, 16% to congenital malformations, and almost 10% to intrapartum anoxia. Some of these conditions still cause death after the first month of life. Among the postneonatal deaths the common causes of death were Sudden Infant Death syndrome (31.3%), congenital malformation (29.1%), infection (14.4%) and immaturity (11.4%).

Ultrasound is extremely helpful for diagnosing abnormalities, the biophysical score and color Doppler for fetal wellbeing.[14,15]

Routinely four ultrasounds should be asked for in all pregnancies. The parameters to be checked in all four ultrasounds are mentioned. They are:

FROM 06–09 WEEKS

- Uterine size
- Location of gestational sac
- Number of gestational sacs
- Size of gestational sac
- Yolk sac
- Size of yolk sac
- Embryo/fetus size
- Menstrual age
- Cardiac activity
- Heart rate
- Trophoblastic reaction
- Any uterine mass
- Any adnexal mass
- Corpus luteum (present/absent).

FROM 10–14 WEEKS

- Placental site
- Liquor amnii
- Fetal crown-rump length
- Menstrual age
- Fetal movements and cardiac activity
- Any gross anomalies
- Nuchal translucency
- Nasal bone (Present/absent)
- Ductus Venosus flow
- Internal os width
- Length of cervix
- Any uterine mass
- Any adnexal mass.

FROM 18–22 WEEKS

- Placenta
- Liquor amnii
- Umbilical cord
- Cervix
- Lower segment
- Myometrium
- Adnexa
- Nuchal skin thickness
- Cerebellar transverse diameter
- Cisterna magna depth
- Width of body of lateral ventricle
- Inter-hemispheric distance
- Ratio of the width of body of lateral ventricle to inter-hemispheric distance
- Ocular diameter
- Interocular distance
- Binocular distance
- Biparietal diameter
- Occipitofrontal distance
- Head perimeter
- Abdominal perimeter
- Femoral length
- Humeral length
- Foot length
- Fetal movements and cardiac activity
- Ductus venosus flow velocity waveform.

FROM 35–40 WEEKS

- Placenta
- Liquor amnii
- Umbilical cord
- Cervix
- Lower segment
- Myometrium
- Adnexa
- Biparietal diameter
- Occipitofrontal distance
- Head perimeter
- Abdominal perimeter
- Femoral length
- Distal femoral epiphysis

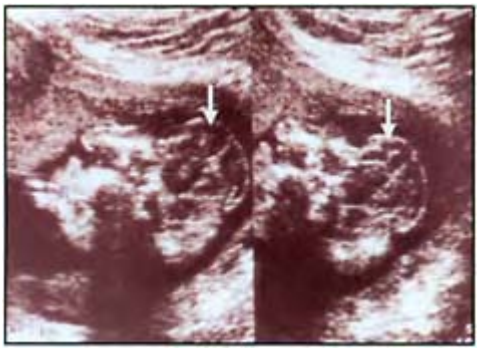

Figure 8.25: Abnormalities like Acrania can and should be now diagnosed as early as 10–11 weeks of gestation

- Biophysical profile
- Color Doppler-arterial (Umbilical artery, Middle cerebral artery, Descending aorta and Both maternal uterine arteries)
- Color Doppler-venous (Umbilical vein, Inferior vena cava and Ductus venosus)

CONGENITAL MALFORMATION

Fetal major abnormalities occur in about 1 in 50 pregnancies and result in spontaneous abortions, *perinatal morbidity and mortality,* and postnatal mental and physical

disabilities. The detection of anatomic congenital anomalies is one of the primary goals of prenatal care (Figs 8.25 to 8.30).[16,17]

With the introduction of screening biochemical and by routine ultrasound it has resulted in the identification of the majority of neural tube defects at such a period of gestation when the women can be offered termination of pregnancy. This has resulted in a decrease in perinatal mortality but an increase in therapeutic termination for this condition.[18–20]

Fortunately, remarkable technological progress in equipment resolution of ultrasound scanners and rapidly increasing sonographer expertise has resulted in an increased detection of significant fetal anomalies in the past decade. A detailed sonographic evaluation of the fetus, and follow

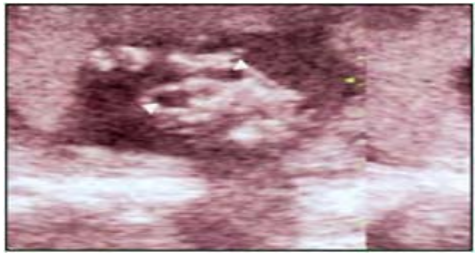

Figure 8.26: Case of Anencephaly with no brain or bone seen superior to the orbits diagnosed at 11 weeks of gestation

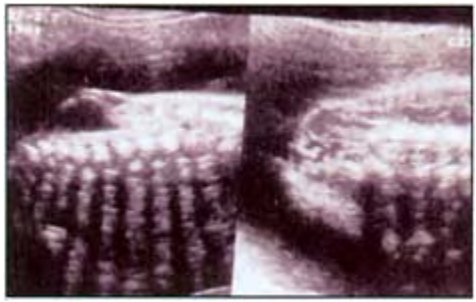

Figure 8.27: Meningomyelocele seen in a 22 weeks fetus with tethering of the spinal cord

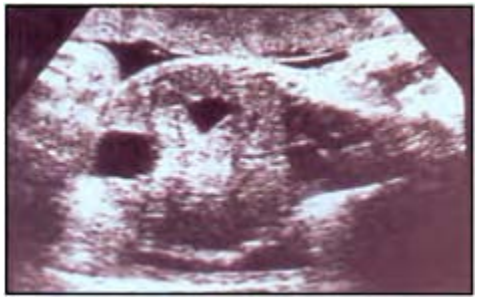

Figure 8.28: Case of a narrow thorax in a 28 weeks fetus bound to have difficulty in breathing after delivery

up invasive diagnostic procedures, are now crucial to obstetric management and outcome, and in the long term, to patient counselling.

A detailed anatomic evaluation of the fetus and its environment is listed in Table 8.1.

After the detailed analysis the need for invasive/biochemical procedures is viewed so as to decide whether the pregnancy should be continued or terminated and the need for follow up/2nd opinion sonography.

With improved technology, in particular the development of transvaginal ultrasound probes, it has become possible to examine the fetal anatomy in detail in the first trimester. The optimum gestational age would appear to be around 12–13 weeks, whether using the vaginal or abdominal route.

The overview of the normal embryological development with three-dimensional ultrasound

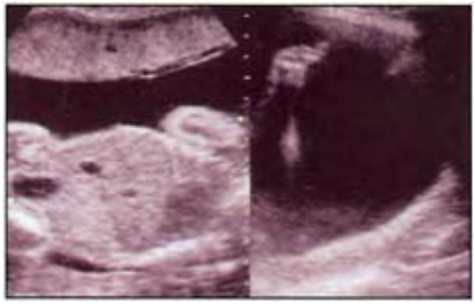

Figure 8.29: Esophageal atresia (absent stomach bubble with gross polyhydramnios)

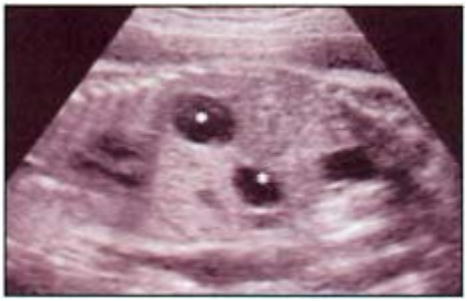

Figure 8.30: Double bubble sign (duodenal atresia) in a 32 weeks fetus

and with computers handling the pre- and postprocessing of the ultrasound images it gives us a future insight of the dynamic developmental changes during the first trimester.

ANTEPARTUM FETAL DEATH

Fetal asphyxia may occur before the onset of labor because of premature separation of the placenta (placental abruption) which can be diagnosed and assessed on ultrasound. The other important cause is inadequate placentation whereby the fetus is exposed to chronic hypoxia. These fetuses when subjected to the stress of labor can lead to asphyxia during labor.

Fetal growth directly depends on a steady supply of nutrients and oxygen from the mother, and so a normal uteroplacental and fetoplacental circulation is essential.

Table 8.1: Schematic analysis for fetal anoma ies

EXTRA-FETAL EVALUATION		
PLACENTA	**UMBILICAL CORD**	**LIQUOR AMNII**
Thickness	Number of vessels	Echotexture
Location	Origin and Insertion	Quantity
Morphology Focal Masses	Masses Length	Amniotic bands
CERVIX	**LOWER SEGMENT**	**PELVIS**
Internal os	Thickness	Masses
Length		
Serial evaluation		
FETAL EVALUATION		
CHOROID PLEXUS	**CEREBELLUM**	**CISTERNA MAGNA**
Cysts	Cerebellar transverse diameter	Depth

Hydrocephalus	Superior and inferior cerebellar vermis	Posterior fossa cyst
Isolated dilatation	Communication between fourth ventricle and cisterna magna	
ORBITS	**FACE**	**NUCHAL SKIN**
Hypo- and hypertelorism	Lips	Thickness
Lens	Nostrils	Septations
	Ear	
SPINE	**HEART**	**THORAX**
Coronal	Situs	Diaphragm
Longitudinal	Size	Lung length
Axial	Rate	Lung echoes
Ossification	Rhythm	Ribs
Soft Tissues	Cofiguration Connections	Masses Cardio-thoracic ratio
ABDOMEN	**SKELETON**	**BIOMETRY**
Gastrointestinal	Cranium	Biparietal diameter
Hepatobiliary	Mandible	Occipitofrontal distance
Genitourinary	Clavicle	Head perimeter
Pancreas	Spine	Abdominal perimeter
Spleen	Extremeties	Femur length
The optimal time to visualize fetal anatomy is 18–22 weeks.		

Doppler ultrasound is now a chosen non-invasive modality of evaluation of blood flow in the fetoplacental and uteroplacental circulation in normal and complicated pregnancies.[21] This leads to a timely termination of pregnancies, thus reducing maternal and perinatal morbidity and mortality. The cost of a nursery ICU and the facilities available always pose a dilemma for the termination of pregnancy to give the parents an alive neonate or to wait for an intrauterine demise to occur. Color Doppler effectively provides for the most appropriate time to deliver and the time available for the administration of steroids. There is clear evidence that giving steroids to the mother before preterm delivery reduces the baby's risk of developing respiratory distress syndrome, and thus reduces perinatal mortality. Steroids need to be given at least 24 hours before delivery and sometimes it is only the Color Doppler which lets us know whether we have those 24 hours or not.

Uteroplacental Circulation

During pregnancy there is a hyperplasia and hypertrophy of the uterine wall and the arteries elongate and become coiled. At the base of the placenta, the endometrium is progressively thinned as it is invaded by the trophoblast. The trophoblast migrates along

the entire length of spiral arterioles and strips it of its muscular elastic coat by the 20th postmenstrual week. This has the effect of reducing resistance to blood flow at this level.

Uterine artery color flow mapping and duplex Doppler evaluation is now accepted as a reliable method of evaluating the low-risk mother for the prediction of a hypertensive disorder in pregnancy and for a high-risk mother for prediction of perinatal morbidity and mortality.[22,23] It is important to obtain right and left uterine artery flow velocity waveforms in the 'terminal portion of the arterial course, distal to the origin of the tubal branch and proximal to the "fanning" out of arcuate arteries. Indices used to predict adverse outcome should be deployed after 24 to 26 weeks of pregnancy (Fig. 8.31). The variables includes a Resistive

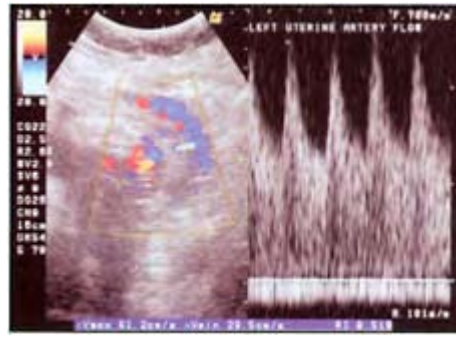

Figure 8.31: Normal uterine artery flow velocity waveform with no notching and a good amount of diastolic flow

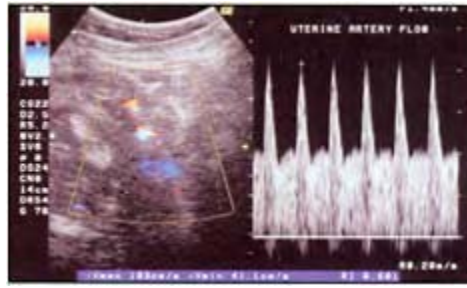

Figure 8.32: Abnormal uterine artery flow velocity waveform. Indices used to predict adverse outcome should be deployed after 24 to 26 weeks of pregnancy. The variables includes a Resistive Index of >0.55, a

Systolic/Diastolic ratio of >2.60, a notch in early diastole, a systolic notch and a large difference of the right and left sides of the uterine circulation

Index of >0.55, a Systolic/Diastolic ratio of >2.60, a notch in early diastole, a systolic notch and a large difference of the right and left sides of the uterine circulation (Fig. 8.32).

Fetoplacental Circulation

The fetal circulation is characterized by a high blood flow and a low vascular resistance. Umbilical blood flow increases with gestational age and pressure gradient driving the blood from the descending aorta through the placenta and back to the inferior vena cava.

DOPPLER SAMPLING SITES IN THE FETUS

1. Umbilical arteries
2. Middle cerebral artery
3. Ductus venosus
4. Descending abdominal aorta

Umbilical Artery

With increasing placental resistance, the diastolic flow decreases (Fig. 8.33). The absence of diastolic flow and especially reversal of flow in diastole (Fig. 8.34) indicates that the fetus is at risk for intrauterine death. These changes are most likely due to increased placental villous vasoconstriction and placental villous infarction.[24]

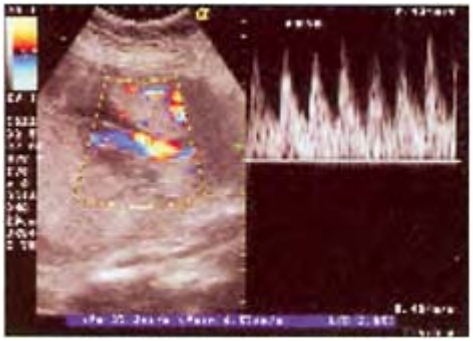

Figure 8.33: Normal umbilical artery flow velocity waveform with good amount of diastolic flow

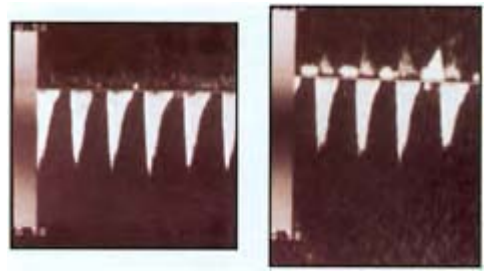

Figure 8.34: Absent and reversal of end diastolic flow in the umbilical artery flow velocity waveform

The non-stress test along with the fetal biophysical profile are presently used to assess fetal wellbeing. The umbilical artery waveform analysis detects fetal compromise more accurately than does fetal heart rate monitoring. As mentioned, if the Doppler waveform from the umbilical artery shows no flow in diastole, then this has a grave prognostic significance for the fetus.[25,26] This is especially if there is retrograde flow in diastole.

Middle Cerebral Artery

The fetal middle cerebral artery is easy to locate with Doppler ultrasound. As hypoxemia supervenes within the fetus, dilatation of the cerebral vessels leads to a lowered resistance to blood flow,[27] and it is this low resistance which can be detected by cerebral flows (Figs 8.35 and 8.36).

A fetus with a single umbilical artery abnormal reading, with a normal middle cerebral artery

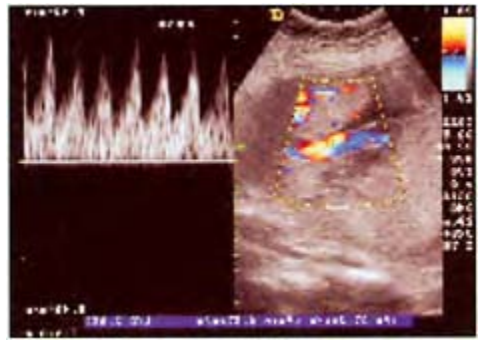

Figure 8.35: Normal middle cerebral artery flow velocity waveform

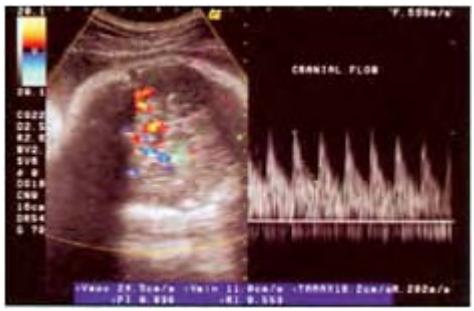

Figure 8.36: Abnormal middle cerebral artery flow velocity waveform with rise in diastolic flow as a manifestation of brain-sparring effect

reading in the presence of normal fetal heart rate testing, can be treated expectantly. A fetus with abnormal readings in the umbilical artery and the middle cerebral artery[28,29] clearly needs further assessment to determine whether or not immediate delivery is required.

Ductus Venosus

The ductus venosus connects the left hepatic vein to the inferior vena cava. It is easily visualized in the transverse plane using color to identify and follow the umbilical vein until the ductus divides from the hepatic vein. With worsening hypoxemia, the dilatation of the ductus becomes such that the reverse flow in atrial systole in the inferior vena cava is transmitted to the ductus flow also (Figs 8.37 and 8.38). Preliminary data from the ductus venosus would suggest that retrograde flow at any

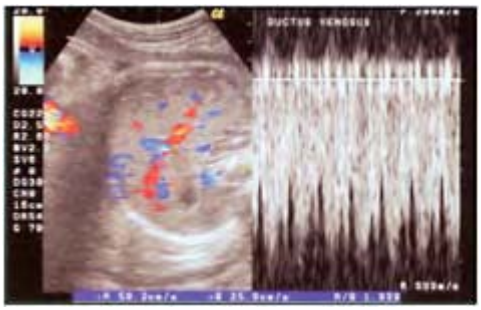

Figure 8.37: Normal ductus venosus flow velocity waveform with plenty of flow in diastole and a good Sino-Atrial ratio

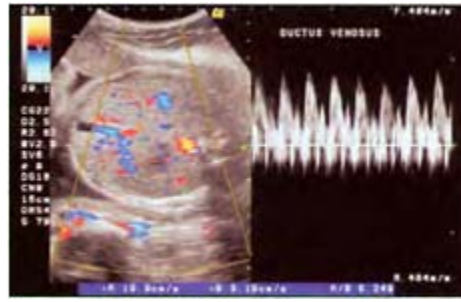

Figure 8.38: Abnormal ductus venosus flow velocity waveform with reduction of forward flow in diastole

point of the cycle (most commonly during arterial contraction) is indicative of a extremely high chance of perinatal morbidity in terms of metabolic academia and a greater than 50% mortality within 3 days.[30] The advantage of the ductus venosus, unlike the umbilical artery and middle cerebral flows, is that the measurement appears not to be altered by gestation and therefore is useful throughout pregnancy.

Descending Aorta

The flow represents the summation of flow to the kidneys, bowel, placenta and lower extremities.[31] The Pulsatility Index of the descending aorta is constant throughout gestation (Fig. 8.39).

The use of color Doppler to measure flow velocity waveforms within the fetoplacental circulation to predict increased perinatal morbidity

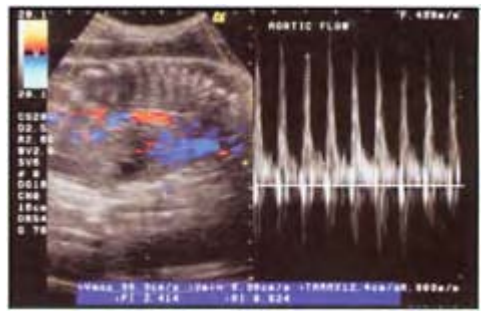

Figure 8.39: Normal descending aorta flow velocity waveform

and mortality should be undertaken in a stepwise manner. Pregnancies that are identified as being at risk can be investigated by the use of umbilical artery waveforms. In the absence of an acute maternal illness, a pregnancy with a fetus with growth parameters

above the 2.5 percentile and normal umbilical artery flows should be managed expectantly.

In a pregnancy with a fetus with abnormal umbilical artery flows, a repeat assessment of the placental resistance should be made twice per week to determine the trend of the Systolic/ Diastolic ratio. An assessment of middle cerebral artery flows should also be made. Normal middle cerebral artery flows and a slow improvement in the umbilical artery flows, requires no intervention. In the presence of abnormal middle cerebral artery flows delivery should be considered. If prolongation of the pregnancy is desirable, flow in the ductus venosus should be determined. If the ductus venosus flows are normal then reassessment of fetal condition with color Doppler and cardiotocography should be undertaken twice a week. Should the ductus venosus flows become abnormal, then consideration for delivery should be made at any gestation.

The 11–14 Weeks Scan

Each pregnancy was scanned to accurately assess the viability and the gestation and the problems of first trimester. In the last few years the machine resolution has improved to such an extent that it is now possible to accurately assess sonoembryology. This has enabled workers to shift the timing of an anomaly scan from 14 to 20 weeks.

The period of 11–14 weeks offers many significant embryological markers and is a very important period to assess almost all congenital anomalies specially chromosomal markers.

At 11–14 weeks we can study

1. Gestational age
2. Early oligohydramnios
3. Early fetal brain development
4. Nuchal translucency
5. Fetal nasal bone ossification
6. Fetal gut herniations
7. Fetal G.I. tracts
8. Fetal kidney and bladder
9. Fetal echocardiography and heart rate
10. Fetal ductus venosus blood flows
11. Major anomaly
12. Fetal iliac crest angles.

Looking at multiple ultrasound markers at 11–14 weeks it is possible to pick up trisomes and chromosomal anomalies to the tune of 81%.

A 11–14 weeks scan should be incorporated as a routine scanning of each and every pregnancy.

CONCLUSIONS

With good equipment resolution and operator expertise ultrasound is definitely the modality of choice to detect abnormalities and complications and with good obstetric care the maternal and perinatal morbidity and mortality can be reduced to quite an extent even in developing countries. There is a strong case for doing or atleast offering a routine antenatal ultrasound to all pregnant women even in developing countries and we propose this routine scan to be done at 14 weeks by transvaginal ultrasound and to be repeated at 24 weeks when color Doppler or 3D-4D can be offered to high-risk suspicious cases.

REFERENCES

1. Pittrof R. The sorry of reproductive health of women: a global overview. Contemporary Reviews in Obstetrics and Gynaecology 1996; 8:93–97
2. Kaunitz AM, Spence C, Danielson TS, Rochard RW, Grimes DA. Perinatal and maternal mortality in a religious group avoiding obstetric care. American Journal of Obstetrics and Gynecology 1994; 150:826–31
3. Loudon I. Death in childbirth: an international study of maternal care and maternal mortality 1800–1950. Oxford: Clarendon Press, 1992.
4. Chervenak F, Mccullough L. Ethical dimensions of maternal mortality. In: Weinstein D, Chervenak F: The first World Congress on Maternal Mortality, Monduzzi Editore, International Proceedings Division, Bologna (Italy) 1997.
5. Kurjak A, Breyer B. The use of ultrasound in developing countries. Ultrasound in Med & Biol 1986;12:611.
6. Goldstein S, Warson C et al: Very early pregnancy detection with endovaginal ultrasound. Obstet Gynecol 1998; 72:200–04
7. Doubilet PM, Benson CB. Embryonic fetal heart rate in the early first trimester. What rate is normal. J Ultra Med 1995; 14:431–34.
8. Nyberg DA, Mack LA, Laing FC et al: Distinguishing normal from abnormal gestational sac growth in early pregnancy. J Ultra Med 1987; 6:23–26
9. Lindsay DJ, Lovett IS, Lyons EA, Levi CS et al. Yolk sac diameter & shape at endovaginal US: prediction of pregnancy outcome in the first trimester. Radiology 1992; 183:115–18
10. Mc Kenna KM, Feldsten VA, Goldsten RB, Fily RA. The empty amnion: or sign of pregnancy failure. J Ultrasound Medicine 1995; 14:117–21
11. Confidential Enquiry into Stillbirth and Deaths in Infancy. Fifth Annual Report, London: Maternal and Child Health Research Consortium, 1998.
12. Liljenstrand J. Reducing perinatal and maternal mortality in the world: the major challenges (RCOG). Br J Obstet Gynecol 1999; 106:877.
13. UNFPA. Reducing maternal mortality and morbidity. Programme Advisory Note No 5. New York: UNFPA, 1998.
14. Kurjak A, Levene M. Rational use of high technology in perinatal medicine. J Perinat Med 1994; 22:453.
15. Kurjak A. Diagnostic ultrasound in developing countries. Mladost, Zagreb, 1986.
16. Opitz JM. The developmental analysis of human congenital anomalies. In: Papadatos CJ, Bartsocas CS (Eds). Skeletal Dysplasias. New York: Alan R Liss; 1982; 15–43
17. Romero R, Pilu G, Jeanty P et al. Prenatal Diagnosis of Congenital Anomalies. Norwalk, Conn: Appleton & Lange; 1988; 1–466.
18. Manning FA, Lempe R, Morrison I et al. Determination of fetal health: Methods for antepartum and intrapartum fetal assessment. Curr Probl Obstet Gynecol 1983; 7.

19. Levi S, Hyjazi Y, Schaaps JP et al. Sensitivity and specificity of routine antenatal screening for congenital anomalies by ultrasound: The Belgian multicentric study. Ultrasound Obstet Gynecol 1991; 1: 102–10.
20. Sabbagha RE, Sheikh Z, Tamura RK et al. Predictive value, sensitivity, and specificity of ultrasonic targeted imaging for fetal anomalies in gravid women at high risk for birth defects. Am J Obstet Gynecol 1985; 152–822.
21. Bower S, Schuchter K, Campbell S. Doppler ultrasound screening as part of routine antenatal scanning: Prediction of pre-eclampsia and intrauterine growth retardation. Br J Obstet Gynaecol 1993; 100:989–94.
22. Bower S, Bewley S, Campbell S. Improved prediction of preeclampsia by two-stage screening of uterine arteries using the early diastolic notch and color Doppler imaging. Obstet Gynecol 1993; 82:78–83.
23. Chan FY, Pun TC, Lam C et al. Pregnancy screening by uterine artery Doppler velocimetry-Which criterion performs best? Obstet Gynecol 1995; 85:596–602.
24. Trudinger BJ, Stevens D, Connelly A et al. Umbilical artery flow velocity waveforms and placental resistance: The effects of embolization of the umbilical circulation. Am J Obstet Gynecol 1987; 157:1443–49.
25. Fleischer A, Schulman H, Farmakides G et al. Umbilical velocity wave ratios in intrauterine growth retardation. Am J Obstet Gynecol 1985; 151:502–06.
26. Devoe LD, Gardner P, Dear C et al. The significance of increasing umbilical artery systolic-diastolic ratios in third-trimester pregnancy. Obstet Gynecol 1992; 80:684–87.
27. Vyas S, Nicolaides KH, Bower S et al. Middle cerebral artery flow velocity waveforms in fetal hypoxemia. Br J Obstet Gynaecol 1990; 97:797–803.
28. Mari G, Deter RL. Middle cerebral artery flow velocity waveforms in normal and small for gestational age fetuses. Am J Obstet Gynecol 1992; 166:1262–70.
29. Richardson BS, Rurak D, Patrick JE et al. Cerebral oxidative metabolism during sustained hypoxaemia in fetal sheep. J Dev Physiol 1989; 11:37–43.
30. Goncalves LF, Romero R, Silva M et al. Reverse flow in the ductus venosus: An ominous sign. Am J Obstet Gynecol 1995; 172(1):266 (abstr 33).
31. Mari G. Arterial blood flow velocity waveforms of the pelvis and lower extremities in normal and growth-retarded fetuses. Am J Obstet Gynecol 1991; 165: 143–51.

Section 2
Obstetrics

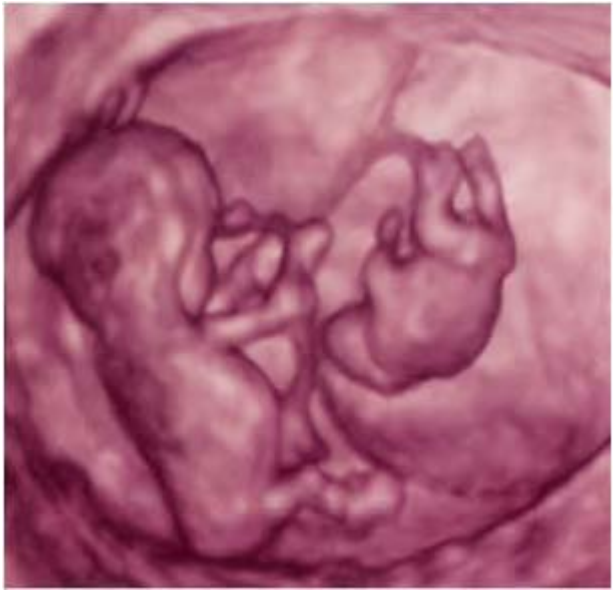

Chapter 9
Development of the Human Embryo

Ljiljana Kostovic-Knezevic, Srecko Gajovic

INTRODUCTION

In humans, like in other species, new life starts as a single cell—a fertilized egg. During development the fertilized egg divides repeatedly to produce many different cells and tissues in a final complex pattern, which is determined by its genome. Special feature of mammalian embryo is that its development is hidden within the uterus. Therefore, sophisticated methods are now available to monitor it in humans, and experimental approaches include a variety of *in vitro* methods and molecular and genetic modifications in animals. The obtained data helped us to get insight in the amazing process in which in the minute details our body plan is set up.

GESTATIONAL AGE

Two different systems for dating pregnancies have evolved. One used by embryologists, dates pregnancy from the time of fertilization—referred as fertilization age. The other system used by clinicians and obstetricians dates pregnancy from the last menstrual bleeding—referred as menstrual age. As the difference between these two is rarely exactly 14 days and the date of conception is frequently not known, the early embryonic period age data can be very imprecise.

In order to define morphological features characteristic to the given age, extensive work on staging of human embryos started at the beginning of 20th century. There is an internationally accepted system based on Carnegie collection of human embryos, which comprises embryonic stages according to Streeter,[1–4] and O'Rahilly and Müller,[5,6] referred as Horizons or Carnegie stages. The use of these stages enables to determine exact age of the embryo according to its morphological characteristics (Table 9.1).

PREIMPLANTATION PERIOD—FIRST WEEK OF DEVELOPMENT

Fertilization

Human pregnancy begins with the fusion of an egg and a sperm. This event requires a range of preparations to be previously established:

1. Female and male germ cells pass through a long series of changes (gametogenesis) to be converted into mature gametes, capable to participate in the process of fertilization;
2. Spermatozoon and oocyte meet in the ampullar part of the uterine tube;
3. Process of gamete recognition involves development of species-specific receptors on both spermatozoon and oocyte.[7–9]

The process of fertilization includes:

1. Penetration of the spermatozoon into the corona radiata;
2. Adhesion of the spermatozoon to the zona pellucida, where the surface glycoproteins of the plasmalemma and zona pellucida are essential;
3. Spermatozoon acrosomal reaction and penetration into the zona pellucida;
4. Binding and fusion of the plasmalemmas of both spermatozoon and oocyte;

Table 9.1: Developmental carne egie stages

Carnegie stage	*Crown rump length—CRL (mm)*	*Age (days after fertilization)*	*Sequence of events*
Preimplantation period			
1			
2		1	fertilization; zygote
3		1, 5–3	cleavage: morula—compaction
4	0.1	4–4, 5	free blastocyst: embryoblast+trophoblast
		5, 5–6	blastocyst: attachment to the endometrium
Implantation			
5a	0.1–0.2	7	blastocyst: partially implanted, bilaminar embryonic disc, primary yolk sac, proliferation of the extraembryonic mesoderm
5b	0.2	9	bilaminar embryonic disc, enlargement of the amniotic cavity
5c	0.2	11–12	late blastocyst
6a	0.3	13	primitive streak, secondary yolk sac
Gastrulation			
6b	0.3	14–15	beginning of the gastrulation, intraembryonic mesoderm
7	0.4	16	completed gastrulation, notochord, prechordal plate
Organogenesis			
8	1.0–1.5	18	presomite embryo: blood islands, beginning of neurulation: neural plate, neural fold and groove

9	1.5–2.5	20	1–3 somites; deep neural groove, paired heart tubes
10	2.0–3.5	22–23	4–12 somites; beginning of neural tube formation, 2 pharyngeal arches
11	2.5–4.5	24–25	13–20 somites; closure of rostral neuropore, mesonephritic duct
12	3–5	26–27	21–29 somites; closure of caudal neuropore, 4 pharyngeal arches, secondary neurulation, appearance of upper limb buds
13	4–6	28	30 somites; lens placode, otic vesicle, appearance of lower limb buds, cardiac primordium: septum primum, foramen primum, respiratory diverticulum

Carnegie stage	*Crown rump length—CRL (mm)*	*Age (days after fertilization)*	*Sequence of events*
14	5–7	32	lens vesicle, optic cup, nasal pits, ureteric bud
15	7–9	33	development of hand plates, urogenital sinus, cerebral vesicles, primary bronchi
16	8–11	37	development of foot plates, visible retinal pigment, auricular hillock
17	11–14	41	appearance of finger rays, formation of nasolacrimal groove, 6 auricular hillocks, chondrogenesis, segmental bronchial buds
18	13–17	44	development of the face: formation of eyelids and tip of nose, heart: septum secundum, foramen ovale
19	17–20	47–48	flexion of hands, beginning of herniation of midgut into umbilical cord, metanephrogenic blastema
20	21–23	50–51	perforation of anal membrane, dorsal flexion of legs, beginning of glomeruli differentiation
21	22–24	52	indifferent external genitalia, 2nd and 3rd generation of glomeruli
22	25–27	54	4th and 5th generation of glomeruli
23	28–30	56–57	beginning of ossification

Cleavage and Morula Formation (Fig. 9.1)

5. Cortical reaction i.e. zona reaction of the oocyte. The secretory products of the cortical granules secreted by the oocyte eliminate the ability of other spermatozoa to adhere to and penetrate through the zona pellucida. That is the control mechanism to prevent the polispermy;
6. Metabolic activation of the oocyte includes: early release of Ca^{++}, followed by exchange of extracellular Na^{++} and intracellular H^{+} through the plasma membrane, which is followed by an increase of oxidative metabolism;
7. Completion of meiosis of the oocyte;
8. Development of the male and female pronuclei;
9. Syngamy of both pronuclei.

The process of fertilization results in the formation of zygote (Carnegie stage 1) with the diploid number of chromosomes. The zygote is genetically unique product of chromosomal reassortment, important for the viability of human species. The zygote first divides 24–36 hours after fertilization, resulting with two daughter cells or blastomeres. As the successive divisions continue, new blastomeres become smaller and smaller. Eventually, 3–4 days after fertilization, they form a morula (Carnegie stage 2). At this stage the morula is still inside the zona pellucida. At the 8-cell stage the morula enters into a phase called compaction, during which the individual blastomeres express cell-cell interactions through intercellular gap and tight junctions.[10,11] Experiments in mammalian embryos have demonstrated that cadherins are main adhesion molecules. Besides compaction, E-cadherin (uvomorulin) is involved in the other morphogenetic events in early embryo such as gastrulation and neurulation.[12]

Early Blastocyst (Carnegie Stage 3)

Compaction contributes to the formation of a continuous epithelial layer on the surface of the morula. Through activity of ATPase based Na^{+} transport system water accumulates inside the morula and forms a fluid filled space blastocoele. At this stage embryo is called blastocyst consisting of an outer superficial layer—trophoblast, and a small inner group of cells called inner cell mass or embryoblast. The trophoblast cells will contri-bute only to the extraembryonic membranes, while the inner cell mass will contribute to the extraembryonic membranes and the embryo proper.

Implantation (nidation) starts between 5th and 6th day of development (Carnegie stage 4) and it is completed at 12th day of gestation (Carnegie stage 5c), when the primitive uteroplacental circulation is established.

The preparation period for the implantation starts shortly after fertilization, during preimplan-tation period, through both local and systemic signaling. Substances from embryo deposited freely in the uterine lumen are involved in signaling to maternal host and in preparing the site to impending implantation (decidualization). The synchrony of maternal/embryo communi-cation includes numerous signal molecules, factors and receptors from the embryo as well as from the endometrium.[13] In the past years the morpho-logical, biochemical and molecular investigations are focused to the optimal

period of the endometrial receptivity for blastocyst, known as “implantation window”. Structural parameters such as cell processes on the apical part of endo-metrial surface are regulated by Hoxa 10 gene.[14] Biochemical analysis confirmed integrins as surface

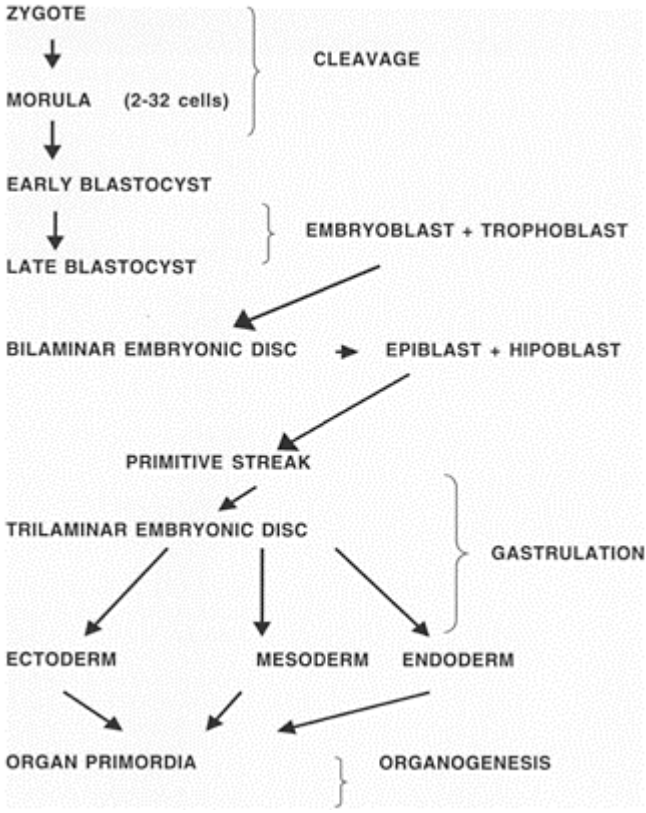

Figure 9.1: Key events during embryogenesis

receptors expressed on the endometrial epithelia at the opening of the “implantation window”.[15]

After the blastocyst reaches the uterine cavity, some important changes occur:

1. The zona pellucida is enzymatically loosened by means of a trypsin-like enzyme, secreted by the trophoblast;
2. The blastocyst “hatches” out;
3. The blastocyst attaches by the area above the inner cell mass (embryonic pole) to the endometrial surface epithelia.

4. The next stage of implantation (7th day of development, Carnegie stage 5a) is an active penetration ("invasion") of the uterine epithe-lium. By that time the trophoblast undergoes its differentiation into inner cellular layer—cytotrophoblast, and outer multinucleated syncytiotrophoblast, which is at the embryonic pole highly invasive.

Lacunar or Previllous Stage

By 9th day of development (Carnegie stage 5b) syncytiotrophoblast progresses and invades endometrial stroma. Vacuoles appear in the syncytiotrophoblast at the embryonic pole of the blastocyst. A few vacuoles coalesce and form intercommunicating cavities. Their fluid-filled spaces develop in the lacunae.

Between 10th and 13th days trophoblast pene-trates *deeper* into endometrial stroma and erodes the adjacent maternal capillaries. Syncitial lacunae become filled with a mixture of maternal blood and secretion products from eroded endometrial glands.

Some investigations demonstrated that the implantation is a very balanced process, controlled by molecules such as plasminogen activators and family of matrix metalloproteinases.[16–18]

Bilaminar Embryonic Disc

During the implantation period and differentiation of the trophoblast, the inner cell mass or embryo-blast rearrange into two epithelial layers: the epiblast or primitive ectoderm and the hypoblast or primitive endoderm. Epiblast and hypoblast form bilaminar embryonic disc. Approximately 7 days after fertilization, amniotic cavity appears. Exactly how it is formed in humans is not known, but studies on primate embryos indicate that the amniotic cavity arises from cavitations within the epiblast layer.[19] Meanwhile the hypoblast cells migrate along the inner side of the wall of the blastocoele cavity forming the extraembryonic endoderm called primary yolk sac. Starting about 12 days after fertilization the extraembryonic mesoderm appears. The extraembryonic mesoderm supports the epithelium of yolk sac and amnion as well as the chorionic villi, which arise from the trophoblast. This mesoderm has an important role in differentiation of the first primitive blood vessels.

GASTRULATION—THIRD WEEK OF DEVELOPMENT

Primitive Streak

Third week is the period of the trilaminar embryonic disc (Carnegie stage 6a and 6b). The

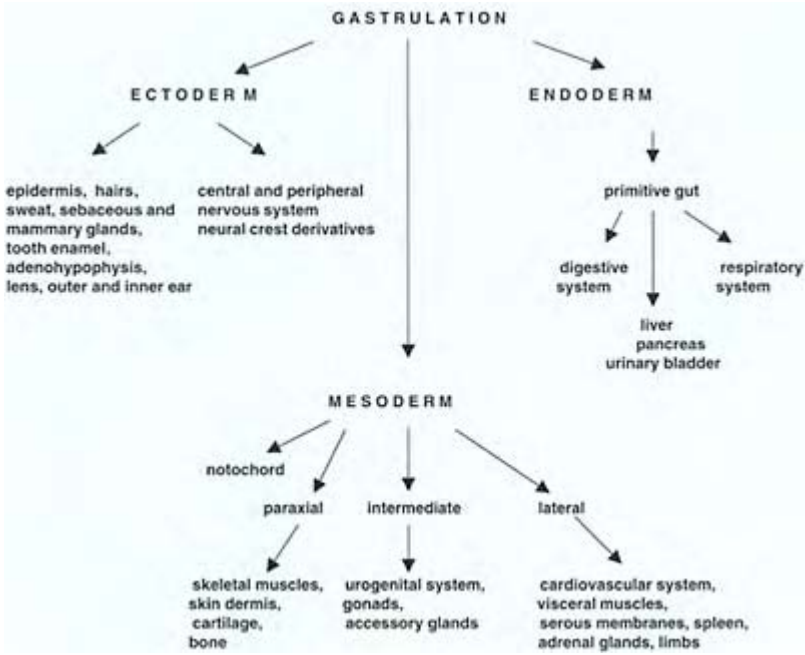

Figure 9.2: Derivatives of the germ layers

embryonic disc at this stage is slightly elongated. Caudally situated cells of the ectoderm migrate along the median plane and form the primitive streak. Through the primitive streak and subsequent primitive groove cells proliferate and migrate downwards and laterally to form embryonic mesoderm and endoderm. That process is called gastrulation (Fig. 9.2).

Gastrulation starts 14th and 15th day by formation of the primitive streak, which appears as a thickening in the midline on the dorsocaudal part of the ectoderm. Cells of the epiblast in the primitive streak region change shape and pass through it to form a new cell layers beneath the epiblast. While in the epiblast, the cells have the properties of typical epithelial cells with apicobasal polarity and a basal lamina. As they enter the primitive streak, the cells elongate, loose their basal lamina and take on a characteristic morphology referred as bottle cells. The cell movements and the changes in cell shape and adhesiveness is modulated by the cytoskeleton and adhesive molecules on the cell surface. Subsequent spreading out of the mesoderm cells is under the influence of extracellular matrix molecules secreted by the epiblast cells.[20,21] Experimental investigations *in vivo* and *in vitro* demonstrate that cells of the epiblast in early gastrulation produce hyaluronic acid, fibronectin and laminin.[22,23]

The most prominent feature of the human gastrulation is formation of the mesoderm. Some cells that migrate give rise to the extraembryonic mesoderm of the body stalk, which connects caudal part of embryo to the other extraembryonic structures. The

majority of cells passing through the primitive streak spread out between the epiblast and the hypoblast to form embryonic mesoderm.

At the cranial end of the primitive streak a small accumulation of cells is called primitive or Hensen's node. This structure is important for the formation of the notochord, the primitive axial skeleton of the embryo.

Notochord

Notochord arises from a population of epiblast cells, which migrate through the primitive node in the cranial direction and form in the medial line the notochordal process (Carnegie stage 7, approximately 16 days). The notochordal process continues to grow cranially until it reaches a small circular area of columnar endodermal cells called prochordal plate. The notochordal process develops into the notochordal plate (Carnegie stages 9 and 10) and finally becomes the notochord (Carnegie stage 11, 24 days) when the primitive axis of the embryo is formed.

The notochord plays an important role in series of signaling episodes (inductions) that transform undifferentiated embryonic cells into tissues and organs. The most important role of the notochord is induction of the surface ectoderm into neuroectoderm, a source of the nervous system.

After its initial appearance primitive streak expands cranially until 18th day of gestation. After formation of mesoderm, it regresses and normally disappears. In rare instances large tumors called teratomas appear in the sacrococcygeal region. Teratomas often contain mixture of many different types of tissues, because they arise from the remnants of the primitive streak.

ECTODERM DIFFERENTIATION—NEURULATION

The neural tube develops by a complex process called neurulation. The inductive relationship between the notochord and the overlying ectoderm in the genesis of the nervous system was recognized in the early 1900s.[24] These early original experiments done on amphibians, and later in higher vertebrates including mammals showed that the notochordal process acts as a neural inductor on the overlying ectoderm.

Primary Neurulation

The first stage in the formation of the neural tube is transformation of the ectoderm into the neuroectoderm and formation of the neural plate (Carnegie stage 8, 18 days). The second stage is further proliferation of neural plate cells, growth of the plate in the anterior-posterior axis, and formation of the neural groove and neural folds (Carnegie stage 9). The next stage consists of an apposition of two lateral apical surfaces of the neural folds, their fusion and formation of the neural tube. The closure of the neural tube starts 22nd day in the midline region and it proceeds in both cephalic and caudal directions resembling to the closing of a double-headed zipper. The unclosed cephalic and caudal parts of the neural tube are called the anterior (cranial) and posterior (caudal) neuropores (Carnegie stage 10). The anterior neuropore closes between 24th and 25th

day, and the posterior between 26th and 27th day of development. The neural tube in the brain-forming region undergoes three dilatations con-sisting of the forebrain (prosencephalon), midbrain (mesencephalon) and hindbrain (rhombe-ncephalon).

The process of neural plate formation divides common ectodermal layer into two cell lineages: one of them will give rise to the neural tissue, and other to the epidermal cells.[25,26] The neural tube formation includes the changes of cell shape by their extension, adhesion and contraction. The intracellular microtubules and actin filaments have the essential role in this process. Neuroepithelial cells express at their surface transmembrane adhesive glycoproteins molecules such as N-cadherins.[27]

Secondary Neurulation

The caudal portion of the neural tube as well as the notochord (caudally to the sacrococcygeal region) develop from an undifferentiated mass of cells known as the caudal eminence (or end-bud) by a different morphogenetic mechanism without formation of the neural plate and the groove. The cells of the caudal eminence region aggregate in the medullary cord and rearrange later into the lumen of the secondary neural tube.[28,29] Different morphogenetic mechanisms of primary and secondary neurulation and body formation explain the congenital disorders in human, e.g. various types of spina bifida are located in the sacrococcygeal region.[30]

The Neural Crest

During the process of neurulation, a population of neuroepithelial cells situated in the neural folds, separates from the common position and migrates away. They spread throughout the body of the embryo and give rise to: cranial ganglia, autonomic ganglia, the adrenal medulla, Schwann cells, meninges, melanocytes, ectomesenchyme of the head and neck, and conotruncal cushions of the heart.[31]

Mesoderm Differentiation

During the process of gastrulation, the ectodermal cells migrate through the primitive streak and form a new layer of mesenchymal cells between ecto-derm and endoderm—the embryonic mesoderm. After formation of the notochord, mesodermal cells proliferate and differentiate lateral to the notochord and the neural tube in a column of mesenchymal cells known as paraxial mesoderm (Carnegie stage 8). This tissue is soon segmented into somites. Continuous with the paraxial mesoderm is a lateral region of the intermediate mesoderm, which gives rise to the excretory units of the urinary system. Beyond that, the lateral mesoderm splits into two layers, forming the parietal (somatic) and visceral (splanchnic) sheath. Between them the intraembryonic coelom develops.

Somites

The formation of somites as columnar blocks of cells within the paraxial mesoderm is called somitogenesis. The precursors of somites are called somitomeres, which play in the cranial part of the embryo significant role in head development. Somites develop

successively in the craniocaudal direction of the embryo. Gradually increasing somite number is used as one of criteria for determining the age of the early embryo. In human somitogenesis proceeds until there are 42–44 pairs of the somites. The most caudal 5–7 somites disappear and those cranial to this fuse to form sacrococcygeal region. The ventral part of each somite will differentiate in the sclerotome, and give rise to the vertebral column, ribs, sternum and skull. The dorsomedial region of the somite develops in the dermomyotome, which subdivides in dermatome and myotome. Dermatome gives rise to the dermis, and myotome to the skeletal muscles. Somitogenesis is strongly controlled process by signals from the overlying ectoderm and the notochord.[32] At the cellular level somito-genesis involves changes in cellular adhesive properties and the secretion of the extracellular matrix components such as fibronectin and glycosaminoglycans.

ENDODERM DIFFERENTIATION

The endodermal germ layer transforms from the flat intraembryonic endodermal sheet into the tubular gut as a result of the lateral and craniocaudal folding of the embryonic body. A major morphological consequence of these folding processes is the delineation of the yolk sac from the digestive tube.

At the end of the fourth week the region of the yolk sac is reduced by constriction to form the yolk stalk (i.e. omphalomesenteric or vitelline duct). The intraembryonic endoderm forms the foregut, midgut and hindgut. The midgut is through the yolk stalk opened into the yolk sac.

The anterior end of the foregut is temporarily attached to the surface ectoderm. They together form a bilayer called oropharyngeal membrane. This membrane separates the ectodermaly derived stomodeum (the future mouth) from the endodermal part of the foregut. In the caudal region another ectodermal-endodermal bilayer is called the cloacal membrane. It is included in the formation of the cloaca, which in the early embryo represents a common outlet for the both digestive and the urogenital systems.

From the simple tubular gut, the development of digestive tract includes the elongation, folding and twisting of the primitive gut itself. The series of inductions and tissue interactions provide the basis for further development of the digestive glands, and secretory and absorptive functions of intestine.

VASCULOGENESIS AND FORMATION OF THE EARLY CIRCULATORY SYSTEM

Vasculogenesis

The process of differentiation of multipotential mesenchymal progenitors (angioblasts) into blood vessels *in situ* is named vasculogenesis.

The vascular system develops when the embryo is not any more able to answer nutritional requirements by diffusion. The formation of blood and blood vessels begins in the extraembryonic structures: in the mesodermal wall of the yolk sac as well as in the

chorion and connecting stalk (Carnegie stage 7–8, 16–18 days). Blood vessels develop as mesenchymal aggregations known as blood islands. By an inductive interactions with the endoderm of yolk sac, blood islands differentiate into the centrally located blood forming cells—hemocytoblasts, and into the marginal cells which form the primitive endothelial lining as the primitive vessel wall.[33–35] These vessel precursors interconnect and establish a primitive vascular net work of sinusoid appearance. The hemocytoblasts differentiate into the primitive blood cells.

The embryonic vasculogenesis starts separately from the extraembryonic network by identical process. The first blood vessels are formed in the embryonic parietal mesoderm of the floor of the intraembryonic coelom. With the development of the embryo the extraembryonic as well as intraembryonic vessel networks grow by budding, sprouting and extending of already present vessels. This process is called angiogenesis. The connection of the extraembryonic and intraembryonic vessel networks forms the primitive circulatory system.

Development of Heart Primordia

The heart is derived from the splanchnic mesoderm as bilateral tubular primordium, called cardiogenic plate, and located rostrally to the oropharyngeal membrane and primitive foregut (18 days of gestation). The myocardium develops from cardiogenic cells derived from the cardiogenic plate. Between the myocardial primordium and endoderm of the primitive gut, isolated paired mesodermal vesicles appear forming endocardial tubes. As the embryo takes shape by both lateral and cranioventral folding, the bilateral endocardial tubes fuse to form a single primitive tubular heart. At its caudal end, the endocardial tubes do not fuse, but rather extend toward the posterior part of the embryo as a venous inflow region of the heart. At the cranial part of the embryo, heart tube produces vascular arches around the primitive pharynx.

Embryonic Circulation

When is the cardiac function and blood flow established, is the fundamental question in the human embryogenesis. The experimental investigations reveal that early maturation of the circulation follows a tightly coordinated process programmed by molecular and cellular signal.[36,37] *In situ* hybridization demonstrated that the beginning of the heartbeats is coincident with appearance of the yolk sac derived erythroblasts.[38]

MOLECULAR BASIS OF DEVELOPMENT

The whole blueprint of a new human being is already present in the genome of the fertilized egg. The activity of hereditary information, organized in genes, leads tightly controlled sequence of events, which results with astonishing precision with the formation of a new member of our society. Just recently, fragments of this whole process started to be delineated, in order to understand how activity of genes shapes the embryo.

The progress in this field was facilitated by the fact that genes that control development are conserved during evolution. The developmentally regulated genes in

insects (Drosophila melanogaster) or even in worms (Caenorhabditis elegans) were shown to have their counterparts in humans. In addition, even in the same species the same gene could have different function in different periods of development and in different organs. These genes are active during normal, but as well abnormal development. In contemporary cancer research, the mutant forms of developmentally important genes are highly investigated.

The developmentally important genes and their products—proteins, can be functionally divided in relatively small number of categories. Transcription factors are proteins, which regulate other genes, and in this way control onset of complex activities during morphogenesis. Intercellular signalling molecules leave the cells that produce them and exert their effects on other cells enabling inductive interactions. Receptor molecules permit to the cells, which carry them on their surface to respond to the signals. Molecules involved in intracellular signalling pathways process the received signals in order to provide adequate answer through subsequent cell behavior.

As a result of these molecular activities, a molecular pattern is built. The morphogenesis is a consequence of this pre-built molecular pattern.[39] Currently, we are far away to understand the molecular pattern in the same extent, as it is our knowledge about morphology of the development. However, clear examples of this already exist in e.g. Hox code, a defined combination of different Hox genes, which settle the identity for every vertebra in the vertebral column.[40] Taking in account the current outcomes of sequencing human genome, it is reasonable to believe that molecular understanding of embryology is conceivable future.

REFERENCES

1. Streeter GL. Developmental horizons in human embryos. Description of age group XI, 13 to 20 somites, and age group XII, 21 to 29 somites. Carnegie Inst Wash Publ 541, Contrib Embryol 1942; 30:211–45
2. Streeter GL. Developmental horizons in human embryos. Description of age group XIII, embryos about 4 or 5 millimeters long, and age group XIV, period of identation of the lens vesicle. Carnegie Inst Wash Publ 557, Contrib Embryol 1945; 31:27–63
3. Streeter GL. Developmental horizons in human embryos. Age groups XI to XXIII. Carnegie Inst Wash Publ 541, Embryology Reprint Vol II, 1951.
4. Streeter GL, Heuser CH, Corner GW. Developmental horizons in human embryos. Description of age groups XIX, XX, XXI, XXII and XXIII. Carnegie Inst Wash Publ 592, Embryol Reprint Vol II, 1951; 165–96.
5. O'Rahilly R. Developmental stages in human embryos. Part A: Embryos of the first three weeks (stages 1 to 9). Carnegie Inst Wash Publ 1973; 631
6. O'Rahilly R, Müller F. Developmental Stages in Human Embryos, Including a Revision of Streeter's "Horizons" and a Survey of the Carnegie Collection. Carnegie Inst Wash Publication 1987; 637
7. Bookbinder LH, Cheng A, Bleil JD. Tissue- and species-specific expression of sp56, a mouse sperm fertilization protein. Science 1995; 269:86–89
8. Sinowatz F, Plendl J, Kolle S. Protein—carbohydrate interactions during fertilization. Acta Anat 1998; 161:196–205
9. Cohen N, Wasserman PM. Association of egg zona pellucida glycoprotein mZP3 with sperm protein sp56 during fertilization in mice. Int J Dev Biol 2001; 45:569–76

10. McLachlin JR, Caveney S, Kidder GM. Control of gap junction formation in early mouse embryos. Dev Biol 1983; 98:155–64
11. Sueoka K, Shiokawa S, Miyazaki T et al. Integrins and reproductive physiology:expression and model in fertilization, embryogenesis and implantation. Fertil Steril 1997; 67:799–811
12. Duc-Goiran P, Mignot TM, Burgeois C et al. Embryo-maternal interactions at the implantation site: a delicate equilibrium. Eur J Obs Gyn Rep Biol 1999; 83:85–100
13. Bagot CN, Kliman HJ, Taylor HS. Maternal hoxa 10 is required for pinopod formation in the development of mouse uterine receptivity to embryo implantation. Dev Dyn 2001; 222:538–44
14. Maclntry DM, Lim HC, Ryan K et al. Implantation-associated changes in bovine uterine expression integrins and extracellular matrix. Biol Rep 2002; 66:1430–36.
15. Thomas K, Thomson AJ, Wood SJ et al. Endometrial integrin expression in women undergoing IVF and ICSI: a comparis on of the two groups and fertile controls. Hum Reprod 2003; 18:364–69.
16. Bischof P, Martelli M, Campana A et al. Importance of matrix metalloproteinases in human trophoblast invasion. Early Preg Biol Med 1995; 1:263–69.
17. Hines RS. Molecular analysis of implantation. Sem Reprod Med 2000;18:91–96.
18. Carlson BM. Human Embryology & Developmental Biology, Mosby, 1999.
19. Klinowska TC, Ireland GW, Kimber SJ. A new in vitro model of murine mesoderm migration:the role of fibronectin and laminin. Differentiation 1994; 57: 7–19.
20. Yang JT, Bader BL, Kreidberg JA, et al. Overlapping and independent functions of fibronectin receptor integrins in early mesoderm development. Dev Biol 1999; 215:264–77
21. Lopez-Sanchez C, Garcia-Martinez V, Schoenwolf GC. Localization of cells of the prospective neural plate, heart and somites within the primitive streak and epiblast of avian embryos at intermediate primitive-streak stages. Cells Tissues Organs 2001; 169:334–46
22. Canning DR, Amin T, Richard E. Regulation of epiblastic cell movements by chondroitin sulfate during gastrulation in the chick. Dev Dyn 2000; 219:545–59
23. Mullegger J, Lepperdinger G. Hyaluronan is an abundant constituent of the extracellular matrix of Xenopus embryos. Mol Reprod Dev 2002; 61:312–16
24. Speman H, Mangold H. Über Induktion von Embryonenanlagen durch Implantation ortfremder Organisatoren. Arch Mikrosop Anat Entw-Mec 1924; 100:599–638.
25. Hammati-Brivanlou A, Melton D. Vertebrate embryonic cells will become nerve cells unless told otherwise. Cell 1997; 88:13–17
26. Weinstein DC, Hammati-Brivanlou A. Neural induction. Ann Rev Cell Dev Biol 1999; 15:411–33
27. Colas JF, Schoenwolf GC. Towards a cellular and molecular understanding of neurulation. Dev Dyn 2001; 22:117–45
28. Kostovic-Knezevic LJ, Gajovic S, Švajger A. Morphogenetic features in the tail region of the rat embryo. Int J Dev Biol 1991; 35:91–95
29. Gajovic S, Kostovic-Knezevic LJ. Ventral ectodermal ridge and ventral ectodermal groove:two distinct morphological features in the developing rat embryo tail. Anat Embryol 1995; 192:181–87.
30. Haque M, Ohata K, Takami T et al. Development of lumbosactral spina bifida: three dimensional computer graphic study of human embryos at Carnegie stage twelve. Pediatr Neurosurg 2001; 35:247–52
31. Gallo R, Zazzeroni F, Alesse E et al. REN: a novel developmentally regulated gene that promotes neural cell differentiation. J Cell Biol 2002; 19:731–40.
32. Schnell S, Maini PK, McInerney D et al. Models for pattern formation in somitogenesis: a marriage of cellular and molecular biology. C R Biol 2002; 325:179–89.
33. Baron MH. Molecular regulation of embryonic hema-topoiesis and vascular developments novel pathway. J Hematother Stem Cell Res 2001; 10:587–94
34. Liao HJ, Kume T, McKay C et al. Absence of erythrogenesis and vasculogenesis in Plcg1-deficient mice. J Biol Chem 2002; 277:9335–41

35. Baron M. Induction of embryonic hematopoietic and endothelial stem/progenitor cells by hedgehog-mediated signals. Differentiation 2001; 68:175–85
36. Jonker L, Arthur HM. Endoglin expression in early development is associated with vasculogenesis and angiogenesis. Mech Dev 2002; 110:193–96.
37. Palis J, Chan RJ, Koniski A et al. Spatial and temporal emergence of high proliferative potential hemato-poietic precursors during murine embryogenesis. Proc Natl Acad Sci USA 2001; 98:4528–33
38. Ji RP, Phoon CK, Aristizabal O. Onset of cardiac function during early mouse embryogenesis coincides with entry of primitive erythroblasts into the embryo proper. Circ Res 2003; 7:133–35
39. Zernicka-Goetz M. Patterning of the embryo:the first spatial decisions in the life of a mouse. Development 2002; 129:815–29
40. Christ B, Huang R, Wilting J. The development of the avian vertebral column. Anat Embryol 2000; 202:179–94

Chapter 10
Ultrasound Evaluation during the First Trimester of Normal Pregnancy

Maher G Sarraf

INTRODUCTION

In general, ultrasonography, and in particular the transvaginal route of ultrasound examinations, has become the method of choice in the examination and evaluation of obstetrics patients in the first trimester of pregnancy. In this period a dramatic sequence of events occur; ovulation, fertilization, formation of morula and blastocyst, and gastrulation.

The Embryonic Period and the Fetal Life

The first trimester examination is performed either within the routine obstetric visit of the pregnant women or as a result of the patient complaining of bleeding or pain.

Accordingly, sonography has the following emergency clinical questions to answer:

- Where is the pregnancy localized (is it intrauterine or ectopic)?
- Is the embryo/fetus alive?
- What is the probability of consequent demise of a living embryo/fetus?

The other goals of first trimester sonography are:

- Estimation of menstrual age of pregnancy
- Assessment of multiple pregnancy
- Evaluation of nuchal thickening and nasal bone
- Screening at 14 weeks

In order to be able to read the ultrasound images correctly, it is important to review and understand the embryologic development of the embryo and later the fetus.

In this chapter, the first trimester sonography will be tackled week-by-week, explaining the important milestones of embryonic development and highlighting the corresponding appearance on the ultrasound screen.

It should be pointed out that all dates presented are expressed in menstrual age *(embryologic age +two weeks)* as used in obstetric literature, rather than presenting it in embryologic age as used by embryologists.

Furthermore, all measurements, values, descriptions and structural appearances that will be cited in the chapter have been carried out using the transvaginal approach, unless stated otherwise, i.e. abdominal approach.

Most of the brief information addressing the embryology in this chapter is referenced mainly from *Before we are Born by K L Moore and Persaud;*[1] *and Langman's Medical Embryology by TW Sadler*.[2]

WEEKS 1–2

The first half of the menstrual cycle: preovulatory and periovulatory phase.

Menstrual Phase

The length of the average menstrual cycle is 28 days; the first menstrual day is designated as day 1 of the cycle. The menses usually lasts 4–5 days. After menstruation, the eroded endometrium is thin: it is less than 4 mm in width.

Proliferative Phase

The proliferative phase lasts about 9 days. It starts from the last day of the bleeding.

A gonadotrophin-releasing hormone (GnRH) is synthesized by the hypothalamus and carried to the anterior lobe of the pituitary gland. GnRH causes the release of two hormones by this gland. Both of them act on the ovary.

- Follicle stimulating hormone (FSH) stimulates the development of ovarian follicles, which in turn produce estrogen.
- Luteinizing hormone (LH) serves as the trigger for ovulation (It also stimulates corpus luteum to produce progesterone in the secretory phase).

During these 9 days FSH acts on the primary follicle, forming the secondary follicle, in which the primary oocyte is pushed to one side, where it becomes surrounded by a mound of follicular cells forming the cumulus oophorus. The follicle containing the follicular fluid continues to enlarge until it becomes a mature ovarian follicle.

Ovulation

At day 14 of the menstrual cycle, the ovulation is triggered by a surge of LH production. Ovulation usually follows the LH peak by 12 to 24 hours. The expelled secondary oocyte goes to the tube and the follicular wall is then transformed into a glandular structure: the corpus luteum.

Placement of the ultrasound probe into the vagina means that the ovaries are only 3 to 5 cm away, which enables the sonographer to clearly visualize the ovaries themselves as

well as the follicles. The follicle appears as an echofree structure around the ovarian tissue, which is more echogenic (Fig. 10.1).

When the ovulation occurs, the leading follicle enlarges from a diameter of 3 to 5 mm at the end of menstrual cycle to over 20 to 24 mm. Besides follicular size, visualization by ultrasound of the cumulus oophorus—a few millimeter bleb on the wall of the follicle—means that ovulation will occur within following 36 hours.

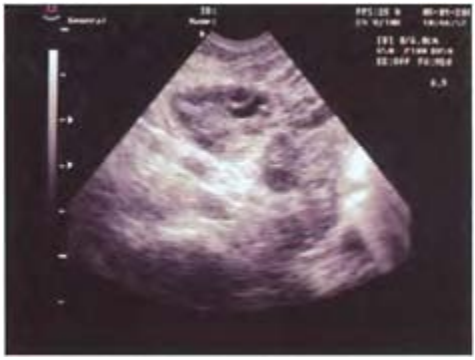

Figure 10.1: The ovary by vaginal ultrasonography

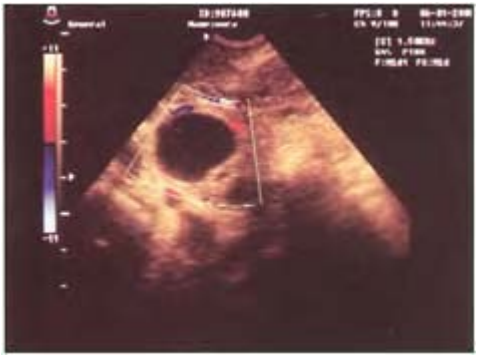

Figure 10.2: Ripe follicle and the cumulus oophorus, surrounded by perifollicular vessels (blue and red)

Kurjak et al described a ring of angiogenesis around the dominant follicle at the moment of the presumed ovulation. The velocity of perifollicular blood flow tends to increase, while the resistance to blood flow decreases[3] (Fig. 10.2).

Endometrium

After menstruation the endometrium is demonstrated as a single echogenic line (Fig. 10.3). The estrogen biosynthesis by the dominant follicle leads to stimulation of the endometrium with growth of the glands and stroma. This change is visualized as the "triple-line" (Fig. 10.4). The interface between the two leaves of the endometrium is the central echogenic line. The

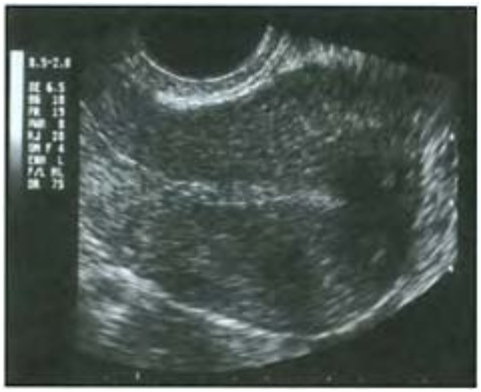

Figure 10.3: An ultrasound image of a thin endometrium portraying a single echogenic line

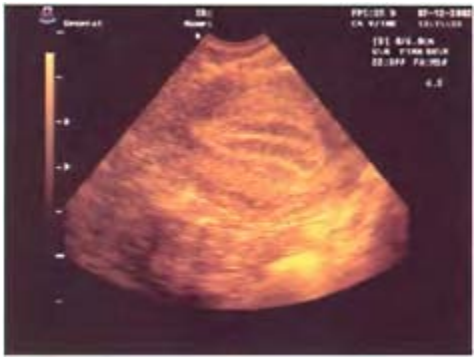

Figure 10.4: Visualization of the triple-line sign of the endometrium at the period ovulation

two outer lines represent the basalis of the developing endometrium. The endometrium appears hypoechoic compared to the echogenic lines. The thickness of the endometrium

can reach 6 to 10 mm, around the time of ovulation, which represents a two to three fold increase in its original thickness.[4]

WEEKS 3–4: CONCEPTUS

Embryonic Events

Day 14: Ovulation, changing in the endometrium, becoming soft, thick and edematous in response to progesterone

Day 15: Fertilization.

Day 18: Morula stage.

Day 20: Blastocyst stage—beginning of implantation.

Day 23: Implantation complete.

Days 27–28: Formation of secondary yolk sac. It is the secondary rather than the primary yolk sac that can be identified by ultrasound.

Days 21–28: Proliferation of syncytiotrophoblast formation of primary chorionic villi.

(Modified from Levi CS, Dashefsky SM and Lyons EA et al First Trimester Ultrasound. In McGahan JP and Porto M: Diagnostic Obstetric Ultrasound, J B Lippincott Company 1994; 2)

With the formation of the corpus luteum the production of progesterone starts the secretory phase of the endometrium. The glands of the endometrium increase in number and length and through the secretion of glycogen-rich material they become wide and tortuous. If fertilization occurs, the zygote, will be formed.

This highly specialized totipotent cell is the beginning of the embryonic development. Despite this fact the duration of pregnancy described in clinical medicine is calculated from the commencement of the mother's last menstrual period, which is about 14 days before conception occurs. This is the gestational age, which overestimates the actual embryonic age by 2 weeks.

The usual site of fertilization is the ampulla of the tube. Cleavage of the zygote results in a rapid increase in the number of its cells. These cells are called blastomeres; they become smaller with each division. When the total number of blastomeres reaches 12–15, the developing human is called a morula. It is formed 3 days after ovulation, which is day 18 of the menstrual cycle.

After the morula enters the uterus, fluid passes through it to form the blastocyst cavity. And the fluid continue to enter the cavity until the blastocyst is separated into two parts:

The trophoblast: A thin outer cell layer that gives rise to the embryonic part of the placenta.

The inner cell mass: A group of blastomeres that give rise to the embryo.

On day 20 of the cycle the blastocyst attaches to the endometrium usually on the site of the inner cell mass.

The trophoblast starts to proliferate rapidly and differentiate into two layers:

- Cytotrophoblast: Inner layer of cells.
- Syncytiotrophoblast: Outer layer of cells.

The Syncytiotrophoblast extends through the endometrium and invades the endometrial connective tissue. By day 21 of the menstrual cycle the blastocyst is superficially implanted, and by day 23 it is completely implanted into the endometrium.

Isolated cavities called lacunae appear in the Syncytiotrophoblast, the uterine vessels erode and come in contact with these lacunae to build the beginning of the uteroplacental circulation. The Syncytiotrophoblast begins to produce a hormone, the human chorionic gonadotrophin (hCG), which enters the aforementioned lacunae to the maternal blood. As the conceptus implants, cells of the endometrium swell because of accumulation of glycogen and lipids. These changes in the endometrium are known as the decidual reaction. Carlson stated that this transformation occurs to provide an immunologically privileged site for the conceptus.[5]

ULTRASOUND FINDINGS

By the time the blastocyst is implanted in the endometrium, the conceptus measures 0.1 mm and cannot be detected by the available ultrasound equipment. However Yeh et al identified a focal echogenic zone of decidual thickening at the site of implantation during this stage of pregnancy (3.5 to 4 weeks of menstrual age).[6] This sign may be difficult to demonstrate, in addition to the fact that its predictive value has never been published.

More reliable evidence of the presence of pregnancy is the demonstration of trophoblastic flow with Transvaginal Color Flow Doppler (TVCFD),[7,8] which is characterized by a high-velocity, low-impedance signal. Cartier and colleagues' findings suggest that blood flow can be demonstrated before TVS demonstration of the gestational sac.[9]

It has been suggested that the increased blood flow velocity in the endometrium is due to the invasion of the decidua by the chorionic villi.[10] The peak flow velocity in a normal pregnancy ranged from 8 to 30 cm/sec before TVS visualization of the intradecidual sac.[8]

Secretary Phase

The "triple-line" disappears and is replaced by an echogenic pattern. At this stage the endometrium is at its maximum thickness as it reaches up to 14 mm.

Corpus Luteum

At the time of ovulation the graafian follicle experiences some changes to form the corpus luteum. If pregnancy does not occur the corpus luteum decreases gradually in its size and atrophies to become the corpus luteum albicans, which cannot be identified sonographically.

In case of pregnancy, the corpus luteum will increase in size and produce progesterone to support the pregnancy until the placenta takes over its hormonal function. Corpus luteum can be sonographically identified in the majority of patients; however, it may vary considerably in its appearance. It appears usually as a thin walled, unilocular cyst with a diameter of less that 5 cm.[11] Occasionally internal septation, thickening of the cyst wall and echogenic debris may be demonstrated by ultrasound examination due to internal

hemorrhage of the cyst. In some circumstances the corpus luteum may reach a size greater than 10 cm.

These changes cause difficulty for the sonographer when attempting to differentiate between it and other pathologic masses that may be present in the first trimester. For instance such as ovarian neoplasm which is very rare in pregnancy, and dermoid cysts that demonstrate focal calcification revealing different echogenicity within the cystic area.[12]

Color Doppler may help differentiating between the different ovarian cysts. Due to the high metabolic activity, color flow imaging may demonstrate a ring of increased vascularity known as a "ring of fire".

Torsion and rupture may occasionally happen. If surgical intervention is necessary, it should be performed in the second trimester to minimize the likelihood of inducing abortion.

WEEK 5

Embryonic Events

Days 29–30: Gastrulation; formation of the three primary germ layers—ectoderm, endoderm, mesoderm.

Days 31–42: Neurolation; formation of the neural plate and neural tube.

Day 35: Primitive cardiovascular system consisting of the heart and a vascular network in the embryo, yolk-sac, connecting stalk, and chorion. *(Modified from Levi CS, Dashefsky SM and Lyons EA et al. First Trimester Ultrasound. In McGahan JP and Porto M: Diagnostic Obstetric Ultrasound, J B Lippincott Company 1994:2)*

Start of the 5th Week

The first few days after the completion of the 4th week of GA are the days during which usually the menstruation is expected. The cessation of this menstrual period is the first sign for the woman that she is pregnant. At this stage the conceptus is comprised from the chorionic sac, amniotic sac, yolk sac and the embryonic disc.

At this time the gastrulation process begins, which is the conversion of the bilaminar embryonic disc into the trilaminar one: endoderm, mesoderm and ectoderm. Each of the three germ layers will give rise to specific tissues and organs.

Gastrulation is the beginning of the development of the embryonic body—morphogenesis. The neurolation process starts, which is the transformation of the neural plate into the neural tube; the lateral edges of the neural plate become more elevated to form neural folds. In the mean time, the depressed mid-region forms a groove. Gradually, the neural folds approach each other in the midline to fuse and form the neural tube. Certain drugs can produce neural tube anomalies if administered during the fifth week (the week of the missed period).

In addition to neurolation, the heart, toward the end of the fifth week, is represented by paired endothelial heart tubes; and a primordial cardiovascular system formed by the end of the same week.

ULTRASOUND FINDINGS

Gestational Sac

Calculating from the first menstrual day, using transvaginal probe with frequencies of at least 5 MHz, a tiny gestational sac with a size of 2–3 mm can be detected between 4 weeks and 3 days to 4 weeks and 5 days. It is essential to recognize that this is the first definitive sonographic finding to suggest early pregnancy.[6,13] Further on, GA measurements are expressed using the MSD (Mean Sac Diameter), which is the average linear measurement of a gestational sac, obtained from three dimensions (length, width and depth) measured from the inner edge to the other inner edge.

It appears as a small fluid collection surrounded completely by an echogenic rim (Fig. 10.5). The central fluid collection corresponds to the chorionic cavity and the surrounding echoes are due to the chorionic decidual complex. Normalcy is indicated with the following:

- The echogenicity of the rim should exceed the level of myometrial echoes
- The position of a normal gestational sac should be found in the fundus or in the mid to upper uterus and is always abutting the endometrial canal.

The GA should be distinguished from:

1. Nabotion cyst that may lie in the upper cervix.

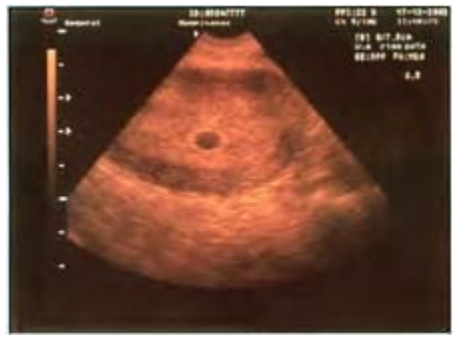

Figure 10.5: Intradecidual gestational sac

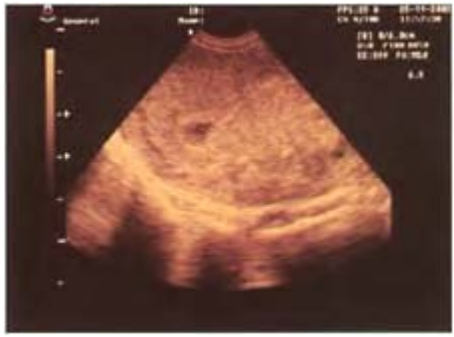

2. Decidual cyst which do not abut the endometrial canal.
3. Fluid collection within the endometrial canal surrounded by only a single decidual layer, referred to as a decidual cast or pseudo-gestational sac (Fig. 10.6).

Gestational sacs are usually round, but as they grow they frequently become elliptic and they may get irregular in shape as a result of:

- Uterine myoma
- Uterine contraction
- Bleeding surrounding the implantation site
- Distended maternal bladder.

As the blastocyst is completely burrowed in the endometrium, it is completely surrounded by the chorion. As pregnancy advances, villi on the embryonic pole (toward the myometrium) continue to grow and expand. Thus giving rise to the chorion frondosum (bushy chorion). The decidua, which is adjacent to the chorion frondosum, is called the decidua basalis. It consists of a compact layer of large cells with abundant amounts of lipids and glycogen. This part of the decidua with the chorion frondosum forms the placenta.

Villi on the abembryonic pole (the pole near the endometrium) degenerate, it is known as the chorion laeve. The decidual layer surrounding this part of the chorion is known as the decidua capsularis.

All the remaining parts of the decidua, on both sides of the endometrium are called decidua vera or decidua parietalis (Fig. 10.7).

Figure 10.7: Schematic representation clarifying the formation of the double-decidual sign (decidua parietalis and the decidua capsularis)

An excellent correlation exists between levels of hCG and the identification of the presence of a gestational sac and its size.

There are two β-hCG levels:

1. The threshold level: this is the lowest β-hCG level by which a normal intrauterine gestational sac is possible to be identified.
2. The discriminatory level: this is the level above which a gestational sac must be visualized. This measurement is a more important one than the former and has more clinical significance.

Nyberg and associates identified a discriminatory level for transvaginal sonography at 1000 MlU/ml (Second International Standard SI), which is equivalent to 1700 to 2000 MlU/ml (International Reference Preparation).[14] Note that the Second International Standard SI is numerically about half the International Reference Preparation.

It is obvious that the discriminatory level also depends on the resolution of the ultrasound scanner.

Yolk Sac

The yolk sac is the initial source of exchange between the mother and the embryo. It provides nutritive, metabolic, endocrine, immunological and hematopoietic functions.

The yolk sac is spherical in shape, with a welldefined echogenic rim and sonolucent center (Fig. 10.8). It is the first anatomical structure identified within the gestational sac. The yolk sac is visible using the transvaginal ultrasound by 5.5 weeks GA, when the MSD is 8 mm;[15] while using the transabdominal technique the yolk sac may not be seen before the 6th week of gestation. However, it will be demonstrated by 7 weeks GA when the MSD is 20 mm. The yolk sac diameter increases steadily (0.1 mm per day) until 10 weeks GA to a maximum of 5 to 6 mm.[16–18]

The demonstration of the yolk sac confirms that the sac represents an early intrauterine pregnancy,

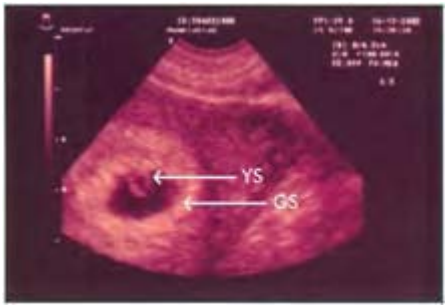

Figure 10.8: The gestational sac (GS), demonstrating the yolk sac (YS) which is the first intragestational structure

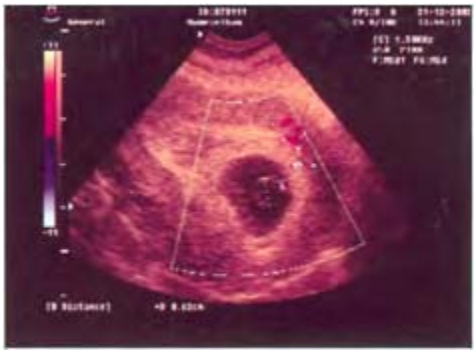

Figure 10.9: Cardiac activity demonstrated adjacent to the yolk sac

as opposed to a pseudosac appearance with an ectopic pregnancy. Yolk sac also serves as an anatomical landmark to locate the embryonic disc and detect early cardiac activity (Fig. 10.9).[15,19,20]

WEEKS 6 to 10: EMBRYONIC PERIOD

This section will discuss the embryologic and ultrasound findings during the embryonic period (organogenesis), where all internal and external structures in the adult form are present and develop in parallel as demonstrated below.

Organogenesis will be dealt with in some detail; however, neurolation, will not be addressed again as it has been mentioned thoroughly in week 5.

EMBRYONIC EVENTS

Musculoskeletal System

5.5–6 weeks	Formation of limb buds.
7.5–8 weeks	Digital rays are distinct upper limbs one bent at elbows.
8 weeks	Center of ossification is present in clavicle.
9 weeks	Center of ossification is present in mandible and palate and Vertebral center and neural arches begin to ossify.
10–11 weeks	Frontal bones begin to ossify.

CV System

6 weeks	Blood flow is unidirectional.
8 weeks	Heart attains its definitive form.
10 weeks	Completion of the development of the peripheral vascular system.

GI System

6 weeks	Formation of the primitive gut.
8–12 weeks	Mid-gut herniates into the umbilical cord.
8 weeks 10 weeks	Rectum separates from the urogenital sinus. Anal membrane perforates.

(Modified from Levi CS, Dashefsky SM and Lyons EA et al. First Trimester Ultrasound. In McGahan JP and Porto M: Diagnostic Obstetric Ultrasound, J B Lippincott Company 1994; 5)

ULTRASOUND FINDINGS

It should be noted that although this section is primarily dealing with the period spanning from 6 to 10 weeks GA; it is necessary to indicate that week 6, specifically, has great importance in terms of sonographic and landmarks for the purpose of providing sufficient evidence of a normal intrauterine pregnancy.

As the sac enlarges the gestational sac that is now abutting the endometrial canal (Fig. 10.10), starts to protrude into the canal, displacing it

Figure 10.10: Schematic representation of the gestational sac abutting the endometrial canal

Figure 10.11: Schematic representation of the gestational sac protruding the endometrial canal

towards the other side. When the mean gestational sac diameter (MSD) is 10 mm or more, the decidua capsularis approaches the decidua parietalis squeezing it and finally obliterating it (Fig. 10.11). As the two echogenic rims approach each other: *decidua capsularis and decidua parietalis,* the so called double-decidual sac sign is formed. This sign can confirm intrauterine pregnancy.[21] However, with the introduction of the transvaginal sonography this sign becomes less important (Fig. 10.12).

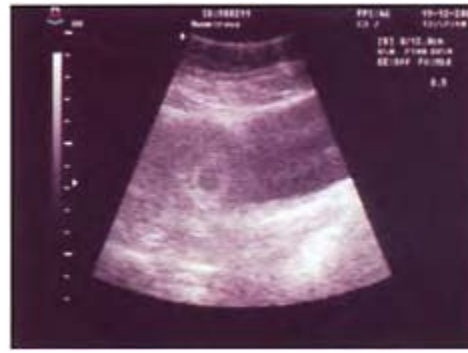

Figure 10.12: Double-decidual sac sign seen on the left hand side of the sac

Embryo, Amnion and Cardiac Activity

Sonographically, heart motion can be detected at approximately 5.5 weeks GA, when the crown-rump length (CRL) is 2 to 3 mm. As the human eye is sensitive to cardiac activity, it can be

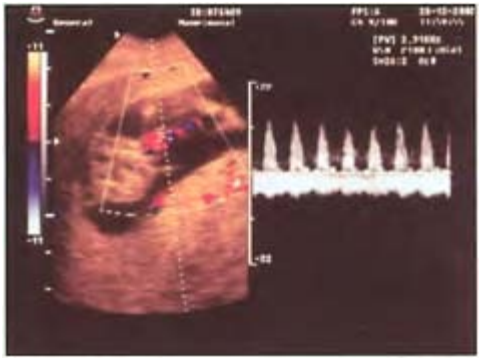

Figure 10.13: Color flow Doppler used to confirm cardiac activity

occasionally seen before the embryo itself is identified (Figs 10.9 and 10.13).[22] The amniotic cavity is too small to be clearly visualized at this stage, so that the heart beat is seen adjacent to the secondary yolk sac and looks as if there is no space between the yolk sac and the embryo.

Using the transvaginal probe the amniotic membrane is routinely visualized after 5.5 weeks GA. The amniotic sac with the yolk sac are approximately equal in size (Fig. 10.14) with the embryonic disc between them lying within the gestational sac create a shape known as double bleb sign.[23] However this double bleb sign is transient and disappears at 7 weeks GA due to

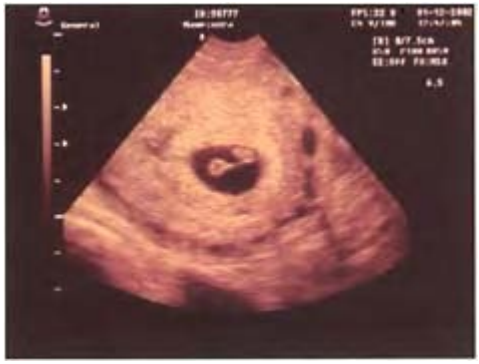

Figure 10.14: Yolk sac (left) and embryo (right) connected by the viteline duct

the developmental changes affect the size and configurations of each sac. In a normal pregnancy the amnion may be visualized when the crown-rump length is 5 mm and is routinely detectable when the CRL is 7 mm or more. From this age onwards the amniotic sac diameter as well as the CRL increase by 1 mm per day.

When the embryo reaches a gestational age of 7 weeks, the gestational sac appears to occupy 1/3 of the uterine volume.

Musculoskeletal System

The skeletal system begins to develop during the 6th week of gestation. It begins with the upper limbs followed by the lower extremities. The spine is developing in the embryonic period. Sonographically, parallel echogenic lines can be demonstrated at 7 to 8 weeks of gestation. Crown-rump length can be measured with certainty at this age. Its length is about 10 mm.

Using the transvaginal approach, the limb buds can be demonstrated starting from the 7th week (Fig. 10.15), beginning with upper limbs. At 8 weeks, the lower limb buds can be seen more clearly, while the upper limb buds are harder to visualize. The feet and hands are completely developed by the end of the 10th week of gestation (Fig. 10.16), while the fingers and toes cannot be detected until the 11th week of gestation. Discreet

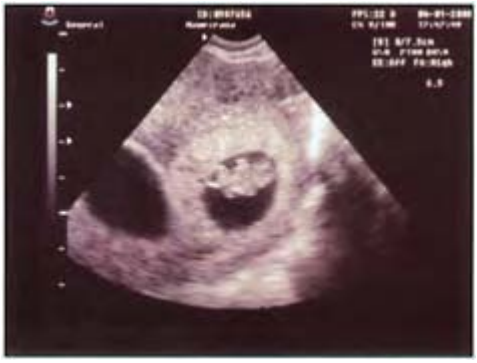

Figure 10.15: Limb buds seen in an embryo at 7 weeks GA

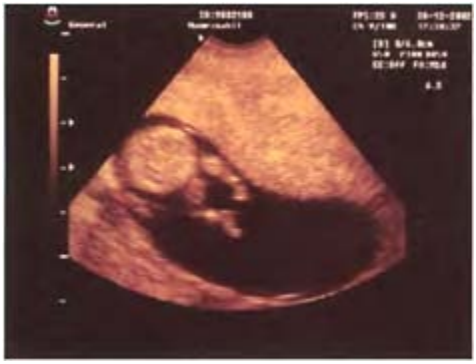

Figure 10.16: Lower limbs visualized in a 10 week old fetus

movements can be sporadically demonstrated at the end of the 8th week GA.

The embryonic face cannot be seen with diagnostic detail. By the 9th week, the maxilla and mandible are ossified and appear as brightly echogenic structures.

Brain

At the beginning of the embryonic period three primary brain vesicles are formed. The first vesicle detected represents the rhombencephalon, which later, after division into the metencephalon and the myelencephalon, both contributes to form the normal fourth ventricle and should not be mistaken for a posterior fossa cyst of pathologic significance (Fig. 10.17). The mesencephalon (or

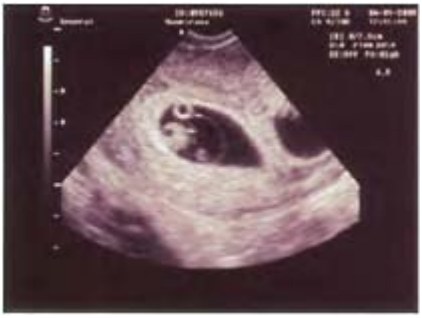

Figure 10.17: A normal brain vesicles during the embryonic development—not to be mistaken as a pathologic feature

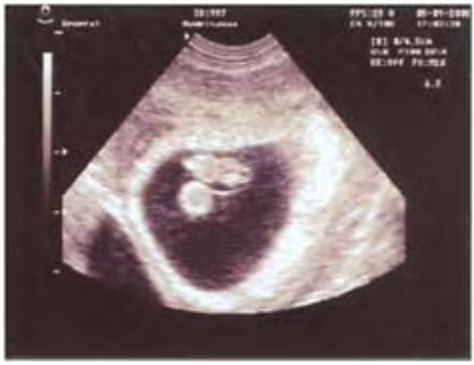

Figure 10.18: A demonstration of the head-trunk relation

midbrain) lies between rhombencephalon and prosencephalon; without division it later forms the aqueduct. The prosencephalon is divided into two portions: the telencephalon, which is the anterior part that forms the lateral ventricle, and the posterior diencephalon that form the third ventricle.

At 7.5 weeks the embryonic cranium can be distinguished from the embryonic abdomen. The head is now much larger in relation to the trunk (Fig. 10.18). At 9 to 10 weeks, the head size is almost half of the size of the embryo; it surpasses the diameter of the yolk sac. The lateral ventricles extend to reach the inner table of the skull by 12 weeks GA. Sonographically, only a small rim of the cerebral cortex can be seen. Furthermore, the choroid plexus fills the lateral ventricles completely and it appears echogenic (Fig. 10.19). The choroid plexus are imaged as hyperechoic structures in the ventricles.

Gastrointestinal System (Physiologic Midgut Herniation)

The developing embryo is transformed from a flat disc to a cylindrical shape by the folding of the cranial, caudal, and lateral ends of the embryo simultaneously. At the same time the fetal organs develop.

With the development of the cranial folds, the base of the yolk sac becomes incorporated as part

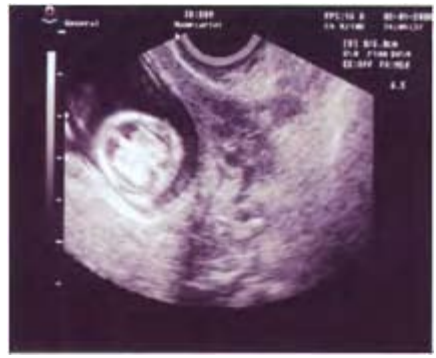

Figure 10.19: Hyperechoic choroid plexus filling the lateral ventricles

of the foregut. This develops into the proximal gestrointestinal (GI) tract. Another part of the yolk sac is incorporated into hindgut, as the caudal folds develop. The two lateral folds form the lateral end of the anterior abdominal wall. The midgut forms from the roof of the yolk sac to become the part of the gastrointestinal from the distal duodenum to the proximal two-thirds of the transverse colon. At this time the liver and kidneys occupy the majority of the abdomen, and the small bowel grows rapidly, to the extent that it cannot be accommodated by the abdominal cavity. The midgut grows faster than the abdominal cavity thus it herniates in the umbilicus. This physiologic umbilical herniation occurs at the beginning of the 8th menstrual week. The size of the hernia in this

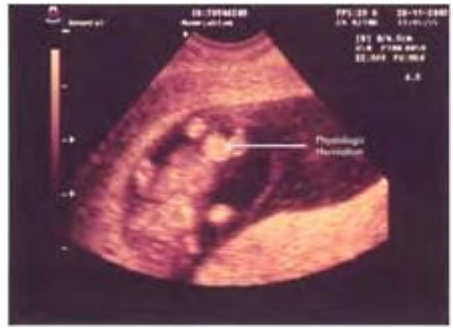

Figure 10.20: Physiologic herniation visualized by transvaginal ultrasound at the 11th week GA

area is at least 1.5 times the size of the cord (Fig. 10.20).

At 12 menstrual weeks, the transient physiologic herniation ends as the small bowel returns into the abdomen. Timor-Tritsch et al reported that they could not find any physiologic herniation after this age. Research has identified that any measurement of the

physiologic herniated bowel above 7 mm, is considered in the grounds of pathology. They also could not demonstrate any physiologic herniation in any embryo with a crown rump length over 44 mm.

It is essential to keep in mind that any organ seen outside the abdomen other than the small bowel indicates an abdominal wall defect even before 12 weeks gestation, rather than a physiologic herniation.

Doppler

Using Power Doppler, Kupesic demonstrated aorta and umbilical blood flow at 7 to 8 weeks gestation. In addition, features of early vascular anatomy at the base of the skull were depicted.[24]

Between 9 to 10 weeks gestation, the major branches of the aorta (the common iliac and renal arteries) (Fig. 10.21) and the circle of Willis has been depicted by the Power Doppler technique. The color Doppler waveform is characterized by an absent end-diastolic flow and pulsatiled venous flow.[24]

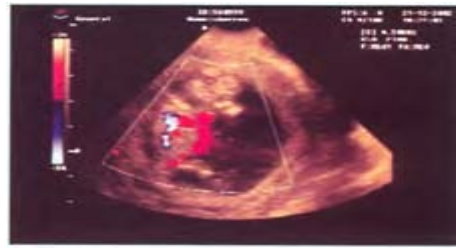

Figure 10.21: Aorta (left) and umbilical cord (right) demonstrated by color Doppler at 11th week GA

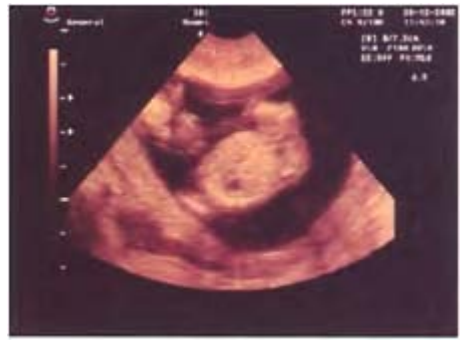

Figure 10.22: Stomach (middle) and bladder (right) demonstrated after the 10th week GA

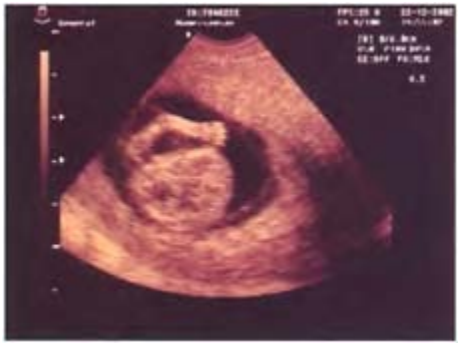

Figure 10.24: Spine and ribs clearly visualized at the 11th week gestation

WEEK 11 AND AFTER

With advanced ultrasound technology, specifically high frequency transvaginal probes; one can now demonstrate most fetal organs before 13 weeks. By the 12th week GA, a sonographer can demonstrate the fetal stomach in 93% of fetuses, and the bladder in 50% of them (Fig. 10.22). Moreover, urine starts to form and is excreted in the amniotic fluid. In the mean time, ossification is progressing in general, and at this age it starts in the long bones of the fetus. What's more, the biparietal diameter is now more accurate to measure, thus giving rise to an easier and more accurate fetal biometry assessment. From then on, a more detailed anatomical survey can be

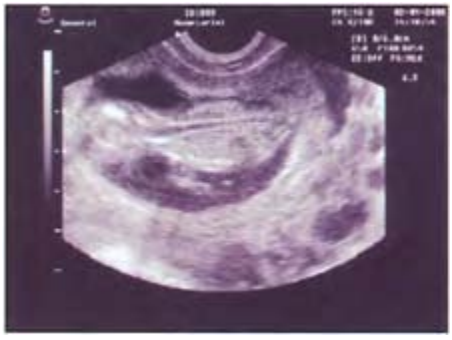

Figure 10.23: Fingers seen in the late first trimester

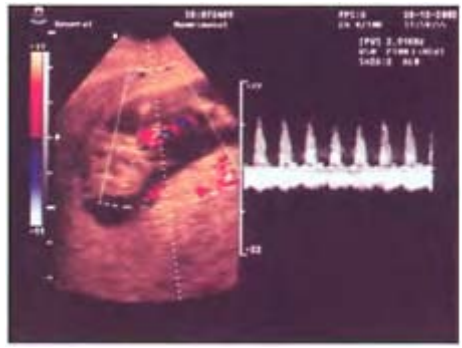

Figure 10.25: Color flow Doppler showing an absent end-diastolic flow and pulsatile venous flow

achieved, including the cerebral and cardiovascular systems and the digestive tract. Liver, stomach and heart can be seen in the trunk. The midgut is no longer herniated at this stage; it is now situated back in the abdomen. The neck is well defined, and the face is in general indistinct. As aforementioned, fingers (Fig. 10.23), toes and the spine (Fig. 10.24) are clearly recognized during the 11th week. In regards to the placenta, during this period, about half of it seems to partly or completely occupy the lower pole of the uterus.

Kupesic and Kurjak reported measuring the end-diastolic velocities of the umbilical artery at 11–12 weeks gestation (Fig. 10.25).[24]

In addition to the examination of the embryonic and fetal structures listed above, any fetus screened in the late first trimester should be evaluated for both nuchal translucency and nasal bone, as there are measures for identifying aneuploidy.

ACKNOWLEDGEMENT

I wish to express my sincere thanks to Dr Muna Al-Abdulla and Mr Khaled M Sarraf who have spared no effort in assisting with the preparation of this chapter.

REFERENCES

1. Moore KL, Persaud TVN. Before We Are Born. Philadelphia, Pennsylvania, USA, W.B. Saunders Co. 1998; 5th edition
2. Sadler TW. Langman's Medical Embryology. Williams & Wilkins, Baltimore, USA, 1995. Mass Publishing Co. Egypt 1996, Middle East Edition.
3. Kurjak A, Kupesic S. Color Doppler in Obstetrics, Gynecology and Infertility. Art studio Azinovic-Medi-sone, Zagreb-Seoul, 1999. Infertility Chapter 18–34.
4. Lyons EA, Gratton D, Hamington C. Transvaginal sonography of normal pelvic anatomy. Radiol Clin North Am 1992; 30:663
5. Carlson BM. Human Embryology and Developmental Biology. St Louis, CV Mosby, 1994.

6. Yeh H-C, Goodman JD, Carr L et al. Intradecidual sign: A US criterion of early intrauterine pregnancy.g Radiology 1986; 161:463–67
7. Pellerito JS, Taylor KJW, Quedens-Case C et al. Ectopic pregnancy: Evaluation with endovaginal colour flow imaging. Radiology 1992; 183:407–11
8. Emerson DS, Cartier MS, Altieri LA et al. Diagnostic efficacy of endovaginal colour flow imaging in an ectopic pregnancy screening program. Radiology 1992; 183:413–20
9. Cartier MS, Altieri LA, Emerson DS et al. Diagnostic efficacy of endovaginal color flow Doppler in an ectopic pregnancy screening program. Radiology 1990; 177(p):117
10. Taylor KJW, Ramos IM. Fey cock AL et al. Ectopic pregnancy: Duplex Doppler evaluation. Radiology 1989; 173:93–97
11. Fleischer AC, Boehm FH, James AE Jr. Sonographic evaluation of pelvic masses and maternal disorders occurring during pregnancy. In Sanders RC, James AE Jr (eds): The Principles and Practice of Ultrasonography in Obstetrics and Gynecology, 3rd ed. Norwalk, CT: Appleton-Century-Crofts, 1985:435–47.
12. Pennes DR, Bowerman RA, Silver TM: Echogenic adnexal masses associated with first-trimester pregnancy: Sonographic appearance and clinical significance. J Clin Ultrasound 1985; 13:391–96
13. Rossavik IK, Torjusen GO, Gibbons WE. Conceptual age and ultrasound measurements of gestational sac and crown-rump length in Vitro fertilization pregnancies. Fertil Steril 1988; 49:1012–17
14. Nyberg DA, Filly RA, Laing FC et al. Ectopic pregnancy: Diagnosis by sonography correlated wiht quantitative hCG levels. J Ultrasound Med 1987; 6(3):145–50.
15. Levi CS, Lyons EA, Lindsay DJ. Early diagnosis of nonviable pregnancy with transvaginal US. Radiology 1981; 67:383–85
16. Lindsay DJ, Lovett IS, Lyons EA et al. Yolk sac diameter and shape at transvaginal US: Predictors of pregnancy outcome in the first trimester. Radiology 1992; 183:115–18
17. Stampone C, Nicotra M, Muttinelli C et al. Transvaginal sonography of the yolk sac in normal and abnormal pregnancy. J Clin Ultrasound 1996; 24: 3–9.
18. Jauniaux E, Jurkovic D, Henriet Y, et al. Development of the secondary human yolk sac: Correlation of sonographic and anatomical features. Hum Reprod 1991;6:1160–66.
19. Cadkin AV, McAlpin J. Detection of fetal cardiac activity between 41 and 43 days of gestation. J Ultrasound Med 1984; 3:499–503
20. Nyberg DA, Laurence MA, Harvey D et al. Value of the yolk sac in evaluating early pregnancies. J Ultrasound Med 1988; 7:129–35
21. Nyberg DA, Laing FC, Filly RA et al. Ultrasonographic differentiation of the gestational sac of early intrauterine pregnancy from the pseudogestational sac of ectopic pregnancy. Radiology 1983; 146:755–59.
22. Laing FC, Frates MC. Ultrasound evaluation during the first trimester of pregnancy. In: Callen PW (Ed): Ultrasonography in Obstetrics and Gynecology. Philadelphia: WB Saunders Company, 2000; 105–45.
23. Yeh HC, Rabinowitz JG. Amniotic sac development: Ultrasound features of early pregnancy-the double bleb sign. Radiology 1988; 166:97–103
24. Kupesic S, Kurjak A, Bjelos D. Power Doppler in prenatal diagnosis. The Ultrasound Review 2002; 2: 261–73.

Chapter 11
Sonographic Determination of Gestational Age

Robin B Kalish

IMPORTANCE OF ACCURATE GESTATIONAL AGE ASSESSMENT

Accurate assessment of gestational age is fundamental in managing both low and high risk pregnancies. In particular, uncertain gestational age has been associated with adverse pregnancy outcomes including low birth weight, spontaneous preterm delivery and perinatal mortality, independent of maternal characteristics.[1] Making appropriate management decisions and delivering optimal obstetric care necessitates accurate appraisal of gestational age. For example, proper diagnosis and management of preterm labor and post-term pregnancy requires an accurate estimation of fetal age. Many pregnancies considered to be preterm or postterm are wrongly classified. Unnecessary testing such as fetal monitoring and unwarranted interventions including induction for supposed postterm pregnancies may lead to an increased risk of maternal and neonatal morbidity. In addition, pregnancies erroneously thought to be preterm may be subject to avoidable and expensive hospitalization stays as well as excessive and potentially dangerous medication use including tocolytic therapy. In one study by Kramer et al that assessed over 11,000 pregnant women who underwent early ultrasound, one-fourth of all infants who would be classified as premature and one-eighth of all infants who would be classified as postterm by menstrual history alone would be misdiagnosed.[2] Accurate pregnancy dating may also assist obstetricians in appropriately counseling women who are at imminent risk of a preterm delivery about likely neonatal outcomes.

Precise knowledge of gestational age is also essential in the evaluation of fetal growth and the detection of intrauterine growth restriction. During the third trimester, fundal height assessment may be helpful in determining appropriate fetal growth by comparing the measurement to a known gestational age. In addition, dating a pregnancy is imperative for scheduling invasive diagnostic tests such as chorionic villus sampling or amnio-centesis, as appropriate timing can influence the safety of the procedure. Certainty of gestational age is also important in the interpretation of biochemical serum screening test results and may help avoid undue parental anxiety from miscal-culations and superfluous invasive procedures, which may increase the risk of pregnancy loss. Assessment of gestational age is also crucial for counseling patients regarding the option of pregnancy termination.

ASSESSING GESTATIONAL AGE USING LAST MENSTRUAL PERIOD

Traditionally, the first day of the last menstrual period (LMP) has been used as a reference point, with a predicted delivery date 280 days later. The estimated date of confinement (EDC) can also be calculated by Nägele's rule by subtracting three months and adding seven days to the first day of the last normal menstrual period. However, there are inherent problems in assessing gesta-tional age using the menstrual cycle. One obstacle in using the LMP is the varying length of the follicular phase and the fact that many women do not have regular menstrual cycles. Walker et al evaluated 75 ovulatory cycles using luteinizing hormone levels as a biochemical marker and found that ovulation occurred within a wide range of 8–31 days after the LMP.[3] Similarl y, Chia zz al collected over 30,000 recorded menstrual cycles from 2316 women and found that only 77% of women have average cycle lengths between 25 and 31 days.[4] Another barrier in using a menstrual history is that many women do not routinely document or remember their LMP. Campbell et al demonstrated that of more than 4000 pregnant women, 45% were not certain about their LMP as a result of poor recall, irregular cycles, bleeding in early pregnancy or oral contraceptive use within two months of conception.[5]

CLINICAL METHODS FOR DETERMINING GESTATIONAL AGE

Other methods used to assess gestational age have included uterine size assessment, time at quickening and fundal height measurements. However, these clinical methods are often suboptimal. Robinson noted that uterine size determination by bimanual examination produced incorrect assessments by more than two weeks in over 30% of patients.[6] Similarly, fundal height estimation does not provide a reliable guide to predicting gestational age. Beazly et al found up to eight weeks variation in gestational age for any particular fundal height measurement during the second and third trimesters.[7] In addition, quickening, or initial perception of fetal movement can vary greatly among women. While these modalities may be useful adjuncts, they are unreliable as the sole tool for the precise dating of a pregnancy.

ULTRASOUND ASSESSMENT OF GESTATIONAL AGE

In recent years, ultrasound assessment of gestational age has become an integral part of obstetric practice.[8] Correspondingly, prediction of gestational age is a central element of obstetric ultrasonography. Fetal biometry has been used to predict gestational age since the time of A-mode ultrasound.[9] Currently, the sonographic estimation is derived from calculations based on fetal measurements and serves as an indirect indicator of gestational age. Over the past three decades, numerous equations regarding the relationship between fetal biometric parameters and gestational age have been described and have proven early antenatal ultrasound to be an objective and accurate means of establishing gestational age.[10–15]

FIRST TRIMESTER ULTRASOUND

Ultrasound assessment of gestational age is most accurate in the first trimester of pregnancy. During this time, biological variation in fetal size is minimal. The gestational sac is the earliest unequivocal sonographic sign of pregnancy.[16–19] Historically, gestational sac size and volume had been used as a means to estimate gestational age.[20,21] This structure sonographically resembles a fluid filled sac surrounded by a bright echogenic ring, the developing chorionic villi, within the endometrial cavity (Fig. 11.1). This sac can be visualized as early as five menstrual weeks using transvaginal sonography.[22–24] More recently,

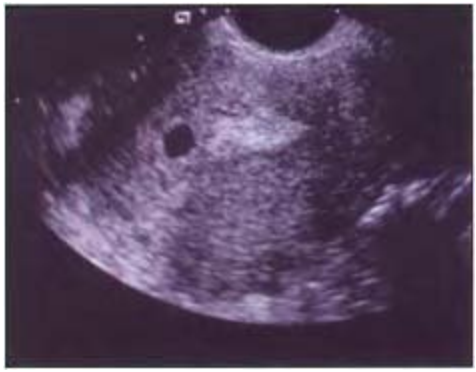

Figure 11.1: Transvaginal ultrasound image demonstrating an early gestational sac prior to the visualization of a fetal pole

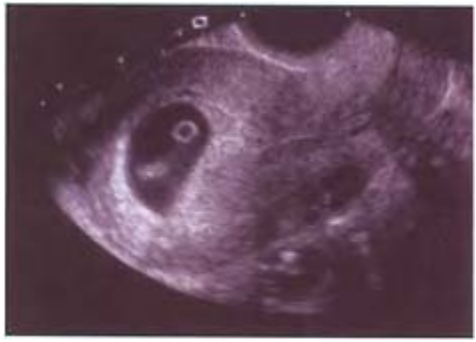

Figure 11.2: Transvaginal ultrasound image demons-trating an early embryo with a visible yolk sac at approximately 7 weeks gestation

studies have shown that fetal age assessment by gestation sac measurement is not reliable, with a prediction error up to two weeks.[6,25] Another imprecise yet often used modality is the sonographic visualization of distinct developing structures.[26] During the fifth menstrual week, the yolk sac, the earliest embryonic structure detectable by sonography, can be visualized prior to the appearance of the fetal pole. And, by the end of the sixth menstrual week, a fetal pole with cardiac activity should be present (Fig. 11.2). Subsequently, the presence of limb buds and midgut herniation can be seen at approximately 8 weeks gestation. However, these developmental landmarks can only provide rough estimates to the actual fetal age.

In 1973, Robinson reported using the crown-rump length (CRL) for determining gestational age.[27] Since that time, ultrasound equipment, techniques and prediction formulas have substantially improved and allow for more rapid and precise measurement of the crown rump length and determination of gestational age.[28,29] For the best results, the fetus should be imaged in a longitudinal plane. The greatest embryonic length should be measured by placing the calipers at the head and rump of the fetus (Fig. 11.3). Three adequate CRL measurements should be taken and the average used for gestational age determination.[30] The accuracy of the CRL

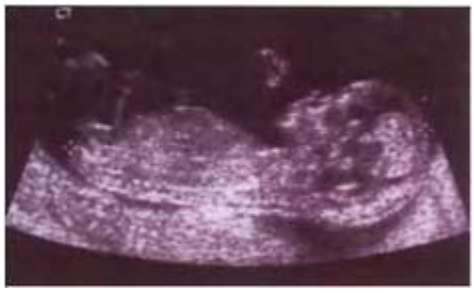

Figure 11.3: Ultrasound image demonstrating the fetal crown-rump length measurement in the first trimester

measurement has been well documented in the medical literature. Specifically, gestational age can be estimated safely with a maximal error of three to five days in the first trimester.[6,31,32]

In summary, first trimester ultrasound is a useful and reliable tool in the assessment of gestational age. In particular, sonographic measurement of the CRL during the first trimester is the best parameter for estimating gestational age and is accurate within five days of the actual conception date.[31]

SECOND TRIMESTER ULTRASOUND

Although routine ultrasonography at 18–20 weeks gestation is controversial,[33] it is practiced by many obstetricians in the United States.[34] In addition to screening for fetal anomalies, sonographic gestational age assessment may be of clinical value in that it has been shown to decrease the incidence of postterm as well as preterm diagnoses and thus the administration of tocolytics.[35,36] In addition, uncertain gestational age has been associated with higher perinatal mortality rates and an increase of low birth weight and spontaneous preterm delivery.[1]

Ultrasound Parameters

When choosing the optimal parameter for estimating gestational age, it is essential that the structure has little biologic variation, is growing at a rapid pace, and can be measured with a high degree of reproducibility.[37] In the past, the biparietal diameter (BPD) had been described as a reliable method of determining gestational age.[9,12] While the BPD was the first fetal parameter to be clinically utilized in the determination of fetal age in the second trimester, more recent studies have evaluated the use several other biometric parameters including head circumference (HC),[38] abdominal circumference (AC),[39] femur length (FL),[40] foot length,[41] ear size,[42] orbital diameters,[43,44] cerebellum diameter[45,46] and others. In a large study by Chervenak et al that evaluated pregnancies conceived by *in vitro* fertilization and thus had known conception dates, head circumference was found to be the best predictor of gestational age compared with other commonly used parameters (Table 11.1).[47] This finding is in agreement with that of Hadlock,[10] Ott[11] and Benson[48] who compared the performance of HC, BPD, FL and AC in different populations.

Table 11.1: Comparison of ste regression in estimation of fet age for singletons using different second trimester biometric parameters by Chervenak et al*

Biometric parameters	*Random error (days)*
HC	3.77
AC	3.96
BPD	4.26
FL	4.35
HC+AC	3.44
HC+FL	3.55
HC+AC+FL	3.35

*(Adapted from Chervenak FA, Skupski DW, Romero R, et al. How accurate is fetal biometry in the assessment of fetal age? American Journal of Obstetrics and Gynecology 1998; 178:678–87)

The head circumference should be measured in a plane that is perpendicular to the parietal bones and traverses the third ventricle and thalami (Fig. 11.4).[30] The image should also demonstrate smooth and symmetrical calvaria and the presence of a cavum septum pellucidum. The calipers should be placed on the outer edges of the calvaria and a computer-generated ellipse should be adjusted to fit around the fetal head without

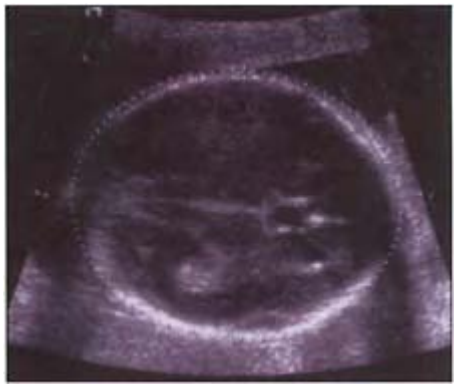

Figure 11.4: Ultrasound image demonstrating the head circumference measurement in a second trimester fetus

including the scalp. The biparietal diameter can be taken in the same plane by placing the calipers on the outer edge of the proximal calvarium wall and on the inner edge of the distal calvarium wall.[49] The BPD, while highly correlated with HC, is less accurate as a predictor of gestational age as a result of variation in head shape.[47]

Multiple parameters have been shown to improve the accuracy of gestational age assessment.[47] Along with head circumference, the addition of one parameter (AC or FL) or two parameters (AC and FL) is slightly superior to head circumference alone in the prediction of fetal age. Table 11.1 demonstrates the relative error associated with the use of different biometric parameters. The use of multiple parameters also reduces the effect of outliers caused by biologic phenomena (i.e. congenital anomalies or growth variation) or technical error in measurement of a single structure. Still, with multiple parameters, it is important to take the images in the proper plane and place the calipers appropriately. For example, when assessing FL, the long axis of the femur should be aligned with the transducer measuring only the osseous portions of the diaphysis and metaphysis of the proximal femur. While not included in the FL measurement, the proximal epiphyseal cartilage (future greater trochanter) and the distal femoral epiphyseal

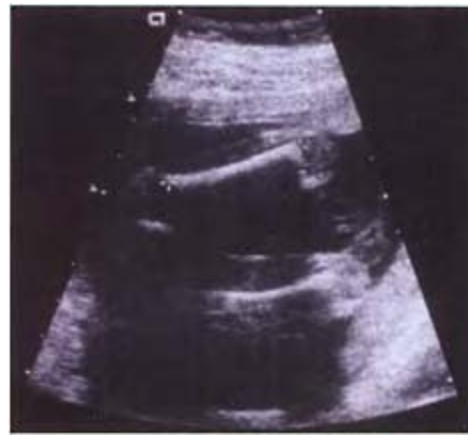

Figure 11.5: Ultrasound image demonstrating the femur length measurement in a second trimester fetus

cartilage (future distal femoral condyle) should be visualized to assure that the entire osseous femur can be measured without foreshortening or elongation (Fig. 11.5).[30,50] Similarly, the AC must be measured appropriately in order to obtain an accurate estimate. The image should taken in a plane slightly superior to the umbilicus at the greatest transverse abdominal diameter, with the liver, stomach, spleen and junction of the right and left portal veins visualized (Fig. 11.6).[30]

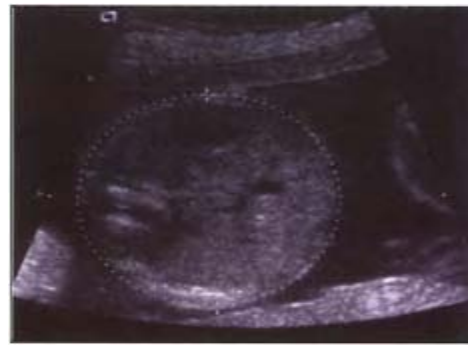

Figure 11.6: Ultrasound image demonstrating the abdominal circumference measurement in a second trimester fetus

Most modern ultrasound machines are equipped with computer software that will automatically calculate the estimated gestational age based on the entered measurements. Using a large singleton *in vitro* fertilization (IVF) population from 14–22 weeks, Chervenak et al derived an optimal gestational age prediction formula using stepwise linear regression with a standard deviation (SD) of 3.5 days between the predicted and true gestational age.[47] This formula was compared it to 38 previously published equations. Nearly all equations produced a prediction within one ent of gestational age is applicable and accurate across populations and institutions. Clinically, when a discrepancy greater than seven days (2SD) exists between the menstrual and ultrasound dating in the second trimester, the biometric prediction should be given preference.

THIRD TRIMESTER ULTRASOUND

While ultrasound has proven to be useful in the assessment of gestational age in the first and second trimesters, accuracy in the third trimester is not as reliable. Biologic variation can be a major factor that affects accuracy in gestational age prediction, and this variability greatly increases with advancing pregnancy. Doubilet and Benson evaluated late third trimester ultrasound examinations of women who had also received a first trimester exam and found the disparity in gestational age assessments to be three weeks or greater.[51] Thus, third trimester sonographic estimates of gestational age should be used with caution, if at all.

MULTIPLE PREGNANCIES

Dating equations generated for singletons can be applied to twins and triplets in order to accurately predict fetal age. Chervenak et al used multiple linear regression to determine an optimal dating formula for multiple gestations.[47] In twin pregnancies, a single averaged prediction of the gestational age of each fetus is appropriate and was found to yield the most accurate results. This approach of averaging the two fetal age estimates is reasonable as the combined biologic and measurement variability among twins is larger than the decrease in average size of twins relative to singletons. In contrast, using the maximum or minimum estimate in a twin set yielded a slightly larger systematic error than an averaged prediction (Table 11.2). In the case of triplets, one day can be added to the average of the largest and shortest gestational age prediction among these fetuses for the most accurate gestational age assessment.

Slightly larger deviations in the predictions are not unexpected for individual twins or triplets as the formulae have been derived from a singleton population. However, this imprecision is partially compensated for by the fact that multiple pregnancy predictions are based on more information, namely two or three times as many measurements as for singletons. As singleton and multiple gestations grow at similar rates during the second trimester, the difference in the uncertainty of the prediction for gestational age is small using a singleton gestation formula.

Table 11.2: Application of a singleton multip regression form ula for estimation of fetal is by Chervenak et al*

Pregnancy type	*Prediction type*	*Mean error (days)*
Twins	GA of larger twin	0.8
	GA of smaller twin	−1.3
	Mean GA of both fetuses	−0.3
	GA of larger twin	2.2
	GA of smaller twin	
Triplets	GA of largest triplet	0.8
	GA of smallest triplet	−3.4
	Mean GA of all fetuses	−1.3
	GA of largest triplet	4.2
	GA of smallest triplet	

GA=gestational age
*(Adapted from Chervenak FA, Skupski DW, Romero R, et al. How accurate is fetal biometry in the assessment of fetal age? American Journal of Obstetrics and Gynecology 1998; 178:678–87)

CHOOSING A DUE DATE

When the date of conception is unequivocal, as in cases of in *vitro* fertilization, the estimated date of confinement should not be changed based on ultrasound. However, more often than not, this is not the case. In the first trimester, an estimated date of confinement (EDC) based on the LMP that is greater than five days different from the crown-rump length measurement should be changed to the sonographically derived EDC (Fig. 11.7).[27,31,32] In the second trimester, a combination of biometric parameters that includes the head circumference should be used to predict the EDC. In the face of a discrepancy of more than 7 days in the second trimester, the sonographic biometric prediction should be given preference, provided there is no anomaly or severe growth delay (Fig. 11.8).[47] In fact, some authors argue that biometric prediction in the first and second trimesters should be given preference in every case.[52–55]

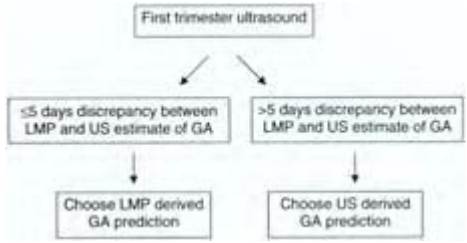

Figure 11.7: Gestational age assessment using first trimester ultrasound (LMP=last menstrual period, US=ultrasound, GA=gestational age)

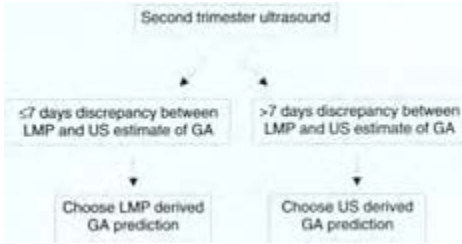

Figure 11.8: Gestational age assessment using second trimester ultrasound (LMP=last menstrual period, US=ultrasound, GA=gestational age)

One of the most common and serious mistakes made when determining gestational age is changing the due date based on a second or subsequent ultrasound exam. The inaccuracy of ultrasound dating increases with gestational age. If the LMP and clinical findings suggest a gestational age within 5 days of a first trimester scan or within 7 days of a second trimester scan, no further investigation is necessary. If the initial first or second trimester sonographically determined gestational age is outside these ranges, the due date should be changed. However, as the pregnancy progresses, revision of a due date that was based on a previous ultrasound is never warranted. If there is a discrepancy between the gestational age assessments of two ultrasound examinations, considering explanations such as intrauterine growth retardation (IUGR), macrosomia or other pathological conditions may be appropriate.

ULTRASOUND PITFALLS

Recent advances in ultrasound image quality and the wide availability of accurate biometric formulas have greatly improved physicians' ability to calculate gestational age. However, properly dating a pregnancy sonographically still depends on adherence to good ultrasound technique. Obtaining a clear and precise image of each bio-metric indicator is essential. Errors in estimation may arise from technical difficulties including obtaining the proper axis for measurement, movement of the mother or fetus, machine sensitivity settings or caliper placement. If a certain biometric indicator is not well visualized or is difficult to measure, it is better to use an alternative indicator rather than include a suboptimal measurement. In addition, it is helpful to obtain several measurements of each indicator and use an average to ensure a more precise calculation of fetal age.

CONCLUSIONS

Knowledge of gestational age is of great impor-tance in obstetric practice. Optimal assessment requires good judgment by the obstetrician caring for the patient. Since clinical data such as the menstrual cycle or uterine size often are not reliable, the most precise parameter for pregnancy dating should be determined by the obstetrician early in the pregnancy. Ultrasound is an accurate and useful modality for the assessment of gestational age in the first and second trimester of pregnancy and, as a routine part of prenatal care, can greatly impact obstetric management and improve antepartum care.

REFERENCES

1. Hall MH, Carr-Hill RA. The significance of uncertain gestation for obstetric outcome. Br J Obstet Gynaecol 1985; 92:452–60
2. Kramer MS, McLean FH, Boyd ME, Usher RH. The validity of gestational age estimation by menstrual dating in term, pre-term and post-term pregnancies. JAMA 1988; 260:3306–08
3. Walker EM, Lewis M, Cooper W, Marnie M, Howie PW. Occult biochemical pregnancy: fact or fiction? Br J Obstet Gynaecol 1988; 95:659–63
4. Chiazze L Jr, Brayer FT, Macisco Jj J, Parker MP, Duf BJ. The length and variability of the human menstrual cycle. JAMA 1968; 203:377–80
5. Campbell S, Warsof SL, Little D, Cooper DJ. Routine ultrasound screening for the prediction of gestational age. Obstet Gynecol 1985; 65:613–20
6. Robinson HP Gestational age determination: First trimester. In Cherevenak FA, Isaacson GC, Campbell S (Eds). Ultrasound in Obstetrics and Gynecology. Boston: Little, Brown and Company, 1993; 295–304
7. Beazley JM, Underhill RA. Fallacy of the fundal height. Br Med J 1970; 4:404–06
8. Kalish RB, Chervenak FA. Ultrasound assessment of gestational age. Optimal Obstetrics 2002; 1:1–6.
9. Campbell S. The prediction of fetal maturity by ultrasonic measurement of the biparietal diameter. J Obstet Gynaecol Br Commonw 1969; 76:603–06
10. Hadlock FP, Deter RL, Harrist RB, Park SK. Es fetal age: computer assisted analysis of multiple fetal growth parameters. Radiology 1984; 152:497–501

11. Ott WJ. Accurate gestational dating revisited. Am J Perinatol 1994;6:404–08.
12. Kurtz AB, Wapner RJ, Kurtz RJ, Dershaw DD, Rubin CS, Cole-Beuglet C et al. Analysis of biparietal diameter as an accurate indicator of gestational age. J Clin Ultrasound 1980; 8:319–26
13. Mul T, Mongelli M, Gardosi J. A comparative analysis of second-trimester ultrasound dating formulas in pregnancies conceived with artificial reproductive techniques. Ultrasound Obstet Gynecol 1996; 8:397 402.
14. Campbell S, Newman GB. Growth of the fetal biparietal diameter during normal pregnancy. J Obstet Gynaecol Br Commonw 1971; 78:513–19
15. Persson PH, Weldner BM. Reliability of ultrasound fetometry in estimating gestational age in the second trimester. Acta Obstet Gynecol Scand 1986; 65 481–83.
16. Goldstein I, Zimmer EA, Tamir A, Peretz BA, Paldi E. Evaluation of normal gestational sac growth: Appearance of embryonic heartbeat and embryo body movements using the transvaginal technique. Obstet Gynecol 1991; 77:885–88
17. Yeh HC, Rabinowitz JG. Amniotic sac development: Ultrasound features of early pregnancy-the double bleb sign. Radiology 1988; 166:97–103
18. Selbing A. Gestational age and ultrasonic measurement of gestational sac, crown-rump length and biparietal diameter during the first 15 weeks of pregnancy. Acta Obstet Gynecol Scand 1982; 61: 233–35.
19. Bernaschek G, Rudelstorfer R, Csaicsich P. Vaginal sonography versus human chorionic gonadotropin in early detection of pregnancy. Am J Obstet Gynecol 1988; 158:608–12
20. Kohorn EI, Kaufman M.Sonar in the first trimester of pregnancy. Obstet Gynecol 1974; 44:473–83
21. Donald I, Abdulla U. Ultrasonics in obstetrics and gynaecology. Br J Rad 1967; 40:604–11
22. Hellman LM, Kobayashi M, Fillitri L, Lavenhar M, Cromb E. Growth and development of the human fetus prior to the twentieth week of gestation. Am J Obstet Gynecol 1969; 103:789–800
23. Nyberg DA, Filly RA, Mahony BS, Monroe S, Laing FC, Jeffrey RB Jr. Early gestation: Correlation of HCG levels and sonographic identification. AJR 1985; 144:951–54.
24. de Crispigny LC, Cooper D, McKenna M. Early detection of intrauterine pregnancy with ultrasound. J Ultrasound Med 1988; 7:7–10
25. Warren WB, Timor-Tritsch I, Peisner DB, Raju S, Rosen MG. Dating the early pregnancy by sequential appearance of embryonic structures. Am J Obstet Gynecol 1989; 161:747–53
26. Steinkampf MP, Guzick DS, Hammond KR, Bla RE. Identification of early pregnancy landmarks by transvaginal sonography: analysis by logistic regression. Fertility and Sterility 1997; 68:168–70
27. Robinson HP, Fleming JEE. A critical evaluation of sonar “crown-rump length” measurements. British Journal of Obstetrics and Gynaecology 1975; 82:702 10.
28. Daya S. Accuracy of gestational age estimation by means of fetal crown-rump length measurement. Am J Obstet Gynecol 1993; 168:903–08
29. MacGregor SN, Tamura RK, Sabbagha RE, Minogue JP, Gibson ME, Hoffman DI. Underestimation of gestational age by conventional crown-rump length curves. Obstet Gynecol 1987; 70:344–48
30. Filly RA, Hadlock FP. Sonographic determination of menstrual age. In Callen PW (Ed). Ultrasonography in Obstetrics and Gynecology. Philadelphia: WB Saunders, 2000; 146–70.
31. Wisser J, Dirschedl P, Krone S. Estimation of gestational age by transvaginal sonographic measurement of greatest embryonic length in dated human embryos. Ultrasound in Obstetrics and Gynecology 1994; 4:457–62
32. Drumm JE, Clinch J, MacKenzie G. The ultrasonic measurement of fetal crown-rump length as a method of assessing gestational age. British Journal of Obstetrics and Gynaecology 1976; 83:417–21
33. Ewigman BG, Crane JP, Frigoletto FD, LeFevre ML, Bain RP, McNellis D. Effect of prenatal ultrasound screening on perinatal outcome. N Engl J Med 1993; 329:821–27

34. Chervenak FA, McCullough LB. Should all pregnant women have an ultrasound examination? Ultrasound Obstet Gynecol 1994; 4:177–79
35. Romero R. Routine obstetric ultrasound. Ultrasound Obstet Gynecol 1993; 3:303–07
36. Taipale P, Hiilesmaa V. Predicting delivery date by ultrasound and last menstrual period in early gestation. Obstet Gynecol 2001; 97:189–94
37. Campbell S. Gestational age determination: Second trimester. In Cherevenak FA, Isaacson GC, Campbell S (Eds). Ultrasound in Obstetrics and Gynecology. Boston: Little, Brown and Company, 1993; 305 10.
38. Hadlock FP, Deter RL, Harrist RB, Park SK. F circumference: Relation to menstrual age. Am J Radiol 1982; 138:649–53
39. Hadlock FP, Deter RL, Harrist RB, Park S abdominal circumference as a predictor of menstrual age. Am J Radiol 1982; 139:367–70
40. O'Brien G, Queenan JT, Campbell S. Assessment of gestational age in the second trimester by real-time ultrasound measurement of the femur length. Am J Obstet Gynecol 1981; 139:540–45.
41. Mercer BM, Sklar S, Shariatmadar A, Gillieson MS, D'Alton ME. Fetal foot length as a predictor of gestational age. Am J Obstet Gynecol 1987; 156: 350–55.
42. Chitkara U, Lee L, El-Sayed YY et al. Ultrasono-graphic ear length measurement in normal second-and third-trimester fetuses. Am J Obstet Gynecol 2000; 183:230–34
43. Mayden KL, Tortora M, Berkowitz RL, Bracken M, Hobbins JC. Orbital diameters: A new parameter for prenatal diagnosis and dating. Am J Obstet Gynecol 1982; 144:289–97
44. Goldstein I, Tamir A, Zimmer EZ, Itskovitz-Eldor J. Growth of the fetal orbit and lens in normal preg-nancies. Ultrasound Obstet Gynecol 1998; 12:175–79
45. Davies MW, Swaminathan M, Betheras FR. Measurement of the transverse cerebellar diameter in preterm neonates and its use in assessment of gestational age. Australasian Radiology 2001; 45: 309–12.
46. Smith PA, Johansson D, Tzannatos C, Campbell S. Prenatal measurement of the fetal cerebellum and cisterna cerebellomedullaris by ultrasound. Prenat Diagn 1986; 6:133–41
47. Chervenak FA, Skupski DW, Romero R et al. How accurate is fetal biometry in the assessment of fetal age? American Journal of Obstetrics and Gynecology 1998; 178:678–87
48. Benson CB, Doubilet PM. Sonographic prediction of gestational age: Accuracy of second- and third-tri-mester fetal measurements. AJR 1991; 157:1275–77
49. Manning FA. General principles and applications of ultrasonography. In Creasy RK, Resnik R (Eds). Maternal-Fetal Medicine. Philadelphia: WB Saunders Company, 1999; 169–206.
50. Goldstein RB, Filly RA, Simpson G. Pitfalls in femur length measurements. J Ultrasound Med 1987; 6 203–07.
51. Doubilet PM, Benson CB. Improved prediction of gestational age in the late third trimester. J Ultrasound Med 1993; 12:647–53
52. Geirsson RT. Ultrasound: the rational way to determine gestational age. Fetal and Maternal Medicine 1997; 9:133–46
53. Geirrson RT, Have G. Comparison of actual and ultrasound estimated second trimester gestational length in in-vitro fertilized pregnancies. Acta Obstet Gynecol Scand 1993; 72:344–46
54. Geirrsson RT. Ultrasound instead of last menstrual period as the basis of gestational age assignment. Ultrasound Obstet Gynecol 1991;1:212–19.
55. Mul T, Mongelli M, Gardosi J. A comparative analysis of second trimester ultrasound dating formulas in pregnancies conceived with artificial reproductive techniques. Ultrasound Obstet Gynecol 1996; 8:397 402.

Chapter 12
Ultrasound Markers of Chromosomal Anomalies in First Trimester

Giovanni Monni, Maria Angelica Zoppi

INTRODUCTION

The most common chromosomal abnormality at birth is trisomy 21 that affects approximately one out of 700 neonates. However, the frequency of chromosomal abnormalities is higher at earlier stages of pregnancies, considering that a large part of affected fetuses die during the pregnancy. It has been estimated that about 80% of fetuses with trisomy 18, 13 and Turner syndrome spontaneously miscarry from 10 weeks to birth, and in trisomy 21 about 30% of affected fetuses alive at 12 weeks and about 20% of fetuses alive at 16 weeks, die before 40 weeks.[1,2] This means that the probability of encountering a chromosomally abnormal fetus during a first trimester scan is higher than for other gestational stages.

In normal pregnancies, during the first trimester scan by transabdominal or transvaginal technique, it is possible to obtain a lot of information about the placenta, the amniotic fluid, the cord, to visualize some fetal structures, evaluate fetal growth, measure the heart rate and to assess some fetal functional aspects.

Fetuses with abnormal karyotype frequently have structural malformations, whose recognition is possible at the first trimester, or manifest some slight variations of morphological or functional parameters, occasionally manifesting as transient markers, that are not always obvious, and which require at times more specific investigation carried out by definite techniques.[1]

By 10 weeks onwards, it is possible to offer a safe and accurate technique for prenatal diagnosis of chromosomal abnormalities using the first trimester chorionic villus sampling.[3] The recognition of fetuses at higher risk for chromo-somopathies, by first trimester ultrasound, either in a general population or in high risk groups, could give the unique opportunity to the clinician and the parents to know the fetal karyotype early in pregnancy by perfoming first trimester diagnosis.

FETAL GROWTH

An impaired fetal growth could be associated with chromosomal abnormalities. In the first trimester, the measurement of the crown- rump length (CRL) is useful to detect this

finding. Drugan et al reported that a fetal CRL smaller more than 7 mm indicate a three time higher risk for chromosome abnormalities than the maternal background risk.[4]

HEART RATE

Fetal heart rate is detectable by transvaginal ultrasound at the end of the 6th week. Mean heart rate is about 100 beats per minute at 6 weeks, and increases to a peak (about 160–170 beats per minute) at 9 weeks and then slightly decreases. Abnormal heart rate patterns can be found in several chromosomal abnormalities at 10–14 weeks of gestation. A significant mean increase in the fetal heart rate has been shown in fetuses with trisomy 21, trisomy 13 and Turner syndrome, while in trisomy 18 and triploidy the cardiac frequency is significantly reduced.[5] The differences

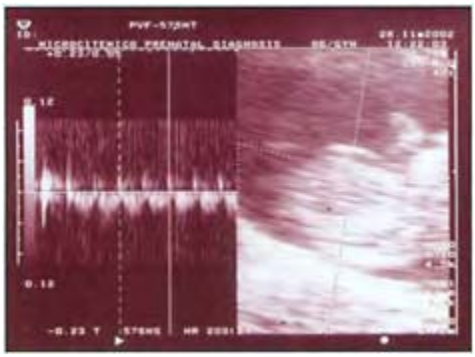

Figure 12.1: Fetal heart rate in a first trimester fetus with trisomy 13:208 beats per minute

in mean fetal heart rate are not used at present to discriminate in practice affected fetuses from normals (Fig. 12.1).

FETAL STRUCTURAL MALFORMATIONS

Most part of fetuses with an abnormal karyotype have structural malformations that are evident at ultrasound examination in the second and third trimester.[1] First trimester studies of fetal anatomy is limited, due to technical problems and to the natural development of fetal organs, but some malformation and phenotypical expressions of chromosomal abnormalities could be detected by transabdominal and transvaginal examination, especially at 11–14 weeks scan: malformations in the skull and face as holoprosencephaly (occurs

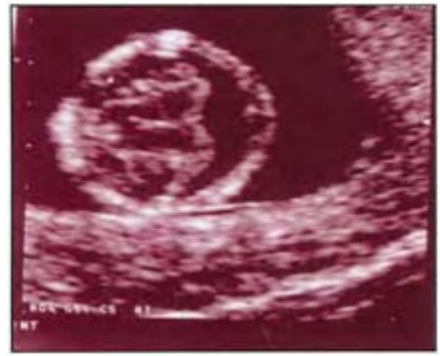

Figure 12.2: Holoprosencephaly

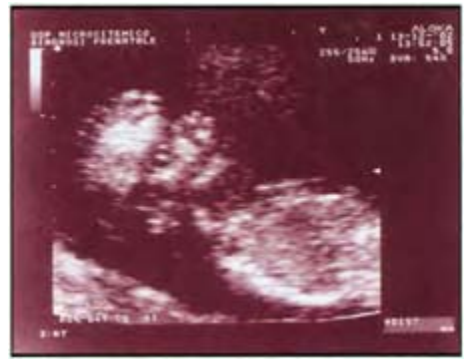

Figure 12.3: Facial cleft

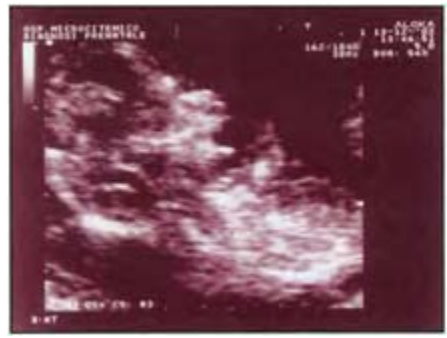

Figure 12.4: Micrognathia

in about 3% of trisomy 18, 39% of trisomy 13) (Fig. 12.2), facial clefts (Fig. 12.3) (occur in about 1% of trisomy 21, 10% of trisomy 18, 39% of trisomy 13, 2% of triploidy), micrognathia (Fig. 12.4) (occurs in about 1% of trisomy 21, 53% of trisomy 18, 9% of

trisomy 13, 44% of triploidy); malformation in the neck as cystic hygromata (occurs in about 88% of Turner syndrome); malformations of the chest as cardiac abnormalities (occur in about 26% of trisomy 21, 52% of trisomy 18, 43% of trisomy 13, 48% of Turner syndrome, 16% of triploidy); malformations of the abdomen as exomphalos (Fig. 12.5) (occurs in about 31% of trisomy 18, and 17% of trisomy 13).

NUCHAL TRANSLUCENCY

The first trimester nuchal translucency (NT) is the

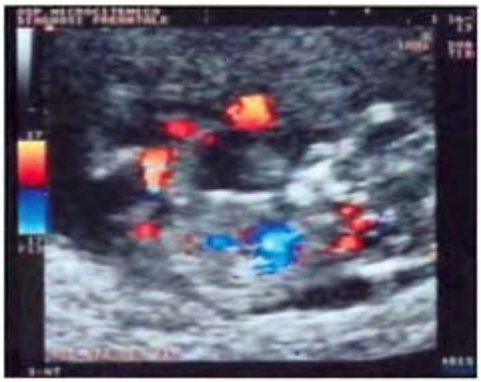

Figure 12.5: Exomphalos

anechoic space located behind the fetal neck, that is visible and measurable in almost all fetuses from 10 to 14 weeks (Fig. 12.6).[6] The original technique for the detection and measurement of NT includes: fetal crown-rump length between 38 mm and 84 mm (between 10.3 and 13.6 weeks). For a better definition of the fetal anatomy, it was subsequently preferred to measure the NT for the screening of aneuploidies from a CRL of 45 mm (11th weeks).[7] The fetus should be imaged in a sagittal section; with a magnification of the fetal image at 75% of the screen; and the amnion has to be clearly distinguished from the fetal skin. The measurement should be performed at the level of the maximum thickness of the subcutaneous

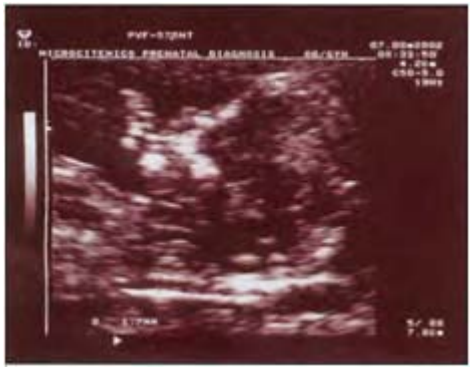

Figure 12.6: Nuchal translucency

translucency between the skin and the soft tissues overlying the cervical spine, with calipers placed “on to on” in the transonic space and the measurement taken at least 0.1 mm. The biggest of three measurements has to be considered. The scanning is preferably done by transabdominal probe, but in some difficult cases the transvaginal probe is employed.

About 75–80% of fetuses with trisomy 21 at 11–14 weeks scan present an enlarged nuchal translucency, while it is visible in about 5–10% of normal karyotype fetuses (Fig. 12.7). An enlarged fetal nuchal translucency can also be found in other chromosomopathies such as trisomy 18, trisomy 13, Turner syndrome, Klinefelter syndrome and triploidy.[7,8]

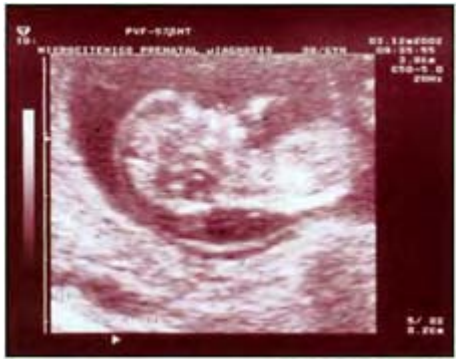

Figure 12.7: Enlarged nuchal translucency

Several are the potential causes related to the accumulation of fluid in the fetal nuchal: cardiac abnormalities and other structural defects, failure or delay in the development of the lymphatic system (Turner syndrome), alterations in the extracellular matrix of the

skin (trisomy 21 fetuses). First trimester nuchal translucency is a transient marker, that in most part of the cases disappears by the end of the first trimester.

The maternal age-related risk for trisomy 21, combined with the likelihood ratio calculated from the thickness of nuchal translucency in trisomy 21 and normal fetuses, has been proposed for the screening for trisomy 21. For a risk greater than or equal to 1 in 300, the sensitivity for trisomy 21 has been estimated to be 82%, with 8% false positive rate.[7] There is evidence that the nuchal translucency could be used as a reliable screening test only if the measurement is performed according to the standard technique, with adequate training of operators and a constant audit of the results.[9,10] In order to increase the sensitivity and reduce the false-positive rate, the risk obtained by maternal age and nuchal translucency could be combined with some maternal serum markers, such as first trimester PAPP-A and free beta-hCG levels. With a false-positive rate of about 3%, the sensitivity for trisomy 21 cases increased to 90%.[11]

MEGACYSTIS

At 10–14 weeks, the fetal bladder is visible in almost all fetuses of at least 67 mm of CRL, and first trimester megacystis is considered when the longitudinal diameter is 6–8 mm or the bladder diameter/CRL ratio is 13% or more (Fig. 12.8). First trimester megacystis has a frequency of about 1 case in 1633, and it resolves in about 60% of cases.[12] Chromosomal abnormalities occur in about 20% of cases of megacystis, and spontaneous resolution of megacystis in the second trimester is not considered as a reassuring finding.

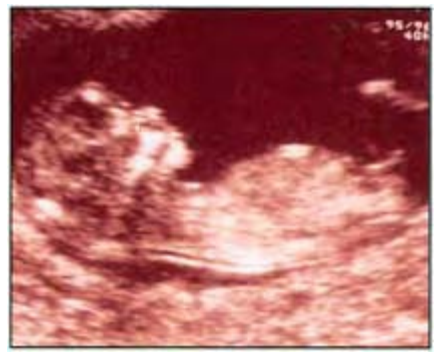

Figure 12.8: Megacystis

ABSENT NASAL BONE

Trisomy 21 fetuses, among other skeletal abnormalities described by radiological and anatomical

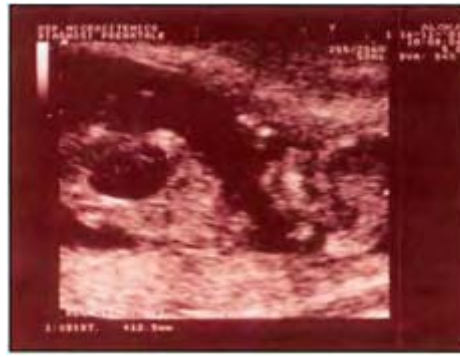

Figure 12.9: Nasal bone

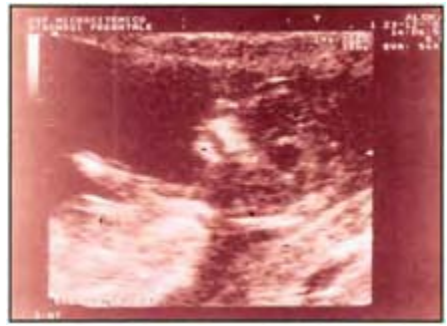

Figure 12.10: Absent nasal bone

studies, present an absence or delay in the development of the nasal bones. The absence of nasal bone is recognizable by prenatal ultrasound in first and second trimester fetuses, and about two-thirds of fetuses with trisomy 21 show an absent nasal bone (Figs 12.9 and 12.10).[13–15] There is evidence that an appropriate technique is required to visualize the fetal nasal bone by ultrasound. As the absence of nasal bone does not appear to be related to the fetal nuchal translucency thickness, the two signs could be combined in a single test for prenatal screening of trisomy 21 that seems to be very accurate (about 90% of sensitivity with 3% of false-positive rate). The absence of nasal bone has been recognized also in first trimester fetuses affected by trisomy 18, Turner syndrome, and trisomy 9.

UMBILICAL CORD DIAMETER

The measurement of the umbilical cord diameter at 10–14 weeks scan, can identify fetuses at higher risk for aneuploidies. An incresed diameter (above the 95th centile of reference values) is more frequent among abnormal karyotype fetuses than in normal fetuses.[16]

UMBILICAL ARTERY PULSATILITY INDEX

In the third trimester, the placenta of trisomic fetuses demonstrate a significantly lower small muscular artery number and a small muscular artery/villi ratio, which is associated with abnormal values of impedance in the umbilical cord arteries, detectable by pulsed Doppler. Conflicting results have been obtained about associating a higher than normal umbilical artery pulsatility index (UAPI) in fetuses with trisomy 21 in the first trimester. Martinez et al reported values of UAPI significantly higher in cases of trisomy 21 compared to normal fetuses,[17] whilst Brown et al,[18] in 19 trisomy 21 fetuses with enlarged NT, and Jauniaux et al,[19] in 11 cases of trisomy 21, reported that UAPI in these fetuses was not significantly different from normal. Our research did not reveal a significant difference in the UAPI values of trisomy 21 fetuses with enlarged NT and normal fetuses, with large and normal NT.[20] These differences could be explained in the limited number of each series.

DUCTUS VENOSUS VELOCIMETRY

The presence of congenital heart defects or the delayed development of certain cardiovascular structures, that are frequent in chromosomal abnormalities, could determine a perturbation of fetal hemodynamics, sometimes temporary, that are detectable at the first trimester study of fetal circulation by Doppler velocimetry. At 11–14 weeks, in the same fetal position for NT measurement, ductus venosus is visualized by color Doppler and the flow waveform is obtained by placing the pulsed Doppler sample volume on the portion immediately above the umbilical sinus.

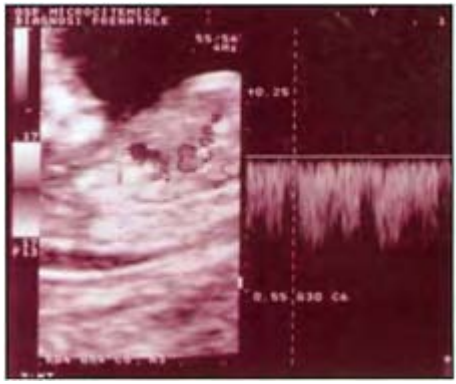

Figure 12.11: Ductus venosus flow waveform

Figure 12.12: Absent flow velocity during the atrial contraction in the ductus venosus

The ductus venosus waveform shows a peak of forward flow in sistole, a second lower peak in diastole and a small forward velocity during atrial contraction (ACV) (Fig. 12.11). An increase of the end-diastolic pressure in the right atrium cause an alteration of the ductus venosus waveform, with an ACV that becomes absent (Fig. 12.12) or inverted (Fig. 12.13).

Fetuses with enlarged NT, show in about 40% of cases an abnormal flow in the ductus venosus, probably because this percentage is the proportion of enlarged NT caused by abnormal circulation

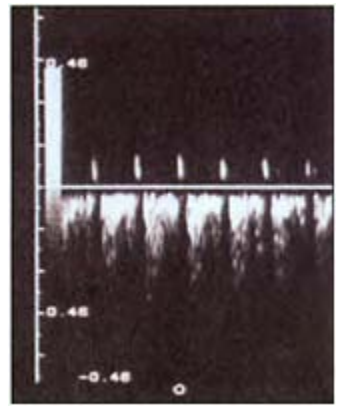

Figure 12.13: Reverse flow during the atrial contraction in the ductus venosus

factors. Absence or inversion of ductus venosus ACV has been seen in about 70–90% of fetuses with a chromosomal abnormality. Abnormal ductus venosus flow waveform analysis has been proposed to discriminate cases at higher risk of chromosomopathies and heart defects among fetuses with enlarged NT, and to decrease the rate of false-positives and the number of prenatal invasive procedures.[21,22]

REFERENCES

1. Snijders RJM, Nicolaides K. Ultrasound markers for chromosomal defects. London, UK: Parthenon Publishing, 1996.
2. Snijders RJM, Sundberg K, Holzgreve W, Henry G, Nicolaides K. Maternal age and gestation-specific risk for trisomy 21. Ultrasound Obstet Gynecol 1999; 13:167–70.
3. Monni G, Ibba RM, Lai R, Cau G, Mura S, Rosatelli C, Olla G, Cao A. Early Transabdominal chorionic villus sampling in couples at high genetic risk. Am J Obstet Gynecol 1993; 168:170–73
4. Drugan A, Johnson MP, Evans MI. Ultrasound screening for fetal chromosome anomalies. Am J Med Genet 2000; 90:98–107
5. Liao AW, Snijders R, Geerts L, Spencer K, Nicolaides K. Fetal heart rate in chromosomally abnormal fetuses. Ultrasound Obstet Gynecol 2000; 16:610–13
6. Nicolaides KH, Azar G, Byrne D, Mansur C, Marks K. Fetal nuchal translucency screening for chromosomal defects in first trimester of pregnancy. Br Med J 1992; 304:867–69
7. Snijders RJM, Noble P, Sebire N, Souka A, Nicol KH. UK multicentre project on assessment of risk of trisomy 21 by maternal age and fetal nuchal-translucency thickness at 10–14 weeks of gestation. Lancet 1998; 352:343–46
8. Zoppi MA, Ibba RM, Putzolu M, Floris M, Monni G. Assessment of risk for chromosomal abnormalities at 10–14 weeks of gestation by nuchal translucency and maternal age in 5210 fetuses carried out at a single center. Fetal Diagn Ther 2000; 15:170–73
9. Monni G, Zoppi MA, Ibba RM, Floris M. Fetal nuchal translucency test for Down's syndrome. Lancet 1997; 350:1631
10. Zoppi MA, Ibba RM, Floris M, Monni G. Fetal nuchal translucency screening in 12,495 pregnancies in Sardinia. Ultrasound Obstet Gynecol 2001; 18: 649–51.
11. Spencer K, Souter V, Tul N, Snijders R, Nicolaides A screening program for trisomy 21 at 10–14 weeks using fetal nuchal translucency, maternal serum free beta-human chorionic gonadotropin and pregnancy-associated plasma protein-A. Ultrasound Obstet Gynecol 1999; 13:231–37
12. Sebire NJ, Von Kaisenberg C, Rubio C, Snijders RJ, Nicolaides KH. Fetal megacystis at 10–14 weeks of gestation. Ultrasound Obstet Gynecol 1996;8: 387–90.
13. Cicero S, Curcio P, Papageorghiou A, Sonek J, Nicolaides KH. Absence of nasal bone in fetuses with trisomy 21 at 11–14 weeks of gestation: an observational study. Lancet 2001; 358:1665–67
14. Monni G, Zoppi MA, Ibba RM. Absence of nasal bone and detection of trisomy 21. Lancet 2002; 359:1343
15. Monni G, Zoppi MA, Ibba RM, Floris M, Manca F, Axiana C. Absence of nasal bone and aneuploidies at 11–14 weeks in an unselected population. Ultrasound Obstet Gynecol 2002; 20(S1):89
16. Ghezzi F, Raio L, Di Naro E, Franchi M, Buttarelli M, Schneider H. First trimester umbilical cord diameter: a novel marker of fetal aneuploidy. Ultrasound Obstet Gynecol 2002; 19:235–39.
17. Martinez Crespo JM, Comas C, Ojuel H, Puerto B, Borrell A, Fortuny A. Umbilical artery pulsatility index in early pregnancies with chromosome anomalies. Br J Obstet Gynaecol 1996; 103:330–34.

18. Brown R, Di Luzio L, Gomes C, Nicolaides KH. The umbilical artery pulsatility index in the first trimester: i there an association with increased nuchal trans-lucency or chromosomal abnormality? Ultrasound Obstet Gynecol 1998; 12:244–47.
19. Jauniaux E, Gavril P, Khun P, Kurdi Wesam, J, Nicolaides KH. Fetal heart rate and umbilicoplacental Doppler flow velocity waveforms in early pregnancies with a chromosomal abnormality and/ or an increased nuchal translucency thickness. Hum Reprod 1996; 11:435–39
20. Zoppi MA, Ibba RM, Putzolu M, Floris M, Monni G. First trimester umbilical artery pulsatility index in fetuses presenting enlarged nuchal translucency. Prenat Diagn 2000; 20:701–04
21. Matias A, Montenegro N. Ductus venosus blood flow in chromosomally abnormal fetuses at 11 to 14 weeks of gestation. Semin Perinatol 2001; 25:32 37.
22. Zoppi MA, Putzolu M, Ibba RM, Floris M, Monni G. First trimester ductus venosus velocimetry in relation to nuchal translucency thickness and fetal karyotype. Fetal Diagn Ther 2002; 17:52–57

Chapter 13
Ultrasound Evaluation of Abnormal Early Pregnancy

Asim Kurjak, Sanja Kupesic, Ana Tripalo

The first trimester is characterized by many important landmarks with regard to the ultimate outcome of pregnancy and is mostly defined by the first 100 days of pregnancy. Woman becomes aware of her pregnancy after missing her last period and in that time she is already at least 4 weeks pregnant.[1]

A positive pregnancy test opens Pandora's box, offering more questions than answers. Although, a positive pregnancy test most likely suggests an intrauterine pregnancy, production of human cho-rionic gonadotropin (hCG) occurs also by tumors (dysgerminoma, choriocarcinoma) or maldevelopment of pregnancy (ectopic pregnancy or mola hydatidosa).[2] Falsely positive results are mainly obtained in the case of proteinuria, erithrocyturia or some drug intake (e.g. tranquilizers). The role of the ultrasonographer in these situations is to help the practicing clinician to evaluate pregnancy and determine the exact pregnancy status.

INTRODUCTION

Ultrasound evaluation of an early pregnancy includes detection of the pregnancy location (extrauterine or intrauterine), the type of pregnancy (one—fetus pregnancy, multiple pregnancy, molar pregnancy), the viability of the pregnancy and establishment of the gestational age. Evaluating pregnancy, the ultrasonographer also recognizes the complications that may occur in first trimester. Ultrasound examination has become the "golden standard" in follow-up of the development and complications of early pregnancy. With introduction of transvaginal sonography (TVS), a possibility for early morphological and biometrical ultrasound examinations has been significantly improved. Application of color Doppler ultrasound has enabled functional hemodynamic presentation and evaluation soon after implantation.

Basic ultrasound markers for normal pregnancy are intrauterine gestational sac, morphologically normal embryo and its heart action (Scheme 13.1). Normal embryonic echo, in 90% of the cases suggests normal pregnancy.

The possibility of early pregnancy loss is very high and can be related to fetal biometry (Table 13.1).[3]

There is discordance between the clinicians' and embryologists' statements in determining the

Scheme 13.1: Basic ultrasound markers for normal intrauterine pregnancy

Table 13.1: The risk of early pregnancy loss relation to CRL values

CRL *(mm)*	*Possibility for pregnancy loss (%)*
<5	8
6–10	3–4
>10	below 1
Adapted from ref. 3.	

gestational age. Clinicians define gestational age from the first day of the last menstrual period. However, embryologists define the gestational age from the time of conception. Therefore, when talking about embryonic period embryologists define it as a period of organogenesis from the 3rd to the 8th week after conception, while obstetricians define it as a period from 5th to 10th week after first day of the last menstrual period.[4] Fetal period begins after 8th week according to embryologists, i.e. after 10th week according to clinicians. As the onset of marrow formation in the humerus (the end of embryonic period according to the embryologists that occurs 56–57 day after ovulation)[5] is not visible by the ultrasound, for ultrasound examination and evaluation of the embryo/fetus, Blass[6] suggests that disappearance of the physiological midgut herniation could be orientation as the end of embryonic period. The physiological midgut herniation is a macroscopically visible process, which starts after 7 completed weeks. The retraction of the bowel into the abdominal cavity occurs between approximately 10.5 to 12 completed weeks.[7] Application of 3D and 4D ultrasound seems to be advantageous in determining the points for differentiation of the embryo and the fetus.

EARLY PREGNANCY FAILURE AND VAGINAL BLEEDING

Early pregnancy failure is defined as a pregnancy that ends spontaneously before the embryo is detected by ultrasound at the gestational age in which visualization of viable embryo should occur. The most common pathological symptom of the early pregnancy failure is the vaginal bleeding. One of the main problems in diagnosis of early pregnancy failure is why vaginal bleeding occurs. When it happened, all clinicians should answer several questions that can radically alter the management:

1. Is the patient pregnant?

2. Is the embryo viable or not?

3. What is the gestational age?

4. Is there any evidence to suggest that the pregnancy is ectopic?

5. If an abortion occurs, is it complete or incomplete?

6. Is there any associated pelvic mass?

Only differentiation and accurate estimation of the pregnancy status and embryo/fetus status make it possible to obtain appropriate therapeutic measures to cases where a normal outcome of the pregnancy can be expected. At this moment, ultrasonography is considered to be the best diagnostic method for detection of early pregnancy complications. For these patients the skill of the ultrasonographer is very important, since the accurate diagnosis of pregnancy failure will often result in surgical intervention.

Clinical presentation of the symptoms such as vaginal bleeding and abdominal pain, with or without the expulsion of products of conception[8] is suspected of a spontaneous abortion. For ultrasound evaluation, it is important to distinguish threatened, complete and incomplete abortion.

Threatened Abortion (Abnormal Vaginal Bleeding)

Threatened abortion is the clinical term used to describe symptom such as vaginal bleeding during the first 20 weeks of pregnancy in women who, on the basis of clinical evaluation, are considered to have a potentially living embryo/fetus. The main problem in the management of these patients is in confirming the accurate diagnosis. The threatened and spontaneous abortions together present the most common complications of early pregnancy. Sometimes we are not even aware that a woman has been pregnant and that she aborted. If we take into the consideration these cases also, incidence of spontaneous abortions is estimated up to 70%.[9] Only 1/3 of embryos continue further development, and 50% of abortions occur before the term of expected menstruation.[9,10] These types of abortion usually cause the symptoms of sterility rather than infertility, because it seems

that a woman is not even able to conceive. Thirty to forty percent of pregnancies fail after implantation, and only 10–15% manifest with clinical symptoms.[10,11]

In patients with a normal intrauterine pregnancy, bleeding from the chorion frondosum is undoubtedly the most common source of vaginal bleeding during the first trimester.

The development of transvaginal sonography has allowed the improved assessment of patients presenting vaginal bleeding during the first half of pregnancy, clarifying the differential diagnosis of missed abortion, ectopic pregnancy, blighted ovum and threatened abortion with a living embryo. Embryo vitality can be established reliably by documenting cardiac activity on realtime, B-mode or color Doppler ultrasonography.

Sonographic evidence of vaginal bleeding can be identified as a perigestational hemorrhage in 5–22% of women with symptoms of threatened abortion. However, some precautions must be taken, because the perigestational hemorrhage is occasionally difficult to distinguish from a blighted twin. The prognostic significance of identifying perigestational hemorrhage during the first trimester remains uncertain. Most of the small hemorrhages resolve without clinical sequelae, while in some cases spontaneous abortion may occur.

Incomplete and Complete Spontaneous Abortion

As a definition, **incomplete abortion** is the passage of some, but not all fetal or placental tissue through the cervical canal. In **complete abortion,** all products of conception are expelled through the cervix.[12] In incomplete abortion, the uterine debris may consist of a combination of products of conception, blood and decidua.[13]

Transvaginal ultrasonography plays important role in evaluating uterine cavity in spontaneous abortion due to detection of the retained products of conception. Retained products of conception after abortion may cause bleeding or chorio-amnionitis.[14] An echogenic and vascularized mass within the uterine cavity supports the diagnosis of retained products of conception.[15] Wong and co-workers[16] reported 100% sensitivity and 80% specificity of the transvaginal sonographic exami-nation in differentiation of the complete from incomplete spontaneous abortions. The sono-graphic definition of incomplete abortion is a bilayer endometrial thickness of more than 8 mm. In 29% of patients with incomplete abortion transvaginal sonography obviated the need for surgical intervention, but in 30% of patients with complete abortion detected retained products of conception. Adding color Doppler examination to basic transvaginal 2D ultrasound examination increases detection rate of the retained tropho-blastic tissue.[17–19] In their recent paper, Alcázar and co-workers[20] suggested that transvaginal color Doppler is a helpful method for detecting retained trophoblastic tissue in patients with first-trimester spontaneous abortion. They analyzed 62 patients with positive urine pregnancy test and history of heavy vaginal bleeding whose gestational age was less than 14 weeks. In each patient transvaginal ultrasound (TV US) and βHCG serum measure-ments were performed at the time of admission to the hospital. Retained trophoblastic tissue was suspected in the presence of low resistance flow (RI<0.45) within the myometrium or just beneath the endometrial- myometrial interface. In 29% of women retained trophoblastic tissue was suspected and in 88.9% of these patients pathological analysis was positive for retained trophoblastic tissue. The authors suggested to perform B mode and color

Doppler examination when there is suspicion on retained trophoblastic tissue (Figure 13.1).

Recent studies demonstrate that risk for *repea-ted* spontaneous abortion depends exclusively on the number of previous spontaneous abortions and their cause. Even though, many different risk factors have been thoroughly researched, around

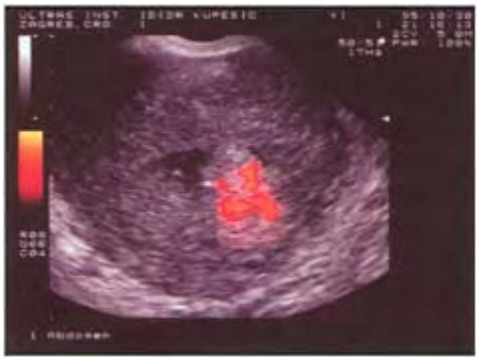

Figure 13.1: Transvaginal power Doppler Image of an irregular uterine cavity. Note abundant vascularity demonstrating residual placental tissue

60% of unsuccessful pregnancies remain a "causa ignota".[21] The important criteria for evaluation of pregnancy loss are:[22]

- Always to keep in mind that the risk of spontaneous miscarriage is higher in older women;
- Try to uncover causes for repetitive first-trimester miscarriages. Karyotyping of couples will reveal that 3 to 8% have some abnormality, most frequently balanced chromosomal rear-rangement, a translocation (other abnormali-ties: sex chromosome mosaicism, chromosome inversions or ring chromosomes). Besides spontaneous miscarriages, these abnormalities are associated with high risk of malformations and mental retardation. Karyotyping is espe-cially vital if the couple has had a malformed infant or fetus in addition to miscarriages in previous pregnancies.
- Smoking, alcohol, and heavy coffee consump-tion have been reported to be associated with an increased risk of recurrent pregnancy losses.[23]
- Patients with thyroid disease or uncontrolled diabetes mellitus may suffer spontaneous miscarriages although these diseases are not causes of recurrent miscarriages.
- Uterine abnormalities can result in impaired vascularization of a pregnancy, limited space for a fetus due to distortion of the uterine cavity, and incoordinate uterine contractility (See the chapter: Sonographic imaging in infertility).
- Looking at the first trimester miscarriage, a firm correlation with bacterial vaginosis-associated microorganisms was found in the study of Donders and colleagues.[24]

• The major cause of thrombosis in pregnancy is an inherited predisposition for clotting, especially the factor V Leiden mutation.

Immunological problems can be classified into two groups: autoimmunity (self antigens), and alloimmunity (foreign antigens). In the autoimmu-nity, a humoral or cellular response is directed against a specific component of the host. The lupus anticoagulant and anticardiolipin antibodies are antiphospholipid antibodies, which arise as the result of an autoimmune disease. Several series demonstrated that 10–16% of women with recurrent miscarriages have had anti-phospholipid antibodies.[9,25] These antibodies are also associated with growth retardation and fetal death in addition to recurrent miscarriages. Preferred treatment for significant titers of antiphospholipid antibodies consists of the combination of low-dose aspirin (80 mg daily) and low-dose heparin as soon as pregnancy is diagnosed.[26,27] Unfortunately, treatment is not always successful. Alloimmunity refers to all causes of pregnancy losses related to an abnormal maternal immune response to antigens on placental or fetal tissues.

MISSED ABORTION

The diagnosis of missed abortion is determined by the ultrasound identification of an embryo/fetus without any heart activity. It is relatively easy to make this diagnosis by means of the transvaginal color Doppler ultrasound. The main parameter is the absence of the heart beats and the lack of color flow signals at its expected position after the 6th gestational week (Fig. 13.2).

With the aid of sensitive color Doppler equipment it is possible to demonstrate two types

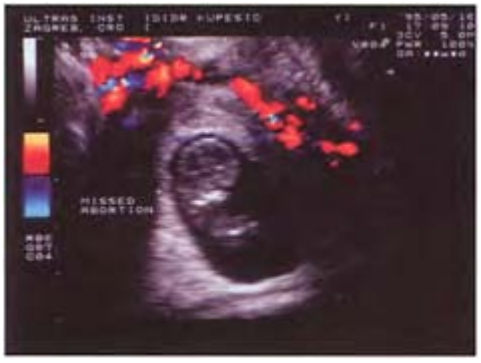

Figure 13.2: Transvaginal color Doppler scan of a missed abortion. Prominent blood flow signals are obtained from the spiral arteries, while absence of heart activity is noted by color Doppler

of blood flow velocity waveforms from the intervillous space[28] (pulsatile arterial-like and continuous venous-like patterns) in both, normal and abnormal early pregnancies. Studies did not show any difference in terms of RI and PI of the intervillous arterial blood flow between women with missed abortion and those with normally developing pregnancy. In long-standing demise, the cessation of the embryonic portion of placental circulation leaves the fluid pumping action of the trophoblast unaffected, as it remains nourished by the maternal side of circulation. As a consequence, the embryonic circulation no longer drains a trophoblast-conveyed fluid in the villous stroma. Progressive accumulation of the fluid may result in a significant reduction of the intervillous blood flow impedance. Lower impedance to blood flow, observed in spiral arteries, indicates that a massive and continuous infiltration of the maternal blood without effective drainage causes further disruption of the maternal embryonic interface resulting in abortion. These changes can be effectively studied by 2D and 3D power Doppler. Histological studies of the material obtained after spontaneous abortions have shown insufficient trophoblastic invasion into the spiral arteries. Such findings suggest defective transformation of spiral arteries as a possible cause of spontaneous abortion in these cases. Being aware that chromosomal abnormalities are one of the most important factors for spontaneous abortion occurring in more than 50% it is not surprising that Doppler studies do not demonstrate any significant difference in terms of vascular resistance between normal pregnancies and those with missed abortions. Pellizzari and co[29] pointed out that blood flow analysis of uterine artery does not have any clinical role in the management of early pregnancies complicated by uterine bleeding.

Acharya and Morgan[30] compared 2D and 3D ultrasound findings in the first trimester normal and abnormal pregnancies. 3D ultrasound volume measurements of intrauterine contents in normal and failed pregnancies correlated well with conventional 2D ultrasound. 3D volumetric assessment does not improve the diagnosis of abortion, but it can help in predicting pregnancies that will fail and gives possibility to determine the appropriate management regime.

BLIGHTED OVUM (ANEMBRYONIC PREGNANCY)

Blighted ovum (anembryonic pregnancy) refers to a gestational sac in which the embryo either failed to develop or died at a stage too early to visualize. The diagnosis of anembryonic pregnancy is based on the absence of embryonic echoes within the gestational sac, large enough for such structures to be visualized, independent of the clinical data or menstrual cycle. Advances in transvaginal sonography allow us to detect this kind of abnormality at a mean sac diameter of 1.5 cm.[31] If the volume of the sac is less than 2.5 ml and is not increasing in size by at least 75% over a period of 1 week, the definition of this pathological condition in early pregnancy is a blighted ovum. A large empty sac usually measures between 12 and 18 mm in mean diameter. To confirm the diagnosis, these findings should be correlated with other clinical and sonographic data including the presence of a yolk sac.

Transvaginal sonography can clearly detect existing, but a non-living embryo (embryonic demise) in some cases that undoubtedly would have been diagnosed as a blighted ovum if trans-abdominal sonography was the only examination performed. What

the ultrasonographer would detect on his screen depends on gestational age and when the resorption process begun.

In anembryonic pregnancy, a fertilized ovum develops into a blastocyst, but the inner cell mass and resultant embryonic pole never develops. The gestational sac invades the endometrium and acts partly like a normally developing pregnancy. The sincytiotrophoblast invades the endometrium and produces human chorionic gonadotropin. Therefore, pregnancy tests are positive and clinical signs of the pregnancy occur. But, the gestational sac fails to grow and develop normally, and the uterus fails to develop as expected. In this condi-tion, the incidence of chromosomal abnormality is high. Generally, one can estimate that about 15–20% of all human pregnancies diagnosed before the end of the first trimester terminate in spontaneous abortion.

With falling levels of human chorionic gonado-tropin, progesterone and estrogen, the feeling of being pregnant and the associated clinical signs of pregnancy that occurred earlier are lost. The diagnosis of a blighted ovum is in 100% of cases by 2D real-time ultrasonography examinations when performed a week apart after absence of embryo development has been confirmed.

Using color Doppler ultrasound in evaluation of the normal and abnormal pregnancies, Kurjak and Kupesic[28] hypothesized that lower PI from the intervillous space of the anembryonic pregnancy may reflect changes in the placental stroma, where individual villi are prone to edema. Sometimes even the embryos that measure 1 cm by trans-vaginal sonography may be absorbed totally after prolonged retention. Consequently, a trophoblast conveyed embryonic circulation no longer drains fluid in the villous stroma. Ongoing processes result in disruption of the maternal-embryonic interface, and finally abortion (Fig. 13.3).

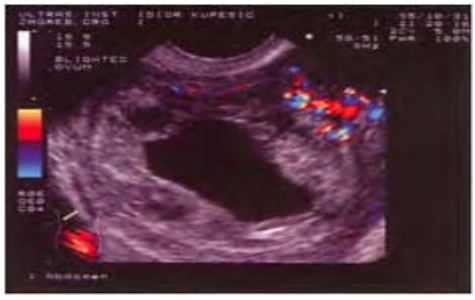

Figure 13.3: Transvaginal sonogram of an anembryonic pregnancy. Note the absence of the living embryo and the yolk sac indicative of an anembryonic pregnancy. Color Doppler image presents signals obtained from the spiral arteries and other maternal vessels

Analyzing intervillous circulation as one of the first ultrasonographic signs of the pregnancy, studies demonstrated lower vascular resistance of the arterial-like signals in the patients with blighted ovum when compared with the normal pregnancies.

Scheme 13.2 offers way of menagement for women presented with vaginal bleeding.

INTRAUTERINE HEMATOMAS

Intrauterine hematomas are defined as sonolucent crescent or wedge-shaped structures between chorionic tissue and uterine wall, or fetal mem-branes.[32] By localization we can divide them into retroplacental, subchorionic, marginal and supracervical. The most severe are large, central, retroplacental hematomas in which separation of chorionic tissue from basal deciduas occurs by mechanism similar to a mechanism of abruption of the placenta.

The most common causes of intrauterine hematoma are:

- Disturbed trophoblast invasion and defect in spiral arteries transformation
- Infection
- Mechanical factors
- Autoimmune factors
- Hematological factors.

It is important to stress that finding of an intrauterine hematoma does not immediately indicate the likelihood of a spontaneous abortion. As the measure of precaution rather classify this pregnancy into a high-risk group with additional necessity for further intensive monitoring. Prognostically, there are two main elements, which determine the pregnancy outcome. First one is the location of the hematoma. According to Kurjak and associates, location is more predictive sign than the volume of hematoma.[32,33] It is likely that if the bleeding occurs at the level of the definitive placenta (under the cord insertion), it may result in placental separation and subsequent abortion.[34] Conversely, a subchorionic hematoma detaching only a membrane opposite to the cord insertion could probably reach a significant volume before it affects normal pregnancy development.[35] Supracervical hematoma has much better prognosis because it is easily drained into the vagina and for this reason it doesn't represent mechanical factor for compression of the uteroplacental vessels. Higher incidence of spontaneous abortions has been reported in the cases where hematoma has been localized in the fundal or corporal region, which could be attributed to placental location in that area.[33] Retropla-cental or central hematomas have the worst prognosis because they cause the largest incident of the uteroplacental circulation and placental tissue (Fig. 13.4).[36] The pathological mechanism is probably placental abruption, in which retro-placental clots are located between the placenta and myometrium, and pre-placental clots are found between the amniotic fluid and the placenta later in the second trimester.

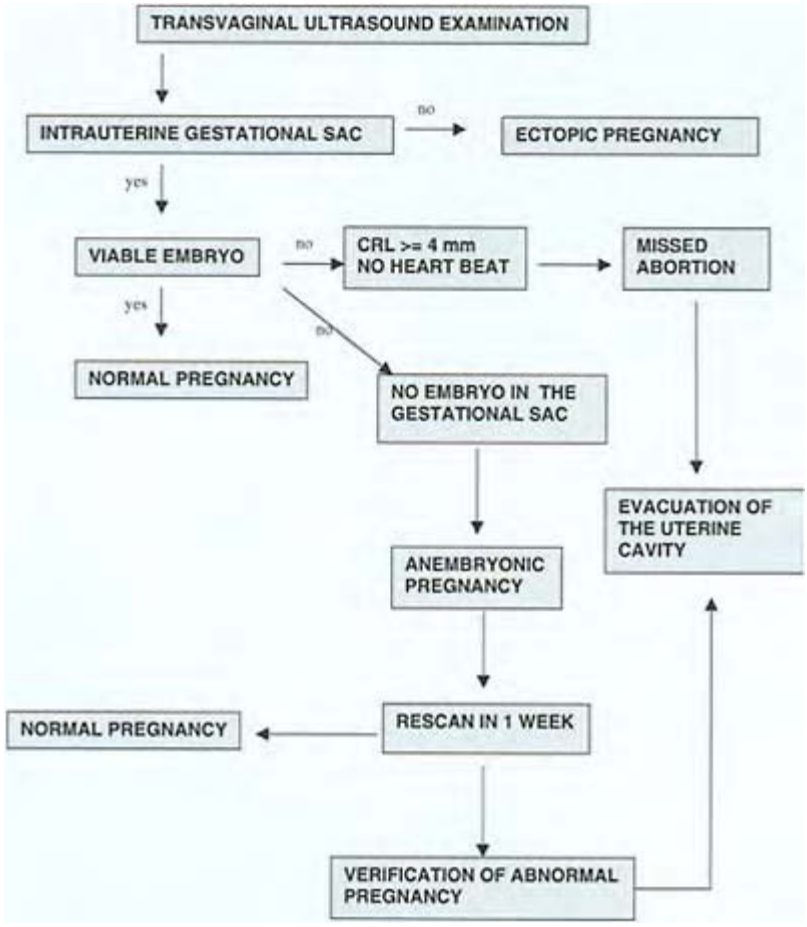

Scheme 13.2: Ultrasound revaluation of women with vaginal bleeding and positive pregnancy test

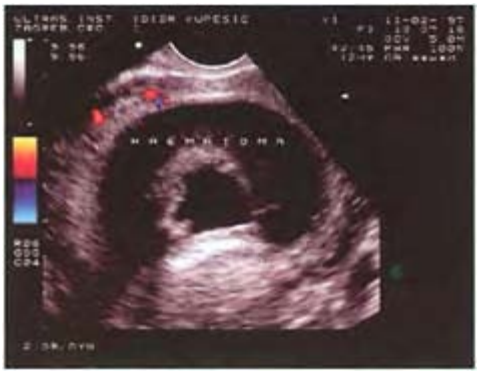

Figure 13.4: Transvaginal sonogram of a large-volume hematoma located in fundal-corporeal region. Note the uterine blood flow signals on the side of the hematoma

Table 13.2 presents data on hematoma site and pregnancy outcome.[32] Kurjak and co-workers reported on increased resistance to blood flow and decrease in velocity through spiral arteries on the side of subchorionic hematoma, which is a consequence of mechanical compression of hematoma itself.[32,37] With the progression of pregnancy and growth of the trophoblastic tissue most of the hematomas gradually disappear, and circulation normalizes, but the pregnancy remains

Table 13.2: Hematoma site and pregnancy outcome

Hematoma site	*Spontaneous abortion*			*Preterm delivery*	
Site	*N*	*n*	*%*	*n*	%
Supracervical	30	2	6.7	2	6.7
Fundus-corpus	29	8	27.5	1	3.4
Total	59	10	17.5	3	5
Fisher exact test: one-tail P=0.01, two-tail P=0.03. From ref. 33, with permission					

in the high-risk group with necessity for intensive monitoring.

Second element in diagnosis of intrauterine hematoma is its size. The modern ultrasonographic machines with transvaginal approach enable accurate evaluation of the size of the intrauterine hematoma. Intrauterine hematoma should be analyzed in relation to the trophoblast tissue, and its distance from the internal cervical os.[38] Furthermore, software of the newest machines makes possible the spatial three-dimensional image of hematomas and surrounding structures as well as measuring their volume and dynamic follow-up of biometric changes (Fig. 13.5). At the same time Doppler measurements can evaluate compression effect on adjacent uteroplacental circulation.[32,33]

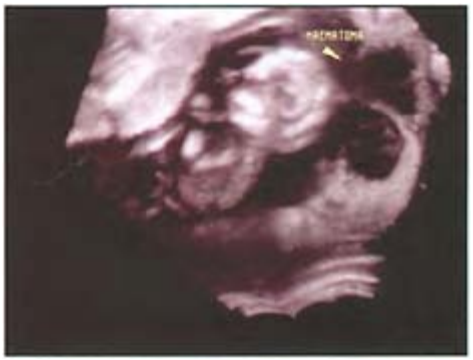

Figure 13.5: Three-dimensional transvaginal sonogram of the subchorionic hematoma in a close proximity to the gestational sac

Table 13.3: Clinical outcome of pregnancies complicated by subchorionic hematoma

Correlation among variables				
Variable	*Gestational weeks*	*Resistance index*	*Peak systolic velocity*	*Volume*
GW	1.000			
RI	−0.304	1.000		
PS	0.702	−0.791	1.000	
V	0.157	0.527	−0.276	1.000

From ref. 40, with permission. GW—Gestational weeks; RI—Resistance index; PS—Peak systolic; V—Volume

Kupesic and co-workers[39] used color Doppler to visualize the spiral arteries in the patients affected with intrauterine hematoma. Blood flow velocity waveforms were analyzed by means of pulsed Doppler. Parameters used in the study were the resistance index (RI) and peak-systolic velocity (PVS). Table 13.3 presents the effect of the subchorionic hematoma on the local hemodynamics.[39]

The essential finding is that in the presence of hematomas, RI in the ipsilateral spiral arteries was increased and blood flow was decreased. Doppler measurements showed lack of the diastolic flow (RI=1.0) in most of the patients (Fig. 13.6). The subchorionic hematoma compresses the spiral arteries and reduces the peak-systolic velocity. With continuation of pregnancy and reabsorption of the hematoma, impedance to blood flow returns to normal values. This statistical relationship suggests that the changes in blood flow velocity are secondary, and not the cause of

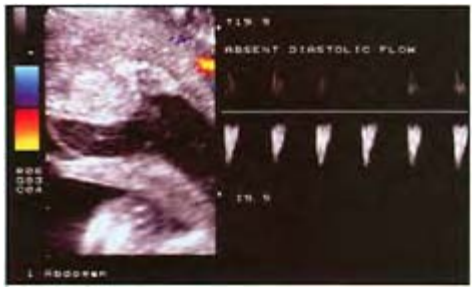

Figure 13.6: Transvaginal color Doppler scan of a hematoma. Note the absence of diastolic flow (RI=1.0) detected in spiral arteries close to the perigestational hemorrhage

subchorionic hematoma. It means that the improvement of blood flow is predictive for normal pregnancy outcome, while decreased spiral artery perfusion indicates increased risk of first and early second trimester loss. Since no increased risk for preterm delivery was found in patients with subchorionic hematoma, it is expected that the elevated impedance to blood flow is a transitory consequence of a compression of the arterial walls by the hemorrhage itself.

ECTOPIC PREGNANCY

When the endometrium is abnormally thick or has irregular echogenicity, and intrauterine sac is not detected in the patient with the positive urinary pregnancy test, one should always think of an ectopic pregnancy. More about this entity an interested reader can find in a separate chapter.

EARLY PREGNANCY LOSS

Nowadays, there is possibility to determine pregnancy outcome or to detect possible maldevelopment of the embryo by evaluating early pregnancy ultrasound signs. As the result of the abnormal development of an early pregnancy structures, early pregnancy loss could occur. Evaluation should include analysis of structures by the time of their ultrasound appearance (Scheme 13.3):

- Gestational sac
- Yolk sac
- Crown-rump length
- Embryonic heart rate
- Amnion.

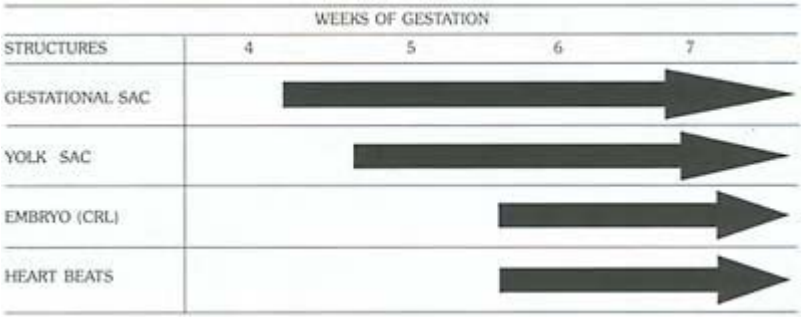

Scheme 13.3: Time of appearance of important developing structures in first trimester as assessed by transvaginal ultrasound

Gestational Sac

The first visible structure within the uterus is a gestational sac. During the 5th gestational week, it measures 2 to 3 mm in diameter [40,41] as estimated by transvaginal ultrasound. The measurement should be obtained from the inner-to-inner part of the gestational sac. The gestational sac grows approximately 1–2 mm in size per day.[42]

Biometric and morphological characteristics of gestational sac and embryonic echo can be used as a predictive factor in diagnosis of abnormal early pregnancy. Decreased values of gestational sac diameter and/or its irregular shape can suggest upcoming incident and may be used as a marker for chromosomopathies. For example, early spontaneous abortion as one of the complications in early pregnancy usually connected with triploidy and trisomy is followed by abnormal gestational sac growth.[43,44]

By transabdominal approach abnormal gestational sac criteria include:

- Impossibility to detect double decidual sac when sac diameter is 10 mm or greater,
- Impossibility to detect yolk sac when sac diameter is 20 mm or greater, and/or
- Impossibility to detect an embryo with cardiac activity when sac diameter is 25 mm or greater.[45,46]

By transvaginal approach abnormal gestational sac criteria include:

- Impossibility to detect yolk sac when sac diameter is 8 mm or greater, or
- Impossibility to detect cardiac activity when sac diameter is 16 mm or greater.[47]

When growth rate fails to increase at least 0.7 mm/day, abnormal sac and early embryo failure should be considered.[48]

Color Doppler evaluation of the supposed gestational sac is important for obtaining additional information and differentiation between the pseudogestational sac and intrauterine gestational sac. Pseudogestational sac is characterized by either absent flow around it or very low velocity flow (<8 cm/s peak systolic velocity) and moderate resistance to blood flow (RI>0.50).[49] Normal or abnormal intrauterine gestational sac is

characterized by high velocity and low resistance pattern (RI<0.45) (Fig. 13.7). As mentioned, there is no difference in blood flow between normal and abnormal gestational sac.[50,51]

Measurement of the gestational sac volume by 3D US can be used for the estimation of gestational age in the early pregnancy. An abnormal measurement of gestational sac could potentially be used as a prognostic marker for pregnancy outcome.[52]

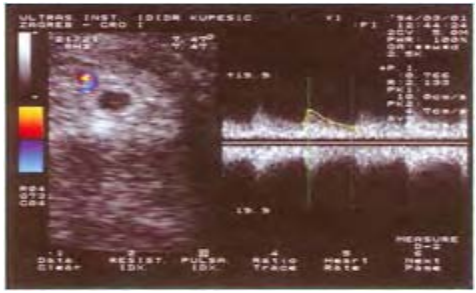

Figure 13.7: Transvaginal color Doppler image of an early gestational sac. Blood flow signals derived from spiral arteries demonstrate low vascular resistance (PI=0.77)

Yolk Sac

Yolk sac is the first recognizable structure inside the gestational sac and should be obtained as a regularly rounded extra-amniotic structure when gestational sac reaches 8–10 mm.[53] Normal biometric values of yolk sac diameter during the first trimester are 3–6 mm (inner diameter) (Fig. 13.8).

Figure 13.8: Three-dimensional transvaginal imaging at 7–8 weeks of

gestation by surface mode. Note regular shape of the yolk sac

Following changes assessed by 2D US are related to spontaneous abortion prediction.[53]

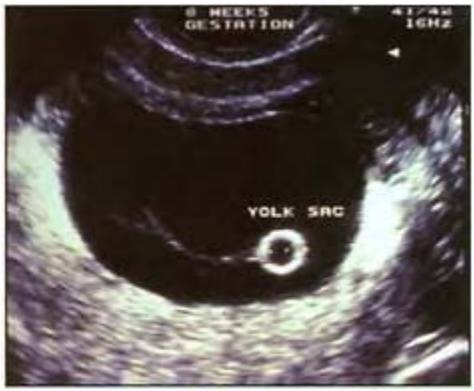

Figure 13.9: Transvaginal sonogram of vitelline duct and yolk sac characterized with increased echogenicity

- Absence of the yolk sac,
- Too large—more than 6 mm (over 2SD, sensitivity 16%, specificity 97%, PPV60%),
- Too small—less than 3 mm (below 2SD, sensitivity 15%, specificity 95%, PPV 44%),
- Irregular shape—mainly wrinkled with indented walls,
- Degenerative changes—abundant calcifications with decreased translucency of the yolk sac (Fig. 13.9), and
- Number of yolk sacs—has to be equal to the number of the embryos.

It is, nowadays, supposed that yolk sac abnormalities are rather the consequence than the cause of altered embryonic development.[54,55] Table 13.4 refers on yolk sac diameter and vascularity between 6 and 12 weeks of gestation in normal pregnancies.[54]

The ultrasound appearance of the yolk sac has already been proposed as a prognostic parameter for the outcome of pregnancy. Kurjak and co-workers[32] established sonographic criteria for distinguishing between “normal” and “abnormal” yolk sac appearance. In their experience, yolk sac should always be visible before the viable embryo; yolk sac measures 4.0–5.0 mm in diameter until 7–8 weeks of gestation and reaches 6.0–6.5 mm by the end of the 9th week. After that period yolk

Table 13.4: Yolk sac diameter and vascularity between 6 and 10 weeks of gestation in normal pregnancies

Gestational age (weeks)	N	*Yolk sac* diameter		*Yolk sac vascularity*		
		Mean (range) (mm)	Significance	N	*%*	Significance
6	9	3.1 (2.5–3.8)		3	33.33	
7	15	3.6 (2.9–4.4)	p<0.05	12	80.00	p< 0.005
8	19	4.1 (3.6–5.1)	p<0.05	17	89.47	p<0.05
9	18	4.5 (4.1–5.9)	p<0.05	15	83.33	p<0.05
10	14	5.3 (4.3–6.0)	p<0.001	8	57.14	p<0.001
11	12	5.0 (4.1–5.9)	p<0.05	3	25.00	p< 0.005
12	10	4.3 (3.4–4.9)	p<0.001	0	0	p<0.001
Total	87	. 4.2 (2.5–6.0)		58	66.67	
From ref: 55, with permission						

sac starts its regression and disappears at 12 weeks of gestation.[56]

The sonographic detection of abnormal yolk sac morphology may predict abnormal fetal outcome. Attempts have been made to identify abnormal parameters. Parameters of abnormal yolk sac findings listed above are predictive indicators of early pregnancy failure. All these parameters should be defined and assessed prior to 10 gestational weeks.

Abnormal yolk sac size may be the first sonographic indicator of associated failure. Primarily, the presence of an embryo without the visible yolk sac before the 10th gestational week is mostly an abnormal finding. According to some authors, the inner diameter of the yolk sac is always less than 5.6 mm in a normal pregnancy before the 10th week of gestational age. Lyons[57] established that for a mean gestational sac diameter of less than 10 mm, the yolk sac diameter should be less than 4 mm. In 15 patients who had abnormally large sacs, six had no embryo, five aborted spontaneously and only one conceptus survived. Out of nine others with embryo and large yolk sac, eight patients aborted and in one patient trisomy 21 was detected at the 24th gestational week.

The yolk sac can be too small, and this is accepted as a marker of poor pregnancy outcome. Green and Hobbins[58] analyzed a group of patients between 8 and 12 weeks' gestational age, and found out that patients with a yolk sac diameter less than 2 mm were associated with an adverse pregnancy outcome.

Most often, the shape of the yolk sac is changed when compressed by an enlarging fetus after the 10th gestational week. The normal spherical shape

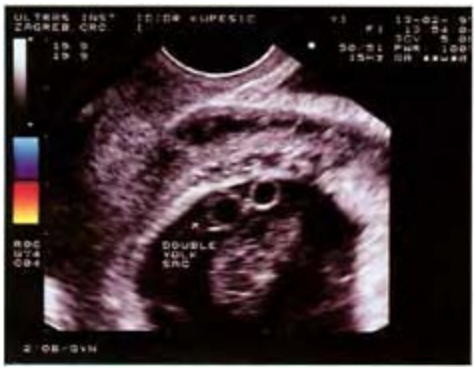

Figure 13.10: Transvaginal color Doppler scan of an 8-week embryo. Note the double yolk sac close to the embryonic body

of the yolk sac could *be* distorted even earlier, requiring intensive follow-up within the next few weeks. The most difficult diagnostic *puzzle* is the double yolk sac (Fig. 13.10). Each singleton pregnancy should have a single yolk sac. A double yolk sac is an extremely rare finding. The diagnostic *puzzle* includes the morphological differentiation of a retarded disappearance of physiological midgut herniation or an early abdominal wall defect.

It is unknown whether abnormalities of the yolk sac are related primarily to the yolk sac or secondary to embryonic maldevelopment. According to the present data is seems that the yolk sac plays an important role in maternofetal transportation in early pregnancy. Changes in size and shape could indicate or reflect the significant dysfunction of this system, and therefore could influence early embryonic development. Currently, the major benefits of the sonographic evaluation of the yolk sac are:

1. Differentiation of potentially viable and nonviable gestations,
2. Confirmation of the presence of an intrauterine pregnancy vs. a decidual cast, and
3. Indication of a possible fetal abnormality.

Kurjak and associates[54] performed a transvaginal color Doppler study of yolk sac vascularization. They examined 105 patients whose gestational age ranged from 6–10 weeks from the last menstrual period. Transvaginal color and pulsed Doppler examination was performed before the termination of pregnancy for psychosocial reasons. The overall visualization rate for yolk sac vessels was 72.38%. A characteristic waveform profile included low velocity (5.8±1.7 cm/s), and the absence of diastolic flow was found in all examined yolk sacs. The pulsatility index showed a mean value of 3.24±0.94 without significant changes between the subgroups.

Kurjak and co-workers [59,60] also analyzed the vascularization of yolk sac in abnormal pregnancies. Study included 48 patients with missed abortion between 6 and 12 weeks' gestation. Yolk sac blood flow was detected in 18.54% of missed abortions. Three types of abnormal vascular signals were obtained from the yolk sac: irregular blood flow,

permanent diastolic flow and venous blood flow signals. Changes in vascularization of the yolk sac noticed in missed abortions in this study are probably a consequence of embryonic death and reabsorption of the embryo through the vitelline duct. Abnormal patterns of the yolk sac vascularity can be related to decreased vitelline blood flow, which may cause progressive accumulation of nutritive secretions not utilized by the embryo. This process ends with enlargement of the yolk sac indicative of an early pregnancy failure. In 28.57% of missed abortions yolk sac vascularity was detected with large diameter of the yolk sac, and 20.00% with normal yolk sac diameter.

Yolk sac calcification was reported to result from the typical dystrophic changes that occur in nonviable cellular material.[61] Recognition of a calcified yolk sac without blood flow signals suggests long-standing demise in the first trimester, which directs the clinician for further diagnostic work-up.

Kurjak and Kupesic[60] presented data indicating that there is an interaction between the yolk sac vascularity and intervillous circulation in patients with missed abortion. In patients with long standing demise, vascular signals could not have been extracted from the hyperechoic walls of the yolk sac. Parallel assessment of the intervillous circulation demonstrated numerous color-coded areas within the intervillous space indicating low mesenchymal turgor and progressive disruption of the maternoembryonic interface. Therefore, the changes in the intervillous circulation noticed in some missed abortions are rather the consequence of embryonic death and inadequate drainage than being the primary cause of early pregnancy failure. Independent Doppler studies from three institutions using sensitive conventional and power Doppler velocimetry found that continuous and pulsatile blood flow can be extracted from intervillous space in both normal pregnancies and those with adverse outcome.[62–64]

Data presented by Kurjak and Kupesic[60] support the concept that establishment of the intervillous circulation is a progressive process during the first trimester of pregnancy. Between the 6th and 10th week of gestation clear blood flow signals are derived from the walls of the yolk sac supporting the hypothesis that yolk sac is responsible for optimal delivery of nutrients and oxygen to developing embryo up to 10 weeks of gestation. Later on intervillous circulation becomes more prominent indicating a possible switch from the vitelline towards intervillous circulation.

Three-dimensional ultrasound (3D US) significantly contributes to *"in vivo"* observation of the yolk sac surface pattern, enabling reduced scanning time and observation of the honeycomb surface pattern of the yolk sac. Automatic volume calculation allows us to estimate precise relationship between the yolk sac and gestational sac volumes, as well as to obtain the correlation between yolk sac volume and CRL measurements.[65] Distinguishing the yolk sac and embryo in 6th and 7th week of gestation decreases possibility of CRL measurement error (Fig. 13.10).

Table 13.5 reveals normal and abnormal yolk sac features.[66]

Crown-rump length (CRL)

Crown-rump length is used to estimate growth of the embryo and define exact gestational age. Measurement of CRL is performed in midsagittal section from the top of the head (crown) to the end of the rump of embryo by transvaginal probe.

Reliability of CRL measurements depends on embryo size and the fact that the measurements are only precise when the greatest long axis reaches 18–22 mm. In smaller embryos, a mistake in few millimeters means a large deviation. In embryos over 18 mm, when the real CRL is measured and the anatomic structures are visible, the possibility of a mistake is smaller.

The median CRL in fetuses with trisomies 21 and 13 or sex chromosome aneuploidies is not significantly different from the normal fetuses as reported by Kuhn and co-workers.[67] This is the reason why routine pregnancy dating should be by measurement of CRL as well as interpretation

Table 13.5: Normal and abnormal yolk sac characteristics

Yolk sac characteristics		
	Normal yolk sac	*Abnormal yolk sac*
Size	5–6 mm up to 9th week of gestation	< 2 mm in 8 to 12 weeks (to small) > 6 mm after 10th week (to large)
Shape	Round	Oval, distorted
Ultrasound finding	Echoic rim, hypoechoic center	Hyperechoic
Doppler	Absence of diastolic flow	Irregular blood flow Permanent diastolic flow Venous blood flow
From ref. 67, with permission		

of the results from nuchal translucency or biochemical screening.

However, some results suggest that the measurement of fetal CRL may be useful predictor of spontaneous miscarriage and SGA in pregnancies with threatened abortion.[68]

Embryonic Heart Rate

The cutoff CRL for detecting cardiac activity by transvaginal probe is 4 mm,[69] and by transabdo-minal 9 mm.[70] Heart rate progressively increases to 120 to 160 beats/minute after 6 to 7 weeks.[71] Embryonic heart rate demonstrates certain physiologic variability within its normal range of frequencies that is 150–190 beats/minute for embryos bigger than 10 mm at 8–12 weeks of gestation. An embryonic heart rate less than 100 beats per minute (bpm) 7 weeks is recognized as embryonic bradycardia.[72] An embryonic heart rate less than 70 bpm has been reported to result in a fetal demise in 100% patients.[73] Bradycardia or arrhythmia could be considered as predictors for heart action cessation. In these cases, an early hemodynamic heart failure was noticed with consequential gestational sac enlargement, yolk sac enlargement (more than 6 mm) and initial generalized hydrops. This type of hemodynamic disturbances can occur in patients presenting with massive intrauterine hematomas prior to fetal demise.[74] Doubilet[75] reported that pregnancies in which the embryos have a slow heart rate at or before 7

weeks of gestation and which continue beyond the first trimester, have a high likelihood (90%) of congenital anomalies, but than embryos with normal heart rates. Reduced body move-ments of the embryo during first and second trimester are also considered possible predictors of early pregnancy complications.[74]

Amnion Evaluation

At 6 to 8 weeks of gestation by transvaginal probe, amniotic membrane is visualized as a thin rounded structure encircling embryo. It could appear before 6th week of gestation as a linear echogenic interface projected within the gestational sac in proximity to the embryo.[41]

When the amniotic membrane is clearly visua-lized or its thickness and echogenicity approach that of yolk sac, it should be always suspicious to abnormal amnion development.[76] Mean amniotic sac diameter is approximately equal to the CRL in normal early pregnancy. Enlarged amniotic cavity related to the CRL suggests early pregnancy abnormality.[76]

Horrow[77] presented data on the difference between the CRL and amniotic cavity diameter and stated that in normal pregnancies was approximately 1 mm but reached almost 9 mm in abnormal pregnancies.

In normal early pregnancy embryo is usually detected before amniotic membrane. Cases of "empty amnion" with gestational sac greater than 16 mm are highly suggestive of abnormal pregnancy and require further analysis.[78]

OBJECTS IN FIRST TRIMESTER SCREENING FOR CHROMOSOMOPATHIES

Nuchal Translucency

Increased nuchal translucency (NT) thickness at 10–14 weeks of gestation is associated with fetal chromosomal defects and many genetic syndro-mes and abnormalities.[79,80] Measurement of NT may be obtained by transvaginal or transabdo-minal approach. The elements that should be kept in mind during NT measurement are:

- Embryo/fetus presented in sagittal section,
- Magnification of the embryo/fetus image occupies at least 75% of the screen,
- Ability to distinguish between fetal skin and amnion,
- Measurement of the maximum thickness of the subcutaneous translucency, between the skin and the soft tissues overlying the cervical spine,[79]
- CRL between 38 and 84 mm.

Pajkrt and co-workers[81] determined the normal range for the NT measurement in chromosomal and phenotypicaly normal fetuses. They demonstrated normal physiological variation in the NT thickness between 9th and 14th week of gestation. Cross-sectional data in Braithwhite's study[82] demonstrated an increase in NT measurement between 9th and 12th week, followed by the decrease at 13 and 14 weeks of gestation. Because of the change of the value of NT with CRL fixed cut of value is

inappropriate and each measurement of the NT should be compared with adequate CRL value.[83] According to results of many studies NT measurement in first trimester presents one of the best ultrasonographic markers for detection of chromosomal abnormalities.[84,85]

Limitations of NT measurement by 2D US are:

- Suboptimal fetal position,
- Observation of inappropriate median sagittal section of the embryo,
- Attachment of the nuchal region to the amniotic membrane,
- Small size of the structure to be measured[86] and
- Long lasting examination.

Performing 3D US seems to overcome some of these limitations. After storing the volume data

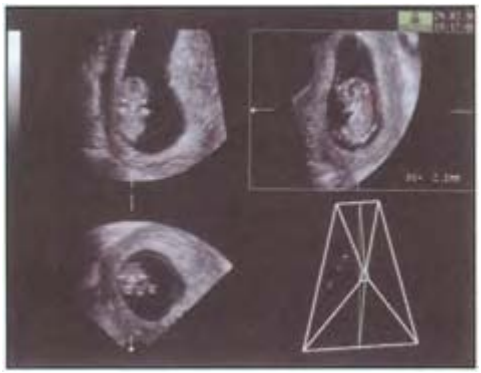

Figure 13.11: Three-dimensional scan of a fetus at 12 weeks gestation. Three perpendicular planes: plane A allows a frontal view of the fetal nuchal region; plane B shows an ideal mid-sagittal view of the fetus; plane C gives a symmetrical transverse section of the fetus. These planes make measurement of the nuchal translucency much easier and more accurate

examiner may repeat volume scanning and perform the assessment of the nuchal region from all directions (Fig. 13.11).[87] Correlation of the 2D and 3D transvaginal ultrasound examinations indicated that 3D ultrasound is superior to 2D US, since using 3D US technique the midsagittal section of the fetus can be visualized with 100% success rate. Further more, the initial scan of the patient may be performed by a less experienced ultrasonographer and stored values analyzed by an expert in settled conditions. 3D US improves the accuracy of NT measurement, producing an appropriate midsagittal section

of the fetus and making a clear distinction of the nuchal region from the amniotic membrane. Similarly, 3D US measurements of the NT present better intra-observer reproducibility than that conventional 2D US, increasing the effectiveness of the screening programs.[86,88]

One of the most often pitfalls in evaluation of the NT is cystic hygroma. Cystic hygroma is most often associated with chromosomopathies especially Down syndrome in the first trimester, and with Turner syndrome in the second trimester. It is caused by abnormality of lymphatic system. Cystic hygroma presents fluid accumulation in the cervical region with or without septa. The presence of the septations within a nuchal fluid accumula-tion is considered ominous. The fetuses with non-septated cystic hygroma in diagnosis had better life prognosis than the fetuses with septated cystic hygroma.

Ductus Venosus and Heart Failure

Ductus venosus (DV), foramen ovale and ductus arteriosus Botali present specific shunts during the intrauterine life. Function of ductus venosus is connecting to umbilical circulation with inferior vena cava. DV originates from the umbilical vein and enters the inferior vena cava at the level of the hepatic veins, just below the diaphragm, for-ming the subdiaphragmatic venous vestibulum.[89] The main function of DV is distribution of the oxygenated blood through foramen ovale into the left atrium. In normal conditions approximately 53% of the umbilical blood flows into the DV,[90] but during the state of hypoxia rises to 70% with decrease in intrahepatic hepatic blood flow.[91] Ductus venosus blood flow signals can be depicted in the right sagittal section of the fetal abdomen as a continuation of the umbilical vein towards inferior vena cava.[92]

In normal fetuses the DV waveform shows a peak velocity during ventricular systole, another peak during ventricular diastole and a nadir during atrial contraction. The DV pulsatility index is independent of the insonation angle and proved to be the most reproducible parameter.[93] Changes in the DV waveform have been reported in different hemodynamic situations. In cardiac failure without structural defects, reversed flow during atrial contraction has been detected.[94] Similar findings have been reported in growth-restricted fetuses.[95,96] An abnormally increased DV pulsatility index may indicate a chromosomal defect.[58] Because NT is independent ultrasonographic marker, authors combined NT and DV measurement. The results from Antolín et al[97] demonstr ate usefulness of DV pulsatility index in an unselected population. Combining DV pulsatility index and NT measurement, overall sensitivity decreased to 55%, but specificity reached 99.3%, with a negative predictive value of 99.3%. When only autosomal trisomies were considered, the detection rate was similar to NT with decrease in the false-positive rate. Similar effectiveness was found during the early gestational age period. These results suggest that NT may be used as a first line-screening test in order to maintain the sensitivity, while examination of the DV waveforms is useful as a second line test in order to decrease the false-positive rate, reducing the need for invasive testing to less than 1%.[98] Increased DV pulsatility index (using 95th centile) can be explained by an early cardiac failure.[99] Transient changes in DV waveform have been noted in chromosomally abnormal fetuses in early pregnancy, with a reversed flow during atrial contraction. Suggesting a temporary phenomenon Huisman and Bilardo[100] found a twin pregnancy discordant for trisomy 18 where the affected fetus at 13 weeks' gestation had an

increased nuchal translucency thickness and reversed end-diastolic DV flow.[100] Transient cardiac failure has been involved in the physiology of the NT thickness. It can be hypothesized that the same early cardiac dysfunction can produce a transient fluid accumulation in the back of the neck and a temporary increase in DV pulsatility index.[100] Normal DV hemodynamics has been reported in the pathology involving the left atrium or ventricle, although blood flow from this vessel is preferentially directed across the foramen ovale into the left heart. Abnormal DV parameters have been demonstrated in association with right ventricular pathology.[101] Malformations involving the right ventricular inlet or outlet are more commonly associated with changes in the DV waveform during atrial contraction than isolated septal defects[93] Zoppi and all[102] found reduced absent or reversed flow in the DV during late diastole, coinciding with atrial contraction. This was considered a sign of early fetal cardiac function impairment and was observed in the first-trimester fetuses with chromosomal abnormalities that are expected to carry a more frequent rate of cardiac defects than normal. Because of the prevalence of the cardiac defects in fetuses carrying chromosomal abnormalities, it is clear that some signs of heart failure may be evident in the first trimester, and DV seems to be an essential site where this impairment could be manifested. The conclusion of this study is that DV pulsatility index should not be used as a first line screening test at 10–16 weeks' gestation because it does not increase the number of cases detected by NT, but can be useful as a second line test in screen-positive cases with increased NT thickness in order to increase the specificity, reducing the need for invasive testing. In chromosomally normal fetuses with an abnormal DV waveform pattern, a careful follow-up scan, including fetal echocardiography, should be mandatory.

Umbilical Artery Assessment

Analysis of the embryo/fetal umbilical artery flow shows variable results. While Zoppi and co-workers[102] demonstrated no alterations in the umbilical artery flow in embryo/fetuses with increased NT and normal karyotype and those with increased NT and trisomy 21, Borrell and co-workers[103] presented alarming data that Doppler ultrasound finding of a reversed end-diastolic flow in the umbilical artery during the first trimester of pregnancy may indicate structural and/or chromosomal defect. However, the impor-tance of the umbilical artery flow measurements has yet to be established.

Nasal Bone

2D-ultrasound evaluation of the nasal bone in first trimester day—by -day becomes more important but also encourages academic discussion. In combi-nation with NT, DV and biochemical markers, absence of the nasal bone indicates possibility of a chromosomal anomaly. The most common chromosomal anomaly connected with absence of the nasal bone is Down syndrome (trisomy 21). Screening regarding to this problem takes place between 11 and 14 weeks.[104] Visualization of the nasal bone should be done by transabdominal ultrasound in mid-sagittal view of the embryo/fetal profile, in an adequately magnified image, with an angle of insonation about 45 or 135° between the ultrasound beam and the line traced from the top of the chin of the embryo/fetus.[104,105]

Most recent observations suggest it is the best to visualize nasal bone in sagittal section in medial orbital angle. Cicero and co-workers in their study analyzed nasal bone at 11th to 14th week of gestation.[104]

In 99.5% of chromosomally normal fetuses nasal bone was visible. In 73% of cases with trisomy 21 nasal bone was not found. Cicero and co-workers suggests than nasal bone screening in combination with NT thickness and maternal serum biochemical analysis sensitivity could achieve 90%.[104]

Heart Analysis

Simpson and Sharland[106] analyzed association between congenital heart defects and increased NT. Their data indicate that a normal nuchal scan in no way excludes karyotype abnormalities or serious cardiac malformations. For fetuses with increased nuchal translucency, the median gestational age at time of the diagnosis of the congenital heart disease was 20 weeks. Bronshtein and Zimmer[107] suggest that transvaginal ultrasound examination of the heart in at least two main planes of four chambers and three specific images of the vessels (X, P, Y) in a period between 14th-16th week of gestation increases possibility of detecting heart defects. Earlier diagnosis preser-ves entire specter of diagnostic and therapeutic options including genetic studies when indicated or therapeutic abortion. In cases of severe fetal malformations, early detection may prevent unnecessary invasive procedures.[107]

Umbilical Cord Diameter

Ghezzi and co-workers[108] analyzed NT and umbilical cord diameter in 784 patients between 10 and 14 weeks of gestation. The umbilical cord diameter was measured as outer to outer border at the maximal magnification. As the umbilical cord diameter increases with gestational age, 95th centile was cut off for enlarged diameter. The proportion of fetuses with enlarged umbilical cord diameter was higher in presence of fetal or placental chromosomal abnormalities.

Introduction of umbilical cord diameter as the ultrasonographic marker for chromosomal abnormalities slowly enters in everyday practice.

COMBINED STRATEGIES FOR ANEUPLOIDY SCREENING

Unfortunately, definitive diagnosis of the aneu-ploidy still can only be accomplished by invasive procedures. Certain ultrasonographic markers such as abnormal NT, DV and nasal bone refer to possibility of existence of chromosomal abnormality. Trying to create an efficient non-invasive screening test clinicians combined ultrasonographic and non-ultrasonographic markers. Sabria and co-workers[109] presented data from their 13 years long experience in prenatal screening with detection rate of 90.0% at 5.5% false-positive rate for trisomy 21, detection rate of 75.0% at 1.0% false-positive rate for trisomy 18 and detection rate of 87.5% at 5.2% false-positive rate for all-aneuploidies. Their suggestion for first trimester ultrasound screening is to combine:

- Maternal age,

• NT as ultrasound marker, and
• PAPP-A and free ßHCG as biochemical markers.

This combination detects between 85 and 90% of Down's syndrome, at the 5% false-positive rate.[110–112] Similar results are presented in retro-spective studies for trisomy 13 and Turner's syndrome, while sex trisomies are usually not detectable.[113,114]

Introducing nasal bone as the independent ultrasonographic marker and using color Doppler evaluation of DV, as a second line marker Sabria suggests that detection rate for trisomy 21 will be 98% at 5% false-positive rate.

Comas and co-workers[115] suggested for lowrisk population single NT measurement or selective screening by NT and DV assessment, and for the high risk population combined simultaneous screening (including all sonographic, Doppler and biochemical parameters), all in sense of reducing invasive testing procedures.

CONCLUSION

Ultrasound examination has become the "golden standard" in follow-up of the development and complications in early pregnancy. With introduction of transvaginal sonography a possibility for early morphological and biometrical ultrasound examinations has been significantly improved. The essential aim of an early pregnancy ultrasound is not only to diagnose a pregnancy, but also to differentiate between normal and abnormal pregnancy. Application of color Doppler ultrasound has enabled functional hemodynamic presentation and evaluation soon after implantation.

Early pregnancy failure is defined as a pregnancy that ends spontaneously before the embryo is detected by ultrasound at the gestational age in which visualization of viable embryo should occur. The most common pathological symptom of the early pregnancy failure is the vaginal bleeding. Only differentiation and accurate estimation of the pregnancy status and embryo/fetus make it possible to obtain therapeutic measures to cases where a normal outcome of the pregnancy can be expected.

The development of transvaginal sonography has allowed improved assessment of the patients presenting vaginal bleeding during the first half of pregnancy, clarifying the differential diagnosis of missed abortion, ectopic pregnancy, blighted ovum and threatened abortion with a living embryo. Embryo vitality can be established reliably by documenting cardiac activity on realtime, B-mode and/or color Doppler ultrasonography.

Threatened abortion is the clinical term used to describe vaginal bleeding during the first 20 weeks of pregnancy in women who, on the basis of clinical evaluation are considered to have a potentially living embryo/fetus. With a normal intrauterine pregnancy, bleeding from the chorion frondosum is undoubtedly the most common source of vaginal bleeding during the first trimester and should be considered in the diagnosis of threatened abortion.

As a definition, incomplete abortion is the passage of some, but not all fetal or placental tissue through the cervical canal. In complete abortion, all products of conception are expelled through the cervix. Transvaginal ultrasonography plays an important role in evaluating uterine cavity in spontaneous abortion since it enables detection of the retained products of conception. Retained products of conception after abortion may cause bleeding or endometritis. Recent studies demonstrate that the risk for

repeated spontaneous abortion depends exclusively on the number of previous spontaneous abortions, their cause, maternal age, chromosomal abnormalities, uterine anomalies, etc. Even though, many different risk factors have been thoroughly researched around 60% of unsuccessful pregnancies remain unknown.

In patients with a suspicion on a spontaneous abortion it is suggested to perform not only 2D but also color Doppler sonographic evaluation of the retained trophoblastic tissue.

The diagnosis of missed abortion is determined by the ultrasound identification of an embryo/fetus without any heart activity. It is relatively easy to make this diagnosis by means of the transvaginal color Doppler ultrasound. The main parameter is the absence of the heartbeats and the lack of a color flow signals at its expected position after the 6th gestational week.

Blighted ovum (anembryonic pregnancy) refers to a gestational sac in which the embryo either failed to develop or died at a stage to early to be visualized. The diagnosis of anembryonic pregnancy is based on the absence of embryonic echoes within the gestational sac large enough for such structures to be visualized independent of the clinical data or menstrual cycle. Advances in transvaginal sonography allow us to detect this kind of abnormality at a mean sac diameter of 1.5 cm. To confirm the diagnosis, these findings should be correlated with other clinical and sonographic data including the presence of a yolk sac.

Intrauterine hematomas are defined as sonolucent crescent or wedge-shaped structure between chorionic tissue and uterine wall, or fetal membranes. By localization intrauterine hematomas can be divided into retroplacental, subcho-rionic, marginal and supracervical. The most severe are large, central, retroplacental hema-tomas. Prognostically, there are two main elements which determine the pregnancy outcome: location and the size of the hematoma. The essential color Doppler finding is that in the presence of hematomas, vascular resistance in the ipsilateral spiral arteries is increased and blood flow is decreased. Doppler measurements showed lack of the diastolic flow in most of hematomas resulting in RI of 1.0. Since no increased risk for preterm delivery was found in patients with subchorionic hematoma, it is expected that the elevated impedance to blood flow is a transitory consequence of a compression of the spiral arterial walls by the hemorrhage itself.

Biometric and morphological characteristics of gestational sac and embryonic echo can be used as predictive factors in diagnosis of abnormal early pregnancy. Decreased values of gestational sac diameter and/or its irregular shape can suggest upcoming incident and could be used as markers for chromosomopathies. When growth rate fails to increase at least 0.7 mm/d an early embryo failure should be considered.

Yolk sac is the first recognizable structure inside the gestational sac in early pregnancy. Following changes assessed by 2D US are related to the prediction of the spontaneous abortion: absence of yolk sac, too large yolk sac (more than 6 mm), too small yolk sac (less than 3 mm), irregular shape of the yolk sac (mainly wrinkled with indented walls), degenerative changes of the yolk sac (abun-dant calcifications with decreased translucency of yolk sac), and number of yolk sacs (has to be equal to the number of the embryos).

Crown-rump length (CRL) is used to estimate growth of the embryo and define exact gestational age. The median CRL in fetuses with trisomies 21 and 13 or sex chromosome

aneuploidies is not significantly different from that of the normal fetuses. An embryonic heart rate less than 100 beats per minute (bpm) before 7 weeks is recognized as embryonic bradycardia. Brady-cardia or arrhythmia could be considered as predictors for heart action cessation. In these cases, an early hemodynamic heart failure is usually noticed with consequential gestational sac enlargement, yolk sac enlargement (more than 6 mm) and initial generalized hydrops.

Mean amniotic sac diameter is approximately equal to the CRL in normal early pregnancy. Enlarged amniotic cavity related to the CRL suggests early pregnancy abnormality.

Increased NT thickness at 10–14 weeks of gestation is associated with fetal chromosomal defects, many genetic syndromes and abnormalities. Because of the change of the value of NT with CRL, each measurement of the NT should be compared with adequate CRL value. First trimester ultrasound screening should include: maternal age, NT as ultrasound marker and PAPP-A and free βHCG as biochemical markers. These parameters have detection rate of 90.0% at 5.5% false-positive rate for trisomy 21, detection rate of 75.0% at 1.0% false-positive rate for trisomy 18 and detection rate of 87.5% at 5.2% false-positive rate for all-aneuploidies.

In normal fetuses the DV waveform shows a peak velocity during ventricular systole, another peak during ventricular diastole and a nadir during atrial contraction. Results of different studies suggest that NT should be used as a first linescreening test in order to maintain the sensitivity, while examination of the DV waveforms can be useful as a second line test in order to decrease the false-positive rate, reducing the need for invasive testing to less than 1%.

In combination with NT, DV and biochemical markers absence of the nasal bone indicates possibility of a chromosomal anomaly. Introducing nasal bone as the independent additional ultrasonographic marker and using color Doppler evaluation of DV, as a second line markers it is suspected that detection rate will be 98% at 5% false-positive rate for trisomy 21.

REFERENCES

1. Kurjak A. Ultrasound in early pregnancy. In: Kurjak A (Ed). Diagnostic Ultrasound in Developing Countries. Mladost. Zagreb 1986; 65–75
2. Jukic S. Pathology of women's reproductive system. AGM, Zagreb, 1999.
3. Goldstein SR. Embryonic death in early pregnancy: a new look at the first trimester. Obstet Gynecol 1994; 84:294–97.
4. Sadler TW. Langman's Medical Embriology, 7th Williams and Wilkins, 1994.
5. Streeter GL. Developmental horizons in human embryo (4th issue). A review of the histogenesis of cartilage and bone. Contr Embryol Carneg Inst 1949; 220:150–73
6. Blaas HGK. The examination of the embryo and early fetus: how and by whom? Ultrasound Obstet Gynecol 1999; 14:153–58
7. Blaas HG, Eik-Nes SH, Kiserud T, Hellevik LR. Early development of the abdominal wall, stomach and heart from the 7 to 12 weeks of gestation: a longitudinal study. Ultrasound Obstet Gynecol 1995; 6 240–49.
8. Cetin A, Cetin M. Diagnostic and therapeutical decision-making with transvaginal sonography for first trimester spontaneous abortion, clinically thought to be complete or incomplete. Contraception 1998; 57 393–97.

9. Edmonds DK, Lindsky KS, Miller JF. Early embryonic mortality in women. Fertil Steril 1982; 38:447–53
10. Hakim RB, Gray RH, Zacur H. Infertility and early pregnancy loss. Am J Obstet Gynecol 1995; 172: 1510–17.
11. Alberman E. The epidemiology of repeated abortion. In: Beard RW, Bishop F (Eds). Early pregnancy loss: mechanism and treatment. New York: SpringerVerlag 1988; 9–17
12. Kurtz AB, Shlansky-Goldberg BB. Detection of retained products of conception following spontaneous abortion in the first trimester. J Ultrasound Med 1991; 10:387–95
13. Chung TKH, Cheung LP, Sahota DS, Haine Chang AMZ. Evaluation of the accuracy of transvaginal sonography for the assessment of retained products of conception after spontaneous abortion. Gynecol Obstet Invest 1998; 45:190–93
14. Kaakaji Y, Nghiem HV, Nodel C. Sonography of obstetric and gynecologic emergencies. AJR Am J Roentgenol 2000; 174:641
15. Moore L, Wilson SR. Ultrasonography in obstetric and gynecologic emergencies. Radiol Clin North Am 1994; 32:1005
16. Wong SF, Lam MO, Ho LC. Transvaginal sonography in the detection of retained products of conception after first-trimester spontaneous abortion. J Clin Ultrasound 2002; 30:428–32
17. Achiron R, Goldenberg M, Lipitz S, Mashiach S. Transvaginal duplex Doppler sonography in bleeding patients suspected on having residual trophoblastic tissue. Obstet Gynecol 1993; 81:507–11
18. Dillon EH, Case CQ, Ramos IM, Holland CK, Taylor KJW. Endovaginal ultrasound and Doppler findings after first-trimester abortion. Radiology 1993; 186:87 91.
19. Tal J, Timor-Tritsch Y, Degani S. Accurate diagnosis of postabortial placental remanant by sonohystero-graphy and color Doppler sonographic studies. Gynecol Obstet Invest 1997; 43:131–34
20. Alcázar JL, Ortiz CA. Transvaginal color Doppler ultrasonography in the management of first-trimester spontaneous abortion. Eu J Obstet Gynecol Reprod Bio 2002; 102:83–87.
21. Kos M, Kupesic, S Latin V Diagnostics of spontaneous abortion. In: Kurjak A (Eds). Ultrasound in Gynecology and Obstetrics. Zagreb: Art Studio Azinovic. 2000; 314–21
22. Reccurrent early pregnancy loss. In: Speroff L, Glass RH, Kase NG (Eds). Clinical Gynecologic Endocrinology and Infertility. London: Williams and Wilkins 1999; 1043–55.
23. Windham GC, Voin Behren J, Fenster L, Schaefer C, Swan SH. Moderate maternal alcohol consum-ption and risk of spontaneous abortion. Epidemiology 1997; 8:509–14
24. Donders GGG, Odds A, Veercken A, van Bulck B, Caudron J, Londers L, Selembier G, Spitz P Abnormal vaginal flora in the first trimester, but not full blown bacterial vaginosis, is associated with preterm birth. Prenat Neonat Med 1998; 3:558–93
25. Kupesic S, Kurjak A, Chervenak F. Doppler studies of subchorionic hematomas in early pregnancy. In: Chervenak F, Kurjak A (Eds). Current Perspectives on the Fetus as a Patient. Carnforth, UK: Parthenon Publishing 1996; 33–39
26. Cowchock FS, Reece EA, Balaban D, Branch DW, Plouffe L. Repeated fetal losses associated with anti-phospholipid antibodies: a collaborative randomized trial comparing prednizone with low-dose heparin treatment. Am J Obstet Gynecol 1992; 166:1318–23
27. Rai R, Cohen H, Dave M, Regan L. Randomized controlled trial of aspirin and aspirin plus heparin in pregnant women with recurrent miscarriage associated with phospholipid antibodies. Br Med 1997; 314:253–57
28. Kurjak A, Kupesic S. Doppler assessment of the intervillous blood flow in normal and abnormal early pregnancy. Ultrasound Obstet Gynecol 1997; 89:252 56.
29. Pellizari P, Pozzan C, Marchiori S, Zen T M. Assessment of uterine artery blood flow in normal first trimester pregnancies and those complicated by uterine bleeding. Ultrasound Obstet Gynecol 2002; 19(4):366–70.

30. Acharya G, Morgan H. First-trimester, three-dimensional transvaginal ultrasound volumetry in normal pregnancies and spontaneous miscarriages. Ultrasound Obstet Gynecol 2002; 19:575–79.
31. De Crepigni L. Early diagnosis of pregnancy failure with transvaginal sonography. Am J Obstet Gynecol 1988; 159–408
32. Kurjak A, Schulman H, Kupesic S, Zudenigo D, Kos M, Goldenberg M. Subchorionic hematomas in early pregnancy: clinical outcome and blood flow patterns J Matern Fetal Med 1996; 5:41–44
33. Kurjak A, Chervenak F, Zudenigo D, Kupesic S. Early pregnancy hemodynamics assessed by transvaginal color Doppler. In: Chervenak F, Kurjak A (Eds). The Fetus as a Patient. Carnforth UK: Parthenon Publishing 1994; 435:55
34. Jauniaux E, Gavril P, Nicolaides KH. Ultrasono-graphic assessment of early pregnancy complication. In: Jurkovic D, Jauniaux E (Eds). Ultrasound and early pregnancy. Carnforth, UK: Parthenon Publishing 1995; 53–64
35. Kurjak A, Kupesic S. Blood flow studies in normal and abnormal pregnancy. In: Kurjak A, Kupesic S (Eds). An Atlas of Transvaginal Color Doppler. London: Parthenon Publishing 2000; 41–51
36. Laurini RN. Abruptio placentae: From early pregnancy to term. In: Chervenak F, Kurjak A (Eds). The Fetus as a Patient. Carnforth UK: Parthenon Publishing 1996; 433–44
37. Mantoni M, Pedersen JF. Intrauterine hematoma: a ultrasound study of threatened abortion. Br J Obstet Gynecol 1981; 88:47–50
38. Falco P, Milano V, Pilu G, David C, Grisolia N, Bovicelli L. Sonography of pregnancies with first-trimester bleeding and viable embryo: a study of prognostic indicators by logistic regression analysis. Ultrasound Obstet Gynecol 1996; 7:65–69
39. Kupesic S, Kurjak A. Physiology of uteroplacental and embryonic circulation. In: Kurjak A (Ed). Textbook of Perinatal Medicine. Parthenon Publishing 1998; 482–90.
40. Timor-Tritsch IE, Farine D, Rosen MG. A close look at the embryonic development with the high frequency transvaginal transducer. Am J Obstet Gynecol 1988; 159:676–81
41. de Crespigny LC, Cooper D, McKenna M. Early detection of intrauterine pregnancy with ultrasound. 1988; 10.
42. Fleischer AC, Kepple DM. Transvaginal sonography of early intrauterine pregnancy. In: Fleischer AC, Manning FA, Jeanty P, Romero R (Eds). Sonography in Obstetrics and Gynecology Principles & Practice (sixth edition). The McGraw-Hill Companies. 2001; 61–88.
43. Bromley B, Harlow BL, Laboda LA, Benacerraf BR. Small sac size in the first trimester: a predict or of poor fetal outcome. Radiology 1991; 178:375–77
44. Dickey RP, Gasser R, Oltar TT, Taylo Relationship of initial chorionic sac diameter to abortion and abortus karyotype based in new growth curves for the 16th to 49th postovulation day. Hum Reprod 1994; 9:559–65
45. Nyberg DA, Laing FC, Filly RA. Threatened abortion: Sonographic distinction of normal and abnormal gestational sac. Radiology 1986; 158:397–400.
46. Nyberg DA, Laing FC, Filly RA. Ultrasonographic differentiation of the gestational sac of early intrauterine pregnancy and pseudogestational sac of ectopic pregnancy. Radiology 1983; 146:755–59.
47. Levi CS, Lyons EA, Lindsay DJ. Early diagnosis of normal pregnancy with transvaginal ultrasound. Radiology 1988; 167:383–85.
48. Nyberg DA, Mack LA, Laing FC, Patten RM. Distinguishing normal from abnormal gestational sac growth in early pregnancy. J Ultrasound Med 1987; 6:23–27
49. Dillon EH, Feyock AL, Taylor KJW. Pseudogestational sacs: Doppler US differentiation from normal or abnormal intrauterine pregnancies. Radiology 1990; 176:359–64
50. Kurjak A, Zalud I, Predanic M, Kupesic S. Transvaginal and pulsed Doppler study of uterine blood flow in the first and early second trimesters of pregnancy:normal versus abnormal. J Ultrasound Med 1994; 13:43–47

51. Jaffe R, Warsof SL. Color Doppler imaging in the assessment of uteroplacental blood flow in the abnormal first trimester intrauterine pregnancies: An attempt to define etiologic mechanisms. J Ultrasound Med 1992; 11:41–44
52. Benoit B, Hafner T, Bekavac I, Kurjak A. Three-dimensional sonoembryology. Ultrasound Rev Obstet Gynecol 2001; 1:111–1
53. Lindsay DJ, Lovett IS, Lyons EA. Endovaginal appearance of the yolk sac in pregnancy:normal growth and usefulness as a predictor of abnormal pregnancy. Radiology 1992; 183:115–1
54. Kurjak A, Kupesic S, Kostovic Lj. Vascularization of yolk sac and vitteline duct in normal pregnancy studied by transvaginal color Doppler. J Perinat Med 1994; 22:433–40
55. Kurjak A, Kupesic S, Kos M, Latin V, Kos MA. Ultrasonic and Doppler studies of human yolk sac. In: Chervenak F, Kurjak A (Eds). The Fetus as a Patient. Carnforth UK: Parthenon Publishing 1996; 345–47.
56. Jauniaux E, Moscoso JG. Morphology and signi-ficance of the human yolk sac. In: Barnea E (Ed). The first twelve weeks of gestation. Heidelberg: Springer 1992;192–216.
57. Lyons EA. Endovaginal sonography of the first trimester of pregnancy. Proceedings of the 3rd International Perinatal and Gynecological Ultrasound Symposium Ottawa, Ontario, 1994; 1–25.
58. Green JJ, Hobbins JC. Abdominal ultrasound examination of the first trimester fetus. Am J Obstet Gynecol 1988; 159:165–75
59. Kurjak A, Kupesic S. Parallel Doppler assessment of yolk sac and intervillous circulation in normal preg-nancy and missed abortion. Placenta 1998; 19:619–23.
60. Kurjak A, Kupesic S, Kos M. Early hemodynamics studied by transvaginal color Doppler. Prenatal and Neonatal Medicine 1996; 1:38–49.
61. Harris RD, Vincent LM, Askin FB. Yolk sac calcification: A sonographic finding associated with intrauterine embryonic demise in the first trimester. Radiology 1988;166:109–16.
62. Merce L T, Barco MJ, Bau S. Color D Doppler sonographic assessment of placental circulation in the first trimester of normal pregnancy. J Ultrasound Med 1996; 15:135–42
63. Valentin L, Sladkevicius P, Laurini R. Uteroplacental and luteal circulation in normal first-trimester preg-nancies: Doppler ultrasonographic and morphologic study. Am J Obstet Gynecol 1996; 174:768–75
64. Kurjak A, Dudenhausen JW, Hafner T et al. Intervillous circulation in all three trimesters of normal pregnancy assessed by color Doppler. J Perinat Med 1997; 25:373–80
65. Kurjak A, Kupesic S, Kos M. Three-dimensional Sonography for Assessment of Morphology and Vascularization of the Fetus and Placenta. J Soc Gynecol Investig 2002;9:186–202.
66. Kurjak A, Kupesic S. Blood flow studies in early pregnancy. In: Kurjak A, Kupesic S (Eds). Color Doppler in obstetrics, gynecology and infertility. Art Studio Azinovic-Medison Zagreb-Seoul 1999; 87 108.
67. Kuhn P, Brizot M, Pandya PP, Snijders RJ, Nicolaides KH. Crown-rump length in the chromosomally abnormal fetuses at 10 to 13 weeks' gestation. Am J Obstet Gynecol 1995; 172:32–35
68. Reljic M. The significance of crown-rump length measurement for predicting adverse pregnancy outcome of threatened abortion. Ultrasound Obstet Gynecol 2001; 17:510–12
69. Levi CS, Lyons EA, Zheng XH. Transvaginal US: Demonstration of cardiac activity in embryos less than 5.0 mm in crown-rump length. Radiology 1990; 176:71–74.
70. Pennell RG, Needelman L, Pajak T. Prospective comparison of vaginal and abdominal sonography in normal early pregnancy. J Ultrasound Med 1991; 1 0:63–67.
71. Laboda LA, Estroff JA, Benacerraf BR. First trimester bradycardia: A sign of impending fetal loss. J Ultrasound Med 1989; 8:561–63
72. Albayram F, Hamper UM. First-Trimester Obstetric Emergencies: Spectrum of sonographic findings. J Clin Ultrasound 2002; 3:161–77
73. Benson CB, Doubilet PM. Slow embryonic heart rate in early first trimester: indicator of poor pregnancy outcome. Radiology 1994; 192:343

74. Birnholz JC, Kent FB. The embryo as a patient: early pregnancy loss. In: Chervenak F, Kurjak A (Eds). The Fetus as a Patient. Carnforth UK: Parthenon Publishing 1996; 345–47
75. Doubilet PM, Benson CB, Chow JS. Long term prognosis of pregnancies complicated by slow embryonic heart rates in early first trimester. J Ultrasound Med 1999; 18:537–41.
76. Laing FC, Frates MC. Ultrasound evaluation during the first trimester of pregnancy. In: Callen PW (Ed). Ultrasound in Obstetrics and Gynecology 4th edition Sounders Company. 2000; 105–45.
77. Horrow MM. Enlarged amniotic cavity: A new sonographic sign of early embrionic death. AJR Am J Roentgenol 1992; 158:359–62
78. McKenna KM, Feldstein VA, Goldstein RB, Filly RA. The “empty amnion”: a sign of early pregnancy failure. J Ultrasound Med 1995; 14:117–21.
79. Nicolaides KH, Azar G, Byrne D, Mansur C, Marks K. Fetal nuchal translucency screening for chromosomal defects in first trimester of pregnancy. Br Med J 1992; 034:867–69
80. Pandya PP, Snijders RJM, Johnson SP, Brizot ML, Nicolaides KH. Screening for fetal trisomies by maternal age and fetal nuchal translucency thickness at 10–14 weeks of gestation. Br J Obstet Gynecol 1995; 102:957–62
81. Pajkrt E, Bilardo CM, van Lith JMM. Nuchal translucency measurement in normal fetuses. Obstet Gynecol 1995; 86:994
82. Braithwhite JM, Kadir RA, Economides DL. Nuchal translucency measurements frequency distribution and changes with gestation in a general population. Br J Obstet Gynecol 1995; 103:1201.
83. Taipale P, Hiilesma V, Salonen R, Ylostalo P Increased nuchal translucency as a marker for fetal chromosomal defects. N Eng J Med 1997; 337:1654–58
84. Monni G, Ibba RM, Zoppi MA. Antenatal screening for Down’s syndrome. Lancet 1998; 352:1631–32
85. Zoppi MA, Ibba RM, Putzolu M, Floris M, Monni G. Nuchal translucency and the acceptance of invasive prenatal chromosomal diagnosis in women aged 35 and older. Obstet Gynecol 2001; 97:916–20
86. Kurjak A, Kupesic S, Kosuta-Ivancevic M. Three-dimensional transvaginal ultrasound improves mea-surement of nuchal translucency. J Perinat Med 1999; 27:97–102.
87. Kurjak A, Matijevic R. Three-dimensional ultrasound markers of chromosomal anomalies. In: Kurjak A, Kupesic S (Eds). Clinical Application of 3D sonogra-phy. Parthenon Publishing London NY. 2000; 143–50.
88. Chung BL, Kim YP, Nam. Three-dimensional ultrasound for nuchal translucency measurement at 10–14 weeks of gestation. In: Kurjak A, Kupesic S (Eds). Clinical application of 3D Sonography. Parthenon Publishing London NY 2000; 151–54.
89. Huisman TWA, Gittenberger-De Groot AC, Wladimiroff JW. Recognition of fetal subdiaphrag-matic venous vestibulum essential for fetal venous Doppler assessment. Pediatr Res 1992; 32:338–41
90. Edelstone DI. Regulation of blood flow through the ductus venosus. J Dev Physiol 1980; 2:219–38
91. Meyers RL, Paulick LP, Rudolph CD, Rudolph AM. Cardiovascular responses to acute, severe hemor-rhage in fetal sheep. J Dev Physiol 1991; 15:189–97
92. Antolin E, Comas C, Carrera JM. Doppler velocimet of the ductus venosus in the first trimester of pregnancy. In: Kurjak A, Chervenak FA, Carrera JM (Eds). The Embryo as a Patient, Parthenon Publishing Group, New York London, 2001; 181 85
93. Hecher K, Campbell S, Snijders R, Nicolaides K. Reference ranges for fetal venous and atrioventricular blood flow parameters. Ultrasound Obstet Gynecol 1994; 4:381–90
94. Kiserud T, Eik-Nes SH, Hellevik LR, Blaas HG. Ductus venosus blood velocity changes in fetal cardiac diseases. J Matern Fetal Invest 1993; 3:15–20

95. Kiserud T, Eik-Nes SH, Blaas HG, Hellevik LR, Simensen B. Ductus venosus blood velocity and the umbilical circulation in seriously growth-retarded fetus. Ultrasound Obstet Gynecol 1994;4:109–14.
96. Hecher K, Campbell S, Doyle P, Harrington K, Nicolaides KH. Assessment of fetal compromise by Doppler ultrasound investigation on the fetal circulation. Arterial, intracardiac and venous blood flow velocity studies. Circulation 1995; 91:129–38
97. Antolion E, Comas C, Torrents M, Munoz A, Figueras F, Echevarría M, Cararach M, Carrera M. The role of ductus venosus blood flow assessment in screening for chromosomal abnormalities at 10–16 week of gestation. Ultrasound Obstet Gynecol 2001; 17:295300.
98. Montenegro N, Matias A, Areias JC, Castedo S, Barros H. Increased nuchal translucency: possible involvement of early cardiac failure. Ultrasound Obstet Gynecol 1997; 10:265–68.
99. Huisman TWA, Bilardo CM. Transient increase in nuchal translucency thickness and reversed end-diastolic ductus venosus flow in a fetus with trisomy 18. Ultrasound Obstet Gynecol 1997; 10:397–99.
100. DeVore GR, Horenstein J. Ductus venosus index:a new method for evaluating right ventricular preload in the second trimester fetus. Ultrasound Obstet Gynecol 1993; 3:338–42
101. Zoppi MA, Putzolu M, Ibba RM, Floris M, Monni G. First trimester ductus venosus velocimetry in relation to nuchal translucency thickness and fetal karyotype. Fetal Diagn Ther 2002; 17:52–57
102. Zoppi MA, Ibba RM, Putzolu M, Floris Marcella, Monni G. First trimester umbilical artery pulsatility index in fetuses presenting enlarged nuchal translucency. Prenat Diagn 2000; 20:701–04
103. Borrell A, Martinez JM, Farre T, Azulay M, Cararach V, Fortuny A. Reversed end-diastolic flow in first trimes-ter umbilical artery: An ominous new sign for fetal outcome. Am J Obstet Gynecol 2001; 185:204–07
104. Cicero S Curcio, Papageorghiou A, Sonek J, Nicolaides K. Absence of nasal bone in fetuses with trisomy 21 at 11–14 weeks of gestation:an observational study. Lancet 2001; 358(9294):1665–67
105. Sonek J, Nicolaides K. Prenatal ultrasound diagnosis of nasal bone abnormalities in the three fetuses with Down syndrome. Am J Obstet Gynecol 2002; 186:139–41.
106. Simpson JM and Sharland GK. Nuchal translucency and congenital heart defects:heart failure or not? Ultrasound Obstet Gynecol 2000; 16:30–36.
107. Bronshtein M, and Zimmer EZ. The sonographic approach to the detection of fetal cardiac anomalies in the early pregnancy. Ultrasound Obstet Gynecol 2002; 19:360–65
108. Ghezzi F, Raio L, di Naro E, Franchi M, Buttarelli M, Schneider H. First trimester umbilical cord diameter: a novel marker of fetal aneuploidy. Ultrasound Obstet Gynecol 2002; 19:235–39
109. Sabria J, Cabrero D, Bach C. Aneuploidy screening: ultrasound versus biochemistry. Ultrasound Rev Gynecol 2002; 2:221–28.
110. Wald NJ, Hacksaw AK. Combining ultrasound and biochemistry in first trimester screening for Down's syndrome. Prenat Diagn 1997; 17:821–29
111. De Graaf IM, Pajkrt E, Bilardo CM. Early pregnancy screening for fetal aneuploidy with serum markers and nuchal translucency. Prenat Diagn 1999; 19:458–62.
112. Spencer K, Souter V, Tul N. A screening program for trisomy 21 at 10–14 weeks using fetal nuchal translucency, maternal serum free ß-human chorionic gonadotropin and pregnancy—associated plasma protein-A. Ultrasound Obstet Gynecol 1999; 13 231–37.
113. Spencer K, Ong C, Skentou H. Screening for trisomy 13 by fetal nuchal translucency, maternal serum free β-HCG and PAPP- A at 10–14 weeks of gestation. Prenat Diagn 2000; 20:411–16.
114. Spencer K, Tul N, Nicolaides KH. Maternal serum free ß-HCG and PAPP- A in fetal sex chromosome defects in first trimester. Prenat Diagn 2000; 20:390–94

115. Comas C, Antolin E, Torrents M, Munoz A, Figueras F, Echevarria, Gomez O, Carrera M. Early screening for chromosomal abnormalities:new strategies combining biochemical, sonographic and Doppler parameters. Prenat Neonat Med 2001; 6:95–102

Chapter 14
Ectopic Pregnancy

Sanja Kupesic, Alenka Aksamija, Asim Kurjak

Ectopic pregnancy represents implantation of the fertilized ovum outside the uterine cavity. In 95% of the cases it is localized in the fallopian tube (95%), but sites like abdominal cavity, ovary, intraligamentous location, cornual, intramural or cervical sites are not unusual (Table 14.1).[1–4] The exact cause of blastocyst implantation and development outside the endometrial cavity is not fully understood. Increased incidence of ectopic pregnancy was found during the last decades,[5,6] mainly attributed to greater degree of socially acceptable sexual behavior, which led to increased incidence of the pelvic inflammatory disease (PID). Fortunately, the fatal outcomes have been reduced up to 75% for the reason of early diagnosis and less invasive treatment techniques. Mechanical factors predisposing pathomorphological site of implantation are: low-grade pelvic infection (main cause for the faulty implantation), peritubal adhesions (result of the previous PID), and salpingitis with the partial or total destruction of the tubal mucosa. It has been reported that ectopic pregnancies do occur in totally normal tubes, suggesting that abnormalities of the conceptus or maternal hormonal changes may act as etiological factors.[7,8]

Table 14.1: Locations of ectopic pregnancy

• Tube
• Abdomen
• Ovary
• Interligamentous location
• Uterine horn
• Cervix

Risk factors for ectopic pregnancy are STDPID (sexually transmitted diseases-pelvic inflammatory disease),[9,10] assisted reproductive techniques, abnormalities of the conceptus, maternal hormonal changes, surgical procedures in pelvis,[11] IUD (intrauterine device),[12] previous ectopic pregnancy, fibroids, uterine malformations, cigarette smoking, etc. In addition to providing an accurate description of the sites of implantation of ectopic

pregnancy some authors showed that current IUD use 'protects' against interstitial pregnancies, which are the most difficult to manage and that subsequent fertility tends to be higher in women with distal EP.[13] It is essential to identify risk so we can provide patients with adequate information, diagnose and treat an ectopic pregnancy early, and possibly to develop preventive strategies (Table 14.2).[14–16]

Table 14.2: Risk factors for ectopi

• STD-PID
• Assisted reproductive techniques
• Abnormalities of the conceptus
• Uterine malformations
• Maternal hormonal changes
• Surgical procedures in pelvis
• IUD
• Previous ectopic pregnancy
• Fibroids
• Cigarette smoking

The main problem of ectopic pregnancy is clinical presentation.[17] Symptoms can vary from vaginal spotting to vasomotor shock with hematoperitoneum.[18,19] The classic triad of delayed menses, irregular vaginal bleeding and abdominal pain is most commonly **not** encountered, but the exact frequency of clinical symptoms and signs is hard to assess.[1] Both typical and atypical clinical presentation can mimic all kinds of diseases, which have no connection with pathology of reproductive system, such as appendicitis, diverticulitis, non-specific mesenterial lymphadenitis, or diseases of the urinary system. In most cases ectopic pregnancy is confused with an early spontaneous abortion because of the similar symptoms in both processes (delayed menses, enlarged and softened uterus and bleeding). Other conditions that should be considered in differential diagnosis of ectopic pregnancy are: normal intrauterine pregnancy, salpingitis, torsion or rupture of the ovarian cyst, adnexal torsion, bleeding corpus luteum, endometriosis, appendicitis, gastroenteritis, diverticulitis, conditions affecting urinary tract, etc. (Table 14.3). Therefore, early and reliable diagnosis of ectopic pregnancy is major challenge for every clinician. Significance of early diagnosis lays in the possibility for application of the conservative methods of treatment, which are crucial for preserving further reproductive capability, and in severe cases the life itself.[20] Diagnostic procedures are divided into two groups:

Non-invasive: History, general clinical and gynecological examination, hormonal and other laboratory markers and ultrasound diagnostics.

Invasive: Culdocenthesis,[21] curettage[22] and laparoscopy.

Table 14.3: Differential diag is of ectopic pregnancy

• Intrauterine pregnancy
• Spontaneous miscarriage
• Torsion or rupture of ovarian cyst
• Bleeding corpus luteum
• Endometriosis
• Salpingitis
• Adnexal torsion
• Perforated appendicitis
• Gastroenteritis
• Diverticulitis

THE ROLE OF BIOCHEMICAL MARKERS IN ECTOPIC PREGNANCY

Beta hCG (human chorionic gonadotropin) is the glycoprotein hormone released into circulation by human placental trophoblastic cells. From the 8th day after conception its concentration in blood rises 1, 7 times everyday.[23] As so on as implan occurs the trophoblast starts producing beta hCG. Common urine beta hCG tests react at concentrations higher or equal to 1000 IU/l of urine, which means that they become positive 10–14 days after conception.[1] Falsely positive results are mainly obtained in the case of proteinuria, erythrocyturia, gynecological tumors, tuboovarian abscess,[24] or some drug intake (e.g. tranquilizers). Embryo in cases of an ectopic pregnancy usually disappears, gets resorbed and we normally visualize an empty gestational sac producing smaller amounts of beta hCG. Normal levels of beta hCG could be found only in cases of a still living embryo which occurs in 5–8% of ectopic pregnancies.[23] For the reason of low concentrations of human chorionic gonadotropin only 40–60% of ectopic pregnancies have the positive urine test, therefore the more sensitive blood test should be performed, which becomes positive already 10 days after conception.[23] Absolute value of beta hCG levels in circulation are much lower than the levels of the same hormone in normal intrauterine pregnancies of the same gestational age.[25,26] Dynamics of the titer show slower increase of circulating concentrations and prolongate the time for doubling its values. The most important use of the quantitative beta hCG determination in conjunction with ultrasonography is that of understanding the value of “discriminatory zone” of beta hCG. The discriminatory zone represents the level of beta hCG above which all normal intrauterine chorionic sacs will be detected by ultrasound. There is now almost a consensus in considering the discriminatory zone to be about 1000 mIU/ ml with the use of transvaginal probe of at least 5 MHz.[27–30]

THE ROLE OF ULTRASOUND IN THE DIAGNOSIS OF ECTOPIC PREGNANCY

With recent technological development ultrasonography (but more precisely, transvaginal sonography) has become the "gold standard" diagnostic modality for the effective and fast detection of ectopic pregnancy. An important advantage of most currently used transvaginal transducers is the ability to perform simultaneous and spectral Doppler studies, allowing easy identification of the ectopic peritrophoblastic flow. In comparison to transvaginal sonography, transabdominal ultrasound, as a method for detecting ectopic gestation is restricted for a very small number of oddly located ectopic pregnancies, mainly high up in the pelvis-outside the effective reach of 5 MHz vaginal probe.[31]

Transabdominal Ultrasound

The absence of gestational sac inside the intrauterine cavity at 6 weeks' gestation raises the suspicion of an ectopic pregnancy. Transabdominal ultrasonography cannot reliably diagnose ectopic pregnancy, except when a live fetus is demonstrated in the abdominal cavity. In only 3–5% of the cases an ectopic gestational sac with embryonic echoes and clear heart activity can be demonstrated.[32] Probe with frequency of 3.5 MHz and large contact area is used for transabdominal ultrasonographic imaging and full bladder plays a role of an acoustic window. Resolution of this probe is somewhat lower, but the penetration is much deeper than one of the transvaginal probe.

The best results in confirming the intrauterine pregnancy are achieved using following criteria:

1. Normal size, shape and location of the gestational sac in the uterine cavity,
2. Double ring surrounding the gestational sac,
3. Embryonic parts with eventual,
4. Heart action.

Signs for ectopic pregnancy could be divided into uterine and extrauterine, some of them being diagnostic or just suggestive.

Diagnostic signs include: absence of the intrauterine gestational sac surrounded with double ring, absence of the yolk sac and/or fetal structures inside the gestational sac and presence of extraovarian adnexal structure.

Suggestive signs are: uterine enlargement with thickened endometrium and blood or coagulum in the retrouterine space.[32]

Low sensitivity, specificity, positive and negative predictive values for detection of ectopic pregnancy are shortcomings of transabdominal ultrasound.[33,34] This modality still has some value in successful detection of a small proportion of ectopic pregnancies with bizarre location, such as high in the pelvis.

Transvaginal Ultrasound

In comparison with transabdominal approach, transvaginal ultrasound enables much better image of the morphological features in pelvis thanks to higher frequencies and probe location in immediate vicinity of the examined area. Sensitivity of transvaginal

sonography was found to be 96%, the specificity reached 88%, the positive predictive value 89% and the negative predictive value 95%.[35] Intrauterine gestational sac surrounded with double ring with clear embryonic echo is considered to be strong evidence against ectopic pregnancy because heterotopic, pregnancy (intrauterine and ectopic), coincide rarely, but shouldn't be so easily ignored, especially in the patients undergoing some of the methods of assisted reproduction.[36]

Intrauterine sonographic findings in women with ectopic pregnancy are variable. These include:

1. Empty uterus, with or without increased endometrial thickness,
2. Central hypoechoic area, or a sac like structure inside the cavity—the so called pseudogestational sac, and
3. Concurrent intrauterine pregnancy.

Early intrauterine pregnancy and recent spontaneous abortion may present themselves on transvaginal sonography with empty uterus and endometrial layer variable in thickness.[3] Therefore, they are considered to be suggestive signs. Pseudogestational sac can be demonstrated in 10–20% of patients with ectopic pregnancy[3] as a mixed echo pattern of endometrium that results from a decidual reaction, fluid, or both. Careful examination of the uterine cavity usually allows a reliable distinction to be made between the pseudogestational sac and normal gestational sac. The pseudogestational sac is detected in the middle of the uterine cavity, its shape changes, owing to myometrial contractions. In differentiating a real gestational sac from a pseudogestational one, transvaginal color and pulsed Doppler ultrasound proved to be very useful.

Adnexal sonographic findings in women with ectopic pregnancy are variable. Gestational sac located inside adnexa with clear embryonic echo and heart activity directly proves ectopic pregnancy, but is seen in only 15–28% of the cases. Less rare is visualization of an adnexal gestational sac with or without embryonic echo (without heart action).[37] Such a finding is detected in 46–71% of reported cases if tube is unruptured,[38] while the most common finding is an unspecific adnexal tumor. Free fluid in the retrouterine space is seen in 40–83% of cases.

Accurate ultrasound diagnosis of ectopic pregnancy depends strongly on examiner's experience. Adnexal abnormalities may be difficult to identify because of confusion with loops of bowel or other pelvic structures.[39]

There are four adnexal structures that may resemble an ectopic pregnancy and should be correctly identified.[40] One is the corpus luteum, which is eccentrically located within the ovary, surrounded by ovarian tissue and possibly creating the impression of a sac-like structure. About 85% of ectopic pregnancies are formed on the same side as the corpus luteum.[41] This is important to bear in mind while trying to distinguish tubal pregnancy from the ipsilateral corpus luteum. Corpus luteum is found in the ovary and its echogenicity is slightly (or at times even substantially) lower than that of trophoblastic tissue of the tubal ring. Furthermore, hemorrhagic corpus luteum usually shows a hypoechoic rather than a cystic central region.[42] Other three conditions than need to be correctly differentiated from an ectopic gestation are a thickwalled ovarian follicle, the small intestine, and tubal pathology conditions, in such as hydrosalpinx containing fluid (Table 14.4).

Using the protocol of combination of clinical examination, serum beta hCG assay and transvaginal ultrasound examination it is possible to diagnose ectopic pregnancy with a sensitivity of 100% and specificity of 99%.[43]

Another problem in detection of an ectopic pregnancy in adnexal region arises in patients

Table 14.4: Sonographic features of intrauterine and ectopic pregnancy

<table>
<tr><th>Intrauterine pregnancy</th><th colspan="3">Ectopic pregnancy</th></tr>
<tr><td rowspan="2">• Gestational sac of normal size and shape inside the uterine cavity</td><td>UTERINE FINDING</td><td>DIAGNOSTIC SIGNS</td><td>• Absence of gestational sac located in cavity
• Absence of embryo or its parts in the cavity</td></tr>
<tr><td rowspan="2">• Double ring
• Clear embryonic echo
• Positive heart action</td><td rowspan="2">SUGGESTIVE SIGNS</td><td rowspan="2">• Enlarged uterus
• Thick endometrium
• Free fluid in Cul-de-sac</td></tr>
<tr><td>ADNEXAL FINDINGS</td><td colspan="2">• Ectopic gestational sac with or without living embryo
or
• Mixed solid and cystic mass</td></tr>
</table>

undergoing assisted reproductive procedures or simple hormonal superovulation. Besides the increased risk for ectopic pregnancy in these patients, a large number of artificial corpora lutea will be seen that resemble the tubal ring of an ectopic pregnancy. Sometimes cystic adnexal masses (ovarian cystadenoma, cystadenofibroma, endometrioma, teratoma and pedunculated fibroids) may also rise differential diagnostic problems.

Free intraperitoneal fluid is seen in 40–83% the women with ectopic pregnancy, but also in up to 20% of normal intrauterine pregnancies.[38] In case of tubal abortion echogenic echoes suggesting the presence of blood clots are demonstrated, while tubal rupture is associated with a homogeneous, hypoechoic retrouterine echo that represents blood collection. The possibility of an ectopic pregnancy increases if the amount of fluid is moderate to large, but the absence of blood does not exclude its diagnosis.

Serial serum beta hCG assay may rise a suspicion on ectopic pregnancy at a very early gestation, while transvaginal ultrasound scan may not be able to demonstrate the site of the pregnancy. Under these circumstances sometimes it is necessary to perform laparoscopic examination to exclude the possibility of ectopic pregnancy. However, even laparoscopic examination may not be able to achieve a precise diagnosis, especially when the ectopic pregnancy is very small or when there are co-existing pathologies such as hydrosalpinges, adhesions or fibroids. Some reports demonstrated that laparoscopic ultrasound can facilitate the diagnosis of the site of ectopic pregnancy intraoperatively, even if it is as small as 3.9 mm.[44] The number of negative laparoscopies can be decreased and repeat laparoscopy avoided. Therefore, laparoscopic ultrasound should be used when the site of ectopic pregnancy cannot be determined or is obscured by other pathologies during laparoscopic examination.

Color Doppler Facility

Ultrasound machine with color Doppler facility is an excellent guide in search for blood flow signals

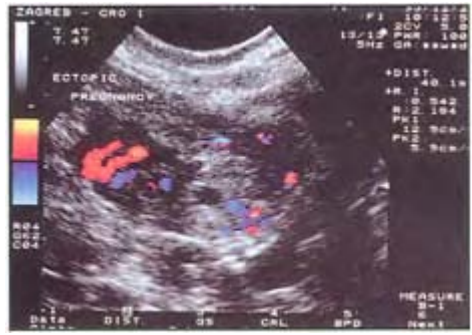

Figure 14.1: Transvaginal color Doppler scan of a small gestational sac in the adnexal region measuring 8–10 mm. Note the dilated tubal vessels, indicating the pathophysiological site of the pregnancy (within the tube)

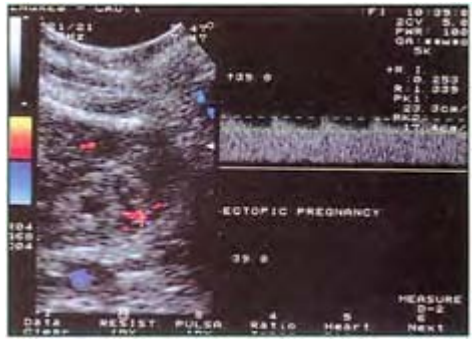

Figure 14.2: The same patient as in previous figure. Blood flow velocity waveforms depicted from the area of peritrophoblastic flow show high velocity (23.3 cm/ s) and low vascular resistance (RI=0.25)

within the entire pelvis. The color flow pattern associated with ectopic pregnancy is variable. It usually presents randomly dispersed multiple small vessels within the adnexa

(Fig. 14.1), showing high-velocity and low impedance signals (RI=0.36–0.45) clearly separated from the ovarian tissue and corpus luteum (Fig. 14.2). The sensitivity of transvaginal color and pulsed Doppler in diagnosis of ectopic pregnancy reported in several studies ranges from 73–96%, and specificity from 87–100%.[3,4,38,45]

Visualization of ipsilateral corpus luteum blood flow may aid in diagnosis of ectopic pregnancy

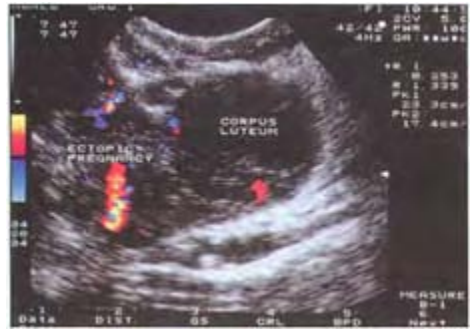

Figure 14.3: The same patient as in the previous figures. An ipsilateral corpus luteum is demonstrated laterally to the ectopic gestational sac

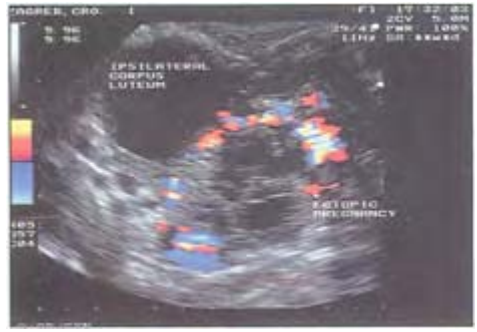

Figure 14.4: Color Doppler facilitates visualization of randomly dispersed tubal arteries indicating prominent trophoblastic vitality and invasiveness. Note the ipsilateral corpus luteum

(Fig. 14.3). The RI of luteal flow in the cases of ectopic pregnancy has been reported to be 0.48 ±0.07, which is between the values of the non-pregnant women (0.42±0.12) and those with normal early intrauterine pregnancy (0.53± 0.09).[46] In majority of patients

with proven ectopic pregnancy, luteal flow is detected on the same side as the ectopic pregnancy. This observation could be used as a guide in searching for ectopic pregnancy (Fig. 14.4).

The between-side difference in tubal artery blood flow was also documented. There was a significant increase in the tubal artery blood flow on the side of tubal gestation. The mean reduction

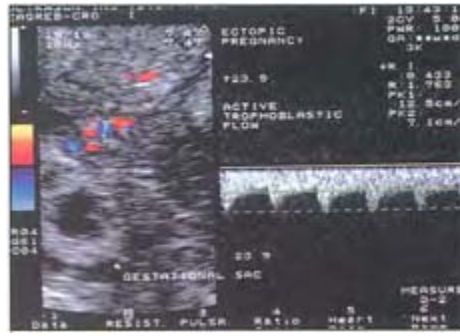

Figure 14.5: Transvaginal color Doppler imaging of a left sided ectopic pregnancy. Note the color signals indicative of invasive trophoblast (left). Pulsed Doppler waveform analysis (right) demonstrates low resistance index (RI=0.43)

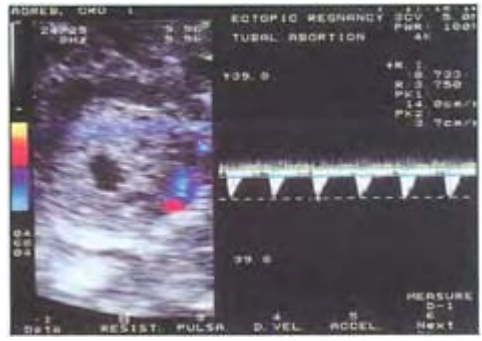

Figure 14.6: Gestational sac measuring 12 mm visualized in the left adnexal region. Color Doppler depicts a small area of angiogenesis characterized by a high resistance

index (RI=0.73). This finding is indicative of tubal abortion

of the RI on the side with the ectopic pregnancy compared to the opposite side was 15.5%.[4] These changes appear to be due to trophoblastic invasion, and showed no dependence on gestational age. Bright color on the screen while using the pulsed Doppler facility is due to very high speed of the peritrophoblastic blood flow and low impedance (Fig. 14.5). It should be stressed out that the patients with tubal abortion demonstrate significantly higher vascular impedance of peritrophoblastic flow (RI>0.60), and less prominent color signals (Fig. 14.6).

The main diagnostic importance of transvaginal color and pulsed Doppler is in differentiating the nature of non-specific adnexal masses. Doppler blood flow indices in the uterine, spiral arteries and corpus luteum arteries in ectopic and intrauterine pregnancies showed that the mean uterine and spiral artery RI decreased with increased gestational age of the intrauterine pregnancies, but remained constantly high in ectopic pregnancies.[47] The peak systolic blood flow velocity in the uterine artery increased with increasing gestational age in intrauterine pregnancies, and the values were significantly higher than in ectopic pregnancies.[48] The difference in peak systolic velocity reflects a decreased blood supply to the ectopic pregnancy. Intrauterine gestational sac shows prominent peritrophoblastic vascular signals (RI=0.44–0.45), while pseudogestational sacs do not demonstrate increased blood flow (RI>0.55). It has been suggested that velocities below 21 cm/s are diagnostic for pseudogestational sac and can successfully rule out trophoblastic flow of a normal intrauterine pregnancy.[49]

The intravascular ultrasound contrast agent has a recognizable effect on Doppler ultrasonographic examination of the adnexal circulation. It appears to be helpful when the finding in color flow imaging is ambiguous. The use of the contrast agent may also facilitate localization of trophoblastic tissue in hemorrhagic adnexal lesions.[50]

As with other diagnostic methods, transvaginal color and pulsed Doppler studies include both, false-positive and false-negative findings. A falsepositive diagnosis arises predominantly from the corpus luteum, but in exceptional cases some adnexal lesions may mimic ectopic pregnancy. A false-negative result may arise from technical inadequacy, lack of experience or patients' non-compliance. The other possibility of fault diagnosis is non-vascularized ectopic gestation, as these are associated with low beta hCG values.

Some authors compared technical errors with improper setting of color flow parameters.[51] The color velocity scale, color priority, color gain, color sensitivity and color wall filter should be adjusted to optimize color flow information. Technical errors may result in false diagnosis of ovarian torsion, malignancy and ectopic pregnancy.

The diagnosis of ectopic pregnancy still remains a challenge to the clinician despite advances in ultrasound and biochemical technology. Frequently the diagnosis remains uncertain until laparoscopy or D&C are performed. With the increasing tendency towards conservative therapy, the distinction between ectopic pregnancies that will resolve spontaneously and those that will rupture is essential.[52] Usually patients without acute symptoms and with declining beta hCG values are treated conservatively.[53] However, secondary ruptures have been reported in patients with low initial beta hCG concentrations.[54] The differentiation between viable ectopic pregnancies with

trophoblastic activity and dissolving tubal abortions could facilitate the decision to proceed with conservative or operative treatment.

After implantation in the mucosa of endosalpinx, the lamina propria and then the muscularis of the oviduct, the blastocyst grows mainly between the lumen of the tube and its peritoneal covering.[55] Growth occurs both parallel to the long axis of the tube and circumferentially around it. As the trophoblast invades surrounding vessels, intensive blood flow and/or intraperitoneal bleeding occur. The intensive ring of vascular signals could be a criterion for viability of an ectopic pregnancy that can be determined rapidly and easily and seems to be independent of beta hCG values.[56] In patients with a viable ectopic pregnancy who demand a conservative treatment, this method could provide an aid, in addition to beta hCG values; for supervising the efficiency of treatment, especially in those cases where beta hCG levels slowly normalize. In this way duration of hospitalization could be shortened, the patients uncertainty diminished, and the cost of the treatment reduced. In cases of persisting high beta hCG levels after operative removal of the ectopic, color Doppler sonography can provide evidence for the presence of viable trophoblast remnants. On contrary, in asymptomatic patients with hypoperfused and/or avascular ectopic gestational sac and decreased values of beta hCG expectative treatment can be established.

3D Ultrasound in the Assessment of Tubal Ectopic Pregnancy

Three-dimensional (3D) ultrasound technology offers some advantages over conventional twodimensional (2D) sonographic imaging.[57,58] Modern systems are capable of generating surface and transparent views depicting the sculpture-like reconstruction of surfaces or the transparent images structure's content.

Planar mode tomograms are helpful in distinguishing the early intraendometrial gestational sac from a collection of the fluid between the endometrial leaves (pseudogestational sac).

A prospective follow up study was conducted in order to evaluate the potential utility of 3D ultrasound to differentiate the intrauterine from ectopic gestations.[59] Fifty-four pregnancies with a gestational age <10 weeks and with an intrauterine gestational sac <5 mm in diameter formed the study group. The configuration of the endometrium in the frontal plane of the uterus was correlated with pregnancy outcome. After exclusion of three patients with a poor 3D image quality, the endometrial shape was found to be asymmetrical with regard to the median longitudinal axis of the uterus in 84% of intrauterine pregnancies, whereas endometrium showed symmetry in the frontal plane in 90% of ectopic pregnancies. Intrauterine fluid accumulation may distort the uterine cavity, thus being responsible for false-positive, as well as false-negative results. The evaluation of the endometrial shape in the frontal plane appeared to be a useful additional mean of distinguishing intrauterine from ectopic pregnancies, especially when a gestational sac was not clearly demonstrated with conventional ultrasound. Similarly, preliminary data of other authors suggested that 3D sonography is an effective procedure for early diagnosis of ectopic pregnancy in asymptomatic patients before 6 weeks of amenorrhea.[60]

The possible use of 3D power Doppler is the monitoring of the vascularity of ectopic pregnancy. The hypoperfusion, quantified by indices of vascularity (VI) and flow (FI),

could indicate that the ectopic pregnancy is spontaneously being resolved, and that laparoscopy should be postponed. This way, the conservative approach to ectopic pregnancy would rely on more precise and easily obtainable data. Conversely, in case of hyperperfusion, the patients should be subjected to laparoscopy or medical treatment immediately.

Shih and colleagues[61] described the use of 3D color/power angiography in two cases in which an arteriovenous malformation of mesosalpinx was diagnosed following involution of an anembryonic ectopic gestation. The diagnosis of arteriovenous malformations has traditionally been made by arteriography. Recently, it has also been diagnosed by non-invasive methods such as contrast enhanced CT, MRI and color Doppler ultrasound. The advantage of 3D reconstruction of color/ power angiography images is better spatial and anatomic orientation and quick demonstration of the vessels, usually within one minute, especially in the areas where complex structures are present. Therefore, unlike MRI, digital subtraction angiography or contrast enhanced CT, 3D color/ power angiography allows the physician to examine vascular anatomy immediately and without radiation exposure.

Most tubal gestations are not ongoing viable gestations. They are usually in the involutional phase of abortion within a confined area which results in the extrusion of products of conception through a ruptured site or fimbriae. In the two reported cases, the serum assays of beta hCG in both patients increased to significant levels which precluded intrauterine missed abortion.[61] Besides, there were neither retained products of conception *in uterus* nor heavy vaginal bleeding (indicating process of abortion in progress) prior to the diagnosis of arteriovenous malformation. Therefore, authors speculated that there might be an ectopic gestation occurring somewhere, although they could find only a pelvic arteriovenous malformation rather than an adnexal gestational sac.

The major difference between uterine implantation and tubal gestation is that endosalpingeal stroma usually falls to undergo decidualization. The chorionic villi of the tubal implantation may than invade into the tubal wall and mesentery (mesosalpinx) more directly and rapidly. The vascularization within the ectopic pregnancy is an analog of placenta increta.[62] In such situations cytotrophoblast may invade the contiguous artery and vein of mesosalpinx with destruction of these vessels' walls, and thus may induce an arteriovenous malformation *in situ* or nearby. Possibly, the secretion of angiogenic factors (by trophoblast) and the increasing afterload of an arterioventricular shunt existing in the tubal gestation can induce the rapid growth of a small pre-existing congenital arteriovenous malformation. However, two unusual cases of adnexal arteriovenous malformations associated with "vanishing" ectopic gestation where congenital etiology seemed unlikely have also been reported.[61] B-mode ultrasound and color Doppler provided information on the hemodynamics of the vascular tumor and led to the diagnosis of arteriovenous malformation. Three-dimensional color/power angiography further improved understanding of the complex vascular anatomy and refined the diagnosis.

Even though the exact role of 3D ultrasound in the pathology of early pregnancy is yet to be established, a promising results of already published papers are encouraging. Unlimited numbers of sections are easily obtained without the need for excessive manipulation with the probe. Additional progress has been made, owing to the permanent

possibility or repeated analysis of previous stored 3D volumes and Cartesian elimination of surrounding structures and artifacts. Three-dimensional reconstruction of stored image without any degradation is the most impressive benefit of 3D scanning.

OTHER SITES OF IMPLANTATION

About 5% of ectopic pregnancies implant in sites other than the tubes.[1] These are at times more difficult to detect and some, owing to strategic sites of implantation, may cause rupture, significant bleeding and higher morbidity and mortality than the tubal gestations.

Interstitial pregnancy occurs in 1.1–6.3% of all ectopic pregnancies.[1,63] This location of ectopic pregnancy usually occurs following *in vitro* fertilization (IVF) and previous salpingectomy,[63] but in most cases there are no apparent risk factors. Interstitial pregnancy clinically presents with abdominal pain and a tender asymmetrically enlarged uterus. The major problem of this location lies in late diagnosis, because it is commonly diagnosed after the rupture of the cornu has occurred and this may result in massive hemorrhage. Previously, interstitial pregnancies were diagnosed only at laparotomy following the rupture. For the reason of major hemorrhage, hysterectomy rate was as high as 40%.[60] In recent years, the routine use of ultrasound for the assessment of women with early pregnancy complications has enabled a non-invasive diagnosis of interstitial pregnancy to be made. Earlier diagnosis made before serious complications, allows the use of more conservative management, such as medical treatment or laparoscopic surgery.

A viable interstitial pregnancy may occasionally be misinterpreted as a normal intrauterine pregnancy. Therefore, it is important that strict diagnostic criteria are used in every case:[64]

1. Empty uterine cavity, and
2. Chorionic sac that is seen separately and more than 1 cm from the most lateral edge of the uterine cavity and surrounded by a thin myometrial layer.

It is worth to mention that approximately 15% of patients with interstitial pregnancy have heterotopic pregnancy.[64] In these cases, intrauterine findings may be misleading and should be interpreted with caution, rather than being used as primary diagnostic criterion. Visualization of the interstitial part of the tube in close proximity of the endometrium and depiction of the trophoblastic tissue improves the diagnosis of interstitial pregnancy.[65] It also confirms that pregnancy is located outside the uterine cavity, facilitating the differential diagnosis between an interstitial pregnancy and unusual forms of intrauterine pregnancy such as angular pregnancy or pregnancy in the cornu of an anomalous uterus. This sign is particularly helpful in women with small intramural fibroids located in vicinity of the interstitial part of the tube, which may be misinterpreted as a solid interstitial pregnancy.[66] In women with fibroids, the intramural part of the tube is displaced and can be visualized bypassing the mass, thus preventing the false-positive diagnosis of the interstitial pregnancy. Color Doppler facilitates the diagnosis of a cornual pregnancy by exposing low resistance peritrophoblastic flow (Fig. 14.7).

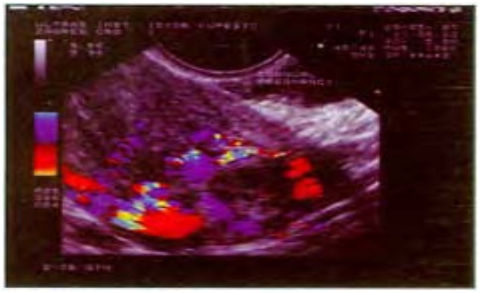

Figure 14.7: Transvaginal color Doppler scan of interstitial pregnancy. Color signals facilitate early diagnosis of this ectopic pregnancy location by exposing low resistance peritrophoblastic flow

Three-dimensional ultrasound has the advantage of providing views of the uterus, which can rarely be obtained by conventional 2D ultrasound scan.[67] In the coronal section, the position of the interstitial pregnancy in relation to the uterine cavity can be studied in detail. Visualization of the proximal section of the interstitial tube is also facilitated, which increases diagnostic confidence.[65] It is believed that 3D ultrasound is a helpful diagnostic tool in women with suspected interstitial pregnancy and should be considered in the cases where the diagnosis is not certain on conventional 2D transvaginal ultrasound scan.[68]

Most cornual/interstitial ectopic pregnancies are treated by laparoscopy and laparotomy using various surgical procedures (excision, suturing, etc.). Lately, transvaginal sonographic puncture and local injection of methotrexate, has been used to treat both viable and non-viable interstitial pregnancies.[64,65] There have been very few reported side-effects after treatment with low-dose local injection of methotrexate.[69] Data reported in the literature suggest the superiority of local therapy, with regard to both safety aspect and the success rate. In general, a likely explanation for the increased effectiveness of local injection is in higher concentration of therapeutic agent achieved in the target tissue. Although absorption of methotrexate into the circulation occurs after both local and systemic administration, a lower dose of methotrexate is used locally, leading to lower systemic levels and therefore fewer sideeffects.[70] Color Doppler plays an extremely important role providing an aid in approaching the cornual pregnancy from the medial aspect and traversing the thicker myometrial layer so rupture or bleeding are less likely to occur.[71] In these cases, color Doppler guidance during the instillation of methotrexate enables better visualization of blood vessels and avoidance of intraprocedural complications.

Viable heterotopic/interstitial pregnancies are often treated by local injection of potassium chloride, as this is not teratogenic. All six reported cases of heterotopic pregnancies in the literature were successfully treated in this way, with three (50%) intrauterine pregnancies progressing normally to full term.[4]

Expectant management of the interstitial pregnancy has also been reported.[64,66] All three non-viable interstitial pregnancies managed in this way were resolved spontaneously without any need for intervention. Expectant management can therefore, be useful option in selected cases.

Cervical pregnancy is defined as the implantation of the conceptus below the level of the internal os. It is the rare condition that occurs in one in 50,000.[4] Intrauterine adhesions, uterine anomalies, previous cesarean sections, fibroids, previous therapeutic abortions and IVF treatment have all been associated with cervical implantation. Traditionally the diagnosis of cervical pregnancy was based solely on clinical findings and history reports after hysterectomy. Therefore, it is likely that only the most severe cases were diagnosed, and a number of cervical pregnancies went undiagnosed or were treated as incomplete miscarriages. In the past two decades, ultrasound has become the method of choice for diagnosis of early pregnancy disorders and certainly contributed to the recent increase in number of reported cervical pregnancies.

The diagnosis of cervical pregnancy can be made on the following criteria:

1. No evidence on intrauterine pregnancy,
2. An hour glass uterine shape with ballooned cervical canal,
3. Presence of a gestational sac or placental tissue within the cervical canal, and
4. Closed internal os.

Early diagnosis may also explain the milder clinical symptoms and better prognosis of cervical pregnancy today as compared to pre-ultrasound era.

Transvaginal ultrasound approach has become the accepted standard for the examination of patients with suspected early pregnancy abnormalities. Apart from providing superior images of pelvic anatomy, addition of color Doppler enables simultaneous visualization of the pelvic blood vessels (Fig. 14.8). The level of the insertion of the uterine arteries should be used to identify the internal os and thus facilitate the diagnosis of cervical pregnancy.[71] The extensive vascular blood supply to the trophoblastic tissue originating from

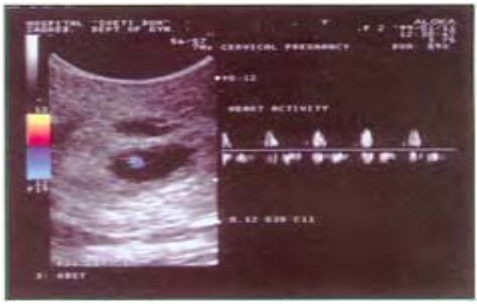

Figure 14.8: Transvaginal color Doppler scan of a cervical pregnancy. Blood flow signals are derived from

the fetal heart and demonstrate regular heart action

the adjacent maternal arteries at the implantation site (within the cervix) is easily visualized by transvaginal color Doppler. The products of conception in transit through the cervix after the failure of a normally implanted pregnancy are detached from their implantation site and maternal vascular supply. It is therefore impossible to detect any peritrophoblastic blood flow in these cases.[72] Conversely, even a small amount of placental tissue in a true cervical pregnancy remains highly vascularized on color Doppler examination.[73] This facilitates the differential diagnosis between the cervical pregnancy and incomplete miscarriage. Color Doppler analysis may also improve selection of the patients for primary surgical removal of cervical pregnancy and assist in planning D&C following medical treatment. It is necessary to stress out the potential of 3D sonography in diagnosis of cervical gestation and include: better anatomic orientation and multiplanar sections of the investigated area.

Local injection of methotrexate or potassium chloride appears to be most effective way of treating an early viable cervical pregnancy regardless of the gestational age. There are no data on the use of local injection in non-viable pregnancies, and it is uncertain whether the treatment would be as effective as in viable pregnancies. Systemic treatment in these cases is simple and highly effective and local injection would offer a very little advantage.

The regiments and dosages of methotrexate used for systemic therapy have varied considerably. There is no clear correlation between the dose and therapeutic success, and it is therefore logical to use as little methotrexate as possible to minimize side-effects. The usual regiment should be two intramuscular injections of 1 mg/kg methotrexate followed by folic acid. For local injection, 25 mg methotrexate into gestation sac appears to be sufficient. Potassium chloride 3–5 mEq is equally successful and less likely to cause sideeffects.[4]

The place of surgery should be limited to those cases where medical treatment has failed. Dilatation and curettage in combination with cervical cerclage or the insertion of a Foley catheter is probably the best choice for a general gynecologist and is as effective as more complicated and expensive methods for the prevention of uncontrollable hemorrhage.[71]

The sonographic diagnosis of **ovarian pregnancy** is extremely difficult to establish. It has been calculated that ovarian pregnancy accounts for less than 3% of ectopic pregnancies.[1,2] The sonographic diagnosis is made upon the finding of a hyperechoic trophoblastic ring detected within ovarian tissue, and the fact that it is impossible to separate the ectopic gestational sac from the ovary by transabdominal pressure from either examiner's hand or transvaginal ultrasound probe.[2] Color Doppler facilitates detection of the peritrophoblastic flow, which can speed up the entire diagnostic procedure.

Intra-abdominal pregnancy is a rare condition, constituting only 1% of all ectopic gestations.[74] Its complications, however, can be devastating. These include massive hemorrhage due to disseminated intravascular coagulation (DIG) and placental separation complicating fetal demise, or infection with abscess formation. The outlook for the fetus is even worse, and perinatal mortality may reach 75% with up to 90% of the surviving

infants having serious malformations.[75] The diagnosis of the abdominal pregnancy is not easy, especially in the early stages. Characteristically, patients present with abdominal pain, vaginal bleeding and gastrointestinal complaints. Ultrasonography together with beta hCG estimations have made early diagnosis easier. The problem still exists, however, as a patient subgroup with an ambiguous presentation remain.[76]

Ultrasound seems to be the most valuable diagnostic tool to localize this rare type of ectopic pregnancy.[2] Primary abdominal pregnancy is condition where fertilized egg implants itself directly into the peritoneal surface of abdominal cavity. If, however, an early tubal pregnancy dislodges and aborts into the pelvis, adhering to peritoneal surface, it is termed a secondary abdominal pregnancy through the secondary nidation. The sonographic presentation of abdominal pregnancy is no different from any other ectopic pregnancy, i. e. showing a hyperechoic ectopic gestational sac containing embryonic/fetal structures and extraembryonic structures with or without active heart beats. Oligohydramnion is the rule and there is no uterine mantle around the fetus.

Surgery is a time-honored treatment for abdominal pregnancy following its diagnosis, with placenta left *in situ*. This is mainly because, in many instances, the placenta is attached to the vital organs or vascular sites, which could be seriously damaged during placental separation. No serious complications occur when it's left *in situ*.[77] An additional important factor is that most abdominal pregnancies are diagnosed relatively late in pregnancy, when the placenta and its area of attachment are larger. Recently, abdominal pregnancies have been diagnosed earlier and in one case the diagnosis was made at 6 weeks of amenorrhea.[74] This made it possible for these pregnancies to be removed laparoscopically. The possible advantages of such therapeutic approach include lower morbidity and mortality, as well as better fertility outcome. However, only a limited number of cases of abdominal pregnancy have been reported early in pregnancy and the safety of operative laparoscopy can be guaranteed only in appropriately selected cases.[74] Similar cases demonstrate further the importance of first trimester ultrasound examination in diagnosing early pregnancy complications. The importance of sonographic imaging in cases of acute abdomen in pregnancy cannot be over-stressed.[78]

Although there are no available data on the use of color Doppler and 3D ultrasound in this field, we believe that these modalities may add additional information on the implantation site and attachment of the placenta to surrounding structures.

THERAPY

Throughout the years, the treatment of ectopic pregnancy has been emergency laparotomy, including salpingectomy. In order to preserve fertility, alternatives to laparotomy and salpingectomy include observation, laparoscopic removal of ectopic pregnancy and systemic or local use of methotrexate or other feticidal agents. As medical therapy for ectopic pregnancy becomes a common practice, familiarity with its side effects may lead to greater success rates. The decision to abandon medical treatment and proceed with surgery should be based on defined guidelines, such as development of peritoneal signs, decreasing hemoglobin levels, or hemodynamic instability.[79]

Methotrexate may be administered systemically,[80] locally[81,82] or in combination. Local application is performed either laparoscopically or transvaginally under ultrasound needle

puncture.[40] In the latter approach, methotrexate is injected directly into the gestational sac. The success rate of systemic, single-dose methotrexate (83–96%) is similar to that of local administration under laparoscopic guidance (89–100%), but the success rate of methotrexate under ultrasound guidance seems to be lower (70–83%).[83] Local injection of methotrexate under control of color Doppler imaging may increase the success rate.[4] The use of color and pulsed Doppler enables visualization of the trophoblastic adnexal flow with highvelocity and low impedance pulsed Doppler (RI<0.40). The needle can be inserted into the area of maximum color signal, which marks trophoblastic invasiveness and vitality.

Pharmacological management of an unruptured, size-appropriate ectopic pregnancy is now an established standard of care. The present protocol recommends systemic use of methotrexate in a single-dose.[84] This form of methotrexate has proven to be successful and cost-effective alternative to traditional surgical management of ectopic pregnancy.[85] In view of the risk of standard therapy and patients desire for fertility, methotrexate treatment may be a therapeutic alternative in cervical pregnancy as well. Recent reports have affirmed that ectopic pregnancy has become, a medical rather than a surgical disease.[2,4,69,72,79,83,84,86]

Puncture injections are valid and reasonable alternative to a traditional surgical approach, especially in patients with an interstitial, cervical or heterotopic pregnancy. In these particular cases, puncture procedures guided by transvaginal ultrasound can efficiently replace surgical treatment and save the patient from unnecessary hysterectomy.

Early diagnosis is the key to effective non-surgical treatment. Diagnostic algorithms using serial beta hCG measurements and transvaginal ultrasound examinations make definitive diagnosis possible without laparoscopy. As stated before, with help of color Doppler it is possible to identify the activity, invasiveness and vitality of trophoblast. These represent the most important characteristics for making the decision for more selective management of ectopic pregnancy. Three-dimensional ultrasound seems to be an even more effective procedure for early diagnosis of ectopic pregnancy in asymptomatic patients, even before 6 weeks of amenorrhea.[59]

Laparoscopic salpingostomy, the surgical gold standard, is an effective therapy in patients who are hemodynamically stable and wish to preserve their fertility. The reproductive performance after salpingostomy appears to be equal to, or better than salpingectomy, but the recurrent ectopic pregnancy rate is slightly higher.[3] A variable systemic dose of methotrexate produces outcomes close to those of laparoscopic salpingostomy in similar patients.[87] Methotrexate treatment is recommended in the asymptomatic patient with serum beta hCG levels of less than 2000 IU/ml, a tubal diameter of <2 cm, and absence of fetal heart activity. The patient's understanding of her condition and compliance are mandatory. However, in many cases, ectopic pregnancy does not meet suitable medical criteria and still requires surgery. In cases suspicious of tubal abortion with a high impedance signal (RI>0.55) and beta hCG below 1000 IU/ml, local administration of methotrexate is not advised.

CONCLUSION

The introduction of beta hCG testing and transvaginal ultrasound has changed our approach to the patient suspected of ectopic pregnancy. An important advantage of the most currently used transvaginal transducers is the ability to perform simultaneous color and spectral Doppler studies, allowing easy identification of the ectopic peritrophoblastic flow. Therefore, color should be applied whenever a finding is suggestive of ectopic pregnancy.

Further progress in diagnostic procedures was made when 3D ultrasound was introduced. Transvaginal 3D ultrasound enables the clinician to perceive the true spatial relations and thus easily distinguish the origin of an adnexal mass, while 3D power Doppler allows detailed analysis of the vascularization.

Transvaginal color and pulsed Doppler imaging may be potentially used for detection of the patients with less prominent tubal perfusion, suitable for the expectant management of ectopic pregnancy. It is expected that increased sensitivity of the serum beta hCG immunoassay and the quality of transvaginal B-mode, color Doppler ultrasound and more recently 3D with color and power Doppler facilities will allow even earlier detection and conservative management of ectopic pregnancies. Furthermore, it seems that fertility outcomes and number of women attempting to conceive after ectopic pregnancy will further increase.

REFERENCES

1. Ectopic pregnancy. In: Speroff L, Glass RH, Kase NG (Eds). Clinical Gynecologic Endocrinology and Infertility. London: Williams and Wilkins, 1999; 1149–67.
2. Timor-Tristch IE, Monteagudo A. Ectopic pregnancy. In: Kupesic S, de Ziegler D (Eds). Ultrasound and Infertility. UK: Parthenon Publishing Group, 2000; 215–39.
3. Kurjak A, Kupesic S. Ectopic pregnancy. In: Kurjak A (Eds). Ultrasound in Obstetrics and Gynecology. Boston: CRC Press, 1990; 225–35
4. Kupesic S, Kurjak A. Color Doppler assessment of ectopic pregnancy. In: Kurjak A. Kupesic S (Eds). An Atlas of Transvaginal Color Doppler. London: Parthenon Publishing, 2000; 137–47.
5. Boufous S, Quartararo M, Mohsin M, Parker J. Trends in the incidence of ectopic pregnancy in New South Wales between 1990–1998. Aust NZJ Obstet Gynaecol 2001; 41:436–3
6. Rajkhowa M, Glass MR, Rutherford AJ, Balen AH, Sharma V, Cuckle HS. Trends in the incidence of ectopic pregnancy in England and Wales from 1966 to 1996. BJOG 2000; 107:369–74
7. Nederlof KP, Lawson HW, Saftlas AF, Atrash HK, Finch EL. Ectopic pregnancy surveillance. Morbid Mortal Weekly Rep 1990; 39:9
8. Strandell A, Thorburn J, Hamberger L. Risk factors for ectopic pregnancy in assisted reproduction. Fertil Steril 1999;2:282–86.
9. Kamwendo F, Forslin L, Bodin L, Danielsson D. Epidemiology of ectopic pregnancy during a 28 year period and the role of pelvic inflammatory disease. Sex Transm Infect 2000; 76:28–32
10. Barlow RE, Cooke ID, Odukoya O, Heatley MK, Jenkins J, Narayansingh G, Ramsewak SS, Eley A. The prevalence of Chlamydia trachomatis in fresh tissue specimens from patients with ectopic pregnancy or tubal factor infertility as determined by PCR and in-situ hybridisation. J Med Microbiol 2001; 50:902 08.
11. Brown WD, Burrows L, Todd CS. Ectopic pregnancy after cesarean hysterectomy. Obstet Gynecol 2002; 99:933–34.

12. Bouyer J, Rachou E, Germain E, Fernandez H, Coste J, Pouly JL, Job-Spira N. Risk factors for extrauterine pregnancy in women using an intrauterine device. Fertil Steril 2000; 74:899–908
13. Bouyer J, Coste J, Fernandez H, Pouly JL, Job-Spira N. Sites of ectopic pregnancy: a 10 year populationbased study of 1800 cases. Hum Reprod 2002; 17:3224–30.
14. Mol BW, van der Veen F, Bossuyt PM. Symptom-free women at increased risk of ectopic pregnancy: should we screen? Acta Obstet Gynecol Scand 2002;81:661–72.
15. Kalinski MA, Guss DA. Hemorrhagic shock from a ruptured ectopic pregnancy in a patient with a negative urine pregnancy test result. Ann Emerg Med 2002; 40:102–05
16. Mertz HL, Yalcinkaya TMJ. Early diagnosis of ectopic pregnancy. Does use of a strict algorithm decrease the incidence of tubal rupture? Reprod Med 2001; 46:29–33
17. Sagaster P, Zojer N, Dekan G, Ludwig HA. Paraneoplastic syndrome mimicking extrauterine pregnancy. Ann Oncol 2002; 13:170–72
18. Hick JL, Rodgerson JD, Heegaard WG, Sterner S. Vital signs fail to correlate with hemoperitoneum from ruptured ectopic pregnancy. Am J Emerg Med 2001;19:488–91.
19. Birkhahn RH, Gaeta TJ, Bei R, Bove JJ. Shock index in the first trimester of pregnancy and its relationship to ruptured ectopic pregnancy. Acad Emerg Med 2002; 9:115–19
20. Wong E, Suat SO. Ectopic pregnancy—a diagnostic challenge in the emergency department. Eur J Emerg Med 2000; 7:189–94
21. Dart R, McLean SA, Dart L. Isolated fluid in the culde-sac: how well does it predict ectopic pregnancy? Am J Emerg Med 2002; 20:1–4
22. Barnhart KT, Katz I, Hummel A, Gracia CR. Presumed diagnosis of ectopic pregnancy. Obstet Gynecol 2002; 100:505–10
23. Sheppard RW, Patton PE, Novy MJ. Serial beta hCG measurements in the early detection of ectopic pregnancy. Obstet Gynecol 1990; 7:417–20
24. Levsky ME, Handler JA, Suarez RD, Esrig ET. Falsepositive urine beta-HCG in a woman with a tuboovarian abscess. J Emerg Med 2001; 21:407–09
25. Dumps P, Meisser A, Pons D, Morales MA, Anguenot JL, Campana A, Bischof P Accuracy of single measurements of pregnancy-associated plasma proteinA, human chorionic gonadotropin and progesterone in the diagnosis of early pregnancy failure. Eur J Obstet Gynecol Reprod Biol 2002; 100:174–80.
26. Poppe WA, Vandenbussche N. Eur Postoperative day 3 serum human chorionic gonadotropin decline as a predictor of persistent ectopic pregnancy after linear salpingotomy. J Obstet Gynecol Reprod Biol 2001; 99:249–52.
27. Timor-Tristch IE, Rottem S, Thale I. Review of transvaginal ultrasonography: description with clinical application. Ultrasound Q 1988; 6:1–32
28. Peisner DB, Timor-Tritsch IE. The discriminatory zone of beta hCG for vaginal probes. J Clin Ultrasound 1990; 18:280–85
29. Fossum GT, Dvajan V, Kletzky DA. Early detection of pregnancy with transvaginal ultrasound. Fertil Steril 1988; 49:788–91
30. Bernascheck G, Euaelstorfer R, Csaicsich P. Vaginal sonography versus serum human chorionic gonadotropin in early detection of pregnancy. Am J Obstet 1988; 158:608–12
31. Albayram F, Hamper UM. First-trimester obstetric emergencies: spectrum of sonographic findings. J Clin Ultrasound 2002; 30:161–77
32. Kurjak A, Zalud I, Volpe G. Conventional B-mode and transvaginal color Doppler on ultrasound assessment of ectopic pregnancy. Acta Med 1990;44:91–103.
33. Rubin GL, Petersin HB, Dorfman SF. Ectopic pregnancy in the United States 1970–1978. J Am Med Assoc 1983; 249:1725–29
34. Bolton G, Cohen F. Detecting and treating ectopic pregnancy. Contemp Obstet Gynecol 1981; 18:101–04.
35. Hopp H, Schaar P Entezami M. Diagnostic reliability of vaginal ultrasound in ectopic pregnancy. Geburtshilfe Frauenheilkd 1995; 55:666–70

36. Hertzberg BS, Kliewer MA. Ectopic pregnancy: ultrasound diagnosis and interpretive pitfalls. South Med J 1995; 88:1191–98
37. Thoma ME. Early detection of ectopic pregnancy visualizing the presence of a tubal ring with ultrasonography performed by emergency physicians. Am J Emerg Med 2000; 18:444–48.
38. Nyberg D. Ectopic pregnancy. In: Nyberg DA, Hill LM, Bohm-Velez M (Eds). Transvaginal Sonography. St. Luis: Mosby Year Book, 1992:105–35.
39. Wojak JC, Clayton MJ, Nolan TE. Outcomes of ultrasound diagnosis of ectopic pregnancy. Dependence on observer experience. Invest Radiol 1995; 30 115–17.
40. Timor-Tritsch IE, Yeh MN, Peisner DB, Lesser KB, Slavik TA. The use of transvaginal ultrasonography in the diagnosis of ectopic pregnancy. Am J Obstet Gynecol 1989; 161:167–70
41. Pellerito JS, Taylor KJW, Quedens-Case C. Ectopic pregnancy: evaluation with endovaginal color flow imaging. Radiology 1992; 183:831–33
42. Fleischer AC, Pennell RG, McKee MS. Ectopic pregnancy: features at transvaginal sonography. Radiology 1990; 174:375–78
43. Bernhart K, Mennuti MT, Benjamin D, Jacobson S, Goodman D, Contifaris C. Prompt diagnosis of ectopic pregnancy in an emergency department setting. Obstet Gynecol 1994; 84:1010–15
44. Leung TY, Ng PS, Fung TY. Ectopic pregnancy diagnosed by laparoscopic ultrasound scan. Ultrasound Obstet Gynecol 1999; 13:281–86
45. Kurjak A, Zalud I, Shulman H. Ectopic pregnancy: transvaginal color Doppler of trophoblastic flow in questionable adnexa. J Ultrasound Med 1991; 10:685–89.
46. Zalud I, Kurjak A. The assessment of luteal blood flow in pregnant and non-pregnant women by transvaginal color Doppler. J Perinat Med 1990; 18:215–21
47. Jurkovic D, Bourne TH, Jauniaux E, Campbell S, Collins WP Transvaginal color Doppler study of blood flow in ectopic pregnancies. Fertil Steril 1992; 57:68 73.
48. Wherry KL, Dubinsky TJ, Waitches GM, Richardson ML, Reed S. Low-resistance endometrial arterial flow in the exclusion of ectopic pregnancy revisited. J Ultrasound Med 2001; 20:335–42
49. Dillon EH, Feyock AL, Taylor KJW. Pseudogestational sacs: Doppler US differentiation from normal or abnormal intrauterine pregnancies. Radiology 1990; 176:359–64.
50. Orden MR, Gudmundsson S, Helin HL, Kirkinen P. Intravascular contrast agent in the ultrasonography of ectopic pregnancy. Ultrasound Obstet Gynecol 1999; 14:348–52.
51. Pellerito JS, Troiano RN, Quedens-Case C, Taylor KJW. Common pitfalls of endovaginal color Doppler flow imaging. Radiographics 1995; 15:37–47.
52. Lurie S, Katz Z. Where a pendulum of expectant management of ectopic pregnancy should rest? Gynecol Obstet Invest 1996; 45:145
53. Stovall TG, Link WF. Expectant management of ectopic pregnancy. Obstet Gynecol Clin North Am 1991; 18:135–44
54. Laurie S, Insler V. Can the serum beta hCG level reliably predict likelihood of a ruptured tubal pregnancy? Isr J Obstet Gynecol 1992; 3:152–44
55. Budowich M, Johnson TRB, Genadry R. The histopathology of developing tubal ectopic pregnancy. Fertil Steril 1980; 34:169–73
56. Kemp B, Funk A, Hauptmann S, Rath W. Doppler sonographic criteria for viability in symptomless ectopic pregnancies. Lancet 1997; 349:1220–21
57. Baba K, Stach K, Sakamoto S, Okai T, Shiego I. Development of an ultrasonic system for three dimensional reconstruction of the fetus. J Perinat Med 1989; 17:19–24
58. Fredfelt KE, Holm HH, Pedersen JF. Three dimensional ultrasonic scanning. Acta Radiol Diagn 1995; 25:237–40
59. Rempen A. The shape of the endometrium evaluated with three-dimensional ultrasound: an additional predictor of extrauterine pregnancy. Hum Reprod 1998; 13:450–54
60. Harika G, Gabriel R, Carre-Pigeon F, Alemany L, Quereux C, Wahl P Primary application of threedimensional ultrasonography to early diagnosis of ectopic pregnancy. Eur J Obstet Gynecol Reprod Biol 1995; 60:117–20

61. Shih JC, Shyu MK, Cheng WF, Lee CN, Jou HJ, Wang RM, Hseih FJ. Arteriovenous malformation of mesosalpinx associated with a vanishing ectopic pregnancy: diagnosis with three-dimensional color power angiography. Ultrasound Obstet Gynecol 1999; 13:63–66
62. Mazur MT, Kurman RJ. Disease of the fallopian tube. In: Kerman RJ (Ed). Blaustein's Pathology of the Female Genital Tract (4th edn). New York: SpringerVerlag, 1994:541–43.
63. Agarwal SK, Wisot AL, Garzo G, Meldrum DR. Cornual pregnancies in patients with prior salpingectomy undergoing in vitro fertilization and embryo transfer. Fertil Steril 1996; 65:659–60
64. Timor-Tritsch IE, Monteagudo A, Matera C, Veit C. Sonographic evaluation of cornual pregnancies treated without surgery. Obstet Gynecol 1992; 79:1044–49.
65. Ackerman TE, Levi CS, Dashefsky SM, Holt SC, Lindsay DJ. Interstitial line: sonographic finding in interstitial (cornual) ectopic pregnancy. Radiology 1993; 189:83–87
66. Hafner T, Aslam N, Ros JA, Zosmer N, Jurkovic D. The effectiveness of non-surgical management of early interstitial pregnancy: a report of ten cases and review of the literature. Ultrasound Obstet Gynecol 1999; 13:131–36
67. Jurkovic D, Geipel A, Gruboeck K, Jauniaux E, Natucci M, Campbell S. Three-dimensional ultrasound for the assessment of uterine anatomy and detection of congenital uterine anomalies. A comparison with hysterosalpingography and two dimensional sonography. Ultrasound Obstet Gynecol 1995; 5:233–37
68. Lawrence A, Jurkovic D. Three-dimensional ultrasound diagnosis of interstitial pregnancy. Ultrasound Obstet Gynecol 1999; 14:292–93.
69. Ben-Sholmo I, Eliyahu S, Yanai N, Shalev E. Methotrexate as a possible cause of ovarian cyst formation: experience with women treated for ectopic pregnancies. Fertil Steril 1997; 67:786–88
70. Schiff E, Tsabari A, Shalev E, Maschiach S, Bustan M, Weiner E. Pharmacokinetics of methotrexate after local tubal injection for conservative treatment of ectopic pregnancy. Fertil Steril 1992; 57:688–90
71. Timor-Tritsch IE, Monteagudo A, Mandeville EO, Peisner DB, Parra-Anaya G, Pirrone EC. Successful management of viable cervical pregnancy by local injection of methotrexate guided by transvaginal ultrasonography. Am J Obstet Gynecol 1994; 170:737–39.
72. Jurkovic D, Hacket E, Campbell S. Diagnosis and treatment of early cervical pregnancy: a review and a report of two cases treated conservatively. Ultrasound Obstet Gynecol 1996; 8:373–80
73. Jauniaux E, Taidi J, Jurkovic D, Campbell S, Hustin J. Comparison of color Doppler features and pathological findings in complicated early pregnancy. Hum Reprod 1994; 9:2432–37
74. Morita Y, Tsutsumi O, Kurmochi K, Momoeda M, Yoshikawa H, Taketeani Y. Successful laparoscopic management of primary abdominal pregnancy. Hum Reprod 1996; 11:2546–47.
75. Ahmed B, Fawzi HW, Abushama M. Advanced abdominal pregnancy in the developing countries. J Obstet Gynecol 1996; 16:400–05.
76. Angtuaco TL, Shah HR, Meal MR, Quirk JG. Ultrasound evaluation of abdominal pregnancy. Crit Rev Diagn Imaging 1994; 35:1–59
77. Bajo JM, Garcia FA, Huertas MA. Sonographic follow-up of a placenta left in situ after delivery of the fetus in abdominal pregnancy. Ultrasound Obstet Gynecol 1996; 7:285–88
78. Zaki ZMS. An unusual presentation of ectopic pregnancy. Ultrasound Obstet Gynecol 1998; 11:456–58.
79. Thoen LD, Crenin MD. Medical treatment of ectopic pregnancy with methotrexate. Fertil Steril 1997; 68:727–30.
80. Lipscomb GH, Meyer NL, Flynn DE, Peterson M, Ling FW. Oral methotrexate for treatment of ectopic pregnancy. Am J Obstet Gynecol 2002; 186:1192–95
81. Haimov-Kochman R, Sciaky-Tamir Y, Yanai N, Yagel S. Conservative management of two ectopic pregnancies implanted in previous uterine scars. Ultrasound Obstet Gynecol 2002; 19:616–19.

82. El-Lamie IK, Shehata NA, Kamel HA. Intramuscular methotrexate for tubal pregnancy. J Reprod Med 2002; 47:144–50
83. Yao M, Tulandi T. Current status of surgical and non-surgical management of ectopic pregnancy. Fertil Steril 1997; 67:421–33
84. Powell MP, Spellman JR. Medical management of the patient with an ectopic pregnancy. J Perinat Neonat Nurs 1997; 9:31–43
85. Luciano AA, Roy G, Solima E, Ann NY Ectopic pregnancy from surgical emergency to medical management. Acad Sci 2001; 943:235–54
86. Morlock RJ, Lafata JE, Eisenstein D. Costeffectiveness of single-dose methotrexate compared with laparoscopic treatment of ectopic pregnancy. Obstet Gynecol 2000; 95:407–12
87. Tulandi T, Sammour A. Evidence-based management of ectopic pregnancy. Curr Opin Obstet Gynecol 2000;12:289–92.

Chapter 15
Trophoblastic Disease

Kazuo Maeda

INTRODUCTION

Trophoblastic diseases are more in Asia than Europe. Choriocarcinoma is preceded by hydatidiform mole, and characterized by metastases to the tissues and organs, and many patients died of the metastases. The metastatic and primary foci are so effectively supppressed by chemotherapy, patients are cured from the death and hysterectomy. At present choriocarcinoma is rare by the postmolar chemotherapy. Molar pregnancy also decreased, possibly due to ultrasound diagnosis and termination in early pregnancy. Outcome of trophoblastic diseases is greatly improved by the introduction of ultrasound diagnosis and intensive chemotherapy.

CLASSIFICATION,[1] DEVELOPMENT AND PATHOLOGY[1]

(Japan Society of Obstetrics and Gynecology and Japanese Pathological Society, 1995)

Trophoblastic diseases are roughly divided into hydatidiform mole and choriocarcinoma, both are classified into subgroups in the pathological classification. There are also clinical classification (Tables 15.1 and 15.2) and FIGO staging (Table 15.3) in the diseases.

Total Hydatidiform Mole

It is abnormal pregnancy, where all placental villi change to molar vesicles and fill uterine cavity, while there is no embryo, fetus, nor umbilical cord (Fig. 15.1). Amnion is, however, found in

Table 15.1: Clinical classification of trophoblastic diseases

I.	Hydatidiform mole	
	A.	Total hydatidiform mole
		(1) non-invasive total mole
		(2) invasive total mole
	B.	Partial hydatidiform mole
		(1) non-invasive partial mole
		(2) invasive partial mole
II.	Choriocarcinoma	
III	Persistent trophobiastic disease	
Appendix: Every disease from I to III is further divided into metastatic or non-metastatic disease.		

Table 15.2: NCI/NIH clinical classification[28]

1. Benign GTD:
   - A. Complete hydatidiform mole
   - B. Partial hydatidiform mole
2. Malignant GTD
   - A. Nonmetastatic GTD
   - B. Metastatic GTD
     1. Good prognosis, low-risk—absence of any risk factor.
     2. Poor prognosis, high-risk—presence of any risk factor.
3. Risk factors are:
   - a. Duration of disease greater than 4 months.
   - b. Pretherapy ßhCG level greater than 40,000 IU/mL (prior to any chemotherapy).
   - c. Brain or liver metastasis.
   - d. GTD after term gestation.
   - e. Prior failed chemotherapy

some cases.[2] No capillary vessel is noted in the molar cyst which is covered by proliferated trophoblasts (Fig. 15.2). Microscopically found molar cyst of diameter less than 2 mm is called

Table 15.3: FIGO staging for gestational trophoblastic disease (GTD)

I.	Disease confirmed to uterus (IA, B, or C, depending on risk factors).
II.	Metastasis to pelvis or vagina (IIA, B, or C, depending on risk fact
III.	Metastas is to lung (IIIA, B, or C, depending on risk factors).
IV.	Metastasis to distant sites: brain, liver, etc. (IVA, B, or C depending on risk factors)
	A=no risk factors.
	B=one risk factor.
	C=two risk factors.
1.	Risk factors are:
a.	βhCG greater than 100,000 IU/mL.
b.	Duration of disease greater than 6 months from termination of antecedent pregnancy.
2. Note any prior chemotherapy given for GTD. Placental site trophoblastic tumors should be reported separately, and histologic verification of disease is not required.	

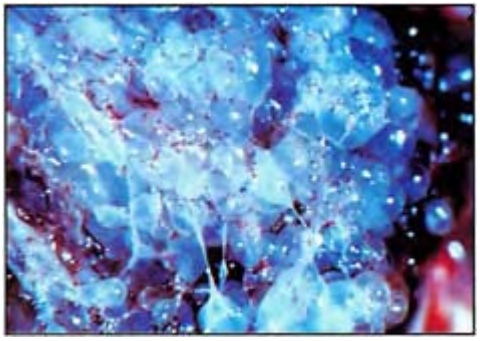

Figure 15.1: The cysts of total hydatidiform mole occupy whole uterine cavity

microscopic mole. Trophoblasts are scattered in the decidua and myometrium, and called syncytial endometritis. Molar cysts may spread into blood vessel, which is the intravascular mole, and rarely metastasis appears in distant organ. Chromosomes are usually diploid 46, XX, where the XX are both male origin, that is called androgenesis (Kaji and Ohama,[3] 1977). Its developmental mechanism is the fertilization of two X sperms into a vacant ovum without nucleus.[3] The chromosome is rarely 46, XY, where both X and Y are male origin.[4] Total mole develops also in one conceptus of the twins or triplets by the androgenesis (Figs 15.3 and 15.4). Risk of the repeated molar pregnancy is

less than 1%, the risk increased in blood group B and in some Asians, while repeated molar pregnancy is not an indication for chemo-

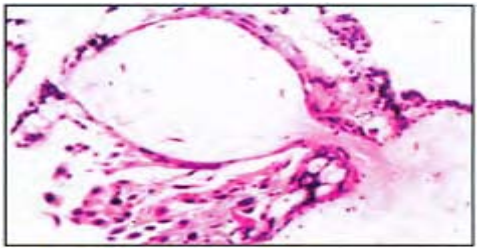

Figure 15.2: Microscopic view of a daughter villus of total mole, which is covered by proliferated trophoblasts, while no capillary blood vessel is found in the molar cyst

therapy.[5] The presence of telomerase activity in total moles is associated with the development of invasive mole and choriocarcinoma.[6]

Ovarian theca lutein cysts are found in trophoblastic diseases, particularly in developed total and invasive moles (Fig. 15.5). The incidence of ultrasonographic lutein cyst is low in the first trimester.[7] Since theca cell cyst is benign, it is not a trophoblastic disease, and disappear after the remission, no surgical removal is appropriate.

Partial Hydatidiform Mole

It is partial change of placental villi into the mole, which is associated with embryo, fetus or fetal parts (Fig. 15.6). Fetal anomalies are common. Chromosomes are usually triploids, 69, XXX, 69,

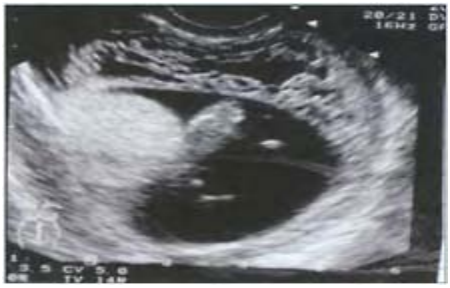

Figure 15.3: One twin changes into total hydatidiform mole. F—fetus,

M—mole. *Courtesy* Dr M Utsu of Seirei Mikatahara Hospital

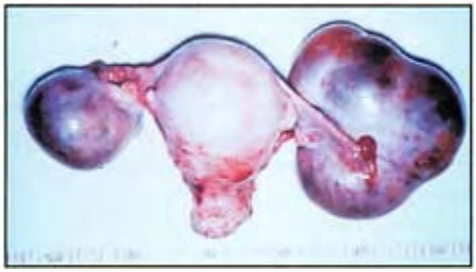

Figure 15.5: Ovarian theca lutein cysts associated with invasive mole, which were removed in 1960 before the knowledge of their benign nature

XXY, or 69, XYY.[8] DNA analysis confirmed the androgenetic mechanism.[9] Capillary vessels are found in molar interstitium.

Invasive Hydatidiform Mole

It is the invasion of molar cysts into myometrium with destruction and hemorrhage. Intravascular mole and placental polyp are excluded from the invasive mole. The lesion is formed either in total or partial mole, usually after the molar evacuation, although the invasion may develop before the termination. The change is visually noted in surgical specimen (Fig. 15.7) and microscopically confirmed, where the trophoblasts proliferate,

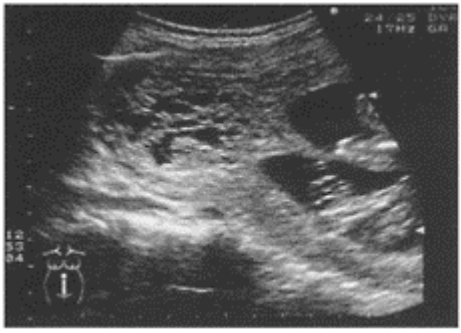

Figure 15.4: One triplet changes into total hydatidiform mole. F1, F2—two triplet fetuses, M—mole. *Courtesy* Dr M Utsu

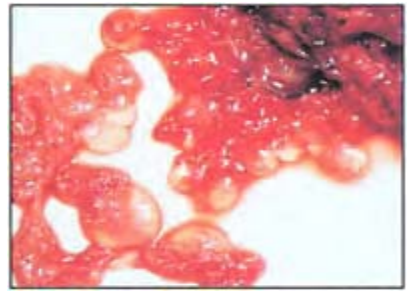

Figure 15.6: Partial hydatidiform mole. Normal placenta is shown at upper right corner

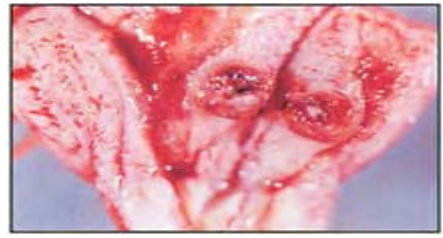

Figure 15.7: Invasive mole found in hysterectomized specimen (two arrows)

hemorrhage and necrosis are found in the myometrium (Fig. 15.8). Invasive mole metastasis

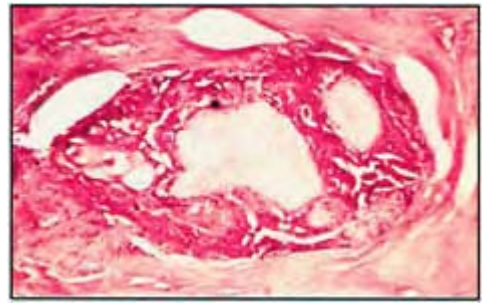

Figure 15.8: Low power microscopic view of villus pattern of the invasive mole

is rare and of low malignancy, e.g. spontaneous pulmonary focus regression was experienced after hysterectomy of invasive mole. The outcome is more favorable than choriocarcinoma.

Choriocarcinoma

It is solid trophoblastic tumor developed primarily in myometrium (Fig. 15.9), or in distant organs and tissues,[10–15] usually after the removal of or partial hydatidiform mole, and also infrequently after the abortion or deliveries. They are gestational choriocarcinoma or gestational trophoblastic disease (GTD). Non-gestational choriocarcinoma develops from germ cells or other cancer cells in children.[10] Other papers also reported primary choriocarcinoma in reproductive as well as in non-reprodctive organs, e.g. vulva,[11] uterine cervix,[12] lung, stomach and pancreas,[13,14] gall-

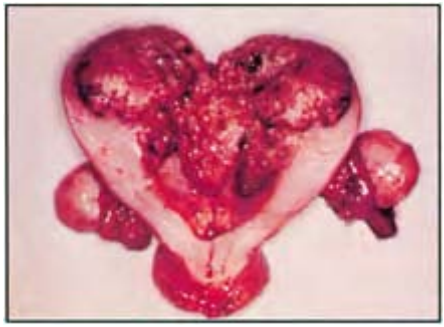

Figure 15.9: Uterine choriocarcinoma. The uterus was hysterectomized in the period before introduction of effective chemotherapy

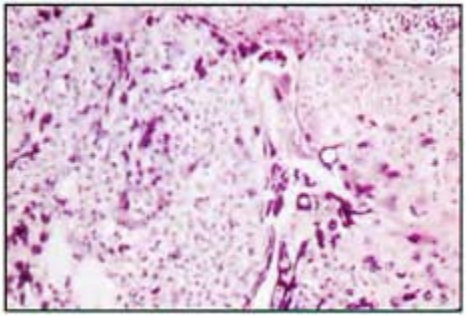

Figure 15.10: Microscopic view of choriocarcinoma. Note the trophoblast

proliferation and absence of villus pattern

bladder,[15] or urinary bladder.[16] We also treated uterine cervical choriocarcinoma with internal iliac arterial infusion of methotrexate.[17]

Choriocarcioma is constructed of syncytio- and cyto-trophoblasts, and shows no villus pattern at all (Fig. 15.10). Since villus pattern is characteristic sign of invasive mole, and its outcome is less ominous than choriocarcinoma, microscopic studies should be detailed on whole specimen after hysterectomy.

Wide spread distant metastases of choriocarcinoma were common before the introduction of effective chemotherapy in this field. The interval of its diagnosis and metastases was about half to one year. Early metastases were dark red tumors at external genitalia and vaginal wall (Fig. 15.11).

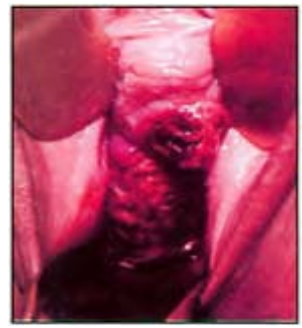

Figure 15.11: Vaginal wall metastasis of choriocarcinoma. Note the dark red tumor (arrow)

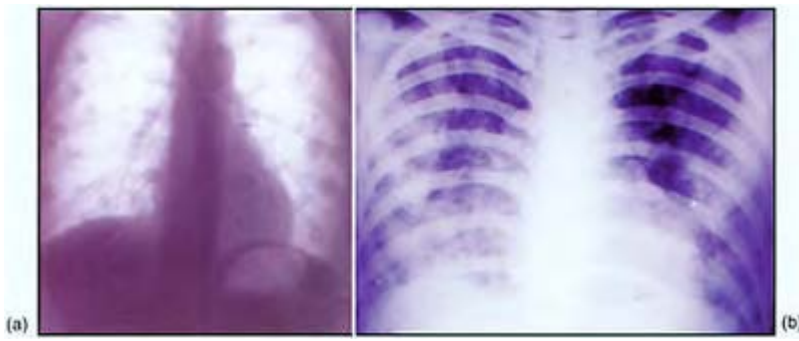

Figure 15.12: Left panel (a) shows typical pulmonary metastasis of choriocarcinoma. Note multiple round

foci with irregular size. Right (b) diffuse shadows show multiple emboli of choriocarcinoma in pulmonary arterioles. Her symptom was dyspnea

Subsequent frequent spread was the lung, where typical foci showed round shape of irregular size (Fig. 15.12a), resembled to snow balls or cannon balls, while diffuse pulmonary shadow is found in multiple trophoblast emboli in pulmonary arterioles (Fig. 15.12b). Any organs or tissues were affected after pulmonary metastasis, e.g. skin,[18] subcutaneous tissue, intestine, liver, spleen, kidney, heart,[19,20] and finally brain (Figs 15.13 and 15.14). Tumor cells were found also in blood vessels (Fig. 15.15). Every organ is damaged by the trophoblasts and hemorrhage. Intraperitoneal bleeding appeared in hepatic lesion. Patients died from brain metastasis and multiple metastases due

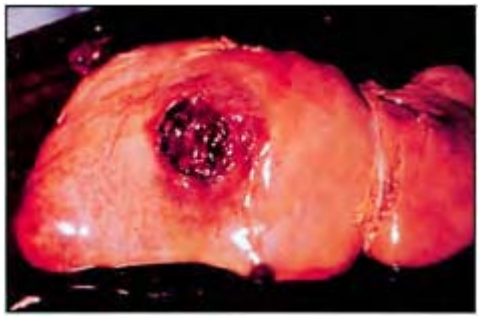

Figure 15.13: Choriocarcinoma metastasis on the right lobe of liver. Autopsy finding

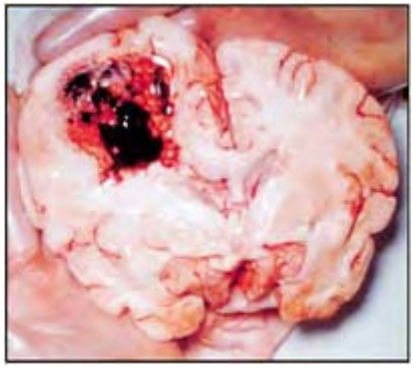

Figure 15.14: Brain metastasis of choriocarcinoma, cerebral hemorrhage

and brain edema. Autopsy finding before introduction of effective chemotherapy

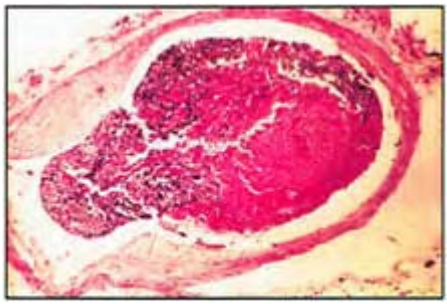

Figure 15.15: Choriocarcinoma cells found in the coronary artery in an autopsy

to the damage and dysfunction. Choriocarcinoma is divided into three subtypes:

1. *Gestational choriocarcinoma* development is related to pregnancy, and three categories are further classified.

    a. *Uterine choriocarcinoma* is the most common, developed in the uterus after hydatidiform mole, and rarely after abortion or normal delivery. A choriocarcinoma with an intact pregnancy was reported.[21]
    b. *Extrauterine choriocarcinoma* develops primarily at the place of ectopic pregnancy, while there is no tumor in the uterus.
    c. *Intraplacental choriocarcinoma* is found in the placenta mainly after delivery. Intraplacental choriocarcinomas were reported to be associated with viable pregnancy.[22]

2. *Non-gestational choriocarcinoma* is not gestational origin, and divided into two categories.

    a. *Choriocarcinoma of germ cell origin* is subtype of germ cell tumor developed in the ovary or testis. Common germ cell tumor may be associated with choriocarcinoma. The disease develops even in the woman before marriage or adult male, and the tumor is more resistant to chemotherapy than gestational one.
    b. *Choriocarcinoma derived from dedifferentiation of other carcinoma* is choriocarcinomatous change of other cancers, which may excrete hCG.

3. *Unclassified choriocarcinoma* is unclassified tumor into gestational or non-gestational.

Placental Site Trophoblastic Tumor (PSTT)

It is rare uterine tumor of proliferated intermediate trophoblasts that play critical role in implantation.[23] There is seldom contribution of syncitioor cyto-trophoblast. The tumor is preceded by normal delivery, abortion, or hydatidiform mole. The hCG titer is low, and HPL is higher than βhCG.[28] Final diagnosis is made by histology. Metastasis and recurrence are many.[23–25,27] PSTT is reported to be highly malignant, and can be deadly.[28] A case of PSTT in mother and child was reported.[26]

Persistent Trophoblastic Disease (PTD)

It is either postmolar metastatic mole, invasive mole or choriocarcinoma, where no specimen is obtained or pathological finding is unknown. Three subdivisions are classified.

1. *Post-molar persistent hCG* shows abnormal type II hCG regression pattern after complete removal of hydatidiform mole, i.e. urinary hCG is higher than 1,000 mIU/mL after 5 weeks, serum hCG higher than 100 mIU/mL after 8 weeks, or serum hCGß higher than 1.0 mIU/ mL (hCGß-CTP 0.5 mIU/mL), that is cut-off level after 20 weeks, where the focus is unknown.
2. *Clinical invasive mole or metastatic mole* is estimated by the modified Ishizuka score (Table 15.4), or by the persistence of metastatic molar focus.
3. *Clinical choriocarcinoma* is the disease estimated from the existing focus and Ishizuka score (Table 15.4), or by the post-molar state where hCG elevates again, except for new pregnancy, after the complete remission, which is confirmed by the hCG lower than the cut-off level.

SYMPTOMS

Hydatidiform mole shows amenorrhea similar to common pregnancy. Typical symptoms of well developed total hydatidiform mole are: severe nausea and vomiting (hyperemesis), hypertension and proteinuria (pre-eclampsia), no fetal movement, no fetal heartbeat detected by auscultation or Doppler detector, greater uterine size than normal pregnancy, abdominal pain, hemorrhage, and expelling molar vesicles in some cases, and higher urinary or serum hCG level usually than 100,000 mIU/mL. Typical symptoms are infrequent at present, after introduction of ultrasound diagnosis,. Ultrasonic screening of the first trimester of pregnancy changed the situation, particularly with transvaginal scan, where early stage hydatidiform mole is detected by common real-time B-mode and evacuated before its development. Ovarian theca lutein cysts is also detected by the ultrasound.

Partial hydatidiform mole associated with living fetus was similar to common pregnancy except for hyperemesis, enlarged uterus and high titer hCG. The situation changed also after the use of ultrasonic screening by the detection of partial molar changes of the placenta with the embryo, fetus or fetal particles (Fig. 15.16).

Twenty percent of the total mole are followed by the sequelae, and choriocarcinoma develops in 2% of total mole after its evacuation, whereas partial moles show 5% incidence of sequelae, and rare progress to choriocarcinoma.[28]

Table 15.4: Scoring system for the diagnosis of choriocarcinoma[1]

Score	0	1	2	3	4	5
Possibility to be choriocarcinoma	50	60	70	80	90	100
Antecedent*[1] pregnancy	Molar				Abortion	Term delivery
Latency*[2]	<6 months				6m-3years	3years<
Primary focus	Uterus, vagina, parametrium		Ovary, F-tube Cervix	Outside pelvis		
Metastasis	No, pelvis, lung				Outside pelvis (Except lung)	
Lung foci						
diameter	<20 mm			20–30	mm 30 mm <	
irregular size*[3]	No				Yes	
number	<20				20 <	
Urinary hCG (mIU/ml)	$<10^6$	$10^{6–7}$		10^7		
Basal body Temperature Chart	irregular, or monophasic				di-phasic	
Menstruation	irregular				regular*[4]	

Clinical invasive mole or metastatic mole: Sum of the scores; 4 or less
Clinical choriocarcinoma: Sum of the scores; 5 or more
*1 Immediately antecedent pregnancy
*2 Between the end of antecedent pregnancy and the diagnosis
*3>1 cm difference in the diameter of foci
*4 Diphasic BBT or regular menstruation for at least a few months after the antecedent pregnancy. Add 5 points too, if serum hCG is less than cut-off level in the period of regular menstruation.

Invasive mole is usually found after removal of total or partial mole, and shows vaginal bleeding, enlarged uterus, bilaterally enlarged ovaries, and high urinary or serum hCG. The symptom resembles choriocarcinoma, and needs differential diagnosis. The interval from antecedent pregnancy

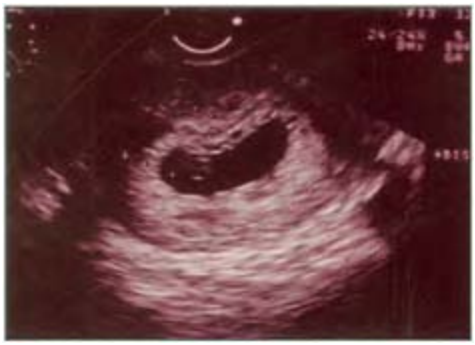

Figure 15.16: Partial hydatidiform mole at 11 weeks of pregnancy. *Courtesy* Dr M Utsu

is shorter than choriocarcinoma, and it is usually within half year in invasive mole. Urinary hCG shows continuous elevation after the molar evacuation, and the hCG titer is relatively lower than choriocarcinoma. Ultrasonic study discloses the presence of molar cysts in the uterine mass.

Choriocarcinoma Common gestational choriocarcinoma is preceded by total or partial hydatidiform mole, or abortion or even by term delivery. Interval from antecedent pregnancy is long, and it can be more than one year in typical uterine choriocarcinoma. It is longer than invasive mole, and there may be the period of partial remission and low hCG titer in some cases. The interval is more than 10 years in case of extrauterine choriocarcinoma, e.g. in a primary tumor developed in the lung.

Clinical symptoms are vaginal bleeding, enlarged uterus, high hCG titer, ovarian masses, and irregular basal body temperature (BBT) chart. Choriocarcinoma is strongly supposed by the presence of metastasis, which is found at external genitalia or vaginal wall in early stage. Multiple round radiological foci in the lung show the progress of malignancy. In non-gynecological case also, hCG should be checked when pulmonary round foci are found in female patient.

The symptoms due to distant metastases suggest choriocarcinoma, e.g. abdominal pain and hemorrhage in hepatic lesion, or persistent headache and vomiting followed by unconsciousness and apnea in the brain metastasis. A patient losed her personality after metastasis to the frontal lobe of the brain in our experience.

Placental site trophoblastic tumor (PSTT) is preceded by any gestational process. Enlarged uterus and vaginal bleeding is clinical symptoms. Metastasis is frequently found. The disease often recurrences after chemotherapy or surgery. The disease is highly malignant and can be deadly.[28]

Persistent trophoblastic disease (PTD) includes three categories, i.e. postmolar persistence of hCG, clinical invasive or metastatic mole, and clinical choriocarcinoma. Although the focus is unknown in the postmolar state and it is known in the clinical invasive mole and clinical choriocarcinoma, all three show persistence of abnormally high hCG titer.

DIAGNOSIS

Total hydatidiform mole is diagnosed by its symptoms, high urinary and serum hCG titer, and particularly by ultrasonic B-mode, color Doppler and Doppler fllowmetry. Transvaginal scan is useful in the first trimester. Ultrasonic B-mode detects mole cysts in the uterine cavity without detecting the fetus or embryo or its particle (Fig. 15.17). Amniotic membrane and fluid are, however, occasionally detected by the B-mode. An embryo with heart beat was found in gestational sac in a report, and the total hydatidiform mole with 45, XX chromosome was detectd 4 weeks later.

The total hydatidiform mole is detected in the most early stage at the screening of the first trimester. Empty gestational sac, of which wall showed small cystic change without embryo was ultrasonically confirmed before the typical growth of total hydatidiform mole (Fig. 15.18). Early total mole resembles to a blighted ovum, whereas vomiting and high urinary hCG titer of molar case are contradictory to blighted ovum. The GS wall increases, and typical molar cysts develop within

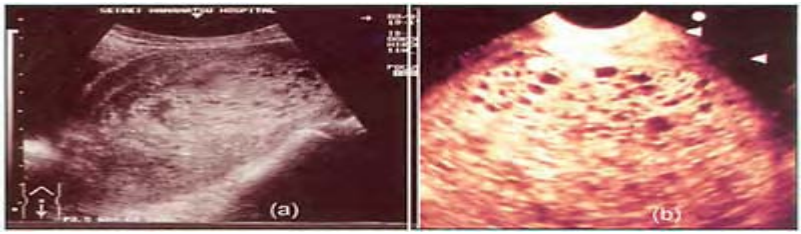

Figure 15.17: Left (a) shows total hydatidiform mole in 11 weeks of pregnancy. *Courtesy* Dr M Utsu, and Right (b) shows established total mole. *Courtesy* Prof S Kupesic of University of Zagreb

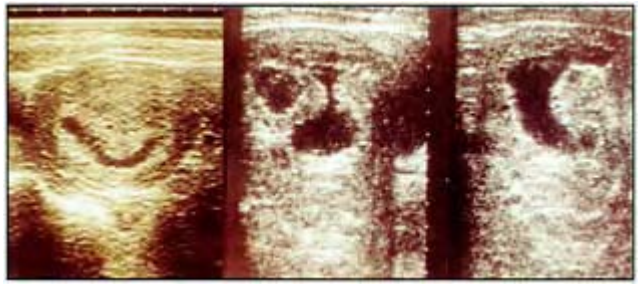

Figure 15.18: Ultrasonograms of three total hydatidiform moles in early pregnancy

1 to 2 weeks in early pregnancy. It is cystic but not snow-storm pattern in the use of modern B-mode device. The diastolic flow is large and RI is lower in uterine, arcuate, radial and spiral arteries than normal pregnancy (Fig. 15.19).[29] Also in the intervillous space, RI is low in molar pregnancy.[30] Total mole is recognized these morphological and functional characters which are detected by ultrasound techniques.

Total mole is diagnosed when urinary or serum hCG is higher than 100,000 mIU/mL that is the higher normal range of early pregnancy. Total mole is, however, not totally denied by lower hCG level. Postmolar state is monitored every 1 to 2 weeks by the hCG, ultrasound and local condition, after the complete mole removal by repeated curettages, until the hCG reaces low cut-off level.

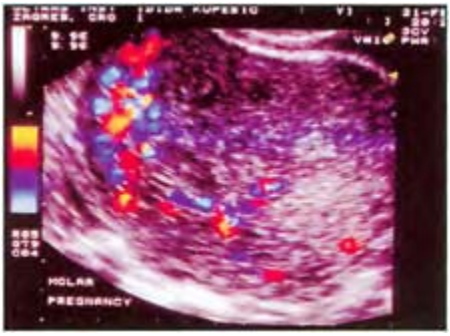

Figure 15.19: Color flow mapping of total hydatidiform mole. *Courtesy* Prof S Kupesic

Abnormal regression of hCG or the persistent trophoblastic disease receives chemotherapy for the prophylaxis of choriocarcinoma.

Total hydatidiform mole developes in one of twins or triplets. It is diagnosed in ultrasonic study by the molar tissue separated by the septum originated from the fetus (Figs 15.3 and 15.4). Chromosome diploidy and DNA analysis reports androgenetic origin. Partial mole in singleton pregnancy is differentiated from the total mole of multiple pregnancy by the partial molar change of placental villi without separating septum, or by the triploid chromosome.

Partial hydatidiform mole is diagnosed by the subjective symptoms, high urinary hCG and the ultrasound findings, which show the presence of the fetus, or the partial image of the fetus and partial changes of the placental villi into molar cysts. Anomalies are frequent in the fetus. Chromosomal examination shows triploidy. Post-molar changes of urinary and serum hCG are the same as those of total hydatidiform mole. Chemotherapy in case of abnormal regression and persistent trophoblastic disease is also the same as total hydatidiform mole.

Invasive hydatidiform mole is mainly found after the evacuation of total or partial mole, with short interval after the mole, which is less than half year, although the mole invades the myometrium during its pregnancy. Myometrial invasion may be found by

detailed study on the uterine wall before the termination with B-mode and particularly color flow or power Doppler flow mapping.

Its symptoms are close to choriocarcinoma, i.e. postmolar development, vaginal bleeding, enlarged uterus, and the metastasis can be present. Urinary or serum hCG is positive, but the level is lower than choriocarcinoma. Ultrasound B-mode shows uterine mass. Invasive mole is clear, if molar cysts are imaged in the tumor (Fig. 15.20). Rich blood flow is found by color flow mapping (Fig. 15.21) and by power Doppler image. Doppler flow impedance is low in the invasive mole (Fig. 15.23). On the contrary, Doppler flow impedance is as high as 0.6 in the wall artery of theca luein cyst (Fig. 15.24).

Choriocarcinoma develops after evacuation of hydatidiform mole, abortion or delivery. Clinical symptoms are vaginal bleeding, enlarged uterus, ovarian masses, high gonadotropin titer, and they are similar to the invasive mole, when it is early stage before the metastases. Invasive mole is characterized by its postmolar detection and shorter interval after the mole. Metastases in external genitalia and vaginal wall (Fig. 15.11), as well as a few radiological foci in the lung are found mainly in early stage of choriocarcinoma, but an invasive mole cannot be totally denied from the metastasis.

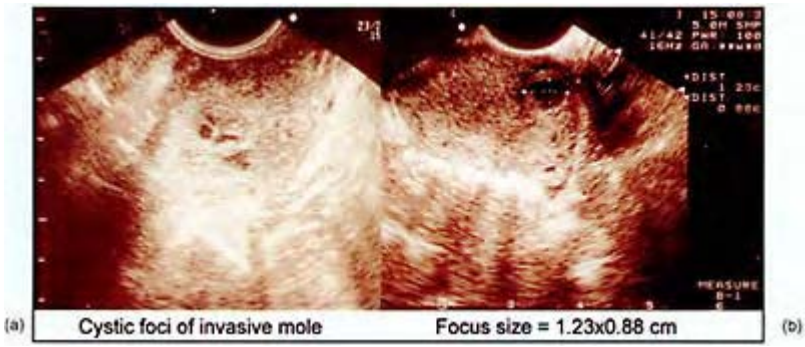

Figure 15.20: Left (a) shows cystic foci of invasive mole. Right (b) shows focus size that is 1.23×0.88 cm. *Courtesy* Dr. S.Yoshida, Dpt. OBGY, Tottori University

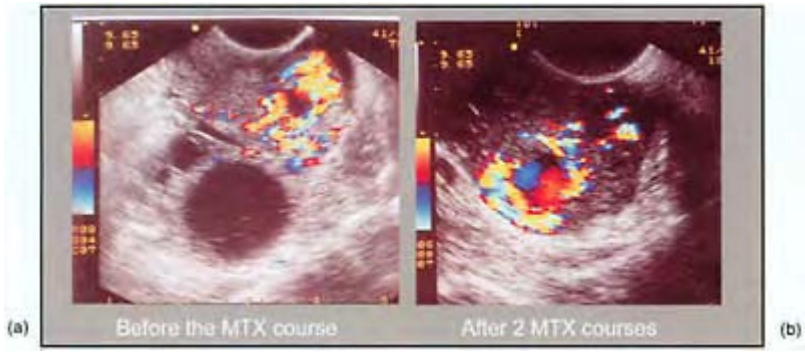

Figure 15.21: Invasive mole (left, a) and mild change after two MTX courses (right, b). *Courtesy* Dr S Yoshida

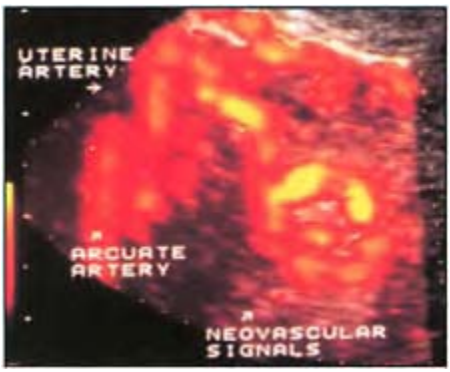

Figure 15.22: Power Doppler image shows rich blood flow in an invasive mole. Courtesy of Prof. S.Kupesic

Differential diagnosis of choriocarcinoma from invasive mole is important, because the outcome is ominous in the former and less risky in the latter, in spite of the similarity of their clinical symptoms. Ultrasonic detection of cystic pattern in the focus (Fig. 15.20) is decisive evidence to invasive mole, i.e. ultrasound is an alternative to X-ray pelvic angiography. Ultrasonic B-mode image shows no cyst pattern in choriocacinoma (Fig. 15.25). Color Doppler flow mapping shows rich blood flow (Fig. 15.26), and flow impedance is usually low in both diseases, but it is lower in choriocarcinoma than invasive mole. The RI of uterine artery is significantly lower in the choriocarcinoma than in

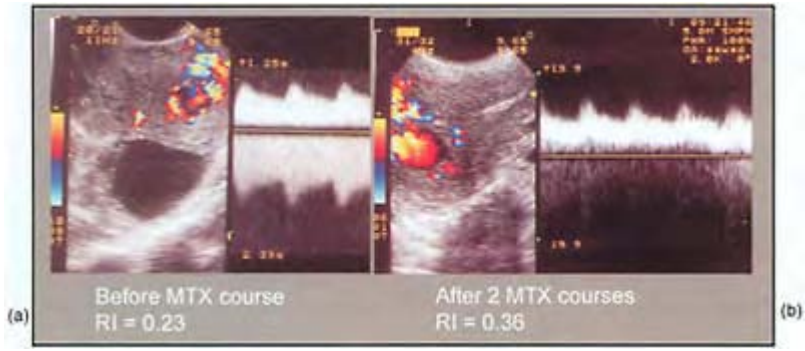

Figure 15.23: Pulsed Doppler flow waves before (left, a) and after (right, b) two MTX courses in the invasive mole of Fig. 15.21. There is mild increase of RI after the course. *Courtesy* Dr. S.Yoshida

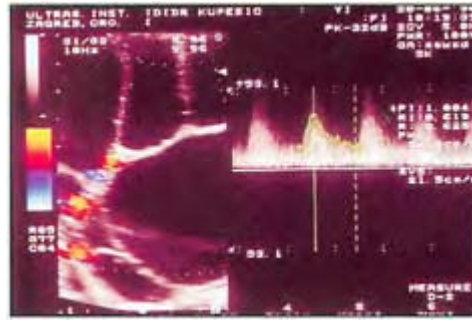

Figure 15.24: Color flow mapping and pulsed Doppler flow wave analysis in theca cell tumor. Courtesy Prof. S.Kupesic

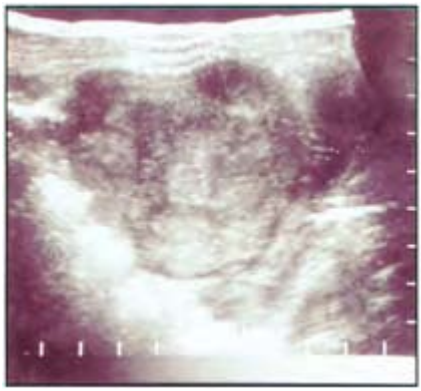

Figure 15.25: Abdominal scan of choriocarcinoma. *Courtesy* Dr. Terahara, Imakyurei Hospital

hydatidiform mole.[31] Differential gene expression pattern is reported between normal trophoblast and choriocarcinoma cells.[32] In vague cases after detailed examination, the disease is suspected by the use of scoring system (Table 15.4). The risk is estimated by NCI/NIH classification (Table 15.2), FIGO staging (Table 15.3) and WHO scoring table (Table 15.5).

The diagnosis of non-gestational choriocarcinoma is based on the tumor formation in the ovary or testis, no existence of antecedent gestation, positive urinary and serum hCG, and ultrasound finding with B-mode and color flow mapping. DNA polymorphism analysis is reported in pure non-gestational choriocarcinoma.[33]

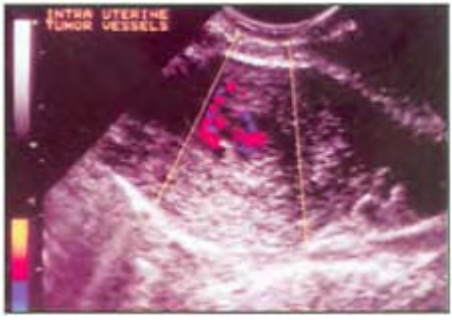

Figure 15.26: Uterine choriocarcinoma with moderate color flow pattern. RI=0.3. *Courtesy* S.Kondo

In the detection of metastatic foci, X-ray image in pulmonary lesion, CT in brain metastasis, MRI in some soft tissues are useful, while the mostly useful are the ultrasonic B-mode, color flow mapping and Doppler flowmetry in the diagnosis and monitoring of the foci in various tissues and organs. Invasive mole is differentiated from choriocarcinoma from its cystic pattern, and the foci size is measured by B-mode and rich blood flow by color flow mapping or power Doppler, and the low flow impedance by the pulsed Doppler flowmetry in malignant trophoblastic diseases. In the chemotherpy course, the reduction of the tumor size in primary and metastatic foci is objectively and quantitatively monitored, and the blood flow reduction is observed during the therapy by these ultrasonic diagnoses. Ultrasound is indispensable in the diagnosis of trophoblastic diseases.

Persistent trophoblastic disease (PTD) Since the PTD patients receive chemotherapy that may lead to complete remission without surgical removal of the foci, no histological diagnosis is made and the clinical diagnosis is the final in the case of complete remission. The foci are found by ultrasonic diagnosis and the size is monitored until the disappearance in the chemotherapeutic courses. Color flow mapping and Doppler flow metry are also useful for the confirmation of tumor reduction. Ultrasonic study is indispensable in the diagnosis and evaluation of trophoblastic diseases. 0

Table 15.5: WHO progrnostic scoring system

	Score[b]			
	0	1	2	4
Age	<=39	>39		
Antecedent pregnancy	hydatidiform mole	abortion	term	
Interval between end of antecedent pregnancy and start of chemotherapy (month)	<4	4–6	7–12	>12
HCG (IU/L)	$<10^3$	10^3–10^4	10^4–10^5	$>10^5$
A, B, and O groups		O or A	B or AB	
Largest tumor, including uterine (cm)	<3	3–5	>5	
Site of metastasis		spleen, kidney	GI tract, live	brain
Number of metastasis	0	1–4	4–8	>8
Prior chemotherapy		1 drug	>=2 drugs	

[a] Most accurate for determining prognosis, especially for stage II and III disease.
[b] Total score is obtained by adding individual scores.
Total score< =4 is low risk, 5–7 is medium risk, >=8 is high risk.

Placental site trophoblastic tumor (PSTT) The long interval after the antecedent gestation, symptoms including vaginal bleeding and enlarged uterus, and the lack of high

hCG titer, suggest the presence of the disease. Differential diagnosis from other malignant trophoblastic disease is needed. Also due to the rarity of PSTT, the diagnosis tends to be incorrect, e.g. diagnosed as spontaneous abortion. Final correct diagnosis is made after histology.

Other than common examination and B-mode imaging, color Doppler flow mapping documents marked increase of uterine vascularity, which is characterized by low resistance to flow, without regression after successful chemotherapy, when negative βhCG plasma levels are obtained. Serial transvaginal color Doppler sonography is useful in monitoring the patients during chemotherapy and in detecting residual tumor, and increase the accuracy of diagnosis of PSTT.[34]

THERAPY

Total hydatidiform mole is treated primarily by the evacuation and curettage, where well-developed massive total mole should be carefully treated, i.e. the cervix is slowly dilated as large as possible and followed by uterine contraction induced by prostaglandin before the expulsion and curettage of molar tissue, for the prevention of excessive hemorrhage and the damage of thin and soft myometrium. Ultrasonically diagnosed early stage evacuation is easier than the later stage of developed molar mass. The curettage is repeated for complete evacuation that leaves no mole in the uterine cavity. Ultrasound monitoring is useful for the prevention of uterine injury and molar residue. Hysterectomy is uncommon in the intrauterine mole, except for the patient's request in our past experience (Fig. 15.1). Surgery is performed in the refractory molar metastasis to chemotherapy.

Partial hydatidiform mole Labor is induced by prostaglandin and followed by curettage, for the expulsion of the fetus and evacuation of the mole.

Postmolar monitoring is indispensable for the detection of any sequela and prevention of malignant trophoblastic disease. After ultrasonically confirmed complete evacuation of the uterus, local state, ultrasonic transvaginal scan sonography, and urinary or serum human chorionic gonadotropin (hCG) are studied for every 1 to 2 weeks until hCG decreases to normal cut-off level, then 1 to 2 months for a year.[28] X-ray image is studied by any concern of pulmonary change. Contraception is not so long as the past, because new pregnancy is easily detected by ultrasound. Clinical care, however, lasts for 3 years, because 85% of choriocarcinoma develop at 3 years after the mole.

Postmolar hCG regression pattern is normal and called type I, when urinary hCG decreased to 1,000 mIU/mL or less after 5 weeks, serum hCG is 100 mIU/mL or less after 8 weeks, and serum hCG is 1 mIU/ml or less with hCGß system and 0.5 mIU/mL or less with hCGß-CTP system, that is the cut-off level, after 20 weeks. Abnormal regression is type II, of which hCG level is higher than type I regular regression.[1] The type II or hCG re-elevation after transient remission should be treated by prophylactic chemotherapy[35] for the prevention of choriocarcinoma, where methotrexate (MTX) is common. We[36] studied prophylactic chemotherapy for the choriocarcinoma in a controlled study, and found significantly less choriocarcinoma (actually zero) in the study group than the control.

Choriocarcinoma is treated by primary chemotherapy, which means the first choice of chemotherapy for the treatment of choriocarcinoma. In old period, hysterectomy was common but frequently followed by metastases, which was treated by chemotherapy. Radiation was done but it was also a local therapy. MTX was the first primary chemotherapy in 1960s. It was systemic because we defined choriocarcinoma a systemic disease. Until now, systemic chemotherapy has been main treatment of choriocarcinoma. The effect is further improved by the combined chemotherapy, which is EMA (etoposide, MTX, actinomycin-D),[37] or further combination of CO (cyclophosphamide and vincristine), forming EMA/CO regimen.[38,39] Low risk group, such as postmolar persistent hCG, is treated by single MTX, and high-risk group, e.g. resistant choriocarcinoma, is treated by EMA/CO.[38] The most heavy chemotherapy may be salvage chemotherapy including etoposide or cisplatine.[40] Only in chemotherapy resistant metastasis or the relaps is associated with surgery, e.g. pulmonary lobectomy and craniotomy,[41] and severe vaginal bleeding is treated by hysterectomy, however, active combination of hysterectomy[42] or endoscopic surgery[43] and chemotherapy resulted favorable remission.

Ultrasound technique estimates tumor sensitivity to the chemotherapy, which should be estimated as early as possible in the chemotherapy course. The impedance to intratumoral blood flow, which is RI or PI of pulsed Doppler method, showed clear increase immediately after the start of chemotherapy in the first course, when the choriocarcinoma was sensitive to chemotherapy, while hCG reduces in the second course, and the tumor reduced in further courses. Chemotherapy resistant invasive mole showed no change of RI and PI in tumoral flow.[44] Another chemotherapy resistant invasive mole also showed only mild increase of RI at the end of systemic chemotherapy (Fig. 15.23).

Serum hCG level should be lower than the cut-off level in the complete remission of the disease, that means complete disappearance of the primary and metastatic foci and hCG decrease to the cut-off level. Critical hCG level is confirmed by precise determination. Since there is cross sensitivity of hCG antibody to pituitary luteinizing hormone (LH), hCGβ or hCGβ-CTP antibody, that is more specific for the hCG, is common use in the monitoring of trophoblastic diseases, particularly in the low level hCG for the diagnosis of complete remission.

Recent studies reported, however, the presence of false-positive test in the use of some hCG anti-body including hCGβ and hCGβ-CTP.45,46 The reports suggested repeating tests, urine test instead of serum, serial dilution of the serum for the confirmation of linearity, or removal of interfering substances before the assay, if there is any discrepancy among clinical conditions and the test results. Unnecessary chemotherapy must not be performed by the false-positive test for low titer hCG.

Systemic side effect of intensive chemotherapy are stomatitis, skin eruption, hair-fall, fever, reduced granulocytes, bone marrow damage, hepatic lesion, GI tract damage and others. Heavy life threatening effect is the bone marrow damage and its expression is the leucopenia in peripheral blood. Mild leucopenia is cured by adrenal steroid, while severe damage is cured by bone marrow transplantation and the stem cell support,[42] where the patient is isolated in a clean room.

Intra-arterial infusion chemotherapy was tried in liver metastases which was decreased by the treatment.[47] We[17] tried intra-internal iliac arterial infusion chemotherapy in the

choriocarcinoma patient of uterine cervix, where the tumor changed necrotic and decreased.

Pregnancy outcome after complete remission obtained by intensive chemotherapy was favorable and the treatment showed minimal inpact.[48] As for further long term influence of the chemotherapy, menopause was earlier for 3 years than control women.[49]

Non-gestational choriocarcinoma Germ cell origin choriocarcinoma is treated by its original therapy, usually its resection followed by the adjuvant chemotherapy. Metastasis is surgically removed and treated by adjuvant chemotherapy. Resistive case receives multiple adjuvant therapy, usually EMA/CO therapy (etoposide, MIX, actinomycin-D, cyclophosphamide and vincristine). Other cancer receives its own therapy, extirpation, radiotherapy and chemotherapy.

Persistent trophoblastic disease Postmolar persistence of urinary or serum hCG receives prophylactic chemotherapy for the choriocarcinoma, where it is usually single MTX therapy. Its course is repeated until the hCG reaches normal level. Clinical choriocarcinoma receives the chemotherapy that is the same as the treatment described in the "choriocarcinoma". Clinical invasive mole also receives the MTX therapy until the hCG reaches normal level.

Invasive mole is also treated by systemic chemotherapy, although the sensitivity to chemotherapy tends to be low in invasive mole. It may be explained that invasive mole is composed of the molar tissue that is low malignancy lower than choriocarcinoma. Since higher local dose of chemotherapy agent may be needed in invasive mole than the choriocarcinoma, common systemic dose chemotherapy may not be suitable. Therefore, any local therapy may be needed. Hysterectomy should be avoided as far as possible for the preservation of fertility, and therefore, it may be allowed that the focus of invasive mole is resected or evaporated by laser surgery at the open uterus.

Placental site trophoblastic tumor (PSTT) was treated by hysterectomy where the tumor was limited within the uterus, while for the patiens whose tumor was spread out of the uterus, chemotherapy was indicated, although clinical outcome was variable and it was poor when the patient's precedent pregnancy was more than 2 years before the PSTT.[50]

Recently, Janni et al (1999)[51] recommended cytostatic-surgical approach consisting of cytoreductive surgery and adjuvant chemotherapy for metastatic PSTT. Furthermore, Tsuji et al (2002)[52] reported that open resection of PSTT tumor following EMA/CO (etoposide, MTX, actinomycinD, cyclophosphamide and vincristine) chemotherapy could achieve long-term remission and save fertility of young patients who wish future pregnancy. Other reports53–5 7 also obtained favorable results mainly by the EMA/CO combined chemotherapy, and further use is etoposidecisplatine cycle.[57]

The outcome of patients with FIGO stage I-II disease after hysterectomy were excellent, but FIGO III-IV stage patients survived only for 30%.[55]

In these reports, placental site trophoblastic tumor (PSTT) responses chemotherapy, and complete remission can be expected. Although the PSTT case is rare, the reports show very great progress of chemotherapy for trophoblastic disease. Associated surgery further improves the outcome of PSTT patients.

Other reported treatment Watanabe et al[58] reported the choriocarcinoma in the pulmonary artery, which needed the treatment with emergency pulmonary embolectomy under cardiopulmonary bypass. Kohyama et al[59] reported the sterotactic radiation therapy of the choriocarcinoma in the cranium, and followed by conventional craniospinal

irradiation. Bohlmann et al[17] reported intracardiac resection of a metastatic choriocarcinoma. Brain metastasis is usually treated by intensive chemotherapy.[60] We also experienced massive MTX treatment in a case of brain metastasis, who was successfully treated and survived for more than 20 years.

REFERENCES

1. Japan Society of Obstetrics and Gynecology and Japanese Pathological Society. The General Rules for Clinical and Pathological Management of Trophoblastic Diseases. 2nd edition. 1995, Tokyo, Kanehara Shuppan.
2. Weaver DT, Fisher RA, Newlands ES, Paradinas FJ. Amniotic tissue in complete hydatidiform moles can be androgenetic. J Pathol 2000; 191:67–70.
3. Kajii T, Ohama K. Androgenetic origin of hydatidiform mole. Nature 1977; 268:633–34
4. Ohama K, Kajii T, Okamoto E, Fukuda Y, Imazumi K, Tsukahara M, Kobayashi K, Hagiware K. Dispermic origin of XY hydatidiform mole. Nature 1981; 292: 551–52.
5. Lorigan PC, Sharma S, Bright N, Coleman RE, Hancock BW. Characteristics of women with recurrent molar pregnancies. Gynecol Oncol 200; 78:288–92.
6. Bae SN, Kim SJ. Telomerase activity in complete hydatidiform mole. Am J Obstet Gynecol 1999; 180: 328–33.
7. Lazarus E, Hulka C, Siewert B, Levine D. Sonographic appearance of early complete molar pregnancy. J Ultrasound Med 1999; 18:589–94.
8. Szulman AE, Philippe E, Boue JG, Boue A. Human triploidy. Association with partial hydatidiform moles and nonmolar conceptuses. Hum Pathol 1981; 12: 1016–21.
9. Hirose M, Kimura T, Mitsuno N, Wakuda K, Fujita J, Noda Y. DNA flow cytometric auantification and DNA polymorphism analysis in the case of a complete mole with a coexisting fetus. J Assis Reprod Genet 1999; 16:263–67
10. Suita S, Shono K, Tajiri T, Takamatsu T, Mozote H, Nagasaki A, Inomata Y, Hara T, Okamura J, Miyazaki K, Eguchi H, Tsuneyoshi M. Malignant germ cell tumors: Clinical characteristics, treatment, and outcome. A report from the study group for Pediatric Solid Malignant Tumors in the Kyushu Area, Japan. J Pediatr Surg 2002; 37:1703–06
11. Weiss S, Amit A, Schwartz MR, Kaplan AL. Primary choriocarcinoma of the vulva. Int J Gynecol Cancer 2001; 11:251–54
12. Yahata T, Kodama S, Kase H, Sekizuka N, Kurobayashi T, Aoki Y, Tanaka K. Primary choriocarcinoma of the uterine cervix: clinical, MRI, and color Doppler ultrasonographic study. Gynecol Oncol 1997; 64:274–78
13. Coskun M, Agildere AM, Boyvat F, Tarhan C, Niron EA. Primary choriocarcinoma of the stomach and pancreas: CT findings. Eur Radiol 1998; 8:1425–28
14. Liu Z, Mira, JL, Cruz-Caudillo JC. Primary gastric choriocarcinoma: a case report and review of the literature. Arch Pathol Lab Med 2001; 125:1601–04.
15. Wang JC, Angeles S, Chak P, Platt Abm Nimmag N. Choriocarcinoma of the gallbladder: related with cisplatin-based chemotherapy. Med Oncol 2001; 18: 165–69.
16. Sievert K, Weber EA, Herwig R, Schmid H, Roos S, Eickenberg HU. Pure primary choriocarcinoma of the urinary bladder with long-term survival. Urology 2000; 56:856
17. Koga K, Izuchi S, Maeda K, Noutomi Y. Treatment of chorionepithelioma of uterine cervix with hypogastric arterial infusion of amethopterin. J Jpn Obstet Gynecol Soc 1966; 13:245–49.
18. Chama CM, Nggada HA, Nuhu A. Cutaneous metastasis of gestational choriocarcinoma. Int J Gynecol Obstet 2002; 77:249–50
19. Bohlmann MK, Eckstein FS, Allemann Y, Stauffer E, Carrel TP. Intracardiac resection of a metastatic choriocarcinoma. Gynecol Oncol 2002; 84:157–60

20. Gersak B, Lakic N, Gorjup V, Gulic T, Berden P, Cernic NS. Right ventricular metastatic choriocarcinoma obstructing inflow and outflow tract. Ann Thorac Surg 2002; 73:1631–33
21. Steigrad SJ, Cheung AP, Osborn RA. Choriocarcinoma co-existent with and intact pregnancy: case report and review of the literature. J Obstet Gynecol Res 1999; 25:197–203
22. Jacques SM, Qureshi F, Doss BJ, Munkarah A. Intraplacental choriocarcinoma associated with viable pregnancy: pathologic features and implications for the mother and infant. Perdiatr Dev Pathol 1998; 1: 380–87.
23. Feltmate CM, Genest DR, Goldstein DP, Berkowi RS. Advances in the understanding of placental site trophoblastic tumor. J Reprod Med 2002; 47:337 41.
24. Mangili G, Garavaglia E, De Marzi P, Zanetto F, Taccagni G. Metastatic placental site trophoblastic tumor. Report of a case with complete response to chemotherapy. J Reprod Med 2001; 46:259–62
25. Remadi S, Lifschita-Mercer B, Ben-Hur H, Dgani R, Czernobilsky B. Metastasizing placental site trophoblastic tumor: immunohistochemical and DNA analysis. 2 case reports and a review of the literature. Arch Gynecol Obstet 1997; 259:97–103
26. Placental site trophoblastic tumor (PSTT) in mother and child: first report of PSTT in infancy. Med Pediatr Oncol 2002; 38:187–9
27. Feltmate CM, Genest DR, Wise L, Bernstein MR, Goldstein DP, Berkowitz RS. Placental site trophoblastic tumor: a 17-year experience at the New England Trophoblastic Disease Center. Gynecol Oncol 2001; 82:415–19
28. Santoso JT, Coleman RI (Eds). Handbook of Gyn Oncology, McGraw-Hill, New York, 2001.
29. Kurjak A, Zalud I, Predanic M, Kupesic S. Transvaginal color and pulsed Doppler study of uterine blood flow in the first and early second trimesters of pregnancy: normal versus abnormal. J Ultrasound Med 1994; 13:43–47.
30. Kurjak A, Zalud I, Salihagic A, Cervenkovic G, Maijevic R. Transvaginal color Doppler in the assessment of abnormal early pregnancy. J Perinat Med 1991; 19:155–65
31. Gungor T, Ekin M, Dumanli H, Gokmen O. Color Doppler ultrasonography in the earlier differentiation of benign molehydatidiform from malignant gestational trophoblastic disease. Acta Obstet Gynecol Scand 1998; 77;860–62
32. Vegan GL, Fulop V, Liu Y, Ng SW, Tuncer ZS, Genest DR, Paldi-Haris P, Foldi JM, Mok SC, Berko wit Differential gene expression pattern between normal human trophoblast and choriocarcinoma cell lines: downregulation of heat shock protein-27 in choriocarcinoma in vitro and in vivo. Gynecol Oncol 1999; 75:391–96
33. Shigematsu T, Kamura T, Wake N, Nakano H. DNA polymorphism analysis If a pre non-gestational choriocarcinoma of the ovary: case report.
34. Bettencourt E, Pinto E, Abraul E, Dinis M, De Oliveira CF. Placental site trophoblastic tumor: the value of transvaginal colour and pulsed Doppler sonography (TV-CGS) in is diagnosis: case report. Eur J Gynecol Oncol 1997; 18:461–64
35. Park TK, Kim SN, Lee SK. Analysis of risk factors for postmolar trophoblastic disease: categorization of risk factors and effect of prophylactic chemotherapy. Yonsei Med J 1996; 37:412–19
36. Koga K, Maeda K. Prophylactic chemotherapy with amethopterin for the prevention of choriocarcinoma following removal of hydatidiform mole. Am J Obstet Gynecol 1968; 100:270–75
37. Soto-Wright V, Goldstein DP, Bernstein MR, Berkowitz RS. The management of gestational trophoblastic tumors with etoposide, methotrexate, and actinomycin D. Gynecol Oncol 1997; 64:156–59
38. Newlands ES, Paradinas FJ, Fisher RA. Recent advances in gestational trophoblastic disease. Hematol Oncol Clin North Am 1999; 13:225–44.
39. Nozue A, Ichikawa Y, Minami R, Tsunoda H, Nishida M, Kubo T. Postpartum choriocarcinoma complicated by brain and lung metastases treated successfully with EMA/CO regimen. BJOG 2000; 107:1171–72

40. Okamoto T, Goto S. Resistance to multiple agent chemotherapy including cisplatin after chronic lowdose oral etoposide administration in gestational choriocarcinoma. Gynecol Obstet Invest 2001; 52:139–41.
41. Kang SB, Lee CM, Kim JW, Park NH, Lee HP Chemo-resistant choriocarcinoma cured by pulmonary lobectomy and craniotomy. Int J Gynecol Cancer 2000; 10:165–69.
42. Knox S, Brooks SE, Wong-You-Cheong J, Ioffe O, Meisenberg B, Goldstein DP Choriocarcinoma and epithelial trophoblastic tumor: successful treatment of relapse with hysterectomy and high dose chemotherapy with peripheral stem cell support: A case report. Gynecol Oncol 2002; 85:204–08
43. Chou HH, Lai CH, Wang PN, Tsai KT, Liu HP, Hsu S. Combination of high-dose chemotherapy, autologous bone marrow/peripheral blood stem cell transplantation, and thoracoscopic surgery in refractory nongestational choriocarcinoma of a 45XO/ 46XY female: a case report. Gynecol Oncol 1997; 64:521–25.
44. Maeda K. Gestational trophoblastic disease. Lecture in the Ian Donald Inter-University School of Medical Ultrasound, Dubrovnik, 1995.
45. Cole LA, Butler S. Detection of hCG in trophoblastic disease. The USA hCG reference service experience. J Reprod Med 2002; 47:433–44
46. ACOG committee opinion, Avoiding inappropriate clinical decisions based on false-positive human chorionic gonadotropin test results. Amer J Obstet Gynecol 2002; 100:1057–5
47. Tanase K, Tawada M, Moriyama N, Muranaka K. Intra-arterial infusion chemotherapy for liver metastases of testicular tumors: report of two cases. Hinyokika Kiyo 2000; 46:823–27
48. Woolas RP, Bower M, Newlands ES, Seckel M, Short D, Holden L. Influence of chemotherapy for gestational trophoblastic disease on subsequent pregnancy outcome. Br J Obstet Gynaecol 1998; 105:1032–35.
49. Bower M, Rustin GJ, Newlands ES, Holden L, Short D, Foskett M, Bagshawe KD. Chemotherapy for gestational trophoblastic tumours hastens menopause by 3 years. Eur J Cancer 1998; 34:1204–07
50. Newlands ES, Bower M, Fisher RA, Paradinas FJ. Management of placental site trophoblastic tumors. J Reprod Med 1998; 3:53–59
51. Janni W, Hantschmann P, Rehbock J, Braun S, Lochmueller E, Kindermann G. Successful treatment of malignant placental site trophoblastc tumor with combined cytostatic-surgical approach: case report and review of literature. Gynecol Oncol 1999; 75:164–69.
52. Tsuji Y, Tsubamoto H, Hori M, Ogasawara T, Koyama K. Case of PSTT treated with chemotherapy flowed by open uterine tumor resection to preserve fertility. Gynecol Oncol 2002; 87:303–07.
53. Twiggs LB, Hartenbach E, Saltzman AK, King LA. Metastatic placental site trophoblastic tumor. Int J Gynecol Obst 1998; 60(Suppl 1):S51-S5
54. Swisher E, Drescher CW. Metastatic placental site trophoblastic tumor: long-term remission in a patient treated with EMA/CO chemotherapy. Gynecol Oncol 1998; 68:62–65
55. Chang YL, Chang TC, Hsuen S, Huang KG, Wand PN, Liu HP, Soong YK. Prognostic factors and treatment for placental site trophoblastic tumor report of 3 cases and analysis of 88 cases. Gynecol Oncol 1999; 73:216–22
56. Mangili G, Garavaglia E, De Marzi P, Zanetto F, Taccagni G. Metastatic placental site trophoblastic tumor. Report of a case with complete response to chemotherapy. J Reprod Med 2001; 46:259–62
57. Randall TC, Coukos G, Wheeler JE, Rubin SC. Prolonged remission of recurrent, metastatic placental site trophoblastic tumor after chemotherapy. Gynecol Oncol 2000; 76:115–17
58. Watanabe S, Shimokawa S, Sakasegawa K, Masuda H, Sakata R, Higashi M. Choriocarcinoma in the pulmonary artery treated with emergency pulmonary embolectomy. Chest 2002; 121:654–56

59. Kohyama S, Uematsu M, Ishihara S, Shima K, Tamai S, Kusano S. An experience of stereotactic radiation therapy for primary intracranial choriocarcinoma. Tumori 2001; 87:162–65
60. Landanio G, Sartore-Bianchi A, Giannetta L. Renga M, Riva M, Siena S. Controversies in the management of brain metastases: the role of chemotherapy. Forum (Geneva) 2001; 11:59–74

Chapter 16
Normal Fetal Anatomy

Vincenzo D'Addario, Edoardo Di Naro, Luca Di Cagno

Screening for fetal malformations is one of the main aims of ultrasonography during pregnancy. In most cases fetal anomalies occur as an unexpected event in not- at -risk patients: for this reason the only way to rule out them is to screen every pregnant patient with a systematic evaluation of the fetal anatomy.

Embryonic organogenesis is a complex and evolutive process that cannot be squeezed in a single ultrasonic examination;[1] an accurate evaluation, which would take in account the complex fetal morphological evolution, should require multiple ultrasonic examinations during pregnancy. In the clinical practice, however, a so complicated screening program cannot be applied to the general population of the pregnant women due to the elevated cost and the unjustified use of medical resources. For this reason the ultrasonic screening of fetal malformations has to be based on a single examination that has to be planned at a gestational age which is advanced enough to visualize most fetal anomalies and early enough to plan further diagnostic tests and allow the termination of pregnancy in the most severe cases. The gestational age that constitutes the best compromise between the need of an early diagnosis and the natural history of most congenital malformations is the period ranging from 19 to 21 weeks of gestation. This ultrasonic examination is known as "fetal anomaly scan" or "fetal morphology scan".

In order to obtain a systematic evaluation of the fetal anatomy it is essential to establish:

- The orientation of the ultrasonic images on the screen in regard to the patient lay (i.e. the left border of the screen corresponds to the left side of the patient abdomen in the axial scans and to the cephalic pole in the longitudinal ones).
- The fetal lay in the uterus.

To obtain the latter goal it is necessary to correlate the three-dimensional movements of the probe on the maternal abdomen to the two-dimensional images appearing on the screen and to reconstruct a mental three-dimensional model from the pool of images seen. Once the idea of the fetal lay *in utero* is obtained the probe can be quickly oriented on the correct plane to visualize the desired fetal anatomical structure.[2]

The fetal anatomical figures, which can be visualized by ultrasound, are innumerable and the expert sonographer may carry out a detailed evaluation of the complex fetal anatomy. In order to standardize the fetal morphological examination, several scientific

Societies have suggested guidelines reporting the minimal standards of the fetal structures which should be visualized during a routine scan performed during the second trimester.[3–5]

The guidelines of the Italian Society of Ultrasound in Obstetrics and Gynecology suggest the visualization and measurement of the following structures:[5]

HEAD

- Measurement of the BPD and head circumference (it means that a correct scan of the skull and brain has been obtained showing the integrity of the calvarium, the cavum septi pellucidi, the talami, the falx, the symmetry of the two cerebral hemispheres)
- Measurement of the atrial width (it means that the lateral ventricles have been evaluated)
- Measurement of the transverse cerebellar diameter (it means that the normality of the posterior fossa has been checked)
- Visualization of the orbits.

SPINE

- Longitudinal view of the spine.

CHEST

- Visualization of the lungs on a transverse scan
- "situs cardiacum"
- "Four-chambers" view of the heart (it is recommended to include the outflow tracts evaluation in the next future).

ABDOMEN

- Measurement of the abdominal circumference
- Visualization of the stomach and the anterior abdominal profile
- Visualization of the kidneys and bladder.

LIMBS

- Visualization of the long bones of the four limbs
- Visualization of the hands and feet (present/ absent) without counting the fingers
- Measurement of the femur length.

Following these simple guidelines allows the performance of a good level basic examination. If one of the above mentioned structures is not accurately visualized or seems to be altered, the patient should be referred to a second level centre.

There are some conditions, however, in which the ultrasonic evaluation of the minimal fetal anatomical structures is limited, such as: maternal obesity, oligohydramnios, adverse fetal lay. These limitations, when present, should be described on the report.

The minimal anatomical figures reported above, as well as further thin anatomical details, will be described.

HEAD AND BRAIN

The measurements of BPD and head circumference are obtained on an axial scan of the fetal head showing the thalami, the cavum septi pellucidi and the frontal horns of the lateral ventricles (transthalamic scan) (Fig. 16.1).

By slightly tilting the probe caudally (towards the base of the skull), the atrium and the occipital horn of the lateral ventricle containing the choroid plexus are shown (transventricular scan) (Fig. 16.2); at this level the atrial width is measured: the normal value is </=10 mm.

By further tilting the probe caudally the posterior fossa is shown with the cerebellum and the cisterna magna (transcerebellar scan) (Fig. 16.3). By tilting the probe on the opposite side the orbits can be visualized (transorbitary scan) (Fig. 16.4).

These four simple scans allow an accurate evaluation of the brain anatomy and the recognition of the majority of the brain anomalies. However, further scans can be obtained, which allow a more detailed evaluation of the finest brain structures. Particularly when the fetus is in breech presentation or in transverse lay, sagittal and coronal scans can be obtained. A midsagittal scan shows the corpus callosum above the cavum septi pellucidi as well as the posterior fossa, where the cerebellar vermis and the fourth ventricle can be recognized (Fig. 16.5). A parasagittal scan shows the different components of the lateral ventricle (Fig. 16.6). The coronal scans will show the lateral ventricles with a different appearance, depending on the level of the scan: the anterior one will show the frontal horns with the interposed cavum septi pellucidi (Fig. 16.7); the posterior one will show the occipital horns with their typical round appearance (Fig. 16.8).

The fetal face can be evaluated both by midsagittal scan, showing the profile (Fig. 16.9)

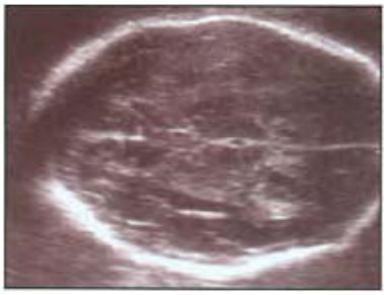

Figure 16.1: Transthalamic scan showing the thalami, with the interposed third ventricle, and the frontal horns

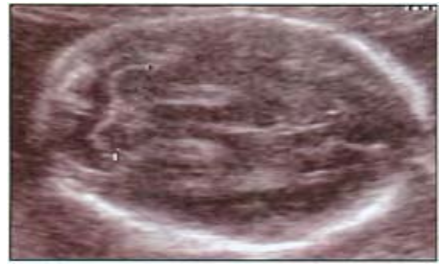

Figure 16.3: Transcerebellar scan showing the cerebellum and the cisterna magna

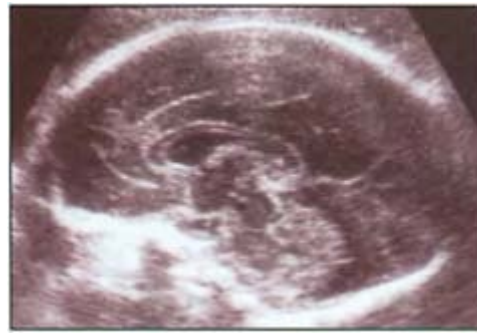

Figure 16.5: Midsagittal scan of the brain, showing the corpus callosum, the cavum septi pellucidi and the posterior fossa where the cerebellar vermis and the fourth ventricle can be recognized

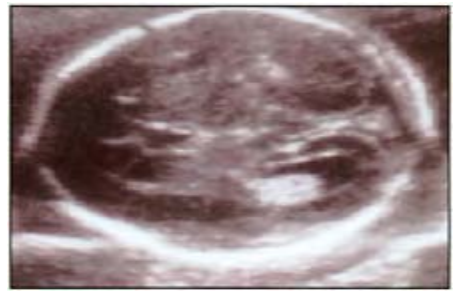

Figure 16.2: Transventricular scan showing the atrium and the occipital horn of the lateral ventricle, containing the choroid plexus

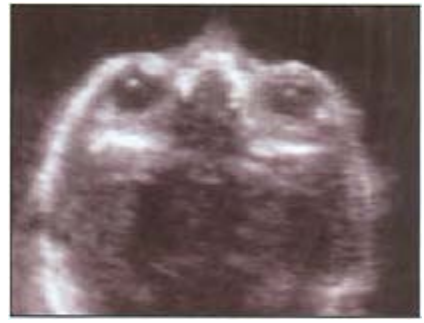

Figure 16.4: Transorbitary scan

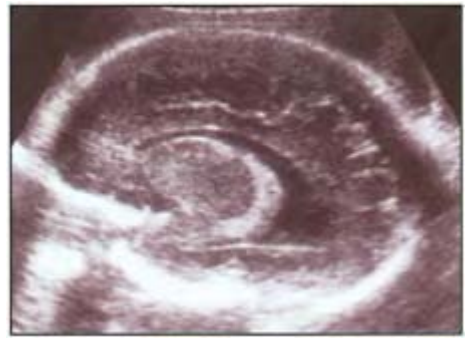

Figure 16.6: Parasagittal scan of the brain showing the different components of the lateral ventricle

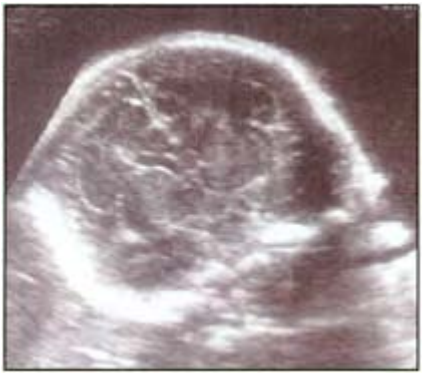

Figure 16.7: Anterior coronal scan of the brain at the level of the frontal horns of the lateral ventricles

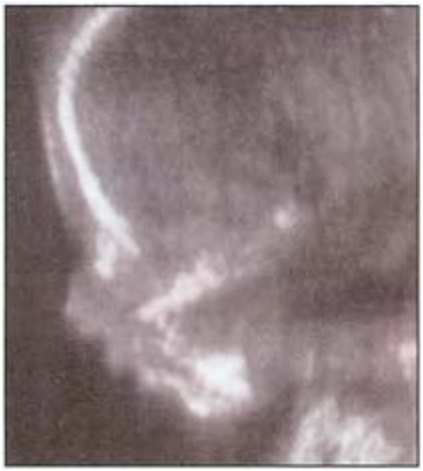

Figure 16.9: Mid-sagittal scan of the face showing the profile

and by coronal scan, showing the lips and nostrils (Fig. 16.10).

SPINE

The spine can be evaluated in longitudinal, coronal and axial scans. The best longitudinal view is that one passing through the spine from the posterior to the anterior aspect (Fig. 16.11), thus showing the vertebral canal; on the contrary an anterior-posterior scan is not good since the shadows caused by the vertebral bodies obscure the spinal canal. An

alternative way to visualize the spinal canal is the coronal scan passing through the laminae (Fig. 16.12). The sonographic appearance of the spine on axial scan varies according to the level of section (Fig. 16.13).

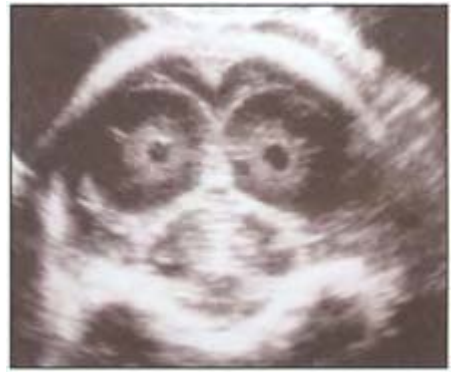

Figure 16.8: Posterior coronal scan of the brain at the level of the occipital horns of the lateral ventricles

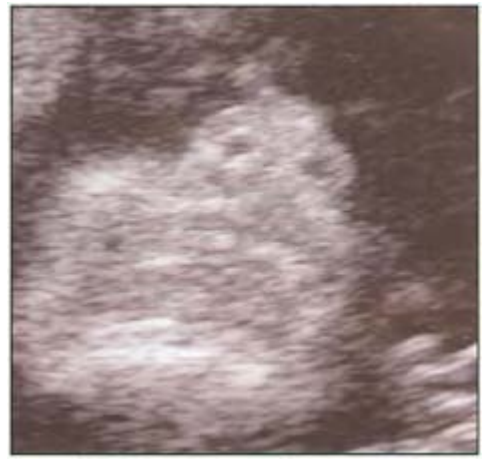

Figure 16.10: Coronal scan of the face showing the lips and nostrils

Close to the spine further bony structures can be seen, such as the clavicles (Fig. 16.14), the scapulae (Fig. 16.15) and the iliac wings (Fig. 16.16).

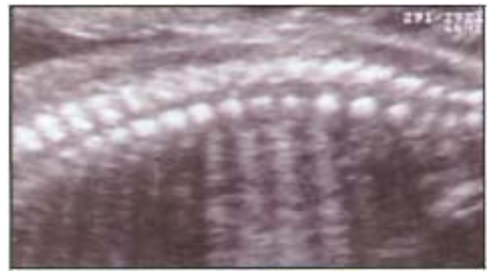

Figure 16.11: Longitudinal scan of the spine

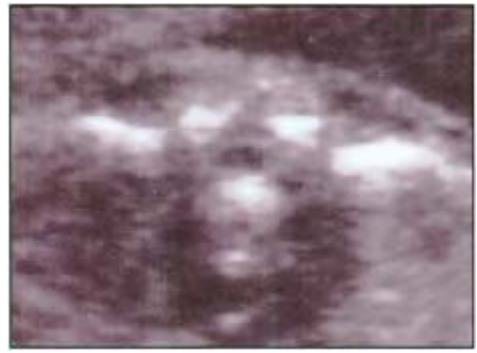

Figure 16.13: Transverse scan of a thoracic vertebra showing the vertebral body and the spinal canal

Figure 16.15: Scapula

Figure 16.12: Coronal scan of the spine passing through the laminae and showing some spinous processes

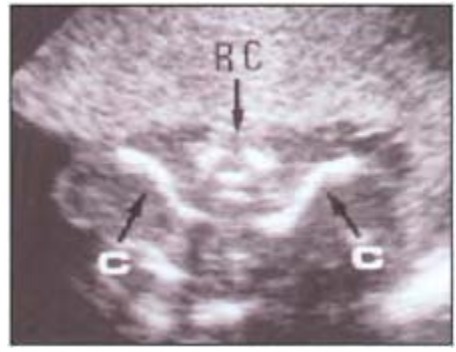

Figure 16.14: Clavicles and a cervical vertebra

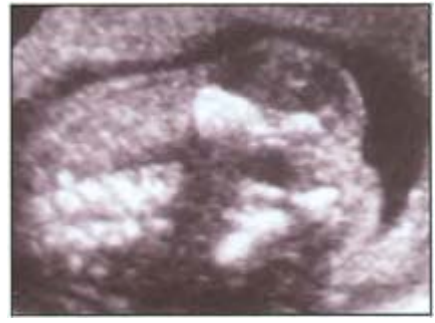

Figure 16.16: Iliac wings

CHEST

The best section to evaluate the chest structures is the axial one, at the level of the heart: this scan shows the hyperechoic lungs "embracing" the cardiac area. In this axial scan the four-chambers view of the heart is looked for. In order to obtain a correct four-chambers view, the first step is to localize the stomach in an axial scan on the abdomen, and then moving the transducer cranially without tilting it: in such a way a confirmation of a normally left-sided heart as well as a correct heart section are easily obtained. The four-chamber view can be "apical" when the ultrasonic beam is parallel and "transverse" when it is perpendicular to the interventricular septum. It is better to try to obtain both scans, since the "apical" is optimal for the atrioventricular valves, and the "transverse" for the interventricular and interatrial septa.

In the "four-chambers" view the following cardiac structures can be seen (Fig. 16.17):

- The atria: they have approximately the same size; the left one is closer to the spine and contains the foramen ovale's valve
- Two of the pulmonary veins opening in the left atrium
- The interatrial septum with the interruption due to the foramen ovale
- The atrioventricular valves: the tricuspid has a slightly lower septal insertion than the mitral valve
- The ventricles: they have approximately the same size but a different shape; the right one is more round and contains the "moderator band" close to the apex
- The interventricular septum.

Once the four-chambers view has been obtained, by simply moving the transducer, it is possible to visualize the outflow tracts and the subaortic part of the interventricular septum.

The left outflow tract (also called left long axis) is obtained from the four-chambers view, by rotating the transducer towards the right fetal shoulder.

In the left long axis the following structures can be evaluated (Fig. 16.18):

- The connection between the left ventricle and the aorta
- The integrity of the subaortic part of the interventricular septum
- The presence and function of the aortic valve.

By rotating the transducer from the long axis view towards the fetal head, the right outflow tract can be visualized.

In the right short axis the following structures can be seen (Fig. 16.19):

- The connection between the right ventricle and the pulmonary artery (moving the transducer from the left to the right axis, the vessels crossover can be seen)
- The presence and function of the pulmonary valve.

For a complete echocardiographic evaluation further scans are need that will be described in another chapter.

ABDOMEN

The best scan to visualize the fetal abdomen is the transverse one at the level where of the abdominal circumference is measured; at this level the following structures can be recognized: the intrahepatic tract of the umbilical vein on the anterior aspect, the stomach on the left side and the spine with the transverse section of the abdominal aorta on the posterior aspect (Fig. 16.20).

Following the course of the umbilical vein the insertion of the umbilical cord on the abdominal wall is seen (Fig. 16.21).

The kidneys are visible on axial scan and appear as two echogenic structures on both sides of the spine (Fig. 16.22); a mild physiological dilatation of the renal pelvis can sometimes be seen. In the coronal scan the kidneys show their typical “bean” shape (Fig. 16.23).

The visualization of the bladder is easy: it appears as a cystic median structure in the lower abdomen (Fig. 16.24).

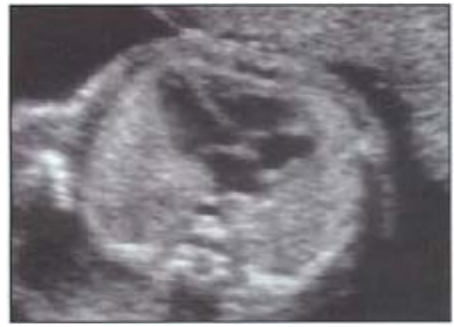

Figure 16.17: Four-chambers view of the heart

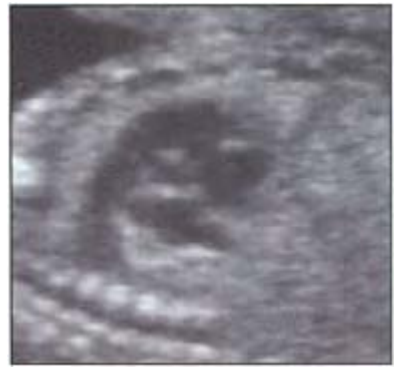

Figure 16.19: Right out-flow tract (right short axis) of the heart

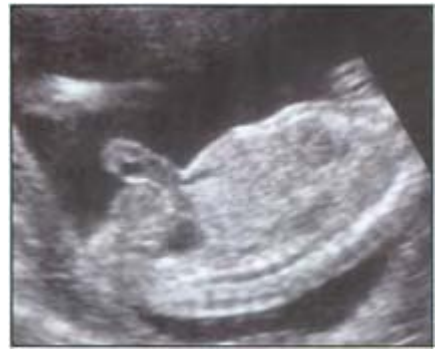

Figure 16.21: Umbilical cord insertion on the abdominal wall

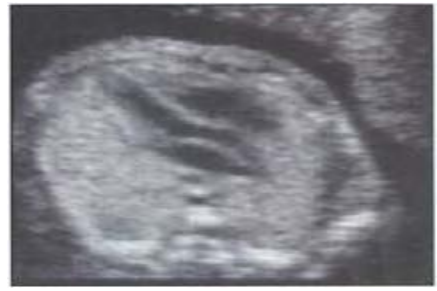

Figure 16.18: Left out-flow tract (left long axis) of the heart

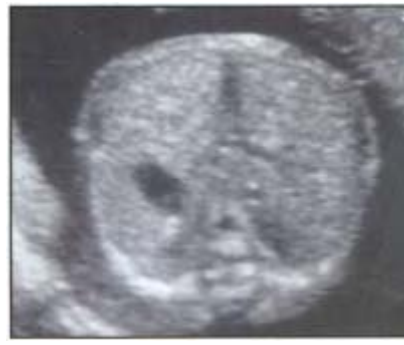

Figure 16.20: Transverse scan of the abdomen showing the stomach and the intrahepatic tract of the umbilical vein

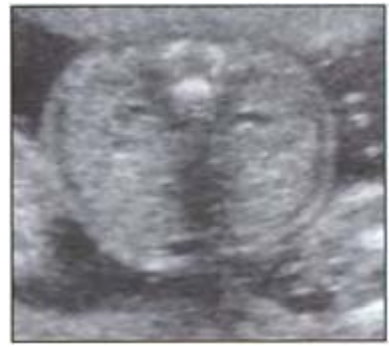

Figure 16.22: Axial scan of the kidneys

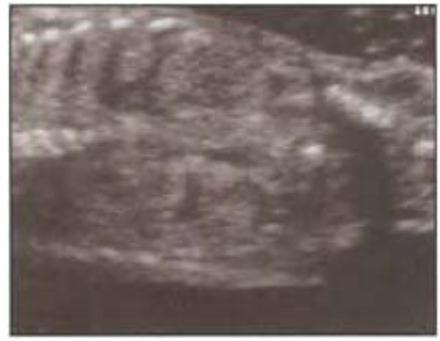

Figure 16.23: Coronal scan of the kidneys

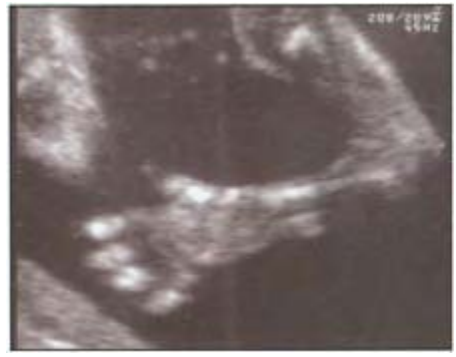

Figure 16.25: Upper limb

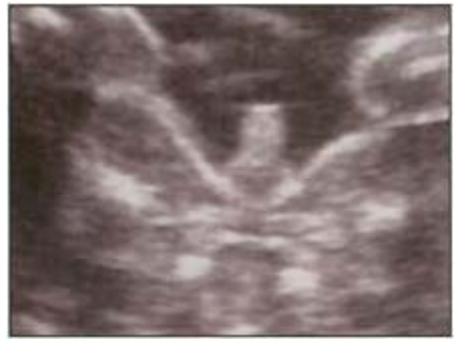

Figure 16.27: Male fetus

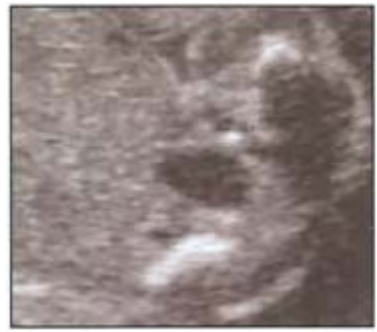

Figure 16.24: Bladder

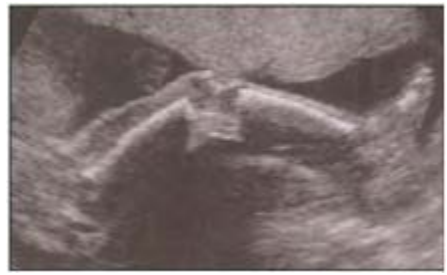

Figure 16.26: Lower limb

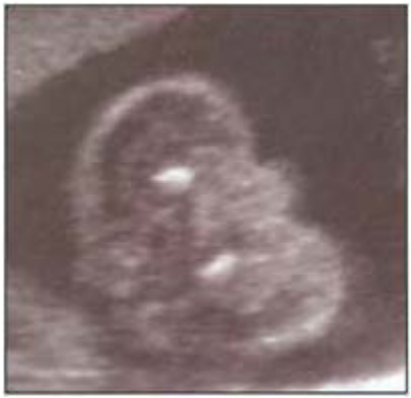

Figure 16.28: Female fetus

LIMBS

The visualization of the limbs requires a correct understanding of the fetal lay *in utero* and some skill in following their movements. The amount of amniotic fluid is very important: in case of oligohydramnios the recognition of the limbs becomes difficult. The long bones should be recognized and the femur length must be measured (Figs 16.25 and 16.26).

The hands and feet should also be visualized but only to define whether they are present or absent. The count of the fingers on the open hand is not always possible since the fetus usually has the hands in the closed position.

GENDER

Although the evaluation of the fetal gender is not included in the minimal standards required by most guidelines, however the patients require knowing it and therefore the ultrasonographer should be able to recognize the fetal penis and scrotum (Fig. 16.27) and the labia majora (Fig. 16.28).

REFERENCES

1. Kalousek DK, Lau AE: Development of the embryo, fetus and placenta. In: Dimmick JE, Kalousek DK (Eds). Developmental Pathology of the Embryo and Fetus. New York, JB Lippincott Co. 1992; 1–25.
2. Staudach A: Fetal echoanatomy. Berlin, Springler-Verlag, 1989.
3. ACOG: Screening Ultrasonography in Pregnancy. Guide to Clinical Preventive Services (2nd edn). Baltimore: Williams & Wilkins 1996; 407–18
4. AIUM: Standards for performance of the antepartum obstetrical ultrasound examination 1994.
5. SIEOG: Linee Guida in Ecografia Ostetrica e Ginecologica. Editeam, 2002.

Chapter 17
Fetal Growth and Biometry

Toshiyuki Hata

INTRODUCTION

Obstetric ultrasonography has substantially improved our understanding of fetal growth and development, and has permitted the prenatal evaluation of a variety of pathologic states of fetal growth. Traditionally, fetal growth has been defined as a change in anatomic parameters with advancing gestation.[1] Initially, fetal weight was the principal parameter used in growth studies.[2] However, the advent of sonographic imaging has made possible the use of a large number of one, two- (2D), and three-dimensional (3D) parameters to study the changes in a variety of fetal anatomic parameters.[3]

Accurate surveillance of fetal growth is the most important task of antenatal care. Timely detection of growth abnormalities is a challenge at the best of times but even more so in multicultural population.[4] It is well known that there are ethnic differences in fetal growth among populations. A number of studies have described ethnic differences in birth weight.[5–9] Several studies have shown that Asian babies tend to lighter than European babies.[6] Babies of women from the Indian subcontinent were generally of lower birth weight at term than white Anglo-Saxon babies.[6,7,10,11] Therefore, it is inappropriate to assess the birth weight of such Asian babies using Anglo-Saxon birth weight standards.[5,12–14]

Multiple pregnancies are known to be at increased risk of a variety of complications during the antepartum and intrapartum periods.[15] The main neonatal complications in multiple pregnan cies result from prematurity,[16] but multiple pregnancy presents a high-risk condition with frequent growth problems. Due to the complexity of multiple pregnancies, fetal growth assessment is more difficult, and thus a means for evaluating its effectiveness is essential.

With recent advances in ultrasound imaging, especially improvements in resolution and focusing, fetal intracranial, intrathoracic, and intra-abdominal organs can now be clearly identified.[17] Numerous reports on fetal organ measurements such as liver, spleen, and adrenal gland have been presented.[18–21]

Recent technical development of 3D ultra-sound machine has led to a self-contained imaging system that can both produce conventional 2D images and generate within seconds a high-quality 3D image without a need for an external work-station or other additional, costly equipment. Potential obstetric applications of 3D ultrasono-graphy for systematic examination of the developmental stages of the fetus, detection of fetal malformations or birth weight prediction have been reported.[22–24]

This chapter presents the state-of-the-art on fetal growth and biometry with the use of conventional 2D and 3D ultrasonography.

BODY PARTS

Multiple and singleton gestations exhibit similar growth through 30 weeks, and the singleton fetus appears to accelerate in growth in a sigmoid manner beyond 30 weeks gestation.[25,26] The

Table 17.1: Fitted centiles, SD and standard errors (SE) for 5th and 95th centiles of biparietal diameter and occipitofrontal diameter (Reprinted with permission from Br J Obstet Gyn aecol 1 999:106:126–135[32])

	Biparietal diameter (mm)					*Occipitofrontal diameter (mm)*				
Week of gestation	*5th*	*50th*	*95th*	*SD*	*SE*	*5th*	*50th*	*95th*	*SD*	*SE*
12	17.0	21.0	25.0	2.43	0.2	20.2	24.6	29.1	2.73	0.3
13	20.8	24.9	29.0	2.50	0.2	24.9	29.6	34.3	2.85	0.3
14	24.5	28.7	32.9	2.56	0.2	29.6	34.5	39.4	2.97	0.3
15	28.2	32.5	36.8	2.63	0.2	34.3	39.3	44.4	3.09	0.3
16	31.8	36.2	40.6	2.69	0.2	38.8	44.1	49.4	3.21	0.2
17	35.3	39.9	44.4	2.76	0.2	43.2	48.7	54.2	3.33	0.2
18	38.8	43.5	48.1	2.82	0.2	47.6	53.2	58.9	3.45	0.2
19	42.2	47.0	51.7	2.89	0.2	51.8	57.7	63.5	3.58	0.2
20	45.6	50.4	55.3	2.95	0.2	55.9	62.0	68.1	3.70	0.2
21	48.8	53.8	58.8	3.02	0.2	59.9	66.2	72.4	3.82	0.2
22	52.0	57.1	62.2	3.08	0.2	63.7	70.2	76.7	3.94	0.2
23	55.1	60.3	65.5	3.15	0.2	67.5	74.1	80.8	4.06	0.2
24	58.1	63.4	68.7	3.22	0.2	71.1	77.9	84.8	4.18	0.2
25	61.1	66.5	71.9	3.28	0.2	74.5	81.6	88.7	4.31	0.3
26	63.9	69.4	74.9	3.35	0.2	77.8	85.1	92.4	4.43	0.3
27	66.6	72.2	77.8	3.41	0.2	80.9	88.4	95.9	4.55	0.3
28	69.2	74.9	80.7	3.48	0.2	83.9	91.6	99.3	4.67	0.3
29	71.7	77.6	83.4	3.54	0.2	86.7	94.6	102.5	4.79	0.3
30	74.1	80.1	86.0	3.61	0.2	89.3	97.4	105.5	4.91	0.3

31	76.4	82.5	88.5	3.67	0.2	91.8	100.1	108.4	5.04	0.3
32	78.6	84.7	90.9	3.74	0.2	94.1	102.5	111.0	5.16	0.3
33	80.6	86.9	93.1	3.80	0.2	96.1	104.8	113.5	5.28	0.3
34	82.5	88.9	95.3	3.87	0.2	98.0	106.9	115.8	5.40	0.3
35	84.3	90.8	97.3	3.93	0.2	99.7	108.8	117.8	5.52	0.3
36	86.0	92.6	99.1	4.00	0.2	101.1	110.4	119.7	5.64	0.3
37	87.5	94.2	100.9	4.06	0.2	102.4	111.9	121.3	5.77	0.4
38	88.9	95.7	102.5	4.13	0.3	103.4	113.1	122.8	5.89	0.4
39	90.1	97.0	103.9	4.19	0.3	104.2	114.1	124.0	6.01	0.4
40	91.2	98.2	105.2	4.26	0.3	104.7	114.8	124.9	6.13	0.5
41	92.1	99.2	106.3	4.33	0.4	105.1	115.3	125.6	6.25	0.5
42	92.9	100.1	107.3	4.39	0.4	105.1	115.6	126.1	6.37	0.6

multiple gestation lacks this acceleration in growth shown by singleton gestations. Triplet growth remains linear throughout the third trimester rather than plateauing as previously suggested.[26] Similarly, the mean birth weight of triplets was slightly below the 10th percentile for singletons as 38 weeks' gestation or later.[27] Therefore, the growth of triplet fetuses as estimated from live born birth weights is slower than that of singletons. Recent study also showed that there was no significant difference in predicted estimated weight between twin and triplet fetuses.[28] However, these values in multiple gestations were slightly lower than that of singleton fetuses. The reason for these differences is currently unknown. It has been suggested that the deposition of soft tissue sees

Table 17.2: Fitted centiles. SD and standard errors (SE) for 5th and 95th centiles of head circumference and cephalic index (Reprinted with permission from Br J Obstet Gynaecol 1999:106:126–13532)

	Head circumference (mm)					*Cephalic index*				
Week of gestation	*5th*	*50th*	*95th*	*SD*	*SE*	*5th*	*50th*	*95th*	*SD*	*SE*
12	59.7	72.1	84.5	7.6	0.9	0.74	0.85	0.95	0.07	0.007
13	73.3	86.1	98.9	7.8	0.8	0.74	0.84	0.94	0.06	0.005
14	86.7	99.9	113.1	8.0	0.7	0.75	0.84	0.93	0.06	0.004
15	99.9	113.5	127.0	8.2	0.6	0.75	0.83	0.92	0.05	0.003
16	112.9	126.8	140.7	8.5	0.6	0.75	0.83	0.91	0.05	0.003
17	125.6	139.9	154.2	8.7	0.6	0.75	0.83	0.90	0.05	0.003

18	138.1	152.7	167.4	8.9	0.6	0.75	0.82	0.89	0.04	0.003
19	150.2	165.2	180.3	9.1	0.6	0.75	0.82	0.89	0.04	0.003
20	162.1	177.5	192.9	9.4	0.6	0.75	0.82	0.89	0.04	0.003
21	173.6	189.4	205.2	9.6	0.6	0.75	0.82	0.88	0.04	0.003
22	184.9	201.0	217.1	9.8	0.6	0.75	0.81	0.88	0.04	0.003
23	195.7	212.2	228.7	10.0	0.6	0.75	0.81	0.88	0.04	0.003
24	206.2	223.1	240.0	10.3	0.6	0.75	0.81	0.88	0.04	0.003
25	216.4	233.6	250.9	10.5	0.6	0.75	0.81	0.88	0.04	0.003
26	226.1	243.7	261.3	10.7	0.7	0.75	0.81	0.88	0.04	0.003
27	235.5	253.4	271.4	10.9	0.7	0.75	0.81	0.88	0.04	0.003
28	244.4	262.7	281.1	11.2	0.7	0.75	0.81	0.88	0.04	0.003
29	252.9	271.6	290.3	11.4	0.7	0.75	0.82	0.88	0.04	0.003
30	280.9	280.0	299.1	11.6	0.7	0.75	0.82	0.89	0.04	0.003
31	268.4	287.9	307.3	11.8	0.7	0.75	0.82	0.89	0.04	0.003
32	275.5	295.3	315.1	12.1	0.7	0.75	0.82	0.89	0.04	0.003
33	282.1	302.2	322.4	12.3	0.7	0.76	0.83	0.90	0.04	0.003
34	288.1	308.7	329.2	12.5	0.7	0.76	0.83	0.90	0.04	0.003
35	293.6	314.5	335.5	12.7	0.8	0.76	0.83	0.91	0.04	0.003
36	298.6	319.9	341.2	13.0	0.8	0.77	0.84	0.91	0.04	0.003
37	303.0	324.6	346.3	13.2	0.9	0.77	0.84	0.92	0.04	0.003
38	306.8	328.8	350.9	13.4	0.9	0.77	0.85	0.92	0.05	0.004
39	310.0	332.4	354.8	13.6	1.0	0.78	0.85	0.93	0.05	0.004
40	312.6	335.4	358.2	13.9	1.2	0.78	0.86	0.94	0.05	0.005
41	314.6	337.7	360.9	14.1	1.3	0.79	0.87	0.94	0.05	0.005
42	315.9	339.4	363.0	14.3	1.5	0.79	0.87	0.95	0.05	0.006

in normal singletons during the third trimester occurs to a much lesser extent in normal twins and triplets.[29,30] Further study is needed to clarify whether this decrease in soft tissue deposition in multiple pregnancies represents a true growth abnormality or merely a physiological adaptation to the energy demands associated with the support of growth in multiple fetuses.[28]

So far, many reference charts and tables have been reported. However, a number of these studies were conducted using old ultrasound machine with low spatial resolution and different ultrasound velocities compared with latest ultrasound machines.[31] With recent advances in ultrasound equipment, the ultrasound image quality has increased enormously, and this has opened up new

Table 17.3: Fitted centiles, SD and standard errors (SE) for 5th and 95th centiles of mean abdominal diameter and abdominal circumference. (Reprinted with permission from Br J Obstet Gynaecol 1999; 106:136–143[33])

	Mean abdominal diameter (mm)					*Abdominal circumference (mm)*				
Week of gestation	*5th*	*50th*	*95th*	*SD*	*SE*	*5th*	*50th*	*95th*	*SD*	*SE*
12	14.5	18.1	21.8	2.23	0.3	45.3	56.6	67.9	6.88	0.9
13	17.9	21.9	25.8	2.38	0.3	56.1	68.2	80.3	7.36	0.9
14	21.4	25.5	29.7	2.53	0.2	66.9	79.8	92.7	7.83	0.8
15	24.8	29.2	33.6	2.68	0.2	77.6	91.3	105.0	8.31	0.7
16	28.2	32.9	37.5	2.83	0.2	88.3	102.7	117.2	8.78	0.7
17	31.6	36.5	41.4	2.98	0.2	98.8	114.0	129.3	9.26	0.7
18	34.9	40.1	45.2	3.13	0.2	109.3	125.3	141.3	9.73	0.7
19	38.2	43.6	49.0	3.28	0.2	119.7	136.4	153.2	10.21	0.7
20	41.5	47.1	52.8	3.43	0.2	129.9	147.5	165.1	10.69	0.7
21	44.7	50.6	56.5	3.58	0.2	140.1	158.5	176.8	11.16	0.7
22	48.0	54.1	60.2	3.73	0.2	150.2	169.3	188.4	11.64	0.7
23	51.1	57.5	63.9	3.88	0.2	160.1	180.0	200.0	12.11	0.7
24	54.3	60.9	67.5	4.03	0.2	169.9	190.6	211.3	12.59	0.7
25	57.4	64.2	71.1	4.18	0.2	179.6	201.1	222.6	13.06	0.7
26	60.4	67.5	74.7	4.33	0.2	189.2	211.5	233.7	13.54	0.8
27	63.4	70.8	78.2	4.48	0.3	198.7	221.7	244.8	14.01	0.8
28	66.4	74.0	81.6	4.62	0.3	208.0	231.8	255.6	14.49	0.8
29	69.3	77.2	85.0	4.77	0.3	217.1	241.7	266.3	14.96	0.8
30	72.2	80.3	88.4	4.92	0.3	226.1	251.5	276.9	15.44	0.8
31	75.0	83.4	91.7	5.07	0.3	235.0	261.1	287.3	15.91	0.8
32	77.8	86.4	95.0	5.22	0.3	243.6	270.6	297.6	16.39	0.8
33	80.5	89.4	98.2	5.37	0.3	252.2	279.9	307.7	16.86	0.9
34	83.2	92.3	101.4	5.52	0.3	260.5	289.0	317.6	17.34	0.9
35	85.8	95.1	104.5	5.67	0.3	268.7	298.0	327.3	17.81	0.9
36	88.4	97.9	107.5	5.82	0.3	276.7	306.8	336.9	18.29	1.0
37	90.9	100.7	110.5	5.97	0.4	284.5	315.4	346.2	18.77	1.1

38	93.3	103.4	113.4	6.12	0.4	292.1	323.8	355.4	19.24	1.2
39	95.7	106.0	116.3	6.27	0.4	299.5	332.0	364.4	19.72	1.3
40	98.0	108.5	119.1	6.42	0.5	306.8	340.0	373.2	20.19	1.5
41	100.2	111.0	121.8	6.57	0.5	313.8	347.8	381.8	20.67	1.6
42	102.4	113.4	124.5	6.72	0.6	320.6	355.3	390.1	21.14	1.8

improved measurement techniques.[32] In addition, many of the earlier publications had methodological flaws, falling short of the ideal attributes of gestational age-related reference curve design. Tables 17.1 to 17.4 show latest reliable reference ranges for biparietal diameter, occipitofrontal diameter, head circumference, cephalic index, abdominal diameter, abdominal circumference, and femur length in Anglo-Saxon fetuses.[32,33]

It is well known that there are ethnic differences in fetal growth among populations. A number of studies have described ethnic differences in birth weight.[5–9] Several studies have shown that Asian babies tend to lighter than European babies.[6]

Table 17.4: Fitted centiles. SD and standard errors (SE) for 5th and 95th centiles of femur length (Reprinted with permission from BR J Obstet Gynaecol 1999:106:136–143[33])

	Femur length (mm)				
Week of gestation	*5th*	*50th*	*95th*	*SD*	*SE*
12	4.1	7.0	9 8	1.73	0.2
13	7.2	10.3	13.4	1.89	0.2
14	10.3	13.6	16.9	2.03	0.2
15	13.3	16.8	20.4	2.15	0.2
16	16.3	20.0	23.7	2.25	0.1
17	19.2	23.0	26.9	2.35	0.1
18	22.1	26.1	30.0	2.43	0.1
19	24.9	29.0	33.1	2.50	0.1
20	27.6	31.9	36.1	2.57	0.1
21	30.3	34.7	39.0	2.63	0.1
22	33.0	37.4	41.8	2.68	0.1
23	35.6	40.1	44.5	2.73	0.1
24	38.1	42.6	47.2	2.78	0.2
25	40.5	45.2	49.8	2.82	0.2

26	42.9	47.6	52.3	2.86	0.2
27	45.2	50.0	54.8	2.89	0.2
28	47.5	52.3	57.1	2.93	0.2
29	49.7	54.5	59.4	2.96	0.2
30	51.8	56.7	61.6	2.99	0.2
31	53.9	58.8	63.8	3.01	0.2
32	55.9	60.9	65.8	3.04	0.2
33	57.8	62.8	67.9	3.06	0.2
34	59.6	64.7	69.8	3.08	0.2
35	61.4	66.5	71.6	3.11	0.2
36	63.1	68.3	73.4	3.13	0.2
37	64.8	70.0	75.1	3.14	0.2
38	66.4	71.6	76.8	3.16	0.2
39	67.9	73.1	78.4	3.18	0.2
40	69.3	74.6	79.9	3.19	0.2
41	70.7	76.0	81.3	3.21	0.3
42	72.0	77.3	82.6	3.22	0.3

Meire and Farrant[34] compared ultrasonic measurements of fetal size during pregnancy in Indian and Anglo-Saxon women and found no difference in biparietal diameter between the two populations. In contrast, the group of Indian fetuses had a significantly lower mean abdominal circumference after 24 weeks of gestation.[35] Spencer et al[36] also suggested that abdominal circumference and estimated fetal weight of the Bangladesh fetuses were smaller than Anglo-Saxon fetuses at 28, 32 and 36 weeks of gestation. Tables 17.5 to 17.8 show latest reliable reference ranges for head circumference, abdominal circumference, femur length, and estimated weight in singleton, twin, and triplet Asian fetuses.[28]

INDIVIDUAL GROWTH ASSESSMENT

As with the growth of both singletons and twins, many of the problems associated with the evaluation of triplet growth can be eliminated by the use of individual growth curve standards.[37–39] The fetal growth model developed by Rossavik and Deter[40] specifies individual growth curve standards for various fetal anatomic parameter, using data from second trimester ultrasound measurements.[37,38,41] Experiences with the model has shown the following: (1) birth characteristics in normally growing fetuses can be accurately predicted from only two second trimester scans separated by an interval of at least 5 weeks,[42–46] (2) healthy fetuses show relatively limited variability in their projected

individual growth curves,[42] and (3) little change in growth occurs after 38 weeks.[47,48] This method is capable of separating healthy infants from those with evidence of fetal growth restriction[49] or excessive growth.50 Mor over, individualized growth assessment should be useful for detection of growth restricted infants with poor perinatal outcomes.[51]

FETAL ORGAN MEASUREMENTS

With recent advances in ultrasound imaging, especially improvements in resolution and focusing, fetal intracranial, intrathoracic, and intraabdominal organs can now be clearly identified.[17] As it is well known, fetal organs have complex shapes. Since these organs are three-dimensional objects, the most appropriate growth parameters would be weight, volume, or surface

Table 17.5: Head circumference value (cm) in singleton appropriate for gestational age fetus (S-AGA). singleton small for gesstational age fetus (S-SGA). twin appropriate for gestational age fetus (Tw-AGA). and triplet appropriate for gestational age fetus (tri-AGA) (Reprinted with permission from Hum Reprod 1999:14:1352–1360[33])

MA (weeks)	*S-AGA*			*S-SGA*			*Tw-AGA*			*Tri-AGA*		
	−2SD	*mean*	*+2SD*	*−2SD*	*mean*	*+2SD*	*−2SD*	*mean*	*+2SD*	*−2SD*	*mean*	*+2SD*
15	8.8	10.8	12.8	8,8	10.6	13.3	9.6	11.3	13.1	9.1	10.7	12.2
16	10.1	12.1	14.1	10.0	11.8	13.5	10.7	12.5	14.3	10.3	11.9	13.4
17	11.3	13.3	15.3	11.2	13.0	15.0	11.9	13.6	15.4	11.5	13.1	14.7
18	12.5	14.5	16.5	12.4	14.1	15.9	13.0	14.7	16.5	12.7	14.3	15.8
19	13.7	15.7	17.7	13.5	15.3	17.0	14.1	15.9	17.6	13.8	15.4	17.0
20	14.8	16.8	18.8	14.6	16.4	18.1	15.2	16.9	18.7	15.0	16.5	18.1
21	15.9	17.9	19.9	15.7	17.5	19.2	16.2	18.0	19.7	16.1	17.6	19.2
22	17.0	19.0	21.0	16.7	18.5	20.2	17.2	19.0	20.8	17.1	18.7	20.3
23	18.1	20.1	22.1	17.7	19.5	21.3	18.2	20.0	21.8	18.2	19.7	21.3
24	19.1	21.1	23.1	18.7	20.5	22.2	19.2	21.0	22.8	19.2	20.7	22.3
25	20.0	22.0	24.1	19.6	21.4	23.2	20.2	21.9	23.7	20.1	21.7	23.3
26	21.0	23.0	25.0	20.5	22.3	24.0	21.1	22.9	24.6	21.0	22.6	24.2
27	21.9	23.9	25.9	21.4	23.1	24.9	22.0	23.7	25.5	21.9	23.5	25.1
28	22.7	24.7	26.7	22.2	23.9	25.7	22.8	24.6	26.4	22.8	24.4	25.9

29	23.5	25.5	27.5	23.0	24.7	26.5	23.7	25.4	27.2	23.6	25.2	26.7
30	24.3	26.3	28.3	23.7	25.4	27.2	24.4	26.2	28.0	24.4	25.9	27.5
31	25.0	27.0	29.0	24.3	26.1	27.8	25.2	27.0	28.7	25.1	26.7	28.2
32	25.7	27.7	29.7	25.0	26.7	28.5	25.9	27.7	29.5	25.8	27.3	28.9
33	26.3	28.3	30.3	25.5	27.3	29,0	26.6	28.4	30.1	26.4	28.0	29.5
34	26.9	28.9	30.9	26.0	27.8	29.5	27.2	29.0	30.8	27.0	28.6	30.1
35	27.4	29.4	31.4	26.5	28.3	30.0	27.9	29.6	31.4	27.5	29.1	30.7
36	27.8	29.9	31.9	26.9	28.7	30.4	28.4	30.2	32.0	28.0	29.6	31.1
37	28.3	30.3	32.3	27.2	29.0	30.8	28.9	30.7	32.5			
38	28.6	30.6	32.6	27.5	29.3	31.0	29.4	31.2	33.0			
39	28.9	30.9	32.9	27.8	29.5	31.3	29.8	31.6	33.4			
40	29.1	31.1	33.1	27.9	29.7	31.4	30.2	32.0	33.8			

MA=menstrual age.

area.[53] However, it is very difficult to determine such parameters because of the complexity of the measurement procedures required.[17] For example, we focused on the growth of fetal liver. The liver occupies most of the upper abdominal cavity, and it is the first organ to be affected by fetal growth restriction.[54] The fetal liver weight is reduced in animal models of fetal growth restriction.[55–58] Therefore, direct measurements of fetal liver size may enhance the early detection of the fetus at risk of fetal growth restriction.[59] There have been a few human studies that have directly measured liver length (LL) using traditional two-dimensional sonography in small-for-gestational-age fetuses, and the results have been conflicting.[21,54,60–62] Murao et al[60] reported that the LL in small-for-gestational-age fetuses was smaller than in appropriate-for-gestational-age fetuses, and that LL measurements may be useful in the detection of small-for-gestational-age fetuses. In their study, however, small-for-gestational-age fetus was defined as an infant with a birth weight 25th percentile, and descriptive statistics were not conducted. In the other two investigations,[21,62]

Table 17.6: Abdominal circumference value (cm) in singleton appropriate for gestational age fetus (S-AGA). singleton small for gesstational age fetus (S-SGA). twin appropriate for gestational age fetus (Tw-AGA). and triplet appropriate for gestational age fetus (tri-AGA) (Reprinted with permission from Hum Reprod 1999:14:1352–1360[33])

MA (weeks)	*S-A*			*S-SGA*			*TW-AGA*			*Tri-AGA*		
	−2SD	*mean*	*+2SD*	*−2SD*	*mea*	*+2SD*	*−2SD*	*mean*	*+2SD*	*−2SD*	*mean*	*+2SD*
15	6.4	8.7	11.1	6.0	8.6	11.2	6.0	8.9	11.2	6.2	8.4	10.7
16	7.5	0.0	12.2	7.1	9.7	12.3	7.7	10.0	12.3	7.4	0.8	11.8
17	8.7	11.0	13.4	8.2	10.8	13.4	8.8	11.2	13.5	8.5	10.7	12.0
18	9.8	12.1	14.5	9.3	11.0	14.5	0.0	12.3	14.6	0.6	11.8	14.0
19	10.9	13.2	15.6	10.4	13.0	16.0	11.0	13.3	15.7	10.7	12.0	15.1
20	11.0	14.3	18.0	11.4	140	10.8	12.1	14.4	16.7	11.7	13.9	16.1
21	13.0	15.3	17.7	12.4	15.0	17.6	13.1	15.4	17.7	12.8	15.0	17.2
22	14.0	16.3	18.7	13.4	104	18.6	14.1	10.4	18.7	13.8	18.0	18.2
23	15.0	17.4	19.7	14.4	17.0	10.6	15.1	17.4.	19.7	14.7	17.0	10.2
24	16.0	18.3	20.7	15.3	17.9	20.5	10.0	18.	20.7	15.7	17.9	20,1
25	17.0	19.3	21.7	10.2	18.8	21.4	16.0	19.3	210	18.6	18.8	21.0
26	17.9	20.3	22.0	17.1	19.7	22.3	17.8	20.2	22.5	17.5	19.7	21.0
27	18.0	21.2	23.5	18.0	20.0	23.2	18.7	21.0	23.3	18.4	20.8	22.8
28	10.8	22.1	24.5	18.8	21.4	24.0	19.6	21.9	24.2	19.2	21.4	23.6
29	20.7	23.0	25.4	19.6	22.2	24.8	20.4	22.7	25.0	20.0	22.2	24.5
30	21.5	23.9	26.2	20.4	23.0	25.6	21.2	23.5	25.8	20.8	23.0	25.2
31	22.4	24.7	27.1	21.1	23.7	26.3	21.9	24.3	26.6	21.5	23.7	28.0
32	23.2	25.6	27.9	21.8	24.4	27.0	22.7	25.0	27.3	22.2	24.4	26.6
33	24.8	26.4	28.7	22.4	25.0	27.6	23.4	25.7	28.0	22.9	25.1	27.3
34	24.8	27.2	29.5	23.1	25.7	28.3	24.1	20.4	28.7	23.5	25.7	27.9
35	25.6	28.0	30.3	23.6	20.2	28.8	24.8	27.1	20.4	24.1	26.3	28.5
36	20.4	28.7	31.1	24.4	20.8	20.4	25.4	27.7	30	24.6	26.8	20.0
37	27.1	29.5	31.8	24.7	27.3	29.9	26.0	28.3	30.6	–	–	–
38	27.8	30.2	32.5	25.1	27.7	30.3	26.6	28.9	31.2	–	–	–

39		28.5	30.0	33.2	25.5	28.1	30.7	27.2	29.5	31.8	–	–	–
40	29.2		31.6	33.9	25.9	28.5	31.1	27.7	30.0	32.3	–	–	–
MA =	**menstrual age**												

most LL measurements of small-for-gestational-age fetuses were within normal ranges (90.5% and 82%, respectively). In the recent study,[63] the LL was also normal in 7 of 10 small-for-gestational-age fetuses (70%) (Fig. 17.1). However, liver volume (LV) values in all small-for-gestational-age fetuses were below 10th percentile (Fig. 17.2). The LL was a one-dimensional parameter. Despite the ease of measurement, it may be apparent that the LL is a rather crude measure for characterizing the growth of an object with a complex shape such as the fetal liver. Therefore, the LL may not be the most appropriate parameter for evaluation of liver growth.[63]

With respect to the fetal LV measurement, Chang et al[64] showed that three-dimensional sonography was superior to two-dimensional sonography in a reproducibility test of fetal LV assessment. Moreover, the LV assessed with the traditional two-dimensional sonographic method was significantly less than that measured with three-dimensional sonography. These authors recommended that three-dimensional sonography instead of two-dimensional sonography should be

Table 17.7: Femur length value (cm) in singleton appropriate for gestational age fetus (S-AGA). singleton small for gesstational age fetus (S-SGA). twin appropriate for gestational age fetus (Tw-AGA). and triplet appropriate for gestational age fetus (tri-AGA) (Reprinted with permission from Hum Reprod 1999:14:1352–1360[33])

MA (weeks)	*S-AGA*			*S-SGA*			*Tw-AGA*			*Tri-AGA*		
	−2SD	*mean*	*+2SD*	*−2SD*	*mean*	*+2SD*	*−2SD*	mean	*+2SD*	*−2SD*	*mean*	*+2SD*
15	1,1	1.5	1.9	1,0	1.5	2.0	0.8	1.5	2.1	1.0	1.5	1.9
16	1.4	1.8	2.2	1.3	1,8	2.3	1.1	1,8	2.5	1.3	1.8	2,2
17.	1.7	2.1	2.5	1.6	2,1	2.6	1.4	2.1	2.8	1.6	2.1	2.5
18	2,0	2.4	2.8	1.9	2.3	2.8	1.7	2,4	3.1	1,9	2.4	2,8
10	2.3	2.7	3.1	2.1	2.6	3.1	2,0	2.7	3.4	2,2	2,6	3.1
20	2.3	3.0	3.4	2.4	2.9	3.4	2.3	3.0	3.6	2.4	2,9	3.4
21	2.9	3.3	3.7	2.7	3.1	3.6	2.6	3.3	3.9	2.7	3.2	3.6
22	3.1	3.5	3.9	2.9	3.4	3.9	2.9	3.5	4.2	3.0	3.4	3.9

23	3.4	3.8	4.2	3.2	3.7	4,1	3.1	3.8	4,4	3.2	3.7	4,2
24	3.6	4.0	4.4	3.4	3.4	4.4	3.3	4.0	4.7	3.5	3.9	4,4
25	3.9	4.3	4.7	3.6	4.1	4,6	3.6	4.2	4.9	3.7	4.2	4.6
26	4,1	4.5	4.9	3.9	4.4	4.9	3.8	4.5	5.1	3.9	4.4	4.8
27	4.3	4.7	5.1	4,1	4.6	5.1	4.0	4.7	5.3	4.1	4.6	5.1
28	4.6	5.0	5.4	4.3	4.8	5.3	4.2	4.9	5.6	4.3	4.8	5.3
29	4.8	5.2	5.6	4.5	5.0	5.5	4.1	5.1	5.7	4.5	5.0	5.5
30	5.0	5.4	5.8	4.7	5.2	5.7	4,6	5.3	5.9	4.7	5.2	5.7
31	5.2	5.6	6,0	4,9	5.4	5.9	4.8	5.4	6.1	4.9	5.4	5.8
32	5.4	5.8	6.2	5.1	5.6	6.1	4,9	5.6	6.3	5.1	5.5	6.0
33	5.6	6.0	6.3	5.3	5.8	6.3	5.1	5.8	6.4	5.2	5.7	6,2
34	5.7	6,1	6.5	5.4	5.9	6.4	5.3	5.9	6.6	5.4	5.9	6.3
35	5.9	6.3	6.7	5.6	6.1	6.6	5.4	6.1	6.7	5.5	6,0	6.5
36	6.1	6.5	6,9	5.7	6.2	6.7	5.5	6,2	6.8	5.7	6.1	6.6
37	6,2	6.6	7.0	5.9	6.4	6.0	5.2	6.3	7.0			.
38	6.4	6,8	7.2	6.0	6.5	7.0	5.3	6,4	7.1			
39	6.5	6.9	7.3	6.1	6.6	7.1	5.8	6.5	7.2		.	
40	6.6,	7.0	7.4	6.2	6.7	7.2	5.9	6.6	7.3	–	–	–

MA=menstrual age.

used for reaching an accurate assessment of fetal LV.[64] Further studies for three-dimensional sono-graphic fetal organ volume measurements would be needed to clarify and confirm suggestion.

SUMMARY

The selection of optimal parameters, the develop-ment of the valid measurement procedures, and the use of mathematical modeling and descriptive statistics are necessary if valid quantitative data on fetal growth and biometry obtained. Moreover, three-dimensional volume measurements of fetal organs are next step for precise evaluation of fetal organ growth *in utero*.

REFERENCES

1. Deter RL, Hadlock FP, Harrist RB. Evaluation of fetal growth and the detection of intrauterine growth retardation. In: Callen PW (Ed). Ultrasonography in Obstetrics and Gynecology. Philadelphia: Saunders, 1983; 113–40.
2. Deter RL, Harrist RB. Assessment of normal fetal growth. In: Chervenak FA, Isaacson GC, Campbell S (Eds). Ultrasound in Obstetrics and Gynecology. Boston; Little Brown and Company, 1993; 361–85

Table 17.8: Estimated weight value (g) in singleton appropriate for gestational fetus (S-AGA). singleton small for gestaional age fetus (S-SGA). twin appropriate for gestational age fetus (Tw-AGA). and triplet appropriate for gestational age fetus (Tri-AGA) (Reprinted with permission from Hum Reprod 199:14:1352–1360[33]).

MA (weeks)	*S-AGA*			*S-SGA*			*Tw-AGA*			*Tri-A*		
	−2SD	*mean*	*+2SD*	*−2SD*	*mean*	*+2SD*	*−2SD*	*mean*	*+2SD*	*−2SD*	*mean*	*+2SD*
15			326			305		*8*	347		37	282
16		62	387		34	371		70	409		89	335
17		129	453		104	440		136	476		147	392
18		200	525		178	514	.	208	548		209	454
19		278	602		256	592		284	624	31	276	252
20	36	361	685	2	338	674	26	366	705	103	349	594
21	125	450	774	88	425	761	112	452	792	181	427	672
22	220	545	869	179	515	852	204	543	883	265	510	755
23	322	646	971	274,	610	947	300	640	980	354	599	844
24	430	754	1079	373	709	1046	402	742	1082	448	694	939
25	544	869	1193	476	813	1149	510	850	1189	549	795	1040
26	666	990	1315	584	920	1257	623	963	1302	656	902	1147
27	794	1119	1443	696	1032	1367	741	1081	1421	769	1015	1260
28	930	1254	1578	812	1148	1485	865	1205	1545	889	1135	1380
29	1072	1397	1721	932	1269	1605	995	1335	1675	1016	1261	1506
30	1223	1547	1871	1057	1393	1729	1131	1470	1810	1149	1394	1640
31	1380	1705	2029	1185	1522	1858	1272	1612	1952	1289	1534	1780
32	1546	1870	2195	1318	1655	1991	1420	1759	2099	1436	1682	1927

33	1720	2044	2368	1455	1792	2128	1573	1913	2253	1591	1836	2081
34	1901	2226	2550	1597	1933	2270	1733	2073	2412	1753	1998	2243
35	2091	2416	2740	1742	2079	2415	1899	2239	2578	1922	2167	2413
36	2290	2614	2938	1892	2229	2565	2071	2411	2751	2099	2345	2590
37	2497	2821	3146	2046	2383	2719	2250	2590	2929			
38	2713	3037	3361	2204	2541	2877	2435	2775	3114			
39	2937	3262	3586	2367	2703	3040	2627	2966	3306			
40	3171,	3496	3820	2534	2870	3206	2825	3165	3505			

MA=menstrual age.

3. Deter RL. Evaluation of studies of normal growth. In: Deter RL, Harrist RB, Hadlock FP (Eds). Quantitative Obstetrical Ultrasonography. New York, Churchill Livingstone, 1986; 65–112
4. Gardosi J. Ethnic differences in fetal growth. Ultrasound Obstet Gynecol 1995; 6:73–74
5. Brooke OG, Butters F, Wood C, Bailey P, Tukmac F. Size at birth from 37–41 weeks gestation: ethnic standard for British infants of both sexes. J Hum Nutr 1981; 35:415–30
6. McFadyen IR, Campbell-Brown M, Abraham A, North WRS, Haines AP. Factors affecting birthweight in Hindus, Moslems and Europeans. Br J Obstet Gynaecol 1984; 91:968–72
7. Chetcuti P, Sinha SH, Levine MI: Birth size in Indian ethnic subgroups born in Britain. Arch Dis Child 1985; 60:868–70
8. Shiono PH, Klebanoff MA, Graubard BI, Berendes HW, Rhoads GG: Birth weight among women of different ethnic groups. JAMA 1986; 255:48–52
9. Overpeck MD, Hediger ML, Zhang J, Trumble AC, Klebanoff MA. Birth weight for gestational age of Mexican American infants born in the United States. Obstet Gynecol 1999; 93:943–47
10. Grundy MFB, Newman GB. Birthweight standards in a racial community of mixed racial origin. Br J Obstet Gynaecol 1978; 85:481–86

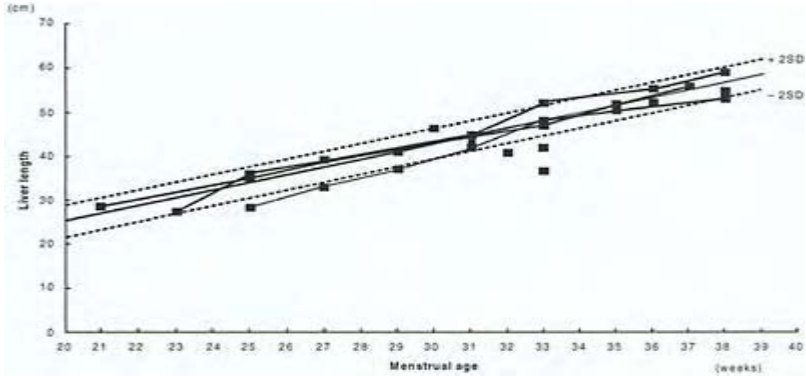

Figure 17.1: Normal range of fetal liver length. Each square represents an SGA fetus. Connected squares represent serial studies for a given

fetus (Reprinted with permission from J Ultrasound Med 2002; 21:361–66)[63]

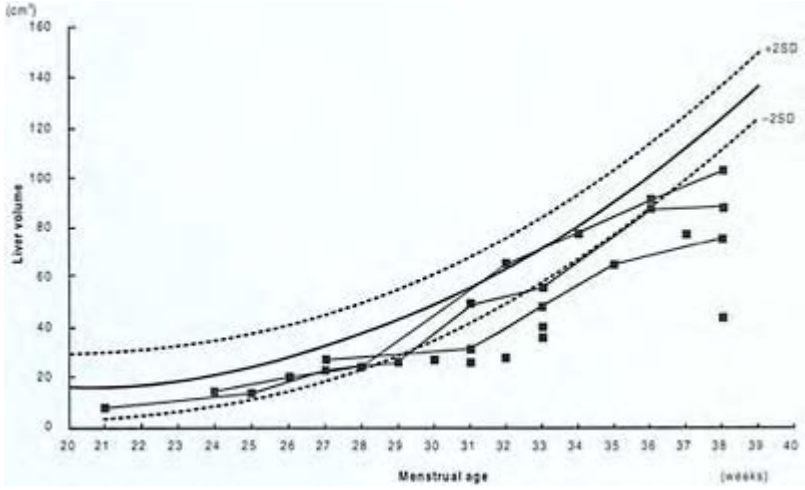

Figure 17.2: Normal range of fetal liver volume. Each square represents an SGA fetus. Connected squares represent serial studies for a given fetus (Reprinted with permission from J Ultrasound Med 2002; 21:361–66)[63]

11. Clarson CL, Barker MJ, Marshall T, Wharton BA. Secular changes in birthweight of Asian babies born in Birmingham. Arch Dis Child 1982; 57:867–71
12. Dawson I, Golder RY, Jonas EG. Birthweight by gestational age and its effect on perinatal mortality in white and Punjabi births. Br J Obstet Gynaecol 1982;89:886–90.
13. Gardosi J, Chang A, Kalyan B, Sahota D, Symonds EM. Customized antenatal growth charts. Lancet 1992; 339:283–87
14. Lei H, Wei SW. Ultrasonographic examination of intrauterine growth for multiple fetal dimensions in Chinese population. Am J Obstet Gynecol 1998; 178 916–21.
15. Landy HJ, Keith LG. The vanishing twin: A review. Hum Reprod Update 1998; 4:177–83
16. Ron-El R, Caspi E, Schreyer P, Weinraub Z, Arieli S, Goldberg MD. Triplet and quadruplet pregnancies and management. Obstet Gynecol 1981; 57:458–6
17. Hata T, Deter RL: A review of fetal organ measurements obtained with ultrasound: normal growth. J Clin Ultrasound 1992; 20:155–74
18. Aoki S, Hata T, Kitao M. Ultrasonographic assessment of fetal and neonatal spleen. Am J Perinatology 1992; 9:361–67.
19. Hata T, Deter RL, Aoki S, Makihara K, Hata K, Kitao M. Mathematical modeling of fetal splenic growth: Use of the Rossavik Growth Model. J Clin Ultrasound 1992; 20:321–27
20. Hata T, Deter RL, Nagata H, Makihara K, Hata K, Kitao M. Mathematical modeling of fetal organ growth using the Rossavik Growth Model: Adrenal gland. Am J Perinatol 1993; 10:97–100

21. Senoh D, Hata T, Kitao M. Fetal liver length measurement does not provide a superior means for prediction of a small for gestational age fetus. Am J Perinatol 1994; 11:344–47.
22. Hata T, Aoki S, Akiyama M, Yanagihara T, Miyazaki K. Three-dimensional Ultrasonographic assessment of fetal hands and feet. Ultrasound Obstet Gynecol 1998; 12:235–39
23. Merz E, Bahlmann F, Weber G. Volume scanning in the evaluation of fetal malformations: A new dimension in prenatal diagnosis. Ultrasound Obstet Gynecol 1995; 5:222–27
24. Merz E, Weber G, Bahlmann F, Miric-Tesanic D. Application of transvaginal and abdominal three-dimensional ultrasound for the detection or exclusion of malformations of the fetal face. Ultrasound Obstet Gynecol 1997; 9:237–43
25. Brenner WE, Edelman DA, Hendricks CH. A standard of fetal growth for the United States of America. Am J Obstet Gynecol 1976; 126:555–64.
26. Jones JS, Newman RB, Miller MC. Cross-sectional analysis of triplet birth weight. Am J Obstet Gynecol 1991; 164:135–40
27. Yuval Y, Seidman DS, Achiron R et al. Intrauterine growth of triplets as estimated from liveborn birth weight data. Ultrasound Obstet Gynecol 1995; 6:345 48.
28. Kuno A, Akiyama M, Yanagihara T, Hata T. Compa-rison of fetal growth in singleton, twin, and triplet pregnancies. Hum Reprod 1999; 14:1352–60.
29. Hata T, Deter RL, Hill RM. Reduction of soft tissue deposition in normal triplets. J Clin Ultrasound 1991; 19:541–45
30. Xu B, Deter RL, Milner LL, Hill RM. Evaluation of twin growth status at birth using individual growth assessment: Comparison with conventional methods. J Clin Ultrasound 1995; 23:277–86
31. Schillinger H, Muller R, Kretzschmar M, Wode J. Best-immung des Gestationsalters in der Spatschwanger-schaft durch Ultraschall. Geburtshilfe Frauenheilk 1976; 36:500–06
32. Kurmanavicius J, Wright EM, Royston P, Wiss er Huch R, Huch A, Zimmermann R. Fetal ultrasound biometry: 1. Head reference values. Br J Obstet Gynaecol 1999; 106:126–35
33. Kurmanavicius J, Wright EM, Royston P, Zimmer-mann R, Huch R, Huch A, Wisser J. Fetal ultrasound biometry: 1. Abdomen and femur length reference values. Br J Obstet Gynaecol 1999; 106:136–43.
34. Gardosi J. Ethnic differences in fetal growth. Ultrasound Obstet Gynecol 1995; 6:73–74.
35. Meire HB, Farrant P Ultrasound demonstration of an unusual fetal growth pattern in Indians. Br J Obstet Gynaecol 1981; 88:260–63
36. Spencer JAD, Chang TC, Robson SC, Gallivan S. Fetal size and growth in Bangladesh pregnancies Ultrasound Obstet Gynecol 1995; 5:313–17
37. Deter RL, Rossavik IK, Harrist RB, Hadlock FP Mathematical modeling of fetal growth: Development of individual growth curve standards. Obstet Gynecol 1986; 68:156–61
38. Stefos T, Deter RL, Hill RM, Simon NV. Individual growth curve standards in twins: Prediction of third-trimester growth and birth characteristics. Am J Obstet Gynecol 1989; 161:179–83
39. Hata T, Deter RL, Hill RM. Individual growth curve standards in triplets: Prediction of third-trimester growth and birth characteristics. Obstet Gynecol 1991; 78:379–84
40. Rossavik IK, Deter RL. Mathematical modeling of fetal growth. I. Basic principles. J Clin Ultrasound 1984; 12:529–34.
41. Deter RL, Rossavik IK. A simplified method for determining individual growth curve standards. Obstet Gynecol 1987; 70:801–06
42. Dijxboorn MJ. Asphyxia at Birth and Neonatal Neurological Morbidity. Groningen The Netherlands: Drukkerij Van Denderen BV; 1986:127. Thesis
43. Simon NV, Deter RL, Shearer DM, Levisky JS. Prediction of normal fetal growth by the Rossavik growth model using two scans before 27 weeks, menstrual age. J Clin Ultrasound 1989; 17:237–43.
44. Stefos T, Deter RL, Simon NV. Effect of timing of initial scan and interval between scans on Rossavik growth model specification. J Clin Ultrasound 1989; 17:319–25.

45. Simon NV, Deter RL, Levisky JS, Stefos T, Shearer DM. Influence of the interval between time points on individual fetal growth curve standards derived from Rossavik models and two ultrasound scans before 26 weeks, menstrual age. J Clin Ultrasound 1989; 17:245–50.
46. Deter RL, Hill RM, Tennyson LM. Predicting the birth characteristics of normal fetuses 14 weeks before delivery. J Clin Ultrasound 1989; 17:89–94
47. Deter RL, Rossavik IK, Carpenter RJ. Development of individual growth standards for estimated fetal weight. II. Weight prediction during the third trimester and at birth. J Clin Ultrasound 1989; 17:83–88
48. Rossavik IK, Deter RL, Wasserstrum N. Mathematical modeling of fetal growth. V. Fetal weight changes at term. J Clin Ultrasound 1988; 16:9–15.
49. Deter RL, Harrist RB, Hill RM. Neonatal growth assessment score: A new approach to the detection of intrauterine growth retardation in the newborn. Am J Obstet Gynecol 1990; 162:1030–36
50. Simon NV, Deter RL, Grow DR, Kofinas AD. Detection of macrosomia by the individual fetal growth curve assessment method. Obstet Gynecol 1991; 77:793–97
51. Ariyuki Y, Hata T, Kitao M. Evaluation of perinatal outcome using individualized growth assessment: Comparison with conventional methods. Pediatrics 1995; 96:36–42
52. Hata T, Kuno A, Akiyama M, Yanagihara T, Manabe A, Miyazaki K. Detection of small-for-gestational-age infants with poor perinatal outcomes using individualized growth assessment. Gynecol Obstet Invest 1999; 47:162–65
53. Deter RL, Harrist RB, Hadlock FP, Carpenter RJ. The use of ultrasound in the assessment of normal fetal growth: A review. J Clin Ultrasound 1981; 9:481–93
54. Vintzileos AM, Neckles S, Campbell WA, Andreoli JW; Jr, Kaplan BM, Nochimson DJ. Fetal liver ultrasound measurements during normal pregnancy. Obstet Gynecol 1985; 66:477–80
55. Naeye R, Burlington VH. Malnutrition. Arch Pathol 1965; 79:284–91.
56. Evans MI, Mukherjee AB, Schulman JD. Animal models of intrauterine growth retardation. Obstet Gynecol Surv 1983; 38:183–92
57. Vatnick I, Bell AW. Ontogeny of fetal hepatic and placental growth and metabolism in sheep. Am J Physiol 1992; 263:R619–23
58. McLellan KC, Bocking AD, White SE, Han VK. Placental and fetal hepatic growth are selectively inhibited by prolonged reductions of uterine blood flow in pregnant sheep. Reprod Fertil Dev 1995; 7:405–10
59. Landy JAM, Janssen MMM, Struyk PC, Stijnen T, Wallenburg HCS, Wladimiroff W. Fetal liver volume measurement by three-dimensional ultrasonography: a preliminary study. Ultrasound Obstet Gynecol 1998; 12:93–96
60. Murao F, Takamiya O, Yamamoto K, Iwanari O Detection of intrauterine growth retardation based on measurements of size of the liver. Gynecol Obstet Invest 1990; 29:26–31
61. Roberts AB, Mitchell JM, Pattison NS. Fetal liver length in normal and isoimmunized pregnancies. Am J Obstet Gynecol 1989;161:42–46.
62. Roberts AB, Mitchell JM, McCowan LM, Barker S. Ultrasonographic measurement of liver length in the small-for-gestational-age fetus. Am J Obstet Gynecol 1999; 180:643–48
63. Kuno A, Hayashi Y, Akiyama M, Yamashiro C, Tanaka H, Yanagihara T, Hata T. Three-dimensional sono-graphic measurement of liver volume in the small-for-gestational-age fetus. J Ultrasound Med 2002; 21:361–66.
64. Chang FM, Hsu KF, Ko HC, Yao BL, Chang CH, Yu CH, Chen HY. Three-dimensional ultrasound assessment of fetal liver volume in normal pregnancy: comparison of reproducibility with two-dimensional ultrasound and a search for a volume constant. Ultrasound Med Biol 1997; 23:381–89

Chapter 18
Ultrasonographic Diagnosis of Intrauterine Growth Restriction

Jose Maria Carrera

INTRODUCTION

Intrauterine growth restriction (IUGR) undoub-tedly is one of the most challenging areas of research for obstetricians today.[1,2] Fetuses with IUGR greatly contribute to perinatal mortality and morbidity due to congenital abnormalities, perinatal asphyxia and other neonatal processes (persistent fetal blood flow, hypothermia, hypo-glycemia, polycythemia, etc.). On the other hand continues to be associated a long-term morbidity: learning problems, abnormal behavior patterns, neurological deficits, etc.[3,4] Even in the adult age, the arterial hypertension and the cardiovascular diseases increase.[5]

Despite marked progress made over the past two decades in both diagnostic procedures and management strategies, the question of what causes growth restriction still remains unanswered in 30–40% of all cases of IUGR.

DEFINITIONS AND INCIDENCE

It is necessary to make a difference between three different concepts: Growth, development and maturity. *'Growth'* is usually defined as the process whereby the body mass of a living being increases in size as a result of the increase in number and/ or size of its cells. *'Development'*, should be understood as the process by which the organs acquire their particular anatomy and their specific functions in living beings, and consequently the progressive anatomical and functional *'Maturity* of all them, as well as its physiological regulations. Thanks to these three processes, that are going on in a parallel way, the fetus reach at the gestation terminus a maturity enough to face the extra-uterine life.

Regarding to the fetal weight anomalies, a clear distinction should be made between the meaning of three different terms: Low birth weight (LBW), Small for gestational age (SGA), and Intrauterine growth restriction (IUGR). *LBW* refers only to newborn infants weighing less than 2500 g. independently of gestational age. Some of these newborns will be premature, and others will be newborns with a growth restriction. *SGA* is a term based on a statistical definition, which includes all newborn infants found below the lower confi-dence limit of normal weight-weeks of gestation curve. Depending upon the type of curve, the lower confidence limit may be the 3rd, 5th, or 10th percentile or −1 or

−2 SD. *IUGR* refers to any process that is capable of limiting intrinsic fetal growth potential *"in utero"*. It is thus a heteroge-neous entity with a variety of possible aetiologies.

Unfortunately, in literature, the terms IUGR and SGA are frequently considered as synonymous. This confusion was increased even more the National Institute of Child Health and Human Development in the USA stated that for "both medical and research purposes, intrauterine growth restriction should be defined as a situation which results in a newborn weight that is lower than 10th percentile for its gestational age".

The *incidence* of IUGR varies greatly in the literature, with reports of figures ranging from 1% to 12%. The reason for this may be found indifferent factors, including the social and economic status of the population studied, different criteria used for discrimination (10th percentile, 5th percentile, etc.), different ways in which standard curves are drawn, data obtained from transverse or longitudinal studies, etc.[6]

CLASSIFICATION OF IUGR

On the basis of sonographic features, Campbell and associates[7,8] proposed a classification of IUGR largely based on the profile of the fetal biparietal-diameter curve. These authors distinguished between IUGR with and "early low profile" in the cephalometric curve and IUGR with a downturn or "late flattening" of the curve. This classification, adopted by most specialists in ultrasonography, was later added to by Levi and colleagues,[9,10] who also took into account the head circumference/ abdominal circumference (HC/AC) index. Follow-ing this classification, IUGR was divided into "har-monious" (or "proportionate") and "dispropor-tionate" (HC greater than AC). Experience soon showed that cases of IUGR classified as harmonious were usually intrinsic and exhibited an early low cephalometric profile; in contrast, cases of IUGR classified as disharmonious were extrinsic and exhibited a late flattening of the cephalometric curve.

Most Anglo Saxon specialists[11] subsequently adopted the classification of symmetrical and asymmetrical IUGR, with some[12] adding a third category known as symmetrical IUGR with "femur sparing", characterized by femur length appro-piate for gestational age but out of proportion to all other biometrical parameters.

Integrated Classification of IUGR

This classification has been proposed by our group[13–19] since 1976, and takes into account all the basic aspects of IUGR, such as onset (early or late), etiology (intrinsically abnormal develop-mental process, etc.), anthropometric data of the newborn infant (weight, length, head circum-ference), general morphology (proportionate, disproportionate, semiproportionate), trophism (eutrophic, hypotrophic, dystrophic), etc. In accordance with these characteristics, three types of IUGR have been recognized (Table 18.1).

Type I implies a decrease in intrinsic fetal growth potential and is also know as intrinsic, harmonious, proportionate, symmetrical or early. In this case, the adverse factor-experts its influence from the time of conception, or at least from the embryonic

stage (hyperplastic stage). Due to the early onset of the process, the three parameters that are usually assessed to determine IUGR are uniformly affected: fetal weight, length and head circumference. Newborn infants are hypoplastic of microsomic, but their appearance is clearly eutrophic. The incidence of congenital malforma-tions is very high (aneuploidy in 25% of fetuses with severe growth retardation in the early stages of gestation).[20] It is thus advisable to carry out routine studies of fetal karyotype. Approximately 20–30% of cases of IUGR are of this type.[13,21,22]

Table 18.1: Types of intrauterine restriction

	Type I	Type II	Type III
Anthropometrical parameters affected	Weight, size and heart perimeter	Weight	Weight and size
General morphology	Harmonious	Non-harmonious	Semi-harmonious
Origin	Intrinsic	Extrinsic pathological	Extrinsic (deficiency)
Starting	Early	Late	Semi-early
Trophism	Hypoplastic eutrophic	Distrophic underfed	Hypotrophic badly fed

Type II is known as extrinsic, disharmonious, disproportionate, asymmetrical or late, and uteroplacental insufficiency is the etiopathogenetic mechanism. Since factors involved in uteroplacental insufficiency are particularly common during the last trimester of pregnancy (hyper-trophic stage), only fetal weight is affected, whilst little or no effect is evident in fetal length or head circumference. The physical appearance of the neonate is characteristic, with a disproportionately large head and dystrophic, undernourished body. Cases of *in utero* fetal death and fetal distress during delivery are most often found in this group. Approximately 70–80% of cases of IUGR are thought to be of this type.[23,24]

Type III is somewhat mixed in comparison with the other two types. While the factors at work are apparently extrinsic and appear relatively early on in pregnancy (nutrient deficiency), the consequen-ces are more akin to those associated with intrinsic IUGR, where fetal weight and length, in particular, are modified. Neonates in this group are characterized by semi-harmonious morphology and a hypotrophic, undernourished appearance.

ANTENATAL DIAGNOSIS OF IUGR

Diagnosis of the Risk of IUGR

Pregnancies at risk for IUGR may be diagnosed on the basis of previous history (low fetal birth weight in earlier pregnancies, etc.), associated disorders (autoimmune diseases, high blood pressure, etc.), toxic habits (regular smoker, etc.). Previous history of IUGR is the most important risk factor.

Attempts have been made to predict the risk of IUGR, in particular in association with pregnancy-induced hypertension, using Doppler velocimetry in maternal uterine arteries.

The Doppler study of the uterine artery at 22–24 weeks' gestation allows detecting the IUGR with a low sensibility (close to 15%). However if we consider the severe IUGR (those that need to finalise the gestation before 32 weeks), the sensibility is then 80%. It does exist some controversy about the impact that the population screening of IUGR could have on the perinatal results. But, as a minimum, it would permit to classify the population in high or low risk of IUGR and to adopt different ultrasound procedures in the two groups.

In our opinion, the presence of a protodiastolic notch in uterine artery velocity waveforms that persist up to 25–26 weeks should alert the possibility of IUGR.[25]

Ultrasound Screening of IUGR

This is perhaps the most important and the most difficult diagnosis to make when we consider that more than 50% of pregnancies are free of any associated conditions that would alert obstetricians to the possibility of IUGR.

The majority of authors are in agreement that patients whose symphysis fundal height does fall below the 5th centile should subsequently undergo testing that will be able to identify fetuses that are at high risk for developing chronic fetal distress, such as Doppler study of the umbilical cord.[26,27]

Serial Measurements of Biparietal Diameter

Initially, and still in many places, the biparietal diameter (BPD) was the only measurement that was routinely taken for the assessment of fetal growth. When pregnancy is normal, this parameter falls within the normal range and can be considered a representative indicator of the growth of other fetal organs and tissues, but when pregnancy is abnormal it may still fall within the normal range (head size is rarely affected in many cases of IUGR) although in this case it is not representative of the growth of other fetal structures. On the other hand, misdiagnoses have been on many occasions in fetuses with marked brachycephaly or dolichocephaly in association with normal development of the rest of the body. In addition, measurement of the BPD does not permit determination of fetal weight and height growth with acceptable reliability. The substitution of BPD by head circumference or cephalic area does not substantially improve the sensitivity of the method.

Measurement of Biparietal Diameter and Length of the Femur

With the purpose of improving the screening method, measurement of the length of the femur has been introduced. It has the advantage that it measures a component of fetal longitudinal growth and does not suffer the sudden flattening out characteristic of cephalic parameters at term, although it has the disadvantage of not being a useful parameter for establishing the diagnosis of IUGR early stages.

Measurement of Biparietal Diameters, Length of the Femur and an Abdominal Parameter

The combination of these three parameters, if they are correctly measured, provides a considerably higher sensitivity than a measurement of BPD alone or in association with the length of the femur. Inclusion of an abdominal parameter (abdominal diameter, abdominal circumference or abdominal area) adds a measurement that is earlier affected by growth restriction than cephalic or longitudinal development. An important limitation, however, is the high variability and low reproductibility of these measurements. Values within the normal or abnormal ranges may be found according to the section site.

Ultrasound screening of abnormal fetal growth is based on results of the three basic sonographic studies generally recognized as necessary in the control of a supposedly normal pregnancy. That is, at 8–12, 18–22 and 34–36 weeks of gestation. Measurement of the crown-rump length (CRL) is obtained in the first examination, so that gesta-tional age is determined with notable accuracy, whereas other biometric parameters are measured on the second and third occasions of echographic study. Comparison of data obtained in both these examinations will permit identification of devia-tions from normality.

Ultrasound Diagnosis of IUGR

The diagnosis of IUGR is based on biometrics parameters recorded during ultrasound scanning. However, for the correct evaluation of those it is fundamental that a correct gestational age has been previously assigned.

It is desirable that this is determined since the first ultrasonography exploration because the reliability of this evaluation decreases as the gestation goes on.

In order the biometrical parameters are useful, the measurements must be standardized (precisely defined cross-sections for ultrasound imaging, clear reference points, etc.), discrimination consis-tent (identical cut-off points to differentiate fetuses and neonates) and appropriate curves used for the different populations under study which should then be correctly interpreted. It should be borne in mind that the independent variable, used to calculate the dependent variable, is located in the abscissa. In order to reduce misreadings to a minimum, gestational age should be precisely determinated. If it is not clinically reliable, it must be determined by using measurements of fetal structures that are affected either little or not all by fetal growth retardation, such as transverse cerebellar diameter.[28,29]

Although there are multiple standardized measurements of fetal parameters for which tables or curves showing normal values have been deve-loped, the following parameters are those used in clinical practice.

Crown-rump Length

This is particularly sensitive biometric parameter that can be measured in the early stages of gestation.[33] The greatest value of this parameter is the early confirmation of the gestational age, which, if measured in all gestations, allows for the early diagnosis of IUGR.

Technically the only limitation is the progressive bending of the embryo which makes measurements less reliable after weeks 10–12 ofgestation. Between weeks 6–12 of gestation there is an exponential increase in CRL although this increase later appears to be linear. The maximum error obtained when calculating this parameter with respect to gestational age is ±5 days in 95% of cases (between weeks 6 and 14, fetal growth is rapid and the limits of confidence are very narrow). If an embryo falls well outside the normal curve, the presence of chromosome anomalies or dysmorphy should be suspected. Fetal surveillance using ultrasound imaging should be instituted and the karyotype determined (Fig. 18.1).

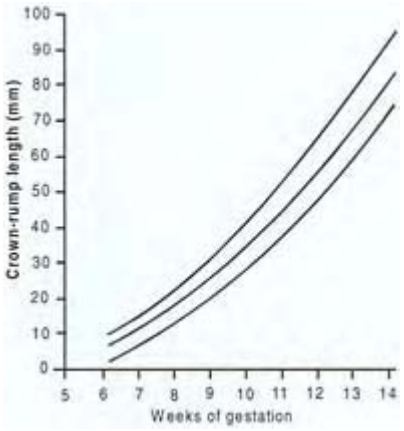

Figure 18.1: Mean ±2 SD fetal crown-rump length for gestational age 6–14 weeks

Biparietal Diameter

This is the most reproducible parameter; it may be determined from weeks 13–14 of gestation (Fig. 18.2). Many would consider this biometric parameter to be the most useful, not only to determine gestational age, but also to diagnose IUGR. Currently, this parameter is not ued alone, but in conjunction with other biometric parameters.

The principal advantage of this measurements is the fact that it is relatively little affected by processes of nutritional deprivation or placental insufficiency, which permits it to be used, in spite of these conditions, for the determination of the probable gestational age.

The sonographic section, from front to back includes[34] the most anterior portion of the

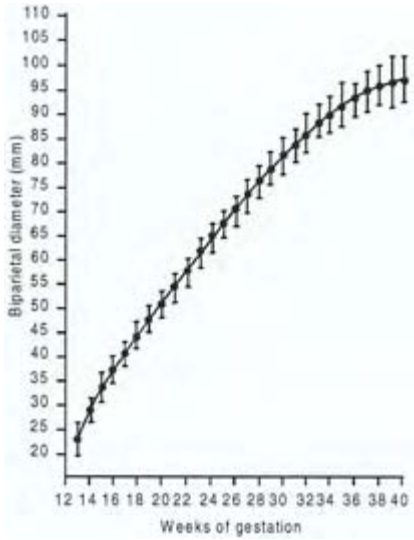

Figure 18.2: Relationship between biparietal diameter (mean ±1 SD) and gestational age

longitudinal fissure, the cavum of the septum pellucidum, the thick line of the third ventricle and quadrigeminal cisterna with the punctiform echo on the pineal body. Frontal horns of the lateral ventricles and thalami on either side of the third ventricle should be visible.[34,35]

Until week 30 of gestation, increases in BPD are reasonably linear, with weekly increases of 3 mm approximately equal to the standard deviation of mean values for this period.[36,37] From weeks 30 to 38, the rate of change gradually slows, with weekly increases of about 1.5.[37,38] From week 38 to term, weekly increases are 1 mm, and virtually nil as from week 42. The sum of the different rates of increase in BPD causes standard deviations to increase as pregnancy reaches-term.

Campbell and Dewhurst[7] reported that when the BPD was lower than the 5th centile, IUGR was confirmed in 68% of cases. Most errors occured when values fell between the 5th and the 10th centiles; in these circumstances, weight at birth was within the normal range in 69% of newborns.

Table 18.2: Comparison of several biometric parameters for detection of the small-for-gestational-age infant at 34 36 weeks of gestation

			Predictive value	
	Sensitivity	*Specificity*	*Positive*	*Negative*
Biparietal diameter	45	74.	23.0	81.5
Cephalic circumference	52	80.0	26.02.03	94.3
Cephalic area	60	80.0	23.0	95.2
Abdominal circumference	83	87.7	43.0	97.8
Abdominal area	85	88.0	44.0	98.1
Femur Length	58	81.0	23.3	95.0

The sensitivity of the BPD as the only cephalometric parameter does not exceed 50%[39] (varying from 26.9% to 48%)[41–44] when determining a small-for-dates fetus below the 10th centile. In our experience, the sensitivity of the BPD between weeks 34 and 36 of gestation is 45% (Table 18.2).

Given the variability of the BPD (at least three different weeks may theoretically be ascribed to each value), serial measurements are recommended. Sabbagha and associates[45] proposed determining the so-called growth-adjusted sonar age in order to determine sonar age precisely and to improve the prediction of IUGR. The ideal evolution of the 226 cases in which serial measurements of BPD were made (the first within the 24th week and the last after the 30th) on an original centile curve is shown in Figure 18.3.

At present, despite the fact that it continues to be the most frequently used biometric parameter, the BPD is not considered to be a reliable indicator of IUGR. This is because head size is rarely affected in many cases of IUGR (in particular type II IUGR, the most commonly occurring) and, moreover, because in the last weeks of pregnancy it is very difficult to determine whether or not the fetus is really growing, since weekly gains in fetal weight are minimal. On the other hand, the BPD should be used when the cephalic index (fronto-occipital diameter divided by BPD and multiplied by 100) falls between 70 and 85.

When the BPD is apparently below the lower limits of confidence, it does not necessarily signify IUGR. There may be an error in the calculation of the estimated day of delivery.

The possibility of an error in the estimated day of delivery can be eliminated by performing an ultrasound examination in the first trimester of gestation (data from the size of the embryo or yolk sac). The diagnosis of IUGR is specially consistent when cephalic measurements are initiated early. If the cephalic curve remains parallel to the standard curve throughout the gestation, then we are dealing with a pregnancy with earlier dates. In contrast, if we are dealing with IUGR, the curve will deviate from the theoretical standard curve at a given moment during the gestation.

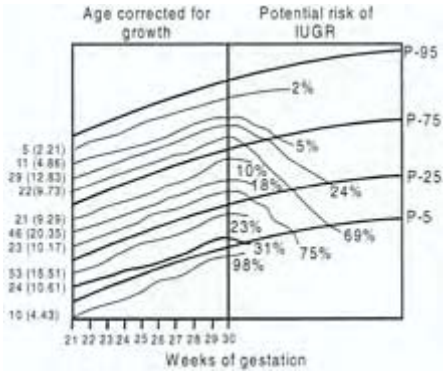

Figure 18.3: Potential risk of intrauterine growth restriction (IUGR) according to the evolution of biparietal diameter (BPD). Curves are shown for the 5th, 25th, 75th and 95th centiles, with 'small', 'medium' and 'large' BPD between them. Number of cases analyzed are shown on the left, with percentage incidence of IUGR in parentheses. The potential risk of IUGR is shown on the right

Nevertheless, it is not always possible to have early measurements to observe the exact moment at which a fetus begins to deviate from the standard growth curve. In practice, we need to resort to the method of weekly increments. We are indebted to Campbell and Newman,[38] who performed serial studies of fetal growth and have established graphs in which the relationship of weekly growth, BPD and gestational age are demonstrated.

It is thus possible to determine in successive weekly measurements whether, in a given case, the weekly growth of the fetus is adequate. In contrast, one can ascertain the gestational age using the data from the weekly increase in growth. If one is dealing with a questionable date of the last menstrual period (LMP), a suspicion for IUGR will arise in any fetus whose weekly increase in the measurement of the BPD is below the 10th centile of the expected measurement and it can almost be confirmed for any increase that is lower than the 5th centile.[46]

If there are any doubts of the LMP or if the BPD is less than that expected for a given gestational age, one can resort to the second graph, which permits the evaluation of the increments as a function of BPD. If the weekly increments remain below those expected for a given BPD, it is most probable that one is dealing with a fetus with IUGR, especially if the weekly increase is below the 5th centile. If the measurements agree, then one is dealing with a miscalculation of the gestational age.

Head Circumference and/or Cephalic Area

Measuring the head circumference of cephalic area is a more complex procedure than measuring BPD since, for measurements to be correct, the sono-graphic section should include both the biparietal and the fronto-occipital diameters. These para-meters, however, have some advantages over the BPD, since they avoid the errors that occur in BPD measurements as a result of brachycephaly or dolichocephaly (e.g. craniosynostosis); and in cases of breech presentation, which often accom-panies a fundic placenta, BPD measurements in normally developed fetuses are abnormally small, while head circumference of cephalic area are within normal limits (Fig. 18.4).

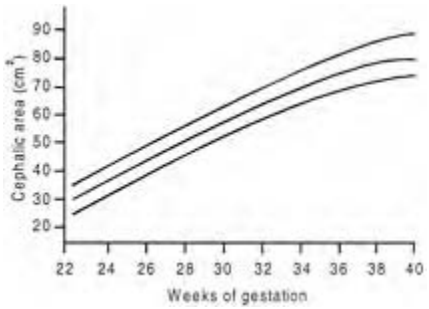

Figure 18.4: Relationship between cephalic area (mean ±2 SD) and gestational age

The sensitivity of head circumference measure-ments is 52% and therefore, somewhat higher than that of BPD. Specificity, however, is similar (80%). Predictive values do not seem to differ greatly whether head circumference or cephalic area are used. In our experience (using our own curve) the sensitivity of cephalic area is 60% and specificity 80% (Table 18.2).

Abdominal Diameters

Both transverse and anteroposterior abdominal diameters have been used to assess fetal develop-ment. Some authors[47,48] consider that measure-ment of abdominal diameters has the advantage over abdominal circumference or abdominal area of being much simpler and open to fewer errors. To ensure the reproducibility of abdominal diameter measurements:

1. A cross-sectional view should be obtained from the appropriate site (the site of Choice is the level at which the umbilical vein leads into the canal of Arantius (ductus venosus). At this point the diameter of the liver is largest and therefore, abdominal circumference should be the greatest at this level;
2. The section should be as close to orthogonal as possible.
3. The measurement should be made during a moment of fetal apnea.

Macler and co-workers,[47] correlating false-positive and false-negative results from the BPD, thoracic diameter and abdominal diameter, have shown that figures were particularly low, throughout gestation, when abdominal diameters were used.

These parameters are considered to be the best indicators of fetal growth, since they reflect the volume of an important complete organ, such as the fetal liver. On the other hand, by comparing them to cephalic parameters, it allows for the phenotypic type if IUGR to be determined.

Measurement of the abdominal circumference or abdominal area of the fetus is facilitated by the cylindrical shape if this body segment and the existence of an excellent point of reference (the umbilical vein). The curve of values for the abdominal circumference during pregnancy shows as almost linear increase until week 36, with a slight decrease from this time on. The tendency for values to fall off suddenly at term, typical of cephalometric parameters is, therefore, not detected (Fig. 18.5).

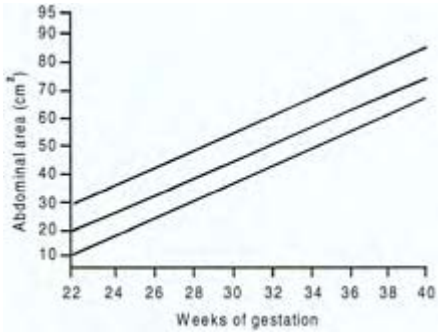

Figure 18.5: Relationship between abdominal area (mean±2 SD) and gestational age

If measurements of abdominal circumference are compared with those of head circumference it may be observed that, although mean abdo-minal circumference measurements are at first smaller than mean head circumference measure-ments are at first smaller than mean head circumference, they equal out at week 36, and from then on the mean abdominal circumference measurements are greater than those of head circumference. According to Campbell and Wilkin[49] the diagnostic accuracy of this parameter in cases of IUGR is remarkable; using a single measurement at week 32 of gestation, 86.7% of newborns who fall below the 5th centile can be identified. Results are less favorable, however, as pregnancy progresses. At week 35 to 36, Campbell and Soothill[50] reported a sensitivity of 83%, specificity of 79%, positive predictive value of 39% and negative predictive value of 87%. Similar results have been reported by other authors.[51,52] In our experience this parameter showed an overall sensitivity of 83% with a specificity of 87.7%; in the case of abdominal area, the sensitivity and specificity were 85% and 88%, respectively.[53]

It should be noted that sensitivity and positive predictive value increase with gestational age, so that week 34±1 of pregnancy is considered to be the best time for differentiating fetuses with IUGR.[54,55]

Unfortunately, both head circumference and head area measurements are subject to greater inter- and intraobserver variations than BPD, owing to the changes that take place in measure-ments as a result of fetal breathing movements and fetal position.[56]

Length of Femur

The femur is the easiest long bone to identify and measure. On the other hand, it offers an advantage over the BPD since it does not change with mor-phological changes of the fetal head, and it also permits the evaluation of certain types of skeletal dysplasias. Its typical "golf club" -like appearance and moderate curvature from week 18 on are unmistakable. The normal curve for length of femur, similar to that of abdominal parameters, does not suffer the sudden flattening out characteristic of cephalic parameters (Fig. 18.6).

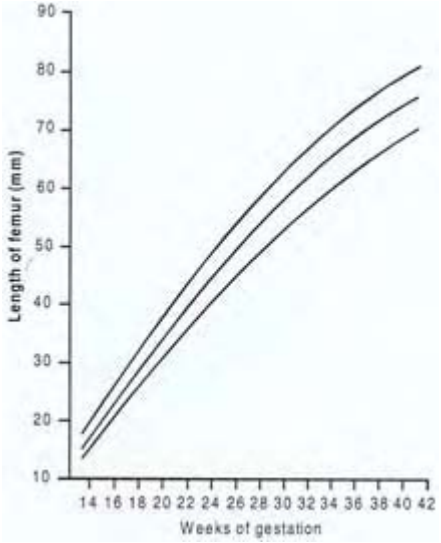

Figure 18.6: Relationship between length of femur (mean±2 SD) and gestational age

O'Brien and Queenan[57,58] showed that fetal femur length values in 60% of cases of IUGR fell below the lower confidence limit. This parameter, just like cephalic parameters, is affected in cases of symmetrical fetal growth restriction (type I) but is hardly or not at all affected in cases of asymmetrical fetal growth restriction (type II). Hadlock and colleagues[59] have emphasized the usefulness if the femur length/abdominal circumference ratio, which not only presents acceptable levels of sensitivity (63%) but

also has the advantage of being independent of gestational age. Indeed, this ratio remains constant (22±2%) as from week 22 of gestation. Its predictive value, however, is less than 30%.[60]

Diagnosis from the Delay of the Growth of BPD and Femur Length

The pregnancy weeks matched to the sizes of sonographic fetal parameters are calculated, and compared to actual pregnancy weeks calculated from the CRL in the first trimester or reliable LMP A common manual method is to compare the measured BPD and femur length to the growth curves of the BPD and femur length standardized in each district or region. It will be appropriate, for example, in Japan to use femur length growth values reported by the Japanese Society of Obstetrics and Gynecology,[61] where fetal femur length value is smaller than the European standard in late pregnancy.[25]

A computerized technique is to calculate the pregnancy weeks from the values of BPD and/or femur length. IUGR is suggested, if the pregnancy weeks determined by the computer programs repeatedly delay in the third trimester from the weeks determined by the CRL or correct LMP

Total Intrauterine Volume

Gohari and co-workers[62] have measured maximum longitudinal (L), transverse (T) and anteroposterior (AP) diameters of the uterus to calculate total intrauterine volume (TIUV=L× T×AP×0.5233). Using measurements obtained from 100 pregnancies at different stages of gestation, they calculated a normal curve. In a series of 96 cases of suspected IUGR (with postnatal confirmation in 28 cases), it was concluded that IUGR is likely when total intrauterine volume corresponds to −1.5 SD of the mean, equivocal when figures fall between −1.5 and+1.5 SD of the mean (one-third of cases of IUGR), or should be excluded when they are over—1SD. The only errors recorded were those caused by severe oligohydramnios. Results of some later studies, however, are less encouraging (sensitivity 60%, positive predictive value 30%).[44]

Fetal Organs Biometry

Currently we study the biometry of certain organs (diameters, estimation of volume, ect) of diverse fetal organs such as the brain, the heart, the lungs, the liver, the spleen, the pancreas, the stomach, the suprarenal glands, the intestine and the bladder.[63] Nevertheless, in general, and with the exception of measuring the volume of the bladder to calculate the production of urine by the fetus, these parameters have little value in diagnosing IUGR.

Diagnosis of Type of IUGR

The prenatal knowledge of the biometric type of IUGR does not have the same importance as it did several years ago, when it was considered that symmetric IUGR was most probably associated with chromosomal or genetic abnormalities, and asymmetric IUGR with a vascular insufficiency of the uteroplacenatal bed. However several studies

have shown that chromosomal abnormalities can be associated with both types of IUGR[64,65] and that the asymmetry is a progressive phenomenon closely related to clinical severity in the restriction of fetal growth.[66] The ultrasonographic identification of the type of IUGR is based on three evaluations: (1) A profile of the cranial parameters, (2) Calculation of the HC/AC ratio, and (3) Calculation of the diameter of the fetal thigh.

The *profile of the curve of cephalometric parameters* (BPD, head circumference, etc.) provide information on the moment when the noxa begin to affect fetal cranial structures (early, late or semi-early onset).

In the case of type I IUGR, the curve of the mean values falls below—2 SD early in pregnancy and continues largely parallel to the latter. In contrast, in type II IUGR, the mean curve of BPD or head circumference coincides with mean values for the normal population until approximately weeks 30 of gestation, when it fall below the mean.

Finally in type III IUGR, the BPD profile shows an intermediate pattern

The study of the head-abdominal circumference ratio (HC/AC ratio) provides data on overall fetal morphology, helping to define growth as proportionate (symmetric or type I IUGR), disproportionate (asymmetric or type II IUGR) or semi-proportionate (or type III IUGR).

The HC/AC ratio decreases throughout pregnancy (values>1.2 at 14 to 16 weeks; <1 after 36 weeks; between 0.9 and 1 at term), owing to the rapid accumulation of fat in subcutaneous and soft tissues in the fetal thorax and abdomen during the last trimester.

Kurjak and Breyer[67] have the HC/AC ratio with the position of the newborn on the centile curve at 36 weeks. When this method was reproduced by our group, similar results were obtained, with the only difference being that, in the group of neonates below the 10th centile, one-third of cases showed a ratio of <1, whereas in the experience of Kurjak and Breyer[67] this occurred in only 5% of infants in this group.

It may be concluded that the HC/AC ratio is inverted after week 36 of gestation (from >1 to <1). Only 7% of normal fetuses do not show this pattern.[25]

Fetuses small for gestational age behave differently depending upon the causes of growth retardation. If the ratio is inverted and, therefore, values are within the confidence interval of the normal curve, it is safe to assume that the case is one of fetal growth retardation of the proportionate or symmetrical type (type I IUGR). The neonate that is small for gestational age is hypoplastic but nor hypotrophic. Only 11.7% of infants do not show this pattern. Fetal growth retardation, however, will not go unnoticed at the time of sonographic examination since, as we have already mentioned, BPD is markedly affected. On the other hand, however, when the ratio is above the upper limit of the confidence interval of this curve and, consequently, is not inverted, the case is probably one of growth retardation of the asymmetrical, disproportionate or extrinsic type (IUGR type II) as a result of which newborn infants will be small for gestational age, hypotrophic and, in some cases, dystrophic. Only 7.14% of infants do not show this pattern.[25] Finally, in the case of IUGR type III (semi-proportionate), the ratio is >1 in 41.7% cases, <1 in 52.94% and equal to 1 in 5.82%.

In spite of the prenatal assignment of IUGR to one type or another, the prognostic importance of this had diminished in comparison to the situation several years ago. It is evident, nonetheless, that the diagnostic importance echograp-hically of the HC/AC ratio means that it is a

	Abnormal ratio (n=56)	*Normal ratio (n=78)*	*Statistical analysis*
Gestational age at delivery (weeks)	34±3.6	36.3±3.6	P*<0.005
Birth weight (g)	1533±635	2022±655	P+<0.0001
Delta birth weight	−2.62±10.73	−2.10±0.67	*P*+<0.0001
Abnormal UA Doppler	29 (52%)	20 (26%)	OR++ 3.1 1 (1.14–6,9
Abnormal biophysical profile	15 (27%)	9 (11%)	OR++ 2.80 (1.04–7.73)
Emergengy Cesarean section	21 (37%)	23 (29%)	OR++ 1.43 (0.65–3.17)
Delivery at <34 weeks**	19 (34%)	10 (13%)	OR++ 3.49 (1.36–9.08)
Perinatal mortality	12 (21%)	6 (8%)	OR++ 3.27 (1.04–9.34)
Chromosomal abnormalities	2	2	

UA—umbilical aretery; *probability level derived from Mann-Whitney U test; +probability level from Student's *t* test; ++odds ratio with 95% confidence interval; **excluding intrauterine deaths.

measurement that should be taken into account when determining the well-being of the fetus. As can seen in Table 18.3, which demonstrates the experience of David and colleagues,[66] there are differences that are statistically significant in the use of various parameters, depending on whether a given ratio is normal or elevated. In both groups, there could be deterioration of the fetal condition, but this possibility is obviously greater in the group of fetuses with IUGR with an elevated HC/AC ratio because, as previously stated, in this case the pathological restriction of ponderal growth is greater.

The quantity and distribution of fat present in the fetus evaluated through *fetal thigh diameter* is, without a doubt, one of the most significant parameters that represents the nutritional status of the fetus.[68] Even when this factor is evaluated indirectly by measuring the abdominal perimeter or area, and calculating the HC/AC ratio, it is evident that the proportion of fat in the fetal extremities, and specially in the thigh, is greater than in the abdomen.[69–71] It must be kept in mind, on the other hand, that the decrease in the abdominal parameters in the presence of asymmetric IUGR is not only due to the loss of fat, but also, and especially, due to the poor development of the liver.

Balouet and colleagues[72] have systematically calculated the cutaneous perimeter and aponeuro-sis of the thigh, proposing a formula to estimate fetal weight, that in addition, takes into account the umbilical perimeter. By this formula, the global precision was 6%, the correlation with fetal weight 0.954 and, in 82% of cases, the margin of error was less than 10%.

The confirmation of normal values should lead one to believe that the fetus is well nourished (if one is dealing with IUGR, it is most likely type I) and values that are

obviously pathological should lead to a diagnosis type II IUGR. Apparently, this procedure is efficacious in all fetal weights and varies little with ethnic conditions.

HEMODYNAMIC STUDY OF FETAL DETERIORATION

The reduction in the number of functional arterio-les in the tertially villi, of progressively increases the circulatory resistance in the umbilical artery, and gives rise to a decrease in the PO_2 in the umbilical vein. Both these events set into motion a phenomenon of circulatory redistribution principally characterized by the centralization of blood flow. The better oxygenated blood goes towards the most vital organs (brain, heart, the adrenals), whilst vasoconstriction limits the blood's arrival at the organs considered less indispensable (digestive system, lungs, skin, skeleton, etc.).[73]

Table 18.4: Haemodynam

	Pattern	
	Normal	*Pathological*
Arterial parameters		
Umbilical artery (PI)	<P-95	>P-95
Aorta artery (PI)	<P-95	>P-95
Carotid artery (PI)	>P-5	>P-5
Middle cerebral artery (PI)	>P-5	<P-5
Venous parameters		
Umbilical vein	Non-pulsating	Pulsating
Inferior vena cava (VPI)	<P-95	>P-95
Ductus venosus (VPI)	<P-95	>P-95
Intracardiac parameters		
Diastolic function		
E/A Transmitral	>P-5	<P-5
E/A Transtricuspid	>P-5	<P-5
Dystolic function		
Aorta (PSV Ao)	>P-5	<P-5
Pulmonary (PSV P)	>P-5	<P-5

The redistribution or centralization of blood flow has been studied in animal experimentation by various resarchers,[74–76] and the above-mentioned mechanical pattern has been confirmed. However, it should be stressed that when fetal hypoxemia was induced by maternal hypoxemia, not only was there an increase in cardiac and cerebral

perfusion, but there was also a significant increase in the umbilical blood flow, and this was not the case when the fetal asphyxia originated from microembolization of the umbilical arteries, thus creating conditions similar to those of a human fetus with a placental lesion.[77–79]

Nowadays, Doppler enables a hemodynamic profile to be drawn up that includes the functionality of vascular (arterial and venous) and cardiac systems (Table 18.4).[80]

Thanks to the Doppler technique it is possible to recognize four periods with relatively well defined hemodynamic, biophysical and biochemical patterns. These are: (1) a silent period of increase in resistance; (2) a period with reduction in umbilical blood flow; (3) a period with centralization of the blood flow; and (4) a period with decentralization of blood flow.

Silent Period of Increase in Resistance

Pathophysiological Basis

The progressive deterioration of the villous microcirculation is reflected in the Doppler study of the umbilical artery, when the functional abstruction reaches 50% of the villous arteriolar system, and significantly modifies the pulsatility index (PI) (Fig. 18.7).[81]

Before this percentage is reached, the capacity of the placental reserves covers the theoretical deficit of gaseous exchange, provided the maternal supply line remains satisfactory.[82]

Doppler Hemodynamic Profile

The hemodynamic profile is completely normal over a certain period (generally 3–6 weeks), and there is no pathology of any kind. The flow velocity waveform (FVW) of the umbilical artery is normal (positive blood flow over the whole cardiac cycle, with normal pulsatility indices, resistance or conductancy.[83,84] Doppler studies on the remaining vessels (aorta, common carotid and middle cerebral arteries) also prove normal. We can therefore speak of a “normal hemodynamic pattern”.

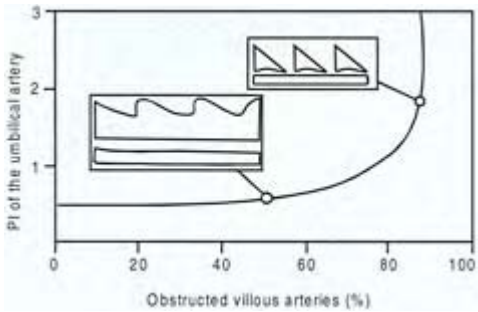

Figure 18.7: Trudinger’s mathematical model,[81] relating the morphology of

the flow velocity waveform of the umbilical artery (Doppler) with the resistance in the villous arteriolar system (percentage of obstructed villous arterioles)

In a Doppler study we carried out on 82 cases of growth retardation confirmed at birth, we demonstrated that 36 of them (43.9%) had a normal umbilical PI; the study of the remaining fetal vessels proved normal in all these cases (Table 18.5). For this reason, we consider it unnecessary in practice to widen the hemodynamic study of the fetus when the umbilical FVW is normal and fetal growth is also apparently normal.

In this period, both the cardiotocography and the remaining parameters of the biophysical profile are normal and the study of fetal blood gases by funiculocentesis is normal. According to the limits of our current experience, such an exploration is therefore not justified when the Doppler study is normal.

For all these reasons, the perinatal mortality rate is not increased.

Reduction in Umbilical Blood Flow

This is the first objective sign of the start of chronic fetal distress brought on by the placental lesion.

Pathophysiological Basis

It has been demonstrated that the functional obstruction of over 50% of the villous arterioles is translated into a clear deterioration of the umbilical FVW.[73]

Although some studies claim that the umbilical artery is not always the first vessel affected,[85,86] in our experience and in that of other authors, an increase in umbilical resistance is usually the firts observable hemodynamic signal when there is a placental lesion affecting the villous microcirculation. In 15–20% of fetuses with growth retardation with a placental cause, the abrupt decrease in PO2 can give rise, through the and carotid chemoreceptors, to an increase in the aortic and/or cerebral PI, which exceeds and/or precedes those observed in the umbilical artery. On the other hand, it is also possible to observe pathological values of the aortic or cerebral PI before an alteration in umbilical perfusion, when the cause of fetal distress does not reside in the placenta but in a disorder in the mother's internal medium (hypoxemia through maternal cardiorespiratory pathology, an acute deficit of specific nutrients, severe anemia, etc.) or in her hemo-dynamics (e.g. hypertensive crises with a renal or endocrine origin). Even in these cases, umbilical conductance may be increased. So, brain-sparring may develop independently of the umbilical artery waveform.[87–89]

Alternatively, there is experimental evidence that a placental lesion is followed by a decrease in umbilical arterial perfusion. Morrow and co-workers.[77,78,92] working with fetal sheep subjected to an embolism of the villous microcir-culation (plastic micropistons 50μm in diameter), observed gradual changes in the FVW of the umbilical artery similar

to those described in human fetuses subjected to growth retardation through villous pathology (reduction in endodiastolic blood flow, zero diastole and, finally, reserve blood flow). The cause, therefore, of the deterioration of the umbilical FVW lies in the increase in microvillous vascular resistance which, whilst primarily inducing a deficit in the perfusion in the umbilical artery, is also the reason for a progressive decrease in the PO_2 in the umbilical vein. Hypoxemia is thus the result and not the cause of the hemodynamic umbilical-placental alteration. This is why a reduction in PO_2 without any placental lesion does not give rise to any change in the umbilical FVW[90,93] and neither does this change occur through an increase in hematic viscosity or a rise in maternal blood pressure.[90,91]

Table 18.5: Cases of intrauterine growth retardation, grouped into four groups according to the pulsatility (PI) results in the umbilical artery and the hemodynamic, profile (FHP): thoracic aorta PI. common carotid artery PI and module cerebral artery. The PH of the umbilical vein was measured at birth

		Cases		*Perinatal mortality*		*pH<7.20*	
Group	*Association*	*N*	*%*	*N*	*%*	*N*	*%*
I	Normal umbilical PI+normal FHP	36	43.9	0	0.0	6	16.6
II	Normal umbilical PI+abnormal FHP	0	0.0	–	–	–	–
III	Abnormal umbilical PI+normal FHP	22	26.8	0	0.0	8	36.3
IV	Abnormal umbilical PI+abnormal FHP	24	29.2	6	25.0	15	62.5
Total		82	100.0	6	7.3	29	35.3

A moderate increase in umbilical resistance is the only finding capable of revealing the onset of chronic fetal distress for a specific period of time, the duration of which largely depends on how quickly the placental lesion takes effect. During this period the Doppler study of the rest of the fetal circulatory system, including the aorta, is usually normal. In our experience 56% of fetuses with growth retardation presented an altered umbi-lical PI, but of these only 52% were accompanied by a pathological hemodynamic pattern.

The umbilical FVW presents positive flow velocities throughout the entire cardiac cycle, but the pulsatility (or conductance) incides reveal values outside the accepted limits for the gestation.

The only compensatory hemodynamic process that can be observed at this time, with the use, in particular, of color Doppler, is the reopening of the ductus venosus, the caliber of which if physiologically reduced at the end of the second trimester. This mechanism makes it possible to extract a significant amount of blood from the fetal liver, and this goes directly to the heart. This “shunt” can delay by some weeks the need for a centralization of the blood flow, but induces the appearance of typical asymmetric growth retardation.[94]

In the cerebral circulation, it is also possible to confirm, in some cases, the experience of a decrease in the PI of the M_2 sector of the middle cerebral artery, with the M_1/M_2 index passing from below 1 (normal) to being over 1 (pathological). This occurrence, secondary to the selective vasodilation of that arterial tract, which can be considered as the subcortical sector of the artery, represents a preservation mechanism for specific areas in the brain, and precedes the authentic brain-sparring effect.

The objective of these two compensatory mechanisms is to delay as far as possible the stimulation of the aortic and carotid chemo-receptors which will set in motion the centralization of flow.

All the parameters of the biophysical profile, including the cardiotocographic study, are normal, as are the results of "vibroacoustic stimulation" (VAS) tests and even the stress tests (test of strength, oxytocin test, etc.). This is because these variable are affected only when hypoxia of the fetal brain on/or heart occurs.

In this period the fetus is normally in normoxia. In our experience it is not necessary to carry out diagnostic funiculocentesis in this phase if there is confirmation that centralization of the blood flow has not begun.

There were no fetal deaths in our statistics for this group but there was a significant increase in the percentage of small-for-dates neonates. For this reason the percentage of neonates with pH below 7.20 reached 38%. In fact, the percentage of intrapartum fetal distress tripled, proof of a greater fetal vulnerability. The *cesarean section* rate rose to 30–40%.[73]

Centralization of Blood Flow

Pathophysiological Basis

As the resistance in the umbilical arterial system increases, there is also a corresponding decrease in the PO_2 in the umbilical vein. This mean that the fetus must carry out, in addition to a reopening of the ductus venosus, a redistribution of its blood flow once a specific PO_2 value has been reached, in order to protect its most important structures from hypoxia. As we have already explained, this redistribution consists of a circulatory centralization with selective vasodilatation of certain organs, such as the brain, the heart and the adrenals, and a vasoconstriction of other sites such as the lung, the intestine, the skin, the kidney or the skeleton. This redistribution can be seen with Doppler, which records a successive increase in the PI of the aorta and the renal artery, and a decreased PI in the common carotid artery and the intracranial vessels.

These changes in the perfusion of the various organs are primarily mediated by neuronal stimulation, whether directly by stimulation of the vagal center or through the aortic and carotid chemoreceptors. In 1969 Dawes and colleagues[95] confirmed that the aortic chemoreceptors in sheep respond to small reductions in arterial oxygen levels. However, it is very probable that these vasoconstriction phenomena are modulated by other factors, such as, for example, the direct effect of hypoxemia vasoactive substances, secretion of catecholamines, or an over all increase in the activity of the autonomic nervous system.

Although the chronological pattern is not well established, it seems that the first vessel to be affected after the umbilical artery is the aorta. The increase in resistance in the

descending thoracic aorta is the result of the combined action of several factors: an increase in umbilical-placental resistance, arterial vasoconstriction resulting in progressive hypoxemia and, finally, a decrease in myocardial contractility.[96] Lingman and co-workers[97] postulate an inverse relationship between myocardial contractility and the aortic and umbilical PI (Fig. 18.8).

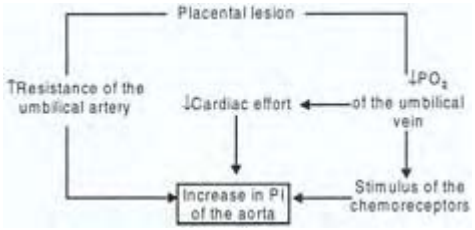

Figure 18.8: Outline of the mechanisms that Influence the pulsatility index (PI) in the aorta after the placental lesion

Doppler Hemodynamic Profile

Doppler study reveals an increase in PI, not only in the umbilical artery but also in the descending thoracic aorta and its branches, such as the renal artery.[98–102] There is a progressive loss of end-dia-stolic velocity in both vessels when the resistance reaches a certain level. At the same time, there is a noticeable decrease in the PI of the cerebral and common carotid arteries, evidence of a further vasodilatation process.

In our previously mentioned study, of the 82 cases of IUGR studied, 46 (56.1%) presented a pathological umbilical PI; 52% of the fetuses also had an abnormal increase in the PI of the thoracic aorta and 41.1% presented further decrease in resistance in the common carotid and/or middle cerebral arteries.

It is often possible to recognize three phases in the centralization of blood flow.

Initial phase The PI in the umbilical artery is high, but there are still positive values in the Doppler frequencies throughout the whole cardiac cycle, even in telediastole.

On the other hand, the FVW of the common carotid artery, which has no end-diastolic frequencies until weeks 32–34,[103] recovers its end-diastolic flow shortly after a proven moderate increase in intracranial perfusion. This suggests that the fall in the PI of the common carotid artery is due to the reduction in the resistance of the cerebral vessels.

The study of the umbilical PI/middle cerebral PI (U/C) relationship can prove particularly helpful in making a definitive assessment of centralization at this stage. Several authors[104–107] maintain that this is the best fluxometric index for tracing IUGR.

Advanced phase The umbilical FVW shows zero diastole. The first to disappear were the teledia-stolic frequencies, but afterwards the lack of blood flow affected the whole diastole. According to Trudinger,[81] the situation occurs when an 80% obstruction in the villous arteriolar system has been attained. The FVW of the aorta also loses its end-diastolic values.

In conjunction with this deterioration in the umbilical blood flow, the vasodilatation of the cerebral vessels arrives at its maximum point, which means that the PI of both the common carotid and the middle cerebral arteries attain their lowest values.

Terminal phase In addition to an absence of end-diastolic flow, there is the onset of a reserve flow, both in the umbilical artery and in the aorta, and this obviously aggravates the prognosis. As well as the arterial hemodynamic findings already described, there are signs in this phase of cardiac insufficiency, revealed by Doppler study of the fetal venous circulation through a decrease both in the velocity peaks in the exit tracts and in the ventricular ejection force, and through a possible visualization of the coronary blood flow.[108,109]

As regards the venous return circulation, there are three signals:

1. Raised reserve blood flow in the inferior vena cava, coinciding with auricular contraction. This finding, which reveals difficulties in the blood flow through the right atrium, can be due both to alterations in the fetal cardiac fre-quency and to deficient auricular contrac-tility.[110–112] The reverse flow can reach up to 30% of the total blood flow (under normal conditions this does not exceed 10%).
2. Reduction in the telediastolic velocity values in the ductus venosus (in the notch which ref-lects the auricular contraction); this reduction can lead to an inversion of the blood flow. This would be secondary not only to the increase in telediastolic; volume determined by the increase in the peripheral resistance, but also to the reduction in the capacity for myocardial response.[113]
3. “Venous pulsation” in the umbilical vein, with an apparent cyclical decrease in the venous flow coinciding with the zero diastole of the umbilical artery.

As regards the exit blood flows, there have been reports of their progressive deterioration in this phase, with a clear reduction in their velocity peaks and decreased cardiac output.[114] The most recent observation in this respect in probably the reduction in the values of the so-called “ventricular ejection force” (VEF).[115]

It has been demonstrated that the VEF values of both the right and the left ventricles are similar and increase throughout gestation in fetuses with normal growth. In contrast, there is a significant decrease in both ventricles, below the 5th centile of the normality curves, in the terminal phase of the centralization of blood flow.[115] Furthermore, there is an excellent correlation between the VEF values and the severity of the acidosis registered by funiculocentesis. It can therefore be stated that this hemodynamic finding is significantly related to a serious fetal compromise.

The visualization of the coronary blood flow, in the context of a severe uteroplacental insuffi-ciency, must be interpreted as a very serious sign of fetal distresss, probably *pre mortem*. The phenomenon is particularly visible in the dias-tole.[116]

The coronary vasodilatation which makes it possible can be the result of three different types of mechanism: a) an attempt at compensation provoked by low myocardial oxygen pressure; b) loss of myocardial contraction force, which causes a reduction in the pressure on the coronary arteries (especially during the diastole), and c) decrease in the velocity of the intracardial blood flows, with the same results as in b).

The first autoregulating mechanism described could be called a heart-sparring effect, and this has been studied in detail.[108]

In the initial phase of centralization, the cardiotocographic readings can still apparently be normal and Manning's biophysical profile proves to be unaltered or boubtful.

The biophysical parameters affected most early or are in correlation with behavior. Changes in the cyclical periods of rest/activity[117] and a decrease in multiple rolling movements (Fig. 18.9).

Although there is an increase in the pathological results of the biophysical stress tests with respect to the previous stage, we have not been

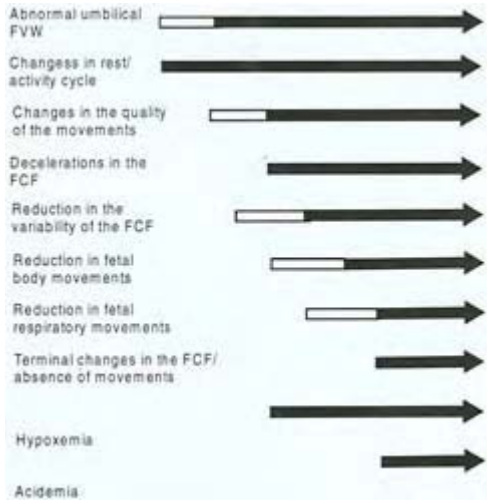

Figure 18.9: Chronological correlation (represented by the different lengths of the arrows) of the biophysical signs of fetal deterioration. The open parts of the arrows represent the silent phase whilst the hatched parts represent the detection phase. FVW, flow velocity waveforms; FCF, fetal cardiac frequency

able to establish whether their comparative percentages are significantly different statistically.

However, in the advanced phase there is a progressive deterioration in the fetal cardiac frequency register and late decelerations appear. The time lapse from the pathological quality of the umbilical PI until the appearance of late decelerations in the register has been evaluated as between 9 and 60 days,[118,119] with a mean of 2–3 weeks.[120–122] Echographically, on the other hand, there is an evident decrease in fetal movements (somatic and respiratory) and in fetal tone. There can be a marked decrease in amniotic

fluid; Phelan and co-workers[123] obtained indices of between 5 and 8. If all these data are marked in accordance with Manning the biophysical profile usually attains a score of under 7. In the phase the number of positive oxytocin tests is already clearly significant, as are the force tests and the vibroacoustic stimulation. We are then confronted with the decompensation of a chronic fetal distress which, until then, could be considered as compensated.

Finally, in the late phase, and owing to the loss of cardiac automatism, not only do apparent late decelerations appear in the cardiotocographic reading, but there is also noticeable loss of reactivity.[124] The ominous readings do not appear until 2–3 weeks after the minimum values of the cerebral PI have been attained. In fact, this interval depends on the ability of the fetus to compensate for the reduction in the metabolic supply.[81,125,126]

The biophysical profile shows very low values, always under 5, owing to the alteration of all its parameters (severe decrease to the alteration of all its parameters (severe decrease in fetal movements and tone, etc.) and an increasingly significant oligohydramnios.

Biochemical Correlation

When the velocimetric values are altered not only in the umbilical artery, but also in the remaining fetal vessels (aorta, common carotid and middle cerebral arteries), there is a risk of low po2 an pH values in the fetal blood obtained by cordocentesis.[105,117,127,128] In fact, centralization gets under way only when the fetus is already suffering from a degree of hypoxemia and acidosis.

In the initial phase, with end-diastolic frequencies still present in both the umbilical artery and the aorta, the percentage of cases with hypoxemia does not generally exceed 25–30%.

The situation changes dramatically in the advanced phase, when the end-diastolic values of the Doppler frequency in those two vessels disappear: in the case 70–80% of the fetuses present hypoxemia, and 40–60% present acidosis.[104,105,128,129] The majority of authors[130–132] consider that the absence of end-diastolic flow signifies pathological results in the acid-base study of the fetal blood.[133]

Finally, in the terminal phase, practically all the fetuses have a po_2 of between 2 and 4 SD below the mean.[134]

Obstetric and Neonatal Outcome

A high number of deaths in fetuses (250 per 1000) and neonates are concentrated in this group, and there is a significant increase in neonates with pH under 7.20 (83.3%). A cesarean section was performed in all our cases. Furthermore, the surviving fetuses present a high number of complications (e.g. necrozating enterocolitis and hemorrhages), which are attributable to the persistent vasoconstriction of specific organs.[135]

Various authors[83,84,136] have observed that the absence of end-diastolic values in the aorta accurately predicts neonatal morbidity.

Arduini and co-workers[137] have designed a test that determines whether fetuses will have a specially bad prognosis if they are not immediatly extracted. The administer oxygen humidified at 60% to the mother, and carry out a fetal hemodynamic study using

Doppler before, just after 20 min after therapy. If the PI values are not substantially modified, the fetuses will suffer a rapid deterioration.

Decentralization of Blood Flow

Decentralization of blood flow is represented by irreversible hemodynamic changes that follow on from the centralization of blood flow and which precede fetal death.

Pathophysiological Basis

If the hypoxia persists, a phenomenon of generalized fetal vascular paralysis will ultimately occur.

We can probably hypothesize that the situation is similar to those described in the fetuses of monkeys[138] and sheep[139] subjected to severe and sustained hypoxemia. The appearance of cerebral edema and the resulting increase in intracranial pressure hinder the mechanism for cerebral blood perfusion. The cerebral edema is probably brought about by the local accumulation of lactic acid resulting from the sustained anaerobic metabolism, which alters the permeability of the cellular membrane, increases the osmotic intracellular pressure and ultimately leads to the edema and eventual tissue necrosis.

The result of all this is that, in addition to the hypoxemia of the cerebral centers, there is a progressively irreversible interference in the control mechanism of the arterial tone. This situation usually occurs when the hypoxemia is extreme: more than 4 SD below the mean.[134,140,141]

Doppler Hemodynamic Profile

The diagnosis of decentralization of blood flow essentially rests on two findings:

1. Confirmation of resistance in the umbilical and peripheral circulation (aorta, renal…) with the presence of reserve end diastolic flow; and
2. Increase, after a brief period of stabilization, in the PI in the intracranial arteries, the values of which can appear normal; there are even FVW without diastoles or with reverse flow.[142]

It is not known how much time can pass from the onset of this picture until *in utero* fetal death, but it is probably no more than 2–3 days, and in many cases only a few hours; this explains the remote possibility of observing in through Doppler.

Biophysical Correlation

If a cardiotocographic examination is carried out at this point, it is certain that a terminal pattern will be observed, indicating the so-called “intrauterine brain death syndrome”.[143–148] The readings invariably show a fixed fetal cardiac frequency, with no variability from one heartbeat to another and a complete absence of accelerations or decelerations, even when contractions are induced by an oxytocin test or an EVA is performed. The biophysical profile, on the other hand, will show an immobile atonic fetus, drawn in on

itself and with hardly any amniotic fluid, although some authors[147–149] have described some cases with hydramnios. The score will not exceed 2 points.

Only on very rare occasions will it be possible by echography to confirm the existence of cystic periventricular cerebral lesions (porencephaly) or evident ventriculomegaly,[148,150,151] the consequence of the hypoxic necrosis.[143,150,152]

Figure 18.10 presents the probable sequence of the pathophysiological mechanisms and biophysical signals, which can be observed through exploration, in a case of IUGR through uteroplacental vascular insufficiency.

Biochemical Correlation

As has already been mentioned above, that a funiculocentis will confirm extreme hypoxemia (values of PO_2–4 SD below the mean and a significant acidosis.

Obstetrical Outcome

This is a situation that results in either fetal or neonatal death, especially if an emergency extraction is carried out. A cesarean section is therefore generally considered unnecessary.[148]

OBSTETRIC MANAGEMENT OF IUGR IN ACCORDANCE WITH THE INFORMATION PROVIDED BY DOPPLER STUDY

The traditional thinking is that pregnancy must be terminated "when possibilities of life for the fetus are less than those which it would have to be converted into a newborn", a concept that is sometimes difficult to establish in practice. The decision as to timing and the method of delivery should be taken with the following borne in mind: 1) The objective data concerning fetal well-being (type of IUGR, absence or presence of congenital malformations, onset of centralization of blood flow, etc.); 2) The degree of fetal lung maturity, and 3) The clinical features of each case (parity underlying diseases, etc.).[153]

Nowadays and thanks to the haemodynamic fetal-placental study provided by Doppler it is possible to establish the following protocol:

IUGR without Hemodynamic Redistribution

Excluding the infectious and chromosomal causes, perinatal results are good. It is required a Doppler control (AU and ACM) echographical and TNS every 1–2 weeks.

IUGR with Hemodynamic Redistribution > 34 Weeks

The increasing evidence of a worse perinatal result in the IUGR group with hemodynamic redistribution does not make justifiable to prolong the gestation more than 34 weeks.

IUGR with Hemodynamic Redistribution Between 32 and 34 Weeks

The presence of a desacelerative TNS pattern, decreased variability (<5 beat/minute), the presence of a diastolic flow absent or reverse in AU and also the alteration of venous flows are criterions for finalising the gestation.

If it is decided to adopt an expectant conduct it is advisable the derivation to a centre with Intensive Neonatal Care Unit and the weekly monitarization of fetal well-being.

IUGR with Hemodynamic Redistribution Between 28 and 32 Weeks

The presence of a desacelerative or silent TNS pattern, the presence of a diastolic flow reverse

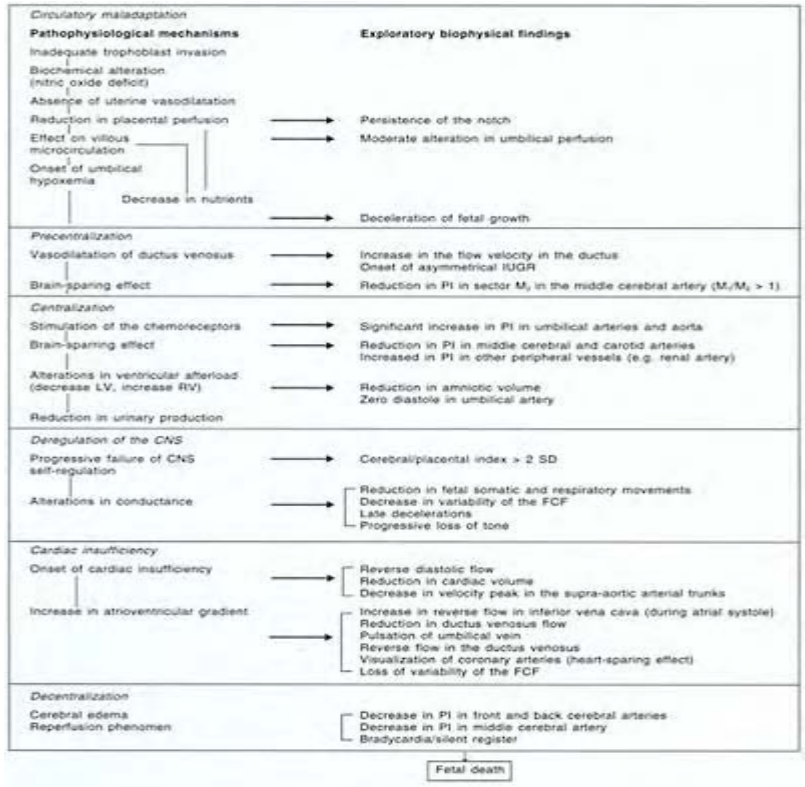

Figure 18.10: Sequence of the pathophysiological mechanisms and biophysical signals. IUGR—intrauterine growth retardation, PI—pulsatility index, LV—left ventricle, RV—right ventricle, CNS—central

nervous system, FCF—fetal cardiac frequency.

in AU and the severe alteration of venous flows are criterions for finalising the gestation.

If it is decided to adopt an expectant conduct it is advisable the derivation to a centre with Intensive Neonatal Care Unit and the monitarization of fetal well-being every 3–4 days.

IUGR with Hemodynamic Redistribution Under 28 Weeks

In this subgroup each case must be evaluated multidisciplinaryly by an Obstetrician with good knowledge about Doppler and by a Neonatologist, but taking into account the opinion of parents.

Only the presence of very altered venous flows or the presence of a desacelerative TNS pattern seem to be justifiable criterions for finalising the gestation.

In those cases in that the grade of fetal compromise is very severe it is possible to agree on an expectant conduct with parents.

REFERENCES

1. Carrera JM. Fetal growth characteristics. In: Kurjak A (Ed). Textbook of Perinatal Medicine. London: The Parthenon Publish, 1998; 2:1129–31
2. Carrera JM. Crecimiento Intrauterino retardado: concepto y frecuencia. En: J.M. Carrera y col., eds-Crecimiento fetal normal y patológico. Barcelona: Editorial Masson 1997; 219–22
3. Spinillo A, Capuzzo E, Piazzi G, Baltaro F, Stranati M, Ornetto A. Significance of low birth weight for gestational age among very preterm infants. Br J Obstet Gynaecol 1997; 104:668–73.
4. Leviton A, Gilles F. Ventriculomegaly, delayed myelination, white matter hypoplasia, and periventricular leukomalacia: how are they related? Pediatr Neurol 1996; 15:127–36
5. Barker DJP The fetal origins of coronary heart disease. Acta Pediatr 1997; Suppl 442:73–7
6. Carrera JM. Definitions, etiology and clinical implications. In: Carrera JM, Mandruzzato GP, Maeda K (Eds). Ultrasound and Fetal Growth. London: The Parthenon Publish, 1999; 17–34
7. Campbell S, Dewhurst CJ. Diagnosis of the small-for-dates fetus by serial ultrasonic cephalometry. Lancet 1971; 2:1002–15
8. Campbell S, Thoms A. Ultrasound measurement of the fetal head to abdomen circumference ratio in the assessment of growth retardation. Br J Obstet Gynaecol 1977; 84:165–79
9. Levi S, Flamme P. Relation entre divers paramètres foeto-maternels et le diamètre biparíétal mesuré par les ultrasons. Fonds National de la Recherche Scient. Med. Group de Perinatologie, Bruxelles 1970; 324 25.
10. Levi S, Maamari R. Ecographic diagnosis of PIFG. In: Salvador! B, Bacchi-Modena A (Eds). Poor Intrauterine Fetal Growth 1977; 251–5 4 (Parm a, Ita Minerva Médica).
11. Warsof SL, Cooper DJ, Little D, Campbell S. Routine ultrasound screening for antenatal detection of intrauterine growth retardation. Obstet Gynecol 1986; 67:33–39.
12. Clark SL. Patterns of intrauterine growth retardation. Clin Obstet Gynecol 1992; 35:194–201
13. Carrera JM. Intrauterine Growth Retardation. Abstracts of VIII World Congress of Gynecology and Obstetrics (FIGO). Mexico, DF, October 17–22, 1976
14. Carrera JM, Barri PN. Diagnosis of the intrauterine growth retardation. In: Salvador! B, Bacchi-Modena A (Eds). Poor Intrauterine Fetal Growth, 1977; Parma, Italy: Minerva Médica; 277–81.

15. Carrera JM. Concepto, selección y clasificación de los recién nacidos pequeños por retardo de crecimiento intrauterino. Prog Obstet Ginecol 1978; 21:197–208.
16. Carrera JM, Mallafré J. Tratamiento “in utero” el retardo de crecimiento fetal. In: Esteban Altirriba J, Perinatología Clínica 3, 1980 (Barcelona: Salvat Editores, S.A.E.).
17. Carrera, JM. Regulation del crecimiento fetal. In: Carrera JM, Biología Y Ecología Fetal 1981; 217 (Barcelona: Salvat Editores, S.A.E.).
18. Carrera JM. Clasificación del crecimiento intrauterino retardado. Tesis doctoral, Santiago de Compostela, 1981.
19. Carrera JM. *Ecografía Obstétrica*, 2nd edition, 1985, Barcelona: Salvat Editores, S.A.E.
20. Weiner CP, Williamson RA. Evaluation of severe retardation using cordocentesis-hematologic and metabolic alterations by etiology. Obstet Gynecol 1989; 73:225–29
21. Lockwood CJ, Weiner S. Assessment of fetal growth. Clin Perinatol 1986; 13:3–35.
22. Mintz M, Landon M. Sonographic diagnosis of fetal growth disorders. Clin Obstet Gynecol 1988; 31:44–52.
23. Carrera JM, Devesa R, Serra B. Classification of intrauterine growth restriction. In: Kurjak A (Ed). Textbook of Perinatal Medicine. London. The Parthenon Publish 1998;1192–1200.
24. Brar HS, Rutherford SE. Classification of intrauterine growth retardation. Semin Perinatol 1988; 12:2–10.
25. Carrera JM, Kaeda K, Comas C, Torrents M. Diagnosis of intrauterine growth restriction. In: Carrera JM, Mandruzzatoand GP Maeda K (Eds). Ultrasound and Fetal Growth. London. Parthenon Publish, 35–70.
26. Theron GB, Pattinsor RC. Management of patients with poor symphysis pubis-fundus growth by Doppler flow velocimetry of the umbilical artery—An effective method to detect the fetus at risk. Int J Gynecol Obstet 1992; 39:93–98
27. Pearce JM, Campbell S. A comparison of symphys-fundal height and ultrasound as screening test for high for gestational age infants. Br J Obstet Gynaecol 1987; 94:100–04
28. Goldstein I, Reece EA, Pilu G, Bovicelli L, Hobbins JC. Cerebellar measurements with ultrasonography in the evaluation of fetal growth and development. Am J Obstet Gynecol 1987; 156:1065–69.
29. Reece EA, Godstein I, Pilu G, Hobbins JC. Fetal cerebellar growth unaffected by intrauterine growth retardation: A new parameter for prenatal diagnosis. Am J Obstet Gynecol 1987; 157:632–38.
30. Reece EA, Hagay Z. Prenatal diagnosis of desviant fetal growth. In: Reece AE, Hobbins JC, Mahoney MJ, Petrie RH (Eds). Medicine of the Fetus and Mother. Filadelfia: Lippincott (Co), 1992; 671–85
31. Duchatel F, Mennesson B, Berseneff H, Oury JF. Antenatal echographic measurement of the fetal cerebellum. Significance in the evaluation of fetal development. J Gynecol Obstet Biol Reprod Paris 1989; 18:879–83
32. Campbell WA, Narci D, Vintzileos AM, Rodis JF, Turner CW, Egan JF. Transverse cerebellar diameter/ abdominal circumference ratio through-out preg-nancy: A gestational age independent method to assess fetal growth. Obstet Gynecol 1991; 77:893–96
33. Drumm JE, Clinch J, Mac Kenzie G. The ultrasonic measurement of fetal crown-rump length as a method of assessing gestational age. Br J Obstet Gynaecol 1976; 83:417–21
34. Shepard M, Filly RA. A standardized plane for biparietal diameter measurement. J Ultrasound Med 1982; 1:145–54.
35. Johnson ML, Dunne MG, Mack LA, Rashbaum CL. Evaluation of fetal intracranial anatomy by static and real-time ultrasound. J Clin Ultrasound 1980; 8:311–18.
36. Campbell S. Ultrasonic fetal cephalometry during the second trimester of pregnancy. J Obstet Gynaecol Br Commonw 1970; 77:1057–63
37. Varma YR. Prediction of delivery date by ultrasound cephalometry. Br J Obst et Gynae col 1973; 80:31

38. Campbell S, Newman GB. Growth of the fetal biparietal diameter during normal pregnancy. J Obstet Gynaecol Br Commonw 1971; 78:513–19
39. Seeds JW. Impaired fetal growth: Ultrasonic evalua-tion and clinical management. Obstet Gynecol 1984; 63:577–82.
40. Carrera JM, Mallafre J. Intrauterine Growth Retardation. In: Kurjak A, Chervenak F (Eds). Fetus. as a Patient. The Parthenon Publish. London, 1994; 251–87.
41. Rosendahl H, Kivinen S. Routine ultrasound screen-ing for early detection of small for gestational age fetuses. Obstet Gynecol 1988; 71:518–21
42. Arias F. The diagnosis and management of intra-uterine growth retardation. Obstet Gynecol 1977; 49 293–98.
43. Kurjak A, Kirkinen P, Latin V. Biometric and dynamic ultrasound assessment of small-for-dates infants. Report of 260 cases. Obstet Gynecol 1980; 56:281–84
44. Geirsson RT, Patel NB, Christie AD. Intrauterine volume, fetal abdominal area and biparietal diameter measurements with ultrasound in the prediction of small-for-dates babies in a high-risk obstetric population. Br J Obstet Gynaecol 1985; 92:936–40
45. Sabbagha R, Hughey M, Depp R. Growth adjusted sonographic age. A simplified method. Obstet Gynecol 1978; 51:383–86
46. Di Renzo GC, Luzi G, Clerici G, Carrera JM. Antenatal diagnosis of Intrauterine Growth Retardation. In: Kurjak A (Ed). Textbook of Perinatal Medicine. The Parthenon Publish, London 1998; 1201–11.
47. Macler J, Rosenthal C, Burgun P, Rena ud R. interest of ecotography measurements of the trans-versal abdominal diameter in the poor intrauterine fetal growth. In: Salvadori B, Bacchi-Modena A (Eds). Poor Intrauterine Fetal Growth. Parma: Minerva Médica, 1977.
48. Zoltan I. Poor intrauterine fetal growth: Constitutional factors/weight and size. In: Salvadori B, Bacchi-Modena A (Eds). Poor Intrauterine Fetal Growth. Parma: Minerva Médica, 1977; 51–55
49. Campbell S, Wilkin D. Ultrasonic measurement of fetal abdomen circumference in the estimation of fetal weight. Br J Obstet Gynaecol 1975; 82(9):689–97
50. Campbell S, Soothill P Detection and management of intrauterine growth retardation. A British approach. In: Chevernack FA, Isaacson J, Campbell S (Eds). Ultrasound in Obstetrics and Gynecology. London: Little Brown, 1993; 1431
51. Jeanty P, Coussaert E, contraine F. Normal growth of the abdominal perimeter. Am J Perinatol 1984; 1:129–35.
52. Wittmann BK, Robinson HP, Aitchis on T, Flem ing The value of diagnostic ultrasound as a screening test for intrauterine growth retardation: Comparison of nine parameters. Am J Obstet Gynecol 1979; 134:30–35.
53. Carrera JM, Alegre M, Torrents M. Ecobiometría anatómica fetal. In: Carrera JM (Ed). Ecografía Obstétrica. Barcelona: Salvat, 1985; 259–86
54. Warsof SL, Cooper DJ, Little D, Campbell S. Routine ultrasound screening for antenatal detection of intrauterine growth retardation. Obstet Gynecol 1986; 67:33–39.
55. Warsof SL, Wolf P, Coulehan J, Queenan JT. Comparison of fetal weight estimation formulas with and without head measurements. Obstet Gynecol 1986; 67(4):569–73
56. Campbell S, Thoms A. Ultrasound measurement of the fetal head to abdomen circumference ratio in the assessment of growth retardation. Br J Obstet Gynaecol 1977; 84(3):165–74
57. O'Brien GD, Queenan JT. Growth of the ultrasound fetal femur length during normal pregnancy. Am J Obstet Gynecol 1981; 141:833–37.
58. O'Brien GD, Queenan JT. Ultrasound femur length in relation to intrauterine growth retardation. Am J Obstet Gynecol 1982; 144:35–39.
59. Hadlock FP, Deter RL, Harrist RB, Roecker E, Park SK. A date independent predictor of intrauterine growth retardation: Femur length/abdominal circum-ference ratio. AJR Am J Roentgenol 1983; 141:979–84.
60. Benson CB, Doubilet PM, Saltzman DH, Jones TB. FL/AC ratio: Poor predictor of intrauterine growth retardation. Invest Radiol 1985; 20:727–30

61. Japanese Society of Obstetrics and Gynecology, Standard ultrasonic values of biparietal diameter and femur length of Japanese fetuses. Acta Obstet Gynecol Jpn 1993; 45:391–94
62. Gohari P, Berkowitz RL, Hobbins JC. In utero prediction of IUGR by determination of total intrauterine volume. Am J Obstet Gynecol 1977; 127(1):255–58.
63. Hata T, Deter RL. A review of fetal organs measurements obtained with ultrasound: Normal growth. J Clin Ultrasound 1992; 20(3):155–7
64. Kramer MS, Mc Lean FH, Olivier M, Willis DM, Usher RH. Body proportionality and head to length "sparing" in the growth-retarded neonates: A critical reappraisal. Pediatrics 1989; 84:717–23
65. Kramer MS, Olivier M, Mc Lean FH, Willis DM, Usher RH. Impact of intrauterine growth retardation and body proportionality on fetal neonatal outcome. Pediatrics 1990; 86:707–13
66. David C, Gabriell S, Pilu G, Bovicelli L. The head-to-abdomen circumference ratio: A reappraisal. Ultrasound Obstet Gynecol 1995; 5(5):256–59
67. Kurjak A, Breyer B. Estimation of fetal weight by ultrasonic abdominometry. Am J Obstet Gynecol 1977; 125(7):962–65
68. Sumners JE, Findley GM, Ferguson KA. Evaluation methods for intrauterine growth using neonatal fat stores instead of birth weight as outcome measures: Fetal and neonatal measurements correlated with neonatal skinfold thicknesses. JCU J Clin Ultrasound 1990;18(1):9–14.
69. Balouet P Estimation du poids foetal. Med Foetal Echogr Gynecol 1994; 17:10–17
70. Leroy B, Ngo C. Evaluation échographique du diamètre des membres fœtaux. Soirées Echogr Gynéco-Obstet 1979; 15:4–8.
71. Warda A, Deter RL, Duncan G, Hadlock FP Evaluation of fetal thigh circumference measurements: A comparative ultrasound and anatomical study. JCU J Clin Ultrasound 1986; 14(2):99–103
72. Balouet P, Speckel D, Herlicoviez M. Estimation échographique du poids fœtal: Intérêt de la mesure de la graisse des membres. J Gynecol Obstet Biol Reprod 1992; 21(7):795–802
73. Carrera JM, Devesa R, Torrents M, Muñoz A, Comas C, Nortera C, Serra B. Natural History of fetal compromise in intrauterine growth retardation. In: Kurjak A (Ed): Textbook of Perinatal Medicine (Vol 2). London, Parthenon Publish, 1226–43
74. Rudolph AM, Heymann MA. The circulation of the fetus "in utero". Methods for studying distribution of blood flow, cardiac output and organ blood flow. Circ Res 1967; 21:163–67
75. Johnson GN, Palahniuk RJ, Tweed WA, Jones MV, Wade JG. Regional cerebral blood flow changes during fetal asphyxia produced by slow partial umbilical cord compression. Am J Obstet Gynecol 1979; 135:48–52
76. Behrman RE, Lees MH, Peterson EN, De Lannoy CW, Seeds AE. Distribution of the circulation in the normal and asphyxiated fetal primate. Am J Obstet Gynecol 1970; 108:956–69
77. Morrow RJ, Adamson SL, Bull SB, Ritchie JWK. Ante hypoxemia does not effect umbilical artery wave-forms in sheep. Obstet Gynecol 1990; 75:590–93.
78. Morrow RJ, Adamson SL, Bull SB, Ritchie JWK. Hypoxia acidaemia, hyperviscosity and maternal hypertension do not affect the umbilical artery velocity waveforms in fetal sheep. Am J Obstet Gynecol 1990; 163:1313–20
79. Hecher K, Bilardo CM, Stigter RH et al. Monitoring of fetuses with IUGR: a longitudinal study. Ultrasound Obstet Gynecol 2001; 18:564–70.
80. Carrera JM, Torrents M, Muñoz A, Figueras F, Comas C. The role of Doppler in prenatal diagnosis. Ultrasound Rev Obstet Gynecol 2002; 2:240–50
81. Trudinger BJ. Doppler ultrasound study and fetal abnormality. In: Drife JO, Donnan D (Eds). Antenatal Diagnosis of Fetal Abnormalities. London: Springer-Verlag, 1991; 113
82. Gruenwald P. The relation of deprivation to perinatal pathology and late sequels. In: Gruenwald P (Ed). The Placenta. Lancaster Gr: Med. Tech. Publish. Co., 1975.
83. Laurin J, Marsal K, Persson PH, Lingman G. Ultrasound measurement of fetal blood in predicting fetal outcome. Br J Obstet Gynaecol 1987; 94:940–48.

84. Laurin J, Lingman G, Marsal K, Persson PH. Fetal blood flow in pregnancies complicated by intrauterine growth retardation. Obstet Gynecol 1987; 69:895–902.
85. Guidetti R, Luzi G, Simonazzi E, Tini M, Chicodi A, Di Renzo GC, Cosmi E. Correlation between cerebral blood flow and umbilical blood flow in the fetus recorded with a pulsed Doppler system. Abstract Book of the XI European congress of Perinatal Medicine. Roma: CIC, 1988; 252
86. Baschat AA, Weiner CP. Umbilical artery Doppler screening for detection of the small fetus in need of antepartum surveillance. Am J Obst Gynecol 2000; 182:154–58.
87. Severi FM, Bocchi C, Viscuti A et al. Uterine and fetal cerebral Doppler predict the outcome of third trimester samll-for-gestational age fetuses with normal umbilical artery Doppler. Ultrasound Obstet Gynecol 2002; 19:225–28
88. Hershkowitz R, Kingdom JC, Geary M, Rodeck CH. Fetal cerebral. Blood flow distribution in late gestations: identification of compromise in samll fetuses with normal umbilical artery Doppler. Ultrasound Obstet Gynecol 2000; 15:209–12.
89. Mc Cowan LM, Harding JE, Roberts AB et al. A pilot randomized controlled trial of two regiments of fetal surveillance for small-for-gestational-age fetuses with normal results of umbilical artery Doppler velocimetry. Am J Obstet Gynecol 2000;182:81–86.
90. Arduini D, Valentise H. Fetal hemodynamics in growth retardation. In: Kurjak A (Ed). Textbook of Perinatal Medicine. The Parthenon Publish, London 1998; 1217–25
91. Laurini R, Laurin J, Marsal K. Placental histology and fetal blood in intrauterine retardation. Acta Obst Gynecol Scand 1994; 73:529–34
92. Morrow RJ, Adamson SL, Ritchie JWK, Pearce JM. The pathophysiological basis of abnormal flow velocity waveforms. In: Pearce JM (Ed). Doppler Ultrasound in Perinatal Medicine. Oxford: Oxford University Press, 1992.
93. De Haan J. Fisiopatología de los cambios de los indices de flujo Doppler en la circulatión fetal. In: Carrera JM (Ed). Doppler en Obstetricia. Barcelona: Masson-Salvat, 1992; 89–97
94. Giorlandino G, Vizzone A. Flussimetria ostetrica materna e fetale. Testo Atlante. Roma: CIC Edizione Inter, 1993.
95. Dawes GS, Duncan SL, Lewis BV, Merlet CL, Owen-Thomas TB, Reeves JT. Cyanide stimulation of the systemic arterial chemoreceptors in foetal lambs. J Physiol 1969; 201:117–28
96. De Vore GR. Examination of the fetal heart in the fetus with intrauterine growth retardation using M-mode echocardiography. Semin Perinatol 1988; 12: 66–79.
97. Lingman G, Legarth J, Rahman F, Stangenberg M. Myocardial contractility in the anemia human fetus. Ultrasound Obstet Gynecol 1991; 1:266–68.
98. Marsal K, Lingman G, Giles W. Evaluation of the carotid, aortic and umbilical blood velocity waveforms in the human fetus. XI Annual Conference of the Society for the Study of Fetal Physiology; Oxford. Oxford: The Nuffield Institute, 1984; C33
99. Marsal K, Lindblad A, Lingman G, Eik-Nes SH. Blood flow in the fetal descending aorta: intrinsic factors affecting fetal blood flow i.e. fetal breathing movements and fetal cardiac arrhythmia. Ultrasound Med Biol 1984; 10:339–48.
100. Wladimiroff JW, Tonge HM, Stewart PA. Doppler ultrasound assessment of cerebral blood flow in the human fetus. Br J Obstet Gynaecol 1986; 93:471–75
101. Arabin B, Bergmann PL, Saling E. Simultaneous assessment of blood flow velocity waveforms in uteroplacental vessels, the umbilical artery, the fetal aorta and the common carotid artery. Fetal Ther 1987; 2:17–26
102. Arabin B, Siebert M, Jimenez E, Saling E. Obstetrical characteristic of a loss of end-diastolic velocities in the fetal aorta and/or umbilical artery using Doppler ultrasound. Gynecol Obstet Invest 1987; 25:173–80
103. Bilardo CM, Campbell S, Nicolaides KH. Mean blood velocity and flow impedance in the fetal descending thoracic aorta and common carotid artery in normal pregnancy. Early Hum Dev 1988; 18:213–17

104. Montenegro CA. Perfil hemodinámico fetal-Diástole-Zero “revisitada”. J Brasileiro Ginecol 1992; 102(10): 375–80.
105. Montenegro CA, Meirelles J, Fonseca AL, Netto MC, Amin Junior J, Rezende-Filho J, Jacyntho C. Cordocentèse et evaluation du bien-être foetal dans une population à très haut risque. Rev Franç Gynecol Obstet 1992; 87:467–77
106. Gramellini P, Folli MC, Raboni S, Vadora E, Merialdi A. Cerebral-umbilical Doppler ratio as a predictor of adverse perinatal outcome. Obstet Gynecol 1992; 79: 416–20.
107. Ferrazi E, Bellotti m, Galan H, Pennati G, Bozzo M, Rigano S, Battaglia FC. Doppler investigation in intrauterine growth restriction—from qualitative indices to flow measurements: a review of the experience of a collaborative group. Ann NY Acad Sci 2001; 943:316–25
108. Gembruch U, Baschat AA. Demonstration of fetal coronary blood flow by color-coded and pulsed wave Doppler sonography: a posible indicator of severe compromise and impending demise in intrauterine growth retardation. Ultrasound Obstet Gynecol 1996; 7:10–16
109. Rigano S, Bozzo M, Ferrazi E, Belloti M, Battaglia FC, Galan HL. Early and persistent reduction in umbilical vein blood flow in the growth restricted fetus: a longitudinal study. Am J Obstet Gynecol 2001; 185:834–38
110. Indik JH, Chen V, Reed KL. Association of umbilical venous with inferior vena cava blood flow velocities. Obstet Gynecol 1991; 77:551–57
111. Reed KL. Venous flow velocities in the fetus. In: Jaffe R, Warson SL (Eds). Color Doppler imaging in obstetrics and gynecology. New York: McGraw-Hill, 1992; 179
112. Rizzo G, Arduini D, Romanini C. Inferior flow velocity waveforms in appropriate and small-for-gestational-age fetuses. Am J Obstet Gynecol 1992; 166:1271–80
113. Antolin E, Carrera JM. Ductus venosus in IUGR. Perinatal outcome. In: Carrera JM, Cabero L, Baraibar R (Eds). The Perinatal Medicine of the New Milunnium. Bolonia. Monduzzi, 2001;691–99.
114. Rizzo G, Arduini D. Fetal cardiac function in intra-uterine growth retardation. Am J Obstet Gynecol 1991; 165:876–82
115. Rizzo G, Capponi A, Rinaldo D, Arduini D, Romanini C. Ventricular ejection force in growth retarded fetuses. Ultrasound Obstet Gynecol 1995; 5:247–55
116. Baschat AA, Gembruch U, Gortner L, Reiss I, Weiner CP, Harman CR. Coronary artery blood flow visualization signifies hemodynamic deterioration in growth-restricted fetuses. Ultrasound Obstet Gynecol 2000; 16:425–31
117. Arduini D, Rizzo G, Romanini C, Mancuso S. Are blood flow velocity waveforms related to umbilical cord acid-base status in the human fetus? Gynecol Obstet Invest 1989; 27:183–87
118. Reuwer PJ, Sijmons EA, Rietman GW, Van Tiel MN, Bruinse HW. Intrauterine growth retardation: prediction of perinatal distress by Doppler ultrasound. Lancet 1987; 2:415–18
119. Bekedam DJ, Visser GH, Van Der Zee AG, Snijders RJ, Poelmann Weesjes G. Abnormal velocity waveforms of the umbilical artery in growth retarded fetuses: relationship to antepartum late heart rate decelerations and outcome. Early Hum Dev 1990; 24:79–89
120. Arduini D, Rizzo G, Romanini C. Changes of Pulsatility Index from fetal vessels preceding the outset of late decelerations in growth retarded fetuses. Obstet Gynecol 1992; 79:605–10
121. Arduini D, Rizzo G. Color Doppler studies of fetal circulation in intrauterine growth retardation. In: Jaffe R, Warson SL (Eds). Color Doppler imaging in obstetrics and gynaecology. New York: McGraw-Hill, 1992; 183
122. Griffin DR, Bilardo K, Diaz-Recasens J, Pearce JM, Wilson K, Campbell S. Doppler blood flow waveforms in the descending thoracic aorta of the human fetus. Br J Obstet Gynaecol 1984; 91:997–1002
123. Phelan JP, Smith CV, Bronssard P, Small M. Amniotic fluid volume assessment with the four-quadrant technique at 36–42 weeks of gestation. J Reprod Med 1987; 32:540–42
124. Niijhuis IJ, Hof J, Mulder EJ, Nijhuis JG et al. Fetal hear rate in relation to its variation in normal and growth retarded fetuses. Eur J Obstet Gynecol Reprod Biol 2000; 89:27–33

125. Manning FA, Harman CR, Menticoglon S, Dayal A, Xic J. Mental retardation: prevalence and etiological factors in a large obstetric population. Am J Obstet Gynecol 2000; 182:S110
126. Baschat AA. Integrated fetal testing in growth restriction: combining multivessel Doppler and biophysical parameters. Ultrasound Obstet Gynecol 2003; 21:1–8
127. Nicolaides KH, Bilardo CM, Soothill PW, Campbell S. Absence of end-diastolic frequencies in the umbilical artery: A sign of fetal hypoxia and acidosis. Br Med J 1988; 297:1026–27.
128. Nicolaides KH, Bilardo CM, Campbell S. Prediction of fetal anaemia by measurement of mean blood velocity in the fetal aorta. Am J Obstet Gynecol 1990; 162:209–12.
129. Hsieh FJ, Chang FM, Ko TM, Chen HY, Chen YP. Umbilical artery flow velocity waveforms in fetuses dying with congenital anomalies. Br J Obstet Gynaecol 1988; 95:478–82
130. Ferrazzi E, Pardi G, Bauscaglia M, Marconi AM, Gementi B, Bellotti M, Makowski EL, Battaglia FC. The correlation of biochemical monitoring versus umbilical flow velocity measurements of the human fetus. Am J Obstet Gynecol 1988; 159:1081–87
131. Tyrrell S, Obais AH, Lilford RJ. Umbilical artery Doppler velocimetry as a predictor of fetal hypoxia and acidosis at birth. Obstet Gynecol 1989; 74:332–37
132. Bilardo CM, Nicolaides KH, Campbell S. Doppler measurement of fetal and uteroplacental circulation: relationship with umbilical venous blood gases measured at cordocentesis. Am J Obstet Gynecol 1990; 162:115–19
133. Ferrazi E, Bozzo M, Rigano S, Belloti M, Morabito A, Pardi G, Battaglia FC, Galan HL. Temporal sequence of abnormal Doppler changes in the peripheral and central circulation systems of the severely growth-restricted fetus. Ultrasound Obstet Gynecol 2002; 19:140–46.
134. Vyas S, Nicolaides KH, Bower S, Campbell S. Middle cerebral artery flow velocity waveforms in fetal hypoxemia. Br J Obstet Gynaecol 1990; 97:797–803
135. Manning FA, Harman CR, Menticoglou S, Morrison J. Assessment of fetal well-being with ultrasound. Obstet Gynecol Clin North Am 1991; 18:891–905
136. Hackett GA, Campbell S, Gamsu H, Cohen-Overbeek T, Pearce JM. Doppler studies in the growth retarded fetus and prediction of neonatal necrotising enterocolitis haemorrhage and neonatal morbidity. Br Med J 1987; 294:13–16
137. Arduini D, Rizzo G, Romanini C, Mancuso S. Haemodynamic changes in growth retarded fetuses during materna oxygen administration as predictors of fetal outcome. J Ultrasound Med 1989; 8:193–96.
138. Myers RE, De Courtney-Myers GM, Wagner KR. Effects of hypoxia on fetal brain. In: Beard RW, Nathanielsz PW (Eds). Fetal physiology and medicine. London: Butterworth, 1984:419.
139. Richardson BS, Rurak D, Patrick IE, Homan J, Carmichael I. Cerebral oxidative metabolism during sustained hypoxaemia in fetal sheep. J Dev Physiol 1989; 2:37–43
140. Vyas S. Pulsed Doppler examination of the normal human fetus. In: Pearce JM (Ed). Doppler Ultrasound in Perinatal Medicine. Oxford: Oxford University Press, 1992.
141. Vyas S, Campbell S. Doppler studies of the cerebral and renal circulations in small-for-gestational age fetuses. In: Pearce JM (Ed). Doppler Ultrasound in Perinatal Medicine. Oxford: Oxford University Press, 1992; 268–78
142. Mari G, Wasserstrum N. Flow velocity waveforms of the fetal circulation preceding fetal death in a case of lupus anticoagulant. Am J Obstet Gynecol 1991; 164:776–78.
143. Adams RD, Prod'Hom LS, Rabinowicz TH. Intrauterine brain death. Acta Neuropathol 1977; 40 41–49.
144. Gaziano EP, Freeman DW. Analysis of heart rate patterns preceding fetal death. Obstet Gynecol 1977; 50:578–82.
145. Van der Moer PE, Gerretsen G, Visser GHA. Fixed fetal heart rate pattern after intrauterine accidental decerebration. Obstet Gynecol 1985; 65:125–27
146. Nijhuis JG, Kruyt N, Van Vijck JAM. Fetal brain death. Two case reports. Br J Obstet Gynaecol 1988; 85:197–200.
147. Nijhuis JG, Crevels AJ, Van Dongen PWJ. Fetal brain death: The definition of a fetal heart rate pattern and its clinical consequences. Obstet Gynecol Surv 1990; 45:229–32.

148. Zimmer EZ, Jakobi P, Goldstein I, Gutterman E. Cardiotocographic and sonographic findings in two cases of antenatally diagnosed intrauterine fetal brain death. Prenatal Diagn 1992; 12:271–76
149. Ellis WG, Goetzman BW, Lindenberg JA. Neuro-pathologic documentation of prenatal brain damage. Am J Dis Child 1988; 142:858–66
150. Nwaesei CG, Pape KE, Martin DJ, Becker LE, Fitz CR. Periventricular infarction diagnosed by ultrasound: A postmortem correlation. J Pediatr 1984; 105:106–10.
151. Hill A. Assessment of the fetus: Relevance to brain injury. Clin Perinatol 1989; 16:413–14
152. Larroche JCL, Droulle P, Delezoide AL, Narey F, Nessmann C. Brain damage in monozygous twins. Biol Neonate 1990; 57:261–78
153. Carrera JM, Mortera C and Comas C. Natural history of fetal compromise in intrauterine growth restriction. In: Carrera JM, Mandruzzato GP, Maeda K (Eds). Ultrasound and Fetal Growth. London, Parthenon Publish 2001; 91–100.

Chapter 19
Fetal Central Nervous System

Ritsuko K Pooh, Kyong H Pooh

INTRODUCTION

Prenatal assessment of the fetal central nervous system (CNS) plays an important role in the field of perinatology. The brain rapidly develops *in utero* and remarkably changes its appearance from the primitive brain structure in early stage to the well-developed brain in late pregnancy.[1] Introduction of high-frequency transvaginal transducer has contributed to establishing "sonoembryology" and recent general use of transvaginal sonography in early pregnancy enabled early diagnoses of major fetal anomalies.[2,3] Furthermore, three-dimensional (3D) ultrasound has added accurate and objective information from early gestation till delivery, with surface anatomy, internal multidimensional analysis, volume calculation and circulatory visualization. Basic anatomical knowledge is essential, and transvaginal technique and

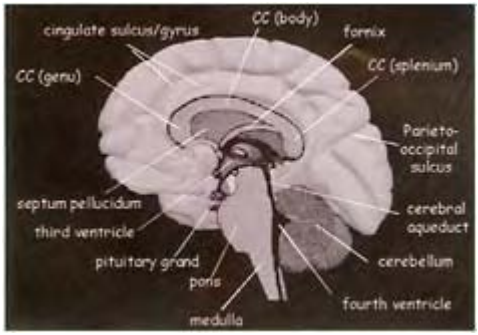

Figure 19.1: Basic anatomical knowledge of sagittal cutting section of the brain. CC—corpus callosum

3D ultrasound are helpful for obtaining orientation of the brain in neuroimaging.

Basic Knowledge of CNS Anatomy

The brain should be evaluated as a three-dimensional structure. One of reasons to make CNS imaging difficult, is little anatomical knowledge. Figures 19.1 to 19.3 show basic knowledge of brain anatomy for neuroimaging diagnosis.

Transvaginal Approach to the Fetal Brain

In the middle and late pregnancy, fetal CNS is generally evaluated through maternal abdominal wall. By transabdominal sonography, fetal brain is mostly demonstrated in transcranial axial sections. Sonographic assessment of the fetal brain in the sagittal and coronal sections, requires an approach from fetal parietal direction. Trans-

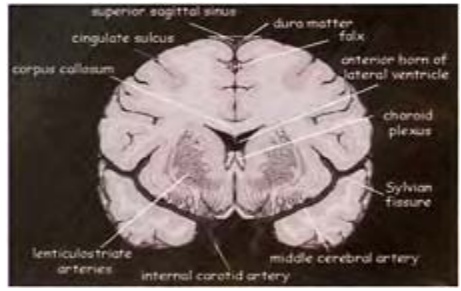

Figure 19.2: Basic anatomical knowledge of coronal cutting section of the brain

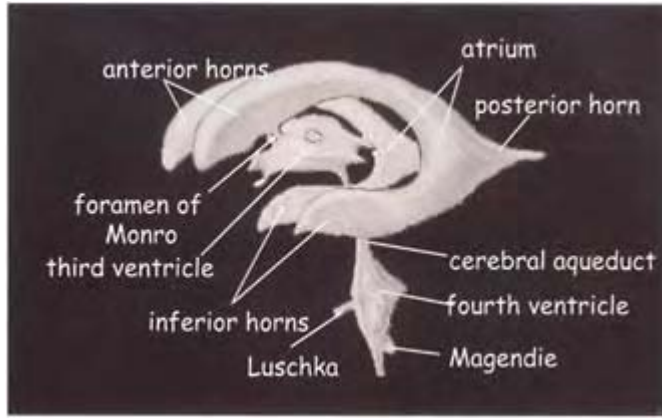

Figure 19.3: Basic anatomical knowledge of ventricular system of the brain

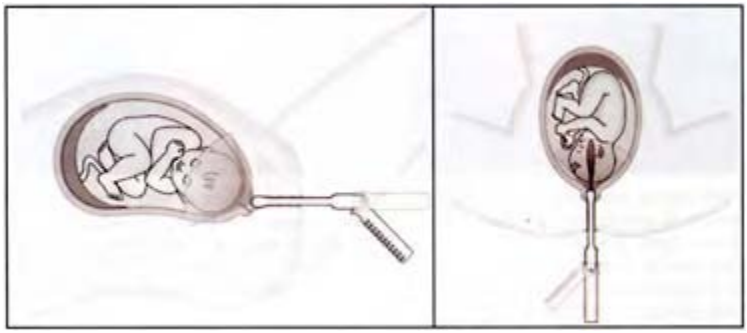

Figure 19.4: Schema of transvaginal sonography. (left) Lateral view of vertex presenting fetus and transvaginal transducer, (right) Frontal view. Clear imaging is possible by rotating and angle-changing of the transducer

vaginal sonography of the fetal brain opened a new field in medicine, "neurosonography".[4] Transvaginal approach to the normal fetal brain during the second and third trimester was introduced in the beginning of 1990s. It was the first practical application of three-dimensional central nervous system assessment by two-dimensional (2D) ultrasound.[5] Transvaginal observation of the fetal brain (Fig. 19.4) offers sagittal and coronal views of the brain from fetal parietal direction[6–10] through the fontanelles and/or the sagittal suture as ultrasound windows. Serial oblique sections via the same ultrasound window reveal the intracranial morphology in detail.[4] This method has contributed to the prenatal sonographic assessment of congenital CNS anomalies and acquired brain damage *in utero*, especially when compared with conventional transabdominal method.

Three-dimensional (3D) Ultrasound Technology

Recent introduction of three-dimensional (3D) ultrasound in obstetrics[11–13] has produced not only objective imaging of fetal superficial structure but also bony structure (Fig. 19.5), multiplanar ana-

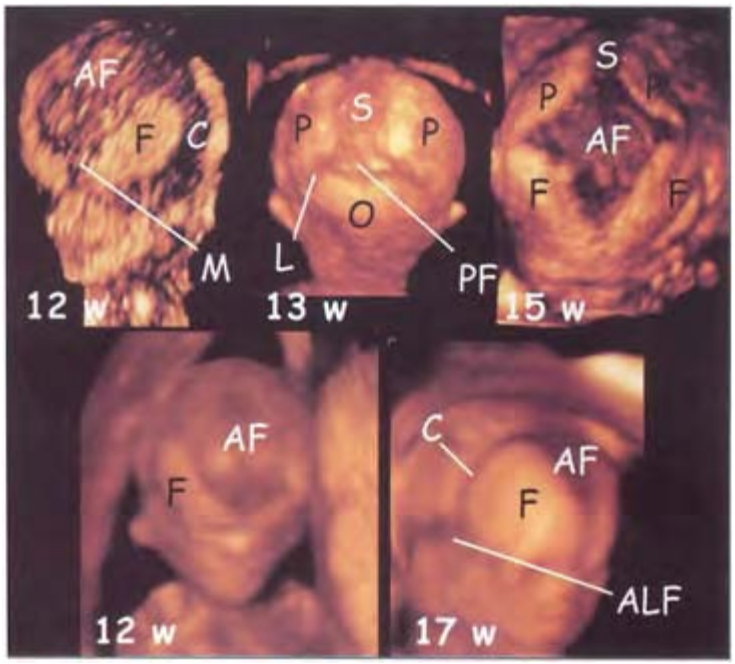

Figure 19.5: Fetal cranial structure in early gestation (3D US images), (upper left) 12 weeks, from the oblique front, (upper middle) 13 weeks, from the back, (upper right) 15 weeks, from the top of head, (lower left) 12 weeks, from the front, (lower right) 17 weeks. Oblique position. Premature shape of cranial bones, sutures, and fontanelles at 12 to 13 weeks change its appearance to the neonatal shape. AF: anterior fontanelle, PF: posterior fontanelle, ALF: anterolateral fontanelle, F: frontal bone, P: parietal bone, O: occipital bone, C: coronal suture, M: metopic suture, S: sagittal suture, L: lambdoid suture

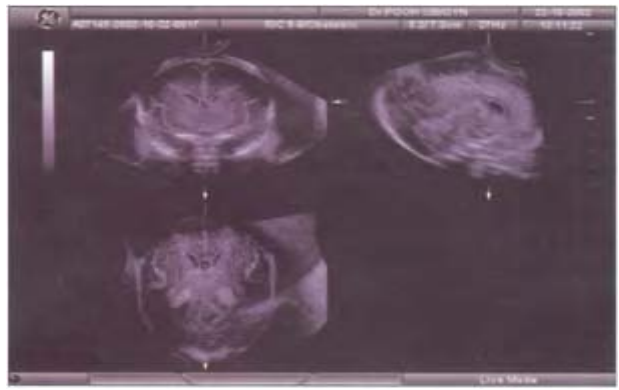

Figure 19.6: 3D multiplanar image analysis. Three orthogonal views are useful to obtain orientation of the brain structure. The raw 3D volume data set can be saved quickly. Saved data can be reviewed on ultrasound devise, and extracted on CD-R(W) or MO disks and sent for consultation. Off line image analysis can be done easily and repeatedly

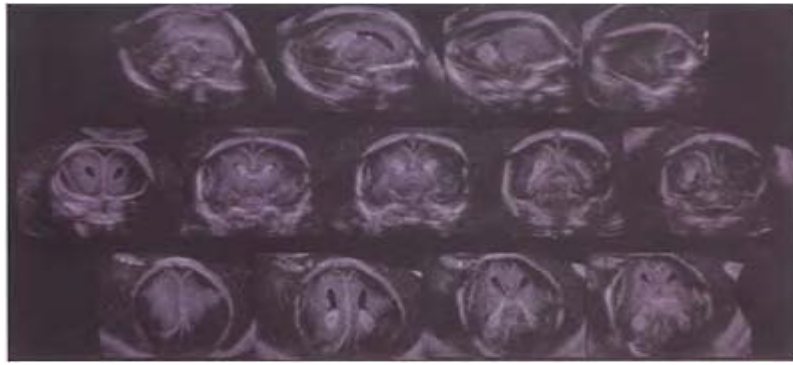

Figure 19.7: Normal intracranial structure at 19 weeks of gestation in parallel cutting slices of three orthogonal views. Sagittal, coronal, axial sections from above

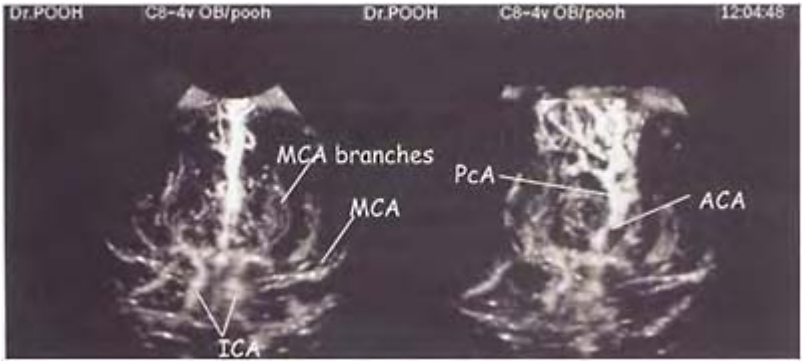

Figure 19.8: 3D power Doppler image of fetal brain circulation, (left) View from the front. Bilateral internal carotid arteries (ICA) and middle cerebral arteries (MCA) and branches of MCA are demonstrated, (right) Oblique view.

lysis of inside morphology (Figs 19.6 and 19.7), sono-angiography (Fig. 19.8), and volume calculation of target organ (Fig. 19.9). Combination of both transvaginal sonography and 3D ultrasound may be a great diagnostic tool for evaluation of three-dimensional structure of fetal CNS.[14–20]

Neuroimaging of Normal Brain Structure

Figures 19.10 to 19.15 shows normal brain imaging in each cutting section of axial, sagittal, parasagittal and coronal sectiions. Axial section (Fig. 19.10) is used to evaluate cerebellar structure, midline, symmetry of both hemispheres. In median sagittal section (Fig. 19.11), the corpus

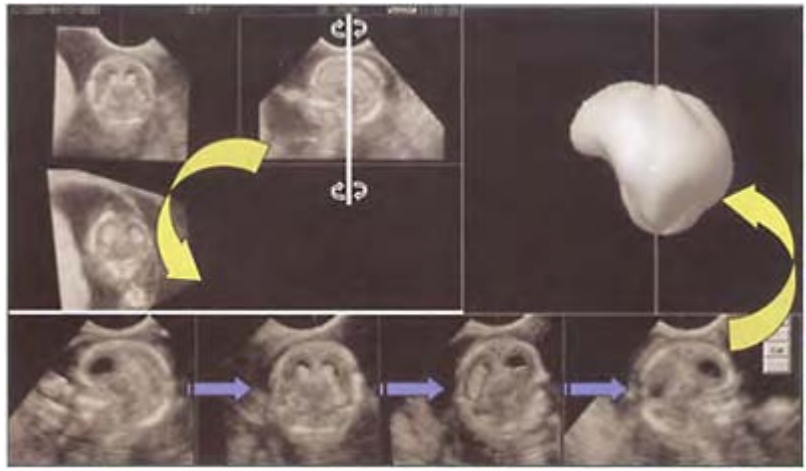

Figure 19.9: 3D volume extraction and volumetric analysis. On three orthogonal sections, the target organ can be traced automatically or manually with rotation of volume imaging data. After tracing, volume extraction image (upper right) can be demonstrated and volume calculation data is shown. 3D volumetry adds objective graphed imaging data.

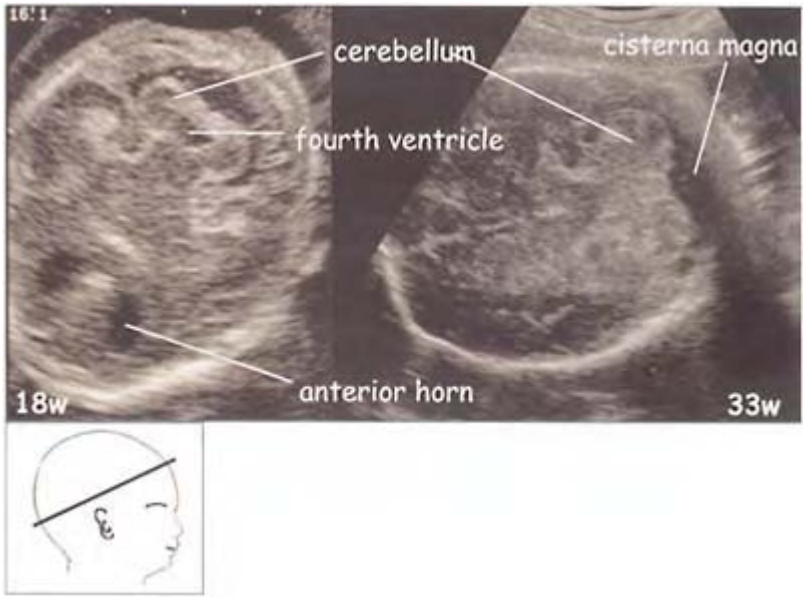

Figure 19.10: Axial sections at 19 and 33 weeks of gestation

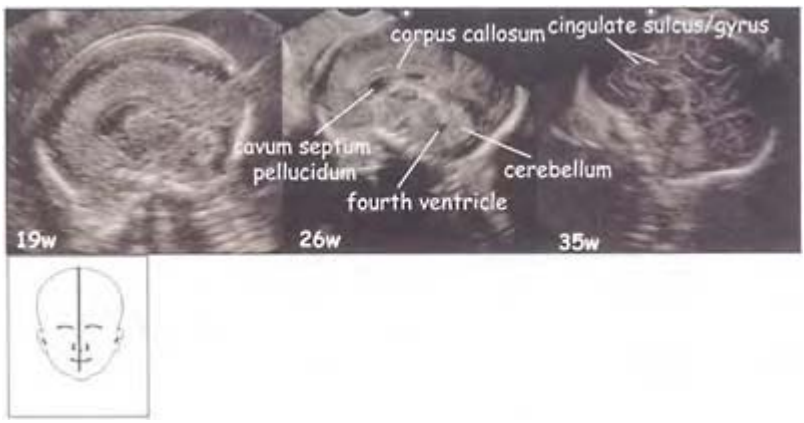

Figure 19.11: Sagittal sections at 19, 26 and 35 weeks of gestation

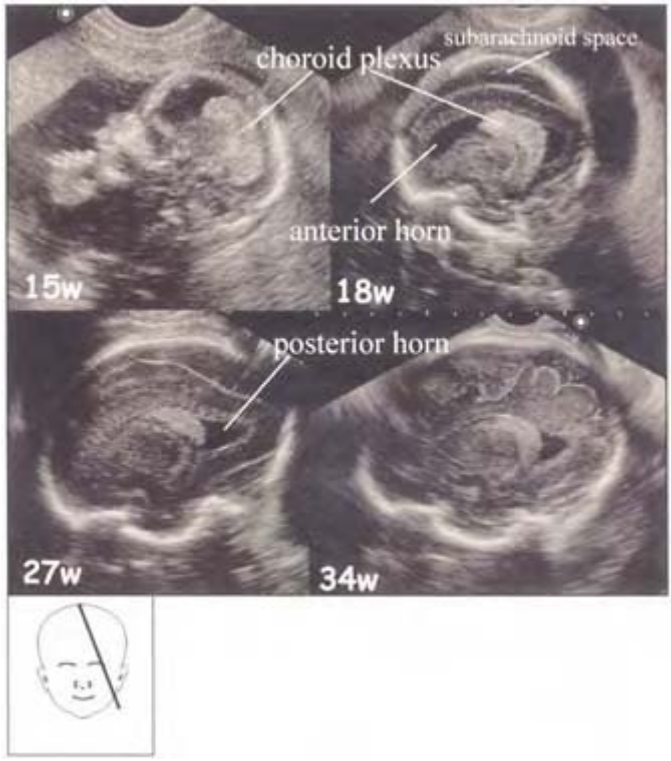

Figure 19.12: Parasagittal sections at 15, 18, 27 and 34 weeks of gestation

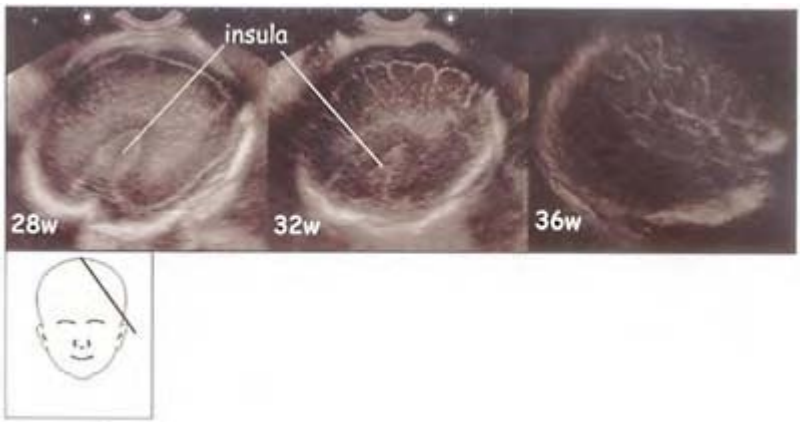

Figure 19.13: Parasagittal sections at 28, 32 and 36 weeks of gestation

callosum (from 18 weeks of gestation), septum pellucidum, fourth ventricle and sagittal section of cerebellum are demonstrated. In parasagittal section (Figs 19.12 and 19.13), lateral ventricle and choroid plexus, subarachnoid space and insula are visualized. In anterior coronal section (Fig. 19.14), anterior horns of lateral ventricle, corpus callosum and Sylvian fissure, and in posterior coronal section (Fig. 19.15), posterior horns and cerebellum are demonstrated. In late pregnancy, gyral formation is clearly demonstrated, as shown in Figure 19.16.

Assessment of Enlarged Ventricles

Hydrocephalus and ventriculomegaly are often used interchangeably to describe dilatation of the fetal lateral ventricles. However, they should be distinguished from each other to assess the enlargement of ventricles. Hydrocephalus is a dilatation of the lateral ventricles resulted from increased amount of cerebrospinal fluid and intracranial pressure, while ventriculomegaly is a dilatation of lateral ventricles without increased intracranial pressure due to hypoplastic cerebrum or other intracerebral abnormalities such as agenesis of corpus callosum. In sonographic imaging, those two intracranial conditions can be differentiated by visualization of subarachnoid space and appearance of choroids plexus. The transvaginal oblique and coronal images demonstrate the obliterated subarachnoid space and the dangling choroid plexus in the case of hydrocephalus (Figs 19.17 to 19.19). In contrast, the subarachnoid space and choroid plexus are well preserved in the case of ventriculomegaly (Fig. 19.20).[21] It is difficult to evaluate obliterated subarachnoid space in the axial section. Therefore, it is suggested that the evaluation of fetuses with enlarged ventricles may be evaluated by parasagittal and coronal views taken by transvaginal way. Furthermore, intracranial venous blood flow may be related to increased intracranial pressure. In normal fetuses, blood flow waveforms of dural sinuses, such as superior sagittal sinus, vein of Galen and straight sinus have pulsatile pattern (Fig. 19.21).[22] However, in cases with progressive hydrocephalus, normal pulsation disappears and blood flow waveforms become flat pattern (Fig. 19.22).[22] In cases with progressive hydrocephalus, there may be seven stages of progression (Fig. 19.23): 1) increased fluid collection of lateral ventricles, 2) increased intracranial pressure,

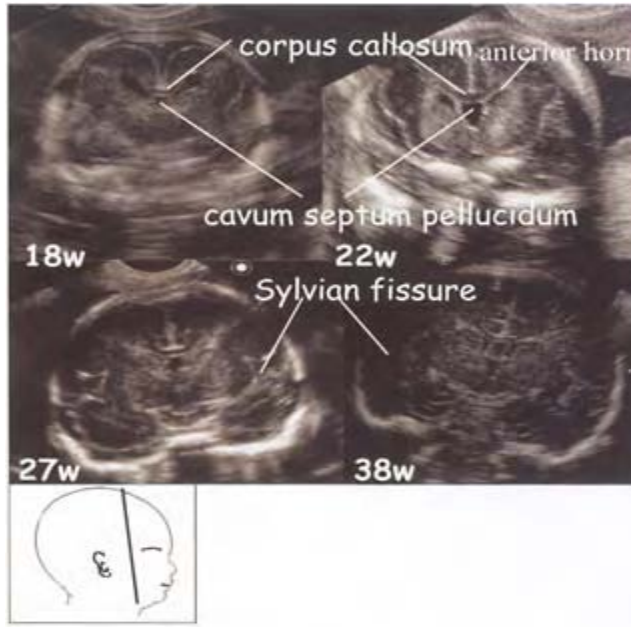

Figure 19.14: Anterior coronal sections at 18, 22, 27 and 38 weeks of gestation

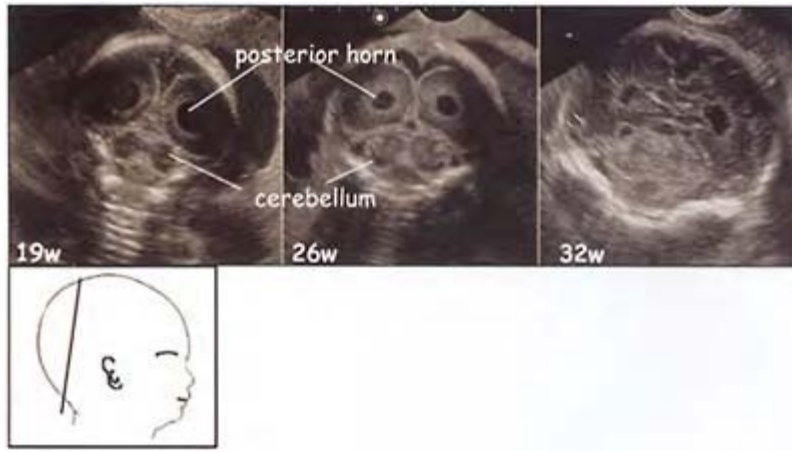

Figure 19.15: Posterior coronal sections at 19, 26 and 32 weeks of gestation

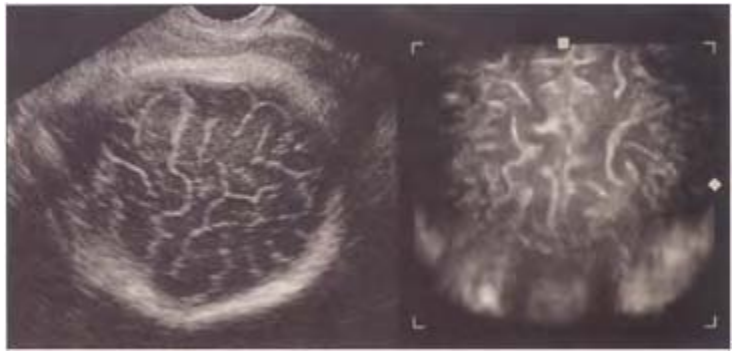

Figure 19.16: Gyral formation in the late pregnancy by 2D (left) and 3D (right) ultrasound

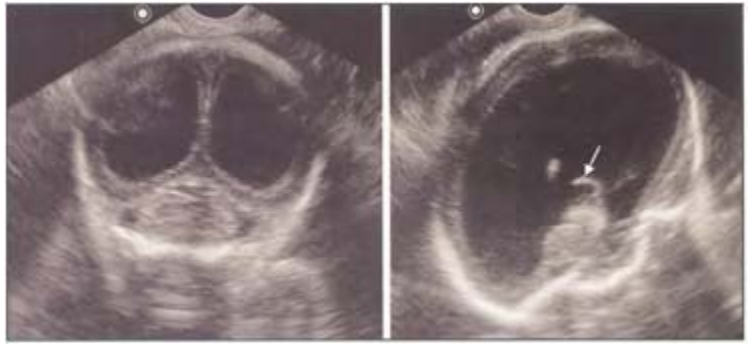

Figure 19.17: US images of fetal hydrocephalus at 34 weeks of gestation, (left) Coronal image. Subarachnoid space is obliterated, (right) Sagittal image. Dangling choroid plexus is demonstrated (arrow)

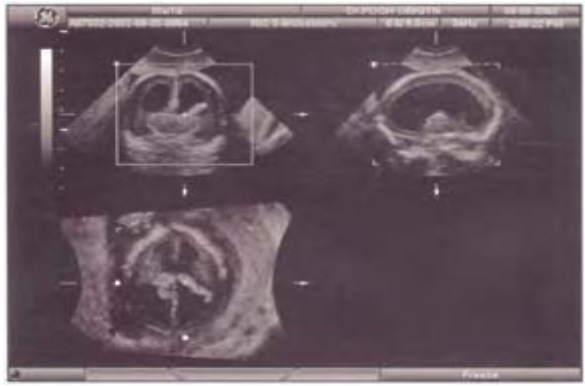

Figure 19.18: 3D orthogonal views of hydrocephalus at 18 weeks of gestation, (upper left) Coronal image, (upper right) Sagittal image, (lower) Axial image. Subarachnoid space is already obliterated and dangling choroid plexus is seen

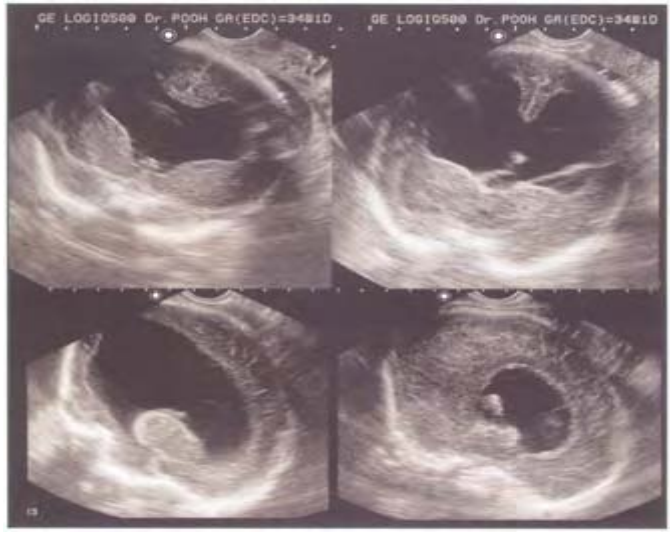

Figure 19.19: US images of hydrocephalus at 34 weeks of gestation, (upper) Coronal Images. Septum pellucidum was destroyed may

be due to enlargement of bilateral ventricles and both ventricles were fused. Dangling choroid plexus is seen, (lower) Parasagittal and sagittal images. Dangling choroid plexus and obliterated subarachnoid space are seen.

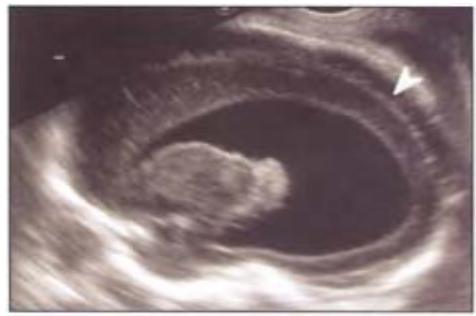

Figure 19.20: US image of ventriculomegaly. Enlarged ventricle exists but subarachnoid space is well preserved and no dangling choroid plexus, which indicates normal intercranial pressure. This condition should be differentiated from hydrocephalus

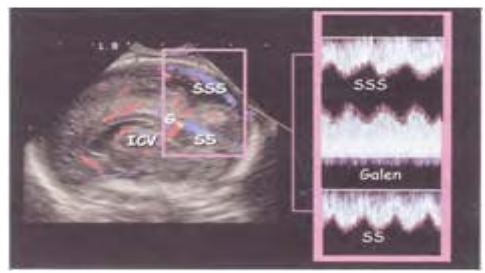

Figure 19.21: Normal cerebral venous circulation, (left) Sagittal image of color Doppler. SSS: superior sagittal sinus, ICV: internal cerebral vein, G: vein of Galen, SS: straight sinus,

(right) Normal blood flow waveforms of dural sinuses. In normal fetuses, venous flow always have pulsations

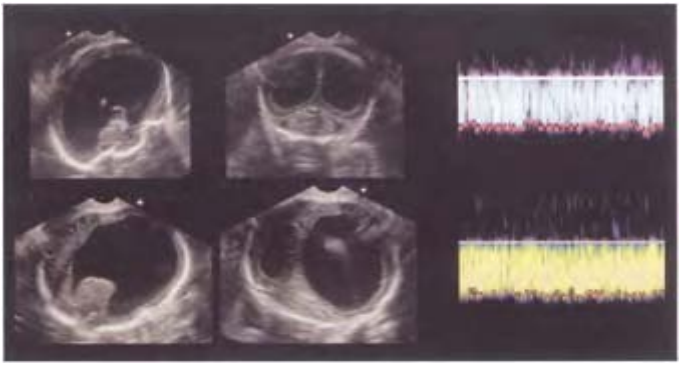

Figure 19.22: Disappearance of venous pulsation in cases with hydrocephalus. Normal dural sinuses have pulsatile patterns of flow waveform. In cases with progressive hydrocephalus, venous pulsation disappeared (right figures) may be because of excessive extension of the dura and dural sinuses

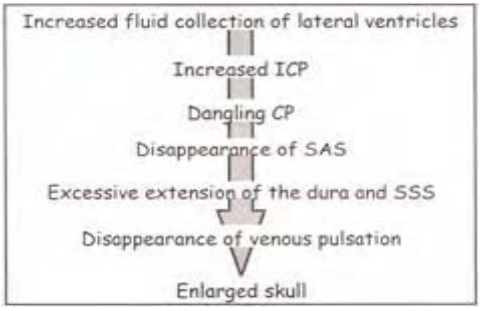

Figure 19.23: Progressive stages of hydrocephalus. ICP: intracranial pressure, CP: choroid plexus, SAS: subarachnoid space; SSS: superior sagittal sinus

3) dangling choroids plexus, 4) disappearance of subarachnoid space, 5) excessive extension of the dura and SSS, 6) disappearance of venous pulsation, 7) enlarged skull.

Congenital CMS Anomalies

Neurulation Disorder (Cranium Bifidum and Spina Bifida)

Cranium bifidum The calvarial ossification started at 10 weeks of gestation and the hyperechogenic skull appears in sonographic image by 11 weeks in normal pregnancy. Cranium bifidum is classified into four types of encephaloschisis (including anencephaly and exencephaly), meningocele, encephalomeningocele, encephalocystocele, and cranium bifidum occultum. Encephalocele occurs in the occipital region in 70–80%. Many reported remarkable reduction of prevalence of NTDs after using folic acid supplementation and fortification,[23–26] although some reported no decline of anencephaly rate.[27] Acrania, exencephaly (Fig. 19.24) and anencephaly (Fig. 19.25), caused by disorder of neurulation, are not independent anomalies. It is considered that dysraphia (absent cranial vault, acrania) occurs in very early stage and disintegration of the exposed brain (exencephaly) during the fetal period results in anencephaly.[28]

Spina bifida Spinal dysraphism is the most common abnormality of the central nervous system. Prevalence rate has been declined due to folic acid supplementation and fortification.

Spina bifida aperta Manifest form of spina bifida. Spina bifida aperta is classified into four types of meningocele, myelomeningocele, myelocystocele, and myeloschisis. Approximately 10–15% of spinal dysraphic defects are closed and normal skin

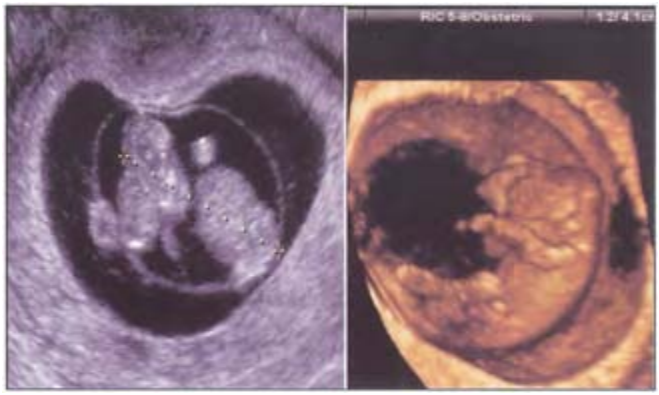

Figure 19.24: Acrania at 10 weeks of gestation, (left) US coronal image at 10 weeks. Note the normal appearance of amniotic membrane, which indicates this condition is not amniotic

band syndrome, (right) 3D US image of the same fetus as left image

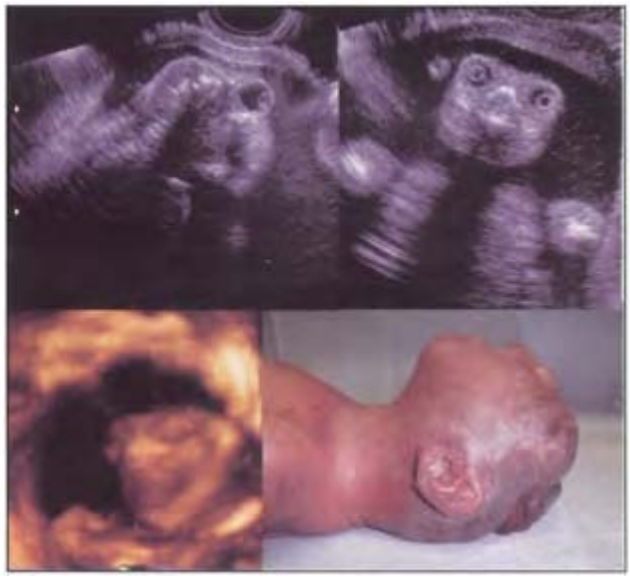

Figure 19.25: Anencephaly in middle gestation (same case as Fig. 19.24). (upper left) US sagittal image at 23 weeks of gestation, (upper right) US coronal image, (lower left) 3D US image, (lower right) External appearances of stillborn fetus at 25 weeks of gestation. It is clear that exencephalic brain tissue scattered in the amniotic space compared with this case at 10 weeks

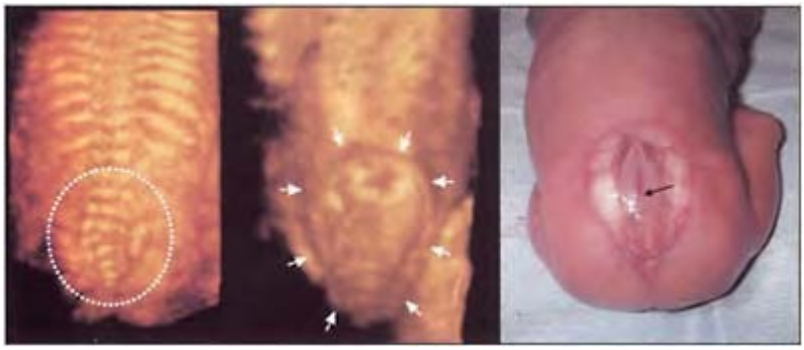

Figure 19.26: Prenatal US image of myelomeningocele, spina bifida at 20 weeks of gestation, (left) 3D bony demonstration of lumbar spina bifida. 3D ultrasound shows the exact level of spina bifida. (middle) 3D surface reconstruction of large myelomeningocele (white arrows), (right) External appearance of aborted fetus at 21 weeks of gestation. Note the central canal of the spinal cord (black arrow) in large myelomeningocele

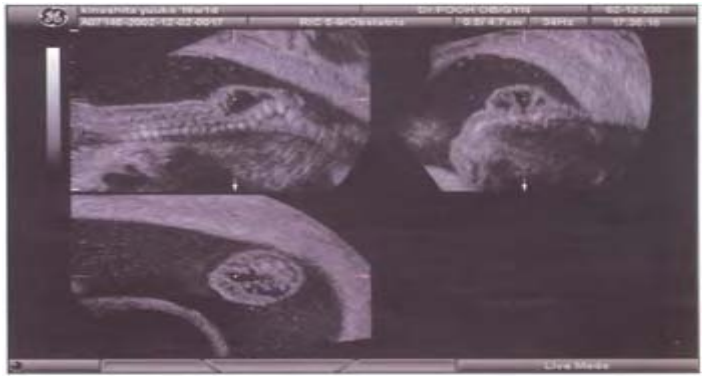

Figure 19.27: 3D US image of myelomeningocele with kyphosis at 16 weeks of gestation. Three orthogonal views and surface reconstruction image, (upper left) Sagittal US image.

Spinal cord completely protrude into the sac surface from spinal canal and severe kyphosis are seen, (upper right) Axial US view. (lower left) Coronal US view of myelomeningocele.

covers the bony defects (spina bifida occulta). The open spina bifida with protrusion of the spinal cord namely occur in the lumbar, thoracolumbar or lumbosacral region. Sonographic appearance of myelomeningocele is shown in Figures 19.26 and 19.27. Chiari type II malformation is present in almost every case of myelomeningocele. This malformation is characterized by inferior displacement of the lower cerebellum through the foramen magnum with obliteration of the cisterna

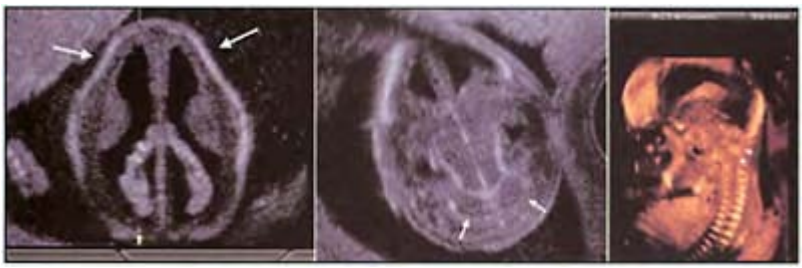

Figure 19.28: Chiari type II malformation at 16 weeks of gestation. Chiari type II malformation is observed in most cases with myelomeningocele and myeloschisis. (left) Typical lemon sign (arrows). (middle) Typical banana sign (arrows), (right) 3D reconstruction internal image of Chiari type II malformation (arrows).

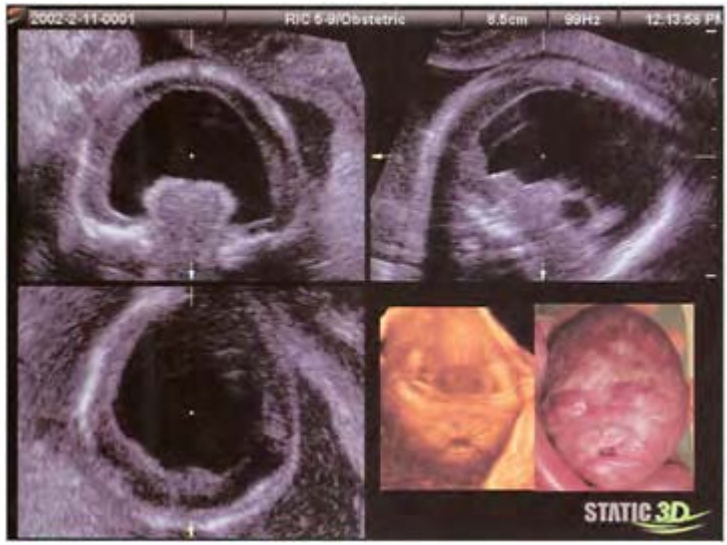

Figure 19.29: Alobar holoprosencephaly at 20 weeks of gestation. Three orthogonal images of intracranial structure show complete single ventricle within a single-sphered cerebral structure, (lower right) 3D US image of fetal face and the face of aborted fetus at 21 weeks of gestation. A flat nose with median cleft lip/palate are seen.

magna (banana sign), inferior displacement of the medulla into the spinal canal, and deformity of the frontal bone with indentation (lemon sign). Both banana sign and lemon sign are detectable by sonography until 24 weeks' gestation (Fig. 19.28) and occasionally the median section of craniovertebral junction demonstrates the medullary kink. Although the banana sign persists during pregnancy, the lemon sign may disappear in many cases with advancing gestational age.[29]

Disorder of Prosencephalic Development

Holoprosencephaly

Holoprosencephaly (Fig. 19.29) is caused by the disorder of prosencephalic development and is divided into the three subtypes: alobar, semilobar and lobar types. Holoprosencephaly is frequently associated with other malformation, chromosomal

aberration or Dandy-Walker malformation. 75% of holoprosencephaly has normal karyotype, but chromosomes 2, 3, 7, 13, 18 and 21 have been implicated in holoprosencephaly. Particularly, trisomy 13 has most commonly been observed The facial anomalies such as cyclopia, cebo cephaly, flat nose and cleft lip are often associated with holoprosencephaly. The characteristic appearance of fused ventricles is detectable from the early pregnancy.[30,32]

Agenesis of the Corpus Callosum

Agenesis of the corpus callosum (complete agenesis, partial agenesis, dysgenesis, Fig. 19.30) leads abnormal induction of medial cerebral convolution. Agenesis of the corpus callosum is associated with additional cerebral anomalies, noncerebral anomalies and chromosomal aberration. It has been described that isolated agenesis of the corpus callosum per se has little consequence on neurological development. Gupta and colleagues[33] reviewed 70 reported cases of agenesis of the corpus callosum detected prenatally and described that 85% of fetuses without other detectable anomalies carried a normal development and 15% had a risk of handicap. Therefore, prenatal findings suggestive of agenesis of the corpus callosum should be followed by a careful search for associated anomalies and counseling parents should be prudent if agenesis of the corpus callosum is an isolated finding. The typical findings of agenesis of the corpus callosum are the medial cerebral sulci demonstrated as a radial arrangement, enlargement of the posterior horns of lateral ventricles, steer-horn appearance of the anterior horns and upward displacement of the third ventricle. In most cases detected prenatally by sonography, diagnosis was made by detection of indirect findings. The transvaginal median section of the brain, however, may be most reasonable to directly document the callosal lesion.

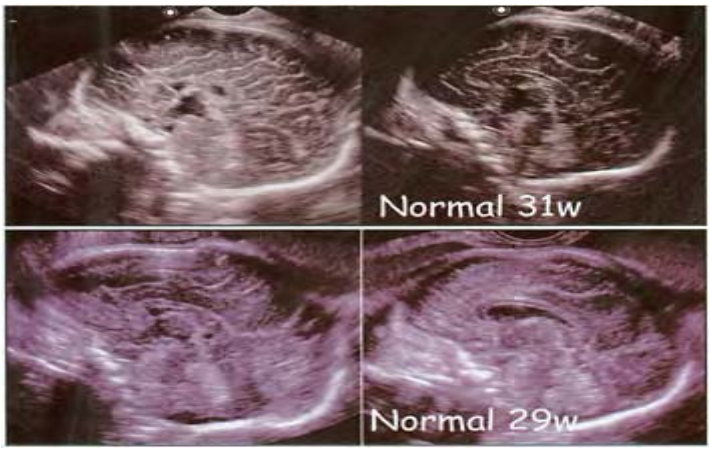

Figure 19.30: Complete agenesis (upper) and hypogenesis (lower) of the corpus callosum. All images are

transvaginal median (mid-sagittal) images. Right images are normal images of the corpus callosum at the same gestational age as each left image

Migration Disorder

Lissencephaly, polymicrogyria, schizencephaly are categorized in migration disorders, with poor prognosis.

Lissencephaly

Lissencephaly is characterized by a lack of gyral development and divided into two types: type I has microcephaly and facial dysmorphism and often associated with Miller-Dierker syndrome and type II have hydrocephalus, retinal dysplasia and muscular dysplasia, associated with Walker-Warburg syndrome and Fukuyama congenital muscular dystrophy. Antenatal diagnosis of syndromes associated with lissencephaly before gyral development in families with prior affected infants has been reported by demonstration of additional abnormalities such as bilateral cataract[34] and hydrocephalus.[35] Sonographic detection of smooth gyral pattern at 31–32 weeks' gestation has been reported.[36] Prenatal sonographic diagnosis of lissencephaly, however, without a previous history cannot be reliably made until 26 to 28 weeks' gestation, when the normal gyri and sulci become well defined.

Posterior Fossa Anomalies

Dandy-Walker Complex

Dandy-Walker complex is used to indicate a spectrum of anomalies of the posterior fossa. Classification of Dandy-Walker complex; (classic) Dandy-Walker malformation; enlarged posterior fossa, complete or partial agenesis of the cerebellar vermis, elevated tentorium;

Dandy-Walker variant; variable hypoplasia of the cerebellar vermis with or without enlargement of the posterior fossa;

Megacisterna magna; enlarged cisterna magna with integrity of both cerebellar vermis and fourth ventricle.

Dandy-Walker malformation occurs as a part of recognizable syndromes such as Mechel's syndrome and Walker-Warburg syndrome, and is frequently associated with chromosomal aberrations. There often exist additional intracerebral or extracerebral anomalies. Congenital hydrocephalus exists in 5–10% of cases,[37] but hydrocephalus develops usually within three months after birth.[38] Antenatal diagnosis should be performed by a careful observation of the posterior fossa in the axial, coronal and sagittal planes. The prenatal diagnosis of Dandy-Walker malformation is possible from 14 weeks' gestation.[39]

The closure of the cerebellar vermis in normal fetuses is demonstrated by sonography from 14 till 18 weeks' gestation. Blomley and colleagues described that 56% of normal fetuses had an open vermis at 14 weeks' gestation, 23% at 15 weeks and 6% at 17 weeks. Thus, the cerebellar vermis develops during early second trimester.[40] The normal sonographic appearance of the open vermis should not be interpreted by developmental change of Dandy-Walker malformation and its variant, which is described as a small defect in the cerebellar vermis without dilatation of the cisterna magna. Prenatal diagnosis of Dandy-Walker variant should not be made before 18 weeks.[40]

Cerebellar Hypoplasia

Cerebellar dysplasia (Fig. 19.31) is often associated with chromosomal abnormalities such as trisomy 18 and others. In late pregnancy, prenatal diagnosis of cerebellar dysplasia is not difficult because of conspicuous enlargement of cisterna magna. However, in the first half of pregnancy, all normal cases have large cisterna magna. In order to detect cerebellar dysplasia, therefore, it is recommended to assess the development of the cerebellum measuring the cerebellar transverse diameter in axial image or posterior coronal section.

Others

Arachnoid Cyst

Arachnoid cyst (Fig. 19.32) is a congenital or acquired cyst, lined by arachnoid membranes, and filled with fluid collection which is the same

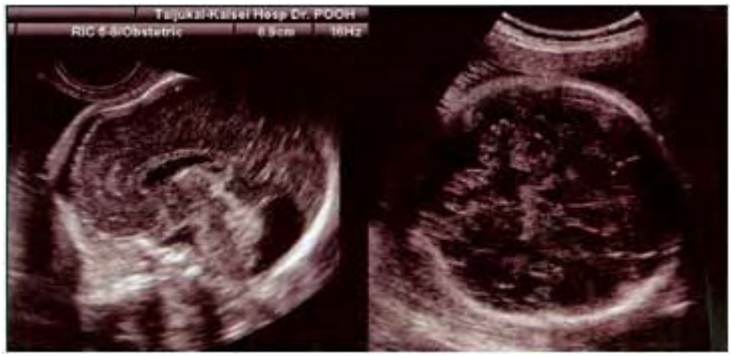

Figure 19.31: Cerebellar dysplasia (28 weeks of gestation), (upper left) Transvaginal median image. Small cerebellum in a normal size of posterior fossa, (upper right) Transabdominal axial image, (lower

left) Fetal MR sagittal image, (lower right) MR axial image. This case has chromosomal aberration of trisomy 18 with other congenital anomalies such as large VSD, overlapping finger, lowset ears, etc.

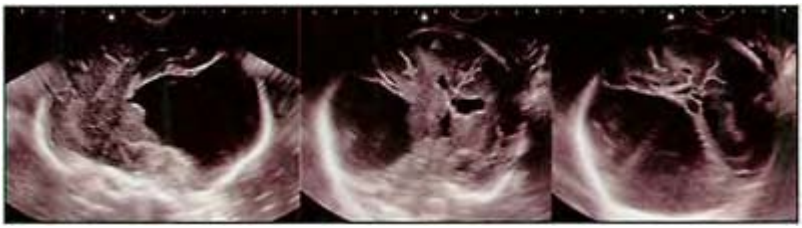

Figure 19.32: Fetal arachnoid cyst at 31 weeks of gestation, (upper) Transvaginal US image. Sagittal (left) and coronal (middle, right) sections, (lower left) Fetal MR sagittal image. The cyst occupis supra- to infratentorial space. Not only cerebrum but also cerebellum are compressed by the cyst, (lower right) Fetal MR coronal image. Midline is conspicuously arcuated. Scalp and skull bone are extended due to the existence of the huge cyst. Note the difference between right and left head size.

character as the cerebrospinal fluid. The number of cysts is mostly single, but two or more cysts can be occasionally observed. Location of arachnoid cyst is various; approximately 50% of cysts occurs from the Sylvian fissure (middle fossa). Interhemispheric cysts are often associated with agenesis or hypogenesis of the corpus callosum. Postnatal prognosis is usually good.

Choroid Plexus Cyst

Choroid plexus cysts are defined as cysts with fluid collection within the choroids plexus with incidence of 0.95–2.8% of all fetuses scanned,[41–43] which may exist unilaterally or bilaterally, associated with chromosomal aberration such as trisomy 18. They are

depicted in the second trimester and usually resolve by the 24th week. Choroid plexus cysts, *per se,* are usually asymptomatic and benign, but rarely, symptomatic and disturbs CSF flow.[44,45] Isolated choroid plexus cysts may be normal variation. Fetal karyotyping examination should be offered if additional abnormalities are found.

Acquired Brain Abnormalities in Utero

Intracranial Hemorrhage

Intracranial hemorrhage in *utero* may be caused by trauma, infections, asphyxia, alloimmune thrombocytopenia, intracranial tumor, cord

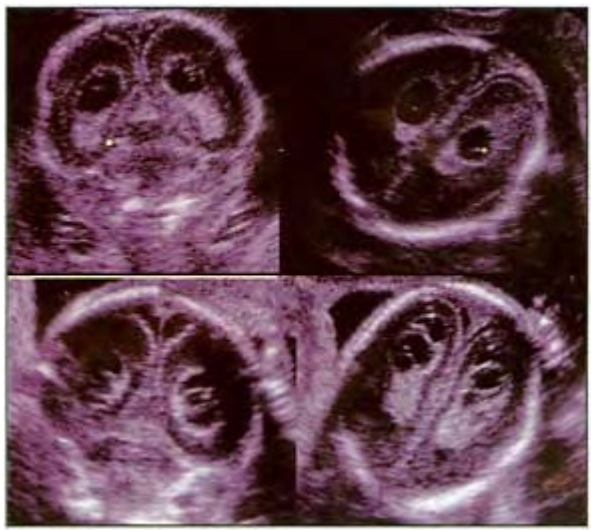

Figure 19.33: Fetal US Images of chorold plexus cysts, (upper) Bilateral choroid plexus cysts In a fetus with trisomy 18. Cardiac ventricular septum defect and overlapping fingers were accompanied, (lower) Bilateral choroid plexus cysts in a normal fetus. Impossible to differentiate between normal and abnormal karyotypes by location and appearance of choroid plexus cyst. Detection of additional anomalies is important for differentiated diagnosis

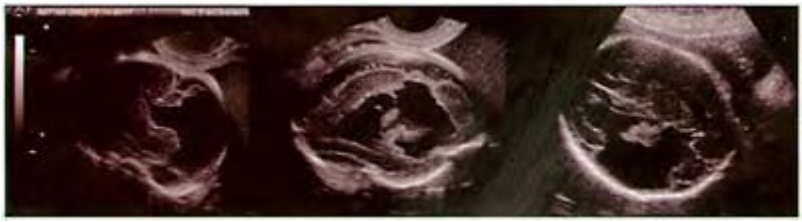

Figure 19.34: Porencephaly at 25 weeks of gestation, (upper left) Transvaginal US coronal image. Defect of parietolateral part of the unilateral cerebrum. This case has also absent septum pellucidum. (upper middle) Parasagittal US image. Porencephalic part connects to unilateral ventricle. Echogenicity of inside ventricular wall indicates intraventricular hemorrhage, (upper right) Transabdominal US axial image

complication, preeclampsia, abruptio placenta and other factors. Hemorrhage is commonly located in the subdural, periventricular and cerebellar regions. Many cases of intracranial hemorrhage detected prenatally have been reported.[46–51] The outcome of fetuses with intracranial hemorrhage has ranged from fetal demise and postnatal death to a good outcome with normal development.[47]

Porencephaly

Porencephaly (porencephalic cyst, Fig. 19.34) is fluidfilled space replacing normal brain parenchyma and may or may not communicate with the lateral ventricles or subarachnoid space. Ischemic episode, trauma, demise of one twin, intercerebral hemorrhage, infection can cause porencephaly. Easy to occur when immature cerebrum has some factors with propensity of dissolution and cavitation. Timing of ischemic injury (may be as early as second trimester) is strongly related to porencephaly.

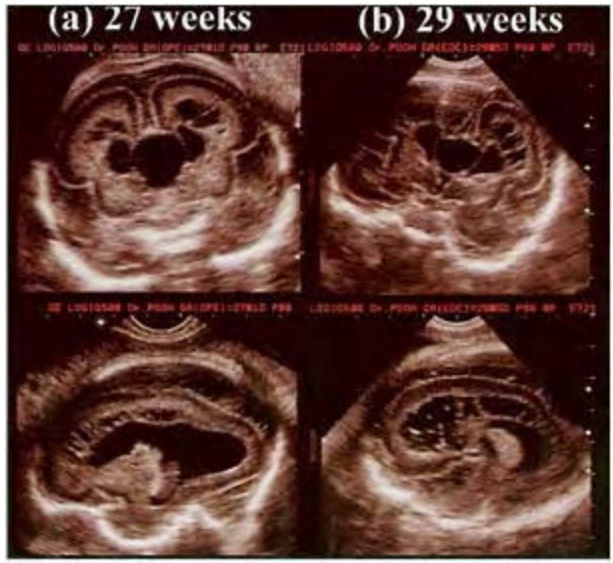

Figure 19.35: Fetal PVL (periventricular leukomalacia). (a)Fetal USG at 27 weeks. Clear bilateral PVL is observed with mild ventriculomegaly and enlargement of cavum septum pellucidum. b) At 29 weeks, PVL was progressive and became wide-spread type

Periventricular Leukomalacia

It had been believed for a long time that infant cerebral palsy was caused by inadequate management of the labor. However, this misleading concept has been recently corrected by the scientists who detected various antepartum causes of cerebral palsy other than those in intrapartum stage.[52] Neonatal brain disturbances, therefore, should be carefully studied in the relation to the brain changes in antepartum stage. Most of the interests of investigation at present in perinatology and neonatology, lie mainly on periventricular leukomalacia (PVL) which has been thought to be the important cause of cerebral palsy. PVL is characterized by the necrotic changes of bilateral periventricular areas of the white matter, which is found in preterm babies and babies with complications during pregnancy, such as multiple pregnancy, cord complication, repeated deceleration of the fetal heart rate and others. Although multiple small cysts appear in the necrotic tissue in typical PVL cases, the cysts disappear two weeks later and the lateral ventricles begin to dilate due to the atrophy of the white matter. Lateral walls of bilateral ventricles show irregular waving when the ventricles dilate.[53] The presence of PVL cysts in neonatal

period may strongly suggest that the periventricular lesion originally starts *in utero*. Prenatal sonographic images of PVL at 27 and 29 weeks are shown in Figure 19.35.

Future Aspects

The assessment of the fetal central nervous system plays an important role for the rest of infant's life. As described in this article, advanced sonography combined with methodology of approaching the fetal brain has improved the assessment of fetal intracranial structure and diagnosis of the prenatal brain abnormalities. Recent remarkable development of three dimensional/four dimensional ultrasound[54–55] and advanced MRI technology will produce more accurate evaluation of the brain morphology. A functional evaluation of the intracranial condition and a prenatal prediction of neurological development after birth are also important points in a proper management for fetuses with intracranial abnormalities, but many uncertain and unknown facts still exist. Further studies on the assessment of cerebral function may be expected.

REFERENCES

1. The nervous system. In: Moore KL, Persaud TVN, Shiota K (Eds). Color Atlas of Clinical Embryology. Philadelphia, USA: WB Saunders 1994; 209–20.
2. Timor-Tritsch IE, Peisners DB, Raju S. Sonoembryology: an organ-oriented approach using a high-frequency vaginal probe. J Clin Ultrasound 1990; 18: 286–98.
3. Pooh RK. B-mode and Doppler studies of the abnormal fetus in the first trimester. In: Chervenak FA, Kurjak A (Eds). Fetal Medicine. Parthenon Publishing, Carnforth 1999; 46–51.
4. Timor-Tritsch IE, Monteagudo A. Transvaginal fetal neurosonography: standardization of the planes and sections by anatomic landmarks. Ultrasound Obstet Gynecol 1996;8:42–47.
5. Monteagudo A, Reuss ML, Trmor-Tritsch IE. Imaging the fetal brain in the second and third trimesters using transvaginal sonography. Obstet Gynecol 1991;77:27–32.
6. Monteagudo A, Timor-Tritsch IE, Moomjy M. In utero detection of ventriculomegaly during the second and third trimesters by transvaginal sonography. Ultrasound Obstet Gynecol 1994; 4:193–98.
7. Monteagudo A, Timor-Tritsch IE. Development of fetal gyri, sulci and fissures: a transvaginal sonographic study. Ultrasound Obstet Gynecol 1997; 9:222–28.
8. Pooh RK, Nakagawa Y, Nagamachi N, Pooh KH, Nakagawa Y, Maeda K et al. Transvaginal sonography of the fetal brain: detection of abnormal morphology and circulation. Croat Med J 1998; 39:147–57.
9. Pooh RK, Maeda K, Pooh KH, Kurjak A. Sonographic assessment of the fetal brain morphology. Prenat Neonat Med 1999; 4:18–38.
10. Pilu G, Falco R Milano V, Perolo A, Bovicelli L. Prenatal diagnosis of microcephaly assisted by vaginal sonography and power Doppler. Ultrasound Obstet Gynecol 1998; 11:357–60.
11. Pretorius DH, Nelson TR. Three-dimensional ultrasound. Ultrasound Obstet Gynecol 1995; 5:219–21.
12. Merz E. Three-dimensional ultrasound—a requirement for prenatal diagnosis. Ultrasound Obstet Gynecol 1998; 12:225–26.
13. Kurjak A, Kupesic S, Banovic I, Hafner T, Kos M. The study of morphology and circulation of early embryo by three-dimensional ultrasound and power Doppler. J Perinat Med 1999; 27:145–57.

14. Pooh RK. Fetal brain assessment by three-dimensional ultrasound. In: Kurjak A, Kupesic S (Eds). Clinical application of 3D sonography. Parthenon Publishing, Carnforth 2000; 171–79.
15. Pooh RK, Pooh K, Nakagawa Y, NishidaS, Ohno Y. Clinical application of three-dimensional ultrasound in fetal brain assessment. Croat Med J 2000; 41:245–51.
16. Monteagudo A, Timor-Tritsch IE, Mayberry P Three-dimensional transvaginal neurosonography of the fetal brain: 'navigating' in the volume scan. Ultrasound Obstet Gynecol 2000; 16:307–13.
17. Timor-Tritsch IE, Monteagudo A, Mayberry P Three-dimensional ultrasound evaluation of the fetal brain: the three horn view. Ultrasound Obstet Gynecol 2000; 16:302–06.
18. Pooh RK, Pooh KH. Transvaginal 3D and Doppler ultrasonography of the fetal brain. Semin Perinat 2001; 25:38–43.
19. Blaas HG, Eik-Nes SH, Kiserud T, Berg S, Angelsen B, Olstad B. Three-dimensional imaging of the brain cavities in human embryos. Ultrasound Obstet Gynecol 1995; 5:228–32.
20. Blaas HG, Eik-Nes SH, Berg S, Torp H. In-vivo three-dimensional ultrasound reconstructions of embryos and early fetuses. Lancet 1998; 352:1182–86.
21. Pooh RK, Maeda K, Pooh KH, Kurjak A. Sonographic assessment of the fetal brain morphology. Prenat Neonat Med 1999; 4:18–38.
22. Pooh RK, Pooh KH, Nakagawa Y, Maeda K, Fukui R, Aono T. Transvaginal Doppler assessment of fetal intracranial venous flow. Obstet Gynecol 1999; 93: 697–701.
23. Martinez de Villarreal L, Perez JZ, Vazquez PA, Herrera RH, Campos Mdel R, Lopez RA, Ramirez JL, Sanchez JM, Villarreal JJ, Garza MT, Limon A, Lopez AG, Barcenas M, Garcia JR, Dominguez AS, Nunez RH, Ayala JL, Martinez JG, Gonzalez MT, Alvarez CG, Castro RN. Decline of neural tube defects cases after a folic acid campaign in Nuevo Leon, Mexico. Teratology 2002; 66:249–56.
24. Ray JG, Meier C, Vermeulen MJ, Boss S, Wyatt PR, Cole DE. Association of neural tube defects and folic acid food fortification in Canada. Lancet 2002; 360:2047–48.
25. Persad VL, Van den Hof MC, Dube JM, Zimmer P. Incidence of open neural tube defects in Nova Scotia after folic acid fortification. CMAJ 2002;167:241–45.
26. Mathews TJ, Honein MA, Erickson JD. Spina bifida and anencephaly prevalence—United States, 1991–2001. MMWR Recomm Rep 2002;51:9–11.
27. Green NS. Folic acid supplementation and prevention of birth defects. J Nutr 2002;132:2356S-60S.
28. Monteagudo A, Timor-Tritsch IE. Fetal Neurosonography of congenital brain anomalies. In: TimorTritsch IE, Monteagudo A, Cohen HL. Ultrasonography of the Prenatal and Neonatal Brain (2nd ed). McGraw-Hill, New York, 2001;151–258.
29. Van den Hof MC, Nicolaides KH, Campbell J, Campbell S. Evaluation of the lemon and banana signs in one hundred thirty fetuses with open spina bifida. Am J Obstet Gynecol 1990; 162:322–27.
30. Pilu G, Perolo A, David C. Midline anomalies of the brain. In Timor-Tritsch IE, Monteagudo A, Cohen HL (Eds). Ultrasonography of the prenatal and neonatal brain. Stamford, USA: Appleton & Lange, 1996;241–58.
31. Bronshtein M, Weiner Z. Early transvaginal sonographic diagnosis of alober holoprosencephaly. Prenat Diagn 1991;ll:459–62.
32. Gonzalez-Gomez F, Salamanca A, Padilla MC, Camara M, Sabatel RM. Alober holoprosencephalic embryo detected via transvaginal sonography. Eur J Obstet Gynecol Reprod Biol 1991;47:266–70.
33. Gupta JK, Lilford RJ. Assessment and management of fetal agenesis of the corpus callosum. Prenat Diagn 1995;15:301–12.
34. Bornemann A, Pfeiffer R, Beinder E, Wenkel H, Schlicker U, Meyermann R et al. Three siblings with Walker-Warburg syndrome. General & Diagnostic Pathology 1997; 141:371–75.
35. Gasser B, Lindner V, Dreyfus M, Feidt X, Leissner P, Treisser A et al. Prenatal diagnosis of WalkerWarburg syndrome in three sibs. Am J Med Genet 1998;76:107–10.

36. Saltzman DH, Krauss CM, Goldman JM, Benacerraf BR. Prenatal diagnosis of lissencephaly. Prenat Diagn 1991; 11:139–43.
37. Volpe JJ. Neural tube formation and prosencephalic development. Neurology of the Newborn. Philadelphia, USA: WB Saunders, 2001; 3–42.
38. Hirsch JF, Pierre-Kahn A, Renier D, Sainte-Rose C, Hoppe-Hirsch E. The Dandy-Walker malformation. A review of 40 cases. J Neurosurg 1984; 61:515–22.
39. Ulm B, Ulm MR, Deutinger J, Bernaschek G. DandyWalker malformation diagnosed before 21 weeks of gestation: associated malformation and chromosomal abnormalities. Ultrasound Obstet Gynecol 1997; 10:167–70.
40. Blomley B, Nadel AS, Pauker S, Estroff JA, Benacerraf BR. Closure of the cerebellar vermis: evaluation with second trimester US. Radiology 1994; 193:761–63.
41. Sullivan A, Giudice T, Vavelidis F, Thiagarajah S. Choroid plexus cysts: Is biochemical testing a valuable adjunct to targeted ultrasonography? Am J Obstet Gynecol 1999; 181:260–65.
42. Reinsch RC. Choroid plexus cysts—association with trisomy: prospective review of 16,059 patients. Am J Obstet Gynecol 1997; 176:1381–83.
43. Morcos CL, Platt LD, Carlson DE, Gregory KD, Greene NH, Korst LM. The isolated choroid plexus cyst. Obstet Gynecol 1998; 92:232–36.
44. Lam AH, Villanueva AC. Symptomatic third ventricular choroid plexus cysts. Pediatr Radiol 1992; 22(6):413–16.
45. Parizek J, Jakubec J, Hobza V, Nemeckova J, Cernoch Z, Sercl M, Zizka J, Spacek J, Nemecek S, Suba R Choroid plexus cyst of the left lateral ventricle with intermittent blockage of the foramen of Monro, and initial invagination into the III ventricle in a child. Childs Nerv Syst 1998; 14:700–08.
46. Forgaty K, Cohen HL, Haller JO. Sonography of fetal intracranial hemorrhage: unusual causes and a review of the literature. J Clin Ultrasound 1989; 17:366–70.
47. Achiron R, Pinchas OH, Reichman B, Heyman Z, Schimmel M, Eidelman A et al. Fetal intracranial haemorrhage: clinical significance of in utero ultrasonographic diagnosis. Br J Obstet Gynaecol 1993; 100:995–99.
48. Anderson MW, McGahan JP Sonographic detection of an in utero intracranial hemorrhage in the second trimester. J Ultrasound Med 1994; 13:315–18.
49. Catenzarite VA, Schrimmer DB, Maida C, Mendoza A. Prenatal sonographic diagnosis of intracranial hemorrhage: report of a case with a sinusoidal fetal heart rate tracing, and review of the literature. Prenat Diagn 1995; 15:229–35.
50. Reiss I, Gortner L, Mller J, Gehl HB, Baschat AA, Gembruch U. Fetal intracerebral hemorrhage in the second trimester: diagnosis by sonography and magnetic resonance imaging. Ultrasound Obstet Gynecol 1996; 7:49–51.
51. Guerriero S, Ajossa S, Mais V, Risalvato A, Angiolucci M, Labate F et al. Color Doppler energy imaging in the diagnosis of fetal intracranial hemorrhage in the second trimester. Ultrasound Obstet Gynecol 1997; 10:205–08.
52. Naeye RL, Peters EC, Bartholomew M, Landis JR. Origins of cerebral palsy. Am J Dis Child 1989; 145:1154–61.
53. Maeda K, Utsu M, Imanishi M, Naruse H, Akaiwa A. Ultrasonic assessment of intrapartum fetal brain damage. Proc. CEcografia nel Decennio del Cervello. 1992; 517–35.
54. Pooh RK, Pooh KH. The assessment of fetal brain morphology and circulation by transvaginal 3D sonography and power Doppler. J Perinat Med 2002; 30:48–56.
55. Pooh RK, Pooh KH. Fetal neuroimaging with new technology. Ultrasound Review Obstet Gynecology 2002; 2:178–81.

Chapter 20
Ultrasound Examination of the Fetal Thorax

Zoltan Papp

THE THORAX

During fetal life the lungs are not inflated and are visualized as solid structures that fill the space between the heart and the rib cage. Examination of the lungs using the same section as for the four-chamber view of the fetal heart is sufficient (Fig. 20.1). Under normal conditions, the fetal lungs are uniformly echogenic. The echogenicity of the lungs varies in comparison to that of the fetal liver along gestation. At 18–23 weeks, the central third of the thoracic area at the level of the four-chamber view is occupied by the heart, and the remaining two thirds by the lungs.[1–3] This scanning plane can also be used for the measurement of the thoracic circumference, which correlates with the development of the lungs.[4] Cardiac dextroposition is an important sign of intrathoracic mass (diaphragmatic hernia, where the hernia contents only solid organs, cystic adenomatoid malfor-

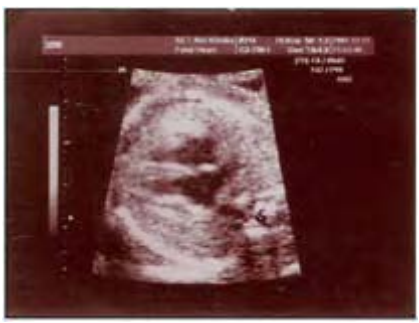

Figure 20.1: Four-chamber view of the thorax

mation of the lungs or extralobar sequestration), significant right lung hypoplasia. A sagittal plane of the fetal trunk usually allows identification of the diaphragm as a thin sonolucent line separating the abdominal from the thoracic cavity. A correct visualization of the chest in the mediosagittal plane is necessary in cases of possible chest hypoplasia (Fig. 20.2). The fetal thymus can be visualized in the transverse section of the fetal chest between the sternum and the great vessels of the heart (the “three vessels view”—

pulmonary artery, aorta and superior vena cava with the trachea to the right of the vessels) and between both lungs (Fig. 20.3). It appears as an oval homogenous structure in the anterior mediastinum, composed of two connected lobes. The importance of prenatal thymus identification and measurement is especially relevant with regard to prenatal diagnosis of DiGeorge syndrome,

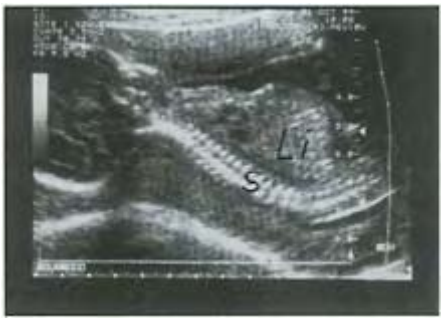

Figure 20.2: Small chest especially when compared to the abdomen (S: spine, Li: liver)

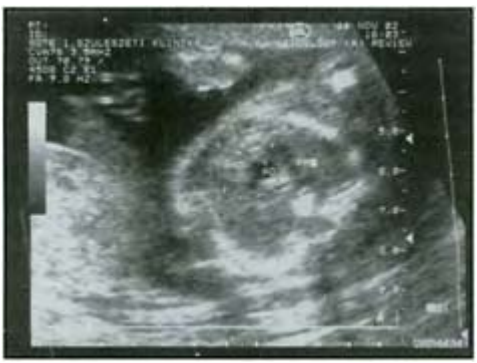

Figure 20.3: Three-vessel view of the thorax for correct measure of the fetal thymus (AO: aorta, AP: pulmonary artery)

chondrodysplasia, severe combined immunodeficiency, acute illnesses, exposure to ethanol, and chorioamnionitis.[5–7]

DIAPHRAGMATIC HERNIA

Diaphragmatic hernia consists of protrusion of the abdominal organs into the thoracic cavity through a diaphragmatic defect. The incidence varies from 0.033 to 0.05% of births. Neonatal surgical series report a frequency of 0.012%. The difference is due to an underestimation of the incidence of the disease because of its association with stillbirth and early neonatal death.[8,9]

The diaphragm is a dome-shaped septum dividing the thoracic and abdominal cavities. It is formed by the fusion of four different structures. The diaphragm is completely formed by the end of the 8th week of conceptional age, with modeling continuing through gestation. The normal diaphragm allows the passage of organs, vessels, and nerves from the thoracic to the abdominal cavity. Congenital diaphragmatic hernias occur when a diaphragmatic defect allows the protrusion of abdominal visceral content into the thoracic cavity. The spectrum of embryologic defects is wide, ranging from complete absence of the diaphragm through pathological orifices to congenital hiatal hernia.

The mechanisms responsible for the origin of diaphragmatic hernia are unknown. The two main hypotheses are delayed fusion of the diaphragm and primary diaphragmatic defect.

Congenital diaphragmatic hernia has been associated with other anomalies (lung hypoplasia and gut malrotation are implied in the diaphragmatic hernia sequence) in 50–57% of cases. These are anomalies of the central nervous, gastro-intestinal, skeletal, genitourinary and cardio-vascular system (23%), as well as chromosomal abnormalities and genetic syndromes (such as Fryns syndrome, de Lange syndrome and Marfan syndrome).[10]

Prenatally the diaphragm is imaged by ultrasonography as an echo-free space between the thorax and abdomen. A definitive diagnosis of diaphragmatic hernia can be made if abdominal organs are seen in the thoracic cavity. Visualization of fluid-filled bowel at the level of the four chamber view of the heart is diagnostic (Fig. 20.4). The ribs and the inferior margin of the scapula can be used as landmarks when trying to establish the intrathoracic location of viscera. These organs can be seen as fluid-filled cystic structures in the thoracic cavity and peristalsis could be observed. The clearest sign of the presence of a congenital diaphragmatic hernia is a shift in the position of the heart within the chest. Polyhydramnios is

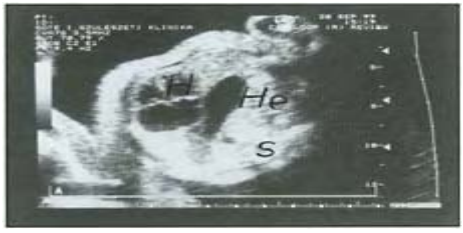

Figure 20.4: Left-sided diaphragmatic hernia. Note dislocation of the fetal heart and the stomach near the left

ventricle (S: spine, H: heart, He: diaphragmatic hernia)

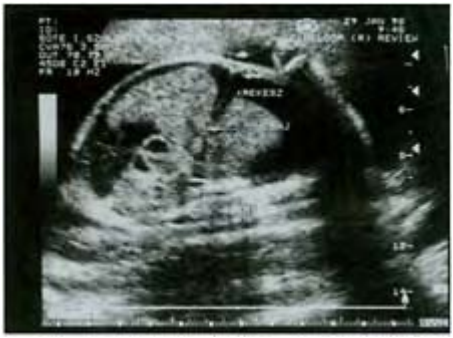

Figure 20.5: Right-sided diaphragmatic hernia, ascites and pleural effusion (diaphragm, liver, spine)

common, usually after 25 weeks. This may be the consequence of impaired fetal swallowing due to compression of the esophagus by the herniated abdominal organs. The diagnosis of right diaphragmatic hernia is extremely difficult because of the similar echogenicity of the liver and lungs. The presence of non-immune hydrops is common with right diaphragmatic hernia (Fig. 20.5). The mechanism of fluid accumulation is thought to be related to an obstruction of venous return. Small congenital diaphragmatic hernias may not be detected *in utero*.

The main differential diagnosis is in the case of cystic lung disease, such as cystic adenomatoid malformation or mediastinal cystic processes (neuroenteric cysts, bronchogenic cysts and thymic cysts). In these cases, in contrast to diaphragmatic hernia, the upper abdominal anatomy is normal.

In humans, the bronchial tree is fully developed by the 16th week of gestation, at which time the full number of airways is established. The alveoli continue to develop even after birth, increasing in number and size until the growth of the chest wall is completed in adulthood. The growth of blood vessels supplying the acinus (intra-acinar vessels) parallels alveolar development, while the growth of pre-acinar vessels follows the development of the airways. In diaphragmatic hernia, the reduced thoracic space is available to the deve loping lung and leads to a reduction in airways, alveoli and arteries. Furthermore, there is an increase in arterial medial wall thickness and extension of muscle peripherally into the small preacinar arteries, offering an explanation for the pulmonary hypertension and persistent fetal circulation observed after neonatal repair.[11–14] Thus, although isolated diaphragmatic hernia is an anatomically simple defect, which is easily correctable, the mortality rate is about 50%.[15] The main cause of death is hypoxemia due to pulmonary hypertension, resulting from the abnormal development of the pulmonary vascular bed.[16,17]

Congenital Cystic Adenomatoid Malformation

Congenital cystic adenomatoid malformation (synonyms: CAM, congenital adenomatoid malformation) of the lung is a hamartoma of the lung cha-racterized by overgrowth of terminal bronchioles (adenomatoid) at the expense of saccular spaces. The respiratory tract includes the conducting airways and the respiratory component. They have different embryologic origins. The conduction airways are derived from the foregut (endoderm), whereas the respiratory component arises from mesenchyma that concentrate around the tips of the growing bronchi. The embryologic problem responsible for cystic adenomatoid malformation is thought to be an arrest of the connection of the two systems and subsequent overgrowth of the terminal bronchioles, occurring before the 5th week of conceptional age. Although the lesion may be bilateral involving entire lung tissue, the lesion is almost always unilateral. It is quite a rare malformation, found in about 1 in 4000 births.[18,19]

Prenatal diagnosis is based on the ultrasonographic finding of a nonpulsatile hyperechogenic pulmonary tumor, cystic or solid consistence. It is often large enough to cause a shift of the mediastinal structures and to compress the contralateral lung. A significant shift can be detected by displacement of the cardiac silhouette. Stocker et al proposed a classification of congenital cystic

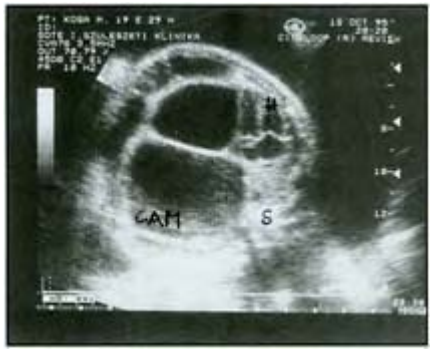

Figure 20.6: CCAM type 1 with especially large cysts on the left side of the fetal chest. The heart is severely dislocated and the right lung is compressed (S: spine)

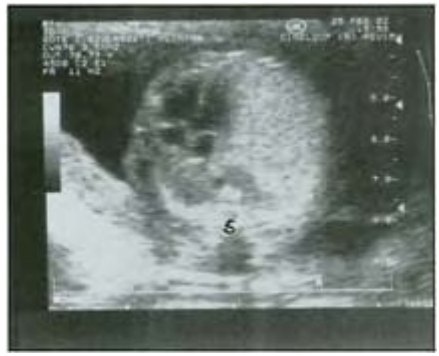

Figure 20.7: Left-sided CCAM type 3. A hyperechogen terime is on the left side of the fetal chest above the diaphragm. (S: spine)

adenomatoid malformation into three subtypes according to the size of the cysts.[20] Type I has large cysts (Fig. 20.6), type II has multiple small cysts of less than 1.2 cm in diameter, and type III consists of a noncystic or microcystic lesion producing mediastinal shift (Fig. 20.7). The worst prognosis is seen in type III lesions. Associated anomalies (renal, gastrointestinal, cardial, bronchial) are frequently present in type II. Polyhydramnios and nonimmune hydrops are frequently present in the cases detected prenatally. Polyhydramnios is probably related to esophageal compression. Fetal hydrops can result from decreased venous return due to vascular compression by the

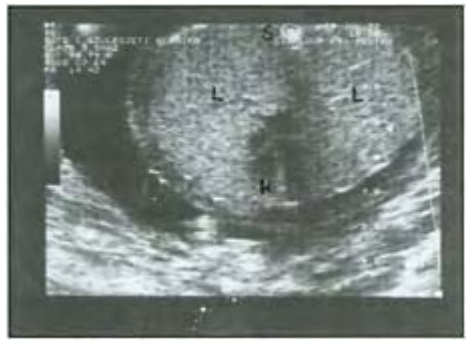

Figure 20.8: Tracheal atresia. Severe overgrowth of both lungs, which are hyperechogenic. The heart is small. Small amount of pleural effusion (H: heart, L: lung, S: spine)

pulmonary mass or decreased myocardial contractility. Hydrops is more commonly associated with the microcystic lesion. Differential diagnosis includes thoracic lesions, as diaphragmatic hernia, bronchogenic cysts, pulmonary sequestration, lymphangio-hemangioma, tracheal atresia (Fig. 20.8). Extralobar pulmonary sequestration can be differentiated because it appears as a solid lesion without cysts, with a pyramidal shape. The management and prognosis depend on the presence of associated hydrops. Serial scans are recommended to monitor the growth of the lesion and to look for early signs of hydrops. The mortality rate of fetuses with hydrops can be as high as 100%. Prognostic features for a poor outcome include major lung compression causing pulmonary hypoplasia, polyhydramnios and development of hydrops fetalis irrespective of the type of the lesion.[21,22] Prenatal diagnosis mandates delivery in a tertiary care center, where immediate thoracic surgery can be performed.

Sequestration of the Lungs

Lung sequestration is one of the bronchopulmonary foregut malformations, a term that refers to a group of anomalies of the respiratory and gastrointestinal tracts that originate from the embryonic foregut. It is a rare and sporadic abnormality. A sequestered lung either originates from a separate outpouching of the foregut or is a segment of a developing lung that has lost its connection with the rest of the tracheobronchial tree. If the accessory lung bud arises before the formation of the pleura, the sequestered lung will be adjacent to the normal lung and surrounded by the same pleura (intralobar sequestration). If the accessory lung bud arises after formation of the pleura, the sequestered lung will have its own pleura (extralobar sequestration). The difference between these two conditions (which is based on the presence or absence of a separate pleural covering from the normal lung) cannot be accurately determined with prenatal ultrasound. In some cases the sequestrated lung connects to the gastrointestinal tract. This occurs when the pedicle of the accessory lung bud does not involute.

The arterial supply and venous drainage are primarily provided by systemic vessels. In intralobar sequestration the venous drainage terminates in the pulmonary veins.

Extralobar sequestration is usually located between the lower lobe and the diaphragm. Other locations include paracardiac, mediastinal, infrapericardial, infradiaphragmatic and abdominal sites (Fig. 20.9).[23]

Foregut malformations are associated with each other more frequently than would be expected by chance. These are: tracheo-esophageal fistula, esophageal duplications, neurenteric cysts, esophageal diverticulum, esophageal cysts, and bronchogenic cysts.[24–27] Extrapulmonary anomalies occur in 10% of patients with intralobar sequestration, and they include: skeletal deformities, diaphragmatic hernia, congenital heart diseases, renal and cerebral anomalies. In extralobar sequestration the incidence of extrapulmonary anomalies is as high as 60%, including diaphragmatic hernia, heart anomalies, funnel chest, vertebral defects and megacolon.

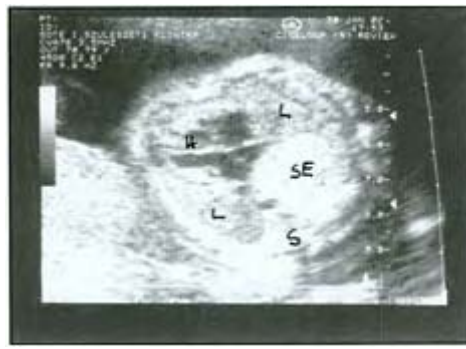

Figure 20.9: Hyperechogen terime is on the right side of the fetal chest, which is an extralobar sequestration. The heart is mildly dislocated (H: heart, L: lung, S: spine, SE: sequestratum)

The sequestrated lung appears as a homogenous, brightly echogenic mass in the lower lobes of the lungs or in the upper abdomen (Fig. 20.10). The diagnosis is confirmed by color Doppler demonstration that the vascular supply of the sequestrated lobe arises from the abdominal aorta. Large lung sequestration may act as an arteriovenous fistula and cause high-output heart failure and hydrops (Fig. 20.13).[28,29] Differential diagnosis should include mediastinal teratomas, whose high density usually causes an acoustic shadowing behind the mass, and cystic adenomatoid malformation of the lung (type III). Extralobar lung sequestration may simulate the

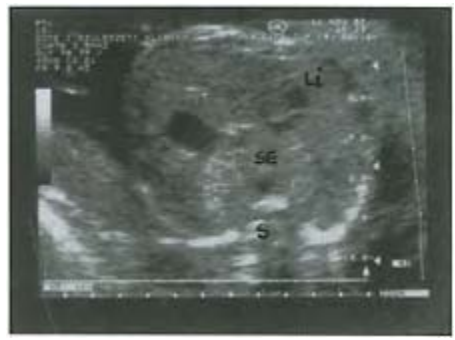

Figure 20.10: A hyperechogen terime around the spine, which is an extralobar pulmonary sequestratum in the abdominal cavity (S: spine, SE: sequestratum, Li: liver)

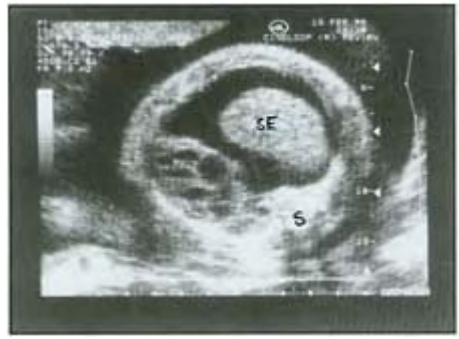

Figure 20.11: Extralobar lung sequestratum is on the right side of the chest with dislocation of the fetal heart and large pleural effusion (S: spine, RV: right ventricle, LV: left ventricle, SE: sequestratum)

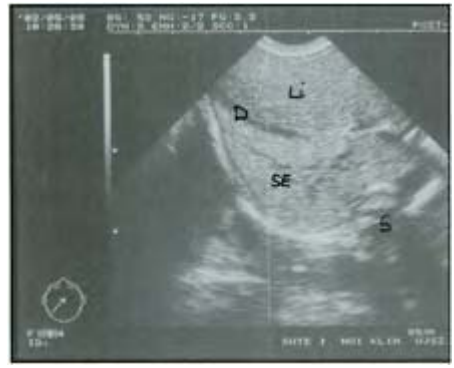

Figure 20.12: At the postnatal ultrasound examination of the prenatally diagnosed extralobar lung sequestration, the sequestratum looks like an echogenic, solid terime above the diaphragm. The diaphragm is a hypoechogenic line between the liver and the sequestratum (S: spine, SE: sequestratum, D: diaphragm, Li: liver)

pyramidal shape of a lower lobe. It should also be considered in the differential diagnosis of intra-abdominal solid masses, such as mesonephroma. There has been some

experience that the size of the hyperechogen mass decreases toward the end of pregnancy. The position of the mediastinum is normal and sometimes there is no sign of the previously detected and documented hyperechogen mass. In such cases postnatal examination is important as there usually is a sonographically detectable mass in the chest (Fig. 20.12).

Pleural Effusions

Fetal pleural effusions, which may be unilateral or bilateral, may be an isolated finding or they occur in association with generalized edema and ascites. Chylothorax is a common cause of pleural effusion. Its prevalence has been estimated to be 1:10,000 deliveries.

Accumulation of lymph within the pleural cavity can result from overproduction or impaired reabsorption of lymph. The latter could be due to either an obstruction to pulmonary lymph drainage or abnormal lymphatic vessels.[29,30]

Chylothorax occurs as a unilateral pleural effusion involving the right side of the lung in most instances. In rare cases, pleural effusions can be bilateral. Chylothorax may lead to lung compression and the development of pulmonary hypoplasia. Unilateral effusion can also shift the mediastinum, impair venous return, and lead to congestive heart failure and hydrops.

Chylothorax may be associated with trisomy 21, congenital pulmonary lymphangiectasis, tracheoesophageal fistula, extralobar lung sequestration and a multiple malformation complex.

Chylothorax should be suspected in the presence of a pleural effusion (Fig. 20.13).

A specific diagnosis is not possible on the basis of a gross appearance of the fluid. Indeed, lymph

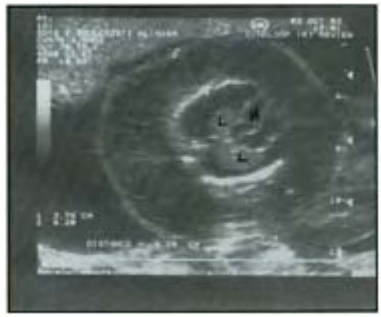

Figure 20.13: Bilateral pleural effusion. The lung is compressed. The pleural effusion is part of a generalized severe hydrops fetalis. (L: lung, H: heart)

looks serous at birth and becomes lactescent only after oral feedings. It has been suggested that identification of abundant lymphocytes (>60%) in pleural fluid indicates

chylothorax. The pleural effusion may be associated with nonimmune hydrops.[31] Polyhydramnios has been noted in all cases diagnosed prenatally. It may be the result of esophageal compression by the pleural effusion. Irrespective of the underlying cause, infants affected by pleural effusions in the neonatal period usually exhibit severe, and often fatal, respiratory insufficiency. This is either a direct result of pulmonary compression caused by the effusions, or is due to pulmonary hypoplasia secondary to chronic intrathoracic compression. The overall mortality of neonates with pleural effusions is 25%, with a range from 15% in infants with isolated pleural effusions to 95% in those with gross hydrops.

The prenatal therapy of repeated thoracocentesis for drainage of pleural effusions has generally been unsuccessful in reversing the hydropic state, because the fluid reaccumulates within 24–48 hours of drainage. A better approach is chronic drainage by the insertion of thoracoamniotic shunts. This is useful for both diagnosis and treatment. The diagnosis of underlying cardiac abnormalities or other intrathoracic lesions may become apparent only after effective decompression and return of the mediastinum to its normal position. The chronic drainage can reverse fetal hydrops, resolve polyhydramnios and thereby reduce the risk of preterm delivery, and may prevent pulmonary hypoplasia. It may help to distinguish between hydrops due to primary accumulation of pleural effusions in which case the ascites and skin edema may resolve after shunting, and other causes of hydrops such as infection, in which drainage of the effusions does not prevent worsening of the hydrops.

REFERENCES

1. Abdullah MM, Lacro RV, Smallhorn J et al. Fetal cardiac dextroposition in the absence of an intrathoracic mass: sign of significant right lung hypoplasia. J Ultrasound Med 2000; 19(10):669–76.
2. Devine PC, Malone FD. Noncardiac thoracic anomalies. Clinics in Perinatology 2000; 27(4):865–99.
3. Crane JM, Ash K, Fink N et al. Abnormal cardiac axis in the detection of intrathoracic anomalies and congenital heart disease. Ultrasound Obstet Gynecol 1997; 10(2):90–93.
4. Chitkara et al. Relationship between the gestational age in weeks and thoracic circumference and length in centimeters. Am J Obstet Gynecol 1987; 156: 1069–72.
5. Zalel Y, Gamzu R, Mashiach S et al. The development of the fetal thymus: an in utero sonographic evaluation. Prenat Diagn 2002; 22:114–17.
6. Toti R De Felice C, Stumpo M et al. Acute thymic involution in fetuses and neonates with chorioamnionitis. Hum Pathol 2000; 31:1121–28.
7. Game E, Haeusler M, Bariscic I et al. Congenital diaphragmatic hernia: evaluation of prenatal diagnosis in 20 European regions. Ultrasound Obstet Gynecol 2002; 19(4):329–33.
8. Adzick NS, Harrison MR, Crombleholme TM et al. Fetal lung lesions: Management and outcome. Am J Obstet Gynecol 1998; 179(4):884–89.
9. Thorpe-Beeston JG, Gosden CM, Nicolaides KH. Prenatal diagnosis of congenital diaphragmatic hernia: associated malformations and chromosomal defects. Fetal Ther 1989; 4:21–28.
10. Paladini D, Palmieri S, Celentano E et al. Pulmonary venous blood flow in the human fetus. Ultrasound Obstet Gynecol 1997; 10:27–31.
11. Chaoui R, Kalache K, Tennstedt C, Lenz F et al. Pulmonary arterial Doppler velocimetry in fetuses with lung hypoplasia. Eur J Obstet Gynecol Reprod Biol 1999; 84:179–85.

12. Laudy JA, Gaillard JL, Anker JN et al. Doppler ultrasound imaging: a new technique to detect lung hypoplasia before birth? Ultrasound Obstet Gynecol 1996; 7:189–92.
13. Laudy JA, Tibboel D, Robben SG et al. Prenatal prediction of pulmonary hypoplasia: clinical, biometric, and Doppler velocimetry correlates. Pediatrics 2002; 109(2):250–58.
14. Fox HE, Badalian IE, Timor-Tritsch et al. Fetal upper respiratory tract function in cases of antenatally diagnosed congenital diaphragmatic hernia: preliminary observations. Ultrasound Obstet Gynecol 1993; 3:164–67.
15. Tanaka T, Yamaki S, Ohno T et al. The histology of the lung in neonates with tricuspid valve disease and gross cardiomegaly due to severe regurgitation. Pediatr Cardiol 1998; 19(2):133–38.
16. Chaoui R.Fetal echocardiography: state of the art of the state of the heart. Ultrasound Obstet Gynecol 2001; 17:277–84.
17. Kassanos D, Christodoulou CN, Agapitos E et al. Prenatal ultrasound detection of the tracheal atresia sequence. Ultrasound Obstet Gynecol 1997; 10(2): 133–36.
18. Winters WD, Effmann EL, Nghiem HV et al. Disappearing fetal lung masses: Importance of postnatal imaging studies. Pediatr Radiol 1997; 27(6):535–39.
19. Stocker JT, Madewell JE, Drake RM: Congenital cystic adenomatoid malformation of the lung. Classification and morphologic spectrum. Hum Pathol 1977; 8:155.
20. Laberge JM, Flageole H, Pugash D et al. Outcome of the prenatally diagnosed congenital cystic adenomatoid lung malformation: a Canadian experience. Fetal Diagn Ther 2001; 16(3):178–96.
21. Crombleholme TM, Coleman B, Hedricj H et al. Cystic adenomatoid malformation volume ratio predicts outcome in prenatally diagnosed cystic adenomatoid malformation of the lung. Journal of Pediatr Surg 2002; 37(3):331–38.
22. Romero R, Chervenak F, Katzen J et al. Antenatal sonographic findings of extralobar pulmonary sequestration. J Ultrasound Med 1982; l:131–33.
23. Gerle RD, Jaretzki A, Ashley CA et al. Congenital bronchopulmonary-foregut malformation. N Engl J Med 1968; 278:1413.
24. Luet'ic T, Crombleholme TM, Semple JP et al. Early prenatal diagnosis of bronchopulmonary sequestration with associated diaphragmatic hernia. J Ultrasound Med 1995; 14:533–35.
25. MacKenzie TC, Guttenberg ME, Nisenbaum HL et al. A fetal lung lesion consisting of bronchogenic cyst, bronchopulmonary sequestration, and congenital cystic adenomatoid malformation: The missing link? Fetal Diagn Ther 2001; 16(4): 193–95.
26. Kousseff BG, Gilbert-Barness E, Debich-Spicer D. Bronchopulmonary-foregut malformations: A continuum of paracrine hamartomas? Am J Med Genet 1997; 68(1):12–17.
27. Favre R, Bettahar K, Christmann D et al. Antenatal diagnosis and treatment of fetal hydrops secondary to pulmonary extralobar sequestration. Ultrasound Obstet Gynecol 1994; 4:335–38.
28. Weiner C, Varner M, Pringle K et al. Antenatal diagnosis and palliative treatment of non immune hydrops fetalis secondary to pulmonary extralobar sequestration. Obstet Gynecol 1986; 68:275–80.
29. Longaker MT, Laberge JM, Danserau J et al. Primary fetal hydrothorax: natural history and management. J Pediatr Surg 1989; 24:573–76.
30. Weber AM, Philipson EH. Fetal pleural effusion: a review and meta-analysis for prognostic indicators. Obstet Gynecol 1992; 79:281–86.
31. Romero R, Pilu G, Jeanty P et al. Prenatal diagnosis of congenital anomalies. Appleton and Lange; 1988; 195–99.

Chapter 21
Ultrasound Evaluation of the Fetal Heart

Paolo Volpe, Maria Angela Rustico, Mattia Gentile

INTRODUCTION

Congenital heart defects are the most common of all birth defects.[1] They alone make up one-third of all malformations and are responsible for 20% of neonatal deaths and up to 50% of infant deaths attributed to malformations.[2] The incidence reported in the literature ranges from 3 to 10 per 1000 live births.[3]

There are two reasons for this admittedly wide range:

1. The criteria adopted for diagnosis, exclusively clinical in the early 1970s now make use of non-invasive techniques such as ultrasound evaluation of the fetal heart, which enable us to identify minor heart malformations (such as small defects of the interatrial or interventricular septum, and minor valvular stenoses that are impossible to detect by auscultation alone).
2. The period of life monitored for the purposes of diagnosis: in some studies, follow-up observation was limited to the first week of postnatal life, while others continued follow-up until the infant was a year old. In fact, this longer followup makes it possible to detect later-onset heart abnormalities (such as interatrial defects) and this has provided an important contribution to our knowledge about the real incidence of cardiac malformations in the live birth population.

IN UTERO EPIDEMIOLOGY

The epidemiological observations regarding the incidence of heart malformations in intrauterine life are based on necroptic studies and echocardiography examinations. Studies of spontaneous abortion have shown that in a percentage ranging between 2.4% and 15.4% of cases, loss of the fetus was attributable to a heart defect. If we add to these cases those deaths in *utero* which occur late in pregnancy, the frequency of heart malformations in intrauterine life appears even greater, and has been estimated as being five times that reported for the live birth population.

Echocardiography examinations have usually been performed in selected pregnancies because of specific risk factors that are now well known. In this at-risk population, the

incidence is high; according to the selection criteria adopted, it can vary from 5 to 10 per 100.[4–5] Congenital heart malformations detected in *utero* are frequently associated with an abnormal karyotype and extracardiac malformations: in fact, the incidence of aneuploidy is twice as high (20%) as the incidence reported in postnatal populations (10%), and in over one-third of cases there is association with extracardiac malformations/ syndromes. The most desirable effect of prenatal diagnosis is to succeed in detecting abnormalities whose early diagnosis should improve prognosis, not just in terms of survival of the fetus, but of the quality of that survival. In this sense, heart defects are among those abnormalities for which prenatal diagnosis can offer the greatest benefits. If a heart defect can be corrected, early detection makes it possible to plan the birth in a level III Centre, and begin suitable treatment immediately. In fact, preliminary reports indicate that prenatal diagnosis of certain forms of heart defect both improves survival and reduces costs.[6] In cases of incurable heart disease and/or association with chromosomal/extra-cardiac abnormalities, early detection can offer couples the chance of opting for termination of the pregnancy; in these cases, the effect of prenatal diagnosis is to reduce the number of live births suffering from heart defects by 20–25%. The diagnosis of heart malformations is performed by means of fetal echocardiography, a complex examination which requires expert operators, sophisticated equipment, and close collaboration between obstetricians and cardiologists: it is usually indicated in cases of pregnancies with a specific high-risk profile where there is a greater likelihood of heart disease. However, only 30% of the fetuses with heart defects are found among these high-risk pregnancies; in fact, around 70% of heart abnormalities developed in the low-risk fetal population. For this reason, it is vital to include a screening test for the low-risk fetal population as an integral part of the routine ultrasound examination to allow us to identify the fetuses with heart anomalies.

THE SCREENING OF THE FETAL HEART DEFECTS

For some time now, the 4-chamber view of the fetal heart has been used as a screening test for congenital heart malformations since it was reported to be the simplest method of detecting most heart defects. Results have been conflicting, and differences in study methodology have made it difficult to compare the various findings.[7,8] Sensitivity varies from 5% to 60%, with ail average of around 35% for the most serious malformations, well below the levels to be expected from an effective screening test. This low performance is especially due to the intrinsic limitations of the 4-chamber view: it explores only the atrioventricular and not the ventricular-arterial junction, whereas possible defects of this junction make up the most important group of duct-dependent heart anomalies which can benefit from prenatal diagnosis, and which can best be checked for by inspecting the outflow tracts. Evaluation of the fetal heart extended to the great vessel connections is not yet considered feasible in low-risk pregnancies since it is time-consuming, difficult both to teach and to learn, and still of unproven cost-benefit. In spite of this, there is increasing pressure on health professionals to include evaluation of the outflow tracts with the 4-chamber view, by training operators to learn how to look at this section.[9] The level of training of the operators is therefore crucial since it is

reasonable to suppose that even a less experienced operator with the right teaching support can learn how to perform an accurate examination of the fetal heart.

The Fetal Heart Scanning

Although by the late first and early second trimesters of gestation,[10] the cardiac connection can be identified in most patients, fetal echocardiography is commonly performed at 18–22 weeks.

The standard projections that should be obtained for a complete evaluation of the fetal heart include:

Transverse and Oblique Views

- The transverse view of the upper abdomen
- The four-chamber view
- The three-vessels view
- The left ventricular outflow tract view
- The right ventricular outflow tract view
- The short axis view of the great vessels
- The aortic and ductal arch view.

Longitudinal Views

- The long axis of the inferior and superior vena cava
- The long axis of the aortic and ductal arch.

Before obtaining these views, it is necessary to identify the position of the fetal head and spine to determine the right and left sides of the fetus.

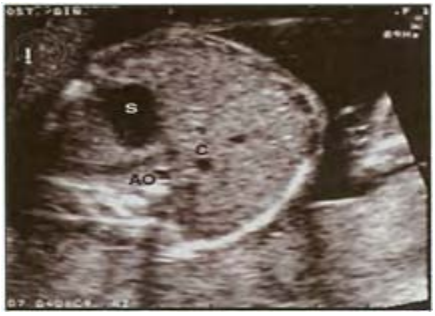

Figure 21.1: The transverse view of the upper abdomen shows the normal relationship of the aorta and inferior vena cava. The aorta (AO) is located anteriorly and to the left of the spine,

the inferior vena cava (C) is anterior and to the right of the aorta. S=stomach

Transverse and Oblique Views

The Transverse View of the Abdomen

This view allows observation of the location of the stomach, liver, abdominal aorta and inferior vena cava which denotes the situs. In the normal arrangement, situs solitus, the stomach is seen on the left half of the abdomen and the larger liver lobe is seen on the right; the aorta is located posteriorly at the left anterior aspect of the spine, and the inferior vena cava is located more anteriorly on the right (Fig. 21.1). In a mirrorimaged arrangement, situs inversus, this left-right relationship is reversed.

In rare cases, the arrangement of the abdominal organs does not conform to the above patterns; an abnormal arrangement is called situs ambiguus, and is almost always associated with asplenia or polysplenia. In cases of asplenia or right isomerism the aorta and inferior vena cava are often on the same side of the spine; in cases of polysplenia or left isomerism, interruption of the suprarenal segment of the inferior vena cava is often present, with continuation through the azygous or hemiazygous vein. The azygous vein is posterior to the aorta (Fig. 21.2).

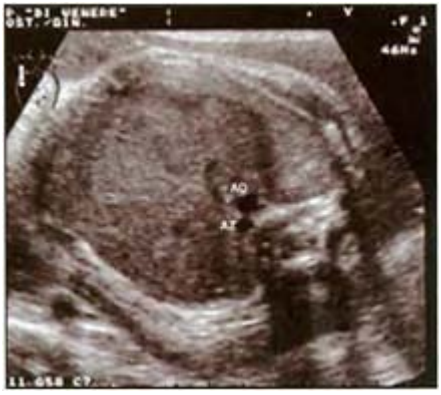

Figure 21.2: Left isomerism: the transverse view of the upper abdomen shows a vessel to the left and posterior to the descending aorta. This appearance is suggestive of the diagnosis of the left atrial isomerism. AZ=azygous vein; AO=aorta

Since it is very difficult at fetal echocardiography to identify the atrial arrangement, because this is in harmony with the arrangement of the abdominal organs in most cases, it is preferable to predict the atrial situs on the basis of the visceral situs. Hence, abnormal arrangements of the abdominal organs will alert the physician to the likely presence of heart defects.

The four-chamber view

Since the fetal heart lies horizontally in the thorax, to obtain a four-chamber view from the lateral section of the upper abdomen it is necessary to slide the transducer toward the fetal chest, maintaining the transverse plane. The fetal rib corresponding to a 4-chamber view plane is the 4th rib. When multiple ribs are visualized along the two lateral chest walls, an oblique rather than a transverse view is obtained.

According to the fetal position, there are three types of four chamber views of the fetal heart. When the left anterior chest wall is closest to the transducer, an apical four-chamber view is obtained; when the fetal spine is anterior and closest to the transducer, a basal four-chamber view is obtained; in these 2 sections the ultrasound beam is almost parallel to the ventricular septum. When the fetal spine is lateral, closer to the lateral uterine walls, a transverse four-chamber view is obtained. Among these three views, the apical and transverse four-chamber views are better projections for evaluating the fetal cardiac axis, position, size, structure.

Axis The fetal cardiac axis is the angle that the ventricular septum forms with the midline of the thorax. The normal axis lies at a 40°±20° angle to the left of the midline (levocardia) (Fig. 21.3). An abnormal angle of the heart can indicate a cardiac malformation; when it is associated with an abnormal heart position, in most cases this is the result of a space-occupying lesion in the thoracic cavity such as diaphragmatic hernia.

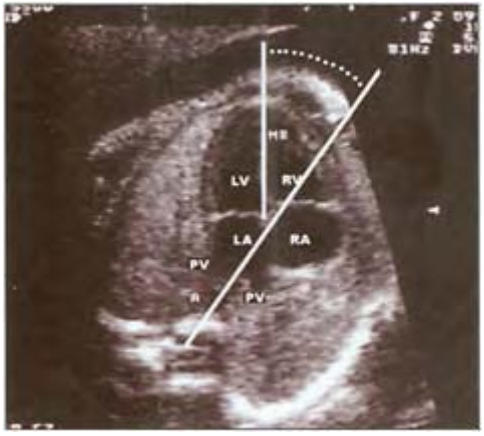

Figure 21.3: The ventricular septum forms an angle of about 40° to the midline of the thorax. LA: left atrium,

LV: left ventricle, RA: right atrium, RV: right ventricle, MB: Moderator band, PV: pulmonary veins

Position Normally 2/3 of the heart lies in the left chest and 1/3 in the right chest. An abnormal position of the heart (dextroposition, etc.) results from extrinsic factors such as a space-occupying lesion within the chest (Fig. 21.4).

Size The heart occupies 1/3 of the thorax. The heart area can easily be compared to the area of the thorax and the ratio should be one-third or less.

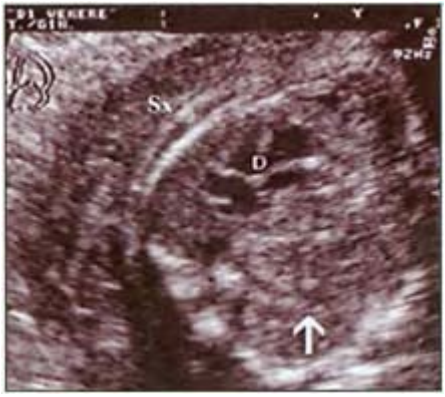

Figure 21.4: The transverse view of the chest in a fetus with a right-sided diaphragmatic hernia, with location of the liver (arrow) in the right chest. The heart is displaced to the left by the liver. D: ventricular septal defect

Structure In the four-chamber view the following structural features should be observed:

- Two equal-sized atria
- Two equal-sized ventricles
- Two atrioventricular valves with complete leaflet excursion and different insertion on the ventricular septum
- The pulmonary veins connected to the left atrium
- Intact inlet and muscular portions of the ventricular septum
- The foramen ovale occupying the middle third of the atrial septum, with its flap valve lying in the left atrium
- The right ventricle can be identified by the presence of a moderator band and by the septal attachment of its atrioventricular valve, that is lower than that of the morphologically left ventricle (Fig. 21.5).

The right ventricle is the chamber closest to the anterior chest wall and the left atrium is the chamber closest to the spine (Fig. 21.5). Near to the term of pregnancy, the right ventricle is mildly predominant with respect to the left ventricle.

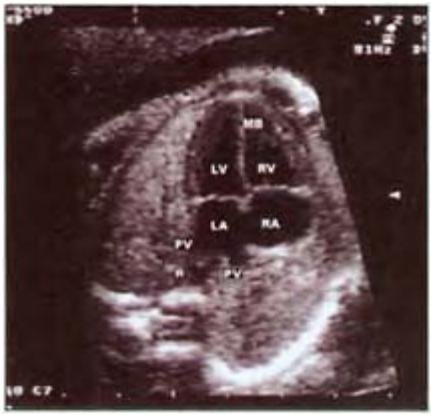

Figure 21.5: Four-chamber view: the right ventricle (RV) lies below the sternum; the left atrium(LA) is anterior to the spine. Note the pulmonary veins (PV) that connect the left atrium and the presence of a moderator band (MB) in the right ventricle. RA: right atrium; LV: left ventricle

The Left Ventricular Outflow Tract View

From a lateral four-chamber view, the left ventricular outflow tract view can be obtained by slight angulation of the transducer towards the fetal right shoulder. In this view it is important to note the continuity between the anterior wall of the ascending aorta with the ventricular septum (Figs 21.6A and 21.6B) and the posterior leaflet of the aortic valve with the anterior leaflet of the mitral valve. The aorta courses from the right to left atria and inferior to the pulmonary artery before it emerges from the heart and turns leftward to form the aortic arch. This projection also shows the perimembranous and outlet portions of the ventricular septum.

The Right Ventricular Outflow Tract View

From the long-axis view of the left ventricle, the right ventricular outflow tract view can be obtained by sliding the transducer slightly upward towards the fetal head. This view shows the pulmonary artery as it arises from the right ventricle (Fig. 21.7) and courses anteriorly and cranially to the aorta, crosses over it, and then divides into the right and

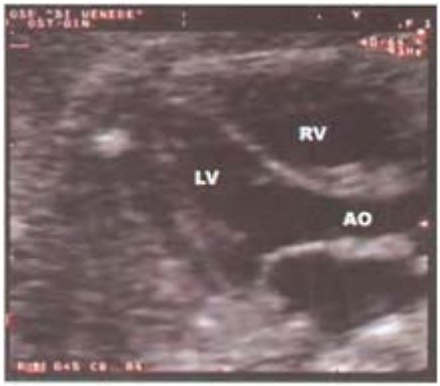

Figure 21.6A: The long axis view of the left ventricle. The anterior wall of the aorta is continuous with the septum; note also the perimembranous and outlet portions of the ventricular septum. LV: left ventricle; RV: right ventricle; AO: aorta

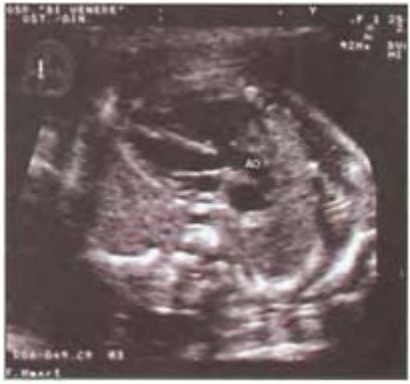

Figure 21.6B: The typical ventricular septal defect and aortic override are seen on a long axis view of the left ventricle in a fetus with tetralogy of Fallot. AO: aorta.

left pulmonary arteries and the ductus arteriosus which connects with the descending aorta. In other words, the long axis of the aorta and of the pulmonary artery are perpendicular to each other as they arise from their respective ventricles. This anatomic

orientation is lost in cases of transposition of the great vessels, in which the two vessels are parallel, not crossing at the level of the semilunar valves (Fig. 21.8).

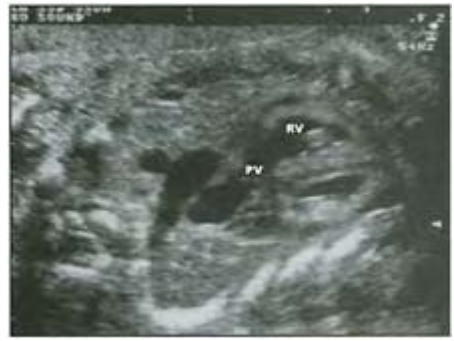

Figure 21.7: The long axis of the right ventricle. Note the pulmonary artery, that arises from the right ventricle (RV), the infundibulum and pulmonary valve (PV)

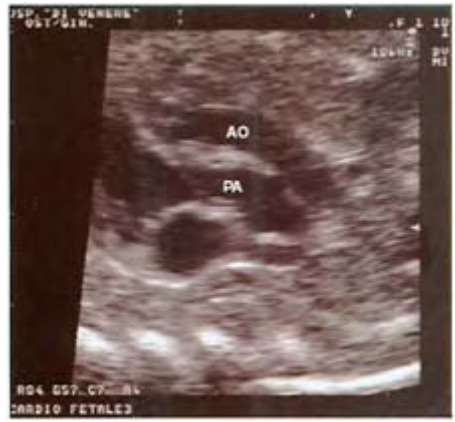

Figure 21.8: Parallel arrangement of the two great arteries in a fetus with transposition of the great arteries. AO: aorta; PA: pulmonary artery

The Short Axis View of the Great Vessels

From a lateral four-chamber view, the short axis view of the great vessels can be obtained by angling the transducer towards the fetal left shoulder. In this view, the aorta

appears as a circular structure with the pulmonary artery coursing over it, before it divides into the right pulmonary artery and the ductus arteriosus (Fig. 21.9). This is also an ideal view for visualizing the normal connection of the right heart segments (or structure), the normal cross-over of the great

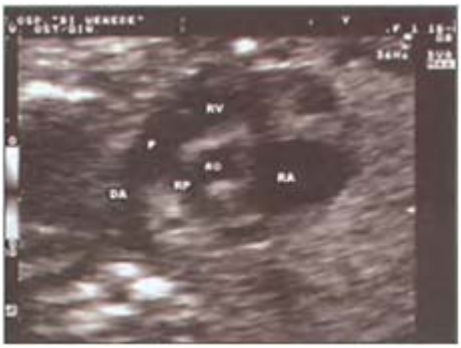

Figure 21.9: Short axis view of the great arteries: the aorta (AO) appears as a circular structure with the pulmonary artery (P) coursing over it before it divides into the right pulmonary artery (RP) and the ductus arteriosus (DA). RA: right atrium; RV: right ventricle

arteries and the normal size relationship of the 2 vessels.

The Three-Vessels View

From a four-chamber view, the three-vessels view is obtained by sliding the transducer cranially, while maintaining the transverse plane; it demonstrates the round cross section of the ascending aorta and superior vena cava and an oblique section of the main pulmonary artery. The pulmonary artery is the largest of the three vessels, and lies furthest to the left anterior, the ascending aorta is next, both in position and size, and the superior vena cava lies furthest to the right posterior (Fig. 21.10).[11] By slight sweeping of the transducer, the right pulmonary artery, the left pulmonary artery and the ductus arteriosus can easily be visualized. In cases of abnormal vessel size, alignment, arrangement and number, a congenital heart disease is present.

The Aortic and Ductal Arch View

The transverse view of the aortic arch is obtained by sliding the transducer upwards towards the fetal head from the three vessels plane. In this view, the aortic arch and the trachea are visualized on the same plane (Fig. 21.11). The aortic arch is

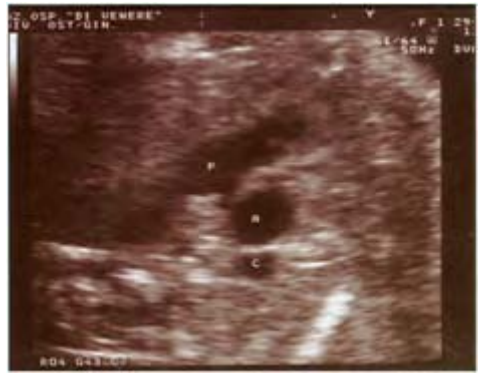

Figure 21.10: Three-vessels view: the pulmonary artery (P) is the largest of the three vessels, the ascending aorta (A) is between the pulmonary artery and superior vena cava in position and size and the superior vena cava (C) is the smallest, most posterior vessel

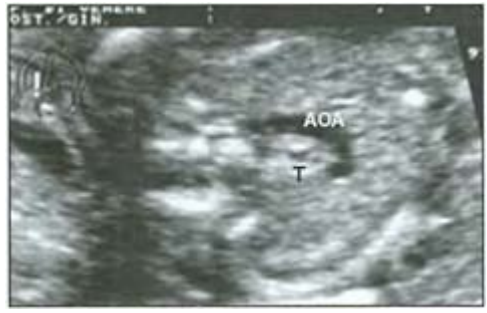

Figure 21.11: The transverse view of the aortic arch: the aortic arch (AOA) and the trachea (T) are visualized on the same plane

visualized in this section as the most superior vessel in the thorax, crossing the midline in front of the spine. It lies superior to the transverse section of the ductal arch.

By a slight caudal tilt of the transducer to the left it is possible to simultaneously visualize the aortic arch and duct. They are of similar size and the direction of blood flow in both vessels is the same. In this view the thymus can be identified as structure in front of the great vessels, between the lungs (Fig. 21.12).

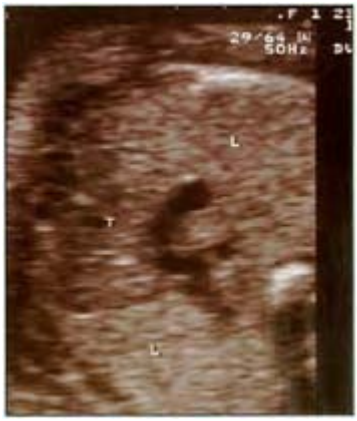

Figure 21.12: A transverse section of the fetal upper thorax shows the thymus (T) between the lung lobes (L) in front of the vessels

Longitudinal Views

By sliding the transducer from the right to the left parasagittal chest, maintaining the same orientation, it is possible to obtain three ultrasonographic planes; the superior and inferior venae cavae, the aortic arch and the ductal arch, respectively.

The Long Axis View of the Aortic Arch

The aortic arch is circular and forms a candy-cane shape; the three head vessels, the innominate, the left common carotid and the left subclavian, arise from the superior aspect of the arch (Fig. 21.13); the right pulmonary artery lies below the arch.[12,13] Of particular importance is the section of isthmus, the distal portion of the transverse aortic arch between the left subclavian artery and the duct, because this is where most *in utero* coarctations occur. However, especially when the coarctation is moderate, the diagnosis is extremely difficult to perform *in utero*. It is also important to control the continuity of the aortic arch.[12,13]

The Long Axis View of the Ductal Arch

From the long axis view of the aortic arch, the long axis view of the ductal arch is obtained by sliding the transducer to the left and anteriorly.

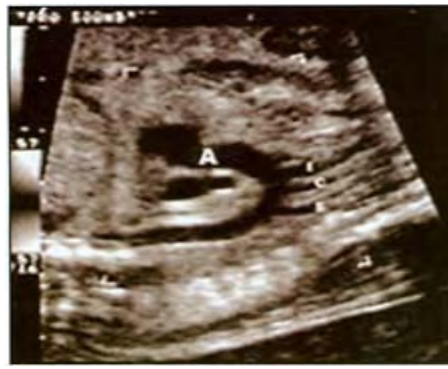

Figure 21.13: The long-axis of the aortic arch: the three neck vessels, the innominate (I), the left common carotid (C) and the left subclavian (S), arise from the superior aspect of the arch. A=aorta

The ductal arch consists of the pulmonary artery, ductus arteriosus and descending aorta; its shape has been likened to that of a hockey stick (Fig. 21.14). The patent duct allows 70–80% of the right ventricular output to bypass the pulmonary bed. Ductal constriction in the fetus can be caused by

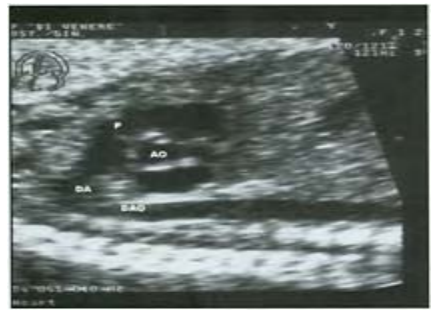

Figure 21.14: The long-axis of the ductal arch: The ductal arch is described as having a “hockey stick” appearance. AO=ascending aorta;

P=pulmonary artery; DA=ductus arteriosus; DAO=descending aorta

indomethacin therapy and other anti-inflammatory agents administered in the mother after 30–32 weeks' gestation. In the majority of cases the constriction regresses when therapy is discontinued.

The Long Axis View of the Inferior and Superior Venae Cavae

By sliding the transducer from the left to the right parasagittal chest, the long axis view of the inferior and superior venae cavae is obtained. This projection demonstrates the inferior vena cava and superior vena cava, that are the same size and connect to the right atrium (Fig. 21.15).

After two-dimensional echocardiography, color Doppler evaluation of the fetal heart is the most important examination method in the diagnosis of cardiac anomalies. In fact, for a detailed study of the fetal heart, color flow mapping is commonly used. Furthermore, in some forms of CHD, the use of pulsed Doppler may also be necessary to complete the evaluation.

Pulsed and color Doppler ultrasound improve the diagnostic accuracy of two-dimensional scanning for the detection of fetal heart defects. Color Doppler is used for the general assessment

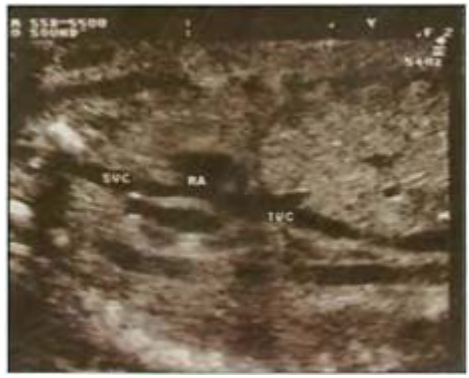

Figure 21.15: The long-axis of the inferior and superior venae cavae: this projection demonstrates the inferior vena cava (IVC) and superior vena cava (SVC), that are similar in size and connect to the right atrium (RA)

of flow in the region of interest, and pulsed Doppler for a targeted examination of flow in a vessel or across a valve.[14] Examination of the fetal heart with color Doppler is

performed along the same planes as gray-scale imaging but the angle of insonation is different; it should be as small as possible.

However, there are confidence limits with even detailed fetal heart scanning, related to the developing or progressive lesions such as aortic and pulmonary stenosis, or to the subtle lesions such as small ventricle defects. In addition, there are some lesions (i.e. a persistent arterial duct and an atrial septal defect), which are undetectable before birth. It should be also noted that confidence limits may be much wider with poor image quality. The image quality is dependent on the combination of operator skill and experience, machine resolution, gestational age, fetal position, and the thickness of the maternal abdomen.

Early Fetal Echocardiography

It is possible to evaluate the normal heart anatomy and recognize many heart defects early on in pregnancy (13–15 weeks) by means of high frequency transvaginal or transabdominal probes.[15] Although this has been proven possible in many case series, and in some studies of both high and low risk fetal populations, the real accuracy of early echocardiography is still unclear and it presents grave limitations. Proof of these limitations in unselected fetal populations has been derived from the observation that some additional cardiac anomalies are missed and suspected anomalies need to be confirmed at a later gestational age. In the high-risk fetal population, the limitations of the early scan are made evident by the type of false-positive emerging (aortic arch defect, ventricular septal defect).[16] The costs in terms of time and equipment and the involvement of operators who are not specifically interested in this field make early screening for fetal cardiac anomalies ill-advised in a low-risk population. This examination should only be performed by expert operators on fetuses specifically at risk for cardiac disease, i.e. extracardiac anomalies, a positive family history.

CONCLUSION

Fetal echocardiography allows the cardiac structures to be visualized from the late first and early second trimesters of gestation onwards, enabling early diagnosis of heart defects,[10] evaluation of their associations with cytogenetic anomalies[17] and formulation of an appropriate management plan for affected fetuses.[6]

Evaluation of the fetal heart with a fourchamber view has become an integral part of the fetal anatomical survey during routine obstetric scanning. However, the four chamber view alone does not enable detection of the great vessels or of aortic arch anomalies, therefore in pregnancies at increased risk of CHD, a complete cardiac evaluation is required.

REFERENCES

1. Ferencz C, Neill CA, Baughman JA et al. Congenital cardiovascular malformations associated with chromosome abnormalities: an epidemiologic study. J Pediatr 1989; 114:79–86.

2. Hoffman JIE, Christiansen R. Congenital heart disease in a cohort of 19502 births with long term follow up. Am J Cardiol 1978; 42:641–47.
3. Mebergh A, Otterstad JE, Froland G et al. Increasing incidence of ventricular septal defects caused by improved detection rate. Acta Pediatr 1994; 83:653–57.
4. Stewart PA, Wladimiroff JW, Reuss A et al. Fetal echocardiography: a review of a six years experience. Fetal Ther 1987; 2:222–31.
5. Wheller JJ, Reiss R, Allen HD. Clinical experience with fetal echocardiography. Am J Dis Child 1990; 144:49–53.
6. Bonnet D, Coltri A, Butera G et al. Detection of transposition of the great arteries in fetuses reduces neonatal morbidity and mortality. Circulation 1999; 99:916–18.
7. Paladini D. Prenatal screening of congenital heart disease between ethics and cost-effectiveness. Time for a change in current prenatal ultrasound screening policies? Ultrasound Obstet Gynecol 1999; 4:225–28.
8. Gembruch U.Prenatal diagnosis of congenital heart disease. Prenat Diagn 1997; 17:1283–98.
9. Achiron R, Glaser J, Gelernter I et al. Extended fetal echocardiographic examination for detecting cardiac malformations in low risk pregnancies. BMJ 1992; 304:671–74.
10. Allan LD. Fetal echocardiography. In. Moller JH, Hoffman JIE (Eds). Pediatric cardiovascular medicine. Philadelphia: Churchill Livingstone 2000:187–202.
11. Yoo SJ, Lee YH, Kim ES et al. Three-vessel view of the fetal upper mediastinum: an easy means of detecting abnormalities of the ventricular outflow tracts and great arteries during obstetric screening. Ultrasound Obstet Gynecol 1997; 9:173–82.
12. Volpe P, Marasini M, Caruso G et al. Prenatal diagnosis of interruption of the aortic arch and its association with deletion of chromosome 22qll. Ultrasound Obstet Gynecol 2002; 20:327–31.
13. Volpe P, Gentile M, Marasini M.Prenatal diagnosis of type A interrupted aortic arch: an unusual association with 22qll.2 deletion. Pren Diagn 2002; 22:371–74.
14. Chaoui R.Fetal echocardiography: state of the art of the state of the heart. Ultrasound Obstet Gynecol 2001; 17:277–84.
15. Bronshtein M, Zimmer EZ, Milo S et al. Fetal cardiac abnormalities detected by transvaginal sonography at 12–16 weeks gestation. Obstet Gynecol 1991; 78:374–78.
16. Rustico MA, Benettoni A, D'Ottavio G et al. Early screening for fetal cardiac anomalies by transvaginal echocardiography in an unselected population: the role of operator experience. Ultrasound Obstet Gynecol 2000; 16:614–19.
17. Clark EB, Nakazawa M, Takao A. Etiology and morphogenesis of congenital heart disease: twenty years of progress in genetics and developmental biology. New York: Futura Publishing CO Inc., 2000.

Chapter 22
Malformations of the Gastrointestinal System

Vincenzo D'Addario, Luca Di Cagno, Riccardo Tamburro

A correct ultrasonic examination of the fetal gastrointestinal tract includes the visualization of the following structures:

- The stomach (Fig. 22.1)
- The small and large bowels (Fig. 22.2)
- The liver with its main vessels and the gallbladder (Fig. 22.1)

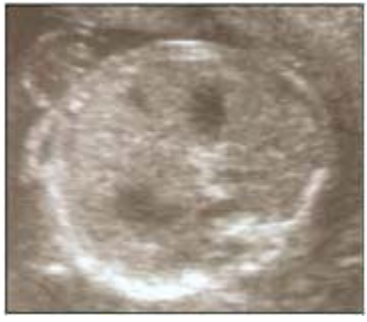

Figure 22.1: Transverse scan of the fetal abdomen showing the stomach, the liver, the intrahepatic tract of the umbilical vein, the gallbladder

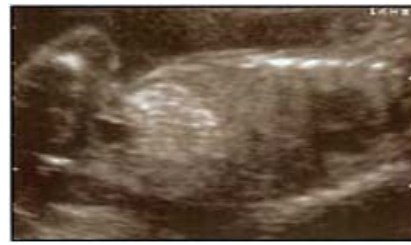

Figure 22.2: Fetal bowel

• The abdominal wall and the insertion of the umbilical cord (Fig. 22.3)
• The diaphragm (Fig. 22.4).

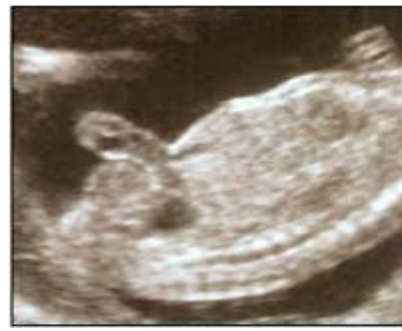

Figure 22.3: Insertion of the umbilical vein into the abdominal wall

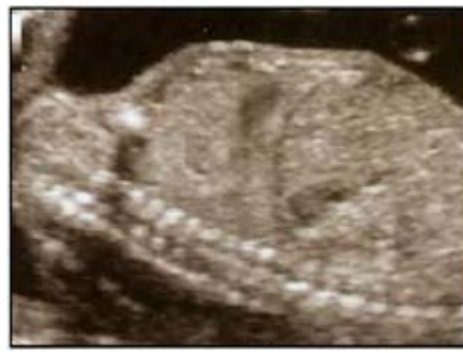

Figure 22.4: Longitudinal scan on the fetal chest and abdomen showing the diaphragm

The malformations of gastrointestinal tract and abdominal wall can be divided in four groups:

1. Anterior abdominal wall defects
2. Diaphragmatic defects
3. Bowel disorders
4. Non-bowel cystic masses.

ANTERIOR ABDOMINAL WALL DEFECTS

The congenital abdominal wall defects include gastroschisis, omphalocele and body stalk anomaly.[1] The ultrasonic prenatal diagnosis of these defects is relatively simple and possible in the first half of pregnancy. However it must be remembered that there is a physiological herniation of the small intestine outside the abdominal cavity between the 5th and the llth weeks of gestation (Fig. 22.5) and therefore a prenatal diagnosis of abdominal wall defect cannot be made in the earliest stage of pregnancy.[2]

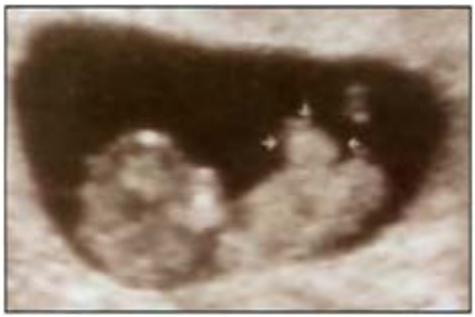

Figure 22.5: Physiological herniation of the midgut at 10 weeks of gestation

Gastroschisis

This malformation consists in a para-umbilical full thickness defect of the anterior abdominal wall which is usually located to the right side of the umbilical cord insertion, associated with evisceration of abdominal organs.

The incidence ranges from 1:10.000 to 1:15.000 live births.

Gastroschisis is considered a sporadic event with a multifactorial etiology, but cases of familial

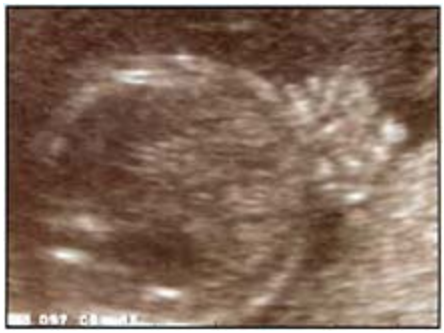

Figure 22.6: Gastroschisis: a cauliflower-like mass protrudes from the abdominal cavity into the amniotic fluid

occurrence have been reported. Young maternal age, maternal cigarette use and vasoactive drugs consumption during first trimester are considered as possible etiological factors.

The malformation results from vascular compromise of either the umbilical vein or the omphalomesenteric artery. The abdominal wall defect is generally small but the amount of bowel protruding from the defect and floating freely in the amniotic fluid may be disproportionately large.

The ultrasonographic diagnosis of gastroschisis is suggested by the finding of a partly solid, partly cystic mass adjacent to the anterior abdominal wall and freely mobile in the amniotic fluid (Fig. 22.6). The differential diagnosis from omphalocele is based on the presence of a normal insertion of the umbilical cord, the lateral location of the mass and the absence of a membrane covering the herniated mass.

In contrast to omphalocele, gastroschisis is rarely associated with other malformations and chromosomal anomalies, but additional gastrointestinal abnormalities (malrotation, atresia, volvulus, infarction) may occur in 20–40% of the cases.[3,4] Intrauterine growth restriction and polyhydramnios are frequently associated. The extent of bowel damage is variable and strictly affects the prognosis Most of the bowel damage is caused by constriction at the site of the abdominal wall defect: the sonographic evidence of small bowel dilatation and mural thickening correlates with severe intestinal damage and poor clinical outcome.

The mode of delivery of fetuses affected by gastroschisis is still controversial although there is no striking evidence for cesarean section over vaginal delivery. Maternal transfer before delivery to a tertiary care centre is recommended. The mortality rate ranges from about 8% to 28%.

Omphalocele

Omphalocele is a ventral wall defect characterized by an incomplete development of abdominal muscles, fascia and skin and the herniation of intra-abdominal organs (bowel

loops, stomach, liver) into the base of umbilical cord, with a covering amnioperitoneal membrane. The defect is thought to be caused by an abnormality in the process of body infolding. The classic omphalocele is a mid-abdominal defect although there is also a high or an epigastric omphalocele (typical of the pentalogy of Cantrell) and a low or hypogastric omphalocele (as seen in bladder or cloacal extrophy), due respectively to cephalic and caudal folding defects. The incidence of omphalocele ranges from 1:4.000 to 1:7.000 live births. It is more frequent in older women; most cases are sporadic, although a familial occurrence with a sex-linked or autosomal pattern of inheritance has been reported.

The ultrasonographic appearance of omphalocele varies according to the type of defect, the presence of ascites and the organs herniated. The principal diagnostic features are: the umbilical cord insertion into the membrane covering the abdominal wall defect, the presence of the intrahepatic portion of the umbilical vein coursing through the central portion of the defect, and the presence of a limiting membrane that can occasionally rupture (Fig. 22.7). There are different syndromes that include omphalocele, such as pentalogy of Cantrell (midline supraumbilical abdominal defect, lower sternum defect, deficiency of diaphragmatic pericardium, anterior diaphragm defect, cardiac abnormality) and Beckwith-Wiedemann syndrome (macroglossia, visceromegaly, omphalocele).

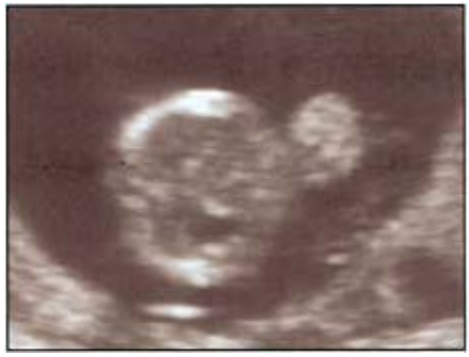

Figure 22.7: Omphalocele: a round solid mass protrudes from the anterior abdominal wall

The most important prognostic variable is the presence of associated malformations (50–70% of cases) or chromosomal abnormalities (30% of cases).[5]

The mode of delivery of fetuses with omphalocele has been debated in literature. The goal in the management is to deliver the fetus as close to term as possible in tertiary care centres. Cesarean section may be necessary to avoid dystocia or sac rupture in large omphaloceles. In the case of small defects vaginal delivery is recommended.

Body Stalk Anomaly

The body stalk anomaly is a severe abdominal wall defect caused by the failure of formation of the body stalk; it is characterized by the absence of umbilical cord and umbilicus and the fusion of the placenta to the herniated viscera. The incidence is 1:14.000 births.

The ultrasonographic diagnosis is suggested by the finding of a large anterior wall defect attaching the fetus to the placenta or uterine wall, the absence of umbilical cord, and the visualization of abdominal organs in a sac outside the abdominal cavity (Fig. 22.8).[6,7] The position of the fetus may lead to scoliosis and kyphosis. Multiple malformations may be associated. The body stalk anomaly is a uniformly fatal condition.

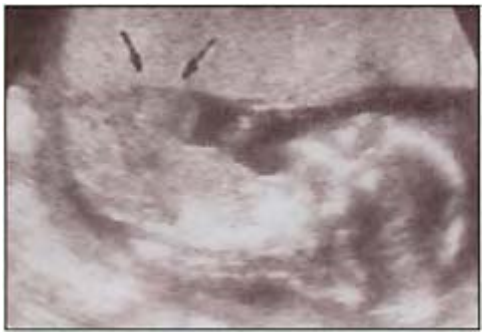

Figure 22.8: Body stalk anomaly: a large anterior abdominal wall defect attaches the fetus directly to the placenta

DIAPHRAGMATIC DEFECTS

The classification of these malformations is based on the location of the diaphragmatic defect:

1. Diaphragmatic hernia (Bochdaleck and Morgagni types)
2. Septum transversum defects (defect of the central tendon)
3. Hiatal hernia (congenital large esophageal orifice)
4. Eventration of the diaphragm
5. Agenesis of the diaphragm.

The incidence of congenital diaphragmatic hernia is 1:3000–1:5000 live births. This entity can be either sporadic or a familiar disorder but its etiology is quite unknown. The most common type of diaphragmatic hernia is the Bochdalek type which is a posterolateral defect mostly located on the left side (80% of cases), less frequently on the right side (15%) or bilateral (5%). This type of defect occurs very early during gestation (9 to 10 weeks) and causes the protrusion of the abdominal organs into the thoracic

cavity. Stomach, spleen and colon are the most frequently herniated organs. The Morgagni type is usually a very small hernia which occurs in 1–2% of cases. It is a parasternal defect located in the anterior portion of the diaphragm; it contains liver, which may limit the degree of herniation. In the case of eventration of diaphragm, this structure appears to be weak

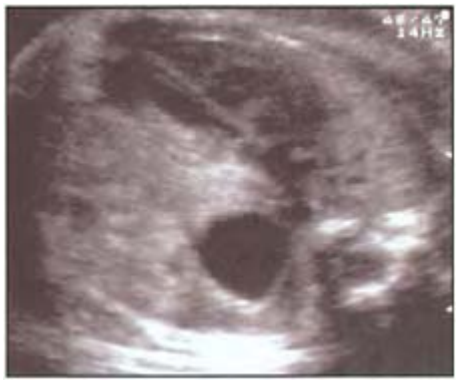

Figure 22.9: Transverse section of the fetal chest in a case of diaphragmatic hernia: the heart is displaced to the right side by the presence of the stomach and bowel loops in the thoracic cavity

so that the abdominal contents are displaced in the thoracic cavity.

The prenatal sonographic diagnosis of diaphragmatic hernia is mainly based on the visualization of abdominal organs at the same level of the four chamber view of the heart in the trasverse section of the fetal chest. The heart is usually shifted on the right side of the chest (Fig. 22.9).

The rate of associated anomalies is 25–75% increasing to 95% in stillborns.

The prognosis for this malformation is still very poor and becomes poorer if other malformations are associated. The poor prognosis mainly depends on the severity of pulmonary hypoplasia induced by the prolonged compression of the lungs by the herniated viscera. For this reason experimental prenatal surgery has been suggested to prevent the lung damage. There are no indications for preterm delivery or for cesarean section. The delivery should be planned in a tertiary care centre.

BOWEL DISORDERS

Esophageal Atresia

This anomaly consists in the absence of a segment of the esophagus and is often associated with a tracheo-esophageal fistula (86–90% of cases). Among different types the most common is the esophageal atresia associated with a fistula connecting the proximal part of the esophagus and the trachea (80% of the cases). The incidence varies between 1:800 and 1:5.000 live births and the etiology is unknown.

The prenatal diagnosis is possible in only 10% of the cases and should be suspected in the presence of polyhydramnios with absent stomach bubble in several and repeated ultrasound examinations (Fig. 22.10); however this malformation can occur even in presence of a normal or small stomach, due to the frequently associated tracheoesophageal fistula.[8]

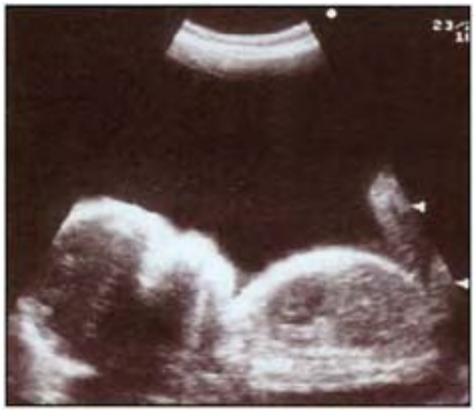

Figure 22.10: Esophageal atresia: the diagnosis is suspected by the association of absent stomach and polyhydramnios

Associated anomalies are present in 50–70% of the cases. A characteristic association is the "VACTER1T (Vertebral, Anorectal anomalies, Cardiac anomalies, Tracheo-esophageal fistula, Esophageal atresia, Renal anomalies, Limb anomalies). Fetal karyotyping is suggested. The prognosis depends on the associated malformations and on the severity of polyhydramnios, which can facilitate preterm delivery.

Duodenal Atresia or Stenosis

The incidence of this malformation is 1:10.000 live births and its genesis goes back to the llth

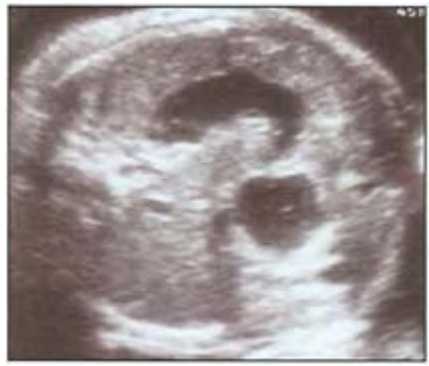

Figure 22.11: Duodenal atresia: the dilatation of the stomach and proximal duodenum produces the typical "double bubble" sign

week of gestation due to a failure of canalization of the primitive bowel. In most cases the etiology is unknown. Atresia is more common than stenosis (70% of cases) and could be associated with chromosomal abnormalities (trisomy 21), skeletal defects and other anomalies.[9]

The most typical sonographic finding is the characteristic "double bubble" sign caused by the simultaneous dilatation of the stomach and the proximal duodenum (Fig. 22.11). The diagnosis is usually made in the late second trimester.[10] Up to half of duodenal atresia cases are complicated by polyhydramnios and this can contribute to preterm labor but the main cause of death are the associated anomalies. This malformation can present late complications and late death even months or years after management.

Bowel Obstruction

The incidence of bowel stenosis and atresia is 2–3:10.000 births and the most common locations are distal ileum (36%) and proximal jejunum (31%). Most cases of intestinal atresias (48%) are characterized by complete separation of blind ends of bowel loops with a corresponding mesenteric defect; sometimes a fibrous band is connecting the blind ends (32%); the presence of a simple transverse diaphragm of the mucosa is less frequent (20%).

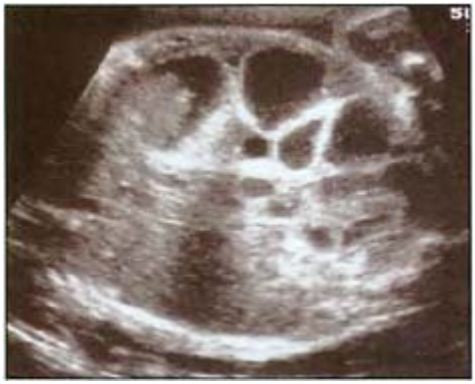

Figure 22.12: Jejunal atresia: multiple dilated bowel loops are present in the fetal abdomen

These defects are usually sporadic, although familial cases have been described.

According to the site of the obstruction the defects are devided in: (1) jejunoileal atresia and stenosis, (2) colonic atresia, and (3) imperforate anus.

The sonographic prenatal appearance varies according to the level of the defect. In the case of jejunoileal atresia multiple dilated bowel loops in the fetal abdomen may be seen in association with polyhydramnios (Fig. 22.12).[11,12] In colon atresia (that usually occurs proximal to the splenic flexure with a significant segment of absent colon with distal microcolon) the sonographic finding is similar to distal ileal occlusion and the differential diagnosis may not be possible. In the imperforate anus dilated intestinal loops with increased peristalsis may be seen as well as intraluminal hyperechogenic small areas referring to meconium (Fig. 22.13).[13]

The diagnosis of bowel obstruction is usually made in the third trimester: the lower is the obstruction the later is the appearance of the sonographic signs.

The prognosis of these malformations mainly depends on the level of obstruction: the lower the obstruction, the better the outcome. Other important prognostic factors are the presence of associated malformations, meconium peronitis and intrauterine growth restriction.

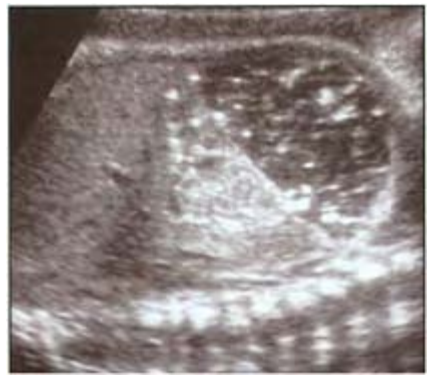

Figure 22.13: Imperforate anus in a third trimester fetus: a dilated distal colon is seen containing multiple small hyperechogenic areas due to meconium

Meconium Peritonitis

This condition is the consequence of *in utero* perforation of the bowel with spread of meconium into the peritoneal cavity leading to a local sterile chemical peritonitis. The peritonitis may be localized, with the development of a dense calcified mass or fibrous tissue, or diffuse, with a fibrous reaction leading to bowel adhesions and pseudocyst formation. Inflammatory reaction leads to an exudative process and ascites. Its incidence is 1:35.000 live births.

The prenatal sonographic appearance of meconium peritonitis varies according to the underlying anatomical finding: main signs are intra-abdominal calcifications (85% of cases), polyhydramnios, fetal ascites caused by exudate and bowel dilatation.

Postanatal management depends on the etiology of meconium peritonitis; up to 1/3 of all cases have cystic fibrosis.

Echogenic Bowel

Sonographically, “echogenic bowel” is defined as echogenicity of the bowel loops equal to or greater than the density of the iliac wing (Fig. 22.14). 1:200 midtrimester fetuses presents this feature which might depend on a slow or delayed transit

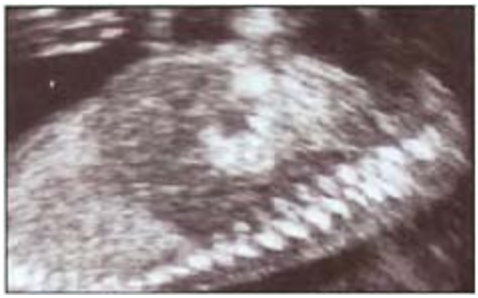

Figure 22.14: Echogenic bowel

of the meconium along the bowel. This finding has been considered as a "soft marker" of chromosomal abnormalities but actually the increased risk of chromosomopathy in the presence of such an isolated marker is extremely low.[14] The risk increases when further sonographic markers are present. The "echogenic bowel" may also be the first sign of cystic fibrosis or can be seen in cases of intra-amniotic bleeding.[15] However it is important to stress that the recognition of hyperechogenic meconium does not always represent a pathological condition but might be a normal variant and an isolated finding.[16]

NON-BOWEL CYSTIC MASSES

Choledochal Cysts

Choledochal cyst is a rare congenital cystic dilatation of the common bile duct. The incidence is about 1:2.000. Its sonographic appearance is that of a cystic structure located in the upper right abdomen with dilated proximal ducts (Fig. 22.15). The cystic size and the association with biliary obstruction affect the prognosis.[17]

Mesenteric and Omental Cyst

This benign malformation consists in cystic structures located in the small or large bowel mesentery or in the omentum filled with serous or chilous fluid. Its sonographic appearance is that of a thin-walled, unilocular or multilocular cystic

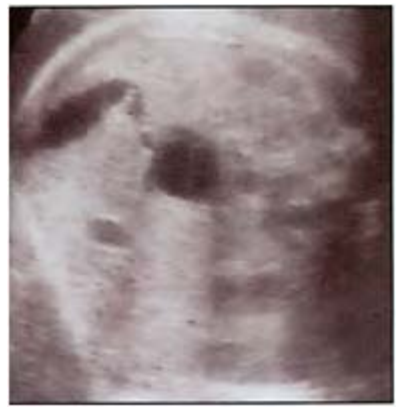

Figure 22.15: Choledochal cyst

mass. It is difficult to make a differential diagnosis with other intrabdominal cystic conditions.

Hepatic Masses

Hepatic masses might origin from an obstruction of the hepatic biliary system or might have a tumoral origin (hemangioma, hamartoma, etc.).

Their sonographic appearance changes depending on the origin: mesenchymal hamartomas usually appear as irregular hyperechoic areas (Fig. 22.16), while hemangioma appears hypoechoic,

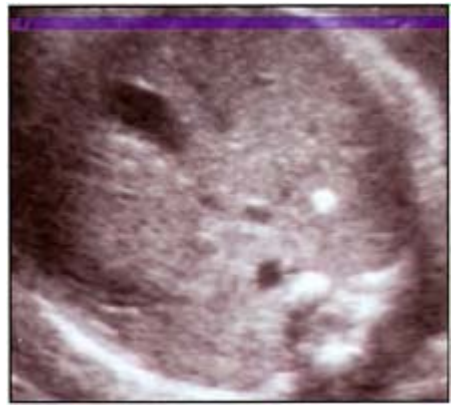

Figure 22.16: Small hepatic hamartoma

hyperechoic or mixed depending on the degree of fibrosis and stage of involution.[18] Hepatoblastomas and adenomas have a solid appearance.

The management is expectant in terms of monitoring the size and evolution of the tumor; for large tumors the cesarean section is indicated.

REFERENCES

1. Martin RW. Screening for fetal abdominal wall defects. Obstet Gynecol Clin North Am 1998; 25: 517–26.
2. Kurkchubasche AG. The fetus with an abdominal wall defect. Med Health RI 2001; 84:159–61.
3. Oguniemy D. Gastroschisis complicated by midgut atresia, absorption of bowel, and closure of the abdominal wall defect. Fetal Diagn Ther 2001; 16: 227–30.
4. Morris-Stiff G, al-Wafi A, Lari J. Gastroschisis and total intestinal atresia. Eur J Pediatr Surg 1998; 8:105–06.
5. Boyd PA, Bhattacharjee A, Gould S et al. Outcome of prenatally diagnosed anterior abdominal wall defects. Arch Dis Child Fetal Neonatal Ed. 1998; 78:F209–13.
6. Ginsberg NE, Cadkin A, Strom C. Prenatal diagnosis of body stalk anomaly in the first trimester of pregnancy. Ultrasound Obstet Gynecol 1997; 10:419–21.
7. Takeuchi K, Fujita I, Nakajima K et al. Body stalk anomaly: prenatal diagnosis. Int J Gynaecol Obstet 1995; 51:49–52.
8. Shulman A, Mazkereth R, Zalel Y et al. Prenatal identification of esophageal atresia: the role of ultrasonography for evaluation of functional anatomy. Prenat Diagn 2002; 22:669–74.
9. Sugimoto T, Yamagiwa I, Obata K et al. Choledochal cyst and duodenal atresia: a rare combination. Pediatr Surg Int 2002; 18:281–83.
10. Lawrence MJ, Ford WD, Furness M et al. Congenital duodenal obstruction: early antenatal ultrasound diagnosis. Pediatr Surg Int 2000; 16:342–45.
11. Uerpairojkit B, Charoenvidhya D, Tanawattanacharoen S et al. Fetal intestinal volvulus: a clinicosonographic finding. Ultrasound Obstet Gynecol 2001; 18:186–87.
12. Ogunyemi D. Prenatal ultrasonographic diagnosis of ileal atresia and volvulus in a twin pregnancy. J Ultrasound Med 2000; 19:723–26.
13. Has R, Gunay S. 'Whirlpool' sign in the prenatal diagnosis of intestinal volvulus. Ultrasound Obstet Gynecol 2002; 20:307–08.
14. Al-Kouatly HB, Chasen ST, Streltzoff J et al. The clinical significance of fetal echogenic bowel. Am J Obstet Gynecol 2001; 185:1035–38.
15. Berlin BM, Norton ME, Sugarman EA et al. Cystic fibrosis and chromosome abnormalities associated with echogenic fetal bowel. Obstet Gynecol 1999; 94:135–38.
16. Slotnik RN, Abuhamad AZ. Study of fetal echogenic bowel (FEB) and its implications. J Ultrasound Med 1999; 18:88.
17. Berg C, Baschat AA, Geipel A et al. First-trimester diagnosis of fetal hepatic cyst. Ultrasound Obstet Gynecol 2002; 19:287–89.
18. Macken MB, Wright JR Jr, Lau H et al. Prenatal sonographic detection of congenital hepatic cyst in third trimester after normal second-trimester sonographic examination. J Clin Ultrasound 2000; 28: 307–10.
19. Tsao K, Hirose S, Sydorak R et al. Fetal therapy for giant hepatic cysts. J Pediatr Surg 2002; 37: E31.

Chapter 23
Fetal Genitourinary Tract: Prenatal Diagnosis and Assessment of Nephrouropathies

Juan M Troyano Luque, Matilde T Clavijo Rodriguez

From January 10, 1991 through January 25, 2002 our team carried out 93 urinary aspirations between week 18 and 32 of pregnancy. In 82% of the punctures, kidney and urinary tract diseases were associated with hydronephrosis. We practiced 22 bladder punctures and 71 aspirative nephrostomies. The concentration of the biochemical markers in urine was always lower in physiological cases than in irreversible pathological cases. Beta2 microglobulin and N-acetil glucosaminidase were found in large quantities in fetal urine and in amniotic fluid in pathological conditions. In this study, a review of kidney and urinary tract disease sonographic markers is assessed along with their biochemical expression.

INCIDENCE AND EPIDEMIOLOGY

Kidney and urinary tract disease make up 34% of all malformations detected in our Fetal Medicine Department.[1] Thirty two percent of these malformations are isolated findings, 20% are associated with other kidney and urinary tract diseases and 48% are found in chromosomopathies and malformation syndromes. Since kidney and urinary tract disease is often linked to a wide spectrum of other diseases (Table 23.1), renal function must be evaluated to assess the prognosis and treatment possibilities. Expertise is needed in this evaluation because many times for a positive outcome, treatment must begin before week 20 of pregnancy. These fetal therapy techniques are only justified when renal function is preserved.

Prenatal diagnosis of kidney and urinary tract disease is hindered, much like the case of congenital heart disease, by the fact that often a highrisk population cannot be targeted. Pelvicalyceal dilatation, whether obstructive or not, occurs in 87% of all kidney and urinary tract disease; thus, in only 13% of the cases of these diseases is this valuable sonographic marker not found since they are isolated parenchymal diseases without pelvicalyceal dilatation (Fig. 23.1)

CLASSIFICATION

It is clear that unanimity in kidney and urinary tract disease classification has not been achieved. Potter's classification concerning renal dysplasia, defines a range of severity.[2,3] Clinical and pathological classifications show great differences.The following describes kidney and urinary tract diseases in which kidney function may be impaired, and which may be suggested by ultrasound examination. These include cystic diseases and renal dysplasia, which fall into a group of parenchymal pathology, and obstructive uropathies.

Parenchymal Pathology and the Ultrasound Markers

A major drawback in the clinical diagnosis of prenatal nephrouropathies occurs when a fetus is suffering from renal dysplasia. Conceptually speaking, this disease presents a kidney with total or partial anomalous differentiation owing to the persistence of mesenchymal heterotopic or

Table 23.1

	Smith-Lemli-Optiz syndrome
	Schwartz-Jampel syndrome
	Ivemark syndrome
NEPHROUROLOGICAL	Lawrence-Bardet-Biedl syndrome
MALFORMATIONS	Miranda syndrome
A) URETER-HYDRONEPHROS1S COMPLEX	
WITH MEGAURETER	ASSOCIATED WITH CHROMOSOME "X"
Vesicoureteral ebb	Ehlers-Danlos syndrome
Unblocked megaureter	Oro-facio-digital syndrome
Megaureter-Megabladder syndrome	
Prune Belly syndrome	MENDELIAN-FREE HEREDITY
Neurogen bladder	Lowe syndrome
Ureteral atresia	Beckwith syndrome
Ureter-vesical stenosis	Goldenhar syndrome
Ureterocele:	Dandy-Walker syndrome
Stenotic	
Sphincteral	METABOLIPATHIES
Mixed	Tyrosinemia
Blind	Galactosemia
Double pyeloureteral systems	E.Von Gierke syndrome

With ureterocele

Without ureterocele

MEGAURETER

Pyeloureteral stenosis

Megacaliosis

Pyelic duplicity

111 rotations

Ectopies

B) CYSTIC KIDNEY

a) GENETIC

Polycystic disease (AR) Locus Cr.16

Prenatal-Neonatal type

Child type

Juvenile type

Polycystic type (AD)

Postnatal

Juvenile nephroptisis

Cyst-Dysmorph ism

MENDELIAN HEREDITY
DOMINANT AUTOSOMIC

Tuberous sclerosis

Von Hippel-Lindau syndrome

Peutz-Jeghers syndrome

RECESSIVE AUTOSOMIC

Meckel syndrome

Jeune (Thoracic-asphyxiating Dysplasia) syndrome

Zellwerger (Cerebro-Hepatic-Renal) syndrome

Goldston syndrome

CHROMOSOMOPATHIES

Trisomy: 21, 13, 18

Turner syndrome

UNRELATED WITH GENES

Multicystic dysplasia

Simple cyst

Multilocular cyst

Acquired cystic renal disease Spongiomedular kidney
Caliceal diverticulosis (Pyelogenic Cyst)

c) MORPHOLOGICAL & POSITIONAL PATHOLOGIES

Renal agenesis

bilateral

unilateral

Renal hypoplasia

Renal ectopy

Horseshoe kidney

Further malformations

d) INFECTIONS

Rubella

Parvovirus (B-19)

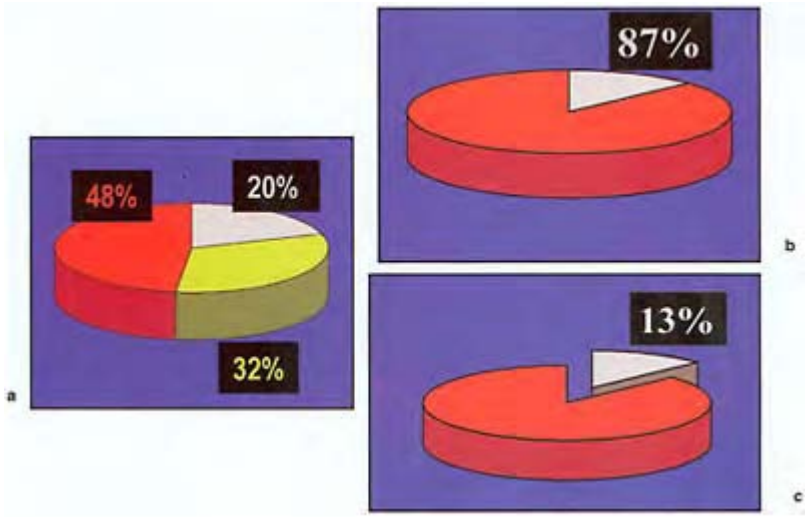

Figure 23.1: Kidney and urinary tract disease detected in our Ultrasound Unit of Fetal Medicine in Tenerife, University Hospital of the Canary Islands (a) isolated findings 32% are associated with other kidney and urinary tract diseases 20%. Are found in chromosomopathies and malformations syndromes 48%. (b) Pelvicalyceal dilatation, whether obstructive or not, accurs in 87% of all cases, (c) Only 13% of the cases are isolated parenchymal diseases without pelvicalyceal dilatation

undifferentiated structures (Fig. 23.2).[2,4,7] It should be stressed that the complexity of Potter classification factors may at times prevent straightforward prenatal assessment.[1]

Renal Agenesis

Renal dysplasia can be assessed in terms of number, size and extent of damage caused to the fetus.[8,9] As early as week 12, in bilateral renal agenesis, anhydramnios can be encountered (Fig. 23.3). By week 16, neither the kidneys nor the bladder can be located. Failure to find the renal arteries is another diagnostic clue. There is pulmonary hypoplasia. The condition is found in 1/5000 births and is always lethal. Unilateral agenesis is found in 1/2000 births. There are usually no effects on the fetus, thus making

ultrasound diagnosis difficult (Fig. 23.4). If suspected, however, no renal artery will be found.

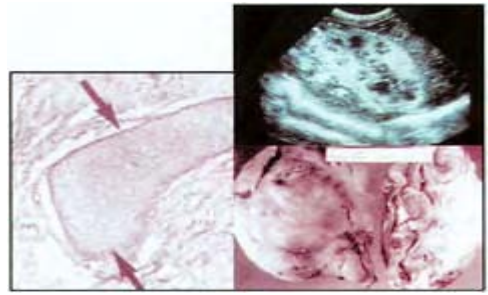

Figure 23.2: General characteristics of renal dysplasia: islets of primordial tubules, fibrous stratum and cartilage metaplasia (arrows). The basic observation on ultrasound is corticomedullar dysplasia which is seen as renomegalia, undefined capsule, loss of corticomedullar stratum and hyperechogenicity

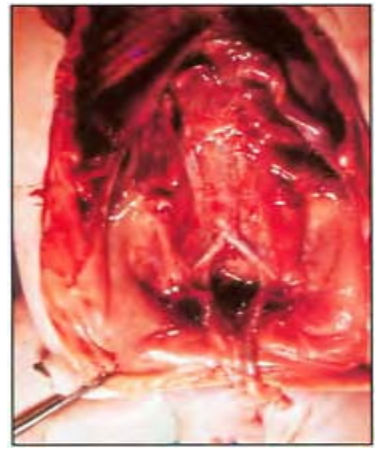

Figure 23.3: Bilateral renal agenesis: postmortem case

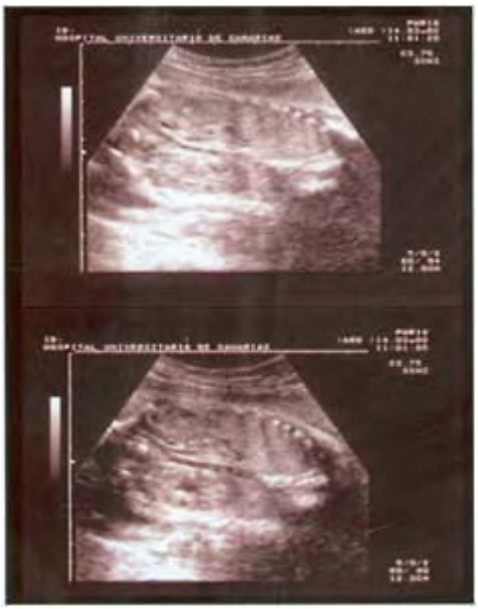

Figure 23.4: Unilateral agenesis, absence of left kidney

Infantile Polycystic Disease: Potter Type I

Infantile polycystic disease is found in 1/14000 births (Fig. 23.5). Criteria for diagnosis consist of large, hyperechogenic and homogenous kidneys with multiple corticomedullary cysts. There is a marked loss of visualization in differentiating the cortex from the medulla. Oligohydramnion may be present, with difficulty in visualization of the bladder, but these are not constant features. The perinatal form of this disease is lethal *in utero* or within a month of birth. The neonatal form causes death within the first year after birth. The infantile and the juvenile forms lead to chronic renal failure and a short live span.[7]

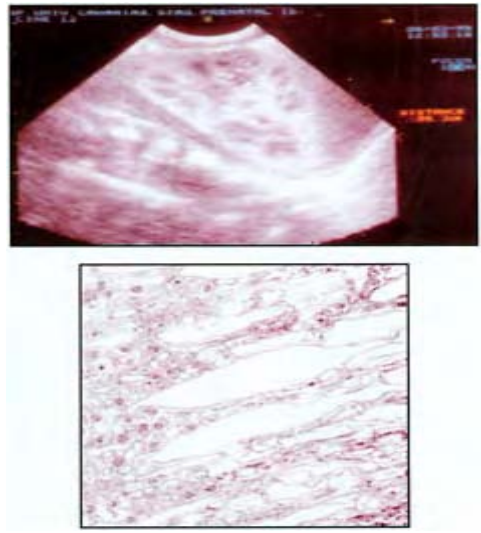

Figure 23.5: Potter Type I disease and corresponding ultrasound image

Multicystic Renal Dysplasia: Potter Type II

This is the most frequent renal disease of the parenchyma in the newborn found in 1/1000

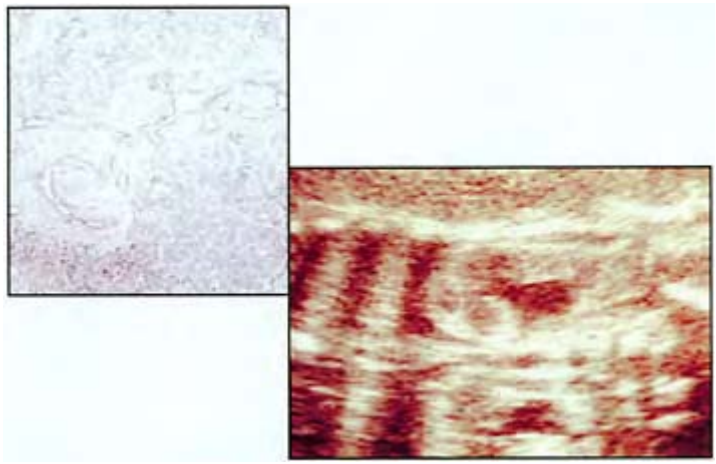

Figure 23.6: Ultrasound image and pathology specimen in Potter type II disease

births. It usually occurs unilaterally (Fig. 23.6) and exceptionally can occur bilaterally (1/10000 births). In unilateral cases, the kidney is usually enlarged and presents multiple round, peripheral cysts that differ in size and deform the renal surface. There is pathological dilatation of the ureter. Bilateral cases are lethal, unilateral cases usually present normal prognosis.[3,4]

Juvenile or Adult Polycystosis: Potter Type III

An autosomal dominant disease, characterized by enlarged, echogenic, irregular kidneys similar to those found in Potter I but smaller, and normal or slightly decreased amniotic fluid. Diagnosis is usually made only by family history (Fig. 23.7).[2]

Dyplasia Kidney Secondary to Obstruction: Potter Type IV

Renal dysplasia can also be caused by a severe and prolonged obstruction that presents ultrasound features later in pregnancy; if the obstruction occurs at the beginning of pregnancy, a multicystic kidney is the outcome. The obstruction can occur at any level from the ureteropelvic

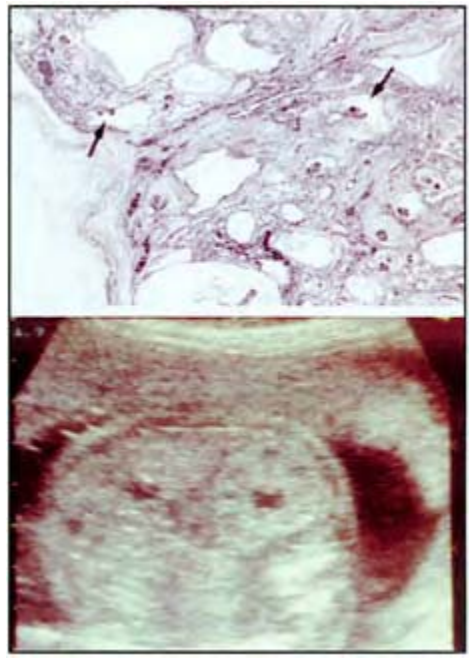

Figure 23.7: Potter Type III disease: ultrasound image and pathology specimen. The arrows indicate fibrosis and collectors cyst

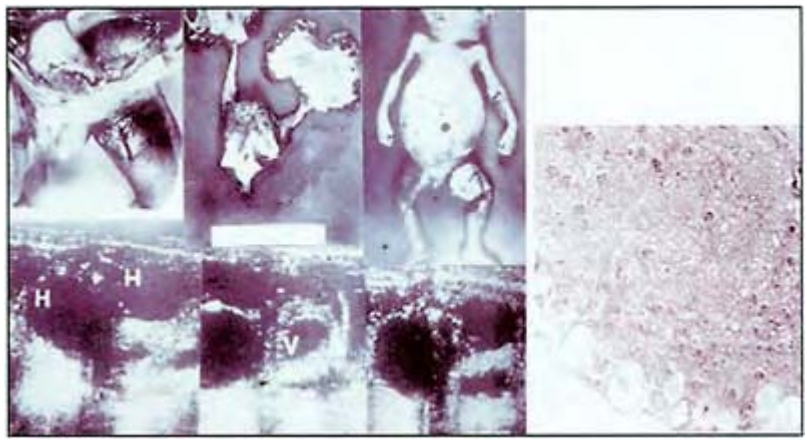

Figure 23.8: Ultrasound image and morphological sequence of Potter Type IV disease: note the presence of subcortical cysts. H: hydronephrosis, V: bladder

junction to the urethra. Ultrasound signs include subcapsular parenchymal cysts or increased echogenicity. The presence of apparently normal parenchyma does not exclude the existence of dysplasia of the obstructed kidney (Fig. 23.8). Sometimes only a segment of the kidney is affected.[3,10,11]

OBSTRUCTIVE UROPATHIES AND THEIR ULTRASOUND MARKERS

The anteroposterior diameter of the renal pelvis should be <5 mm at 15–19 weeks, <6 mm at 20–29 weeks and <8 mm at 30–40 weeks. By 15 weeks gestation, the bladder should be visualised in all fetuses.

Mild hydronephrosis or pyelectasia is defined by the presence of an anteroposterior diameter of the pelvis of >4mm at 15–19 weeks, >5 mm at 20–29 weeks and >7 mm at 30–40 week. Transient hydronephrosis is sometimes due to relaxation of the smooth muscle of the urinary tract, induced by high levels of circulating maternal hormones or maternal-fetal overhydration. Severe hydronephrosis is an easy sonographic marker to obtain, as its presence is obvious on ultrasound examination. Some kidney and urinary tract diseases are so apparent that problems may be diagnosed as early as 10 weeks (Fig. 23.9).[12,13]

The occurrence of renal blockage at the pyeloureteral level, or below, may trigger an initial urinary ectasia and subsequently evolve to hypertension by retrograde flow, which in turn may progress in three ways: persistent dilatation, gradual increase in size of dilated area or changes in the kidney's morphology

In these cases, upon ultrasound examination, an ecentric lacunar area within the renal parenchyma is visualized, even though the resulting dilatation is actually extrarrenal in origin. The morphology of the lacunar area is either lenticular, or spherical with a diameter no greater than 0.8 mm.[13] In severely affected fetuses, the size of the pelvic dilatation may reach up to 4–7 cm, exceeding the size of the abdominal cavity and causing digestive tract problems and other kinds of extrarenal cystic processes (Fig. 23.10).

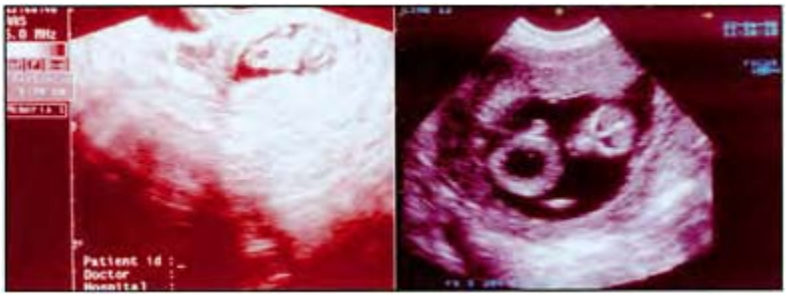

Figure 23.9: Pathology view of bladder in a 9-weeks-old embryo and its evolution to megabladder (Prune Belly syndrome)

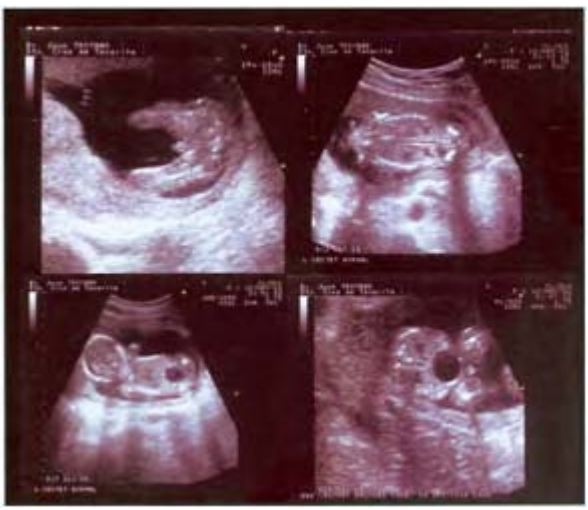

Figure 23.10: Severe obstructive hydronephrosis with loss of parenchyma and calyceal systems due to hypertension

Etiology

Dilatation pathologies can be summarized on the basis of two phenomena.[1] The first is pyeloureteral stenosis, which is primary hydronephrosis consisting of functional and anatomical collapse at the pyeloureteral level. It is frequently associated with extrarenal malformations (cloacal syndrome, anal imperforation), and even urogenital malformations such as hypospadia and renal ectopy. The second pattern is called reflux dilatation, which can be primary as in prune belly syndrome[11] or secondary as in ureteral duplication or megabladder (Fig. 23.11); or refluxless dilatation, which

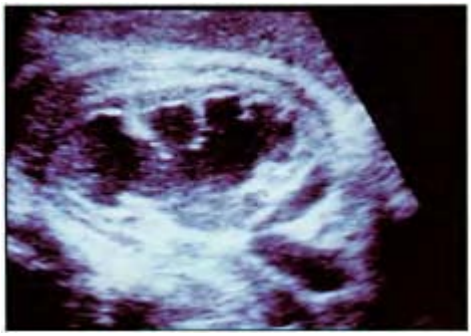

Figure 23.11: Early hydronephrosis (week 11) and development of megabladder: In these cases, distal obstructive pathology such as stenosis, atresia and posterior ureteral valves should be taken into account

again can be primary (obstructive, atresia, stenosis, posterior valves) or secondary (ectopia, ureterocele, vesical diverticulum, extrinsic compression).

Calyceal Dilatation

When the renal pelvis is subjected to increasing hypertension, the dilatation may affect the whole or only a part of the calyceal network, normally the superior area.[1,13,14] Mild hydronephrosis may also have a severe impact on the calyceal system, translating into renal malfunction. However, severe pelvic dilatation may not affect the calyces or the overall renal physiology.

The size of the calyceal area and the thickness of the renal parenchyma of the calyces are both key factors in the assessment of hypertension-derived alterations. In severe cases, such expansion displaces or even destroys the parenchymal area.[12]

Some fetuses undergo a combined process of dilatation of the upper calyceal area (over 1 cm) and a moderate dilatation of the renal pelvis (over 15 mm). In these cases, the obstructive situation worsens throughout the first year after birth, and derivative surgery is frequently needed (Fig. 23.12).[15–17]

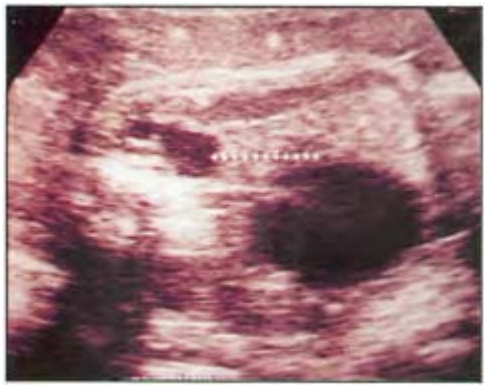

Figure 23.12: Asymmetrical dilatation of the calyceal system. In these cases it is frequent to find an association of a duplicated pyeloureteral system with obstruction or reflux in one of the ureters. In these cases there is evident risk of segmentary kidney hydronephrosis, often requiring surgery after birth.

Ureter Dilatation

Ureter dilatation originates from obstructive processes occurring through the ureteral conduct that brings about an increasing thickness of the prestenotic ureter. This alteration is fairly obvious on examination. The morphology of the dilated area varies according to its etiology, and is found in two forms[1]: static and dynamic.

The static forms can be:

1. Rectilinear, where a long lacunar area (cross-section over 5 mm), stacked on the renal pelvis, is seen, sometimes reaching the bladder. This condition leads to ureteral obstruction. (Fig. 23.13);

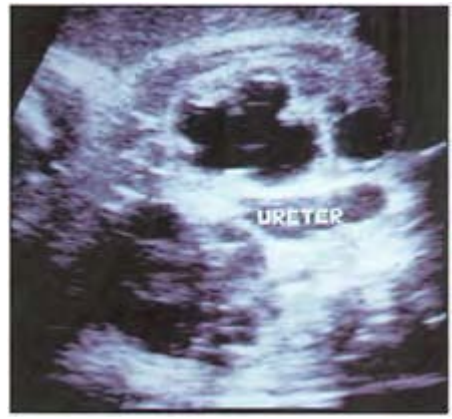

Figure 23.13: Static form of ureteral dilatation, rectilinear type, with a transversal diameter of 5 mm associated with renal pelvis dilatation

2. Winding morphology, where long and sometimes even bent morphology is seen. It is often associated with pseudocystic ultra-sound findings around the ureter, between the kidney and bladder. If this condition progresses, it can be physiologically compromising (Fig. 23.14);
3. Lacunar morphology, where a cystic lacunae can be seen in most of the abdominal cavity of the fetus, even beyond the vertebrae;
4. Sacular shape, where one or various cystic lacunae lay between the kidney and bladder

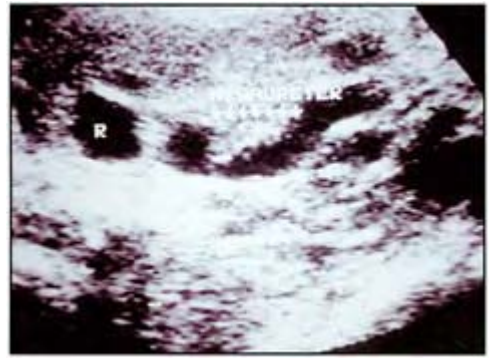

Figure 23.14: Winding form of ureteral dilatation. R: kidney

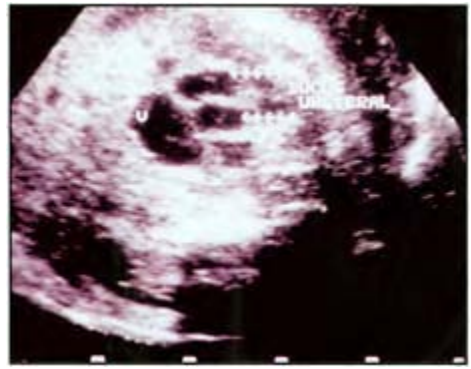

Figure 23.15: Lacunar type of ureteral dilatation where cysts between the kidney and the bladder may be visualized (diverticulum form)

(diverticulum). It is infrequent, but commonly associated with excretory diseases such as ureteral agenesis. Assessment is often difficult when overall renal function remains undamaged (Fig. 23.15).

The dynamic forms are those where there are changes in the pattern, causing pathological stress, and therefore induce changing responses as manifested in the morphology of the ureter in two ways. The first takes the form of episodes, characteristic of pathologies such as vesicoureteral reflux, but sometimes confused with physiological behaviors and premicturation dynamics. It is

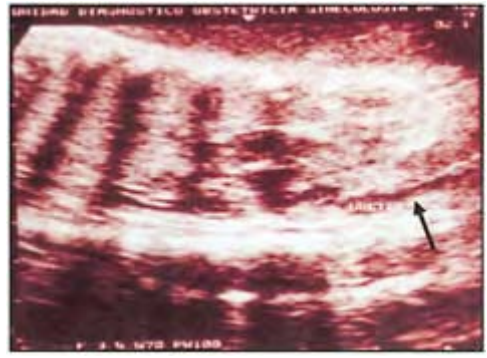

Figure 23.16: Dynamic form, progressing in episodes, with dilatation of the ureter (arrow) because of vesicoureteral reflux. A pulsatile

movement of the ureter can be seen, similar to a pulsating artery

frequently associated with a moderately dilated pelvis (Fig. 23.16). The second dynamic type is peristaltic. The ureter is dilated; sometimes it is cylindrical, showing peristaltic waves from the pelvis to the bladder. Ureter thickness varies considerably during pregnancy. The conditon is frequently associated with the initial phases of prestenotic megaureter (Fig. 23.17).

As mentioned above, dilatation events affecting excretory tissues are particularly harmful to

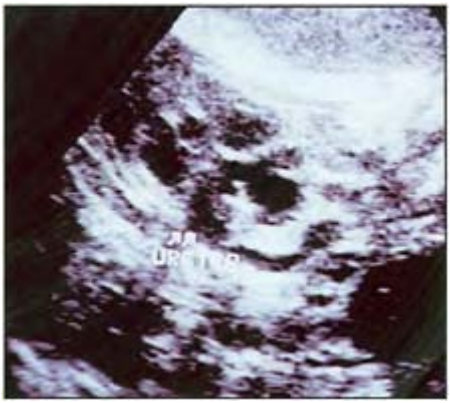

Figure 23.17: Dynamic peristaltic form, where ureteral dilatation with peristaltic waves is seen. This is found in the initial phases of prestenotic megaureter

the fetus' welfare because they may alter the whole renal system, causing severe or irreversible damage. Dilatation of the excretory network may sometimes result in shrinkage of the renal parenchyma. Hence, both ectasia and pressure in the conducts decrease, and thus harm the parenchyma, leading to dysplasia that impacts on overall renal function, particularly in fetuses suffering from the pyelocalyceal dilatation syndrome.[1,13,18]

The above mechanisms of retrograde hypertension may generate a number of different parenchymal states. These include shrinking parenchyma, where calyceal groups grow in size, pelvic volume increases with overlapping between the calyces and pelvis, and parenchymal shrinkage is concentrated around the dilated calyces. Another is laminate parenchyma, where there is extreme shrinkage of the parenchyma as a result of severe hydronephrosis. Parenchyma is not seen by ultrasound. There is gradual evolution to end stages, where there is extreme dilatation of the pelvis and calyceal system (Fig. 23.18).

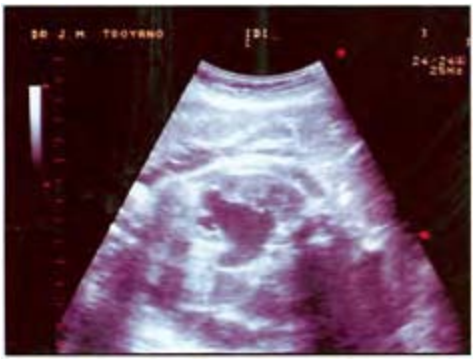

Figure 23.18: Laminate parenchyma with loss of renal morphology due to extreme corticomedullar thinning

Apart from the above, renal function modifications may demonstrate other patterns that deserve separate description. The partial destruction of the renal parenchyma by compressive dilatation is an outstanding example, where an area of healthy parenchyma, calyces and pelvis, varying in size, remain operative. There are two kinds of renal compressive dilatation: superior and inferior. Superior renal compressive dilatation is the most frequent and severe, and presents with round cysts or cysts cluttered on the superior pole, laminate parenchyma due to compression and stable renal volume. This phenomenon takes place in abnormalities such as ureteral duplication and with alteration in the drainage that causes dilatation of the superior pole of the kidney. A vesical cyst (ureterocele) may often be observed accompanying these duplicate systems (ectopic ureter), and can be confused with tumors at the suprarenal level (Fig. 23.19).

INTRAUTERINE TREATMENT OF OBSTRUCTIVE NEPHROUROPATHIES

Diagnosis is often difficult, and many fetuses do not qualify for therapy because of irreversible renal failure.[1,12,16–18] A very small group of fetuses are eligible for prenatal therapy. Renal obstructions do not necessarily trigger irreversible damage. The amniotic volume can be employed as an indirect indicator of renal pathology. Normal quantities of amniotic volume suggest renal excretory function and on-course physiological pulmonary development. Conversely, major excretory problems can be predicted in those cases presenting severe oligohydramnion.[11,12,19]

As stated at the beginning of this article, intrauterine therapy should only be applied to those fetuses with reversible damage to their kidneys. Selection of adequate patients must be undertaken on the basis of the fetus' renal performance.[13,16,17–20]

Renal dysplasia produces irreversible damage, and the type and extent of the disease determine the degree of impact upon renal physiology. A number of parenchymal alterations coexist in dysplastic kidneys: fibrosis, cartilage dysplasia, and sometimes

corticomedullary cysts. In 90% of dysplastic diseases, there is an association with obstructive problems, and this high percentage is enough to question the use of any derivative treatment prior to birth.[3,7,11,17]

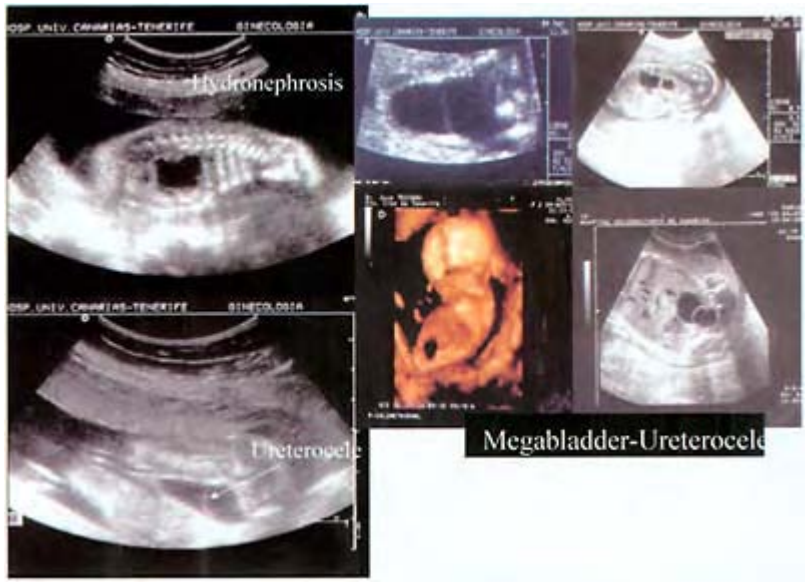

Figure 23.19: Image corresponding to an intravesical ureterocele. This pathology is usually seen with an ectopic ureter causing hydronephrosis that progresses. The bladder should always be examined when hydronephrosis is found

Ultrasound techniques are our main tool for diagnosis of prenatal pathologies. These techniques are continually improving, but still have some limitations (Table 23.2). Since dysplastic kidneys are not always detected by sonographic techniques, further methods are required to differentiate physiological from pathological conditions, and foresee which fetal obstructive uropathies may be eligible for derivative nephrostomy.[1,21–26] An alternative method should be selected according to three kinds of parameters, described below.

Biometric Parameters

In this case the parameters to be evaluated are: longitudinal renal diameter, transverse renal diameter, renal ellipse, renal volume and nephro-

Table 23.2: Prenatal nephrouropathy ultrasound prediction

Marker	*Sensibility*	*Parenchymal specificity*
Cortico-medullar cysts	50%	100%
Hyperechogenicity	60%	90%
Hydronephrosis	35%	70%
Hydronephrosis+cysts	90%	100%
25–30% of false-negatives, i.e. obstructive uropathies displaying ultrasound signs of parenchymal normality		

abdominal index. These parameters, considered together, complement the assessment of renal functionality, maintaining a linear relationship with gestational chronology (Graph 23.1).[27] Throughout pregnancy, there is a steady increase in all of the biometric parameters; the longitudinal

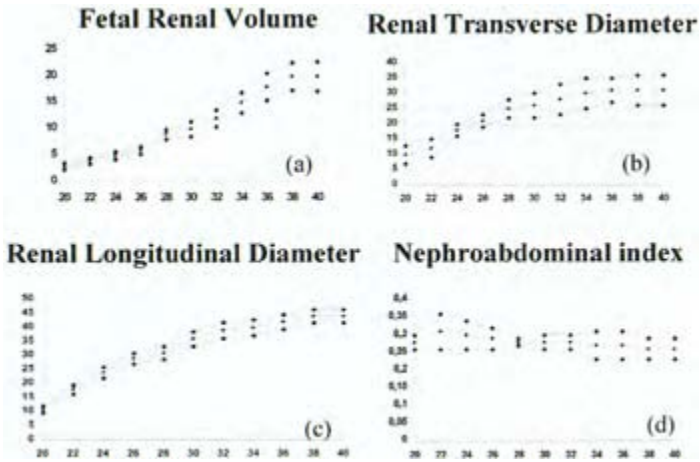

Graph 23.1: Biometric parameters, (a) Fetal renal volume, (b) Renal transverse diameter, (c) Renal longitudinal diameter, (d) Nephroabdominal index

diameter and renal volume increase the most, and the transverse diameter stops growing by week 34 of pregnancy.[27] The nephro-abdominal index increases up to week 22 of pregnancy; the growth rate is greater for the abdomen than for the kidney up to week 22 of pregnancy, and then the growth rates become equal from 36 weeks of pregnancy. Variations in this index are indicative of either enlargement or small kidneys.

Dynamic Parameters

These parameters are urinary excretion (micturation dynamics) and Doppler velocimetry (Graph 23.2). By assessing micturation dynamics, new knowledge may be obtained.[18,19] In the second and third trimesters of gestation, active diuresis occurs at 25–30 minute intervals. Micturation volume per unit increases with gestational age. Clearance, the most intrinsic renal factor, is not clinically quan-

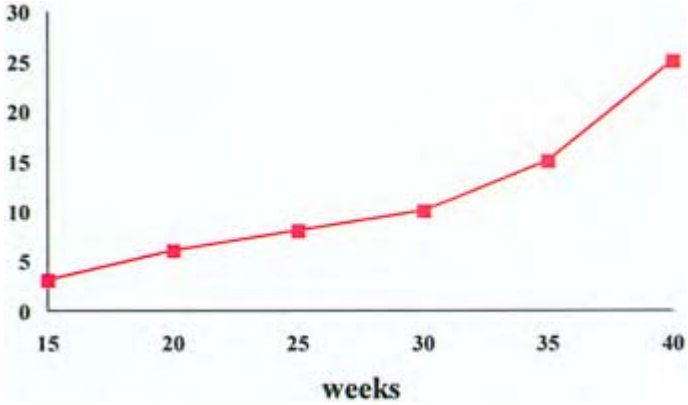

Graph 23.2: Micturation dynamics

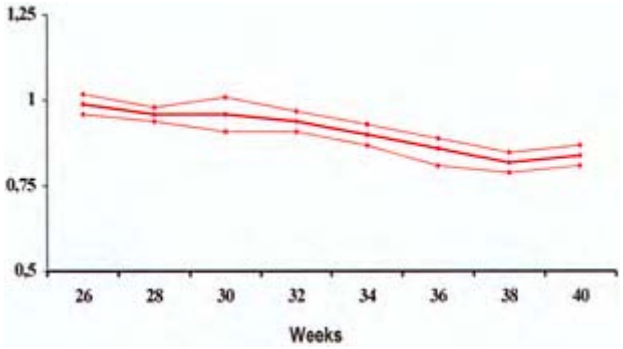

Graph 23.3: Resistance index (Rl) in the renal artery (Curve indicate mean and 5th and 95th centiles)

tified when assessing urinary expenditure rates, so that micturation dynamics, although informative, have a low predictive value in nephrological diagnosis. Wladimiroff found paradoxial cases of polyuria, possibly resulting from a breakdown in the reabsorption dynamics of the proximal tubules.[18,23] Amniotic volume and fetal diuresis give additional diagnostic information (i.e. the fetus is able to urinate). Velocimetry patterns of renal vessels can be also very useful in the assessment of renal function, particularly in

intrauterine growth restriction (IUGR), oligohydramnion and some malformation pathologies (mainly cardiopathies involving circulatory failure in the left ventricle), and in the assessment of hemodynamic responses to drugs (cardiotonics, prostaglandins, etc.).

For example, the resistance index (RI) (Graph 23.3) and the pulsatility index (PI) (Graph 23.4) both decrease with gestational age under physiological conditions. This trend is brought about by centrifugal nephrogenic development, which peaks in week 34 of gestation, when the fetus has already attained considerable functional maturity.[1,29–31]

The plasmatic flow normally amounts to 5% of the total cardiac flow of the fetus. It increases gradually with pregnancy, as intrinsic vascular resistance decreases and systemic resistance increases. Fetal nephrogenesis takes place from week 34 onwards, cortical flow amounting to up to 12% of the cardiac flow by the end of pregnancy.

The hemodynamics of renal flow from the middle third of the renal artery show a pattern

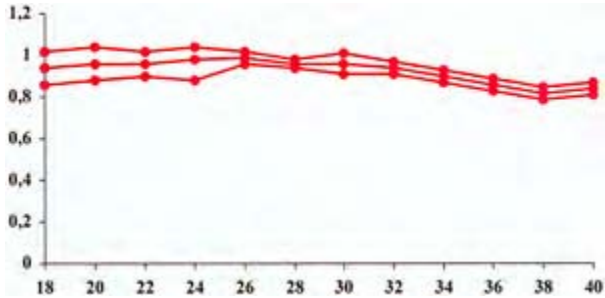

Graph 23.4: Pulsatility index (PI) in the renal artery (Curve indicate mean and 5th and 95th centiles)

of high systolic velocity and lack of diastole for most of pregnancy. Diastolic flow can be first detected from week 34, a consequence of the decrease in intraparenchymal resistance and in nephrogenic maturity. Interestingly, if birth occurs prior to the 34th week of gestation, the preterm newborns' kidneys proceed to mature with total functionality.[1]

Overlapping artery-vein recordings are common in velocimetry studies, but can be prevented by avoiding movements of the trunk of the fetus, and making sure that the angle of the beam, in relation to the longitudinal axis of the renal artery, is equal or less than 40°.

In our unit, IUGR-associated chronic hypoxia is normally associated with increased sympathetic tone, which subsequently leads to overall flow redistribution, noted as an increase in cerebral flow and a decrease in peripheral circulation.[1]

Vyas and colleagues[31] applied funiculocentesis and Doppler ultrasound to assess renal hypoxemia. Their results showed that the PI was significantly higher in pathological cases than in physiological cases, and correlated positively with levels of hypoxemia. Furthermore, increased PI values were recorded in cases associated with oligohydramnion.

Hemodynamic profiles encompassing cerebral and renal flows can be used to explore the severity of renal hypoxemia using the following guidelines:

a. Decreased cerebral PI and increased renal PI: hypoxemia.
b. Normal cerebral PI and decreased renal PI: physiological renal condition.
c. Normal cerebral PI and increased renal PI: renal dysfunction.

Renal flows and glomerular filtration are regulated by PGE_2 and F_2oc prostaglandins. Increases in the concentration of both hormone modulators maintain physiological renal flows (this has been observed in fetal urine samples obtained by intrauterine puncture). PGE_2 prostaglandins act as antagonists to vasopressin in the proximal tubules, thus slowing down the reabsorption of water and solutes. Consequently, severe parenchymal damage leads to a marked increase in vascular resistance. This pattern cannot generalized to all types of obstructive pathologies. Thus, it can be suggested that extraparenchymal hemo-dynamic alterations may play a role in slowing down vascular resistance and glomerular adaptation.

Comparative Assessment of flow patterns from the renal artery in status of IUGR with either euamnion or oligohydramnion

Kidney perfusion has been assessed in fetuses displaying intrauterine growth restriction (IUGR) by contrasting the S/D index from the renal artery in cases of euamnion and severe oligohydramnion.

This hemodynamic approach has been employed to explore the role of renal perfusion in the perinatal evolution of abnormally small fetuses in different amniotic environments.

A total of 96 pregnancies featuring IUGR (P<10) and euamnion (Chamberlain amniotic index >3) were monitored between the 26th and 40th weeks of pregnancy. This group was fairly heterogeneous as a result of differences in the timing of diagnosis and was not surveyed linearly. However, linear monitoring (biweekly) was carried out in a group of nine pregnancies in the period through the 26th to the 34th gestational weeks.

A further 39 pregnant women were diagnosed as cases of lUGR-oligohydramnion between the 26th and 34th gestational weeks. Again, linear monitoring was precluded by the diagnosis timing and also by the time of delivery as required according to the gravity and evolution of individual cases. A group of six pregnancies were studied linearly in the period from the 26th to the 32nd gestational weeks. In the course of which several cesarean were done to counteract some cases of severe fetal compromise. Fetal suffering was the main cause of mortality in this group (perinatal mortality=23%).

Significant differences in the S/D index occurred between lUGR-euamnion vs lUGR-oligo-hydramnion cases. In the other hand the S/D ratio

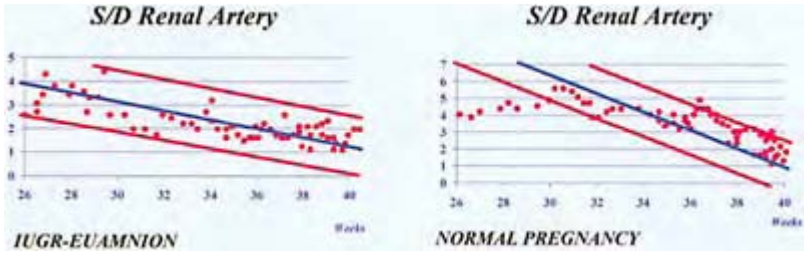

Graph 23.5: It shows S/D index differences between lUGR-Euamnion (a) vs. Normal pregnacy cases (b)

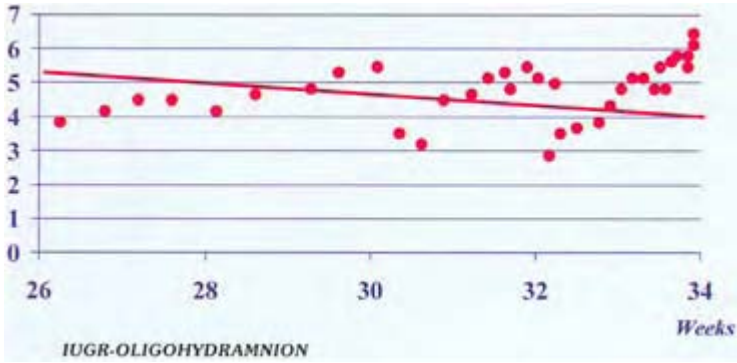

Graph 23.6: S/D Index for IUGR-Oligohydramnion cases

for IUGR-euamnion pregnancies was fairly identical to that of eutrophic gestations in physiological conditions (Graph 23.5).

Concerning to S/D values for IUGR-oligohydramnion cases were regarded as restrictive, such condition being statistically significant (Graph 23.6)

Velocimetry Patterns from the Renal Artery in a Status of Nephrourological Pathology

Patterns of change in the Resistance Index (RI) from renal artery are well known in physiological pregnancies monitored at our research unit. However, approaches are needed to assess such an index in a pathological context.

In our Research Unit of Fetal Medicine, the RI was quantified in a number of cases presenting prenatal kidney pathology, basically obstructive, while an insight was given into the effect of pathological renal parenchyma and excretion upon the flowmetry of the renal artery.

A total of three pathological types were subjected to monitoring:

- Group I—Severe hydronephrosis (dilatation >25 mm, and echographic evidence of shrinkage parenchyma) (Fig. 23.20). In this group 11 patients surveyed between the 28th and 38th weeks of gestation.
- Group II—Light hydronephrosis (dilatation of kidney pelvis <15 mm, and conservative

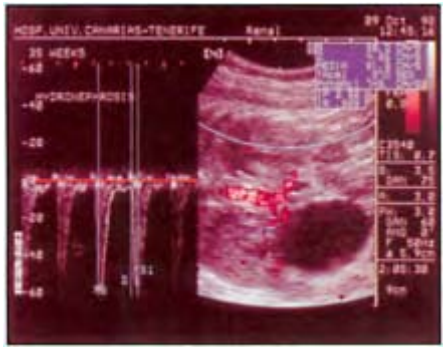

Figure 23.20: Severe hydronephrosis with echographic evidence of shrinkage parenchyma. Hemodynamic profile with restrictive flow

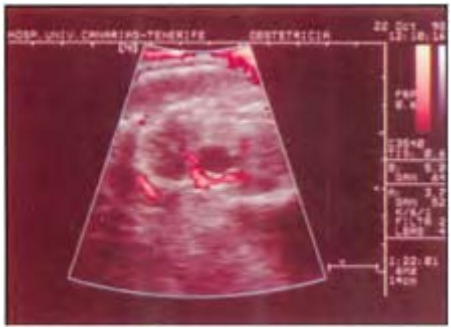

Figure 23.21: Light hydronephrosis. Dilatation kidney pelvis <15 mm and conservative parenchyma

parenchyma). In this group 16 patients surveyed between the 28th and 38th gestational weeks (Fig. 23.21).

- Group HI—Corticomedullar dysplasia associated with oligohydramnion (renomagaly, less of corticomedullar layers, hyperechogenicity, absence of capsular definition). In this group 22 patients surveyed between the 30th and 36th gestational weeks (Fig. 23.22).

In our experience RI from the renal artery were larger in cases of severe hydronephrosis than in cases of light hydronephrosis (though statistically insignificant).

Pathological kidneys in group I and III showed RI values always larger than these from healthy kidneys, statistical differences being as follows:

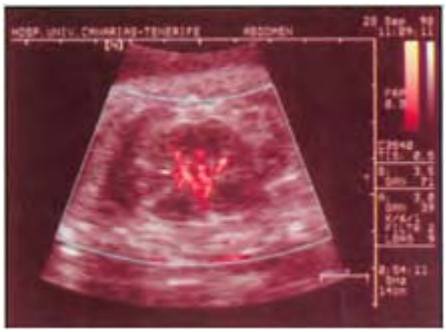

Figure 23.22: Corticomedullar dysplasia (Renomegaly, less of corticomedullar layers, capsula undefined and irregular vascular distribution)

- Insignificant for severe hydronephrosis.
- Very significant for corticomedullar dysplasia associated with oligohydramnion (Group III).
- In our point of view a gradient of increasing restriction in blood flows through the renal artery occurs from physiological conditions, through hydronephrosis, to dysplasia particulary if combined with oligohydramnion.
- The maintenance of optimal levels of both renal perfusion and diuresis may be closely related with a corticomedullar system remaining at least partially functional.

A number of remarkable observations have been made at our research unit,[29,30] by applying Doppler to the middle third of the renal artery (between the aortic anastomosis and the parenchymal area) in situations when the fetus is not moving and the vein and artery recordings do not overlap:

1. RI values decrease from the week 32 due to centrifugal nephrogenesis.
2. This hemodynamic trend correlates positively with the RI for both the middle cerebral (from week 22) and umbilical arteries.
3. There are significant differences in RI between the two renal arteries, the RI being smaller in the right kidney, possibly due to the influence of neighboring splachnic vessels.
4. The systole/diastole rate (S/D) in cases of IUGR associated with oligohydramnion is restrictive in cases of IUGR associated with euamniotic fetuses, the rate in the latter being similar to that in healthy fetuses. The combination of IUGR and

oligohydramnion is linked to renal hypoperfusion mechanisms, and is indicative of corticomedullary hemodynamic failure in the context of visceral centralization.
5. The arterial RI in severe hydronephrosis (dilatation over 3 cm) is larger (although not statistically significant) than that in mild hydronephrosis for fetuses suffering from nephrourological problems (hydronephrosis and/or corticomedullary dysplasia).
6. There are significant differences in RI between severe hydronephrotic fetuses and those presenting healthy kidneys.
7. The RI is significantly higher in cases of corticomedullary dysplasia associated with oligohydramnion than in healthy cases.

Physiological levels of both perfusion and diuresis are possible, providing for the corticomedullary system which stays at least partly functional.[29]

Biochemical Parameters

Biochemical parameters are the cornerstone of clinical assessment of fetus renal function. Fetal urine originates from ultrafiltration of fetal serum, and is characteristically hypotonic owing to active reabsorption of sodium (Na^+) and chlorine ($Cl-$) from the proximal tubule. This condition prevails throughout gestation and can aid in predicting function. In contrast, hypotonic or isotonic fetal urine is indicative of irreversible pathologies of the proximal tubules.[1]

Unlike Na^+ and Cl^-, the fetal clearance mechanism of potassium (K^+) and creatinine has very little clinical predictive value because it overlaps with the placenta clearance process, and also because K^+ ions change in charge constantly during pregnancy and are present in low concentrations in fetal blood due to insulin modulation. Therefore, K^+ filtration and absorption levels are low and irregular in fetal kidneys.[32]

Sodium and chlorine concentrations and osmolarity are the main prediction factors used

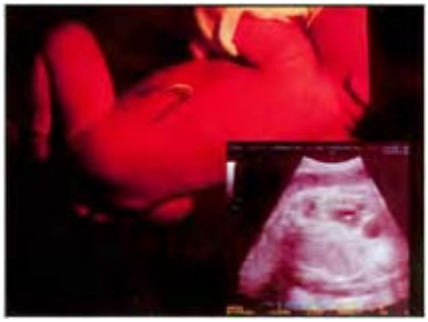

Figure 23.23: Fetal puncture and aspiration to obtain urine depends on fetal position. The dorsoanterior position makes nephrostomy easier while the posterior position makes

vesical puncture the easiest option. This criteria is also used in *in utero* fetal therapy

in assessing renal function.[1] The limits for considering normal kidney function are [Na^+] <100 mEq/l,[Cr]<90mEq/l, and Osmolarity <200–210 mOsm. Potassium and creatinine concentrations have been shown to be indistinguishable for pathological and healthy groups. Intrauterine monitoring of fetal urine is the best technique for assessing renal clearance function.[1,13,32]

Aspiration puncture techniques are carried out by means of standard 16–18 gauge spinal needles. Two different approaches are possible, depending on the fetal position. Vesical punctures are best for fetuses in the posterior position, whereas aspirative nephrostomy is particularly suitable for dorsal or lateral positions (Fig. 23.23). As observed in the ultrasound monitoring of both techniques, nephrostomy-derived hematurias are rare (less than 4% of the interventions) certainly in part because of the expertise of the doctor carrying out the technique.[33,34]

Samples of 2 mm size suffice to detect dysplastic diseases. Suitable samples can be collected in 65% of attempts with 16 gauge needles and in only 38% of punctures with 18 gauge needles.[33,35] On the other hand, aspirative nephrostomy has the advantages that it guarantees the collection of urine samples, enables reassessment of dilated parenchyma and allows safe renal biopsy.[1,33]

A number of biochemical markers of proximal tubule pathologies can be obtained from urine samples. They are all lysosomial proteins featuring two outstanding properties: they are both easily filtered and reabsorbed (β_2 microglobulin) or they are specific elements of tubular tissues (N-acetyl-diglucosaminidase, NAG). The two lysosomial groups present low molecular weights and appear in large quantities in fetal urine and amniotic fluid under pathological conditions.[32]

At the Fetal Medicine Research Unit of the University Hospital of the Canary Islands *(Santa Cruz de Tenerife, Spain)*, our team carried out a total of 93 urinary aspirations including 22 bladder punctures and 71 aspirative nephrostomies. In 82% of cases, nephrouropathies were associated with hydronephrosis. Nephrourological punctures were carried out from week 18 of gestation and beyond week 32. Of the 93 aspirations, healthy and pathological statuses were recorded in 75 and 18 cases, respectively (Table 23.3). The concentration of biochemical markers was always much lower in physiological cases than in irreversible pathological cases. $Beta_2$ microglobulin ($\beta_2$mgG) and NAG behaved the same manner over time (Tables 23.4 and 23.5).[20,32]

Table 23.3: Punctures by nephrourological aspiration. Frequecy distribution according to gestational age

	18–20 weeks	*21–31 weeks*	*>32 weeks*
Physiological	18	46	11
Pathological	3	12	3

Table 23.4: Concentrations of biochemical markers in urine in physiological conditions (Nephrourological aspirations)

	18–20 weeks	*21–31 weeks*	*>32 weeks*
Na+ (mEq/ml)	42±1.7	42±1.7	47±3.0
Cl^- (mEq/ml)	23±2.0	41±2.6	41±2.0
OsM (mOsm)	96±1.2	102±1.6	102±2.1
NAG(U/l)	2.0±1.0	2.7±1.2	2.0±0.9
β_2mG(ml/l)	4.7±1.4	5.1±1.0	5.3±1.0

Table 23.5: Concentrations of biochemical markers in urine in pathological conditions (Nephrourological aspiration)

	18–20 weeks	*21–31 weeks*	*>32 weeks*
Na^+(mEq/mI)	120.0	126.44±11.50	139.60
Cl^-(mEq/ml)	119.0	132.50±7.18	141.00
OsM (mOsm)	240.0	261.50±7.18	281.00
NAG (U/l)	18.0	25.83±0.85	25.73
B2mG(ml/l)	26.0	38.97±1.30	38.72
K^+(mEq/ml)	3.1	3.41±0.66	3.90
Creatinine (ml/l)	1.2	2,54±0.83	3.70

Table 23.6: Physiological concentrations of biochemical indicators sampled from both urine versus amniotic fluids

	18–20 weeks	*21–31 weeks*	*>32 weeks*
Na^+ (mEq/ml)	42/37	42/140	47/140
Cr (mEq/ml)	23/109	47/109	41/108

OsM (mOsm)	98/287	102/273	102/271
NAG (U/l)	2.0/3.6	2.7/3.62	2.0/4.69
B2mcG(ml/l)	4.7/4.5	5.1/5.0	5.3/5.8
K+ (mEq/ml)		41/140	
Creatinine (ml/l)		1.9/0.6	
Urine/Amniotic study			

There were no significant differences between healthy and pathological fetuses in ionic concentrations (Na^+, Cl^-) and osmolarity in both fetal urine and amniotic fluid. Conversely, the concentrations of NAG and $\beta_2$mcG were significantly higher in the amniotic fluid of nephropathological fetuses than in that of healthy fetuses (Tables 23.6 and 23.7).

Table 23.7: Pathological concentrations of biochemical indicators sample from both urine and amniotic fluid

	18–20 weeks	*21–31 weeks*	*>32 weeks*
Na+ (mEq/ml)	120/132	126.4/140	139.6/140
Cr (mEq/ml)	119/107	132.5/149	141/158
OsM (mOsm)	240/267	261.5/273	281/296
NAG (U/l)	18/16.9	25.8/20.3	25.73/20.8
$\beta_2$mcG(ml/l)	26/22.3	38.9/28.7	38.72/30.0
K^+(mEq/mi)	3.1/138	3.4/140.6	3.9/148
Creatinine (ml/l)	1.2/0.7	2.54/0.82	3.7/0.9
Urine/Amniotic values			

We feel that an increase in the concentration of lysosomial markers may well be caused by an increase in the volume of urinary excretion, and also by an accumulative effect resulting from the process of amniotic fluid clearance. Lysosomial clinical techniques avoid physical invasion of the fetus' kidneys, but further research is needed if this technique is to be routinely applied for fetal nephrouropathy therapy. Concentrations of both K^+ and creatinine have shown little predictive value because of the placenta clearance effect and continuous shifts in the K^+ ionic charge during pregnancy. Nephrourological assessment scores are summed up in Table 23.8.[1,32,34]

Table 23.8: Fetal urine: assessment of the nephrourological status of the fetus at any gestational age by means of biochemical markers. Ultrasound observation and quantification of amniotic volume

Prediction	*Unfavorable prognosis*	*Favorable prognosis*
Ultrasound observation	Hyperechogenicity + cysts	Normal
Amniotic volume	Oligoamnios	Normal
Fetal urine		
Na^+ (mEq/ml)	>100	<100
Cl^- (mEq.ml)	>90	<90
Osmolarity (mOsm)	>21G	<210
NAG (U/l)	>8	<8
$\beta_2$mcG(ml/l)	>7	<7
K^+	Negligible	Negligible
Creatinine	Negligible	Negligible

Based on these biochemical results, in the group with conserved renal function (75 cases), surgery was necessary in 62 cases with positive outcomes (eight cases were uretheroceles). In ten cases repeat surgery was necessary and in three cases unilateral nephrectomy was performed owing to renal failure. In the pathological group (18 cases) abortion was performed in three cases, and 12 presented severe renal dysplasia and irreversible function. Three cases were chromosomopathies and none of them survived.

Further Aspects Related to Renal Function

Our study of ultrasound and biochemical markers in kidney and urinary tract disease has enabled us to find other aspects related to renal function, summarized below.

Furosemide administered to the mother, does not cause diuretic responses in the stressed fetuses, as shown by quantitative analysis of bladder storage velocity. In stressed neonates and IUGR cases, this pattern may be caused by an increase in the concentration of antidiuretic hormone, in turn causing water savings and the maintenance of plasmatic volume. Further hormones such as aldosterone and cortisol may play a part in the latter mechanism, since they mediate an increase in urinary flow and excretion rates of Cl, Na^+ and K^+. This modulation is basically fetus-associated, not occurring in the adult kidney unless high concentration dose is given.

Losses of fetal Na^+ trigger polyhydramnios, seen typically in chlorothiazide treated mothers.[36] As such, fetal hyponatremia would possibly account for polyhydramnios in cases of dilatation of the urinary system.[23] Fetuses displaying losses of Na^+ experience reduced capability for tubular absorption of water (polyuria), while fetal losses of water

lead to natriuria.[1] Both polyuria and polyhydramnios are indicators of severe and irreversible tubulopathies (particularly in the proximal area).

Renal Glomerule Filtration (RGF)

Effective renal glomerule filtration starts from week 10–12 of gestation, the normal indices being 0.32–0.24 ml/mm to week 24–26, 1.60–1.46 ml/min to 32–34 weeks gestation, and 4.67–1.72 ml/min to 38–40 weeks gestation. Preterm newborns show functional immaturity when born before week 32, but acquire defined maturity at week 34. This observation indicates that nephrogenesis and kidney function and maturity are in direct relation to gestational age, even after the birth of preterm newborns. The process of nephrogenesis ends at week 34, entailing a build-up of centrifugal (arterial) flows that in turn enhance the maturation of cortical nephrons (the final nephrons to reach maturity).[1]

Tubular Dynamics of Sodium and Chlorine

A number of interesting results have been obtained from experimental animals subjected to saline overloading in their venous system. By dosing 5–15 mEq NaCl per kilogram of animal weight in 30 minutes, and subsequently collecting the excreted urine fluids over a two hour period, it was observed that less than 10% of the dosed amount of NaCl remaind longer than 5 minutes within the intracellular space.

Saline overload in the venous system is very obvious in fetal excretion (reabsorption rates of sodium/chlorine from proximal tubules over 60%) but is not indicative of the actual fetal capacity for physiological excretion.

Increases in glomerular filtration due to water diuresis (i.e. maternal dosage of furosemide)[36] bring about a decrease in proximal reabsorption of Na^+,Cr, CO_3H-, Ca^{2+}, P^{3-}, Glucose, Uric acid and P_2 microglobulin. The magnitude of these changes can shift according to saline levels in both the fetus and the mother, the type of drugs employed and the degree of fetal stress.[1]

Tubular Dynamics of Potassium

Plasmatic concentrations of potassium remain within a rather constant range throughout gestation, and are modulated by two factors: first overall corporal content of potassium acting upon the exterior balance, and second, intra- and extracellular distribution of potassium acting upon the interior balance. Some 98% of the fetus' total potassium is found inside fetal cells (intracellular). Restricted K^+ excretion takes place before the 35th week of gestation. Overall potassium concentration is positively correlated with gestational time.

The modulation network is aided by insulin, controlling the entrance of potassium into the intracellular space, even when the concentration of aldosterone decreases.

Increases in the concentration of K^+ in fetal blood occur in situations of hyperkalemia, resulting from renal failure, indomethacine dosage, congenital renal hyperplasia involving saline losses, pseudohyperaldosteronism, obstructive uropathies, fetal renal thrombosis and IUGR.

Tubular Dynamics of Calcium

Healthy fetuses can be considered to be in a relatively hypercalcemic state combined with hypoparathyroidism counteracting the excess of calcium. Calcium concentrations are further enhanced by metabolic acidosis and increases in the fraction of ionic calcium. Braun and Steranka[37] showed that excretion rates of urinary Ca^{2+} are positively correlated with concentration and excretion rates of Na^{+}, and negatively correlated with calcemia levels.[37]

Furthermore, Goldsmith[38] proved that intravenous inputs of calcium triggered increases in the volume of urinary excretion, while furosemide led to hypercalciuria (resulting from Na^{+} excretion) and decreased reabsorption of calcium. Calcemia levels subside by the end of gestation in relation to prenatal/neonatal maturity. This results in the release of PTH (Parathyroid hormone), which in turn activates the synthesis of Vitamin D and digestive absorption of calcium in the intestines.

Calcium dynamics reflects also sodium dynamics. However, conversely, the reabsorption of calcium is greater than that of sodium in the pars recta of the proximal tubules, while the reverse pattern can be observed in the distal tubules.

Tubular Dynamics of Phosphate

Reabsorption rates of phosphate also vary with gestational age. At 28 weeks there is 85% reabsorption, at 34 weeks, 93%, and at 40 weeks, 98%. Phosphate dynamics are opposite to those of calcium in that reabsorption rates increase towards the end of gestation. Phosphate savings seem to be directly related to PTH levels as suggested by Mulroney and colleagues.[39]

Tubular Dynamics of Uric Acid

Uric acid dynamics depends on the amount of extracellular volume present in the fetus. Its concentration normally ranges within 7.7±2.7 mg/dl (average) in immature fetuses and between 5.2±1.6 mg/dl in mature fetuses. Thus, uricosuria levels are lowest at early gestational ages, so that the release of uric acid increases at the end of pregnancy.[1]

Acid-base Balance

Urine pH increases with gestational age, while Henle net acid excretion decreases even in situations of metabolic acidosis. The limit of bicarbonate excretion range between 14 and 18 mEq/1 in preterm fetuses, whereas it is around 20 mEq/1 at term fetuses.

Net acid excretion and plasmatic bicarbonate concentration levels are positively correlated with gestational age.

Tubular Dynamics of Glucose

The presence of physiological concentrations of glucose (glucosuria) is a characteristic feature of the preterm fetus. Furthermore, urine excretion volume is enhanced by physiological increases in extracellular volume, whereas glucose tubular reabsorption decreases till the end of gestation.

Tuvad and Vesterdal have shown that immature filtering capacity in the glomerules results in decreased levels of tubular reabsorption as well as transport of glucose.[40]

Urinary Concentration Capacity

The kidney's capacity for concentrating urinary fluid is modulated by three factors, all of which trigger decreased urine concentration responses. These factors are vasopressin (present from week 26), PGE2 (acting on the collector tubules) and a weak corticomedullar gradient of both urea and Na^+ (resulting from Henle's loops being very short, underdevelopment of the chlorine pump causing low excretion rates of urea, and increased medullar blood flows).

Urine concentration mechanisms comprise, first, reabsorption of water from the collector tubules, which become more permeable under vasopressin modulation; and second, they are dependant on the intensity of a corticomedullar osmotic gradient (which originates from the accumulation of urinary products in the medullar intersticia in two ways: passive for urea, and active for solutes such as chlorine and sodium).

In contrast, urine dilution mechanisms (synthesis of free water) result from active reabsorption of chlorine and sodium in the descending loops and the proximal tubules, under no vasopressin modulation.[1]

CONCLUSIONS

Since only 25% of the cases with renal dysplasia are detected by means ultrasound techniques, biochemical assessment of fetal urine represents a complementary tool for diagnosing and predicting fetal nephrouropathies of all kinds. Nevertheless ultrasound diagnostic is the main procedure to evaluate this prenatal disease, being necessary to include, not only the parenchyma echostructural characteristics and amniotic volume, but also the Doppler flow evaluation of the renal artery in all cases.[21,24,25,41]

REFERENCES

1. Troyano JM, De la Fuente P Prenatal nephrouropathies and their intrauterine management. In Prenatal Features of Fetal Kidney Physiopathology and their Intra- and Extrauterine Treatment. A Multidisciplinary Problem. Tenerife: University Hospital of the Canary Islands, 1993; 35–39.
2. Potter EL. Normal and abnormal development of the kidney. Chicago Year Bock Med, 1912.
3. Alvarez-Argiielles H, Marin A, Domenech E et al. Caracterfsticas clinico-patologicas del rinon quistico tipo II de Potter con especial referencia a las anomalfas del desarrollo asociadas. Morfol Norm Patol 1981; B:5–117.
4. Baxter TJ. Poly cystic kidney of infants and children: morphology, distribution and relation of cysts. Nephron 1965; 2:15–33.
5. Bernstein J. A classification of renal cysts. In: Gardner KD, Bernstein J (Eds). The Cystic Kidney. Boston: Kluwer Academic Publishers, 1990; 4:147.
6. Mottet KK, Jensen H. The anomalous embryonic development associated with trisomy 13–15. Am Clin Pathol 1965; 6:43–334.
7. Risdon RA. Renal dysplasia. 1. A clinicopathological study of 76 cases. 2. A necropsy study of 41 cases. J Clin Pathol 1971; 24:57–65.

8. Ashey AC, Mostofy FK. Renal agenesis and dysgenesis. J Urol 1960;82:211.
9. Dubbins PA, Kurtz AB, Wapner RJ, Goldberg BB. Renal agenesis: spectrum of in utero findings. J Clin Ultrasound 1981; 9:189–93.
10. Christopher CR, Spinelli A, Servet D. Ultrasonic diagnosis of Prune Belly syndrome. Obstet Gynaecol 1982; 59:391–94.
11. Smythe AR. Ultrasonic detection of fetal ascites and bladder dilation with resulting Prune Belly. J Pediatr 1981; 98:978–80.
12. Click PL, Harrison MR, Golbus MS. Management of the fetus with congenital hydronephrosis. II Prognostic criteria and selection for treatment. J Pediatr Surg 1985;20:376.
13. Golbus MS, Harrison MR, Filly RA. Prenatal diagnosis and treatment of fetal hydronephrosis. Semin Perinatol 1983; 7:102–08.
14. Walzer A, Koenigsberg M. Prenatal evaluation of partial obstruction of the urinary tract. Radiolog 1980; 135:93–94.
15. Harrison MR, Anderson J, Rosen MS. Fetal surgery in the primate. 1: Anesthesic, surgical and tocolytic management to maximize fetal-neonatal survival. J Pediatr Surg 1982; 17:115–42.
16. Harrison MR, Colbus MS, Filly RA. Fetal surgical treatment. Pediatr Ann 1982;l:896–99, 901–03.
17. Harrison MR, Golbus MS, Filly RA. Management of the fetus with a correctable defect. J Am Med Assoc 1981; 246:774–77.
18. Pilu G, Nicolaides KH. Diagnosis of Fetal Abnormalities. Carnforth, UK: Parthenon Publishing, 1999:77–78.
19. Wladimiroff JM, Campbell S. Fetal urine production rates in normal and complicated pregnancy. Lancet 1974; 1:151–54.
20. Kurjak A, Kirkinenl R LatinY, Ivankovic D. Ultrasound assessment of fetal kidney function in normal and complicated pregnancies. Am J Obstet Gynecol 1981; 141:266–70.
21. Vadel HE, Martin S. Realtime sonographic diagnosis of fetal dysplastic kidney. Gynaecol Obstet 1980; 18: 140–43.
22. Friedberg JE, Mitnick JS, Davss DA. Antepartum ultrasonic detection of multicystic kidney. Radiology 1979; 131:131–38.
23. Henderson SC, Van Kolken RJ, Rahatzad M. Multicystic kidney hydramnios. J Clin Ultrasound 1980; 8:249–50.
24. Mahoney BS, Filly RA, Callen PW, Hricak H, Colbus MS, Harrison MR. Fetal renal dysplasia: sonographic evaluation. Radiology 1984; 152:143–46.
25. Pedicelli G, Jequier S, Bowen A, Boisvert 1. Multicystic dysplastic kidneys: spontaneous regression demonstrated with ultrasound. Radiology 1986; 160:23–26.
26. Zerres K, Weiss F, Bulla M, Roth B. Prenatal diagnosis of an early manifestation of autosomal dominant adult-type poly cystic kidney disease. Lancet 1982; 2:988.
27. Jeanty P, Dramaix-Wilment M, Elkazen N, Hibinot C, Van Regemorter. Measurement of fetal kidney growth on ultrasound. Radiology 1982; 144:159–62.
28. Campbell S, Wladimiroff JW, Dewhurst CJ. The antenatal measurement of foetal urine production. Br Obstet Gynaecol 1973; 80:680–85.
29. Troyano JM, Clavijo MT, Marco OY et al. Velocimetry from renal vessels: techniques, results, assessment and interplay with other fetal vessels. Ultrasound Obstet Gynecol 1999; 14.
30. Troyano JM, Clavijo MT, Marco OY et al. Velocimetry patterns from the renal artery in a status of nephrological pathology. Ultrasound Obstet Gynecol 1999; 14:151.
31. Vyas S, Nicolaides KH, Campbell S. Renal artery flow-velocity waveforms in normal and hypoxemic fetuses. Obstet Gynecol 1988; 7:72.
32. Troyano JM, Clavijo M, Feo E, Laynez E, Gomez-Frieiro M. Parameters of renal function by the obtention of fetal urine by intrauterine aspiration. Ultrasound Obstet Gynecol 2000; 16:77.
33. Troyano JM, Padron E, Clavijo M. Fetal biopsy and puncture. Actual status. In: Filipiche DS (Ed). Balkan Ohrid's School of Ultrasound Advanced Ultrasound II. Macedonia: Ohrid, 1996; 9:51–61.

34. Troyano JM. Fetal biopsy and puncture: actual status. In Weiner S, Kurjak A (Eds). Interventional Ultrasound. Progress in Obstetric and Gynecological Sonography Series. Lancaster, UK: Parthenon Publishing, 1999; 81–94.
35. Campbell WA, Yamase HT, Salafia CA, Vintzileos AM, Rodis JE. Fetal renal biopsy: technique development. Fetal Diagn Ther 1993;8:135–43.
36. Wladimiroff JW. Effect of furosemide on fetal urine production. Br J Obstet Gynaecol 1975; 82:221–24.
37. Braun DR, Steranka BH. Renal cation excretion in the hypocalcemic premature human neonate. J Pediatr 1981; 15:1100.
38. Goldsmith MA, Bhatia SS, Kanto WP, Kutner MH, Rudman D. Gluconate calcium therapy and neonatal hypercalciuria. Am J Dis Child 1981; 135:538–43.
39. Mulroney SE, Lumpking MD, Haramati A. Antagonist to growth hormone releasing factor inhibits growth and renal phosphate reabsorption in immature rats. Am J Physiol 1989; 257:F29–34.
40. Tuvad E, Vesterdal L. Sugar reabsorption in prematures and full-term babies. Scand J Clin Lab Invest 1949; 1:281.
41. Stuck KJ, Koff SA, Silver TM. Ultrasonic features of multicystic dysplastic kidney: expanded diagnostic criteria. Radiology 1982; 143:217–21.

Chapter 24
The Umbilical Cord: Sonographic Assessment

Edoardo Di Naro, Luigi Raio, Vincenzo D'Addario

The umbilical cord is an unique structure that connects the fetal circulation with that of the placenta. It contains two arteries and one vein (Fig. 24.1) and the characteristic feature, its helical structure, is already developed as early as eight weeks of gestation. This particular angioarchitecture and the surrounding Wharton's jelly protects the blood against compression, stretching and torsion of the umbilical cord. Moreover, this morphology seems to have an important role in influencing the blood flow from the placenta to the fetus. A huge number of studies published so far have found an association between alterations of the umbilical cord structure and pregnancy outcome. It is therefore important to integrate the umbilical cord sonographic assessment in our prenatal screening programs. The aim of this chapter is to evaluate the role of the sonographic assessment of the umbilical cord during fetal life.

Figure 24.1: Sonographic image of the umbilical cord. It contains two arteries and one vein

UMBILICAL CORD AREA

From the pre-sonographic literature we have learned that a thin umbilical cord is associated with adverse pregnancy outcome and unexplained fetal death. With the technologic improvements of our ultrasound machines it is now possible to study the umbilical cord in its physiologic environment, during fetal life. Recently, it has been shown that the umbilical cord cross-sectional area is correlated with fetal biometry[1] and that a lean umbilical cord, defined as a cross-sectional area below the 10th centile for gestational age, increases considerably the risk of having a small for gestational age fetus at delivery, fetal distress in labor, and operative delivery.[2] Moreover, it has been demonstrated that the umbilical coiling index and the umbilical vein blood flow is lower in growth-retarded fetuses than in healthy fetuses, even in absence of umbilical artery Doppler abnormalities.[3] Therefore, lean umbilical cords differ from normal cords not only from a structural point of view, but also in umbilical vein blood flow characteristics. This fact could explain the increased risk of intrapartum complications and fetal growth restriction among fetuses with a lean or hypocoiled cord.[4] Similar observations have been made in cases with early onset preeclampsia where the umbilical cords are characterized by a reduction of the Wharton's jelly amount and a smaller umbilical vein area.[5] It seems that this morphologic changes of the umbilical cord may be present before fetal growth restriction or preeclampsia is manifest.

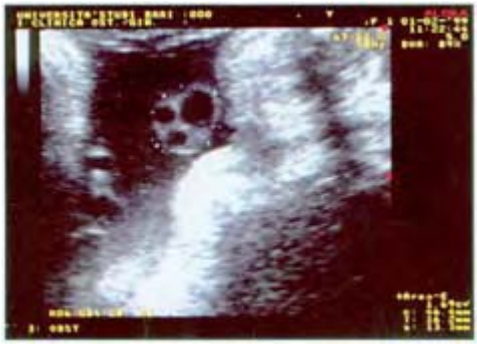

Figure 24.2: The sonographic cross-sectional area of the umbilical cord has to be measured at the maximal magnification in a free loop near the fetal end of the umbilical cord. The ellipse function of the ultrasound machine is used and the best-fitting ellipse is put over the umbilical cord

The sonographic cross-sectional area of the umbilical cord has to be measured at the maximal magnification in a free loop near the fetal end of the umbilical cord. The ellipse function of the ultrasound machine is used and the best-fitting ellipse is put over the

umbilical cord (Fig. 24.2). The cord cross-sectional area increases as a function of gestational age progressively up to 32 weeks of gestation reaching a plateau until term when a progressive reduction (Graph 24.1) occurs.[6,7] This fact can be explained by a progressive reduction of Wharton jelly. Conversely,

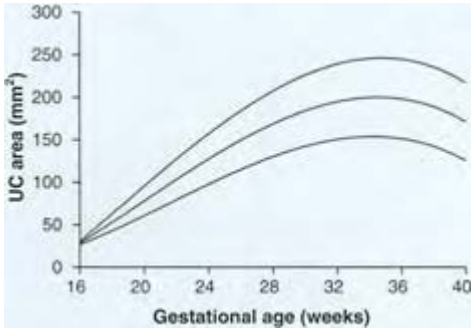

Graph 24.1: The cord cross-sectional area increases as a function of gestational age progressively up to 32 weeks of gestation reaching a plateau until term, when a progressive reduction occurs

in patients with gestational diabetes the umbilical cord has been found to be larger than in uncomplicated pregnancies, with an increased content of fluid and plasma proteins within the empty spaces of Wharton's jelly.[8]

UMBILICAL CORD DIAMETER IN THE FIRST TRIMESTER

Literature and the clinical evidence have shown that the morphometry of the umbilical cord in the second half of gestation might be useful in predicting adverse perinatal outcome. Recently Ghezzi et al[9] in an observational study has investigated the clinical value of the sonographic measurement of the umbilical cord diameter early in gestation (Fig. 24.3). A significant correlation was found between umbilical cord diameter and

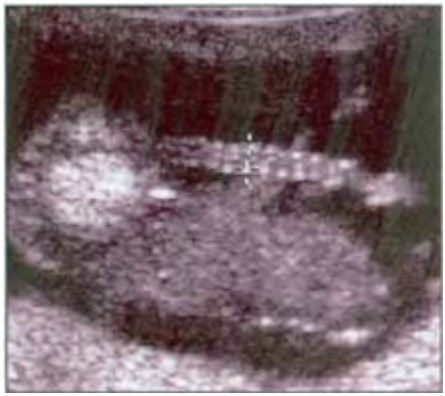

Figure 24.3: Sonographic measurement of the umbilical cord diameter early in gestation

gestational age: umbilical cord diameter increases steadily from 8 to 15 weeks of gestation (Graph 24.2); moreover a significant correlation was found between umbilical cord diameter and crown-rump length and umbilical cord diameter and biparietal diameter; correlation was not found between umbilical cord diameter and birth weight or placental weight. The umbilical cord diameter was found below 2 standard deviations from the mean respectively in 43% and 37% among

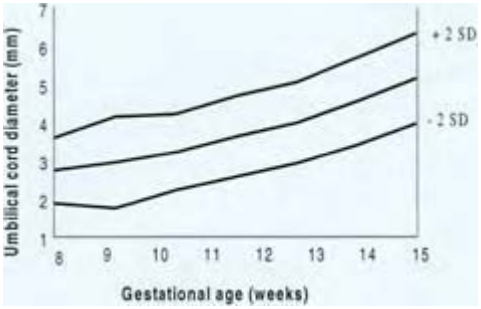

Graph 24.2: Umbilical cord diameter increases steadily from 8 to 15 weeks of gestation

patients with miscarriage and pre-eclampsia, while the proportion of fetuses with an umbilical cord diameter above the 95th centile was higher in fetuses with placental or chromosomal abnormalities than in normal ones.[10] Today the umbilical cord diameter seems to be a marker for identifying a subset of fetuses at risk of spontaneous miscarriage, pre-eclampsia and chromosomal abnormalities.

UMBILICAL CORD COILING

The spiral course of the umbilical cord has been the subject of several investigations since the Middle Ages but the cause and significance of such coiling is still a matter of debate. The helical structure of the umbilical cord is fully developed as early as eight weeks of gestation and the number of umbilical vascular coils present in the first trimester and at term gestation is similar. Currently the standard method to quantify the degree of umbilical vascular coiling is the umbilical coiling index (UCI) (Fig. 24.4), proposed by Strong et al.[11] The UCI is obtained by dividing the total number of complete vascular coils by the umbilical cord length. Hypercoiled (UCI>0.3 coils/cm) and hypocoiled (UCI<0.1 coils/cm) umbilical cords were both associated with increased fetal risk. Some studies conducted postnatally showed that the absence or paucity of umbilical vascular coils

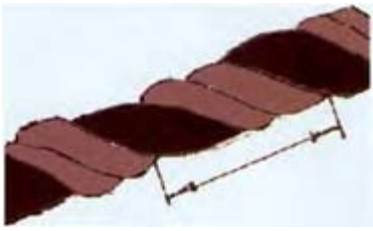

Figure 24.4: The umbilical cord coiling index

is a condition frequently associated with unexplained fetal demise, intrauterine growth disorders, abnormal fetal karyotype, the need of interventional delivery and intrapartum fetal heart rate disturbances.[12,13] Moreover Otsubo et al[14] found an association between hypocoiled cords and abnormal placental insertion of the cord. Abnormal cord coiling is believed to be a chronic state, established in early gestation, that may have chronic and acute effects on fetal well-being. The cause of abnormal cord coiling is not known and its effect on neurological status of survivors are also unknown, but antenatal detection of abnormal cord coiling index by ultrasound could lead to elective delivery of fetuses at risk. An attempt has been made to estimate prenatally the UCI by measuring the sonographic distance between coils. The sonographic UCI was defined as the reciprocal of this distance. Whilst Degani et al[12] found a good correlation between the sonographic UCI at term gestation and the true coiling index at delivery Qin et al[15] found a poor correlation between the UCI in the second trimester and the true UCI at term. Moreover, there are also differences in coiling indices at different segments of the umbilical cord.

DISCORDANT UMBILICAL ARTERIES

Usually both umbilical arteries are of similar diameter. Discordant arteries is a specific entity that has been associated with placental abnormalities, variation of the umbilical

cord insertion and gestational diabetes (Fig. 24.5).[16] Each umbilical artery supplies one lobe of the placenta and

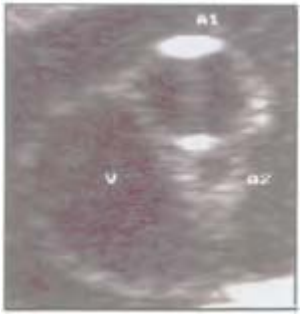

Figure 24.5: Discordant umbilical arteries. A1: larger umbilical artery, A2: smaller umbilical artery, V: umbilical vein

therefore each artery is considered to be an end artery. Only a small interarterial vessel (Hyrtl anastomosis) (Fig. 24.6) located within 3 cm from the placental cord insertion connects both arteries and it is believed that this structure fulfils the function of a pressure-equalizing system between umbilical arteries and between the two lobes of the placenta.[17] Discordant arteries may be caused by a malfunction or absence of the Hyrtl anastomosis and differences in blood flow impedance between both lobes of the placenta. The clinical significance of antenatally detected discordant umbilical arteries is not only its association with placental anomalies, but also an increased risk of

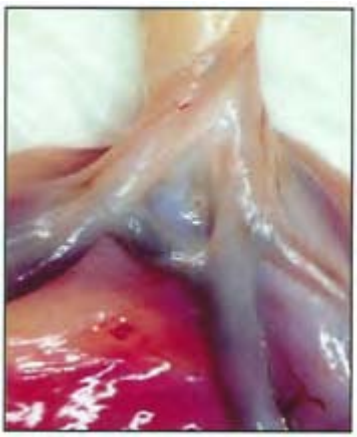

Figure 24.6: Hyrtl anastomosis

SGA infant, low Apgar score and preterm delivery. Abnormal Doppler velocimetry, with high resistance pattern in the smaller one and normal Doppler in the other artery, should be considered with caution, because it does not seem to be associated with poor perinatal outcome.[16]

SINGLE UMBILICAL ARTERY (SUA)

The incidence of SUA (Fig. 24.7) in uncomplicated pregnancy is 0.5–2.5% reaching 5% in twin pregnancies.[18] The most important clinical implication of SUA is its association with a huge number of syndromes and fetal structural and chromosomal abnormalities,[19–21] with IUGR,[18] unexplained fetal death, placental abnormalities and abnormalities of the umbilical cord insertion.[19] Even in the absence of congenital or chromosomal abnormalities fetuses with SUA have a higher perinatal mortality rate.[19] Prenatal sonography can identify only 37% of fetal anomalies associated with SUA[21] and this is important during counselling. Fetal karyotyping should be offered when additional anomalies are present. Moreover, fetal growth should be monitored and pediatricians have to be informed in order to search for

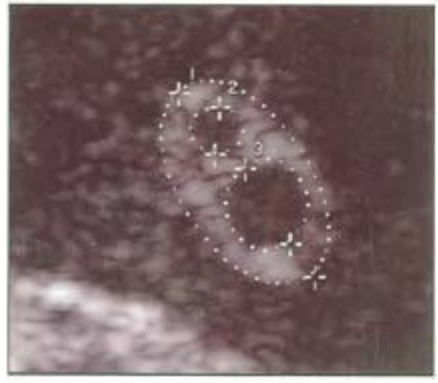

Figure 24.7: Single umbilical artery

The diagnosis is quite easy to carry out. Usually the single artery is larger due to an adaptational dilatation of the single artery and sometimes the diameter may reach that of the umbilical vein.[22] It is important to look at different parts along the umbilical cord to rule out fused arteries. Color Doppler can be used to visualize the single artery as the artery courses around the bladder. Usually the left one is absent.[23]

UMBILICAL CORD TUMORS

Omphalomesenteric duct cyst and allantoid cyst represent the most common cystic lesions of the umbilical cord (Fig. 24.8). They are often located close to the fetal insertion

of the umbilical cord and may vary widely in size. The incidental detection of single umbilical cord cysts in early gestation which usually disappears completely is not associated with adverse pregnancy outcome.[24,25] However, multiple umbilical cord cysts in the first trimester and cysts detected in the second and third trimester of gestation are highly associated with structural and chromosomal abnormalities, especially trisomy 18.[26]

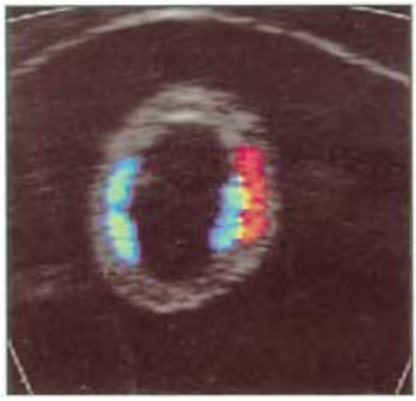

Figure 24.8: Allantoid cyst

Solid tumors of the umbilical cord are extremely rare anomalies. The majority of them are vascular tumors such as hemangiomas which can cause fetal cardiac dysfunction and polyhydramnios.[27] Teratomas of the umbilical cord have also been described.

REFERENCES

1. Raio L, Ghezzi F, Di Naro E. Sonographic measurement of the umbilical cord and fetal anthropometric parameters. Eur J Obstet Gynecol Reprod Biol 1999; 83:131–35.
2. Bruch JF, Sibony O, Benali K. Computerized microscope morphometry of umbilical vessels from pregnancies with intrauterine growth retardation and abnormal umbilical artery Doppler. Hum Pathol 1997; 28:1139–45.
3. Di Naro E, Raio L, Ghezzi F. Longitudinal umbilical vein blood flow changes in normal and growth-retarded fetuses. Acta Obstet Gynecol Scand 2002; 81:527–33.
4. Di Naro E, Ghezzi F, Raio L. Umbilical vein blood flow in fetuses with normal and lean umbilical cord Ultrasound Obstet Gynecol 2001; 17:224–28.
5. Raio L, Ghezzi F, Di Naro E. Altered sonographic umbilical cord morphometry in early-onset preeclampsia. Obstet Gynecol 2002; 100:311–16.
6. Raio L, Ghezzi F, Di Naro E. Umbilical cord area and fetal anthropometric parameters. Am J Obstet Gynecol 1998; 178:164, abstr.578.
7. Ghezzi F, Raio L, Di Naro E. Nomogram of Wharton's jelly as depicted in the sonographic cross section of the umbilical cord. Ultrasound Obstet Gynecol 2001; 18:121–25.
8. Weissman A, Jakobi R Sonographic measurements of the umbilical cord in pregnancies complicated by gestational diabetes. J Ultrasound Med 1997; 16: 691–94.

9. Ghezzi F, Raio L, Di Naro E. First-trimester sonographic umbilical cord diameter and the growth of the human embryo. Ultrasound Obstet Gynecol 2001; 18:348–51.
10. Ghezzi F, Raio L, Di Naro E. First-trimester umbilical cord diameter: a novel marker of fetal aneuploidy. Ultrasound Obstet Gynecol 2002; 19:235–39.
11. Strong TH Jr, Jarles DL, Vega JS, Feldman DB. The umbilical coiling index. Am J Obstet Gynecol 1994; 170:29–32.
12. Degani S, Leibovich Z, Shapiro I. Early second-trimester low umbilical coiling index predicts smallfor-gestational-age fetuses. J Ultrasound Med 2001; 20:1183–88.
13. Georgiou HM, Rice GE, Walker SP. The effect of vascular coiling on venous perfusion during experimental umbilical cord encirclement. Am J Obstet Gynecol 2001; 184:673–78.
14. Otsubo Y, Yoneyama Y, Suzuki S. Sonographic evaluation of umbilical cord insertion with umbilical coiling index. J Clin Ultrasound 1999; 27:341–44.
15. Quin Y, Lau TK, Rogers MS. Second-trimester ultrasonographic assessment of the umbilical coiling index. Ultrasound Obstet Gynecol 2002; 20:458–63.
16. Raio L, Ghezzi F, Di Naro E. The clinical significance of antenatal detection of discordant umbilical arteries. Obstet Gynecol 1998; 91:86–91.
17. Raio L, Ghezzi F, Di Naro E. In-utero characterization of the blood flow in the Hyrtl anastomosis. Placenta 2001; 22:597–601.
18. Leung AKG, Robson WLM. Single umbilical artery. Am J Dis Child 1989; 143:108–11.
19. Heifetz SA. Single umbilical artery: a statistical analysis of 237 autopsy cases and review of the literature. Perspect Pediatr Pathol 1994; 8:345–78.
20. Catanzarite VA, Hendricks SK, Maida C. Prenatal diagnosis of the two-vessels cord: implications for patient counselling and obstetric management. Ultrasound Obstet Gynecol 1995; 5:98–105.
21. Persutte WH, Hobbins J. Single umbilical artery. A clinical enigma in modern prenatal diagnosis. Ultrasound Obstet Gynecol 1995; 6:216–29.
22. Persutte WH, Lenke RR. Transverse umbilical arterial diameter: a new technique for the prenatal diagnosis of single umbilical artery. J Ultrasound M 1994; 13:763–66.
23. Abuhamad AZ, Shaffer W, Mari G. Single umbilical artery: does it matter which artery is missing? Am J Obstet Gyneco 1995; 173:728–32.
24. Sepulveda W, Leible S, Ulloa A. Clinical significance of first trimester umbilical cord cyst. J Ultrasound Med 1999; 18:95–99.
25. Raio L, Ghezzi F, Di Naro E. Society of Gynecol Investigation 2002 abst.
26. Stella A, Babbo GL. Omphalocele and umbilical cord cyst. Prenatal diagnosis. Minerva Ginecol 2000; 52:213–16.
27. Tennstedt C, Chaoui R, Bollmann R. Angiomyxoma of the umbilical cord in one twin with cystic degeneration of Wharton's jelly. A case report. Pathol Res Pract 1998; 194:55–58.

Chapter 25
The Placenta

Ratko Matijevic

INTRODUCTION

The placenta has long been overlooked by medicine. It is essentially a fetal organ and represents the link between the developing fetus and the mother. In the human placenta, trophoblast erodes into the decidua so that endothelium of the maternal blood vessels is destroyed and maternal blood is in direct contact with the chorion. Because of that, placenta enables the fetus to take oxygen and nutritients from the maternal blood and serves as the excretory organ for carbon dioxide and other waste products of fetal metabolites. As well as that the placenta forms a barrier against the transfer of infection to the fetus and secretes a large amount of hormones in maternal circulation.

Many clinical problems are attributed to the placenta despite the fact that they cannot always be explained on pathologic explanation.[1] The interest of sonographers in this short-lived organ is well known and described. As placenta has attained its final thickness and shape at the end of the fourth gestational month, this is an ideal time to perform initial ultrasound examination. In this chapter we will describe some normal and pathologic conditions related to the placenta recognizable by ultrasound.

PLACENTAL THICKNESS, SHAPE AND VOLUME

Placenta has its final thickness and shape after 16 weeks of pregnancy. However, the growth of placenta continues by the meaning of circumferential enlargements throughout second and third trimester. The normal placenta thickness is between 3 to 5 cm. Abnormal placental thickness on ultrasound examination throughout pregnancy was correlated to perinatal mortality and morbidity. A linear increase of placental thickness was found to correlate with gestational age throughout pregnancy. In the presence of intrauterine growth restriction or pre-eclampsia, placenta may be thinner than expected (Fig. 25.1). Thick placenta was determined as placenta that was above the 90th centile. It is usually related to intrauterine infection, hydrops and multiple pregnancy (Fig. 25.2). No correlation was found between placental thickness and maternal age or parity. However, it was found that sonographically thick placenta is associated with increased perinatal risk with

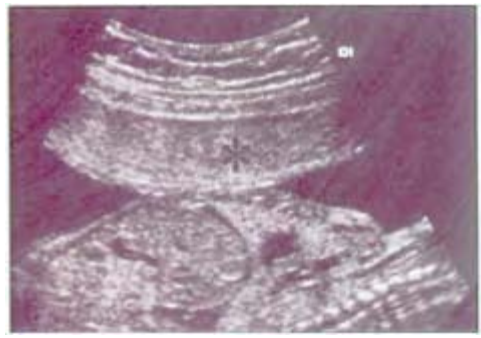

Figure 25.1: Thin placenta in the case of intrauterine growth restriction

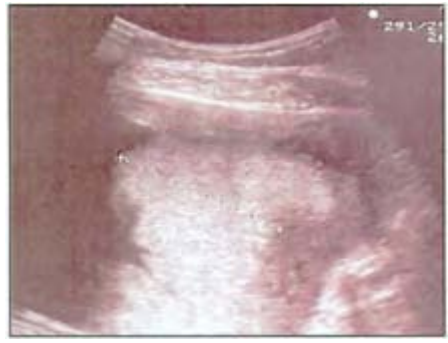

Figure 25.2: Thick placenta in the toxoplasmosis infection

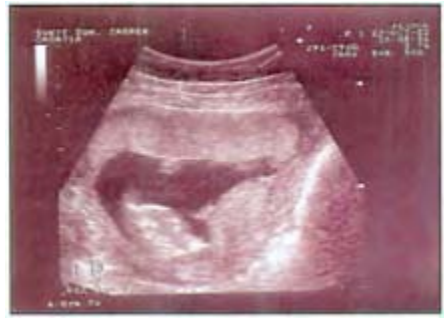

Figure 25.3: Succenturiate placental lobe

increased mortality related to fetal anomalies and higher rates of both small for gestational age and large for gestational age infants at term.[2]

Up to 8% of placentas has succenturiate or accessory lobes.[3] This is a separate mass of chorionic villi connected to the rest of the placenta by vessels. These vessels are within the membranes. The sonographic appearance of succenturiate placenta is presented on Figure 25.3. The antenatal diagnosis of succenturiate placental lobe is of importance, as it may remain retained inside the uterus after delivery. As well as that, it may cause postpartum hemorrhage, but it is not rare that succenturiate lobe of the placenta and connecting vessels can cause antenatal hemorrhage. This is of importance particularly if connecting vessels are present on the projection

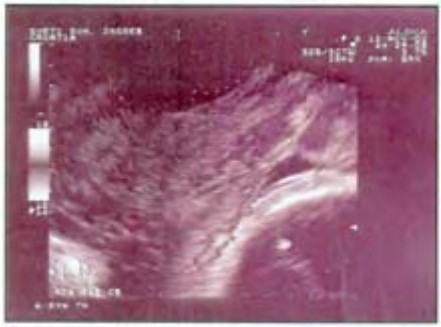

Figure 25.4: Vasa previa

of internal cervical os (Fig. 25.4). This condition is named vasa previa and bleeding in such situation represents direct fetal blood loss which may result in fetal death if the intervention is delayed. It is rarely reported condition in which fetal blood vessel(s) from the placenta or umbilical cord crosses the internal cervical os. The incidence is 1:3000 deliveries with high fetal mortality rate being between 50 and 90%. Such fetal mortality is a result of blood vessel tearing at the time the fetal membranes rupture or in labor. As well as that, vasa previa is associated with inadequate fetal oxygen supply. The veins of the umbilical cord normally run from the middle of the placenta to the baby. Velamentous insertion means that the veins, now unprotected by Wharton's jelly, lay across the membranes before they come together into the umbilical cord. This condition has the umbilical cord insert on the chorioamniotic membranes instead of on the main portion of the placenta. Vasa previa often occurs with a low-lying placenta (due to scarring of the uterine wall by a previous miscarriage or a D&C), an unusually formed placenta (a bilobed placenta or succenturiate-lobed [(accessory) lobe is a second or third placental lobe that is much smaller than the largest lobe] placenta), an in-vitro fertilization pregnancy, and multiple pregnancies (twins, triplets, etc).

Vasa previa may not be suspected until the fetal vessel rupture occurs. When vasa previa is found before labor, the baby has a much greater chance of surviving. Vasa previa can be detected during pregnancy as early as the 16th week of pregnancy with use of transvaginal sonography in combination with color Doppler. Because of the closeness of the vessels to the lower segment of the uterus, rupture of these vessels can happen at

any time, but most often during an amniotomy. When vasa previa is diagnosed, a planned cesarean section before labor begins can save the baby's life. Cesarean section should be done early enough to avoid an emergency, but late enough to avoid problems associated with prematurity.

Other variations of the placental shape include placenta membranacea. This represents annular or ring-shaped placenta. It is associated with antenatal and postnatal hemorrhage. The characteristic ultrasound appearance of such placenta is characterized as a mass of placental tissue which extend over a most of the uterine cavity (Fig. 25.5).[4]

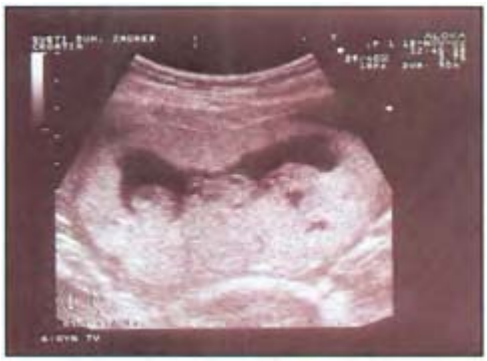

Figure 25.5: Placenta membanacea

Placental volume was speculated to be a useful parameter for the indirect assessment of some fetal conditions. It was investigated as a potential "marker" for chromosomal anomalies. Metzenbauer et al compared first-trimester placental volume in chromosomally abnormal and normal pregnancies. Among 2863 pregnancies evaluated, there were 17 with major chromosomal defects (nine cases of trisomy 21, four of trisomy 18, two of trisomy 13, and one each of Turner syndrome and 48, XXY+21). The median placental quotient in the chromosomally abnormal group (0.67) was significantly lower than that in the normal fetuses (0.98). In nine of the 17 affected pregnancies the quotient was below the 10th centile of the normal range.[5] As well as that, the placental volume was used as second trimester marker to predict birth size. It was found that placental volume in the second trimester was positively associated with all birth measurements, and it was concluded that low birth weight was often preceded by small placental volume in the second trimester. Placental volume was proposed as more reliable predictor of size at birth than fetal measurements, and may be useful in early identification of the fetus at risk in the perinatal period.[6] This is not in concordance to previously published results obtained by three-dimensional ultrasound. This group of authors found placental volume to be insufficient for predicting small for gestational age infants.[7]

NORMAL PLACENTAL LESIONS

All placental lesions are difficult to assess because there is often a discrepancy between the ultrasound findings, clinical diagnosis and pathology. Large placental lesions especially when solid and echogenic on ultrasound may be associated with a high maternal serum alpha-fetoprotein, intrauterine growth retardation or uteroplacental insufficiency. Pathological examination as infarction, hematoma or both may be related to potential problems in pregnancy and it was suggested that the growth of placental lesions during pregnancy may be an important sign related to the severity of the disease and therefore poor outcome.[8]

Subchorionic Fibrin Deposition

Subchorionic hypoechogenic areas are present in normal pregnancy. They represent areas of fibrin deposition in the term placenta.[9] They are characterized as a fibrin collection between

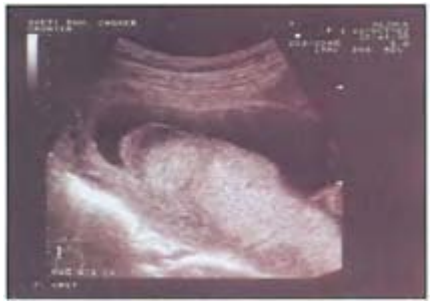

Figure 25.6: Subchorionic fibrin deposition

chorionic plate and placental villi (Fig. 25.6).[1,9] It is result of pooling and stasis of maternal blood in the intervillous space beneath the chorion, which leads to thrombosis and secondary fibrin deposition.[1] Differential diagnosis may include chorioangioma of the placenta.

Intervillous Thrombosis

Intervillous thrombosis represents bleeding from fetal vessels. It is characterized as intraplacental areas of hemorrhage with variable appearance dependant on the age of lesion. Fresh lesions are dark red, with aging become brown, yellow and finally white. Intervillous thrombosis may be found in up to 50% of the term placentas. Ultrasound appearance of intervillous thrombosis is anechogenic or hypoechogenic areas in the placenta of variable size (Fig. 25.7). They can be as small as few millimeters up to few centimeters in size and they may extend to subchorionic space or basal

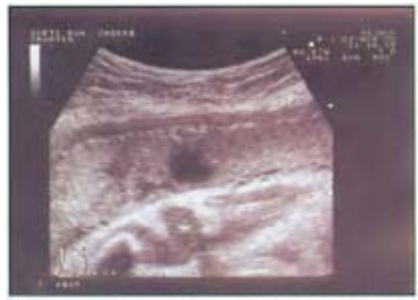

Figure 25.7: Intervillous thrombosis

plate.[10] The clinical significance of intervillous thrombosis is in the possible presence of fetalmaternal hemorrhage. Microscopically, fetal and maternal red blood cells may be present and the incidence is increased in the Rh isoimmunisation.[10]

Perivillous Fibrin Deposition

The incidence of perivillous fibrin deposition is around 20% at the term uncomplicated pregnancy.[1] It is a result of pooling and stasis of blood in intervillous space. Ultrasound appearance of perivillous fibrin deposition consists of several intraplacental lesions of low echogenicity (Fig. 25.8). They are of no clinical significance.

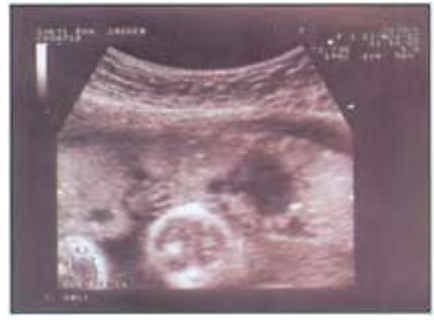

Figure 25.8: Perivillous fibrin deposition

Maternal Blood Lakes

It is possible that maternal lakes represent early stages of intervillous thrombosis.[1] They are of no clinical significance and it is believed that they correspond to blood filled spaces at delivery. Blood flow can be demonstrated in some of these lesions by color and power Doppler technique, while black and white appearance is characterized by anechogenic or hypoechogenis areas in the placenta sometimes surrounded by hyperechogenic echoes (Fig. 25.9).

Placental Infarcts

Placental infarction results from disruption of blood supply to the placenta. As placenta is

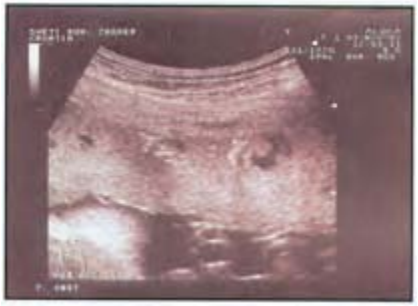

Figure 25.9: Maternal blood lakes

Figure 25.10: Placental infarcts—macroscopis appearance

completely dependent on the maternal blood supply, there is underlying problem in maternal blood supply resulting in coagulation necrosis of villi (Fig. 25.10).[1] In the most circumstances infarcts are present on the placental basis, in the close proximity to the basal plate and they are variable in size (Fig. 25.11). Small infarcts can be found in ¼ of the placenta without clinical significance, but they are frequently related to preeclampsia and essential hypertension. Placental infarcts can be diagnosed by ultrasound only if they are complicated by hemorrhage.[11]

The clinical significance of placental infarction is still unknown, however, some recent reports suggests that, compared to gestational agematched controls, infants born to mothers with maternal floor infarction (MFI) of the placenta had a higher incidence of CNS injury on neonatal cranial ultrasound examinations. As well as that,

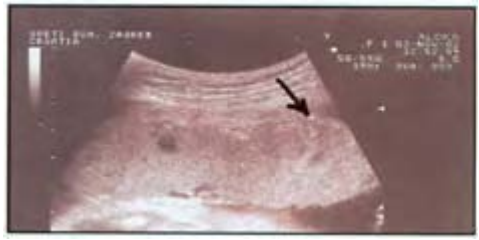

Figure 25.11: Placental infarcts (arrow)

at follow-up they were more likely to have a suspicious or abnormal neurologic examination.[12]

Placental Calcifications

The deposition of calcium in the placenta is normal physiologic process in the pregnancy.[13] Placental calcifications are microscopic during the first two trimesters and they become macroscopically apparent in the third trimester, mostly after 33 weeks.[1,14] Calcifications primary appear on the basal plate and septa, but they can be found in the perivillous space and subchorionic space. Their characteristic is the absence of characteristic significant shadowing otherwise typical for the calcified tissues. By the presence of the calcifications, the placenta can be divided into the four grades. They are present on the Table 25.1.

The significance of placental grading and "aging" is not clear.[13,15] More than 50% of the placentas show some degree of calcifications after 33 weeks and there is no increased calcification in postmature placenta.[16] Possible effects of the morphological changes in the placenta on fetal prognosis and on umbilical artery and uterine artery Doppler indices in late, low-risk pregnancies was investigated in the study of Kara et al.[17] They found that morphological changes of placental aging are common and have no effect on fetus and on Doppler flow of the umbilical and uterine arteries, provided these are not high-risk pregnancies and placental changes are not infarction, villitis or severe structural or localization anomaly. However, colonic and placental stage 3 grading was found to be a reliable and reproducible

Table 25.1: Placental grading

	Grade 0 (Fig. 25.12)	*Grade 1 (Fig. 25.13)*	*Grade 2 (Fig. 25.14)*	*Grade 3 (Fig. 25.15)*
Presence	Early pregnancy, 1st and 2nd trimester	After 28 weeks, in 40% placentas at term	After 36 weeks, in 45% placentas at term	After 38 weeks
Chorion plate	Smooth, well defined	Slightly irregular shape	"notches" which do not reach basal plate	Calcified septa up to basal plate

Placenta	Homogenous tissue	Few “dot like” calcifications without acoustic shadowing	Several notches with calcifications	Circular calcifications with or without central anechogenic areas
Basal plate	No echoes	No echoes	Linear hyperechogenic echoes	Larger echoes with shadowing

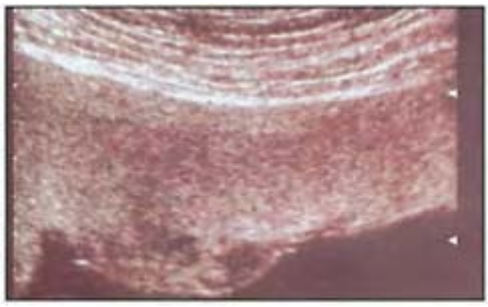

Figure 25.12: Placenta grade 0

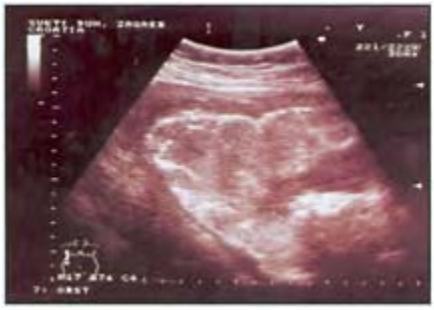

Figure 25.13: Placenta grade 1

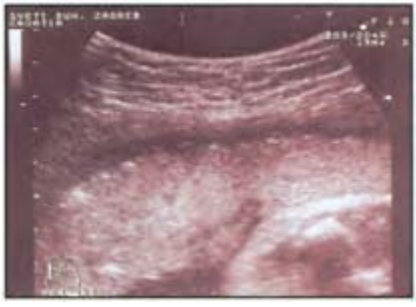

Figure 25.14: Placenta grade 2

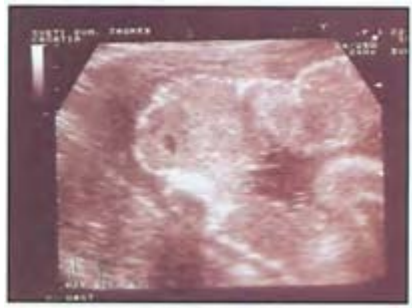

Figure 25.15: Placenta grade 3

ultrasonographic scale that can help predict fetal lung maturity.[18]

ABNORMAL PLACENTAL LESIONS

Tumors (Primary and Secondary)

Placental tumors are relatively rare. Gestational trophoblastic disease is discussed in the chapter of abnormal early pregnancy, and excluding this pathologic condition, there are two non-trophoblastic primary tumors of the placenta. This includes relatively common chorioangioma and the rare teratoma. Ultrasound appearance of chorioangioma is well circumscribed solid intraplacental mass (Fig. 25.16). If large they can be associated with fetal hydrops by congestive heart failure, cardiomegaly, intrauterine growth restriction, and intrauterine fetal death; while small lesions are usually of no clinical significance. The location of placental chorioangioma is usually within the placenta while large tumors may protrude from the fetal surface. Ultrasound appearance includes tumor mass of irregular echogenicity well surrounded from the rest of the placenta. Color and pulsed Doppler ultrasound may demonstrate vascularity of the lesion and color Doppler imaging helps differentiate placental chorioangioma from other placental lesions and may be useful in the prenatal follow-up of chorioangioma.[19,20] In recent study of Zalel et al fifteen cases of placental masses were evaluated; 8 of them were identified as placental hemorrhage

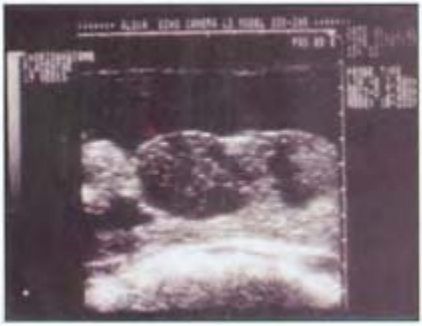

Figure 25.16: Angioma

or subchorionic hematoma on the basis of the sonographic findings. The other 7 cases were identified antenatally as placental chorioangioma, at a mean menstrual age of 23 weeks and a mean maternal age of 29 years. The mean size of the tumor was 6.5 cm (range, 4–13 cm). All cases of chorioangioma showed either substantial internal vascularity or a large feeding vessel within the tumor. Three infants were delivered at term with favorable outcome; 2 of them demonstrated reduction of the intratumoral blood flow during follow-up. The other 4 cases were delivered at or before 32 weeks' menstrual age (1 intrauterine fetal death, 2 terminated pregnancies, and 1 normal infant). No case of placental hematoma demonstrated blood flow within the lesion or was associated with complications of the pregnancy. In severe forms placental chorioangioma can be treated by alcohol ablation of the feeding vessel. This might be helpful in the presence of the large tumor and signs of heart failure and hydrops.[21]

As well as ultrasound, another possible diagnostic method for the evaluation of placental masses includes magnetic resonance.[22]

Placental teratomas are extremely rare.[23]There was only few lesions reported in the literature from 1925 to 2001. They are located between amnion and chorion and usually are of no clinical significance.[13] Teratomas may present throughout the variety of anatomic lesions, including a misdiagnosed acardiac fetus.[24]

Other primary intraplacental tumors are very rare but they may have a significant clinical impact on the mother and fetus. There was described case of an intraplacental, potentially malignant smooth muscle tumor, presenting as intraplacental, hypoechoic area consistent with chorioangioma.[25] Therefore, although ultrasound differentiation is difficult, rare non-trophoblastic tumors should be considered in the differential diagnosis of placental masses. Secondary placental tumors are also very rare and they include metastatic activity of breast and lung carcinoma and melanoma. They can be suspected, but not diagnosed on ultrasound examination, and final diagnosis is usually made on postmortem examination of the suspected placental mass.

Abscess

Macroabscesses of the placenta are very rare.[1] The commonest microorganisms found include beta hemolytic Streptococcus, Mycobacterium tuberculosis and Listeria.

RETROPLACENTAL SPACE

Retroplacental Hematomas

The placenta can easily be recognized from retroplacental space, including the decidua and myometrium (Fig. 25.17). The myometrium is usually hypoechogenic on ultrasound examination with hyperechogenic echoes of the placenta. On the placental-myometrial junction there is intensive blood flow on the opening of spiral arteries into the intervillous space. Retroplacental hematoma are caused by retroplacental hemorrhage. It can manifest by either external bleeding without the formation of excessive intrauterine retroplacental hematoma or formation of retroplacental or marginal hematoma without significant external bleeding, or formation of a submembranous hematoma at a distance from the placenta with or without external bleeding.[1] It should be pointed that in the most of the circumstances ultrasound examination of the women with antenatal hemorrhage will be negative for the presence of hematoma if there is external bleeding.

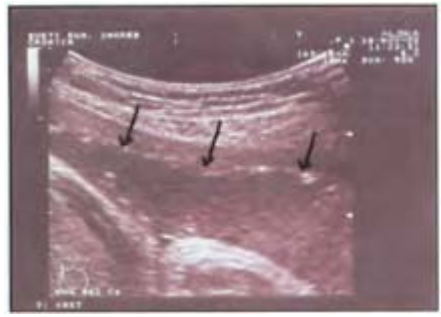

Figure 25.17: Normal retroplacental space

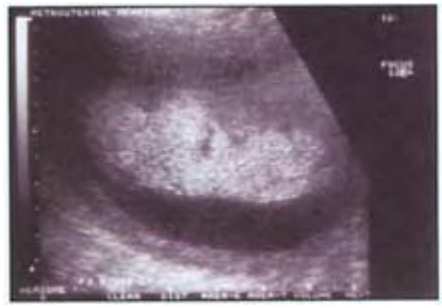

Figure 25.18: Retroplacental hematoma

Subchorionic hematomas may be related to fetal growth restriction and abnormal umbilical blood flow[26] and fetal hydrops.[27] Retroplacental or submembranous hematoma will present on ultrasound examination as a complex or hypoechoic mass usually in the close proximity of the placenta (Fig. 25.18). Such hematoma are the most common in early pregnancy. In this case, if bleeding is not excessive and appropriate management include follow up with repeated ultrasound examination in a week time with the prevention of Rh immunization if indicated.

Placental Abruption

Abruption defines acute placental separation of the placenta from the uterus prior to delivery of the fetus (Fig. 25.19). The symptoms include pain, uterine tenderness and abdominal pain and it is usually accompanied with vaginal bleeding. Such

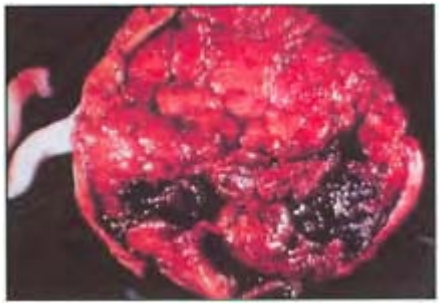

Figure 25.19: Placental abruption—macroscopic appearance

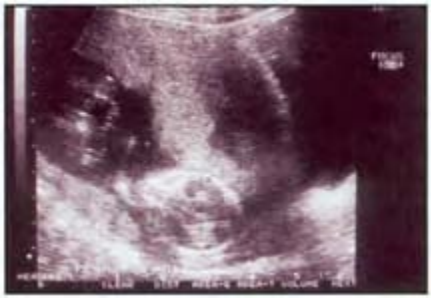

Figure 25.20: Placental abruption

bleeding, if excessive may cause maternal hypovolemia and shock, while severe forms of abruption result in diminished fetoplacental transfer and consequently may cause fetal death *in utero*.

Ultrasound appearance of placenta abruption varies. Usually it is characterized by bizarre echoes between placenta and myometrium variable size and echogenicity (Fig.

25.20). Is should be pointed that small abruption may not be recognizable on ultrasound examination, and in most of the circumstances when abruption can clearly be recognised fetus might be dead.

Subamniotic Hematoma

Subamniotic hematomas are classical placental pathological lesions resulting from the rupture of chorionic vessels near the cord insertion. Most Subamniotic hematomas are found after birth and result from excessive traction on the umbilical cord at delivery. The development of these lesions has been rarely reported in *utero*. The sonographic features were those of a poorly reflective ovalshaped cystic mass overlying the fetal plate of the placenta and covered in a thin membrane.[28]In all the cases, a cystic structure containing a thrombotic mass arising from the amniotic membrane, which was attached to the fetal placental surface, was found after delivery. They may be associated with elevated serum alphafetoprotein and be related to slow fetal growth, vaginal bleeding and polyhydramnios.

PLACENTA PREVIA

It is a placenta inserted partially or wholly in the lower uterine segment. The incidence of placenta previa is around 1% of all deliveries.[29] With the advent of ultrasound up to 45% of placenta previa cases may be diagnosed early in the second trimester.[30] However, this pathologic condition is usually overdiagnosed by ultrasound as the correct diagnosis of placenta previa can not be made before 30–32 weeks as the lower uterine segment is not formed. Formation of the lower uterine segment causes the extension of this part of the uterus and if placenta is not implanted on the both sides of internal cervical os, or in the close proximity of the internal cervical os, it is going to be pulled upwards making internal cervical os free from the placenta. Second reason for overdiagnosing placenta previa represents full urinary bladder and uterine contractions. In such cases it is important to examine the pregnant women after 32 weeks or earlier if antenatal hemorrhage occurs. In the diagnosing placenta previa, transvaginal approach was found to be much better compared to transabdominal ultrasound examination.[31]

This is particularly true in the posteriorly located placenta previa as presenting part of the fetus can obstruct the clear visualization of internal cervical os making precise diagnosis impossible. There are four grades of placenta previa presented on Table 25.2. In the recent years the shape of the placenta in the placenta previa was correlated to pregnancy outcome. Clinical significance of the shape of the lower placental edge in women with transvaginal sonographic diagnosis of placenta previa was assessed. The incidence of major complications in thick-edge or central placenta was compared to that in the thin-edge group, and women having a low-lying placenta with a thick edge had a significantly higher rate of antepartum hemorrhage, abdominal delivery, abnormally adherent placenta and low birth weight.[32]

Table 25.2: Grading of placenta previa

Grade	*Description*
I	The placenta is in the lower uterine segment but its lower edge does not reach the internal os (Fig. 25.21)
II	The lower edge of the low-lying placenta reaches but does not cover the internal os (Fig. 25.22)
III	The placenta covers the internal os asymmetrically (Fig. 25.23)
IV	The placenta covers internal os symmetrically (Fig. 25.24)

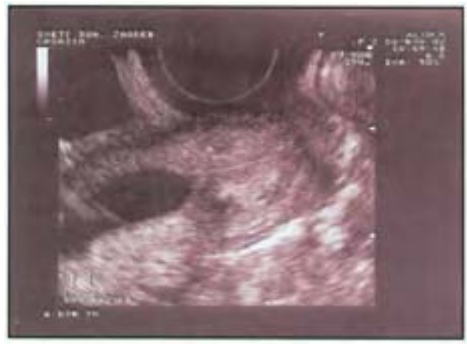

Figure 25.21: Placenta previa grade 1

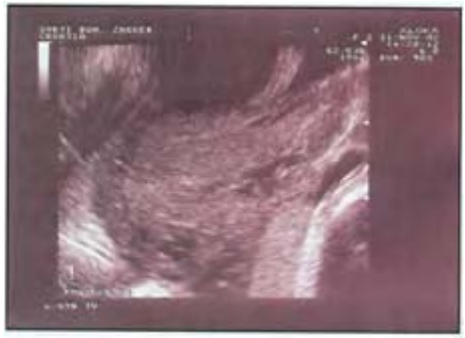

Figure 25.22: Placenta previa grade 2

PLACENTA ACCRETA

Placenta accreta is an abnormal adherence, either in whole or in part, of the placenta to the uterine wall.[33] The incidence is approximately 1:7000

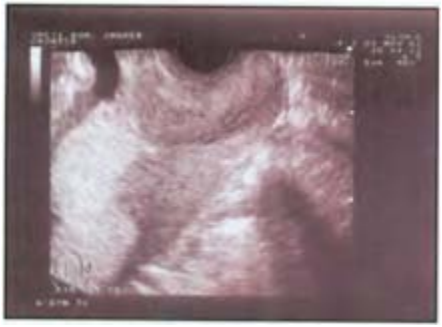

Figure 25.23: Placenta previa grade 3

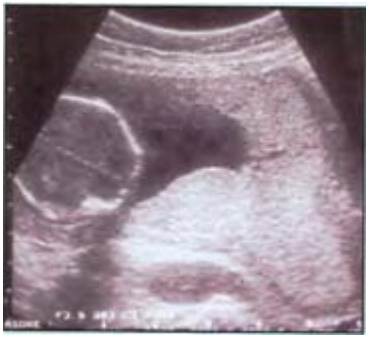

Figure 25.24: Placenta previa grade 4

deliveries. The types of placenta accreta are presented on Table 25.3. Placenta accreta is commonly associated with placenta previa because of a deficiency of decidua in the lower uterine segment. Placenta accreta can be diagnosed by ultrasound, mostly by the absence of retroplacental hypoechogenic zone of the decidua/myometrium.[35]

Table 25.3: The types of placenta accreta[34]

Type	*Characteristics*
Placenta accreta	Pathological adherence due to the paucity of underlying placenta
Placenta increta	The placenta invades the uterine wail
Placenta percreta	The invasion reaches the uterine serosa and may even rupture the uterus

PLACENTAL VESSELS

In recent years, power Doppler technology combined with three-dimensional (3D) ultrasound examinations offers promise in evaluation of placental vascular network in

ongoing pregnancy. These two new developments in ultrasound technology differs from "classical" two dimensional (2D) conventional color Doppler technique with better sensitivity in detecting lower blood flow velocities.[36,37]

Anatomically, the umbilical cord, normally containing two umbilical arteries and one umbilical vein, inserts into the placenta. The umbilical arteries give rise to the fetal circulation of the placenta via vessels that extend along the placental surface. Those vessels are named main stem vessels. They perforate the chorionic plate and give rise to a hierarchy of intraplacental vessels: from largest to smallest, the primary stem, secondary stem, tertiary stem, cotyledonary and villous. Visualization of these vessels is superior using 3D ultrasound with power Doppler technology.[37] Using power Doppler, ultrasound noise is less present as blood flow can be displayed as a homogenous background color rather than different colors as seen with conventional color Doppler.[38] Power Doppler uses color flow mapping, creating integrated signals more dependant on density, rather than blood flow velocity.[39] This make power Doppler more sensitive, providing the ability of visualization of blood vessels smaller in diameter with lower blood flow velocity, which is

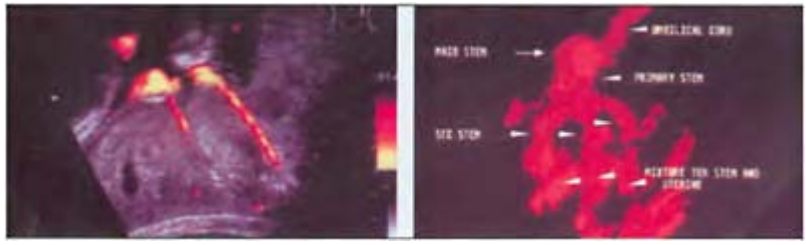

Figure 25.25: Fetal placental vessels by 2D (left) and 3D (right) power Doppler

characteristic of placental vessels. As well as that, there is no need for use of low frequency filters, which may result in the complete absence of the detection of low velocity blood flow signals. Blood flow signal becomes angle independent and smaller vessels analyzed in transverse section will appear on the ultrasound screen, which is not possible using conventional color Doppler technology. However, power Doppler does not have the possibility of detecting the direction of the blood flow. With such characteristics, power Doppler was found to be very useful in the mapping of blood flow in parenchimatous organs as placenta and kidney. In the early days of power Doppler, the use of dehydroepiandrosterone sulphate (DHAS) was suggested as a contrast media in order to visualize placental blood vessels more clearly.[40] Nowadays, it was found that contrast media are not necessary, and the results of our study support this observation.[37,40]

2D power Doppler was found to be sufficient for the analysis of the major placental vessels, including the umbilical cord insertion and superficial placental vessels running on the chorional plate. It is possible to follow umbilical artery and vein from the cord insertion easily but it took a serious effort and experience to follow every single superficial placental vessel from the umbilical cord insertion to the place where it pierce

chorional plate disappearing into the cotyledon (Fig. 25.25). In order to do so, 3D ultrasound with a power Doppler technique is superior compared to the

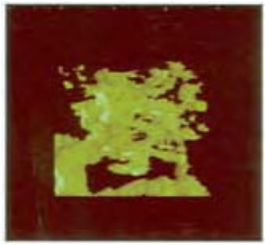

Figure 25.26: Fetal placental vessels by 3D power Doppler

2D ultrasound, being faster and more accurate. This is not only because of the possibility to memorize the segments of examination on the different memory media making subsequent analysis possible. 3D is faster in general, as it can present complete branching of the placental vessels in the defined segment of the placental tissue during the single examination (Fig. 25.26). Therefore, the time of exposure is reduced as well as the energy delivered by ultrasound reducing the potential harmful effect. Disadvantages of 2D ultrasound are obvious. Using even high quality top of the range equipment available on the market, it is still not possible to visualize complete architecture and branching of the stem vessels. Therefore, 2D power Doppler can only partially confirm the results of hystological studies about the branching of umbilical artery on the system of so called stem vessels during on going pregnancy.

3D power Doppler is superior to the 2D in detection and visualization of placental vascular branches.[37] There are several reasons for that. 2D power Doppler ultrasound can present blood vessels mostly if they are examined within their full or partial length. However, if they are examined in transverse section, despite the better visualization by power Doppler compared to color Doppler, those vessels will be displayed on the ultrasound screen as color-coded dots that may easily be missed or misdiagnosed as a motion artefact. Computer reconstruction of the numerous 2D images obtained during 3D examination and their combination can create the perception of third dimension. Those volume rendered images were valuable in allowing the investigator to acquire an improved overall understanding of placental anatomy. On those images, color-coded dots representing transverse section of small placental vessels can be combined together making possible visualization of the full or partial length of the examined blood vessel. Therefore, volume rendered images assisted the investigator in following the continuity of vessels as they wrapped around and twisted through the perception of third dimension. By the rotation of such computer generalized image it becomes much easier to see distal vascular branching of the main stem vessel, as far as to the level of tertiary stem vessel in 75% of cases. Therefore, 3D power Doppler can more precisely display the placental vessels in general, as well as their relationship to the surrounding structures inside the placenta.

The placental vascular system ends with cotyledonary and villous vessels. They were not displayed neither using 2D and/or 3D power Doppler ultrasound. Those vessels are characterized with low blood flow velocities, but more importantly, they are in the close proximity to the intervillous space and opening of the spiral arteries. Therefore, blood flow signals which might originate from them is going to be superimposed with much stronger signal obtained from opening of the spiral arteries making separate analysis impossible (Fig. 25.26).

As well as in singleton pregnancy, 3D power Doppler was found to be useful in the assessment of the placental anastomosis in multiple pregnancy.[41] Welsh et al assessed detection of arterioarterial and arteriovenous placental anastomoses in monochorionic pregnancy. They concluded that detailed anastomotic anatomy can be demonstrated by 3D power Doppler *in vivo*, and given the increasing evidence of implicating various anastomotic configurations in pathological inter-twin transfusion, this technique may prove useful in the antenatal assessment and treatment of monochorionic twin pregnancies. During last few years we also assessed the inter-twin anastomoses in women with twin to twin transfusion syndrome (TTTS) by 3D power Doppler ultrasound. We were able to display entire placental vascular network using 3D power Doppler sonography, including arteriovenous anastomoses responsible for a TTTS. Single unpaired vessel form a donor twin, running on the surface of the placenta, disappearing into the cotyledon can be seen, as well as single unpaired vessels arising from the same cotyledon running to the recipient twin (Fig. 25.27). Further work is in progress in order to confirm this observation on a larger number of women with TTTS. Every single placental unit is independent on the most distal level. They are communicating on the level of main stem vessels, when they join together on the placental surface close to the umbilical cord insertion. Therefore assessment of the blood flow in each of those units is of great importance for understanding the placental physiology and function, which becomes possible by the use of 3D power Doppler. Unfortunately, for a time being, we have the ability to analyze only static images without parallel functional Doppler studies. It is our belief that assessment of the fetal placental vessels in real time will become possible soon. The potential exists to identify high risk pregnancies; i.e. early placental insufficiency, arterial and venous placental thromboses, twin transfusion syndrome,

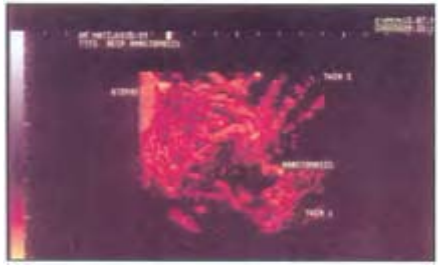

Figure 25.27: Combination of blood flow in the opening of spiral arteries, intervillous spaces and blood flow in terminal parts of fetal placental

placental infarction and placental abruption prior to the development of fetal compromise detectable by traditional methods.

REFERENCES

1. Spirt BA, Gordon LP. Sonography of the placenta. In: Fleischer AC, Manning FA, Jeanty P, Romero R. Sonography in obstetrics and gynecology. Principles and practice. Appleton & Lange 1996; 173.
2. Elchalal U, Ezra Y, Levi Y, Bar-Oz B, Yanai N, Intrator O, Nadjari M. Sonographically thick placenta: a marker for increased perinatal risk—a prospective cross-sectional study. Placenta 2000; 21:268–72.
3. Earn AA. Placental anomalies. Can Med Assoc J 1951; 65:118.
4. Molloy CE, McDowell W, Armour R. Ultrasonic diagnosis of placenta membranacea in utero. J Ultrasound Med 1983; 3:337.
5. Metzenbauer M, Hafner E, Schuchter K, Philipp K. First-trimester placental volume as a marker for chromosomal anomalies: preliminary results from an unselected population. Ultrasound Obstet Gynecol 2002; 19:240–42.
6. Thame M, Osmond C, Wilks R, Bennett FI, Forrester TE. Second-trimester placental volume and infant size at birth. Obstet Gynecol 2001; 98:279–83.
7. Hafner E, Philipp T, Schuchter K, Dillinger-Paller B, Philipp K, Bauer P. Second-trimester measurements of placental volume by three-dimensional ultrasound to predict small-for-gestational-age infants. Ultrasound Obstet Gynecol 1998; 12:97–102.
8. Rodriguez JG, Porter HJ, Andrews HS, Soothill PW. Placental lesions: is growth a predictor of bad outcome? Fetal Diagn Ther 1997; 12:163–66.
9. Spirt BA, Kagan EH, Rozanski RM. Sonolucent areas in the placenta: Sonographic and pathologic correlation. AJR 1978; 131:961.
10. Hooghland HJ, deHaan J, Vooys GP. Ultrasonographic diagnosis of intervillous thrombosis related to Rh isoimmunisation. Gynecol Obstet Invest 1979; 10:237.
11. Harris RD, Simpson WA, Pet LR. Placental hypoechoic/anechoic areas and infarction: sonographic-pathologic correlation. Radiology 1990; 176:75.
12. Adams-Chapman I, Vaucher YE, Bejar RF, Benirschke K, Baergen RN, Moore TR. Maternal floor infarction of the placenta: association with central nervous system injury and adverse neurodevelopmental outcome. J Perinatol 2002; 22:236–41.
13. Fox H. Pathology of placenta. WB Saunders, Philadelphia, 1978.
14. Tindall VR, Scott JS. Placental calcification. A study of 3025 singleton and multiple pregnancies. J Obstet Gynecol Br Commonw 1965; 72:356.
15. Spirt BA, Gordon LP. The placenta as indicator of fetal maturity. Facts and fancy. Semin Ultrasound 1984; 13:501.
16. Sprit BA, Cohen WN, Weinstein HM. The incidence of placental calcifications in normal pregnancy. Radiology 1982; 142:707.
17. Kara SA, Toppare MF, Avsar F, Caydere M.Placental aging, fetal prognosis and fetomaternal Doppler indices. Eur J Obstet Gynecol Reprod Biol 1999; 82:47–52.
18. Loret de Mola JR, Judge N, Entsminger C, DeViney M, Muise KL, Duchon MA. Indirect prediction of fetal lung maturity. Value of ultrasonographic colonic and placental grading. J Reprod Med 1998; 43:898–902.
19. Zalel Y, Gamzu R, Weiss Y, Schiff E, Shalmon B, Dolizky M, Achiron R. Role of color Doppler imaging in diagnosing and managing pregnancies complicated by placental chorioangioma. J Clin Ultrasound 2002; 30:264–69.
20. Sepulveda W, Aviles G, Carstens E, Corral E, Perez N. Prenatal diagnosis of solid placental masses: the value of color flow imaging. Ultrasound Obstet Gynecol 2000; 16:554–58.

21. Wanapirak C, Tongsong T, Sirichotiyakul S, Chanprapaph P. Alcoholization: the choice of intrauterine treatment for chorioangioma. J Obstet Gynaecol Res 2002; 28:71–75.
22. Kojima K, Suzuki Y, Makino A, Murakami I, Suzumori K. A case of massive subchorionic thrombohematoma diagnosed by ultrasonography and magnetic resonance imaging. Fetal Diagn Ther 2001; 16:57–60.
23. Meinhard K, Dimitrov S, Nicolov A, Dimitrova V, Vassilev N. Placental teratoma—a case report. Pathol Res Pract 1999; 195:649–51.
24. Gillet N, Hustin J, Magritte JR Givron O, Longueville E. Placental teratoma: differential diagnosis with fetal acardia. Gynecol Obstet Biol Reprod (Paris) 2001; 30:789–92.
25. Harirah HM, Jones DC, Donia SE, Bahado-Singh R. Intraplacental smooth muscle tumor. A case report. J Reprod Med 2001; 46:937–40.
26. Richards DS, Bennett BB.Prenatal ultrasound diagnosis of massive subchorionic thrombohematoma. Ultrasound Obstet Gynecol 1998; 11:364–66.
27. Uchide K, Suzuki N, Murakami K, Terada S, Inoue M. Subchorial hematoma: a probable cause of reversible nonimmune hydrops fetalis. Am J Perinatol 1997; 14:281–83.
28. Deans A, Jauniaux E. Prenatal diagnosis and outcome of subamniotic hematomas. Ultrasound Obstet Gynecol 1998; 11:319–23.
29. Iyasu S, Saftlas AK, Rowley DL et al. The epidemiology of placenta previa in US. 1979–1987. Am J Obstet Gynecol 1993; 168:1424.
30. Wexler P, Grottersfeld KR. Second trimester placenta previa: An apparently normal presentation. Obstetrics and Gynaecology 1977; 50:521–25.
31. Smith RS, Lauria MR, Comstock CH, Treadwell MC, Kirk JS, Lee W, Bottoms SF.Transvaginal ultrasonography for all placentas that appear to be low-lying or over the internal cervical os. Ultrasound Obstet Gynecol 1997; 9:22–24.
32. Ghourab S. Third-trimester transvaginal ultrasonography in placenta previa: does the shape of the lower placental edge predict clinical outcome? Ultrasound Obstet Gynecol 2001; 18:103–08.
33. Irving FC, Hertig AT. A study of placenta accreta. Surgery, Obstetrics and Gynecology 1937; 64:178–200.
34. Still DK. Postpartum hemorrhage and other problems of the third stage. In: James DK, Steer PJ, Weiner CR Gonik (Eds). High risk pregnancy. Management options. WB Saunders, London, 1996; 1175.
35. Finberg HJ, Williams JW. Placenta accreta. Prospective sonographic diagnosis in patients with placenta previa and prior cesarean section. J Ultrasound Med 1992; 11:333.
36. Pretorius DH, Nelson TR, Baergen RN, Pai E, Cantrell C. Imaging of placental vasculature using three dimensional ultrasound and color power Doppler: a preliminary study. Ultrasound Obstet Gynecol 1998; 1245–49.
37. Matijevic R, Kurjak A. The assessment of placental blood vessels by three—dimensional power Doppler ultrasound. J Perinat Med 2002; 30:26–32.
38. Macsweeney JE, Cosgrove DO, Arenson J. Colour Doppler energy (power) mode ultrasound. Clin Radiol 1996; 51;387–91.
39. Adler RS, Rubin JM, Fowlkes JB, Carson PL, Pallister JE. Ultrasonic estimation of tissue perfusion: a stochastic approach. Ultrasound Med Biol 1995; 21:493–500.
40. Hata T, Manabe A, Yonehara T, Aoki S, Miyazaki K. Power Doppler enhancement of the dehydroepiandrostencione sulphate in term pregnancy. Br J Obstet Gynaecol 1998; 105:360–65.
40. Welsh AW, Humphries K, Cosgrove DO, Taylor MJ, Fisk NM. Development of three-dimensional power Doppler ultrasound imaging of fetoplacental vasculature. Ultrasound Med Biol 2001; 27:1161–65.
41. Welsh AW, Taylor MJ, Cosgrove DO, Fisk NM. Freehand three-dimensional Doppler demonstration of monochorionic vascular anastomoses in vivo: a preliminary report. Ultrasound Obstet Gynecol 2001; 18:317–21.

Chapter 26
Ultrasound Based Diagnosis of Cervical Insufficiency and Evidence to Support the Intervention

Ratko Matijevic, Asim Kurjak, Ozren Grgic

INTRODUCTION

Late miscarriage (LM) and preterm delivery (PD) are two of the most important problems in modern obstetrics. In both cases there is premature expulsion of the fetus and placenta from the uterus before completed 37 weeks of pregnancy. The incidence of PD is between 5 and 10%, but exact incidence of miscarriage can not be precisely determined as the highest proportion of them occurs in early pregnancy around the time of implantation and they remain undiagnosed.[1,2] Earlier, the hypothesis was that recurrence rate of miscarriage and PD in subsequent pregnancies is as high as 100%, but today it is proven that such recurrence rate is between 30 to 55%, and it is dependant on etiological cause leading to miscarriage and PD.

There are numerous etiological factors causing LM and PD. Some of them are isolated but in the most of the cases they are multifactorial.[2] As well as that, some of them we can recognize in advance and act appropriately, however, most of them still can not be diagnosed precisely and therefore there is no appropriate management. Etiologic factors for LM and PD may generally be divided in seven subgroups including: fetal anomalies, female genital tract anomalies, hormonal problems, immunological causes, systemic maternal diseases, infection and cervical insufficiency (CI). CI is going to be discussed in this chapter. The importance of CI is in the second trimester of pregnancy causing LM and PD. It is well known that between 12 and 22 weeks of pregnancy there is progressive extension and growth of the uterus and normal cervix in this circumstances act as a sphincter preventing expulsion of the products of conception from the uterus. In CI, the ability of the cervix to “keep together” lower part of the uterus is reduced and directly responsible for LM and PD.[4]

CERVICAL INSUFFICIENCY: THE DIAGNOSIS

CI is defined as asymptomatic cervical dilatation in second and third trimester of pregnancy. Consequently, amniotic membranes can protrude into the cervical canal (and vagina in later stages), being responsible for further cervical dilatation, membrane rupture and LM and PD. In the absence of therapeutic intervention, this condition is likely to

reoccur in every subsequent pregnancy. There are several conditions related to cervical insufficiency and they are listed on Table 26.1.[2] However, the precise diagnosis of cervical insufficiency is still unclear and very difficult, particularly if it is based only on the patients' history. There are several reasons for that, mostly because of either inconsistent criteria used or non-standardized different methods described for the diagnosis of CI. If we manage to define sole and clear criteria of CI, cerclage would be a method of choice with potential reduction of perinatal mortality and morbidity related to LM and PD. CI can be suspected on the patient history including:

Table 26.1: Etiologic fact of cervical insufficiency

Inherited	*Acquired*
– Developmental malformations of Muller duct Septate uterus, subseptate uterus, bicorneate uterus, "T" shape uterus	– Mechanical D & C, laser treatment, knife cone biopsy, amputation
– Intrauterine exposure to DES	– Hormonal—relaxin

- LM or PD before 34 weeks of pregnancy
- Prelabor preterm rupture of membranes (PPROM) before 32 weeks
- History of the surgical procedure on the cervix (amputation, D and C, termination of pregnancy, knife cone biopsy, etc.)
- Intrauterine exposure to DES
- Congenital anomalies of the uterus, vagina, fallopian tubes and ovaries either isolated or related to urinary tract anomalies.

As well as patients' history, there are other diagnostic procedures described in the literature in order to make diagnosis of CI. The most of them are performed before pregnancy, and include hysterosalpingography, dilatation of the cervix assessed by the insertion of Hegars dilatators and possibility of the expulsion of Foleys catheter balloon in the second phase of menstrual cycle.

As well as that, classical bimanual clinical examination as a screening method for CI is traditionally used in the routine practice during on going pregnancy. Nowadays, we are clearly aware that none of these methods has sensitivity, specificity, positive and negative predictive value of use in the screening for CI which would justify its use in screening of general population of asymptomatic pregnant women. Elective cerclage, indicated by the above mentioned "diagnostic" test is still a part of the routine clinical practice. However, nowadays it is used less frequently compared to the previous years. In such cases, elective cerclage can be performed either early (between 11 to 14 weeks) or late (between 14 to 24 weeks). In both cases, there is no scientific evidence that elective cerclage helps improving perinatal mortality and morbidity. This is mostly because the absence of evidence that cerclage performed based on the patients history is really indicated as there is no proper diagnosis of CI. This diagnostic and therapeutic approach changes after 14 weeks of pregnancy, as we do have the possibility of cervical assessment in order to recognize asymptomatic changes suggestive of CI. These changes can not be recognized by earlier mentioned "classical" methods, but they are detectable by cervical assessment using transvaginal ultrasound—so called cervical measurement or cervicometry (CM).[6] CM can provide important information about the cervical condition and changes in

pregnancy. It should be performed in all women at risk for CI starting from 14 weeks. Earlier examination is of no particular use as uterine cervix acting as a sphincter is not fully formed. The examination should be repeated in two weeks intervals finishing at 24 weeks as this is upper limit of gestational age to perform cerclage.[7] Clinical effectiveness of these two approaches, elective cerclage in the cases of suspected CI based on the history and selective cerclage based on CI suspected by CM is presented on the Table 26.2. In all three studies included in analysis, elective cerclage did not perform better compared to the selective cerclage in the terms of reduction of perinatal mortality and morbidity. Therefore, we believe that CM with an intervention if indicated is an excellent alternative to elective cerclage in women with suspected CI based on the risk factors and previous history. CM can directly visualize uterine cervix including internal and external

Table 26.2: Comparison of the effectiveness: early elective cerclage and cerclage indicated with the signs of cervical insufficiency based on ultrasound examination

Study	*Method*	*Aim of study*	*Entry criteria*	*No women included*	*Elective cerclage*	*Results*	*Selective cerclage*	*Results*	*p*
To MS et al[9]	RS	No PL<34 weeks	History of LM and PL 16–33 weeks	90	43	6/41* 14.6%	47/28	9/43* 20.9%	.64
Berghella et al[27]	RS	No PL <35 weeks PL <33 weeks	History of LM 14–24 weeks	177	66	23% 21%	111/40	30% 26%	.30 .50
Kelly et al[6]	RS	AGA	History PL	106	45	35.1 weeks	61	36.1 weeks	
RS—retrospective study LM—late miscarriage				PL—preterm labor AGA—average gestational age				No—number	
* 6 women excluded because of fetal death and provoked PL									

cervical os. It can display the shape of the cervix and present different planes for the measurements of all cervical segments. Two ultrasound based criteria are found to be related to cervical insufficiency. These are the length of the closed part of the cervical canal (Fig. 26.1), the shape of the internal cervical os (“T”, Fig. 26.2; “V” or “Y”, Fig. 26.3, with so called “funneling”, Fig. 26.4.).[8] Follow up of women at risk should be in two weeks intervals, as this period is sufficient enough to detect significant changes. With this

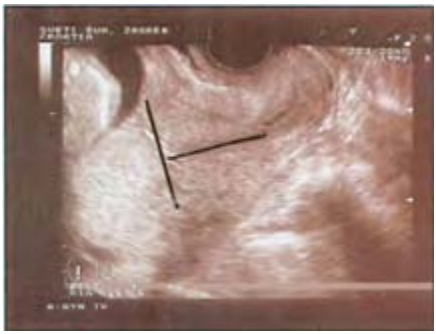

Figure 26.1: The ultrasound assessment of the cervix in pregnancy. Normal “T” shape of the cervix and placenta previa

approach we can significantly reduce the incidence of unnecessary elective cervical cerclage which are proven to be of no use in reducing perinatal mortality and morbidity. As well as that, there was no increase in the risk of LM and PD. The only problem in the CM is the lack of standardized diagnostic criteria of CI indicating cerclage, and we do not know which diagnostic criterion performs best. At the present time the evidence supports the measurements of the length of closed part of cervical canal (Fig. 26.1.) Unfortunately, the evidence in the literature still does not specify the clear cut of point value suggestive of CI to be generally accepted. The most frequently

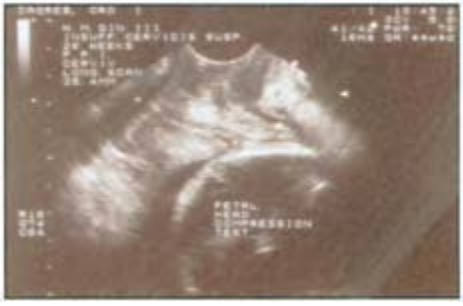

Figure 26.2: Normal “T” shape of the cervix

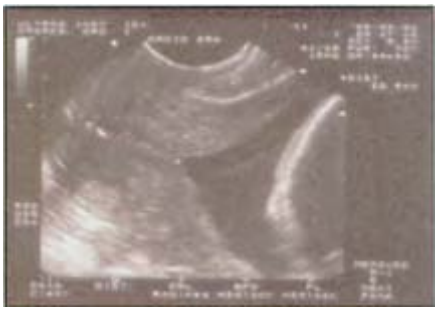

Figure 26.3: Suspicious “V” or “Y” shape of the cervix

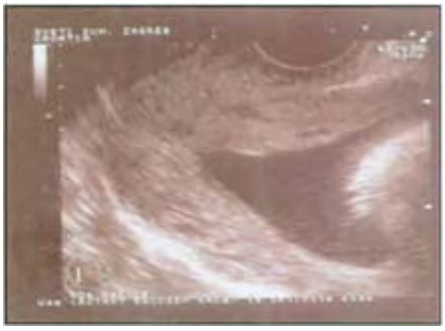

Figure 26.4: Funneling, or “U” shape cervix suspicious for Cl

reported normal values are 25 mm and more, but some authors suggests that the length of closed part of cervical canal of 15 mm and more is still considered to be normal.[9] The relationship of the length of the closed part of the cervix in pregnancy to the incidence of PD is presented on Table 26.3. In all included studies CI was diagnosed by ultrasound in the groups of high risk or low risk women, with the history indicative of CI, but without clinical signs of CI in the present pregnancy. Nairn et al found that cervical length <30 mm before 16 weeks of pregnancy and significant dynamic reduction in the cervical length are related to PL,[29] while study of Owen et al proved that cervical length <25 mm carries 3.3 relative risk (RR) of PL.[7] Odibo et al found that cervical length <25 mm carries statistically significant higher incidence of PPROM.[30] Similarly, To et al found the relationship of cervical length <15 mm with PL.[31] Althuisimus et al proved that cervical length <25 mm before 27 weeks caries 46% increase of the PL risk.[33]

In the case of isolated CI the intervention is advocated and should not be delayed. It was proven that unnecessary waiting without intervention in the cases of CI suspected on CM has negative effect on pregnancy outcome. In

Table 26.3: The relationship between cervical length measured by ultrasound and preterm labor

Study	*Method*	*Entry criteria*	*Weeks at inclusion*	*Cervical length (mm)*	*Outcome assessed*	*%*	*P*
Naim et al[29]	PS n=154	HRP	16	<30	PL <37 weeks	23	<.05
Odibo et al[30]	RS n=69	LRP	14–24	<25	PPROM	39	<.04
To et al[31]	PS n=6819	LRP	23	<15	PL <33 weeks		<.0001
Althuisimus et al[33]	PS n=35	HRP	<27	<25	PL <34 weeks	46	<.006
Owen et al[7]	PS n=183	HRP	16–19	<25	PL <35 weeks	26	RR 3.3
PS-prospective study LRP—low risk pregnancy PL-preterm labor		RS-retrospective study HRP—high risk pregnancy history of PL PPROM- prelabor preterm rupture of membranes					

cervical length significantly shorter than 25 mm and presence of so called “funneling” above 25%, cerclage does not significantly improves pregnancy outcome. Funneling is defined as the relationship of the dilatation of internal cervical os and closed part of the cervical canal. In this circumstances the risk of PPROM is around 40%.[10,11] In cervix with the length of the closed part <15 mm, cerclage does not reduce the incidence of LM and PL, but significantly increases the risk of PPROM from 36.4% to 65.2%.[12] Therefore, it is imperative to intervene “on time” as prolapsed membranes through the internal cervical os into the cervical canal are directly related to the shortening of cervical length. In cervices with length of the closed part between 15 and 25 mm there are clear signs of CI and prolapsed membranes are extremely rare. Therefore, this is a group of patients to consider for selective cerclage.[13,15] If we found prolapsed membranes into the cervical canal and the length of the closed part of the cervix shorter than 15 mm there is 50% risk of PL with high perinatal mortality.[14] But, it should be pointed that responsibility for such high mortality is not solely on CI and there is a significant contribution of clinical and sub-clinical infection.[13]

Dynamic changes and shortening of the cervix differs from one pregnant woman to another. Mean reduction in cervical length in mid second trimester of pregnancy is around 1.1 mm, but it may be as high as 2.7 mm weekly.[16] This data may be used only for primiparous patients as multiparous patients has different dynamic of cervical shortening.[16] It was found that every pregnant women has its own dynamic of cervical shortening and it is very difficult to make general conclusions.[17,18]

Finally, if we do not succeed to recognize the asymptomatic phase of the CI and the first presentation of the pregnant women occurs on the labor ward with clinical signs of cervical insufficiency (dilatation and prolapsed membranes on clinical examination) the

intervention is still possible in the form of emergency cerclage. However, in such cases all possible efforts should be made to

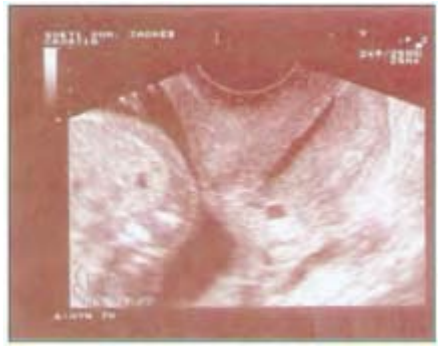

Figure 26.5: The presence of cervical mucus and glands as s normal finding

confirm isolated CI and all other possible etiologic factors must be excluded especially infection and uterine contractions. Despite positive experience of some studies, the results are still doubtfull.[15]

In recent years, we found new ultrasound based parameters of CI. With well known cervical length and shape, nowadays we have presence of cervical gland and cervical mucus proposed to be a parameter used in order to define CI. The absence of cervical glands and cervical mucus detected by ultrasound can be one of the early signs for CI (Fig. 26.5).[19]

As well as transvaginal ultrasound approach, transabdominal ultrasound examinations can also help in the detection of CI. However, transvaginal one was found to be significantly better, as there is no need for full urinary bladder which might change anatomical relationships and change the shape of the cervix.[20] In recent years even three-dimensional ultrasound was introduced in the screening program for detection of CI. It was not found significantly better regarding the measurements of the cervical length but it introduced the new term of cervical volumetry that my be of help in the further assessment programs.[21,22]

Cerclage and Cervical Insufficiency

We have already described potential complications of the delaying cerclage in the CI. It is our proposal to perform the procedure between 16 and 24 weeks. Despite some reports in the literature which favor cerclage to bed rest in defined CI, there are no clear conclusion which approach performs better. Comparison of the cerclage to conservative management is presented on Table 26.4. In all listed studies, cerclage is compared to common management without cerclage. In all presented studies women included had CM and based on the finding they have been diagnosed to have CI and intervention based outcome was assessed. Study of Berghella et al found that despite

Table 26.4: Comparison of the effectiveness of cerclage compared to the non-cerclage in the cervical insufficiency detected by ultrasound

				Cerclage		*Pregnancy outcome*			
Study		*Entry criteria*	*No*	*YES*	*NO*	*Assessed*	*Cerclage*	*No cerclage*	*p*
Berghella et al[10]	PS	HRP Cx <25	69	39	30	PP	23%	27%	>.7
Hassan et al[12]	RS	Cx<15	70	25	45	PPROM	65.2%	36.4%	<.03
1 Rust et al[32]	PS	HRP Cx <25	61	31	30	GA PM	34.7 weeks 12.9%	33.5 weeks 10%	>.05 >.05
2 Rust et al[13]	PS	HRP Cx<25	135	55	58	PO			N.S.
CIPRACT Althuisimus et al[28]	PS	HRP Cx<25	18	10	8	PP<34t	1/10	5/8	<.05
CIPRACT Althuisimus et al[33]	PS	HRP Cx<25	35	19	16	PP<34t NS NM	1/19 19/19 1/19	7/16 13/16 8/16	=.002 >.05 =.005

PS—prospective study
GD—gestational age
PM—perinatal mortality
PL—preterm labor
NM—neonatal morbidity
RS—retrospective study
HRP—high risk pregnancy history of PL
PO—pregnancy outcome
NS—neonatal survival
PPROM—preterm prelabor rupture of membranes

cerclage there was no significant change in the PL.[10] However, there was no randomization preformed in the named study and cerclage is offered based on the opinion of the clinician. It is interesting observation that group with cerclage had significantly lower gestational age compared to the group without cerclage on inclusion. Study of Hassan et al did not assess the influence of cerclage on prolongation of the pregnancy but its influence on PPROM.[12] The authors described statistically significant higher incidence of PPROM in the cerclage group, but without difference in the rate of PL. Similarly as in the study of Berghelle et al there was no proper randomization and all women included in the cerclage group were of lower gestational age at inclusion compared to non-cerclage group.[10,12] Two studies of Rust et al, found that cerclage has no beneficial effect compared to conservative management in the reduction of PL and perinatal outcome,[13,32] however, CIPRACT trial results found that cerclage significantly reduces the PL and has beneficial effect on neonatal morbidity but no difference in neonatal mortality and survival rate.[28,33] Recently published systematic review of Odibo et al assessed studies listed in Cochrane Database and Science Citation Index from 1966 to 2002.[34] They included all randomized trials that evaluated the effectiveness of cervical cerclage in

preventing preterm birth. A total of 2190 women enrolled into the trials were identified with 1110 receiving cerclage and 1080 managed expectantly. There were a total of 278 of 2190 (12.7%) deliveries before 34 weeks of gestation. The meta-analysis demonstrated a trend toward cervical cerclage preventing preterm delivery at less than 34 weeks (OR 0.77, 95% CI, 0.59, 0.99; P=.049). However, there was no demonstrable improvement in neonatal mortality (OR of 0.86, 95% CI, 0.56, 1.33; P=.50). There is a trend toward cervical cerclage reducing preterm births before 34 weeks. The use of cerclage is, however, associated with an increased risk of postpartum fever. Cochrane database of systematic reviews assessed effectiveness and safety of prophylactic cerclage (before the cervix has dilated), emergency cerclage (where cervices have started to shorten and dilate) and then labor halted, and determined whether a particular technique of stitch insertion is better than others. Six trials with a total of 2175 women were analyzed. Prophylactic cerclage was compared with no cerclage in four trials. There was no overall reduction in pregnancy loss and preterm delivery rates, although a small reduction in births under 33 weeks' gestation was seen in the largest trial (relative risks 0.75, 95% confidence interval 0.58 to 0.98). Cervical cerclage was associated with mild pyrexia, increased use of tocolytic therapy and hospital admissions but no serious morbidity. Two trials examined the role of therapeutic cerclage when ultrasound examination revealed short cervix. Pooled results failed to show a reduction in total pregnancy loss, early pregnancy loss or preterm delivery before 28 and 34 weeks in women assigned to cervical cerclage.[35]

As well as in the diagnosis of CI ultrasound can be used in the further assessment of the women with cerclage. The stitch can clearly be seen on ultrasound examination and allows the assessment of the placement and potential further changes on the cervix in ongoing pregnancy (Figs 26.6 and 26.7). This may be of help in identifying patients at higher risk for premature rupture of the membranes and preterm delivery.[36]

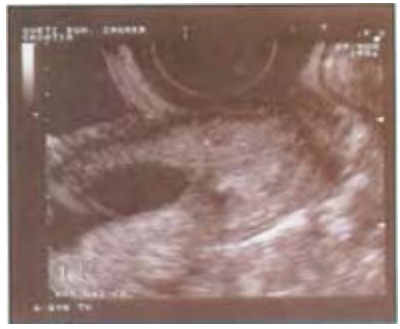

Figure 26.6: Cerclage assessed by ultrasound

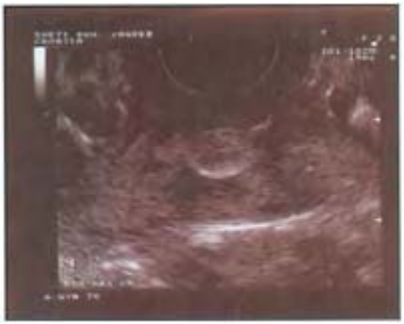

Figure 26.7: Cerclage assessed by ultrasound

Finally, it may be concluded that there is a place for ultrasound examination of the cervix in modern obstetric practice. This can significantly reduce the incidence of elective cervical cerclage without increasing the risk of LM and PL, without influence on perinatal mortality and morbidity. As well as that, cerclage performed before 24 weeks of pregnancy in the group of high risk pregnant women selected by CM, compared to the routine rest but without cerclage, may have some beneficial effect in reducing the incidence of PL but the data of available trials are still inconclusive.

REFERENCES

1. Beckmann R, Ling F, Herbert W. Obstetrics and Gynecology: Lippincott Williams & Wilkins: 1998.
2. Dražančić A (Ed). Porodništvo: Školska knjiga: 1998.
3. Benson R, Pernoll M. Handbook of Obstetrics and Gynecology: McGraw-Hill, Inc. 1994.
4. Cunningham F, MacDonald P, Gant F. Williams Obstetrics: Appleton & Lange 1989.
5. Šimunic V (Ed). Ginekologija: Nak. Lijevak 2001.
6. Kelly S, Pollock M, Maas B, Lefebvre C, Manley J, Sciscione A. Early transvaginal ultrasonography versus early cerclage in women with an unclear history of incompetent cervix. Am J Obstet Gynecol 2001; 184:1097–99.
7. Owen J, Yost N, Berghella V, Thom E, Swain M, Dildy GA 3rd, Miodovnik M, Langer O, Sibai B, McNellis D. Mid-trimester endovaginal sonography in women at high risk for spontaneous preterm birth. JAMA 2001; 286:1340–48.
8. Rozenberg R Gillet A, Ville Y. Transvaginal sonographic examination of the cervix in asymptomatic pregnant women: review of the literature. Ultrasound Obstet Gynecol 2002; 19:302–11.
9. To MS, Palaniappan V, Skentou C, Gibb D, Nicolaides KH. Elective cerclage vs ultrasound-indicated cerclage in high-risk pregnancies. Ultrasound Obstet Gynecol 2002; 19:475–77.
10. Berghella V, Daly SF, Tolosa JE, DiVito MM, Chalmers R, Garg N, Bhullar A, Wapner RJ. Prediction of preterm delivery with transvaginal ultrasonography of the cervix in patients with high-risk pregnancies: does cerclage prevent prematurity? Am J Obstet Gynecol 1999; 181:809–15.
11. Macdonald R, Smith P, Vyas S. Cervical incompetence: the use of transvaginal sonography to provide an objective diagnosis. Ultrasound Obstet Gynecol 2001; 18:211–16.

12. Hassan SS, Romero R, Maymon E, Berry SM, Blackwell SC, Treadwell MC, Tomlinson M. Does cervical cerclage prevent preterm delivery in patients with a short cervix? Am J Obstet Gynecol 2001; 184:1325–29; discussion 1329–31.
13. Rust OA, Atlas RO, Reed J, van Gaalen J, Balducci J. Revisiting the short cervix detected by transvaginal ultrasound in the second trimester: why cerclage therapy may not help. Am J Obstet Gynecol 2001; 185:1098–105.
14. Benham BN, Balducci J, Atlas RO, Rust OA. Risk factors for preterm delivery in patients demonstrating sonographic evidence of premature dilation of the internal os, prolapse of the membranes in the endocervical canal and shortening of the distal cervical segment by second trimester ultrasound. Aust N Z J Obstet Gynaecol 2002; 42:46–50.
15. Matijevic R, Olujic B, Tumbri J, Kurjak A. Cervical incompetence. The role of selective and cerclage. J Perinat Med 2001; 29:31–35.
16. Groom KM, Shennan AH, Bennett PR. Ultrasoundindicated cervical cerclage: outcome depends on preoperative cervical length and presence of visible membranes at time of cerclage. Am J Obstet Gynecol 2002; 187:445–49.
17. Bergelin I, Valentin L. Patterns of normal change in cervical length and width during pregnancy in nulliparous women: a prospective, longitudinal ultrasound study. Ultrasound Obstet Gynecol 2001; 18:217–22.
18. Bergelin I, Valentin L. Normal cervical changes in parous women during the second half of pregnancy—a prospective, longitudinal ultrasound study. Acta Obstet Gynecol Scand 2002; 81:31–38.
19. Yoshimatsu K, Sekiya T, Ishihara K, Fukami T, Otabe T, Araki T. Detection of the cervical gland area in threatened preterm labor using transvaginal sonography in the assessment of cervical maturation and the outcome of pregnancy. Gynecol Obstet Invest 2002; 53:149–56.
20. To MS, Skentou C, Cicero S, Nicolaides KH. Cervical assessment at the routine 23-weeks' scan: problems with transabdominal sonography. Ultrasound Obstet Gynecol 2000; 15:292–96.
21. Strauss A, Heer I, Fuchshuber S, Janssen U, Hillemanns P, Hepp H. Sonographic cervical volumetry in higher order multiple gestation. Fetal Diagn Ther 2001; 16:346–53.
22. Vendittelli F, Mamelle N, Munoz F, Janky E. Transvaginal ultrasonography of the uterine cervix in hospitalized women with preterm labor. Int J Gynaecol Obstet 2001; 72:117–25.
23. Althuisius SM, Dekker GA, Hummel P, Brkedam DJ, van Geijn HP Final results of the Cervical Incopetence: Prevention Randomized Cerclage Trial: therapeutic cerclage with bed rest versus bed rest alone. Am J Obstet Gynecol 2001; 185:1106–12.
24. Pastorek JG II. Obstetric and Gynecologic infectious disease. Raven Press, 1994.
25. Dowd J, Permezel M, Garland S, de Crespigny L. Is there an interaction between cervical length and cervical microbiology in the pathogenesis of preterm labour? Aust N Z J Obstet Gynaecol 2001; 41:177–81.
26. Gire C, Faggianelli P, Nicaise C, Shojai R, Fiori A, Chau C, Boubli L, D'Ercole C. Ultrasonographic evaluation of cervical length in pregnancies complicated by preterm premature rupture of membranes. Ultrasound Obstet Gynecol 2002; 19:565–69.
27. Berghella V, Haas S, Chervoneva I, Hyslop T. Patients with prior second-trimester loss:prophilactic cerclage or serial transvaginal sonograms?. Am J Obstet Gynecol 2002; 187:747–51.
28. Althuisius SM, Dekker GA, van Geijn HP, Bekedam DJ, Hummel P Cervical incompetence prevention randomized cerclage trial (CIPRACT): study. Design and preliminary results. Am J Obstet Gynecol 2000; 183:823–29.
29. Nairn A, Haberman S, Burgess T, Navizedoh N. Changes in cervical length and the risk of preterm labor. Am J Obstet Gynecol 2002; 186:887–89.
30. Odibo AO, Berghella V, Reddy U, Tolosa JE. Does transvaginal US of the cervix predict preterm premature rupture of membranes in a high risk population? Ultrasound Obst Gynecol 2001; 18: 223–27.

31. To MS, Skentou C, Liao AW, Cacho A. Cervical length and funnelling at 23 weeks of gestation in the prediction of spontaneous early preterm delivery:Ultras Obste Gynecol 2001; 18:200–03.
32. Rust OA, Atlas RO, Jones KJ, Benham BN, Balducci J. A randomized trial of cerclage versus no cerclage among patients with ultrasonographically detected second-trimester preterm dilatation of the internal os. Am J Obstet Gynecol 2000; 183:830–35.
33. Althuisius SM, Dekker G, Hummel P, Bekedam D, Kuik D, van Geijn H. Cervical Incompetence Prevention Randomized Cerclage Trial (CIPRACT): effect of therapeutic cerclage with bed rest vs. bed rest only on cervical length. Ultrasound Obstet Gynecol 2002;20:163–67.
34. Odibo AO, Elkousy M, Ural SH, Macones GA. Prevention of preterm birth by cervical cerclage compared with expectant management: a systematic review. Obstet Gynecol Surv 2003; 58:130–36.
35. Drakeley AJ, Roberts D, Alfirevic Z. Cervical stitch (cerclage) for preventing pregnancy loss in women (Cochrane Review). Cochrane Database Syst Rev 2003; (1):CD003253.
36. O'Brien JM, Hill AL, Barton JR. Funneling to the stitch: an informative ultrasonographic finding after cervical cerclage. Ultrasound Obstet Gynecol 2002; 20:252–55.

Chapter 27
Ultrasound Evaluation of the Multifetal Gestation

Sriram C Perni

INTRODUCTION

Multiple gestation pregnancies have proven to be a challenge to obstetricians for many years. They have increasingly accounted for a greater proportion of total pregnancies in the developed world today, owing to the expanded utilization of fertility treatments and advanced maternal age at childbirth.[1] Twin gestations account for 1–2% of all pregnancies, with approximately two-thirds being dizygotic and one-third monozygotic.[2] One-third of monozygotic twins and all dizygotic twin gestations are dichorionic; therefore, approximately 20% of all twins are monochorionic.[2] Multiple gestation pregnancies are at risk for a range of both antepartum and intrapartum complications compared to their singleton gestation counter– parts. Some of these complications include intrauterine growth restriction, premature delivery, congenital anomalies, cord accidents, malpresentations, placenta previa, and abruptio placentae.[3] The most serious of this myriad of complications is premature delivery, which is associated with short-term and long-term neonatal morbidity and increased perinatal mortality.[4] Twin pregnancies have higher perinatal death rates compared to singleton gestations at all gestational ages.[5] In order to optimize the outcome for these pregnancies, early diagnosis of multiple gestation is of paramount importance. Routine, quality ultra-sound, which should detect every twin gestation, in the first or second trimester, has the potential to decrease perinatal morbidity and mortality.[6] In addition, serial ultrasound surveillance can be beneficial in assessing a spectrum of potential fetal complications, which upon detection can subsequently be appropriately managed.

EARLY ASSESSMENT OF MULTIFETAL GESTATIONS

With the increasing incidence of multiple gestations, it is essential for the obstetrician to appreciate the benefit of ultrasound with twins.[7] Although the conclusions of the routine antenatal diagnostic imaging ultrasound study (RADIUS), a randomized, prospective clinical trial, failed to demonstrate a reduction in perinatal morbidity or mortality in the low-risk population, and actually reported excessive costs for routine clinical ultra-sound,

these results have definitely been subject to significant controversy.[8] The benefit to the detection of fetal anomalies and early diagnosis of twin gestation on ultrasound were overlooked. The efficacy of a universal screening program in the second trimester to obtain early diagnosis of a twin pregnancy has been demonstrated.[9]

Certain clinical clues allow the obstetrician to have a high index of suspicion for a multiple pregnancy. These include a uterus that is larger than expected for gestational age, hyperemesis gravidarum, auscultation of multiple fetal heart tones, surging serum alpha-fetoprotein levels, or unexplained maternal anemia. Since multifetal gestation is associated with increased risks of almost every potential complication of pregnancy, with the exception of macrosomia and postdate gestation.[10] early diagnosis is the key. Ultrasound is the only safe, reliable, and consistent way in which to diagnose a twin pregnancy. Again, the efficacy of a universal screening program for early diagnosis of twin gestations by ultrasound has been demonstrated.[9]

With the advent of transvaginal ultrasound, it is now possible to visualize the landmarks in twin gestations earlier than with transabdominal scanning. During early gestation, it is possible to delineate separate gestational sacs by six weeks from the last menstrual period with transabdominal ultrasound. While an embryo in each gestational sac and a pulsating fetal heartbeat can be detected abdominally by seven and 7.5 8 weeks respectively from the last menstrual period, endovaginally these become apparent as early as six weeks estimated gestational age.[3] See Figure 27.1 to view separate gestational sacs in this early monochorionic, diamniotic pregnancy. A and B indicate the respective membrane of each twin.

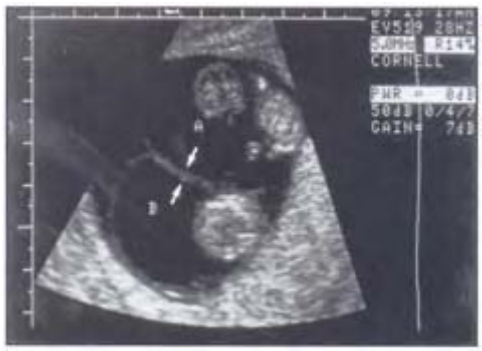

Figure 27.1: Separate gestational sacs in an early monochorionic, diamniotic twin pregnancy. Letters A and B indicate the respective membranes of each twin (*Courtesy* of Frank A.Chervenak MD and Jane Streltzoff, BS, ROMS)

Although it is possible for early diagnosis of multifetal gestations, the natural progression of twin pregnancies and potential sources of ultrasonic error must be taken into

consideration when making a diagnosis of twins. For example, the phenomenon of the "vanishing twin" should be recognized. The spontaneous reduction from a twin gestation to a singleton gestation is not uncommon. In one study of 549 twin pregnancies by Dickey et al, spontaneous reduction to one sac (i.e. the "vanishing twin") occurred in 36% of pregnancies previously diagnosed as twins prior to the 12th week of gestation.[11] The only way to conclusively diagnose this with absolute certainty is visualization of cardiac activity of this fetus in a previous scan, with subsequent absence of this cardiac motion on a follow-up sonogram. An empty gestational sac, usually depicted by an echolucent area, does not always imply a previous twin gestation. In fact, the vast majority of these areas are the result of a variety of other conditions. It is crucial for the obstetrician and sonologist to appreciate this, given the extreme psychological anxiety it could provoke in parents, who believe only one fetus survived the twin pregnancy. Parental self-blame and feelings of fault could potentially arise from such an unfortunate situation.

Other potential sources of errors in the first trimester that must be recognized by the sonologist are the "decidual pseudosac" and refraction errors. A false diagnosis of a multiple gestation can be made when a decidual reaction is evident in a uterus with a mullerian anomaly. A normal gestational sac can be visualized in a uterine horn, and the contralateral horn can contain the aforementioned decidual reaction, which can potentially be confused for a twin gestation. In addition, refraction errors are also frequently encountered in multiple pregnancies. When the ultrasonic acoustic beam traverses the abdominal wall tissues, a refraction zone can appear, altering the anatomic structures distal to this area.[12, 13] This can subsequently produce a ghost artifact, which falsely will be reported as a twin, triplet, or higher-order pregnancy.[14] Therefore, when performing an ultrasound examination in the first trimester for a potential multiple gestation pregnancy, it should be done meticulously and with great care to minimize these confounding variables.

EMBRYOLOGY AND CLINICAL CHARACTERISTICS OF MULTIFETAL GESTATIONS

Of all twin gestations, approximately two-thirds of twin pregnancies are dizygotic and one-third are monozygotic. Dizygotic twinning rates vary tremendously across various ethnic groups and populations, ranging from three per thousand to 16 per thousand.[15, 16] In contrast, the frequency of monozygotic twinning is relatively constant across various populations, approximately four in 1,000 births.[17, 18] Dizygotic twinning rates are lowest in Japan and China, highest in Africa (i.e. especially Nigeria) and intermediate in Europe and the United States of America. Dizygotic twinning rates vary from three per thousand in Asians to 16 per thousand in Africans, with Caucasians at eight per thousand. The proportion of dichorionic versus monochorionic gestations within a population also varies. Although Nigerians have the highest incidence of dizygotic twinning, only 5% of the twins are monochorionic.[15, 18]

Monozygotic twinning is independent of maternal age, race, and parity. In contrast, dizygotic twinning varies with maternal age, parity, the use of assisted reproductive technologies, and genetic factors.[15, 17] Dizygotic twinning rates are highest for maternal

age between 35 and 39 years and rates increase with increasing parity.[15], [17], [19] Higher twinning rates are observed in women who have previously given birth to twins. The increased stimulation of ovarian tissue by the pituitary gland, leading to multiple ovulations, has been implicated as the mechanism behind this increased incidence.[19] Higher rates of dizygotic twin gestations are also the result of ovarian hyperstimulation with follicle-stimulating hormone and luteinizing hormone reproductive technologies, owing to multiple ovulations. An eightfold increase has been demonstrated in the rate of monozygotic twin gestations, with the aid of assisted reproductive technologies.[20]

Dizygotic or "fraternal" twins result from fertilization of two discrete ova. Each member of the dizygotic twin pair develops embryologically like a singleton gestation forming its own blastocyst, which eventually gives rise to the placenta, chorionic membrane, amnion, yolk sac, umbilical cord, and fetus.[21] Dizygotic twin gestations result in implantation of two blastocysts; thus, they are, dichorionic and diamniotic. Monozygotic or "identical" twins result from fertilization of a single ovum, which subsequently divides. In a monozygotic twin gestation, the number of amnions and chorions is determined by the timing of the division of the fertilized ovum. Division of the zygote prior to day four results in a dichorionic, diamniotic gestation and accounts for approximately 25% of monozygotic twins. The division of the inner cell mass between day 4 and day 8 after fertilization, results in a monochorionic, diamniotic gestation and accounts for 75% of all monozygotic twin gestations. Division of a monozygotic gestation after 8 days' post-fertilization results in a monochorionic, monoamniotic gestation and occurs in 1% of monozygotic twins. Division of the embryonic disk greater than 13 days' after fertilization results in incomplete division and results in conjoined twins, who share one chorion and one amnion.

DETERMINATION OF AMNIONICITY AND CHORIONICITY

An early and accurate assessment of amnionicity and chorionicity in a multifetal pregnancy is essential. The impact of chorionicity, in particular, can have profound consequencies for a pregnancy. Owing to the presence of fetoplacental vascular anastomoses in most monochorionic twin gestations, these pregnancies are at much higher risk for poor perinatal complications and outcomes.[22] Monochorionic placentas usually are ellipsoidal in shape; however, other configurations have been described.[23] Utilizing colored milk for injection studies in monochorionic placentas, Schatz created extensive illustrations and drawings depicting the relative frequencies of these vascular anastomoses.[23] Of the superficial connections, the networking between arteries was the most common, and between veins was uncommon. Connections between arteries and veins via villi was more likely in the deep connections.[23] For example, hemodynamic imbalances can occur in monochorionic placentations, potentiating severe neurological complications or even fetal death. In addition, fetal demise in a monochorionic pregnancy can result in significant hemodynamic alteration, profound hypotension in the surviving twin, and eventual demise of the co-twin.[22] However, these vascular networks are invariably absent in their dichorionic counterparts. Further-more, monochorionic pregnancies are at significantly increased risk of early pregnancy loss (i.e. prior to 24 weeks gestation), and increased risks of preterm labor and birth among twins,[24] and up to

10–15% will develop the twin-twin transfusion syndrome.[25] Given the extensive array of potential complications that can develop with particular placentation patterns in twin pregnancies, establishment of chorionicity in early pregnancy is paramount. Chorionicity is usually definitively established after delivery by pathological examination of the placenta. However, prenatal ultrasound examination at 10–14 weeks of gestation has a high reliability in determining chorionicity in a twin pregnancy.[26] In fact, given the high accuracy rate for determining chorionicity at 10–14 weeks gestation with ultrasound, many ultrasound centers throughout the United Kingdom are performing this in conjunction with first trimester fetal nuchal translucency examination.[27] In one study by Stenhouse et al on 138 twin pregnancies at Glasgow Royal Maternity Hospital, chorionicity was correctly determined by ultrasound in 95% (n=131) of the cases; 91% of the monochorionic and 96% of the dichorionic pregnancies were correctly diagnosed. When the chorionicity was evaluated prior to 14 weeks gestation in this study, only one case resulted in an incorrect assessment of chorionicity. Therefore, ultrasonic evaluation of chorionicity has a high sensitivity and specificity, especially if performed before 14 weeks gestation.[28]

Ultrasound determination of chorionicity relies on the assessment of the number of placental masses, the fetal gender, and characteristics of the dividing membrane.[26], [29] The presence of two placental masses or twins of different sex provides reliable evidence of a dichorionic twin pregnancy on diagnostic ultrasound.[29] See Figure. 27.2 to visualize an example of two placental masses. P^a refers to the placenta of twin A, and P^b indicates the placenta of twin B.

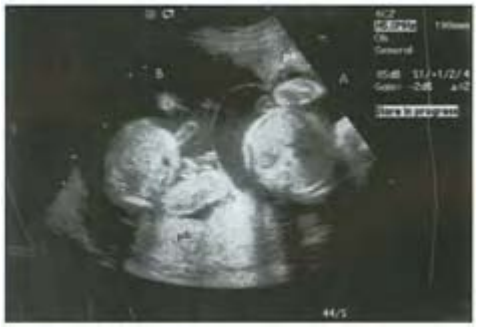

Figure 27.2: Two separate placental masses (*Courtesy* of Frank A.Chervenak MD and Jane Streltzoff, BS, ROMS)

The challenge, however, to the sonologist in assessing chorionicity lies in the setting of concordant fetal gender or presence of a single placental mass. Under such circumstances, evaluation of the thickness of the dividing membrane is useful in predicting chorionicity.[26], [27], [29] In dichorionic twin gestations, the membranes separating gestational sacs consist of two layers of amnion plus two layers of chorion. However, in monochorionic, diamniotic pregnancies, there are only two layers of amnion.

The determination of chorionicity on ultrasonic evaluation in a multifetal pregnancy should be determined in a systematic way between 10–14 weeks gestation. First, if separate placental masses are visualized, the placentation is dichorionic. If only one placental mass is appreciated, a careful attempt should be made to evaluate the fetal genders. If the external genitalia of the twins are discordant, placentation again can be assumed to be dichorionic. When the situation is encountered where only one placental mass is noted and the fetuses are of similar sex, the sonologist can utilize other clues to determine the chorionicity of the pregnancy. Careful identification and examination of the intertwin septum or dividing membrane is particularly useful in assessing chorionicity in those circumstances mentioned above. In a study performed by D'Alton and Dudley on 69 twin gestations, actual counting of the layers in the dividing membrane was performed to evaluate for chorionicity. If two layers were identified, a mono-chorionic-diamniotic placentation was diagnosed. Similarly, if four layers were demonstrated, a dichorionic-diamniotic placentation was made. If only three layers were visualized, once again a dichorionic placentation was established, given the possibility of being unable to see one of the layers of the membrane. If no dividing septum was evident on at least two separate ultrasonic evaluations, a monochorionic-monoamniotic placentation was determined. Precautions were undertaken to minimize the possibility of misdiagnosis, including visualization of the membrane near its insertion into the placenta, magnification of the area of interest as required, and repeating ultrasonic examinations until adequate diagnosis of chorionicity was established. Chorionicity determination was definitively diagnosed much easier earlier in gestation. In this study of chorionicity determination utilizing this counting technique, 51 of 51 (100%) dichorionic gestations were accurately diagnosed and 1.7 of 18 (94.4%) monochorionic placentations were accurately made based on pathologic evaluation of the placenta after delivery. The overall antenatal predictive accuracy in this study was 98.5%.[29] Some studies have indicated that the intertwin membrane is more echogenic and thicker in dichorionic placentas; however, this determination is somewhat arbitrary and subjective.[30] Others have demonstrated that an intertwin membrane thickness of 2 mm or greater is associated with a dichorionic pregnancy.[31] However, the reproducibility of this measurement is dependent on a multitude of extraneous factors, including

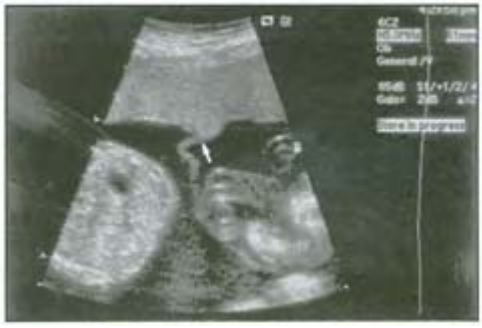

Figure 27.3: Demonstration of the Lambda sign (*Courtesy* of Frank

A.Chervenak MD and Jane Streltzoff, BS, ROMS)

gestational age and technical aspects of the ultrasound examination itself.[32]

Another potential feature on ultrasound examination that can help delineate chorionicity in a twin pregnancy is evaluation for the twin peak or lambda sign. The twin peak or lambda sign is a triangular projection of placental tissue extending up into the base of the dichorionic intertwin membrane (Fig. 27.3 where the arrow points to the lambda sign). Finberg described this in 1992 as proliferating chorionic villi growing into the potential space between the layers of chorion, and thus its presence would indicate dichorionicity.[33] A study by Sepulveda et al at the Harris Birthright Research Centre for Fetal Medicine in the United Kingdom prospectively evaluated 369 twin pregnancies at 10–14 weeks gestation to evaluate chorionicity on ultrasound, utilizing the lambda sign. Pregnancies were classified as dichorionic if a single placental mass was noted with the presence of the lambda sign at the intertwin membrane-placental junction or two discrete placentas were visualized, or monochorionic if a single placental mass was observed without observation of the lambda sign. All pregnancies that were classified as dichorionic resulted in delivery of different-sex pairs and all gestations classified as monochorionic resulted in delivery of same-sex pairs.[26] However, in this

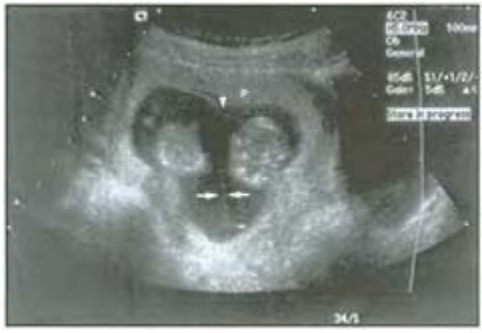

Figure 27.4: Demonstration of the T sign (*Courtesy* of Frank A.Chervenak MD and Jane Streltzoff, BS, ROMS)

study, follow-up placental pathology was not performed. Nevertheless, these findings demonstrate the reliability of determining chorionicity in multiple gestation pregnancies by ultrasonic evaluation of the lambda sign at 10–14 weeks gestation. In a prospective trial by Carroll et al on 150 twin pregnancies assessing chorionicity at 10–14 weeks gestation, prenatal ultrasound evaluation correctly identified chorionicity on 149 (99.3%) of these cases. In this study, a combination of the lambda sign or separate placentas resulted in a sensitivity and a specificity for diagnosing a dichorionic gestation by ultrasound to 97.4% and 100%, respectively.[27] In addition, the T sign (i.e. fusion of two amniotic membranes) in monochorionic gestations was associated with a sensitivity of 100% and a specificity of 98.2% in predicting chorionicity accurately (Fig. 27.4).[27] The

arrow head is pointing to the T-sign and the two arrows point to the dividing membrane. P refers to the placenta.

The establishment of amnionicity in a multifetal gestation is determined by sonographic visualization or non-visualization of the intertwin membrane.[6] This is best accomplished in the first trimester. With advancing gestational age, visualization of this membrane can become increasingly difficult. This may be due in part to fetal crowding, oligohydramnios, or continual thinning of the intertwin membrane. If an intertwin membrane is not apparent sonographically, possibilities include a normal twin gestation in which the membrane is unable to be visualized, monoamniotic twinning, or a stuck twin secondary to severe oligohydramnios.[34] Therefore, the inability to identify an intertwin membrane does not conclusively prove a monoamniotic gestation. In a study by Mahony et al, identification of an intertwin membrane was observed in 55 of 65 diamniotic twin gestations, yielding a sensitivity and a positive predictive value of 85% and 100%, respectively.[34] In 11 pregnancies in which the intertwin membrane was unable to be visualized, only one of the pregnancies resulted in a monoamniotic gestation, yielding a 9% accuracy rate.[34] Other potential clues to a monoamniotic twin gestation include close insertion of two umbilical cords into the placenta, close intrauterine positioning of the two fetuses close to each other, and presence of one yolk sac only.[2] Figure 27.5 demonstrates only one yolk sac (YS) in a conjoined twin pregnancy. L indicates the lower limb of each twin. Definitive signs of a monoamniotic multifetal gestation include umbilical cord entanglement and conjoined twins. Umbilical cord entanglement can have severe consequences in a monoamniotic multifetal gestation. In a review of three cases of cord entanglement by Arabin et al, the role of antenatal ultrasound diagnosis was explored to potentially

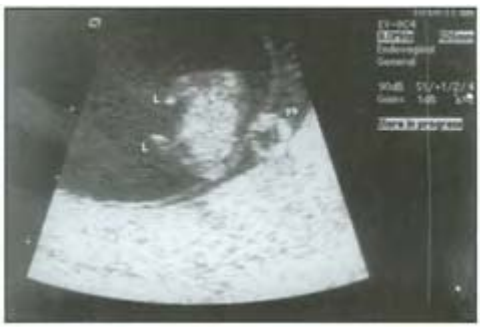

Figure 27.5: Single yolk sac in a conjoined twin pregnancy (*Courtesy* of Frank A.Chervenak MD and Jane Streltzoff, BS, ROMS)

impact on subsequent counseling and management of these pregnancies.[35] In this review, umbilical cord entanglement was detected between 10–18 weeks gestation by color Doppler and pulsed Doppler velocimetry,[35] with a variety of resultant outcomes. In one of the cases, cord entanglement was detected by color Doppler velocimetry at 10 weeks

gestation. Unfortunately, by 15 weeks gestation, intrauterine demise of both twins was apparent.[35] In another case, color Doppler detected a side-by-side insertion of the umbilical cord and Doppler velocimetry revealed an entanglement of the cord at the chorionic plate at 18 weeks gestation. Although this pregnancy was further complicated by polyhydramnios, a successful cesarean section was performed at 36 weeks gestation, and cord entanglement was confirmed at the chorionic plate; subsequent development of the twins was normal.[35]

Monoamniotic twin pregnancies are associated with a high rate of perinatal death and fetal abnormalities, and mortality rates are higher than previously perceived.[2] Therefore, early detection of a monoamniotic twin pregnancy is crucial. A monoamniotic pregnancy should only be considered when the following are observed on ultrasonic evaluation: no intertwin membrane is visualized, both fetuses are of similar gender, only one placental mass is observed, both fetuses appear to move without hindrance within the amniotic cavity, and both fetuses are surrounded by adequate amniotic fluid volume.[36]

Establishment of chorionicity and amnionicity in a multifetal gestation by ultrasound assessment is of paramount importance. Ultrasound evaluation yields a high level of accuracy in delineating amnionicity and chorionicity when performed in the first or second trimester. However, the certainty with which this can be diagnosed is less accurate in the later gestation, especially in circumstances of severe oligohydramnios. Observation of discordant genders in late gestation is the most reliable indicator of a dichorionic, diamniotic pregnancy. Obviously, the determination of amnionicity and chorionicity is much more difficult when the genders are concordant. In addition, the thickness of the intertwin membrane also becomes less useful as pregnancy advances because its thickness becomes less apparent.[29] Performing first and second trimester ultrasound examination routinely would diagnose all twin gestations, and provide the optimal time to evaluate the chorionicity and amnionicity of twin gestations.[6]

ASSESSMENT OF AMNIOTIC FLUID VOLUME

The amniotic fluid volume should be routinely assessed when performing an ultrasonic evaluation in a multifetal pregnancy. Amniotic fluid changes, at times, may serve as the only useful diagnostic clue to potential pathological conditions developing in *utero*. Significant increases in perinatal morbidity, mortality, and congenital anomalies become apparent with upward or downward fluxes in the amniotic fluid volume.[37], [39] Traditionally, measurement of amniotic fluid volume in singleton pregnancies has been fairly routine and straightforward. In singleton gestations, amniotic fluid is assessed by either measurement of the deepest vertical pocket of fluid, subjective evaluation of the total fluid, or the ultrasonic calibration of the amniotic fluid index (API).

Standards for ultrasonic evaluation of the amniotic fluid volume in multifetal pregnancies have not been established. Less data are available in determining amniotic fluid volume (AFV) in multiple gestations. A sonographic standard for determination of AFV in normal twin pregnancies was provided by Watson et al.[40] In this prospective study, 210 uncomplicated twin pregnancies were evaluated. The AFV was assessed ultrasonographically, by measuring the single deepest vertical pocket in each sac and by measuring the API. The API in this study steadily increased to 27 weeks gestation, and

then declined. This correlated well with the technique of measuring the deepest vertical amniotic fluid pocket in each sac ($r=0.71$; $p<0.0001$). The mean API was also greater in multifetal gestations compared to their singleton pregnancy counterparts. In singleton gestations, polyhydramnios can potentially be a harbinger for significant future sequelae. However, in Watson's study, 9.8% of the cases between 26 and 32 weeks gestation had a fluid pocket of at least 8 cm and no pathological state was appreciated.

Other studies have evaluated AFV in multiple gestation pregnancies. In a study of 91 normal diamniotic twin gestations by Chau et al, a single API for the twin pair was determined, and the maximum depth and width of each twin's largest pocket was measured every 4–6 weeks between 15 and 40 weeks gestation. The API changed tremendously with gestational age. Between 15 to 24 weeks gestation, API steadily increased, plateaued until 36 weeks, and then declined. However, the depths and two-diameter pockets did not significantly change with gestational age.[41] These findings can have potential clinical significance in the management of twin pregnancies. At this time, definitive standards are available for assessing AFV in singleton pregnancies. However, although it is established that evaluation of AFV is crucial in multiple gestations as well, the exact methodology to be utilized is still subject to debate. Most authors believe that either measurement of AFI or determination of the deepest vertical pocket is acceptable.

ULTRASONIC EVALUATION OF FETAL GROWTH IN MULTIFETAL GESTATIONS

Frequent evaluation and survey of fetal well-being and growth is crucial to optimal management of a multiple gestation. Evaluation of growth in twins is vital, because these pregnancies are at increased risk for growth restriction and perinatal mortality three times that of their singleton counterparts.[42] In addition, monozygotic twin pregnancies and second twins are particularly vulnerable.[42] Intrauterine growth restriction (IUGR), defined as birth weight less than the 10th percentile for gestational age, complicates approximately 7% to 10% of singleton pregnancies; however, in twin gestations, IUGR can potentially affect up to 47% of these gestations.[7] The etiology of growth restriction in one or both members or abnormal growth can result from constitutional variability, fetal/placental crowding, placental insufficiency, chromosomal or structural problems, or early infection. Abnormal growth should be defined as either a discrepancy of 20% or greater between the larger and smaller twin or an estimated fetal weight (EFW) less than the 10% using singleton growth curves. Concordant IUGR would be missed if only growth discordancy calculations were employed.

The pattern of fetal growth in twin pregnancies is not entirely certain, and fetal growth in uncomplicated twin pregnancies remains controversial. Although some studies indicate no difference between growth in multifetal and singleton gestations, others have suggested decreased fetal growth in normal twin pregnancies.[43] This dilemma is important given that different growth curves should be utilized if normal twin gestations have a different growth pattern than singleton pregnancies.

Clinically, it is difficult to evaluate for abnormal growth in a multiple gestation pregnancy. In singleton pregnancies, a discrepancy between fundal height and gestational age is a potential harbinger for abnormal growth; however, this principle cannot be

accurately applied for a twin gestation.[44] Some authors believe that twin gestations grow at a similar rate to singleton gestations until 28 weeks gestation, with a subsequent decline even in uncomplicated pregancies.[43] However, a recent retrospective study by Ong et al of 1,011 twin pregnancies made some interesting conclusions. In this study, ultrasonic measurement of growth of the abdominal circumference followed closely to that of singleton gestations until 32 weeks gestation. Thereafter, there was an obvious decline away from singleton measurements. The growth patterns for femur length were similar between twin pregnancies and singleton standards. Interestingly, the biparietal diameter of twins was greater than that of singletons from the mid to early third trimester.[45] In another study by Smith *et* al, prospective ultrasound evaluations were performed on 162 patients with a twin pregnancy every two weeks from 16 weeks gestation until delivery. In this study, abdominal circumference, femur length, and biparietal diameter all under-went significant decreases in growth velocity after 32 weeks of gestation.[42] No substantial differences in growth velocity were appreciated between twins of different zygosity, chorionicity, gender, or birth order. Both monozygotic and dizygotic twin gestations sustained a decline in growth velocity as gestation progressed.[42]

Although studies have evaluated growth parameters in twin gestations, many of these are not reliable, because chorionicity was not considered. The influence of chorionicity on growth potential can be significant. In a recent study by Senoo in Japan, 115 twin pregnancies were enrolled. 70 cases of concordant twins (24 monochorionic, 46 dichorionic) and 45 cases of discordant twins (25 monochorionic, 20 dichorionic) were evaluated. Growth was monitored ultrasonographically by biometric measurements of biparietal diameter (BPD), fetal trunk area, and femur length (FL). No differences were noted in incremental growth between concordant monochorionic and dichorionic twins. In addition, this growth curve was similar to singletons until 34 weeks gestation. However, in discordant twins, the growth of the smaller twin gradually decreased to the range of growth restriction; conversely, the larger twin's growth was similar to the growth curve of a singleton gestation on a concordant twin. In the monochorionic discordant twins, discrepancy between growth became marked at 20–22 weeks gestation in some cases (i.e. greater than 40% difference in EFW). In addition, when discordancy developed at 25 weeks gestation or later in monochorionic gestations, in some cases this developed rapidly within 1–2 weeks.[46] This study illustrates the importance of determining chorionicity by ultrasound early in twin gestations and observing longitudinal fetal growth curves appropriately for each chorionicity.

A significant body of literature addressing growth in multifetal gestations has been reported. However, these studies have usually evaluated growth in twins by ultrasound in the late second and third trimesters of pregnancy. With the advent of high-resolution transvaginal ultrasound, it is now possible to evaluate for growth in multiple pregnancies as early as the first-trimester. In a retrospective study by Weissman et al from 1992–1993 on twin pregnancies, significant size variation was observed in five cases. Discordant embryonal growth in this study was defined as a variation in the crown-rump length (CRL) of five or more days, reflecting more than two standard deviations of the mean gestational age from any CRL at 6–13 weeks gestation. In all of these cases, major congenital anomalies were diagnosed in the smaller twin in the second trimester. These malformations included partial schizencephaly, diaphragmatic hernia with a two vessel-cord, severe ventriculomegaly, aortic atresia, and sacral agenesis.[47] Therefore, an early

ultrasonic discrepancy between CRL in twin gestations may suggest future growth delays and diagnosis of congenital anomalies in the smaller fetus.[47]

Establishment of growth curves for twin gestations has been limited. Attempts at establishment of growth curves specifically for twin gestations has been hindered by small populations, limited studies, and studies performed without regard to chorionicity and outcome. At this time, singleton growth curves are the best predictors of adverse outcome in multiple gestations, and should be utilized for evaluating abnormalities in growth in twin pregnancies.[48]

There is no clear consensus among the obstetrical community as to the optimal frequency of obtaining ultrasounds for evaluation of growth and AFV among twin gestations. Some investigators advocate that ultrasonic evaluations should be tailored to specific clinical circumstances. For example, recommendations by Rode et al support that dichorionic pregnancies should be evaluated at 26 to 28 weeks gestation by ultrasound and every three to four weeks thereafter to evaluate AFV and interval growth. In monochorionic pregnancies, however, because of the 10–15% chance of developing the twin-twin transfusion syndrome (TTTS), ultrasonic surveillance should be initiated at 23 to 24 weeks gestation.[36] Chasen et al, however, recommend performing ultrasound every 4–6 weeks in dichorionic pregnancies after 20 weeks gestation and increasing surveillance accordingly. Additionally, monochorionic twin pregnancies should be evaluated every 2–3 weeks from the second trimester. Therefore, optimal frequency for evaluation of a multifetal gestation has not yet been established. Each twin pregnancy should be ultrasonographically evaluated according to the specific circumstances present.

THE TWIN-TWIN TRANSFUSION SYNDROME

The twin-twin transfusion syndrome (TTTS) is a potential devastating complication of a monozy-gotic-monochorionic twin pregnancy. The TTTS, also referred to as feto-fetal transfusion syndrome, is present in 10–15% of all monochorionic multiple gestations. The overall prognosis for untreated severe cases of TTTS is extremely dismal. In a recent multicenter study by Dickinson and Evans on 112 cases of TTTS revealed high rates of perinatal morbidity and mortality (38%), preterm delivery (90%), abnormal head ultrasound (27%), neonatal renal failure (7.7%), hypertrophic cardiomyopathy (3.3%), and severe lower limb ischemia requiring amputation (2.7%).[49] Perinatal complications can occur despite invasive treatment (laser coagulation of anastomotic vessels and serial amniocentesis). The shared circulation in these multifetal gestations is the reason for these significant perinatal complications. Anastomoses have been demonstrated between arteries and veins of each twin, and arteriovenous anastomoses that proceed through a placental cotyledonary capillary bed.[50] In the classic model of the TTTS, an artery from one twin supplies a placental cotyledon, which is drained in turn by a vein returning to the co-twin.[51] According to this model, blood is shunted from one of the twins, the donor, and towards the transfused co-twin, the recipient. A placental injection study in twin pregnancies was performed by Robertson et al on 278 twin pairs at Jackson Memorial Hospital.[52] In this study, anastomoses were almost universally present in monochorionic placentas (55 of 56 placentas), and very infrequently in dichorionic placentas (67 of 68 placentas without communications). However, the TTTS occurred rarely in spite of the

high frequency of occurrence of the cross-placental vascular communications (three cases of the 55 cases in monochorionic placentas, 5.5%).[52] According to Blickstein, a new composite definition of TTTS is as follows: sonographic signs (intertwin difference of abdominal circumference greater than 18 mm, polyhydramnios-oligohydramnios, and signs of monozygosity), Doppler velocimetry of the umbilical arteries (intertwin difference in systolic/diastolic ratios above 0.4), intertwin birth weight discrepancy of 15% or more, intertwin differences in hemoglobin of 5 gm/dL or greater, and demonstration of a transplacental vascular shunt.[53] However, these standard criteria for diagnosis of TTTS have been challenged. In a study by Danskin et al at The Queen Mother's Hospital in Glasgow, Scotland from August 1984 to February 1988,178 consecutive twin pregnancies were evaluated to reexamine the standard diagnostic criteria of diagnosing chronic TTTS utilizing an intertwin difference of greater than 5 gm/dL and birth weight discrepancy of greater than 20%. Hemoglobin differences of greater than 5 gm/dL were demonstrated in six monochorionic pregnancies; however, this was also observed in seven dichorionic placentas. In addition, a birth weight discordance of greater than 20% was noted in 17.4% of the pregnancies; However, this phenomenon did not occur more frequently in monchorionic than in dichorionic pregnancies. Furthermore, in this study, four pregnancies had a hemoglobin difference of greater than 5 gm/dL and a birth weight discordance of greater than 20%, and none of these gestations demonstrated evidence of oligohydramnios or polyhydramnios in either amniotic sac; one of these pregnancies was a monochorionic gestation.[54] Interestingly, a recent study by Nores et al of thirty-seven twin pregnancies at New England Medical Center reported a significant female preponderance in multiple gestations complicated by severe TTTS. Of these 37 twin pairs, 33 (89%) were female.[55]

When TTTS is diagnosed postpartum, treatment is geared directly towards the respective twins. However, the clinician faces a real dilemma if the diagnosis is made antenatally, between expectant management and therapeutic intervention. Expectant management can be associated with a perinatal mortality rate approaching 100%.[53] In cases in which one of the monozygous twins dies in utero, the surviving twin may be exposed to the morbidities of brain damage and other structural defects.[53] In a study of thirteen consecutive pregnancies affected by the "stuck twin" phenomenon, the potential benefit of serial amniocentesis was investigated. This study was performed by Mahony et al in Seattle, Washington.[56] The "stuck twin" is described as a diamniotic pregnancy whereby one fetus resides against the uterine wall in a severely oligohydramniotic sac (see Fig. 27.6, where H refers to head and SP to spine), and the co-twin is severely polyhydramniotic (Fig. 27.7). Figure 27.7 depicts the largest vertical pocket in the recipient twin and Figure 27.8 demonstrates oligohydramnios and measurement of the only amniotic fluid pocket between the arrows in the "stuck" twin. "Stuck twin" affects up to 35% of all monochorionic, diamniotic gestations. In this trial, 8 of 13 pregnancies underwent serial amniocentesis, and the other five were managed expectantly. The survival rate for the serial amniocentesis group was 69% compared to 20% in the non-amniocentesis group at the same institution (p=0.01). Complications, however, did occur in the serial amniocentesis group, including brain infarction and renal tubular necrosis.[56] Other therapies include selective feticide, hysterotomy

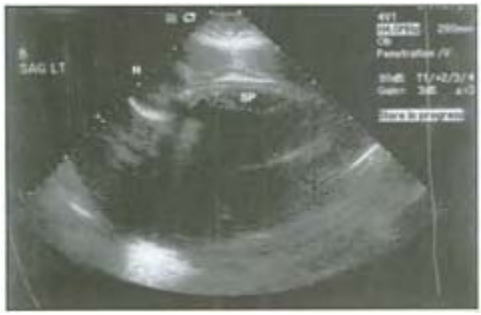

Figure 27.6: Example of a "stuck twin" in a pregnancy complicated by the twin-to-twin transfusion syndrome (*Courtesy* of Frank A.Chervenak MD and Jane Streltzoff, BS, ROMS)

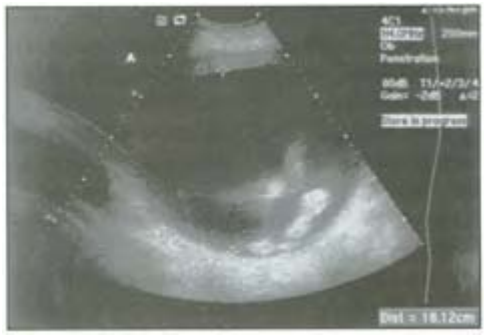

Figure 27.7: Evidence of polyhydramnios in the recipient twin of a pregnancy complicated by the twinto-twin transfusion syndrome (*Courtesy* of Frank A. Chervenak MD and Jane Streltzoff, BS, ROMS)

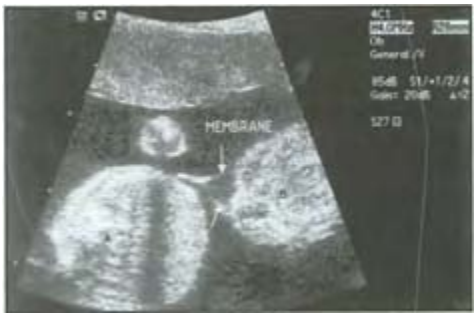

Figure 27.8: Demonstration of oligohydramnios in the "stuck twin" of a twin-to-twin transfusion syndrome pregnancy (*Courtesy* of Frank A.Chervenak MD and Jane Streltzoff, BS, RDMS)

| for umbilical cord ligation of one twin, bloodletting from a placental vessel, and laser coagulation of placental anastomotic vessels.[56]

The best available method, at this time, for evaluation of the progression of TTTS is serial ultrasonographic assessments of fetal growth and AFV in conjuction with Biophysical Profile. Doppler velocimetry also may be of diagnostic and prognostic value. In a study by Taylor et al, visualization of an arterioarterial anastomosis by Doppler was associated with a low probability of TTTS and survival of both twins. However, absent or reversed end-diastolic flow in the donor twin's umbilical artery or abnormal pulsatility of the venous system of the recipient twin was associated with poor survival.[57]

ANOMALIES IN MULTIPLE GESTATIONS

Multiple gestation pregnancies deserve the same careful ultrasonic evaluation for fetal aneuploidy and congenital anomalies as do singleton gestations. The goal of identifying pregnancies at risk for trisomy 21 and congenital anomalies is no different for multiple gestations. As previously stated, the prevalence of twin pregnancies increases with advancing maternal age, and thus, the risk for aneuploidy is also increased.

Congenital anomalies can cause significant fear and anxiety in parents. This can further be compounded by the presence of such a situation in a multiple gestation. Although no universal definition for a congenital anomaly exists and the true incidence of anomalies is subject to debate, congenital anomalies occur approximately twice as common in twin gestations compared to singleton gestations.[58] Careful attention should be made to the proper classification of the various anomalies, including malformation, deformation, and disruption. A malformation is a defect in an organ or area of the fetal body resulting from an abnormal intrinsic process of development.[21] A deformation is an abnormality resulting from extrinsic mechanical forces, which affects the position, shape,

or form of a fetal body part.[21] One example of a deformation is that the umbilical cord length on average in twin pregnancies is 7.90 cm shorter than in singleton pregnancies.[59] This was demonstrated by Soernes et al on 59 twin births in a study between 1979 and 1985.[59] Mean cord length of the 118 twins was 49.63 cm and 57.52 cm in the singleton neonates.[59] A disruption results from deterioration of previously normal tissue.[21]

Specific anomalies are unique to multiple gestations, and others are present in singleton pregnancies as well. Some studies have suggested an increased frequency of congenital anomalies in monozygotic twins, especially monochorionic compared to dichorionic placentations.[60] Congenital anomalies unique to the twinning process include acardia, conjoined twinning, and the twin-twin transfusion syndrome previously discussed.[58], [61] Acardia, or chorioangiopagus parasiticus, occurs in approximately one out of every 100 monozygotic twin pregnancies or one in 34,600 deliveries,[62] and presents in a spectrum of ways. It can present as an incomplete, but well-developed fetus to a mass of nebulous debris. Although the pathogenesis of this condition is not entirely certain, two theories have been proposed, including a primary malfunction of the cardiac pump development or heart atrophy subsequent to passive perfusion and reversal of circulation,[60] the twin reversed arterial perfusion (TRAP) sequence. The TRAP phenomenon, unique to monochorionic gestations, is characterized by a 50% mortality rate for the "pump" twin secondary to high-output heart failure, and the presence of lethal anomalies, acephaly and acardia, in the "recipient" twin.[63] Interestingly, in a literature review of 22 cases of cardiac twinning by Arias et al, mortality for the "pump" twin was reduced from 50% to 13.6% with invasive fetal surgery (i.e. endoscopic laser coagulation before 24 weeks gestation and umbilical cord ligation after 24 weeks gestation).[63]

Although it remains uncertain as to the absolute rate of conjoined twinning, it is believed that approximately one in 200 monozygotic twin

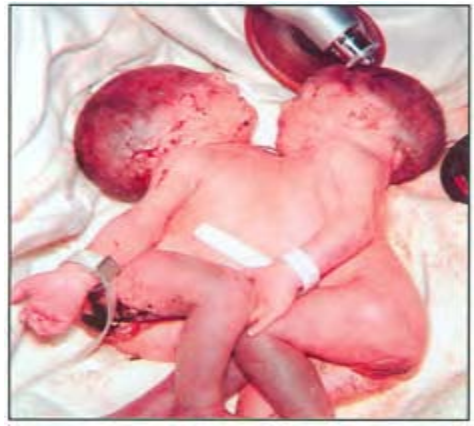

Figure 27.9: Post-natal conjoined thoracopagus twins. (*Courtesy* of Rebecca N.Baergen, MD)

pairs or one in 50,000 total births (range of one in 25,000 to one in 80,000) are affected,[58,60,64] with thoracopagus (chest union) being the most common, representing three-fourths of all cases.[58] No environmental factor can be consistently linked to the conjoined twinning process. This phenomenon occurs in monozygotic twins as a result of incomplete division of the zygote, after formation of two embryonic disks, on days 13 and 15 after conception. No consistent predisposing factors are obvious in conjoined twinning. Five major types of conjoined twins, classified according to the predominant site of attachment, are thoracopagus (74–75%), craniopagus (1–2%), omphalopagus (0.5%), pygophagus (18%), and ishiopagus (6%).[58,65] In thoracopagus twinning, a high incidence of congenital heart disease (e.g total anomalous pulmonary venous return, endocardial cushion defect, single ventricle, conotruncal abnormalities) is appreciated.[60] It should be noted that most conjoined twin pairs are female. See Figures 27.9 to 27.12 for conjoined twinning. Figure 27.9 depicts a gross picture of postnatal conjoined thoracopagus twins. Figures 27.10 and 27.11 demonstrate examples of conjoi

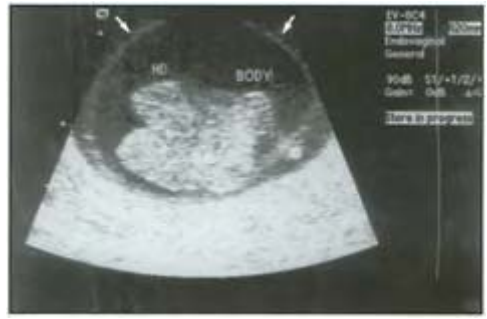

Figure 27.10: Example of conjoined twinning (*Courtesy* of Frank A.Chervenak MD and Jane Streltzoff, BS, ROMS)

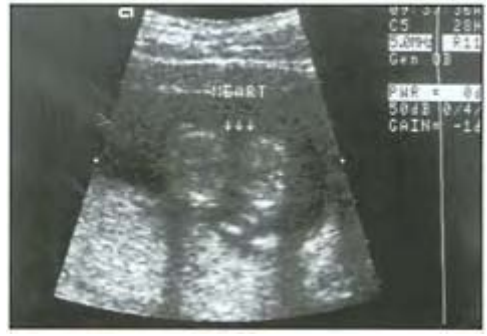

Figure 27.11: Conjoined twinning with cardiac union (*Courtesy* of Frank

A.Chervenak MD and Jane Streltzoff, BS, RDMS)

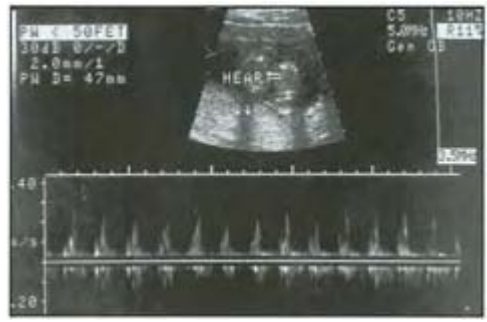

Figure 27.12: Pulsed Doppler on cardiac union (*Courtesy* of Frank A.Chervenak MD and Jane Streltzoff, BS, RDMS)

ned twinning evident on ultrasound with Figure 27.11 showing union at the heart. Figure 27.12 shows pulsed Doppler on the conjoined heart.

Congenital anomalies also exist that are not unique to the twinning process. However, a few of these anomalies may be more prevalent in multiple gestations. These include neural tube defects (encephaloceles and anencephalus in likesex twins), congenital heart disease, single umbilical artery, tracheoesophageal fistula, genitourinary defects, and the VACTERL association.[61] These malformations usually manifest as a clinically affected twin, with a normal co-twin. Much controversy exists as to whether twin gestations truly have an increased incidence of congenital heart disease. Many studies evaluating for congenital heart disease in multiple gestations have not controlled for the many confounding variables present in these pregnancies (e.g. zygosity). Single umbilical artery and hydrocephalus have also been demonstrated to be present more often in twin pregnancies compared to singletons.[60]

Each individual fetus is at the same risk for aneuploidy and Down's syndrome as a singleton fetus; however, the overall pregnancy is at a higher risk than a singleton pregnancy given that more than one fetus is present. Counseling for prenatal diagnosis of trisomy 21 is indicated for pregnant women with a twin gestation at age 33 or greater, because the risk of aneuploidy is similar to that of a 35 year-old woman with a singleton gestation.[66] In singleton gestations in the first trimester of pregnancy, screening for trisomy 21 by a combination of fetal nuchal translucency measurement and maternal serum pregnancy-associated plasma protein-A (PAPP-A) and free (5-human chorionic gonadotrophin has been demonstrated to identify approximately 90% of the cases of trisomy 21, with only a 5% false-positive rate.[67] This combination of fetal nuchal translucency thickness and maternal biochemical screening can also detect trisomy 21 in twin gestations at a rate similar to singleton gestations.[67] No statistical difference has

been demonstrated between monochorionic and dichorionic twin pregnancies in relation to maternal serum screening.[67]

REFERENCES

1. Luke B. The changing pattern of multiple births in the United States: maternal and infant characteristics, 1973 and 1990. Obstet Gynecol 1994;84:101–09.
2. Sebire NJ, Souka A, Skentou H et al. First trimester diagnosis of monoamniotic twin pregnancies. Ultrasound Obstet Gynecol 2000;16(3):223–25.
3. Chitkara U, Berkowitz RL. "Assessment of multiple pregnancies." Ultrasound in Obstetrics and Gynecology. In: Chervenak FA, Isaacson GC, Campbell S (Eds). United States of America: Little, Brown and Company, 1993.
4. Roberts WE, Morrison JC, Hamer C. The incidence of preterm labor and specific risk factors. Obstet Gynecol 1990;76:85S-89S.
5. Devoe LD, Ware DJ. Antenatal assessment of twin gestation. Semin Perinatol 1995; 19(5):413–23.
6. Chasen ST, Chervenak FA. What is the relationship between the universal use of ultrasound, the rate of detection of twins, and outcome differences. Clin Obstet Gynecol 1998;41:66–77.
7. Hendrix NW, Chauhan SR Sonographic examination of twins. From first trimester to delivery of second fetus. Obstet Gynecol Clin North Am 1998;25 (3): 609–21.
8. Ewigman BG, Crane JP, Frigoletto FD et al. Effect of prenatal ultrasound screening on perinatal outcome. N Engl J Med 1993;329:821–27.
9. Persson PH, Kullander S. Long term experience of general ultrasound screening in pregnancy. Am J Obstet Gynecol 1983; 146:942–47.
10. Spellacy WN, Handler A, Ferre CD. A case-control study of 1253 twin pregnancies from a 1982–1987 perinatal data base. Obstet Gynecol 1990;75:168–71.
11. Dickey RP, Taylor SN, Lu PY et al. Spontaneous reduction of multiple pregnancy: incidence and effect on outcome. Am J Obstet Gynecol 2002; 186:77–83.
12. Robinson DE, Wilson LS, Kossoff G. Shadowing and enhancement in ultrasonic echograms by reflection and refraction. J Clin Ultrasound 1981;9:181–88.
13. Pierce G, Golding RH, Cooperberg PL. The effects of tissue velocity changes on acoustical interfaces. J Ultrasound Med 1982;1:185–87.
14. Buttery B, Davison G. The ghost artifact. J Ultrasound Med 1984;3:49–52.
15. MacGillivray I. Epidemiology of twin pregnancy. Seminars in Perinatology 1986;10(1):4–8.
16. Bomsel-Helmreich O, Al Mufti W. "The mechanism of monozygosity and double ovulatlon." In: Keith LG, Papiernik E, Keith DM et al (Eds). Multiple Pregnancy. Camforth, UK: The Parthenon Publishing Group, 1995.
17. Hrubec Z, Robinette CD. The study of human twins in medical research. N Engl J Med 1984;310(7):435–41.
18. Benirschke K, Kim CK. Multiple pregnancy (First of two parts). N Engl J Med 1973;288(24): 1276 84.
19. Milham S. Pituitary gonadotrophin and dizygotic twinning. Lancet 1964;2:566.
20. Wenstrom KD, Syrop CH, Hammitt DG et al. Increased risk of monochorionic twinning associated with assisted reproduction. Fertil Steril 1993;60(3): 510 14.
21. Callen PW. Ultrasonography in Obstetrics and Gynecology. Philadelphia, PA, USA: WB Saunders Company, 2000.
22. Sepulveda W. Chorionicity determination in twin pregnancies: double trouble? Ultrasound Obstet Gynecol 1997;10:79 81.
23. Johnson SF, Driscoll SG. Twin placentation and its complications. Seminars in Perinatology 1986;10(1): 09 13.

24. Dube J, Dodds L, Armson BA. Does chorionicity or zygosity predict adverse perinatal outcomes in twins? Am J Obstet Gynecol 2002;186(3):579 83.
25. Sebire NJ, Snijders RJ, Hughes K et al. The hidden mortality of monochorionic twin pregnancies. Br J Obstet Gynaecol 1997;104:1203 07.
26. Sepulveda W, Sebire NJ, Hughes K et al. The lambda sign at 10 14 weeks of gestation as a predictor of chorionicity in twin pregnancies. Ultrasound Obstet Gynecol 1996;7:421 23.
27. Carroll SG, Soothill PW, Abdel-Fattah SA et al. Prediction of chorionicity in twin pregnancies at 1014 weeks of gestation. Br J Obstet Gynaecol 2002; 109:182 26.
28. Stenhouse E, Hardwick C, Maharaj S et al. Chorionicity determination in twin pregnancies: how accurate are we? Ultrasound Obstet Gynecol 2002; 19(4):350 52.
29. D'Alton ME, Dudley DK. The ultrasonographic prediction of chorionicity in twin gestation. Am J Obstet Gynecol 1989; 160(3):557 61.
30. Barss VA, Benacerraf BR, Frigoletto FD. Ultrasonographic determination of chorion type in twin gestation. Obstet Gynecol 1985;66(6):779 83.
31. Winn HN, Gabrielli S, Reece EA et al. Ultrasonographic criteria for the prenatal diagnosis of placental chorionicity in twin gestations. Am J Obstet Gynecol 1989; 161 (6Ptl): 1540 42.
32. Stagiannis KD, Sepulveda W, Southwell D et al. Ultrasonographic measurement of the dividing membrane in twin pregnancy during the second and third trimesters: a reproducibility study. Am J Obstet Gynecol 1995;173(5):1546 50.
33. Finberg HJ. The "twin peak" sign: reliable evidence of dichorionic twinning. J Ultrasound Med 1992; ll(ll):571 77.
34. Mahony BS, Filly RA, Callen PW. Amnionicity and chorionicity in twin pregnancies: prediction using ultrasound. Radiology 1985;155(1):205 09.
35. Arabin B, Laurini RN, van Eyck J. Early prenatal diagnosis of cord entanglement in monoamniotic multiple pregnancies. Ultrasound Obstet Gynecol 1999;13(3):181 86.
36. Rode ME, Jackson M. Sonographic considerations with multiple gestation. Seminars in Roentgenology 1999;34(l):29 34.
37. Manning FA, Hill LM, Platt LD. Qualitative amniotic fluid determination by ultrasound: Antepartum detection of intrauterine growth retardation. Am J Obstet Gynecol 1981;139(3):254 58.
38. Chamberlain PF, Manning FA, Morrison I et al. Ultrasound evaluation of amniotic fluid volume I. The relationship of marginal and decreased amniotic fluid volumes to perinatal outcome. Am J Obstet Gynecol 1984; 150(3):245 49.
39. Chamberlain PF, Manning FA, Morrison I et al. Ultrasound evaluation of amniotic fluid volume II. The relationship of increased amniotic fluid to perinatal outcome. Am J Obstet Gynecol 1984; 150(3):250 54.
40. Watson WJ, Harlass FE, Menard MK et al. Sonographic assessment of amniotic fluid in normal twin pregnancy. Am J Perinatol 1995; 12(2): 122 24.
41. Chau AC, Kjos SL, Kovacs BW. Ultrasonographic measurement of amniotic fluid volume in normal diamniotic twin pregnancies. Am J Obstet Gynecol 1996;174(3):1003 07.
42. Smith AP, Ong S, Smith NC. A prospective longitudinal study of growth velocity in twin pregnancy. Ultrasound Obstet Gynecol 2001;18(5):485 87.
43. Divon MY, Weiner Z. Ultrasound in twin pregnancy. Seminars in Perinatology 1995;19(5):404 12.
44. Egan JF, Vintzileos AM, Turner G et al. Correlation of uterine fundal height with ultrasonic measurements in twin gestations. J Matern Fetal Med 1994;3: 18 22.
45. Ong S, Lim MN, Fitzmaurice A. The creation of twin centile curves for size. Br J Obstet Gynaecol 2002;109(7):753 58.
46. Senoo M, Okamura K, Murotsuki J et al. Growth pattern of twins of different chorionicity evaluated by sonographic biometry. Obstet Gynecol 2000; 95(5):656 61.
47. Weissman A, Achiron R, Lipitz S et al. The firsttrimester growth-discordant twin: an ominous prenatal finding. Obstet Gynecol 1994;84(1):110 14.

48. Hamilton EF, Platt RW, Morin L et al. How small is too small in a twin pregnancy? Am J Obstet Gynecol 1998; 179(3Pt1):682–85.
49. Dickinson JE, Evans SF Obstetric and perinatal outcomes from the Australian and new Zealand twintwin transfusion syndrome registry. Am J Obstet Gynecol 2000; 182(3):706–12.
50. Urig MA, Clewell WH, Elliott JR Twin-twin transfusion syndrome. Am J Obstet Gynecol 1990; 163(5Pt1): 1522–26.
51. Bruner JP, Rosemond RL. Twin-to-twin transfusion syndrome: A subset of the twin oligohydramniospolyhydramnios sequence. Am J Obstet Gynecol 1993; 169(4):925–30.
52. Robertson EG, Neer KJ. Placental injection studies in twin gestation. Am J Obstet Gynecol 1983; 147(2): 170–74.
53. Blickstein I. The twin-twin transfusion syndrome. Obstet Gynecol 1990; 76(4):714–22.
54. Danskin FH, Neilson JP Twin-to-twin transfusion syndrome: What are appropriate diagnostic criteria? Am J Obstet Gynecol 1989; 161(2):365–69.
55. Nores J, Athanassiou A, Elkadry E et al. Gender differences in twin-twin transfusion syndrome. Obstet Gynecol 1997; 90(4): 580–82.
56. Mahony BS, Petty CN, Nyberg DA et al. The “stuck twin” phenomenon: Ultrasonographic findings, pregnancy outcome, and management with serial amniocenteses. Am J Obstet Gynecol 1990; 163(5Pt1): 1513–22.
57. Taylor MJ, Denbow ML, Duncan KR et al. Antenatal factors at diagnosis that predict outcome in twin-twin transfusion syndrome. Am J Obstet Gynecol 2000; 183(4):1023–28.
58. Malone FD, D’Alton ME. Anomalies peculiar to multiple gestations. Clin Perinatol 2000; 27(4): 1033–46.
59. Soernes T, Bakke T. The length of the human umbilical cord in twin pregnancies. Am J Obstet Gynecol 1987; 157(5):1229–30.
60. Little J, Bryan E. Congenital anomalies in twins. Semin Perinatol 1986; 10(l):50–64.
61. Burn J. “Twins and twinning.” In: Chervenak FA, Isaacson GC, Campbell S (Eds). Ultrasound in Obstetrics and Gynecology. United States of America: Little, Brown and Company, 1993.
62. Aggarwal N, Suri V, Saxena S et al. Acardiac acephalus twins: a case report and review of literature. Acta Obstet Gynecol Scand 2002; 81(10):983–84.
63. Arias F, Sunderji S, Gimpelson R et al. Treatment of a cardiac twinning. Obstet Gynecol 1998; 91(5Pt2): 818–21.
64. Hanson JW. Incidence of conjoined twinning. Lancet 1975; 1257.
65. van den Brand SF, Nijhuis JG, van Dongen PW. Prenatal ultrasound diagnosis of conjoined twins. Obstet Gynecol Surv 1994; 49(9):656–62.
66. American College of Obstetricians and Gynecologists. Prenatal diagnosis of fetal chromosomal abnormalities. ACOG practice bulletin #27. American College of Obstetricians and Gynecologists, Washington, D.C. 2001.
67. Spencer K. Screening for trisomy 21 in twin pregnancies in the first trimester: does chorionicity impact on maternal serum free beta-hCG or PAPP-A levels? Prenat Diagn 2001; 21(9):715–17.

Chapter 28
General Aspects on Ultrasound Screening of Congenital Anomalies

Vincenzo Pinto, Mira Wankelmuth, Vincenzo D'Addario

INTRODUCTION

Fetal malformations represent an important public health problem because of the severe disabilities as well as the social consequences and financial charges they present for the family and the community. The prevalence of the congenital anomalies (CAs) is of difficult evaluation since only the most severe and evident cases are diagnosed at birth, while those considered of "minor importance", or diagnosed after months or years, escape the notification and are excluded therefore from the registry of CAs data. Despite their relatively low prevalence (ranging from 1.5 to 3% of all births) CAs account in developed countries for 20–30% of perinatal death, 50% of deaths in infancy and 50% of severe mental and physical handicaps in children.

PREVENTION OF FETAL MALFORMATIONS

The prevention of fetal malformation has an immediate reply on the affected individual, on the parents who wish to have a healthy child and on the community, which has to consider the high social costs of many CAs. The primary prevention programs used in prenatal medicine permit the prevention of congenital defects for which the pathogenesis is known. They can be organized on a large scale or for limited high risk groups. By definition, the primary prevention is apt to eliminate or limit an event for which the pathogenesis is known and therefore it is applicable only for some CAs. Furthermore its organization is difficult and necessitates an aimed intervention of the sanitary politics.

The realization of primary prevention programs for some CAs does not exclude the possibility to also apply secondary prevention programs. The secondary prevention is the detection of a malformation or a risk factor in the prenatal age. It is an imperfect prevention aimed to point out a disease, although at an early stage; nevertheless its achievement offers a series of therapeutic options and allows to institute, at birth or even prenatally, management strategies to improve survival or minimize morbidity.

SONOGRAPHIC SCREENING OF CONGENITAL ABNORMALITIES

Sonography is the most effective diagnostic tool in the recognition of CAs. Throughout the ’60 and the first half of the ‘70 the first applications of sonography in obstetrics were limited to the fetal biometry even though there were isolated detections of fetal malformations. The first ultrasonographic report of a fetal malformation was published in 1961 by Donald and Brown who described a case of hydrocephaly.[1] In 1964 Sunden described a case of acrania[2] and Campbell, in 1972, published the sonographic features of the anencephaly.[3] Subsequently, the remarkable improvements of the equipment and the accreditation that this technique acquired, permitted the application of screening programs which initially were limited to risk pregnancies. The inclusion criteria in these screening programs usually included previous CAs in the obstetric anamnesis, maternal malformations or high blood titers of α-feto protein in the mother. The further technical development of the equipment with the reduction of the costs, the pressing request from the parents of a morphological evaluation of their fetus and above all the statistic evidence that congenital malformations in 80–90% of the cases occur in infants without any risk factor,[4] has led the scientific community to advocate ultrasonographic screening of the whole obstetric population to allow prenatal diagnosis of structural birth defects. The utility to recognize in prenatal age the presence of CAs is currently amplified by other factors such as the availability of new invasive procedures, the progress in the management of the premature infants, the increased skill in pediatric surgery and the greater safety of the techniques of termination of pregnancy.

CAs represent a group of pathologies for which the organization of a prenatal screening is justifiable for its significant prevalence (1.5–3%), the severe and invaliding consequences and the high social cost. Furthermore in some cases the prenatal diagnosis permits the application of measures which can modify the natural history of the illness. An ideal screening test should be quickly performed, repeatable, safe, non-invasive, well accepted, cheap, sensitive and specific. Sonography is a non-invasive, safe procedure with limited cost and wide availability.

Its accuracy in detecting CAs varies between the population at high risk and the one at low risk. Pregnant women affected by CAs, with a former fetus with CAs, having risk factors for CAs (age, infectious diseases, teratogens exposure) or with positivity for biochemical tests are considered at high risk for CAs. According to Levi and Montenegro[5] the definition of the risk level characterizing the population of pregnant women studied has not been clearly established. A population of pregnant women “at low risk” should only include the group cleared from the women at risk. The unselected, geographical areabased population, which could be called “at regular risk” is the population submitted for screening. The prevalence of the CAs is thus expected to be the one observed in geographical area-based populations “at regular risk”.[5] Nevertheless in literature the term “low risk” usually means the normal, unselected population of pregnant women at “regular risk”.

Targeted studies performed on high risk group of pregnant women appear to be simpler, being often known the anomalies to seek, and has shown an excellent sensitivity (89–99%) and specificity (99–100%).[6] On the contrary the sonographic screening of fetal CAs in a low risk population results more difficult because it needs an accurate and

systematic evaluation of the whole fetal anatomy. The major studies that have evaluated the US accuracy denoted a high specificity and an equally satisfying positive and negative predictive value, but they showed discordant results for the sensitivity that ranges between 34.8% of the RADIUS Study Group[7] and 85% of the Luck study (Table 28.1).[8]

Table 28.1: Diagnostic accuracy (%) of sonographic screenings in detecting CAs

	Sensitivity	*Specificity*	*PPV*	*NPV*
Chitty[91]	71.4	99.9	97.9	99.6
Luck[92]	85.0	99.9	–	–
Shirley[92]	60.7	99.9	–	–
RADIUS[93]	34.8	–	–	–
Levi[95]	44.5	99.9	94.2	98.6
Anderson[95]	58.3	99.9	89.4	99.2
Carrera[95]	78.3	99.9	99.2	99.3
Chambers[95]	50.9	–	–	–
Stoll[95]	37.8	99.8	97.7	98.4
Boyd[98]	54.6	99.5	–	–
Stefos[99]	85.2	99.5	–	–
Eurofetus[99]	61.4	–	–	–

FACTORS THAT INFLUENCE THE RESULTS

The sensitivity of a screening tool for detecting CAs is the expression of the capability to recognize prenatally a fetal malformation. The results ideally should be prevalence independent, and therefore not bound to the values of the prevalence of the CAs to be screened. The results should also be unrelated to the subjective interpretation of the operator.

However, the published studies of sonographic detection of fetal abnormality have reported wide variations in the rate of detection. There are several potential sources for bias in any fetal abnormality audit study:

1. Origin of the data/examiners' experience
2. Inclusion or exclusion criteria
3. Prevalence of CAs in the population screened
4. Features of the audit
5. Postnatal identification of CAs
6. Number of scans and their timing.

Origin of the Data/Examiners' Experience

There is a discrepancy between the results of the multicenter studies and the ones obtained in one single center. Data from primary, secondary and tertiary level centers often consider also referred patients. It causes a higher prevalence of abnormalities in the population to be evaluated which will improve the detection rate. Therefore it will not be representative of what we can aspect to achieve in a non-selected population.[9]

The studies undertaken in one single center, show a higher sensitivity compared to the multicenter studies which are an expression of the experiences of many operators, because they reflect the skill of only one or a small group of selected operators. These aspects may justify the differences found among the multicentric trials performed by primary level operators[7,10] and those undertaken in secondary level centers by specially trained personnel.[8,11,12] Moreover the personnel involved in prenatal screening programs is not homogeneous in expertise. The trials in fact may have been carried out by radiographers with the overall supervision of a radiologist,[8,12] by nurses under the close supervision of consulting doctors,[13] by radiologists[14] or obstetricians.[15] The RADIUS study has been conducted in 28 ultrasound laboratories by technicians, physician sonologists, obstetricians and radiologists.[7]

Concerning the origin of the data, they should be collected in a short period. Long lasting trials may increase the bias due to changes in diagnostic procedures and equipments.[5]

Inclusion or Exclusion Criteria

The reporting criteria of inclusion or exclusion vary widely and are not clearly stated in many studies; the different detection rates reported are related to the lack of an explicit definition of "major" and "minor" congenital birth defects and to the arbitrary exclusion of the latter from some statistics. Minor abnormalities are traditionally considered unusual morphologic features that are of no serious medical or cosmetic consequence to the patient. Major abnormalities are considered as producing significant long-term disability and/ or death; the word minor should not underestimate the significance of the abnormality because often it just means "less severe". In some studies, as the RADIUS trial,[7] the overall sensitivity has considered all CAs undetected. Other studies have excluded the "minor" or US undetectable defects and did not count them as false-negatives if screening failed their detection. The latter trials showed in most of the studies a higher detection rate. These methodological errors may be suspected if there is a high sensitivity but low prevalence of CAs at birth or at termination of pregnancy.[10]

On the contrary, some trials, as the series reported by Luck, whose overall sensitivity was as high as 85%, are considered to be unrepresentative because of the abnormally high proportion of hydronephroses, which are among the best detected.[16] In fact the sensitivity of the sonographic screening of CAs differs according to the affected organ system and is related to the relative prevalence of the abnormalities. The detection of CAs is high for the central nervous system and urinary tract but remains poor for craniofacial, skeletal and, above all, cardiac malformations, which are the most frequent ones at birth but also the most difficult to diagnose prenatally (Table 28.2).

Table 28.2: Sensitivity (%) of sonographic screenings in detecting CAs according to the organ system

	CNS	*GE*	*GU*	*Skel.*	*CV*
Chitty	95.0	57.1	84.0	54.5	63.6
Luck	100.0	86.0	100.0	60.0	36.0
Bernaschek	68.3	46.0	73.0	53.0	30.0
Levi	77.8	51.0	72.6	34.3	35.2
Anderson	92.0	69.0	69.0	35.0	31.0
Carrera	75.1	84.1	90.8	67.8	66.6
Chambers	92.1	24.0	88.4	25.0	18.4
Stoll	76.7	47.3	64.1	18.2	16.5
Stefos	93.1	85.2	85.7	84.6	45.2
Eurofetus	88.3	53.7	88.5	36.6	27.7

CNS: central nervous system; GE: gastrointestinal system; GU: genitourinary system; Skel: skeletal system; CV: cardiovascular system

Chromosomal anomalies must not be considered in assessing the detection rate of a screening program for CAs. Their inclusion is an important bias in the evaluation of the audit.

Prevalence of CAs in the Population Screened

The percentage of abnormalities detected is influenced by the prevalence of CAs in the population screened. The percentage of abnormalities detected is a ratio of anomalies detected, divided by the prevalence reported. Thus, a high percentage can be achieved with a small number of abnormalities detected if the reported prevalence is low.[14]

Features of the Audit

The ranking of detection is strongly influenced by the reporting method. Some studies in fact report the number of CAs detected, others the number of babies with CAs detected. The Eurofetus study for example, showed a sensitivity of 61.4% in detecting malformed fetuses. It decreased to 56.2% considering the anomalies detected.[16]

Postnatal Identification of CAs

In most of the studies the abnormalities detected after the postpartum hospitalization period are not recorded. It is known that many CAs, especially those of the heart and digestive tract, become apparent in the first month of life or even later.[16] Therefore if the

postnatal follow-up includes only the postpartum examination, CAs are underreported and the overall screening accuracy may be slightly overestimated. This possibility is supported by the fact that the detection rate for lethal and severely handicapping anomalies are similar in most of the studies.[7]

Number of Scans and Their Timing

The most important second trimester trials have been performed at a gestational age ranging between the 16th and the 24th week.

Trials which use scans in the second and third trimester show a higher detection rate compared to the ones that consider only one scan in the Second trimester (Table 28.3).

Table 28.3: Sensitivity (%) of sonographic sereenings in detecting CAs according to the gestational age

	Second trimester	*Second and third trimester*
Shirley	60.8 (≤22 wk)	66.7
RADIUS	16.6 (≤24 wk)	34.8
Bernaschek	18.0 (≤24 wk)	50.0
Levi	33.6 (≤23 wk)	44.5
Carrera	59.4 (≤22 wk)	78.3
Chambers	32.5 (≤24 wk)	50.9
Eurofetus	44.0 (≤24 wk)	61.4

The positive predictive value and the specificity were not cited in all the studies because the value of the false-positive cases is not always available and sometimes has methodological errors.

In the studies carried out in unselected low risk populations the negative predictive value is always very high (>98.4%) (Table 28.1). It should not be surprising because the prevalence of the CAs is relatively low in these populations and even when ignoring systematically all of the fetal CAs, with a prevalence of about 2%, the negative predictive value cannot be inferior than 98%.

CLINICAL USE OF THE SONOGRAPHIC SCREENING OF CAs

The results of the sonographic screening of CAs in the low risk population have been critically reviewed and the advantages of a routine or indication-based ultrasound investigation are still under debate. The Cochrane Pregnancy and Childbirth Group[17] has compared routine versus selective sonography within the 24th week of pregnancy. It stated that routine US examination was associated with earlier detection of multiple pregnancies and reduced rates of induction of labour for post-term pregnancy. There was

no statistical evidence of a better clinical outcome, and where the detection of CAs was a specific aim of the examination, the number of terminations of pregnancy for fetal anomaly increased.

The Helsinki Group[13] demonstrated a significant reduction of the perinatal mortality; therefore the only practical application of the screening within the 24th week would consist in the recognition of undetected CAs at an age where it is still possible to terminate the pregnancy.

Nevertheless the reduction of the perinatal death cannot be considered the only end-point in evaluating the utility of US screening of CAs. In fact we have to consider other undoubtable advantages of the prenatal diagnosis on the neonatal outcome. Prenatal detection of CAs allows the opportunity for prenatal counselling with a multidisciplinary team of experts. It may also influence antepartum and intrapartum management and permit the planning of the mode and site of delivery. Furthermore the psychological preparation of the family receiving a child with a CA is better if it is acquired gradually during the pregnancy.

SONOGRAPHIC SCREENING TRIALS OF CONGENITAL MALFORMATIONS

The CAs sonographic screening must address the entire population of pregnant women to be efficient on a public health basis, because a primary selection of high risk pregnancies is unsatisfactory. To be efficient, any screening program should address the entire population of pregnant women. Any preliminary selection aimed to reduce the number of patients to be screened and to direct only high risk pregnant women towards specialized labs would leave about 75% of the affected fetuses undiagnosed causing a considerable reduction of the mean sensitivity.[5]

Screenings should be performed by trained and motivated personnel using excellent equipment with sufficient time allocated for examination.

For the best chances of CAs detection, an adequate timing for the ultrasound should objectively be fixed, taking into account that there are ideal gestational ages for specific diagnoses when the anomaly becomes sufficiently clear. Since a single evaluation does not guarantee a satisfactory sensitivity in the screening of CAs, more than one scan is necessary during the pregnancy. Considering that the accuracy of a screening method increases with the number of examinations, the best results would be obtained-theoreticallyapplying monthly evaluations. Such a program is not justifiable because of its high cost. The CAs screening has to be carried out in a sufficiently advanced period of the pregnancy where most of the CAs are recognized. On the other hand it should be performed sufficiently early to program eventual further diagnostic tests and permitting the entire spectrum of management choices, including termination within the legal time period. Although sonographic surveys employing the transvaginal[18] or the transabdominal and the transvaginal route[19] have detected the majority of CAs already in the first trimester of the pregnancy, the gestational age which represents the best compromise between the need of an early diagnosis and the natural history of many structural birth defects is the period between the 19th and the 22nd week.

All the major studies[7,12,15,16,18,21,22] have shown a considerable and often statistically significant increase of the detection rate when the Second trimester screening is associated with a further evaluation in the third trimester (Table 28.3). These results are related to the detection of some pathologies (as for example microcephaly, lissencephaly, porencephaly, obstructive hydrocephaly, obstructive uropathy, gastrointestinal tract stenoses and atresias) that may become apparent later on.

The recognition of minimal requisites which the screening has to assure and the uniformity of the postnatal audit should lead to a higher homogenicity of the results.

The specificity of the US screening on unselected pregnancies has always shown excellent performances and cannot improve. On the contrary the sensitivity of routine screening is steadily improving and might rapidly approach the levels of the referral trials.[20] This may allow to reach the final goal of the sonographic screening of the CAs, which is reassuring the expecting mother with the exclusion of the US detectable diseases. As the negative predictive value is high we may expect relief of anxiety when a screening test is announced as normal. If a CA is detected the prenatal medicine unit should be able to offer the widest range of management choices.

REFERENCES

1. Donald I, Brown TG. Demonstration of tissue interfaces within the body by ultrasonic echo sounding. Br J Radiol 1961; 34:539 46.
2. Sunden B. On the diagnostic value of ultrasound in obstetrics and gynecology. Acta Obstet Gynecol Scand 1964; 43(suppl):6.
3. Campbell S, Holt EM, Johnstone FD et al. Anencephaly: early ultrasonic diagnosis and active management. Lancet 1972; 2:1226 27.
4. Kurjak A, Kirkinen P, Latin V et al. Diagnosis and assessment of fetal malformations and abnormalities by ultrasound. J Perinat Med 1980; 8:219 35.
5. Levi S, Montenegro NA. Eurofetus: an evaluation of routine ultrasound screening for the detection of fetal defects: aims and method. Annals of the New York Academy of Sciences 1998; 847:103 17.
6. European Association of Perinatal Medicine. Recommendations and protocols for prenatal diagnosis, 1994; 18.
7. Crane JR LeFevre ML, Winborn RC and the RADIUS study group. A randomized trial of prenatal ultrasonographic screening: impact on the detection, management and outcome of anomalous fetuses. Am J Obstet Gynecol 1994; 171:392 99.
8. Luck CA. Value of routine ultrasound scanning at 19 weeks: a four year study of 8849 deliveries. Br Med J 1992; 304:1474 78.
9. Eik-Nes SH. Fetal structural disorders -the large series are emerging. Ultrasound Obstet Gynecol 1995; 5: 364 65.
10. Levi S, Hyjazi Y, Schaaps JP et al. Sensitivity and specificity of routine antenatal screening for congenital anomalies by ultrasound: The Belgian Multicentric Study. Ultrasound Obstet Gynecol 1991; 1:102 10.
11. Chitty LS, Hunt GH, Moore J et al. Effectiveness of routine ultrasonography in detecting fetal structural abnormalities in a low risk population. Br Med J 1991; 303:1165 69.
12. Shirley IM, Bottomley F, Robinson VR Routine radiographer screening for fetal abnormalities by ultrasound in an unselected low-risk population. Br J Radiol 1992; 65:564 69.

13. Saari-Kemppainen A, Karjalainen O, Ylostalo P et al. Fetal anomalies in a controlled one-stage ultrasound screening trial. A report from the Helsinki Ultrasound Group. J Perinat Med 1994; 22:279 89.
14. Anderson N, Boswell O, Duff G. Prenatal sonography for the detection of fetal anomalies: results of a prospective study and comparison with prior series. AJR 1995; 165:943 50.
15. Bernaschek G, Stuempflen I, Deutinger J. The value of sonographic diagnosis of fetal malformations: different results between indications-based and screening-based investigations. Prenat Diagn 1994; 14:807 12.
16. Grandjean H, Larroque D, Levi S and the Eurofetus Study Group. The performance of routine ultrasonographic screening of pregnancies in the Eurofetus Study. Am J Obstet Gynecol 1999; 181:446 54.
17. Neilson JP Routine ultrasound in early pregnancy. Pregnancy and Childbirth Module of the Cochrane Database of Systematic Reviews 2000;(2) CD000182.
18. Kurjak A, Kupesic S, Matijevic R et al. First trimester malformation screening. Eur J Obstet Gynecol Repr Biol 1999; 85:93 96.
19. Withlow BJ, Chatzipapas IK, Lazanakis ML et al. The value of sonography in early pregnancy for the detection of fetal abnormalities in an unselected population. Br J Obstet Gynecol 1999; 106:929.
20. Levi S, Schaaps JP, De Havay P et al. End-result of routine ultrasound screening for congenital anomalies: the Belgian Multicentric Study 1984 92. Ultrasound Obstet Gynecol 1995; 5:366 71.
21. Carrera JM, Torrents M, Mortera C et al. Routine prenatal ultrasound screening for fetal abnormalities: 22 years' experience. Ultrasound Obstet Gynecol 1995; 5:174–79.
22. Chambers SE, Geirsson RT, Stewart RJ et al. Audit of a screening service for fetal abnormalities using early ultrasound scanning and maternal serum alpha feto protein estimation combined with selected detailed scanning. Ultrasound Obstet Gynecol 1995; 5:168–73.
23. Stoll C, Dott B, Alembik Y et al. Evaluation of routine prenatal diagnosis by a registry of congenital anomalies. Prenat Diagn 1995; 15:791–800.

Chapter 29
Fetal Hydrops

Ratko Matijevic

INTRODUCTION

Fetal hydrops is defined as edema plus an accumulation of the fluid in at least one visceral cavity. It is not a defined disease but a morphologic description of underlying problem. It can be divided into two groups: immune and non-immune.[1] Nowadays, there is significant reduction in the incidence of immune hydrops secondary to Rhesus disease, mostly by Immune Globulin prophylaxis. As well as that, the results of treatment by intrauterine transfusion significantly improves survival rate being as high as 90%.[2] However, non-immune fetal hydrops still significantly contributes to fetal mortality and morbidity.

The main fetal risks related to hydrops are:

- Perinatal death, being 25–30% in immune and as high as 90% in non-immune fetal hydrops[3]
- Consequence of the underlying cause
- Complications of various diagnostic and therapeutic procedures.[4]

As well as fetal, there are several potential maternal complications arising mostly from diagnostic and therapeutic procedures, but also from anemia, cesarean section, postpartal hemorrhage and retained placenta.

DIAGNOSIS

Presentation of fetal hydrops can be through either routine ultrasound screening program, detection of polyhydramnios, uterus larger than expected for the named gestational age; or hydrops can be found during the investigation of maternal diabetes, pre-eclampsia and as a part of follow up of placental abruption. The various presumed causes of hydrops are summarized on Table 29.1.

Pathophysiologic mechanism of fetal hydrops include:

- Inadequate cardiac output resulting from obstructed or diverted outflow and inadequate cardiac return

• Diffuse lymphatic malformation
• And/or liver or peritoneal disease causing an exudative ascites and hypoproteinemia.[5,6]

Ultrasound identification of fetal hydrops should initially focus on the presence or absence of fluid accumulation in thoracic, pleural or pericardial space (Fig. 29.1). It should be pointed that any amount of free fluid in the fetal thorax or abdomen is abnormal,[7] while pericardial space may be filled with some free fluid (up to 2 mm) in normal circumstances (Fig. 29.2).[8] Everything above this is considered to be abnormal and called preicardial effusion or hydropercard. Intraperitoneal collection of free fluid is commonly identified within peritoneum surrounding the liver or spleen (Figs 29.3 and 29.4). However, it should be pointed that the abdominal wall muscles, particularly if examined by high-resolution machines, can appear as hypoechogenic band in the close proximity to the umbilical cord insertion.[9] In these circumstances, the area of the abdomen near the insertion of umbilical cord should be examined carefully, and if both sides of umbilical vein can be seen clearly than hypoechogenic area very probably represents free fluid.

Table 29.1: Abnormalities associated with hydrops[4]

Immune	*Infection (intrauterine)*
• Anti-D Rhesus antibodies	• parvovirus B19 (either by anemia myocarditis or hepatitis)
• Antibodies to K in the Kell system	
• Antibodies to Fya in the *Duffy* system	• syphilis
• Antibodies to C and E in the Rhesus system	• cytomegalovirus
	• toxoplasmosis
Non-Immune	• herpes simplex
• Idiopathic/Unknown	• leptospirosis
• Chagas disease	
Anemia	
• homozygous alpha-thalassemia	*Liver*
• chronic feto-maternal transfusion	• hepatic calcifications
• twin-twin transfusion and variants	• hepatic fibrosis
• erythroleukemia	• congenital hepatitis
• cholestasis	• polycystic disease
	• biliary atresia
Cardiovascular	• familiar chirosis
• severe congenital heart disease (ASD, VSD, hypoplastic left heart, pulmonary valve insufficiency Ebstein anomaly, subaortic stenosis, A-V canal defect	

- Tetralogy of Fallot
- premature closure of foramen ovale
- premature closure of ductus (? indomethacin therapy not reported)
- myocarditis (coxsackie, CMV, parvovirus B19)
- large A-V malformation
- tachyarrhythmias (SVT, atrial flutter)
- bradyarrhythmias (heart block)
- Wolff-Parkinson-White syndrome
- intracardiac tumors (teratoma, rhabdomyoma)
- cardiomyopathy (e.g. fibroelastosis)
- myocardial infarction
- arterial calcification

Chromosomal

- trisomies
- Turner's syndrome (45 XO)
- triploidy

Pulmonary

- cystic adenomatous malformation
- pulmonary lymphangiectasia
- pulmonary hypoplasia
- diaphragmatic hernia
- chondrodysplasia
- bronchogenic cyst and other tumors
- pulmonary sequestration
- congenital hydro-/chylo-thorax

Renal

- congenital nephrosis (Finnish type)
- renal vein thrombosis

Genetic metabolic disease (many have their effect via the liver)

- Gaucher disease
- GMI gangliosidosis
- mucopolysaccharidosis (types IVa and VII)
- iron-storage disease

Anomalies *(associated with fetal immobility)*

- achondroplasia
- achondrogenesis type 2
- thanatophoric dwarfisrn
- sacrococcygeal teratoma
- arthrogryposis
- multiple pterygium syndrome
- Neu-Laxova syndrome
- Pena-Shokeir type I syndrome
- Noonan syndrome
- myotonic dystrophy

Miscellaneous

- cystic hygroma
- meconium peritonitis
- fetal neuroblastosts
- tuberous sclerosis
- small bowel volvulus
- amniotic band syndrome
- torsion of ovarian cyst
- poly splenia syndrome

Placental

- umbilical vein thrombosis

• urethral obstruction (atresia, posterior valves)	• chorangioma
• spontaneous bladder perforation	• true cord knots
• cloacal malformation	
• prune belly	*Maternal*
• neuronal degeneration	• diabetes mellitus
	• pre-eclampsia
	• severe anemia
	• hypoalbuminemia

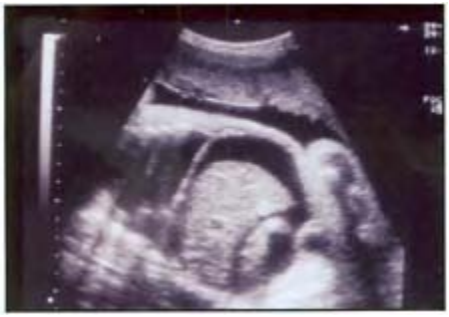

Figure 29.1: Fetal ascites and hydrothorax

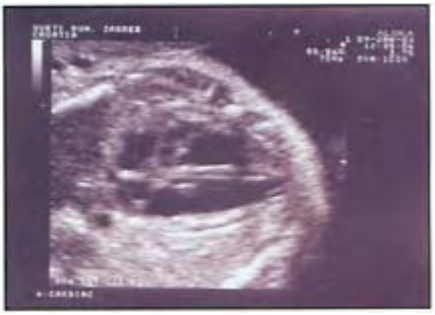

Figure 29.2: Normal amount for free fluid in pericardial space

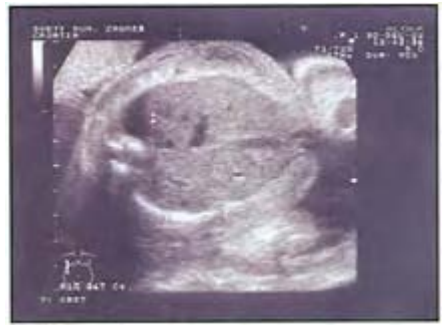

Figure 29.3: Intraperitoneal fluid collection (arrows) and edema

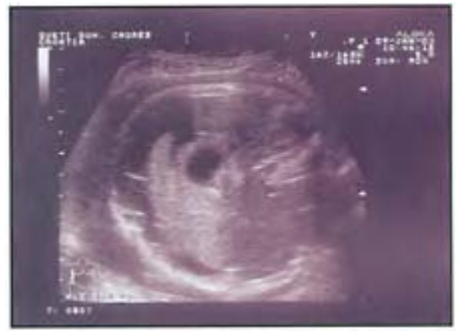

Figure 29.4: Fetal ascites

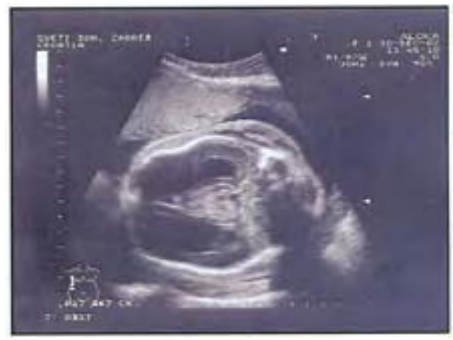

Figure 29.5: Fetal skin edema on the head. Note ventriculomegaly as associated anomaly in the presence of parvo B19 infection

Fetal skin edema as a part of the fetal hydrops is defined as a skin thickness greater than 5 mm. It is commonly recognized on the fetal head (Fig. 29.5). It also can be diagnosed on the fetal abdomen but fat in the subcutaneous layer can cause the mistakes (Fig. 29.6). Polyhydramnios, placental edema and alterations of the fetal umbilical vessels are commonly seen with fetal non-immune hydrops. Polyhydramnios is described as a subjective increase of amniotic fluid volume, i.e. single pocket with vertical measurement greater than 8 cm, or amniotic fluid index greater than 20 cm.[10] Placental edema is defined as thickness of the placental tissue greater than 4 or 6 cm (Fig. 29.7).[11] We use the cut of point of 5 cm, but the caution should be used as in the cases of gross polyhydramnios placenta can be compressed towards the uterine wall and consequently the placental thickness cannot be adequately assessed.

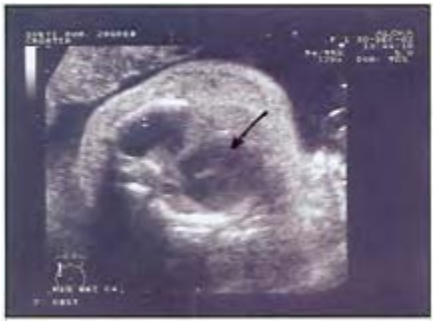

Figure 29.6: Fetal skin edema on the fetal abdomen. Hydrothorax (white arrows) and hydropericard (black arrow)

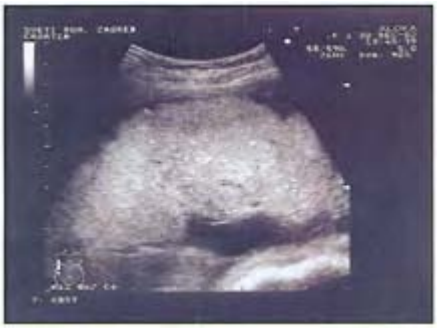

Figure 29.7: Placental hydrops

There are certain conditions which may mimic the presence of fetal hydrops. Those include:

• Extensive body fat of a macrosomic fetus

- Urinary ascites secondary to bladder or renal collecting system rupture
- Intraperitoneal fluid associated to the rupture of the viscous organ
- Chlylothorax resulting from the accumulation of lymphatic fluid secondary to thoracic duct rupture
- Intraperitoneal and pleural effusions seen with cystic hygromas.[4]

In these circumstances certain features may suggest the difference. They include:

- Distension of the bladder and renal collecting system associated with urinary ascites
- Abnormally distended loops of the bowel in meconium peritonitis
- Unilateral hydrothorax located on the left side associated with thoracic duct rupture.

However, in all cases the experienced sonographer with best available ultrasound equipment should examine the pregnant woman with suspected or diagnosed fetal hydrops and referral in tertiary specialized center is mandatory for further management.

MANAGEMENT

The investigation of diagnosed case of fetal hydrops should start with maternal investigation including:

- Detailed history (previous hydrops, diagnosis causing hydrops) previous baby with jaundice, ethnic origin
- Blood tests:
    - Full blood count, blood group and antibody screen
    - Electrophoresis (depending on ethnic origin)
    - Renal tests (urea, electrolytes, urate)
    - Liver tests (including albumen)
    - Lupus anticoagulant and anticardiolipin antibodies
    - Alpha fetoprotein
    - Keihauer Bethe test
    - Serology (syphilis, Parvo B19, toxoplasmosis, CMV, Herpes virus).

After precise diagnosis mostly by B/W ultrasound and color/pulsed Doppler as well as 3D ultrasonography if available[12,13] fetal investigations include:

- Exclusion of accompanied anomalies (See Table 29.1)
- Echocardiography
- Assessment of amniotic fluid volume
- Biophysical profile
- Invasive testing:
    - Karyotype
    - Umbilical venous pressure
    - Fetal full blood count
    - Fetal hemoglobin electrophoresis
    - serologic test for specific antibodies (IgM class)

• in the suspected fetal hypoxia assessment of pH and blood gases.

The treatment of fetal hydrops is mostly related to the underlying cause. Immune fetal hydrops is usually managed by fetal blood transfusion and the results are promising. Nowadays, the survival rate of alloimmune fetal hydrops diagnosed before 24 weeks is up to 74% while if the diagnosis is made after 24 weeks survival rate can be up to 90%.[4]

The survival rate is significantly lower in the hydrops of non-immune origin. Prenatal evaluation of non-immune hydrops is summarized on the Table 29.2. Detailed counseling is mandatory as a prognosis is relatively poor and the pregnant women should be aware of the potential risks and possible fetal death. In the circumstance when the diagnosis is made before 24 week the termination of the pregnancy should be considered as a potential option. If the diagnosis is made later in pregnancy, the fetal survival rate is higher and different therapeutic options should be considered. As most of them require experienced and highly equipped unit the referral to tertiary fetal center is mandatory. Treatment is dependent on the cause. In the case of anemia causing fetal hydrops, therapeutic option is fetal blood transfusion. Taking a sample of fetal blood provides the diagnosis but in the recent years non-invasive diagnosis by color/pulsed Doppler is becoming a challenging alternative.[14]

In non-immune fetal anemia the results of intrauterine blood transfusion are not as good as

Table 29.2: Antenatal evaluation of non-immune fetal hydrops[4]

Type	*Test*	*Possible etiology*
Ultrasound	Real time B-mode	Structural malformations Fetal arrhythmia Assessment of severity of hydrops Response to therapy Biophysical profile (BPP)
Maternal	Full blood count Hb electrophoresis Blood chemistry Kleihauer test VDRL, TORCH, P B19 Glucose tolerance test	Hematological disorders Hematological disorders Metabolic disease Fetal-maternal transfusion Fetal infection Maternal diabetes
Amniocentesis	Fetal karyotype Amniotic fluid microbiology Amniotic fluid AFP Metabolic tests	Chromosomal anomalies Fetal infection Congenital nephrosis Metabolic disorders
Cordocentesis	Rapid fetal karyotype Metabolic tests Hemoglobin chain analysis Specific IgM Plasma albumin Full blood count Reticulocytes	Chromosomal anomalies Metabolic disease Thalassemias Fetal infection Hypoalbuminemia Anemia Erythroid status

	Blood gases	Fetal well being
Needle catheter fetal surgery	Serous fluid culture	Infection
	Fetal karyotype	Chromosomal anomalies
	Body cavity decompression	Hemodynamc disturbances

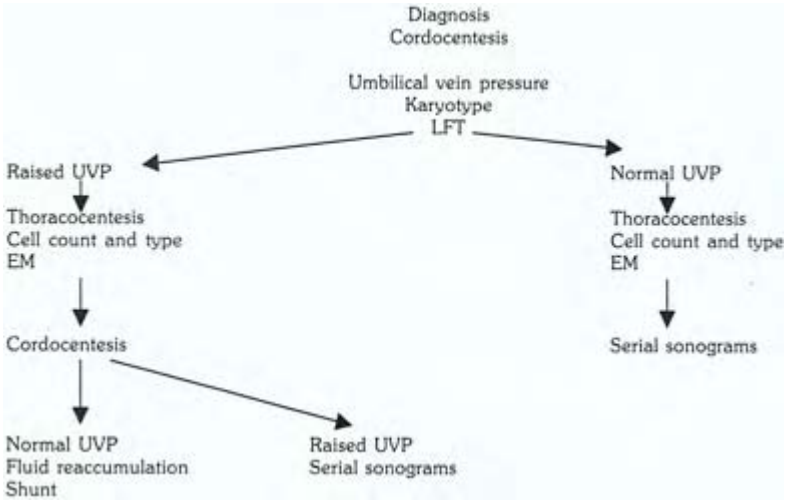

Figure 29.8: Algorithm for management of non-immune fetal hydrops associated with hydrothorax (by Weiner, 1993)[5]

in the cases of immune anemia. Survival rate is around 25% independently on the age of presentation.[4] The principles for the fetal blood transfusion are identical as in the immune fetal hydrops, and there is no difference even if the hydrops is caused by fetal infection, i.e. parvo B19.[15]

If fetal hydrops is caused by underlying cardiovascular problem, the general treatment is advocated (i.e. treatment of fetal heart arrhythmia, tachycardia, etc.). Before treatment, fetal echocardiography should confirm the presence of structurally normal heart. If fetal hydrops is caused by underlying chromosomal problem, termination of the pregnancy is appropriate management within legal limits.

In fetal hydrops of pulmonary origin the prognosis is generally poor with the main exception of isolated hydrothorax in the absence of another detectable cause. They usually present after 24 weeks gestation after the lung development has entered the canalicular phase.[4] Therefore the treatment is aimed to improve cardiac function. Thoracic drainage permits the heart to return to its midline position and elevated umbilical vein pressure associated with elevated intrathoracic pressure caused by fluid accumulation can normalize after the drainage.[4] If single drainage is not successful the placement of thoracic shunt is advocated. The management of non-immune hydrops with hydrothorax is presented on Figure 29.8.[5]

In recent paper, the outcome of fetal hydrops was assessed in relation to gestational age at diagnosis and following investigation and treatment. During seven year period in large Fetal Medicine Unit in UK there was 87 cases of fetal hydrops among 13,980 referred cases, giving the incidence of 0.6%. The cases were examined for gestational age at presentation according to etiology and fetal survival following investigation and treatment. The cause of hydrops was determined antenatally in 71 of the 87 (82%) cases. Of the 51 cases presenting before 24 weeks' gestation, 23 (45%) were due to chromosomal abnormality. After 24 weeks, fetal tachyarrhy-thmias and hydrothorax were the most common causes and accounted for 14 (38%) of the 36 cases. Thirty-four cases (39%) of hydrops received intrauterine treatment. The survival rates excluding chromosomal abnormalities in the nonimmune cases before and after 24 weeks' gestation were 31% and 48%, respectively, and were not significantly different.[16] Detailed treatment of some of the underlying

conditions is not further discussed here and can be found in numerous publications about fetal therapy.

REFERENCES

1. Warsof S, Nicolaides KH, Rocedk C. Immune and non-immune hydrops. Clin Obstet Gynecol 1986; 29:532–33.
2. Hussey RM, Clarke CA. Death from Rh haemolytic disease in England and Wales in 1988 and 1989. BMJ 1991; 303:445–56.
3. Skoll MA, Sharland GK, Allen LD. Is the ultrasound definition of fluid collections in non-immune hydrops fetalis helpful in defining the underlying cause or predicting outcome? Ultrasound Obstet Gynecol 1991; 1:309–12.
4. James D, Smoleniec J, Weiner CP. Fetal Hydrops. In: James DK, Steer PJ, Weiner CR Gonik B (Eds). High risk pregnancy. Management Options. WB Saunders, 1994; 804.
5. Weiner CP, Umbilical pressure measurement in the evaluation of nonimmune hydrops fetalis. Am J Obstet Gynecol 1993; 168:817–23.
6. Winderbank KP, Bridges NA, Ostman-Smith I, Stevens JE. Hydrops fetalis due to abnormal lymphatics. Arch Dis Child 1987; 62:198–200.
7. Bruner JP, Fleischer AC, Leanty P, Bohem FH. Sonography of nonimmune hydrops fetalis. In: Fleischer AC, Manning FA, Jeanty P, Romero R (Eds). Sonography in obstetrics and gynecology. Principles and Practice. Appleton & Lange 1996; 565.
8. Shenker L, Reed K, Anderson CF Fetal pericardial effusion. Am J Obstet Gynecol 1989; 160:1505.
9. Mallmann R Gembruch U, Mallmann R. Investigation into a possible immunological origin of idiopathic non-immune hydrops fetalis and initial results of prophylactic treatment of subsequent pregnancies. Acta Obstet Gynecol Scand 1991; 70:35.
10. Phelan JP, Smith CV, Broussard P. Amniotic fluid volume assessment using the four-quadrant technique in pregnancy between 36 and 42 weeks gestation. J Reprod Med 1987; 32:540.
11. Hoddick WK, Mahoney BS, Callen PW. Placental thickness. J Ultrasound Med 1985; 4:479.
12. Cosmi E, Mari G, Delle Chiaie L, Detti L, Akiyama M, Murphy J, Stefos T, Ferguson JE 2nd, Hunter D, Hsu CD, Abuhamad A, Bahado-Singh R. Noninvasive diagnosis by Doppler ultrasonography of fetal anemia resulting from parvovirus infection. Am J Obstet Gynecol 2002; 187:1290–93.
13. Machado LE, Osborne NG, Bonilla-Musoles F Twodimensional and three-dimensional ultrasound of fetal anasarca: the glass baby. J Perinat Med 2002; 30:105–10.

14. Abdel-Fattah SA, Soothill PW, Carroll SG, Kyle PM. Noninvasive diagnosis of anemia in hydrops fetalis with the use of middle cerebral artery Doppler velocity. Am J Obstet Gynecol 2001; 185:1411–15.
15. Dembinsk J, Haverkamp F, Maara H, Hansmann M, Eis-Hubinger AM, Bartmann P Neurodevelopmental outcome after intrauterine red cell transfusion for parvovirus B19-induced fetal hydrops. BJOG 2002; 109(11): 1232–34.
16. Sohan K, Carroll SG, De La Fuente S, Soothill P, Kyle P. Analysis of outcome in hydrops fetalis in relation to gestational age at diagnosis, cause and treatment. Acta Obstet Gynecol Scand 2001; 80(8): 726–30.

Chapter 30
Ultrasound in the Management of the Alloimmunized Pregnancy

Daniel W Skupski

Introduction

The diagnosis and treatment of red blood cell (RBC) alloimmunization is arguably the quintessential success story in obstetrics. The patho-physiology is well described, the diagnosis is easily and reliably established, and life-saving treatment for the fetus is available both in *utero* and after delivery with a high degree of success. This has only been possible with the advent of ultrasound imaging. Ultrasound has been used as an adjunct for diagnosis and treatment of RBC alloimmunization for several decades and the applications for ultrasound are continuing to expand. This chapter will outline the current uses of ultrasound in the setting of the alloimmunized pregnancy.

History

The modern era of fetal therapy began with the introduction of amniocentesis for testing of the amniotic fluid for bilirubin levels by spectrophotometry. The degree of change in the optical density at a wavelength of 450 nm (delta OD450) of light during spectrophotometry of amniotic fluid correlates with the level of bilirubin in the fluid due to the preferential absorption of light at this wavelength by bilirubin. High levels of bilirubin in amniotic fluid correlate with the severity of RBC alloimmunization, and have been used to guide therapy. This was first described by Sir Richard Liley in 1961.[1] Treatment for severe RBC alloimmunization was also instituted by Liley, which consisted of either percutaneous intraperitoneal fetal transfusion (IPT) or early delivery.[2] At that time, imaging to guide the needle placement for IPT was in the form of amniography—placement of radio-opaque dye into the amniotic cavity followed by fluoroscopy, using radiation, to outline the fetus and guide needle placement into the fetal abdominal cavity. Once real-time ultrasound was available, it replaced amniography as the imaging study of choice.

Real-time ultrasound allowed the development of percutaneous intravascular blood transfusion to the fetus, which occurred first by fetoscopy, and later by cordocentesis or percutaneous umbilical blood sampling (PUBS), which was an ultrasound guided procedure.[3,4] PUBS allowed more accurate diagnosis of fetal anemia (and the need for intrauterine therapy) by directly testing the fetal hematocrit. The ability of ultrasound to

image the necessary structures has continued to improve, allowing the procedures to be technically easier. As a result of advances in image quality, intrauterine transfusion (IUT) can now be performed in the early second trimester for the rare cases that present with severe fetal anemia very early in gestation.

Diagnosis

The diagnosis of the alloimmunized pregnancy rests upon the identification of antibodies in maternal serum. Ultrasound has traditionally been used after a pregnancy is known to have RBC alloimmunization in order to identify hydrops fetalis (Fig. 30.1). Hydrops fetalis occurs when fetal anemia is very severe, and is probably produced by a combination of pathophysiologic factors including hypoalbuminemia and hepatic damage from extramedullary hematopoiesis.[5] The fetal hematocrit is usually below 15% when hydrops is present. When immune hydrops fetalis is present, IUT is life-saving, and usually needs to be performed within 1–7 days. Hydrops fetalis is present when two or more factors listed in Table 29.1 are present. When only one factor is present, this may be an early sign of hydrops, particularly in the alloimmunized pregnancy.

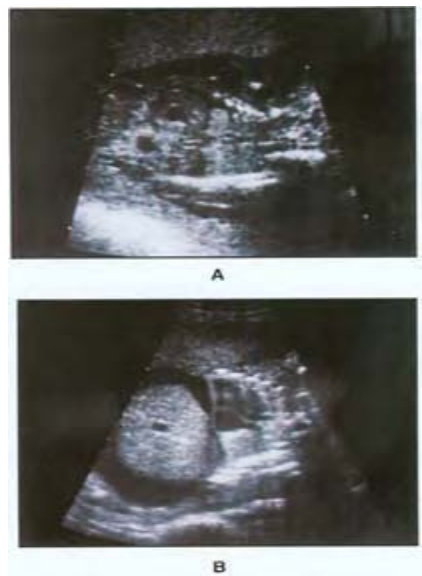

Figure 30.1: Ultrasound image of immune hydrops. A Longitudinal or coronal scan of the fetal thorax (toward the right of the image) and abdomen (toward the left of the image) showing bilateral pleural effusions above the diaphragm. B Longitudinal or coronal

scan of the fetal thorax and abdomen (same orientation) showing ascites

When fetal anemia becomes extremely severe, there can also be changes in fetal behavior. During severe fetal anemia, oxygen delivery to fetal tissues may be restricted, and the fetus may conserve

Table 30.1: Diagnosis of hydrops fetalis*

Polyhydramnios
Thickened placenta (>6 cm)
Pericardial effusion
Ascites
Skin edema
Pleural effusion
*Findings are listed in the order of usual progression of disease

energy by limiting its movements. The biophysical profile can possibly identify the fetus who is decompensating, but may not be reliable for this purpose. The biophysical profile does not dis¬ tinguish between severe acidemia, severe anemia, advanced fetal sepsis and severe central nervous system anomaly, nor does it determine the cause of the fetal decompensation.

Ultrasound has been commonly used to guide the diagnostic procedure of cordocentesis or PUBS (Fig. 30.2). Ultrasound is used first to identify the umbilical cord insertion into the placenta, then a 20 or 22 gauge needle is placed percutaneously through the maternal abdomen into the fetal umbilical vein at the level of the placental cord insertion. The placental cord insertion is chosen because the cord is anchored at this point, allowing the needle to puncture the cord easily.[6]

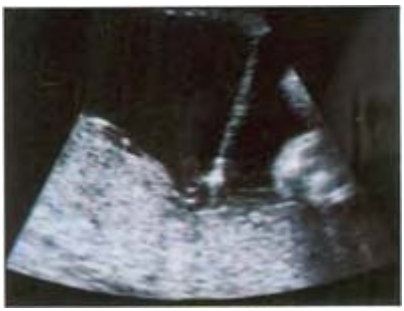

Figure 30.2: Percutaneous umbilical blood sampling or cordocentesis for intrauterine fetal transfusion:

Ultrasound image of a needle being placed in the umbilical vein at the placental cord insertion in a pregnancy with a posterior uterine placental attachment. Fetal parts are seen on the right

Because of their mobility, free loops of umbilical cord have rarely been used as the access point to the umbilical vein. The venous vessels are chosen because they have a larger caliber and usually allow a shorter procedure time. It is also thought that puncture of the arterial vessels is more likely to produce fetal bradycardia.

Non-invasive Diagnosis

A revolution occurred during the 1960's when we became able to diagnose and treat erythroblastosis fetalis. Another revolution is now occurring in fetal medicine with the introduction of non-invasive ultrasound (Doppler) diagnosis of fetal anemia. During the past two decades many fetal vessels and morphologic findings have been evaluated for ultrasound or Doppler findings that would allow a specific diagnosis of severe fetal anemia prior to the development of hydrops fetalis. An excellent review of this experience is available.[7] The optimal time for diagnosis of severe anemia is prior to the development of hydrops fetalis, because the mortality increases once hydrops has occurred.[8] A group of investigators working consistently during the decade of the 1990's has now identified that the fetal middle cerebral artery peak systolic velocity (MCA-PSV) reliably predicts fetal anemia and can be performed by sonographers consistently with technical accuracy.[9,13] Viscosity of blood is inversely correlated with the speed of blood flow in vessels. Assuming the same pumping force is applied, the lower the viscosity of blood in vessels, the higher the velocity. When fetal anemia becomes severe, the viscosity of blood is markedly decreased, and this leads to a markedly increased peak systolic velocity. Because the angle of incidence at which the ultrasound beam intersects the flowing blood in a vessel affects the results of many Doppler measurements, most Doppler indices include angle correction as a feature of the software that performs the calculations. For optimal accuracy—i.e. low intraobserver and interobserver variability, the measurement of peak systolic velocity of blood in a vessel requires that no angle correction be performed.[9] With a zero degree angle of incidence no angle correction is needed, and the measurement of peak systolic velocity is then very accurate.

The specific technique for performing MCA-PSV measurements includes magnifying the image on the screen, using color Doppler to visualize the middle cerebral artery of the fetus and adjusting the transducer on the maternal abdomen so that the angle of incidence of the beam to the artery is zero degrees, i.e. the direction of blood flow in the vessel should be aimed directly at the transducer or directly away from the transducer (Fig. 30.3) Measurements should be taken when there is an absence of marked fetal body and breathing movements. Several measurements should be obtained at each visit. The highest MCA-PSV should be reported and used for management decisions.

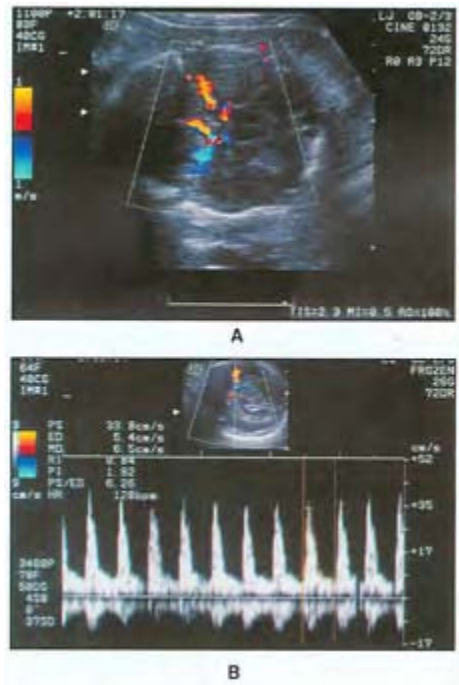

Figure 30.3: Color and pulsed wave Doppler measurement of the peak systolic velocity of the fetal middle cerebral artery. **A** Magnified image with color Doppler ultrasound that is obtained first. **B** Pulsed wave Doppler image obtained subsequently showing the peak systolic velocity (PS) in centimeter per second

The Collaborative Group for Doppler Assessment of the Blood Velocity in Anemic Fetuses has reported the results of a large number of patients with fetuses at risk for anemia who have undergone fetal MCA-PSV testing.[10,12] In their first report, they studied 110 consecutive pregnant women carrying 111 fetuses at risk for fetal anemia due to red blood cell alloimmunization evaluated between 15 and 36 weeks of gestation.[10] They performed MCA-PSV measurements at the time of initial referral and every two weeks thereafter, including immediately prior to cordocentesis. Since hemoglobin concentration in fetuses increases with gestational age, they developed nomograms for hemoglobin concentration from 265 fetuses undergoing cordocentesis for other reasons (suspicion of fetal infection, alloimmune thrombocytopenia, immune thrombocytopenia purpura and chromosomal anomalies) who did not have anemia. The expected values for MCA-PSV were based on nomograms produced previously.[9] The results from cordocentesis showed

that 41 of 111 fetuses at risk for anemia did not have anemia, 35 had mild anemia, 4 had moderate anemia and 31 had severe anemia. Of the 31 fetuses with severe anemia, 12 had hydrops fetalis. The sensitivity of MCA-PSV in detecting moderate or severe anemia was 100% (35/35) and the 95% confidence intervals were 86–100%. Receiver-operator curve characteristics for the MCA-PSV showed that a level of 1.5 multiples of the median (MOM) or greater allowed a sensitivity of 100% while only producing a false-positive rate of 12% (4/35). They concluded that, in fetuses at risk of anemia due to RBC alloimmunization, moderate and severe anemia can be reliably detected by non-invasive Doppler assessment using the middle cerebral artery peak systolic velocity.

In a follow-up prospective multi-center trial with intent-to-treat, MCA-PSV was found to be highly predictive of moderate to severe anemia at delivery, with a sensitivity of 88%, specificity of 87%, positive predictive value of 53% and negative predictive value of 98%.[13] The diagnosis of severe anemia was missed in one fetus, but the final outcome was good. They concluded that MCA-PSV will minimize fetal complications associated with invasive testing in pregnancies affected by RBC alloimmunization, and recommended a Doppler testing interval of seven days.[13]

The same investigators also assessed the ability of MCA-PSV in determining severe anemia longitudinally in 34 fetuses, where measurements were performed serially. They calculated the slope of the MCA-PSV in each fetus over time and determined the average rate of change as a function of gestational age in 3 groups of fetuses: normal, mildly anemic and severely anemic. The estimated average slope increased significantly in the severely anemic fetuses. This demonstrated that the MCA-PSV can by used to follow fetuses at risk for severe anemia over the course of the pregnancy.[12] In addition, MCA-PSV has been evaluated in fetuses at risk for anemia in suspected cases of fetal parvovirus B-19 infection (non-immune hydrops fetalis).[14]

The current status of MCA-PSV as a reliable method for the noninvasive determination of fetal anemia has also been confirmed by meta-analysis.[15] This study showed that the likelihood ratio for a positive test was 8.45 and for a negative test was 0.02. These results are consistent with both clinical and statistical significance.

Management

Ultrasound has progressed from a useful adjunct to an indispensable diagnostic tool in the evaluation and treatment of the alloimmunized pregnancy. A management scheme that is significantly less invasive than previous schemes is now possible. The author's algorithm for management is shown in Figure 30.4.

With the advent of DNA testing for the RhD locus—a highly reliable diagnostic test—we have been able to identify those fetuses who are truly at risk, i.e. separate the fetuses who are antigen

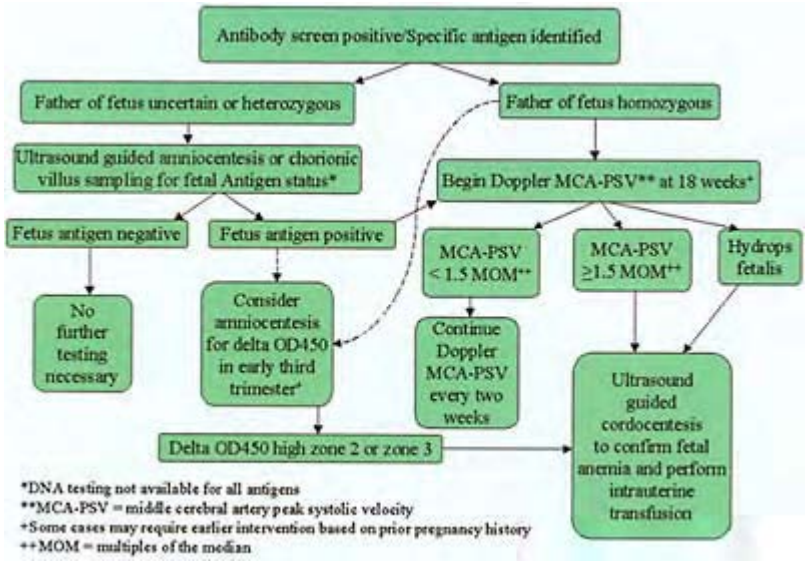

Figure 30.4: Management of the alloimmunized pregnancy

negative from antigen positive.[16] This can occur whenever fetal DNA can be obtained at any time in gestation (first or second trimester is preferable), and is irrespective of the paternal zygosity status. RhD DNA testing by polymerase chain reaction (PCR) is reliable even if paternity is unknown. Fetal tissue can be obtained by amniocentesis or chorionic villus sampling (CVS) in early gestation, and further invasive procedures can be avoided in those fetuses who are antigen negative and are thus not at risk for severe anemia.[16] For fathers who are heterozygous for the offending antigen, this includes 50% of fetuses. Ultrasound is used to guide the procedures of amniocentesis and CVS.

For those fetuses who are antigen positive and there is no prior pregnancy history of severe fetal anemia, the patient can be followed with ultrasound to rule out hydrops fetalis and a MCA-PSV measurement performed every one or two weeks beginning at 18 weeks of gestation. If the MCA-PSV is greater than 1.5 multiples of the median (MOM) for the gestational age at which it is performed, this indicates a severe fetal anemia, and is an indication for cordocentesis and possibly IUT. Similarly, if hydrops fetalis is identified, cordocentesis for IUT would be chosen (Fig. 30.4).

For those fetuses who are antigen positive, management can be tailored based on their prior pregnancy history. Generally, invasive testing in a subsequent pregnancy begins before the time in gestation when the fetus was deemed to be affected in a prior pregnancy. For example, if amniocentesis showed delta OD450 in Liley zone 3 at 28 weeks of gestation (or cordocentesis showed severe fetal anemia) in one pregnancy, then invasive testing would be recommended at 20–26 weeks of gestation in the next pregnancy in previous schemes of management. Using the MCA-PSV, earlier testing would not be required (because all patients would begin testing at 18 weeks of gestation)

unless an earlier pregnancy was affected prior to 18 weeks. An excellent review of the current state of treatment for RBC alloimmunization is available.[17]

Alloimmune Thrombocytopenia

Fetal and neonatal alloimmune thrombocytopenia is the platelet corollary to RBC alloimmunization. The natural history of the disease is similar to that of RBC alloimmunization in that each subsequent pregnancy is generally more severely affected, including antenatal intracranial hemorrhage and fetal demise.[18] Life saving fetal treatment is available in the form of intravenous immune globulin or gamma globulin (IVIG) given on a weekly or twice weekly basis to the mother, which is believed to act at least in part by limiting the placental transfer of anti-platelet IgG antibody that attaches to fetal platelets.[19–21] In alloimmune thrombocytopenia, anti-platelet IgG is thought to coat fetal platelets and enhance the rapid elimination of fetal platelets by the fetal reticuloendothelial system. Diagnosis of the most severely affected cases rests on the ultrasound guided procedure of PUBS. PUBS allows fetal blood to be obtained so that a severely low fetal platelet count can be diagnosed and prenatal treatment can be instituted. A review of the diagnosis and treatment of alloimmune thrombocytopenia is available.[22]

Summary

From its beginnings as a research tool to its current indispensable status as both a diagnostic tool and an adjunct to therapy, ultrasound is a cornerstone in the fight against alloimmunization. Ultrasound has advanced our knowledge of the pathophysiology and the fetal effects of disease, and our ability to manage the alloimmunized pregnancy. The Doppler MCA-PSV measurement is a major advance in our ability to diagnose and thus manage the alloimmunized pregnancy. We should expect additional advances in ultrasound imaging quality and knowledge in the near future.

REFERENCES

1. Liley AW. Liquor amnii analysis in the management of pregnancy complicated by rhesus immunization. Am J Obstet Gynecol 1961; 82:1359–66.
2. Liley AW. Intrauterine transfusion of foetus in haemolytic disease. BMJ 1963; 2:1107–13.
3. Rodeck CH, Kemp JR, Holman CA, Whitmore DN, Karicki J, Austin MA. Direct intravascular fetal blood transfusion by fetoscopy in severe thesus isoimmunization. Lancet 1981; 1(8221):625–27.
4. Rodeck CH, Nicolaides KH, Warsof SL, Fysh WJ, Gamsu HR, Kemp JR. The management of severe rhesus isoimmunization by fetoscopic intravascular transfusions. Am J Obstet Gynecol 1984; 150:769–74.
5. Bowman JM. Hemolytic disease (erythroblastosis fetalis). In: Creasy RK, Resnik R (Eds). Maternal-Fetal Medicine: Principles and Practice. Philadelphia: W.B. Saunders Company, 1994; 719.
6. Grannum PA, Copel JA, Plaxe SC, Scioscia AL, Hobbins JC. In utero exchange transfusion by direct intravascular injection in severe erythroblastosis fetalis. N Engl J Med 1896; 314:1431–34.

7. Whitecar PW, Moise KJ. Sonographic methods to detect fetal anemia in red blood cell alloimmunization. Obstet Gynecol Survey 2000; 55:240–50.
8. Schumacher B, Moise KJ. Fetal transfusion for red blood cell alloimmunization in pregnancy. Obstet Gynecol 1996; 88:137–50.
9. Mari G, Adrignolo A, Abuhamad AZ, Pirhonen J, Jones, DC, Ludomirsky A, Copel JA. Diagnosis of fetal anemia with Doppler ultrasound in the pregnancy complicated by maternal blood group immunization. Ultrasound Obstet Gynecol 1995; 5:400–05.
10. Mari G, Deter RL, Carpenter RL, Rahman F, Zimmerman R, Moise KJ, Dorman KF et al for the Collaborative Group for Doppler Assessment of the Blood Velocity in Anemic Fetuses. Noninvasive diagnosis by Doppler ultrasonography of fetal anemia due to maternal red cell alloimmunization. N Engl J Med 2000; 342:9–14.
11. Mari G, Rahman F, Ologsson P, Ozcan T, Copel JA. Increase of fetal hematocrit decreases the middle cerebral artery peak systolic velocity in pregnancies complicated by rhesus alloimmunization. J Matern Fetal Med 1997; 6:206–08.
12. Detti L, Mari G, Akiyama M, Cosmi E, Moise KJ, Stefor T, Conaway M, Deter R. Longitudinal assessment of the middle cerebral artery peak systolic velocity in healthy fetuses and in fetuses at risk for anemia. Am J Obstet Gynecol 2002; 187:937–39.
13. Zimmerman R, Carpenter RJ, Durig P, Mari G. Longitudinal measurement of peak systolic velocity in the fetal middle cerebral artery for monitoring pregnancies complicated by red cell alloimmunisation: a prospective multicentre trial with intention-to-treat. BJOG 2002; 109:746–52.
14. Cosmi E, Mari G, Delle Chiaie L, Detti L, Akiyama M, Murphy J, Stefos T, Ferguson JE 2nd, Hunter D, Hsu CD, Abuhamad A, Bahado-Singh R. Noninvasive diagnosis by Doppler ultrasonography of fetal anemia resulting from parvovirus infection. Am J Obstet Gynecol 2002; 187:1290–93.
15. Divakaran TG, Waugh J, Clark TJ, Khan KS, Whittle MJ, Kilby MD. Noninvasive techniques to detect fetal anemia due to red blood cell alloimmunization: a systematic review. Obstet Gynecol 2001; 98:509–17.
16. Bennett PR, Le Van Kim C, Colin Y, Warwick RM, Cherif-Zahar B, Fisk NM, Cartron JP Prenatal determination of fetal RhD type by DNA amplification. N Engl J Med 1993; 329:607–10.
17. Moise KJ. Management of rhesus alloimmunization in pregnancy. Obstet Gynecol 2002; 100:600–11.
18. Bussel JB, Zabusky MR, Berkowitz RL, McFarland JG. Fetal alloimmune thrombocytopenia. N Engl J Med 1997; 337:22–26.
19. Lynch L, Bussel JB, McFarland JG, Chitkara U, Berkowitz RL. Antenatal treatment of alloimmune thrombocytopenia. Obstet Gynecol 1992; 80:67–71.
20. Bussel JB, Berkowitz RL, Lynch L, Lesser ML, Paidas MJ, Huang CL, McFarland JG. Antenatal management of alloimmune thrombocytopenia with intravenous gamma-globulin: a randomized trial of the addition of low-dose steroid to intravenous gamma-globulin. Am J Obstet Gynecol 1996; 174:1414–23.
21. Urbaniak SJ, Duncan JI, Armstrong-Fisher SS, Abramovich DR, Page KR. Transfer of anti-D antibodies across the isolated perfused human placental lobule and inhibition by high-dose intravenous immunoglobulin: a possible mechanism of action. Br J Haematol 1997; 96:186–93.
22. Skupski DW, Bussel JB. Alloimmune thrombocytopenia. Clin Obstet Gynecol 1999; 42:335–48.

Chapter 31
Post-termination Fetopathology

Tamás Marion, Zoltán Bán, Zoltán Papp

INTRODUCTION

Fetopathology is mainly a postmortem speciality concerned with causes and mechanisms of reproductive loss. Increasing interest in this field has come when the numbers of deaths in the perinatal have decreased to 10/1000 births in developed countries. In late first and early second trimester, diagnosis of fetal anomaly by ultrasound became a major factor leading to termination. Even in centres with high rate of accurate prenatal ultrasound, a high percentage of fetuses with correctly diagnosed anomalies have additional defects that were not recognized by ultrasound. At the post-termination autopsy the fetopathologist must concentrate on small, even minute anatomic details to find these additional defects to refine the pre-termination diagnosis. Microscopic sections should be made of several organs. The detection of clinically unsuspected malformation and details of dysmorphic features is essential to the correct estimation of the risk of recurrence, so that the appropriate plan for surveillance of subsequent pregnancies can be instituted. Improved management of other similar cases as a result of knowledge gained in the one case will be to the benefit also of other parents in the future. Discussion of postmortem findings at regular fetal pathology meetings is a further means of providing valuable training of medical personnel. In these ways fetopathology serves to promote the quality of individual, family and public health.

The goal of this chapter is to create a good survey of the most significant fetal syndromes. The diagnostic potential of prenatal ultrasound scan has developed enormously in the past decades but it still has its limits, which means that frequently it is impossible to give a precise diagnosis, but our target is to estimate the prognosis of the disease. The second aim of the screening is to indicate further diagnostic procedures such as molecular genetic investigations and/or fetal karyotyping. Recently the prenatal diagnostic procedure requires teamwork, demands involvement of other specialities, the clinical geneticists, pediatric surgeons and specialists in rehabilitation.

The syndrome consists of three or more symptoms. Therefore, developmental abnormality associated with syndrome is characterised by complex and specific features. Usually a syndrome is the result of a single cause and the symptoms are primarily (direct) consequence of the original cause. The “single cause” can be a single gene mutation, a chromosome abnormality, or a teratogene effect. The features of the syndrome are often specific and an experienced sonographist or a skilled pathologist who is good at dysmorphology can determine the etiology.

The sequence has a complex appearance too, but the abnormalities are secondary to a primary cause that results in a dysmophic sequel. A simple example to illustrate the syndrome and sequence. Potter syndrome as a diagnosis is reserved for the kidney agenesis and consequent phenotypic signs. All the other disorders determined by oligoanhydramnios are summarized under the term Potter sequence, when the common cause of the features are secondary to the reduced space in the uterus. In Potter sequence

the lack of amniotic fluid not primary but secondary. Polycystic kidney, multicystic kidney, urethra obstruction sequence, or premature rupture of the membranes (PROM) can stay behind it.

Syndromes develop with time. Some of them produce diagnostic hallmarks early in the first trimester while others show just very mild or hardly any alterations and the ultrasonographic alterations become diagnostic only later. The constituents of individual syndromes can vary, as the penetrance of the syndrome is different from individual to individual.

NEURAL TUBE DEFECT (NTD)

The neuropore closes on the 26th day after conception. The closure of the neural tube is a multicentric procedure.[1] Depending on the site of the defective closure the result is anencephaly or spina bifida or combined in craniorachischisis. The prevalence of NTD is approximately 0.1%. Because of the periconceptional folate substitution a decreasing trend was observed in the number of neural tube defects. Folic acid has no preventive effect after the closure of the neuropore—after the 5–6th post-menstruation week. The etiology of NTD is multifactorial. However, recently a thermolabile mutation of the methylene tetrahydrofolate reductase gene has been associated with NTD. It

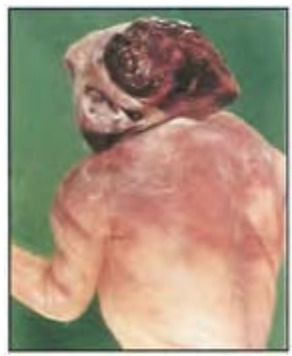

Figure 31.1: Posterolateral view of anencephaly

may be that NTD is partly related to this mutation possibly in occipital, cervico-lumbar localization.[2] Occasionally anencephaly or spina bifida is part of the malformation spectrum, observed in common trisomies (trisomy 13 and 18). Although, NTD is typically solitaire malformation, in rare instances NTD is associated to a multiplex malformation syndrome.

Anencephaly: Initially the missing cranial vault results in exencephaly. The uncovered brain floats in the amniotic fluid. Later as a result of unknown causes (most obviously mechanical trauma) the neural tissue disappears and a blood vessel rich loose connective tissue replaces it, the so called area cerebrovasculosa. In this final stage the head is flat,

and resembles a “frog head”. The eyes and the tongue are relatively large. The most important associated alteration is the hypoplasia of the adrenal glands. If the NTD affects the entire length of the neural tube, it results in a so-called craniorachischisis (Figs 31.1 to 31.5).

Spina bifida: Missing closure of the neural tube most frequently in the lumbo-sacral region. A child born with spina bifida has often devastating clinical consequences. *In utero* often ventriculomegaly is the first sign, later “banana sign” or “lemon shaped head” might be a clue to search for missing closure of the lower end of the vertebral canal. Another characteristic is a type II Arnold-Chiari malformation, which is a herniation and slide of

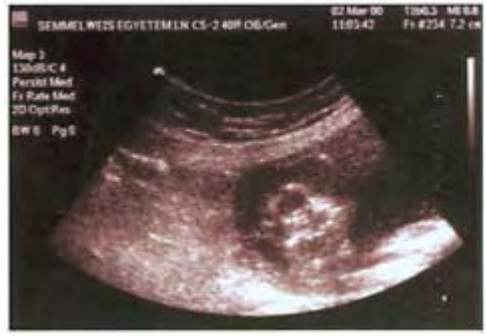

Figure 31.2: Ultrasound image of anencephaly

Figure 31.3: Anterior view of a fetus with exencephaly

Figure 31.4: Frontal section of an exencephalis fetal head

the pons and medulla though the foramen magnum, resulting in a Z shape of the area. Sometimes the only ultrasound sign of a NTD is a widening of the lumbar vertebral canal. In some cases it is quite difficult to investigate the hydrocephalus and different other etiologies have to be born in mind such as primary hydrocephaly, especially with X-linked inheritance. In X-linked hydrocephalus flexed adducted thumbs should be searched (Figs 31.6 and 31.7).

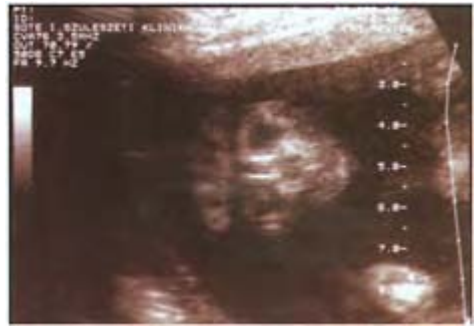

Figure 31.5: Ultrasound Image of exencephaly

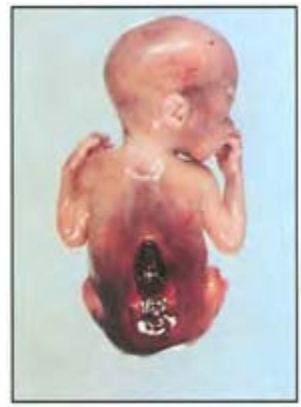

Figure 31.6: Mid-trimester fetus with extensive thoracolumbar spina bifida

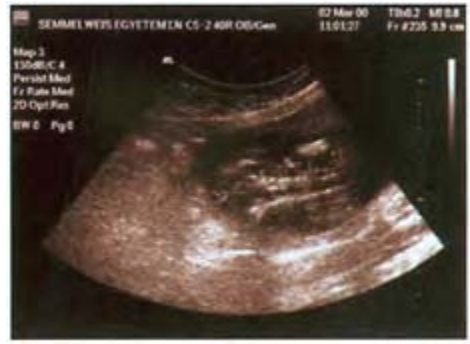

Figure 31.7: Ultrasound image of lumbar spina bifida

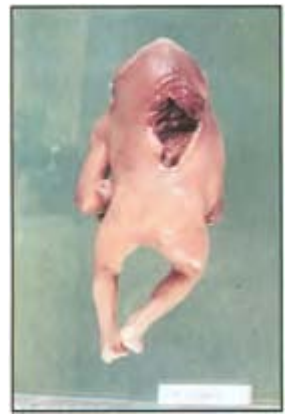

Figure 31.8: Iniencephaly, posterior view with open cervicothoracic defect

Iniencephaly: It is a peculiar form of cervical neural tube defect. The cervical, cervicothoracic vertebrae are disorganized and several of them are fused. Brain tissue is herniated through an enlarged foramen magnum. A severe lordosis of the vertebral column results in the characteristic "star seeking" position of the head, short thorax, trunk and a result of these, lung hypoplasia.[3]

There are two distinctive types of spina bifida. The open type leaves the vertebral canal open, and the spinal cord can be seen on the bottom of the lesion. Spina bifida tecta means that the vertebral canal is covered to some extent. Frequently shows a meningomyelocele, a bulk of the affected area. In sacral localisation it is a differential diagnosis of a sacral teratoma (Figs 31.8 and 31.9).

Meckel syndrome is a specific condition. It is inherited in an autosomal recessive trait. Three genetic loci have been identified so far on different chromosomes: 17q22–23, 11q and 8q. Phenotypically it constitutes of posterior (occipital) encephalocele, polydactyly (typically post-axial), cystic kidneys, hepatic cysts and dysplastic portal areas.[4] Occasionally bowing of the lower extremities is also present. The expression of the features is variable (Fig. 31.10).[5]

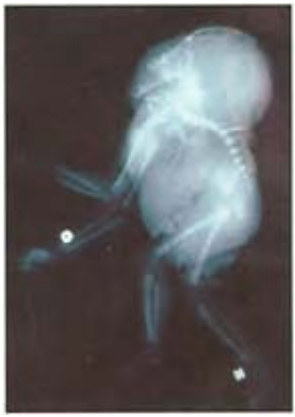

Figure 31.9: Iniencephaly—lateral X-ray

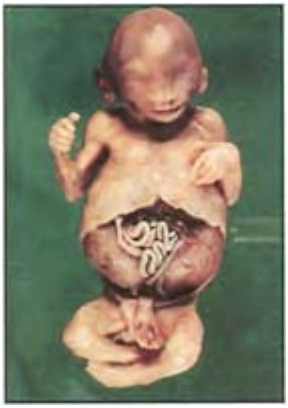

Figure 31.10: Multicystic kidneys in Meckel's syndrome

COMMON CHROMOSOME ABNORMALITIES

Trisomy 13 results in Patau syndrome. This syndrome has a great variety of malformations. The head is small, microcephaly, and different brain anomalies can be seen. The most frequent is holoprosencephaly (HPE). In HPE the two hemispheres are not divided, the cortex is continual between the two brain halves and so are the lateral ventricles resulting in a single sickle shaped ventricle. The missing midline signal in early embryonal stage is the cause of HPE. Facial anomalies are commonly associated with HPE and they include: low set ears, hypotelorism or cyclopia (single, midline eye), cleft of the lip or palate, dysmorphism of the nose, possibility of a proboscis (midline protrusion of the face replacing the nose) and microphthalmia.

There are several other malformations typical for trisomy 13: post axial polydactyly, great variety of congenital heart diseases (ventricular septal defect, truncus arteriosus, transposition of the great arteries, pulmonary or aorta stenosis, double outlet right ventricle), kidney diseases (horseshoe kidney, cystic dysplasia of the kidney, pelvic dilatation), and omphalocele. Reduced fetal size of the trisomic conceptuses is common and in growth-retarded fetuses (Fig. 31.11).

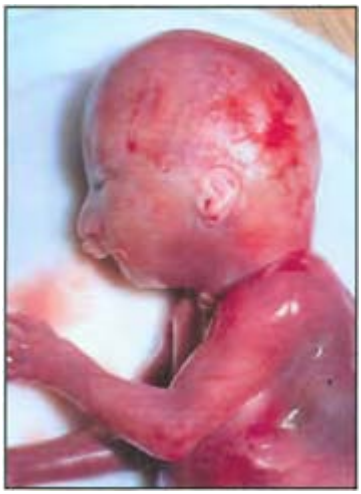

Figure 31.11: Trisomy 13: profile showing short, thick neck, high cranial vault, deep-set eyes, cleft lip with prominent premaxilla, moderate micrognathia

While investigating a HPE case several other syndromes than trisomy 13 has to be excluded, which are less common:[6]

- There are several familial HPE's inherited with different traits. In these cases the HPE is isolated and the only associated sign is a possible consequent facial dysmorphism or clefts.
- Pseudotrisomy 13 is characterized by malformations seen in trisomy 13 but the patient has a normal karyotype.[7] Autosomal recessive inheritance and onset as a new mutation have been described.

The appearance of **trisomy 18,** Edwards syndrome is characterized by low set, posteriorly rotated ears, prominent occiput, and microcephaly. The heart is almost always affected, the majority of the cases has a subaortic (membranous) ventricular defect, tetralogy of Fallot, or transposition of the great arteries. Single umbilical artery is common. Omphalocele, oesophagus atresia, horseshoe kidney, cystic, hypoplastic kidneys, hydronephrosis can occur. The central nervous system can present meningocele, anencephaly or even holoprosencephaly, however it is much less frequent than in trisomy 13. Other features are postaxial polydactyly, other limb abnormalities, facial clefts (Fig. 31.12).

The malformations in **trisomy 21,** Down syndrome appear to be less severe but carries specific characteristics. A thickened nuchal fold

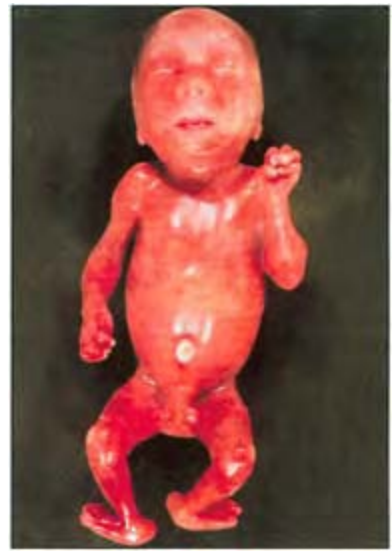

Figure 31.12: Trisomy 18: microcephaly with distal limb defects

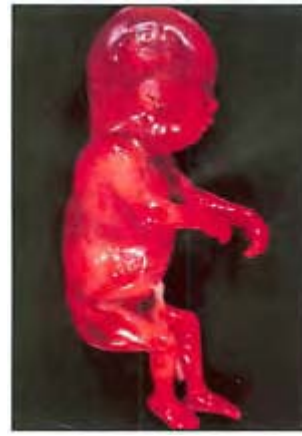

Figure 31.13: Trisomy 21: nuchal edema, abnormal ear, characteristic facial profile

is observable during the first trimester of pregnancy. In approximately half of the cases congenital heart disease is present, within this, the vast majority of the cases has atrioventricular septal defect (the vitium affects the inlet proportion of the ventricular septum, usually with a single atrioventricular orifice). The other ultrasonographically

recognizable alteration is the “double bubble”—which is consequence of the stenotic or atretic duodenum. Fetus with trisomy 21 are often growth retarded. Several other malformation can occur in Down syndrome, but these are rare (Fig. 31.13).

The main feature of **monosomy X** (Turner syndrome, 45,X0) is a generalized edema with female phenotype. The fetus is usually growth retarded and dies *in utero*. The edema on the back often manifests in huge cystic hygroma, which can be septated. The following malformations can occur: Horseshoe kidney, agenesis of the kidney, cystic kidneys, low set ears, aortic stenosis or hypoplastic aortic arch (Fig. 31.14).

Triploidy (69,XXX or 69,XXY) is characterized by a severe, otherwise unexplained growth retardation, with a striking discordance between the head and the body size. The gravida often develops oligohydramnios and midtrimester of preeclampsia. These fetuses are not viable and

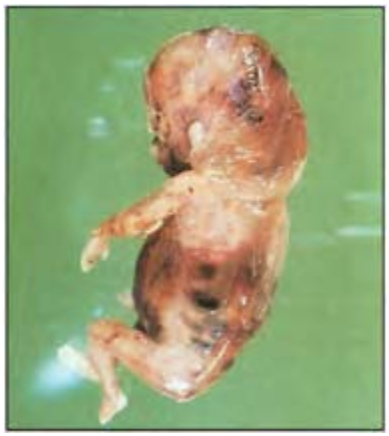

Figure 31.14: X-monosomy with typical hygroma

most of them die *in utero*. The placenta can present partial hydatidiform changes. About two-third of the cases have congenital heart disease. The features of the fetus include syndactily of the 3rd and 4th fingers. In the central nervous system hydrocephalus, holoprosencephaly, spina bifida and meningomyelocele can occur. The kidneys can be hypoplastic, cystic or hydronephrotic(Fig. 31.15.)[8]

DiGeorge syndrome (CATCH-22) is caused by the microdeletion of the 22q11.2 region that can be diagnosed with fluorescent *in situ* hybridization (Fig. 31.16). It presents with micrognathia, hypertelorism, low set ears and conotruncal

Figure 31.15: 69, XXX karyotype from cultured amniotic fluid cells

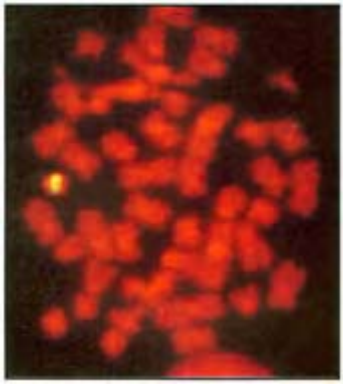

Figure 31.16: Deletion of the CATCH22 region in DiGeorge syndrome can be visualized by FISH (fluorescent signal on only one copy of the two chromosome 22)

cardiac abnormalities. Other phenotypic signs are not recognizable on prenatal screening. DiGeorge syndrome is often inherited in an autosomal dominant way and the affected parent carries mild features (Fig. 31.16).

OLIGOHYDRAMNIOS AND RELATED MALFORMATIONS

The intrauterine assessment of these cases is challenging, because the oligoanhydramnios makes the orientation sometimes extremely difficult. The common in anhydramnios is the external appearance, which is described with the term Potter phenotype. Postnatally the

following hallmarks can be identified: flat face, low set ears, flexion contractures of the extremities, often skin webs in the axilla and elbow. The lungs are hypoplastic as a consequence of the reduced fetal breathing movements. The micrognathia with short tongue, and cleft of the soft palate is called Pierre Robin sequence. The main recognizable disorder according the fetal phenotype is the lack of amniotic fluid, the reduced space for fetal movements. It is crucial to investigate the causes that have led to the anhydramnios.

Agenesis of the kidneys is most often sporadic. The adrenal glands are discoid shape, as the kidneys are missing. Together with the Potter phenotype it is the classic Potter syndrome.

Cystic kidneys are white on the scan and often enlarged. Oligohydramnios does not occur in cases of autosomal dominant cystic kidney, whereas it is frequent in cases of autosomal recessive one. It is impossible to differentiate between the **diffuse cystic dysplastic kidney** and **autosomal recessive cystic kidney** on the scan, as both appear as large white reniform masses with anhydramnios (Fig. 31.17). The diffuse cystic dysplastic kidney is frequently part of a malformation syndrome and is inherited according to the determinant malformation. The **multicystic kidney dysplasia** has to be distinguished too (Fig. 31.18.) This hyperechogenic kidney is not reniform, but has the appearance of a branch of grapes that consists of different sized cysts. On the end of this disease spectrum stays the **aplastic dysplastic kidney,** which is small, reniform and has no urine producing parenchyma. Obstruction in the lower urinary tract affects mainly male fetuses. The anatomic basis is either urethra atresia or posterior urethral valve. The result is oligohydramnios, megaurocystis, ureter and pyelon dilatation. The parenchyma of the kidneys is also altered, histologically a so-called **obstructive kidney dysplasia** is seen. After a

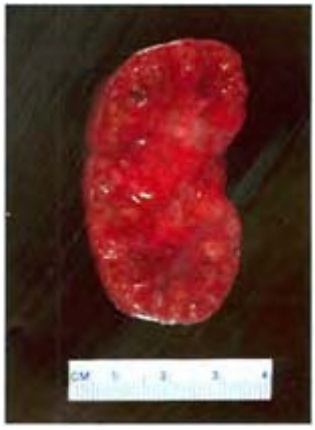

Figure 31.17: Infantile type polycystic kidney: small cysts, no connective tissue proliferation

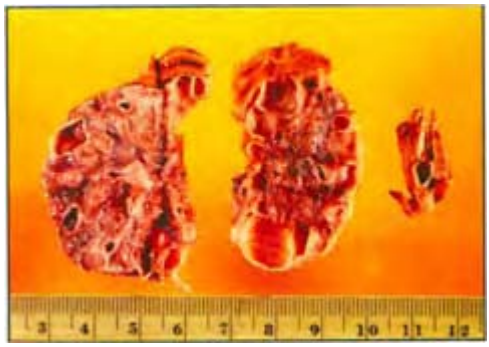

Figure 31.18: Multicystic dysplastic kidneys: loss of normal embryonic lobulation, cysts of varying diameter

certain period of time the kidney changes are irreversible and drainage of the bladder does not cure the fetus. It is important to differentiate the huge bladder from other cysts (such as duplication cysts of the gastrointestinal system or a cyst of the ovary). In rare cases ACE inhibitor non-steroid anti-inflammatory drug (NSAID) use of the mother can lead to fetal renal failure and **tubular dysgenesis.** The possibility of a **premature rupture of the membranes** in all oligohydramnios cases has to be investigated and excluded with clinical investigations.

In **Caudal regression syndrome** the lower body half bears different developmental abnormalities as a consequence of a disruption. It constitutes of kidney agenesis, abnormalities of the anogenital region and involvement of the lower limbs. The legs are mostly joined (siernomelia) and different extent of limb reduction is also present. It is almost always combined with single umbilical artery (Fig. 31.19).

Association is a looser term, which accounts for a range of malformations that occur more frequently together but the cause is not yet known. Associations are signed by acronyms that refer to the organs involved. The individual components associate more or less often than just by chance. *VATER association:* Vertebral defect (e.g. spina bifida), Anal atresia, TE-Tracheoesophageal fistula/Esophagus atresia, R-Radial or Renal abnormality.[9] The VATER association became expanded to the acronym VACTERL.[10] VACTERL is an acronym for vertebral anomalies, anal atresia, cardiac malformations, tracheoesophageal fistula, renal anomalies (including urethral atresia with hydronephrosis), and limb anomalies. The MURCS association consists of Müllerian duct aplasia, Renal aplasia, and Cervicothoracic Somite dysplasia.[11] MURCS shows overlapping with VACTERL. The CHARGE association is the combination of the following abnormalities: **C**hoanal atresia, **C**oloboma of the eye; **C**ongenital **H**eart **D**isease; **A**tresia of the choana; Retardation of mental and somatic development; Genital anomaly (microphallus); Ear abnormalities. Tracheoesophageal fistula, **M**icrognathia, **C**left lip or palate; **O**mphalocele; **H**oloprosencephaly could be associated. CHARGE shows overlap with VACTERL too. Schisis association refers to the association of neural tube defect, cleft lip and palate, omphalocele, cardiac defect, limb abnormality, and diaphragmatic hernia.[12] The significance of the associations is that the scanner has to be

aware of the various association possibilities and has to search for the different constituents in the fetus.

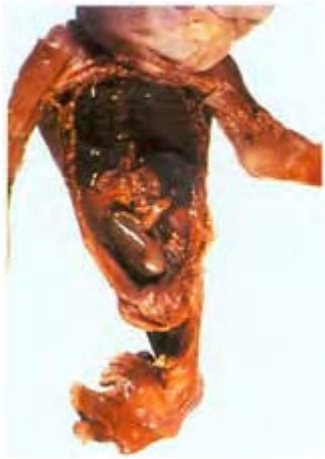

Figure 31.19: Caudal regression syndrome (siernomelia sequence) with bilateral renal agenesis

ADAM complex is an acronym for Amniotic Deformities, Adhesions and Mutilations. In contrast to the associations it consists of a range of abnormalities, that are not related, often affect distant parts of the body. Etiology of the ADAM complex is not known. An early rupture of the amnion is thought to be a keyfactor in its development. The bodystalk defect (called limb bodywall complex too) belongs to this group. The fetus is attached to the placenta with different parts of its body and has a very short or no umbilical cord. The body wall is open, the vertebral column is scoliotic. It appears to be a bodystalk modeling defect and the role of homeobox genes cannot be excluded.[13]

FETAL INFECTIONS: TORCH

TORCH is an acronym for congenital Toxoplasmosis, Other (syphilis and virus infections), Rubella, CMV and Herpes simplex virus. These organisms can cause severe disruption of the fetal development.

Congenital toxoplasmosis results in progressive hydrocephalus or microcephalus, cerebral calcifications, microphthalmia. The placenta is frequently edematous and enlarged (Fig. 31.20).

Congenital rubella infection can stay behind microcephaly, microphthalmia and congenital heart defect.

CMV infection causes microcephaly with calcifications, hydrocephaly, and hyperechogen liver. The placenta enlarged and calcified.

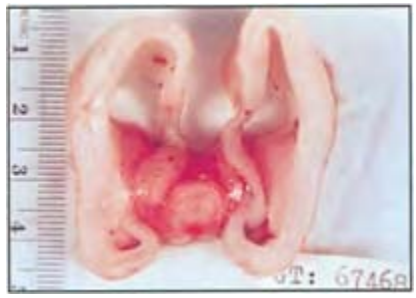

Figure 31.20: Intrauterine toxoplasmosis with internal hydrocephalus

REFERENCES

1. Van Allen MI, Kalousek DK, Chernoff GF, Juriloff D, Harris M, McGillivray BC et al. Evidence for multisite closure of the neural tube in humans. Am J Med Genet 1993; 47(5):723–43.
2. Wenstrom KD, Johanning GL, Owen J, Johnston KE, Acton S, Oliver S et al. Amniotic fluid homocysteine levels, 5,10-methylenetetrahydrafolate reductase genotypes, and neural tube closure sites. Am J Med Genet 2000; 90(1):6–11.
3. Marton T, Tanko A, Mezei G, Papp Z. Diagnosis of an unusual form of iniencephaly in the first trimester of pregnancy. Ultrasound Obstet Gynecol 2001; 18(5):549–51.
4. Fraser FC, Lytwyn A. Spectrum of anomalies in the Meckel syndrome, or: “Maybe there is a malformation syndrome with at least one constant anomaly”. Am J Med Genet 1981; 9(1):67–73.
5. Seller MJ. Phenotypic variation in Meckel syndrome. Clin Genet 1981; 20(1):74–77.
6. Munke M. Clinical, cytogenetic, and molecular approaches to the genetic heterogeneity of holoprosencephaly. Am J Med Genet 1989; 34(2):237–45.
7. Cohen MM, Jr., Gorlin RJ. Pseudo-trisomy 13 syndrome. Am J Med Genet 1991; 39(3):332–35.
8. Ban Z, Nagy B, Papp CS, Toth-Pal E, Papp Z. Rapid diagnosis of triploidy of maternal origin using fluorescent-PCR and DNA fragment analysis in the third trimester of pregnancy. Prenat Diagn 2002; 22:984–87.
9. Quan L, Smith DW. The VATER association. Vertebral defects, Anal atresia, T-E fistula with esophageal atresia, Radial and Renal dysplasia: a spectrum of associated defects. J Pediatr 1973; 82(1):104–07.
10. Khoury MJ, Cordero JF, Greenberg F, James LM, Erickson JD. A population study of the VACTERL association: evidence for its etiologic heterogeneity. Pediatrics 1983; 71(5):815–20.
11. Duncan PA, Shapiro LR, Stangel JJ, Klein RM, Addonizio JC. The MURCS association: Mullerian duct aplasia, renal aplasia, and cervicothoracic somite dysplasia. J Pediatr 1979; 95(3):399–402.
12. Czeizel A. Schisis-association. Am J Med Genet 1981; 10(1):25–35.

13. Kitamura K, Miura H, Miyagawa-Tomita S, Yanazawa M, Katoh-Fukui Y, Suzuki R et al. Mouse Pitx2 deficiency leads to anomalies of the ventral body wall, heart, extra- and periocular mesoderm and right pulmonary isomerism. Development 1999; 126(24): 5749–58.

Chapter 32
Doppler Sonography in Obstetrics

A Kubilay Ertan, H AlperTanriverdi, Werner Schmidt

One of the main aims of routine antenatal care is to identify the 'at risk' fetus in order to apply clinical interventions which could result in reduced perinatal morbidity and mortality. Doppler sonography in obstetrics is a widely accepted functional method of examining the uterofetoplacental unit.

Doppler ultrasound is a non-invasive technique whereby the movement of blood (usually in a vessel) is studied by detecting the change in frequency of reflected sound. Doppler ultrasound has been used in obstetrics since 1977 to study the fetoplacental (umbilical) circulation,[1] and since the 1980s to study the uteroplacental (uterine) circulation[2] and fetal circulation.[3] Recently, this method became an important tool for qualifying high risk pregnancies.

Information obtained with Doppler sonography helps obstetricians managing patients in situations like pregnancies complicated by intrauterine growth restriction (IUGR), Rhesus alloimmunization, multiple pregnancies, and anamnestic risk factors. Examination of the uteroplacental and fetomaternal circulation by Doppler sonography in the early second trimester helps predicting pregnancy complications like preeclampsia, IUGR and perinatal death.[4–12]

This chapter aims to introduce Doppler sonographic examinations in modern obstetrics. Doppler blood flow velocity waveforms (FVWs) of the fetal side (umbilical artery, aorta descendens, middle cerebral artery) and maternal side (uterine arteries) are discussed and nomograms for routine obstetric practice are presented.

The Safety of Doppler Ultrasound in Obstetrics

The safety of Doppler ultrasound in Obstetrics remains a concern. The data available to date suggests that diagnostic ultrasound has no adverse effects on embryogenesis or fetal growth. In addition, ultrasonographic scanning has no long term effects on cognitive function or change visual or hearing functions. However, although B and M mode scans are safe during pregnancy, color, power and pulsed Doppler procedures should be performed with caution due to possible thermal effects. Lastly, a new method, the three dimensional technique, was introduced. While there are no studies regarding the safety of this novel topic, the short acquisition time and the post-processing analysis may decrease exposure and thus unknown effects of the ultrasound waves on fetal development.[13]

In particular the use of pulsed Doppler involves the use of higher intensities compared to diagnostic ultrasound, and hence may cause significant tissue heating and thermal effects. However these thermal effects depend on the presence of a tissue/ air interface and may therefore not be clinically significant in obstetric ultrasound examinations.[14] Clearly, while there is continuing concern regarding the safety of Doppler ultrasound, it should only be used in cases of proven value.

Dependency of Doppler Flow Velocity Waveforms on Gestational Age

The amount of perfusion in trophoblastic tissue is related to gestational age. For this reason, in interpreting the Doppler sonographic findings, gestational age should be taken into account as well. That is, nomograms for Doppler sonographic measurements should be standardized according to gestational age. In general, the accepted time for starting Doppler sonographic examinations is the beginning of the second trimester. This is the right time that allows modifications in antenatal care in a high risk pregnancy. For specific conditions, earlier timing of measurements may be considered.[15]

The main objective in constituting fetomaternal Doppler sonographic nomograms is to improve perinatal outcome in high risk pregnancies. Curves presented below depict normal fetal and maternal Doppler sonographic values, and can be used in routine practice.

Indices

Blood flow velocity in the fetal circulating system depends on the type of vessel: The arteries always have a pulsatile pattern, whereas veins have either a pulsatile or continuous pattern.

Analysis of Doppler sonographic FVWs quantitatively, is more difficult than analysing qualitatively. Qualitative analysis also overcomes erroneous measurements in small vessels. There are plenty of indices for qualitative analysis.

Following are the most frequently used indices:

- Systolic/Diastolic ratio (S/D ratio, Stuart 1980)
- Resistance index (RI, Pourcelot 1974)
- Pulsatility index (PI, Gosling and King 1977)

In analyzing sonographic results and calculating indices, following characters are used:

S=Temporal peak of maximum frequency
D=End-diastolic maximum frequency
C=Temporal average of maximum frequency, F_{mean}
I=Instantaneous spatial average frequency
E=Temporal average of spatial average frequency.
Calculations of formulae are as follows (Fig. 32.1):
S/D ratio=S/D

$$RI=(S-D)/S$$

$$PI=(S-D)/C$$

While calculating PI values, in some sonographic devices, E values are used instead of C values. As a result PI values increase slightly.

The above presented indices overcome also a very serious problem involved with the angle

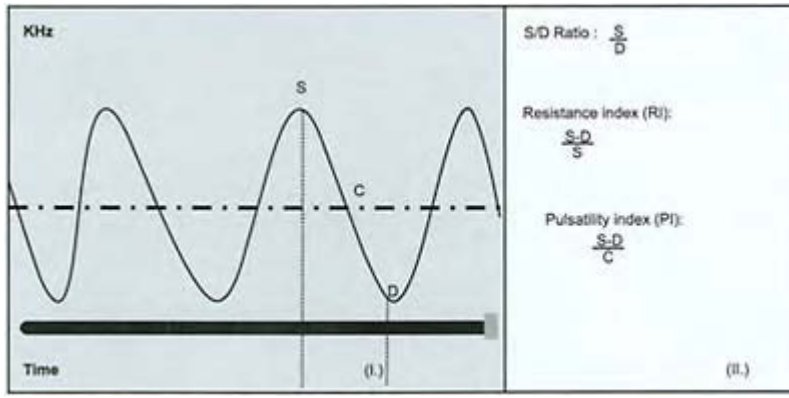

Figure 32.1: Scheme of the Doppler curve (I). S: systolic, D: diastolic, C: Temporal average of maximum frequency. Calculation of formulae of the main Doppler sonographic indices (II)

between the ultrasound beam and the direction of blood flow (insonation angle). These indices are relatively angle independent and are therefore easily applied in clinical practice.

In practice, none of the indices is superior to the other[16–18] and any index may be used. Although S/D ratio is easily calculated, RI is the easiest to interpret. RI values approach to zero if the resistance decreases and approach to one if resistance increases. If end-diastolic flow is absent, PI is the only index making evaluation of blood flow possible, because in this situation S/D will equal to infinite and RI to one. The PI is more complex because it requires the calculation of the mean velocity, but modern Doppler sonographic devices provide those values in real time.

Doppler sonographic nomograms are used for differentiation of normal and abnormal blood FVWs, which helps to determine high risk pregnancies. By taking threshold values of pathologic pregnancies into consideration, nomograms are capable to differentiate between normal and abnormal. The nomograms are presented for meeting this target.[19] While confronting with these nomograms, it must always kept in mind that the values on these nomograms should not be taken as mathematical equations, and that limitations of sensitivity and specifity exist.

Using Nomograms in Practice

Just like the defense mechanism of peripheral vasoconstriction in an adult in the face of hemorrhagic shock, the "brain sparing" mechanism (Brain sparing effect) becomes active in a fetus with hypoxia or chronic placental insufficiency. As a result of the brain sparing effect, resistance either in the umbilical artery (UA) and fetal descending aorta (FDA) increases. As a consequence Doppler indices related to these vessels increase. The end-diastolic blood flow increases in middle cerebral arteries (MCA) by the same effect. Doppler indices for this vessel decreases consequently.

Some points should be considered while using Doppler sonographic nomograms:

1. Among the measurements performed on the UA and FDA, values between 90–95th percentiles should be considered as borderline and repeat follow-ups should be planned. Values exceeding the 95th percentile are considered abnormal.
2. Doppler values between 5–10th percentiles in MCA should be considered as borderline and repeat follow-ups should be planned. Values below the 5th percentile are considered abnormal.
3. Measurements taken after 24 weeks' gestation from uterin arteries are more valuable. The early diastolic notching, and values exceeding the 95th percentile are considered as abnormal. One point to remember is notching by itself predicts of elevated risk of preeclampsia.

Changes in Doppler sonographic results during the course of pregnancy and complicated pregnancies:

During the course of pregnancy and in some specific pregnancy complications, Doppler sonographic results of fetomaternal vessels display changing values.

Umbilical Artery (UA)

It has been shown in a longitudinal, observational study that Doppler ultrasound of the UA is more helpful than other tests of fetal wellbeing (e.g. heart rate variability and biophysical profile score) in distinguishing between the normal small fetus and the 'sick' small fetus.[20] However its exact role in optimizing management, particularly timing of delivery, remains unclear, and is currently being investigated by many study groups. The optimal timing of delivery in pregnancies complicated by highly pathological Doppler flow findings is still an issue to be resolved. The established approach to resolve this question and to improve the perinatal morbidity and mortality by the use of Doppler examination is being investigated in multicenter clinical trials,[21] e.g. the trial of umbilical and fetal flow in Europe Group (TRUFFLE-Protocol, unpublished data).

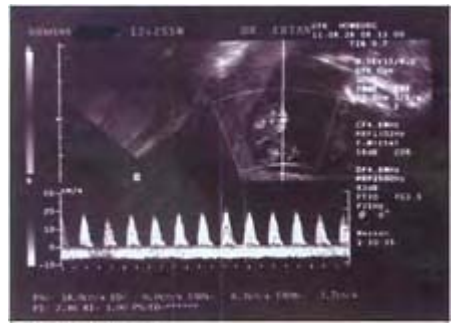

Figure 32.2: Absent end-diastolic flow of the umbilical artery in the first trimester (physiologic) with pulsations of the umbilical vein (physiologic)

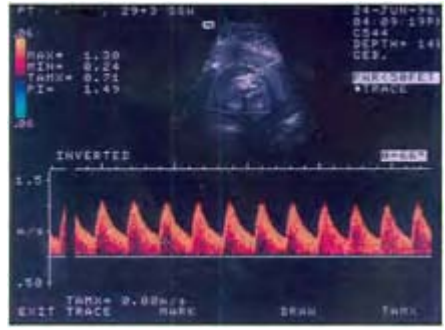

Figure 32.3: Normal flow velocity waveforms of the umbilical artery in the third trimester

Blood flow velocity in the UA increases with the advancing gestation. As a result impedance to blood flow continuously decreases due to increasing arterial blood flow in the systole and diastole. End-diastolic velocity is often absent in the first trimester (Fig. 32.2)[1,2] and the diastolic component increases with advancing gestation (Fig. 32.3).[23] With advancing gestational age end-diastolic flow becomes evident during the whole heart cycle (Fig. 32.3), proven with previous longitudinal studies of Fogarty et al[18] and Hiinecke et al,[24] as with many cross-sectional studies.[23,25]

Trudinger et al[26] explained this phenomenon with the following mechanisms:

- Continuous maturation in placental villi
- Continuous widening of placental vessels cause a continuous decrease in vascular resistance
- Continuous increase in fetal cardiac output

• Continuous changes in the vessel compliance
• Continuous increase in fetal blood pressure.

Especially in the third trimester of pregnancy, depending on the above factors normal values become scattered on nomograms (Fig. 32.7). This scattering is more prominent in the S/D ratio than the PI. Resistance index is not affected by above factors after 28 weeks' gestation (Figs 32.7 to 32.9).

Flow velocity waveforms of the UA are slightly different at the abdominal wall and the placental site, with indices higher at the fetal abdominal wall than the placental insertion.[27] The difference, however, is minimal, and therefore in clinical practice it is not important to obtain the FVWs always at the same level. FVWs must always be obtained during fetal apnea periods because fetal breathing affects the waveforms.

In case of an abnormal test, clinical experience and randomized controlled trials showed significant association with an adverse perinatal outcome.

Intrauterine Growth Restriction

The IUGR fetus is a fetus that does not reach its potential growth. Environmental factors responsible may be due to maternal, uteroplacental and fetal factors (Table 32.1). Many authors have reported on the association between an abnormal UA Doppler FVW and IUGR.

Differentiating the fetus with pathologic growth restriction that is at risk for perinatal complications from the constitutionally small but healthy fetus has been an ongoing challenge in obstetrics. Not all infants whose birth weight is below the 10th percentile have been exposed to a pathologic process in utero; in fact, most small newborns are constitutionally small and healthy. Doppler sonography has become the most important investigation method to differentiate between these fetuses.

Table 32.1: Factors responsible for intrauterine growth restriction

Maternal factors
Cardiorespiratory diseases
Renal disease
Anemia
Drugs (Antineoplastic agents, narcotics)
Smoking
Alcohol abuse
Uteroplacental factors
Impaired Uteroplacental blood flow
Chronic hypertension
Preeclampsia

Gestational diabetes
Collagen vascular disease
Uterine anomalies
Leiomyomatosis
Placental factors
Abruptio placentae
Placenta previa
Placental infarction
Placentitis, vasculitis
Placental cysts, tumors (chorioangioma)
Fetal factors
Infections
Cardiac disease
Chromosomal anomalies

Pathophysiology of abnormal FVWs in placental insufficiency[28] In the presence of placental insufficiency, there is greater placental resistance, which is reflected in a decreased end-diastolic component of the UA FVWs.[29–33] An abnormal UA FVW has a S/D ratio above the normal range. As their placental insufficiency worsens, the end-diastolic velocity decreases (Fig. 32.4), then become absent (Fig. 32.5), and finally it is reversed (Fig. 32.6). Some fetuses have decreased end-diastolic velocity that remains constant with advancing gestation and never become absent or reversed, which may be due to a milder form of placental insufficiency (Fig. 32.4). Pitfalls can be caused due to e.g. fetal breathing (Fig. 32.10).

Abnormal UA Doppler studies, but not normal results were found to be associated with lower arterial and venous pH values, an increased

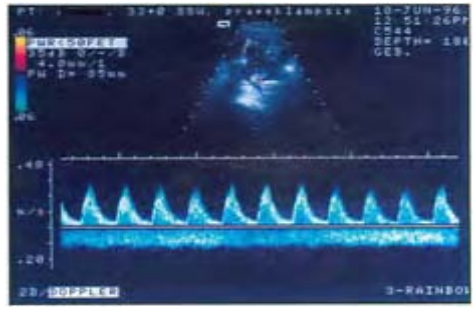

Figure 32.4: Abnormal flow velocity waveforms of the umbilical artery in

the third trimester (high resistance index)

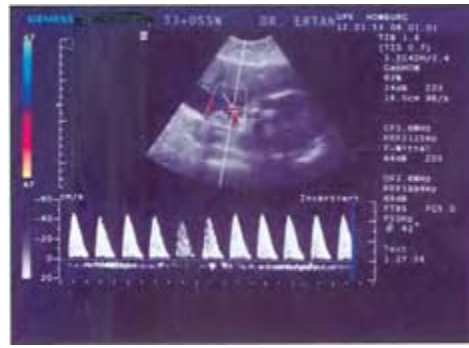

Figure 32.5: Absent end-diastolic flow (AEDF) of the umbilical artery in the third trimester

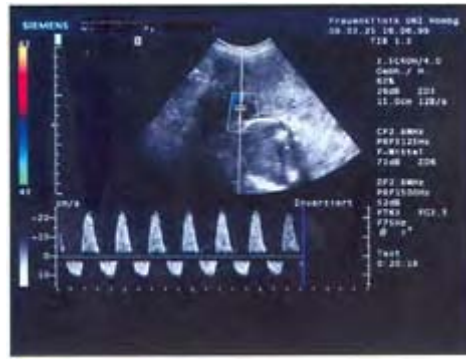

Figure 32.6: Reverse flow (RF) of the umbilical artery

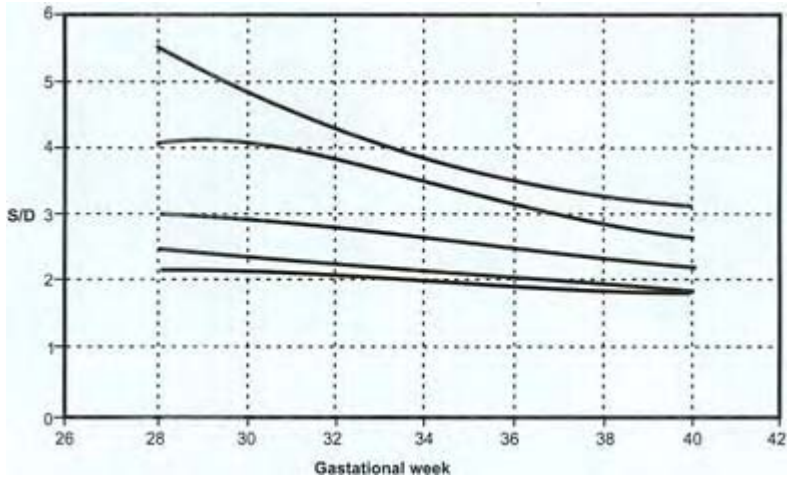

Figure 32.7: Umbilical artery Systolic/Diastolic (S/D) ratio nomogram

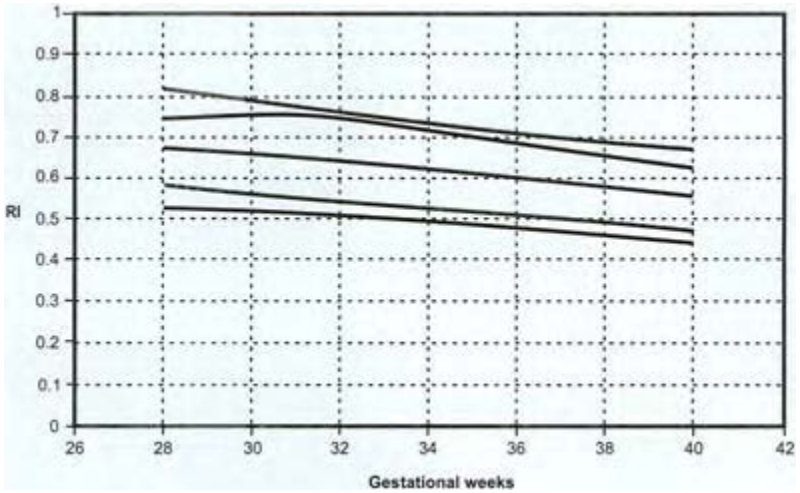

Figure 32.8: Umbilical artery Resistance index (RI) nomogram

likelihood of intrapartum fetal distress, more admissions to the neonatal intensive care unit (NICU), and a higher incidence of respiratory distress in IUGR fetuses.[34] Therefore, intensive antenatal surveillance in fetuses with suspected IUGR if the UA Doppler FVWs are normal was not recommended by the authors. Conflicting data were presented by McCowan et al.[35] They confirmed that abnormal UA Doppler studies are associated with

a poor perinatal outcome in IUGR fetuses but also concluded that the perinatal outcome in small for gestational age fetuses with

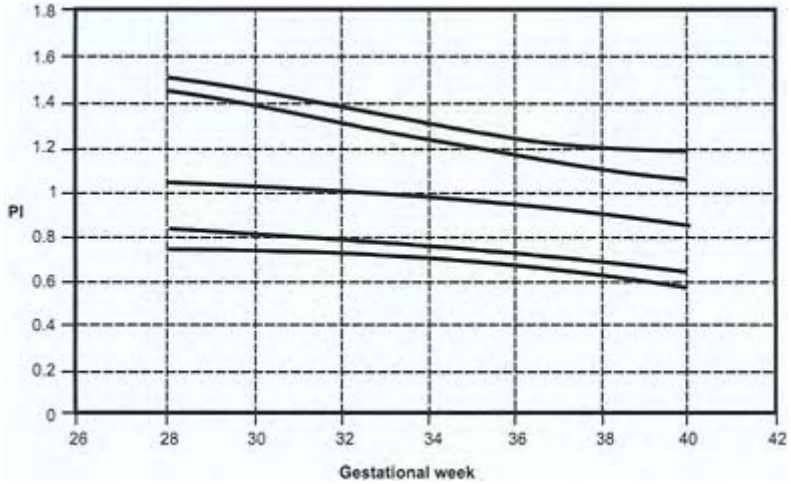

Figure 32.9: Umbilical artery Pulsatility index (PI) nomogram

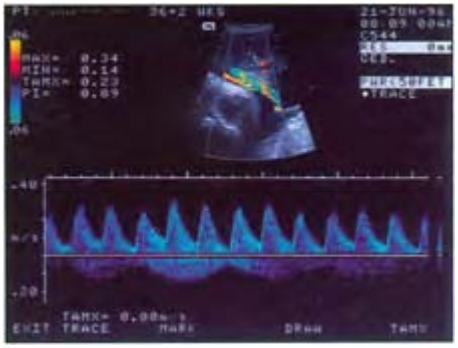

Figure 32.10: Pitfalls in umbilical artery Doppler velocimetry (fetal breathing)

normal UA Doppler studies is not always benign (i.e. low ponderal index, postnatal hypoglycemia, admission to the NICU). Recently, Ertan et al[36] suggested that reversed flow should be seen as a particular clinical entity with higher incidences of perinatal and overall mortality, and severe intrauterine growth restriction compared to absent end-diastolic flow (Figs 32.5 and 32.6).

In our clinical experience, when an IUGR fetus is suspected, the UA, FDA and MCA are the first fetal vessels to be assessed. The ductus venosus (DV), umbilical vein,

inferior vena cava doppler examinations are secondary vessels to be examined, only when an abnormal FVW is detected on the arterial vessels. Adding serial Doppler evaluation of the UA, MCA and DV to IUGR surveillance will enhance the performance of the biophysical score in the detection of fetal compromise and therefore optimizing the timing of intervention.[37]

Chromosomal Abnormalities

It was shown that absent end-diastolic flow in the UA is associated with chromosomal abnormalities like trisomies, triploidies or chromosomal deletions.[38] Setting out from the point that structural anomalies are more frequent in fetuses with chromosomal aberrations, the authors recommended a rapid acquisition of a karyotype in fetuses with congenital anomalies and an absent end-diastolic flow in the UA.[39]

Impact on Perinatal Consequences

Abnormal UA FVWs are associated in IUGR fetuses with one of the following outcomes: early delivery, reduced birth weight, oligohydramnios, NICU admission, and prolonged hospital stay.[28,40] In a meta-analysis it was shown that the use of UA Doppler sonography in pregnancies complicated by IUGR reduces perinatal mortality up to 38% and improves perinatal outcome.[41] A review consisting of 7000 high risk pregnancies[42] found that Doppler ultrasound was associated with a trend toward reduction in perinatal death especially in pregnancies complicated with preeclampsia or IUGR. The Doppler ultrasound use was also associated with fewer inductions of labor and fewer hospital admissions, without reports of adverse perinatal effects. The reviewers concluded that the use of Doppler ultrasound in high risk pregnancies is likely to reduce perinatal mortality.

Neonatal Intraventricular Hemorrhage

Fetal status as well as neonatal complications of prematurity in IUGR both contribute to adverse perinatal outcome and increase the risk for the development of intraventricular hemorrhage (IVH). Data suggest that absent and reversed end-diastolic flow in the UA early in gestation carries a high risk of subsequent neonatal IVH.[43] However, this observation is not independent of other perinatal variables: prematurity and difficult births remain the most important determinants of this complication.

Neuromotoric Outcome

Valcomonico et al[40] evaluated the association of UA Doppler velocimetry with long term neuromotoric outcome in IUGR fetuses with normal (n=17), reduced (n=23) and absent or reversed (n=31) UA end-diastolic flow. The infants who survived the neonatal period were observed for a mean of 18 months. Their postural, sensorial and cognitive functions were evaluated at 3, 6, 9, 12 and 18 months of age. Although, due to small number of cases the results did not reach statistical significance, the incidence of permanent neurological sequelae increased as the UA end-diastolic flow decreased (35% with absent or reversed flow, 12% with reduced flow, and 0% with normal flow). Recently, in

another study[44] twenty three IUGR fetuses with absent or reversed UA end-diastolic flow were matched with fetuses with appropriate growth. All children were followed for 6 years, and intellectual development, neuromotoric development was significantly diminished in fetuses with abnormal FVWs. Only social development was not impaired in fetuses with abnormal UA FVWs. Similar results were previously published by our working group, too.[45,46]

Intrapartum Studies

A review of intrapartum UA Doppler velocimetry for adverse perinatal outcome gave disappointing results.[47] Out of 2700 pregnancies, which were evaluated for the intrapartum use of Doppler velocimetry showed that it is a poor predictor for measures like low Apgar scores, intrapartum fetal heart rate abnormalities, umbilical arterial acidosis, and cesarean section for fetal distress.

Umbilical Artery Doppler Ultrasound in Unselected Patients

Theoretically, the use of routine UA Doppler ultrasound in unselected or low risk pregnancies would be to detect those pregnancies in which there has been failure to establish or maintain the normal low-resistance umbilical and uterine circulations, (a pathological process leading to placental dysfunction and associated with intrauterine growth retardation and preeclampsia), before there is clinical evidence of fetal compromise. In practice, observational and longitudinal studies of Doppler ultrasound in unselected or low risk pregnancies have raised doubts about its application as a routine screening test, and authors have cautioned against its introduction into obstetric practice without supportive evidence from randomized trials.[48–50] The relatively low incidence of significant, poor perinatal outcomes in low risk and unselected populations presents a challenge in evaluating the clinical effectiveness of routine UA Doppler ultrasound, as large numbers are required to test the hypothesis.

Multiple Gestation

The S/D ratio of twins at the UA are in agreement with singleton pregnancies in the third trimester.[51] Twins with an abnormal UA FVW tend to be born earlier, have a higher perinatal mortality and morbidity, and have more frequent structural anomalies than fetuses without abnormal Doppler results.[52]

In cases of twin-twin transfusion syndrome, a poor placental implantation site, or chromosomal anomalies discordant growth between the twins may occur. This is a very high risk situation, with a high perinatal mortality and morbidity. The diagnosis is made mainly by ultrasound biometry. The best predictor for diagnosis of discordant twins appears to be the presence either a difference in the UA S/D ratio greater than 15% or a different estimated fetal weight greater than 15%.[53] Recently it has been reported that abnormal UA velocimetry can be observed in small twins more often in monochorionic than dichorionic twins.[54] Doppler ultrasound abnormalities of the UA in either twin are associated with poor perinatal outcome in twin-twin transfusion syndrome.

The Biophysical Profile and Multivessel Doppler Ultrasound in IUGR

Biophysical profile scoring (BPS) and Doppler surveillance are the primary methods for fetal assessment in IUGR. As placental insufficiency worsens, the fetus adapts by progressive compensation. Previously it has been suggested that the sequential changes in arterial and venous flow occur before some biophysical parameters (fetal tonus, movement, breathing, amniotic fluid volume and non-stress test) decline.[55,56] Baschat et al[37] evaluated whether multivessel Doppler parameters (UA, UV, MCA, DV, and inferior vena cava) precede biophysical fetal parameters in fetuses with severe IUGR. They found that combining multivessel Doppler and composite BPS will provide significant early warning and a definitive indication for action in the management of severe IUGR, and suggested that delivery timing may be based on this new gold standard.

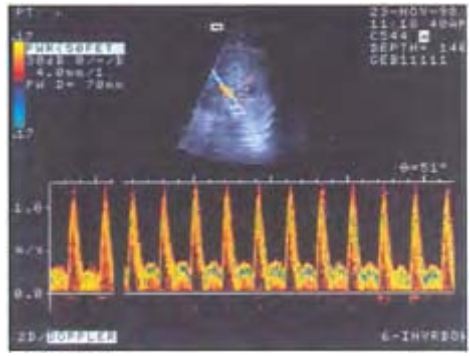

Figure 32.11: Normal flow velocity waveforms of the fetal descending aorta in the third trimester

Fetal Descending Aorta (FDA)

Beside the UA, routine Doppler sonographic examination at the descending fetal aorta is possible. FVWs of the FDA are usually recorded at the level of the diaphragm. In fact, FVWs at the level of the diaphragm and distally to the origin of the renal arteries are different.[57] Normal blood FVWs in the FDA is highly pulsatile, with a minimal diastolic component (Fig. 32.11). The descending part of the aorta provides perfusion to the fetal abdominal organs, umbilical-placental circulation, and lower extremities. The flow velocity waveform of the FDA shows a continuous forward stream during the whole heart cycle, but when compared to the FVW of the UA, the end-diastolic flow is less than the systolic component. Due to this reason the S/D ratio in the fetal aorta goes far than the S/D ratio in the UA. As pregnancy advances, the fetal aortic diameter gets wider, which decreases peripheral resistance and increases diastolic flow component. Nevertheless, this does not cause a significant S/D ratio decrease in the FDA.[58] Resistance and Pulsatility indices in the last trimester are also not affected significantly, and show a similar course as in the UA.

Increased placental impedance combined with redistribution of blood flow from nonvital to vital organs may result in changes in the aortic FVWs. An elevated S/D-ratio, RI and PI (Figs 32.12, 32.15

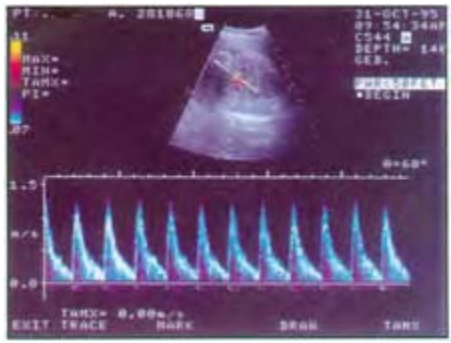

Figure 32.12: Abnormal flow velocity waveforms of the fetal descending aorta in the third trimester (high resistance index)

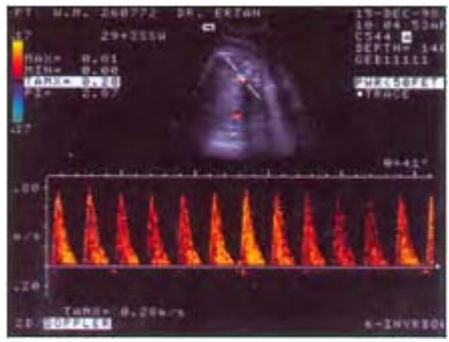

Figure 32.13: Absent end-diastolic flow (AEDF) of the fetal descending aorta (FDA) in the third trimester

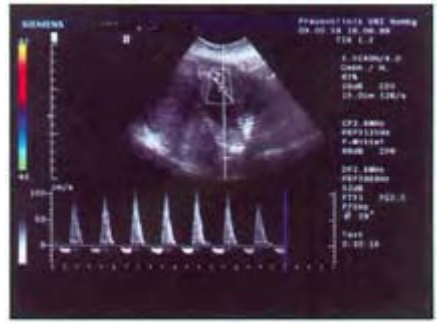

Figure 32.14: Reverse flow (RF) in the fetal descending aorta

to 32.17) is associated with both IUGR and adverse perinatal outcomes, such as severe growth restriction, necrotizing enterocolitis, fetal distress, and perinatal mortality.[59–66] Absent end-diastolic flow at the FDA is also a predictor of fetal heart rate abnormalities (Fig. 32.13). It was shown that absent flow in the FDA were detected 8 days prior to the onset of decelerations at fetal heart rate monitoring.[63] The sensitivity and specificity of absent end-diastolic flow in the FDA for prediction of IUGR with fetal heart rate abnormalities are 85% and 80%, respectively.[65,66]

Abnormal FVWs of the FDA were also evaluated for intellectual function, and minor

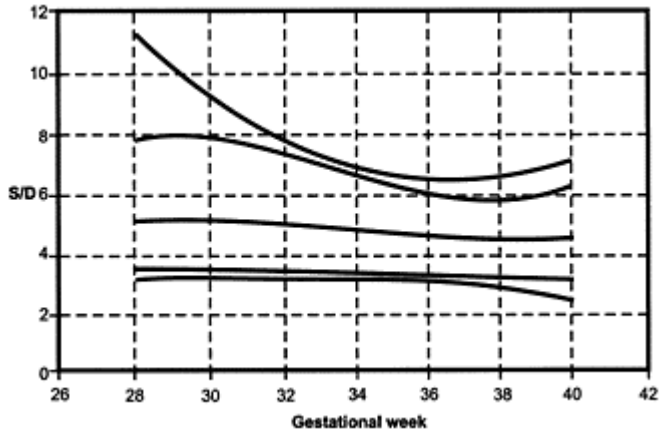

Figure 32.15: Fetal descending aorta S/D ratio nomogram

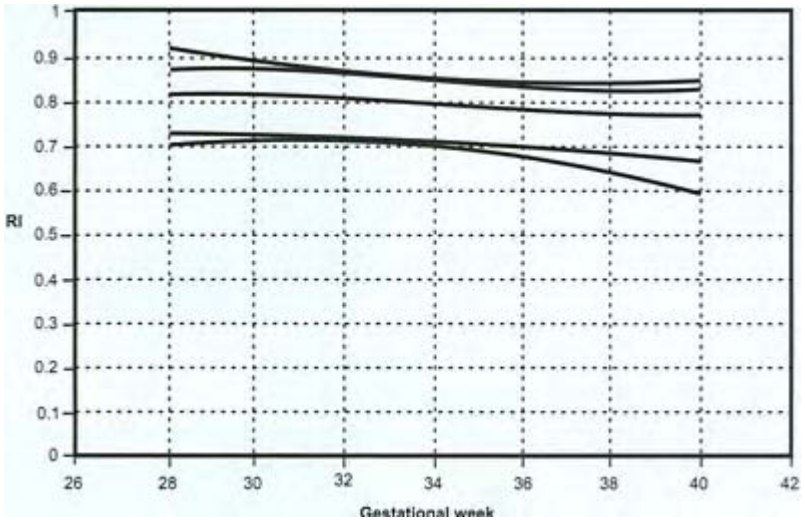

Figure 32.16: Fetal descending aorta RI nomogram

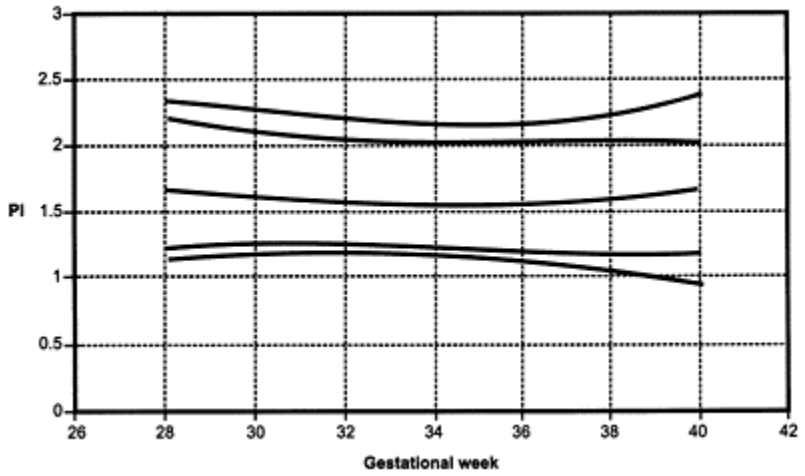

Figure 32.17: Fetal descendings aorta PI nomogram

neurological dysfunction.[45,46,67,68] At 7 years of age, verbal and global performances as well as neurological examination were significantly better in the fetuses with normal aortic FVWs.

Albeit, most of the studies showed Doppler velocimetry abnormalities of the FDA is a predictive test for the onset of decompensation due to placental insufficiency in the IUGR

fetuses (Figs 32.13 and 32.14), it cannot be recommended as a screening or diagnostic test for IUGR in an unselected obstetric population.[69]

Middle Cerebral Artery (MCA)

The circle of Willis is composed anteriorly of the anterior cerebral arteries (branches of the internal carotid artery that are interconnected by the anterior communicating artery) and posteriorly of the two posterior cerebral arteries (Branches of the basilar artery that are interconnected on either side with internal carotid artery by the posterior communicating artery).[70] These two trunks and the MCA, another branch of the internal carotid artery, supply the hemispheres on each side (Fig. 32.18). All of the defined arteries have different FVWs, therefore, it is important to know which artery is being examined during clinical practice.[71]

Figure 32.18: Circulus villisii and middle cerebral artery visualized with color Doppler

The most favorably positioned vessel for Doppler sonographic examination of fetal brain perfusion is the MCA. As the pregnancy advances, the vascular resistance in the MCA decreases (Fig. 32.19),[72] and the Doppler indices change (Figs 32.22 to 32.24). During the early stages of pregnacy, end-diastolic flow velocities in cerebral vessels are small or absent, but velocities increase towards the end of gestation. In the normal developing fetus, the brain is an area of low vascular impedance and receives continuous

Figure 32.19: Normal flow velocity waveforms of the middle cerebral artery in the third trimester

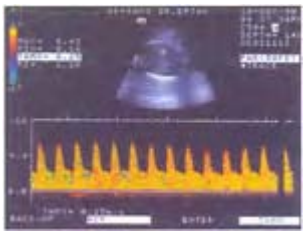

Figure 32.20: Abnormal flow velocity waveforms of the middle cerebral artery in the third trimester (brain sparring effect)

forward flow throughout the cardiac cycle. IUGR due to placental insufficiency is likely to be caused by redistribution of fetal blood flow in favor of the fetal brain and "stress organs", at the expense of less essential organs such as subcutaneous tissue, kidneys, and liver. Finally, the already low resistance to blood flow in the brain drops further to enhance brain circulation (Fig. 32.20). This results with increased end-diastolic velocities, and a decrease in the S/D ratio of the MCA (Brain sparring effect).[73]

Abnormalities of the UA flow correlated with fetal compromise better than intracerebral artery blood flow impairment. This suggests that high placental impedance precedes the onset of the "brain sparring effect". In a study, in which 576 high risk pregnancies were evaluated for the UA and MCA velocimetry, neither test was able to predict adverse perinatal outcome in the normal growing fetus.[74] Results showed that simultaneous assessment of UA and MCA velocimetry in IUGR fetuses did not improve the perinatal outcome. When the UA velocimetry was normal, the MCA velocimetry did not improve the prediction of IUGR or adverse perinatal outcome. However, when both arteries velocimetric values were abnormal, the risk of being growth restricted and having an adverse perinatal outcome was doubled.

It has been reported that the MCA PI is below the normal range when PO_2 is reduced.[75] Maximum reduction in PI is reached when the fetal PO_2 is 2–4 standard deviations below normal for gestation. When the oxygen deficit becomes greater, there is a tendency for the MCA PI to rise; this presumably reflects the prefinal stage due to development of brain edema (Fig. 32.21).

Hyperactivity of fetus, increase of intrauterine pressure (e.g. polyhydramnios), and external pressure to the fetal head (e.g. by the probe) might erroneously increase end-diastolic flow velocities

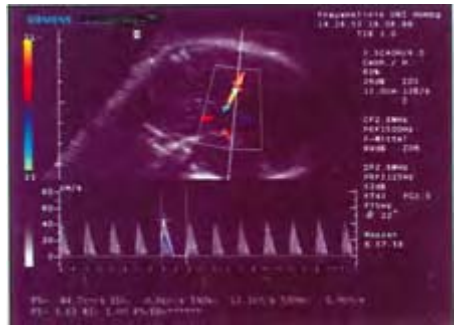

Figure 32.21: Absent end-diastolic flow after the brain sparing effect (decentralization) this presumably reflects the prefinal stage due to development of brain edema

in the MCA.[76] Different investigators have undertaken studies—utilizing data obtained from the UA and MCA—to develop indices for evaluation of intrauterine risk.[70]

Prediction of Fetal Hemoglobin in Red Cell Alloimmunization

Fetal anemia caused by red cell alloimmunization can be detected noninvasively by Doppler

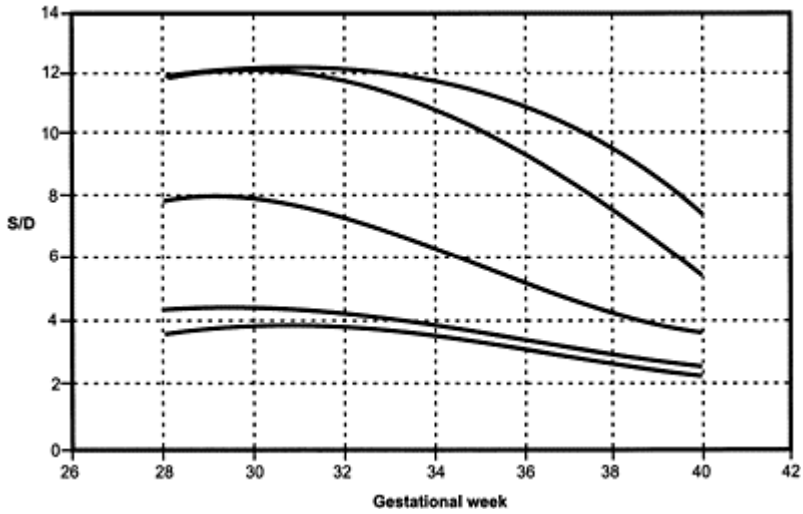

Figure 32.22: Middle cerebral artery S/D ratio nomogram

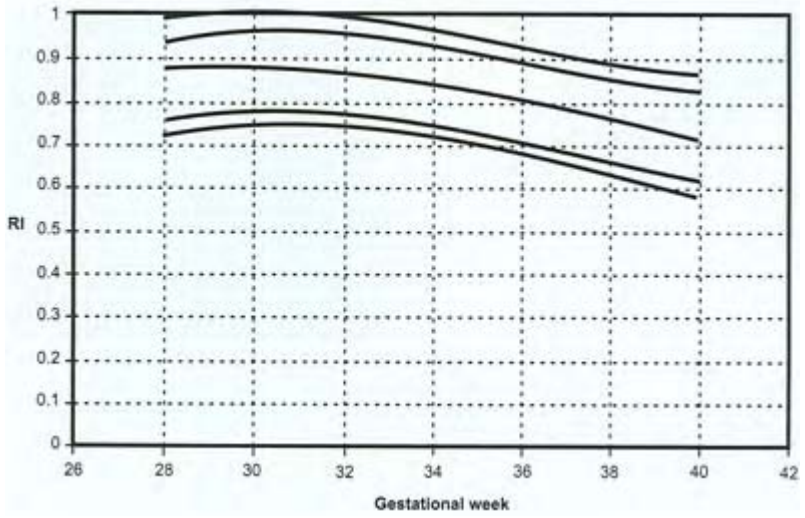

Figure 32.23: Middle cerebral artery RI nomogram

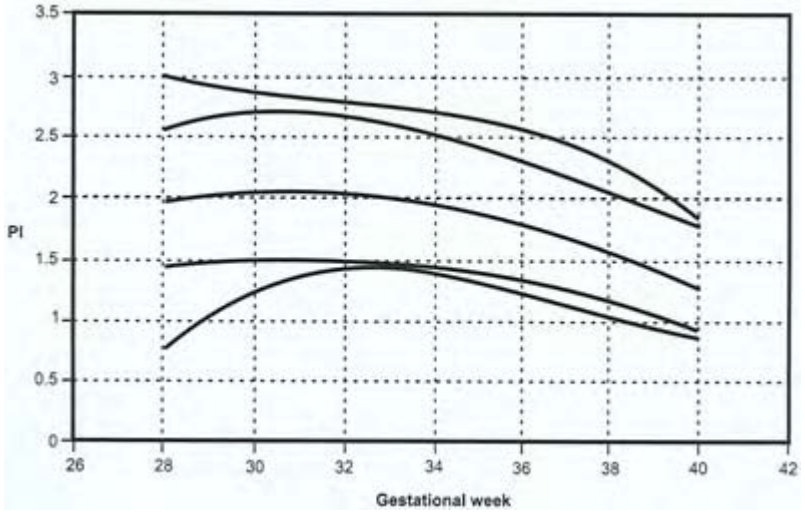

Figure 32.24: Middle cerebral artery PI nomogram

ultrasound on the basis of an increase in the peak systolic velocity in the MCA.[77,78] Although there is not a strong correlation between these two parameters when the fetus is nonanemic, the correlation becomes stronger as the hemoglobin levels decrease.[78] Prospective evaluation of the MCA peak systolic velocity to detect fetuses at risk for

anemia in red cell alloimmunization showed that 90 of the 125 anticipated invasive procedures could be avoided.[79]

In anemic fetuses, change in hematocrit lead to a corresponding alteration in blood viscosity and to an impaired release of oxygen to the tissues. Increased cardiac output and vasodilatation are the main mechanisms by which the fetus attempts to maintain the oxygen and metabolic equilibrium in various organs. It is likely that when the fetus is nonanemic or mildly anemic, there are only minor or insignificant hemodynamic changes. Therefore, the blood velocity does not change. When the fetus becomes more anemic, various mechanisms compensate to maintain the oxygen and metabolic equilibrium in the various organs. The MCA peak systolic velocity changes proportionally to the hemoglobin deficiency.

Doppler measurements appear to be valuable for estimating hemoglobin concentration in fetuses at risk for anemia. Doppler sonography of the MCA has the potential to decrease the need for invasive testing (amniocentesis, cordocentesis) and its potential risks.[80]

Fetal Venous Circulation

In recent years research on the fetomaternal circulation has focused more on the venous side of the fetal circulation. Physiologically, blood flow velocities in the umbilical vein (UV) and the portal circulation are steady and non-pulsatile. However, it has been shown that both fetal body and breathing movements can interrupt the FVWs. In a recent review, it was concluded that several pathologic conditions such as non-immune hydrops, severe IUGR, and cardiac arrhythmias also result in an abnormal, pulsatile venous blood flow.[81] However, the relationship between fetal venous blood flow patterns and imminent fetal asphyxia or fetal death is still unknown. Recently, studies on venous circulation in the fetal brain[82] and pulmonary venous circulation in the diagnosis of pulmonary hypoplasia were performed.[83]

Umbilical Vein (UV)

Oxygenated blood returning from the placenta runs from the UV through the ductus venosus (DV), and inferior vena cava. Approximately 20–30% of the blood in the UV goes through the DV,

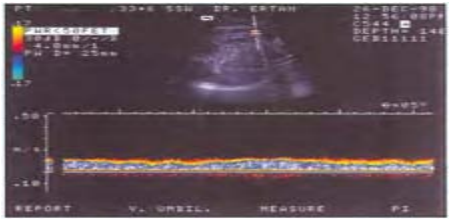

Figure 32.25: Normal flow in the umbilical vein in the third trimester (without pulsations)

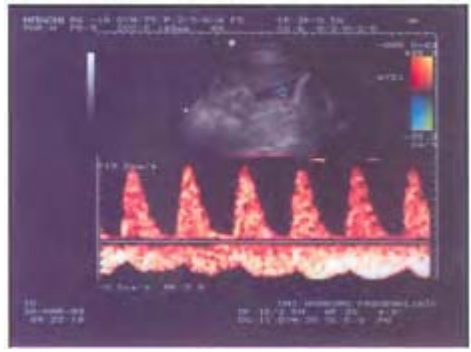

Figure 32.26: Abnormal flow in the umbilical vein (single pulsating pattern during the heart cycle)

and the remaining well oxygenated blood perfudes the left lobe of the liver (Fig. 32.25 to 32.27).[84]

The presence of UV FVW pulsatility has been associated with increased perinatal morbidity and mortality.[85,86] In an animal model, Reed et al evaluated the UV Doppler flow patterns and concluded that pulsations of the UV velocity reflect atrial pressure changes that are transmitted in a retrograde fashion.[87] In some studies, it was also observed that UV pulsations are detected in fetuses with abnormal UA FVWs and/or fetal heart rate abnormalities.[86] More recently, Ferrazzi et al[88] showed that UV blood flow is reduced in IUGR fetuses and suggested that long term studies be performed to evaluate the clinical implications of

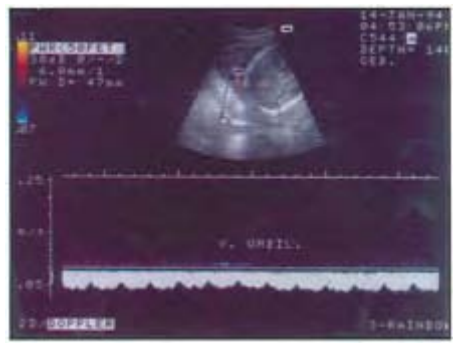

Figure 32.27: Highly pathological flow velocity waveforms of the umbilical vein (double pulsating pattern during the heart cycle)

their finding. UV pulsations were also reported in pregnancies with non-immune hydrops fetalis.[89] In this study, all the fetuses without venous pulsations survived, but only 4 of the 14 fetuses with pulsations survived. Fetuses with pulsation in the UV in late gestation have a higher morbidity and mortality, even in the setting of normal UA blood flow.[90]

Inferior Vena Cava

The flow profile within this vessel is complex: it consists of two phases of forward flow (Systolic and early diastolic), followed by a component of reversed flow in late diastole (Figs 32.28 and 32.29).[81] Like other venous flow patterns, the

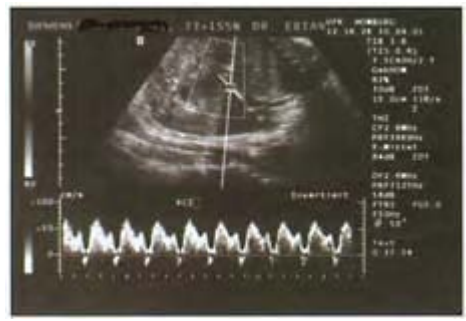

Figure 32.28: Normal flow velocity waveforms of the inferior vena cava (with reverse flow during the end-diastole)

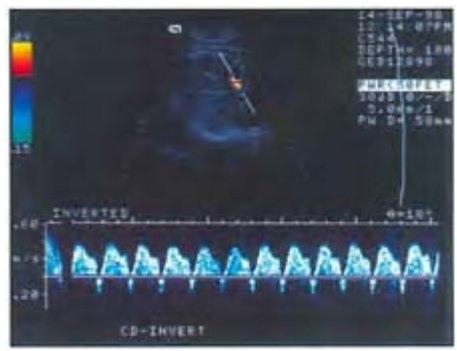

Figure 32.29: Abnormal flow velocity waveforms of the inferior vena cava (with increasing reversed flow during end-diastole)

FVWs are affected by fetal body and breathing movements. The FVW can be used for diagnosis of fetal arrhythmias, by comparing it with the FVW of the fetal aorta due to its proximity.[91] In IUGR fetuses the FVW is characterized by an increased reversed flow during atrial contraction.[92] The mechanism of this increase is attributed to abnormal ventricular filling characteristics, an abnormal ventricular wall compliance, or abnormal end-diastolic pressure.

Ductus Venosus (DV)

The DV transports oxygenated blood from the UV directly through right atrium and foramen ovale to the left atrium and ventricle, and then to the myocardium and brain.[93–99]

The DV originates from the portal sinus. Thus, the frequently expressed concept that the DV originates from the left portal vein or UV is anatomically inaccurate.[100] No anatomical continuity between the UV and DV exists, as incorrectly described, in recent Doppler ultrasound studies.[101] It is well accepted that the DV plays a major role in the regulation of fetal circulation by modifying the volume of its flow depending on the pressure gradient between the UV and the heart.[84]

In normal fetuses, color Doppler demonstrates the DV as a vessel bridging the left portal vein

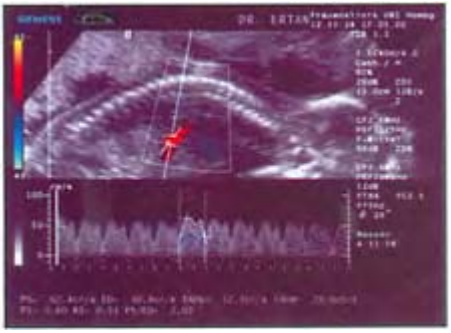

Figure 32.30: Visualization of the ductus venosus with color Doppler and normal flow velocity waveforms (with forward flow during diastole and A-wave: corresponding to atrial contraction during the late diastole)

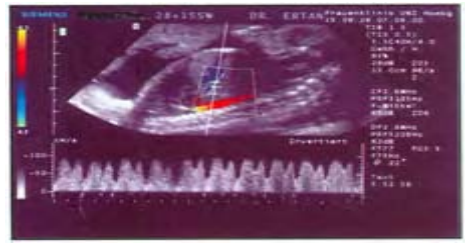

Figure 32.31: Normal flow velocity waveforms in the ductus venosus (with forward flow during diastole and A-wave)

and the inferior vena cava with an obvious gradient in velocity compared with the left portal vein.[84] A common error is the sampling of the left hepatic vein rather than the DV.[70] Physiologically, this FVW shows continuous forward flow during the heart cycle, mimicking the pattern of the inferior vena cava (Figs 32.30 and 32.31). The high pressure gradient between the UV and the DV results in high blood flow velocities within this vessel. In contrast to other venous FVWs, reversed flow in the DV is an abnormal finding, except for the first trimester due to immaturity of the sphincter of ductus venosus. However, abnormal FVWs of the DV between 11–14 weeks' gestation was suggested to be a screening test of fetal chromosomal abnormalities and/or cardiac defects.[102]

In IUGR fetuses, reversed flow in the DV is an ominous sign (Figs 32.32 to 32.35). Recently, it was reported that reverse flow patterns of the DV in IUGR fetuses is the only significant parameter associated with perinatal death.[103]

It has been suggested that changes in DV blood flow pattern precede the appearance of abnormal fetal heart rate patterns in pregnancies complicated with placental insufficiency.[55,104] One should bear in mind, however, that these studies are technically difficult and that blood flow patterns

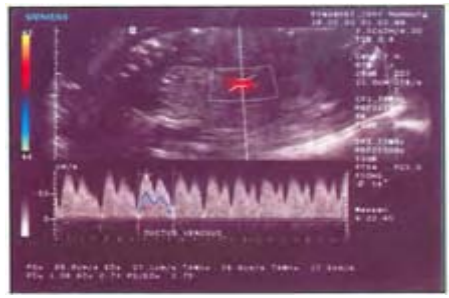

Figure 32.32: Initial pathological flow velocity waveforms of the ductus

venosus (with forward flow and decreasing A-wave)

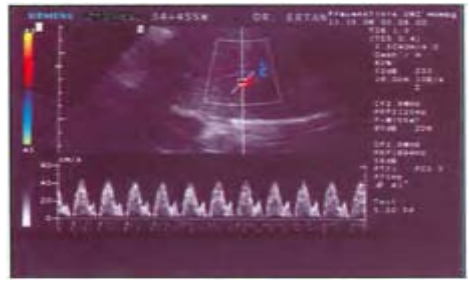

Figure 32.33: Abnormal flow velocity waveforms of the ductus venosus (absent A-wave)

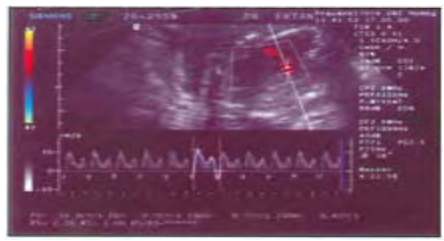

Figure 32.34: Highly pathological flow velocity waveforms of the ductus venosus (reversed A-Wave)

Figure 32.35: Highly pathological flow velocity waveforms of the ductus venosus (pre-final situation)

within the DV are also modulated by fetal behavioral states, breathing movements, and cardiac anomalies/arrhythmias.[69,105,106]

Timing of Delivery in Pregnancies Complicated with IUGR

The optimal timing of delivery in pregnancies complicated by IUGR is stiil an issue to be resolved. Clinicians have to balance the risks of prematurity against the risks of prolonged fetal exposure to hypoxemia and acidemia, possibly resulting in fetal damage or death. In a cross sectional Doppler study of the fetal circulation, the appearance of significant changes in venous Doppler FVWs from the DV, inferior vena cava and hepatic veins was observed after fetal arterial blood flow redistribution from the FDA to the MCA was established.[55] Furthermore, the changes in the venous circulation seemed to be closely related to the onset of abnormal fetal heart rate patterns. Reduced fetal heart rate variation and occurrence of fetal heart rate decelerations have been associated with fetal hypoxemia,[107] whereas extremely low values of short term variation were found to be a reliable predictor of metabolic acidemia at delivery or fetal death.[108] In a longitudinal study,[109] the DV pulsatility index and short term variation of fetal heart rate were found to be important indicators for the optimal timing of delivery before 32 weeks' gestation, and delivery was advised if one of these parameters becomes persistently abnormal.

In another study,[110] to determine time for delivery, the changes in the hepatic vein, DV and UV were investigated. Results of this study suggested that adding venous Doppler ultrasound to the arsenal of fetal surveillance in IUGR fetuses might assist in timing of delivery with less morbidity and mortality. The venous indices of the right hepatic vein and the DV, and double UV pulsations were found to be the most useful tools for this condition. Finally it was stated that venous Doppler evaluation could give valuable clinical information for surveillance in high risk pregnancies.

Uteroplacental Perfusion

In order to evaluate Uteroplacental perfusion, examinations performed at uterine arteries (UtA) give more accurate information than the arcuate arteries.[18] Velocities obtained from UtA are higher than from arcuate arteries (Fig. 32.36). This is important in interpreting Doppler study results, and it should always be paid attention on which vessel examinations were performed.

In the nonpregnant uterus, the UtA FVWs are characterized by high impedance blood flow, and almost always early diastolic notches. Kurjak et al reported the average UtA RI at the proliferative phase to be 0.88±0.04 (2SD).[111] A high resistance to flow during the midluteal phase

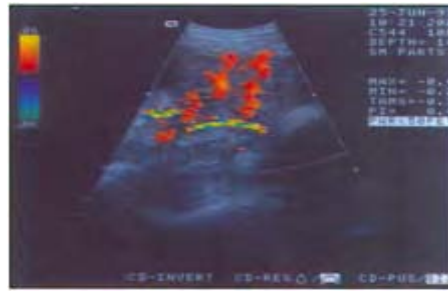

Figure 32.36: Uterine and arcuate arteries, visualized with color Doppler

of the cycle (day 21) has been associated with infertility.[112] In women undergoing in *vitro* fertilization, those with a higher PI on the day of follicular aspiration have a lower probability of successful pregnancy.[113] Such findings suggest a potential value for UtA Doppler velocimetry in identifying endometrial receptivity in infertile patients.

In the first trimester, the intervillous maternal circulation is established at 11 to 12 weeks.[114] A very limited amount of maternal blood reaches the intervillous space and color Doppler signals are usually not seen on the placenta in this period. Detection of blood flow in the intervillous space during the first trimester is associated with higher pregnancy loss rates.[115] After 12 weeks, blood flow can be systematically detected by color Doppler of the placenta. From 6 to 12 weeks, FVWs obtained from the UtA are characterized by a high systolic and low diastolic component (elevated S/ D ratio), and the presence of a notch in the early diastolic period (Fig. 32.37). FVWs of the arcuate arteries also show notching, but with a higher diastolic component.[116]

In the second and third trimester of pregnancy the UtA diameter enlarge,[117] the systolic peak velocity and volume flow rates increase,[118,119] and a progressive fall in impedance to blood flow.[120]

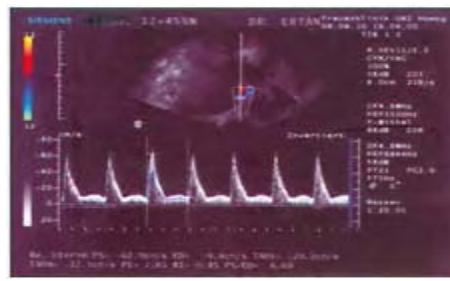

Figure 32.37: Normal flow velocity waveform of the uterine artery in the first trimester (high resistance with an early diastolic notch)

The early diastolic notch and the difference between S/D ratios of the placental versus nonplacental sites should disappear after 24–26 weeks' gestation.[118,121]

Blood flow velocities in uterine arteries depend on the localization of placenta and gestational age.[122] If the placenta is laterally located, blood flow velocities in the ipsilateral uterine artery are more important than the flow velocities of the contralateral vessel. Differences between flow velocities of the right and left uterine artery are evident at early stages of pregnancy. But in the third trimester, the difference between the S/D ratio of the vessels decrease to a minimum (Fig. 32.38).[18] If an abnormal flow pattern is observed in the uterine arteries, this most probably indicates the defective perfusion of fetoplacental unit, which predicts a high probability for developing preeclampsia, resulting with intrauterine growth retardation (Fig. 32.39).[4]

At early stages of pregnancy end-diastolic flow velocities in placental arteries are low, but systolic flow is evident.[18] With trophoblastic invasion and maturation of the uteroplacental vessels, beyond the second trimester the high pressure system is converted to a low pressure system, and vascular resistance declines.[123] The biologic variability after 20–24 weeks' gestation becomes almost stable (Figs 32.40–32.42).

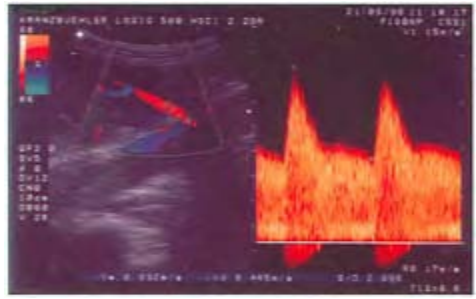

Figure 32.38: Normal flow velocity waveform in the uterine artery in the third trimester (high end-diastolic flow, without notching)

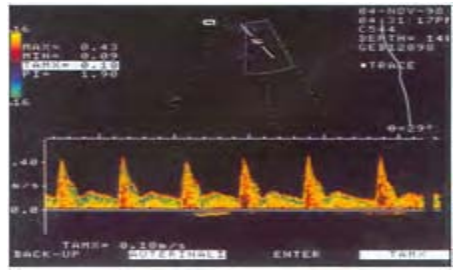

Figure 32.39: Abnormal flow velocity waveform in the uterine artery in the

third trimester (low end-diastolic flow, with an early diastolic notch)

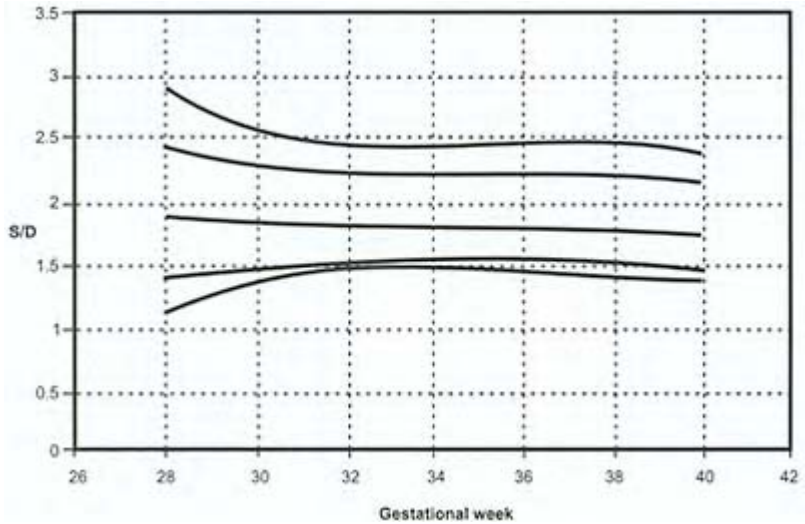

Figure 32.40: Uterine artery S/D ratio nomogram

Before 24 weeks' gestation early diastolic notching, due to the immature uteroplacental vascular system, is normally observed. Beyond this gestational age, persistant early diastolic notching is associated with preeclampsia.[6,9,11] Elevated RI, PI, or S/D ratios and the presence of a diastolic notch are considered as abnormal UtA FVWs.

Prediction of Complicated Pregnancies with Uteroplacental Doppler Velocimetry

Pregnancies complicated with preeclampsia and IUGR show evidence of impaired trophoblastic invasion and maturation.[124] Several studies were reported about the potential role of uteroplacental Doppler sonography to identify the risk for preeclampsia, IUGR, preterm delivery, or adverse

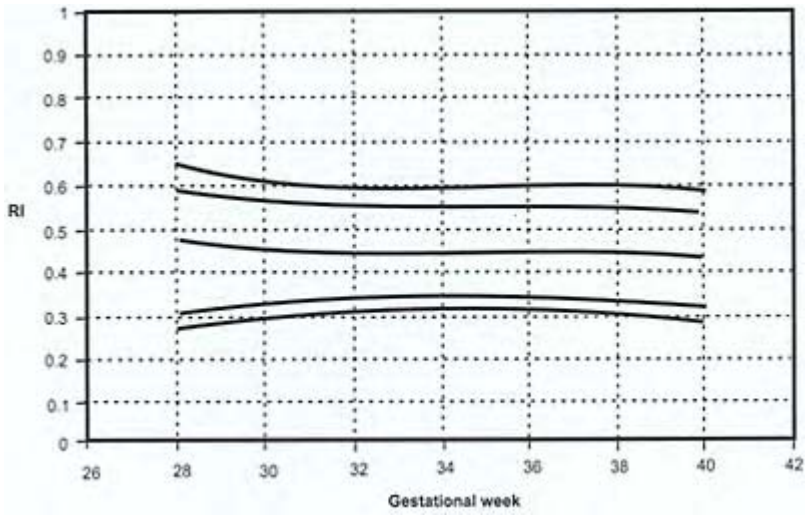

Figure 32.41: Uterine artery RI nomogram

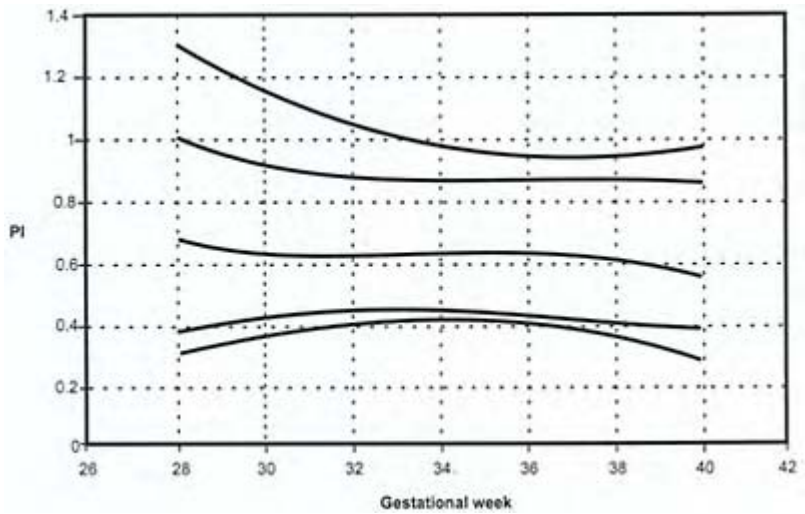

Figure 32.42: Uterine artery PI nomogram

perinatal outcome. In most of the studies uteroplacental Doppler was advocated as effective in predicting a high risk population for preeclampsia and IUGR,[5,7,8,10,12] whereby some were indecisive, and others did not support this result.[125,126] The paradoxical results were attributed to differences in patient selection, gestational ages for

screening, type of equipment, multiple definitions of FVWs, different vessels examined, and heterogeneous outcome criteria.[127] The sensitivity of the examination improved as the gestational age approached to 26 weeks, when examinations on the UtA were performed, and when persistent diastolic notch was one of the criteria for analysis.[126] Bower et al[4] proposed a two stage screening protocol for preeclampsia with UtA Doppler at 18–22 weeks and when abnormal reevaluation at 24 weeks. In their study, 59% of the re-examined patients showed normal UtA Doppler FVWs.[128] Persistence of an abnormal FVW increased the relative risk for developing preeclampsia by 24-fold. Persistent notch in the early diastolic component of the FVW increased the predictive value (from 4.3% to 28%) and was associated with a 68-fold risk for developing preeclampsia.

There were also some studies suggesting Doppler assessment of the UtA can be carried out at 11–14 weeks' gestation and that screening at this early gestation can also identify pregnancies at risk of developing complications associated with impaired placentation.[129] Chromosomal defects are associated with IUGR,[130] and in the case of trisomy 18 and 13, but not in trisomy 21, the IUGR is evident from the first trimester of pregnancy.[131,132] In a study, in which UtA Doppler between 11–14 weeks of gestation was performed to examine whether the high lethality and IUGR is associated with chromosomal abnormalities, the authors showed that UtA impedance is not associated with chromosomal anomalies,[133] and suggested that the placental histological changes may be responsible for increased impedance in the UA, but not in the UtA.

The relationship between abnormal uterine artery Doppler velocimetry and pre-eclampsia, IUGR and adverse perinatal outcome are well established. However, whether its use as a routine screening test ultimately results in a decrease in maternal and perinatal morbidity and mortality remains questionable. This is due to a number of factors, including the low positive predictive value of the test, the lack of an accepted standardized analysis of the uterine artery waveform, and the dependence on operator skill.[134] Furthermore, screening is only worthwhile if an effective preventive treatment is available. The debate about the benefit of prophylactic treatment with low dose aspirin may not be completely resolved, but the results of the two largest multicenter randomized trials (Collaborative Low-Dose Aspirin Study-CLASP[135] and ECPPA[136]) were not encouraging.

SUMMARY

Doppler ultrasound is a noninvasive technique that is commonly used to evaluate maternal and fetal hemodynamics. Examination of fetomaternal vessels using Doppler sonography has been subject of intensive investigation in recent years. However, to date, randomized controlled trials were able to establish only limited clinical value of Doppler velocimetry in obstetrics to improve perinatal outcome in high risk situations. Umbilical artery, fetal descending aorta and middle cerebral artery Doppler velocimetric studies are acceptable tools in the diagnosis and management of intrauterine growth restricted fetuses, and in the reduction of perinatal mortality in high risk pregnancies. The majority of severely compromised fetuses also show pathological venous velocimetry, which might give valuable clinical information for surveillance in high risk pregnancies and their optimal perinatal management. In addition, Doppler sonography might have a role

in predicting long term neuromotoric outcome. Large scale randomized controlled trials are needed to establish the clinical utility of Doppler ultrasound in obstetrics.

REFERENCES

1. FitzGerald DE, Drumm JE. Non-invasive measurement of human fetal circulation using ultrasound: a new method. Br Med J 1977;2:1450–51.
2. Campbell S, Diaz-Recasens J, Griffin DR et al. New doppler technique for assessing uteroplacental blood flow. Lancet 1983; 1:675–77.
3. Eik-Nes SH, Marsal K, Brubakk AO et al. Ultrasonic measurement of human fetal blood flow. J Biomed Eng 1982;4:28–36.
4. Bower S, Schuchter K, Campbell S. Doppler ultrasound screening as part of routine antenatal scanning: prediction of pre-eclampsia and intrauterine growth retardation. Br J Obstet Gynaecol 1993; 100:989–94.
5. Caforio L, Testa AC, Mastromarino C et al. Predictive value of uterine artery velocimetry at midgestation in low- and high-risk populations: A new perspective. Fetal Diagn Ther 1999; 14:201–05.
6. Campbell S, Pearce JM, Hackett G et al. Qualitative assessment of uteroplacental blood flow: early screening test for high-risk pregnancies. Obstet Gynecol 1986; 68:649–53.
7. Harrington K, Cooper D, Lees C et al. Doppler ultrasound of the uterine arteries: the importance of bilateral notching in the prediction of pre-eclampsia, placental abruption or delivery of a small-for-gestational-age baby. Ultrasound Obstet Gynecol 1996; 7:182–88.
8. Harrington K, Goldfrad C, Carpenter RG et al. Transvaginal uterine and umbilical artery Doppler examination of 12–16 weeks and the subsequent development of pre-eclampsia and intrauterine growth retardation. Ultrasound Obstet Gynecol 1997; 9: 94–100.
9. Hoffmann H, Chaoui R, Bollmann R et al. [Potential clinical application of Doppler ultrasound in obstetrics]. Zentralbl Gynakol 1989; 111:1277–84.
10. Irion O, Masse J, Forest JC et al. Prediction of preeclampsia, low birthweight for gestation and prematurity by uterine artery blood flow velocity waveforms analysis in low risk nulliparous women. Br J Obstet Gynaecol 1998; 105:422–29.
11. Trudinger BJ, Giles WB, Cook CM. Uteroplacental blood flow velocity-time waveforms in normal and complicated pregnancy. Br J Obstet Gynaecol 1985; 92:39–45.
12. Zimmermann R Eirio V, Koskinen J et al. Doppler assessment of the uterine and uteroplacental circulation in the second trimester in pregnancies at high risk for pre-eclampsia and/or intrauterine growth retardation: comparison and correlation between different Doppler parameters. Ultrasound Obstet Gynecol 1997; 9:330–38.
13. Hershkovitz R, Sheiner E, Mazor M. Ultrasound in obstetrics: a review of safety. Eur J Obstet Gynecol Reprod Biol 2002; 101:15–18.
14. Barnett S, Kossoff G, Edwards M. Is diagnostic ultrasound safe? Current international consensus on the thermal mechanism. Med J Aust 1994; 160:33–37.
15. Mires GJ, Christie AD, Leslie J et al. Are ‘notched’ uterine arterial waveforms of prognostic value for hypertensive and growth disorders of pregnancy? Fetal Diagn Ther 1995; 10:111–18.
16. Deutinger J. Physiology of Doppler blood flow in maternal blood vessels in pregnancy. Gynakologe 1992; 25:284–91.
17. Fendel H, Fendel M, Pauen A et al. Doppler studies of arterial blood flow in the uterus during labor. Z Geburtshilfe Perinatol 1984; 188:64–67.
18. Fogarty FJ Beattie B, Harper A et al. Continuous wave Doppler flow velocity waveforms from the umbilical artery in normal pregnancy. J Perinat Med 1990; 18:51–57.
19. Ertan AK, Hendrik HJ, Tanriverdi HA et al. Fetomaternal doppler sonography nomograms. Clin Exp Obstet Gynecol. 2003; In press.

20. Soothill PW, Ajayi RA, Campbell S et al. Prediction of morbidity in small and normally grown fetuses by fetal heart rate variability, biophysical profile score and umbilical artery Doppler studies. Br J Obstet Gynaecol 1993; 100:742–45.
21. Romero R, Kalache K, Kadar N. Timing the delivery of the preterm severely growth-restricted fetus: venous Doppler, cardiotocography or the biophysical profile? Ultrasound Obstet Gynecol 2002; 19:118–21.
22. Stuart B, Drumm J, FitzGerald DE et al. Fetal blood velocity waveforms in normal pregnancy. Br J Obstet Gynaecol 1980; 87:780–85.
23. Thompson RS, Trudinger BJ, Cook CM. Doppler ultrasound waveform indices: A/B ratio, pulsatility index and Pourcelot ratio. Br J Obstet Gynaecol 1988; 95:581–88.
24. Huneke B, Hoist A, Schroder HJ et al. Normal values for relative Doppler indices. A/B ratio, resistance index and pulsatility index of the uterine artery and umbilical artery in normal pregnancy. A longitudinal study. Geburtshilfe Frauenheilkd 1995; 55:616–22.
25. Schulman H, Fleischer A, Stern W et al. Umbilical velocity wave ratios in human pregnancy. Am J Obstet Gynecol 1984; 148:985–90.
26. Trudinger BJ, Giles WB, Cook CM et al. Fetal umbilical artery flow velocity waveforms and placental resistance: Clinical significance. Br J Obstet Gynaecol 1985; 92:23–30.
27. Maulik D, Yarlagadda AP, Youngblood JP et al. Components of variability of umbilical arterial Doppler velocimetry—a prospective analysis. Am J Obstet Gynecol 1989; 160:1406–09.
28. Ertan AK, Hendrik HJ, Schmidt W. Perinatologische Auffalligkeiten bei hochpathologischen Doppler-Flow-Befunden. In: Schmidt W, Kurjak A (Eds). Farbdopplersonographie in Gynakologie und Geburtshilfe 2000; Stuttgart: Thieme Verlag.
29. Fleischer A, Schulman H, Farmakides G et al. Umbilical artery velocity waveforms and intrauterine growth retardation. Am J Obstet Gynecol 1985; 151:502–05.
30. Devoe LD, Gardner P, Dear C et al. The significance of increasing umbilical artery systolic-diastolic ratios in third-trimester pregnancy. Obstet Gynecol 1992; 80:684–87.
31. Rochelson B, Schulman H, Farmakides G et al. The significance of absent end-diastolic velocity in umbilical artery velocity waveforms. Am J Obstet Gynecol 1987; 156:1213–18.
32. Trudinger BJ, Cook CM, Giles WB et al. Fetal umbilical artery velocity waveforms and subsequent neonatal outcome. Br J Obstet Gynaecol 1991; 98:378–84.
33. Gudmundsson S, Marsal K. Umbilical and uteroplacental blood flow velocity waveforms in pregnancies with fetal growth retardation. Eur J Obstet Gynecol Reprod Biol 1988; 27:187–96.
34. Baschat AA, Weiner CP. Umbilical artery doppler screening for detection of the small fetus in need of antepartum surveillance. Am J Obstet Gynecol 2000; 182:154–58.
35. McCowan LM, Harding JE, Stewart AW. Umbilical artery Doppler studies in small for gestational age babies reflect disease severity. BJOG 2000; 107:916–25.
36. Ertan AK, He JP, Tanriverdi HA et al. Comparison of perinatal outcome in fetuses with reverse or absent enddiastolic flow in the umbilical Artery/fetal descending aorta. J Perinat Med 2003; In press.
37. Baschat AA, Gembruch U, Harman CR. The sequence of changes in Doppler and biophysical parameters as severe fetal growth restriction worsens. Ultrasound Obstet Gynecol 2001; 18:571–77.
38. Rizzo G, Pietropolli A, Capponi A et al. Chromosomal abnormalities in fetuses with absent end-diastolic velocity in umbilical artery: analysis of risk factors for an abnormal karyotype. Am J Obstet Gynecol 1994; 171:827–31.
39. Ertan AK, He JP, Hendrik HJ et al. Perinatal events of cases with severely abnormal Doppler flow measurements. J Perinat Med 2003; In press.
40. Valcamonico A, Danti L, Frusca T et al. Absent end-diastolic velocity in umbilical artery: risk of neonatal morbidity and brain damage. Am J Obstet Gynecol 1994; 170:796–801.
41. Alfirevic Z, Neilson JP. Doppler ultrasonography in high-risk pregnancies: systematic review with metaanalysis. Am J Obstet Gynecol 1995; 172:1379–87.

42. Neilson JP, Alfirevic Z: Doppler ultrasound for fetal assessment in high risk pregnancies (Cochrane Review). In: The Cochrane Library, Issue 3, (2002). Oxford: Update Software.
43. Baschat AA, Gembruch U, Viscardi RM et al. Antenatal prediction of intraventricular hemorrhage in fetal growth restriction: what is the role of Doppler? Ultrasound Obstet Gynecol 2002; 19:334–39.
44. Wienerroither H, Steiner H, Tomaselli J et al. Intrauterine blood flow and long-term intellectual, neurologic, and social development. Obstet Gynecol 2001; 97:449–53.
45. Ertan AK, Jost W, Hendrik HJ et al. Perinatal events and neuromotoric development of children with zero flow in the fetal vessels during the last trimester. In: Cosmi E, Di Renzo GC (Eds). 2nd World Congress of Perinatal Medicine. 1993; Milano: Monduzzi Editore.
46. Ertan AK, Jost W, Mink D et al. Neuromotoric development of children after AED-Flow during pregnancy. In: Kurjak A, Latin V, Rippmann E (Eds). Advances on the Pathophysiology of Pregnancy, 1995; Milano: CIC Edizioni internazionali.
47. Farrell T, Chien PF, Gordon A. Intrapartum umbilical artery Doppler velocimetry as a predictor of adverse perinatal outcome: a systematic review. Br J Obstet Gynaecol 1999; 106:783–92.
48. Sijmons EA, Reuwer PJ, van Beek E et al. The validity of screening for small-for-gestational-age and low-weight-for-length infants by Doppler ultrasound. Br J Obstet Gynaecol 1989; 96:557–61.
49. Beattie RB, Dornan JC. Antenatal screening for intrauterine growth retardation with umbilical artery Doppler ultrasonography. BMJ 1989; 298:631–35.
50. Goffinet F, Paris-Llado J, Nisand I et al. Umbilical artery Doppler velocimetry in unselected and low risk pregnancies: a review of randomised controlled trials. Br J Obstet Gynaecol 1997; 104:425–30.
51. Giles WB, Trudinger BJ, Cook CM et al. Umbilical artery flow velocity waveforms and twin pregnancy outcome. Obstet Gynecol 1988; 72:894–97.
52. Gaziano EF! Knox H, Ferrera B et al. Is it time to reassess the risk for the growth-retarded fetus with normal Doppler velocimetry of the umbilical artery? Am J Obstet Gynecol 1994; 170:1734–41.
53. Divon MY, Girz BA, Sklar A et al. Discordant twins—a prospective study of the diagnostic value of realtime ultrasonography combined with umbilical artery velocimetry. Am J Obstet Gynecol 1989; 161:757–60.
54. Gaziano E, Gaziano C, Brandt D. Doppler velocimetry determined redistribution of fetal blood flow: correlation with growth restriction in diamniotic monochorionic and dizygotic twins. Am J Obstet Gynecol 1998; 178:1359–67.
55. Hecher K, Campbell S, Doyle P et al. Assessment of fetal compromise by Doppler ultrasound investigation of the fetal circulation. Arterial, intracardiac, and venous blood flow velocity studies. Circulation 1995; 91:129–38.
56. Senat MV, Schwarzler P, Alcais A et al. Longitudinal changes in the ductus venosus, cerebral transverse sinus and cardiotocogram in fetal growth restriction. Ultrasound Obstet Gynecol 2000; 16:19–24.
57. Lingman G, Marsal K. Fetal central blood circulation in the third trimester of normal pregnancy—a longitudinal study. I. Aortic and umbilical blood flow. Early Hum Dev 1986; 13:137–50.
58. Hecher K, Spernol R, Szalay S et al. [Reference values for the pulsatility index and the resistance index of blood flow curves of the umbilical artery and fetal aorta in the 3d trimester]. Ultraschall Med 1989; 10:226–29.
59. Soothill PW, Nicolaides KH, Bilardo K et al. Uteroplacental blood velocity resistance index and umbilical venous pO2, pCO2, pH, lactate and erythroblast count in growth-retarded fetuses. Fetal Ther 1986; 1:176–79.
60. Jouppila P, Kirkinen P. Blood velocity waveforms of the fetal aorta in normal and hypertensive pregnancies. Obstet Gynecol 1986; 67:856–60.

61. Laurin J, Lingman G, Marsal K et al. Fetal blood flow in pregnancies complicated by intrauterine growth retardation. Obstet Gynecol 1987; 69:895–902.
62. Hackett GA, Campbell S, Gamsu H et al. Doppler studies in the growth retarded fetus and prediction of neonatal necrotising enterocolitis, haemorrhage, and neonatal morbidity. Br Med J (Clin Res Ed) 1987; 294:13–16.
63. Arabin B, Siebert M, Jimenez E et al. Obstetrical characteristics of a loss of end-diastolic velocities in the fetal aorta and/or umbilical artery using Doppler ultrasound. Gynecol Obstet Invest 1988; 25:173–80.
64. Tonge HM, Wladimiroff JW, Noordam MJet al. Blood flow velocity waveforms in the descending fetal aorta: comparison between normal and growth-retarded pregnancies. Obstet Gynecol 1986; 67:851–55.
65. Bonatz G, Schulz V, Weisner D et al. Fetal heart rate (FHR) pathology in labor related to preceeding Doppler sonographic results of the umbilical artery and fetal aorta in appropriate and small for gestational age babies. A longitudinal analysis. J Perinat Med 1997; 25:440–46.
66. Marsal K, Laurin J, Lindblad A et al. Blood flow in the fetal descending aorta. Semin Perinatol 1987; 11:322–34.
67. Ley D, Laurin J, Bjerre M et al. Abnormal fetal aortic velocity waveform and minor neurological dysfunction at 7 years of age. Ultrasound Obstet Gynecol 1996; 8:152–59.
68. Ley D, Tideman E, Laurin J et al. Abnormal fetal aortic velocity waveform and intellectual function at 7 years of age. Ultrasound Obstet Gynecol 1996; 8:160–65.
69. Divon MY, Ferber A. Doppler evaluation of the fetus. Clin Obstet Gynecol 2002; 45:1015–25.
70. Mari G, Detti L. Doppler ultrasound application to fetal medicine. In: Fleischer A, Manning F, Jeanty P et al (Eds). Sonography in Obstetrics and Gynecology (Principles and Practice) 2001; New York, USA: McGraw Hill.
71. Mari G, Moise KJ, Jr., Deter RL et al. Doppler assessment of the pulsatility index in the cerebral circulation of the human fetus. Am J Obstet Gynecol 1989; 160:698–703.
72. Vetter K. The significance of Doppler blood flow measurement in recognizing placental insufficiency. Arch Gynecol Obstet 1988; 244 Suppl:S12-S18.
73. Arabin B, Bergmann PL, Saling E. Simultaneous assessment of blood flow velocity waveforms in uteroplacental vessels, the umbilical artery, the fetal aorta and the fetal common carotid artery. Fetal Ther 1987; 2:17–26.
74. Strigini FA, De Luca G, Lencioni G et al. Middle cerebral artery velocimetry: different clinical relevance depending on umbilical velocimetry. Obstet Gynecol 1997; 90:953–57.
75. Sepulveda W, Shennan AH, Peek MJ. Reverse end-diastolic flow in the middle cerebral artery: an agonal pattern in the human fetus. Am J Obstet Gynecol 1996; 174:1645–47.
76. Vyas S, Nicolaides KH, Bower S et al. Middle cerebral artery flow velocity waveforms in fetal hypoxaemia. Br J Obstet Gynaecol 1990; 97:797–803.
77. Mari G, Adrignolo A, Abuhamad AZ et al. Diagnosis of fetal anemia with Doppler ultrasound in the pregnancy complicated by maternal blood group immunization. Ultrasound Obstet Gynecol 1995; 5: 400–05.
78. Mari G, Deter RL, Carpenter RL et al. Noninvasive diagnosis by Doppler ultrasonography of fetal anemia due to maternal red-cell alloimmunization. Collaborative Group for Doppler Assessment of the Blood Velocity in Anemic Fetuses. N Engl J Med 2000; 342:9–14.
79. Zimmerman R, Carpenter RJ, Jr., Durig P et al. Longitudinal measurement of peak systolic velocity in the fetal middle cerebral artery for monitoring pregnancies complicated by red cell alloimmunisation: a prospective multicentre trial with intention-to-treat. BJOG 2002; 109:746–52.
80. Mari G, Detti L, Oz U et al. Accurate prediction of fetal hemoglobin by Doppler ultrasonography. Obstet Gynecol 2002; 99:589–93.
81. Huisman TW. Doppler assessment of the fetal venous system. Semin Perinatol 2001; 25:21–31.

82. Laurichesse-Delmas H, Grimaud O, Moscoso G et al. Color Doppler study of the venous circulation in the fetal brain and hemodynamic study of the cerebral transverse sinus. Ultrasound Obstet Gynecol 1999; 13:34–42.
83. Yoshimura S, Masuzaki H, Miura K et al. Diagnosis of fetal pulmonary hypoplasia by measurement of blood flow velocity waveforms of pulmonary arteries with Doppler ultrasonography. Am J Obstet Gynecol 1999; 180:441–46.
84. Contratti G, Banzi C, Ghi T et al. Absence of the ductus venosus: report of 10 new cases and review of the literature. Ultrasound Obstet Gynecol 2001; 18:605–09.
85. Arduini D, Rizzo G, Romanini C. The development of abnormal heart rate patterns after absent end-diastolic velocity in umbilical artery: analysis of risk factors. Am J Obstet Gynecol 1993; 168:43–50.
86. Damron DP, Chaffin DG, Anderson CF et al. Changes in umbilical arterial and venous blood flow velocity waveforms during late decelerations of the fetal heart rate. Obstet Gynecol 1994; 84:1038–40.
87. Reed K, Chaffin DG, Anderson CF et al. Umbilical venous pulsations are related to atrial contraction pressure waveforms in fetal lambs. Obstet Gynecol 1997; 89:953–56.
88. Ferrazzi E, Rigano S, Bozzo M et al. Umbilical vein blood flow in growth-restricted fetuses. Ultrasound Obstet Gynecol 2000; 16:432–38.
89. Gudmundsson S, Hunta J, Wood DC et al. Venous Doppler in the fetus with nonimmune hydrops fetalis. Am J Obstet Gynecol 1991; 164:33–37.
90. Nakai Y, Miyazaki Y, Matsuoka Y. Pulsatile umbilical venous flow and its clinical significance. Br J Obstet Gynaecol 1992; 99:977–80.
91. Chan FY, Woo SK, Ghosh A et al. Prenatal diagnosis of congenital fetal arrhythmias by simultaneous pulsed Doppler velocimetry of the fetal abdominal aorta and inferior vena cava. Obstet Gynecol 1990; 76:200–05.
92. Rizzo G, Arduini D, Romanini C. Inferior vena cava flow velocity waveforms in appropriate and small-for gestational age fetuses. Am J Obstet Gynecol 1992; 166:1271–80.
93. Kiserud T, Eik-Nes SH, Blaas HG et al. Ultrasonographic velocimetry of the fetal ductus venosus. Lancet 1991; 338:1412–14.
94. Kiserud T, Hellevik LR, Eik-Nes SH et al. Estimation of the pressure gradient across the fetal ductus venosus based on Doppler velocimetry. Ultrasound Med Biol 1994; 20:225–32.
95. Kiserud T. In a different vein: the ductus venosus could yield much valuable information. Ultrasound Obstet Gynecol 1997; 9:369–72.
96. Kiserud T, Rasmussen S. How repeat measurements affect the mean diameter of the umbilical vein and the ductus venosus. Ultrasound Obstet Gynecol 1998; 11:419–25.
97. Kiserud T, Crowe C, Hanson M. Ductus venosus agenesis prevents transmission of central venous pulsations to the umbilical vein in fetal sheep. Ultrasound Obstet Gynecol 1998; 11:190–94.
98. Kiserud T. Ductus venosus blood velocity in myeloproliferative disorders. Ultrasound Obstet Gynecol 2001; 18:184–85.
99. Kiserud T. The ductus venosus. Semin Perinatol 2001; 25:11–20.
100. Mavrides E, Moscoso G, Carvalho JS et al. The anatomy of the umbilical, portal and hepatic venous systems in the human fetus at 14–19 weeks of gestation. Ultrasound Obstet Gynecol 2001; 18:598–04.
101. Bellotti M, Pennati G, De Gasperi C et al. Role of ductus venosus in distribution of umbilical blood flow in human fetuses during second half of pregnancy. Am J Physiol Heart Circ Physiol 2000; 279:H1256–63.
102. Matias A, Montenegro N. Ductus venosus blood flow in chromosomally abnormal fetuses at 11 to 14 weeks of gestation. Semin Perinatol 2001; 25:32–37.
103. Ozcan T, Sbracia M, d'Ancona RL et al. Arterial and venous Doppler velocimetry in the severely growth-restricted fetus and associations with adverse perinatal outcome. Ultrasound Obstet Gynecol 1998; 12:39–44.

104. Hecher K, Hackeloer BJ. Cardiotocogram compared to Doppler investigation of the fetal circulation in the premature growth-retarded fetus: longitudinal observations. Ultrasound Obstet Gynecol 1997; 9:152–61.
105. Kiserud T. Fetal venous circulation—an update on hemodynamics. J Perinat Med 2000; 28:90–96.
106. Kiserud T. Liver length in the small-for-gestational-age fetus and ductus venosus flow. Am J Obstet Gynecol 2000; 182:252–53.
107. Ribbert L, Snijders RJ, Nicolaides KH. Relation of fetal blood gases and data from computer assisted analysis of fetal heart rate patterns. Br J Obstet Gynaecol 1991; 98:820–23.
108. Dawes GS, Moulden M, Redman C. Short term fetal heart rate variation, decelerations, and umbilical flow velocity waveforms before labor. Obstet Gynecol 1992; 80:673–78.
109. Hecher K, Bilardo CM, Stigter RH et al. Monitoring of fetuses with intrauterine growth restriction: a longitudinal study. Ultrasound Obstet Gynecol 2001; 18:564–70.
110. Hofstaetter C, Gudmundsson S, Hansmann M. Venous Doppler velocimetry in the surveillance of severely compromised fetuses. Ultrasound Obstet Gynecol 2002; 20:233–39.
111. Kurjak A, Kupesic-Urek S, Schulman H et al. Transvaginal color flow Doppler in infertile women. Fertil Steril 1991; 56:870–73.
112. Deutinger J, Rudelstorfer R, Bernaschek G. Vaginosonographic Doppler velocimetry in both uterine arteries: elevated left-right differences and relationship to fetal haemodynamics and outcome. Early Hum Dev 1991; 25:187–96.
113. Goswamy R, Williams G, Steptoe P. Decreased uterine perfusion—A cause of infertility. Hum Reprod 1989; 3:955–60.
114. Hustin J, Schaaps JP, Lambotte R. Anatomical studies of the uteroplacental vascularization in the first trimester of pregnancy. Am J Obstet Gynecol 1987; 157:167–71.
115. Khong T, Liddell L, Robertson W. Defective haemochorial placentation as a cause of miscarriage: A preliminary result. Br J Obstet Gynaecol 1987; 94:649–53.
116. Coppens M, Loquet P, Kollen M et al. Longitudinal evaluation of uteroplacental and umbilical blood flow changes in normal early pregnancy. Ultrasound Obstet Gynecol 1996; 7:114–21.
117. Thaler I, Manor D, Itskovitz J et al. Changes in uterine blood flow during human pregnancy. Am J Obstet Gynecol 1990; 162:121–25.
118. Kofinas AD, Espeland MA, Penry M et al. Uteroplacental Doppler flow velocity waveform indices in normal pregnancy: a statistical exercise and the development of appropriate reference values. Am J Perinatol 1992; 9:94–101.
119. Palmer SK, Zamudio S, Coffin C et al. Quantitative estimation of human uterine artery blood flow and pelvic blood flow redistribution in pregnancy. Obstet Gynecol 1992; 80:1000–06.
120. den Ouden M, Cohen-Overbeek TE, Wladimiroff JW. Uterine and fetal umbilical artery flow velocity waveforms in normal first trimester pregnancies. Br J Obstet Gynaecol 1990; 97:716–19.
121. Tekay A, Jouppila P. A longitudinal Doppler ultrasonographic assessment of the alterations in peripheral vascular resistance of uterine arteries and ultrasonographic findings of the involuting uterus during the puerperium. Am J Obstet Gynecol 1993; 168:190–98.
122. Schneider KT, Loos W. The 10th anniversary of obstetric Doppler sonography—development and perspectives. Geburtshilfe Frauenheilkd 1989;49:407–15.
123. Brosens I, Dixon HG, Robertson W. Fetal growth retardation and the arteries of the placental bed. Br J Obstet Gynaecol 1977; 84:656–64.
124. Hitschold T, Ulrich S, Kalder M et al. Blood flow profile in the uterine artery. Correlation with placental morphology and clinico-obstetrical data within the scope of pre-eclampsia. Z Geburtshilfe Perinatol 1995; 199:8–12.
125. Hanretty KP, Primrose MH, Neilson JP et al. Pregnancy screening by Doppler uteroplacental and umbilical artery waveforms. Br J Obstet Gynaecol 1989; 96:1163–67.

126. Newnham JP, Patterson LL, James IR et al. An evaluation of the efficacy of Doppler flow velocity waveform analysis as a screening test in pregnancy. Am J Obstet Gynecol 1990; 162:403–10.
127. Goncalves LF, Romero R, Gervasi M et al. Doppler velocimetry of the uteroplacental circulation. In: Fleischer A, Manning F, Jeanty P et al (Eds). Sonography in Obstetrics and Gynecology (Principles and Practice) 2001; New York, USA: McGraw Hill.
128. Bower S, Bewley S, Campbell S. Improved prediction of preeclampsia by two-stage screening of uterine arteries using the early diastolic notch and color Doppler imaging. Obstet Gynecol 1993; 82:78–83.
129. Martin AM, Bindra R, Curcio P et al. Screening for pre-eclampsia and fetal growth restriction by uterine artery Doppler at 11–14 weeks of gestation. Ultrasound Obstet Gynecol 2001; 18:583–86.
130. Snijders RJ, Sebire NJ, Cuckle H et al. Maternal age and gestational age-specific risks for chromosomal defects. Fetal Diagn Ther 1995; 10:356–67.
131. Kuhn P, Brizor M, Pandya P et al. Crown-rump length in chromosomally abnormal fetuses at 1–13 weeks' gestation. Am J Obstet Gynecol 1995; 172:32–35.
132. Schemmer G, Wapner RJ, Johnson A et al. First trimester growth patterns of aneuploid fetuses. Prenat Diagn 1997; 17:155–59.
133. Bindra R, Curcio P, Cicero S et al. Uterine artery Doppler at 11–14 weeks of gestation in chromosomally abnormal fetuses. Ultrasound Obstet Gynecol 2001; 18:587–89.
134. Aquilina J, Harrington K. Pregnancy hypertension and uterine artery Doppler ultrasound. Curr Opin Obstet Gynecol 1996; 8:435–40.
135. CLASP: A randomized trial of low dose Aspirin for prevention and treatment of preeclampsia among 9364 pregnant women. Lancet 1994; 343:619–22.
136. ECPPA: Randomized trial of low dose Aspirin for prevention of maternal and fetal complications in high risk pregnant women in Brazil. Br J Obstet Gynaecol 1996; 103:39–47.

Chapter 33
Doppler Study of Fetal Arterial Circulation

Giampaolo Mandruzzato, Gianpaolo Maso, Yoram Jacob Meir

Doppler ultrasound technology enables us to investigate with good accuracy the hemodynamic characteristics observable at the level of the fetal, placental and uterine circulation. As a consequence it has become possible to study blood flow patterns and their changes in normal pregnancies and complicated as well. Considering that in many adverse conditions, the most frequent being chronic hypoxemia, the fetus adapts by altering blood flow redistribution it is easy to believe that the possibility that Doppler investigation offers for studying this phenomenon is of great value in clinical assessment and management when a condition of increased risk for the fetus has been identified.

First of all it is necessary to remember some characteristics of the Doppler assessment. By using that technique and spectral analysis it is possible to obtain a Doppler Velocity Waveform (DVWF) that have a characteristic shape. The first part is representing the systolic phase of the cardiac cycle while the second reflects the diastolic phase. The latter is mainly influenced by the resistance downstream the investigated segment of the vessel. This is of course true only in regard to arteries. As the evaluation of flow velocities is strongly dependent on the angle of insonation (the angle between the ultrasound beam and the vessel) the so called “angle independent parameters” have been introduced. They are mainly based on the calculated ratio between systolic and diastolic velocities, therefore being at a certain extent not influenced by the angle of insonation. Anyway some conditions must be respected and the angle should be comprised between 30 and 60 degrees. The offered information is more “qualitative” than quantitative. The more commonly used parameters are: the S/D ratio, the resistance index (RI) and the pulsatility index (PI).Their formulas are represented in Figure 33.1. The PI probably offers a more complete information of the characteristics of the DVWF as it takes into account not only systolic and diastolic velocities but also the mean of the velocities. As already said the pattern of the diastolic phase is strongly influenced by the peripheral resistance

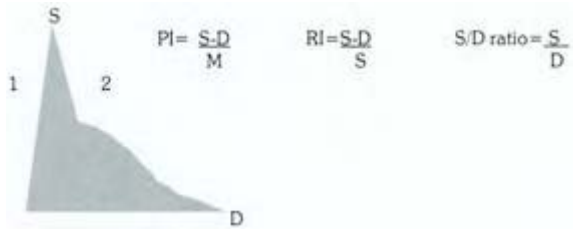

Figure 33.1: Angle independent parameters

that can be increased in case of vasoconstriction or obstructive vasculopathy or decreased in case of vasodilatation or shunting. In case of extreme peripheral resistance the diastolic velocity can be absent (EDFA) or even reversed (RF) these conditions are called ARED (Absent Reverse End Diastolic flow). When observing an apparent end diastolic flow absent it is necessary to set the highpass filter at the lowest possible level in order to avoid false-positive results due to the fact that some frequencies have not been considered. Moreover when using the PI it is necessary to remember that significant differences in the results can be obtained when using different equipments and as a consequence it is necessary or to use always the same equipment on the same patient or to have reference curves for any equipment.[1]

The fetal abnormal condition in which Doppler study can offer the best information for clinical use is represented by the chronic hypoxemia. The hemodynamic adaptation to this condition is well known since a long time from animal experiments.[2] The availability of a non-invasive technique, like Doppler, has offered the possibility to study this phenomenon also in the human fetus.

FETAL ARTERIES

The first step of the adaptation to chronic hypoxemia is represented by blood flow redistribution. After the introduction of Color Flow Mapping (CFM) it has become possible to identify and sample also very tiny vessels. In this way it is now available a map of the hemodynamic patterns observable on fetal and umbilical arteries and their changes along normal pregnancies and when chronic hypoxemia occurs. Object of studies have been: internal-carotid, cerebral arteries (middle, anterior and posterior), coronary and coronary sinus, aortic isthmus and aorta, superior mesenteric, renal, splenic, adrenal, iliac and femoral and anterior tibial arteries.

In normal cases the peripheral resistance is fairly constant in the fetal arteries while is progressively reduced in umbilical. When hypoxemia occurs the scenario is different as a consequence of blood flow redistribution. Somatic splanchnic and musculoskeletal arteries show an increased PI according to the presence of peripheral vasoconstriction while cerebral arteries depict a reduced PI subsequent to vasodilatation. This phenomenon is called “brain sparing effect” and has the target to reserve more

oxygenated blood to the very sensible central nervous system. A possible “sparing effect” has also been suggested for adrenal, splenic and coronaric arteries.[3-6]

A schematic representation of the Doppler patterns in fetal and umbilical arteries is given in Figure 33.2.

UMBILICAL ARTERIES

In the umbilical arteries through normal pregnancy a progressive reduction of the PI index is observable. When obliterative placental vasculopathy occurs, the principal cause of intrauterine growth

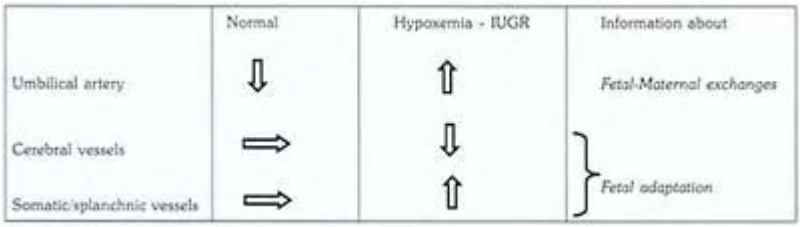

Figure 33.2: Peripheral and cerebral resistance (Pulsatility Indices) in normal and complicated pregnancies by hypoxemic IUGR

restriction (IUGR) and chronic hypoxemia, the peripheral resistance is increases as indicated by elevated PI.

It is necessary to remember a fundamental point: the hemodynamic characteristics and their changes in the umbilical arteries represent the normality of blood supply from the mother to the fetus and their possible reduction that is the cause of the fetal hypoxemia. On the contrary the hemodynamic patterns observable in fetal vessels indicate the normality of his oxygenation and when altered the response and adaptation to hypoxemia.

Due to the capacity of Doppler ultrasound, given a good equipment, a good expertise and a lot of patience and time it is practically possible to identify and sample also very tiny arteries offering a very comprehensive overview of fetal and placental hemodynamic.

CLINICAL APPLICATIONS

But going to the possible clinical application it is necessary to clarify which vessels must be investigated according to the existing evidence that the perinatal outcome is improved in risk pregnancies particularly in case of chronic fetal hypoxemia. This situation can occur in many clinical conditions but the most frequent is represented by IUGR. In fact

this situation can be observed in about 15% of the pregnancies and hypoxemia can be expected in about 30% of the cases and it is the principal cause of the poor outcome.

At the moment being only the Doppler study on the umbilical arteries has proofed to be effective in modulating the management and improving the outcome.[7–8] As already said umbilical arteries blood flow characteristics offers information regarding the maternal-fetal exchanges and how they can be potentially reduced by placental obliterative vasculopathy. It has been shown that the PI in umbilical arteries is proportional to the obliteration of the placental vascular bed[9] but also that the DVWF becomes altered when at least 60% of this obliteration has occurred.[10] Moreover it has been shown that DVWF of the umbilical arteries correlate with intravillous blood volume.[11] Nevertheless the information offered by umbilical arteries can be considered as only partial because it indicates the possible cause of fetal hypoxemia but not the effects on the fetus. It is easy to believe that studying also fetal arterial circulation it is possible to have a better and more comprehensive understanding of the clinical situation and therefore also the clinical management and outcome can be improved.

The first fetal vessel that has been sampled with Doppler has been the thoracic descending aorta.[12] It is easy to recognize and sample also without CFM and the first studies have shown that the peripheral resistance is increased in hypoxemia.[12] This increase reflects mainly the vasoconstriction at the level of somatic, splanchnic and musculoskeletal vessels and at a lesser extent also the increased impedance in the placenta. In fact a significant amount of the aortic blood flow goes to the umbilical arteries.

A group of IUGR fetuses underwent Doppler evaluation on the UA and FA.[13] According to the results they have been divided into 4 groups. In the 1st are the cases presenting ARED flow, in the 2nd are collected those with PI over the 2nd SD in both UA and FA, in the 3rd UA values were normal while FA showed abnormal PI and in the 4th both vessels depicted PI values in the range of normality. The prevalence of hypoxemia and/ or fetal distress (FD: defined as abnormal fetal heart rate variability by computer assisted cardiotochography, late decelerations and/or fetal acidemia in labor) has been calculated for each group (Table 33.1). It is easy to observe that the difference is statistically significant being 100% in the 1st group is progressively reduced moving to the 2nd, 3rd and 4th. It is clear that when ARED flow are present (group 1) severe hypoxemia always occurs and perinatal mortality is also observed and that when PI are normal in both vessels (group 4) hypoxemia has a lower prevalence even in IUGR.

Table 33.1: IUGR outcome according to Doppler characteristics in UA and fetal aorta (n. 653)

ARED	71	Fetal Distress (CS or IUD)	100%
UA-Ao >2SD	64	Fetal Distress (CS)	74%
UA normal, Ao>2SD	85	Fetal Distress (CS)	39%
UA-Ao normal	433	Fetal Distress (CS)	12%

Sensitivity and specificity of abnormal Doppler in UA and FA in predicting FD has been also calculated and it has been found that sensitivity is higher in FA than in UA while

specificity is much higher in UA as in FA. The reasons of this difference is clear when considering the background of abnormal DVWF already presented.

What is wise to discuss is the difference between group 2 and 3.

In both groups PI values for FA were abnormal while values over the 2nd SD in UA were only observed in the 2nd group. The difference in hypoxemia and FD requiring cesarean delivery is marked. As no cases of bad outcome have been observed in the 2 groups the conclusion is that by observing also FA Doppler a certain number of intervention has been avoided in the 2nd group and that using the same methodology a certain number of necessary interventions has been made in the 3rd.

Practically looking also at fetal hemodynamic and not only umbilicoplacental the clinical approach can be improved avoiding unnecessary interventions and/or performing without delay active management when necessary.

Cerebral arterial vessels (internal carotid, middle and anterior cerebral) have been also object of extensive study. The results are still conflicting. In fact the brain sparing effect (reduced PI in cerebral vessels together with increased PI in FA) should be considered as an adaptative phenomenon to hypoxemia. It has been observed that it is associated with accelerated shortening of visual evoked potential latency as an expression of accelerated neurophysiologic maturation being therefore a beneficial adaptative process.[14] Moreover it has been shown that in IUGR the presence of brain sparing effect is associated with a lower risk of intraventricular hemorrhage as compared to preterm infants.[15] Anyway it has been also suggested that sampling the anterior cerebral artery can offer better results as compared to the middle cerebral.[16]

CONCLUSIONS

As a conclusion it is possible to believe that Doppler assessment on UA and FA offering a more comprehensive overview of the maternal fetal blood supply and of the fetal response when used in risk pregnancies is in condition to:

1. Identify the group of fetuses that are or not suffering of chronic hypoxemia.
2. Assess the level of risk and to modulate the characteristics of the clinical management.

REFERENCES

1. Duggan PM, McCowan LME, Mitchell JM. Intermachine error in fetal Doppler velocity waveform analysis: a preliminary report. J Matern Fetal Invest 1994;4:15.
2. Dawes GS. Foetal and Neonatal Physiology Year Book Medical Publishers Inc. Chicago 1968
3. Mari G, Uerpairojkit B, Abuhamad AZ, Copel JA. Adrenal artery velocity waveform in the appropriate and small-for-gestational-age fetus. Ultrasound Obstet Gynaecol 1996;8:82.
4. Abuhamad AZ, Mari G, Bogdan D, Evans AT. Doppler flow velocimetry of the splenic artery in the human fetus:Is it a marker of chronic hypoxia? Am J Obstet Gynaecol 1995;172:82.
5. Gembruch U, Baschat AA. Demonstration of fetal coronary blood flow by color-coded and pulsed wave Doppler sonographyia possible indicator of severe compromise and impending demise in intrauterine growth ratardation. Ultrasound Obstet Gynaecol 1996;7:10.
6. Chaoui R. The fetal “heart sparing effect” detected by the assessment of coronary blood flow: a further ominous sign of fetal compromise? Ultrasound Obstet Gynaecol 1996; 7:5.

7. Alfirevic Z, Neilson JR Doppler ultrasonography in high-risk pregnancies: Systematic review with meta-analysis. Am J Obstet Gynaecol 1995; 172: 1379.
8. Westergaard HB, Langhoff-Ross J, Marsal K et al. A critical appraisal of the use of umbilical artery Doppler ultrasound in high-risk pregnancies: use of meta analyses in evidence-based obstetrics. Ultrasound Obstet Gynaecol 2001; 17:466.
9. Giles W, Trudinger B, Baird F PBP et al. Umbilical flow velocity waveform and placental resistance: pathological correlation. Br J Obstet Gynaecol 1985; 92:31.
10. Trudinger B, Cook CM. Doppler umbilical and uterine flow waveforms in severe pregnancy hypertension. Br J Obstet Gynaecol 1990; 97:142.
11. Hitshhold TR Doppler velocity waveform of the umbilical arteries correlates with intravillous blood volume. Am J Obstet Gynaecol 1998; 179:540.
12. Jouppila P, Kirkinen R Increased vascular resistance in the descending aorta of the human foetus in hypoxia. Br J Obstet Gynaecol 1984; 91:853.
13. Mandruzzato GP, Meir YJ, Natale R, Maso GR Antepartal assessment of IUGR fetuses. J Perinat Med 2001; 29:222.
14. Scherjon SA, Oosting H, Ongerboer BW et al. Fetal brain sparing is associated with accelerated shortening of visual evoked potential latencies during early infancy. Am J Obstet Gynaecol 1996; 175:1569.
15. Mari G, Abuhamad AZ, Heller M et al. Is the fetal brain-sparing effect a risk factor for the development of intraventricular hemorrhage in the preterm infant? Ultrasound Obstet Gynaecol 1996; 8:329.
16. Dubiel M, Gunnarsson GO, Gudmundsson S.Blood redistribution in the fetal brain during chronic hypoxia. Ultrasound Obstet Gynaecol 2002; 20:117.

Chapter 34
Doppler Study of Fetal Venous System

Gianpaolo Maso, Giancarlo Conoscenti, M Piccoli

INTRODUCTION

Fetal blood flow measurements have become an important tool in the surveillance of high risk pregnancies. There is a vast amount of literature on umbilical arteries and fetal arterial system, but fetal venous circulation has only recently been evaluated.

The introduction of high-resolution ultrasonography, combined with color-Doppler imaging, offered a breakthrough in the study of the fetal venous system, considerably enhancing our understanding in normal physiologic conditions, as well as in abnormal circumstances.

This review will focus on the embryologic, anatomic and physiological characteristics of the fetal venous circulation. The knowledge of the development and physiology represents the basis to understand the structural anomalies and the hemodynamic changes that occur in the venous district in pathological conditions.

EMBRYOLOGY OF THE FETAL VENOUS SYSTEM

In a 4-week embryo three pairs of veins are found.

The vitelline veins run from the yolk sac to the sinus venosus via liver sinusoid, and are connected to each other via anastomoses around the duodenum.

The umbilical veins transport oxygenated blood from the chorion to the sinus venosus, bypassing the liver. They merge with the cardinal veins, the third pair of embryonic veins, that originate from the body of the embryo and open into the right and left horns of the sinus venosus of the primitive heart.

The fetal liver and its development in the septum transversus play an important role in modifying the primitive vitelline and umbilical veins into their final morphology.

With the rapid growth of the liver, the umbilical veins (UV) connect with the liver sinusoids. The asymmetric development of the heart and the rotation of the intestinal tract cause the major change in the venosus circulation by forming a single venosus blood stream from left to right.

In the 6 mm long embryo, the complete right umbilical vein, the cranial part of the left umbilical vein, the left vitelline vein and part of the anastomoses obliterate and a new

vessel, the ductus venosus (DV), develops. This is a shunt vessel between the left umbilical vein and the right hepatocardinal channel, that will become the upper inferior vena cava (IVC). At this stage all the placental blood enters the right atrium through the left distal umbilical vein, ductus venosus and proximal right vitelline vein, which by pass the liver sinusoids. The upper two anastomoses of the distal vitelline veins fuse to form the portal vein, whereas the distal anastomoses form the superior mesenteric and splenic veins and the proximal parts become the hepatic veins.

Inferior vena cava and superior vena cava (SVC) originate from the cardinal veins that are the main drainage system of the embryo's body. The anterior and posterior cardinal veins drain the cranial and caudal part of the body of the embryo, respectively. The left brachiocephalic vein is formed during the eighth week from the right anterior and right common cardinal veins, through left to right anastomoses, whereas the left anterior cardinal vein disappears. Azygos and hemyazigos veins originate from upper portion of the division of the supracardinal veins, whereas the caudal part becomes the caudal part of the IVC.[1–4]

ANATOMY OF THE FETAL VENOUS SYSTEM

Two venous systems can be identified within the fetal liver: an afferent system, or umbilical-portal system, taking blood from the placenta and gut to the liver, and an efferent system, given by the hepatic veins, taking blood from the liver to the heart (Fig. 34.1). The DV shunts oxygenated blood from the umbilical-portal system directly to the heart.

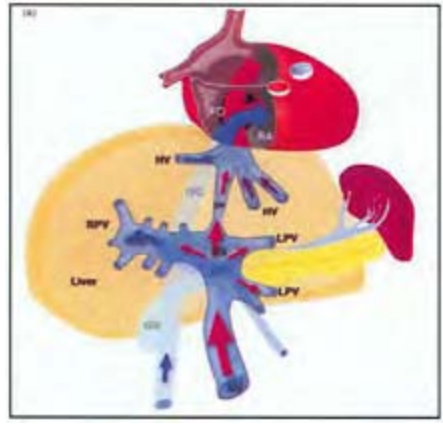

Figure 34.1: Representation of fetal umbilical and hepatic venous system. The arrow indicates the direction of flow. The color shows the degree of oxygenation (red=high, purple=

medium, blue=low). FO: foramen ovale; RA: right atrium; DV: ductus venousus; UV, umbilical vein; HV: hepatic veins; JVC: inferior vena cava; PS: portal sinus; LPV: left portal vein; RPV: right portal vein; EPV: extrahepatic portal vein; GB: gallbladder (reprinted with permission from Ultrasound Obstet Gynecol 2001; 18:598–604)

In the afferent venous system, the UV enters the abdomen within the falciform ligament, ascending steeply towards the liver and runs along its surface in cephalad direction. It then joins a confluence of vessels termed the portal sinus. This is a wide L-shaped vessel at the distal part of the UV, connecting the right and left intrahepatic portal veins. These perfuse the right and left hepatic lobes, respectively. There are two main left (superior and inferior) intrahepatic portal veins. The right intrahepatic portal vein shows a more abundant branching pattern. The vein originating from the confluence of the splenic and superior mesenteric veins outside the liver represents the extrahepatic portal vein.

The DV originates from the portal sinus as the latter turned at an almost right angle into the right lobe of the liver. The diameter of the DV is approximately one-third that of the UV. This is a branchless, hourglass-shaped vessel ascending in the direction of the diaphragm, which joins distally with the hepatic left vein and the IVC, just proximal to the entrance into the right atrium. The existence of a "sphincter" that regulates the blood flow through the DV to the heart has been postulated, and it has been supposed that the control of this anatomic structure is oxygen concentration-dependent.

The efferent system is represented by a number of vessels arising from the right and left hepatic lobes (right, middle and left hepatic veins), which drains into the subdiaphragmatic vestibulum. The funnel-shaped of the hepatic veins, DV and IVC open into the subdiaphragmatic vestibulum, an inverted, funnel shaped, vascular space just below the diaphragm, ending into the right atrium.[3–5]

PHYSIOLOGY OF THE FETAL VENOUS SYSTEM

The anatomical relationship in the hepatic afferent venous system supports the well established concept that oxygenated blood flow from the placenta is distributed through the UV to the portal sinus, which supplies the left and right intrahepatic portal veins and DV. Deoxygenated blood from the extrahepatic portal vein is diverted almost exclusively to the right hepatic lobe. The alignment of UV and DV, although not in anatomical continuity for the interposed portal sinus, favors the preferential streaming of oxygenated blood to the DV and consequently to the heart. Approximately 50% of the UV blood flow enters the DV and accounts for 98% of blood flow through the DV. The portal blood is mainly directed to the right lobe of the liver.

As far as the vessels of the efferent venous system is concerned, it is possible to observe that the right hepatic vein runs parallel to the IVC, while the left and middle hepatic veins run parallel to the DV. It has been postulated that this spatial rearrangement is the consequence of distribution of more oxygenated blood flow. The left hepatic lobe, in fact, is primarily supplied with the blood flow from the UV via the left portal vein.

Moreover it has been shown that there is streamlining of blood flow within the thoracic IVC: blood flow from DV and left hepatic vein flows in the dorsal and leftward part, whereas blood from the right lobe from the distal IVC and the right hepatic lobe flows in the ventral and rightward stream part of IVC. The ventral and rightward stream, together with blood from SVC, is directed to the right atrium and through the tricuspid valve into the right ventricle, ejected into the main pulmonary artery and shunted, via ductus arteriosus, into the descending aorta. The dorsal and leftward stream is directed towards the foramen ovale thereby delivering well-oxygenated blood flow directly to the left heart and, via ascending aorta, to the myocardium and the brain.[3,6,7]

NORMAL DOPPLER FINDINGS

The application of high resolution and color Doppler ultrasonography has allowed the structural and functional evaluation of fetal venous system.

At sonography, the UV can be detected in a sagittal or transverse section of the abdomen. At transverse section it curves towards the right side of the upper abdomen margin with the right portal vein.

The DV can be visualized in its full length in a midsagittal longitudinal section of the trunk or in an oblique transverse section through the upper abdomen. Its origin from UV can be found where color Doppler indicates higher velocities compared with the flow in UV, and sometimes this produces an aliasing effect. The blood flow velocities accelerates due to the narrow lumen of the ductus venosus, the maximum inner width of the narrowest portion being 2 mm (Figs 34.2 and 34.3).

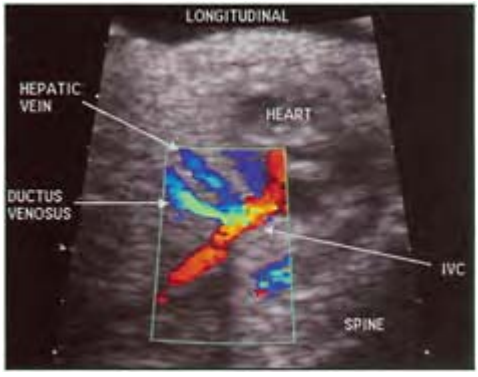

Figure 34.2: Oblique section of the fetal upper abdomen. DV and hepatic vein merge into IVC forming the

subdiaphragmatic infundibulum, a funnel shaped, vascular space just below the diaphragm, ending into the right atrium

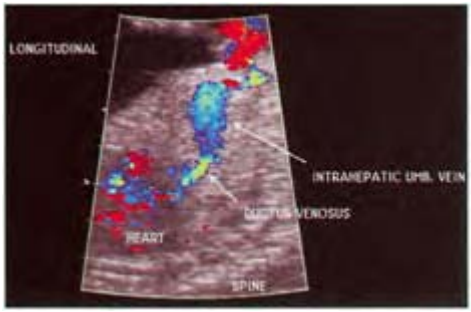

Figure 34.3: Midsagittal longitudinal section of the fetal trunk: DV is visualized in its full length arising from UV, where color Doppler indicates higher velocities compared with the flow in UV: aliasing effect is present

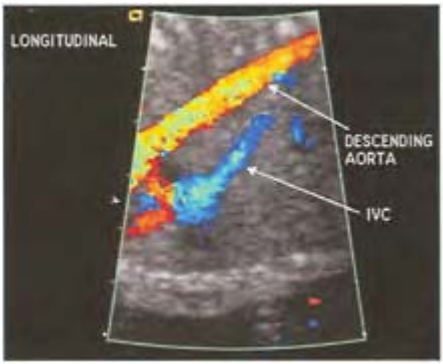

Figure 34.4: Longitudinal coronal plane of the upper abdomen: IVC runs anterior, to the right of and nearly parallel to the descending aorta

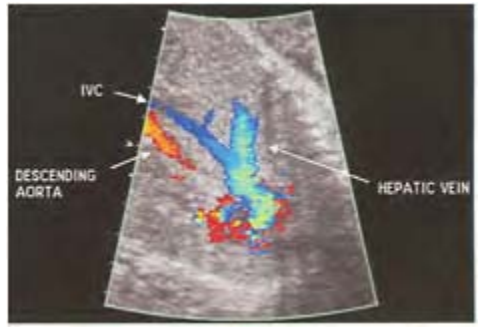

Figure 34.5: Sagittal-coronal section through the right hepatic lobe. The right hepatic vein and IVC merge into the subdiaphragmatic infundibulum

The best ultrasound plane to evaluate IVC is a longitudinal coronal plane, where it runs anterior, to the right of and nearly parallel to the descending aorta (Fig. 34.4).

The hepatic veins can be visualized either in a transverse scan section through the upper abdomen or in a sagittal-coronal section through the hepatic lobes (Fig. 34.5).

The typical waveform for blood flow in venous vessels, excluding UV and portal veins, consists in three phases related to the cardiac cycle (Fig. 34.6). The highest pressure gradient between the venous vessel and the right atrium occurs during ventricular systole (S), resulting in the highest blood flow velocities forward the fetal heart during that part of the cardiac cycle. Early diastole (peak D or e) with opening of the atrioventricular valves and passive early filling of the ventricles (peak E of the biphasic atrioventricular flow waveform) is associated with a second forward peak flow. The lowest velocities (a) in fetal venous vessels can be observed during the atrial contraction of the late diastole (peak A of the biphasic atrioventricular flow waveform).

The DV flow pattern is characterized by a triphasic forward flow (Fig. 34.7): It is directed toward the heart through the whole cardiac cycle.

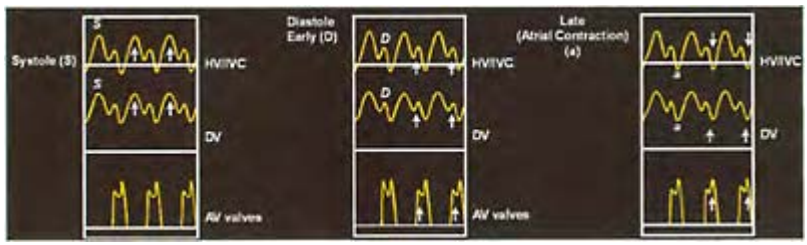

Figure 34.6: Ductus venosus (DV), hepatic veins (HV) and inferior vena cava (IVC) Doppler waveforms pattern

and their relation with the cardiac cycle (AV: atrioventricular valves; S: systole; D: early diastole). A physiologic reverse flow is evident in IVC/HV during atrial contraction (a). (With permission from Hecher K. The fetal venous circulation. In Harrington K. and Campbell S (Eds). A Colour Atlas of Doppler Ultrasonography in Obstetrics, 71–79)

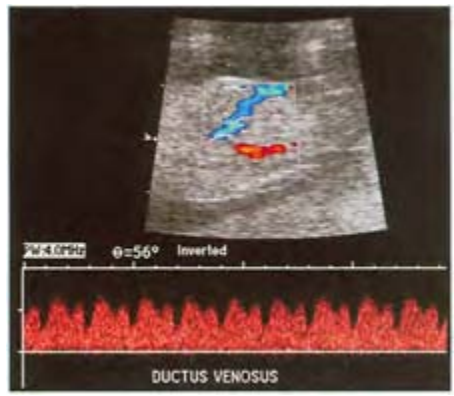

Figure 34.7: The triphasic forward Doppler flow waveform of DV. It is directed toward the heart through the whole cardiac cycle. A nadir of forward flow is observed during atrial contraction

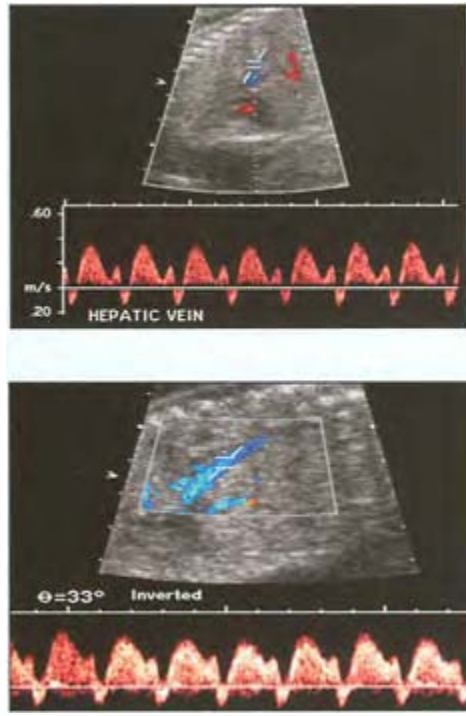

Figures 34.8 and 34.9: Doppler flow waveform of hepatic vein and IVC: a physiological slight reversal flow is recorded during atrial contraction (a).

Even in early pregnancy, there is no retrograde flow during atrial contraction (a).

In IVC and hepatic veins (Figs 34.8 and 34.9) a physiological reverse flow during atrial contraction (a) is observed. The percentage of reverse flow in IVC decreases with advancing gestational age.

As for the site of sampling, this is of main importance in the evaluation of fetal venous system.

It has been shown that the highest velocities of the DV are at the inlet, immediately above the UV, respect to the outlet into IVC. It has been established that the inlet part of DV should be evaluated for Doppler waveform analysis.

As for IVC, a large standard deviation for various Doppler waveform variables and a mixture of overlapping signals from different bloodstreams have been shown at the subdiaphragmatic venous infundibulum. It has been established that the site of sampling is between the renal vein and DV: this is the place of highest reproducibility.[6–9]

More than ten different angle-independent indices form the IVC and DV have been proposed and references ranges have been built (Fig. 34.10). Even if flow volume and absolute velocity measurements can be evaluated, it has been

Figure 34.10: Representation of Doppler velocity waveform of IVC and DV: angle-independent indices reported in the literature. S: systole; D: diastole; A: atrial contraction; TVI: time velocity integral; PV: peak velocity; PLI: preload index; PVIV: peak velocity index for vein; PIV: pulsatility index for vein

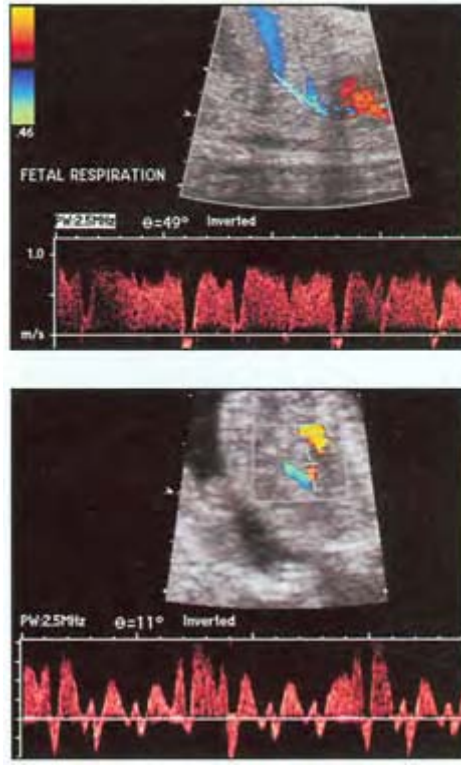

Figures 34.11 and 34.12: Doppler flow waveforms during breathing movements in DV e IVC. The shape of Doppler waveforms shows persistent changes: a raised abdominal-thoracic pressure gradient is responsible of an increase of flow during breathing movements with a vessel collapse during inspiration

demonstrated to have higher inaccuracies and intraobserver variations compared to velocity ratios. This is mainly due to vulnerable errors of the evaluation of vessel diameter measurements and unreliable or high angle of insonation.

The mean and peak velocities increase significantly in venous vessels with advancing gestational age. Velocities are highest in DV and lowest in the right hepatic vein.

Conversely, the angle-independent indices decrease during gestation and this is consistent with a decrease in cardiac afterload due to the decrease in placental resistance. It may also reflect increased ventricular compliance. The decrease in cardiac afterload

causes a decrease in enddiastolic ventricular pressure and therefore an increase in venous blood flow velocity towards the heart during atrial contraction.[10,11]

As shown for arterial Doppler evaluation, from a methodological point of view, it is essential to avoid measurements during fetal breathing movements. Changes in intrathoracic pressure during breathing movements have significant effects on Doppler waveforms. Inward movement of the abdominal wall during inspiration is accompanied by an increase of blood flow velocities, whereas a decrease in velocities is evident during expiration. As the shape of Doppler waveforms shows persistent changes during breathing movements, indices or velocity ratios should be evaluated during fetal apnea (Figs 34.11 and 34.12).[6,7,12]

The easiest vessel to investigate is the UV. References ranges for quantitative umbilical vein blood flow has been also built, according to the formulas: UV volume flow (mL/min)=Time Averaged Velocity (mm/s) x Cross-sectional vessel area (mm^2); UV absolute flow (mL/min)= vessel cross-sectional area (mm^2) x Mean velocity x 60. However, methodological differences in blood flow study have limited its evaluation in clinical practice. Qualitative analysis of the UV waveform shows physiologically a continuous forward flow without pulsations after the first trimester (Fig. 34.13). Mild sinusoidal pulsations synchronous with the fetal heart rate has been described in

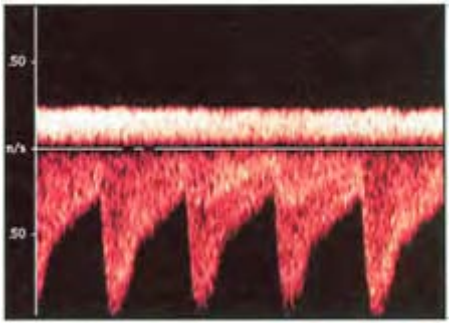

Figure 34.13: Qualitative analysis of the UV waveform: a physiologic continuous forward flow without pulsations is observed after the first trimester

some normal fetuses between 34 and 38 weeks and during fetal breathing movements (20% of the cases in the free-loop portion). These have to be distinguished from the pathological pulsations in cases of severe fetal compromise and nonimmune hydrops.[6,13,15]

STRUCTURAL ANOMALIES OF THE FETAL VENOUS SYSTEM

A short review of the embryologic landmarks has been given in order to understand the fetal venous system structural anomalies (second subtitle of this chapter).

The abnormal development of fetal venous vessels may be related to either of two different pathogenesis: the primary failure to transform or to form the critical anastomoses and the secondary occlusion of an already transformed system.

On the basis of the etiology (primary or secondary), the vessel involved, and the embryologic precursor, four major groups of anomalies can be identified (Table 34.1): 1. Abnormal connection of the cardinal veins; 2. Abnormalities of the UV; 3. Abnormalities of the vitelline veins; 4. Anomalous pulmonary venous connection (not discussed in this chapter).

Table 34.1: Classificatii of fetal venous system anomalies (reprinted with permission from J Ultrasound Med 2002; 21:1145–1158)

A. Cardinal veins
a. Complex malformations, heterotaxic syndrome
b. Isolated malformation
B. Umbilical veins
a. Primary failure to create critical anastomoses
• Complete: abnormal connection of UV (venosus shunts) into iliac vein, JVC, SVC, and right atrium
• Partial: Persistent of right umbilical vein (PRUV) with or without DV
b. Secondary occlusion
C. Vitelline veins
a. Primary failure to create critical anastomoses
• Complete agenesis of portal system
• Partial agenesis of right or left portal branch (portosystemic shunt)
D. Anomalous pulmonary venous connection (total or partial)

Anomalies of the fetal venous system may be also classified simply considering either 1. the abnormalities of the caval venous system, or 2. the anomalies of umbilical, portal and hepatic veins.

The abnormal connections of the cardinal veins are part of the heterotaxy syndromes.

An interrupted or absent IVC with azygos vein continuation or the persistence of left SVC are the result of primary failure to create the anastomoses in embryologic period and may be a sign of cardiosplenic syndromes.

The anatomical correlations of aorta, to IVC and the spine, and the venous connections to the atria are very helpful to diagnose left and right atrial isomerism. In situs solitus the

aorta is located to the left of the spine, whereas in situs inversus the location is reversed. In right isomerism the aorta and IVC are on the same side of the spine, either right or left. Aplasia of the spleen should be a sign of right isomerism. In the left isomerism the aorta runs medial to the spine, the IVC is not identified and the azygos vein runs dorsal and lateral to the aorta, either on the right or on left side. In this subtype of heterotaxy syndrome, multiple spleen are usually present. A situs ambiguus is a common finding in both types of isomerism: the stomach can be in a left, or right, or medial position. The position of the liver can be variable, as well.[2–4,6,16]

Abnormalities of the IVC and SVC, are often associated with major impairments of the heart development, intestinal tract and body symmetry, influencing significantly the prognosis.[2–4,6]

The anomalies of the umbilical veins represent the major and most common group of the fetal venous system structural anomalies.

Primary failure to form the critical anastomoses results with an aberrant vessel that shunts the blood flow from the placenta to the systemic veins. This spectrum of anomalies may involve the iliac vein, the IVC or SVC, or the direct connection with the right atrium. Agenesis of DV is a common feature of these group of anomalies. Two forms may be identified.

The first one is represented by the direct connection of the UV with the systemic venous circulation, by passing the liver. This is often associated with Noonan syndrome, pleural effusion and hydrops.

The second form includes cases in whom the UV is adequately connected with portal vein, but fails to establish a communication with the persistent proximal part of the right vitelline vein. The result is a prolonged hypoperfusion of the liver that may lead to portal hypertension.[2–4,17,18]

Partial failure to form critical anastomoses in left and right veins is quite common. Persistence of the right umbilical vein (PRUV) is the most common anomaly observed. Three types may be identified: the intrahepatic form (the UV is connected with the right portal vein instead of the left portal vein), the form connected directly to the iliac vein, IVC or right atrium, and the type in which both UVs persist.[19]

The first type is commonly identified as an isolated finding, and is considered a benign variant, whereas the other two are often associated with complex anomalies, especially cardiac malformations.

The pathophysiologic mechanisms, primary or secondary, of PRUV seems to be related to occlusion by thromboembolic events arising from the placenta. Teratogenic agents have been advocated as inducing primary failure of the critical anastomoses.

The anomalies of the vitelline veins are extremely rare and only few cases have been reported in prenatal literature. Primary failure to form the critical anastomoses may lead to complete agenesis of the portal system or to partial agenesis of the right or left portal vein. In the complete form, enterohepatic circulation is shunted systemically.

Partial forms of absence of the portal system might a more benign form of the vitelline veins abnormalities.[2–4]

VENOUS SYSTEM DOPPLER AND FETAL DISEASES

Umbilical vein pulsations with moderate to severe notches synchronous with atrial contraction has been described as an ominous sign. They are associated with various fetal pathological conditions such as, non-immune hydrops (NIH), fetal arrhythmia, fetal congestive heart failure, placental anomalies, fetal growth restriction (FGR), absent/reverse end diastolic flow (ARED) in umbilical artery (UA) and abnormal fetal heart rate patterns.

Different pathophysiological mechanisms may lead to UV pulsations. Single pulsation, caused by changes in forward flow from the placenta, might be related to ARED flow in UA during diastole or bradycardia, umbilical cord occlusion and true knot on the cord during systole. Diphasic pulsations, due to increased central venous pressure and/or opening of the DV, can be secondary to congestive heart failure or imminent fetal hypoxemia/acidemia (Fig. 34.14).[20]

Non-immune hydrops fetalis (NIHF) is a severe clinical condition of varying etiologies with poor prognosis. Differentiating between NIHF caused by congestive heart failure and other non-cardiac causes is essential to formulate a prognosis.

In presence of NIHF and umbilical pulsations, the right ventricular shortening fraction is significantly decreased, and abnormal venous return to the heart is consistent with decreased cardiac output, leading to congestive heart failure and poor fetal outcome.

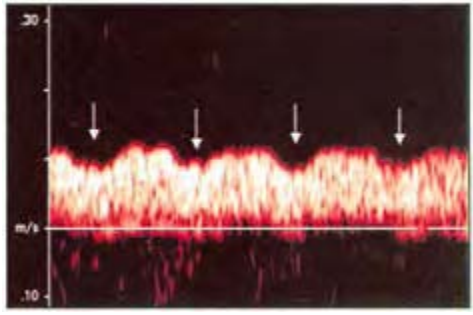

Figure 34.14: Umbilical vein pulsations with notch synchronous with atrial contraction. Diphasic pulsations due to the increased central venous pressure and/or opening of the DV may be secondary to congestive heart failure or imminent fetal hypoxemia/acidemia

Structural heart diseases involving ventricular outflow, with or without hydrops, are frequently associated with abnormal venous blood flow. Altered pump function with increased workload causes a decrease, or even the reversal blood flow during atrial contraction. Increased reversed phase in IVC, in cases with tricuspid regurgitation is

frequently associated to fetal hydrops. Increased central venous pressure due to regurgitant flow into the atrium can cause hydrops, which implies poor prognosis.

The diagnosis of the different types of fetal arrhythmias is possible by simultaneous waveform recordings from abdominal aorta and IVC. Highvelocity reverse flow due to increased right pressure is found either in atrial contraction against a closed tricuspid valve, or in tricuspid regurgitation. The first occurs during premature atrial contraction and with complete atrioventricular block, the second during premature ventricular contraction.

Premature beats of supraventricular or ventricular origin can be differentiated depending on the characteristic differences in blood flow velocity waveforms of the venous vessels (IVC) during atrial contraction. During premature beats of atrial origin an exaggerated reverse flow is recorded earlier than expected during the heart cycle. In cases of premature beats of ventricular origin, the reverse flow is evident at the moment of end diastole, with a typical lag pattern in blood flow velocity after ventricular premature beat.[6–20]

Venous Doppler analysis is also essential to manage supraventricular tachycardia. From the observation of venous flow patterns (IVC, DV), it is possible to delay antiarrhythmic treatment if the heart rate is below 210 beats/mm. Above this critical heart rate frequency, an abnormal monophasic forward flow is observed in DV and IVC. This pattern is related to direct impediment of diastolic filling causing elevation of atrial and venous pressure. Due to the presence of a parallel fetal flow circuitry, the increase of the left atrial pressure leads to right side congestive heart failure and ventricular dysfunction.[6–21]

Fetuses with *intrauterine growth restriction (IUGR)* are usually delivered on the basis of abnormal results of non-stress tests such as fetal heart rate (FHR) monitoring, biophysical profile or the presence of maternal pathological conditions. Although introduction of arterial Doppler ultrasound evaluation has resulted in a significant decrease in perinatal mortality and morbidity, the transition between adaptation and decompensation due to fetal hypoxaemia/acidemia is difficult to identify accurately.

The decision regarding the optimal time of delivery, to avoid iatrogenic delivery of a mild affected premature neonate before irreversible asphyxia-related damage, is still a dilemma. The arterial multivessel evaluation (umbilical artery, descending aorta, middle cerebral artery) is commonly used in clinical practice to assess fetal well-being in high risk pregnancy. However this assessment has a limited value in determining the time of delivery.[6,22–24]

Although maximal decrease in vascular cerebral resistance has been found to precede the onset of late decelerations by an average of two weeks, it has been insuitable to monitor IUGR fetuses closely during the last two weeks preceding the occurrence of acute distress or intrauterine death.

The Doppler study of the fetal venous blood flow in IVC and DV and other venous vessels (sinus transversus, right hepatic vein) have raised new expectations by investigating fetal hemodynamic changes more accurately.

Two mechanisms can be considered for the onset of abnormal venous Doppler waveform: the increase of right ventricular afterload, and the myocardial failure. As long as the fetus is able to compensate for reduced placental supply by redistribution, preferential myocardial oxygenation delays the development of right heart failure, despite

an increasing afterload. Progressive changes in fetal venous circulation may indicate failure of the compensatory mechanism and herald the development of right heart failure due to myocardial hypoxemia.[6,9,10]

It has been shown that evaluation of Doppler venous waveforms are correlated to computerized

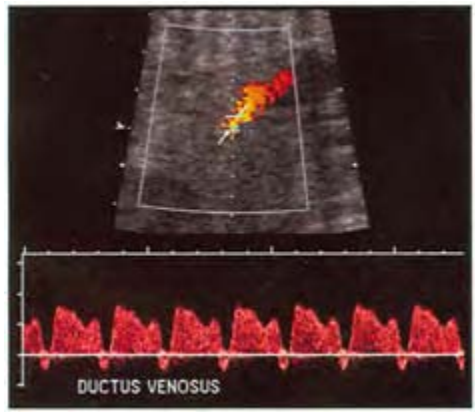

Figure 34.15: Abnormal DV waveform: reversal flow during atrial contraction is the consequence of increased end-diastolic pressure

analysis of FHR monitoring: reverse flow in DV is significantly correlated with values of short-term variation below 3.5 ms, ominous sign of hypoxemia/acidemia (Fig. 34.15).

Despite of promising results, the use of these venous parameters has not yet found widespread application in assessing FGR fetuses. Several reasons can be advocated. Firstly, the technical difficulty of the examination confines its use to few highly specialized units. Secondly, the venous vessel that best predict acidosis has not yet established. Moreover, within the same vessel, it is not which Doppler index has the highest discriminatory value to predict hypoxemia/acidemia.

Besides recent longitudinal studies on venous Doppler, biophysical profile, and computerized FHR monitoring, it has not been yet assessed what is the best method for timing the delivery of preterm severe growth restricted fetuses.[25–29]

The widely held view that, in any case, venous Doppler abnormalities would precede deterioration of biophysical parameters has not been observed.

Ferrazzi et al[29] reported that more than 50% of the fetuses delivered because of an abnormal FHR pattern did not have venous Doppler abnormalities.

Hecher et al[27] observed that among fetuses born before 32 weeks' gestation, persistent abnormalities in FHR tracings preceded the occurrence of an abnormal DV pulsatility index in about 53% of the cases and simultaneous anomalies were detected in 5% of the cases.

Muller et al[24] found that absent/reverse flow in DV in a group of cases with umbilical artery ARED flow is significantly predictive of poor outcome. Delivery was indicated by non reassuring status defined as either CTG pathological pattern or when suspicious FHR traces were associated with absent or reverse flow during atrial contraction. However it is not indicated how many cases of normal DV Doppler flow waveforms were delivered for abnormal CTG pattern.

Baschat et al[30] reported that the deterioration of arterial/venous parameters occurred before an abnormal biophysical profile within 24 hours in the majority of the cases.

This data show that hemodynamic changes of redistribution of flow and decompensation, as detected by an abnormal FHR trace, biophysical profile or venous Doppler, are widely variable among fetuses and does not follow a predictable physiopathological cascade.

Probably the combination of Doppler evaluation of the fetal circulation, to assess cardiac function, and biophysical parameters/computerized CTG, as a reflect of central nervous system involvement, should allow a more precise information about the pathophysiology and assessment of fetal growth restriction.

A multicenter randomized clinical trial should be addressed to assess what is the best method to monitoring and timing the delivery of severe premature growth restricted fetuses.[31]

CONCLUSIONS

In recent years, high resolution sonography, combined with Color-coded Doppler, has advanced our ability to investigate the fetal venous system. This non-invasive technique has enhanced our understanding of the fetal venous circulation in physiologic condition and provide us the possibility to evaluate circulatory changes in abnormal circumstances.

From the literature, it can be concluded that fetal venous Doppler may be an helpful diagnostic tool and may influence the management of fetal diseases such as cardiovascular pathologies, hydrops and fetal growth restriction.

As for the latter condition, the longitudinal Doppler analysis of fetal arterial and venous districts provide us essential information about the progressive deterioration that occurs in chronic hypoxemia. It is clear that abnormal venous Doppler has a high likelihood of perinatal mortality/morbidity. However further studies are needed to clarify the role of fetal venous Doppler in the timing of delivery. The understanding of the variables that affect the physiopathological changes in severely compromise fetuses should provide us this crucial information.

REFERENCES

1. Hamilton WJ, Mossman HW. Human Embriology (4th ed). Cambridge: Heffer 1972;272–82.
2. Hoffstetter C, Plath H., Hansmann M. Prenatal diagnosis of abnormalities of the fetal venous system. Ultrasound Obstet Gynecol 2000; 15(3):231–41.
3. Fasouliotis SJ, Achiron R, et al. The human fetal venous system: normal embryologic, anatomic, and physiologic characteristics and developmental abnormalities. J Ultrasound Med 2002; 21(10):1145–58.

4. Achiron R, Hegesh J, Yagel S et al. Abnormalities of the central veins and umbilico-portal system: prenatal ultrasonographic diagnosis and proposed classification. Ultrasound Obstet Gynecol 2000; 16:539–48.
5. Mavrides E, Moscoso G, Caravalho JS et al. The anatomy of the umbilical, portal and hepatic venous systems in the human fetus at 14–19 weeks of gestation. Ultrasound Obstet Gynecol 2001; 18:598–604.
6. Hecher K, Campbell S. Characteristics of fetal venous blood flow under normal and during fetal disease. Ultrasound Obstet Gynecol 1996;7:68–83.
7. Moll W. Venous return in the fetal-placental cardiovascular system. Eur J Obstet Gynaecol 1999.
8. Hecher K, Campbell S, Snijders R et al. Reference ranges for fetal venous and atrioventricular blood flow parameters. Ultrasound Obstet Gynecol 1994;4:381–90.
9. Hecher K, Snijders R, Campbell S et al. Fetal venous, intracardiac, and arterial blood flow velocities in intrauterine growth restriction: relationship with fetal blood gases. Am J Obstet Gynecol 1995;173:10–15.
10. Rizzo G, Capponi A, Arduini D et al. The value of fetal arterial, cardiac and venous flows in predicting pH and blood gases measured in umbilical blood at cordocentesis in growth retarded fetuses. Br J Obstet Gynecol 1995;102(12):963–69.
11. DeVore GR, Horenstein J. Ductus venosus index: a method for evaluating right ventricular preload in the second trimester fetus. Ultrasound Obstet Gynecol 1993;3:338–42.
12. Reed KL, Anderson CF. Changes in umbilical venous velocities with physiologic perturbation. Am J Obstet Gynecol 2000;182(4):738–40.
13. Ferrazzi E. Measurement of venous blood flow in the human fetus: a dream comes true, but now for some standardization. Ultrasound Obstet Gynecol 2001; 18:1–4.
14. Ferrazzi E, Rigano S, Bozzo M et al. Umbilical vein blood flow in growth-restricted fetuses. Ultrasound Obstet Gynecol 2000; 16:432–38.
15. Barbera A, Gakan HL, Terrazzi E et al. Relationship of umbilical vein blood flow to growth parameters in the hum fetus. Am J Obstet Gynecol 1999;18(1): 174–79.
16. Patel CR, Lane JR, Muise KL. In utero diagnosis of obstructed supracardiac total anomalous pulmonary venous connection in a patient with right isomerism and asplenia. Ultrasound Obstet Gynecol 2001; 17: 268–71.
17. Gembruch U, Baschat AA, Caliebe A et al. Prenatal diagnosis of ductus venosus agenesis: a report of two cases and review of literature. Ultrasound Obstet Gynecol 1998;ll:185–9.
18. Jaeggi ET, Fouron JC, Hornberger LK et al. Agenesis of the ductus venosus that is associated with extrahepatic vein drainage: prenatal features and clinical outcome. Am J Obstet Gynecol 2002;187(4): 1031–37.
19. Wolman I, Gull I, Fait R, et al. Peristent right umbilical vein: incidence and significance. Ultrasound Obstet Gynecol 2002; 19:562–64.
20. Gudmunsson S. Importance of venous flow assessment for clinical decision-making. Eur J Obstet Gynecol Reprod Biol 1999;84(2):173–78.
21. Gembruch U, Krapp M, Germer U et al. Venous Doppler in the sonographic surveillance of fetuses with supraventricular tachycardia. Eur J Obstet Gynecol Reprod Biol 1999;84(2):187–92.
22. Hecher K, Campbell S, Doyle R et al. Assessment of fetal compromise by Doppler ultrasound investigation of fetal circulation. Arterial, intracardiac, and venous blood flow velocity study. Circulation 1995;91(l):129–38.
23. Hofstaetter C, Gudmundsson S, Hansmann M. Venous Doppler velocimetry in the surveillance of severely compromised fetuses. Ultrasound Obstet Gynecol 2002; 20(3):233–39.
24. Muller T, Nanan R, Rehen M, et al. Arterial and ductus venosus Doppler in fetuses with absent or reverse end-diastolic flow in the umbilical artery: correlation with short-term perinatal outcome. Acta Obstet Gynecol Scand 2002;22:786–91.

25. Senat MV, Schwarzler P, Alcais A et al. Longitudinal changes in the ductus venosus, cerebral transverse sinus and cardiotocogram in fetal growth restriction. Ultrasound Obstet Gynecol 2000;16(1): 19–24.
26. Machlitt A, Waur RR, Chaoui R. Longitudinal observation of deterioration of Doppler parameters, computerized cardiotocogram and clinical course in a fetus with growth restriction. J Perinat Med 2001; 29:71–76.
27. Hecher K, Bilardo CM, Stigler RH et al. Monitoring of fetuses with intrauterine growth restriction: a longitudinal study. Ultrasound Obstet Gynecol 2001; 18(6):564–70.
28. Hecher K, Hackeloer BJ. Cardiotocogram compared to Doppler investigation of the fetal circulation the premature growth-retarded fetus: longitudinal observation. Ultrasound Obstet Gynecol 1997;9(3):152–61.
29. Ferrazzi E, Bozzo M, Rigano S et al. Temporal sequence of abnormal Doppler changes in the peripheral and central circulatory systems of the severely growth-restricted fetus. Ultrasound Obstet Gynecol 2002;19:140–46.
30. Baschat AA, Gembruch U, Harman CR et al. The sequence of changes in Doppler and biophysical parameters as severe growth restriction worsens Ultrasound Obstet Gynecol 2001; 18(6):598–604.
31. Romero R, Kalache KD, Kadar N. Timing the delivery of the preterm severely growth-restricted fetus: venous Doppler, cardiotocography or the biophysical profile? Ultrasound Obstet Gynecol 2002;19(2):118–21.

Chatper 35
Postpartum Ultrasound

Ajlana Mulic-Lutvica

INTRODUCTION

Postpartum period usually includes six subsequent weeks during which normal pregnancy involution occurs and the uterus returns to the non-pregnant state. Our knowledge about postpartum changes in the uterus comes from clinical examinations by abdominal palpation as well as from histological studies from the end of the 19th century and the early part of the present century when maternal mortality was high.[1]

Since its introduction into clinical practice in 1958 by Ian Donald et al[2] ultrasound has made the more extensive examinations of the postpartum uterus possible. Although puerperal uterus was one of the first organs to be examined by ultrasound[3–7] it is surprising that little advantage have been taken of this opportunity. In previously published studies concerning the involution process, the length,[4,6–11,13] width,[8] AP-diameter,[4] area[9] and thickness of the uterine wall[8] have been used as a measure of uterine involution. Majority of the studies described pathological conditions without knowledge about normal findings, they were restricted to the early puerperium and designs were cross-sectional.[3–7,12] Recently a few studies concerning uterine cavity during normal puerperium have been published.[14–16]

Postpartum complications involving the uterus occur in about 8–10% of cases. Immediate and late postpartum hemorrhage, puerperal sepsis, and septic pelvic thromboembolism are still potentially life-threatening conditions. Thus whenever puerperal complication occurs, the question is to be raised: “Is there any usefulness to switch on ultrasound machine?”

NORMAL PUERPERIUM

A description of normal ultrasound changes of the uterus and uterine cavity during puerperium is a prerequisite for ultrasound diagnosis of pathological conditions. We can follow the physiological destruction of the uterus weighing more than 1 kg soon after delivery to an organ weighing about 80 grams at the end of the puerperium by means of ultrasound. The involution changes concerning the size, shape, position, and texture of the uterus have been relatively well examined by ultrasound.[6,7,9–11,14] The influence on the

involution process of parity,[8–10,13,14] route of delivery,[11] oxytocin administration during labor[7] breast-feeding[9,11,13,14] or the infant's weight[11,13,14] have been studied. Previously published studies involving sonographic examination of uterine cavity are not unambiguous.[11,14–16]

In the early and middle puerperium (in the first 2 weeks) the transabdominal approach is to be recommended. A relatively short focal length of the vaginal probe limits its use during the early postpartum period when the uterus is too large and lies near to abdominal wall. In contrast, during the late postpartum period (>2 weeks) a high frequency transvaginal probe, which better distinguishes minor details, should be used. At that time the uterus is considerably decreased in size and it lies in the true pelvis. The postpartum uterus should be examined in three standard sections: sagittal, transverse and coronal (Fig. 35.1 and Figs 35.2a to c). Urinary bladder should be moderately filled. Gentle compression with the probe should be used in order to avoid uterine distortion.

We can differentiate three typical ultrasound pictures during normal puerperium: in the early, middle and late puerperium (Fig. 35.3). The involution of the uterus is a dynamic process that has no parallel in normal adult life. There are two physiological lifesaving processes occurring soon after placenta delivery: thrombotamponade (enhanced blood clotting activity) and myotamponade (compression of the vessels by myometrial contraction).

The appearance of ultrasound finding *in the early postpartum period* reflects these physiological changes. The uterus has an angulated form (Fig. 35.4A). It lies in a slightly retroverted position and arches over the sacral promontory. Wachsberg et al[13] pointed out the impact of uterine angulation on the measurement of uterine length and recommended segmental measurement. This angulated form of the early puerperal uterus has been previously described as a "hockey stick".[13] This form of the uterus is typical only in early puerperium and it is artificial. An extremely great (Fig. 35.3a). Sometimes this line can be irregular degree of uterine deformability is caused by a and thicker which probably depends on the heavy uterine corpus, a hypotonic lower uterine amount of retained decidua (Fig. 35.4a). The segment and supine position of the examined separation of the placenta and membranes woman. Lifesaving uterine contraction approaches generally occurs in the spongy layer, however the anterior and posterior uterine walls and just virtual level varies. Already in the 1931 Williams wrote cavity appears. The uterine cavity is empty and concerning the line of separation of the placenta decidua appears as a thin white line from the and membranes: "*While separation generally occurs in the spongy layer, the line is very irregular*

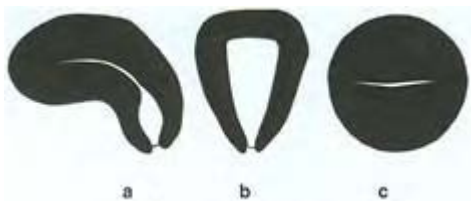

Figure 35.1: Three standard ultrasound sections of the puerperal

uterus: a longitudinal (a), a coronal (b) and a transverse (c)

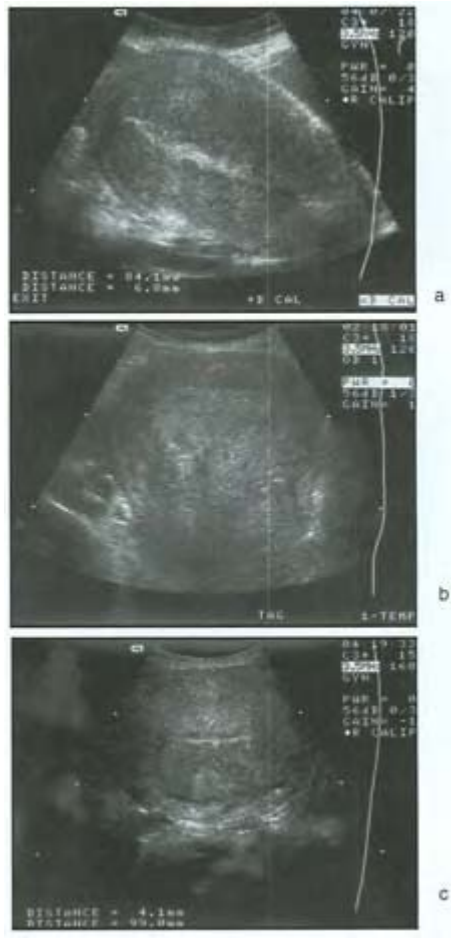

Figure 35.2: Transabdominal ultrasound scans of a normal puerperal uterus on day 1; a longitudinal scan (a), a coronal scan (b), and a transverse scan (c)

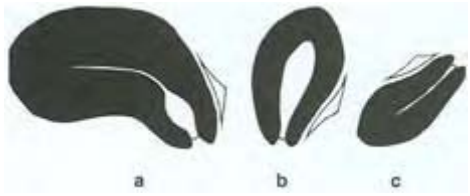

Figure 35.3: The normal ultrasound appearance of the uterus and uterine cavity during the puerperium: transabdominal approach during the early puerperium (a), and during the middle part of the puerperium (b), transvaginal approach during the late puerperium (c)

so that in places a thick layer ofdecidua is retained, in others only a few layers of cells remain, while in still others the muscularis is practically bare".[17] The variation in sonographic appearance of the cavity could be seen as a demonstration of these physiological variations in retained decidua. The white thin line seen on ultrasound might possibly represent cases in which only the basal decidual layer is retained or if the muscularis is practically bare. Whereas the thicker and more irregular lines might represent cases with retention of more spongy decidual layer and perhaps fragments of membranes.

Fluid or echogenic mass is not common finding in the cavity in the early postpartum period.[14] Small echogenic or echolucent dots in the cavity are harmless physiological findings.[18] A heterogeneous mass with fluid and solid components can be seen in the cervical area.[12,14,19] This finding has no clinical significance and the mass is usually expelled spontaneously. It probably reflects a collection of blood, blood clots and parts of membranes. On the posterior wall of the uterus the prominent uterine vascular channels are regularly seen.[11] They usually disappear during the 2nd and 3rd postpartum weeks as a result of

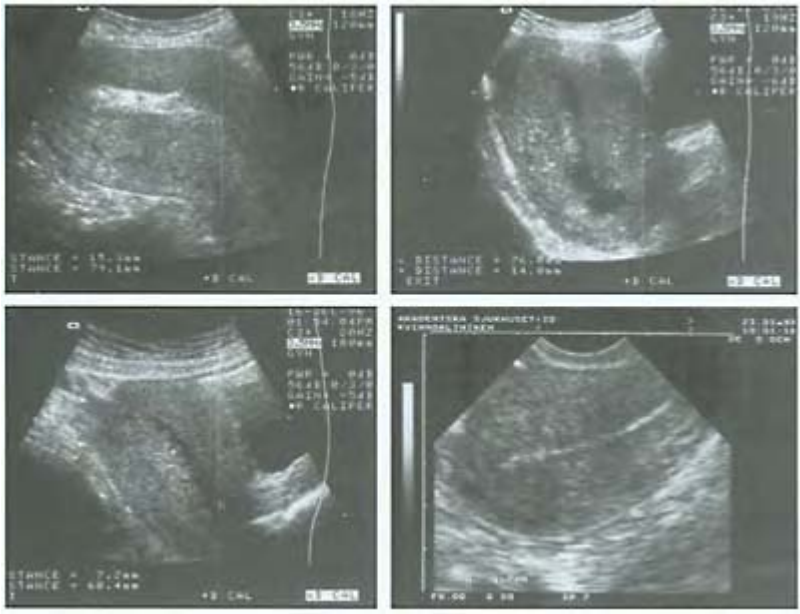

Figure 35.4: Transabdominal, longitudinal scans of the uterus from an uncomplicated puerperium on day 1(a), on day 7 (b), on day 14 (c) and on day 28 (d)

involution process, which decreases both the size and the amount of uterine vessels. Gas in the cavity is not common finding in the early postpartum period although it can be occasionally seen.[14] Wachsberg detected gas in 19% of normal population during the early postpartum period.[20]

Besides conventional ultrasound, Doppler technology is used to study hemodynamic events occurring during the puerperium. Normal preg¬ nancy requires the growth of many new vessels. Consequently during puerperium dramatically regressive changes occur. The physiological destruction of the uterus involves not only muscle cells and decidua but also the arteries. The mean pulsatility index of uterine arteries started to increase within 2 days after delivery.[15] The prediastolic notch is also detected in the early puerperium and these hemodynamic changes can be partly explained by the immediate contraction of the uterus.[15,21]

In the middle part of the puerperium (1–2 weeks postpartum) the uterus is somewhat diminished, the shape of the uterus is oval. It rotates along its internal cervical os towards an anteverted position probably due to forming a firm isthmus.[14] The vascular channels are not so prominent. Either pure fluid or mixed echo with fluid and solid components can be seen in the whole cavity not only in the cervical area (Fig. 35.4b and c). This finding reflects a normal healing process of the placental site inside uterine cavity,

necrotic changes of retained decidua and an abundant shedding of lochia. Echogenic mass or gas are not common findings during middle part of the puerperium. In contrast Edwards et al[16] found an echogenic mass in a great proportion of normal puerperal women. Tekay[15] and Kirkinen[21] studied the changes in vascular resistance of the uterine arteries in the puerperium and they reported that during the mid stable phase of 6 weeks the pulsatility indexes remain unchanged.

During late puerperium (1–2 weeks postpartum) the uterus is considerably diminished. It lies in an anteverted position in 88% of cases.[14] In 12% of cases the uterus has a retroverted position corresponding well to normal prevalence of retroversion of the uterus in general population. The uterine cavity is again empty. Decidua and necrotic vessel ends are exfoliated, the placental site is recovered and a new endometrium is regenerated from the basal layer of the decidua adjacent to the myometrium. In 1953 Sharman performed endometrium biopsies and identified fully restored endometrium from the 16th postpartum day.[22] Ultrasonically the cavity appears as a thin white line (Fig. 35.4d). This corresponds to an inactive endometrium and reflects the hypoestrogenic state of the puerperium (the physiologic menopause). Sometimes a small amount of fluid or echogenic dots can be seen. As regard to the hemodynamic changes during late puerperium, the pulsatility indexes in uterine arteries begin to increase.[15]

RETAINED PLACENTAL TISSUE

Both ultrasound diagnosis of retained placental tissue and appropriate management for late puerperal bleeding is still controversial issue.

Late postpartum hemorrhage occurs in about 1–2% of cases. In developed countries, half of postpartum women who are admitted to hospital with this condition undergo uterine surgical evacuation. In developing countries it is a major contributor to maternal death.[23] Alexander et al[23] identified 45 papers about the management of women with secondary postpartum hemorrhage and they concluded that no information was available from randomized trials to inform the management of women with this condition. Late postpartum hemorrhage is most often the result of abnormal involution of the placenta site in the uterine cavity and endometritis, but it may be caused by retention of placental tissue. It is well known that in only 30% of cases of postpartum bleeding is any placental retention present.[26] First studies concerning retained placental tissue performed with old compound ultrasound equipment showed high rate of false-positive diagnosis.[3,5] On the other side ultrasound appears as a valuable tool to confirm an empty cavity. Lee and Mandrazzo[8] found empty cavity in 20 of 27 patients with late puerperal bleeding. In only one case retained placental tissue was confirmed. The same authors reported that histological confirmation was obtained in eight of nine patients with ultrasound suspected retained placenta tissue. On the other hand last report about late postpartum hemorrhage identified two etiological factors as risk factors, namely primary postpartum hemorrhage and a history of manual removal of a retained placenta.[23] Uterus curettage was performed in 63% of cases. Histological confirmation of residual placental tissue was obtained in 37% following ultrasound diagnosis and in 33% without previous ultrasound examination. The decision whether to perform uterine evacuation for retained placental tissue depends on both, clinical finding and the ability to visualize retained placenta by

ultrasound. Although prompt curettage seems to be necessary in many cases it usually doesn't remove identifiable placental tissue.[24] Moreover it is more likely to traumatise the implantation site and incite more bleeding. Consequently the complications rate is high. Hoveyda et al reported in his review regarding secondary postpartum hemorrhage that the frequency of perforation of the uterus was 3% and hysterectomy about 1%.[25] Although ultrasound technology becomes considerably improved the diagnosis of retained placental tissue is still difficult. Results of previously published studies are confusing and inconclusive.[8,12,18,19,26] Ultrasound finding of retained placental tissue may vary depending on many different factors. We cannot expect the same ultrasound picture during early (Fig. 35.5a) and late period of the puerperium (Fig. 35.5c). The presence of blood, blood clots, necrotic decidua or membranes can give various ultrasound pictures and a proper diagnosis is sometimes difficult. Nevertheless the most common ultrasound finding associated with retained placental tissue is an echogenic mass surrounded by a distinct halo (Fig. 35.5a).[8,12,14,18–20,26]In contrast Edwards found in his study an echogenic mass on day 7 in 51% of normal cases, in 21% on day 14 and in 6% on day 21.[16] He questioned ultrasound finding of an echogenic mass in uterine cavity as a sign of retained placental tissue. However the definition of an echogenic mass was not specified and we may hypothesise that others investigators would probably classify many of his "echogenic mass" as "heterogeneous patterns". A heterogeneous pattern is a common and insignificant finding of the involuting uterus. It is located in the cervical area in the early puerperium, in the whole uterine cavity in the middle part of the puerperium and it is not common during late postpartum period.[14] If dysfunctional postpartum bleeding persists for a long time, retained placental tissue is highly suspected. Hertzberg described so-called "stippled pattern" of scattered hyperechogenic foci that later on became increasingly generalized echogenic, reflected secondary regressive changes in retained placental tissue (Fig. 35.5c).[12]

If ultrasound finding shows an empty cavity with thin white decidua/endometrium during early or late puerperium, pure fluid/heterogeneous content in the cavity during the middle part of the puerperium, or only small echolucent or hyperechogenic dots throughout whole postpartum period, a clinically significant amount of retained placental tissue is unlikely.

Ashiron advocates transvaginal ultrasound with high frequency probe to better differentiate intrauterine puerperal pathology.[19] A few studies investigated transvaginal pulsed and Color Doppler in order to improve diagnostic accuracy of ultrasound regarding retained placental tissue. Some investigators observed low resistance blood flow around intracavitary contents (Fig. 35.5a and b).[14,19] Ashiron measured resistance index (RI) in relation to retained placental tissue and found that diagnosis is highly suspected if RI is below 0.35 (Fig. 35.5b). These patients are suitable for invasive treatment. RI above 0.45 should exclude diagnosis. Values between 0.35 and 0.45 form a "grey zone". Conservative treatment and repeated ultrasound examinations should be performed. Power Doppler seems to be new unexplored modalities that could improve our abilities to

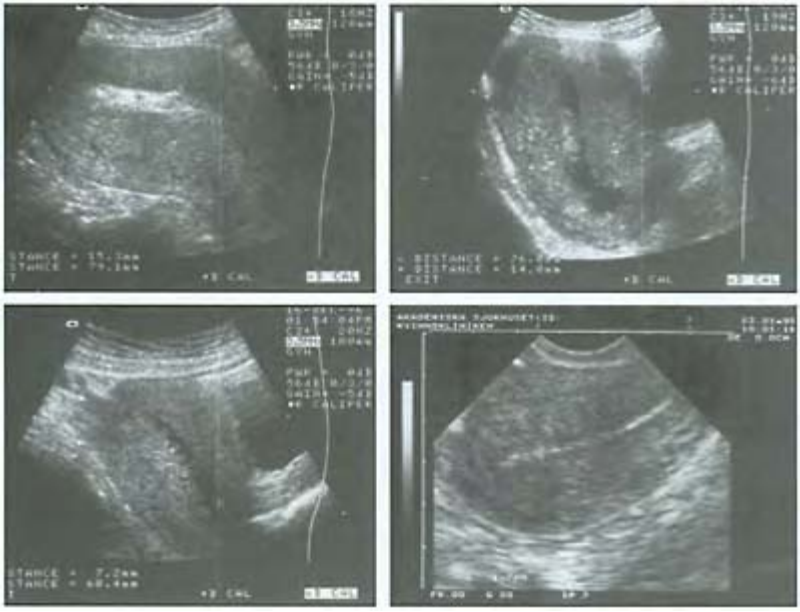

Figure 35.5: Puerperal abnormalities revealed by ultrasound: retained placental tissue 2 days postpartum (a), blood flow in relation to retained placental tissue (b), retained placental tissue 6 weeks postpartum (b) after curettage a thin, echogenic endometrium (c)

diagnose clinically significant retained placental tissue. Transvaginal sonohysterography is also a relatively new method that seems to be more effective for assessment of pathology in uterine cavity particularly concerning residual trophoblastic tissue.[27]

POSTPARTUM ENDOMETRITIS

Postpartum endometritis is the most common clinical condition that develops in 2–5% women following delivery. Cesarean section is the leading predisposing factor. Previously it has been considered that typical ultrasound finding of endometritis is the presence of gas in uterine cavity. Madrazo found gas in uterine cavity in 15% of patients with puerperal endometritis.[10] Nowadays infections caused by gas-forming organisms *Clostridium perfringens are* very rare and large gas-bubbles are almost never seen. Moreover Wachsberg detected gas in about 19% of normal cases, which is in accordance with results of a computed tomographic study performed within 24 hours of

uncomplicated vaginal delivery (21%).[20] Ultrasound appearance of gas is seen as an intensively hyperechogenic focus equivalent in echogenicity to bowel gas with clean and dirty shadowing or a reverberation artifact.[28] According to our experience gas is mostly observed following intrauterine manipulations although it is occasionally observed after normal vaginal delivery (Fig. 35.6a).[14]The detection of gas within the uterine cavity may be a normal finding during the puerperium and doesn't necessarily indicate the presence of endometritis or retained placental tissue.[14,20]After cesarean section or intrauterine manipulations highly echogenic foci can obscure an existing mass in the uterine cavity or be mistaken for retained placental tissue. Thus when

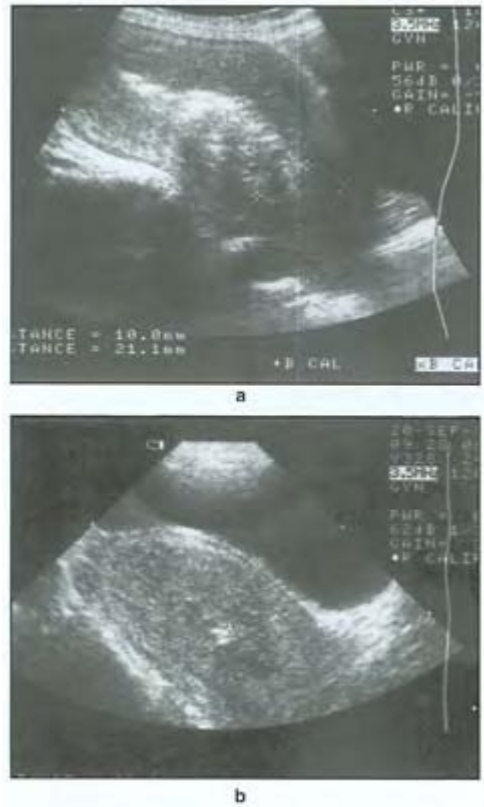

Figures 35.6a and b: Gas in uterine cavity one-day post curettage (a), six days post curettage (b)

ever highly echogenic foci are present in the uterine cavity the physician who interprets ultrasound finding must be aware of recent uterine manipulations and perform follow-up ultrasound to confirm its disappearance. Gas usually disappears within 1–2 weeks after instrumentation (Fig 35.6b). Furthermore it has been thought that ultrasound picture of

retained placental tissue and endometritis overlap. The presence of retained placental tissue may result in intrauterine infection and in these cases ultrasound examination can help us to select patients suitable for invasive treatment. In the vast majority of cases of isolated endometritis, ultrasound findings are normal and have no pathognomonic picture. Kirkinen found that blood flow to the infected uterus could be different from normal.[21] Deutchman and Hartman described postpartum pyometra as a lucent area within the uterus.[29] They also advocated the usage of ultrasound to assist in guiding a drainage procedure. Septic pelvic thrombophlebitis, well known as an "enigmatic puerperal fever" is another uncommon complication of the puerperium. It most commonly presents in early postpartum period and antibiotic treatment is usually unsuccessful. Rudoff et al[30] suggests ultrasound examination in case of clinical suspicion of pelvic thrombophlebitis. Although ultrasound diagnosis of ovarian vein thrombophlebitis is well described[31–33] the diagnosis is still difficult and an ultrasound expertise is needed. Asymmetric dilatation of the ovarian or other pelvic vein may sometimes be observed.[32] Furthermore a complex or hypoechoic mass near the lower pole of the kidney particularly in clinical setting of an "enigmatic puerperal fever" should suggest thrombophlebitis. An echogenic intracaval mass is considered diagnostic and anticoagulation treatment should be added.[33]

CESAREAN SECTION

Nowadays when Cesarean section rates are continuously rising, higher incidence of all puerperal complications should be expected.

The ultrasound image of the uterus following cesarean section usually shows three distinctive patterns: (1) gas in the cavity, (2) a small rounded area at the incision site that reflects tissue reaction due to localized edema and (3) some echogenic dots at the incision site, which is related to the type of closure and the suture material used (Figs 35.7a and b).[34]AH these characteristics are normal findings and no correlation with pathological conditions is found. The involution rate of the uterus following cesarean section is not different from the involution rate after vaginal delivery. Nakay et al[35] studied uterine blood flow resistance after cesarean section and concluded that the resistance index for the uterine artery didn't show any change during the early postpartum period.

The significant infectious morbidity is associated with cesarean section. Ultrasound may be useful in postpartum women with clinical suspicion of a postoperative complication like phlegmona,[36] abscess, pyometra, hematometra (Fig. 35.7c), wound infection, subfascial hematoma or intra-abdominal postoperative hemorrhage. Baker et al described bladder flap hematoma after a low uterine transverse cesarean section.[37] A solid or complex mass between the posterior bladder wall and the anterior uterine wall may be observed by ultrasound. An abscess appears as a cystic structure with internal debris surrounded by thicker irregular walls. An infected hematoma initially has similar ultrasound appearance. During the resolution process, it may change and appears more solid. However the physician must be aware that ultrasound diagnosis is just a complement and clinical condition of the patient should guide the therapeutic approach.

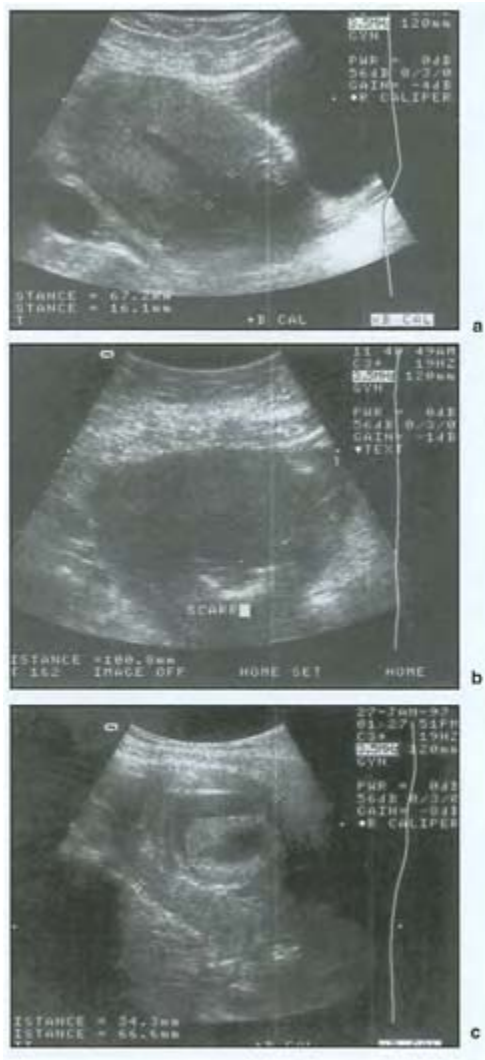

Figures 35.7a to c: The uterus after cesarean sectionlongitudinal section (a), coronal section—hyperechogenic scar in lower uterine segment, and hematometra (c)

CONGENITAL UTERINE MALFORMATIONS

The prevalence of the congenital uterine malformations in general population is largely unknown. Failed fusion of the two Miillerian ducts to form the genital organs may cause reproductive, fetal and maternal hazards (infertility, premature labor, abnormal fetal presentations, retained placental tissue and postpartum hemorrhage). It is well known that uterine anomalies may remain undiscovered except when they are associated with reproductive or obstetric problems. Already in 1976 Bennett suggested puerperal ultrasonic hysterography as a screening procedure prior to radiological examination in women whose reproductive performance suggests a diagnosis of congenital malformation of the uterus.[38] Since that a few studies concerning the issue were published. Szoke and Kiss examined in 1977 patients where manual examination revealed a uterus differing in shape from normal, the patient had a breech presentation in her previous or present pregnancy and the involution of the uterus was slow. The ultrasound echo technique was applied and uterine anomalies were found in five cases postpartum.[39] In 1984 Land et al performed ultrasonic

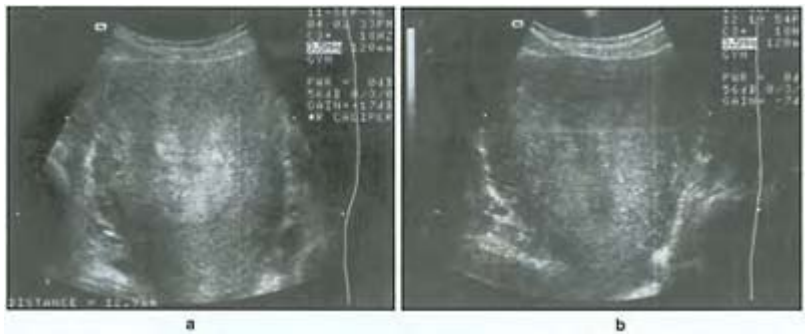

Figures 35.8a and b: A coronal section shows a subseptate uterus 1 day after manual evacuation of the placenta (a), the uterus of the same patient 8 days later (b)

hysterography in 104 patients between the 2nd and 5th postpartum day. An unexpectedly high number of women (16%) showed an abnormal uterine configuration.[40]

The coronal section seems to be the most appropriate section in order to reveal uterine cavity anatomy (Figs 35.8a and b). It is difficult to obtain the coronal section by abdominal examination in non-pregnant patients. However the puerperium when the uterus is extremely large makes an exception. The ultrasound examination should perform in the early puerperium because a large uterus lies in near proximity to the ultrasound probe and highly echogenic decidua outlines well the shape of the cavity. Puerperal ultrasound can detect uterine developmental abnormality, providing an explanation for complications in labor and the puerperium.

POSTPARTUM URINARY RETENTION

Postpartum urinary retention is a relatively common condition and incidence ranges between 1–18%.[41] According to the International Continence Society, 100 ml is considered as the upper limit of residual urine.

Ultrasound is the method of choice when assessing urinary bladder and residual urine postpartum. Invasive catheterization with the discomfort and the risk of infection can be avoided. Conventional bladder scanner is not to be recommended during the puerperium. Large uterus may content fluid and thus a misinterpretation may be done. Many different techniques for bladder volume measurement are used and the accuracy of the method varies widely.

We prefer a method where the longest distance of the maternal bladder (d.l) is measured in a longitudinal section, and then two perpendicular diameters (d2, and d3) are measured in the transverse section. The estimated amount of residual urine can be calculated using the formula for approximation of the ellipsoid:

Volume (ml)=(d1×d2×d3)/2 (Fig. 35.9).[41]

CONCLUSION

Present ultrasound technology with high image resolution has made ultrasound a valuable diagnostic tool for assessing numerous postpartum clinical conditions. Suspicion of retained placental tissue, unknown cause of the puerperal sepsis, surgical complications or acute abdominal pain are some of the possible reasons to switch on ultrasound machine. Not only the involution changes of the uterus or pathological changes in uterine cavity but also the other organs like kidneys, urinary bladder, gallbladder, ovaries and abdominal cavity can be easily examined by ultrasound during postpartum period.

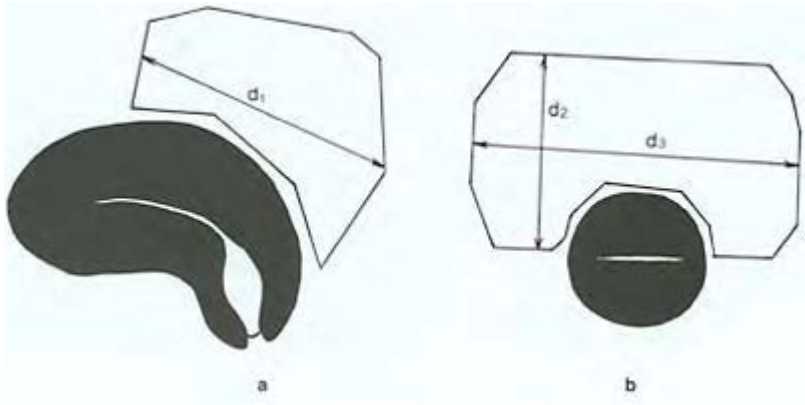

Figure 35.9: Residual urine volume measurement

Color, Pulsed and Power Doppler have improved our ability to study for the first time the vascular changes of the uterine involution noninvasively.[15,17]

Sonohysterography may better differentiate intrauterine pathology by injecting saline under sonographic control and so improve the accuracy of the diagnosis of puerperal pathology.[27]

More studies are required in this important area and some new modalities need further evaluation. Moreover the knowledge obtained through ultrasound examinations can help us to better understand both the physiology and pathophysiology of the puerperium.

REFERENCES

1. Hytten F. The Clinical Physiology of the Puerperium. London, UK: Farrand Press, 1996.
2. Donald I, MacVicar J, Brown TC. Investigation of abdominal masses by pulsed ultrasound. Lancet 1958;1:1188.
3. Robinson HP Sonar in the puerperium. Scott Med J 1972;17:364.
4. Szoke B, Kiss D. The use of the ultrasonic echo technique in examining the normal and pathological involution in the puerperium. Int J Gynaecol Obstet 1976;14:513–16.
5. Malvern J, Campbell S. Ultrasonic scanning of the puerperal uterus following postpartum hemorrhage. J Obstet Gynaecol Br Commonw 1973;80:320–24.
6. Rodeck CH, Newton JR. Study of the uterine cavity by ultrasound in the early puerperium. Br J Obstet Gynaecol 1976;83:795–801.
7. Defoort P, Benijts G, Thiery M et al. Ultrasound assessment of puerperal uterine involution. Eur J Obstet Gynaecol 1978;8:95–97.
8. Lee CY, Madrazo B, Drukker BH. Ultrasonic evaluation of the postpartum uterus in the management of postpartum bleeding. Obstet Gynaecol 1981;58:227–32.
9. VanRees D, Bernstine RL, Crawford W. Involution of the postpartum uterus. An ultrasonic study. J Clin Ultrasound 1981;9:55.
10. Madrazo BL. Postpartum Sonography. The principle and Practice of Ultrasonography in Obstetrics and Gynecology (3rd ed). East Norwalk: AppletonCentury-Crofts, 1985;449–56.
11. Lavery JP, Shaw LA. Sonography of the postpartum uterus. J Ultrasound Med 1989;8:481–86.
12. Hertzberg BS, Bowie JD. Ultrasound of the postpartum uterus, prediction of retained placental tissue. J Ultrasound Med 1991;10:451–56.
13. Wachsberg RH, Kurtz AB, Levine CD, et al. Realtime ultrasonographic analysis of the normal postpartum uterus: technique, variability and measurements. J Ultrasound Med 1994;13:215–21.
14. Mulic-Lutvica A, Bekuretzion M, Axelsson O, et al. Ultrasonic evaluation of the uterus and uterine cavity after normal, vaginal delivery. Ultrasound Obstet Gynecol 2001;18:491–98.
15. Tekay A, Jouppila P. A longitudinal Doppler ultrasonographic assessment of the alterations in peripheral vascular resistance of uterine arteries and ultrasonographic findings of the involuting uterus during the puerperium. Am J Obstet Gynecol 1993;168:190–97.
16. Edwards A, Ellwood DA. Ultrasonographic evaluation of the postpartum uterus. Ultrasound Obstet Gynecol 2000; 16:640–43.
17. Williams JW. Regeneration of the uterine mucosa after delivery with special reference to the placental site. Am J Obstet Gynecol 1931;22:664.
18. Sakki A, Kirkinen P Ultrasonography of the uterus at early puerperium. Eur J Ultrasound 1996;4:99–105.
19. Achiron R, Goldenberg M, Lipitz S et al. Transvaginal duplex Doppler Ultrasonography in bleeding patients suspected of having residual trophoblastic tissue. Obstet Gynecol 1993;81:507–11.

20. Wachsberg RH, Kurtz AB. Gas within the endometrial cavity at postpartum US. A normal finding after spontaneous vaginal delivery. Radiology 1992; 183: 431–33.
21. Kirkinen P, Dudenhausen J, Baumann H, et al. Postpartum blood flow velocity waveforms of the uterine arteries. J Reprod Med 1988;33:745–74.
22. Sharman A. Reproductive Physiology of the PostPartum Period. Livingstone: Edinburgh E. & S. 1966.
23. Alexander J, Thomas P, Sanhghera J. Treatments for secondary postpartum hemorrhage. The Cochrane Library, Issue 4:2002.
24. Dewhurst C. Secondary postpartum hemorrhage. J Obstet Gynaecol Br Commonwealth 1966;73:53–58.
25. Hoveyda F, MacKenzie IZ. Secondary postpartum hemorrhage: incidence, morbidity and current management. Br J Obstet Gynaecol 2001; 108:927–30.
26. Carlan SJ, Scott WT, Pollack R et al. Appearance of the uterus by ultrasound immediately after placental delivery with pathologic correlation. J Clin Ultrasound 1997;25(6):301–08.
27. Wolman I, Hartoov J, Amster R et al. Transvaginal sonohysterography for the early detection of residual trophoblastic tissue. Ultrasound Obstet Gynecol 1986; 8:37.
28. Carson PL. Clean and dirty shadowing at US: a reappraisal. Radiology 1991;181:231–36.
29. Deutchman ME, Hartmann KJ. Postpartum pyometra: a case report. J Fam Pract 1993;36:449–52.
30. Rudoff JM, Astranskas LJ, Rudoff JC et al. Ultrasonographic Diagnosis of Septic Pelvic Thrombophlebitis. J Ultrasound Med 1988;7:287–91.
31. Warhit JM, Fagelman D, Goldman MA et al. Ovarian vein thrombophlebitis: diagnosis by ultrasound and CT J Clin Ultrasound 1984;12:301.
32. Wilson PC, Lerner RM. Diagnosis of ovarian vein thrombophlebitis by Ultrasonography. J Ultrasound Med 1983;2:187.
33. Sherer DM, Fern S, Mester J et al. Postpartum ultrasonographic diagnosis of inferior vena cava thrombus associated with ovarian vein thrombosis. Am J Obstet Gynecol 1997;177(2):474–75.
34. Burger NF, Dararas B, Boes EGM. An echogenic evaluation during the early puerperium of the uterine wound after cesarean section. J Ultrasound Med 1983;2:18.
35. Nakai Y, Imanaka M, Nishio J et al. Uterine blood flow velocity waveforms during early postpartum course following cesarean section. Eur J Obstet Gynecol Reprod Biol 1997;74(2):121–24.
36. Lavery JP, Howell RS, Shaw L. Ultrasonic demonstration of a phlegmona following Cesarean section—case report. J Clin Ultrasound 1985;13:134–36.
37. Baker ME, Bowie JD, Killan AP Sonography of postcesarean-section bladder-flap hematoma. Am J Roentgenol 1984;144:757–59.
38. Bennett MJ. Puerperal ultrasonic hysterography in the diagnosis of congenital uterine malformations. Br J Obstet Gynaecol 1976;83(5):389–92.
39. Szoke B, Kiss D. The use of ultrasonic echo technique in the diagnosis of developmental anomalies of the uterus.
40. Land JA, Stoot JE, Evers JL. Puerperal ultrasonic hysterography. Gynecol Obstet Invest 1984; 18(3): 165–68.
41. Weissman A, Grisarn D, Shenhav M et al. Postpartum surveillance of urinary retention by Ultrasonography: the effect of epidural analgesia. Ultrasound Obstet Gynecol 1995;6:130–34.

Chapter 36
Three-Dimensional Sonoembryology

Bernard Benoit, Tomislav Hafner, Asim Kurjak

INTRODUCTION

Three-dimensional sonography has gained significant popularity among the experts interested in prenatal diagnostics. Although being originally developed in the early 1980s,[1,2] three-dimensional sonography reached its full establishment in recent few years. This was mostly due to the exceptional development of the computer processor technology that is essential for three-dimensional imaging systems.

Modern three-dimensional systems are capable to generate surface and transparent views depicting the sculpture-like reconstruction of fetal surface structures or the X-ray-like images of fetal skeletal anatomy. Main advantages of this new technology in obstetrics include improved assessment of complex anatomic structures, surface scan-analysis of minor defects, volumetric measuring of organs, spatial presentation of blood flow information and three-dimensional examination of fetal skeleton.[3–8] Operating in planar mode, three-dimensional orientation of tomograms is unlimited, despite the limited probe manipulation or inadequate position of fetal structures. These imaging capabilities are extremely important during the first trimester of pregnancy when the manipulation of the vaginal probe is restricted and obtainable ultrasound sections are limited.[9] During the transabdominal scanning, frontal planes parallel to the fetal abdominal wall are also visible. These views are not available with conventional ultrasound. An additional progress is achieved owing to the permanent possibility of repeated analysis of previously saved three-dimensional volumes and with elimination of surrounding structures.[1,10] We like to emphasize that three-dimensional technique is complementary, but not alternative technology to the conventional two-dimensional technique in the field of prenatal diagnosis.[11] However, 3D imaging is superior in the specific diagnostic problems. A comparison of 2D and 3D techniques shows that 3D provides a diagnostic gain in a large percentage of cases owing to the possibility of surface and transparent mode imaging. Therefore, the accurate topographic depiction of desired image plane is much easier.[1,12,13]

Zagreb experience does confirm that detailed sonogram of the fetus during the first trimester can be obtained due to large amount of amniotic fluid. Moreover, we found three-dimensional sonography absolutely superior to the standard two dimensional sonography in the assessment during the first trimester of pregnancy. This is due to several facts. Firstly, three-dimensional sonography tremendously reduces time of

exposure of embryo to the ultrasound beam. Volume acquisition takes only few seconds. Image processing and analysis is done off-line, without any time limitations. Sonographer can choose among two principal modes of imaging: the planar mode and the full three-dimensional image. In the planar mode the object is being simultaneously projected to three perpendicular planes (Fig. 36.1). There is no limit in object rotation and in number of tomograms of different sections of the analyzed

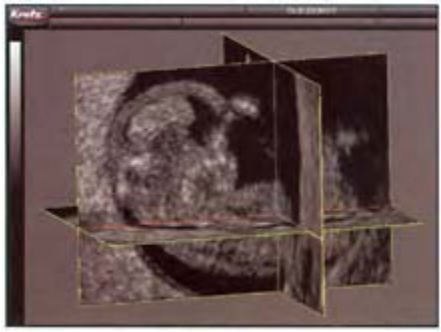

Figure 36.1: Three section planes of three-dimensional ultrasound. These three planes (frontal, transverse, mid-sagittal) are perpendicular with one another at the three-axial center of rotation

object. Planar mode enables a superb precision of measurement. Full three-dimensional mode is particularly useful in presenting three-dimensional interrelationship of different organs or skeleton. Sonographer can optionally change different modalities of image rendering emphasizing the outer surface or presenting inner structures through the transparent mode.

Multicentric studies showed some limitations of three-dimensional ultrasound scanning.[1,14] Fetal and maternal movements during the scanning process lead to motion artifacts that can degrade quality of image. Fetal surface rendering primarily depends on a sufficient amniotic fluid volume in front of the region of interest. In some cases, oligohydramnios and superimposed structures make surface view rendering impossible. Finally, three-dimensional examination of stored volumes is a time-consuming operation. Beginners will need plenty of time and assisted education to become routine in data acquisition, orientation and manipulation what is mandatory for three-dimensional ultrasound imaging.

TYPICAL EMBRYONIC FEATURES DURING FIRST TRIMESTER PREGNANCY AS SEEN BY THREE-DIMENSIONAL SONOGRAPHY

Five Weeks

Gestational sac can be visualized from the middle of the fifth week of amenorrhoea as a small spherical anechoic structure placed inside one of the endometrial leafs. Planar mode tomograms are helpful in distinguishing early intraendometrial gestational sac from collection of free fluid between the endometrial leafs (pseudogestational sac). Three-dimensional sonography enables precise measurement of exponentially expanding gestational sac volume during the first trimester (Table 36.1, Fig. 36.3). Except gestational sac volume, amniotic cavity volume can be obtained in correlation with crown-rump length (CRL) measurements (Fig. 36.4). At the beginning of the fifth week small secondary yolk sac is visible as the earliest sign of the developing embryo. Planar mode tomograms are useful for detecting the embryonic pole inside the gestational sac. Adjacent to the yolk sac, embryo can be seen as a small straight line when it reaches 2–3 mm in length at the end of the fifth week.

Six Weeks

Three-dimensional image of an embryo during the 6th week of pregnancy is characterized by rounded bulky head and thinner body. The head is prominent due to the developing forebrain. Limb buds are rarely visible in this stage of pregnancy. However, umbilical cord and vitelline duct are always clearly visible.

Seven Weeks

During the 7th week of pregnancy fast development of rhombencephalon (hindbrain) takes place. This process gives even more prominence to the head. By the use of planar mode developing vesicles of the brain can be depicted as anechoic structure inside the head. The biggest and usually the only visible is rhombencephalon placed on the top of the head (vertex). Diencephalon and its cavity becomes visible few days later. The head is strongly flexed anteriorly being in the contact with the chest (Fig. 36.2). Limb buds are often visible laterally to the body. Amnion that can be seen as a spherical

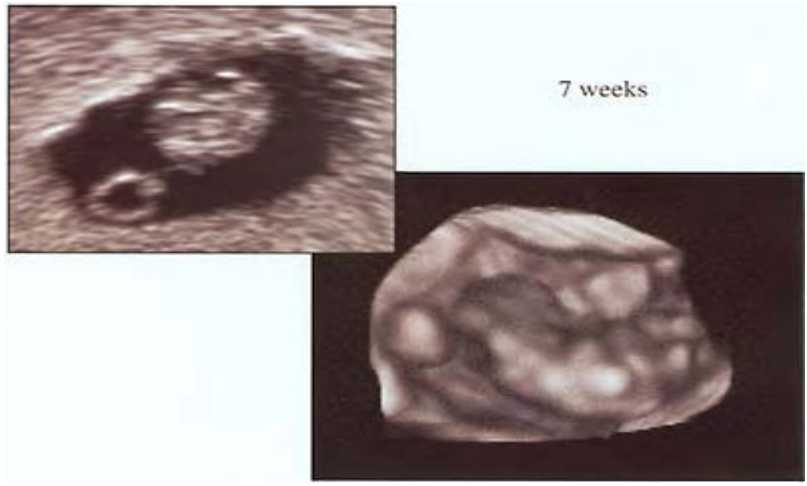

Figure 36.2: Normal embryo at 7 weeks' gestation. Note the anterior flexion of the head being in contact with the chest. Adjacent to the embryo, yolk sac can be seen

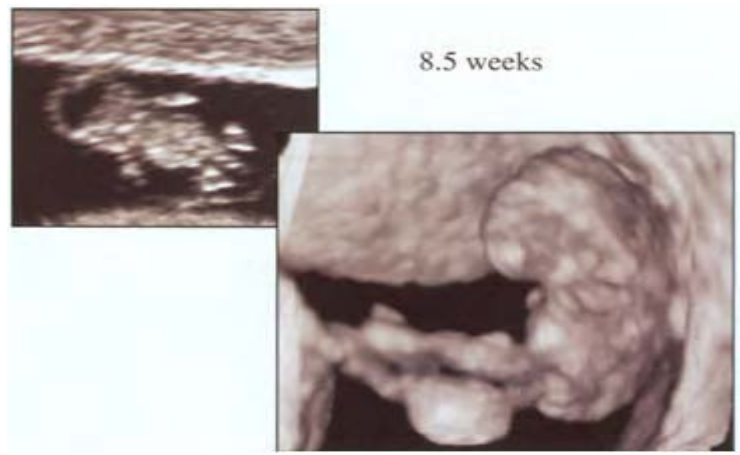

Figure 36.3: A normal embryo at 8.5 weeks' gestation. The developing intestine is herniated into proximal umbilical cord

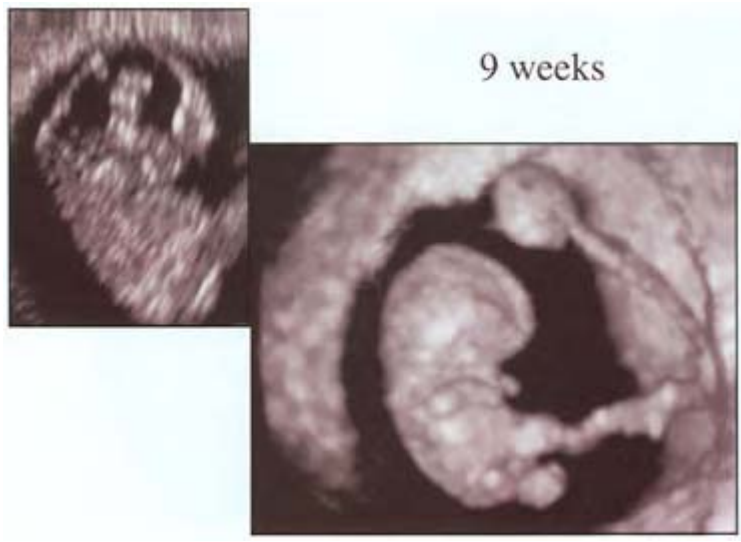

Figure 36.4: A normal embryo at 9 weeks' gestation. The size of lateral ventricles increases rapidly. While the third ventricle is still relatively wide at the beginning of this week, owing to the growth of the thalami. In the fetuses of 25 mm in CRL and more, there is a clear gap between the rhombencephalic and the mesencephalic cavity, owing to the growing cerebellum.

hyperechoic membrane is still close to the embryo, Chorion frondosum can be distinguished from chorion laeve.

Eight Weeks

During the 8th week of pregnancy there is expansion of the ventricular system of the brain (lateral, third and midbrain ventricles). Due to these processes the head erects from the anterior flexion. The vertex is now located over the position of the midbrain. Structures of the viscerocranium are not visible due to the small size. Arms and feet are clearly visible (Fig. 36.3). Insertion of the umbilical cord is visible on the anterior abdominal wall. During the 8th and 9th week developing intestine is being herniated into the proximal umbilical cord (Fig. 36.7).

Nine to Ten Weeks

Cerebral hemispheres continue with development during the 9th and 10th weeks of pregnancy. Visible are lateral ventricles containing hyperechoic choroid plexuses. The head is clearly divided from the body by the neck. External ear is sometimes depicted in the 3D surface image. Herniation of the midgut is present. Dorsal column, the early spine, can be examined in its whole length. The arms with elbow and legs with knee are clearly visible (Fig. 36.4). Feet can be seen approaching the midline.

Eleven to Twelve Weeks

In the llth week of pregnancy development of the head and neck continues. Herniated midgut returns into the abdominal cavity. Planar mode enables detailed analysis of embryonic body with visualization of the stomach and urinary bladder. Kidneys are also often visible. Arms and legs continue with development (Fig. 36.5). Long bones can be visualized as hyperechoic elongated structures inside upper and lower extremities. Fingers and toes are visible. Facial details as nose,

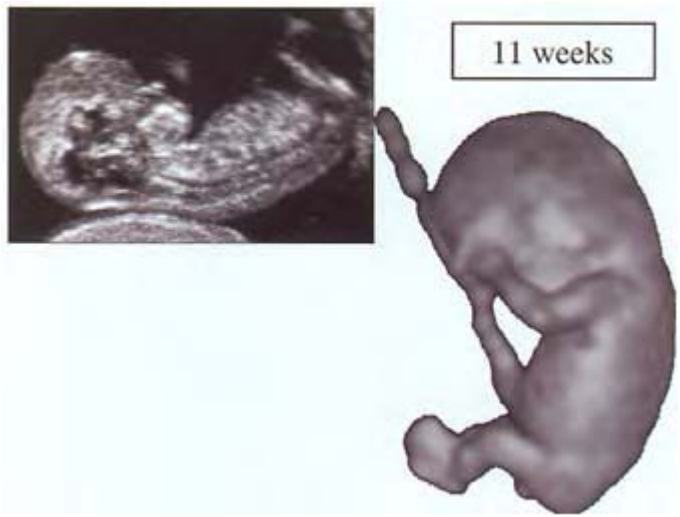

Figure 36.5: Embryo at 11 weeks' gestation. Note the regularity of the front abdominal wall, since the herniated mid gut has returned into the abdominal cavity

orbits, maxilla and mandibles are often visible. Detailed three-dimensional analysis of fetal spine, chest and limbs is obtainable by using the transparent, X-ray-like mode.

MULTIPLE PREGNANCY

Determining chorionicity and amnionicity during the end of first trimester may be much easier by 3D surface rendering (Figs 36.6 and 36.7). All of the relevant criteria can be used. These include: counting the number of placentas; determining whether each embryo is within his own amniotic sac, describing the appearance of the dividing membrane; and looking for the presence of a triangular projection of placental tissue beyond the chorionic surfaces (lambda or twin peak sign).[15,16]

High-resolution 3D sonography enables early and precise detection of abnormal multiple pregnancy. The most often is the early spontaneous demise of one of the fetuses, wanishing twin (Fig. 36.8). It is possible to diagnose a variety of

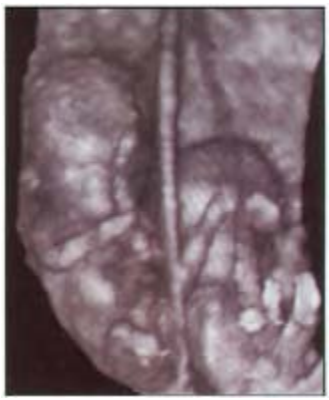

Figure 36.6: Dichorionic/biamniatic twins at 11 weeks' gestation. Dividing membrane is visualized by transvaginal surface-mode reconstruction

anomalies involving one of a twin pair. Twins have a higher incidence of structural anomalies when compared to singletons. The types of malformations affecting twins can be divided into those unique to twins, especially monochorionic twins, like conjoined twins (Fig. 36.9) and acardiac twins

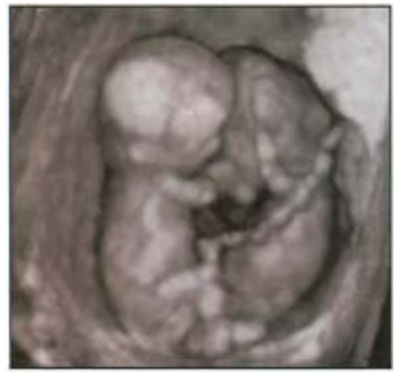

Figure 36.7:
Monochorionic/monoamniatic twins at 11 weeks' gestation

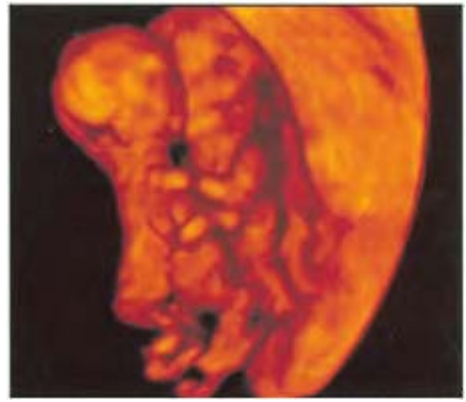

Figure 36.9: Three-dimensional ultrasound scan of conjoined twins. They are sharing chest and abdomen

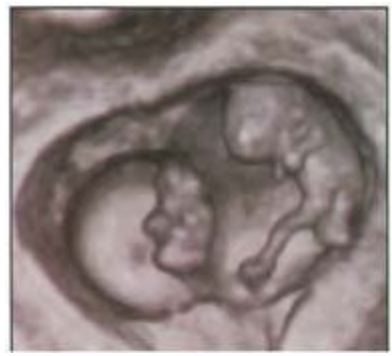

Figure 36.8: Three-dimensional ultrasound scan of the first trimester complication. The discrepancy between the sizes of the two embryos is noticed, and the diagnosis was a vanishing twin

(Fig. 36.10), and those anomalies not unique to twins, such as neural tube defects and congenital heart defects. Conjoined twins result from a postimplantation division of the zygote between the 13th and 16th day after conception, and the most common type is thoracoomphalopagus (28%).[28] More recently, Meizner and co-workers[29] reported on the prenatal diagnosis of thoraco-omphalopagus conjoined twins at 9 weeks' gestation. Early and accurate prenatal diagnosis of conjoined twins is still a challenge, important in planning a treatment options for both the mother and the infants

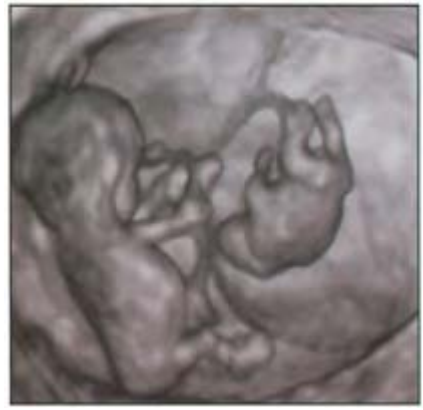

Figure 36.10: MC/MA twins assessed by 3D US. One twin is morphologicaly normal and the other is bizarre -

acardiac (right). Note that the acardiac twin is smaller, than the normal twin and appears to be composed of lower extremities and a trunk

Due to the superb quality of images, three-dimensional sonography enables detection of developmental anomalies.[17,23] Three-dimensional sonography will certainly improve early detection of fetal anomalies, and possibly become the screening method for them. Three-dimensional sonography can improve accuracy and success rate of nuchal translucency measurement in pregnancy between 10 and 14 weeks' gestation.

In a series of 120 pregnancies Kurjak and Kupesic[24] were able to obtain the mid-sagittal section and measure nuchal translucency in 100% of cases using three-dimensional transvaginal sonography. By the use of standard two-dimensional sonography this was possible in only 85% of cases. In addition, three-dimensional sonography produced better intraobserver reproducibility of results. Three-dimensional sonography with the potential of complex and sophisticated post-processing of images has proved to be a useful tool in experimental embryology. Using a special off-line imaging computer device Blaas et al[25] produced a series of *ex vivo* obtained images of human embryo emphasizing development of the brain cavities during the first trimester. This new technology moved embryology from *postmortem* studies to *in vivo* environment.

THE YOLK SAC

Three-dimensional ultrasound imaging may give additional data to functional Doppler studies for research in developmental anatomy and embryology. This method allows a detailed morphologic and volumetric analysis of extraembryonal static structures. Conventional methods for measuring volumes of fluid-filled spaces include modeling of shapes (e.g. using an ellipsoidal approximation). Using three-dimensional planar mode, the position of the yolk-sac wall is accurately spatially assessed. Measurement of the volume, rather than estimation from a simple geometric model increases the accuracy of the measurement. Growth and appearance of the yolk sac were correlated with the outcome of the pregnancy.[26] Kupesic and Kurjak[27] measured gestational sac volume and yolk sac volume and vascularity in 80 women with uncomplicated pregnancy between 5 and 12 weeks of gestation. Regression analysis revealed an exponential growth of the gestational volume throughout the first trimester of pregnancy.

EARLY DETECTION OF FETAL ANOMALIES

Anencephaly and Exencephaly (Acrania)

Anencephaly and exencephaly have in common the absence of the calvaria—the bones that cover the cranial vault. The incidence is about 1:1000 births. Because many

similarities, it was postulated that the exencephaly is a precursor or a variant of the anencephaly.[30,32] Natural history of anencephaly starts with the developmental failure of closure of the cephalic end of the neural tube. This implies the absence of the telencephalon, mesencephalon, and maldevelopment of the cranial vault, including the frontal, parietal and occipital bones. In some cases a certain amount of brain tissue or angiomatous stroma may develop.[33] Some authors hypothesized that the primary event is the lack of development of the neurocranium.[31,32] This results in subsequent degeneration and disappearance of the brain tissue that is exposed to the amniotic fluid. Ultrasound diagnosis is made when no bones can be visualized above the orbits, regardless to the amount of the neural soft tissue.[33]

Three-dimensional sonography is a very powerful tool for anomaly detection during the first trimester. Multiplanar imaging enable accurate analysis of fetal shape and anatomical details. Surface mode rendering depicts the morphology with sculpture-like appearance, leaving no doubt on diagnosis. The lack of cranial development can be detected precisely. Surface/maximum rendering depicts the anomalous shape of the cranium and a complete absence of the calvarian bones development (Figs 36.11a and b).

Encephalocele

Defect of the ossification and closure of the neural tube can affect any region. Lack of ossification of the rostral part of the neural tube causes the encephalocele. Mostly, the defect is positioned posteriorly and in the midline, causing herniation

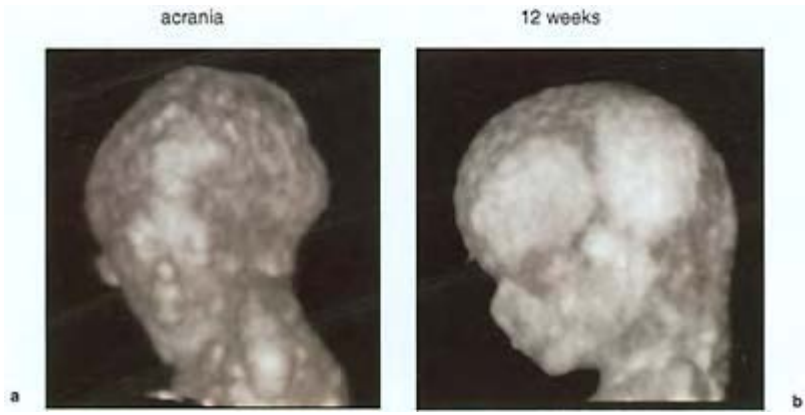

Figures 36.11 a and b: Surface rendered fetal head with acrania (a) compared to a normal fetal head (b)

of the meninges and the brain tissue. Diagnosis of an encephalocele at the end of the first trimester can be found in the literature.[30] Diagnosis was made upon the finding of the bulging meningeal and brain tissue through the defect of the bone.

Three-dimensional sonography can precisely depict the abnormal outline of the head in case of an encephalocele (Fig. 36.12). Both, multi-planar imaging and surface rendering can be used for this task.

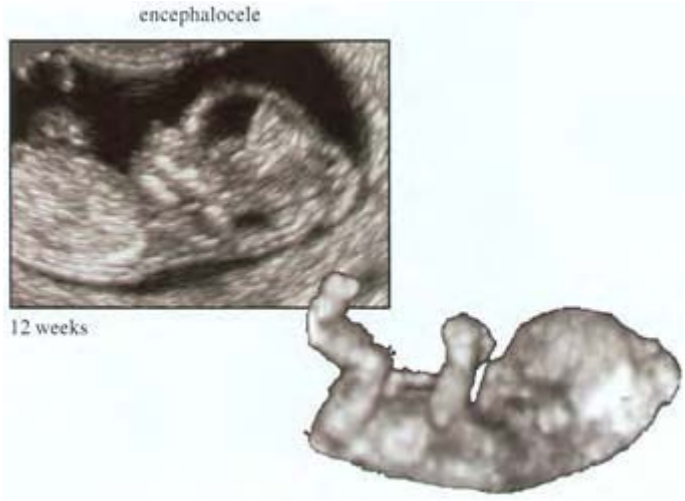

Figure 36.12: Fetus with an occipital encephalocele in sagittal section and surface rendered with the background removed by "electronical scalpel"

Intracranial Abnormalities

Hydrocephaly

Hydrocephaly is characterized by an abnormal accumulation of the cerebrospinal fluid in the ventricular system of the brain. The obstruction can be positioned at different locations. The most common location is the obstruction of the aqueduct of Sylvius. This cause accumulation of the cerebrospinal fluid in the lateral and the third ventricles resulting in enlargement of the ventricles due to the increased pressure of the fluid. The process of enlargement of the ventricles is gradual, and due to this fact it was considered that the diagnosis of hydrocephaly is not possible before the mid-pregnancy.[34] Diagnosis was made if an abnormal hemisphere width to lateral ventricle width was found. Development of high-resolution ultrasound devices enabled diagnosis of hydro-cephaly in early pregnancy.[35,36] Visualization and measurement of the choroid plexus is possible from the llth week of gestation. In normal brain choroid plexus fills the atrium and the body of the lateral ventricle. When pressure of the cerebrospinal fluid rises the dilatation of the lateral ventricles gives a particular appearance to the choroid plexus (Fig. 36.13).[37] Multiplanar three-dimensional analysis is helpful for fast selection of the adequate section of the fetal head in which the "dangling" choroid plexus can be visualized.

Holoprosencephaly

Holoprosencephaly results from absent or incomplete division of the prosencephalon in two cerebral hemispheres and lateral ventricles. Holoprosencephaly is categorized into alobar, semilobar and lobar types.[28]

Alobar holoprosencephaly is the most severe type that occurs after a complete failure of prosencephalon cleavage. This causes a formation of a monoventricular cavity with thalamus and basal ganglia fused in the midline, while the midbrain, brainstem and cerebellum are structurally normal. Alobar holoprosencephaly is often associated with severe facial anomalies such as

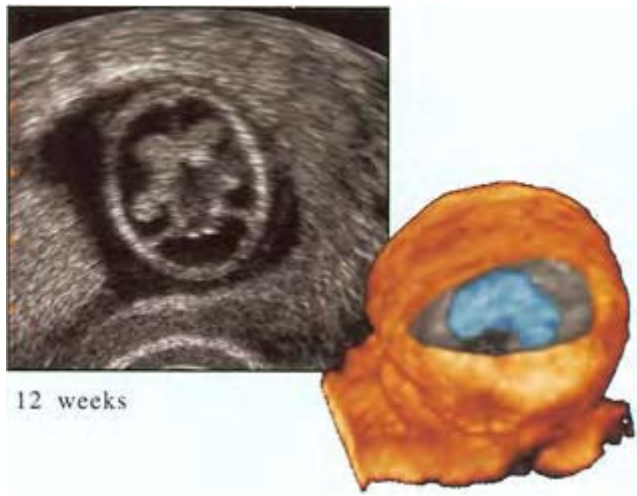

Figure 36.13: Top left: Transverse axial section of the fetal head with early developed hydrocephalus. Note the "dangling" appearance of the choroid plexi. Bottom right: Surface rendered head of the same fetus. "Electronic scalpel" was used to remove a part of the skull, for choroid plexus to be visible

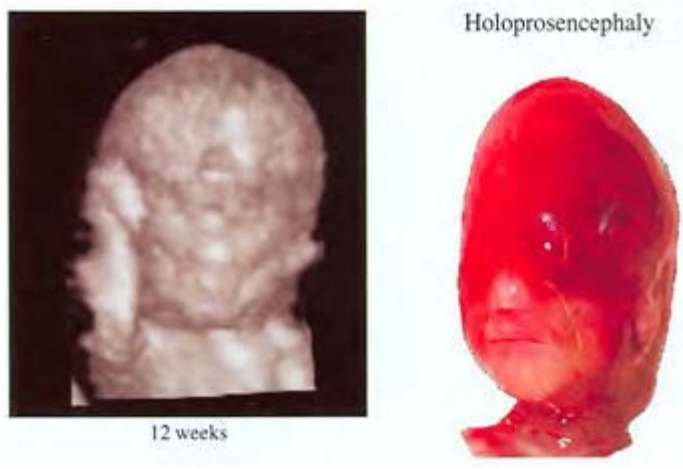

Figure 36.14: Alobar holoprosencephaly at 12 weeks of gestation (Trisomy 13). Compare the ultrasound finding of hypotelorism with the postmortem fetus

cleft lip and palate, severe hypotelorism and cyclopia, arhinia with proboscis.[38] This anomaly can be found in some aneuploidies, usually trisomy 13. Trisomy 18 can also be connected to holoprosencephaly. In the semilobar holoprosencephaly a frontal monoventricle is present and there is a posterior partial formation of the occipital lobes. In the lobar holoprosencephaly the hemispheres may be fused and the lateral ventricles may widely communicate due to the absence of the septum pellucidum.

Due to a severe disruption of the normal intracranial anatomy ultrasound diagnosis of holoprosencephaly is possible at the end of the first trimester, after the 10th week of pregnancy.[39] The lack of normally developed telencephalon containing hyperechoic choroid plexi, frontaly positioned monoventricle, and facial anomaly (severe hypotelorism) are features that should lead to the adequate diagnosis (Fig. 36.14). Threedimensional sonography enables meticulous analysis of anatomical features in very early pregnancy making the diagnostic process accurate and fast

CONCLUSION

Many details involved in this process are still obscure to our knowledge. We believe that studies including a combination of *in vivo* three-dimensional data with postmortem histology specimens can yield new and interesting facts about this period of human development full of incomparable intensity. Undoubtedly, rapid technological development will allow real-time 3D ultrasound to provide improved patient care on the one hand, and increased knowledge of developmental anatomy on the other

REFERENCES

1. Baba K, Satch K, Sakamoto S et al. Development of an ultrasonic system for three-dimensional reconstruction of the fetus. J Perinat Med 1989; 17:1924.
2. Fredfelt KE, Holm HH, Pedersen JF Threedimensional ultrasonic scanning. Acta Radiol Diagn 1984;25:237–39.
3. Merz E, Bahlaman F, Weber G et al. Threedimensional ultrasonography in prenatal diagnosis. J Perinat Med 1995;23:213–22.
4. Gregg A, Steiner H, Staudach A et al. Accuracy of 3D sonographic volume measurements. Am J Obstet Gynecol 1993; 168:348–50.
5. Kossof G, Griffiths KA, Warren PS et al. Three dimensional volume imaging in obstetrics. Ultrasound Obstet Gynecol 1994;4:196–99.
6. Kou HC, Chang FM, Wu CH et al. The primary application of three-dimensional ultrasonography in obstetrics. Am J Obstet Gynecol 1992; 166:880–84.
7. Merz A, Macchiela D, Bahlamann F et al. Threedimensional ultrasound for the diagnosis of fetal malformations. Ultrasound Obstet Gynecol 1992;2: 137–39.
8. Chiba Y, Hayashi K, Yamazaki S et al. New techniques of ultrasound, thick slicing 3D imaging and the clinical aspects in perinatal field. Ultrasound Obstet Gynecol 1994;4:195–97.
9. Feichtinger W. Transvaginal three-dimensional imaging. Editorial. Ultrasound Obstet Gynecol 1993; 3:375–78.
10. Baba K, Okai T. Clinical applications of threedimensional ultrasound in obstetrics. In: Baba K, Jurkovic D (Eds). Three-dimensional Ultrasound in Obstetrics and Gynecology. New York—London: The Parthenon Publishing Group, 1997,29–44.
11. Miric-Tesanic D, Kurjak A. Trodimenzionalni ultrazvuk u ginekologiji i porodnistvu. Ginekol Perinatol 1997;6:43–46.
12. Merz E, Bahlmann F, Weber G et al. Volume 3D scanning—a new dimension in the evaluation of fetal malformations. Ultrasound Obstet Gynecol 1993;3: 131–34.
13. Merz E, Bahlmann F, Weber G. Volume 3D scanning in the evaluation of fetal malformations—A new dimension in prenatal diagnosis. Ultrasound Obstet Gynecol 1995; 4:222–25.
14. Pretorius DH, Nelson TR. Three-dimensional ultrasound. Opininon. Ultrasound Obstet Gynecol 1995;5:219–21.
15. Benoit B. Three-dimensional surface mode for demonstration of normal fetal anatomy in the second and third trimester. In: Merz E (Ed). 3D Ultrasound in Obstetrics and Gynecology. Philadelphia.Lippincott Williams and Wilkins, 1998;95–100.
16. Kurjak A, Kos M. Three dimensional ultrasonography in prenatal diagnosis. In: Chervenack FA, Kurjak A (Eds): Fetal Medicine. Carnforth; UK: Parthenon Publishing, 1999;102–08.
17. Pretorius DH, Nelson TR. Three-dimensional ultrasound of fetal surface features. Ultrasound Obstet Gynecol 1992;2:166–68.
18. Lee A, Deutinger J, Bernaschek G. Three-dimensional ultrasound: abnormalities of the fetal face in surface and volume rendering mode. Br J Obstet Gynaecol 1995;102:40–43.
19. Lee A, Deutinger J, Bernaschek G. Voluvision: Threedimensional ultrasonography of fetal malformations. Am J Obstet Gynecol 1994;170:1312–14.
20. Lee A, Kratochwil, Deutinger J et al. Threedimensional ultrasound in diagnosing phocomelia. Ultrasound Obstet Gynecol 1995;5:238–40.
21. Bonilla-Musoles F, Raga F, Osborne N, Blanes J. The use of three-dimensional (3D) ultrasound for study of normal pathologic morphology of the human embryo and fetus: preliminary report. J Ultrasound Med 1995;14:757–65.
22. Bonilla-Musoles F Three-dimensional visualization of the human embryo: a potential revolution in prenatal diagnosis. Editorial. Ultrasound Obstet Gynecol 1996; 7:393–97.

23. Maymon J, Halperin Z, Weinraub A, Herman A, Schneider D. Three-dimensional sonography of conjoined twins at 10 weeks: a case report. Ultrasound Obstet Gynecol 1998; 11:292–94.
24. Kurjak A, Kupesic S. Three-dimensional transvaginal ultrasound improves measurement of nuchal translucency. J Perinat Med 1999; 27:91–96.
25. Blaas HG, Eik-Nes SH, Berg S, Torp H. In-vivo threedimesional ultrasound reconstructions of embryos and early fetuses. Lancet 1998;352:1182–86.
26. Lindsay DJ, Lyons EA, Levi CS, Zheng XH. Endovaginal appearance of the yolk sac in early pregnancy: normal growth and usefulness as a predictor of abnormal pregnancy outcome. Radiology 1988; 166:109–12.
27. Kupesic S, Kurjak A. Volume and vascularity of the yolk sac studied by three-dimensional ultrasound and color Dopller. J Perinat Med 1999;27:97–102.
28. Edmonds LD, Layde PM. Conjoined twins in the United States 1970–1977. Teratology 1982;25:301–08.
29. Meizner I, Levy A, Katz M, Glezerman M. Early ultrasonic diagnosis of conjoined twins. Harefuah 1993;124:741–44,196.
30. Achiron R, Achiron A. Transvaginal fetal neurosonography: the first trimester of pregnancy. In: Chervenak FA, Kurjak A, Comstock CH (Eds). Ultrasound and the Fetal Brain. Parthenon Publishing, London New York, 1995, 95–108.
31. Achiron R, Malinger G, Tadmor O, Diamant Y, Zakut H. Exencephaly and anencephaly: a distinct anomaly or an embryologic precursor: in utero study by transvaginal sonography. Israel J Obstet Gynecol 1990;l:60–63.
32. Goldstein RB, Filly RA, Callen PA. Sonography of anencephaly: pitfalls in early diagnosis. J Clin Ultrasound 1989;17:397–402.
33. Hudgins RJ, Edwards MSB, Goldstein R, Callen PW, Harrison MW, Filly RA, Golbus MS. Natural history of fetal ventriculomegaly. Pediatrics 1988;82:692–97.
34. Cardoza JD, Goldstein RB, Filly RA. Exclusion of fetal ventriculomegaly with a single measurement: the width of the lateral ventricular atrium. Radiology 1988;169:711–14.
35. Goldstein RB, LaPidus AS, Filly RA, Cardoza J. Mild lateral cerebral ventricular dilatation in utero: clinical significance and prognosis. Radiology 1990;176:237–42.
36. Bronstein M, Ben-Shlomo I. Cholorid plexus dysmorphism detected by transvaginal sonography: the earliest sign of fetal hydrocephalus. J Clin Ultrasound 1991;19:547–53.
37. Cohen M, Jirasek J, Guzman R, Gorlin R, Peterson M. Holoprosencephaly and facial dysmorphia: nosology, etiology, and pathogenesis. Birth Defects 1971;7:125–35.
38. Nelson LH, King M. Early diagnosis of holopros-encephaly. J Ultrasound Med 1992;ll:57–59.
39. Achiron R, Achiron A, Lipitz S, Maschiach S, Goldman B. Holoprosencephaly: alobar. Fetus 1994:4:9–12

Chapter 37
Three-Dimensional (3D) Ultrasound in Obstetrics

Asim Kurjak, Milan Kos, Nika Kalogjera

GENERAL OVERVIEW

Prenatal two-dimensional ultrasonography enables detailed visualisation of fetal anatomy but also detection of fetal growth and structure abnormalities. Improved two-dimensional technique offers high resolution images, but still remains the fact that three-dimensional structures are imaged and analyzed in two-dimensional planes. It is up to sonographer to construct a three-dimensional mental-picture and spatial orientation from few two-dimensional images. Although some have predicted that ultrasound technology has already reached its theoretical limits, the recent introduction of three-dimensional ultrasonography may lead to the development of entirely new clinical applications. Three-dimensional ultrasonography is still relatively new diagnostic imaging technique undergoing rapid advances in recent few years, particularly in the field of obstetrics and prenatal diagnosis. The first generation of 3D technology, during the early 1980s, had provided a pseudo3D image by the simultaneous display of the three ortogonal planes and offered some advantages over conventional 2D imaging. Modern 3D systems are capable to generate surface and transparent views depicting the sculpture like reconstruction of fetal surface structures or the X-ray-like images of fetal skeletal anatomy. These are the most impressive products within the modern three-dimensional ultrasound imaging. Main advantages of three-dimensional technology in perinatal medicine and antenatal diagnosis include scanning in coronar plane, improved assessment of complex anatomic structures, surface scan-analysis of minor defects, volumetric measuring of organs, “plastic” transparent imaging of fetal skeleton, spatial presentation of blood flow arborization and finally, storage of scanned volumes and images. With arbitrary sectional display in 3D-ultrasonography, the orientation of tomograms is unlimited, despite the limited probe manipulation or inadequate position of fetal structures. These facts are extremely important in the first trimester of pregnancy when the manipulation of the vaginal probe is restricted and obtainable ultrasound sections are limited. During the transabdominal scanning, coronar or frontal planes parallel to the fetal abdominal wall are also visible. These views are not available with conventional ultrasound. An additional progress is achieved owing to the permanent possibility of repeated analysis of previously saved three-dimensional volumes and

"kartesian" elimination of surrounding structures and artifacts. Three-dimensional reconstruction of stored image (surface and volume rendering) is the most impressive beneffit of three-dimensional scanning. The region of interest (ROI) is first identified and manually delineated, followed by an automatic process of echo extraction. In this way, the surface of the organ of interest is displayed in three dimensions. This enables a detailed morphological analysis of structures such as fetal face or minor defects. A transparency mode is another way of showing ultrasound images in three dimensions. In this mode, only the strongest and lowest signals are displayed, so that the internal structure of the organ of interest can be analyzed.

Although various systems have capacity for 3D ultrasound data acquisition a 3D image generation, the best three-dimensional images are obtained using a special three-dimensional, automatically drived, transabdominal and transvaginal transducers. These transducers have to be connected to a two dimensional high resolution machine with an integrated three-dimensional control processor and storage unit.

The main advantages of this new technology in obstetrics include improved assessment of complex anatomic structures and malformations, coronal plane scanning, spatial plastic imaging of surface and inner structures, spatial presentation of blood flow arborization and volume measurements. This technique does not only offer the third plane that is not available with 2D ultrasound, but also provides the examiner with a tomographic approach and the possibility to view the fetus in a true 3D surface image. The orthogonal display presents all three orthogonal planes simultaneously, allowing a detailed tomographic examination of the embryo or fetus in a non-moving position. Three-dimensional ultrasound offers several advantages over 2D ultrasound in the detection of specific small defects of the brain, face, spine, distal extremities and gender.

It has to be emphasized, rather than representing an alternative, that the three-dimensional technique is complementary to the conventional technique in the field of prenatal diagnosis. However, 3D imaging is evidently superior in specific diagnostic problems. A comparison of 2D and 3D techniques shows that in a large percentage of cases, 3D offers a diagnostic gain owing to the possibility of surface and transparent mode imaging. Some limitations are also present as with any new technique. For example, fetal and maternal movements during the scanning process lead to motion artefacts that can degrade the image quality. Fetal surface rendering primarily depends on sufficient amniotic fluid volume in front of the region of interest. In some cases, oligohydramnios and superimposed structure make surface rendering impossible. The most common difficulties are related to visualization of: face (mandible, lip, palate and tooth germs), skeleton, distal parts of extremities and body surface malformations.[1,4] Therefore, additional information can be provided by 3D US in these cases. Data presented in Table 37.1 indicate that 3D examination should be preformed whenever 2D US is incapable for visualization of these structures.

MODALITIES OF 3D IMAGING

Three-dimensional sonography (3D US) provides completely new modalities of sonographic scanning including coronar section imaging, three-dimensional spatial

reconstruction and volumetric calculations. Improved visualization rate, depiction of spatial relationship, “sculpture like” plastic

Table 37.1: Diagnostic information provided by 2D US and 3D US in 58 malformations

		Value of 3D US, No, *Malformation, (%)*		
Location of malformation	Total No. *malformations*	Superior *to 2D US*	Same as *2D US*	*Inferior to 2D US*
Cranium or face	13	9(69)	4(31)	0
Neck	2	1(50)	1(50)	0
Thorax	8	1(12)	7(88)	0
Abdomen	24	14(58)	10(42)	0
Spine and extremities	5	5(100)	0(0)	0
Body surface	6	5(83)	1(17)	0
Total	58	35(60)	23(40)	0

With permisson from reference 4.

imaging and volume measurement are the main benefits of new technology.

Multiplanar imaging offers an option of synchronous scanning in three orthogonal sections, including even coronar section. Computer data processing provides numerous sections unobtainable by two-dimensional sonography (2D US). Multiplanar view will result in simultaneous depiction of three sections orthogonal one the others. Two of them (transverse and longitudinal) are dependent on angle of insonation, whereas the third one (coronar) is not. This section is orthogonal to the insonation beam. Integration of data obtained by volume scanning can be used to depict 3D plastic (sculpture-like) reconstruction of region of interest (ROI). **Three-dimensional spatial reconstruction** can be presented in **surface or transparent mode** (Fig. 37.1). In the surface mode, only the signals from the surface of ROI are extracted and displayed in plastic appearance. In the transparent mode, the signals of highest and lowest echogenicity are extracted from the entire volume, resulting in possibility of spatial reconstruction of internal structure of ROI.[5] This mode is particularly useful for spatial reconstruction and imaging of fetal skeletal parts and their topographic relationship.

Three-dimensional **angio-mode** operates on technological basis of high-energy power Doppler. Its greater sensitivity is related to directionindependent scanning and better detection of smaller vessels. This mode provides optimal visualization and selective 3D reconstruction even of tortuous parts of vessels and blood flow arborization. More recently, three-dimensional reconstruction of the vascular channels has been accomplished utilising the Doppler amplitude mode.[6,7] The implementation of the 3D power Doppler imaging permits the physician to investigate the anatomy and topography of homodynamic within particular organ or ROI.

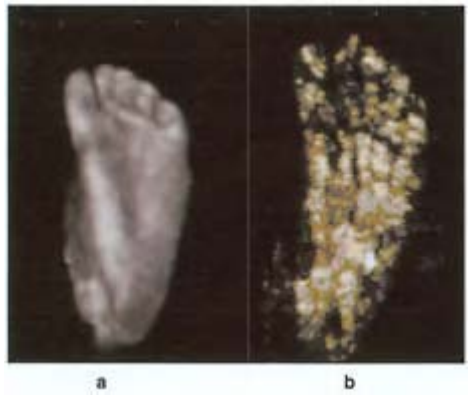

Figure 37.1: Modalities of 3D spatial reconstruction: Surface redered imaging provides the reconstruction of external structure (a), whereas transparent mode provides the reconstruction of the skeletal parts (b).

Three-dimensional measurement of organ volume (volumetry) is obtainable using sequential slice-stepping measurements of areas through the volugram of targeted organ. The volume assessment by two-dimensional sonography (2D US) includes the approximation of volume based on assumption that fetal organs have an ideal geometric shape, however it could be erroneous.

3D EVALUATION OF NORMAL FETAL ANATOMY

Head and Face

Assessment of fetal head is an essential part of routine sonographic examination.[8] Even under optimal conditions, the position of fetal head makes it difficult to obtain adequate images with two-dimensional ultrasonography, and many cross sectional images are required to imagine the complete impression of normal structure. 3D US can demonstrate two basic anatomic parts of the head: the neurocranium, containing the brain, and viscerocranium, composed of facial structures and skeleton. The shape of fetal head with flat cranial bones can be easily visualized and evaluated on single image at the end of the first trimester. Normal anatomy or major anomalies such as anencephaly, encephalocele and holoprosencep-haly can be recognized by detailed observation of skull shape.[9] There are numerous reports about the diagnosis of these anomalies with high frequency 2D transvaginal sonography at the end of the first trimester.[10,12] On surface rendered image the shape of the fetal head, cranial flat bones, orbits, ears, nose, and lips can be investigated clearly, and malformations can be easily excluded.[13] However, 3D

sonography does not provide significant improvement in earlier diagnosis of major malformations.

Assessment of cranial bones and sutures is an important step in confirming the normal morphology of fetal skull. Cranial sutures and fontanels are spaces between the fetal skull plates that allow progressive growth of the brain and skull bones during fetal development. At 12 weeks, premature cranial bones and sutures in between are detectable. The sagittal suture, lambdoid sutures and posterior fontanele can be recognized from 13 weeks. Portions of many sutures and fontanels can be identified with 2D sonography when experienced sonographer targets them. Unfortunately, sometimes it is difficult to assess structural continuity of sutures and fontanels with 2D US in a single plane because of physiological cranial curvature.[14,15] Three-dimensional surface rendering of neurocranium allows the visualization of sutures, fontanels and flat bones on single reconstructed image. Therefore, anomalies such as craniosynostoses can be excluded in early pregnancy.[14] Merz and colleagues studied 125 fetuses to examine the effect of 3D imaging on the axis of facial profile.[16] They found in 30.4% of the results that the profile section of head a bias off by 3–20° compared with optimal midsagittal section. As a result, only in 69.6% of the cases a true profile was obtained. The importance of this finding should not be underestimated. When a midsagittal plane is failed, anomalies may be missed or overlooked.

Previously mentioned data undoubtfully indicate that main improvement of 3D US is primarily related to facilitated visualization of morphological details and complex anatomical structures (Fig. 37.2).[17–19]

It is generally agreed that anomalous shape,

Figure 37.2: Spatial reconstruction of fetal face, surface rendering, plastic depiction of details is available during simultaneous visualization of mouth, nose and eyelids

size and position of fetal ears are associated with a number of known morphological and chromosomal syndromes. Prenatal assessment of ear includes the evaluation of its morphology and position. Unfortunately, due to the complex shape of ear, examination can be performed only to limit extent by 2D US and images obtained are inadequate for the evaluation morphology. Since only auricular geometry is visualized, the differentiation between variants of normal morphology and dimorphic ear is difficult. Surface rendering provides spatial reconstruction of auricle appropriate for the evaluation of ear morphology. Therefore, 3D US provides possibility to detect ear abnormalities by the end of second trimester. Shih and co-workers showed new possibilities of 3D US in systematic analysis of fetal ear and achieved better detection rate in visualization (84% versus 52.8%).[19]

Spatial information such as location and axis orientation can only be evaluated with 3D US. The major axis of normal auricula is vertical and parallel to the head. The normal orientation is anterolateral with superior border pointing toward the cranium. Therefore spatial information allowed detection of low ear set and ears asymmetry such as differences in implantation and size.[19]

Fetal Thorax and Abdomen

Nelson and Pretorius stated that the evaluation of the complete anatomy of the thoracic skeleton in the developing fetuses often is difficult with 2D US because of the curvature of the bones.[20] Ribs can be completely observed using 3D US transparency mode. This modality reduces the echogenicity of the soft tissues, leaving behind echogenic structures, namely the bones. The curvature and relationship of the rib ends to the vertebral bodies and the anterior chest wall can be demonstrated as well as the entire length.

Three-dimensional surface mode enables sculpture-like reconstruction of the abdominal wall and normal umbilical cord insertion. The complete abdominal surface is invisible by conventional 2D technology, with the only means abdominal surface survey involving serial tomographic sections in sagittal and transverse planes. Using the 3D surface mode we are able to visualize the complete abdominal surface and complete umbilical cord insertion in a single image depicting their natural appearance. On the surface rendering image continuity of the fetal skin can be easily confirmed. Normal appearances of these two entities are changed in abdominal wall defects. Post processing possibilities of picture offers a possibility for surface imaging of intraabdominal structures. It is possible to construct any slice nearly parallel to the mother's abdominal wall in arbitrary section or orthogonal triple-section display, thus making it possible to observe the esophageal-gastric junction and pylorus. The electronic pen or electronic rubber is used to "cut out" the overlying body segments, producing either a longitudinal or transverse section. Once this has been done, pathologic organ can be evaluated separately.

Heart

Congenital heart disease is the one of the most commonly occurring congenital malformation. The four-chamber view of the fetal heart is currently used for screening

and is included in the standard ultrasound examination. By visualization of normal four-chamber view only 40% or less fetal congenital heart defects can be excluded.[21] There is still search for more improved type of cardiac examination that provides better assessment of cardiac anatomy especially in low-risk population.

3D US, owing to its motion poorly display the heart. Bonila-Musoles and co-workers visualized heart in 11% of cases with 3D US. Only contours were seen, but no internal structures. With 2D US heart was evaluated in 97% of cases, observing the four chambers.[22] However, there are some publications of 3D US use in the fetal cardiovascular system. Zosmer and co-workers observed intracardiac anatomy by transparency display and obtained good cardiac images at 20 weeks of gestation.[23] In 3D US examination of the adult heart with the regular rhythm, 3D data are generally acquired over a period of many heart beatings, monitored by an electrocardiogram (ECG). A 3D image at each part of the cardiac cycle is constructed using data only for that particular part. For a fetus, an ECG for synchronization is not obtainable. Nelson and coworkers solved this problem by using the movement of a heart wall/valve instead of the ECG, and constructed 3D images of the fetal heart without distortion due to beating.[24] These authors also measured the cardiac output based on voluminal change in the lumen of the heart.[25] However, much time was required to obtain 3D data and fetal movements were a significant problem. Meyer-Wittkopf and co-workers have developed a novel 3D US system with Doppler based phasing of the fetal cardiac cycle.[26] Image acquisition time is reduce to < 30s and provides spatial and temporal assessment of the beating fetal heart. Using this technique scanning time is much reduced and does not require specialized scanning skills to obtain standard views. Unfortunately 3D US with this new technique enabled visualization of standard cardiac views in only 19 of 30 fetuses. These views were well visualized in all but one fetus using 2D US. However, there is some additional information provided with 3D US. They are structural depth, dynamic 3D perspective of valvular morphology and ventricular wall motion.

Skeleton and Extremities

3D US give clear display of curved structures such as the spine, ribs, skull and extremities in a single rendered image. [1,27–29] Using these techniques it is possible to assess skeletal development and related abnormalities. Particular importance is related to the visualization of malformations of fetal skeleton by volume rendering using transparent mode, maximum mode and “X-ray-like” imaging. This technique includes the volume rendering combining minimum and maximum intensity mode. Transparent mode of 3D US allows imaging of fetal skeleton, depicting malformations in spatial orientation.

The vertebral column is originally curved anteroposteriorly. If it is pathologically curved laterally, it is impossible to display the whole vertebral column in one 2D dimensional tomogram. The advantage of 3D ultrasound is the ability to visualize both curvatures at the same time.

Congenital malformations of fetal spine and ribs can be identified easier using 3D surface imaging and transparent mode reconstruction together. Specific vertebral body level may be accurately identified by simultaneous evaluating of axial planes of the spine within a volume rendered image or within the coronal plane image. It is difficult to acquire the entire spine in a single volume and thus multiple volumes are often necessary

to evaluate the spine completely. The most impressive transparent mode reconstruction will result in complete skeletal "babygram".[13,15] Extremities consist of three parts: proximal, medial and distal. With this mode all three segments and spatial relationships between them could be analyzed in three-dimensions. Therefore, the deviation of normal anatomical axis such as pathological angulations of hands and foots can be excluded by 3D US examination.[30]

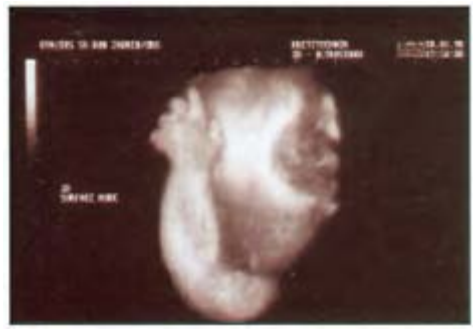

Figure 37.3A: Normal fetal hand reconstructed in surface rendered mode

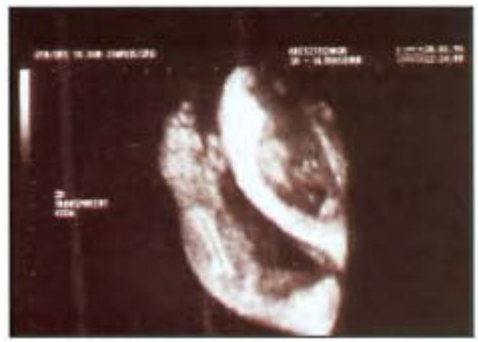

Figure 37.3B: Transparent mode reconstruction of the same hand with clearly visible skeletal structures and soft tissue

Three-dimensional images can be presented in two modes. If one interests spatial relationship between segments of fetal extremity than surface rendering mode should be used (Fig. 37.3A). However, if in the focus of interests is relationship between bone elements of fetal extremity than transparent mode should be used (Fig. 37.3B). By combination of these two modalities more detailed analysis of fetal anatomy can be performed. This illustrates, that fetal skin, subcutaneous tissue and bone structures can be

evaluated. As fingers are clearly visible in the surface mode, this technique is very useful in demonstrating the normal morphology of these structures.

Spatial relations between medial and distal segment of fetal leg can be assessed on surface rendering mode. Normal anatomical axis and her deviations can be confirmed. The number and position of toes are clearly demonstrated on surface mode. Using two modalities of the threedimensional ultrasound step-by-step we can evaluate fetal foot from external appearance to complex bone inner- and intra-topographic relations. Surface of the skin and external spatial relations are shown on surface rendering image. Complex anatomy of bone elements is confirmed on transparent mode image.

Volumetry—Organ Volume Measurements

Before the introduction of 3D US organ volume measurements have not been widely used for assessment of fetal growth and organ abnormalities, because of limitations of 2D US in estimating volumes of irregular structures. Comparing with 2D US, 3D US enables organ volume measurement by stepping through organs slice-by-slice. The area could be traced by means of a cursor in each plane of the object. Building the sum of each slice's volume can perform total volume calculation (Fig. 37.4). Riccabona and colleagues have shown, both *in vitro* and in *vivo*, that 3D US provides more accurate volume estimation of structures with irregular shapes compared with 2D US.[31,32]

The feasibility of calculating volumes of the following structures and organs has been reported: fetal lungs and fetal heart from second trimester to full term, placental volume, fetal arms, thighs, renal and cerebellum volume for estimation of the fetal weight.[33,35] Of special interest are measurements of fetal lung volume in order to confirm or exclude fetal lung hypoplasia or immaturity.[36]

Since 3D US offers more sophisticated volume measurements it is possible to measure volume in spite of irregular shape of organs.[33,34] Lung and hepatic volume normograms have been published, showing that volumes of these increase with gestational age and weight.[34,36]After upper abdominal circumference the best prediction of fetal growth restriction is hepatic volume.[37] Therefore it could be new useful parameter in assessment of fetal growth. For many years taking abdominal

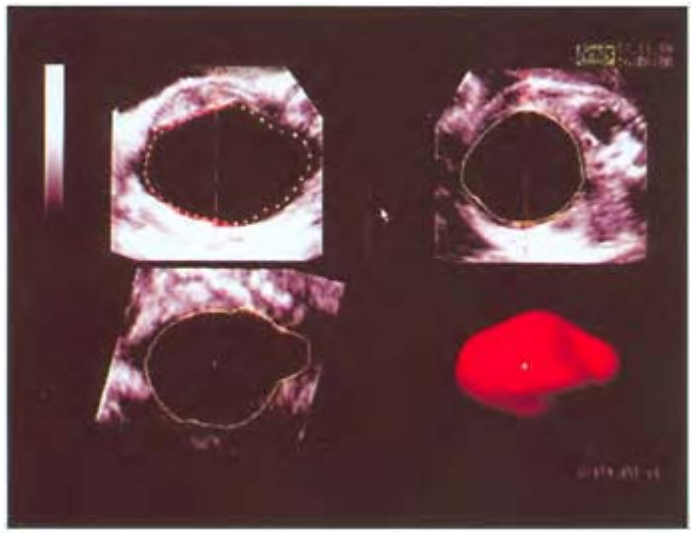

Figure 37.4: Technique of volume measurement. The margins of full bladder are traced with cursor in three orthogonal planes. Volume of the bladder is automatically calculated

circumference has assessed fetal weight. Among all possible sections and parameters of fetal trunk abdominal circumference has been chosen because it reflects changes of liver size. This method does not consider the amount of fetal fat tissue and there is still missing better discriminator for fetal growth aberrations.[38,40] Although, neonatal fat mass represents only 14% of birth weight, it explains 46% of its variance.[41] Birthweight predictions based on limb volumetry (upper arm and thigh) with new formulas are far more accurate.[42,43]

3D ASSESSMENT OF FETAL MALFORMATIONS

Head and Neck

Fetal head is an important part of the sonographic examination due to various physiological variations and association with malformations and chromosomal abnormalities.[8,44,45]

Dysmorphic appearance of fetal anencephaly and acrania can be understood better presenting the fetal head and neck in three-dimensional volume scanning. The visualization of the absence of fetal brain as well as the defect of the vault of the skull in anencephaly is better by 3D than by 2D US.[44] In acrania we can clearly differentiate fetal

brain as area cerebrovasculosa covering the skull and orbits as protuberances on the top of the head.

Simultaneous display of three orthogonal planes provides better visualization of encepha-locele.[46] Despite its relatively high sensitivity, 2D US is inferior over 3D US in the evaluation of the exact location of extracranial mass and amount of extracranial tissue.

Fetal hydrocephaly is one of the most common malformations detected by ultrasonography, also assessed by 3D US (Fig. 37.5).[44,45] 3D reconstruction of intracranial contents offers insight view of dilated bilateral ventricles and thin brain mantle. A dilated lateral ventricle and a dilated atrium in cases of unilateral ventriculomegaly can be assessed better with 3D US. This technique provides much better delineation of the exact nature and anatomic level of the brain malformations.

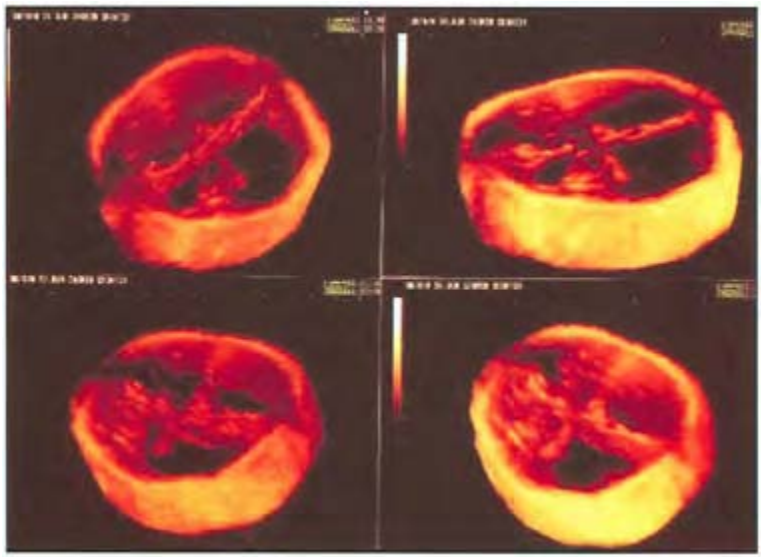

Figure 37.5: Hydrocephalus, 3D surface rendered mode. It is visible abnormal intracranial anatomy. The midline echo is normal but the brain tissue is significantly reduced

Intracranial echo-free spaces such as dilated ventricles, enlarged cisterna magna and Dandy -Walker cyst are necessary for obtaining the 3D acoustic window in almost all cases.[45]

If holoprosencephaly is present, 3D surface images of CNS structures can be obtained by electronically eliminating the calvaria from the image. Absent interhemispheric fissure, common ventricle and extend of thalamic fusion are evident in this malformation by 2D US. Although 3D US do not change the diagnosis of holoprosencephaly made by

2D US, it can assist in defining the seventy and extend of holoprosencephaly.[47] Most fetuses with holoprosencephaly have associated craniofacial fusion defects such as cleft lip/palate, hypotelorism, cyclopia, cebocephaly, and ethmo-cephaly.[48] The most severe facial malformations are associated with alobar holoprosencephaly. Since the 3D US is the method of choice for the evaluation of the fetal face, the 3D examination could be useful in determination of severity and extend of this malformation.[47]

Visualization of fetal face became one of major interest in three-dimensional ultrasonography. Detection of all details of normal facial anatomy and malformations became more available using 3D US. Region of special interest still remains fetal maxilla, mandible arch, ear and nose particularly due to their affection in malformation syndromes and chromosomal abnormalities. One of the first investigators who reported about 3D ultrasound imaging of the fetal face were Pretorius and coworkers.[17] They were able to obtain satisfactory images of the fetal face in 24 of 27 studied fetuses. Higher quality images were produced in scans after 19 weeks of gestation than scans obtained earlier, possibly due to the limits in sonographic resolution and anatomic definition of details. The possibility to analyze fetal face stimulates ultrasonographers for further investigations of this area. Palate and lips are important parts of the face for analysis. Malformations of palate and lips (fetal cleft lip/palate) are among the most frequent craniofacial malformations with an estimated incidence of about 0.1% births.[49] Before the introduction of 3D US, detection rates of cleft lip/ palate were very low (21%-30%).[50] Three-dimensional ultrasound can be helpful in the visualization of these abnormalities. Operator can rotate the image to gain even an impression of the depth of the defect. A simple cleft lip, for example, can be reliably differentiated from a more severe cleft involving the lip, maxilla, and palate. With the time, multiplanar view became fundamental in detection of these malformations. Volume rendered data offers a real benefit for analysis of some “subsurface” structures inside the head. It is possible to obtain three orthogonal slices of palate, pharynx and soft tissues regardless of intrauterine head position. In evaluation of these anomalies, lips could be assessed better with 3D US. Johnson and co-workers correctly detected cleft lip in all affected fetuses with 3D and in 93% with 2D US.[51] The opportunity to see the fetal face in the standard anatomic orientation on surface rendered image allows a more confident interpretation. Sequential transverse views may be obtained easily with 3D US and in the area of the upper lip they could confirm the presence of a cleft lip and help in precise detection of location. Appearance of the tooth germs can provide important diagnostic clues for cleft palate and they can be evaluated as parameters of normal development. In affected fetuses underdeveloped, supernumerary, or missing lateral maxillary incisors can be found. Ulm and co-workers reported that 3D US allowed visualization of tooth germs in 31% of studied fetuses.[3] On the other hand, only in 8.8% fetuses, the visualization has been obtained with 2D ultrasonography. In assessing the palate there are also several advantages of 3D US. By using interactive display, planar views may be manipulated without concern for fetal movement. Also surface-rendering image in combination with planar views could ensure us that the loss of signal in the palate defect was not due to transducer angulation and that the view of the face is symmetric. With combination of these modalities it is easy to differentiate maxilla and mandible. The next important advantage is the information that life-like rendered image could give to parents. It allows the family to see that their fetus has an abnormality and help them to understand

associated anomalies if they are present.[51] Primary cleft palate could be diagnosed in 86% of the cases by 3D US.[51] Therefore 3D US are not only a good tool for identification but also for a better localization of these malforma-tions. Lee and co-workers proposed a standardized approach for the evaluation of the cleft lip and palate by 3D US.[52] They used the multiplanar view for the examination of the upper lip, axial views to visualize maxillary tooth bearing alveolar ridge and anterior tooth socket alignement. Combination of the multiplanar view and surface rendering view were obtained for detection of premaxillary protrusion. Incomplete integrity of the alveolar ridge was used as a sign of cleft palate and a presence of premaxillary protrusion as a sign of bilateral cleft lip and palate. Surface rendering in their study increased diagnostic confidence by confirming findings that had been initially suspected by multiplanar views. They analyzed 7 fetuses with facial clefting anomalies using the method described above. For example, in fetuses with unilateral cleft lip/palate positive predictive value was up to 100%. On the other hand in the group with bilateral cleft lip/palate, positive predictive value was only 75%. These results are encouraging in spite of the low number of examined fetuses.

Combined use of different 3D US modalities gives opportunity to easily assess rare morphological anomalies such as single nostril, flat nose, proboscis, cyclopia, hypertelorism and hypotelorism.[3,19,28,53]

The anomalies of fetal mandible can also be recognized and confirmed by 3D US. They are a common feature of many chromosomal and genetic syndromes.[54] For example micrognathia is associated with Robins, Tracher-Collins, PenaShokier, Seckel and many other syndromes. Advantages of 3D US in visualization of fetal mandible are: 1) once the volume of interest is stored, the time to visualize fetal mandible is reduced; 2) there is no need to exclude any case because 3D US gives opportunity to perform relevant measurements in all cases. The diagnosis of posterior displacement and restriction in size of the fetal mandible is more precise; 3) multi-planar images and ability to store volume provide opportunity to make objective diagnosis.[54]

Surface rendered and multiplanar modality of the 3D US were used by Rotten and co-workers to assess separately the most common anomalies of fetal mandible such as retrognatia and micrognathia. They assessed retrognatia (displacement of fetal mandible) through measurement of the inferior facial angle. All fetuses with mandible anomalies had inferior facial angle below cut off value of 50 degrees. The sensitivity for predicting retrognatia was 100%, specificity 98%, positive predictive value 75% and negative predictive value 100%.[54]

It is generally agreed that anomalous shape, size and position of fetal ears are associated with a number of known morphological and chromosomal syndromes. Dysplastic ears are present in 60% fetuses with Down syndrome.[55] Therefore in cases with detected ear anomalies systematic examination should be performed to determine suptile anomalies that are usually combined with chromosomophaties such as clenched hand in cases of trisomy 18. Chang and co-workers developed normal charts of fetal ear-growth indexes (ear length, ear width and ear area) and evaluated their efficacy in the diagnosis of fetal aneuploidias.[56] Combination of these three measurements elevated the sensitivity in detecting fetal trisomies up to 57.1% and specificity to 83.2%.

Finally, in the following cases we can expect the higher quality of imaging and detection rate of fetal anomalies comparing to the 2D US:

1. Fetal cleft lip and palate; they are easily recognizable following the instruction for optimal technique of scanning;
2. Abnormal curvature of fetal face in a profile reconstruction;
3. Minor defects of face related to chromosomal abnormalities;
4. Fetal face/profile dysmorphism related to systematic or metabolic disorders (pterygium syndrome, skeletal dysplasias);
5. Facial profile investigation: micrognathia, absent nose, frontal bossing;
6. Fetal tooth germs investigations (oligodentia or anodentia).

In the neck region transabdominal scanning can detect changes like larger cystic hygromas, occipital cephalocele, thyroid tumours etc.[57] A same success rate of 100% for prenatal diagnosis of fetal cystic hygroma can be achived by 2D US and 3D US.[58] With the 3D image presented by various modes of reconstruction, the individua-lized variation in understanding the lesion can be reduced and, therefore, better prenatal consultation can be obtained.

Fetal Thorax and Abdomen

3D surface rendering in fetuses with dorsal cleft anomalies permits an accurate surface analysis that can clearly differentiate level and extent of protrusive lesion.[28] Complete rachischysis, isolated spina bifida, myelomeningocele, and some other defects of the spinal column can be easily depicted (Fig. 37.6). Optimal period for evaluation of fetal spine is between 12 and 16 weeks by transabdominal sonography. Sometimes the examination of the area of interest is not possible due to unfavorable fetal position. Therefore, indirect signs of spinal malformations are used such as lemon and banana signs. Screening for these signs of spinal malformations are part of routine prenatal sonographic examination. Banana sign is present up to 70% of cases with open spina bifida in second trimester with sensitivity of this sign is up to 99%.[59] False-negative findings are connected with smaller and skin-covered lesions and that is one of advantages in evaluation of central nervous system anomalies where 3D US may be benefitial. They are identification of level and extend of neural tube defects, visualization of scoliosis and subtle neurotube defects with minimal or no changes in bone structures. It is acomplished by using simultaneous multiplanar imaging in combination with volume rendered image.

Furthermore 3D US provides, for less experienced sonographer, helping detection of this anomaly especially in work with low-risk population. Accurate identification of the level of spina bifida and extent of this neurotube defects is very important in counselling the families and has significant impact on decision about termination of pregnancy and obstetric management.

It can be determinated by using the surface rendered image and sagittal and/or coronal planar view as help for the assessment of transverse view through vertebral bodies. Simultaneous multi-planar view throughout the same vertebral body give chance for more accurate identification of specific level of neurotube defect.[60] Moreover, in a case of myelomeningocele, the sac can be “electronically resected” to demonstrate the actual surface defect, even if the orifice is quite small.

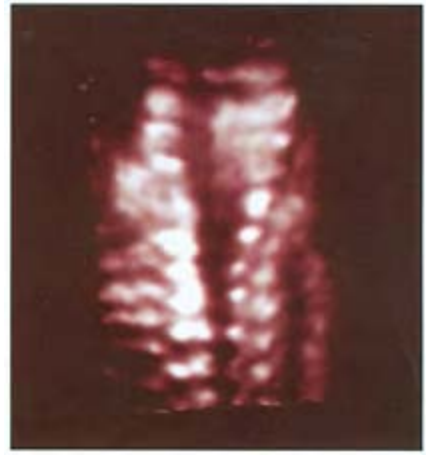

Figure 37.6: Severe rachischysis assessed by 3D transparent mode technique. Spatial presentation of "opened" neural tube. Widening of ossification centers of the vertebral arches are visualized in the upper thoracic spine

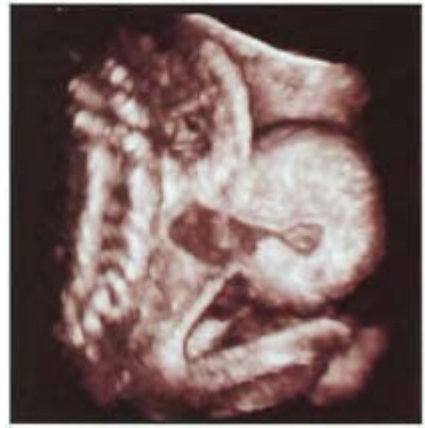

Figure 37.7: Omphalocele, 3D reconstruction in surface rendered mode. Fetal stomach is reconstructed just between peritoneal cavity and omphalocelic sac

Omphalocele and gastroschisis are the most commonly identified malformations of abdominal wall. Other ventral abdominal wall defects (cloacal exstrophy, bladder exstrophy, body-stalk syndrome, and pentalogy of Cantrell) occur in a much lower incidence than gastroschisis and omphalocele but they are much more severe. Distinction between these two anomalies has prognostic implications and can usually be accomplished with 2D US.[46] The diagnosis of omphalocele is based on the evidence of an adjacent mass in direct contact with anterior abdominal wall and surrounded by a thin membrane, which forms the hernia (Fig. 37.7). Herniation occurs through umbilicus. The whole defect and its contents can be observed with 2D US.[61]

On contrary in gastroschisis intestinal loops float freely in the amniotic fluid without any membrane thought a small paraumbilical defect that involves all layers of the abdominal wall. It is usually an isolated entity, rarely associated with other malformations and chromosomophathies. In contrast omphalocele is usually associated with chromosomal abnormalities such as trisomy 18 and 13, triploidy and Klinefelter's syndrome. Furthermore it could appear in a variety of syndromes, most notably, Beckwith-Wiedmann syndrome (omphalocele, macroglossia, organomegaly and neonatal hypoglycemia), pentalogy of Cantrell (midline supraumbilical abdominal defect, sternal defect, intracardiac anomaly, deficiency of diaphragmatic pericardium and anterior diaphragm) and cloacal exstrophy (OEIS complex: omphalocele, exstrophy of the bladder, imperforate anus and spina bifida).

In fetuses with ventral body clefts 3D US offers new capabilities for visualization of the defect and prolapsed organs.[28] Although most of these defects are large and well depicted by 2D US, the rotating display enables the defect to be viewed from multiple angles and often provides better impression of severity of the anomaly. Even in omphalocele and gastroschisis where 2D US depiction rate is 100%, there are still some advantages of 3D US. Some of them enables surface rendering mode with possibility of sculpture like reconstruction of abdominal wall defects. Using this modality, the type and extension of the defect are precisely demonstrated, depicting the size of defect involved organs, umbilical cord position and amnioperi-toneal coverage. In some cases such as ompha-locele volumetric evaluation of exteriorizated abdominal contents can be better carried out with 3D US than 2D US. It is important for the prognosis.

Structural changes of fetal skin surface also can be evaluated, emphasizing the possibilities of visual demonstration of congenital ichthyosis.[62]

Three-dimensional ultrasound cofirms diagnosis of multicystic dysplastic kidney, as well as 2D US, and provides additional information that can help in comprehension of the severity and extend of malformations.[63]

A surface rendered image provides an easily recognized anatomic detail of normal genitalia. However for identification of fetal gender it is best to obtain midsagittal plane.[64] Abnormalities of genital system such as ambiguous genitalia, hypospadias and bipartite scrotum could be assessed easily by 3D US.[65]

Skeleton and Extremities

3D US give clear display of curved structures such as the spine, ribs, skull and extremities in a single rendered image.[1,27,29] Extremities consist of three parts: proximal, medial and distal. Using surface and multiplanar mode together all three segments and spatial relationships between them could be analyzed in three dimensions. Surface rendering mode give clear displays of changes of the normal anatomical axsis. With 3D US, two orthogonal section can be displayed together. The section at the exact midpoint of the limb can be obtained. Using this orientation reversible or irreversible pathological angulations of the normal anatomical axis can be visualized. Precise topographic relationship among three segments of each limb, but also of the wrist, hand and finger could be assessed. Fetal position and neurological damage could cause congenital deformities and contrac-tures of joints and limbs. Their spatial relationship may be evaluated sinchronously in three orthogonal planes.

The vertebral column is originally curved anteroposteriorly. The advantage of 3D ultrasound is the ability to visualize both curvatures at the same time.[60] Anomalies such as scoliosis, kyphosis, lordosis and spina bifida may be overlooked by 2D ultrasound, but are easy to recognize using three-dimensional maximum mode. The overall incidence of congenital skeletal anomalies is about 20 cases per 100,000 births.[66] A number of these disorders are lethal such as thanatophoric dys-plasia, achondrogenesis, osteogenesis imperfecta—type II, etc. Therefore, confident antenatal diagnosis would give option to patient to terminate pregnancy. Other skeletal dysplasias are associated with mental retardation and this information is important in prenatal counselling. Furthermore correct and precise prenatal diagnosis in most cases could not be obtained with 2D ultra-sonography. Among all other skeletal disorders shortened ribs and narrow chest have been seen in fetuses with skeletal dysplasias. Such finding is significant because chest restriction leads to pulmonary hypoplasia, a frequent cause of death in these conditions. These malformations can be depicted better using 3D surface imaging and transparent mode reconstruction together.[67] The curvature and relationship of the rib ends to the vertebral bodies and sternum can be visualized as well as the entire length. The transparent mode is useful for detecting abnormalities of the fetal thorax, but in some conditions, such as a very narrow thorax, surface mode could be of additional clinical importance. Rotation of rendered volume data is helpful in detecting significant thoracic disproportion relative to the abdomen.

Abnormalities of the hands or feet are associated with skeletal dysplasia and chromosomopathies such as trisomy 13, 18 and 21.[1,2–29]3D US gives clear display of normal and abnormal extremities.[1,27] Therefore, may allow improved evaluation of fetal hand and feet. Using these technique it is possible to assess malformations and deformations of fetal extremities and related structures.

With 3D US fingers and toes are also very well observed. Therefore it is helpful for detecting syndactyly, polydactyly and overlapping fingers (Figs 37.8A to C).[1,27]

Ploeckinger-Ulm and co-workers studied 72 fetuses from low-risk pregnancies and showed that 3D US enables a complete visualization of all fingers in significantly more fetuses that 3D US (74.3% versus 52.9%, $p<0.05$).[2] The optimal time for evaluation is between 20 and 23 weeks of gestation. With 2D US one hand was visualized in 93% of cases. Budorick et al studied hands of 44 fetuses from high-risk pregnancies.[27] Hands and fingers were correctly diagnosed in all cases of normal and abnormal anatomy on both 3D US and 2D US. According to the authors 3D advantages were: 1) rotation of stored

3D volume rendered images allows a more comprehensive evaluation of fetal toes and fingers; 2) storage of data that allowed for systematic review of any structure of interest; 3) flexed fingers could be assessed as normal; 4) the thumb could be evaluated simultaneously with the other fingers;

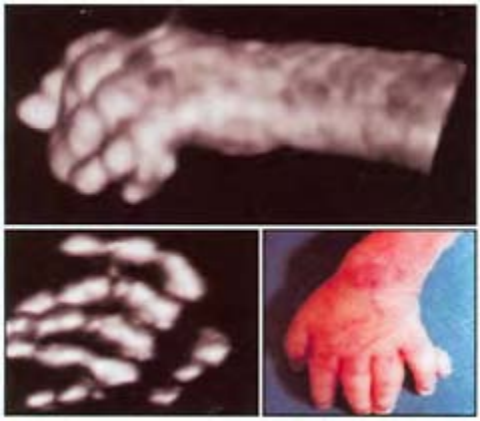

Figures 37.8A to C: (A) Reconstruction of forearm, wrist and fingers with postaxial polydactyly by surface rendered mode. (B) Fetal metacarpals and phalanges by transparent mode. Hypoplastic skeleton of an extra digit is clearly visible. (C) Pathomorphological specimen of the aborted fetus

5) the phalanges and metacarpals could be accurately counted and measured in normal hands, included even when fingers were flexed. In the study of Hata and co-workers, percentage of visualization of the fetal digits with 3D US was 74%, which is in fair agreement with the report of Ploeckinger-Ulm and co-workers.[2,29] Optimal visualization of the fetal digits was achieved between 28 and 35 weeks of gestation. One of the reason for this difference could be that Hata et al used only the surface-rendering mode. Before 15 weeks or after 36 weeks the respective percentages decreased. According to their results the ability to evaluate fetal fingers was better with 3D US than 2D US in the late first trimester and early second trimester.

Evaluation of the distal parts of legs is difficult with 2D US, because of a need to observe the relationship between tibia/fibula to the hindfoot and forefoot. Optimal 2D US evaluation of the distal extremities requires obtaining the sagittal plane through lower part of the leg. This plane is of crucial importance for evaluation of relationship of the tibia and fibula to the ankle. On that way we can evaluate pathological angulations of the normal anatomical axis such as clubfoot.

According to Budorick and co-workers normal legs were better assessed with 3D US than 2D US (85% versus 52%).[1] Rotation of the rendered volume of the distal extremities provided additional information in assessing and understanding foot position. Although 3D US did not significantly improve ability to diagnose normal from abnormal distal extremities, authors stress that significant improvement may be seen in less experienced centers in evaluating lower limb anomalies. The list of abnormalities of distal extremities included: clubfoot, rocker bottom feet, polydactyly and single bone short leg.

Kos et al studied 41 out of 347 high-risk patients with suspected initial diagnosis of limb abnormalities by 2D US.[68] The abnormal distal extremities were observed in 28 out of 41 suspected cases. The following anomalies were detected using 3D US: 17/28 clubfoot, 3/28 handpolydactyly, 2/28 upper limb contractures, 1/28 lower limb contracture, 4/28 micromelia, 1/28 overlapping fingers (Table 37.2). According to the authors positive predictive value for 2D US in detection of clubfoot was lower in comparison to the positive predictive value of 3D US (67.8% versus 89.9%). Therefore, 3D US accurately visualized angular limb deformities (clubfoot), contracture of limbs, shortening and bowing of

Table 37.2: Suspected diagnosis obtained by two modes of sonography compared by two modes of sonography compared to the perinatal outcome

Suspected anomaly	*2D findings*	*3D findings*	*Perinatal outcome*
Clubfoot	28	17	19
Hand polydactyly	5	3	3
Overlapping finger	0	1	1
Upper limb contractures	3	2	2
Lower limb contractures	1	1	1
Micromeiia	4	4	4
Total	41	28	30
With permission from reference 68			

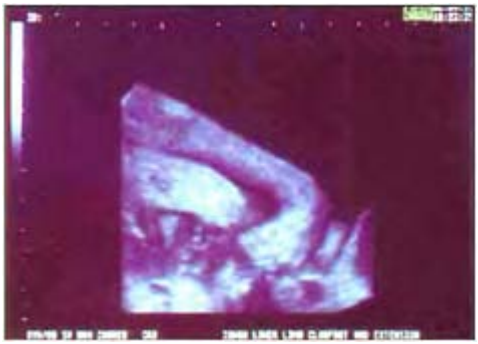

Figure 37.9A: Clubfoot is easily recognized in spatial relationships, surface mode imaging. Severe medial angulation of the foot is clearly visible as a main topographic disorder

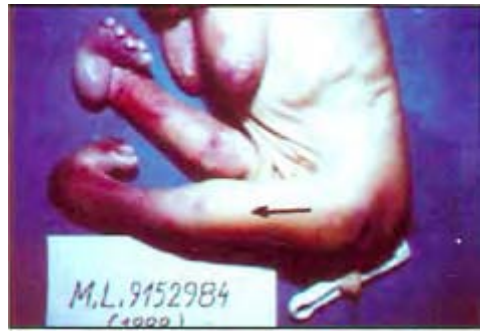

Figure 37.9B: Pathomorphological specimen of the aborted fetus

limbs, polydactyly and overlapping fingers (Figs 37.9A and B). Best spatial reconstruction was achieved in the case of fetal arthrogryposis associated with extremely reduced movements. According to the authors 3D US additional advantages include: 1) Transparent-mode reconstructions that are useful in detection of polydactyly pronouncing strong reflecting surfaces of additional finger and related skeleton; 2) Surface mode provided additional help in assessment of surface anatomy and integrity of skin cover. It was the most efficient modality in the diagnosis of angular deformation and joint contractures especially in cases where it is optimal amount of amniotic fluid.

Particular importance is related to the visualization of malformations of fetal extremities within the group of systematic skeletal dysplasias. Bone structures of the fetal skeleton can be depicted only in the 3D transparent mode, maximum mode and "X-ray like" mode, providing only an image of the structures with highest echogenicity. Using these modalities of 3D imaging we are able to make a spatial reconstruction of affected skeletal parts. These techniques enable detailed analysis to be made of the normal skeletal anatomy, but also the reconstruction of structural and topographic abnormalities included in systemic skeletal dysplasias. Using maximum mode imaging, volume rendering of the data allows visualization of the surface features, soft tissues and internal skeletal structures. The most advanced application of three-dimensional sonography is "real-time 3D" or "4D ultrasonography", which enables us to introduce better functional evaluation of fetal joints and related segments of musculoskeletal systematic reconstruction of shortened and curved—"bulky" extremities, in the cases of severe micromelic dwarfism. Using "maximum-mode" or "X-ray-like" post processing of imaging, the reconstruction of skeleton will result in a complete "baby-gram".

Main advantages of three-dimensional sonography in prenatal diagnosis:

- Improved visualization and diagnosis—Valuation of image planes that cannot be obtained with conventional 2D US due to anatomic constraints and/or fetal position.
- Easy demonstration of the coronar plane—the third plane which cannot be displayed by conventional 2D ultrasonography.
- Better recognition of minor defects related to fetal aneuploidies and realistic depiction of fetal surface anatomy.
- Transparent mode—New dynamic imaging of fetal skeleton.
- Improved orientation in spatial anatomic relationships by interactive rotation of volume rendered images, even including the powere doppler imaging of fetal and placental vessels —particularly in the cases of multiple and severe fetal malformations.
- Volumetry of fetal organs and placenta.
- Data collection, retrospective analysis, consultation and education.

REFERENCES

1. Budorick NE, Pretorius DH, Johnson DD, Nelson TR, Tartar MK, Lou KV. Three-dimensional ultrasonography of the fetal distal lower extremity: normal and abnormal. J Ultrasound Med 1998; 17:649–60.
2. Ploeckinger-Ulm B, Ulm MR, Lee A, Kratochwil A, Bernaschek G. Antenatal depiction of fetal digits with three-dimensional ultrasonography. Am J Obstet Gynecol 1996; 175:571–74.
3. Ulm MR, Kratochwil A, Ulm B, Lee A, Bettelheim D, Bernaschek G. Three-dimensional ultrasonographic imaging of fetal tooth buds for characterization of facial clefts. Early Hum Dev 1999; 55:67–75.
4. Xu HX, Zhang QR Lu MD, Xiao XT. Comparison of two-dimensional and three-dimensional sonography in evaluating fetal malformations. J Clin Ultrasound 2002; 30:515–25.
5. JurkovicD,JauniauxE,CampbellS.Three-dimensional ultrasound in obstetrcs and gynecology. In: Kurjak A,ChervenakF(Eds).TheFetusasaPatient.Carnforth, UK:Parthenon Publishing, 1994; 135–40.
6. Downey DB, Fenster A, Williams JC. Clinical utility of three-dimensional US. Radiographics 2000;20: 559–71.
7. Downey DB, Fenster A. Vascular imaging with a three-dimensional power Doppler system. Am J Roentgenol 1995; 165:665–68.
8. Baba K, Okai T. Clinical applications of threedimensional ultrasound in obstetrics. In: Baba K, Jurkovic D (Eds). Three-dimensional Ultrasound in Obstetrics and Gynecology. Carnforth, UK: Parthenon Publishing, 1997; 29–44.
9. Benoit B, Hafner T, Kurjak A, Kupesic S, Bekavac I, Bozek T. Three-dimensional sonoembryology. J Perinatal Med Med 2000; 30:63–73.
10. Achiron R, Achiron A. Transvaginal fetal neurosonography: the first trimester of pregnancy. In: Chervenak FA, Kurjak A, Comstock CH (Eds).Ultrasound of the fetal brain. Parthenon Publishing, London—New York 1995; 95–102.
11. Pooh RK. B-mode and Doppler studies of the abnormal fetus in the first trimester. In: Chervenak FA, Kurjak A. Fetal Medicine: The clinical care of the fetus as a patient. Parthenon Publishing, London New York 1999; 46–51.
12. Weissman A, Achiron R. Ultrasound diagnosis of congenital anomalies in early pregnancy. In: Jurkovic D, Jauninaux E (Eds). Ultrasound and Early Pregnancy. Canforth, UK: Parthenon Publishing 1996; 95–119.
13. Benoit B. Three-dimensional surface mode for demonstration of normal fetal anatomy in the second and third trimester. In: Merz E (Ed). 3D Ultrasound in Obstetrics and Gynecology. Philadelphia: Lippincott Williams and Wilkins, 1998; 95–100.

14. Patel MD, Swinford AE, Filly RA. Anatomic and sonographic features of fetal skull. J Ultrasound Med 1994; 13:251–57.
15. Pretorius DH, Nelson TR. Prenatal visualization of cranial sutures and fontanelles with three-dimensional ultrasonography. J Ultrasound Med 1994; 13:871–76.
16. Merz E, Weber G, Bahlmann F, Miric-Tesanic D. Application of transvaginal and abdominal threedimensional ultrasound for the detection or exclusion of malformations of the fetal face. Ultrasound Obstet Gynecol 1997; 9:237–43.
17. Pretorius DH, Nelson TR. Fetal face visualization using three-dimensional ultrasonography. J Ultrasound Med 1995; 14:349–56.
18. Pretorius DH, Nelson TR. Prenatal visualization of cranial sutures and fontanelles with three-dimensional ultrasonography. J Ultrasound Med 1994; 13:871–76.
19. Shih JC, Shyu MK, Lee CN, Wu CH, Lin GJ, Hsieh FJ. Antenatal depiction of the fetal ear with threedimensional ultrasonography. Obstet Gynecol 1998; 91:500–05.
20. Nelson TR, Pretorius DH. Visualization of the fetal thoracic skeleton with three-dimensional sonography: A preliminary report. AJR 1995; 164:1485–88.
21. Hess DB, Hess LW, Carter GA, Floyd RC, Fraser RF. Obtaining the four-chamber view to diagnose fetal cardiac anomalies. Obstet Gynecol Clin North Am 1998; 25:499–515.
22. Bonila-Musoles F, Machado LE, Osborne NG et al. Three-dimensional visualization of the normal fetuspart II. In:Bonila-Musoles F, Machado LE, Osborne NG (Eds). Three-dimensional ultrasound for the new millennium. Text and atlas. Madrid, Marco Grafico SL, 2000; 89.
23. Zosmer N, Gruboeck K, Jurkovic D. Threedimensional fetal cardiac imaging. In: Baba K, Jurkovic D (Eds). Three-Dimensional Ultrasound in Obstetrics and Gynaecology. New York: Parthenon, 1997; 45–53.
24. Nelson T, Sklansky M, Pretorius DH. Fetal heart assessment using three-dimensional ultrasound. In: Merz E (Ed). 3-D Ultrasound in Obstetrics and Gynecology. Philadelphia, Lippincott Williams and Wilkins 1998; 125–33.
25. Nelson TR. Three-dimensional fetal echocardiography. Prog Biophys Mol Biol 1998; 69:257–72.
26. Meyer-Wittkopf M, Rappe N, Sierra F, Earth H, SchmidtS. Three-dimensional (3D) ultrasonography for obtaining the four and five chamber view: comparison with cross-sectional (2D) fetal sonographic screening. Ultrasound Obstet Gynecol 2000; 15:397–402.
27. Budorick NE, Pretorius DH, Johnson DD, Tartar MK, Lou KV, Nelson TR. Three-dimensional ultrasound examination of the fetal hands: normal and abnormal. Ultrasound Obstet Gynecol 1998; 12:227–34.
28. Merz E, Bahlmann F, Weber G et al. Fetal malformations-assessment by three-dimensional ultrasound in surface mode. In: Merz E (Ed). 3D Ultrasound in Obstetrics and Gynecology. Philadelphia, Lippincott Williams and Wilkins 1998; 109–20.
29. Hata T, Aoki S, Akiyama M, Yanagihara T, Miyazaki K. Three-dimensional ultrasonographic assessment of fetal hands and feet. Ultrasound Obstet Gynecol 1998; 12:235–39.
30. Kurjak A, Hafner T, Kos M, Kupesic S, Stanojevic M. Three-dimensional sonography in prenatal diagnosis: a luxury or a necessity? J Prenatal Med 2000; 28:194–209.
31. Riccabona M, Nelson TR, Pretorius DH, Davidson TE. Distance and volume measurement using three-dimensional ultrasonography. J Ultrasound Med 1995; 14:881–86.
32. Riccabona M, Nelson TR, Pretorius DH. Threedimensional ultrasound:accuracy of distance and volume measurements. Ultrasound Obstet Gynecol 1996;7:429–34.
33. Pohls UG, Rempen A. Fetal lung volumetry by three-dimensional ultrasound. Ultrasound Obstet Gynecol 1998; 11:6–12.
34. Laudy JA, Janssen MM, Struyk PC, Stijnen T, Wallenburg HC, Wladimiroff JW. Fetal liver volume measurement by three-dimensional ultrasonography: a preliminary study. Ultrasound Obstet Gynecol 1998; 12:93–96.

35. Lee W, Deter RL, Ebersole JD, Huang R, Blanckaert K, Romero R. Birth weight prediction by three-dimensional ultrasonography: fractional limb volume. J Ultrasound Med 2001; 20:1283–92.
36. Osada H, litsuka Y, Masuda K, Sakamoto R, Kaku K, Seki K, Sekiya S. Application of lung volume measurement by three-dimensional ultrasonography for clinical assessment of fetal lung development. J Ultrasound Med. 2002; 21:841–47.
37. Boito SM, Laudy JA, Struijk PC, Stijnen T, Wladimiroff JW. Three-dimensional US assessment of hepatic volume, head circumference, and abdominal circumference in healthy and growth-restricted fetuses. Radiology 2002; 223:661–65.
38. Deter RL, Nazar R, Milner LL. Modified neonatal growth assessment score: a multivariate approach to the detection of intrauterine growth retardation in the neonate. Ultrasound Obstet Gynecol 1995; 6:400–10.
39. Vintzileos AM, Campbell WA, Rodis JF, Bors-Koefoed R, Nochimson DJ. Fetal weight estimation formulas with head, abdominal, femur, and thigh circumference measurements. Am J Obstet Gynecol 1987; 157: 410–14.
40. McLean F, Usher R. Measurements of liveborn fetal malnutrition infants compared with similar gestation and with similar birth weight normal controls. Biol Neonate 1970; 16:215–21.
41. Catalano PM, Tyzbir ED, Allen SR, McBean JH, McAuliffe TL. Evaluation of fetal growth by estimation of neonatal body composition. Obstet Gynecol 1992; 79:46–50.
42. Liang RI, Chang FM, Yao BL, Chang CH, Yu CH, Ko HC. Predicting birth weight by fetal upper-arm volume with use of three-dimensional ultrasonography. Am J Obstet Gynecol 1997; 177:632–38.
43. Chang FM, Liang RI, Ko HC, Yao BL, Chang CH, Yu CH. Three-dimensional ultrasound-assessed fetal thigh volumetry in predicting birth weight. Obstet Gynecol 1997; 90:331–39.
44. Kurjak A, Kos M. Three-dimensional ultrasonography in prenatal diagnosis. In: Chervenak FA, Kurjak A (Eds). Fetal Medicine. New York, Parthenon Publishing Group, 1999; 102–68.
45. Hata T, Yanagihara T, Matsumoto M, Hanaoka U, Ueta M, Tanaka Y, Kanenishi K, Kuno A, Yamashiro C, Ohnishi Y, Tanaka H, Hayashi K. Three-dimensional sonographic features of fetal central nervous system anomaly. Acta Obstet Gynecol Scand 2000; 79:635–39.
46. Dyson RL, Pretorius DH, Budorick NE, Johnson DD, Sklansky MS, Cantrell CJ, Lai S, Nelson TR. Three-dimensional ultrasound in the evaluation of fetal anomalies. Ultrasound Obstet Gynecol 2000; 16:321–29.
47. Lai TH, Chang CH, Yu CH, Kuo PL, Chang FM. Prenatal diagnosis of alobar holoprosencephaly by two-dimensional and three-dimensional ultrasound. Prenatal Diagn 2000; 20(5):400–03.
48. Bonila-Musoles F, Machado LE, Osborne NG et al. Three-dimensional visualization of the normal fetus-part I. In: Bonila-Musoles F, Machado LE, Osborne NG (Eds). Three-dimensional ultrasound for the new millennium. Text and atlas. Madrid, Marco Grafico SL, 2000; 89.
49. dementi M, Tenconi R, Bianchi F, Stoll C. Evaluation of prenatal diagnosis of cleft lip with or without cleft palate and cleft palate by ultrasound: experience from 20 European registres. EUROSCAN study group. Prenat Diagn 2000; 20:870–75.
50. Crane JP, LeFevre ML, Winborn RC et al. A randomized trial of prenatal ultrasonographic screening: impact on the detection, management, and outcome of anomalous fetuses. Am J Obstet Gynecol 1994; 171:392–99.
51. Johnson DD, Pretorius DH, BudorickNE, Jones MC, Lou KV, James GM, Nelson TR. Fetal lip and primary palate: three-dimensional versus two-dimensional US. Radiology 2000; 217:236–39.
52. Lee W, Kirk JS, Shaheen KW, Romero R, Hodges AN, Comstock CH. Fetal cleft lip and palate detection by three-dimensional ultrasonography. Ultrasound Obstet Gynecol 2000; 16:314–20.
53. Pretorius D. The fetal face: 3-D ultrasound. 2nd World Congress on 3-D Ultrasound in Obstetrics and Gynecology (syllabus). Las Vegas, Nevada USA, 1999.

54. Rotten D, Levaillant JM, Martinez H, Ducou le Pointe H, Vicaut E. The fetal mandible: a 2D and 3D sonographic approach to the diagnosis of retrognathia and micrognathia. Ultrasound Obstet Gynecol 2002; 19:122–30.
55. Hall B. Mongolism in newborn infants. An examination of the criteria for recognition and some speculations on the pathogenic activity of the chromosomal abnormality. Clin Pediatr (Phila) 1966; 5:4–12.
56. Chang CH, Chang FM, Yu CH, Liang RI, Ko HC, Chen HY. Fetal ear assessment and prenatal detection of aneuploidy by the quantitative three-dimensional ultrasonography. Ultrasound Med Biol 2000; 26:743–49.
57. Bonilla-Musoles F, et al. First-trimester neck abnormalities: three-dimensional evaluation. J Ultrasound Med 1998; 17:419–25.
58. Kang L, Chang CH, Yu CH, Cheng YC, Chang FM. Prenatal depiction of cystic hygroma using three-dimensional ultrasound. Ultrasound Med Biol 2002; 28:719–23.
59. Watson WJ, Cheschier NC, Katz VL, Seeds JW The role of ultrasound in the evaluation of patiens with elevated maternal serum alpha-fetoprotein: A review. Obstet Gynecol 1991; 78:123–28.
60. Riccabona M, Johnson D, Pretorius DH, Nelson TR.Three-dimensional ultrasound: display modalities in the fetal spine and thorax. Eur J Radiol 1996; 22:141–45.
61. Bonila-Musoles F, Machado LE, Osborne NG et al. Three-dimensional (3D) ultrasound detection of abdominal wall defects. In: Bonila-Musoles F, Machado LE, Osborne NG (Eds). Three-dimensional ultrasound for the new millennium. Text and atlas. Madrid, Marco Grafico SL, 2000; 215–27.
62. Benoit B. Three-dimensional ultrasonography of congenital ichtyosis. Ultrasound Obstet Gynecol 1999; 13:380–83.
63. Chang LW, Chang FM, Chang CH, Yu CH, Cheng YC, Chen HY. Prenatal diagnosis of fetal multicystic dysplastic kidney with two-dimensional and three-dimensional ultrasound. Ultrasound Med Biol 2002; 28:853–58.
64. Lev-Toaff AS, Ozhan S, Pretorius D, Bega G, Kurtz AB, Kuhlman K. Three-dimensional multiplanar ultrasound for fetal gender assignment: value of the mid-sagittal plane. Ultrasound Obstet Gynecol 2000; 16:345–50.
65. Merz E, Miric-Tesanic D, Bahlmann F, Sedlaczek H. Prenatal diagnosis of fetal ambiguous gender using three-dimensional sonography. Ultrasound Obstet Gynecol 1999; 13:217–19.
66. Pilu G, Rizzo N, Perolo A: Anomalies of the skeletal system. In: Chervenek FA, Isaacson GC, Cambell S (Eds). Ultrasound in obstetrics and gynecology. Little Brown and Co. Boston 1993; 2:981–97.
67. Nelson TR, Pretorius DH. Visualization of the fetal thoracic skeleton with three-dimensional sonography: A preliminary report. AJR 1995; 164:1485–88.
68. Kos M, Hafner T, Funduk-Kurjak B, Bozek T, Kurjak A. Limb deformities and three-dimensional ultrasound. J Perinat Med 2002; 30:40–47.

Chapter 38
Three-Dimensional Visualization of Fetal Malformations

Fernando Bonilla-Musoles, Luiz Eduardo Machado, Francisco Raga

INTRODUCTION

Many aneuploidies, including Down's syndrome (DS)-the most frequent chromosomal abnormality in newborns—have the benefit of a diagnosis during the first and second trimesters,[1,2] thanks to the use of a series of echographical markers first applied to 2D, with much clearer results using 3D.

Among such markers are:

1. *Morphological markers:*

- nuchal translucency
- early fetal growth restriction
- heart defects, ventriculomegaly
- intracardiac echogenic focus
- omphalocele, encephalocele and other anomalies
- choroid plexus cysts
- short femur and/or humerus
- pyelectasis
- echogenic bowel
- anatomic and positional anomalies of the extremities
- low ear implantation
- craniofacial anomalies
- flat nose with absent nasal bone
- increased iliac wing angles
- enlarged cisterna magna

2. *Hemodynamic markers:*

- Cardiac rhythm anomalies
- Vascular anomalies of the umbilical cord
- Fetal vascular anomalies
- Uterine vessel anomalies

3. *Placental markers:*

- Non-homogeneous, excessively thick and irregular placenta

4. *Adnexal markers:*

- Single umbilical artery
- Umbilical cord cysts and tumours
- Excessively thick umbilical cord
- Yolk sac anomalies
- Early poly and oligohydramnion

Useful information by 3D evaluation of the fetus can be obtained by using transvaginal 3D transducers from week 5 onward and with abdominal 3D transducers from 14–16 gestational weeks onward. However, with the advance of gestational age, as formerly seen with 2D, the complete observation of the fetus and the obtention of good quality images becomes increasingly difficult. This is especially the case after week 28.

The following conditions are necessary in order to obtain clear and sharp images of the fetus:

- Use of the most sophisticated and advanced 4D and 3D-real time multiplanar equipments, capable of simultaneously combining 2D and 3D real time frame images.[3]
- Use of pouches of amniotic fluid.
- Non-performance of imaging (except for 4D) during periods of fetal activity, including maternal movements and, if necessary, breathing.
- Selection of moment and fetal position that is optimal for imaging of the desired structure.
- Disregard for the time that is necessary to achieve the optimal conditions for a meticulous and systemic exploration. Speed is usually counterproductive in 3D imaging: be reminded of the Spanish proverb "go slowly because I am in a hurry".

Table 38.1

AUTHOR	*CASES*	*3D>2D*	*3D=2D*	*3D<2D*	*COMMENTS*
Merz[4]	204	62%	36%	2%	<Heart defects
Nelson[5]	103	51%	45%	4%	<Polymalformations
Bonilla-Musoles[5]	41	65%	35%	0%	<Heart defects, oligohydramnios

CURRENT STATUS

Although the three more comprehensive and classical sets of statistics of use of 3D for fetal malformations do show an improvement in the rate of diagnostic certainty, this is not applicable to all cases: for instance, the results are completely contrary with regard to congenital heart defects, despite the fact that the heart is one of the most important organs when attempting to arrive at a diagnosis of chromosomal abnormality, specifically DS (Table 38.1).

It is interesting to note that the above results have not been reproduced in recent years despite existing an important experience.

There are some who believe that the advantages in terms of better diagnostic rates would be too small[6] and that they would only be perceived in certain malformations such as cleft lip, superficial tumours, etc.[7]

It must be highlighted that, despite having been built on cases which form part of the authors' personal experience, all recent publications based on the latest technological software agree with us that 3D provides a much better resolution and a subtler picture in the diagnosis of complex malformations.[7–11]

DIAGNOSTIC AREAS IN WHICH 3D PROVIDES THE MOST INFORMATION

FETAL HEAD

Fetal head abnormalities such as anencephalyexencephaly-acrania, an osseous evolutive malformation, or hydrocephaly, are anomalies which can be observed with 3D as of week 11 and week 16 respectively.[15,66] Although the 3D image quality is much more realistic, this technology is not essential for arrival at a diagnosis, 2D allows also the diagnosis (Fig. 38.1).

CRANIOFACIAL MALFORMATIONS

Craniofacial malformations, together with skeletal anomalies, form part of a wide ranging set of defects of difficult diagnosis by the echographer in the absence of data on the mechanisms of embryological formation.

The problem is aggravated further by the need, on many occasions, to take a medical decision (including, at times, abortion) which pose ethical, moral or clinical problems.

Such defects are associated, with a frequency ranging between 25% and 66%, with other major or minor malformations or are part of polymalformative syndromes.

Cleft lip (CL) with or without Cleft Palate (P) is the most frequent and typical example thereof, despite having a seemingly low incidence (1 per every 700 to 1000 live newborns).

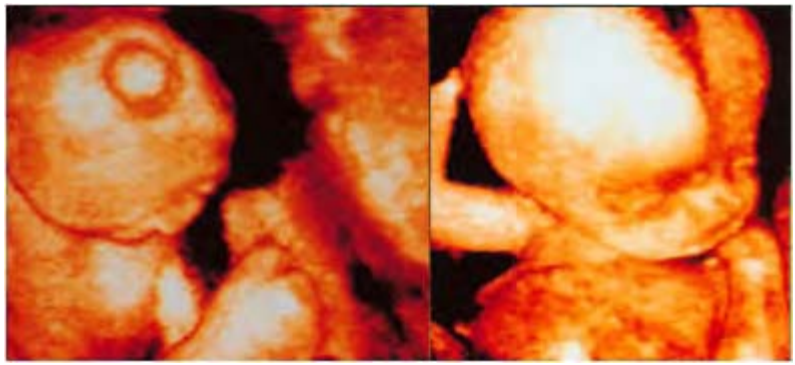

Figure 38.1: 16th week anencephaly with low set ears (left) and 17th week hydrocephaly (right)

The Spanish proverb “the face is the mirror of the soul” can be equated in Medicine with “the face predicts the brain”.[12] This has been shown in a recent publication[13] which reveals that, with the exception of the isolated cleft lip with hardly any repercussions, 90% of the cases are associated with malformations of the central nervous system (CNS), the heart, the kidneys, the skeleton or the intestines.

The problem becomes more complicated in the light of the variations in type and incidence of the malformations.[14] Associated defects are more frequent in fetuses with central (100%) and bilateral (72%) clefts than in those with unilateral clefts (48%). Fetuses with unilateral CL-P also have a better survival rate (52%) than those with a bilateral (35%) or central (0%) CL-R[14]

This is one of the most recommended applications of 3D technology[15–25] since its introduction.

The picture is far more realistic and bears no comparison to 2D, enabling better observation of the fetal face as well as of any lesion in the frontonasal area and the lips. All authors with experience therein agree on this point.[15–25]

The use of orthogonal planes, transparency systems, X-rays or 4D are of great assistance in the diagnostic process enabling observation, simultaneously on screen, of the three bidimensional planes required in any exploration (orthogonal planes) and 3D rendering.

There have, however, been recent comments[13] regarding the possible exceptional occurrence of false-positives, although false-negatives have not been reported.

3D technology, especially real time 3D, can be applied to the routine examination of the mouth and palate.

In addition to a greater diagnostic sensitivity—although not bearing a direct relation to cleft lip—a comparative 2D/3D case study has been published recently[25] of a harlequin fetus. The 3D images of the face, as well as exceptional, have proven to be of incredible assistance in the diagnosis.

ECHOGRAPHICAL CLASSIFICATION

We owe the best existing echographical classification, as yet unsurpassed, to Nyberg.[27] It is based on 65 cases, with no false-positives, of which 97% were correctly classified. It was likewise the first to indicate that the type and bilaterality correlate with fetal evolution, with associated defects and karyotype anomalies (Fig. 38.2):

The use by other authors of this classification has resulted in diagnostic rates ranging between 88%[17] and 100% (Fig 38.3).[13,17,28]

FRONTAL TUMOURS

Prenatal diagnosis of paranasal facial masses is important given the different possible prognoses.

The differential diagnosis includes:[29] frontal encephalocele, epignathus, vascular and lymphatic hemangiomas, teratoma, retinoblastoma, dacryocystocele, hygroma colli, goitre and nasal glioma,[30] but the use of 2D ultrasound for this purpose might prove difficult due to the scarce rendering of distinguishing features.

Some of these (encephalocele, teratoma, hemangioma) are often accompanied by other

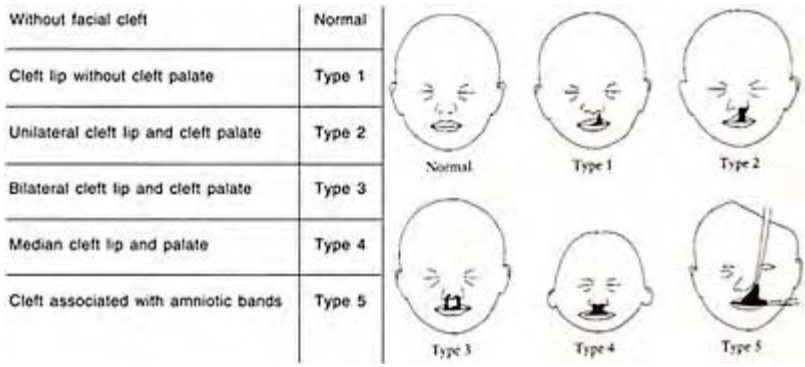

Figure 38.2: Fetal cleft lip with and without cleft palate—echographical classification or sonographic

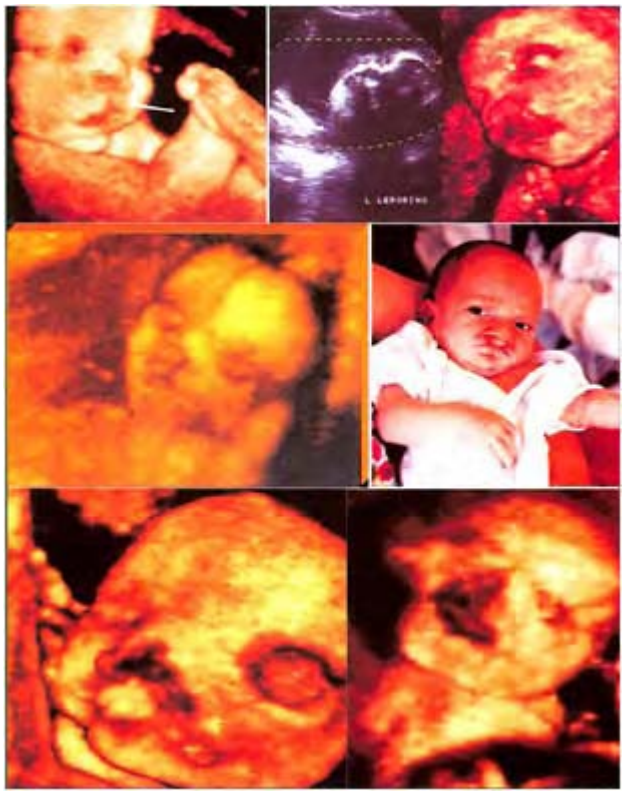

Figure 38.3: In top left an isolated CL is shown. In top right a CL-P is depicted. The central two images show a bilateral CL-P with the typical frontal protrusion. In bottom left a bilateral CL-P is shown. In bottom right a median CL-P can be clearly observed

CNS or generalized malformations, whereas the remainder are well defined and have a better prognosis.

The combined use of 2D ultrasound (localization, morphology and sonolucency), the identification of other accompanying malformations with the use of color Doppler and, when possible, 3D ultrasound technology, is recommended as a set of tools to assist in establishing a diagnosis.[29]

3D Ultrasound

A frontal encephalocele appears as a midline cyst, a solid-cystic or a solid mass projecting as a frontal skull defect.The size and form can be very variable, but it is normally round in shape and always accompanied by other CNS anomalies.

The best way to establish the final diagnosis is the combined use of 2D and 3D. Twodimensional ultrasound will help determine the CNS anomalies and 3D the outer limits and extension (Fig. 38.4).

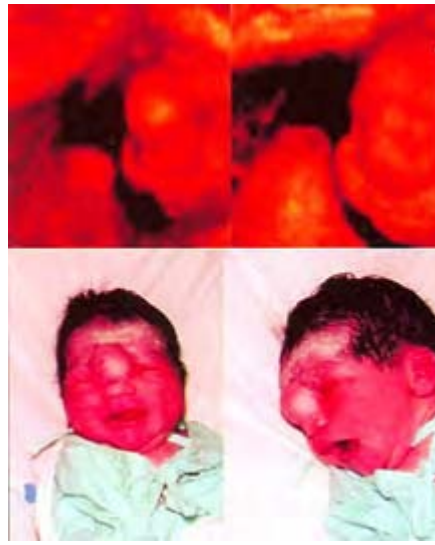

Figure 38.4: The image shows the frontal and mldsagittal view with 3D of the frontal omphalocele intrautero and in the newborn. The 3D image provides a practically life-like picture of the tumor

PROBOSCIS

The cyclops or *"polyphemus"* is a fetus with a frontonasal malformation characterized by one single eye with or without proboscis, and dermocartilaginous appendix or appendices located above anlage of the eyes, which gives it a monstrous appearance.

Despite its rarity, it has been a popular image since Homer's description thereof in the Odyssey in 800 BC.

Undoubtedly and, given its extremely high mortality, even in the cases of lesser severity—if indeed any can be so considered—reaching 97.5% in all cases within one

year of life,[30] the survival of any one of such cases belongs more to the realms of myth and legend than that of reality.

It is therefore not surprising that cases described in humans and animals are associated with mythology, fairy tales and anatomy or zoology museums, where they become the most visited exhibits.

The most severe facial malformations, such as cyclopia, are always accompanied by alobar holoprosencephaly, in which there is total absence of the division in the prosencephaly, hence its disastrous prognosis.[39]

Cyclopia, with or without proboscis, is undoubtedly the most severe variant, almost always accompanied by holoprosencephaly.[30,31]

Classification of the Anomalies of the Facies

Anomalies of the face are classified into four types:[31,32]

a. Cyclopia wih a single eye or several eye anlage bend degrees, with or without proboscis and no nose:

b. Ethmocephaly with hypotelorism and proboscis located between the eyes, nose absent.

c. Cebocephaly with hypotelorism and rudimentary nose with only one narine

d. Cleft lip with median cleft palate, that is, with premaxillary agenesia and hypotelorism.[5]

The use of 3D (Fig. 38.5) is particularly interesting in these types of malformations, which involve defects which alter the surface of the face, as 3D allows a much more realistic vision than 2D as well as helping to highlight proboscis.[32–33]

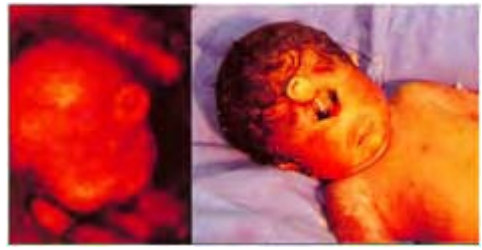

Figure 38.5: Cyclops with proboscis

NASAL BONE

In 1866 Langdom Down noted that newborns with trisomy 21 showed poor skin elasticity which gave the appearance of being too large for the body, and a "flat face with a small nasal bridge and nose". The excess of skin can be seen in the first trimester as an increased nuchal translucency.

The absence of, or an excessively small sized, nose is nowadays considered a new and extremely interesting marker of Down syndrome (DS).[34–41] This new marker is of special interest because:

- It is independent of mother's age
- It is independent of gestational age or BPD
- It is independent of, but can be combined with, nuchal translucency
- It is independent of the biochemical tests
- It appears in different aneuploidies.

The nasal bone has to be examined with 2D and 3D in a midsagittal view of the fetal profile with the beam being parallel to the nose (Figs 38.6 and 38.7).

The relationship with chromosomal syndromes (Trisomies 21, 18, 9, Turner, polyploidies and fragile X) is established when the nasal septum bone is absent in week 14 or beyond, or when its size is less than 4.5 mm after week 20, irrespective of gestational age (Fig. 38.7).

Hence, the relationship between the BPD/nasal bone length=10 would help to identify 81% of DS, in addition to an even more interesting

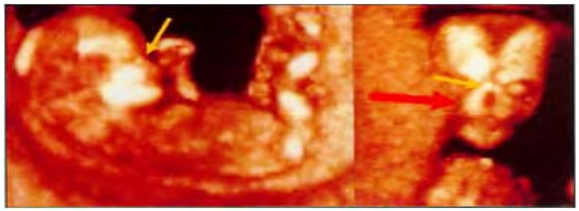

Figure 38.6: 3D ultrasound of a fetus aged 12 weeks and one aged 14

weeks. The yellow arrow indicates the nasal bone. The red arrow shows the maxillary cartilages

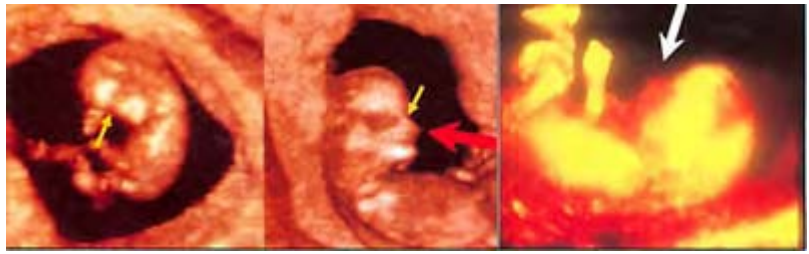

Figure 38.7: 3D ultrasound of 3 cases of fetuses of 11 and 12 weeks with no nasal bone (the left and the right) or is smaller than the norm. In the photograph on the left the yellow arrow indicates the point at which the nasal bone should be present. In the photograqph in the centre, the nasal bone marked by the yellow arrow is too small. The red arrow indicates mouth and nose. The image on the right, obtained with the minimal transparency system, reveals a clear absence of nasal bone

advantage: some of the DS fetuses without nuchal translucency could benefit from this new marker.

This bone can be observed clearly by using 3D with the three-orthogonal planes, thus facilitating the obtention of the correct midsagittal plane (Figs 38.6 and 38.7).

EAR MALFORMATIONS

Two-dimensional ultrasound examination of fetal ears is complex. It involves determination of location, axis orientation, length and shape. Most reports regarding chromosomal anomalies such as trisomies 21, 18, 13, Turner syndrome and fragile X syndrome show that they are associated with ear abnormalities.

Other syndromes are also associated with abnormal fetal ears, like first and second pharyngeal arch syndromes, holoprosencephaly, anencephaly, Crouzon's dysostosis and arthrogryposis.

There are very few publications on 3D and ear abnormalities, but they all show advantages when using this technology. 3D allows the visualization of the following ear anomalies:[42,43]

- Excessive length (Fig. 38.8)
- Excessive shortness
- Abnormal and irregular ears (Fig. 38.8)
- Angle anomalies (Fig. 38.8)
- Low implanted ears (Fig. 38.8).

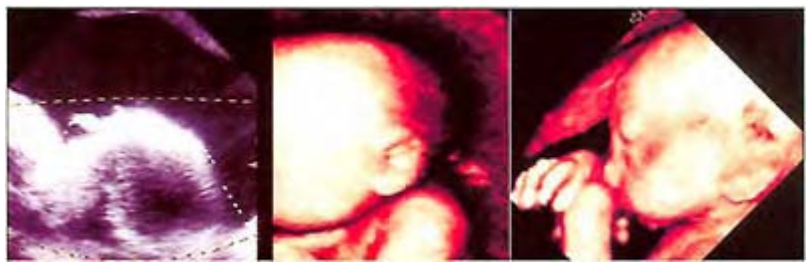

Figure 38.8: To the left a normal fetus with an excessively large ear. To the right, a trisomy 21 with low-set and abnormal ear

MANDIBLE

Anomalies in the mandible are not infrequent and are associated with more than 100 genetic syndromes, of which we highlight the main body of morphological manifestations:

- Pierre Robin sequence
- Treacher Collins syndrome
- Pena-Shokeir and Seckel syndromes
- Various chromosomal anomalies (trisomies 13 and 18, triploidies, translocations and genetic deletions)[44–46]

The mandible develops from the mesenchyme which covers the Meckel cartilage, in the first pharyngeal or brachial arch. Although the latter disappears, its mesenchymal surface develops the mandible. Its development, therefore, is not related at all to the alveolar or osseous maxillary, and anomalies in the mandible may appear with no presence of nasofacial alterations.

Developmental Anomalies

Many of them are part of the syndrome known as first arch pharyngeal or brachial syndrome, consisting of a series of malformations which occur as a result of the disappearance or abnormal development of several components of this first arch. The origin of the defects probably lies in a deficiency in the cells of the neural crest as a result of insufficient migration, cellular necrosis or reduction in proliferation.

The factors which contribute to these defects may be genetic or environmental. For example, a deficiency in vitamin A can cause severe defects in the face and thymus due to interference in the development of the cells of the neural crest. Moreover, given that such cells help to form the walls of the aorta and pulmonary arteries, the syndrome of the first arch is often accompanied by heart anomalies, such as transposition of the large vessels or an interruption in the aortic arch.

Among the first arch syndromes we include the above mentioned Treacher Collins (mandibulofacial dysostosis), Pierre Robin (hypoplasia of the mandible, palatal fissure, defects in the eye and ear) and that of Di George (absence of thymus and parathyroid glands, malformations in the mouth, short subnasal groove or fish mouth, nasal clefts and cardiac anomalies). It has also been associated with chromosomal abnormalities and mendelian defects.

The tongue may cause respiratory obstruction at birth.

However, the degree of mandibular anomaly is not related with either the mechanical problem caused at birth nor with the nature of the underlying syndrome. For this reason, an intrauterine diagnosis must, whenever possible, be carried out. Among these we must differentiate between simple anomalies of position or retraction **-retrognathia-**(Fig. 38.9) and the anomaly of development and size or **micrognathia** (Fig. 38.10). The first is simple mandibular retraction, whereas the second is a developmental defect of a varying severity.

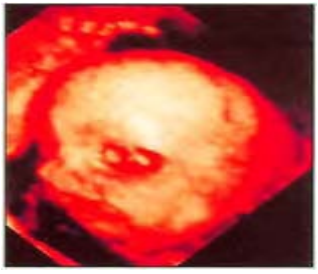

Figure 38.9: Retrognathia

EYE ANOMALIES

Aside from the anomalies mentioned as part of holoprosencephaly with cyclopia, fetuses may present other anomalies of the eyes.

During development and up to week 12, the normal situation of the eyes is that of

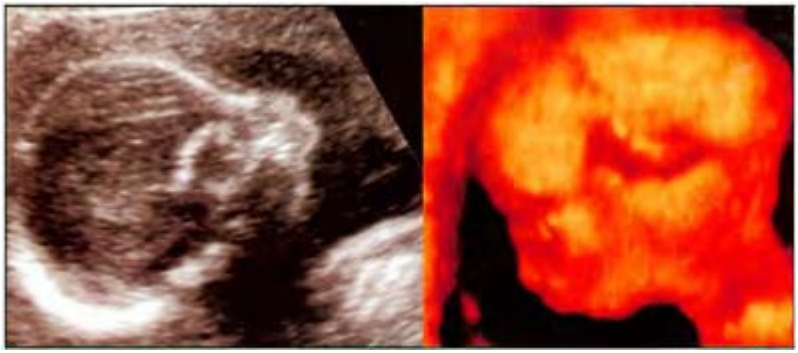

Figure 38.10: Comparison in 2D and 3D of a case of micrognathia in fetus with trisomy 18. The diagnosis can be established with either technique, but the anomaly is more evident when viewed with 3D

hypertelorism with exophthalmia, which is then progressively reduced.

Sporadic cases of mutations have been described, in addition to pathologies of the steroidogenesis (luteomas, congenital adrenal hyperplasia, hyperandrogenism) which could cause such lesions. We show a case of the AntleyBixler syndrome which gives a clear picture of the diagnostic possibilities of 3D (Fig. 38.11).[47]

NECK ANOMALIES

Nuchal Translucency

2D and 3D Measurements of Nuchal Translucency

The thickness of NT, which measures the subcutaneous edema of the fetal neck between weeks 11 and 14 of gestation, has nowadays become the most accepted parameter as a screening method for estimation of the risk of chromosomal anomalies.

This risk increases with maternal age, thickness of the translucency, age of onset during pregnancy, family history and previous pregnancy with chromosomal anomalies.

It is associated with the measurement of the crown-rump diameter and with the cardiac frequency of the fetus.

The rate of detection when combining maternal age, crown-rump length and NT reaches 80% of DS.

Nuchal translucency increases physiologically with age. 95% of the cases show that it varies from an average 2.4 mm in week 12 (crown-rump

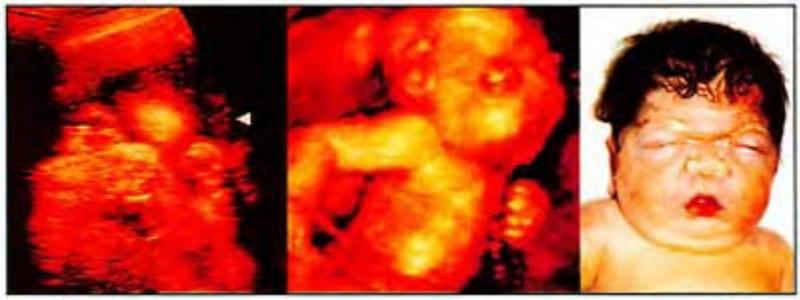

Figure 38.11: On the left, hypertelorism, palpebrate edema and exophthalmia in a case of Antley-Bixler syndrome

length of 45 mm) to 2.9 mm in week 14 (crown -rump length 84 mm). This means that measurements should be very precise.

The use of 3D ultrasound for examination of NT during the first trimester dates back to 1998,[48] when it was first performed in order to differentiate NT from cystic hygroma. Subsequent studies[49–52] have revealed that the inter- and intraoperator reproducibility, as well as measurements obtained with 3D, are much more reliable than with 2D.[49–52]

It has been shown that 3D[50] clearly identifies the structures to be measured (edema) and differentiated (amnion), thus improving diagnostic certainty.

The use of 3D increases the number of successful measurements, enables repetition thereof and shortens the time of exploration by accurately and rapidly locating the axis of the fetus.

Although a high correlation has been noted between 2D and 3D in comparative studies,[50,51] the possibility of storing measurements in optical disks, of documenting the cases and of repeating measurements are significant advantages over and above those of 2D.

The determination of the CRL and nuchal translucency is made using the three orthogonal planes and a complete picture of the fetus by sagittal section.

The ideal abdominal plane on screen is usually that marked as a green square divided into parallel sections,[6,51] easily obtained with 3D. When the most representative midsagittal plane appears in A, measurement of nuchal translucency is performed both in A and in a transversal section. If performed correctly, the transversal section of nuchal

translucency has proven to be as efficient as the sagittal section,6 yet another advantage of 3D ultrasound.

Measurements are obtained by maximum magnification of the image on screen, so that any increase in the distance between gauges is equivalent to 0.1 mm. This enables measurements to be carried out in tenths of a millimeter, achieving image enlargements which are impossible using 2D (Fig. 38.12).

INIENCEPHALY

Iniencephaly is a very rare and complex malformation, first described by von Saint-Hilaire in 1836, consisting of an apertus or clausus neural tube defect with a skull malformation in the area of the occiput.

A part of the occipital bone is missing or has a large hole connecting it to the foramen magnum, making it extremely wide and irregular. This defect

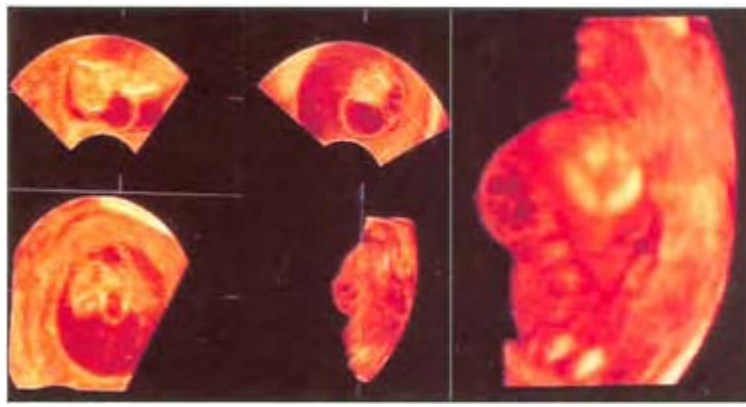

Figure 38.12: Three-orthogonal planes and 30-rendering of a neck hygroma. The 3D rendering clearly shows two big irregular neck bubbles

is often associated with an outward protrusion of the brain.

All cases show a neural tube defect at least affecting the cervical vertebrae, although cases have been reported in which the entire medullary canal is open.[3]

The cervical/cervicothoracic part of the spinal column exhibits extreme lordosis as a consequence of the desintegration of the affected vertebrae, which are reduced in size and number and have fused with the cranium and opened. These vertebral anomalies give rise to a reduction in the crown-rump length.

The consequences of these vertebral defects are:

• An extreme extension of the head, which may be fixed, thus giving the affected fetuses (and newborns) their characteristic appearance.
• The face looks upwards in a so called “stargazing” position
• Protrusion and torsion of the chest
• Lung hypoplasia (occasionally)
• Polyhydramnion (40%), due to swallowing difficulty

Iniencephaly is both rare and heterogeneous in terms of associated intracraneal and skeletal anomalies. Female fetuses are more commonly affected (Fig. 38.13).

MALFORMATIONS OF THE MEDULLARY CANAL

These malformations have a very adverse prognosis of quality of life of the newborn. Even the mildest forms of spina bifida occulta manifest some type of urinary incontinence.

Most of them are diagnosed using 2D during the second trimester,[53] but 3D, especially with transparency systems and X-rays, proves to be much better at defining the severity of the condition and helping the Neonatology team prepare for birth (Fig. 38.14).

Figure 38.14, as well as the iniencephaly shown in Figure 38.13, is an example of the possibilities offered by this technology. When compared to 2D, both show a much more complete vision of the extent of the lesion and number of affected vertebrae.

More severe lesions of the thorax, abdomen and other areas affecting the medulla[54] may be determined with this new system.

TERATOMAS

Fetal tumors are difficult to diagnose during prenatal life. They can appear in any organ, although sacrococcygeal teratomas represent 50%[55] of the total.

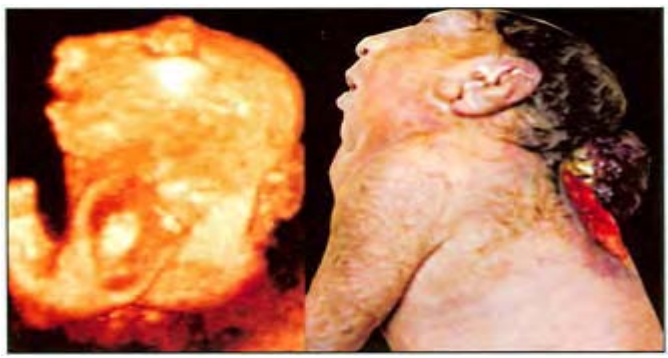

Figure 38.13: 3D rendering and macroscopic view of an iniencephaly in week 14

Figure 38.14: Two clear examples of open spina bifida. To the left a lumbar open spinal anomaly with 5 affected vertebrae. To the right 2D and real time 3D image of a second case of open spina bifida. The 3D picture shows the size and extension of the open canal much more clearly

The much clearer picture of the skeleton and pelvic bones obtained using 3D enables a better definition of these tumors, as well as of the possible involvement of the sacrum and pelvic viscera, which will have a bearing on the prognosis. In this sense 3D seems to be of great assistance.

CONJOINED TWINS

These are variations of monozygotic twins produced by incomplete dissociation of the cells of the internal cellular mass of the embryonic button, between days 9 and 13 of development.

The incidence is of 1 per every 50,000 to 100,000 newborns, with many variants which have been studied and defined with 3D.[56] Of all the variants, the thoracopagus, xiphopagus and omphalopagus are the most frequent.

Although an early diagnosis may be made via vaginal 2D or Doppler, as evidenced in many publications, most of them can reach delivery with no diagnosis or an incomplete diagnosis of conjoined organs, which leads to lack of preparation of suitable medical teams and the resulting disastrous prognosis.

3D ultrasound, combined with Doppler during the first trimester or during the second (Fig. 38.15) nowadays provides diagnostic certainty and differentiation of variants, which is of vital importance in the establishment of the prognosis.

FETUS ACARDIUS (TRAP SYNDROME)

Fetus acardius is an extremely rare complication of monozygotic multifetal gestation that is thought to be due to what is known as the ‘twin reversed arterial perfusion sequence’. These very malformed fetuses may have rudimentary heart tissue (pseudocardia) or may completely lack a heart (holoacardia). This anomaly is always present with other severe fetal malformations. It occurs in 0.3% of monozygotic twin gestations, which amounts to a frequency of about 1 per 35,000 deliveries.[54] Although most cases occur among monozygotic twins, there are reports of acardiac fetuses in triplet and even quintuplet gestations.[54]

Fetus acardius is a consequence of vascular anastomases in the placenta that result in fetofetal transfusion. Until recently, it was thought that the twin with a heart perfused the acardiac twin through at least 2 anastomases, 1 artery to artery and 1 vein to vein, and that circulation of the acardiac twin was therefore reversed. There is evidence, however, that vascular anomalies in these cases may be more complex. Twin-to-twin transfusion may disrupt organogenesis in the recipient in such a way that development of certain "nonessential" organs such as heart, brain, and arms may not occur. The donor twin may have cardiac hypertrophy, cardiac failure, intrauterine growth restriction, or intrauterine death.

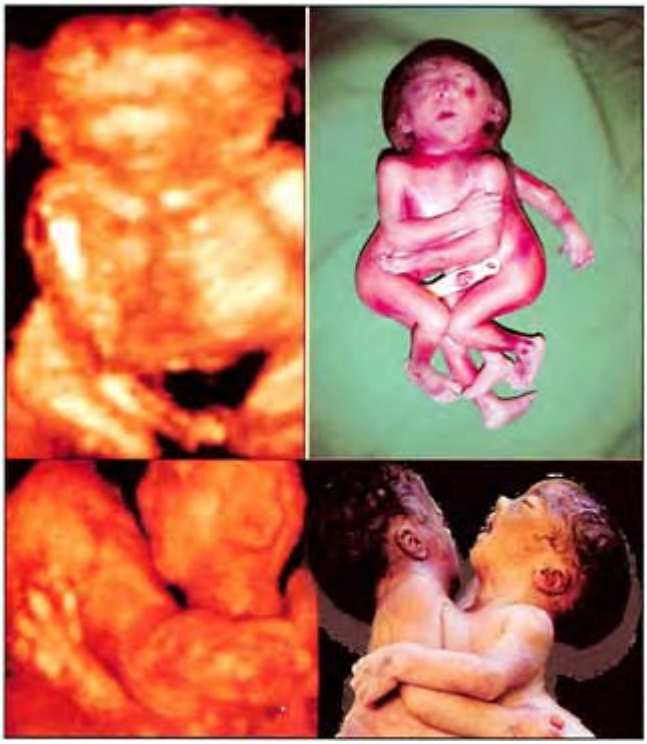

Figure 38.15: Two cases of conjoined twins. Observe that the 3D picture clearly shows the conjoined organs exactly as they are in reality

Diagnosis is now possible during the first trimester of pregnancy by detecting inversion of vascular flow in the recipient acardiac fetus on transvaginal Doppler ultrasonography. The presence of holoacardia or pseudocardia in one of the twins may be associated with obstetric complications such as oligohydramnion, polyhydramnion,

premature rupture of membranes, prematurity, uterine rupture, and hemorrhage. Early diagnosis of fetus acardius may allow measures to be taken that may help reduce the risk of some of these complications or even prevent them (Fig. 38.16).

ABDOMINAL WALL DEFECTS

Normal development of the fetal abdomen depends on the correct fusion of four ectomesodermic folds. Defects in the closure leads to these malformations with an incidence of 1 per every 3000 deliveries.[57]

Omphalocele, linked to trisomy 18, and gastroschisis—almost always unrelated to chromosomal anomalies—are the two most frequent and have been studied with 2D.

There are other abdominal wall defects, such as ectopia cordis, extrophy of the bladder or the cloaca, Beckwitz-Wiedemann syndrome, body stalk or Cantrell pentalogy, which have all been described with 3D.[15]

Although viewing is feasible with 2D, a recent publication[57] reveals the great advantages of 3D ultrasonographic diagnosis of such defects (Fig. 38.17).

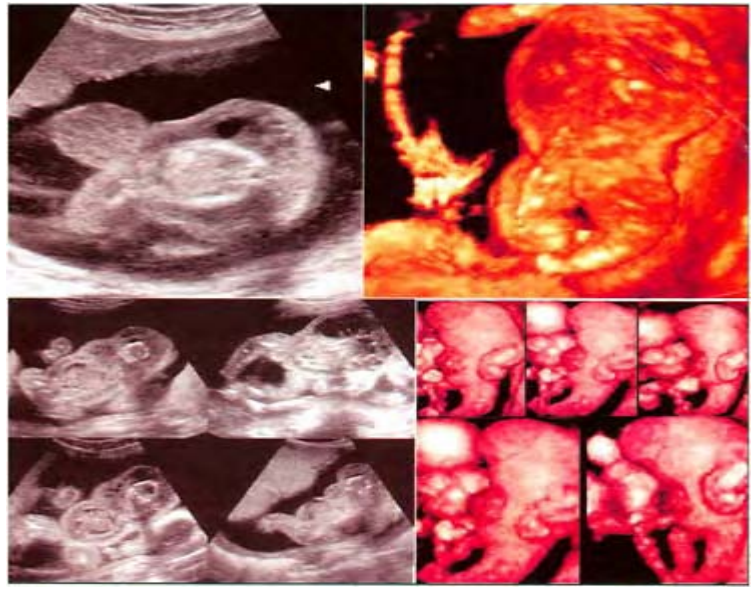

Figure 38.16: Two cases of fetus acardius

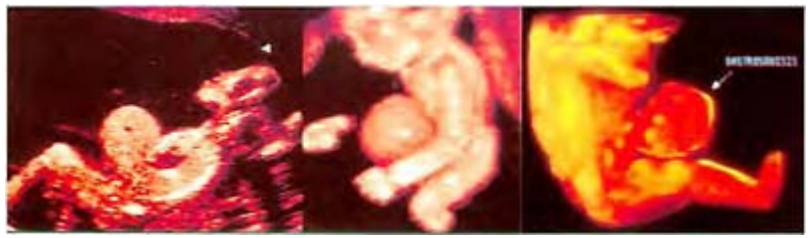

Figure 38.17: The left and central pictures show a case of omphalocele. The right one shows a gastroschisis

FETAL LIMB ABNORMALITIES

The extremities, their size and shape, the toes and the fingers can be evaluated with abdominal 3D from week 14 onwards. A complete visualization should be able to evaluate images of the open hands with flexed and clenched fingers as well as the fetal palms and feet.

Frequently an image of the extended fingers is difficult to obtain before the 20th week because the fetus tends to keep a closed fist during the first half of pregnancy.

A sagittal view of the leg and foot should be obtained along with vision of the plantar surface while observing the feet, in order to rule out anomalies of angulation or prominent calcaneus or astragalus, important for the diagnosis of anomalies such as "rocker bottom feet" or clubfeet.

All varieties of limb, finger and toe anomalies (Fig. 38.18) can be studied with 3D during the second trimester.[15]

3D has been proven to allow visualization of hands and feet[5] between weeks 26 and 36 in almost 100% of the cases (Fig. 38.19).[5,59]

In this regard, the diagnosis of thanatomorphism and achondroplasia[58] which are performed late in gestation and with difficulty using 2D (weeks 24 to 28) can be brought forward thanks to the observation of the "clover" forehead, short thorax, prominent abdomen and short, thick extremities with bent bones (Fig. 38.19).

POSITIONAL ANOMALIES AND CONTRACTURES

Multiple congenital contractures belong to a heterogeneous group of skeletal disorders that have in common multiple joint contractures at birth. These contractures result from limitation of articular motion secondary to peripheral or central neurologic anomalies, muscular abnormalities, connective tissue anomalies, amniotic bands or primary skeletal abnormalities.

The newborn babies with congenital contractures reveal that 55% are associated with disorders of the nervous system, 11% with connective tissue and dermatologic anomalies, 8% with neuromuscular problems and 7% with oligohydramnios.[60]

Fixed articular contractures, lack of mobility and abnormal positioning of extremities are the 3D markers used in the diagnosis (Fig. 38.20).

KIDNEY MALFORMATIONS

Although the definitive kidney, the metanephros, is formed by week 9, urinary production may only be observed as of week 10.

The visualization of malformations in the kidneys or urinary tract is thus postponed to week 13. Very few of these malformations can be seen with 2D and 3D during the first trimester.[61] Among them is the "prune belly" syndrome, consisting of a hyperdistension of the abdominal wall with a megabladder due to the obstruction of urethral valves (Fig. 38.21). This anomaly can be clearly observed using 3D and when it occurs so early in pregnancy it can conclusively damage the union of the glomeruli with the convoluted kidney tubules, with a disastrous prognosis.

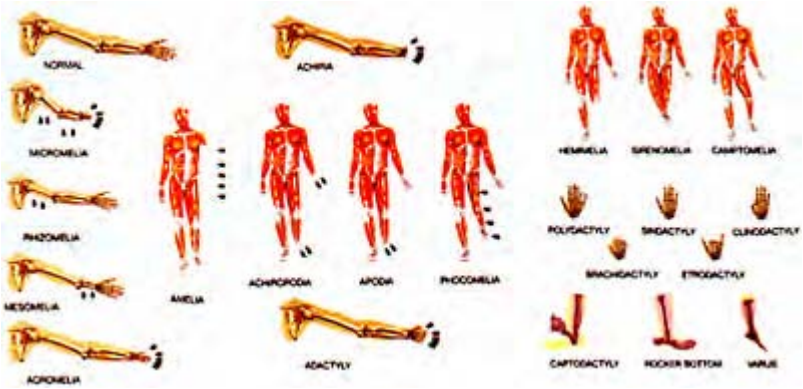

Figure 38.18: Limb, finger and toe anomalies

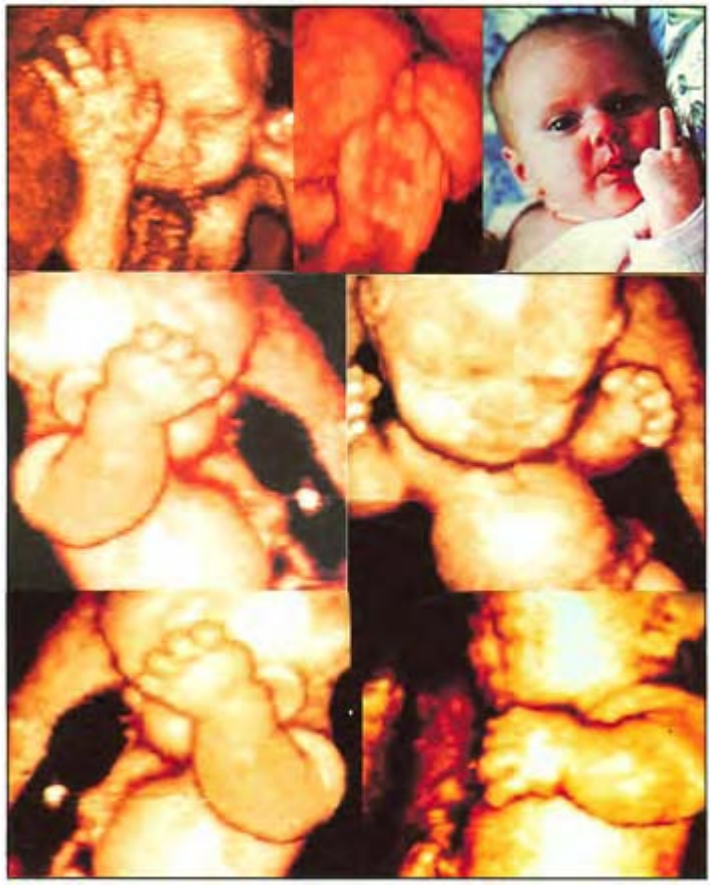

Figure 38.19: The two photographs above show a fetus with only 4 fingers, and a normal fetus with the middle finger pointing upwards. The four lower pictures show cases of thanatophoric dwarfism. Note the large head, “clover-like” forehead and short and thick arms, swollen, leaning against a short thorax with a prominent abdomen

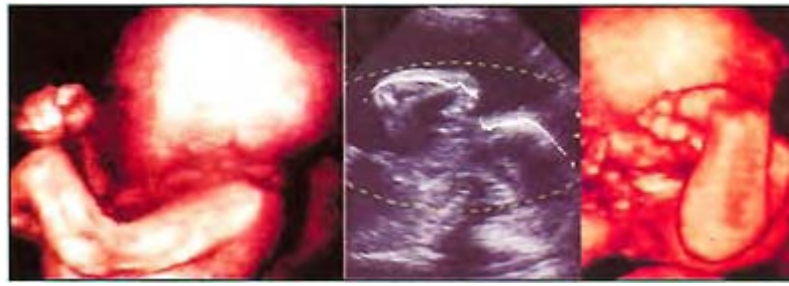

Figure 38.20: Multiple congenital contractures. Note anomalous contracture of elbows and hands (trisomy 18)

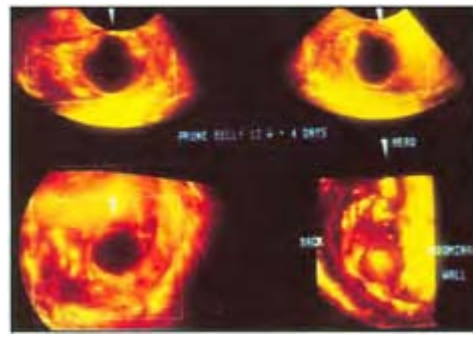

Figure 38.21: Three-orthogonal planes and 3D-rendering of a case of prune belly detected on week 13th. The orthogonal planes show the hyperdistended urinary bladder. The 3D rendering (bottom right) shows the distension in the fetal abdomen

UMBILICAL CORD ANOMALIES

Numerous anomalies of the umbilical cord, placenta, yolk sac and amnion can be diagnosed using 3D ultrasonography during the pregnancy and especially during the first trimester.[67]

We highlight those affecting the umbilical cord in the light of the recently discovered relationship with chromosomal anomalies.

The observation of the umbilical cord using 3D enables[67] the study of physiological variations such as herniation, length of the cord, its thickness, coiling, true and false knots, absence of cord, single umbilical artery, cysts and tumors.

It is worth noting that any cyst appearing near the abdominal or placentary wall, if thick or irregular and remaining after week 12, are associated in 50% of the cases with chromosomal abnormality (Fig. 38.22).[67]

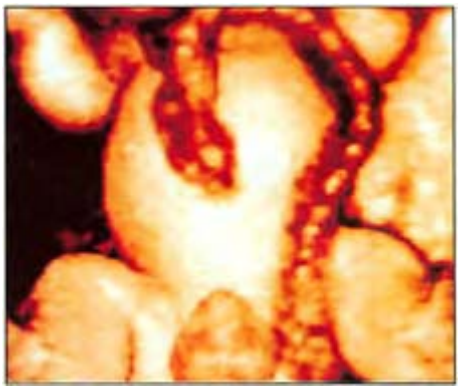

Figure 38.22: Normal umbilical cord depicted in 3D.The length, thickness and coiling can be estimated

REFERENCES

1. Benacerraf BR, Neuberg D, Frigoletto FD Jr. Humeral shortening in second trimester fetuses with Down syndrome. Obstet Gynecol 1991; 77:223–27.
2. Benacerraf BR, Cnann A, Gelman R. Laboda LA, Frigoletto FD Jr. Can sonographers reliably identify anatomic features associated with Down syndrome in fetuses? Radiology 1989; 173:377–80.
3. Campbell S. 4D or not 4D, that is the question. Ultrasound Obstet Gynecol 2002; 19:l-4.
4. Merz E. 3-D ultrasound in Obstetrics and Gynecology. Lippincott Williams and Wilkins. Philadelphia, 1998.

5. Nelson TR, Downey DB, Petrorius DH, Fenster A. Three-dimensional ultrasound. Lippincott Williams and Wilkins. Philadelphia, 1999.
6. Bonilla-Musoles F. Ecografia vaginal, Doppler Y tridimension. Panamericana Ed. Madrid, 2000.
7. Carlson DE. The ultrasound evaluation of cleft lip and palate: a clear winner for 3D. Ultrasound Obstet Gynecol 2001; 16:299–301.
8. Viora E, Sciarrone A, Bastonero S, Errante G, Botta G, Campogrande M. Three-dimensional ultrasound evaluation of short rib polydactyly syndrome type 11 in the second trimester; a case report. Ultrasound Obstet Gynecol 2002; 19:88–91.
9. Koelble N, Sobetzko D, Ersch J, Stallmach T, Eich G, Huch R, Superti-Furga A, Wisser J. Diagnosis of skeletal dysplasia by multidisciplinary assessment: a report of two cases of thanatophoric dysplasia. Ultrasound Obstet Gynecol 2002; 16:92–98.
10. Chen C, Shih JC, Tzen CL, Wang W. Three-dimensional ultrasound in the evaluation of complex anomalies associated with fetal ventral midline defects. Ultrasound Obstet Gynecol 2002; 16:102–08.
11. Xn HX, Thang QP, Lu MD, Xiao XT. Comparison of two-dimensional and three-dimensional sonography in evaluating fetal malformations. J Clin Ultrasound 2002; 30:515–25.
12. De Myer W, Zeman W, Palmer CG. The face predicts the brain.Diagnostic significance of median facial anomalies for holoprosencephaly arhinencephaly. Pediatrics 1964; 43:256–63.
13. Berge SJ, Plath H, Van De Vondel T, Appel T, Niederhagen B, Von Lindern JJ, Reich RH, Hansmann. Fetal cleft lip and palate;sonographic diagnosis, chromosomal abnormalities, associated anomalies and postnatal outcome in 70 fetuses. Ultrasound Obstet Gynecol 2001;18:422–31.
14. Milerad J, Larson O, Hagberg C, Ideberg M. Associated malformations in infants with cleft lip and palate: a prospective, population-based study. Pediatrics 1997; 100:180–86.
15. Bonilla-Musoles F, Machado L,Osborne NG. Three-Dimensional visualization of the normal fetus.Part II. In: Bonilla-Musoles F, Machado L, Osborne NG: Three-Dimensional Ultrasound for the New Millenium Aloka Madrid 2000; 93–113.
16. Ghi T, Perolo A, Banzi C, Contratti G, Valeri B, Savelli L, Morselli GFJ Bovicelli L, Pilu G. Two-dimensional ultrasound is accurate in the diagnosis of fetal craniofacial malformation. Ultrasound Obstet Gynecol 2002; 19:543–51.
17. Pretorius DH, House M, Nelson TR, Hollenbach KA. Evaluation of normal and abnormal lips in fetuses: comparison between three- and two-dimensional sonography. Am J Roentgenol 1995; 165:1233–37.
18. Pretorius DH, Nelson TR. Fetal face visualisation using three-dimensional ultrasonography. J Ultrasound Med 1995; 14:349–56.
19. Devonald KJ, Ellwood DA, Griffiths KA. Volume imaging: three-dimensional appreciation of the fetal head and face. J Ultrasound Med 1995; 14:919–25.
20. Rotten D, Levaillant JM, Martinez H, Ducou LE, Pointe H, Vicaut E. The fetal mandible: a 2D and 3D sonographic approach to the diagnosis of retrognathia and micrognathia. Ultrasound Obstet Gynecol 2002; 19:122–30.
21. Pilu G, Reece EA, Romero R, Bovicelli L, Hobbins JC. Prenatal diagnosis of craniofacial malformations with ultrasonography. Am J Obstet Gynecol 1986;155:45–50.
22. Johnson DD, Pretoris DH, Budorick NE, Jones MC Lou KV, James GM, Nelson TR. Fetal lip and primary palate: three-dimensional versus two-dimensional US. Radiology 2000; 217:236–39.
23. Lee W, Kirk JS, Shaheen KW, Romero R, Hodges AN, Comstock CH. Fetal cleft lip and palate detection by three-dimensional ultra-sonography. Ultrasound Obstet Gynecol 2000; 16:314–20.
24. Merz E, Bahlmann F, Weber G, Macchiella D. Three-dimensional ultrasonography in prenatal diagnosis. J Perinat Med 1995; 23:213–22.
25. Merz E, Weber G, Bahlmann F, Miric-Tesanic D. Application of transvaginal and abdominal three-dimensional ultrasound for the detection or exclusion of malformations of the fetal face. Ultrasound Obstet Gynecol 1997; 9:237–43.

26. Bongain A, Enoit B, Ejnes L, Lambert JC, Gillet JY. Harlequin fetus: three-dimensional sonographic findings and new diagnostic approach. Ultrasound Obstet Gynecol 2002; 20:82–85.
27. Nyberg DA, Sickler GK, Hegge FN, Kramer D. Fetal cleft lip with and without cleft palate: US classification and correlation with outcome. Radiology 1995; 195: 677–84.
28. Cash C, Set P, Coleman N. The accuracy of antenatal ultrasound in the detection of facial clefts in a low-risk screening population. Ultrasound Obstet Gynecol 2001; 18:432–36.
29. Chmait RH, Pretorius DH, Hull AD. Nasal glioma Ultrasound Obstet Gynecol 2002;20;417–18.
30. Blaas HGK, Eriksson AG, Salvesen KA, Isaksen CV, Christensens B, Mollerlokken G, Eik-Nes SH. Brains and faces in holoprosencephaly: pre- and postnatal description of 30 cases. Ultrasound Obstet Gynecol 2002; 19:24–38.
31. Nyberg DA, Mack LA, Bronstein A, Hirsch J, Pagan RA. Holoprosencephaly: Prenatal sonographic diagnosis. AJR 1987; 149:1051–58.
32. Blaas HGK, Eik-Nes SH, Vainio T, Isaksen CV. Alobar holoprosencephaly at 9 weeks gestational age visualized by two- and three-dimensional ultrasound. Ultrasound Obstet Gynecol 2000; 15:62–65.
33. Bonilla-Musoles F, Machado L, Osborne N. Proboscis. In: Three-Dimensional ultrasound of the new Millenium. Aloka Madrid 2000; 75–92 and 281–82.
34. Nyberg DA, Souter VL, El Bastawissi A, Young S, Luthhardt F, Luthy DA. Isolated sonographic markers for the detection of fetal Down syndrome in the second trimester of pregnancy. J Ultrasound Med 2001; 20:1053–63.
35. Bromley B, Lieberman E, Benacerraf BR. The incorporation of maternal age into the sonographic scoring index for the detection at 14–20 weeks of fetuses with Down's syndrome. Ultrasound Obstet Gynecol 1997; 10:321–24.
36. Cicero S, Curcio P, Papageorghiou A, Sonek J, Nicolaides K. Absence of nasal bone in fetuses with trisomy 21 at 11–14 weeks' gestation: an observational study. Lancet 2001; 358:1665–67.
37. Cicero S, Bindra G, Rembouskos G, Tripsanas C, Nicolaides KH. Fetal nasal bone length in chromosomally normal and abnormal foetuses at 11–14 weeks of gestation. J Maternal Fetal Neonat Med 2002; 11:400–02.
38. Sonek JD, Nicolaides KH. Prenatal ultrasonographic diagnosis of nasal bone abnormalities in three fetuses with Down syndrome. Am J Obstet Gynecol 2002; 186:139–41.
39. Bromley B, Lieberman E, Shipp TD, Benaferraf BR. Fetal nose bone length. A marker for Down syndrome in the second trimester. J Ultrasound Med 2002; 21: 1387–94.
40. Monni G, Zoppi MA, Ibba RM. Absence of the nasal bone and detection of trisomy 21. Lancet 2002; 359:1343.
41. Monni G, Zoppi MA. New ultrasonographic markers of aneuploidies: nasal bones. Ultrasound Rev Obstet Gynecol 2002; 2:229–34.
42. Chitkara U, Lee L, Oehlert JW, Bloch A, Holbrook RH Jr, El-Sayed YY, Druzin ML. Fetal ear length measurement: a useful predictor of aneuploidy? Ultrasound Obstet Gynecol 2002; 19:131–35.
43. Shimizu T, Salvador L, Hughes-Benzie R, Dawson L, Nimrod C, Allanson J. The role of reduced ear size in the prenatal detection of chromosomal abnormalities. Prenat Diagn 1997; 17:545–49.
44. Rotten D, Levaillant JM, Martinez H, Ducou Le Pointe H, Vicaut E. The fetal mandible: a 2D and 3D sonographic approach to the diagnosis of retrognathia and micrognathia. Ultrasound Obstet Gynecol 2002; 19:122–30.
45. Merz E. 3D-Ultrasound in prenatal diagnosis. Curr Obstet Gynecol 1999; 9:93–100.
46. Tanaka J, Miyazaki T, Kanenishi K, Tanaka H, Yanagihara T, Hata T. Antenatal three-dimensional sonographic features of Treacher Collins syndrome. Ultrasound Obstet Gynecol 2002; 19:414–15.
47. Machado LE, Osborne NG, Bonilla-Musoles F Antley-Bixler syndrome. Report of a case. J Ultrasound Med 2001; 20:73–77.

48. Bonilla-Musoles F, Raga F, Villalobos A, Osborne N, Blanes J. First trimester neck abnormalities: three-dimensional evaluation. J Ultrasound Med 1998; 17:419–26.
49. Kurjak A, Kupesic S, Ivancic-Kosuta M. Three-dimensional transvaginal ultrasound improves measurement of nuchal translucency. J Perinat Med 1999; 27:97–102.
50. Clementschitsch G, Hasenohrl G, Schaffer H, Steiner H. Comparison between two- and three-dimensional ultrasound measurements of nuchal translucency. Ultrasound Obstet Gynecol 2001; 18, 475–80.
51. Paul C, Krampl E, Skentou C, Jurkovic D, Nicolaides KH. Measurement of fetal nuchal translucency thickness by three-dimensional ultrasound. Ultrasound Obstet Gynecol 2001; 18:481–84.
52. Chung EL, Kim HJ, Lee KH. The application of three-dimensional ultrasound to nuchal translucency measurement in early pregnancy (10–14 weeks): a preliminary study. Ultrasound Obstet Gynecol 2000; 15:122–25.
53. Bonilla-Musoles F, Machado L, Osborne N, Mufioz E, Raga F, Blanes J, Bonilla Jr. Two- and three-dimensional ultrasound in malformations of the medullary canal: report of four cases. Prenat Diagn 2001; 21:622–26.
54. Bonilla-Musoles F, Machado L, Raga F, Osborne N. Fetus acardius. J Ultrasound Med 2001; 20:1117–27.
55. Bonilla-Musoles F, Machado L, Bailao L, Osborne N, Raga F, Blanes J, Bonilla Jr. Prenatal diagnosis of sacrococcygeal teratomas by two- and three-dimensional ultrasound. Ultrasound Obstet Gynecol 2002; 19:124–30.
56. Bonilla-Musoles F, Machado L, Osborne N, Raga F, Blanes J, Bonilla Jr F, Machado. Two-dimensional and three-dimensional sonography of conjoined twins. J Clin Ultrasound 2002; 30:68–75.
57. Bonilla-Musoles F, Machado L, Bailao L, Osborne N, Raga F, Blanes J. Abdominal wall defects. Two-versus three-dimensional ultrasonographic diagnosis. J Ultrasound Med 2001; 20:379–89.
58. Machado L, Bonilla-Musoles F, Raga F, Bonilla M Jr, Machado F, Osborne N. Thanatophoric dysplasia: Ultrasound diagnosis. Ultrasound Quaterly 2001; 17:235–43.
59. Machado L, Bonilla-Musoles F, Osborne N. Fetal limb abnormalities;ultrasound diagnosis. Ultrasound Quaterly 2000; 16:203–14.
60. Bonilla-Musoles F, Machado LE, Osborne NG. Multiple congenital contractures (congenital multiple arthrogryposis). J Perinat Med 2002; 30:99–104.
61. Bonilla-Musoles F, Raga F, Osbornoe N, Blanes J. Three-dimensional evaluation of embryonic and fetal malformations: comparison with two dimensional ultrasound. In: Kurjak A. Perinatology. Parthenon Publsh Lanes. UK 1998; 228–35.
62. Osborne N, Bonilla-Musoles F, Raga F, Bonilla Jr. Umbilical cord cysts: Color Doppler and three-dimensional ultrasound evaluation. Ultrasound Quarterly 2000; 16:133–39.
63. Merz E, Bahlmann AF, Weber G. Volume scanning in the evaluation of fetal malformations: a new dimension in prenatal diagnosis. Ultrasound Obstet Gynecol 1995; 5:222–27.
64. Merz E. 3-D Ultrasound In Obstetrics and Gynecology. Lippincott Williams and Wilkins. Philadelphia, 1998.
65. Pretorius DH, Nelson TR. Three-dimensional ultrasound in Gynecology and Obstetrics, A review. Ultrasound Quaterly 1999; 14:218–33.
66. Bonilla-Musoles F, Machado L, Osborne N, Raga F, Chamusca L, Chagas K, Bonilla Jr F, Cadete C. Ultrasound diagnosis of facial and cephalic pole malformations: comparative study of different three-dimensional modalities and two-dimensional ultrasound. Ultrasound Quaterly 2000; 16:97–105.
67. Bonilla-Musoles F, Machado L, Osborne N, Raga F, Bonilla Jr F, Puig MJ, Machado F. Morphological assessment of the umbilical cord with three-dimensional ultrasonography. Ultrasound Rev Obstet Gynecol 2002; 1:217–42.

Chapter 39
Fetal Behavior: Ontogenesis and Clinical Applications

Kotaro Fukushima, Shoji Satoh, Hitoo Nakano

WHAT IS "FETAL BEHAVIOR"?

Investigation on the central nervous system in developing animals has shown that anatomical function occurs first in the caudal segments, then in the rostral segments, in a manner similar to the development of the spinal cord followed by the caudal brainstem.[1,2] For humans, the brain is highly developed at birth with numerous functions, although development from the anatomical perspective continues for an additional year or two.[3] Visser *et al*[4] investigated anencephaly and found that the lack of normal movement patterns due to a neural tube defect indicated the necessity of anatomically correct neuronal arrangement.[4] The mammalian suprachiasmatic nucleus functions as the pacemaker master clock behind the rhythm of various biological phenomena. These neurons are able to generate and sustain circadian rhythm without any external input. Lesions in the coupling site between the clock and overt activity may result in arrhythmia.[5,6] Thus, it could be assumed that these anatomical defects are manifested as functional defects.

On the other hand, according to Lorenz,[7] the observation of various movements in an organism shows us its brain function manifestation. We can deduce brain function from "behavior" and possibly adapt this to human fetuses. Fetal movement can be felt in the womb starting early in the second trimester. Interestingly, until quite recently this was the only method to characterize the *in utero* status of the fetus before acoustic detection of the fetal heartbeat. Although experienced obstetricians, midwives and, above all, mothers have noticed changes in fetal movement patterns, complexities, and strength during pregnancy, a method for scientific analysis of these movements was lacking. However, during the past decade, real-time ultrasound has facilitated the *in vivo* observation of human fetal movements. Consequently, behavioral patterns in *utero* can be assessed as a one-to-one match between the manifestation of an individual motor activity and its corresponding brain function.

We have described the ontogeny of fetal behavior not only through observing the developmental process of each movement during gestational advances, but also by the investigation of various movements in relation to or in concurrence with one another, gradually integrating into more complex movements. Furthermore, based on these

physiological results, the extent and timing of detection and localization in *utero* of functional brain impairment becomes applicable in obstetrics.[8] We, as well as others, have investigated "fetal behavior" from the viewpoint that the fetus exists in an environment relatively free of external physiological and social influences.[9] However, there is data to support that fetuses can sense external stimulations, including vibro-acoustic stimulus,[10] lights,[11,12] smells,[13] tastes,[14,15] and temperatures,[16,17] and may memorize them.[18] Advances in fetal neural biology indicated that this sensory ability and its integration might have important effects on neural development during both the perinatal and neonatal period[19] and that both intrinsic and extrinsic factors are involved in fetal development. Here, we introduce both physiological and clinical aspects of "fetal behavior" ontogeny. In addition, we will discuss the relationship between fetal behavior and CNS functional development, and "fetal learning" as a possible method for assessing human fetal "extrinsic stimulation".

THE ONTOGENESIS OF HUMAN FETAL BEHAVIOR

As mentioned above, every fetal behavior could be a manifestation of the CNS. However, for clinical utilization, there are some conditions that must be fulfilled, i.e. visible and recordable using Medical Electronics. In general, fetal body movements, including the trunk, peripheral, eye, pupil, mouthing, voiding, and penile tumescence could be observable parameters by ultrasound. The fetal cardiotocogram is also utilized to sample the fetal heartbeat as well as heart movement. In this section, we focus on the relationship and ontogeny of eye movements, pupillary change, mouthing movements, and micturition.

Eye Movement and its Ultradian/ Circadian Rhythm

Eye Movement Patterns

Fetal eye movement is observable by real-time ultrasound[20,21] rather than evaluation of eye movement in the periphery of the sonolucent area and in the retro-occular echo-rich area.[20] The fetal lens can clearly be identified as a pair of small dotted echoes, originating from the near and far lens margins. Thus, this ultrasound image is considered suitable for precise eye movement quantification (Fig. 39.1).[21] Eye movement generally becomes observable at 16–18 weeks of gestation: however, its onset is sporadic and in many instances, remains limited in frequency. Eye movements not only increase but also begin to consolidate at 24–26 weeks of gestation, after which this tendency becomes more distinct and movement consolidation grows into a long-term cluster of eye movement along with a gradual increase in highfrequency eye movement (> 20 per minute) at approximately 30 weeks of gestation. There appears to be almost no relation between the presence and absence of movement by 35–36 weeks of gestation, after which time sporadic onset and low-frequency eye movements (< 5 per minute), both seen as early as 20 weeks of gestation, disappear. Thus, this demonstrates that these two periods, eye movement (EM) and noneye movement (NEM), begin to discernibly alternate (Fig. 39.2).[22] Since low-frequency eye movements are characterized by a sporadic and random

onset, a decrease in low-frequency eye movement would indicate association by 34–37 weeks with the tonic system maturation by which the eye is held in an eccentric position.[23] Therefore, periods of NEM with a considerable duration near term essentially have a different biological meaning compared with that in early pregnancy, especially in cases with less than 29 weeks of gestation, where NEM would imply an immature oculomotor system, leading to a longterm lack of eye movement. Moderate-frequency eye movements seem related to poor consolidation of eye movement, suggesting that this transitional state proceeds into high-frequency eye movement.

Ultradian Rhythm

The hypothesis, based on observing human infants, was proposed that the alternation of rapid eye movement (REM) and non-rapid eye movement (NREM) sleep is the manifestation of a fundamental ultradian rhythm in the central nervous system, namely the 'basic rest-activity cycle',[24] which is unaffected by time of day.[9,25,26] In the mature human fetus, somatic activity periods are also associated with REM periods, alternating with NREM periods, for a combined 30–50 minute cycle.[27,29] The ontogenesis of alternative changes in the duration of both the eye movement (dEM) and non-eye movement (dNEM) periods in the human fetus with advancing gestational age indicates that two critical points for dEM are at 29–30 and 37–38 weeks of gestation. For dNEM, the two critical points reside at 31–32 and 37–38 weeks of gestation (Fig. 39.3). The mean values of both dEM and dNEM increase with gestational age from early in the third trimester until about 37 gestational weeks. However, the gestational age at which dEM and dNEM begin to increase from relatively constant levels is different. dEM increases at 29–30 weeks of gestation, while dNEM increases after 31–32 weeks. The gestational age differences, where increases in dEM and dNEM are initiated, could infer the developmental start of two separate mechanisms, one for maintaining the dEM period and another for maintaining the dNEM period.[30] These findings agree with a preterm infant study by Mirmiran *et al*,[6] which stated that a human biological clock capable of generating a certain circadian rhythm is present as early as 29 gestational weeks. The constant mean values of dEM and dNEM starting at 37–38 gestational weeks indicate that both the switching and maintaining mechanisms responsible for the ultradian rhythm that begin early in the third trimester and produce a regular alternation between dEM and dNEM periods, have matured by this gestational age. The mean values of dEM and dNEM after 37 weeks of gestation were 27–29 and 23–24 minutes, respectively, and are similar to neonatal values.[31,32] Also, they show similarity to the alternative changes in fetal heart rate patterns of 'active' and 'quiet' phases.[29,33,37]

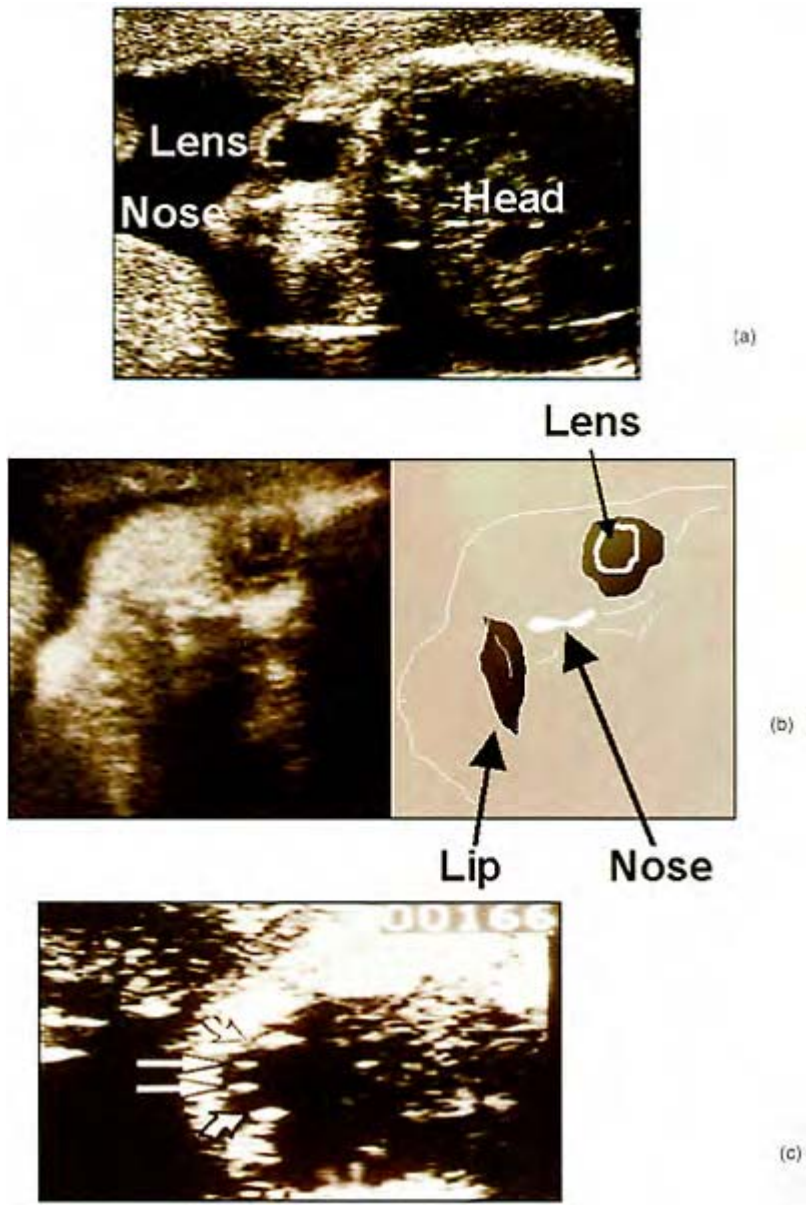

Figure 39.1: Ultrasound image for investigation on fetal eye movement, (a) Ultrasound image for observation of fetal eye

movement, (b) Ultrasound image for observation of fetal mouthing movement, (c) Ultrasound image for observation of fetal pupil. Curved and straight arrows indicate the margins of the lens and pupil, respectively (reproduced from Horimoto et al[78])

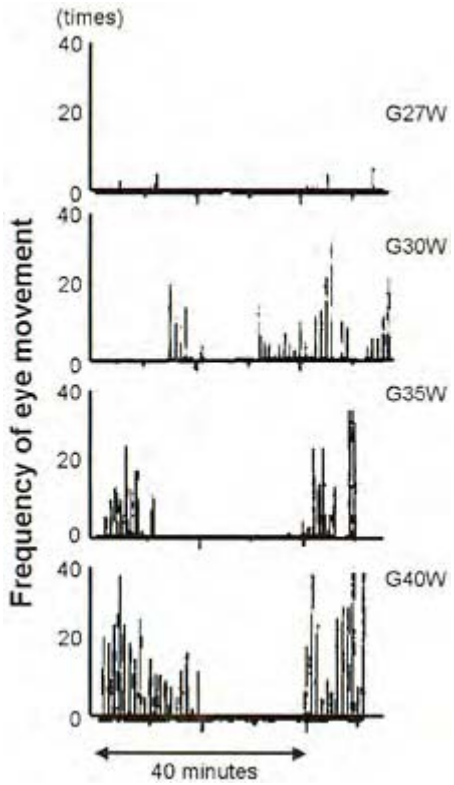

Figure 39.2: Chronological sequences of fetal eye movement. The horizontal and vertical axes indicate the 1

minute epoch and the corresponding frequency of the eye movement, respectively (Reproduced from Inoue et al[22])

Circadian Rhythm

As discussed above, the fetal eye movement pattern, depicted as having EM/NEM phases according to the presence and absence of movement, also appears in a similar fashion called ultradian rhythm.[30] Diurnal rhythms in the human fetus in various physiological parameters, i.e. fetal heart rate (FHR), body movement, and breathing movement have been described.[33,34,38,39] Using the [^{14}C]-labeled deoxyglucose method to measure neuronal activity in the fetal squirrel monkey, Reppert and Schwartz demonstrated the diurnal pattern of glucose utilization in the suprachiasmatic nucleus (SCN). These results indicated that this part of the brain plays an essential role in the generation of diurnal rhythms in the fetus as well as in adults.[40] Recently, diurnal change in fetal eye movement was investigated.[41,42] In this study, diurnal variation and fetal heart rate (FHR) variability were continuously observed for 24 hours using real-time ultrasound and Doppler cardiotocogram, respectively, in 5 full-term fetuses. The time series data of eye movement or lack thereof and mean FHR values for each minute were analyzed using the maximum entropy method (MEM) and subsequent nonlinear least squares fitting.

According to the power value of eye movement, all 5 cases were classified into two groups: 3 cases in the large power group and 2 cases in the small power group (Fig. 39.4). The acrophases of eye movement and FHR variability in the large power group were similar, thereby implying diurnal rhythm in both of these parameters and synchronization. In the small power group, the acrophases were separated. Diurnal rhythm in eye movement was observed in 60% of the cases (three out of five), which is compatible with reports that diurnal rhythm in heart rate variability was detected in 73% of fetuses,[39] and in 2/3 of adult cases.[43] Although all 5 cases showed comparable power values in FHR, they were divided into two groups based on eye movement power values: the large power group where eye movement showed clear diurnal rhythm and the small power group where eye movement failed to exhibit any distinct diurnal rhythm. The acrophases of eye movement and FHR variability in the large power group were close, thereby implying that these two parameters are synchronized. Conversely, in the small power group, the acrophases of the two parameters separated, indicating that they are unsynchronized. The 1/f characteristics difference in acrophase for eye movement and FHR varied from 2.2–4.2 hours in Cases 1, 2, 3, and 5, while Case 4 was 19.3 hours. In 4 cases, the power spectra slope values for both eye movement frequency and FHR ranged between 0.5 and 1.8, indicating diurnal variation, where the slopes tended to have higher values during the day and conversely, lower values at night (Fig. 39.5).

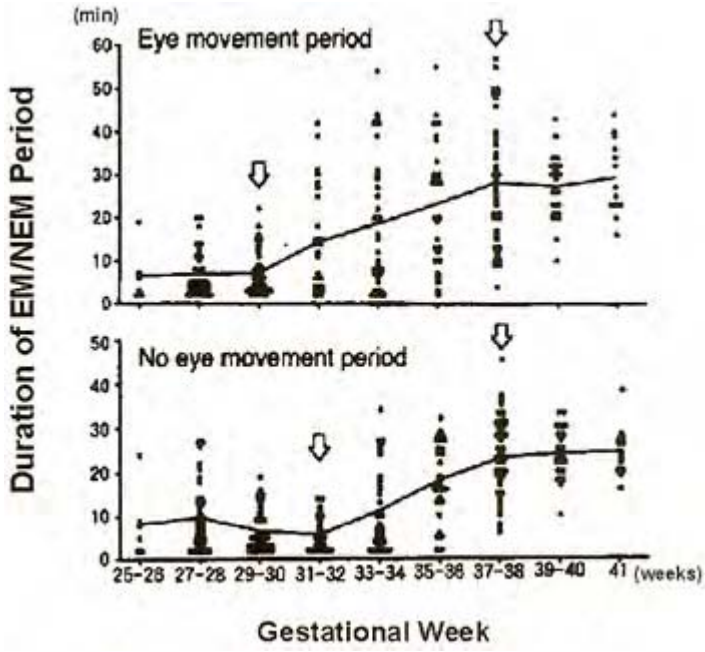

Figure 39.3: Age related distribution of EM/NEM periods. The horizontal axes indicate the gestational age, in 2 week interval. The solid lines indicate the mean values of EM/NEM periods. The arrows indicate the statistically critical points revealed using "piecewise linear regression".[130] (Reproduced from Koyanagi et al[100])

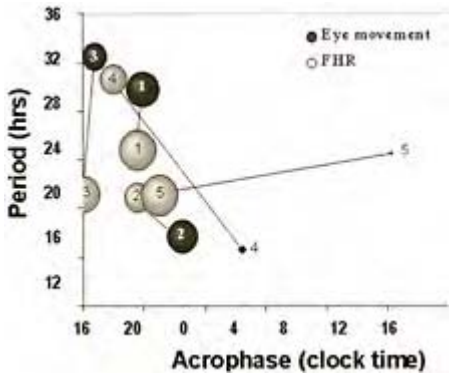

Figure 39.4: Components of periodicity for the best fitting curve. The horizontal and vertical axes show acrophase and period, respectively. The diameter of each circle indicates the magnitude of spectrum power. Since the unit of power for eye movement and FHR are different, only the diameters of like circles (same parameters) can be compared. The lines connect the circle for eye movement and FHR obtained from the same case. Numbers represent the case number. (Reproduced from Morokuma et al[42])

It has been reported that diurnal change is observed in fetal SCN activity,46 and cortisol is one of the most probable factors that causes diurnal rhythm before birth.47 However, it remains to be elucidated whether the daily rhythm of maternal CRF and/or cortisol influence fetal SCN activity through a high amount of glucocorticosteroid receptors present during early development in the SCN or by direct action of cortisol on uterine and fetal activities.47 Although the SCN activities in these fetuses were not clarified, the synchronization of eye movement and FHR variability in the large power

group suggests that these phenomena are governed by a common central mechanism related to diurnal rhythm generation. These findings suggest that in the human fetus at term, eye movement and FHR are under the control of a common central mechanism, and this center changes its complexity, which is seen through diurnal rhythm.

Possible REM/NREM Sleep in the Human Fetus

Rapid Eye Movements and Slow Eye Movements

Two types of eye movements are present during sleep in the adult human: REM, which is characterized by rapid and jerky motions of relatively short arc, and slow eye movements, which are slow and lateral.[48,49] One statistically significant critical point in the human fetus was evident at 0.62 and 0.76 seconds in the duration of the eye movement unit during 33–36 and 37–41 weeks of gestation, respectively. Theses results indicated two distinct types of eye movements in both gestational age groups: one with a short duration from 0.07 to 0.6–0.8 seconds and a second with duration from 0.6–0.8 to 4–5 seconds (Fig. 39.6).[50] These findings are compatible with those of Aserinsky and Kleitman,[51] who defined REM and slow eye movement (SEM) by their duration, in which the former lasts approximately 1 second and the latter lasts 3–4 seconds. Therefore, the fetal eye movements with durations greater than 0.07 to 0.6–0.8 seconds and those of 0.6–0.8 to 3–4 seconds could correspond to REM and slow eye movement, respectively. The age-related

Table 39.1: Slope value js of power spectra (β) for both eye moveme nt frequency and FHR. The slope values of power sped ra (β) for both eye movement frequency and FHR range were indicated. Reproduced from Morokuma et al[42]

	Eye movement			*FHR*		
	median	*90% range*	*acrophase (hrs)*	*median*	*90% range*	*acrophase (hrs)*
Case 1	1.36	0.57–1.84	10.6	1.42	0.51–1.75	8.3
Case 2	1.20	0.68–1.69	9.2	1.11	0.53–1.60	13.4
Case 3	1.28	0.58–1.64	9.1	1.24	0.64–1.68	6.5
Case 4	1.11	-0.04–1.52	14.1	1.26	0.50–1.81	18.5
Case 5	1.24	0.44–1.64	18.5	0,99	0.47–1.48	20.9

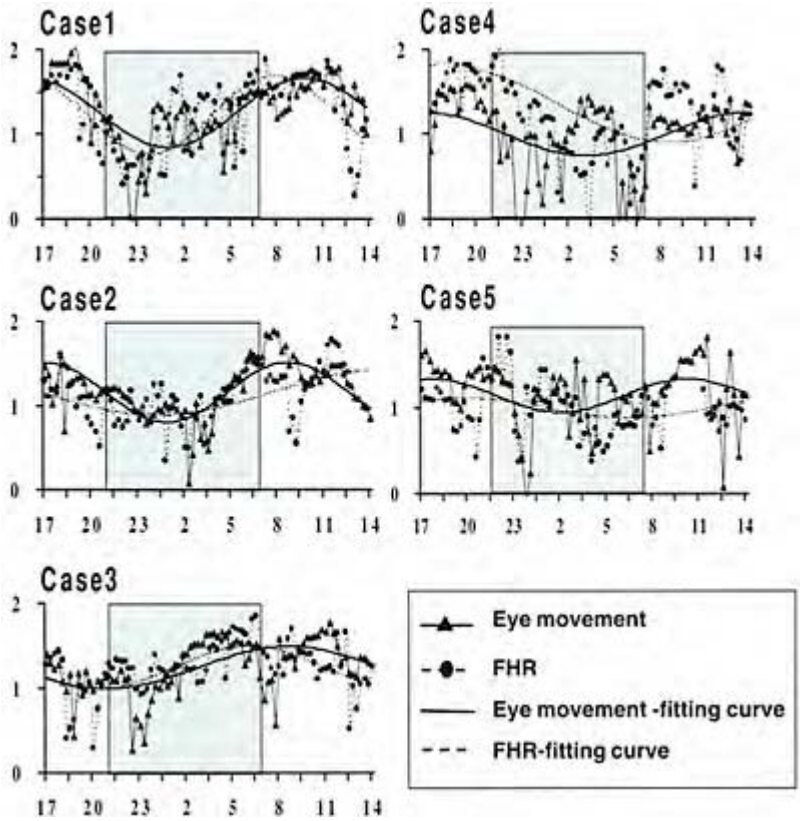

Figure 39.5: Diurnal changes in the slopes of eye movement frequency and FHR variation obtained from each of the 5 cases. The horizontal axis indicates clock time, and triangles and circles are located at the midpoint of each 3-hr time segment. Vertical axis shows b (slope of power spectrum calculated from each 3-hr segment). Solid and broken lines represent the fitting curve to eye

movement and FHR b values, respectively. Shaded areas indicate the period where the room light was off (Reproduced from Morokuma et al[42])

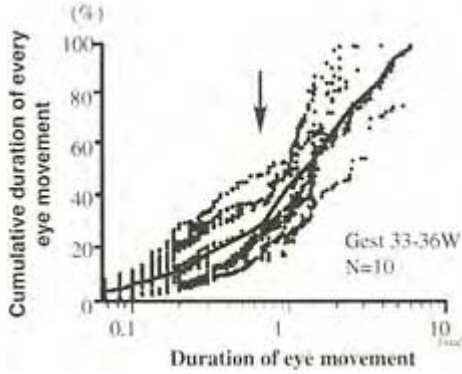

Figure 39.6: Duration of eye movement obtained from fetuses at 33–36 weeks' gestation. The horizontal and vertical axes indicate duration of eye movement and cumulative duration of every eye movement, respectively. The solid line indicates the mean value of the cumulative duration of every eye movement. The arrow indicates the statistically critical point (Reproduced from Horimoto et al[50])

difference between 33–36 and 37–41 weeks of gestation is seen by an increase in the proportionate amount of time maintaining REM.[50] At the latest, the coexistence of REM and slow eye movement becomes apparent by 33 weeks of gestation. This strongly suggests that the start of REM sleep and its related neural mechanisms, including the

locus coeruleus in the pons, controlling the phasic (REM), and the tonic (SEM) phenomena.[51,52]

Due to the anatomical configuration of the extraocular muscles attached to the orbital socket, when the supranuclear control necessary for extremely fine integration of neural activity is absent, extraocular muscles become hypotonic with incoordinate waxing and waning, resulting in slow eye movements.[51] Thus, SEM reflects decreased skeletal muscle tone, which represents the tonic phenomenon during REM sleep, and its control mechanism differs from that of the phasic phenomenon, such as REM. Studies have also reported that infants delivered at 33–35 weeks show reduced muscle action potentials during REM sleep.[52,53] Therefore, the coexistence of rapid and SEM is a minimum requirement for further supporting the existence of REM sleep in the human fetus starting from 33 weeks of gestation.[54] This chronological profile with respect to eye movement between 33 and 41 weeks of gestation supports the reports that REM and SEM are organized in activity episodes and become linked with other variables into coherent behavioral states at about 36–38 weeks of gestation.[55,56]

Mouthing Movement, Pupillary Changes, Penile Tumescence, and Micturition, including their Relation to the EM/NEM Periods

Mouthing

Regular mouthing can be observed in the human fetus *in utero* (Fig. 39.1).[55] From 28 to 31 weeks of gestation, the pattern of the incidence percentage of the interval between two consecutive mouthing movements showed a uniform distribution within the 60 minute observation period (Fig. 39.7).[57] This implies that the mouthing movement occurs in a random manner during this gestational stage. During the eye movement period starting at 35 weeks of gestation, the mouthing movement was uniform and random. Conversely, during the non-eye movement period, a high incidence of mouthing movement was closely repeated every 0.3–0.6 seconds. This regular mouthing closely concurred with the noneye movement period from 35 weeks of gestation to term. In contrast, the random mouthing movement was predominantly observed during the eye movement period and unrelated to gestational progression. From 32 to 34 weeks of gestation, the incidence patterns of mouthing movement intervals transitioned at 28–31 weeks of gestation and 35–41 weeks of gestation (Fig. 39.8). In infants born at or after 35–36 weeks of gestation, the regular mouthing movement was only observed during NREM sleep.[58,61] NREM sleep may indicate thalamocortical pathway function[62] so that *in utero* the fetal brain is functioning to the same extent as in the newborn. This phenomenon relates to behavioral neonatal ‘state 1’[60] and fetal ‘state IF’.[55]

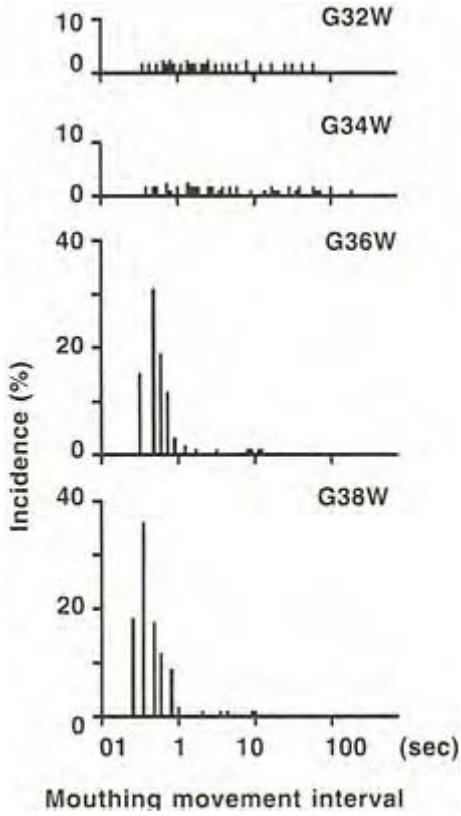

Figure 39.7:
Chronological sequences of fetal patterns in incidences of the mouthing movement interval. The horizontal and vertical axes indicate the interval between two successive mouthing movements and the percentage incidence at a given movement interval, respectively (Reproduced from Horimoto et al[57])

Penile Tumescence

Real-time ultrasound could visualize fetal genitalia with a positive observation rate as high as 90% after 24 weeks of gestation,[63] whereas an uninterrupted image of the fetal penis occurred in only 52% full-term fetuses (Fig. 39.9). Penile tumescence is closely related to REM sleep in the neonate as well as in infants.[51,64,70]Although there were some penile tumescence incidences during the non-eye movement period, they were minimal and brief. Penile tumescence duration was significantly longer in all fetuses during the eye movement period than during the non-eye movement period (Fig. 39.10).[71] Penile tumescence was found to make up 78% of the eye movement period in the fetus, 84% in the neonate,[66] and 80–95% of REM sleep in the adult.[67,69] Penile tumescence was also noted, albeit slightly, during the non-eye movement period with a 16% duration, compatible with neonate penile tumescence.[66] However, penile tumescence occurrences during the non-eye movement period were concentrated during the transitional phases from eye movement to non-eye movement periods and *vice versa*. There is little documentation indicating fetal penile tumescence during the midstage of the non-eye movement period. This suggests that changes in the penis appear to be related to an underlying mechanism that occurs during the transition between both periods. In addition, part of the eye movement period lacks penile tumescence in the human fetus, implying that the fetal penis could not remain tumescent for a considerable duration due to immature neural control of penile erection.

Pupillary Change

Birnholz[72] first identified the pupil in the human fetus *in utero* starting at 26 weeks of gestation (Fig. 39.1). Also, he stated that the pupillary diameter was relatively small and without recognizable dilatation or periodic change. In the adult human as well as in animals, the pupil is more constricted during NREM sleep than in REM sleep.[73,77] Horimoto et al[78] observed pupillary dilatation and constriction in the human fetus at term and reported on pupillary diameter changes in relation to both eye and non-eye movement periods (Fig. 39.11). In all fetuses at 36–41 weeks of gestation, pupillary diameters were statistically differentiated into two groups, thus demonstrating the existence of two different conditions characterized by pupil dilatation (9.7%) and constriction (90.3%). The median values of pupillary diameter at constriction (1.7 mm) and at dilatation (3.0 mm) were compatible with those of the neonate.[79] It was also noted that the median percentage of pupillary dilatation (14.3%) during the eye movement period was significantly greater (2.3%) than during the non-eye movement period, suggesting a close relation between pupillary dilatation and the eye movement period. From this point of view, it is interesting to note that while the pupillary light reflex is present in all neonates born at 35 weeks of gestation or greater, it is absent for the first week after birth in infants born with less than 30 weeks of gestation. Thus, this reflex is thought to gradually develop from this gestational point.[79,81] A correlation between these findings and those from adult humans demonstrating characteristic pupillary size changes from sleep to alertness, where adult pupillary diameters during REM and NREM sleep were 45% and 35% of the alert state diameter, respectively, is currently lacking.[75,76]

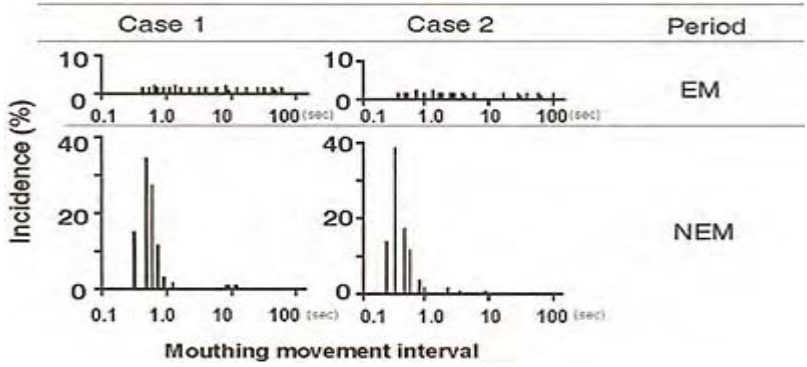

Figure 39.8: Patterns in incidence of the mouthing movement interval in EM/NEM period. Patterns in incidence of the mouthing movement interval in 2 fetuses at 37 weeks, divided into eye movement (EM, upper column) and non-eye movement (NEM, lower column) periods. The horizontal and vertical axes indicate the interval between two successive mouthing movements and the percentage incidence at a given movement interval, respectively. (Reproduced from Horimoto *et al*[57])

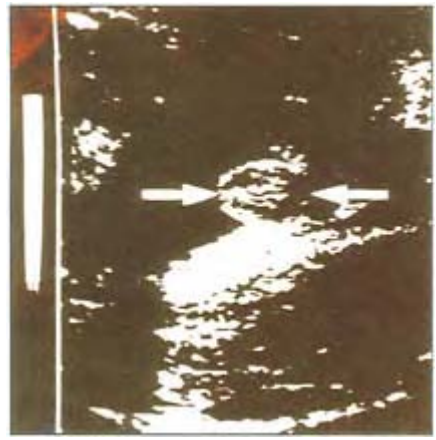

Figure 39.9: Ultrasound image of the feral penis. The arrows indicate the penile length measured from the radix penis to the tip of praeputium (Reproduced from Koyanagi et al[71])

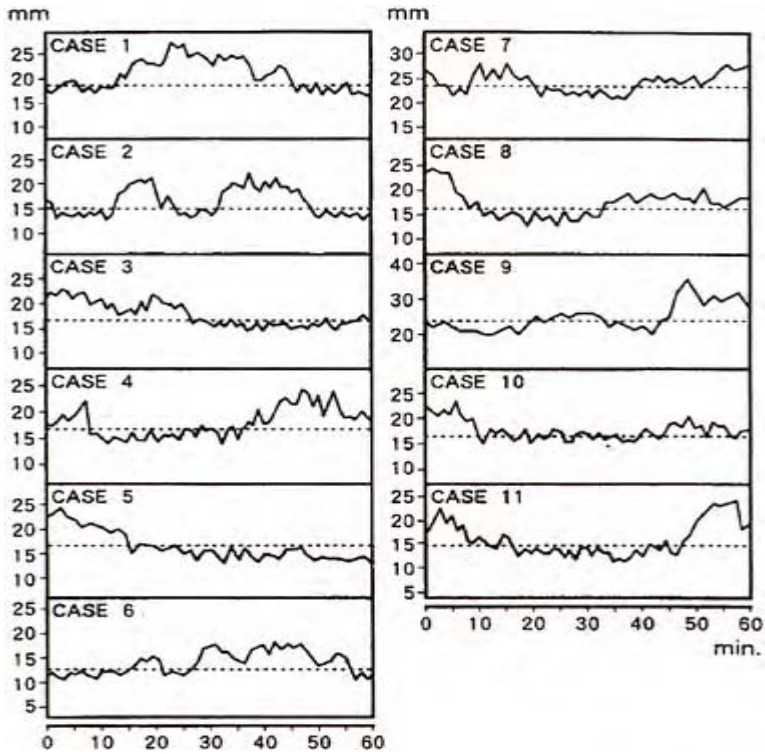

Figure 39.10:
Relationship between change in penile length and EM/NEM periods in fetuses from 36 to 41 weeks' gestation. Shaded and non-shaded areas show non-eye movement and eye movement periods, respectively. The solid lines represent the change in penile length, and the broken lines the 200/o value of the penile length range for each case; values on or above and those below the broken lines indicate

penile tumescence and flaccidity, respectively (Reproduced from Koyanagi et al[71])

Micturition

The time at which the human fetus empties its bladder is significantly associated with the transition between the low and high heart rate variation period, especially with the first part of high variation episodes.[82] Micturition was observed more frequently during the 'active' phase than during the 'quiet' phase of fetal heart rate (FHR) variation.[83] These two FHR phases correspond to the eye and non-eye movement periods, respectively.[29,84] Micturition becomes periodic around 20 weeks of gestation and the median intervals between successive micturitions at 33–36 and 37–41 weeks of gestation are 34 and 39 minutes, respectively.[82,85,87] The median values of one

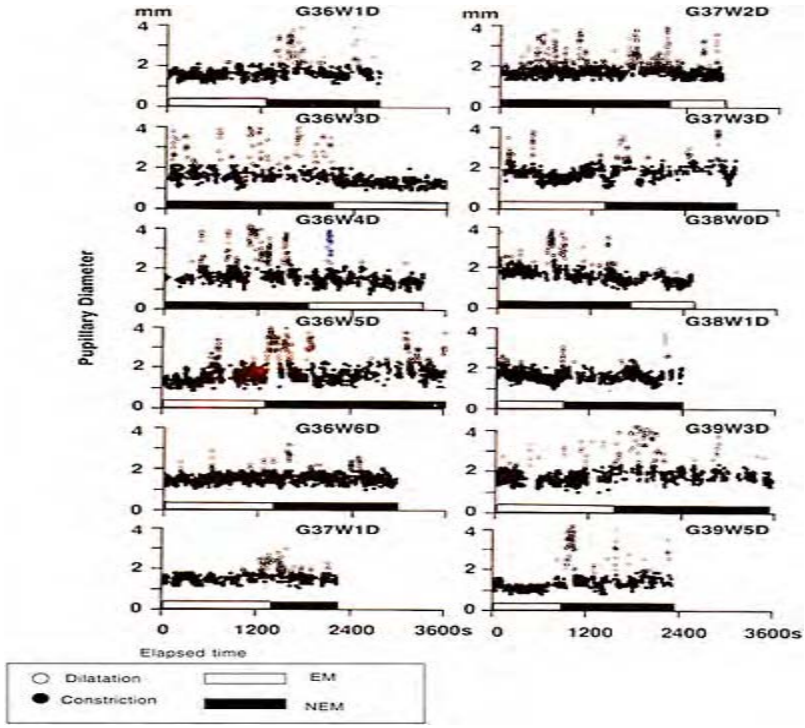

Figure 39.11: The chronological sequences in scattergrams of pupillary diameter. The horizontal and vertical

axes indicate elapsed time and corresponding pupillary diameter, respectively. Open and solid squares indicate EM and NEM period respectively. Open and solid circles indicate pupillary dilatation and constriction respectively, analyzed using "least meadian of squares regression".[131] (Reproduced from Horimoto et al[78])

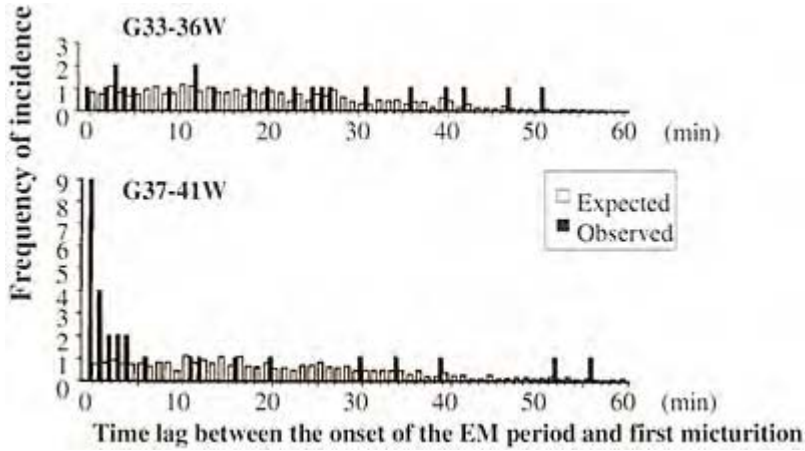

Figure 39.12: Histograms of statistically expected and observed frequencies of the time lag between the onset of the eye movement period and micturition. Histograms of statistically expected (Open bars), and observed (solid bars) frequencies of

the time lag between the onset of the eye movement period and first micturition in fetuses at 33–36 (upper panel) and 37–41 (lower panel) weeks' gestation, revealed using "goodness-fit-test".[132] The horizontal and vertical axes indicate the time lag in 1 minute epochs and frequency of incidence per 1 minute epoch, respectively (Reproduced from Koyanagi et al[87])

complete eye movement/non-eye movement period were 29 and 56 minutes for the same two gestational periods.[87] Accordingly in the earlier age group, the eye movement/non-eye movement periods and micturition cycle were similar. Although this suggests that these cycles occur in a seemingly synchronized fashion, the lag time between the two phenomena showed no statistical significance, indicating that their occurrence is unrelated (Fig. 39.12). On the contrary, with the results obtained from 37 to 41 weeks of gestation, different periodicities were noted between the onset of the eye movement period and micturition. Nevertheless, a statistically significant relationship was evident between the onset of the eye movement period and micturition, with a high frequency of micturition (72%) occurring within 8 minutes (as much as 31% within the first minute) after the eye movement period begins. Therefore, in the human fetus at term, micturition becomes biologically concurrent with the onset of the eye movement period.[87]

Wlodek et al[88] concluded that the voiding associated with REM sleep, which is electrocorticographically assessed, indicates the development of descending control of the fetal voiding process with REM sleep and micturition under neural control of the locus coeruleus and peri-alpha,[89] and the dorsolateral tegmentum,[90,91] respectively. With the pons location of these neurons, synaptic transmission is often incomplete and the neuronal axons and/or synapses may grow either to the wrong target or to an inappropriate region.[92] The relationship between REM sleep and penile erection occurs due to the spread of activation or an overflow phenomenon between controlling neural centers in close proximity.[65] The finding that there is a relationship between the onset of the eye movement period and the first micturition during 37–41 weeks of gestation, but not 33–36 weeks, suggests a similar underlying mechanism whereby such a phenomenon in the pons becomes manifested in the human fetus at term.

Can We Define REM/NREM Sleep *In Utero?*

Here, assuming that behavior reflects brain function[93] in the developing human fetus, we review fetal behavior ontogenesis from its relationship with the EM/NEM period. REM and SEM coexistence is apparent by 33 weeks of gestation. This strongly suggests the start of REM sleep and its related neural mechanisms, including the locus coeruleus in the pons, controlling the phasic (REM) and the tonic (SEM) phenomena. The close association between fetal penile tumescence and the eye movement period at term provides circumstantial evidence for this hypothesis. Concurrence of the regular mouthing movement and the NEM period becomes clearly evident by 35–36 weeks of gestation. This implies the start of NREM sleep and its related neuronal activities with pathways rostral to the pons through the thalamocortical connection to the cerebral cortex by which, together with the tonic system maturation, the fetal eye could be held in an eccentric position. Two conditions exist at 35 weeks of gestation or greater: short-duration pupil dilatation and long-duration constriction, with the former significantly occurring during the eye movement period. Referring to data on adult humans, the pupillary diameter change is almost proportional to the range of states from sleep to alertness. Studies on fetal pupillary change are key to further discussion on the existence of the *in utero* waking state. Significantly evident is the relationship between the EM period onset and the first micturition thereafter, which starts at 37 weeks of gestation. This phenomenon may be explained by the close proximity of the control neurons in the pons, the locus coeruleus, and peri-alpha for the eye movement, and the dorsolateral tegmentum controlling micturition, whereby the axons in part, may grow to and act on an inappropriate region. At term, this phenomenon is described as more mature. This data suggests that the particular statuses, including both REM/NREM "sleep", have already started in the human fetus. Moreover, we have described various movements in relation to or in concurrence with one another, gradually integrating into more complex movements throughout gestation. Therefore, it could be assumed that each center of movements also gradually integrates into a common central mechanism, which may be the center of REM/NREM sleep. However, fetal behavior has only been described in conjunction with variables relating to and/or concurring with several cognizant movements during ultrasound examinations with limited observable variables. This leads to the precarious discussion of whether or not to actually use the terms 'sleep state' and 'waking state' in order to describe conditions in *utero*. Presently, we should restrict ourselves to the terms 'eye movement period' and 'non-eye movement period' while waiting for additional studies.

RELATIONSHIP BETWEEN ABNORMAL BEHAVIORAL PATTERNS *IN UTERO* AND FUNCTIONAL BRAIN IMPAIRMENT

The search for causes of brain impairment in newborns has predominantly focused on intrapartum and postpartum events[94] for the past three decades. Recently, we have provided strong evidence that most cerebral palsy cases are not the result of perinatal asphyxia in full-term infants, but rather the consequence of prenatal intrauterine problems, which are usually unpreventable.[95,98] Ellis et al[94] reported that neuropathological findings of prenatal brain damage were in 25% of infants that died at 7

days of age or less. According to data from the Neurological Collaborative Perinatal Project of the National Institute of Neurological and Communicative Disorders and Stroke, birth asphyxia accounted for only 6% of all cerebral palsy cases.[99] Some attempts have been made to initiate a prenatal screening system in order to discriminate fetuses from the general population with compromised central nervous system function.[100]

Fetuses were considered to have potential *in utero* brain function impairment when exhibiting any of the following three indicators: decrease or lack of fetal movement, persistent non-reactive FHR pattern, and/or central nervous system malformation (Table 39.2).[101] Upon screening 1426 fetuses delivered between 37 and 41 weeks of gestation at the Maternity and Perinatal Care Unit of Kyushu University Hospital in Japan, 24 cases were selected as suspicious. These cases were subjected at 35 36 weeks of gestation to extensive ultrasound observation, especially designed to assess whether functional brain impairment had prenatally occurred by the utilization of five different behavioral patterns (Table 39.2). Following these examinations, eight cases were believed to have abnormal behavioral patterns during the intrauterine period. In an attempt to explain the rationale behind the fetal behavior examination leading to *in utero* abnormality identification, we present the first case as a model.

In case 1, movement in all four extremities was lacking; however, alternations of eye movement and non-eye movement periods as well as breathing movements were not evident (Table 39.3).[100]

Table 39.2: Indicators for possible fetal brain function impairment and extensive US evaluation of fetal brain function impairment

Indicators for possible feral brain function impairment
1. Decrease or lack of fetal movement The mother reports feeling fewer than three fetal movements per 12 hour period or experiences a complete cessation of fetal movement over the same amount of time (Sadovskv et al 1983)
2. Persistent non-reactive FHR pattern A non-reactive FHR pattern consists of the heart rate ranging between 120 and 160 beats per minute (bpm) with a decreased baseline variability of 5 bpm or less and no accelerations in response to fetal movement (Rochard et al 1976). A persistent non-reactive FHR pattern is defined as a non-reactive FHR pattern continuing for 120 minutes or more (Brown & Patrick 1981)
3. Central nervous system malformations Central nervous system malformations diagnosable in *utero* include holoprosencephaly, encephalocele, arachnoid cyst, porencephaly, agenesis of the corpus callosum, intracranial tumor, and the group of congenital brain diseases accompanying ventriculomegaly
Indicators for extensive ultrasound evaluation of fetal brain function impairment
1. Movement of extremities Less than one episode of motion, involving extension, flexion, external and internal rotation or

abduction and adduction of all four extremities during a 60 minute observation is considered abnormal (De Vries et al 1985)

2. **Breathing movement**

   Breathing movement is considered abnormal when this movement cannot be detected during a 120 minute observation period (Trudinger & Knieht 1980)

3. **Rapid eye movement and slow eye movement patterns**

   REMs and SEMs are defined as those having durations of less than, and equal to or more than, the critical value of 0.6 0.8 seconds, respectively. The lack of REMs coexisting with SEMs is considered an abnormal eye movement pattern (Horimoto et al 1990)

4. **Alteration of the EM and NEM periods**

   The 25 75% ranges for the duration of the EM and NEM periods with a 60 90 minute observation are 230 and 2 25 minutes, respectively. The alternation of the EM and NEM periods is considered abnormal when either duration is outside of these ranges (Koyanagi et al 1993b)

5. **Concurrence of regular mouthing movement with the NEM period**

   When repetitive mouthing movements are not observed at a regular interval of 300 600 ms during the NEM period for a 90 minute observation period, the concurrence of regular mouthing with the NEM period is considered abnormal (Horimoto et al 1989)

Table 39.3: Summary of eight cases antenatally diagnosed abnormal behavioral patterns

Antenatally diagnosed abnormal behavioral patterns								
	Fetal behavioral patterns							
Case	*Movement of extremities*	*Breathing movement*	*EM/NEM alteration*	*REM/SEM (EM pattern)*	*Regular mouthing in NEM*	*Postnatal diagnosis*	*Localization*	*Neurological signs*
1	Present	Absent	Present	Present	NA	Mobius synd. with central hypoventilation	Pons medulla	MR Respiration disturbance
2.	Absent	Present	Present	Present	Present	Spinal cord hemorrhage	Spinal cord (C5 6)	Quardriplegia sensory disturbance
3.	Present	Present	Present	Present	Absent	Undetermined	Cerebral white matter	MR,CP

4.	Present	Present	Present	Present	Present	Arachnoid cyst	Rt frontal lobe	None
5.	Present	Present	Present	Present	Present	Arachnoid cyst	Rt quadrigeminal cystern to intrahemispheric fissure lobe	None
6.	Present	Present	Present	Present	Present	Hydrocephalus Encephalocele	Occipital lobe	None
7.	Present	Present	Present	Absent Present	Present	Normal	None	None
8.	Present	Present	Absent Present	Present	Present	Normal	None	None

EM: eye movement; NEM: non-eye movement, REM: rapid EM, SEM: slow EM, NA: not available, MR: mental retardation, CP: cerebral palsy (Reproduced from Koyanagi *et* al)[100]

It is thought that the controlling mechanism of fetal breathing movements is similar to that of adult respiration.[102,103] It has also been reported that medulla decompression in the case of the Chiari I malformation with central apnea, results in a marked reduction in the number of sleep apnea episodes.[104] Gilmore et al[105] documented that since the location of the dorsal and ventral respiratory neurons and pontine respiratory neurons are in close proximity to the cranial nerve VI and VII nuclei and/or nerves, lesions in the pons and medulla lead to or produce central sleep apnea. The neural center, which generates the ultradian rhythm of the eye movement and non-eye movement periods, is known from animal studies to lie within the pons and/or medulla oblongata.[9] Therefore, the prenatal assessment in this case that there was an absence of breathing movement together with a lack of eye movement/non-eye movement alternation suggests a lesion involving the pons and/or medulla oblongata. This prenatal diagnosis was compatible with brain computerized tomography (CT) findings after birth, which demonstrated a calcified lesion spreading from the pons to the medulla oblongata, corresponding to the fasciculus longitudinalis medialis et lateralis (Fig. 39.13). This case is in accordance with a report on a neonate where in *utero* brainstem ischemia was suggested as a mechanism for the Mobius syndrome based on finding pontomedullar calcifications in the fourth ventricle floor in a brain CT scan.[106]

In case 2, despite a normal breathing pattern, no movements in any of the four extremities were observed. Postnatal findings confirmed the localized lesions in the spinal cord at C_5–C_6 that were prenatally diagnosed. In case 3, the concurrence of regular mouthing with the non-eye movement

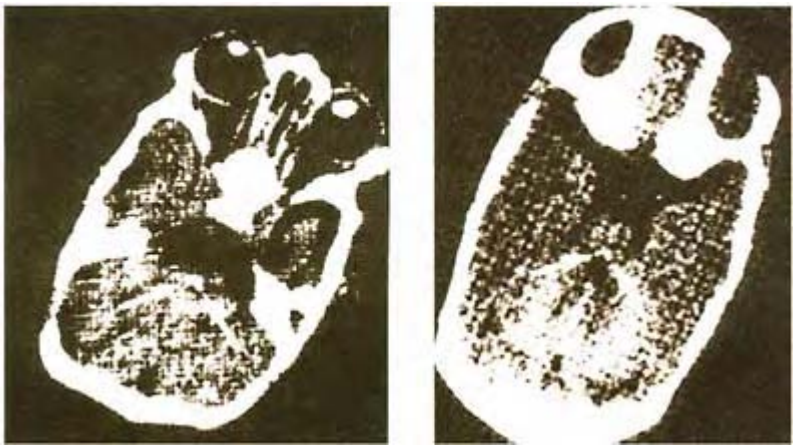

Figure 39.13: Brain CT In case 1 indicates symmetric calcified lesions (arrows) at the pons (left panel), and the medulla oblongata (right panel)

period was absent. Prenatal assessment was limited to lesions cephalad to the pons. Postnatal examination revealed diffuse lesions spreading from the pons through the thalamus to the cerebral cortex. Cases 4, 5, and 6 showed normal behavioral patterns from the intrauterine to early neonatal period in spite of having congenital lesions in the cerebral hemisphere. In both cases 7 and 8, the first extensive examination showed abnormal behavioral patterns in the eye movement/non-eye movement period alternation and REM/slow eye movement patterns. However, findings were normal during the second observation and postnatal physical examinations indicated no neurological abnormalities.

Each of the five indicator behavioral patterns has its own developmental characteristics. De Vries et al[107] reported that isolated arm and leg movements, as well as hand-face contact movement, were clearly visible starting from 12 weeks of gestation. Others have documented that the sighing movement with multiple inspiratory efforts, which coincides with a neuronal discharge from the medullary centre, is frequently seen starting at 32 weeks of gestation in the human fetus, indicating the maturation process of the breathing movement controlling center.[108,109] Eye and non-eye movement periods alternate with relatively consistent durations by 35 36 weeks of gestation, implying that the neural center related to ultradian rhythm, located from the medulla oblongata to the pons, begins to function at this gestational stage.[22,30] In addition, regular mouthing only concurs with the non-eye movement period by 35 36 weeks of gestation,[57] demonstrating functional maturation of the neural area rostral to the pons through the thalamocortical connection to the cerebral hemisphere.[62] Therefore, starting at 35 36

weeks of gestation, the motor systems pertaining to these indicators are considered functional. All eight cases in Table 39.3 were within this gestational period and abnormal behavioral patterns were repeatedly detected in every ultrasound examination, providing convincing evidence of a persistent lesion in the central nervous system during intrauterine life. Thus, the fetuses with suspected functional central nervous system impairment could be classified into four groups: (1) cases with lesion sites at, and caudal to, the pons-medulla (cases 1 and 2), prenatally identified by abnormal behavioral patterns; (2) a case with a diffuse and unlocalized brain lesion (case 3), representing behavioral abnormality in utero; (3) cases with a localized lesion in the cerebral hemisphere(s), *i.e.* arachnoid cyst and encephalocele (cases 46), indicating no abnormal behavior during the intrauterine period; and (4) cases with temporally abnormal behavior in *utero* (cases 7 and 8), finally changing over to a normal pattern without neonatal neurological abnormalities.

Applying this system in a population screen, it was evident that five out of 1426 fetuses (0.4%) could be prenatally diagnosed with a positive predictive value of 62.5% (five out of eight cases). Although this incidence is comparable with that seen in the Rosen & Dickinson review,[110] our results were highly influenced by the high number at risk referred to our perinatal care unit. A clinically apropos system of screening and perceiving fetuses with abnormal behavior as an indication of prenatal brain impairment is still in the early stages and constant revision of the abnormal indicators is mandatory.

FETAL LEARNING AS A NEW PARAMETER TO ASSESS FETAL CNS DEVELOPMENT

The Possible Significance of "Fetal Learning" in the Developing Fetus

As discussed in the previous section, fetuses indicating functional central nervous system (CNS) impairment could be categorized into one of four groups: (1) a lesion at the brainstem, (2) a diffuse brain lesion, (3) a localized lesion in the cerebral hemisphere(s), and (4) cases with temporally abnormal behavior in utero.[100] In one sense, these results might suggest that in the developing human fetus, the CNS is not completely functioning. Therefore, in cases where the lesion exists in a temporarily non-functioning area, no corresponding behavioral abnormality may be observed (Table 39.4). However in another sense, inappropriate choice of behavioral parameters might be misleading in higher brain function assessment. Equally important is the effect of external influences. So far, we hypothesized that the fetal pacemaker must be organized at a basic level during intrauterine life. In this regard, fetal behavior should be considered as an expression of intrinsic CNS function. On the contrary, there is data that fetuses can sense external stimulations, including vibro-acoustic stimulus,[10] lights,[11,12] smells,[13] tastes,[14,15] temperatures[16,17] and may memorize them.[18] For many years, it was thought that the newborn infant lacked a functioning memory. Instead, memory developed over time after birth. However, studies on newborns and premature infants in recent years have changed this view. Newborns have been shown via a variety of learning paradigms, such as habituation,[111,112] classical conditioning,[113] associative learning,[114] and imitation[115] to possess a functioning memory.[116] Memory begins prenatally and the period of birth

merely marks an *in utero* to *ex utero* memory function transition. In this context, it would be incorrect to hypothesize that fetal behavior is an expression of intrinsic CNS function.

Table 39.4: Summary of behavioral pattern and corresponding CNS function

Behavioral pattern	*Corresponding CNS level*	*GW to start functioning*	
Alteration of the eye EM and NEM periods	Pins to medulla	29	31
Possible REM sleep			
HEM and SEM patterns	Pons	33	
Pupillary constriction and dilatation	Controvertial	36	
Micturition at onset of EM period	Pons	37	
Possible NREM sleep			
Concurrence of regular mouthing movement with the NEM period	Pons to thalamocortical	35	
FHR pattern Active/Quite phase alteration	Pons to medulla	30	

Learning is believed to occur in the absence of overt behavior just after stimulation, but actual occurrence can only be inferred from behavioral changes. When a sensory organ receives a stimulus, it sends some signals to the sensory system in the brain, leading to the activation of related areas, including both the learning and memory centers. After these centers determine the intensity and type of response, they send a signal to the motor system, resulting in a response, such as movement. Therefore, learning might reflect more integrated brain function and the cortical development should be involved in a learning process. Habituation is defined as a decrease leading to cessation of a behavioral response that occurs when an initial novel stimulus is repeatedly presented.[117] Habituation is considered the simplest learning, but regarded as one of the most universal and essential learning forms. Although it is unclear how cerebral cortices are involved in this process, it is widely accepted that they play an important role.[118,120] In human fetuses, there is data that they have already acquired this ability *in utero*.[121] Moreover, impaired habituation has been reported in fetuses with Down's syndrome, in pathologic neonates,[122,125] and adults with such abnormalities as unconsciousness, schizophrenia, and severe depression. In the human fetal state, behavioral development[126] and well-being,[127] gestational age,[128] sedative drugs;[121] maternal smoking,[120] maternal hypoxia[129] are factors that may influence habituation. Habituation as well as other types of learning could be behavioral parameters *in utero* to assess fetal CNS function. However, it should be verified how the behavioral development can influence fetal habituation. In this section, we introduce our recent work on the relationship between fetal habituation and functional CNS development assessed with other behavioral parameters (Morokuma and Fukushima, manuscript in preparation).

The relationship between fetal learning and functional CNS development in utero

Included in this study were 18 fetuses from 32 to 37 weeks of gestation with no detected abnor malities during pregnancy. This study was approved by the Ethical Committee of Kyushu University Medical Sciences and written informed consent was obtained from each patient prior to testing.

First, fetal behavioral patterns were assessed by ultrasonographic observation (ALOKA SSD5500, Tokyo) of fetal eye and mouthing movements (Table 39.5). Then, the fetuses were exposed to vibration stimuli, their movement observed, and recorded on videotape. Fetal response was detected using real-time ultrasound with a 5.0 MHz convex transducer positioned to provide the best possible view of the upper torso, at least one extremity, and the head. Movements of the fetal trunk, head, or limb within 1-second of the stimulus application were scored as a positive response. Each trial was ranked according to the nature of the behavioral response: fast, general (3); fast, local (2); slow (1) and no response (0). All scoring was done during video playback. A lack of response to five consecutive stimuli was defined as habituation, with the trial after habituation scored as zero. The stimuli were produced by a fetal vibro-acoustic stimulator (ALOKA SSD-5500, Tokyo). A stimulus of 0.3second duration was repeatedly applied to the maternal abdomen above the fetal legs every 10 seconds for a total of 20 trials. Stimuli were applied after the NREM period for at least two minutes. Vibration stimulus was programmed in the PC and stimulated at the fetal femoral through the maternal abdominal wall. A response decrement curve was constructed by determining the mean fetal response score following each stimulus application. Repeated variance measuring was used to test for behavioral pattern differences between the trials.

The behavioral developmental profile is shown in Table 39.5. All fetuses showed EM/NEM alteration, REM, and SEM. However, regular mouthing in the NEM period, indicating that the thalamocortical pathway is functional, was seen in 5 out of 13 fetuses at 32 34 weeks of gestation. Thus, there are two different statuses in these fetal subjects. For further analysis, the fetuses were first divided into two groups by gestational age of 32 to 34 weeks and 35 to 37 weeks. Both groups showed significant habituation ($P<0.05$). The advanced fetuses seemed to habituate earlier, but not significantly (Fig. 39.14). Next, comparison among the three groups divided not only by gestational weeks, but also by behavioral developmental profile, showed that the fetuses with regular mouthing in the NEM period before 35 weeks, habituated earlier than who failed to show regular mouthing (Figs 39.15 and 39.16). Taken together, there apparently is a relationship between behavioral development and habituation. These results suggested that “fetal learning” might be applicable as a new method to evaluate fetal CNS development.

Table 39.5: Behavioral development. The fetuses were divided into 3 groups by gestational age and fetal behavioral development, assessed with ultrasonographic observation for alteration of EM/NEM, REIW SEM pattern (see text) and concurrence of regular mouthinq in NEM

				Mouthing in NEM	
Gest.	*No. of case*	*EMINEM alteration*	*REM/SEM*	*Positive*	*Negative*
32–34	13	13	13	5	8
35–37	5	5	5	5	0
Total	18	18	18	10	8

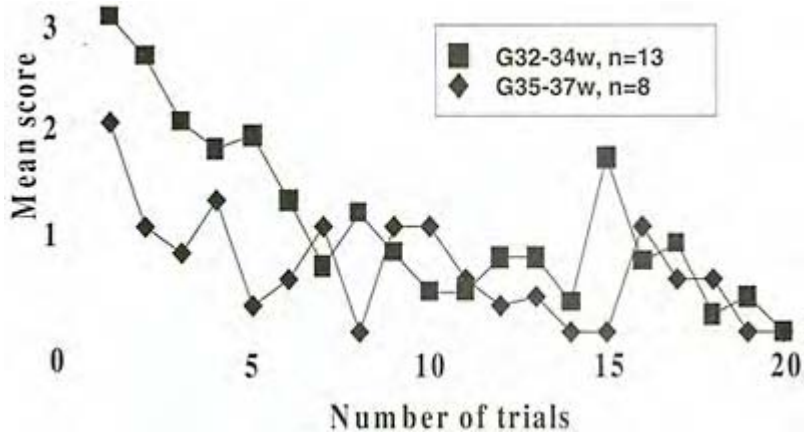

Figure 39.14: Fetal habituation to vibration stimuli; Comparison by gestational age. Eighteen fetuses were stimulated with vibro-acoustic stimulator for 20 times and given points for each response depending on their movement (see text).

The fetuses were divided into two groups by gestational age of 32 to 34 weeks (■) and 35 to 37 weeks (♦).The horizontal and vertical axes indicate the number of stimulations and the mean points, respectively

SUMMARY

Here, we presented the ontogenesis of fetal behavioral development, mainly from its relationship to possible REM/NREM sleep. The ontogeny of fetal behavior shows not only that the development

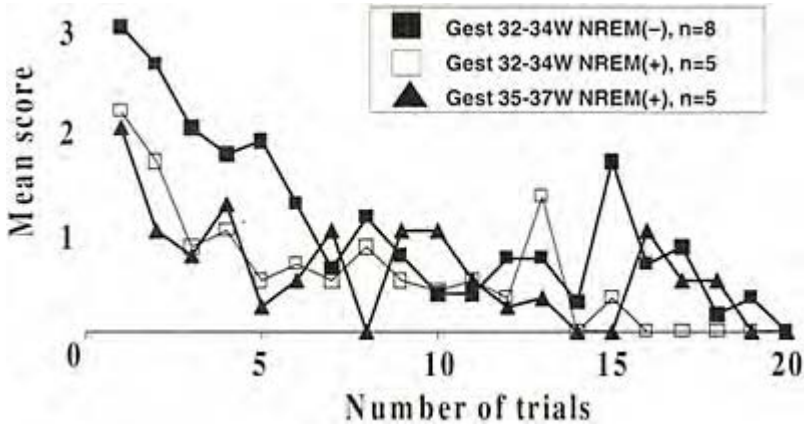

Figure 39.15: Fetal habituation to vibration stimuli; Comparison by behavioral development. Eighteen fetuses were stimulated with vibro-acoustic stimulator for 20 times and given points for each response depending on their movement (see text). The fetuses were

divided into three groups by gestational age and behavioral pattern, depending on the presence or absence of concurrence of regular mouthing movement. ■ □ ▲ indicate gestational age of 32 to 34 weeks with concurrence, without 35 to 37 weeks. There were no fetuses who does not show concurrence after 35 weeks gestation. The horizontal and vertical axes indicate the number of stimulations and the mean points, respectively

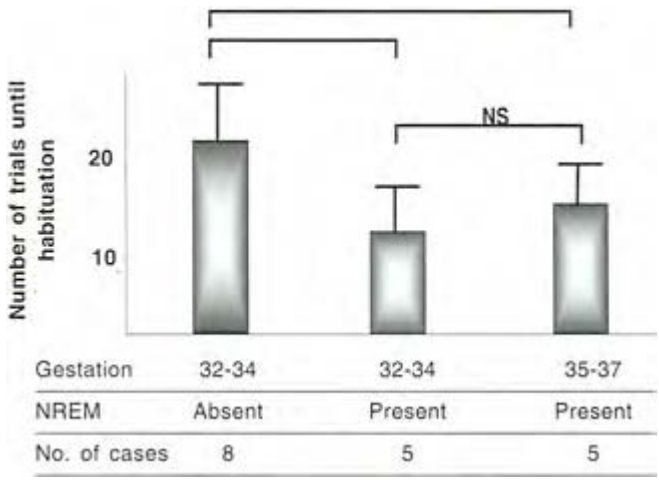

Figure 39.16: The number of stimulus required for habituation. The fetuses were divided into three groups by gestational age and

behavioral pattern, as described. The data are the mean±SD numbers of stimuli required to habituation, judged when no response was seen after sequential five times of stimuli. *: statistically significant, P<0.05, NS: not significant

of each movement proceeds with gestational advances, but also that various movements in relation to or in concurrence with one another, gradually integrate into more complex ones. Furthermore, based on these physiological results, the timing and extent of detection and localization in *utero* of functional brain impairment becomes applicable in obstetrics. However, recent data have suggested that it is insufficient to hypothesize that fetal behavior is a reflection of intrinsic CNS function. Fetal learning might be a new indicator of higher CNS function. Additional studies are necessary on fetal functional CNS development to understand fetal physiological abilities, such as memory and higher brain function.

REFERENCES

1. Humphrey T. Function of the nervous system during prenatal life. In: Stave U (Ed). Perinatal Physiology. Plenum Press, New York, 1978; 651–83.
2. Martin JH. Development as a guide to the regional anatomy of the brain. In: Kandel ER, Schwartz JH (Eds). Principles of neural science (2nd ed). Elsevier, New York, 1985;244–58.
3. Dobbing J, Sands J. Quantitative growth and development of human brain. Archives of Disease in Childhood 1973;48:757–67.
4. Visser GHA, Laurini RN, De Vries JIP et al. Abnormal motor behaviour in anencephalic fetuses. Early Human Development 1985;12:173–82.
5. Kawamura H, Ibuka N. The search for circadian rhythm pacemakers in the light of lesion experiments. Chronobiologia 1978;5:69–88.
6. Mirmiran M, Kok JH, Boer K et al. Perinatal development of human circadian rhythms: role of the foetal biological clock. Neuroscience and Biobehavioral Reviews 1992; 16:371–78.
7. Lorenz K Der Kumpan in der Umwelt des Vogels. Der Artgenosse als auslosendes Moment sozialer Verhaltensweisen. Journal of Ornithology 1935;83: 137–213, 289–413.
8 Koyanagi T, Nakano H. Functional development of the fetal central nervous system. In: Levene MI, Lilford RJ (Eds). Fetal and neonatal neurology and neurosurgery. Churchill Livingstone, London, 1994;31–44.
9. Rasmussen DD. Physiological interactions of the basic rest-activity cycle of the brain: pulsatile luteinizing hormone secretion as a model. Psychoneuroendocrinology 1986; 11:389–405.
10 Hepper PG. Fetal psychology: an embryonic science. In: Nijhuis JG (Ed). Fetal Behavior Developmental and Perinatal Aspects, Oxford University Press, Oxford, 1992; 129–56.
11. Peleg D, Goldman JA. Fetal heart rate accekeratuib ub response to light stimulation as a clinical measure of fetal well being. A preliminaly report. Journal of Perinatal Medicine 1980;8:38–41.

12. Polishuk WZ, Laufer N, Sadovsky E. Fetal reaction to external light. Harefuah 1975;89:395–97.
13. Tucker D. Physical variables in the olfactory stimulation process. Journal of General Physiology 1963;46:453–89.
14. De Sono K Das Trinkende kind im Uterus. Monatsschr. Geburtsh Gynaekol 1937; 105:88–97.
15. Liley AW. The fetus as a personality Australian and New Zealand Journal of Psychiatry 1972;6:99–105.
16. Timor-Tritsch IE. The effect of external stimuli on fetal behaviour. European Journal of Obstetrics and Gynecology and Reproductive Biology 1986;21:321–29.
17. Walker D. Temperature of the human fetus. Journal of Obstetrics and Gynecology of the British Commonwealth 1969;76:503–11.
18. Hepper PG. An interface between psychology and medicine; the antenatal detection of handicap. In: Klimek R (Ed). Pre and Perinatal Psycho-medicine 1992;133–38.
19. Nabekura J, Kawamoto I, Akaike N. Developmental change in voltage dependency of NMDA receptormediated response in nucleus tractus solitarii neurons. Brain Research (Brain Res) 1994;648(1):152–56.
20. Bots RSGM, NijhuisJG, Martin CB Jr et al. Human fetal eye movements: detection in utero by ultrasonography. Early Human Development 1981;5:87–94.
21. Birnholz JC. The development of human fetal eye movement patterns. Science 1981;213:679–81.
22. Inoue M, Koyanagi T, Nakahara H. Functional development of human eye movement in utero assessed quantitatively with real-time ultrasound. American Journal of Obstetrics and Gynecology 1986;155:170–74.
23. Bridgeman B. Phasic eye movement control appears before tonic control in human fetal development. Investigative Ophthalmology and Visual Science 1983;24:658–59.
24. Kleitman N. Basic rest-activity cycle—22 years later. Sleep 1982;5:311–17.
25. Othmer E, Hayden MFJ Segelbaum R. Encephalic cycles during sleep and wakefulness in humans: a 24-hour pattern. Science 1969; 164:447–49.
26. Kripke DR Ultradian rhythms in behavior and physiology. In: Brown FM, Graeber RC (Eds). Rhythmic aspects of behavior. Lawrence Erlbaum, Hillsdale, 1982; 313–43.
27. Roffwarg HR Muzio JN, Dement WC. Ontogenetic development of the human sleep-dream cycle. Science 1966; 152:604–19.
28. Sterman MB, Lucas EA, MacDonald LR. Periodicity with in sleep and operant performance in the cat. Brain Research 1972; 38:327–41.
29. Timor-Tritsch IE, Dierker LJ, Hertz RH et al. Studies of antepartum behavior in the human fetus at term. American Journal of Obstetrics and Gynecology 1978; 132:524–28.
30. Koyanagi T, Horimoto N, Takashima T et al. Ontogenesis of ultradian rhythm in the human fetus, observed through the alternation of eye movement and no eye movement periods. Journal of Reproductive and Infant Psychology 1993b; 11: 129–34.
31. Stern E, Parmelee AH Jr, Akiyama Y et al. Sleep cycle characteristics in infants. Pediatrics 1969; 43:65–70.
32. Parmelee AH, Wenner WH, Akiyama Y et al. Sleep states in premature infants. Developmental Medicine and Child Neurology 1967; 9:70–77.
33. Patrick J, Campbell K, Carmichael L et al. Patterns of gross fetal body movements over 24 hour observation during the last 10 weeks of pregnancy. American Journal of Obstetrics and Gynecology 1982; 142:363–71.
34. Visser GHA, Carse EA, Goodman JDS et al. A comparison of episodic heart-rate patterns in the fetus and newborn. British Journal of Obstetrics and Gynaecology 1982; 89:50–55.
35. Carmichael L, Campbell K, Patrick J. Fetal breathing, gross fetal body movements, and maternal and fetal heart rates before spontaneous labor at term. American Journal of Obstetrics and Gynecology 1984; 148:675–79.

36. Arduini D, Rizzo G, Parlati E et al. Are the fetal heart rate patterns related to fetal-maternal-endocrine rhythms at term pregnancy? Journal of Foetal Medicine 1986; IV:53–57.
37. Honnebier MBOM, Swaab DF, Mirmiran M. Diurnal rhythmicity during early human development. In: Reppert SM (Ed). Development of circadian rhythmicity and photoperiodism in mammals. Perinatology Press, Ithaca, 1989;221–44.
38. Patrick J, Natale R, Richardson B. Patterns of human fetal breathing activity at 34 to 35 weeks' gestational age. Am J Obstet Gynecol 1978; 132:507–13.
39. Lunshof S, Boer K, Wolf H, van Hoffen G, Byram N, Mirmiran M. Fetal and maternal diurnal rhythms during the third trimester of normal pregnancy: Outcomes of computerized analysis of continuous twenty-four-hour fetal heart rate recordings. Am J Obstet Gynecol 1998; 178:247–54.
40. Reppert SM, Schwartz WJ. Functional activity of the suprachiasmatic nuclei in the fetal primate. Neurosci Lett 1984; 46:145–49.
41. Morokuma S, Horimoto N, Satoh, S et al. Diurnal variation of eye movement and heart rate variability in the human fetus at term. Early Hum Dev 2001; 63: 123–30.
42. Morokuma S, Horimoto N, Nakano H. Diurnal changes in the power spectral characteristics of eye movements and heart rate variability in the human fetus at term. Early Hum Dev. 2001; 64:27–36.
43. Otsuka K. Chronome & Janus-Medicine. Tokyo: Medical Review Co. Ltd, 1998.
44. Karin J, Hirsch M, Akselrod S. An estimate of fetal autonomic state by spectral analysis of fetal heart rate fluctuations. Pediatr Res 1993; 34:134–38.
45. Shono H, Yamasaki M, Muro M et al. Chaos and fractals which 1/f spectrum below 10(-2)Hz demonstrates full-term fetal heart rate changes during active phase. Early Hum Dev 1991; 27:111–17.
46. Teich MC, Heneghan C, Lowen SB et al. Fractal character of the neural spike train in the visual system of the cat. J Opt Soc Am [A] 1997; 14:529–46.
47. Bozoki Z. Chaos theory and power spectrum analysis in computerized cardiotocography. Eur J Obstet Gynecol Reprod Biol 1997; 71:163–68.
48. Aserinsky E, Kleitman N. Regularly occurring periods of eye motility, and concomitant phenomena during sleep. Science 1953; 118:273–74.
49. Robinson PC. Control of eye movements. In: Brookhart JM, Mountcastle VB, Brooks VB (Eds). Handbook of Physiology. American Physiological Society, Bethesda, 1981;vol 11:1275–1320.
50. Horimoto N, Koyanagi T, Satoh S. Fetal eye movement assessed with real-time ultrasonography: are there rapid and slow eye movements? American Journal of Obstetrics and Gynecology 1990; 163: 1480–84.
51. Aserinsky E, Kleitman N. Two types of ocular motility occurring in sleep. Journal of Applied Physiology 1955; 8:1–10.
52. Parmelee AH, Stern E. Development of states in infants. In: Clemente CD, Purpura DP, Mayer FE (Eds). Sleep and the maturating nervous system. Academic Press, New York, 1972; 199–215.
53. Petre-Quadens O. Ontogenesis of paradoxical sleep in the human newborn. Journal of the Neurological Sciences 1967; 4:153–57.
54. Prechtl HFR, Lenard HG. A study of eye movements in sleeping newborn infants. Brain Research 1967; 5: 477–93.
55. Nijhuis JG, Prechtl HFR, Martin CB Jr et al. Are there behavioural states in the human fetus? Early Human Development 1982; 6:177–95.
56. Prechtl HFR, Nijhuis JG. Eye movements in the human fetus and newborn. Behavioural Brain Research 1983; 10:119–24.
57. Horimoto N, Koyanagi T, Nagata S et al. Concurrence of mouthing movement and rapid eye movement/ non-rapid eye movement phases with advance in gestation of the human fetus. American Journal of Obstetrics and Gynecology 1989; 161:344–51.

58. Wolff PH. The serial organization of sucking in the young infant. Pediatrics 1968; 42:943–56.
59. Dreyfus-Brisac C. Ontogenesis of sleep in human prematures after 32 weeks of conceptional age. Developmental Psychobiology 1970; 3:91–121.
60. Prechtl HFR. The behavioural states of the newborn infant (a review). Brain Research 1974; 76:185–212.
61. DeHaan R, Patrick J, Chess GF et al. Definition of sleep state in the newborn infant by heart rate analysis. American Journal of Obstetrics and Gynecology 1977; 127:753–58.
62. Watanabe K, Iwase K. Spindle-like fast rhythms in the EEGs of low-birth weight infants. Developmental Medicine and Child Neurology 1972; 14:373–81.
63. Birnholz JC. Determination of fetal sex. New England Journal of Medicine 1983; 309:942–44.
64. Ohlmeyer P, Brilmayer H, Hullstrung H. Periodische Vorgange im Schlaf. Pfluegers Archiv European Journal of Physiology 1944; 248:559–60.
65. Fisher C, Gross J, Zuch J. Cycle of penile erection synchronous with dreaming (REM) sleep. Archives of General Psychiatry 1965; 12:29–45.
66. Karacan I. The developmental aspect and the effect of certain clinical conditions upon penile erection during sleep. Excerpta Medica ICS 1966; 150:2356–59.
67. Karacan I, Hursch CJ, Williams RL et al. Some characteristics of nocturnal penile tumescence during puberty. Pediatric Research 1972a; 6:529–37.
68. Karacan I, Hursch CJ, Williams R L et al. Some characteristics of nocturnal penile tumescence in young adults. Archives of General Psychiatry 1972b; 26:351–56.
69. Karacan I, Williams RL, Thornby JI et al. Sleeprelated penile tumescence as a function of age. American Journal of Psychiatry 1975; 132:932–37.
70. Kessler WO. Nocturnal penile tumescence. Urologic Clinics of North America 1988; 15:81–86.
71. Koyanagi T, Horimoto N, Nakano H. REM sleep determined using in utero penile tumescence in the human fetus at term. Biology of the Neonate 1991; 60: 30–35.
72. Birnholz JC. Ultrasonic fetal ophthalmology. Early Human Development 1985; 12:199–09.
73. Berlucci G, Moruzzi G, Salvi G et al. Pupil behavior and ocular movements during synchronized and desynchronized sleep. Archives Italiennes de Biologic 1964; 102:230–44.
74. Hodes R. Ocular phenomena in the two stages of sleep in the cat. Experimental Neurology 1964; 9:36–42.
75. Yoss RE, Moyer NJ, Hollenhorst RW. Pupil size and spontaneous pupillary waves associated with alertness, drowsiness and sleep. Neurology 1970; 20: 545–54.
76. Lavie P. Ultradian rhythms in alertness—a pupillometric study. Biological Psychology 1979; 9:49–62.
77. Schmidt HS. Pupillometric assessment of disorders of arousal. Sleep 1982; 5:8157–64.
78. Horimoto N, Koyanagi T, Takashima T et al. Changes in pupillary diameter in relation to eye-movement and no-eye-movement periods in the human fetus at term. American Journal of Obstetrics and Gynecology 1992; 167:1465–69.
79. Robinson J, Fielder AR. Pupillary diameter and reaction to the light in preterm neonates. Archives of Disease in Childhood 1990; 65:35–38.
80. Robinson RJ. Assessment of gestational age by neurological examination. Archives of Disease in Childhood 1966; 41:437–47.
81. Lind N, Shinebourne E, Turner P et al. Adrenergic neuron and receptor activity in the iris of the neonate. Pediatrics 1971; 47:105–12.
82. Visser GHA, Goodman JDS, Levine DH et al. Micturition and the heart period cycle in the human fetus. British Journal of Obstetrics and Gynaecology 1981; 88:803–05.
83. Arduini D, Rizzo G, Giorlandino C et al. The fetal behavioural states: an ultrasonic study. Prenatal Diagnosis 1985; 5:269–76.
84. Junge HD. Behavioral states and state related heart rate and motor activity patterns in the newborn infant and the fetus antepartum—a comparative study. I. Technique, illustration of recordings and general results. Journal of Perinatal Medicine 1979; 7:85–107.

85. Campbell S, Wladimiroff JW, Dewhurst CJ. The antenatal measurement of fetal urine production. Journal of Obstetrics and Gynaecology of the British Commonwealth 1973; 80:680–86.
86. Rabinowitz R, Peters MT, Vyas S et al. Measurement of fetal urine production in normal pregnancy by realtime ultrasonography. American Journal of Obstetrics and Gynecology 1989; 161:1264–66.
87. Koyanagi T, Horimoto N, Satoh S et al. The temporal relationship between the onset of rapid eye movement period and the first micturition thereafter in the human fetus with advance in gestation. Early Human Development 1992; 30:11–19.
88. Wlodek ME, Thorburn GD, Harding R. Bladder contractions and micturition in fetal sheep: their relation to behavioral states. American Journal of Physiology 1989; 257:1526–32.
89. Sakai K. Anatomical physiological basis of paradoxical sleep. In: McGunity DJ, Drucker-Colin R, Morrison A (Eds). Brain Mechanisms of Sleep. Raven Press, New York, 1985; 111–37.
90. Satoh K, Shimizu N, Tohyama M et al. Localization of the micturition reflex center at dorsolateral pontine tegmentum of the rat. Neuroscience Letters 1978; 8: 27–33.
91. Sugaya K, Matsuyama K, Takakusaki K et al. Electrical and chemical stimulations of the pontine micturition center. Neuroscience Letters 1987; 80:197–201.
92. Cowan WM, Fawcett JW, O'Leary DDM et al. Regressive events in neurogenesis. Science 1984; 225: 1258–65.
93. Hobson JA, Steriade M Neuronal basis of behavioral state control. In: Bloom FE (Ed). Handbook of Physiology, vol II. American Physiological Society, Bethesda, 1981; 70:1 823.
94. Ellis WG, Goetzman BW, Lindenberg JA. Neuropathologic documentation of prenatal brain damage. American Journal of Diseases of Children 1988; 142: 858–66.
95. Adams RD, Prod'horn LS, Rabinowicz T. Intrauterine brain death. Acta Neuropathologica (Berlin) 1977; 40: 41–49.
96. Mann LI. Pregnancy events and brain damage. American Journal of Obstetrics and Gynecology 1986; 155:6–9.
97. Bejar R, Wozniak P, Allard M et al. Antenatal origin of neurologic damage in newborn infants. I. Preterm infants. American Journal of Obstetrics and Gynecology 1988; 159:357–63.
98. Naeye RL, Peters EC, Bartholomew M et al. Origins of cerebral palsy. American Journal of Diseases of Children 1989; 143:1154–61.
99. Nelson KB, Ellenberg H. Antecedents of cerebral palsy. Multivariate analysis of risk. New England Journal of Medicine 1986; 315:81–86.
100. Koyanagi T, Horimoto N, Maeda H et al. Abnormal behavioral patterns in the human fetus at term: correlation with lesion sites in the central nervous system after birth. Journal of Child Neurology 1993a; 8:19–26.
101. Horimoto N. Annual report on Maternity and Perinatal Care Unit, Kyushu University Hospital, 1992; 1:68–75 [in Japanese].
102. Maloney JE, Adamson TM, Brodecky V et al. Modification of respiratory center output in the unanesthesized fetal sheep "in utero". Journal of Applied Physiology 1975; 39:552–58.
103. Dawes GS, Walker DW, Johnston BM. The central control of fetal breathing and movements. The Fetus and Independent Life. Pitman, London, 1981; 295–307.
104. Levitt P, Cohn MA. Sleep apnea and the Chiari I malformation: case report. Neurosurgery 1988; 23: 508–10.
105. Gilmore RL, Palace P, Kanga J et al. Sleep-disordered breathing in Mobius syndrome. Journal of Child Neurology 1991; 6:73–77.
106. Govaert R Vanhaesebrouck FJ De Praeter C. Experience and reason-briefly recorded: Moebius sequence and prenatal brainstem ischemia. Pediatrics 1989; 84:570–73.
107. De Vries JIP, Visser GHA, Prechtl HFR. The emergence of fetal behavior. II. Quantitative aspects. Early Human Development 1985; 12:99–120.
108. Lewis P, Boylan P Fetal breathing: a review. American Journal of Obstetrics and Gynecology 1979; 134:587–98.

109. Trudinger BJ, Knight PC. Fetal age and pattern of human fetal breathing movements. American Journal of Obstetrics and Gynecology 1980; 137:724–28.
110. Rosen MG, Dickinson JC. The incidence of cerebral palsy. American Journal of Obstetrics and Gynecology 1992; 167:417–23.
111. Slater A, Morison V, Rose D. Habituation in the newborn. Infant Behav Devel 1984; 7:183–200.
112. Slater A, Morison V, Town C et al. Movement perception and identity constancy in the newborn baby. Br Devel Psychol 1985; 3:211–20.
113. Blass EM, Ganchrow JR, Sterner JE. Classical conditioning in newborn humans 2–48 hours of aee. Infant Behav Devel 1984:7:223–35.
114. Fifer WP, Moon C. Psychobiology of newborn auditory preferences. Seminars in Perinatology 1989: 13:430–33.
115. Anisfeld M. Neonatal imitation. Devel Rev 1991: 11:60–97.
116. Hepper PG, Leader LR. Fetal Habituation Fetal and Maternal Medicine Review 1996; 8:109–23.
117. Thompson RF, Spender WA. Habituation: a model for the study of neuronal substrates of behavior Psychology Review, 1966; 73:16–43.
118. Brackbill Y. The role of the cortex in orienting. Orienting reflex in an anencephalic human infant Dev Psychobiol 1971; 5:195–201.
119. Buchwald JS, Humphrey GL. An analysis of habituation in specific sensory systems. Prog Physiol Psychol 1973; 5:1–75.
120. Hepper PG. Fetal Memory Does it exist? What does it do? Acta Pediatr Suppl 1996; 416:16–20.
121. Leader LR, Bennett MF. Fetal habituation and its clinical applications. In: Levene MI, Lilford-RJ (Ed). Fetal and neonatal neurology and neurosurgery. Churchill Livingstone, London, 1994; 31–44.
122. Hepper PG, Shahidullah S. Habituation in normal and Down's syndrome fetuses. Q J Exp Psychol B 1992; 44:305–17.
123 Eisenberg R, Coursin DB, Rupp NR. Habituation to an acoustic pattern as an index of differences among human neonates. Journal of Auditory Research 1966; 6:239–48.
124. Hutt SJ, Hutt C. Hyperactivity in a group of epileptic and some non-epileptic brain damaged children. Epilepsia 1964; 5:334–51.
125. Dustman RE, Callner DA. Cortical evoked responses and response decrement in non retarded and Down's syndrome individuals. American Journal of Mental Deficiency 1979; 83:391–97.
126. Prechtl HFR Ultrasound studies of human fetal behavior. Early Human Development 1985; 12:91–98.
127. Leader LR, Baillie P, Martin B et al. Fetal responses to vibrotactile stimulation: a possible predictor of fetal and neonatal outcome. Australian and New Zealand Journal of Obstetrics and Gynaecology 1984; 24:251–56.
128. Leader LR, Baillie P, Martin B et al. The assessment and significance of habituation to a repeated stimulus by the human fetus. Early Human Development 1982a; 7:211–19.
129. Leader LR, Bailie P, Martin B et al. Fetal habituation in high risk pregnancies. British Journal of Obstetrics and Gynaecology 1982; 89:441–46.
130. Draper N, Smith H (Eds). Applied Regression Analysis (2nd ed). Wiley, New York, 1981; 294–379.
131. Rousseeuw PJ. Least median of squares regression. Journal of American Statistical Association 1984; 79: 871–80.
132. Dixon WHJ, Brown MB, Engleman L et al. BMDP statistical software. University of California Press, Berkeley 1985.
133. Sadovsky E, Ohel G, Havazeleth H et al. The definition and the significance of decreased fetal movements. Acta Obstetrica et Gynecologica Scandinavica 1983; 62:409–13.

134. Brown R, Patrick J. The nonstress test: how long is enough? American Journal of Obstetrics and Gynecology 1981; 141:646–51.

Chapter 40
Ultrasound-Guided Fetal Invasive Procedures: Current Status

Juan MTroyano Luque, Matilde T Clavijo Rodriguez

Since the early eighties a varied amount of experiences and trials of fetal puncture (fine needle aspiration) have been carried out with diagnostic aims.[1–5] At the beginning, the only possible way to enter the fetal evironment was with the support of a fetoscope but the spectacular development of the already well known ultrasonography has permited the invasion of the intrauterine environment with tools that are more and more harmless in the use, especially in the gradually tighter sections and the evolution of certain characteristics of the new needles that are now being incorporated into the new biopsy techniques.[3,6,7]

Fetal puncture with diagnostic aims is technically possible, provided it is done by adequately trained hands, but the essential problem lies in establishing the correct indications which are not yet quite defined.[8]

TECHNIQUE GENERALIZATION

Whatever the location of the fetal puncture may be, a certain number of requirements are imperative.

1. The operator must have sufficient working experience in invasive echography.
2. The room should have surgical consideration or rank, it is necessary to have an aseptic room for echographic intervention. A sterile wrap is recommended for the ultrasound probe. We use a surgical glove for an airtight seal.
3. The characteristics of the surgical equipment or the obtaining of the sample.

As the tendency is to obtain samples with the maximum diagnostic guarantee and a minimal risk to the integrity of the pregnancy, it is of capital importance, with few exceptions, to use sectio needles no smaller than 18 g.

It is clear that depending on the tissue sample we are aiming to obtain, it is not always possible to use innocuous tools. A clear example are the devices used to date for skin biopsies to diagnose some types of *Genodermatosis*, which consist on clipper forceps measuring 2.5 mm.

These methods in many cases require the use of an anesthetic, including in some, general anesthesia, previous to proceeding to the incision in the maternal abdomen, with a scalpel, and the introduction of a trocar sheath enquivalent in sectio to a Verre needle that serves as a guide vehicle for the mentioned system or method.

The complications derived from the use of 2.5 mm sectio needles and the transabdomen forceps method are closer to those of the fetoscope, added to the fact that the great flexibility in many cases of the method itself, having the availability of a great variety of needles of relatively small calibre (18 g standard), obtaining very good biopsies, including skin samples and visceral solid areas (Fig. 40.1).[2,7]

Within the organs that are intrauterinally reachable, with worthy guarantees, the one that follows in difficulties after the skin

Figure 40.1: Different types of needles and systems for fetal biopsy

sampling, is the kidney, fundamentally due to its histological parenchymal stratum constitution.[9]

We can only consider satisfactory the samples or cylinders that include corticomedullar stratum. The fetal availability in respect of its intrauterine position, the distance and the interposed tissue to the kidney (skin, muscle) as well as perirenal fat and the capsule, are the elements that obstruct the obtaining of valid samples.

The use in these cases of a catheter of 14–16 g calibre with isometric aspiration techniques with constant vacuum, allow to obtain valid samples, between 69–80%, while the use of 18–20 g calibre catheter obtains the very best specimens between 25–30%. This means that isometric (fine needle) puncture-aspiration techniques do not always offer the results hoped for on solid organs, fundamentally the kidney, unless wider catheters are used, that are far from the "harmless philosophy" that should prevail in these processes.

For these cases and others that are similar that could present themselves, depending on the tissue characteristics, the use of methods such as the *Aspiration Biopsy Set* that includes an 18 g bisided trocar syringe in all its circumference, acting as a circular blade, and a conical sheath with vacuum suction embolous contriving through its interior which allows to obtain cylinders of 2–5 mm in maximum length, with optimal safety conditions and histological quality, similar to those of the *TruCut* method.

Of all the viscus solid organs within reach, the one that offers the least problem is the liver, its spongy tissue constitution and its great size and volume in the fetal abdomen allows optimal accessability and consequently offers samples in practically 100% of all cases, using a conventional fine needle of 18–20 g.

The obtention of muscle tissue samples offers one of the main difficulties due to the topographic and anatomical characteristics of the skeleton, also the important motorous innervation. For this reason it is necessary to correctly select the spot and the muscular area least suspectible to provoke indelible functional lesions.

The most accessible topographic areas are the external face of either thigh, but it is technically more attainable the vastus externus muscle (Fig. 40.2); it is a zone covered by the subtrochanteric fascia-lata in an oblicular direction descending towards the fetal femur, The use of the *sure cut* systems 18 g with incorporated vacuum aspiration allows a success rate over 75%. Conventional spinal needles with complementary aspiration by

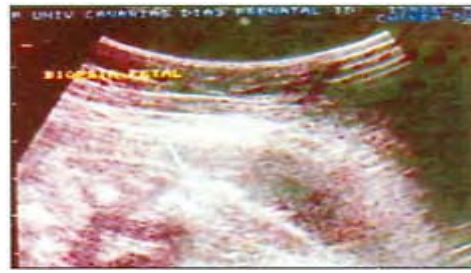

Figure 40.2: Subtrochanteric muscle biopsy: echographic monitoring. The arrow indicates the puncture position obliquely to the fetal femur

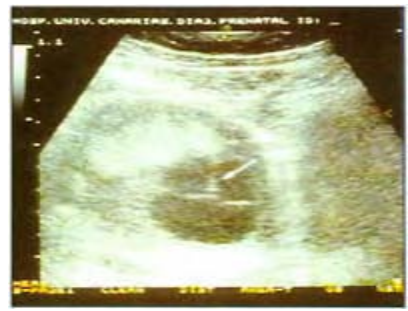

Figure 40.3: Cystic lynphangioma: percutaneous puncture determines qualitative and

genetic characteristics
(lymphocytes)

50 cc syringe vacuum allows to obtain sample with great difficulties.

When the puncture area has liquid characteristics, the echographic view is wide ranged, allowing a large field of action.

4. In general, technically it is precise to choose the most direct route, avoiding any interpositing obstacles, being also of interest to avoid the placenta if at all possible.

5. Once the crucial point to puncture has been determined, the needle should be introduced within the field of view of the probe, frame by frame until reaching the fetus.

6. It is recommended to approximate the puncture point without making direct contact with it in the first instance, until quite certain of the needles angle to the chosen spot, being of capital importance to enter with only one *sudden jab* to avoid sudden fetal jolts or movements.

7. It is advisable in all *free-hand* fetal punctures carried out, that the operator should take into account the dynamic variations of fetal positions.

8. For better manipulation, an assistant should be in charge of carrying out the isometric aspiration process at a prudential distance, approximately a metre away from the surgical table, interplacing a serum of the same length between the needle and the syringe.

9. Except in exceptional circumstances such as pericardic and pleural overflow that need an operating time of about 15–30 minutes, it is absolutely feasible to carry out without any anaesthetic procedures.

Aspiration in cystic disorders will fundamentally orientate the diagnosis. Aspiration on ovarian cysts is only indicated in complex cases derived from its dynamic volume or due to rare structural types with therapeutic aims more than to diagnostic ones.

We collect suspicious chylous collections, where the presence of high lymphocyte concentrations practically give a sure diagnosis also the fact that it allows a genetic study in very few days, justifies this type of procedures (Fig. 40.3).

The puncture of pericardic discharges has also the same diagnostic aims as well as being therapeutic.

Concerning brain punctures, the most representative, the *ventriculocentesis*, also allow us to accomplish serological marker studies, independant to any derived therapeutic attitude, although in this last case the efficiency of the derivative procedures in hydrocephalia is uncertain (Fig. 40.4).

Of all the structurally cystic processes, obtainable fetal urine in dilated urological pathology represents the greatest and highest interest for diagnosis value. The biochemical analysis of the fetal urine allows us to detect irreversible tubular lesions from those which have a normal renal function.

There is no doubt that the incorporation of biological molecular techniques and DNA studies allow to establish in many of the cases, the alterations of any determined genetic locus.[10–13]

Occasionally, we may find that we do not have enough material due to the lack of family records, in these cases the absence of this previous information constitutes a serious inconvenience in order to establish a prenatal diagnosis, as this is based only on a small corionic-villi, funicular or amniotic sample.[11,14]

This situation is where sampling directly from the fetal tissue is of special relevance for the diagnose of one or the other, or in order to rule out any pathological suspicion of family inheritance that are being submitted to any particular study.

"The taking of fetal samples by biopsy techniques is justified only in cases when the prenatal diagnosis of any specific pathological illness is not possible, or is frankly difficult, using any of the existing conventional techniques."

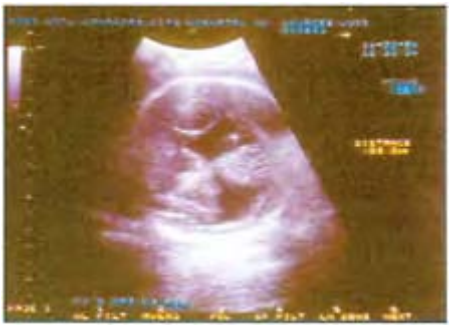

Figure 40.4: Ventriculocentesis: obtaining cephaloraquideus liquid determines the presence of viral bodies by polymerase chain reaction

LIVER BIOPSY

Technique

Fetal transabdominal aspiration-puncture using 18 g needles with conic catheter or spinal needles of the same sectio with isometric vacuum aspiration using a 50 cc syringe and serum system. Once introduced into the fetal liver, soft brief *inward outward* movements should be made in the same direction as the puncture.

Firstly the aspiration system should be extracted and last of all the needle, to avoid contaminating any other tissue. The spot to be punctured should be situated between the belly bottom and the border of the rib. This fate is helped by the physiological hepatomegalia, introducing the needle aproximately one centimetre under strict echographic monitoring. Preferably the external third of the right lobe, should be chosen, as it offers a minor principal vascularization, if not, the suprahepatic vessels should be avoided (Fig. 40.5).

If the diagnosis being sought for is histological, the cylinder should be conserved in formaldehyde if on the contrary it is enzymatic, it should then be airtight sealed in carbonic snow.

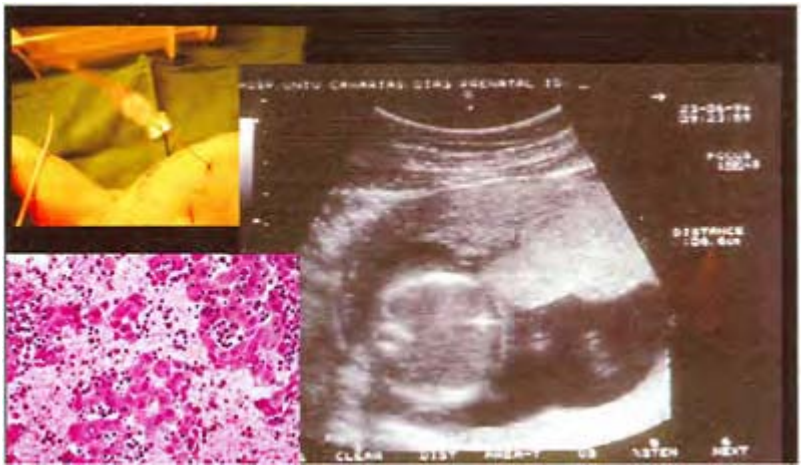

Figure 40.5: Liver biopsy: echographic monitoring and histological samples of fetal liver (19 weeks). Extramedullar hematopoietic foci can be detected

The gestational age recommended should be around 20 weeks, provided that the hepatic metabolism and main enzymatic processes are well, or practically established.

Indications

Prenatal diagnosis, fundamentally of enzymatic alterations and of lethal metabolic characteristics.[15,16]

Ornitil Transcarbamylase Deficiencies (OTC)

This mithocondrial enzyme of the urea cycle is synthesized in the liver or the intestines. Sex-linked disorders tied to the sex, are shown on the screening data of mothers who have urine excretion of orotic acid.

Primary Hyperoxaliuria (PH)

This is severe, charted renal insufficiency of rapid evolution, that is characterized by the presence of Calcic oxalate deposits in the renal tubule, microlithiasis and interstitial fibrosis. The hepatic level is accompanied by a total absence of alanine, inactivity of the catalitic gliosilate aminotransferase and immunoreactive proteins. This is incompatible with life.

For diagnosis it is fundamental to have the previous family clinical history available.

Carbamoyl Phosphate Synthetase Deficiency

This is an enzymatic defect of the urea cycle with recessive autosomic inheritance.

Other autosomic recessive disorders may be detected by means of hepatic biopsy, including:

- Non-ketotic hyperglycinemia.
- Prenatal diagnosis of infantile neuronal ceroidlipofuscinosis.
- Biliary atresia (type I cysts).
- Long-chain 3-hydroxyacyl-CoA dehydrogenase.[17–20]

Complications

The prenatal liver biopsy has few risks on a tissular level, due to its own visceral characteristics. Those risks are derived from the main vascular tears which will have great bleeding resulting in fetal death. In our experience (7 prenatal punctures), we have observed no complications (Table 40.1).

Table 40.1: Experience with seven prenatal punctures for liver biopsy

Reasons for biopsy	*Number of cases*
OTC diseases in the same family	4
Previous affected brother	1
Mitochondrial respiratory deficit	1
Non-ketosic hyperglycinemia	1
Results	
Prenatally confirmed diagnosis of OTC deficiency	2
Prenatally non-confirmed diagnosis with neonatal exitus by hyperammonemia	1
Prenatally confirmed as non-affected fetuses	4

FETAL PUNCTURE IN THE EVALUATION OF RENAL STATUS

The correction of a theoretic renal obstruction problem is possible, in spite of the difficulties and risks that it holds, even if in the majority of cases it is not necessary. We should start by stating that an ultrasound echography diagnosis of the obstructed renal pathology does not necessarily imply an irrevesible function alteration. In this sense the amniotic volume can be used as an indirect marker of the actual renal function, but this does have the inconvenience that it includes the possible measuring of the intrinsic clearance function.

When taking into account the possibility of practising an intrauterine derived therapy, this can only be justifiable in those fetus in whose kidneys there has been no irreversible damage. However, this makes it essential to establish a precise evaluation of the renal

function, in order to adequately select those fetuses that will benefit from prenatal therapy.

The most conflictive situation is the renal dysplasia. In the latter coexist tissular phenomena

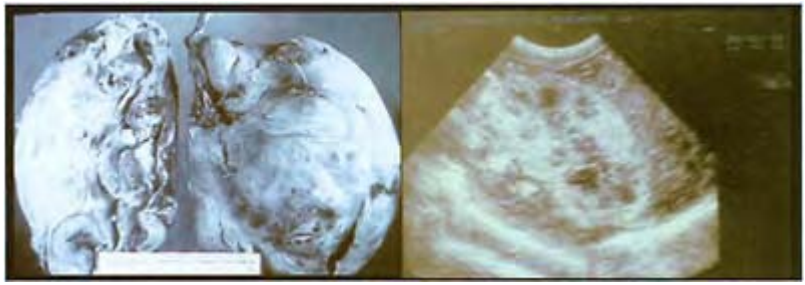

Figure 40.6: Fibro-cortical dysplasia associated with corticomedullar cyst and renomegalia.

that are characterized by fibrosis, dysplasia, cartilaginosis, frequently associated to corticomedullar cysts, although not always so (Fig. 40.6).

Aproximately 90% of all kidney dysplasias is associated to dilated or obstructive disorders. In these cases it can be remarked that any derived therapeutic action is unnecessary.

The high resolution echography has turned into the unquestionable kidney evaluation processes, however, it does have a few diagnostic limitations: (Table 40.2):

Table 40.2: Fetal nephropathy. Echographic prediction

Tissue marker	*Sensibility*	*Specificity*
Corticomedullar cysts	70%	100%
Hyperechogenicity	60%	90%
Hydronefrosis	75%	70%
Hydronefrosis + cysts	90%	100%

In our experience the obstruction of a kidney without objectible cysts or hyperechos does not, however, exclude dysplasia. This quite alarming fact occurs approximately in 25–30% of all cases.[8–21]

From this we can deduce that the echography on its own does not diagnose all renal dysplasias, and for this reason fetuses with pelvic dilation are subsidiary of derived drainage.

A biochemical study of fetal urine is capital data in the managing of these fetuses. The composition of the fetal urine stays constant, prac tically throghout the pregnancy and with hypotonic characteristics. This fact has automatically demonstrated an optimal and reliable renal function and on the contrary isotonic or hypertonic urine, a deficiency in renal function with an unfortunate prediction.

The biochemical markers that have close relation with a renal function are defined by the Na^+, Cl^- and osmotic urine.

Another determining factor in the normal renal clearance function derived from the near high reabsorbative tubular activity, is the establishing of specific proximal tubular lesion selective markers.

These markers correspond to lisosomial proteins exclusive of the proximate tubular structure and become expressed by NAG (N-acetil Dglucosaminidase). Low molecular weight proteins filtered by the glomerular system and reabsorbed practically in their totality by the proximal tube, if it is present in fetal urine and in the amniotic fluid in large quantities (higher than 8 U/l), it is indicative of tubular tissue destruction.

The detection of β-2 microglobuline would be considered in the same manner (Figs 40.7 and 40.8).

We found that the levels of biochemical markers are sensibly low in the physiological urine in comparison with the cases affected with irreversible renal disorder. The same outcome occurs with the tissular markers, NAG and β2 microglobuline (Table 40.3).

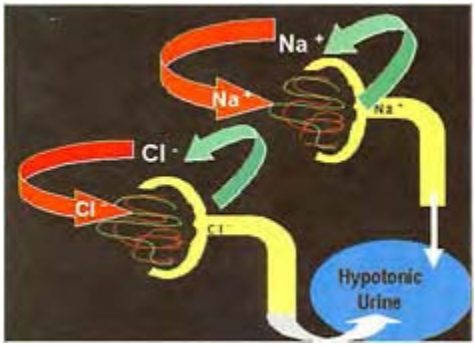

Figure 40.7: Biochemical markers that have close relation with a renal function are defined by the Na^+, Cl^- and osmotic urine derived from the near high reabsorbative tubular activity. Fetal urine stays constant, practically through the

pregnancy and with
hypotonic characteristics

Table 40.3: Fetal urinary aspiration: pathological biochemical markers

	Pathological urine values		
	Weeks		
	18–20	20–30	>32
Na^+ (mEq/ml)	120.0	126.44±11.50	139.60
Cl? (mEq/ml)	119.0	132.50±7.18	141.00
OsM (mOsm)	240	261.50±24.20	281.00
NAG (U/l)	18.0	25.83±0,85	25.73
$ß_2$/µG (ml/1)	26.0	38.97+1.30	38.72
K^+ (mEq/ml)	3.1	3.41±0.66	3.90
Creatinine (ml/1)	1.2	2.54±0.83	3.70

When we compare the relationship between the ionic concentrations and the osmolarity (Na^+ and Cl^-) of the fetal urine, and those of the amniotic liquid, we do not find significant differences between fetuses with conserving and fetuses with pathological functionalities. But comparing the levels of NAG and β2-microglobuline, a significantly greater concentrations of the two markers in the amniotic liquid of the affected fetuses have been observed (Tables 40.4 and 40.5).

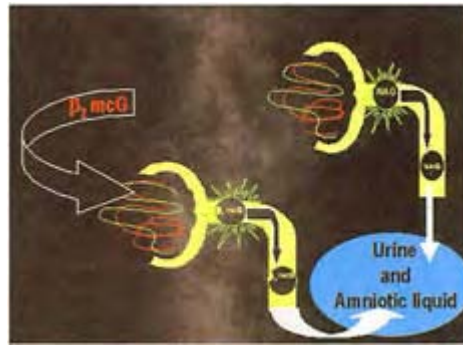

Figure 40.8: Another determining factors in the normal renal clearance function correspond to lysosomial proteins exclusive of the proximate

tubular structure (NAG), if it is present in fetal urine and in the amniotic fluid in large quantities, it is indicative of tubular tissue destruction. Beta-2-microglobuline would be considered in the same manner

Table 40.4: Physiological values: urine vs. amniotic:liquid

Urine/Amn. liquid	*Weeks*		
	18–20	*20–30*	*>32*
Na+ (mEq/ml)	42/137	42/140	47/140
Cl−(mEq/ml)	23/109	47/109	41/108
OsM (mOsm)	98/267	102/273	102/271
NAG (U/l)	2.0/3.6	2.7/3.62	2.0/4.69
ß$_2$µG (ml/1)	4.7/4.5	5.1/5.0	5.3/5.8
K^+ (mEq/ml)		41/140	
Creatinine (ml/1)		1.9/.6	

Table 40.5: Pathological values: urine *vs.* amniotic liquid

Urine/Amn. Liquid	*Weeks*		
	18–20	*20–30*	*>32*
Na^+ (mEq/ml)	120/132	126.4/140	139.6/140
Cl−(mEq/ml)	119/107	132.5/149	141/158
OsM (mOsm)	240/267	261.5/273	281/296
NAG (U/l)	18/16.9	25.83/20.34	25.73/20.8
ß$_2$µG (ml/1)	26/22.3	38.9/28.74	38.72/30.0
K^+ (mEq/ml)	3.1/138	3.4/140.6	3.9/148
Creatinine (ml/1)	1.2/0.7	2.54/0.82	3.7/0.9

The increase in concentration of NAG and β2 microglobuline increase possibly due to the cumulative effect of the amniotic clearance mechanism.

This opens the field of study of nephrouropathies through the determination of these and other parameters in the amniotic liquid, without the need for invasive study of the fetal urine.[21]

The K^+ and creatinine concentrations are different in their predictive evaluation as there exists a great clearance effect in the placenta and great variability in its ionic charge, that makes the potassium filtration very disperse, in the other hand 90% of the K^+ concentration are intracellular.[8,21]

Summarizing, we can adventure a prediction of renal viability in relation to those parametres expressed. In Table 40.6 taking into account that these values are applicable to any gestational age.

Table 40.6: Fetal urine: biochemical marker applicable to any gestational age and echographic image and amniotic liquid volumeto determine a renal function status.

Prediction	*Bad*	*Good*
Echographic image	Hyperechog. +Cyst	Normal echography
Amniotic liquid	Oligoamnios	Normal
	Fetal Urine	
Na^+	>100 mEq/ml	<100 mEq/ml
Cl^-	>90 mEq/ml	<90 mEq/ml
Osmolarity	>210	<210
NAG	>8 U/l	<8 U/l
β-2 microglob.	>4 mg/l	<4 mg/l
K^+	Indifferent	Indifferent
Creatinine	Indifferent	Indifferent

The intrauterine determination of the characteristics of fetal urine offers absolute diagnostic possibilities about the normal renal clearance function.

Urine aspiration puncture with diagnostic aims is technically feasible, using conventional spinal needles of 18 g having an aspiration system connected to a 20 cc syringe.

The way to aproach this depends on the fetal position available.

If at the posterior back position we would not find any great inconveniences in functioning the bladder whilst for a lateral or anterior back where a nephrostomic aspiration is chosen (Fig. 40.9).

In neither one nor the other, can any noticeable complications be found, at least in our experience.[8,21]

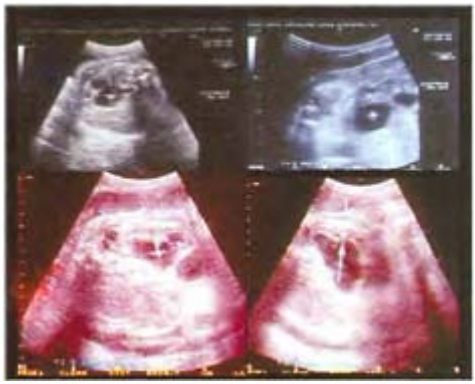

Figure 40.9: Aspirative nephrostomy: echographic monitoring

The nephrostomy aspiration allows us firstly to re-evaluate the echostructural characteristics of the expanded kidney parenchyma, and secondly, as long as we use the 16 g *sure cut* aspiration system, to carry out at the same time a renal biopsy without any technical difficulties.

For this, once the nephrostomy urine aspiration has been done, without taking the needle out move it towards the renal parenchyma and carry out the aspiration with a *swing* movement over the corticomedullar area.

The obtaining of samples of 2 mm in length is enough for the detection of the histological characteristics that define a kidney dysplasia.[8,9,21,23]

But the use of 16 g catheters Aspiration Biopsy *Set* (Fig. 40.3), once the technical problems of involving tissues have been solved, allows to obtain samples in the 65% of the cases. If conventional 18 g catheters are used but inocuous, only 30% of the cases are obtained *(J. Troycmo, Ian Donald, School Inter university of Medical Ultrasound, Dubrovnik August 1996, unpublished observations).*

SKIN BIOPSY

As already stated in the generalization section about fetal biopsies, the skin biopsy entails the most serious difficulties in the obtaining of adequate or sufficient samples that would allow correct histopathological diagnosis or prediction.

The most important aspect is the obtention of valid samples, for this we need at least 1 mm strips of skin and no smaller in surface area and that also include a thickness of the epithelial stratum, and comprising of conjunctive areas and basal membrane. Only by this can an acceptable reading be obtained.[24]

The second aspect to be taken into account is the surgical biopsy material. We have already exposed previously that the use of section 2.5 mm clipping tongs (forceps/clippers) introduced into the amniotic evironment by trocar, will allow the obtention of skin samples in 100% of all cases, and it is true that the residual skin lesions

and any pregnancy complications there may be, will not render any noticeable benefits in relation to the diagnostic data.

The use of conventional needles and isometric aspiration practising the *slice* technique, that consists in inserting the needle sidelongly over the skin and make scratch ing or scraping movements, as this will allow us to obtain skin strips of optimum quality with minimum damage to the integrity of the pregnancy (Fig. 40.10).[25–28]

The third aspect to consider is the place selected to proceed for the taking of the sample, as depending on the disorder that we aim to diagnose prenatally, the biopsy area would be different. Not always the same area of the fetal skin wrap will be valid, or will suit the purpose of the biopsy.

Technique

Skin samples should, if possible, be taken from different areas of the fetus.

The pregnancy stage recommended for this is around 20 weeks, as after this time, the pilose follicles and keratinization mechanisms begin to develop. The study of the elements involved in the keratinization (keratohyalin and tonofibers), initially give suspicions of the disorder.

On the other hand, at this stage in the pregnancy the dermoepidermical junction has definitively been established, and the gradual rise of intercellular desmosomes, is a great help for the diagnosis of different forms of epidermolysis.

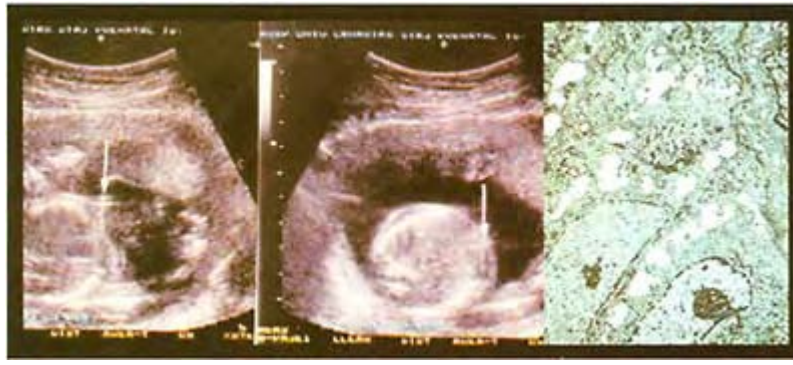

Figure 40.10: Left: skin biopsy in fetal abdomen, sidelong scratching. Right: mature histological cutaneous samples where keratohyalin and hemidesmosomes are detected

The sequence should follow the following steps:
- Echographic monitoring.
- If it is possible, the placenta must be avoided
- Take into consideration the fetal position as on some occasions it will be necessary to obtain samples from different skin areas.
- Rigorous sterilization.
- Optional local anesthesia, depending on the surgical timing.
- Oblique needle incidence in the thickness and surface of the skin, making a scraping or scratching movement without pulling back.
- Try to obtain at least 1 mm strips. The use of the vacuum needles allow the collection of various fragments from the interior without the need of withdrawing the needle.
- Immediately proceed to swim the samples in saline serum for their histological staining and fixing process or for electronic microscopy analysis.

Indications

They are most frequently based on the diagnosis of some type of genodermatosis or congenital dermoepidermic disorders, of dominating autosomic transmission as well as recessive types, the majority being lethal in short or medium terms. These disorders can be classified as follows:
- Bullous epidermolysis: Fetuses with large scale blistered areas that once the blisters break, set off intensive erosive zones with a fast loss of electrolytes are affected.6,10,29,30
- Anhidrotic ectodermic dysplasias: Recessive disorder linked to the sex. The fetuses are born without pilose follicles, without any hair or sudoriparous glands. They develop hyperthermic affectation by disregulation and general dryness syndromes.31
- Keratinization disorders: Also called Colodion baby syndrome, characterized by the appearance of reptile skin due to epidermic membranes that are of quick shedding. Severe and lethal dehydrating disorders.32,33
- Pigmentary atopies: Ocular syndromes with severe intolerance to light and early or premature development of skin cancers.31,34,35

The diagnostic problems faced with these dermatosis are due to the development of the lesion has different topographic origins, so the need to select the puncture spot has to be in accordance to the illness that one is trying to detect.

The diagnostic possibilities of skin biopsies are summarized as shown in Table 40.7.

Table 40.7. Diagnoses possible from fetal skin biopsies

Keratinization disorders:
Harlequin fetus.
Colodion baby.
Sjögren-Larsson syndrome.
Congenital ichthyosis.

The puncture spot is in trunks and buttocks (Fig. 40.11)

Ampollous diseases:

Herlitz ampollous junctional disease.

Hallopeau-Siemens ampollous dermolytic disease.

Inverse dystrophic ampollous disease.

Cockayne-Touraine dystrophic ampollous disease.

The puncture spot is in waist, skin folds, abdomen and buttocks (Fig. 40.12)

Pigmentary disorders:

Negative tirosinase oculocutaneous albinism.

Chediak-Higashi disease.

Anhidrotic ectodermic disease.

The puncture spot in the skin-head (scalp) (Fig. 40.13)

It is fundamental to have objective family history in order to determine the biopsy spot.[34,36,37]

Figure 40.11:
Keratinization disorder

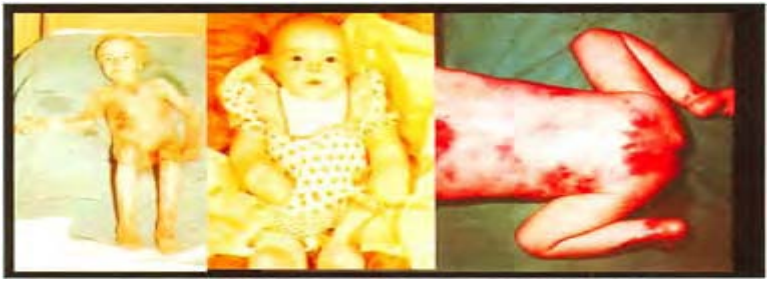

Figure 40.12: Ampollous disease

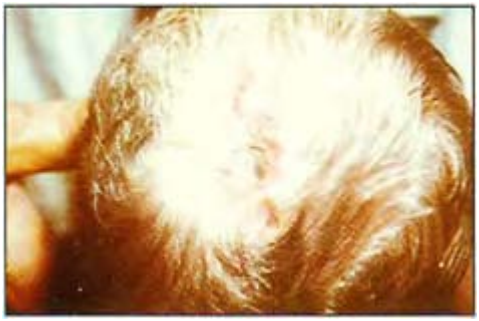

Figure 40.13: Pigmentary disorder (scalp lesions)

Complementary Requirements

The study of the samples will be based on the ultrastructural features stated beforehand. A great deal of experience in fetal dermatology using electronic microscopy is required to make the diagnosis.

It is fundamental to have objective family history knowledge in order to determine the prenatal dermoepidermic structural markers.

It is recommended to have kept previous samples in order to be used as a *study bank*.

Complications

Now the tendency is to propose minimally invasive techniques by the use of conventional needles 7 g.[38]

The use of conventional needles does not withhold more risks than the amniocentesis. On the other hand, the trocar techniques and the 2.5 mm sectio biopsy provoke around 5% of miscarriages due to iatrogenic amniorrhexis, although similarly some indelible fetal skin lesions have been described (Fig. 40.14). This does not occur in cases where the *scalp* technique is carried out with the use of conventional needles.

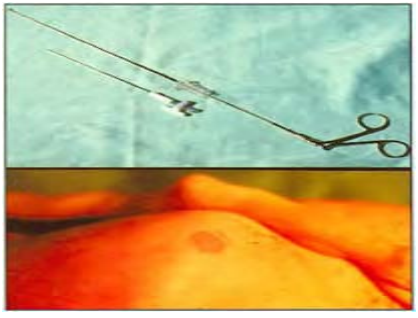

Figure 40.14: Residual cutaneous lesion after

biopsy with clipper system

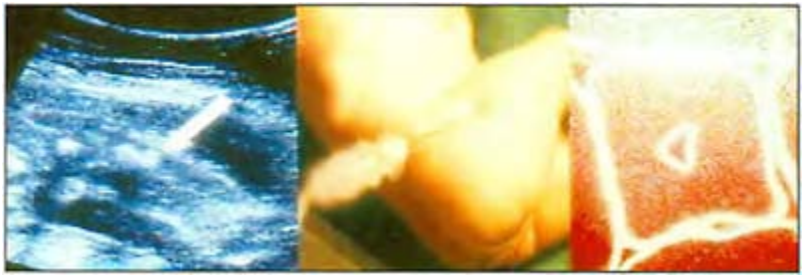

Figure 40.15:
Subtrochanteric muscle biopsy; the detection of dystrophin by immunofluorescence determines healthy muscle

MUSCLE BIOPSY

This is carried out preferably for the prenatal diagnosis of Duchenne's muscular dystrophy (DMD), although it is also possible to detect other hereditary myopathies as long as there is some clinical family history of these disorders.[11,38,39]

For the diagnosis of Duchenne's muscular dystrophy, it is usual for the DNA analysis to be used. When the recombinations within the DMD gene or the DNA analysis are not sufficiently informative, or if from the family history it is not clear if there are possible carriers, so the direct examination of the muscle and its analysis is the only way to give the basis of an objective prenatal diagnosis.

The marker used is the dystrophine, its determination by means of immunofluorescence allows to differentiate the features of affected muscles from those of the healthy ones. The absence of this protein from the skeleton muscles is practically pathognomonic of DMD (Fig. 40.15).[11,14,39,40]

Some other times the prenatal diagnosis of DMD may be impossible when there is only one previously affected male in the family, and there is no identificable detection.

The absence of dystrophine in a skeleton muscle, is worth in itself the determination of the screening of the DMD. Nevertheless this diagnosis can be reinforced by detecting a rise in phosphocreatinekinase of more than 10 times its normal value in fetal blood.

Within the possibilities that can reinforce a prenatal DMD diagnosis or prediction we have:

- Sex linked
- High values of phosphocreatinekinase
- Absence of dystrophine
- Degenerated muscle

• Fat infiltration
• Connective infiltration
• Nuclear and cellular morphological alterations (Fig. 40.16).

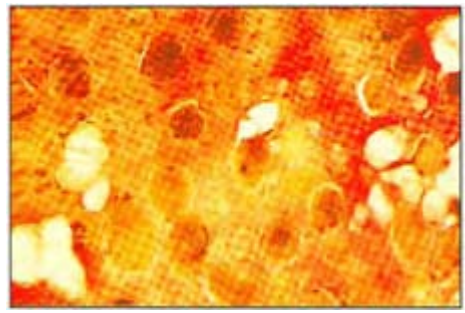

Figure 40.16: Duchenne's muscular dystrophy; degenerated muscle as an associated sign: fat and connective infiltration, and morphological cellular alterations and leucocytes infiltration

Technique

Any muscular skeleton area is good, preferably of the external face of any of the thighs or nuchal areas, avoiding topographic places with innervation or vital vascularization, in this manner functional lesions will not be provoked. Preferably using 18 g conventional needles or even better, the *sure cut* method that have already been described.[8,38,41–43]

Carrying out subtrochanteric punctures in a descending obliquest manner as possible, orientated towards the fetal femur (Fig. 40.2).

The puncture success rate is of 75%.

It is essential to determine muscle dystrophy by immunofluorescence, being advisable but not determining the detection of phosphocreatinekinase and the study of the muscular structure at a morphological muscular level, fat and connective infiltration.

No complications are described.

The fetus is susceptible to study by invasive techniques. These techniques are only justified by the seriousness of a possible inherited illness, or by any other disorder detected during pregnancy; in the latter the need for biopsy diagnosis is exceptional, as the thoracocentesis, pericardiocentesis and punctures of other thoracoabdominal, primary seek a therapeutic attitude, using the extracted material for studying its analytical components.

Other punctures on fetal tumor formations (sacrococcygeal teratomas, solid cervical teratomas, etc.), or liquid collections, such as pericardiocentesis, do not have an acceptable justification from a therapeutic or diagnostic point of view, as the echographic evaluation and the present application of biophysical methods (color Doppler amongst them) give an acceptable identification of their vascularization and origin, including those of suspicious neoplasm.[44,45] (A Kurjak, In: Ian Donald, University School of Medical Ultrasound 16th Course,—Granada, Spain, June 14th-16th 1993, Unpublished).

In agreement with our conduct, we would like to express this thought: *The fetus has been endowed by nature to surpass several inconveniences provided by its forty weeks of developing.*

It is a "Real Titan" front any adversity and, its adaptability is exceptional.

Don't we disturb it!

Don't we invade its privacy agressively!

Let's observe it minutely and, only when it need us, which generally happens in few occasions, it will advise us, then, let's help it.

J.M.Troyano-Luque (1993)

REFERENCES

1. Bahado-Singh RO, Morotti R, Pirhoren J, Lopez JA, Mahoney MJ. Invasive techniques for prenatal diagnosis: current concepts. J Assoc Acad Minor-Phys 1995; 6:28–33.
2. Cadrin C, Golbus MS. Fetal tissue sampling indications, techniques, complications and experience with sampling of fetal skin, liver and muscle. West J Med 1993; 159:269–72.
3. Golbus MS, Sagebield RW, Filly RA et al. Prenatal diagnosis of congenital icthyosiform erythroderma (epidermolytic hyperkeratosis) by fetal skin biopsy. N Engl J Med 1980; 302:93.
4. Kouseff BG, Matsouca LY, Stenn RS et al. Prenatal diagnosis of Sjogren-Larsson syndrome. J Pediatr 1982; 101:998.
5. Robjn AJ, David B, Gardner A, Rodeck CH. Prenatal diagnosis of oculocutaneous albinism by electron microscopy of fetal skin. J Invest Dermatol 1983; 80:210–12.
6. Dolan CR, Smith LT, Syber UP Prenatal detection of epidermolysis bullosa fetalis with pyloric atresia in a fetus by abnormal ultrasound and elevated alphafetoprotein. Am J Genet 1993; 47:395–400.
7. Rodeck CH. Fetoscopy guided by real time ultrasound for pure fetal samples, fetal skin samples and examination of the fetus in utero. Br J Obstet Gynaecol 1980; 87:449–56.
8. Troyano JM, Padron E, Clavijo M. Fetal biopsy and puncture. Actual status. Balkan Ohrid's School of Ultrasound. Advanced Ultrasound II, Vol. 9. Ohrid, Macedonia: Dobri S.Filipche, 1996:51–61.
9. Campbell WA, Yamase HT, Salafia CA, Vintilizeos AM, Rodis JF. Fetal renal biopsy: technique development. Fetal Diagn Ther 1993;8:135–43.
10. Dunnill MG, Rodeck CH, Richards AJ et al. Use of type VII collagen gene (COL7A1) markers in prenatal diagnosis of recessive dystrophic epidermolysis bullosa. J Med Genet 1995; 32:749–50.
11. Evans MI, Farrell SA, Greb A, Ray P, Johnson MP, Hoffman EP In utero fetal muscle biopsy for the diagnosis of Duchenne muscular dystrophy in a female fetus' suddenly at risk'. Am J Med Genet 1993; 46:309–12.
12. Fox J, Hack AM, Fenton WA et al. Prenatal diagnosis of ornithine transcarbamylase deficiency with the use of DNA polymorphisms. N Engl J Med 1986; 315:1205.

13. Matilla I, Corral J, Miranda M et al. Prenatal diagnosis of Werdnig-Woffmann disease: DNA analysis of a mummified umbilical cord using closely linked microsatellite markers. Prenat Diagn 1994; 14:219–22.
14. Kuller JA, Hoffman EP, Fries MH, Golbus MS. Prenatal diagnosis of Duchenne muscular dystrophy by fetal muscle biopsy. Hum Genet 1992; 90:34–40.
15. Ilium N, Lavard L, Danpure ZJ, AerenlundJensen H, Skovby F Primary hyperoxaluria type 1: clinical manifestation in infancy and prenatal diagnosis. Child Nephrol Urol 1992; 12:225–27.
16. Rodeck CH, Patrick AD, Pembrey ME, Tzannatos C, Whitfield AE. Fetal liver biopsy for prenatal diagnosis of ornithine carbamyl transferase deficiency. Lancet 1982; 1:297–99.
17. Goebel HH, Vesa J, Reiter B et al. Prenatal diagnosis of infantile neuronal ceroidlipofuscinosis: a combined electron microscopic and molecular genetic approach. Brain Dey 1995; 17:83–88.
18. Murotsuki J, Vehara S, Okamura K, Yajima A, Oura I, Miyabayashi S.Fetal liver biopsy for prenatal diagnosis of carbamoyl phosphate synthetase deficiency. Am J Perinatol 1994; 11:160–62.
19. Tsushida Y, Kawarasaki H, Iwanaka T, Uchida H, Nakanishi H, Uno K. Antenatal diagnosis of biliary atresia (type 1 cyst) at 19 weeks gestation: differential diagnosis and etiologic implications. J Pediatr Surg 1995; 30:607–09.
20. Von Dobeln V, Venizelos N, Westgren M, Hagenfeldt L.Long chain 3-hydroxylacyl-CoA dehydrogenase in chorionic villi, fetal liver, and fibroblasts and prenatal diagnosis of 3-hydroxylacyl-CoA dehydrogenase. J Inherit Metab Dis 1994;17:185–88.
21. Troyano JM, de la Fuente P (Eds). Prenatal features of fetal kidney physiopathology and their intra and extrauterine treatment. A multidisciplinary problem. Santa Cruz de Tenerife: University Hospital of the Canary Islands, 1993;35–39.
22. Greco P, Loverro G, Carusso G, Clement R, Selvaggi L. Diagnostic potential of fetal renal biopsy. Prenat Diagn 1994;14:415.
23. Gubler MC, Levy M. Prenatal diagnosis of NailPatella syndrome by intrauterine kidney biopsy. Am J Med Genet 1993;47:122–24.
24. Elias S, Emerson DS, Simpson JL, Shulrnan LP, Holbrook KA. Ultrasound-guided fetal skin sampling for prenatal diagnosis of genodermatoses. Obstet Gynecol 1994;83:337–41.
25. Bakharev VA, Aivazyan AA, Karetnikova NA, Mordovtsev VN, Yantousky Y. Fetal skin biopsy in prenatal diagnosis of some Genodermatoses. Prenat Diagn 1990;10:1–12.
26. Buckshee Li, Parveen S, Mittal S, Verma K, Singh M.Percutaneous ultrasound-guided fetal skin biopsy: a new approach. Int J Gynaecol Obstet 1991;34:267–70.
27. Holbrook KA, Wapner R, Jackson L, Zaeri N. Diagnosis and prenatal diagnosis of epidermolysis bullosa herpetiformis (Dowling-Meara). In a mother, two affected children and an affected fetus. Prenat Diagn 1992; 12:725–39.
28. Suzumori K, Kanzak I.Prenatal diagnosis of Harlequirn Ichthyosis by fetal skin biopsy; report of two cases. Prenat Diagn 1991; 11:451–57.
29. McGrath JA, McMillan JR, Dunnill MG et al. Genetic bases of lethaljunctional epidermolysis bullosa in an affected fetus: implications for prenatal diagnosis in one family. Prenat Diagn 1995; 15:647–54.
30. Shirnizu H, Onodera Y, Ikeda S, Ogawa H, Suzumori K, Nishikawa T.Prenatal diagnosis of epidermolysis bullosa: first successful trial in Asia. Dermatology 1994; 188:46–49.
31. Shimizu H, Ishko A, Kikushi A, Akiyarna M, Susumori K, Nishikawa I.Prenatal diagnosis of tyrosinase negative oculocutaneous albinism by an electron microscopic dopa-reaction test of fetal skin. Prenat Diagn 1994; 14:442–50.
32. Akiyama M, Kim DK, Main DM, Otto CE, Holbrook KA. Characteristic morphologic abnormality of harlequin ichthyosis detected in amniotic fluid cells. J Invest Dermatol 1994; 102:210–13.
33. Rizzo WB. Sjogren-Larsson syndrome. Semin Dermatol 1993; 12:210–18.
34. Akeo K, Shirai S, Okisaka S et al. Histology of fetal ages with oculocutaneous albinism. Arch Ophthalmol 1996; 114:613–16.

35. Shimizu H, Niizeki H, Suzumori K et al. Prenatal diagnosis of oculocutaneous albinism by analysis of the fetal tyrosinase gene. J Invest Dermatol 1994; 103:104–06.
36. Holbrook KA, Smith LI, Elias S. Prenatal diagnosis of genetic skin disease using fetal skin biopsy samples. Arch Dermatol 1993; 129:1437–54.
37. Normand J, Karasek MA. A method for the isolation and serial propagation of keratinocytes, endothelial cells and fibroblasts from a single punch biopsy of human skin. In Vitro Cell Dey Biol Anim 1995; 31:447–55.
38. Evans MI, Krivchenia EL, Johnson MP et al. In utero fetal muscle biopsy alters diagnosis and carrier risks in Duchenne and Becker's muscular dystrophy. Fetal Diagn Ther 1995; 10:71–75.
39. Fanin M, Pegoraro E, Angelini C. Absence of dystrophin and spectrin in regenerating muscle fibers from Becker dystrophy patients. J Neurol Sci 1994; 123:88–94.
40. Lindahl M, Backman E, Henriksson KG, Gorospe JR, Hoffman EP Phospholipase A2 activity in dystrophinopathies. Neuromusc Disord 1995; 5:193–99.
41. Benzie RJ, Ray P, Thompson D, Hunter AG, Ivey B, Salvador L. Prenatal exclusion of Duchenne muscular dystrophy and fetal muscle biopsy. Prenat Diagn 1994; 14:235–38.
42. Evans MI, Hoffman ER Cadrin C, Johnson MP, Quintero RA, Golbus MS. Fetal muscle biopsy: collaborative experience with varied indications. Obstet Gynecol 1994; 84:913–17.
43. Evans MI, Quintero RA, King M, Kureshi F, Hoffman ER Johnson MP Endoscopically assisted, ultrasound-guided fetal muscle biopsy. Fetal Diagn Ther 1995; 10:167–72.
44. Troyano JM, Clavijo MT, Clemente I, Marco OY, Rayward J, Mahtani VG. Kidney and urinary tract diseases: Ultrasound and biochemical markers. The Ultrasound Review of Obstetrics and Gynecology. 2002;2(2):92–109.
45. Bebatar A, Vaughan J, Nicolini U, Trotter S, Corrin B, Lincoln C. Prenatal pericardiocentesis: Its role in the management of intrapericardial teratoma. Obstet Gynecol 1992; 79(5);(Pt2):859.

Chapter 41
Chorionic Villus Sampling

CihatSen

Chorionic villus sampling (CVS) has been used to perform first-trimester prenatal diagnosis. The technique of sampling procedure is well documented. In experienced centers, chorionic villus sampling is safe and can be utilized as a primary prenatal diagnostic tool. Due to, more likely, the more technically demanding aspects of sampling, chorionic villus sampling has still not replaced amniocentesis in many centers.

Chorionic villus sampling as a prenatal diagnostic test was first reported from China in 1975. This procedure was performed by inserting the catheter blindly into cervical canal and aspirating villi.[1] Later on, the techniques evolved into transcervically ultrasound-guided procedure. Following to the transcervical approach, transabdominal ultrasound-guided technique has been introduced and has been widely being used because of the higher risk for infections and bleeding complications in transcervical sampling.[2] Since last ten years, early chorionic villus sampling is not being used due to increased risk for limb reduction such as not earlier than 11 weeks of gestational age.[3,4] In some conditions such as posterior low lying placenta and retroflexed uterus, transcervical approach can be preferred, but after 11 weeks of gestation chorionic tissue is reachable by transabdominal approach in experienced hand. On the other hand, delaying until this gestational age will avoid the high spontaneous miscarriage rate in earlier pregnancy.

Prior to performing the procedure, a detailed scanning is performed to assess fetal anatomy, viability, and gestational age and to identify the location of the chorion. The presence of twins as well as other pregnancy-related pathology such as a subchorionic hematoma or co-existing anembryonic pregnancy should be identified since they could potentially affect the interpretation. Preferably the procedure should be performed after the 11th-12th weeks of gestation because some major fetal defects can be identified after this period. At the time of this examination, a detailed genetic counselling is given and the procedure explained to the parents and discussed with them. After counselling, a written consent has to be taken.

TECHNICAL ASPECTS OF THE PROCEDURE

For transcervical CVS, the patient is put in lithotomic position. After exposing the cervix, the vagina and the cervix are prepared with an iodine solution. Tenaculum is not usually necessary. A polyethylene catheter (app. 16-gauge) with an obturator (malleable stainless steel) is directed to the trophoblastic area under ultrasound guidance. Operator should pay more attention to avoid the tip of the catheter close to the fetal membranes

because of the possibility to rupture of the membrane and the decidua, which can cause bleeding and making the procedure difficult. During this insertion procedure, the patient can feel a cramp-like pain, but anesthesia is usually not necessary. After removing the obturator, a 20-ml syringe is attached to the catheter, negative pressure applied and then the catheter is withdrawn slowly. The sample taken is transferred into transport media and performed separation process, which is very important step.

Transabdominal CVS is performed like amniocentesis. After a detailed scanning and locating the chorion, the insertion site on the skin and the course of the needle to enter into amniotic cavity is defined and planned. The skin surface is treated with antiseptic solution and a local anesthetic injected. Trajectory of the needle should be chosen as much as parallel to the long axis of the trophoblast. The needle (20-gauge needle) is inserted into the chorionic villi (single needle technique). In some centers, it is used double needle technique. With this technique, 18-gauge needle is inserted into chorionic villi and the stylet removed, then a smaller needle (20 gauge) with the aspirating syringe through this needle to obtain a sample, moderate suction is applied. Therefore if the sample is not adequate, sampling procedure with this smaller needle through 18-gauge needle can be repeated as necessary. Most centers use the single needle technique. With single needle technique, a sampling path is chosen so that the tip of the needle should pass within the chorion frondosum parallel to the chorionic membrane. The tip of needle is inserted into the myometrium and then advanced into the frondosum. The needle is then redirected so that the tip will course parallel to the membrane through as much as villus tissue as possible. Insertion of the needle into the decidua or myometrium, rather than the frondosum, will result in a “gripping” feeling and in this case adjustment of the tip back into the frondosum should be made. After placement the tip of the needle in the chorionic villi, the stylet is removed and a 20-ml containing 2–3 ml of media is attached and negative pressure applied. The needle is moved up and down four or five times in the frondosum parallel to the chorionic plate, then removed. Some operators use a biopsy guide with a computer-generated needle path. It is quite helpful in determining the anticipated biopsy path and in assuring correct initial needle placement. However, once the needle is within the frondosum, the guide apparatus becomes cumbersome and restricts the motion required to retrieve an adequate sample. Therefore we do choose to use one operator-single needle technique, which is so easy and flexible technique in experienced hand.

Both transabdominal single and double-needle techniques appear to be equally safe. The double-needle technique is theoretically less traumatic since the outer trocar remains still during sampling. It also has the advantage of allowing the operator to obtain additional villi by reinserting the sampling needle without requiring a second puncture and needling. During the learning period of operator, double-needle technique is most appropriate approach to make the sampling procedure easy and less traumatic. On the other hand, the single-needle approach is quicker, less uncomfortable, and able to retrieve adequate tissue with minimal insertions.

After aspiration, the chorionic villi retrieved can be easily identified in the syringe by holding it up to a light or by putting the media in a Petri dish. Operator should confirm the presence of adequate villus tissue by visual inspection. If insufficient villi are obtained on the first attempt, a second pass should be made. Pregnancy loss rates increase significantly when more than two insertions are required, and may be as high as 10% if

three attempts are made.[5] Prior to performing the procedure, the patient should be evaluated carefully, the correct placental location should be confirmed, interfering contractions identified. Experience is important in determining which approach is preferred for an individual patient. An anteverted or mid-position uterus with a posterior or anterior placenta is most easily sampled, also retroverted uterus with anterior placenta easily sampled. However, sampling of a retroverted uterus with posterior placenta is difficult. If the placenta is located on postero-lateral position, CVS can be performed easily by redirection of the tip of the needle in the myometrium by the double-needle technique in experienced hand. In these difficult cases, the double-needle technique is so helpful and makes the procedure safe and quicker. In some retroverted and very rare case, the procedure could not be possible and in this case the CVS procedure is postponed to one week later to allow the uterus move up and the chorionic tissue grow and then the procedure would be possible.

Performing an atraumatic procedure can minimize the incidence of fetal loss. Operator should attempt to avoid areas of venous lakes or slow venous flow. Direct perforation of these will frequently lead to significant post-procedure hemorrhage and hematoma formation.

Decreasing the number of needling improves pregnancy outcome. If there is a local contraction that makes the correct direction and the movement of the needle difficult, it should be waited. Passing needle parallel to the chorionic plate increases sample size by maximizing the amount of frondosum sampled. Insertion perpendicular to the membrane may only result in membrane injury and also will frequently limit the amount of tissue. Accurate demarcation of the placental boundaries is mandatory. Inserting the sampling instrument too lateral to the bulk of the villus tissue will lead to sampling failure. Scanning in a transverse plane in addition to the routine sagittal plane is quite helpful in avoiding this problem. Inadvertent injury of the membranes can be avoided by continuous monitoring of the needle tip. It should be cautioned that the tip of the needle must be imaged rather than a portion of the shaft. The operator carefully observing the scan as the catheter is advanced can make this differentiation. If the ultrasound image of the tip moves when the catheter is advanced this assures a correct view. After sampling, the separation process is immediately carried out. This separation process is very important. Because the chorionic villi should be carefully separated from decidual or any other maternal cells and tissue if available. Villi are free-floating, white tissue with filiforme branches. Contaminating decidual tissue is more amorphous in shape, lacks branches and is usually easily differentiated from villi on gross inspection. Chorionic villus samples consist of a mixture of placental villi and maternal decidual cells and blood. Although washed and dissected some maternal cells may remain and grow in culture but not in direct preparation, a careful dissection and use of enzymatic digestion prior to culture are reduced it. Then the sample is transferred to the transfer media.

COMPLICATIONS, PREGNANCY LOSS, SAFETY

Post-procedure complications following CVS are rare. Vaginal bleeding is the most common complication, occurring in 7–10% of transcervical cases but less frequently following transabdominal CVS.[6] In up to 4% of cases, a small hematoma may be identified at the sampling site immediately following procedure.[7] Other complications

such as infection, oligohydramnios occur only rarely. Infection following CVS occurs very rarely unless a hematoma forms or significant tissue trauma occurs.

The procedure-related risk of pregnancy loss following chorionic villus sampling appears to be the same as midtrimester amniocentesis when performed in experienced centers. The Canadian collaborative experience (a prospective, randomized study comparing CVS to second trimester amniocentesis), published in 1989, showed no significant increase in fetal loss following CVS when compared to midtrimester amniocentesis.[8] There were 7.6% fetal losses (spontaneous abortions, induced abortions and late losses) in the CVS group and 7.0% in the amniocentesis group. Thus an excess loss rate of 0.6% for CVS over amniocentesis was obtained; this difference was not statistically significant.

Shortly thereafter, American collaborative study showed no significant difference in loss between CVS and amniocentesis.[9] This was a prospective, non-randomized trial of over 2200 women who chose either transcervical CVS or second trimester amniocentesis. Patients in both groups were requited in the first trimester of pregnancy. An excess pregnancy loss rate of 0.8% referable to CVS over amniocentesis was seen, which again was neither clinically nor statistically significant.

In contrast, a collaborative European Trial (a prospective, randomized comparison of over 3200 pregnancies sponsored by the European MRC Working Party on the Evaluation of CVS reported a 4.6% increased loss rate following CVS as compared to midtrimester amniocentesis.[10] This difference reflected more spontaneous deaths before 28 weeks' gestation (2.9%), more terminations of pregnancy for chromosomal anomalies (1.0%), and more neonatal deaths (0.3%) in the CVS group. After examining of the studies, it appears that MRC study was performed at a greater number of centers and with more practitioners than the other studies. In addition, each practitioner performed fewer procedures. Thus, it has been suggested that the relative lack of experience might have contributed to the increased loss rate in the MRC study. While the American trial consisted of seven centers and the Canadian trial 11 centers, the European trial included 31 sampling sites. There were, on average, 325 cases per center in the United States study, 106 in the Canadian study, and only 52 in the European trial. While no significant change in pregnancy loss rate was demonstrated during the course of the European trial, the learning curve for both transcervical and transabdominal CVS exceeds 400 or more cases.[11] Operators who have performed fewer than 100 cases may have two or three times pregnancy loss rate of operators who have performed more than 1000 procedures. Chorionic villus sampling was compared to early amniocentesis (prior to 14 weeks' gestation). Nicolaides and colleagues compared transabdominal CVS to amniocentesis performed between 10 and 13 weeks' gestation. In this prospective comparison, the pregnancy loss rate was significantly higher after early amniocentesis (5.3%) than after CVS (2.3%).[12] Recently, Cederholm reported their comparison of transabdominal CVS and early amniocentesis.[13] Spontaneous fetal loss occurred in 6.8% of the amniocentesis and in 1.7% of the CVS group ($p<0.05$). Nineteen percent of the early amniocentesis patients required a second procedure due to culture and sample failure while 5.2% of the CVS group was re-sampled because of ambiguous results. Present information seems to indicate that CVS is the preferred prenatal diagnostic procedure under 14 weeks' gestation.

Smidt-Jensen, one of the pioneers of transabdominal CVS, have added additional information to the safety of the procedures.[14] In a prospective, randomized study they found no difference in pregnancy loss between transabdominal CVS and second trimester amniocentesis, but did demonstrate an increased risk for transcervical CVS.

There has been much discussion in the literature regarding the association of CVS and fetal limb reduction following the report by Firth in 1991 of five infants born with limb reduction defects following CVS in a series of 539 women.[15] Four of the infants had the oromandibular-limb hypogenesis syndrome and one had a terminal transverse limb reduction defect. All of the CVS procedures in the affected infants were between 55 and 66 days of gestation and done by transabdominal sampling. Oromandibular-limb hypogenesis syndrome is hypothesized to be secondary to fetal vascular disruption providing a possible etiological link to CVS.

Using the Italian multicenter birth defects registry, Mastroiacovo and colleagues reported a case-control study with an odds ratio of 11.3 (CI 5.6–2.13) for transverse limb abnormalities following first trimester CVS.[16] The cases, which were sampled prior to 70 days, had a 19.7-fold increased risk of transverse limb reduction defects, while patients sampled later did not demonstrate a significantly increased risk. Brambati and colleagues, an extremely experienced group with no increased risk of limb defects in patients sampled beyond 9 weeks, had a 1.6% incidence of severe limb reduction defects in patients sampled at 6 and 7 weeks.[7] This rate decreased to 0.1% for sampling at 8–9 weeks. Many other small series have also reported an increased incidence of limb reduction defects following CVS. The most common association seems to be with procedures performed early (prior to 70 days of gestation).[17]

There are some reports in the literature in which the question continues to be debated of whether CVS sampling after 10 weeks' gestation has the potential of causing more subtle defects, such as shortening of the distal phalanx or nail hypoplasia.[18,19] On the contrary, most experienced centers performing CVS after 10 weeks have not seen an increase in limb defects of any type. Recently a review of the almost 140,000 CVS procedures reported to the World Health Organization registry demonstrated no increase in the overall incidence of limb reduction defects following CVS nor in any specific type or pattern of defects between 9 and 12 weeks of gestation.[20] In one study which was consisted of the period of 1985–1991 reported that there was no any difference between the group of transcervical CVS performed at the 10th week of gestation and the group of amniocentesis performed at the 16th week of gestation in terms of short and long-term outcomes including limb defects and any other.[21] In another study for the period of 1986–1998 with the cases of more than 2700 CVS procedure after 11 weeks of gestation, there were no any significant differences between the group of patients at the 11–12 weeks, 13–14 weeks and 15–20 weeks of gestation in terms of feasibility, effectiveness and risk of prenatal diagnosis.[22] The fetal loss rates were 1.02%, 0.86% and 0.46% respectively. Thus it appears that procedures performed after 10 weeks of gestation in experienced centers carry no increased risk of limb reduction defects.

Papp et al reported their experience on CVS over 15 years practice. They performed transcervical CVS between 1984 and 1993 and transabdominal CVS thereafter until 1999 in 1149 cases between the 10th and 32nd gestational week. The fetal loss rate of 4.8% in the period of 1984–1993, occurring within 3 weeks from the date of sampling, dropped to 1.7% in the period rf 1994–1999. Premature births (6.4%) and stillbirth rates (1.1%) did

not exceed normal rates observed in the general population. They concluded that transabdominal CVS is a real alternative method of midtrimester amniocentesis and it is recommended for use at any stage of the pregnancy.[23]

MULTIPLE PREGNANCY

The prevalence of twin pregnancy increases with maternal age and also increased by assisted reproductive techniques. There has not been a screening method for chromosomal abnormalities in multiple pregnancies other than maternal age that has been used as a screening method such as older than 35 years old, until the nuchal screening was introduced as a screening method for chromosomal abnormalities in multiple pregnancy.[24] By this screening method it has been possible to calculate the risk of Trisomy-21 for each fetus in multiple pregnancy. Also by this policy, the fetal anatomy and some major fetal anomalies can be evaluated and diagnosed in first trimester that can make this pregnancy at risk for chromosomal abnormalities. Therefore the chorionic villus sampling makes early prenatal diagnosis possible in multiple pregnancies as earlier. But one should remember that the fetal loss rate after CVS in twin pregnancy is high compared to amniocentesis and is about 2%. If one uses two entry and needling technique to sample in both CVS and amniocentesis, the fetal loss rate is about the same.[25]

Therefore the proper genetic counselling should be given to the family according to the procedure-related fetal loss rate and the risk of Trisomy-21 in twin pregnancy, then the family can make a decision based on the information available. In twin pregnancy, CVS in the first trimester in a patient at risk for chromosomal abnormality (by nuchal screening) gives an opportunity to make selective feticide earlier if there is chromosomal abnormality in the fetus. One of the benefits of an earlier result from CVS allowing for earlier selective feticide is a lesser risk of miscarriage against the higher risk of the CVS procedure in comparison to amniocentesis.

Chorionic villus sampling has been demonstrated to be both safe and effective method for sampling twin gestation and has the advantage of an earlier diagnosis than amniocentesis.[26] Initial scanning identifies the locations of the individual chorion frondosum sites, confirms viability and gestational age, and the location and characteristics of the dividing membrane (Monochorionic or dichorionic). Sampling of each gestation is performed by needling each distinct frondosum. To assure sampling of each frondosum, continuous ultrasound localization of the needle tip is required. A combination of both sagittal and transverse views is utilized to confirm that individual samples are being retrieved. If the chorions are fused and the borders of the frondosums are indistinct, sampling near to cord insertion sites is suggested. If there is a doubt, a follow-up procedure should be performed as a repeat CVS performed immediately, or a second trimester amniocentesis. However, the need for a second procedure in experienced hand is rare.[27] Contamination of one sample with villi from the second occurs most frequently when sampling is performed close to the dividing membrane. Twin-twin contamination can also occur if a needle is dragged through one frondosum while attempting to sample another. In two twin series,[26,27] fetal karyotype abnormalities occurred in 2.0% and 3.1% of fetuses. Therefore, documentation of the location of the fetuses is important. If there is later doubt as to the location of the affected fetus a repeat placental biopsy can be performed prior to selective termination and a direct villous

preparation or FISH technique utilized to confirm correct fetal location. As with amniocentesis, there is the possibility of one fetus having an abnormal result. This discrepancy may occur somewhat more frequently with CVS than following amniocentesis since chromosomal abnormalities are more common in earlier gestations.

Until recent years, the karyotyping was carried out by the method of short-term culture in cytotrophoblast cells obtained by chorionic villus sampling, but this karyotyping method was abandoned due to false-positive results in this technique. In some studies, it was reported that FISH analysis could be used for confirmation.[28] In certain manner, the chorionic villi should be processed for long-term culture for karyotyping. Reported false-negative findings in the latter series of over 62,000 chorionic villus samples were extremely rare (0.03%) and most occurred with only one exception, after direct preparation alone.[29,30]

The tissue obtained from chorionic villus sampling can also be used for a variety of biochemical and DNA diagnoses (such as hemoglobinopathies, hemophilia, Duchenne dystrophy, cystic fibrosis, etc). The quantity of tissue is usually sufficient to allow an analysis without the need for tissue culture. In this type of analysis there is the concern of maternal cell contamination. This can be minimized by careful initial separation of the tissue by a technician experienced in handling chorionic villi.

PLACENTAL CONFINED MOSAICISM

The chorionic villi obtained are composed of three cell types, syncytiotrophoblast, cytotrophoblast and a central mesenchymal core. The mesenchymal core is grown out in long-term culture and produces a fibroblast-like cell type that is similar to amniocytes. On the other hand, the trophoblast cells are divided very quick and actively, and may be analyzed for karyotyping after 24 to 48 hours culture (short-term culture). Although this short-term culture gives a rapid result, there have been discrepancies with the true fetal karyotype. If we do use short-term culture, we should make long-term culture to make the results sure in any case. Most centers are not using the short-term culture technique any more because rely on the long-term culture result.

The major source of diagnostic error in CVS is placental confined mosaicism that is caused by the result of non-disjunction occurring during embryogenesis, presence of aneuploid cells in the extraembryonic tissue but not in the fetus. Most common type of placental confined mosaicism (PCM) involves the mosaicism in the direct preparation but normal results in culture and the fetus (Postzygotic non-disjunction in trophoblast cell line). Rare type PCM involves mosaicism in the culture but not in the direct preparation and the fetus (Postzygotic non-disjunction in the inner cell mass that will migrate into the villi). Very rare type involves PCM in the direct preparation and the culture but not in the fetus (Mixed type of non-disjunction).

In the case of placental mosaicism, we need to perform amniocentesis or fetal blood sampling to define the karyotype of the fetus. The overall incidence of chromosomal mosaicism ranges from 0% to 4.4% (average 1%). This is four times frequent as compared to amniocentesis.[31] The effect of confined placental mosaicism on the developing embryo is somewhat controversial, although some studies have shown an increased incidence of intrauterine growth restriction and perinatal death.[32] Follow-up ultrasound evaluation may be helpful in assessing this.

ACCEPTANCE

Prenatal diagnosis in the first trimester has rapidly gained approval for a number of reasons. Most important is the advantage of an earlier procedure. This approach not only provides earlier reassurance when results are normal but also allows an easier and more private pregnancy termination when necessary. Additionally, early diagnosis is essential when *in utero* gene or stern cell therapy is contemplated to correct a genetic defect. First-trimester procedures lowered maternal anxiety levels earlier and more consistently than traditional midtrimester amniocentesis. In a study, women undergoing CVS reported greater attachment to the pregnancy than women undergoing amniocentesis. These authors concluded that the benefits afforded by CVS confirmed earlier reports demonstrating a patient preference for CVS.[33] Also the gestational at the time of result is earlier in CVS than in amniocentesis. Earliest time for having the chromosome result is the 14th week with CVS and the 19th week with amniocentesis.

CONCLUSION

Chorionic villus sampling has been demonstrated to be a safe and effective technique that is capable of providing information and diagnosis to couples at genetic risk about their pregnancy. In most cases, the genetic results are reassuring but when abnormal, the medical and psychological complications of second trimester pregnancy termination can be avoided. Despite these advantages, utilization of CVS has failed to become widely available. This lack of complete acceptance has been primarily due to exaggerated reports of the risks of pregnancy loss and possible congenital abnormalities. The etiology of most of these problems can be directly attributed to inexperience with the procedure. Performing CVS is technically demanding, as demonstrated, the relatively long learning curve. As first-trimester screening for chromosomal abnormality with the detection rate of 97% by maternal age, nuchal thickness, nasal bone and free-beta-hCG and PAPP-A became a reality, we do perform more early prenatal diagnosis. Recent developments in laboratory techniques, we can give early result of FISH evaluation even for limited chromosomes on the same day and then complete result within 14–20 days. That makes CVS a requested method of early prenatal diagnosis. Studies suggest that CVS is the procedure of choice resulting in the need for additional centers with expertise in this procedure.

REFERENCES

1. Department of Obstetrics and Gynecology THoAIaSCA, China: Fetal sex predicition by sex chromatin of chorionic villi during early pregnancy. Chin Med J 1975; 1:117–26.
2. Wapner RJ: Chorionic villus sampling. Obstetr Gynecol Clin North Am 1997; 24:83–110.
3. Firth HV, Boyd PA, Chamberlain P et al: Severe limb abnormalities after chorion villus sampling at 56–66 days' gestation(see comments). Lancet 1991; 762–63.
4. Brambati B, Simoni G, Travi M et al: Genetic diagnosis by chorionic villus sampling before 8 weeks: Efficiency, reliability, and risks on 317 completed pregnancies. Prenat Diagn 1992; 12:789–99.
5. Jackson LG, Wapner RJ. Risks of chorionic villus sampling. Clin Obstet Gynecol 1987; 1:513–31.

6. MRC Working Group Party on the evaluation of chorionic villus sampling. Medical Research Council European trial of chorionic villus sampling. Lancet 1991;337:1491–99.
7. Brambati B, Oldrini A, Ferrazzi E et al: Chorionic villus sampling: an analysis of the obstetric experience of 1000 cases. Prenat Diagn 1987; 7:157–69.
8. Canadian Collaborative CVS-Amniocentesis Clinical Trial Group. Multicentre randomized clinical trial of chorion villus sampling and amniocentesis. Lancet 1989; 1:1–6.
9. Rhoads GG, Jackson LG, Schlesseslman SE et al: The safety and efficacy of chorionic villus sampling for early prenatal diagnosis of cytogenetic abnormalities. N Eng J Med 1989; 320:609–17.
10. MRC Working Group Party on the evaluation of chorionic villus sampling. Medical Research Council European trial of chorionic villus sampling. Lancet 1991; 337:1491–99.
11. Saura R, Gauthier, Taine L et al. Operator experiences and fetal loss rate in transabdominal CVS. Prenat Diagn 1994; 14:70–71.
12. Nicolaides K, Brizot M de L, Patel F, Snijders R. Comparison of chorionic villus sampling and amniocentesis for fetal karyotyping at 10–13 weeks' gestation. Lancet 1994; 344:435–40.
13. Cederholm M, Axelsson O. A prospective comparative study on transabdominal chorionic villus sampling and amniocentesis performed at 10–13 weeks' gestation. Prenat Diagn 1997; 17:311–17.
14. Smidt-Jensen S, Permin M, Philip J. Sampling success and risk at transabdominal chorionic villus sampling, transcervical chorionic villus sampling and amniocentesis: a randomized study. Ultrasound Obstet Gynecol 1991; 1:86–90.
15. Firth HV, Boyd PA, Chamberlain P et al: Severe limb abnormalities after chorion villus sampling at 56–66 days' gestation (see comments). Lancet 1991; 337: 762–63.
16. Mastroiacovo R Botto LD, Cavalcanti DP. Limb anomalies following chorionic villus sampling: a registry based case control study. Am J Med Genet 1992; 44:856–63.
17. Hsieh FJ, Shyu MK, Sheu BC et al: Limb defects after chorionic villus sampling. Obstet Gynecol 1995: 85; 84–88.
18. Burton BK, Schultz CJ, Burd LI. Spectrum of limb disruption defects associated with chorionic villus sampling. Pediatrics 1993; 91:989–93.
19. Olney S, Khoury MJ, Alo CJ et al. Increased risk for transverse digital deficiency after chorionic villus sampling: results of the United States Multistate Case-Control Study, 1988–1992. Teratology 1995; 51: 20–29.
20. Kuliev A, Jackson L, Froster U, Brambati B, Simpson et al: Chorionic villus sampling safety. Report of World Health Organization/EURO meeting in association with the Seventh International Conference on Early Prenatal Diagnosis of Genetic Diseases. Am J Obstet Gynecol 1996:174(3); 807–11.
21. Schaap AHR van der Pol HG, Boer K, Leschot NJ, Wolf H. Long-term follow-up of infants after transcervical chorionic villus sampling and after amniocentesis to compare congenital abnormalities and health status. Prenat Diagn 2002; 22:598–604.
22. Early second trimester (13 to 20 weeks) transabdominal chorionic villus sampling (TA-CVS): a safe and alternative method for both high and low risk populations.
23. Papp C, Beke A, Mezei G, Toth-Pal E, Papp Z. Chorionic villus samplings 15-year experience. Fetal Diagn Ther 2002; 17(4):218–27.
24. Sebire NJ, Snijders RJM, Hughes K, Sepulveda W, Nicolaides KH. Screening for trisomy in twin pregnancies by maternal age and fetal nuchal translucency thickness at 10–14 weeks of gestation. Br J Obstet Gynecol 1996; 103:999–1003.
25. Antsaklis A, Souka AP, Daskalakis G, Kavalakis Y, Michalas S. Second-trimester amniocentesis vs. chorionic villus sampling for prenatal diagnosis in multiple gestations. Ultrasound Obstet Gynecol 2002; 20:476–81.
26. Pergament E, Schulman J, Copeland K et al. The risk of and efficacy of chorionic villus sampling in multiple gestations. Prenat Diagn 1992; 12:377–84.

27. Wapner RJ, Johnson A, Davis G. Prenatal diagnosis in twin gestations: a comparison between second trimester amniocentesis and first trimester chorionic villus sampling. Obstet Gynecol 1993; 82:49–56.
28. Schuring-Blom GH, Hoovers JMN, van Lith JMM, Boer K, Knegt AC et al. FISH analysis of fetal nucleated red cells from CVS washings in cases of aneuploidy. Prenat Diagn 2001; 21:864–67.
29. Schuring-Blom GH, Boer K, Knegt AC et al. Trisomy 13 or 18 (mosaicism) in first trimester cytotrophoblast cells: false-positive results in 11 out of 51 cases. Eur J Obstet Gynecol and Rep Bio 2002; 101; 161–68.
30. Hahnemann JM, Vejerslev LO. Accuracy of cytogenetic findings on chorionic villus sampling (CVS)-diagnostic consequences of CVS mosaicism and non-mosaic discrepancy in centres contributing to EUCROMIC 1986–1992. Prenat Diagn 1997; 17:801–20.
31. Goldberg JD, Wohlferd MM: Incidence and outcome of chromosomal mosaicism found at the time of chorionic villus sampling. Am J Obstet Gynecol 1997; 176:1349–53.
32. Johnson A, Wapner RJ: Mosaicism:Implications for postnatal outcome. Curr Opin Obstet Gynecol 1997; 9:126–35.
33. McGovern MM, Goldberg JD, Desnick RJ. Acceptability of chorionic villi sampling for prenatal diagnosis. Am J Obstet Gynecol 1996; 155:25–29.

Chapter 42
Amniocentesis and Fetal Blood Sampling for Prenatal Diagnosis

Aris J Antsaklis

INTRODUCTION

It is widely accepted that at least 3% of all newborns will be presented with a significant birth defect or genetic disorder and many more individuals will be found to have some congenital or genetic defect during childhood and early adult years.

Prenatal diagnosis tests can be divided into three groups: 1) those involving maternal blood tests which are essential screening tests, 2) those tests imaging the fetus mostly by ultrasound which have the characteristics of both invasive screening and diagnostic test and 3) those invasive tests used to obtain fetal tissue. These tests are carried out in women who are already known to be at increased risk.

The most important consideration is the risk for the fetus. The final indication for an invasive prenatal diagnostic procedure occurs when a patient perceives the expected utility of the test to be greater than that of no test.

With invasive procedures, fetal samples such as amniotic fluid, chorionic villi, placental tissue, fetal blood, pleural fluid, urine form the bladder, skin or liver biopsies can be obtained according to the analysis planned.

The time and the source of fetal sampling for prenatal diagnosis can vary according to the malformation or to the genetic disease examined.

Whatever the route utilized, echographic guidance is mandatory for attaining an acceptable level of security and efficiency.

Any sampling procedure should be performed by an obstetrician experienced in the specific methodology and well trained in clinical and echographic gestational pathophysiology.

It has been suggested that ultrasound, has an essential place in the performance of any invasive procedure and is important in avoiding damage to developing tissue. Color Doppler imaging, is sometimes of value in invasive procedures and it is especially suitable for identifying the umbilical cord insertion in difficult cases and to avoid accidental injury to fetal vessels.

AMNIOCENTESIS

Introduction

Amniocentesis, the transabdominal aspiration of amniotic fluid, was introduced more than 100 years ago to relief the symptoms of hydramnios. In the early 1950s Bevis first used the spectrophotometric analysis of the amniotic fluid to predict the severity of Rhesus immunization.[1] By the same time Fuchs demonstrated that the fetal sex can be determined analyzing amniocytes with the implications in the management of the X-linked diseases like hemophilia and Duchenne muscular dystrophy.[2] In 1966 Steele and Breg first reported that second and third trimester amniotic fluid, contains viable cells that can be cultured and studied cytogenetically.[3] Amniotic fluid cells also proved to be useful in diagnosis of inborn errors of metabolism.[4] In 1970s Nadler and Gerbie published their experience with 155 second trimester genetic amniocentesis and since mid 1970s amniocentesis became the procedure of choice for prenatal genetic testing of the fetus[5] and today amniocentesis is the commonest invasive prenatal diagnostic procedure.

Indications

Amniocentesis is indicated for fetal cytogenetic studies but amniotic fluid can be used for biochemical determinations, enzyme study, DNA analysis, hybridization, while amniocentesis in the second and third trimester is usually undertaken for the investigation of Rh alloimmunization or assessment of the fetal lung maturity.

Timing

With the current technology amniocentesis is technically possible from 8 weeks of gestation until term.

For karyotyping, amniocentesis is usually performed between 15–16 weeks' gestation and culture of amniotic fluid cells takes 1–4 weeks, depending on the number of cells required.

Before this gestational age the procedure has a considerable higher fetal loss rate and the amniotic fluid contains lower fetal cell concentrations.[6,7] Therefore the results of an amniocentesis at 16 weeks are available between 18–21 weeks of gestation. Despite the power of midtrimester amniocentesis as a diagnostic tool, a major disadvantage is that it is performed relatively late in gestation. The appropriate week performing a genetic amniocentesis is defined by the need to perform the procedure late enough to obtain the results consistently and successfully, but as early as possible to permit termination of pregnancy if that option was indicated and so desired.[8]

Recently it has been shown that cytogenetic cultures are successful at earlier gestational age at 10 weeks of pregnancy. But it has been shown, that on the first trimester of pregnancy amniocentesis has a miscarriage rate higher than CVS, so this technique is unlikely to become widely used (Nicolaides et al 1994).[9]

Technique

The method of amniocentesis used has been described variously in the literature. Before the procedure, genetic counseling is mandatory and a detailed family history should be obtained. The parents should be informed about the indication, the risks and limitations of the procedure and laboratory analysis, the consequences of the results, the alternative management options, as well as the time required to obtain the final results.

Before amniocentesis, the operator should undertake a detailed ultrasound scan. This examination provides valuable information about the number and the viability of fetuses, the gestational age, and identifies structural abnormalities of the fetus, the location of the placenta and the appropriate insertion site is chosen.

Using the free hand "Single operator's technique" (one hand holds the needle and the other the ultrasound transducer) a 20 gauge needle is guided transabdominally into the correct position under continuous ultrasound control and 15–20 ml of amniotic fluid are aspirated. The advantages of this technique are the flexibility it gives to make adjustments during the procedure and that once learned this technique, the same technique can be used for all ultrasound guided invasive procedures.

The placenta, the area of the umbilical cord insertion and the fetus should be avoided. Since this area of the fetal surface of the placenta contains a large number of thin walled veins, fetal hemorrhage has been documented following amniocentesis and puncture of these vessels.

The anterior placenta rarely covers the entire anterior uterine wall so there is usually a window available for a lateral approach. Although it has been suggested that the risk of pregnancy loss is increased after transplacental amniocentesis, several studies concluded, that neither transplacental needle insertion nor the number of needle insertions, does influence the risk of pregnancy loss.[10–12] It has been reported that there is no difference on pregnancy losses after transplacental needle passage in 1487 cases compared to 3077 cases without transplacental insertion at amniocentesis performed between 15–16 weeks of gestation.[11] A transplacental approach may be appropriate if it provides the only easy access to a pool of amniotic fluid but care should be taken to avoid the cord insertion.

It has been suggested that no increased risk for pregnancy loss after multiple needle insertion at MA whereas other studies found an increased risk.[12,13]

The first 2 ml of amniotic fluid are discarded to reduce the risk of contamination of the sample with maternal cells which could occasionally lead to false-negative diagnosis (1/600 pregnancies). There is a confirmed relationship between higher fetal loss and aspiration of 40 ml of amniotic fluid or more.

In case that amniotic fluid cannot be aspirated, juxtaposes of the needle to the membrane and rotation 180 degrees may solve the problem. If not, reinserting of the stylet and advancing the needle under ultrasound guidance may help, if not a new insertion site should be selected.

When blood or blood stained amniotic fluid is aspirated, the needle tip should be rechecked, and it can be moved into a different pool of amniotic fluid because the needle had not completely transversed the uterine wall.

The dark or brown color of amniotic fluid indicates the presence of old blood into the amniotic cavity and this is associated with an earlier vaginal bleeding or a previous unsuccessful amniocentesis. This is more often associated with failure of amniotic fluid cells culture.

Although the incidence of this complication is less than 1%, patients should be warned in advance of this possibility.

After the procedure the fetal heart rate should be examined and demonstrated to the parents. Both uterine and maternal abdominal wall puncture sites should be observed ultrasonically for bleeding and anti-D should be given to Rh negative women.

In experienced hands the pure amniotioc fluid aspiration has a success rate of 100%.

Complications

Fetal loss is the major risk of second trimester genetic amniocentesis. It is always difficult to generalize about the safety of an invasive procedure since this is influenced by personal skill.

Amniocentesis, as all the invasive procedures for prenatal diagnosis and treatment, should be undertaken only by operators with considerable experience, in other aspects of obstetric ultrasound.

In assessing the amniocentesis-related fetal loss rate, is essential to take into consideration the background loss rate associated with maternal age, parity or other underlying risk factors.

Mckenzie et al (1988)[14] demonstrated that 2% if the ultrasound diagnosed pregnancies are miscarried, specifically in women younger than 35 years of age and 4.5% among women aged 35–39 years.

Gestational age at the procedure is an important determinant of observed fetal loss rate, because the earlier the pregnancy the greater pre-procedure risk of miscarriage. It has been reported that 2% of the ultrasound diagnosed pregnancies in women younger than 35 years old, are miscarriaged at 9–11 weeks, and 4.5% among women between 35–39 years of age, while later in pregnancy the background loss rate should be less.[14] The difficulties in evaluating the post-procedure loss rate have been clearly shown by the controversial results of several multicentre trials.

In 1978 the National Institute of Child Health and Human Development evaluating the safety and accuracy of midtrimester amniocentesis for prenatal diagnosis, reported a fetal loss rate of 3.5% in the amniocentesis group and 3.2% in the controls.[13]

The Medical Research Council in 1978,[15] reported an amniocentesis related fetal loss rate between 1–1.5%, a small but significant association with neonatal respiration (+0.6%) and it has been suggested that this complications could be the result of oligohydramnios following chorionic leakage of amniotic fluid.

In a critical period of the lung development the respiratory complications included RDS, pneumonia and unexplained difficulties at birth which lasted for more than 24 hours and required oxygen therapy.

This British study also found an increase in postural deformities[15] such as talipes and congenital dislocation of the hip. The possible mechanism of this deformity is compression due to oligohydramnios or tissue injury from the amniocentesis needle.

The study was criticized for biases in the selection of the control patients who were younger had less parity entered later in gestations in the study and some of the matched controls were replaced with other controls.

In 1986 the Danish randomized study in women under 35 with no increased genetic risk for abnormalities has suggested that the over all exist risk of miscarriage due to

amniocentesis is 1%.[10] The loss rate in the subject group was 1.7% in contrast to 0.7% in the control group.

In their original paper they stated that the amniocentesis were carried out with a 18 gauge needle. They have subsequently retracted this statement and indicated that a smaller needle was in fact used.

Several studies in 1990s reported an amniocentesis related fetal loss rate between 0.2–0.9%.[16–18]

Brumfield (1996)[20] reported a total fetal loss of 0.2% following amniocentesis at 16–19 weeks' gestation. In the Canadian early and midtrimester amniocentesis randomized trial 2185 MA were performed with a total pregnancy loss of 5.9% including post-procedural intrauterine and neonatal death. They found that the post-procedural fetal loss rate was about 1% while Roper et al (1999)[17] reported an 0.9% risk for miscarriage after MA.

It has been estimated that fetal loss rate following amniocentesis at 15 weeks of gestation was less than 0.5%, at 14 weeks 1% and at 13 weeks 3% respectively. Blood stained amniotic fluid and amniotic fluid leakage were strong predictors for fetal loss.

It is reasonable for an expert in invasive diagnostic procedures to quote patients a procedure related miscarriage rate of the order of 0.3–0.5%. Operator's experience seems to be an important factor in reducing the risk for pregnancy loss. It has been reported a 3.7% miscarriage risk when the operator has performed less than 10 MA versions 0.3% among operators who had performed at least 50 MA.[19] A recent report demonstrated that those doctors undertaking less than 50 procedures in the study period (36 months) had a single pass success rate of 82% compared with those with greater than 50 procedures of 93%.

Operators with adequate levels of training (greater than 50 procedures per year) have a higher success rate and lower "bloody tap" rate than operators with limited experience.

Adequate training and maintenance skills are of crucial importance. Specific training should include ultrasound experienced. Before practicing on patients the trainee has to practice on clinical skills model and once is confident they can move on to undertake amniocentesis under supervision. For the maintenance of skills about 50 amniocenteses a year required for a satisfactory level of success.

Uterine contractions and vaginal spotting are quite common after a midtrimester amniocentesis, however they are almost always transitory and self limited whereas chorioamnionitis rate is about 0.1% and rupture of the membranes with leakage of amniotic fluid is expected in about 1%.

In cases of amniotic fluid infection induction of labor is requires in order to prevent underlying sepsis. In cases of amniotic fluid leakage without any signs of infections conservative management should be the first option since the rare possibilities of resealing of the membranes within 7 days.[21,22]

Major needle injuries, including cutaneous scarring, brain injury, occurs damage were reported early in the literature when amniocentesis was performed without any ultrasound guidance.

Fetomaternal hemorrhage of sufficient volume of blood to result Rh sensitization occurs in 5% of patients after amniocentesis and is more significant after transplacental amniocentesis performed by unexperienced operators.[10]

The effectiveness of anti-D immunoglobulin in preventing Rh sensitization after midtrimester amniocentesis is proved by several studies. The American College of Obstetricians and Gynecologists recommends the administration of 300 μg of Rh immunoglobulin following genetic amniocentesis.

In the literature there are papers reported cases with severe craniofacial and limb abnormalities or umbilical cord compression, associated with amniotic band syndrome as a sequel of a difficult invasive procedure.

Early Amniocentesis

In recent years some investigators have begun to offer amniocentesis earlier in pregnancies before 15 weeks including the first trimester. The major advantage of early amniocentesis, is that the results are known much earlier than with second trimester amniocentesis.

The technique of early amniocentesis is similar to midtrimester amniocentesis, requiring precise ultrasound directed biopsy, similar to that necessary for transabdominal CVS resulting to no advantages over CVS in terms of early sampling.

Before 12 weeks chorion and amnion are separated and this causes difficulties in performing the amnio because the membrane tenting. Penetration of the membranes can be achieved with a rapid thurst with a 20–22 gauge needle. Aspiration of 1 ml amniotic fluid per week of gestation provides a sufficient concentration of amniocytes for genetic analysis.

The 15 ml amniotic fluid at this week of pregnancy is a significant amount, while the extremities are in a critical period for their development.

This amount represents the 20–25% of the total volume and this is regrated in 7–10 days. It has been reported that there is a culture failure, ranging from 0.5–2.5%.[23,24]

Fetal complications after early amniocentesis were expected to be higher than that with mid-trimester amniocentesis, because the proportion of the removed amniotic fluid in earlier procedures is greater than with MA.

Fetal loss rate related to early amniocentesis ranges from 1.06% to 5%. At 13–14 weeks the pregnancy loss rate is comparable with that of mid-trimester amniocentesis. The pregnancy loss is higher when early amniocentesis is performed between 11 and 13 weeks.[9,25]

Fetal loss rate seems to be higher in cases of difficult procedures with extremely retroverted uterus, increased body mass index, uterine fibroids or amniotic membrane tenting.

The Canadian early amniocentesis trial, found that tenting occurred in 29.4% of trisomy 21 fetuses and only in 8.3% when the karyotype was normal.[26,27]

Early amniocentesis has a higher rate of amniotic fluid leakage than midtrimester amniocentesis with a fetal rate of 40%.

Operator’s experience must be also taken into consideration.

It has been suggested that may be a link between early amniocentesis and postural abnormalities.

Talipes equinovarus is a severe side affection of EA that dements intensive treatment within the first years of life. Until the 10th week of pregnancy the feet are placed with the soles against each other and might be more vulnerable to the fall of the intraamniotic

pressure after the procedure. It has been reported an incidence of talipes equinovarus of 1.6% after an early amniocentesis.

The amniotic fluid leakage seems to increase the incidence of talipes.

The Canadian Early and Midtrimester Amniocentesis Trial Group reported an incidence of talipes of 1.3% in the EA group, without post-procedural amniotic fluid leakage, and an incidence of 15% in the EA group with leakage.[27]

It is not clear yet if the relative oligohydramnios created after EA could influence the lung development and function, but it has been reported an incidence of pulmonary compromise in 6.1% of the neonates after EA.[24]

Although a higher proportion of infants after EA required admission to the NICU because of respiratory problems, this was not due to an excess of infants with respiratory distress syndrome or pneumonia.[28]

The only randomized study has been published in 1994 by Nicolaides.[9] This study includes 488 pregnancies randomized between early amniocentesis and CVS for fetal karyotyping at 10–13 weeks' gestation. They found a significant higher pregnancy loss rate in EA group compared with the CVS group (5.9% vs 1.2%) and the incidence of talipes equinovarus was higher in the amniocentesis group than in the CVS group (1.62% vs 0.56%).

The post-procedural vaginal bleeding seems to be higher in the CVS group whereas the early amniocentesis patients have a higher occurrence of amniotic fluid leakage. CVS has a higher rate of mosaicism (0.8%) and of maternal cell contamination (1.9%) than amniocentesis.

Amniotic fluid in the second trimester contains 10^6 cells per ml, but only 1 to 5 cells/ml are viable and will grow in culture. Amniotic fluid cells are mainly consisted of epithelial cells and fibroblasts.

Before 15 weeks gestation, 70% of the amniotic fluid cells originate from the extraembryonic membranes. The viable cell number is decreased in blood stained amniotic fluid. Tissue culture may fail if the specimen is contaminated with bacteria. The cells not respond to the laboratory conditions or the sample is inadequate. In early amniocentesis the culture failure rate ranges between 0.5% and 2.5% whereas with midtrimester amniocentesis the culture failure rates is between 0.2% and 0.6%.[10,23,29]

On 1997 was proposed the use of a filter technique in order to improve the yield in cell cultures in early amniocentesis, but it has been found an increased fetal loss rate using this technique (Sumberg et al 1997).[30]

Maternal cell contamination can lead to a false diagnosis. The risk of maternal cell contamination can be minimized, by discarding the first few milliliters of the aspirated fluid. The incidence of maternal cell contamination with MA and EA varies between 0.3% and 0.5%.

The presence of multiple cell lines with different chromosomal constitution in the cell culture, is considered as a mosaicism and compose a diagnostic dilemma. The mosaicism may be representative of the fetal karyotype, or is secondary to an *in vitro* event maternal contamination, or may be a cytogenetic aberration that is confined to the extra embryonic membrane. The finding of a true mosaic should be confirmed with a second sampling procedure from a different tissue. Mosaicism is found in 0.25% of MA samples, while EA sample, have a higher rate because higher rate of the cytogenetic aberrations that are confined to the placenta.[18,31]

Mosaic trisomy 16 is not a benign finding. Being associated a high incidence of intrauterine growth retardation, congenital heart disease developmental delay and minor anomalies.

First trimester amniocentesis will also not overcome the problem of placental mosaicism because amniotic fluid early in pregnancy contains a very high proportion of trophoblast derived cells and culture is prove to failure before 12 weeks gestation.

The identification of a balanced translocation, a small inversion or supernumery marker, may require the evaluation of prenatal karyotypes, to determine the significance of this finding.

The risk of limb reduction defects must also be considered and assessed.

In conclusion early amniocentesis before 14 weeks' appears to be associated with significant problems, including increased fetal loss rates, fetal talips and a reduced amniotic culture rate compared to those 4 procedures performed at 15 weeks or later. This procedure should only be undertaken in the presence of extenuating circumstances and only if the mother has been made aware of the potential complications.

FETAL BLOOD SAMPLING AND TISSUE BIOPSY

Fetal blood sampling was initially used for prenatal diagnosis of severe inherited diseases. Now days in the field of prenatal diagnosis the most obvious indications are rapid fetal karyotyping and immunological studies.

Fetal blood sampling was traditionally obtained antenatally by fetoscopy, but this technique has been almost completely abandoned in favor of cordocentesis which is a technique for obtaining fetal blood, by direct puncture of the umbilical vein.[30,31] Other suggested targets for fetal blood sampling are fetal heart ventricles and the intrahepatic tract of the umbilical vein.[45]

The latter technique has some advantages in case of fetal intravascular treatment.

Cordocentesis

Cordocentesis is technique, quite easy to perform, either transplacentally, in case of an anterior placenta, or across the amniotic cavity in the case of a posterior placenta.

It has been suggested that ultrasound has an essential role in the performance of fetal blood sampling technique and is very important in avoiding damage to the developing tissues.[40]

Before the procedure a preliminary ultrasound examination is performed to determine the fetal vitality, the amniotic fluid volume, the fetal position and to localize the placental and the cord insertion site.

It seems that the color Doppler system provides the best information and facilitates fetal blood sampling since it makes the identification of the insertion of the umbilical vein into the placenta very much easier.

The insertion site is cleaned with antiseptic solution and local anesthetic is used. The free hand technique most often is used with a 20 gauge spinal needle under continuous ultrasound guidance.

In case of anterior placenta the transplacental approach is the easier way to the placenta cord insertion unless the placenta is posterior and the cord is entered

approximately 1 cm from the placental umbilical cord insertion site after passing through the amniotic cavity.

The needle must be introduced with firm but controlled movement, trying to avoid puncturing of the chorionic plate and damaging the fetal vessels.

This sampling site seems to have a low risk of hemorrhage because of the relatively thick Wharton's jelly.

Attempts to puncture free loops, often result in the cord being pushed away by the needle to enter the umbilical cord, the needle is brought close to the umbilical vein and then advanced sharply into umbilical vein, and 2–4 ml fetal blood withdraw in heparinized syringe. This amount is safely taken at 18 weeks.

If amniotic fluid is obtained, the needle will be either completely through the cord or along site it. The needle should be carefully imaged again to reassess the position of the tip big magnification and color Doppler system can be used to determine which vessel is sampled.

In cases that blood gases studies are needed, the umbilical vessel should be confirmed as artery or vein by inject 1 ml normal saline into the vessel.

Fetal blood can be sampled from intrahepatic umbilical vein. This ultrasound guided technique is as described for the Cordocentesis. Although good results have been reported, this technique is more difficult than FBS at the cord insertion.

Fetal heart is an alternative sampling site and this technique can be used when access to the fetal circulation must be obtained at gestational age less than 17–18 weeks gestation or if an emergency blood transfusion is required. Blood samples must be immediately examined to identify the purity of the sample and the results of the analysis can be significantly altered in case it has been contaminated by maternal blood or amniotic fluid.

In very experienced hands, pure fetal blood may be obtained in 97–98% of cases.

Complications

Complications of FBS are chorioamnionitis, amniotic fluid leakage, fetal exsanguinations and umbilical cord hematoma, while fetal bradycardia often associated with vasospasm after puncture of the umbilical artery.

The fetal loss rate following cordocentesis and fetal blood sampling, excluding elective termination, reported to be as high as 6–7% in centers with little experience, but in experienced hands the rate is as low as 1–2% and this is strongly influenced by the indication for sampling.

Unfortunately no controlled trials are yet available and is not quite clear what is the fetal loss rate to quote to patients, because most clinical series contain many high risk cases, such as malformed fetuses, IUGR, immune and non-immune hydrops.

Fetal Tissue Sampling

Fetal tissue sampling is very rarely required. The methodology is similar to the blood sampling methods and their use is restricted to a limited number of center containing experienced operators.

Fetal liver biopsy is carried out for the diagnosis of specific enzyme deficiencies. The biopsy is carried out by ultrasound guided aspiration through a 19 gauge needle, or by fetoscopic guidance.

Fetal skin biopsy permits the diagnosis of the majority of genodermatoses.

Although the skin biopsy has to be obtained under fetoscopic control, skin biopsies under ultrasound guidance have been performed.

The suggested sampling sites are the back of the fetus, the thigh or the scalp. Skin sampling is performed at approximately 20 weeks when histological aspects of the skin are already pathognomonic for the disorder.

EMBRYOSCOPY-FETOSCOPY CLINICAL APPLICATION

Introduction

The ability to diagnose and identify various congenital anomalies and genetic disorders prenatally has improved with the advanced resolution of ultrasound and the guided diagnostic techniques.

Ultrasonography and fetoscopic techniques have been the tools available for detailed visualization of the fetus and embryo and the intrauterine environment.

Both techniques have proved effective in either the second or third trimester and antenatal diagnosis was reserved for the second trimester.

In late 1970s and early 1980s transabdominal fetoscopy was used during the second trimester of pregnancy for direct visualization of the external anatomy of the fetus and for fetal blood and tissue sampling. Subsequently high resolution ultrasound imaging made second trimester fetoscopy obsolete. New techniques for prenatal diagnosis have changed the practice of perinatal medicine.

Recent developments in the field of fiberoptics have allowed the progressive introductions of smaller visualization equipments. Therefore much interest has been stimulated by the introduction of embryoscopy during the first trimester of pregnancy.

During the past decade, prenatal diagnosis has increasingly moved into the first trimester of pregnancy with the introduction of new techniques as transvaginal sonography, chorionic villus sampling, transcervical and transabdominal embryoscopy.

Transabdominal Fetoscopy

The words embryoscopy and fetoscopy relate to the gestational age at which human pregnancy is endoscopically visualized. Although there has been a tendency to refer to embryoscopy as a synonym for the use of the transcervical route and fetoscopy for the transabdominal approach, we prefer to use gestational age for this terminology.

A transabdominal route for the endoscopic visualization of the fetus was first used by Mandelbaum in 1967. The endoscope carried only optical fibers and the illumination was provided by a device delivered through a second port.

In this technique endoscopes of 1.7 mm to 3.5 mm in diameter have been used. The model we used for several years had an outer diameter of 1.7 mm (Needlescope Dyonics

Inc. Wolburn USA) with an oval outer sheath of 2.2×2.7 mm to accommodate a working channel.

In the 1980s advances in ultrasonography and percutaneus umbilical blood sampling (PUBS) displaced fetoscopy for most clinical purposed, including anatomic visualizations, cordocentesis and fetal tissue biopsy.

Second trimester fetoscopy soon became superceded by other techniques such as ultrasound guided percutaneous umbilical blood sampling (PUBS) particularly after the Daffos' report (1985)[41] in which "cordocentecis" (a new technique) was performed successfully solely under ultrasound guidance for fetal blood sampling in over 600 pregnancies. Transabdominal fetoscopy has since gene probe for DNA analysis on trophoblastic tissue and amniotic fluid fetal cells as well as high resolution ultrasonography have further reduces the indications for fetoscopy remained an alternative tool for special indications and selected procedures, such as fetal skin sampling, for the diagnosis of certain genodermatoses, liver or muscles biopsies, and laser photocoagulation of anomalous communicating vessels in severe cases of twin to twin transfusion syndrome.

Transcervical Embryoscopy

The first of a transcervical endoscopic observation of the human fetus, was made by Westin in Sweden in 1954.[44] He used a 10 mm rigid hysteroscope and performed transcervical fetoscopy in three patients before termination of pregnancy between 16 and 20 weeks.

The transcervical embryoscopy was first used to detect congenital anomalies in the second trimester by Dubuisson (1979) and Roume (1985). While Gallinot in 1978 suggested that the fetus could be best visualized after the seventh week of gestation.

Girardini (1991) pointed out, that to adequately visualize the embryo the chorionic membranes needed to be perforated.

Dumez (1998)[34] in his early work presented in Athens in 1988 performed successfully transcervical endoscopy in continuing pregnancies in more than 50 women, with a pregnancy loss of 70%.

Cullen (1990)[37] used a modification of the Dumez's technique to confirm congenital anomalies suspected by ultrasound during the first trimester of pregnancy. Technique in transcervical first trimester embryoscopy, the patient is in the lithotomy position and a rigid fiberoptic endoscope 30 cm in length with diameter of 2.0–3.5 mm and a 0° to 30° angle connected to a light source, is passed under ultrasound guidance through the cervical canal and apposed by the fetal membranes. The chorionic membrane is penetrated bluntly by a rapid thrust, and the tip of the endoscope enters the extra coelomic cavity leaving the amniotic intact. The yolk sac and the placenta are directly visualized.

The embryo can be observed through the transparent amniotic membrane and structural defects of the head and neck and limbs are expected to be diagnosable with embryoscopy in early pregnancy. Because of the wide in diameter endoscope used, images are very clear but sometimes is difficult to obtain a complete anatomic survey of the fetus. In contrast to midtrimester transabdominal fetoscopy, the wide angle lens and the small size of the embryo often permit visualization of the embryo in toto.

Limitations include trauma to fetal membranes as a result of the relatively large bore of the endoscope, bleeding specialy in cases with placental previa, potential infections complications and the inability to avoid rupturing the amniotic membrane.

Severely anteverted or retroverted uterus it may be inaccessible to the endoscope. Because of these limitations and potential complications, it has been reluctant to offer this procedure to patients at risk for congenital anomalies in ongoing pregnancies.

It was be suggests that transcervical embryoscopy will be replaced by the less traumatic and more practical transabdominal approach.

Transabdominal Embryoscopy

Considering the limitations of transcervical endoscopy and classic fetoscopy, Quintero in 1993[4] developed a transabdominal endoscopic technique to visualize the embryo or fetus in the first trimester of pregnancy with the use of the new submillimetric fiberotic endoscopes. These endoscopes are of such small diameter that they can be passed though the lumen of a thin needle.

The endoscope is passed through the uterine wall and into the amniotic cavity similar to amniocentesis.

The eyepiece of the endoscope is connected to a video camera and the procedure can be viewed video monitor and recorded for subsequent review.

Successful intra-amniotic insertion of this thin endoscope and visualization of both eyes, nostrils, mouth, ears, anterior chest wall umbilicus, hands and feet can be achieved.

Thus abdominal embryoscopy can be performed as early as three conceptional weeks gestation and this technique is useful not only for detecting abnormalities but also for visualizing normal milestones of embryonic developments of the trunk and limbs including complete closure of the neural tube and fully development hand by the age of 7 conceptional week.

Transabdominal embryoscopy has been invaluable identifying additional anomalies not recognized by ultrasound early in pregnancy and confirming others already detected ultrasonographically. Additional application transabdominal embryoscopy is fetal and tissue sampling and this application serves as a basis for further studies into diagnosis and treatment of congenital diseases early in pregnancy. If the concept of human gene therapy and the stem cell transplantation becomes a reality, embryoscopy will permit accessibility to the human embryos are immunologically “naive” and may therefore be receptive to these grafts.

Potential Applications

Current applications of the technique include accurate endoscopic description of the embryonic development, first trimester diagnosis of congenital anomalies and intraluminal endoscopic description of blood flow within fetal vessels in the second trimester.

Fetal Therapy

The next step in the evolution of needle transabdominal embryofetoscopy is fetal surgery. Fetoscopic ligation of the umbilical cord has less complications and does not have the recanalization problems associated with percutaneous ultrasound guided

intraarterial injection of either thrombogenic coils or fibrin in the umbilical cord of the recipient twin.[42]

It has been suggested that fetal cystoscopy using thin transabdominal embryoscopy is useful in the evaluation at treatment of obstructive defects of the urinary system *in utero*.[36,43]

In case the concept of human gene and cell therapy becomes a reality, embryoscopy will permit accessibility to the human embryo at a time when embryos are immunologically naive and may therefore be receptive to these grafts.

Although presently the only human tissue that can be used effectively for gene therapy intrauterine stem cells transplantation it is expected that more will be learned in the future about how to package the DNA, to purify stem cells, and to make DNA tissue specific. Embryoscopy provides an opportunity for us to treat a variety of genetic disorders before their disabling effects are realized.

The introduction of transabdominal visualization of the embryo in the first trimester using a thin gauge embryoscope allows earlier diagnosis of congenital anomalies currently beyond the resolution of ultrasound.[38] In addition it has the true potential of providing access to the fetal circulation at an early age, an accomplishment that would have important diagnostic and therapeutic applications. In the first and second trimester, operative fetoscopy techniques promise to open new frontiers in the diagnosis and management of fetal surgical and medical conditions.

REFERENCES

1. Bevis DCA. The antenatal prediction of haemolytic disease of the newborn. Lancet 1952; 395.
2. Fuchs Fe, Riis P Antenatal sex determination. Nature 1956; 177:330.
3. Steele MW, Breg WR. Chromosome analysis of human amniotic fluid cells. Lancet 1966; 1:383–86.
4. Jeffcoate TNA, Fliegner JRH, Russel SH et al. Diagnosis of adrenogenital syndrome before birth. Lancet 1965; 2:553.
5. Nadler HL, Gerbie AB. Role of amniocentesis in the intrauterine detection of genetic disorders. N Engl J Med 1970; 282:596–99.
6. Golbus MS, Loughman WD, Epstein CJ et al. Prenatal genetic diagnosis in 3000 amniocentesis. N Engl J Med 1979; 300:157.
7. Webb T, Edwards JH, Cameron AH et al. Amniocentesis in the West Midlands: Report on 1000 births. J Med Genet 1980; 17:81.
8. Evans MJ, Jonhson MP, Holzgreve W. Early amniocentesis: what exactly does it mean? J Reprod Med 1994; 39:77–78.
9. Nicolaides KH, Brizot MDL, Patel F, Snijders R. Comparison of chorionic villus sampling and amniocentesis for fetal karyotyping at 10–14 weeks' gestation. Lancet 1994; 344:435–39.
10. Tabor A, Philip J, Madsen M, Bang J, Obel EB, Norgraad-Padersen A. A randomised controlled trial of genetic amniocentesis in 4606 low risk women. Lancet 1986; 1:1287–93.
11. Giorlandino C, Moboli L, Bilancioni E, D'Allesio P, Carcioppolo O, Gentili P et al. Transplacental amniocentesis: is it really a higher-risk procedure? Prenat Diagn 1994; 14:803–06.
12. Mathin T, Liedgren S, Hammar M. Transplacental needle passage and other risk-factors associated with second trimester amniocentesis. Acta Obstet Gynecol Scand 1977; 76:728–32.
13. NICHD. National Registry for Amniocentesis Study Group: Mid-trimester amniocentesis for prenatal diagnosis: safety and accuracy. JAMA 1981; 1:173–81.

14. Mac Kenzie WE, Holmes DS, Newton JR. Spontaneous abortion rate in ultrasonographically viable pregnancies. Obstet Gynecol 1988; 71:81–83.
15. MRC Working Party: An assessment of the hazard of amniocentesis. Br J Obstet Gynecol 1978; 85: 1–41.
16. Owen J. Pregnancy outcome following genetic amniocentesis at 11–14 vs 16–19 weeks' gestation. Obstet Gynecol 1996; 88:114–18.
17. The Canadian Early and Mid-Trimester Amniocentesis Trial (CEMAT) Group 1998: Randomezed trial to assess safety and fetal outcome of early and mid trimester amniocentesis. Lancet 1998; 351:242–47.
18. Roper EC, Konje JC, De Chazal RC, Duchett DP, Oppenheimer CA, Taylor DJ. Genetic amniocentesis: Gestational specific pregnancy outcome and comparison of following early and traditional amniocentesis. Prenatal Diagn 1999; 19:803–07.
19. Verjaal M, Leschot NJ. Risk of amniocentesis and laboratory findings in a series of 1500 prenatal diagnosis. Prenat Diagn 1981; 1:173–81.
20. Brumfield CG, Lin S, Conner W, Cosper P, Davis RO, Owen J. Pregnancy outcome following genetic amniocentesis at 11–14 versus 16–19 weeks gestation. Obstet Gynecol 1996; 88(1):114–18.
21. Hazan Y, Ben-Arie A, Blickstein I, Hayay Z. Reseal of ruptured membranes after genetic amniocentesis. A case report. J Reprod Med 2000; 45(10):847–49.
22. Borgida AF, Mills AA, Feldman DM, Rodis JF, Egan JF. Outcome of pregnancies complicated by rupture of the membranes after genetic amniocentesis. SM J Obstet Gynecol 2000; 183(4):937–39.
23. Henry GF! Miller WA. Early amniocentesis. J Reprod Med Obstet Gynecol 1992;37:395–402.
24. Penso CA, Sandstrom MM, Garber MF, Ladoulis M, Stryker JM, Benaceraff BB. Early amniocentesis: report of 407 cases with neonatal follow up. Obstet Gynecol 1990; 76(6):1032–36.
25. Rooney DE, Mac Lachlan N, Smith J et al: Early amniocentesis: a cytogenetic evaluation. BMJ 1989; 299:25.
26. Johnson JM Wilson RD, Singer J, Winsor E, Harman C, Armson BA, Benzie R, Danserau J, Ho MF, Mohilde P, Natale R, Okun N. Technical factors in early amniocentesis predict adverse outcome. Results of the Canadian Early vs Mid-Trimester Amniocentesis Trial. Prenat Diagn 1999; 19:732–38.
27. Randomised trial to assess safety and fetal outcome of early and mid trimester amniocentesis. The Canadian Early and Mid-Trimester Amniocentesis Trial (CEMAT). Lancet 1998; 351(24):242–47.
28. Greenough A, Yuksel B, Naik S, Cheeseman P, Nicolaides KH. Invasive antenatal procedures and requirement for neonatal intensive care unit admission. Eur J Pediatr 1997; 156:550–52.
29. Hanson FW, Tennant FR, Hune S, Brookhyser K. Early amniocentesis: outcome, risks and technical problems at less than or equal to 12.8 weeks. Am J Gynecol 1992; 166:1707–11.
30. Sunberg K, Bang J, Smidt-Jensen S, Lundsteen C, Parner J, Keiding N, Philip J. Randomised study of risk of fetal loss related to early amniocentesis versus chorionic villus sampling. Lancet 1997; 350(6): 697–703.
31. Hsu LY, Perlis TE. United States survey on chromosome mosaicism and pseudomosaicism in prenatal diagnosis. Prenat Diagn 1984;4:97–130.
32. Hobbins J, Mahoney J. In uterus diagnosis of hemoglobinopathies. N Engl J Med 1973; 290:1065–67.
33. Rodeck C, Campbell S. Sampling pure fetal blood by fetoscopy in second trimester of pregnancy. Br Med J 1978; ii:728–30.
34. Dumez Y, Oury J, Duchetel F. Embryoscopy and congenital malformations. In Proceedings of the International Conference on Chorionic Villus Sampling and early Prenatal Diagnosis Athens, Greece 1988.

35. Quintero R, Abuhanad A, Hobbins JC, Mahoney MJ. Transabdominal thin gauge embryofetoscopy: a technique for early prenatal diagnosis and its use in the diagnosis of case of Meckel-Gruber syndrome. Am J Obstet Gynecol 1993; 168:1552–57.
36. Quindero R, Romero R, Jonhson M, Smith C, Arias F, Guevare F, Cotton DB, Evans M. In utero percutaneous cystoscopy in the management of fetal obstructive uropathy. Lancet 1995; 346:537–40.
37. Cullen MT, Reece EA, Whethom J et al. Embryoscopy: Description and utility of a new technique. Am J Obstet Gynecol 1990; 162:82–86.
38. Reece EA, Homko CJ, Wiznitzer A et al. Needle embryo fetoscopy (NEF) and early prenatal diagnosis. Fetal Diagn Ther 1995; 10:81–82.
39. Reece EA, Goldstein I, Chatwaui A: Tarnsabdominal needle embryofetoscopy. A new technique paring the way for early fetal therapy. Obstet Gynecol 1994; 84: 634–36.
40. Daffos F, Capella-Pavlosvsky M, Forestier F. A new procedure for pure fetal blood sampling in utero. Preliminary results at fifty-three cases. Am J Obstet Gynecol 1983; 146:985–87.
41. Daffos F, Capella-Pavlosvsky M, Forestier F. Fetal blood sampling during pregnancy with use of a needle guided by ultrasound, a study of 606 consecutive cases. Am J Obstet Gynecol 1985; 153:655–60.
42. Delia J, Kuhlmann R, Harsrad T, Gruikshauk D. Fetoscopic laser ablation of placental vessels in severe prevable twin-twin transfusion syndrome. Am J Obstet Gynecol 1995; 172:1202–11.
43. Quindero R, Hume R, Smith C, Johnson M, Cotton D, Romero R, Evans M. Percutaneous fetal cystoscopy and endoscopic fulguration of posterior urethral valves. Am J Obstet Gynecol 1995; 172:206–09.
44. Westin B. Hysteroscopy in early pregnancy. Lancet 1954; 2:872
45. Antsaklis A, Papantoniou N, Mesogitis S, Vintzileos A et al. Cardiocentesis: An alternative method of fetal sampling for the prenatal diagnosis of hemoglobinopathies. Obstet Gynecol 1992; 79:630.

Chapter 43
Invasive Genetic Studies in Multiple Pregnancy

Aris J Antsaklis

INCIDENCE

The incidence of multiple pregnancies has increased over the past two decades. One-third of the increase is due to the use of ovulation induction agents, one-third due to assisted reproduction techniques and the remaining third due to delayed child bearing.

The management and the prenatal diagnosis of a multiple pregnancy is not only related to the number of fetuses, but it is strongly influenced by the chorionicity. More than 30% are monozygotic (MZ) twins and nearly 70% are dizygotic (DZ). MZ twins are the result of a division of a single fertilized ovum. It occurs in about 2.3–4/1000 pregnancies. The rate is constant and is not influenced by heredity, age of the mother or other factors (Monozygotic twins are always of the same sex, have the same physical characteristics and the same genetic features).

In one-third of monochorionic (MC) twins, zygotic splitting occurs within 3 days of fertilization, resulting in separate fetuses with independent placental circulations. Splitting after the third day, is associated with vascular communications between the placentas. In MZ twins chorionicity is subdivided in three categories. Around 20–30% are dichorionic (DC)—diamniotic (DA) with separate or fused placentas. The most common type of MZ twins is MC—DA (two amniotic cavities with a single placenta) accounting for the 70%. Around 1% of MZ twins are MC—MA.[1] Assisted conception is also associated with a 2–8 fold increased incidence of MZ twins.

MZ twins are of high risk of functional and structural abnormalities, which would affect approximately 10–15% of these.[2] Abnormalities unique to the MZ multiple conception include conjoined twinning, fetus in feto, acardia and fetus papyraceous. Explanation for the increased incidence of abnormalities in monozygotic twins, involve the role of hemodynamic imbalance between MC twins through placental vascular anastomoses.

DZ twins are produced from separately fertilized ova released from separate follicles (very rarely from the same follicle) at approximately the same time. Dizygotic twins may be of the same or different sex. Factors influenced dizygotic twinning are included race (most common in blacks, least common in Asians) and nutrition. Parity does not influence the incidence of dizygotic twinning but aging does, with the rate of dizygotic

twinning peaking between 35–40 years of age and then declining sharply. Dizygotic multiple pregnancy trend to be recurrent.

Women who have borne dizygotic twins have a 10 fold increased chance of subsequent multiple pregnancy. Height and weight have a positive influence on twinning.

Induction of ovulation with human pituitary gonadotropin infertile women increase the incidence of multiple pregnancies, while clomiphene citrate increases the occurrence rate of dizygotic pregnancies to about 5–10%.[2]

The overall incidence of abnormalities appears to be higher in MZ compared with DZ twins. Neural tube defects, anencephaly, holoprosencephaly, sirenomelia complex, cloacal exstrophy and abnormalities which fit into the expanded VATER/ VACTERAL associations are more common in MZ twins. The risk of fetal abnormality in twins may be biased because multiple pregnancies are intensively monitored increasing the chances of detecting abnormalities. Advanced maternal age increases the chances of twinning and this group of patients is more likely to have prenatal diagnosis.

The Risk of Aneuploidy in Multiple Gestations

Since the frequency of MZ twinning remains relatively constant with increased age, DZ twins become relatively more frequent as maternal age increases. In DZ twins, each embryo has an independent risk for aneuploidy and therefore the risk that at least one fetus is aneuploid, will be twice the maternal age risk for a singleton. The probability of both fetuses being involved is minimal.[3]

In cases in which zygosity is uncertain, calculation of the probability of an aneuploid fetus requires an estimation of the most likely zygosity which may vary according to maternal age and race. Using these calculations, a 33 years old woman carrying twins has a risk of at least one aneuploid child, comparable to the risk in a 35 years old woman carrying a singleton. On this basis such women should be offered prenatal testing.

In MZ conceptions both fetuses, share the same karyotype, and hence the risk of an aneuploid fetus is the same as the risk for a singleton at the maternal age.

Despite those calculations reported series show a lower risk for fetal aneuploidy in live born twins.

Indications for Prenatal Diagnosis

The indications for prenatal diagnosis in multiple pregnancy are the same as in singleton pregnancies. These include advanced maternal age, a previous conceptus with chromosomal abnormality, a parent with a structural chromosome rearrangement and the presence of gene associated inborn errors of metabolism. In case of an autosomal recessive disorder the risk is increased and has a 3 in 8 chances of at least one affected fetus, and 1 in 8 chances that both will be affected.

Prenatal diagnosis of chromosomal abnormalities in twins is complicated because effective methods of screening such as maternal serum biochemistry are not applicable.

Maternal serum alpha-fetoprotein (MSAFP) level in twin pregnancy is twice as high as that of a singleton pregnancy and 40% of twins are associated with MSAFP levels of more than a 2.5 MOM at 16 weeks.[4]

The presence of multiples which explains the elevation of MSAFP does not preclude the possibility of an open neural tube defect in one or more fetuses.

Where the MSAFP in twins exceeds 5 MOM, amniocentesis should be performed.

Nuchal translucency thickness measurement, is a valid technique in multiple pregnancies.[5] In 448 twin pregnancies the nuchal translucency thickness was above the 95th centile of the normal range for CRL in singletons in 65 of the 896 fetuses, (7.3%) including 7 of 8 (88%) with trisomy 21.

The minimum estimated risk for trisomy 21, based on maternal age and nuchal translucency thickness was 1 in 300 in 19.5% (75/896) of the twins including all eight of those with trisomy 21. Pandya and co-workers (1995) reviewed the usefulness of nuchal translucency in 20, 543 singleton and 392 twin pregnancies. The detection of trisomy 21 in twins has a similar sensitivity to that in singletons.[6]

Nuchal translucency screening in twins may yield higher false-positive results than in singletons. It has been suggested that this increase in MC twins may be an early manifestation of cardiovascular complications due to twin-to-twin transfusion syndrome (TTTS).[7]

O'Brien and associates stated that "current attempts to generate risk figures for aneuploidy in multiple gestations are fraught with imprecision and should be evaluated with great caution".[8]

Prenatal diagnosis in multiple pregnancies differs in several ways from that in a singleton gestation, and is strongly influenced by chorionicity.

In a DC pregnancy there are no direct consequences for the co-twin if a single fetal demise occurs, whereas in MC twins, intrauterine death of one twin might cause a serious complication for the survivor.

In fused placentas chorionicity must be determined by the ultrasonographic appearance of the dividing membrane. The difference on thickness between the thick dichorionic and the thin monochorionic membranes is much more obvious during the first trimester than it is later in pregnancy.

Furthermore the presence of an echogenic chorionic tissue projection into the base of the inter-twin membrane ("twin peak" or "lambda sign") in the first trimester, has been shown to be one of the most specific ultrasound landmarkers of dichorionic placentation. In the second trimester the "lambda sign" is progressively less prominent making prediction at chorionicity more difficult. Its absence after 20 weeks' gestation should be viewed with caution.[8]

Invasive Procedures for Prenatal Diagnosis

All prenatal diagnosis invasive procedures must be preceded by a detailed ultrasounds examination and each fetus must be carefully examined in order to evaluate the relative position, size and anatomy of each fetus and the location of placenta and to determine the chorionicity.

Amniocentesis for prenatal diagnosis is routinely performed from 15 weeks' gestation; there is only limited information on either the efficacy or safety of amniocentesis in twins performed prior to 15 weeks' gestation.

The procedure is usually carried out with a 22 gauge needle introduced transabdominally under ultrasound guidance to retrieve 20 cc of amniotic fluid.

Tapping multiple sacs requires two or more needle insertions. Many maneuvers have been described to facilitate taps in twins, but the most common is probably the use of a dye to avoid tapping the same sac twice.

Use of methylene blue is now contraindicated since it has been at associated with fetal small bowel intestinal atresias and fetal death.[9,10]

The pathophysiology of methylene blue induced bowel atresias is uncertain. However it seems most likely that vascular disruptive is responsible.

Indigo carmine is most commonly utilized. However despite its apparent safety continued surveillance is warranted because of a mild vasoconstrictive effect when it is injected intravenously.

A technical disadvantage with the instillation of indigo carmine is that the dye tents to concetrate at the bottom of the sac, and it takes some time before the stained fluid surrounds the fetus.

As ultrasound technology has improved, it may now be possible to use other approaches.

Jeanty et al[11] described a single needle insertion techniques. The needle entry is made into the proximal sac near the insertion of the dividing membrane, and 20 cc of amniotic fluid removed. The stylet is then replaced and, under ultrasound guidance, the needle is advanced through the membrane into the second sac. After discarding the first few milliliters of amniotic fluid (to avoid contamination), 20 ml of fluid from the second sac is removed.

The advantages of this alternative technique are that: (i) it requires only one needle insertion, (ii) it reduces patient discomfort, (iii) being swifter and shorter does not require the injection of a dye, (iv) it offers positive proof of tapping the two sacs, and (v) may reduce the incidence of complications.

Because the communication created between the two sacs is very small it is likely that it will heal very rapidly. Puncture of the dividing membrane however may result in pseudo monoamniotic twins with a potential for etrapment of fetal parts or the umbilical cord and the formation of the amniotic band syndrome.[12]

Another drawback is the possible contamination of the needle with cells from the first sac, which could lead to an incorrect diagnosis of mosaicism in the second fetus. This complication can be avoided by strictly adhering to the technique by replacing the stylet prior to membrane perforation, and by discarding the first few milliliters from the second sac.

Both these unfavorable events are not considered a clinical contraindication to the procedure.

An alternative approach to ensure sampling from each sac utilizes two needles inserted simultaneously under ultrasound guidance. After aspiration of amniotic fluid from the first sac, the needle is left in place and a second insertion is made into the other sac. The technique seems to be accurate and safe but experience with this approach is limited.

The possibility of chromosomally discordant results requires that amniotic fluid samples be labeled in such a way as to ensure that the specific location of each fetus will remain identifiable. It has been suggested the spatial location of each fetus and placenta, in relationship to each other or to the cervix, should be drawn in a detailed diagram at the time of procedure, to minimize the possibility of confusing the samples.

Most series of pregnancy outcome following second trimester amniocentesis report loss rates before 20 weeks' gestation of between 1% and 2.5%, and a much higher loss rate before 28 weeks. In a multicenter European study the pregnancy loss rate was estimated to be 2.3% and 3.7% before 20 and 28 weeks' gestation respectively.[13]

Ghidini et al[14] reported the results of amniocentesis in 101 twin pregnancies compared with 108 control twin pregnancies. The technique used involved two needle insertions to sample both sacs. They demonstrated no significant difference in the miscarriage rates and the total fetal loss rate in the amniocentesis group was 3.5% compared to 3.2% in the controls.

Chorionic villus sampling (CVS) has been demonstrated to be safe and efficacious for sampling twin gestations. Genetic results can be obtained much more rapidly than with amniotic fluid cells, either in hours by direct preparations of the cytotrophoblast layer, or in 3–7 days by tissue culture of the villus mesenchymal core. CVS is best performed between 10 and 13 weeks of gestation; sampling each sac is performed by either transcervical or transabdominal route under ultrasound guidance. Each approach has advantages and disadvantages. Technically, transcervical CVS, may be more difficult to perform and the "learning curve" appears to involve several hundred patients. Transabdominal CVS is technically similar to midtrimester amniocentesis and is applied more often than the transcervical technique. Also the amount of tissue obtained with transabdominal CVS is smaller than that obtained by the transcervical route.

Since no marker is available to assure sampling of each chorion, continuous ultrasound localization of the tip of the needle or the catheter is required. If in doubt, a follow up procedure should be performed, either by an immediate repeat CVS or by second trimester amniocentesis.

Contamination of one sample with villi from the second sac is possible and poses a serious potential problem leading to failure to diagnose a chromosomal abnormality in one or both twins. Twin-to-twin contamination can occur, if the needle or the catheter is dragged through one chorion in an attempt to sample the second one. Contamination occurs most frequently when CVS is performed close to the dividing membrane, which contains villi from both chorions. Twin-to-twin contamination can be avoided by using a combination of transcervical and transabdominal techniques.

Since there is the possibility of one fetus having an abnormal result, careful location of fetuses is equally as important with CVS as it is with amniocentesis. Although the position of sacs will remain unchanged in 2–3 weeks after sampling it is standard practice to reconfirm the original diagnosis in both fetal and chorionic tissues before selective termination.

The risk of CVS associated fetal loss before 28 weeks' gestation did not seem to differ between twin and singleton pregnancies (4.9% vs 4% respectively).[15] Among these losses were included fetuses with chromosomal aberrations. When only chromosomally normal pregnancies are considered, the overall loss rate found is a study of 202 twin pregnancies from five centers experienced in performing CVS in multiple gestations, becomes 3.7% which is considerably less than that of amniocentesis.

Wapner et al (1993)[16] reported, that the pregnancy loss rate before 20 weeks was 3.3% following CVS, and 2.8% in a control group of women undergoing twin amniocentesis. These two reports, confirm that, in experienced centers, CVS is as safe as amniocentesis for sampling twins. Since CVS and amniocentesis have equal risks of pregnancy loss, the question of which procedure is preferable must be addressed. Amniocentesis is technically easier and more widely available and accepted. Therefore, if the center is not skilled and experienced in CVS, then amniocentesis would be preferred. CVS has certain advantages since the results are available one month earlier and therapeutic termination

as well as selective termination, within the first trimester is safer. We could conclude that the choice of invasive technique should be based on individual risks calculated from the combinations of maternal age and fetal nuchal translucency. When the risk for a chromosomal defect, in at least one of the fetuses, is greater than 1 in 50, it may be preferable to perform CVS. For pregnancies with a lower risk amniocentesis after 15 weeks may be more appropriate. Van den Berg and co-workers (1999)[17] reported their experience with 500 cases of multiple gestations comparing amniocentesis with CVS and they concluded that CVS was the method of choice for prenatal diagnosis in multiple pregnancies.

Fetal blood sampling in twins does not present any difference when compared to this procedure in singletons. Umbilical cords insertion must be identified before sampling. This technique can be used as an alternative to amniocentesis from 20 weeks' gestation onward to confirm an abnormal karyotype in a dichorionic twin pregnancy when selective feticide is considered a few weeks after the initial procedure has been performed.[19]

Invasive procedures for prenatal diagnosis in multiple gestations are safe and effective. First trimester CVS has a lower risk of procedure failure and of fetal loss than amniocentesis but it carries a higher risk of maternal cell or twin-to-twin cell contamination. There are reports suggesting that in experienced centers obstetric safety, efficacy of sampling and accuracy of genetic analysis between CVS and amniocentesis is the same.

The Greek Experience

In the last 20 years, 372 patients with multiple pregnancies underwent genetic amniocentesis (including 365 twin sets). One was lost to follow up, 6 are ongoing pregnancies, and therefore data on 365 pregnancies are available. All patients had an ultrasound examination before the procedure in order to localize the placental site, the fetal position and to determine chorionicity.

The procedures were performed between the llth and 23rd weeks (mean gestational age 17.2 weeks). In seven cases amniocentesis was performed before 14 completed weeks (i.e. first trimester amniocentesis) and in the remaining 358 cases, the procedure was done, between the 16th and 23rd weeks (second trimester amniocentesis). Patients were 19–52 years old (mean maternal age 36.18 years).

All procedures were performed with the double entry technique using a 22 gauge needle and 20 ml of amniotic fluid from each sac were withdrawn successfully. In 102 cases both placentas were posterior, in the 115 both placentas were anterior and in the remaining 148 there were one anterior and one posterior placenta.

In the group of 358 second trimester amniocenteses, 3 pregnancies were terminated (one because of homozygous β-thalassemia, one because of severe twin-to-twin transfusion syndrome and one because of trisomy 21) and 10 women underwent selective feticide (2 because of trisomy 21, one because of 47, XXX, 4 because of homozygous P-thalassemia and 3 because of a neural tube defect). One patient delivered a healthy live newborn at 30 weeks, 9 patients delivered after 37 weeks and there was one neonatal death of a term baby due to a congenital heart defect.

In the 345 remaining patients there were 12 cases with both of fetuses miscarriages before the 28th week of pregnancy and half of them occurred in the first 3 weeks after the

procedure. For the remaining 333 patients, 24 had a fetal loss of only one fetus after the 28th week of pregnancy and in 14 cases there was a neonatal death in one of the twins. One hundred eighty patients out of 343 (343/180) (52.5%) delivered prematurely before 37 weeks of pregnancy 340 fetuses and the remaining 163 patients delivered 316 fetuses after the 37 week of pregnancy. The perinatal loss after 28 weeks was 3.5%. The neonatal mortality was 2.1%. Of the 343 pregnancies 94.6% resulted in at least one live birth.

During the same period, 74 CVS procedures were performed in multiple pregnancies. Six cases were lost to follow up and we present the data of the remaining 68 cases. The procedure was performed transabdominally in all cases between the 9th—15th week of gestation (mean gestational age 10.7 weeks). The patients were 20–43 years of age (mean maternal age 30.7 years) and there was a 11.7% rate of repeat procedure (8/68). There were 5 procedures in pregnancies with more than two fetuses (4 triplets and 1 quadruplet pregnancies) and in these cases the indications for CVS were p-thalassemia n=4 and advances maternal age n=1. There were 6 fetuses affected by homozygous β-thalassemia and 2 fetuses affected by trisomy 21 and in all cases selective feticide were carried out at less than 14 weeks of gestation. In this group there were two spontaneous abortions at 20 and 21 weeks of gestation (40%) and one patient delivered prematurely at 34 weeks (33.3%).

Chorionic villus sampling also was performed in 63 twin pregnancies. The indications were increased risk of choromosomal abnormality in 10 cases (includes advanced maternal age, anxiety, increased nuchal translucency and family history of trisomy 21) and increased risk of genetic syndromes of structural anomalies in 53 women (β-thalassemia, sickle cell anemia, Duchenne syndrome, phenylketonuria).

In seven cases (11%) the parents decided for termination, in six pregnancies because both fetuses had homozygous β-thalassemia and in one case of phenylketonuria the pregnancy was terminated before results became available.

In twelve cases (19%) with fetus affected by homozygous β-thalassemia selective feticide was carried out between 11 and 16 weeks of gestation. One pregnancy (1/12, 8.3%) miscarried at 16 weeks and two patients delivered before 32 weeks healthy neonates (2/11, 18.2%). There were no other cases of fetal loss.

In the remaining 44 twin pregnancies there were 2 miscarriages, at 10 and 22 weeks of gestation respectively (2/44, 2.3%). The rate of preterm delivery before 32 weeks and 35 weeks was 16.66% (7/42) and 23.80% (10/42) respectively. The perinatal loss before and after 28 weeks of gestation was 9.09% (8/88) and 1.25% (1/80) respectively. Overall 42 women (95.45%) delivered at least on healthy live baby. Between 1977 and 2000 in 89 twin pregnancies fetal blood sampling was performed for prenatal diagnosis. Five cases were lost to follow up and we present the data of 84 cases. The patients were 20–44 years old (mean 28.3) and the procedures were performed at 18–29 weeks of gestation (mean 20.3 weeks). For the first 28 cases fetoscopy was carried out for fetal blood sampling where as after 1985 we switched to ultrasound guided cordocentesis (54 cases), except of 7 cases where cardiocentesis was performed.

The indications for fetal blood sampling in 70 cases were the risk for hemoglobinopathies. In 16 of these 70 patients were over 35 years and additionally chromosome analysis was performed. In 2 cases the indication was advanced maternal age, in 4 cases the indication for fetal blood sampling was the increased risk for

congenital infection and in 11 cases there was a suspicion ultrasound finding for fetal structural defect and fetal blood sampling was performed for chromosomal analysis.

Termination of the pregnancy was carried out in 19 cases (20.2%). In 12 cases both fetuses were affected by β-thalassemia or sickle cell anemia and in one case one fetus had severe obstructive uropathy and the other had hydranencephaly. In 7 cases only one fetus was affected, 5 cases by homozygous β-thalassemia, one case by trisomy 21 and one case by bowel obstruction and the parents decided to terminate the pregnancy.

Selective feticide was performed in 11 patients between 20 and 29 weeks of gestation. There were 9 fetuses affected by β-thalassemia, one fetus with chromosomal abnormality (47, XXY), and one with pulmonary hypoplasia. No miscarriages occurred in this group. The rate of preterm delivery before 32 and 35 weeks was 41.66% and 50% respectively.

In the remaining 55 pregnancies there were 2 miscarriages at 20 and 23 weeks of gestation (3.92%). The rate of preterm delivery before 32 and 35 weeks was 16.98% and 28.30% respectively. The perinatal mortality rate before and after 28 weeks was 8.18% and 5.94% respectively. Overall 90.09% of women had at least one live baby.

REFERENCES

1. Benirschke K. Multiple gestation: incidence, etiology and inheritance. In: Creasy RK, Resnik R (Eds). Maternal—fetal medicine principles and practice (4th ed). Philadelphia: W.B. Sanders 1999; 585–15.
2. Benirschke K, Kim CK. Multiple pregnancy. N Engl J Med 1973; 1329–36:357–67.
3. Rodis JF, Egan JF, Craffey A et al. calculated risk of chromosomal abnormalities in twin gestations. Obst Gynecol 1992; 76:1037.
4. Garduer S, Burton B, Johnson AM. Maternal serum alpha-fetoprotein screening: a report of the Forsyth County Project. Am J Ostet Gynecol 1981; 140:250.
5. Sebire NJ, Suijders RJ, Hughes K et al. Screening for trisomy 21 in twin pregnancies by maternal age and fetal nuchal translucency thickness at 10–14 weeks of gestation. Br J Obstet Gynecol 1996; 03: 999–1003.
6. Pandya PP, Snijders RJN, Johnson SJ, Brizot M, Nikolaides K. Screening for fetal trisomies by maternal age and fetal translucency thickness at 10–14 weeks of gestation. Br J Obstet Gynecol 1995; 107:957–62.
7. Okaro E, Gagnon A, Vandenberg K, Ville Y. Aspects of perinatal diagnosis in twin pregnancies. Gynaecology Forum 1998; 3:19–26.
8. O'Brien JE, Dvorin E, Yaron Y, Ayoub M, Johnson MP, Hume RF Jr, Evans MI. Differential increases in AFP, hCG, uE3 in twin pregnancies impact on attempts to quantify Down syndrome screening calculation. Am J Med Genet 1997; 73:109–12.
9. Nicolini U, Monni G. Intestinal obstruction in babies exposed in utero to methylene blue. Lancet 1990; 36:1258–59.
10. Kidd SA, Lancaster PA, Anderson JC, Boogert A, Fisher C, Robertson E, Wais DM. Fetal death after exposure to methylene blue dye during mid-trimester amniocentesis in twin pregnancy. Prenat Diagnon 1996; 6:39–47.
11. Jeanty Ph, Shah D, Roussis P Single needle insertion in twin amniocentesis. J Ultrasound Med 1990; 9:511–17.
12. Megory E, Weiner E, Shalev E et al. Pseudoamniotic twins with cord entanglement following genetic funipuncture. Obst Gynecol 1991; 78:915.
13. Pruggmayer Mr, Jahoda M, Van der Pol G et al. Genetic amniocentesis in twin pregnancies: results of a multricenter study of 529 cases. Ultrasound Obstet Gynecol 1992; 2:6–10.
14. Ghidini A, Lynch L, Hicks C et al. The risk of second trimester amniocentesis in twin gestation; a case control study. Am J Obstet Gynecol 1993; 169:1013–16.

15. Pergament E, Schulman J, Copeland K et al. The risk of efficacy of chorionic villus sampling in multiple gestations. Prenatal Diagn 1992; 12:377–84.
16. Wapner RJ, Johnson A, Davis G. Prenatal diagnosis in twin gestation: a comparison between second trimester amniocentesis and first trimester chorionic villus sampling. Obstet Gynecol 1993; 82:49–56.
17. Van der Berg C, Braat AP, Van Opstal D, Halley KJ, Kleijer WJ, Den Hollander NS. Amniocentesis or Chorionic villus sampling in multiple gestation? Experience with 500 cases. Prenatal Diagn 1999; 191: 234–44.
18. Antsaklis A, Gougoulakis S, Mesogitis S et al: Invasive techniques for fetal diagnosis in multiple pregnancy. Int J Gynecol Obstet 1991; 34:309–14.
19. Al-kouatly H, Skupski D. Twin pregnancy. Current Optima in Obstet Gynecol 1999; 11:129–29.

Chapter 44
MRI: How to Use it during Pregnancy

Ichiro Kawabata, Yuichiro Takahashi, Shigenori Iwagaki

INTRODUCTION

It is possible to get easily and safely various kinds of information about the mother and fetus during pregnancy by using ultrasonography (USG). However, unsatisfactory results are obtained in some cases due to maternal fat tissue, fetal position or some other reasons. Magnetic resonance imaging (MRI), an imaging tool that has been rapidly spreading in medicine can provide clear images from multiple angles without X-ray exposure. We of course understand the usefulness of USG, but believe that it is also important to evaluate the usefulness of MRI and how to use it during pregnancy.

SAFETY OF MRI

It is generally understood that X-ray exposure should be avoided during pregnancy. In contrast, MRI seems to be safe for the fetus, as indicated by the fact that there are no reported harmful effects from its use, including any mutagenic effects.1 One potential problem of magnetic power is that it may lead to an elevation of the temperature especially in a packed cavity like the pregnant uterus. Figure 44.1 shows our experimental values of intrauterine temperature measured during MRI procedure using a pregnant rabbit. This experiment revealed there was almost no temperature changing in the uterine cavity during exposure to magnetic power of 2.0 teslas which is higher than that used clinically. Thus, with respect to temperature, MRI seems to be safe for the fetus.

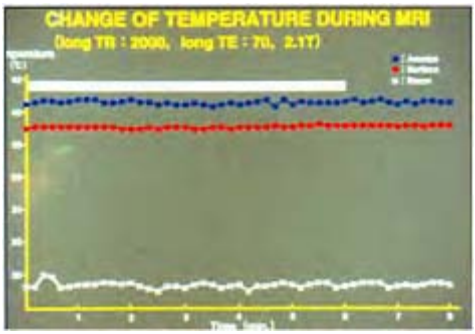

Figure 44.1: Measurement of intrauterine temperature. Results of an animal experiment using a pregnant rabbit. The intrauterine temperature was quite stable during the MRI procedure

We have been administered contrast medium to the mother for MRI in some special cases. Harada reported data from animal experiments in which contrast medium was administered during the first trimester, and concluded that these agents had made no bad effects on the fetus.[2]

Absolute safety of such agents cannot be assured until much more larger studies are available for outcome analysis. Though the National Radiological Protection Board in The United States advises against imaging during the first trimester unless termination of pregnancy is probable, MRI is at least safer than X-ray procedures.

Indication and Procedures for MRI during Pregnancy

What are the indications for MRI during preg- nancy? First of all, MRI is not suitable for screening for fetal anomalies. However there have been many reports of prenatal diagnoses of malformed cases based on MRI.[3] We can divide the indications for MRI into the categories of pelvimetry, fetal anomalies, maternal tumors and others including examinations of the placenta based on our experience. We have performed 485 MRI procedures during pregnancy according to the above indications. The equipment we used was either a SIGNA ADVANTAGE or a SIGNA HORIZON (1.5T, GE Medical Systems, Milwaukee, WI). No drug was administered to the mother or fetus to control fetal movement, because it was not necessary. We sometimes requested mothers to walk around for 15–20 minutes just before the MRI procedure to reduce fetal movement. Because of recent advances in MRI techniques that allow us to obtain a fetal image in a few seconds, it is not necessary to do anything to reduce the fetal movement. If the mother suffers from supine hypotension, the decubitus position is recommended.

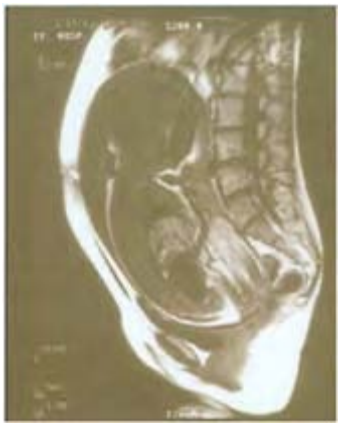

Figure 44.2: MRI pelvimetry, Guthmann's image. This image can be obtained by determining the maternal sagittal image. It is possible to measure the pelvic diameter directly without any calculation

Most MRI specialists might consider that thinslice imaging should be performed, especially in cases of fetal anomaly, to get images from small fetuses. We disagree that thin-slice imaging is optimal in such cases because thin slices result in poorer image quality. Even when the fetus is small, we recommend 10 mm imaging slices. After evaluation by such thick-slice imaging, if necessary or if possible, thin-slice imaging should be performed in cases in which it might yield useful information.

Pelvimetry

Maternal pelvic size and shape has in the past been evaluated by X-ray pelvimetry despite the fact that X-ray exposure should be avoided during pregnancy because there was no other way of evaluation. Several trials of MRI pelvimetry have been reported.[4,5] MRI can be used to delineate pelvic size and shape clearly by obtaining images like the Guthmann and Martius images obtained in X-ray pelvimetry (Figs 44.2 and 44.3). Further- more, the pelvic size can be measured without any calculation such as that necessary in X-ray pelvimetry. Figure 44.4 shows a T1-weighted image of a diabetic macrosomic fetus. In this method of imaging, fat tissue is delineated as a high-intensity, white color. This image revealed that the fetal subcutaneous fat tissue was markedly thickened s

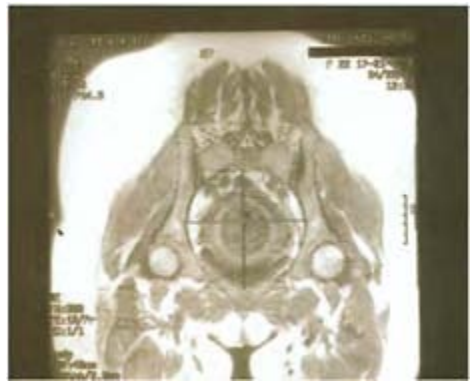

Figure 44.3: MRI pelvimetry, Martius image. The maternal pelvic shape is delineated clearly. We can obtain this image from the maternal sagittal image, which provides a theoretically better method of pelvimetry than X-ray pelvimetry

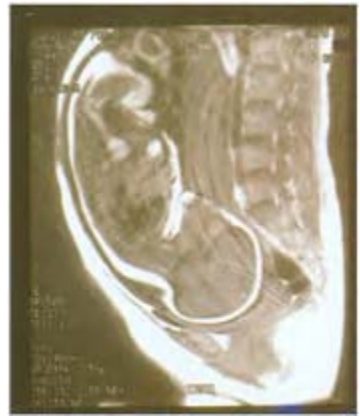

Figure 44.4: Diabetic macrosomia. The macrosomic fetus is rich in fat tissue especially in

cases complicated with a maternal diabetic condition. MRI detects fetal subcutaneous fat tissue as high-intensity substance in T1-weighted images. This image makes it possible to evaluate relative fetal-pelvic disproportion, including disproportion of fetal soft tissue, unlike X-ray evaluation

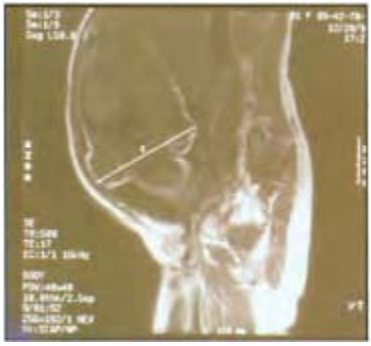

Figure 44.6: Malrotation of fetus. Fetal rotation can be evaluated by X-ray pelvimetry. However, MRI provides information about this condition that is easier to understand

compared with that of a non-diabetic fetus like that in Figure 44.2. Thus MRI pelvimetry makes it possible to make a precise detection of relative cephalo-pelvic disproportion based on the ability to delineate fetal subcutaneous fat tissue as a high-intensity substance. This ability also makes it possible to measure fetal shoulder size (Fig. 44.5).

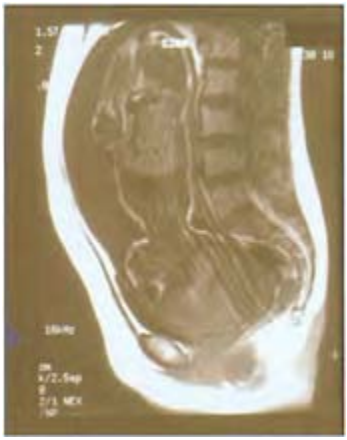

Figure 44.5: Shoulder size evaluation. MRI can image the fetus from multiple angles and thus allows us to measure the fetal shoulder size. Although the fetal shoulder size is flexible, it is an additional potentially important kind of information about the fetus

We can detect fetal malrotation clearly and precisely by MRI because MRI can delineate the whole fetal body in one image even in the late phase of pregnancy (Fig. 44.6).

Maternal Tumors

Maternal tumors are not related to pregnancy but may occur and can be diagnosed during pregnancy. Similarly, luteinizing ovarian cysts related to pregnancy may occur. When a malignant tumor is suspected, the appropriate diagnostic tests should be performed on the mother. MRI which must be performed carefully in the first trimester of pregnancy. It is preference to perform MRI first rather than X-ray imaging after the initial detection by USG because MRI is safer than X-ray imaging.

During pregnancy, obstetricians tend to image the fetus only to evaluate the fetal heartbeat, size, and so on. This tendency sometimes leads to missing the chance to detect maternal tumors in the early phase of pregnancy. With the advance of gestational age, maternal tumors become difficult to diagnose because of the enlarged uterus. It may

become difficult to distinguish between uterine tumors and ovarian tumors, especially when the

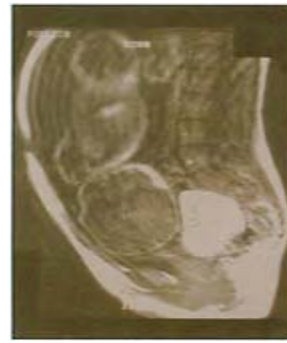

Figure 44.7: Maternal ovarian tumor. Because of the increased size of the uterus, maternal ovarian tumors are sometimes difficult to detect by ultrasonography. MRI can demonstrate such tumors even in the late phase of pregnancy

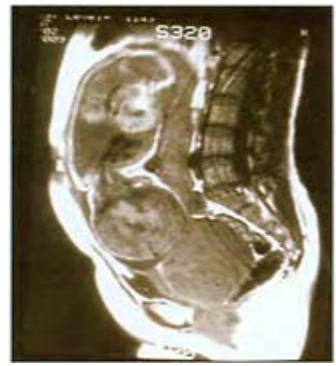

Figure 44.8: Maternal cervical myoma. It is difficult to differentiate between ovarian tumors and cervical myoma in

advanced pregnancy. MRI provides a clear image of the cervical myoma

tumor is located in the Douglas cavity. In such cases, MRI can provide critical information for a precise diagnosis (Figs 44.7 and 44.8).

Fetal Anomalies

There have been many reports about prenatal diagnosis of various fetal anomalies that were detected by USG. USG is convenient and easy to perform and it is the most popular tool for fetal diagnosis. However, this wonderful imaging tool is unfortunately not perfect. Because of maternal fat tissue or fetal position, one sometimes gets unsatisfactory images that are not adequate for making a precise prenatal diagnosis. In such situations, it is necessary to use some other imaging tool to obtain important information about fetal problems.

MRI is an imaging diagnostic tool that provides clear soft tissue images using magnetic power rather than X-rays. Thus, MRI can be performed during pregnancy. It is still widely assumed that it is difficult to obtain clear images of the fetus undisturbed by fetal movement because it takes 1–5 minutes to obtain fetal images by MRI. In the past, fetal MRI was performed while controlling fetal movement with sedatives or muscle relaxants, which in some cases were injected directly into the fetal circulation.[6] This procedure makes fetal MRI an invasive method. Although it is essential to control fetal movement to get a clear image of the fetus, we believe that MRI must ideally be a completely safe and drug-free examination for the pregnant woman and fetus. Accordingly the best way of perform fetal MRI is under condition of "spontaneously controlled fetal movement". When the mother walks around for 15 minutes just before the MRI procedure, the fetal movement markedly decreases. We cannot explain the reason for this decrease of fetal activity, but regular and rhythmic movement of the mother such as occurs in normal walking may produce an effect similar to rocking the baby in a cradle.

Another interference in fetal MRI is maternal breathing. With the advance of gestational age, the maternal breathing style changes to abdominal breathing. The maternal abdomen moves conspicuously, especially in the supine position. For these two reasons, the decubitus position may be recommended for fetal MRI procedures.

Figure 44.9 shows the success rate of fetal MRI using various imaging protocols through our experience. Obtaining superior quality images of the fetus depends on the imaging time, with better images obtained during shorter times. Recently, MRI imaging techniques have rapidly advanced.[7] It takes only a few seconds to get an image using the latest method for imaging, which is called SSFSE or HASTE.[8] Using such an ultra-high-speed imaging method, it is not necessary to control the fetal movement. Using this method of imaging, we could successfully obtain fetal images in all cases.

Figure 44.10 shows the MRI image of a cystic hygroma. It clearly reveals that a huge cystic tumor exists from below the ear to the shoulder, because MRI can delineate the fetal whole body in one image even in the late phase of pregnancy, which is one of the advantages of MRI. From this image, the origin of the tumor was clear, and MRI made it possible to measure the maximum diameter of

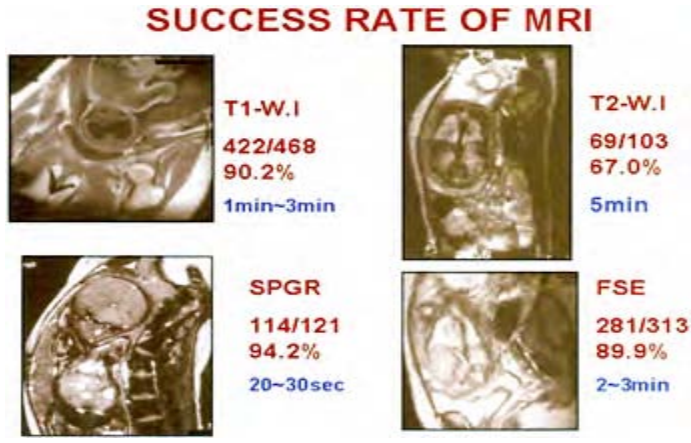

Figure 44.9: Success rate of fetal MRI. We performed fetal MRI without any drug use in the mother or fetus. The success rate of fetal MRI depended on the imaging time

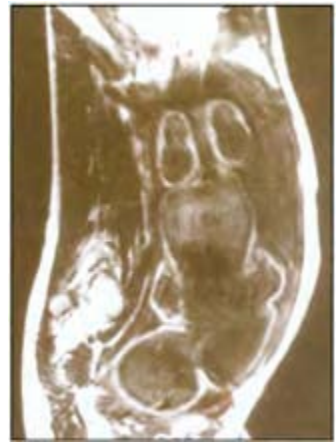

Figure 44.10: Cystic hygroma, T1-weighted image. From below the fetal ear to the shoulder, a

huge tumor was delineated in low intensity. We measured the maximum fetal diameter, including the tumor

the fetus, including the cystic tumor. This information was useful in deciding how to perform the delivery and choosing the shape of the uterine

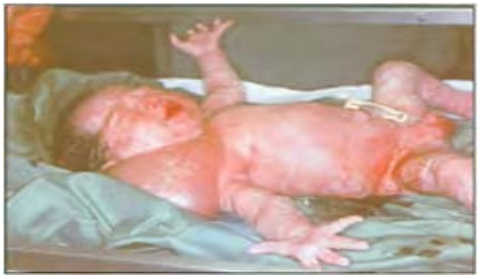

Figure 44.11: Cystic hygroma at birth. Macroscopic findings of the baby at birth. It is easy to see how good the information provided by MRI was

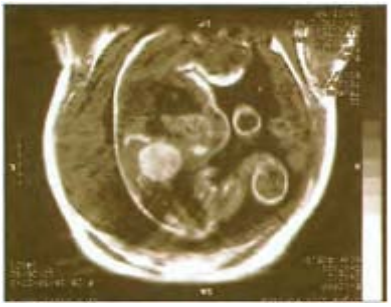

Figure 44.12: Fetal ovarian tumor, T1-weighted image. Fetal

ovarian tumors are usually delineated with low intensity because they are serous tumors arising due to hormonal stimulation from the mother. However, this tumor shows high intensity

incision at cesarean delivery. The quality and usefulness of MRI is clear from the findings of the baby at birth (Fig. 44.11).

The usefulness of MRI for imaging fetal structural anomalies is easily demonstrated. However, MRI also has the ability, unlike USG, to characterize tissues based on the differences of signal intensity that depend on the macromolecules in the tissue under various pulse sequences.[9] Figure 44.12 shows a case of fetal ovarian tumor. Usually fetal ovarian tumors result from maternal hormonal stimulation. Such tumor must be a simple

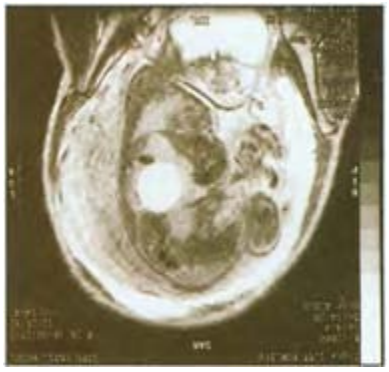

Figure 44.13: Fetal ovarian tumor, T2-weighted image. The tumor is delineated with remarkably high intensity. From this image and it of the Figure 44.10, the contents of tumor must be fat or blood

cystic tumor. However, this MRI showed high-intensity and low-intensity parts in the center of the tumor on the T1-weighted image. The tumor also showed high-intensity on the T2-weighted image (Fig. 44.13). These findings are quite different from those of serous cystic tumors and indicated that the contents of the tumor might be fat or blood.

We then determined the fat-suppressed T1-weighted image which could eliminate the signal from fat tissue (Fig. 44.14).[10] The tumor

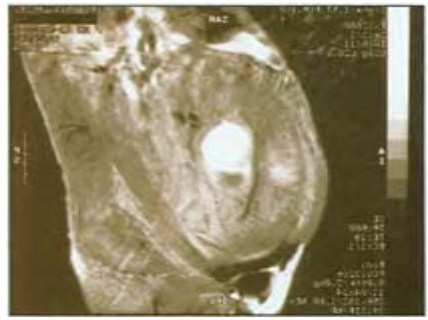

Figure 44.14: Fetal ovarian tumor, fat-suppressed T1-weighted image. While the color of the maternal and fetal skin was changed from white to black, the tumor was still delineated in high intensity. We therefore concluded that this tumor was a hematoma

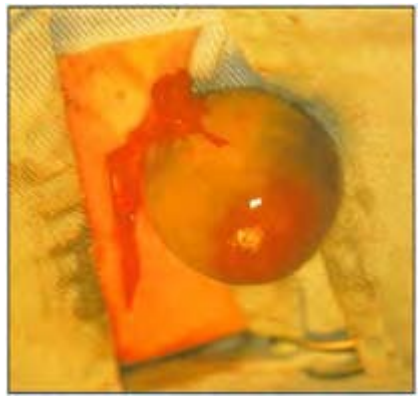

Figure 44.15: Macroscopic findings of the tumor. The

macroscopic findings of this tumor during surgery revealed that it contained 12 ml of degenerated blood

was still delineated with remarkably high intensity, which was consistent with subacute bleeding in the tumor and suggested that there was torsion in the tumor. Operative findings after birth revealed 12 ml of dark-colored blood in the ovarian tumor (Fig. 44.15).

Figure 44.16 shows an SSFSE image of a malformed fetus diagnosed with body-stalk anomaly. The problem of this fetus can be clearly determined from this image. Since MRI is computerized

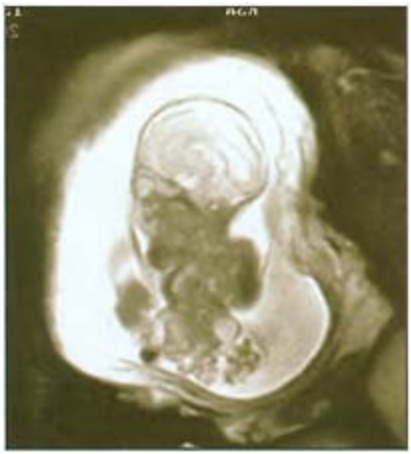

Figure 44.16: Body-stalk anomaly—SSFSE. Severe fetal condition is demonstrated on this image

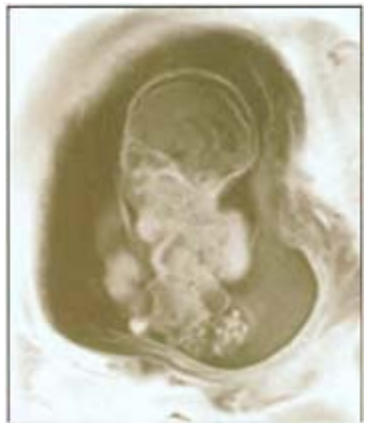

Figure 44.17: Body-stalk anomaly—color-inverted SSFSE. By the technique of color inversion, the color of the amnion was changed from white to black. This image is similar to that obtained by USG, which is more easier to perform for evaluating problems of malformed fetuses

imaging, color inversion can be performed, and we recommend it, as in MRI hydrography, because it makes it much easier to understand what is wrong in cases such as this case, because the signal of the amnion changes from white to black upon color inversion (Fig. 44.17).[11] This image is basically the same as that obtained by USG. The fetal brain is one of the most suitable organs for analysis by MRI.[12] Using the color inversion technique, MRI reveals the fetal brain structure much more clearly than USG, especially for evaluation of the brainstem (Fig. 44.18).

Diaphragmatic herniation is a severe fetal problem because it requires immediate respiratory management after birth. This fetal problem is first suspected based on USG findings. We show MRI findings of this malformation in Figure 44.19. This image clearly reveals that the fetal intestine has herniated into the thoracic cavity. Figure 44.20 also shows a case of suspected diaphragmatic herniation. However, the lower margin of the left lung is sharply delineated and the small intestine remains in the abdominal cavity. We concluded that this case was a diaphragmatic problem, but

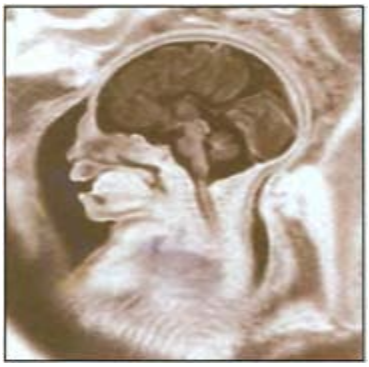

Figure 44.18: Fetal brain, color-inverted SSFSE. The color inversion technique makes clear the findings of the fetal brain. MRI provides high quality image of brainstem which is not easy to detect by USG

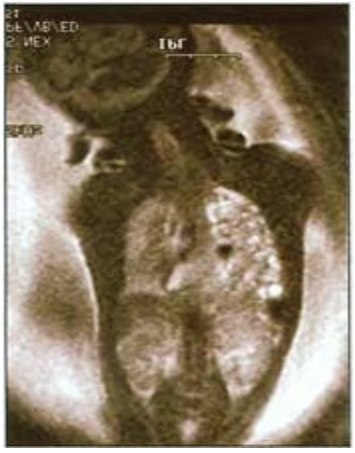

Figure 44.19: Diaphragmatic herniation—SSFSE. MRI revealed the fetal intestine herniated into the thoracic

cavity. It also clearly revealed the size and shape of the fetal right lung

eventration rather than herniation. These images also revealed differences of the findings of the right lung. The right lung in Figure 44.20 was far smaller than that in Figure 44.19. Actually, the outcomes

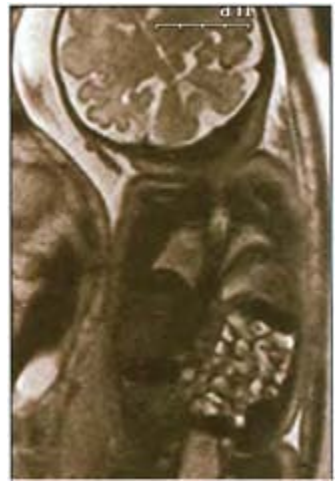

Figure 44.20: Diaphragmatic eventration—SSFSE. The small intestine remained in the abdominal cavity, and the lower margin of the left lung was seen sharply and clearly. These findings are quite different from those of diaphragmatic herniation. We concluded that this was a case of diaphragmatic eventration.

of these two fetuses was opposite: survival and death before surgical treatment in the cases Figures 44.19 and 44.20, respectively. We speculate that the size of the lung may

be a marker of lung hypoplasia. In any case, it seems possible to make differential diagnosis between diaphragmatic herniation and diaphragmatic eventration by MRI.

In our experience, almost half of fetal anomalies could be diagnosed using only USG and the indications for MRI for prenatal diagnosis are limited. However, it is important to note that 12.9% of such cases required MRI (Fig. 44.21).

Placenta

The most common reason for imaging of the placenta is to detect an anomaly of its location, namely placenta previa. However, transvaginal USG is much more convenient than MRI simply detect the location of the placenta.

Placenta percreta is a rare but terrible placental problem.[13] Figure 44.22 shows the MRI findings

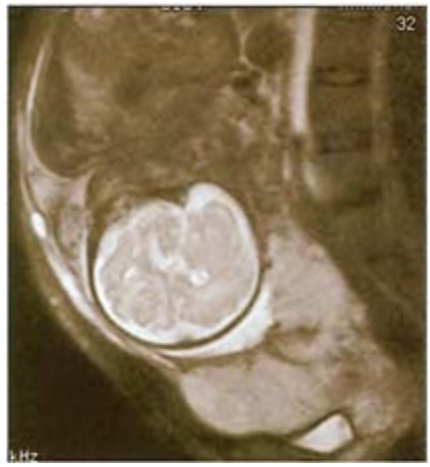

Figure 44.21: Usefulness of MRI, based on our data. In almost half of the cases, MRI was not necessary. On the other hand, the diagnosis of 12.9% of fetal anomalies required MRI. Thus, there are limited but definite indications for the use of MRI to diagnose fetal anomalies is limited

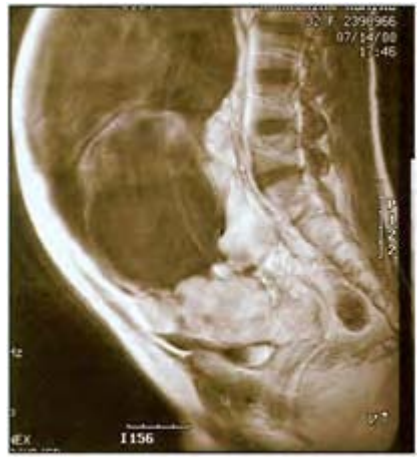

Figure 44.22: Placenta percreta—SSFSE. Deformity of the lower segment of the uterus and discontinuity of the uterine wall are revealed

of placenta percreta. It clearly revealed important findings, including deformity of the lower segment of the uterus and discontinuity of the uterine wall. We also obtained enhanced images (Fig. 44.23).

Figure 44.23: Placenta percreta, enhanced T1-weighted image. By administrating contrast medium, it became clear

that part of the cervix was also invaded by the placenta

They showed deformity of the uterine cervix and revealed that the placenta invaded into the uterine muscle. We had to perform a hysterectomy immediately after cesarean delivery. The macroscopic finding presented on Figure 44.24.

Is MRI useful for diagnosis of fetal anomaly?

(Analysis of 202 cases)

48.5% (98/202)	**Possible to diagnose by USG MRI is not necessary.**
38,6% (78/202)	**MRI helps precise diagnosis.**
12.9% (26/202)	**MRI is necessary.**

Figure 44.24: Macroscopic findings of placenta percreta. We performed hysterectomy immediately after cesarean delivery. The lower segment of the uterus and the cervix were displaced due to invasion by the placenta

CONCLUSION

USG or MRI: which is better for the diagnosis of mother or fetus? This is a very common question.[14] Nobody can deny the usefulness of USG during pregnancy, but this excellent imaging technique is not perfect. When we cannot get useful information about the mother or fetus using USG, we really need some tool not subject to the weak points of USG in order to obtain information vital for the health of the mother and fetus. As we mentioned above, MRI has the ability unlike USG to provide information different from that obtained using USG and useful for diagnosis of anomalies during pregnancy. Of course, MRI is not always superior to USG: indications for MRI during pregnancy are limited but definite. MRI is in general useful as a tool further evaluation of problems that are first detected by USG. When MRI is performed in such cases, we must consider the purpose of the MRI and according determine the appropriate procedure that would provide the most precise and useful diagnostic information.

REFERENCES

1. Geard CR, Osmak RS, Hall EJ et al. Magnetic Resonance Imaging and ionizing radiation: A comparative evaluation in-vitro of congenic and genotoxic potential. Radiology 1984; 152:199.
2. Harada S, Itabashi M. Intravenous Teratology Study of DV-7572 in Rats-Additional Investigation. Jpn Pharmacol Ther 1983; 21(3):123–42.
3. Garel C, Brisse H, Sebag G et al. Magnetic resonance imaging of the fetus. Pediatr Radiol 1998 Apr; 28(4): 201–11.
4. Michel SC, Rake A, Treiber K et al. MR obstetric pelvimetry: effect of birthing position on pelvic bony demension. Am J Roentgenol 2002; 179(4):1063–67.
5. Sporri S, Thoney HC, Raio L et al. MR imaging pelvimetry: a useful adjunct in the treatment of women at risk for dystocia? Am J Roentgenol 2002; 179(l):137–44.
6. Moise KJ. The use of fetal neuro-muscular blockade during intrauterine procedure. Am J Obstet Gynecol 1987; 157:874–78.
7. Ferrucci JT. Advance in abdominal MR imaging. Radiographicsl998; 18(6):1569–86.
8. Chung HW, Chen CY, Zimmerman RA et al. T2weighted fast MR imaging with true FISP versus HASTE: comparative efficacy in the evaluation of normal fetal brain maturation. Am J Roentgenol 2000; 175(5):1375–80.
9. Kawabata I, Imai A, Tamaya T. Antenatal subdural hemorrhage causing fetal death before labor. J Gynecol Obstet 1993; 43:57–61.
10. Adamek HE, Weitz M, Breer H et al. Value of magnetic-resonance cholangio-pancreatography (MRCP) after unsuccessful endoscopic-retrograde cholangio-pancreatography (ERCP). Endoscopy 1997; 29(8):741–44.
11. Jara H, Barish MA, Yucel EK et al. MR hydrography: theory and practice of static fluid imaging. Am J Roentgenol 1998; 170(4):873–82.
12. Merzoug V, Ferey S, Andre Ch et al. Magnetic resonance imaging of the fetal brain. J Neuroradiol 2002; 29(2):76–90.
13. Lam G, Kuller J, McMahon M. Use of magnetic resonance imaging and ultrasound in the antenatal diagnosis of placenta accreta. J Soc Gynecol Investig 2002; 9(1):37–40.
14. Elias P, Zizka J, Balicel P. Current triad: S and MRI diagnosis in the fetus and mother. Perinat Diagn 2002; 22(11):1005–10.

Section 3
Gynecology

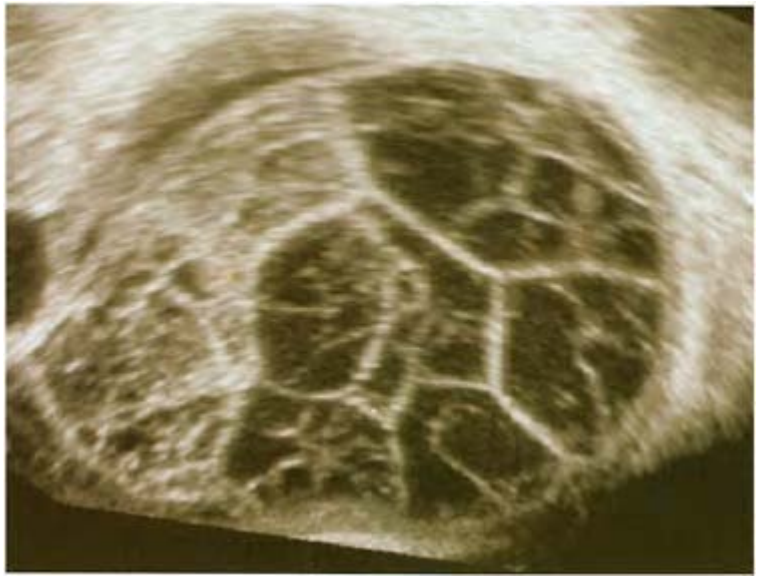

Chapter 45
Normal Pelvic Anatomy Assessed by Ultrasound Methods

Sanja Kupesic, Asim Kurjak, Ana Tripalo

INTRODUCTION

In computer evolution, ultrasonographic diagnostics found good ally. In the last decades ultrasonographic images evoluted from A mode over the 2D B mode to the 3D and 4D computer reconstruction of ultrasonic waves. As the result of this development, we got the possibility to look into the pelvis and obtain high quality real time picture.

Ultrasonographic examination during the reproductive period is most often performed by transvaginal probe. Transvaginal examination starts by placing ultrasonographic gel on the top of the probe and covering it with the condom. Probe is inserted through the introitus into the vagina. Properly placed probe can be manipulated in the coronal and sagittal planes and on the screen we are able to observe the organ in the coronal and/or sagittal section. It is important that patient voids before the examination, because the full urinary bladder may displace the uterus making detailed examination difficult.

Ultrasonographic examination could also be performed by transabdominal, transrectal and transperineal route.

PELVIC ANATOMY

Pelvic bones form firm hoop where uterus, ovaries, Fallopian tubes, vagina, urinary bladder, ureters and part of the colon are placed.

Uterus is a pear-like organ positioned between the urinary bladder in front and the rectum behind it. Uterus has its corpus (body of the uterus) and cervix, having a 2:1 length ratio. Dimensions of the body are commonly 7.5–9 cm length ×4.5–6 cm width×2.5 4 cm thickness. Normal uterine size varies with parity, but after postpartal involution, it stabilizes at an increase of approximately 1.5 cm in all directions.[1] Dimensions of the cervix are 2.5 cm length and 2.5 cm diameter. Cervix presents uterine communication with outer world. The cervix is a cylinder-like structure that consists of a fibrous and elastic connective tissue and smooth muscle. It constitutes a lower third of the uterus in an adult, while in childhood cervix accounts for two-thirds of the uterine length.[2] Since cervix connects upper part of the vagina with the uterine cavity, it serves as a depot for spermatozoa, allowing their migration towards the uterine ostia. After rupture of the follicle and due to the drop of the estrogen level, the cervical canal is closed again.

The entire uterus (its long axis) is bent by threequarters of women towards the symphisis (anteversio) and in relation to cervix closes angle 90°135° towards symphisis (anteflexio). On contrary, when the uterus is bent towards the rectum, it is named

retroversio and in relation to the cervix, uterus closes angle 90°-135° towards the sacrum (retroflexio).

Uterus has a thick muscular-walled body (myometrium) lined internally with columnar epithelium (endometrium) that undergoes changes in addition to the part of the menstrual cycle and age of the female patient. Uterus is supported by uterosacral ligament and the peritoneum is draped over the uterus. The space formed between the uterus and the rectum is the rectovaginal pouch of Douglas. The fold of peritoneum laterally from the uterus in which Fallopian tubes are positioned is known as broad ligament.

Uterine vascularization is complex. The main uterine arteries[3] originate from the internal iliac arteries, and they give off branches, which penetrate in outer third of the myometrium thickness without significant branching. Further, they subdivide into an arcuate wreath encircling the uterus. From this network, smaller branches, called the radial arteries, arise, directed towards the uterine lumen. The radial arteries branch into basal arteries and endometrial spiral arteries as they pass the myometrial-endometrial border. Basal arteries, that are relatively short, terminate in the capillary bed that serves the basal layer of the endometrium. The spiral arteries project further into the endometrium and terminate in a vast capillary network that serves the functional layer of the endometrium. Only spiral arteries undergo substantial anatomical changes during the menstrual cycle.[4] At the time of menstruation, probably because of decreasing estrogen and progesterone levels, the spiral arteries constrict.

Fallopian tubes are tube-shaped organs that origin from the lateral uterine angles toward the corresponding ovary. The Fallopian tubes are approximately 10 to 12 cm long and few millimeters wide. Fallopian tubes consist from dilated part with fimbria positioned most laterally to the ovary (infundibulum), ampular part (5 cm long, meandering with thin walls, varying in diameter), isthmic part (2 cm long) and intramural part (passing through myometrium).

Ovaries present pair of endocrine female sex glands in which follicles develop during the reproductive age. Ovaries are positioned on each side of the cervix, close to the lateral wall of the pelvis in fossa Waldeyer (delimited with ureter and internal iliac vessels). Ovaries are connected with peritoneal leaf -mesovaricum with the backside of the broad ligament. In the direction to the uterus, ovaries are connected with ligamentum ovarii proprium, and ligamentum suspensorium ovarii connects them with the Fallopian tubes. Normal ovaries are ellipsoid in shape, with dimensions approximately 3×2×2 cm in reproductive age. The number of primordial follicles present in the ovaries is inversely proportional to the woman's age. Approaching the menopause, the supply of endocrine responsive follicles becomes depleted causing cycle irregularities. About 7 million of the follicles containing oocytes are present in a female fetus at about 20 weeks gestation.[5] These follicles, called primordial, are microscopic in size and metabolically quiescent. Later in childhood, reproductive age or during oral contraception therapy, they grow from primordial to primary, secondary and tertiary follicles (microscopic in size) forming a fluid-filled antrum. In adequate hormonal conditions (increased local follicle stimulating hormone-FSH levels), follicles continue to grow. Only 100 to 1000 follicles are left until the menopausal period. Most of them are going through the process of atresia, and only some of them ovulate. The small and transient rise in FSH serum levels at the end of each ovarian cycle affects the small antral follicles (size of 1 or 2 mm). These follicles have a

potential to grow further instead to become atretic. During the early follicular phase of the ovarian cycle, hypophyseal FSH affects follicular cells to secrete estradiol and peptide hormone inhibin (reduces FSH production as the follicular phase progresses). The smaller follicles go to regression with the drop in FSH levels, while the larger ones grow regardless. Sometimes two follicles become dominant, producing the substantial amount of estradiol as they grow, while the others become atretic. This turnover happens by the end of the first week of the follicular phase. Atretic follicles can still be visible and can grow, especially in the dominant side, although they are undergoing atresia.

The ovarian vascular system is divided into external and internal part. The external vascular system consists of arteries that start from big abdominal trunks before they enter the ovary and the homologous venous system. Vessels that enter the gland from the ovarian hilus form the internal vascular system. These vessels give rise to the microcirculation and form venous drainage.[6] The cyclic changes of the ovarian vascularization are manifested most intensively in the internal vascular system. The ovary receives its arterial vascularization from two arteries: the ovarian artery and the utero-ovarian branch of the uterine artery.[7] These arteries anastomose, forming an arch parallel to the ovarian hilus, and constitute the vascular genital arcade. The vessels sprouting from the arcade run through the central medullar part of the stroma towards the periphery. In the ovarian cortex, the vessels form vascular arcades in the stroma, surrounding the follicles. In the development of an ovarian follicle during the menstrual cycle, a rich, irregular capillary plexus is progressively formed in the connective tissue layer or theca surrounding the avascular granulosa cell layer of the ovarian follicle. Several hours before ovulation, vessels penetrate the granulosa cell layer. Following ovulation, there is proliferation of the vessels of the theca layer further vascularize the granulosa cell layer and theca cells merge to form the corpus luteum. Within three or four days after the follicular rupture, the corpus luteum is supplied with a dense, multilayered network of sinusoidal capillaries that are drained by numerous superficial venules.

POSTMENOPAUSAL STATE

The size of the cervix and the body of the uterus decreases gradually as menopause progresses. Uterus measures approximately 4.5 cm length × 1.5 cm width × 2.5 cm thickness. Body of the uterus shortens and uterus body/cervix ratio increases almost to 1:1. There is a slight difference between women who are obese or using HRT and other postmenopausal women. Uterus body/cervix ratio is falling much slower in the first group than in second. Due to progressive decrease of the ovarian function in postmenopausal women, the endometrium becomes thin and atrophic not subjected to cyclic changes.

In perimenopausal phase ovarian follicular depletion starts, diminishing the number of antral follicles for recruitment, resulting in lower production of follicular inhibin, and sooner increase of FSH levels (during the late luteal phase) causing earlier start of follicular development (before menstruation takes place). As menopause is approaching, the follicular phase and consequently menstrual cycle get shorter. During the perimenopausal years, it is common to have functional cysts and/or multifollicular appearance of the ovaries. During the postmenopausal period, estrogen and inhibin production falls, resulting in an increase of the FSH levels. The ovaries become small and

homogenous with altered shape, volume and echogenicity. They are ovoid shaped through the next 5 years with significant decrease of the volume. At this time ovaries measure 2 cm × 1.5 cm × 1.5 cm, with maximum volume of 7 cm^3.

NEWBORN AND PREPUBERTY

The newborn *uterus* is tubular in shape with body and cervix length ratio 1:1, poorly differentiated. It can be 0.5 1 cm larger than the uterus in infants because of residuals of pregnancy hormones. Dimensions of the uterus in infants are approximately 3 cm length × 2 cm width × 2 cm thickness, tubular shaped with the same length ratio as in newborn.

During puberty period shape of the uterus changes and corpus enlarges resulting in an adult shape.

The ovaries in newborn period are small sized with small primordial follicles. The ovaries continue to decrease in size for the first two years of childhood and than start growing slowly through the childhood. We can distinguish two periods of the rapid growth: at around 8 years of age during the time of adrenarche and gradually rising levels of FSH; and before and during puberty. It is documented that tall girls have ovaries larger than average.[8]

MENSTRUAL CYCLE

During the reproductive period, all pelvic organs (their size and echogenicity) are changing due to cyclic changes in blood circulating hormone concentrations related to the ovary function. The most obvious changes are evident in the uterus, especially endometrium. Duration of the normal menstrual cycle is 28 days, with about equal time for the preovulatory (follicular) and postovulatory (luteal) phase. In women with normal fertility, duration of the menstrual cycle can vary with the range between 25 and 36 days with variable follicular phase (proliferative phase of the endometrium) and invariable, 14 days long the luteal phase (secretory phase of the endometrium).

Approaching the menopause, the follicular phase becomes shorter, shortening the whole menstrual cycle and bringing the time of ovulation sooner.

PHASES OF THE MENSTRUAL CYCLE ASSESSED BY 2D US

Uterus

Endometrium undergoes changes during the menstrual cycle. Measurement of the endometrial thickness should be performed by transvaginal probe in the sagittal plane of the uterus and should include both anterior and posterior portions of the endometrium (anterior and posterior layer). The hypoechoic part around endometrium presents inner layer of the myometrium and should be excluded from the measurement. The endocervical canal is seen as continuation of the endometrial echo. For most of the patients who do not have significant amount of intraluminal fluid, the endometrium is measured as a double-layer thickness from the proximal myometrial-endometrial junction to the distal myometrial-endometrial junction. The examiner should be careful if

intraluminal fluid is present. Measurement in that case is performed in a way that each endometrial leaf is measured separately, and both layers than summarized with stressing on existence of free fluid within the uterine cavity.

Proliferative Phase

As menstruation ceases, the functional layer of the endometrium responds to small amounts of estrogen secreted by the ovary. Simultaneously with follicular development and rising estrogens production, the endometrial glands in basal layer start to proliferate, elongate and become tortuous.

The image of the early proliferative phase endometrium is a thin echogenic line, measuring 1 to 3 mm. With the progression of proliferative phase, the echogenicity of endometrium decreases in comparison with the surrounding myometrium. The most characteristic sign of the late proliferative phase is the triple-line endometrium (Fig. 45.1). The central echogenic line represents touching of the anterior and posterior endometrial layers. The outer hyperechogenic lines represent endometrialmyometrial junction or echo of the basal layer. The functional layer of endometrium between the two lines becomes hypoechoic and thick during the proliferative phase. The endometrial thickness is normally 4 to 8 mm in the proliferative phase and 8 to 12 mm during the periovulatory period.[9]

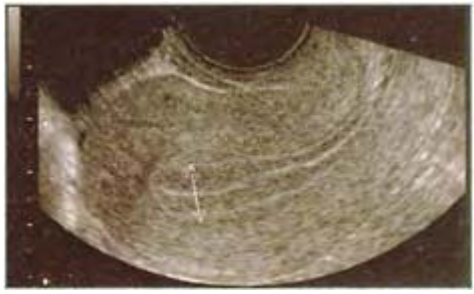

a

Figure 45.1: Transvaginal scan of a triple-line endometrium during a late proliferative phase of the menstrual cycle

Secretory Phase

Progesterone secretion during the luteal phase of the ovarian cycle after ovulation differentiates endometrial glands for secreting glycoproteins. Increased glycoprotein secretion causes disappearing of the three lines present in the late proliferative endometrium. On ultrasound examination,

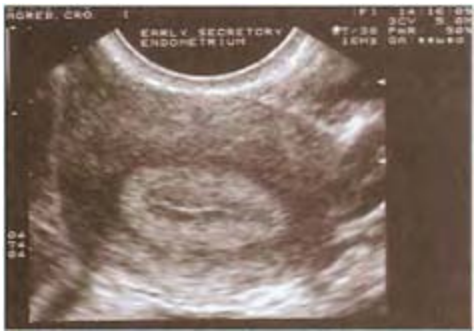

Figure 45.2: Transvaginal scan of a thickened and echogenic endometrium during the luteal phase of the menstrual cycle

the endometrium appears as a homogenous and hyperechogenic layer measuring 8 to 14 mm and stays unchanged till the beginning of the menstrual bleeding or further development of pregnancy (Fig. 45.2).

If pregnancy occurs, echogenicity and thickness are maintained as decidual reaction to implantation starts to progress. If not, endometrium starts to regress in thickness, but not in echogenicity.

Menstrual Phase

Menstruation begins when circulating levels of estrogen and progesterone decrease at the end of the ovarian cycle, causing break down of the functional layer. Ultrasound image varies depending on the amount of blood clots and endometrial fragments, which can be seen as echogenic debris. Basal layers are imaged as thin, irregular, and hyperechogenic lines.

Cervix

The mucus in the endocervical canal is viscous and echogenic, except at the time of ovulation, when it is diluted and seen as an echolucent area on ultrasound examination.

Nabothian cysts are retention cysts of the cervical glands within the intravaginal portion of the cervix undergoing metaplasia from columnar to stratified squamous epithelium. They measure approximately 10 mm in diameter with thin walls and spherical shape containing echolucent fluid. Nabothian cysts have no clinical value even when they are multiple and large, they represent common finding and are not affected by cyclic changes.

Ovaries

The dominant follicle, also called Graafian follicle, is usually detected at 10th day of menstrual cycle (proliferative phase). At that time it measures approximately 10 mm and

increases in size 2 3 mm/day until it reaches about 18 22 mm in size. After that, progressive growth decelerates to 1.3 mm/day.[10] Follicle grows due to increased number of follicle cells and accumulation of fluid inside the follicle cavity (antrum).

Ovulation occurs with dissolution of the part of the follicle wall, liberation of the oocyte and escape of the follicular fluid into the peritoneal cavity that can be easily detected during ultrasound examination as anechogenic accumulation of fluid in retrouterine space. It takes place about 38 hours after the luteinizing hormone (LH) surge begins, as a consequence of pituitary respond to high circulating estrogen levels. At that time, the dominant follicle is 16 23 mm in diameter. Ruptured follicle is now filled with blood and forms first corpus hemorrhagicum, and afterwards corpus luteum. Besides the free fluid imaged on ultrasound, ovulation is presented as sudden disappearance of the echolucent dominant follicle, and after several days formation of the corpus luteum. Corpus luteum begins to secrete progesterone with formation of new blood vessels surrounding the follicle. Commonly, corpus luteum is visualized as a structure containing thick hyperechogenic walls enclosing the hypoechoic center. It can be 5 to 6 cm in diameter, and due to its clot component can be misinterpreted as an endometrioma. Sometimes, corpus luteum can also be hardly seen on transvaginal ultrasound due to the variety of ovarian echogenicity. Because of its atypical ultrasound finding it is called “the great pretender”. If the corpus luteum does not disappear after 2 weeks and is filled with serous fluid, it is called corpus luteum cyst. If luteinization takes place, but the dominant follicle does not release follicular fluid and the oocyte, growing continues toward a diameter of about 3 cm with echogenic or lucent contents. Formed structure is called luteinized unruptured follicle (LUF syndrome). Luteinized unruptured follicles occur in about 5% of normal menstrual cycles and in a higher proportion of abnormal cycles. Progesterone production in LUF syndrome is usually lower comparing to normal subjects, and luteal phase is shorter in relation to controls.

Dominant follicular development is not always sustained by ovulation, especially in early reproductive age when ovulation does not occur, and consequently the entire menstrual cycle becomes longer and irregular (oligomenorrhea or amenorrhea). If ovulation does not occur, the follicle continues to grow resulting in a formation of the follicular cyst. On ultrasound scanning it is demonstrated as a thin-walled cystic lesion filled with lucent fluid, well demarcated from the rest of the ovary which usually regresses spontaneously. If multifollicular appearance of the ovaries means persistence of variable sized developing follicles, some of them are functioning and some atretic. Multifollicular appearance can be normal during adolescence and recovery from weight loss, but in older women is associated with significant ovulation disorder of primarily ovarian origin and/or beginning of the ovarian failure.

Fallopian Tubes

Intramural part of the Fallopian tubes could be visualized by 2D ultrasound as a fine echogenic line arising from the endometrial canal and through the uterine wall. Other parts of the Fallopian tubes could be visualized only in case of tubal pathology.[11] The vascular supply of the tubes is from vascular arch that passes through the mesosalpinx and is formed by the anastomosis of the uterine and ovarian arteries.

COLOR DOPPLER ASSESSMENT OF THE PELVIC BLOOD FLOW

Blood flow in the main pelvic vessels can be easily visualized and recognized. The color Doppler signal from the *main uterine* vessels can be observed as lateral to the cervix at the level of the cervicocorporeal junction.[12,13] Pulsed Doppler waveform profiles of the main uterine artery are characteristic, comprising a high peak-systolic component with a characteristic notch in the protodiastolic part of the cardiac cycle and very low end-diastolic flow (Fig. 45.3). The resistance index varies, because of increased uterine flow associated with estrogen. Uterine artery RI is about 0.88+/− 0.04 in the reproductive age group, and in postmenopausal women is statistically higher and measures 0.89+/− 0.06 and increases with years after menopause.[14]

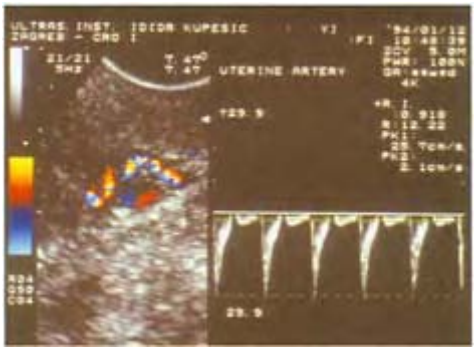

Figure 45.3: Transvaginal color Doppler analysis of the uterine artery blood flow in the proliferative phase of the menstrual cycle. Note a small amount of enddiastolic flow and a characteristic notch (RI=0.92)

Steer and co-workers[15] reported that diastolic flow in the uterine arteries disappear during the day of ovulation. An increasing resistance index and systolic/diastolic ratio during the postovulatory drop in the serum estradiol concentration may be explained by increased uterine contractility[16] and compression of the vessels traversing the uterine wall that decrease their diameter and cause consequently higher resistance to flow. During the

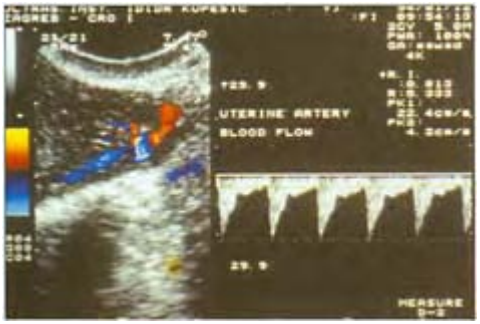

Figure 45.4: Uterine artery blood flow in secretory phase of the menstrual cycle is characterized with sharp increase of an end-diastolic blood flow leading to decrease of the resistance index (Rl=0.81)

normal menstrual cycle there is a sharp increase in end-diastolic velocities between the proliferative and secretory phases of the menstrual cycle. It is interesting that the lowest blood flow impedance occurs during the time of peak luteal function, during which implantation is most likely to occur (Fig. 45.4). It is logical that blood supply to the uterus should be in its maximum in the late luteal phase, as has been reported by Kurjak and colleagues,[16] Goswamy,[17] Battaglia[18] and Steer[15] and their associates. In anovulatory cycles these changes are not present, and a continuous increase in the resistance index is seen. The persistently lower RI in the luteal phase suggests that the relaxation effects on the uterine arteries persist until the onset of menstruation.

The increased endometrial vascularity is highly dependent upon the uterine, arcuate and radial artery blood flow. Doppler sonograms of the arcuate and radial arteries are very similar, with moderate peak-systolic and diastolic components of blood flow. However, differences exist in the values of the resistance (RI) or pulsatility (PI) indices.

The spiral arteries can be visualized in the functional zone of the endometrium in the proliferative phase.[19] The RI of the spiral arteries changes from approximately 0.64 in the follicular phase to 0.50 in the luteal phase (Fig. 45.5).[15]

Blood flow velocity waveform changes in the spiral arteries during normal ovulatory cycles are characterized by lower velocity and lower impedance to blood flow than are those observed in the uterine arteries, with a larger diameter.[18]

Uterine venous channel follows a course similar to that of the arteries.[20] The venous plexus is larger than associated arterial channels and is frequently identified sonographically by both transabdominal and transvaginal approach.

Ovarian arterial blood flow varies according to the stage of the menstrual cycle and patient's age. Before formation of the dominant follicle flow is characterised by low

velocity and high resistance. During the growth of an ovarian follicle, a rich irregular capillary plexus is formed in the connective tissue or theca layer surrounding the avascular granulosa cell layer of the ovarian follicle. At this time RI in perifollicular vessels is 0.50–0.55 and presents important hemodynamic parameter of follicular growth (Fig. 45.6).[13,14]

Several hours before ovulation, vessels penetrate the granulosa cell layer. Reduction of vascular resistance in perifollicular capillaries is significant in the preovulatory phase and shows value of 0.42–0.48. The intrafollicular blood velocity increases 29 hours before the time of follicular rupture, continues for at least 72 hours after the

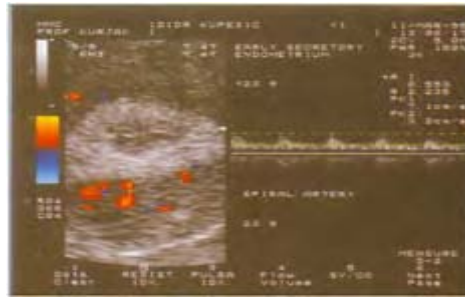

Figure 45.5: Spiral artery blood flow is characterized with significantly lower vascular resistance (Rl=0.55) than are those obtained in main uterine arteries

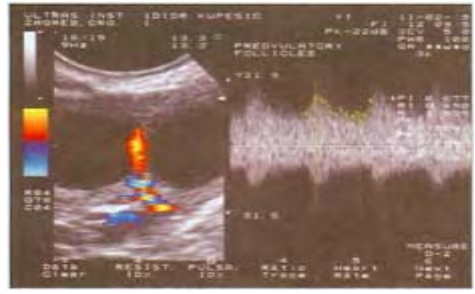

Figure 45.6: Transvaginal color Doppler scan of the preovulatory follicles. Note low-to-moderate

vascular resistance (Rl=0.49) indicative of high oocyte quality

formation of the corpus hemorrhagicum, and is reflected in the color Doppler data obtained at this time (Fig. 45.7). The mean changes in peak systolic velocity appear to follow the mean rise in circulatory LH by approximately 12 hours.[21] The resistance index remains at the same level for 4–5 days after the ovulation, and then gradually rises to 0.50+/− 0.04, still lower than the one measured in the proliferative phase.

The corpus luteum is supplied with a dense, multilayered network of sinusoidal capillaries that are drained by numerous superficial venules. Corpus luteum angiogenesis starts about 24 hours after the LH surge. Using color Doppler, the blood

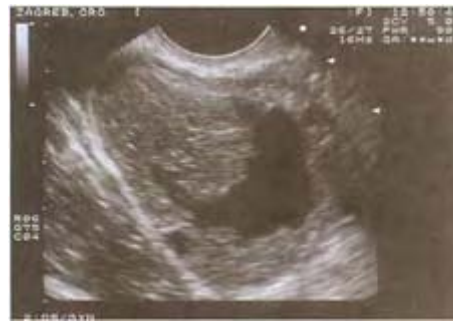

Figure 45.8: Transvaginal color Doppler scan of corpus luteum angiogenesis

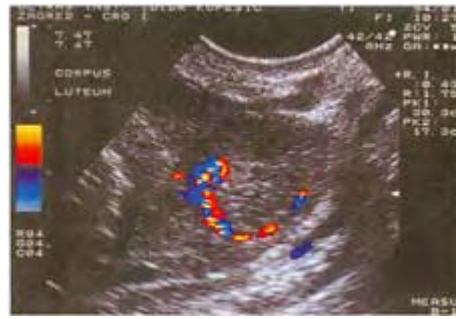

Figure 45.7: Transvaginal scan of an early corpus luteum. Note irregular hypoechogenic walls

enclosing hypoechoic center

supply to the corpus luteum can be clearly seen as a bright colored ring surrounding the corpus luteum and continues to be detectable through the entire functional life of the corpus luteum (Fig. 45.8). It is possible to distinguish three phases of the corpus luteum cycle depending on its vascularization:

1. Organization and vascularization (characterized with RI=0.43±0.04) (Fig. 45.9)
2. Maturation (characterized with RI=0.46± 0.03), and
3. Regression (characterized with RI=0.50± 0.04).

If the corpus luteum is filled with serous fluid and persists more than 2 weeks, it is called corpus luteum cyst.

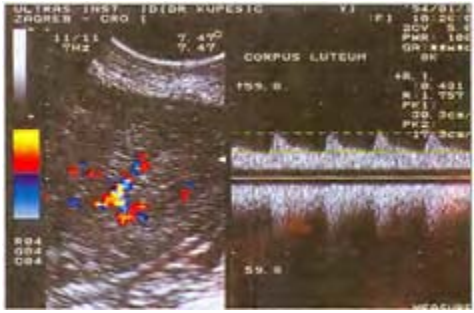

Figure 45.9: Transvaginal color Doppler scan of corpus luteum during stage of organization and vascularization. Low vascular resistance (Rl=0.43) indicates significant perfusion and adequate progesterone production.

Bourne et al[22] found that the changes in PI observed from the wall of the dominant follicle and corpus luteum were less marked than the changes in blood velocity. Kurjak and co-workers[13] detected a lower blood flow velocity waveform index in the dominant ovary during the luteal than in the follicular phase. These blood flow changes reflect changes in vascularization and function of the corpus luteum. The non-dominant ovary[22] presented a slightly higher blood flow velocity waveform index in the follicular and luteal phases. Higher blood flow velocity and lower impedance detected in the vessels of the dominant ovary in the late follicular and early luteal phase indicate increased blood supply to the dominant ovary. The increased blood flow to the ovary containing the dominant follicle and corpus luteum is necessary for delivery of steroid precursors during

the follicular phase and the removal of progesterone in the luteal phase of the menstrual cycle.

In both uterine and ovarian vessels, changes in flow velocity occur before ovulation, implying that these changes are complex and not entirely related to progesterone action. Many other vasoactive compounds (e.g. prostaglandin) are involved in the regulation of the ovarian circulation.

Although the diameter of the follicle is a relatively good predictor of oocyte maturity, it is not a perfect indicator of oocyte quality. Recent studies indicates that follicular vascularity indicated quality of the aspirated oocytes in patients undergoing in *vitro* fertilization.[10,21]

Postmenopausal State

Due to progressive decrease of ovarian hormones in postmenopausal women, the endometrium becomes thin and atrophic not subjected to cyclic changes leading to the mean endometrial thickness of 2.3±1.8 mm.[23] In postmenopausal state ovaries do not secrete estrogens, but still produce androgen hormones, which together with androgens derived from the adrenal glands are converted to estrogens in peripheral adipose cells. Production of estrogens at that way may be responsible for endometrial thickening and proliferation changes showed as hyperplasia or neoplasm. In women taking HRT one can tolerate maximum thickness of 8 mm. In patient receiving sequential HRT the endometrium changes according to the phase of the cyclical therapy. In continuous combined regimens, the endometrium is likely to be relatively thin. An endometrial thickness cut-off level of < 5 mm in a symptomatic patient seems to have a high negative predictive value for the presence of endometrial cancer.[6] Once the endometrial thickness is greater than 8 mm in asymptomatic postmenopausal women not taking HRT, an outpatient biopsy is required to exclude endometrial hyperplasia or malignancy.

Kurjak and Kupesic demonstrated that the RI uterine arteries of postmenopausal women increases with years after menopause.[13] The mean ovarian arterial RI in postmenopausal women is approximately 0.94 in the first 5 years of postmenopause. In older women absent diastolic flow corresponding to RI of 1.0 is usually obtained.[13]

Newborn and Prepuberty

In the childhood transabdominal, transrectal, or transperineal scanning is performed. Uterine length in neonates is 2.0 to 4.4 cm in length with thicker, more echogenic endometrium due to influence of high maternal estrogen levels from the placenta.[24] The size of the uterus does not change till the 7–8 years, but after the stop of maternal estrogen influence, endometrium gets thinner. Uterus starts to grow as said earlier at age 7–8 years, gets bigger during the puberty and approximately at age of 20 years reaches its maximum size.[25]

The ovaries grow slowly through the childhood, increasing in the mean ovarian volume from 0.5 cm^3 at the age of 3, to 2.8 cm^3 at the age of 18 years.[26]

The Role of 3D Ultrasound

Three dimensional ultrasound (3D US) is commonly used for evaluation of the uterine cavity.

It enables estimation of the uterine volume and gives the ability to simultaneously present planar sections of uterus in three different dimensions: transverse, sagittal and coronal. Three-dimensional ultrasound allows a non-invasive and accurate assessment of congenital uterine anomalies, because it provides more accurate spatial visualization and qualitative information on the endometrial cavity and myometrial portion than two-dimensional ultrasound (2D US).[27] Although 2D and 3D endometrial thickness and volume measurement show good reproducibility the reproducibility of 3-D ultrasound is much better than that of 2D ultrasound.[28] By stepping through the volume in multiplanar mode, the outer limits of endometrium are traced, and volume calculations can be performed immediately. The accurateness of this method has been well documented.[29]

Ovarian volume and plastic images of the ovary can be presented by using the 3D ultrasound reconstruction and measurement. The average ovarian volume measurement is between 6 and 10 cm^3 (maximum volume 14–16 cm^3).[30] 3D ultrasound facilitates precise ovarian volume calculation, determination of the antral follicle number, evaluation of the ovarian stroma volume and area, and analysis of the intensity of the ovarian stromal blood flow in a short time and with minimal discomfort for the patient.[31] In reproductive age, detection of cumulus oophorus is important because it virtually excludes empty follicle syndrome. Cumulus oophorus can also be seen by 2D ultrasound, but 3D ultrasound imaging is much more accurate in its' presentation.

3D power Doppler ultrasound enables reconstruction of complete vascularization of the ovary and distinguishes normal from pathological angiogenesis. Image of mesovarium vessels entering the hilus as well as their branches is easily presented during the preovulatory phase. Vessels are usually fewer showing regular type of branching.

By using 3D volume sections and reconstruction it is possible to visualize more precisely pathological processes in Fallopian tubes. Similarly,

Figure 45.10: Three-dimensional power Doppler scan of the regular tubal patency

demonstrated after injection of the echo-enhancing contrast. Note regular spillage of the contrast from the fimbrial end

using 3D power Doppler technology it is possible to visualize changes of the tubal vascularity in patients affected with Fallopian tube malignancy.

Sladkevicius and colleagues[32] presented colorcoded 3D-Power Doppler Imaging of the flow of the contrast through the entire tubal length and its' spill in the retrouterine space. The 3D-PDI method appeared to have advantages over the conventional HyCoSy technique especially in terms of visualization of the spill from the distal end of the tube (Fig. 45.10), which was achieved twice as often comparing to 2D technique.

CONCLUSION

Uterus is a pear-like organ positioned between the urinary bladder in front and rectum behind it. It contains of a corpus (body of the uterus) and cervix. Dimensions of the body are approximately 7.5–9 cm length × 4.5–6 cm width × 2.5–4 cm thickness. Using ultrasound it is possible to monitor the undergoing changes in addition to the part of the menstrual cycle and age of the female patient. Menstrual cycle is divided on proliferative or preovulatory phase, secretory or postovulatory phase and menstrual phase. In between the ovulation occurs. Changes are detectible in the uterus and within the dominant ovary. Ovaries are paired reproductive glands containing follicles, ellipsoid in shape, with dimensions approximately 3×2×2 cm in reproductive age.

In the dominant ovary, the dominant follicle, also called graafian follicle, is usually detected at 10th day of menstrual cycle (proliferative phase). At that time, it measures approximately 10 mm and increases in size 2–3 mm/day until it reaches about 18–22 mm in size. After that, its growth decelerates to 1.3 mm/day.

Ovulation occurs with dissolution of the part of the follicle wall, liberation of the oocyte and escape of the follicular fluid into the peritoneal cavity that can be easily detected during ultrasound examination as anechogenic accumulation of fluid in the retrouterine space. Ruptured follicle is now filled with blood and forms first corpus hemorrhagicum and afterwards corpus luteum.

Perifollicular vessels can be seen by color Doppler ultrasound during the proliferative phase of the menstrual cycle. At this time RI in perifollicular vessels is 0.50–0.55 and presents important hemodynamic parameter of the follicular growth. Several hours before ovulation, vessels penetrate the granulosa cell layer. Reduction of vascular resistance in perifollicular flow is significant in the preovulatory phase and shows values of 0.42–0.48. The resistance index remains at the same level for 4–5 days after the ovulation, and then gradually rises to 0.50+/− 0.04, still lower than the one measured in the proliferative phase.

After ovulation corpus luteum is formed. It is possible to distinguish three phases of the corpus luteum cycle depending on its vascularization:

1. Organization and vascularization (characterized with RI=0.43±0.04)

2. Maturation (characterized with RI=0.46± 0.03), and
3. Regression (characterized with RI=0.50± 0.04).

In proliferative or preovulatory phase, the image of the early proliferative phase endometrium is a thin echogenic line, measuring 1 to 3 mm. With the progression of proliferative phase, the echogenicity of the endometrium decreases in comparison with the surrounding myometrium. The most characteristic sign of the late proliferative phase is the triple-line endometrium. The endometrial thickness is normally 4 to 8 mm in the proliferative phase and 8 to 12 mm in the periovulatory period.

The color Doppler signal from the main uterine vessels can be observed as lateral to the cervix at the level of the cervicocorporeal junction of the uterus. Pulsed Doppler waveform profiles of the main uterine artery are characteristic, comprising a high peak-systolic component with a characteristic notch in the protodiastolic part of the cardiac cycle and very low end-diastolic flow. The resistance index varies since uterine flow is increased with estrogen production and changes during menstrual cycle. The increased endometrial vascularity is highly dependent upon the uterine, arcuate and radial artery blood flow. The spiral arteries can be visualized in the functional zone of the endometrium in the late proliferative and secretory phases.

Three dimensional ultrasound is especially useful for evaluation of the uterine cavity, since it allows simultaneous display of the three ortogonal planes: transverse, sagittal and coronal.

Ovarian volume and plastic images of the ovary can be presented using 3D ultrasound facilities, such as multiplanar imaging and surface reconstruction. 3D power Doppler ultrasound enables reconstruction of the complete vascularization of the ovary and distinguishes normal from pathological angiogenesis and neovascularization. By using 3D volume sections and reconstruction it is possible to precisely distinguish pathological processes of the Fallopian tubes from those occurring in the ovary. With help of 3D power Doppler it is possible to visualize alterations in tubal vascularity and patency.

REFERENCES

1. Ramsay PA, Jansen RPS. Ultrasonography of the normal female pelvis. In: Anderson JC (Ed). Gynecologic Imaging. Churchill Livingstone, London, 1999; 61–80.
2. Suren A, Puchta J, Osmers R. Sonographic evaluation of the cervix uteri. In: Osmers R, Kurjak A (Eds). Ultrasound and the Uterus. New York-London: Parthenon Publishing 1995;13–18.
3. Kurjak A, Kupesic S. Blood flow studies in normal and abnormal early pregnancy. In: Kurjak A, Kupesic S (Eds). An Atlas of Transvaginal Color Doppler (2nd ed). Parthenon Publishing, London 2000;41–43.
4. Templeton AA, Penney GC. The incidence, characteristics and prognosis of patients whose infertility is unexplained. Fertil Steril 1982;37:175–81.
5. Faddy MJ, Gosden RG, Gougeon A. Accelerated disappearance of ovarian follicles in mid-life: implications for forecasting menopause. Hum Reprod 1992;7:1342–46.
6. Nugent D, Smith J, Balen AH. Ultrasound and the ovary. In: Kupesic S, de Ziegler D. Ultrasound in Infertility. Parthenon Publishing, London, 2000; 23–43.
7. Higgins RV, Van Nagell JR Jr, Woods CH et al. Interobserver variation in ovarian measurements using transvaginal sonography. Gynecol Oncol 1990; 39:69–71.
8. Bridges NA, Cooke A, Healy MJR et al. Standards for ovarian volume in childhood and puberty. Fertil Steril 1993;60:456–60.

9. Lyons EA, Gratton D, Hamington C. Transvaginal sonography of the normal pelvic anatomy. Radiol Clin North Am 1992;30:663.
10. Kupesic S, Merce L, Kurjak A. Color Doppler studies from ovulation to implantation. In: Kurjak A, Kupesic S (Eds). An Atlas of Transvaginal Color Doppler (2nd ed). Parthenon Publishing, London, 2000; 15–27.
11. Levi CS, Holt SC, Lyons EA, Lindsay DJ, Dashefsky SM. Normal anatomy of the female pelvis. In: Callen PW (Ed). Ultrasonography in Obstetrics and Gynecology (4th ed), Philadelphia, 2000;781–814.
12. Kurjak A, Kupesic-Urek S. Normal and abnormal uterine perfusion. In: Jaffe R, Warsof LS (Eds). Color Doppler Imaging in Obstetrics and Gynecology. McGraw Hill, New York 1992;255–63.
13. Kurjak A, Zalud I. Normal pelvic blood flow. In: Kurjak A (Ed). Transvaginal Color Doppler. Parthenon Publishing, London 1991;25.
14. Funduk-Kurjak B, Ujevic B, Kurjak A. Ultrasound in postmenopausis. In: Kurjak et al (Eds). Ultrasound in Obstetrics and Gynecology. Art Studio Azinovic 2000;98–105.
15. Steer CV, Mills CV, Campbell S. Vaginal color Doppler assessment on the day of embryo transfer (ET) accurately predicts patients in an in vitro fertilization program with suboptimal uterine perfusion who fail to be pregnant. Ultrasound Obstet Gynecol 1991;! (Suppl), 79.
16. Kupesic S, Kurjak A. Uterine and ovarian perfusion CQO during the periovulatory period assessed by transvaginal color Doppler. Fertil Steril 1993;60:439–43.
17. Goswamy RK, Steptoe PC. Doppler Ultrasound studies of the uterine artery in spontaneous ovarian cycles. Hum Reprod 1988;3:721.
18. Battaglia C, Larocca E, Lanzani A, Valentini M, Genazzani AR. Doppler ultrasound studies of the uterine arteries in spontaneous and IVF cycles. Gynaecol Endocrinol 1990;4:245–50.
19. Applebaum M. The uterine biophysical profile. Ultrasound Obstet Gynecol 1995; 5:67.
20. Splanchology: Reproductive organs of the female. In: Willims PM, Warwick R (Eds): Gray's anatomy. Churchill Livingstone, Edinburgh, 1980; 1423.
21. Bourne TH, Athanasiou S, Bauer B. Ovulation and the Periovulatory Follicle. In: Bourne TH, Jauniaux E, Jurkovic D (Eds). Transvaginal Colour Doppler. (Springer-Verlag: Berlin Heidelberg), 1995; 119–30.
22. Ratmacher RP, Andersson LL. Blood flow and progesterone levels in the ovary of cycling and pregnant pigs. Am J Physiol 1986; 214:1014–18.
23. Kurjak A, Kupesic S. Ovarian senescence and its significance on uterine and ovarian perfusion. Fertil Steril 1995; 64:532–38.
24. Nussbaum AR, Sanders RC, Jones MD. Neonatal uterine morphology as seen on real-time ultrasound. Radiology 1986; 160:641.
25. Holm K, Laursen EM, Broks V. Pubertal maturation of the internal genitalia: An ultrasound evaluation of 166 healthy girls. Ultrasound Obst Gynecol 1995; 6:175.
26. Bridges NA, Cooke A, Healy MJR et al. Standards for ovarian volume in childhood and puberty. Fertil Steril 1993; 60:456–60.
27. Jurkovic D, Geipel A, Gruboeck K, Jauniaux E, Natucci M, Campbell S. Three-dimensional ultrasound for the assessment of uterine anatomy and detection of congenital anomalies: a comparison with hysterosalpingography and two-dimensional sonography. Ultrasound Obstet Gynecol 1995; 5:233–37.
28. Yaman C, Ebner T, Jesacher K, Obermayr G, Polz W. Reproducibility of 3-D ultrasound endometrial volume measurements in patients with postmenopausal bleeding. Ultrasound Obstet Gynecol 2002; 19(3):282–86.
29. Riccabona M, Nelson TR, Pretorius DH. Threedimensional ultrasound: accuracy of distance and volume measurements. Ultrasound Obstet Gynecol 1996; 429–34.
30. Higgins RV, Van Nagell JR Jr, Woods CH et al. Interobserver variation in ovarian measurements using transvaginal sonography. Gynecol Oncol 1990; 39: 69–71.

31. Kupesic S, Kurjak A. Predictors of IVF outcome by three-dimensional ultrasound. Human Reproduction 2002; 17(4):950–55.
32. Sladkevicius P, Ojha K, Campbell S, Nargund G. Three-dimensional power Doppler imaging in the assessment of Fallopian tube patency. Ultrasound Obstet Gynecol 2000; 16(7):644–47.

Chapter 46
Ultrasound of the Uterus

Sanja Kupesic, Asim Kurjak, Drazena Bjelos

INTRODUCTION

No single technique permits complete or precise evaluation of the pelvis. However, ultrasound remains the principal method for imaging the non-pregnant uterus. Pelvic imaging is used to determine whether or not a lesion is present and, if so, its site or origin and does it need biopsy or surgical removal. Ultrasound is the preferred method to assess the uterus due to patient tolerance, repeatability and cost. On the other side, magnetic resonance imaging (MRI) is used to a lesser extent and may clarify the ultrasound findings.

The uterus lies in the middle of the pelvis between the rectum and the bladder with its long axis perpendicularly to the ultrasound probe. Using two-dimensional (2D) ultrasound the examination of the uterine lesions is limited to transverse and sagittal planes, which give an inadequate view of the uterus and uterine pathology. Three-dimensional (3D) ultrasound provides simultaneous display of coronal, sagittal, and transverse planes. Volume data can be viewed using a standard anatomic orientation demonstrating entire volume and continuity of curved structures in a single image. More accurate evaluation of numerous sections through the studied organ becomes possible due to not limited number and the orientation of reformatted planes. When three perpendicular planes are simultaneously displayed on the screen, sagittal plane is chosen for volume measurements, while the other two planes are used to ensure that the entire pathology is included in the measurement. Surface rendering mode allows exploration of the outer or inner contour of the lesion, while “niche aspect” presents detection and analysis of the selected sections of the uterine lesion. Three-dimensional ultrasound offers improved visualization of the lesions, more accurate volume estimation, retrospective review of stored data, assessment of tumor invasion, and using rendered images it can identify more accurately location of abnormalities needing surgical intervention.

Three-dimensional sonohysterography is very useful in the evaluation of the uterine cavity and is more useful than hysterosonography by 2D transvaginal ultrasound in cases of submucous myomas and polyps.

The 3D power Doppler system improves the information available on normal and abnormal (tumoral) vascularity, enabling visualization of the overlapping vessels and assessment of their relationship to other vessels or surrounding tissue. Power Doppler

ultrasound compared to standard color Doppler has the advantage of more sensitivity to low velocity flow overcoming the angle dependence and aliasing. Using contrast agents it is possible to enhance the 3D power Doppler examination of small vessels.

In this chapter we will compare findings of uterine lesions assessed with conventional B-mode and transvaginal color Doppler ultrasound on one side and 3D and power Doppler ultrasound on the other.

NORMAL UTERUS

The components of the uterus are the cervix and the body, separated by a slight constriction, the isthmus. The fundus defines the portion of uterine body cranial to the lateral horns where the Fallopian tubes insert. In longitudinal section, the uterus has a waisted appearance, with a relatively narrow body and more pronounced fundus and cervix. Transvaginal 2D ultrasound imaging of the uterus is limited due to the movement of the transducer in a narrow space of the vagina allowing sagittal and transverse planes through the uterus. Three-dimensional sonography permits multiplanar display of all three perpendicular sections: coronal, sagittal, and transverse plane. The coronal plane of the uterus enables to visualize both horns of the endometrium and the cervix at the same time. A convex shape of the endometrium and myometrium in the fundus usually presents the normal uterus. The uterus receives a dual arterial supply. The uterine artery, a branch of the internal iliac artery, is the major source. Having reached the uterine body via the cardinal ligaments, it gives off vaginal and cervical branches and then runs lateral to the fundus in the broad ligament. Ultrasonically, they look like hyperechoic structures running along the cervix and the isthmic part of the uterus. The minor supply is from the ovarian artery, a branch of the aorta: this anastomoses with the uterine artery to feed the Fallopian tubes. The uterine wall receives blood from the anterior and posterior arcuate arteries (branches of the uterine artery) by a series of radial vessels to the muscular and mucosal layers. Arcuate arteries are tortuotic anechoic structures that spread through myometrium. Radial arteries penetrate vertically the myometrial layers of smooth muscle cells. Blood vessels of the uterus and endometrium can be detected by color and power Doppler ultrasound where endometrium and myometrium constitute an anatomical and functional unit. Spiral arteries supply stratum functionale of endometrium. Their shape and size change during menstrual cycle and they shed during menstruation together with the glandular tissue. During pregnancy, these arteries become uteroplacental decidual arteries. Basal arterioles supply endometrial stratum basale, and they do not change during menstrual cycle. Color Doppler research has determined that every blood vessel in the body has its own typical waveform. This waveform changes under the influence of hormones, ischemia, and internal or external vasoactive factors. The vessels in genital tract undergo cyclic changes dictated by the hormonal cycle. During the menstrual phase, due to hormonal deprivation and alterations in the spiral arteriolar system, spiral arteries undergo increased coiling and cause a circulatory stasis, which leads to tissue ischemia. Vasoconstriction of the spiral arterioles and necrosis of their walls result in bleeding. Anechoic areas that are sometimes visualized indicate endometrial breakdown. Later on, a mixed appearance with anechoic area (indicating blood) and hyperechoic parts (exfoliated endometrium and clots) can be observed. During the late menstrual phase, the endometrium appears sonographically as a thin, single-line, slightly irregular echogenic

interface. In this phase, the uterine artery shows high resistance index (RI). In the early follicular phase, the endometrium is imaged as a hyperechoic line with endometrial thickness of less than 5 mm, but is not always possible to visualize the endometrialmyometrial junction. The total endometrial thickness did not exceed 4 mm on day 4 and 8 mm on day 8 of the menstrual cycle. Paralleling the growth of the follicle and increase of E_2 level, endometrium becomes thick (8–12 mm) with typical triple line appearance. The hyperechoic echo that represents the endometrial-myometrial junction becomes more prominent and does not produce posterior enhancement. The central echogenic interface probably represents refluxed mucus. Doppler velocimetry of the uterine and spiral arteries shows progressive diminution of resistance indices. The hypoechoic halo sometimes seen adjacent to the endometrium should not be included in the measurement. Pathologic correlation shows this ultrasound finding to be due to the inner, compact layer in the myometrium. In the second half of the cycle, the corpus luteum secretes progesterone, mediating glandular enlargement and appearance of secretory vacuoles. The stroma becomes more vascular and edematous and the echogenicity of the functional layer increases as the number of spectral interfaces rises. Secretory phase is characterized by hyperechoic and homogenous endometrium with a loss of the triple-line morphology and surrounding anechoic halo. The endometrial thickness measures between 8 and 12 mm. During this phase of the cycle the ultrasonographic image of the endometrium shows increased echogenicity with respect to the myometrium. The interface of the myometrium with the endometrium is still visible as a hypoechoic zone. Maximum echogenicity is seen in the midluteal phase, when the endometrium appears homogenously hyperechoic. Posterior enhancement is a sonographic characteristic of this phase. Doppler velocimetry demonstrates further decrease of the vascular resistance in uterine and spiral arteries being the lowest in the mid-luteal phase. In the absence of secretion of beta human chorionic gonadotropin (beta hCG) from an implanting blastocyst, which maintains the corpus luteum (and hence the progesterone levels), the glands fragment and undergo autolysis. The necrotic superficial endometrium sloughs off (menstruation). At this time of the cycle, the appearance of the endometrium on TVS is variable. Material of differing echogenicity may be identified within the cavity. Slow subendometrial contraction waves have been noted on real-time sonography. These seem to facilitate sperm transport.

Since changes in the texture and volume of the endometrium can be precisely observed using 3D ultrasound, and retrospectively reviewed or consulted with colleagues, this method may become a method of choice for scanning endometrial pathology in multitude of clinical conditions.

ENDOMETRIAL POLYPS

Endometrial polyps develop as solitary or multiple, soft, sessile and pedunculated tumors containing hyperplastic endometrium.[1,2] Clinically, asymptomatic or symptoms like infertility, bleeding, infection, endometritis or pain are usually present in patients with endometrial polyps. Ultrasonographic appearance of endometrial polyps is best imaged during the early proliferative phase of the menstrual cycle (Fig. 46.1) or during the secretory phase after injection of a negative contrast medium into the uterine cavity. The vascularization of polyps is supported by already existing vessels originating from

terminal branches of the uterine arteries assessed by transvaginal color Doppler ultrasound. It is possible to identify flow in regularly separated vessels and analyze the velocity of blood flow through them. The RI is moderate, usually higher than 0.45 (Fig. 46.2).[13] Infection or necrosis of polyps may lower the impedance to blood flow (RI_{MIN}=0.37). The importance of endometrial polyps lies in the fact that marked reduction in blood flow impedance noted on the periphery and/or within the endometrial polyps may lead an inexperienced ultrasonographer to a false-positive diagnosis of endometrial malignancy.

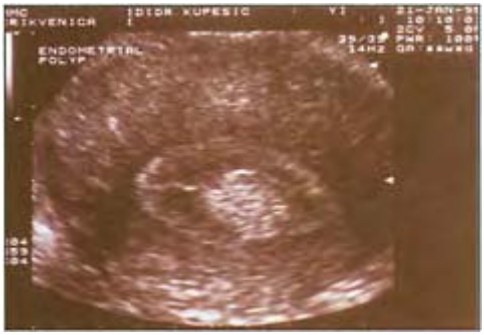

Figure 46.1: Transvaginal scan of the uterus demonstrating a focal area of increased echogenicity in a patient with an endometrial polyp

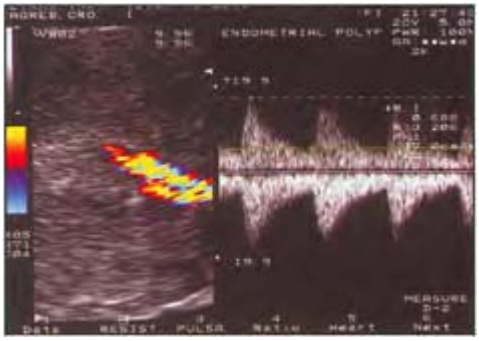

Figure 46.2: Transvaginal color Doppler scan of a patient with an endometrial polyp. Pulsed

Doppler signals isolated from color coded area demonstrate moderate-to-high resistance (RI=0.69) typical of a benign uterine lesion

Tamoxifen is a non-steroidal antiestrogen that is widely used in the hormonal therapy of breast cancer. However, the weak estrogen-like effect that tamoxifen has on the endometrium is a cause of great concern. Patients using tamoxifen should, therefore, be monitored at regular intervals, since numerous studies have described cases of endometrial thickening associated with this therapy. A wide spectrum of pathological uterine findings has been described in association with long-term tamoxifen therapy at a dose of 20 mg/day.[4] These findings include epithelial metaplasia, simple and atypical hyperplasia, endometrial polyps and endometrial carcinoma.[5] Endometrial changes are characterized sonographically by abnormal endometrial thickening and non-homogenous hyperechogenicity, with multiple, small cystic structures. At least three studies have indicated that tamoxifen treatment in postmenopausal breast cancer patients is associated with a high incidence of endometrial polyps.[6–8] Achiron and colleagues[7] found that a peculiar endometrial honeycomb appearance, manifested on gray-scale transvaginal sonography, occurred in 44% of this population, and was associated with the same high incidence (40%) of endometrial polyps. The effect of tamoxifen on endometrial blood flow is less evaluated. Achiron and his group described blood flow changes in the endometrial and subendometrial regions.[7] In asymptomatic postmenopausal patients receiving tamoxifen whose endometrial thickness was less than 5 mm, increased endometrial blood flow with significant reduction of the resistance index compared to untreated, control menopausal women was reported. Another study by the same authors[5] found that women with thick endometrium, and particularly those with endometrial polyps, presented a significantly lower RI, compared to those with thin endometrium (mean RI of 0.39 versus 0.79). The RI values returned to normal following resection of the endometrial polyps, thus supporting a benign transitory effect of long-term tamoxifen therapy on the endometrium.

The data from Goldstein et al[9] suggest that the objective assessment of blood flow impedance (resistance index, pulsatility index) in endometrial polyps and the size of these polyps cannot replace surgical removal and pathologic evaluation to predict histologic type. Patients with nonfunctional polyps in this study were older and less likely to have vaginal bleeding.

Perez-Medina et al[10] evaluated the efficacy of color Doppler exploration for assessing atypia inside endometrial polyps (polyp stalk). Thirty-five polyps (out of 106) with sonographic indications of atypia were pathologically confirmed. Sonographic indications of atypia inside 16 polyps were not confirmed. Three nonquestionable endometrial polyps had atypia inside them. They conclude that low Doppler resistance (RI<0.50) is highly predictive of atypia inside endometrial polyps.

Three-dimensional hysterosonography can better visualize the uterine cavity and the endometrial thickness than with transvaginal sonography, transvaginal sonohysterography, transvaginal color Doppler, or hysteroscopy according to Bonilla-

Musoles et al.[11] Using the multiplanar views polypoid structures can be nicely visualized, allowing for the optimal plane to present their pedicle. Surface rendering mode can suppress undesirable echoes allowing the visualization of the polypoid lesions in continuity with the endometrial lining.[12]

Gruboeck et al[13] performed the measurements of endometrial thickness assessed by conventional 2D ultrasound and endometrial volume assessed with 3D ultrasound in symptomatic postmenopausal patients and they compared the results. The volume measurement was performed using longitudinal plane delineating the whole of the uterine cavity in a number of parallel longitudinal sections 1–2 mm apart. Then, the endometrial volume was calculated automatically by the inbuilt computer software program.

The endometrial thickness was similar in patients with endometrial hyperplasia and polyps, but the endometrial volume in hyperplasia was significantly higher than the volume in patients with polyps. The difference between endometrial hyperplasia and polyps cannot be detected by the measurement of endometrial thickness, but with 3D volume measurement. Polyps are localized thickenings of the endometrium not affecting the whole of the uterine cavity, and therefore their volume is much smaller, while the maximum thickness is similar to that of hyperplasia.

INTRAUTERINE SYNECHIAE (ADHESIONS)

Destruction of the basal layer of the endometrium may result in scarring and development of bands of scar tissue (synechiae) in the uterine cavity. This damage of endometrium may occur as a result of a too vigorous curettage. Tuberculosis may also cause uterine adhesions. Menstrual pattern is characterized by amenorrhea or hypomenorrhea. Ultrasound scan of a patient with Asherman's syndrome shows a mixed picture: in some parts of the uterine cavity no endometrium can be visualized, and in others the endometrium appears normal. If there are adhesions in the uterine cavity, they are visualized as hyperechoic bridges. Intrauterine adhesions do not display increased vascularity on color Doppler examination (Fig. 46.3). They are better visualized during menstruation when intracavitary fluid outlines them. The second option is sonohysterography.

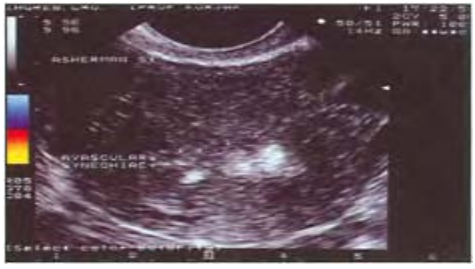

Figure 46.3: Transvaginal color Doppler scan of the intrauterine synechiae. Avascular bridges

occurring in a patient after vigorous curettage reduce the uterine cavity

Sonohysterography performed with 3D ultrasound has several advantages over that with conventional 2D ultrasound. It gives more accurate information about the location of abnormalities, which is very important for preoperative assessment and distinguishing pathologies. Furthermore, the uterus is for shorter time distended compared to the time necessary for 2D examination, which results in better patients' acceptance. However, according to Momtaz et al[14] in cases of intrauterine adhesions, the use of echogenic contrast media (e.g. Echovist, Schering) is more accurate than saline-contrast 3D sonohysterography. Intrauterine synechiae traversing the uterine cavity can be accurately visualized on both multiplanar and rendered imaging.[12] Weinraub et al[12] concluded that surface rendering in cases of equivocal signals confirmed their presence, appearance, actual size, volume, and relationship to the surrounding structures.

Three-dimensional ultrasound is helpful in delineation of intracavitary adhesions and determination of their location which assists in surgical planning. In the cases of bridging adhesions, the degree of cavity obliteration is accurately assessed. Similarly, this technique is beneficial for differentiation between other uterine abnormalities and adhesions.

ADENOMYOSIS

Adenomyosis of the uterus is a condition in which clusters of endometrial tissue grow into the myometrium. It may be localized close to endometrium, or it may extend through the myometrium and serosa. Adenomyosis affects 20% of women, mainly multiparous. The uterus can be normal-sized or enlarged with symptoms such as dysmenorrhea, pelvic pain and menometrorrhagia.

Two-dimensional ultrasound findings include "Swiss cheese" appearance of the myometrium due to areas of hemorrhage and clots within the muscle. Disordered echogenicity of the middle layer of the myometrium is usually present in severe cases (Fig. 46.4). Sometimes the uterus is generally hypoechoic, with the large cysts rarely seen. Using hysterosonography contrast medium penetrates the myometrium. Color Doppler characteristics present increased vascularity by moderate vascular resistance within the myometrium (RI=0.56±0.12), while the RI of the uterine arteries shows a decreased value compared to controls.[15] Statistically significant differences exist between adenomyosis and uterine malignancies in both RI and maximum velocity. However, no significant difference was noted between adenomyosis and myoma in the RI, but a slight difference was observed in the maximum velocity.[16]

In some cases, transonic areas may not represent adenomyosis, but prominent vessels, or other conditions which give rise to hyperemia. Lee et al[17] performed the study which confirmed the superiority of 3D power Doppler sonography compared to transvaginal color Doppler ultrasound in the detection of flow in the areas of adenomyosis. Women with a provisional diagnosis of adenomyosis, listed for hysterectomy were studied. Gray scale ultrasound was first used to screen for the presence of adenomyosis using predetermined ultrasound criteria. Then 3D power Doppler sonography of adenomyotic

areas was performed. Ultrasound findings such as distribution of vessels and pattern of flow in adenomyotic foci were compared with histological results. The same method was used for tracing regular vessels' course in this abnormality. Using 3D power Doppler ultrasound the authors were able to demonstrate the perfusion of adenomyotic foci as well as the vessels' distribution and their branching pattern.

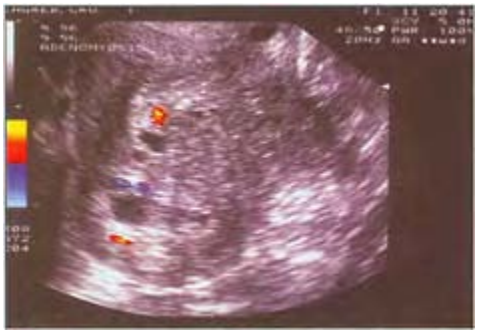

Figure 46.4: "Swiss cheese" appearance of the adenomyosis endometrium with the peripheral vascularity indicates

ENDOMETRIAL HYPERPLASIA

Endometrial hyperplasia, the most common cause of vaginal bleeding in both pre- and postmenopausal women, results from unopposed estrogen stimulation. The endometrial thickness in postmenopausal women is no more than a thin line of 1–3 mm. Abnormal endometrial thickness may be detected in some benign uterine conditions, as well as in patients with endometrial malignancy. Endometrial thickness greater than 14 mm in premenopausal and greater than 5 mm in postmenopausal women should be further investigated.[1] Using B-mode transvaginal sonography alone it is not possible to distinguish endometrial hyperplasia from carcinoma. The proliferation manifests as a pronounced endometrial stripe on ultrasound. It may be indistinguishable from an endometrial polyp or carcinoma, even on transvaginal ultrasound. Hysterosonosalpingography can be definitive, but the diagnosis is usually confirmed by endometrial biopsy. In the

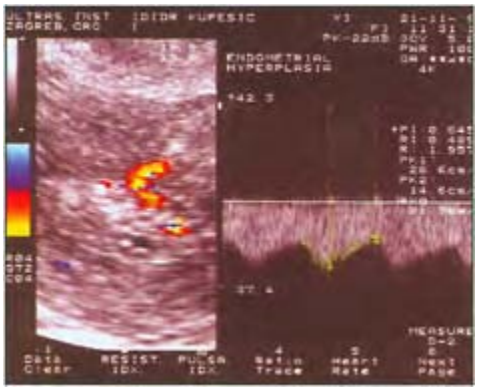

Figure 46.5: Transvaginal color Doppler scan of a hyperplastlc endometrium. Blood flow signals obtained from the periphery of the endometrium revealed moderate vascular resistance (Rl=0.49). Histopathology confirmed endometrial hyperplasia

past, dilatation and curettage (D&C) has been the mainstay for obtaining histologic material for diagnosis. Now, Pipelle biopsy is often used as an office procedure at first referral for vaginal bleeding; D&C and hysteroscopy are reserved more for therapeutic procedures.

More accurate diagnosis of endometrial pathology can be obtained by the use of transvaginal color and pulsed Doppler sonography.[2,3] Color Doppler findings indicative of endometrial hyperplasia include peripheral distribution of the regularly separated vessels with RI significantly higher (mean RI=0.55±0.05) (Fig. 46.5) than in carcinoma (mean RI=0.42±0.02).[18] However, reliable differentiation between endometrial hyperplasia and carcinoma is not possible due to an overlap in the endometrial thickness measurements, as well as to controversial results of blood flow measurements assessed by transvaginal color Doppler ultrasound. Since there is a positive correlation between arterial blood flow impedance and number of years from menopause,[19] one can estimate the risk of uterine malignancy in postmenopausal patients with decreased vascular resistance.

Emoto et al[20] examined the usefulness of transvaginal color Doppler ultrasound in differentiating between endometrial hyperplasia and endometrial carcinoma and in predicting tumor spread in patients with carcinoma. No significant difference was found in the mean value of endometrial thickness between patients with hyperplasia (n= 18

patients; 16.2 mm +/−15.9 mm) and patients with carcinoma (n=53 patients; 18.7 mm +/− 17.1 mm). Intratumoral blood flow was detected in significant number of the patients who had endometrial carcinoma (71.7%, 38 of 53 patients) compared with patients who had endometrial hyperplasia (5.6%, 1 of 18 patients; P<0.0001). For patients with carcinoma, the detection of intratumoral blood flow may be helpful in distinguishing between low-grade and high-grade tumors and predicting myometrial invasion. However, intratumoral blood flow analysis using RI, PI, or PSV may not be useful for predicting tumor spread before surgery.

Jarvela et al[21] evaluated hemodynamic changes in uterine blood flow using transvaginal color Doppler ultrasonography after thermal balloon endometrial ablation therapy. Thermal balloon endometrial ablation therapy induces a rise in uterine blood flow impedance, but not until 6 months after the treatment. The rise in impedance may be due to fibrosis in the uterine cavity following the thermal balloon therapy.

More recently, with the aid of 3D ultrasound, endometrial volume measurements became possible. According to Gruboeck et al[13] endometrial volume was successfully measured in 94.2% of patients, while in others the presence of anterior uterine wall myomas caused acoustic shadowing on 3D records. The volume of the endometrium was measured by delineating the uterine cavity on parallel longitudinal sections 1–2 mm apart. The sections were added together using in-built computer software to calculate the volume. The endometrial volume was significantly lower in patients with benign pathology such as hyperplasia (mean 8.0 ml, SD 7.81 ml) than in patients with endometrial carcinoma (mean 39.0 ml, SD 34.16 ml). Normal endometrial volume in this study was 0.9 ml (SD 1.72 ml).

Our group reported on the use of 3D power Doppler sonography in patients with endometrial hyperplasia.[21] We were able to demonstrate regularly separated vessels at the periphery of the thickened endometrium.

Bonilla-Musoles et al suggest that in patients on hormone replacement therapy or tamoxifen, 3D sonohysterography allows differentiation of normal proliferative from hyperplastic endometrium.[11]

ENDOMETRIAL CARCINOMA

Endometrial carcinoma is the most common gynecological malignancy in many countries with the reported incidence of about 10% in postmenopausal patients presenting uterine bleeding. Early transabdominal sonographic investigations have demonstrated that increased endometrial thickness is associated with endometrial neoplasms in postmenopausal women, but the quality of transabdominal sonographic images is affected by obesity, retroversion of the uterus, and an unfilled bladder, factors that do not influence transvaginal sonographic visualization of the endometrium. Ultrasound findings assessed by conventional B-mode sonography include increased endometrial thickness >5 mm in postmenopausal women or >8 mm in perimenopausal women, hyperechoic endometrium, free fluid in the cul-de-sac, intrauterine fluid or possible invasion in patients with disrupted endometrialsubendometrial layer. In addition, color and pulsed Doppler improves diagnostic accuracy, because the endometrial carcinoma shows abnormal blood flow due to tumor angiogenesis (Fig. 46.6).[22] Endometrial blood flow is absent in normal, atrophic and most cases of endometrial hyperplasia, while, according to

our investigation[18] in 91% of the cases of endometrial carcinoma areas of neovascularization were demonstrated as intratumoral or peritumoral. Neovascular signals

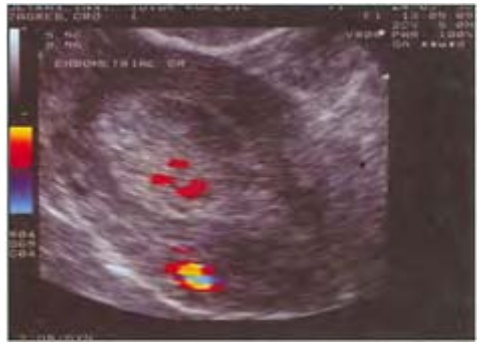

Figure 46.6: Transvaginal color Doppler scan of a thickened endometrium in a postmenopausal patient. Note the intratumoral blood flow signals suggestive of an endometrial malignancy

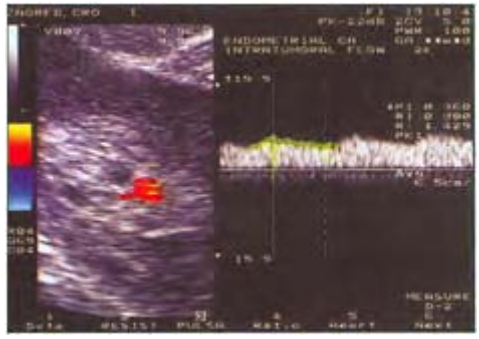

Figure 46.7: Transvaginal color Doppler scan of endometrial carcinoma vessels. Note the low resistance index of intratumoral vessels

(RI=0.30) typical of endometrial malignancy

from the central parts of the lesion demonstrate low vascular resistance (RI=0.42±0.02) (Fig. 46.7), while increased vascularity signals surrounding the lesion are suspected for invasion (Fig. 46.8). If the myometrial vessels are invaded, low vascular resistance is detected due to incomplete or absent membrane and leaky structure.

Conventional 2D ultrasound measurements of endometrial thickness have disadvantages in distinguishing patients with benign and malignant endometrial pathology due to varying thickness, and interference of other pathology like polyps or hyperplasia.

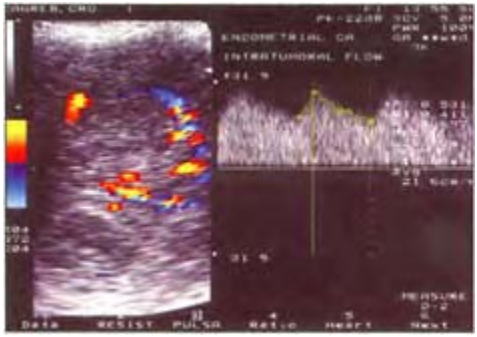

Figure 46.8: Transvaginal color Doppler scan of a richly vascularlzed endometrium in a patient with proven endometrial cancer. Blood flow velocity waveforms obtained from intratumoral vessels demonstrated high velocity (27.9 cm/s) and low resistance (Rl=0.41).

In distinguishing cancer from benign pathology endometrial volume measurements assessed by 3D ultrasound seems to be more helpful. Gruboeck et al[13] compared endometrial thickness and volume in patients with postmenopausal bleeding and examined the value of each parameter in differentiating between benign and malignant endometrial pathology. Each patient underwent 3D ultrasonography for the measurement of endometrial thickness and volume. The results were compared to the histological diagnosis after endometrial biopsy or dilatation and curettage. The mean endometrial thickness in patients with endometrial cancer was 29.5 mm (SD 12.59) and the mean

volume was 39.0 ml (SD 34.16). The optimal cut-off value of endometrial thickness for the diagnosis of cancer was 15 mm, with the test sensitivity of 83.3% and positive predictive value of 54.4%. With a cut-off level of 13 ml, the diagnosis of cancer was made with the sensitivity of 100%. One false-positive result in a patient with hyperplasia gave a specificity of 98.8% and positive predictive value of 91.7%. According to Gruboeck et al[13] the endometrial volume was significantly higher in patients with carcinoma than those with benign lesions. The measurements of endometrial volume were superior to that of endometrial thickness as a diagnostic test for the detection of endometrial cancer in symptomatic postmenopausal women. Increasing volume is associated with the severity or higher grade of the endometrial carcinoma, and progressive myo-metrial invasion. The depth of myometrial invasion showed positive correlation with both endometrial thickness and volume. Only patients with tumor volume larger than 25 ml had evidence of pelvic node involvement at operation.

Yaman et al[23] evaluated the reproducibility of transvaginal 3D endometrial volume measurement in patients with postmenopausal bleeding and compared the reproducibility of this technique to that of 2D endometrial thickness measurement. Endometrial volume and thickness measurements by 3D and 2D ultrasound, respectively, show good reproducibility but the reproducibility of 3D ultrasound is better.

Bonilla et al[11] reported that 3D hysterosonography allows better visualization of myometrial invasion, and may aid in staging malignant endometrial tumors. Using simultaneous display of the transverse plane with 3D ultrasound it is possible to detect infiltration of cervical or endometrial carcinoma into the bladder or rectum. In our study,[24] apart from endometrial volume, other 3D sonographic and power Doppler criteria for the diagnosis of endometrial malignancy included subendometrial hallo irregularity, presence of the intracavitary fluid, chaotic vessel's architecture and branching pattern (Table 46.1). In patients with endometrial carcinoma, mean endometrial volume was 37.0±31.8 ml (Table 46.2). The endometrial volume in hyperplasia had the mean value of 7.82±7.60 ml and was significantly higher than the volume in patients with polyps (mean 2.63±2.12 ml). In patients with normal or atrophic endometrium the mean volume was 0.8±1.51 ml. Subendometrial hallo was regular in all the patients with benign endometrial pathology, whereas 8 out of 12 patients with endometrial carcinoma had irregular endometrial-myometrial border. Intracavitary fluid was present in 4 patients with benign endometrial lesions and in 5 patients with endometrial malignancy. Dichotomous branching and randomly dispersed vessels were detected in 91.67% of the patients with endometrial carcinoma, while single vessel arrangement and regular branching were pathognomonic for benign lesions. Three-dimensional PD ultrasound accurately detected structural abnormalities of the malignant tumor vessels such as microaneurysms, arteriovenous shunts, tumoral lakes, elongation and coiling. Combining morphological and power Doppler criteria, the diagnosis of endometrial carcinoma had a sensitivity of 91.67%. One false-positive result was obtained in a patient with endometrial hyperplasia and one false-negative in a patient with endometrial carcinoma receiving tamoxifen therapy. In this case endometrial lesion demonstrated regularly separated peripheral vessels was falsely interpreted as hyperplasia.

Kupesic et al[25] performed staging of endometrial carcinoma by 3D power Doppler. The objective of this study was to evaluate the accuracy of 3D power Doppler in

determining the depth of myometrial invasion in patients with proved adenocarcinoma of the endometrium, relative to the amount of myometrial invasion as measured by hystopathological analysis (Table 46.3). Thirty-four patients with hystologically proved adenocarcinoma of the endometrium were analyzed. Deep myometrial invasion (>50%) was present at postoperative histology in 5/22 (22.73%) women, while superficial was reported in 17/22 (77.23%). Three-dimensional power Doppler demonstrated

Table 46.1: Three-dimensional sonographic and power Dopplar criteria for the diagnosis of endometrial malignancy

3-D sonographic and power	*Doppter criteria*	*Score*
Endometrial volume	<13 ml	0
	≥13 ml	2
Subendometrial hallo	Regular	0
	Disturbed	2
Intracavitary fluid	Absent	0
	Present	1
Vessel's architecture	Linear vessel arrangement	0
	Chaotic vessel arrangement	2
Branching pattern	Simple	0
	Complex	2
TOTAL SCORE		

From reference 24, with permission.
Total score=sum of individual scores
Cut-off score=greater or equal to 4 is associated with a high risk of endometrial malignancy

Table 46.2: Volume and vascularity of the endometrial lesions (N=57) obtained by 3D PD ultrasound

Histopathohgy	*N*	*V (SD) ml*	*Regular endometrial hallo (%)*	*Intracavitary fluid (%)*	*Neovascular signals (%)*
Normal and/or atrophic endometrium	10	0.8 (1.51)	100	20.00	0
Endometrial hyperplasia	27	7.82 (7.60)	100	37.00	0
Endometrial polyp	28	2.63	100	35.71	3.57

		(2.12)			
Endometrial carcinoma	12	37.0 (31.8)	66.67	41.67	100
From reference 24, with permission.					

Table 46.3: Invasion of endomettrial carcinoma assessed with the aid of 3D PDS

Invasion	*3D Power Doppler*	*Pathohistology*
Superficial *	17	18
Deep **	5	4

From reference 25, with permission
* Invasion into less than a half of the total myometrial thickness
** Invasion into more than a half of the myometrial thickness

a sensitivity of 100% (5/5) and a specificity of 94.44% (17/18) for deep invasion, with a positive predictive value (PPV) of 83.33% (5/6) and a negative predictive value (NPV) of 100% (17/17). In only one patient with adenomyosis, invasion was overestimated by 3D power Doppler. Data showed acceptable accuracy in determining the depth of myometrial invasion in patients with adenocarcinoma. Three-dimensional power Doppler can potentially detect lesions that require aggressive intervention and thus direct to proper treatment.

Lee et al[26] evaluated the relationship between blood flow in the endometrial carcinoma assessed by color Doppler ultrasound, microvessel density assessed by immunohistochemistry, and vascular endothelial growth factor levels. Significantly lower RIs were noted in tumors of stage II or greater (0.37 compared with 0.50, P<.001), of high histologic grade (grade 3) (0.34 compared with 0.49, P=.004), with deep myometrial invasion (one-half depth or greater) (0.39 compared with 0.49, P=.002), with lymphovascular emboli (0.38 compared with 0.49, P <.001), or with lymph node metatasis (0.30 compared with 0.49, P <.001) compared with stage I tumors and tumors of histologic grade 1 or 2, with superficial myometrial invasion, without lymphovascular emboli, or with no lymph node metastasis. Increased vascular endothelial growth factor levels and microvessel density were detected in tumors of stage II or greater, with lymphovascular emboli, or with lymph node metastasis. Resistance index, microvessel density, and vascular endothelial growth factor levels in the tumor showed linear correlations. Blood flow assessed by color Doppler ultrasound showed histologic and biologic correlations with angiogenesis and vascular endothelial growth factor levels and might play an important role in predicting tumor progression and metastasis in patients affected by endometrial carcinoma (Fig. 46.9).

Alcazar et al[27] correlated intratumoral blood flow as assessed by transvaginal color Doppler ultrasound using parameters such as RI and peak systolic velocity (PSV) with tumor histopathologic characteristics, tumoral stage, and risk for recurrence in endometrial carcinoma. Significantly lower RI was found in tumors with the following characteristics: infiltrative growth pattern, grade 3, infiltrating greater than or equal to

50% of the myometrium, cervical involvement, lymphvascular space invasion, lymph node metastasis, stage greater than or equal to Ic, and high risk for recurrence. Significantly higher PSV was found in tumors that were grade 3, infiltrating greater than or equal to 50% of the myometrium, stage greater than or equal to Ic, and with a high risk for recurrence. These data indicate that there is a positive correlation between intratumoral blood

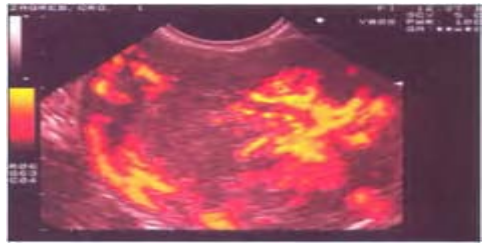

Figure 46.9: Power Doppler imaging of the randomly dispersed vessels in a patient with advanced endometrial carcinoma. Irregular course of the vessels detected within the myometrial portion suggests deep myometrial invasion, which was histopathologically proved following surgery

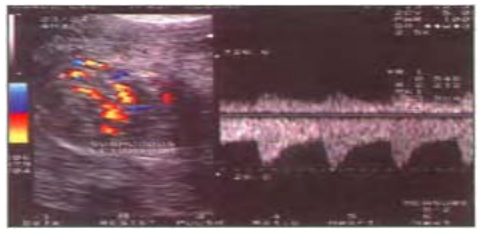

Figure 46.11: The same patient as in Figure 46.10. Peripheral vessels demonstrate moderate

vascular resistance
(RI=0.55)

flow features and histopathological characteristics, tumor stage, and risk for recurrence in patients suffering from endometrial cancer.

LEIOMYOMA

Leiomyomas are the most common tumors of the female pelvis and occur in 20–25% of women of reproductive age, arising from the smooth muscle and soft tissue of the uterine fundus and corpus, while 3% originate from cervix.[28] Myomas are usually multiple and of various sizes. Intramural tumors are the most common, while the submucosal are the least common. If they extend outward, they become pedunculated or subserosal.[29] Symptoms of submucous leiomyomas include metrorrhagia, pelvic pain or infertility, whereas most subserosal leiomyomas are asymptomatic.

On the gray scale ultrasound the uterine leiomyomas may be represented with uterine enlargement, distortion of the uterine contour, and varying echogenicity depending on the amount of connective or smooth muscle tissue.

Transvaginal color Doppler sonography demonstrates vascularization on the periphery of the myoma of uterine origin (Fig. 46.10), with the RI of 0.54±0.08, allowing better delineation of the tumor (Fig. 46.11). Blood vessels in the central part of the myoma in case of necrosis, inflamma-

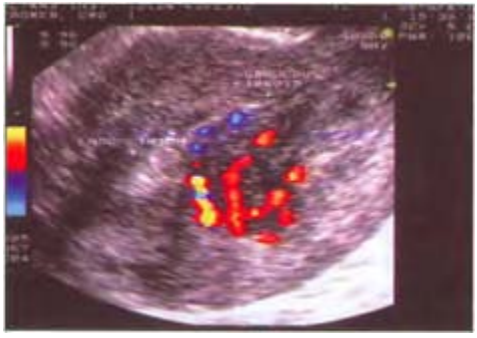

Figure 46.10:
Transvaginal color Doppler scan of a patient with submucous/intramural leiomyoma

tion or other degenerative changes demonstrate lower RI. Uterine arteries present lower impedance to blood flow in patients with myomas (RI= 0.74±0.09) compared to normal group (RI= 0.84±0.09).[30]

Using simultaneous display of three perpendicular planes assessed by 3D ultrasound demonstrates the accurate location of myomas, size, and its relationship to the endometrium that is very important in therapy planning. Patients receiving medical therapy such as gonadotropinreleasing hormone may be followed with serial 3D ultrasound scans to estimate myoma size/ volume and effectiveness of the therapy. Hysterosonography by 3D ultrasound is valuable in obtaining submucosal myomas.[11,12,31,32] Balen et al[31] found that 3D ultrasound and sonohysterography were useful in demonstrating the position of submucosal myomas. They studied both saline and a positive ultrasound contrast agent (Echovist) and found the positive contrast superior when looking at the endometrial cavity. Weinraub et al[12] found that the negative contrast is better for evaluating the contents of the uterine cavity since it enables delineation of the outer surface of lesions, whereas positive contrast creates a cast of the cavity.

One limitation of scanning the uterus with myomas by 2D and/or 3D ultrasound is due to a significant shadowing from calcification. In our recent study[23] we evaluated myometrial lesions regarding their morphology, volume, and vascularization with 3D ultrasound and power Doppler sonography. The mean volume of the leiomyomas undergoing surgery was 78.52±51.8 ml. In 84.38%, 3D power Doppler detected regular vascularity at the periphery, while in cases of secondary degenerative lesions the findings were suggestive of neovascularity, irregular branching and chaotic vascular arrangement, because necrosis, inflammation and degeneration altered the leiomyoma vasculature. We concluded that because of the low positive predictive value of 16.67% this method should not be used for the evaluation of myometrial pathology, both benign and malignant.

LEIOMYOSARCOMA

Uterine sarcoma is a rare tumor, accounting for only 1–3% of all genital tract tumors and 3–7.4% of malignant tumors of the corpus uteri,[33] characterized by early dissemination and poor prognosis for survival. Through the years, several questions regarding these tumors have remained unanswered, and a method for its early and correct diagnosis is still unknown. Uterine sarcoma is expected to be more common in the near future, as gynecologists are more commonly using the conservative treatment of uterine myomas. Abnormal vaginal bleeding is the most common presenting symptom in patients with uterine sarcoma. Lower abdominal pain or pressure and a palpable abdominal mass are additional findings. An enlarged bulky uterus is palpated, and/or the tumor may be seen protruding through the cervix. Dilatation and curettage may be helpful in distinguishing benign from malignant pathology only if the tumor is submucosal. Clinically, a rapid increase in the size of a uterine tumor after the menopause arouses suspicion of sarcoma.

Ultrasonically leiomyosarcoma is presented as solid or solid-cystic structure, altering echogenicity of the myometrium. On transvaginal color Doppler, neovascularization of leiomyosarcoma is detected at the border and/or in the center of the tumor (Fig. 46.12)

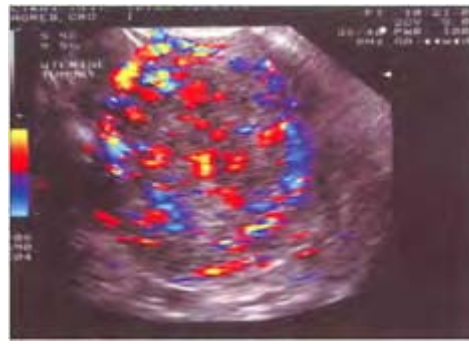

Figure 46.12: Randomly dispersed newly formed vessels as seen by color Doppler imaging in a case of uterine sarcoma

with high blood flow velocity and low impedance to blood flow (RI=0.37±0.03), with irregular, thin, and randomly dispersed vessels (Fig. 46.13). When cut-off value for RI of <0.40 was used, this method reached the sensitivity of 90.91%, specificity 99.82%, positive predictive value 71.43% and negative predictive value of 99.96%.[34] Because of their rarity, uterine sarcomas are not suitable for screening. Transvaginal ultrasound can detect differences in myometrial tissue density, and therefore can be used for detection of uterine sarcoma, but because of low specificity this method is not appropriate as a screening procedure.

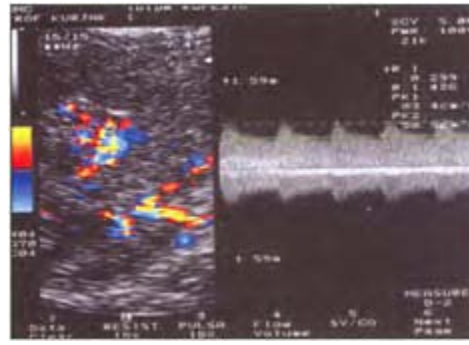

Figure 46.13: Pulsed Doppler waveform analysis demonstrate low impedance to flow (RI=0.30) typical of

uterine sarcoma. This was verified by the time of histopathology

Szabo et al35 investigated uterine vascularity by color and pulsed Doppler in cases of uterine leiomyomas and uterine sarcomas, and determined the efficiency of uterine blood flow analysis in differentiating between them. The mean intratumoral RI and PI were significantly lower and the intratumoral PSV was significantly higher in patients with sarcomas than in patients with uterine leiomyomas. Marked reduction of RI and PI and increased PSV could be found in fast growing leiomyomas and those showing necrotic, degenerative and inflammatory changes. When a cut-off value of 0.5 for the RI was considered, the detection rate for uterine sarcoma was 67% and the false-positive rate was 11.8%. These results suggest that the intratumoral RI detected by color and pulsed Doppler ultrasound is not sensitive enough to be used as a preoperative diagnostic tool for differentiation between leiomyoma and uterine sarcoma.

In our study,23 one patient with uterine leiomyosarcoma was examined with 3D and power Doppler ultrasound. Enlarged volume of the tumor (97.2 ml) and irregular randomly vessels dispersed both in the central and peripheral parts of the tumor were obtained using this method. The diameters of these vessels were “uneven”, with numerous microaneurysms and stenosis.

MISCELLANEOUS PROCESSES

Pelvic inflammatory disease (PID) is rarely confined to uterus; however, the endometrium shows histologic changes of inflammation in more than 70% of women with acute PID[36] and 40% with mucopurulent cervicitis.[37] Discrete endometritis is more likely to be seen postpartum or postinstrumentation. The findings are nonspecific on ultrasound and must, as always, be correlated with the clinical symptoms. They include thickening and irregularity of the endometrium and 606 presence of the fluid, debris, or even gas within the endometrial cavity. On the other side, clinical endometritis may have normal ultrasound findings. Pyometra (pus in the uterine cavity) may complicate cervical stenosis, which frequently involves the internal os.

The acquired causes include infection, neoplasia, and iatrogenic factors (radiation therapy or surgery). The characteristic ultrasound appearance is of a dilated, fluid-filled endometrial cavity. The echogenicity of the cavity varies with the degree of debris or clot.

Nabothian cysts are obstructed and hence dilated inclusion cysts of no clinical relevance, located within the cervix and routinely seen on transabdominal and especially transvaginal ultrasound. Cysts or echogenic foci may also be seen in the myometrium and are of no clinical significance. Mönckeberg’s medial sclerosis, manifesting as peripheral punctate echoes, is due to calcification in the smaller uterine artery branches.

Ultrasound is not especially useful in the diagnosis of cervical disease, including neoplastic conditions. Sonography serves to document the complications of advanced cervical disease and its treatment. Ultrasound can document cervical stenosis and intrauterine fluid retention or hydronephrosis, which may be secondary to large cervical masses or to pelvic radiation.

Systemic malignancies, such as lymphoma or metastases, are likely uncommon in the uterus; when they are present, the sonographic appearance is nonspecific and ultrasound has little to offer in the evaluation of these patients.

Intrauterine contraceptive devices (lUCDs) have been in clinical use for almost 40 years, and there are several different designs. All are detectable by ultrasound since they are highly reflective and cast marked acoustic shadowing. Characteristic appearances may indicate the model of device used. Ultrasound is useful in both confirming intrauterine position of the IUCD and documenting myometrial penetration. When no device is seen in the endometrial cavity and perforation is suspected, then a complementary abdominal radiograph may reveal a peritoneal position anywhere from the pelvis to the direction of the diaphragm.

Finally, uterus in puerperium should return to near normal size within 6 to 8 weeks after delivery. Postpartum ultrasound is usually requested if there is clinical concern about retained products or endometritis. The uterine size is an unreliable variable; the more specific ultrasound finding is visualization of the material within the uterine cavity. Most commonly, the endometrial cavity looks normal. When an abnormality is seen, it may be an echogenic mass, heterogenous mixed-density mass, or fluid. The detection of an echogenic mass in the uterus strongly supports the diagnosis of retained products.[38] A heterogenous mass is sometimes caused by retained placenta but can also be secondary to blood clots or infected or necrotic material in the absence of placental tissue. The detection of gas within the endometrial cavity has been commonly interpreted as indicative of endometritis. But in some cases, gas may be a normal finding in the puerperium, at least until the end of the 3rd postpartum week.[39] B mode ultrasound cannot reliably rule out retained product,[40] but color Doppler ultrasound can detect prominent blood flow signals representing the response of the dilated spiral arteries and venous system to the active trophoblast. Low vascular resistance (RI=0.35±0.08) obtained from the echogenic intracavitary areas indicates presence of the remaining products of conception.

CONCLUSION

Pelvic sonography imaging is the technique of choice for the evaluation of the uterus and is a very commonly performed examination. Transvaginal sonography allows detailed analysis of the endometrial thickness and texture. Blood flow studies can be efficiently used to monitor endometrial development and to distinguish between benign and malignant uterine cavity lesions. It is hoped that color Doppler findings may help to reduce invasive procedures such as dilatation and curettage or hysteroscopy for detection of cavitary lesions. This would decrease both the potential risks and the economic costs. Transvaginal color and pulsed Doppler sonography represents a non-invasive diagnostic tool that can be used repeatedly for assessing vascularity in endometrial lesions. The application of transvaginal color Doppler to the postmenopausal population for the screening of endometrial carcinoma may be a viable option if combined with ovarian screening in the same scan. In this way, the capital costs would be shared and oncological preventive medicine for women could be initiated. The use of this technique could also result in a reduction in dilatation and curettage operations, with considerable reduction of both the potential risks and the economic costs of the operation.

Assessment of vascularization of uterine tumors, if used together with analysis of morphology and size, can increase our accuracy in differentiating between uterine sarcoma and leiomyoma. However, it is unrealistic to expect Doppler studies to clarify confounding histological findings. It seems that the multiparameter sonographic approach, which includes morphology and size depicted by transvaginal ultrasonography and color flow imaging with pulsed Doppler analysis of neovascular signals, can help in the diagnosis of uterine sarcoma in high-risk groups such as postmenopausal patients with a rapidly enlarging uterus. Therefore, serial measurements are recommended for evaluation of myometrial density, follow-up of the tumoral growth and detection of the impedance to blood flow. Only such complex observations can lead to proper diagnosis of these rare tumors, which have an unpredictable prognosis.

Three-dimensional and power Doppler ultrasound is a new diagnostic technique and its role in the assessment of uterine lesions has yet to be investigated. Three-dimensional ultrasound offers improved visualization of uterine lesions providing simultaneous display of coronal, sagittal, and transverse planes, displays entire volume demonstrating continuity of curved structures in a single image, offers more accurate volume estimation using a standard anatomic orientation, retrospective review of stored data, more complete viewing of pathology using rendered images identifying the location of abnormalities, and assessment of tumor invasion. Three-dimensional sonohysterography clearly delineates intrauterine pathology. It seems that 3D power Doppler sonography has brought us a little closer to better understanding of malignant tumor angiogenesis. Interactive rotation of power Doppler rendered images provides improved visualization of the tumor vasculature. This method permits the ultrasonographer to view structures in three dimensions interactively, rather than having to assemble the sectional images in his/her mind. Contrast agents are another possibility for enhancing the three-dimensional power Doppler examination by increasing the detection rate of small vessels.

REFERENCES

1. Kurjak A, Kupesic S, Zalud I, Predanic M. Transvaginal color Doppler. In: Dodson MG (Ed). Transvaginal Ultrasound. New York: Churchill Livingstone, 1995; 325–39.
2. Fleischer AC, Kepple DM, Entman SS. Transvaginal sonography of uterine disorders. In: Timor-Tritsch IE, Rottem S (Eds). Transvaginal Sonography (2nd ed). New York: Elsevier, 1991; 109–30.
3. Kurjak A, Kupesic S. Transvaginal color Doppler and pelvic tumor vascularity: lessons learned and future challenges. Ultrasound Obstet Gynecol 1995; 6:1–15.
4. Ismail SM. Pathology of the endometrium treated with tamoxifen. J Clin Path 1994; 47:827–33.
5. Achiron R, Grisaru D, Golan-Porat N. Tamoxifen and the uterus: an old drug tested by new modalities. Ultrasound Obstet Gynecol 1996; 7:374–78.
6. Lahti E, Blanco G, Kauppila A. Endometrial changes in postmenopausal breast cancer patients receiving tamoxifen. Obstet Gynecol 1993; 81:660–64.
7. Achiron R, Lipitz S, Sivan E. Changes mimicking endometrial neoplasia in postmenopausal, tamoxifentreated women with breast cancer: a transvaginal Doppler study. Ultrasound Obstet Gynecol 1995; 6:116–120.
8. Exacoustos E, Zupi E, Cangi B. Endometrial evaluation in postmenopausal breast cancer patients receiving tamoxifen: an ultrasound, color flow Doppler hysteroscopic and histological study. Ultrasound Obstet Gynecol 1995; 6:435–42.

9. Goldstein SR, Monteagudo A, Popiolek D, Mayberry P, Timor-Tritsch I. Evaluation of endometrial polyps. Am J Obstet Gynecol 2002; 186(4):669–74.
10. Perez-Medina T, Bajo J, Huertas MA, Rubio A. Predicting atypia inside endometrial polyps. Journal Ultrasound Med 2002; 21 (2): 125–28.
11. Bonilla-Musoles F, Raga F, Osborne N, Blanes J, Coelho F. Three-dimensional hysterosonography for the study of endometrial tumors: comparison with conventional transvaginal sonography, hysterosalpingography, and hysteroscopy. Gynecol Oncol 1997; 65:245–52.
12. Weinraub Z, Maymon R, Shulman A, et al. Three-dimensional saline contrast hysterosonography and surface rendering of uterine cavity pathology. Ultrasound Obstet Gynecol 1996; 8(4):277–82.
13. Gruboeck K, Jurkovic D, Lawton F, Savvas M, Tailor A, Campbell S. The diagnostic value of endometrial thickness and volume measurements by three-dimensional ultrasound in patients with postmenopausal bleeding. Ultrasound Obstet Gynecol 1996; 8(4): 272–76.
14. Momtaz M, El Ebrashi A. 3D sonohysterography in the evaluation of the uterine cavity. Syllabus. Las Vegas, October 1999.
15. Fedele I, Bianchi S, Dorta M, Arcaini L, Zanotti F, Carinelli S. Transvaginal ultrasonography in the diagnosis of diffuse adenomyosis. Fertil Steril 1992; 58:94.
16. Hirai M, Shibata K, Sagai H, Sekiya S, Goldberg BB. Transvaginal pulsed and color Doppler sonography for the evaluation of adenomyosis. J Ultrasound Med 1995; 14:529–32.
17. Lee SL, Busmanis I, Tan A. 3D-Angio of Adenomyotic Uteri. Syllabus. Las Vegas, October 1999.
18. Kupesic-Urek S, Shalan H, Kurjak A. Early detection of endometrial cancer by transvaginal color Doppler. EUROBS 1993; 49:46–49.
19. Kurjak A, Kupesic S. Ovarian senescence and its significance on uterine and ovarian perfusion. Fertil Steril 1995; 3:532–7.
20. Emoto M, Tamura R, Shirota K, Hachisuga T, Kawarabayashi T. Clinical usefulness of color Doppler ultrasound in patients with endometrial hyperplasia and carcinoma. Cancer 2002; 94(3):700–06.
21. Jarvela I, Tekay A, Santala M, Jouppila R Thermal balloon endometrial ablation therapy induces a rise in uterine blood flow impedance: a randomized prospective color Doppler study. Ultrasound Obstet Gynecol2001; 17(1):65–70.
22. Folkman J, Cole D, Becker F Growth and metastasis of tumor in organ culture. Tumor Res 1963; 16:453–67.
23. Yaman C, Ebner T, Jesacher K, Obermayr G, Polz W, Tews G. Reproducibility of three-dimensional ultrasound endometrial volume measurements in patients with postmenopausal bleeding. Ultrasound Obstet Gynecol 2002; 19(3):282–86.
24. Kurjak A, Kupesic S. Three-Dimensional Ultrasound and Power Doppler in Assessment of Uterine and Ovarian Angiogenesis: a Prospective Study. Croatian Medical J 1999; 40(3):51–58.
25. Kupesic S, Kurjak A, Zodan T. Staging of endometrial carcinoma by 3-D power Doppler. Gynecol Perinatol 1999; 8(1):1–5.
26. Lee CN, Cheng WF, Chen CA, Chu JS, Hsieh CY, Hsieh FJ. Angiogenesis of endometrial carcinomas assessed by measurement of intratumoral blood flow, microvessel density, and vascular endothelial growth factor levels. Obstet Gynecol 2000; 96(4):615–21.
27. Alcazar JL, Galan JM, Jurado M, Lopez-Garcia G. Intratumoral blood flow analysis in endometrial carcinoma: Correlation with tumor characteristics and risk for recurrence. Gynecol Oncol 2002; 84(2):258–62.
28. Kupesic S, Kurjak A. Color Doppler assessment of uterine leiomyoma and sarcoma. In: Kurjak A, Kupesic S (Eds). An Atlas of Transvaginal Color Doppler. Parthenon Publishing, New York, London, 2000; 179–87.

29. Fleischer AC, Entman SS, Porrath SA, James AE. Sonographic evaluation of uterine malformations and disorders. In: Sanders RC (Ed). The Principles and Practice of Ultrasonography in Obstetrics and Gynecology. Norwalk: Appleton Century Crofts, 1985; 531.
30. Kurjak A, Kupesic-Urek S, Miric D. The assessment of benign uterine tumor vascularization by transvaginal color Doppler. Ultrasound Med Biol 1992; 18:645–48.
31. Balen FG, Allen CM, Gardener JE, Siddle NC, Lees WR. 3-Dimensional reconstruction of ultrasound images of the uterine cavity. Br J Radiol 1993; 66(787):588–91.
32. Lev-Toaff AS, Rawool NM, Kurtz AB, Forssberg F, Goldberg BB. Three-dimensional sonography and 3D transvaginal US: a problem solving tool in complex gynecological cases. Radiology 1996; 201(P): 384.
33. Olah KS, Gee H, Blunt S, Dunn JA, Chan KK. Retrospective analysis of 318 cases of uterine sarcoma. Eur J Cancer 1991; 27:1095–99.
34. Kurjak A, Kupesic S, Shalan H, Jukic S, Kosuta D, Ilijas M. Uterine sarcoma: a report of 10 cases studied by transvaginal color and pulsed Doppler sonography. Gynecol Oncol 1995; 59:342–46.
35. Szabo I, Szantho A, Csabay L, Csapo Z, Szirmai K, Papp Z. Color Doppler ultrasonography in the differentiation of uterine sarcomas from uterine leiomyomas. EJ Gynaecol Oncol 2002; 23(1):29–34.
36. Paavonen J, Aine R, Teisala K. Chlamydial endometritis. J Clin Pathol 1985; 38:726–32.
37. Paavonen J, Kiviat N, Brunham RC. Prevalance and manifestations of endometritis among women with cervicitis. Am J Obstet Gynecol 1985; 152:280–86.
38. Hertzberg BS, Bowie JD. Ultrasound of the postpartum uterus. Prediction of retained placental tissue. J Ultrasound Med 1991; 10(8):451–56.
39. Wachsberg RH, Kurtz AB. Gas within the endometrial cavity at postpartum US: normal finding after spontaneous vaginal delivery. Radiology 1992; 183(2): 431–33.
40. Kurtz AB, Shlansky-Goldberg RD, Choi HY. Detection of retained products of conception following spontaneous abortion in the first trimester. J Ultrasound Med 1991; 10(7):387–95.

Chapter 47
Ovarian Sonography

Asim Kurjak, Matija Prka

Sonography is the diagnostic method of choice for evaluation of pelvic masses, particularly for those thought, on basis of clinical exam, to be benign. Although the sonographic features of a pelvic mass frequently do not permit a specific histopathologic diagnosis, sonography usually provides clinically important parameters for the pelvic mass.[1]

A number of studies proved superiority of the transvaginal approach to transabdominal ultrasonography.[2–4] The resolution as well as the specificity of information about sonographic findings of specific diseases depend on the proximity at which the transvaginal probe can be placed to the pelvic contents, as well as the transducer frequencies used (optimally>5 MHz).

Information gained by transvaginal gray scale sonography, taken into account with other diagnostic modalities, is useful in guiding the gynecologic surgeon through decisions regarding surgical intervention (Table 47.1). Generally, the consensus is that a surgical treatment is required in cases when masses that are over 10 cm in average dimension, contain irregular solid components, or are associated with significant (over 20 mL) of intraperitoneal fluid.[5] Similarly, pelvic masses that are associated with acute pelvic pain may require immediate surgical intervention because they may be associated with adnexal torsion.[6] On the other hand, masses that are completely cystic and smaller than 5 cm may only be observed over a few months with repeated sonograms, to document any change in size. In postmenopausal women, only a low percentage (approximately 3%) of small (less than 5 cm) adnexal masses will represent a malignant neoplasm.[7]

This chapter brings up certain differential points that are clinically important when evaluating a patient with a pelvic mass via transvaginal sonography.

SONOGRAPHIC PARAMETERS

Pelvic sonography has an important role in examining a pelvic mass that may have been palpated or suspected on pelvic examination. It is particularly useful in patients in whom an adequate pelvic examination cannot be performed, or in whom a poorly defined pelvic mass is found on examination.

Since some masses may be outside the range of the examiner's finger, sonography may occasionally detect masses that cannot be palpated adequately. In this situation, a real-time sonographic examination during pelvic examination can be used to demonstrate

the presence or absence of a mass.[8] Transvaginal sonography can be used to particular advantage in the delineation of the uterus and ovaries in obese patients. In fact, sonography has been found to be more reliable than palpation in the identification of normal-sized ovaries—even in the postmenopausal women.[9]

Origin and Size

Transvaginal sonography can provide detailed delineation of a pelvic mass smaller than 10 cm,

Table 47.1: Preoperative investigation and risk assessment for possible malignancy assessment in the diagnosis and treatment of ovarian tumor

Standard investigation	*Risk for malignancy*	*Advanced investigation*
Anamnesis:		
• reproductive data (parity, abortions), menstrual history, oral contraceptive use, infertility treatment, hormonal replacement therapy, earlier operations (ovary)		
Age:		
• premenopausal	*Low*	
• postmenopausal	*High*	
Family history of ovarian and/or breast cancer:		Genetic counseling
• negative	*Low*	
• positive	*High*	
Symptoms (if occur):		Exclude an extraovarian abdominal
• abdominal distension, fullness or pressure in the abdomen or pelvis, abdominal or lower back pain, frequent urination or urgency, constipation, lack of energy, lack of appetite, weight loss	*High*	disease (X-rays, CT, MRI)
Bimanual palpation:		
• smooth, round, mobile, unilateral, <10 cm	*Low*	
• uneven, non-mobile, bilateral, hard, with adhesions, >10 cm	*High*	
Transvaginal gray scale sonography (2D US) *Volume*		*Three-dimensional sonography (3D US) in*

		comparison to 2D US superior in:
• <20 cm^3—premenopausal	*Low*	– showing characteristics of internal
<10 cm^3—postmenopausal		cyst walls
• >20 cm^3—premenopausal	*High*	– identifying the extent of capsular
>10 cm^3—postmenopausal		infiltration of tumors
		– calculating ovarian volume
Morphology		
• smooth cystic wall, thin septa, no solid parts, anechoic	*Low*	
• intracystic growth, papillary projections, thick septa, solid parts, mixed echogenicity	*High*	
Transvaginal color and power Doppler: *Blood flow parameters*		Three-dimensional power Doppler (3D PD) *Qualitative analysis of tumor blood vessels:*
• PI>1.0, RI>0.42	*Low*	– position
• PI<1.0, RI≤0.42	*High*	– structure
		– branching pattern
Location of blood flow		
• peripheral	*Low*	
• central	*High*	
Tumor markers:		
• CA 125<35 U/mL	*Low*	Second generation CA 125,
• CA 125>35 U/mL	*High*	CA 15–3, CA 19–9

and determine its origin.[2,10,11] The uterus serves as a central landmark for identifying the location of a mass within the pelvis. An additional landmark for delineation of its borders is the echogenic endometrial interface within the uterus.[12] Masses within the ovary can usually be identified by the rim of compressed parenchyma ("beak") that is present between the mass and the remaining portion of the ovary. This feature is particularly well depicted with transvaginal scanning.

Abnormally distended tubes originate from the lateral aspect of the uterine cornu and their fusiform enlargement as they extend from the uterus into the pelvis. This is particularly helpful when differentiating between inflammatory disease that may involve the tube or ovary, such as a tuboovarian abscess, and simple hydrosalpinx.

Applying gentle pressure between the mass and the uterus may further elucidate the origin of a mass. For example, pedunculated subserosal fibroids are attached to the uterus

by a pedicle, in contrast to an adnexal mass, which are separable from the uterus. This serves as a differentiating factor between the two.

Occasionally, the size of a pelvic mass can help in differential diagnosis. Physiologic cysts, for example, are rarely larger than between 3 and 5 cm average dimension, while symptomatic ovarian tumors are generally about 10 cm. Exceptions to this may be encountered in acute hemorrhage or torsion of the ovary, when it can quickly enlarge over 24 to 48 hours.

Size alone, however, is not a specific criterion because it depends on when the patient presents for an examination relative to the growth pattern of the mass.

Internal Architecture

In over three-fourths of women studied, transvaginal sonography allows for a detailed delineation of the internal consistency of a pelvic mass, adding diagnostically specific information.[13] The mass that has no internal echoes, has smooth borders, and is enhanced through transmission, can be inferred. Occasionally, low-level echoes may be present within a cyst arising from proteinaceous fluid, blood, or cellular debris. A truly solid mass typically contains internal echoes, whereas a complex mass contains both solid and cystic components.

Generally, ovarian masses are more often cystic, whereas nonovarian masses solid. Thin and echogenic internal septations suggest the diagnosis of an epithelial ovarian neoplasm, usually a cystadenoma. However, the internal interfaces can also be found in hemorrhagic cysts resulting from partial coagulation of an internal clot. Hyperechoic material within an area can be seen in some dermoid cysts that contain sebaceous material, bone tissue, or teeth. Homogenous echogenic internal contents, such as endometriomas that contain clotted blood, may also be encounterd in a mass. Areas of hemorrhagic necrosis present as irregular anechoic regions within a mass. The more solid and irregular components that are present within a mass suggest it is more likely to be malignant.[5,14] Papillary excrescences also usually mean the possibility of malignancy. Irregularities and disruption in the borders of the mass suggest that malignant spread or rupture through the capsule has occurred.

Associated Lesions

Sonography is very accurate in detecting the amount of intraperitoneal fluid sometimes associated with adnexal masses. Although a small amount (3 to 5 mL) of fluid may be present due to physiologic processes, it is uncommon to have more than 10 mL of fluid in the cul-de-sac or peritoneal cavity of a healthy woman. Intraperitoneal fluid associated with pelvic masses increases the likelihood of a lesion to be neoplastic, and the possibility of malignant spread or rupture. In some cases, such as ovarian torsion, however, the fluid can represent a transudate related to obstructed venous and lymphatic return.[6] Rarely, intraperitoneal fluid can be associated with an ovarian fibroma or other benign adnexal masses.

Table 47.2: Sonographic differential dignoses of pelvic masses[a,b]

Cystic	*Complex*	*Solid*
Completely cystic	Predominantly cystic	Ovarian origin
Physiologic ovarian cysts	Cystadenomas	Fibroma
Cystadenomas	Tubo-ovarian abscess	Thecoma
Hydrosalpinx	Dermoid cyst	Uterine origin
Endometrioma	Predominantly solid	Pedunculated subsersal fibroid
Paraovarian cyst	Cystadenoma (carcinoma)	
Hydatid cyst of Morgagni	Germ cell tumor	
Multiple		
Endometriomas		
Multiple follicular cysts		
Septated		
Cystadenoma (carcinoma)		
– mucinous		
– serous		

(Adapted from Fleischer AC, Manning FA, Jeanty P, Romero R (Eds). Sonography in Obstetrics & Gynecology (6th ed), New York, McGraw-Hill, 2001;883–912)
[a]Based on most common appearance.
[b]Pelvic masses with a spectrum of sonographic appearances are mentioned in more than one category.

SONOGRAPHIC DIFFERENTIAL DIAGNOSIS OF PELVIC MASSES

This discussion of the transvaginal sonographic differential diagnoses of pelvic masses is organized according to the most frequently seen sonographic appearance of particular types of a pelvic mass (Table 47.2). If a particular pelvic mass has a spectrum of sonographic appearances, it is mentioned in more than one category.

This differentiating scheme should be used only as a general approach to the sonographic characterization of a pelvic mass. Sonographic findings must be correlated with the clinical ones. The sonographic depiction of morphology is helpful in determining the chance that a mass is malignant. The presences of wall or septal irregularity, or papillary excrescences, correlate with the chance of malignancy.

Cystic Masses

Pelvic masses appearing as cystic adnexal masses on transvaginal sonography most often include physiologic (follicular or luteal) ovarian cysts, hydrosalpinges, endometriomas, and paraovarian cysts. Even with the similar sonographic appearance of several types of cystic adnexal masses, the diagnostic possibilities can usually be narrowed to one or two entities based on clinical presentation and evaluation. In general, most cystic masses that arise within the pelvis are of ovarian origin. Depending on the referral population, physiologic ovarian cysts or hydrosalpinges will be the most common cystic pelvic masses encountered by the sonologist.

Physiologic Ovarian Cysts

Since functional cysts are usually asymptomatic, their precise incidence is unknown. They are most common during the reproductive years, but may occur at any age. Several types of cystic masses can result from abnormalities that occur at different stages of folliculogenesis. In general, follicular cysts occur either due to failure of a mature follicle to rupture at the time of ovulation, or following the collection of blood within the follicle after ovulation occurs (corpus luteum cyst). In most women, a mature follicle average size ranges from 15–20 mm.[7,15] Follicular cysts of the ovary are usually larger than a mature follicle, ranging from 3 to 8 cm in size. Luteal cysts, compared to follicular cysts, usually have a thicker wall and tend to contain hemorrhagic areas. Patients with hemorrhagic cysts may experience the abrupt onset of lower abdominal or pelvic pain.[16,17] Because this history can also pertain to cases of ruptured ectopic pregnancy, it is important to obtain an accurate pregnancy test in these patients.

Sonography has an important role in documenting any change in size of the cyst during and after clinical observation or treatment. At transvaginal sonography, a typical follicular cyst is clear, unilocular, and has a smooth, thin wall (Fig. 47.1). A corpus luteum cyst most commonly has a thick hyperechoic, occasionally crenulated wall, and usually has echogenic content (Fig. 47.2). The

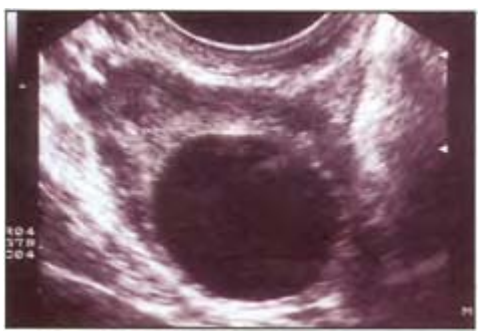

Figure 47.1: Transvaginal sonogram showing follicular cyst. Note smooth, thin cystic wall.

Surrounding ovarian tissue is compressed by cystic structure

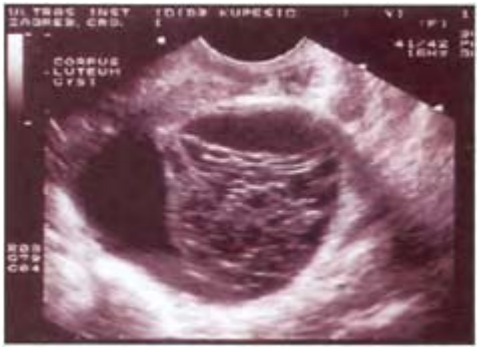

Figure 47.2: Hemorrhagic corpus luteum cyst containing fibrin strands appearing as a web-like complex of thin, branching linear interfaces

increased echogenicity of the cyst wall is probably the result of its higher fat content.[18] The corpus luteum may appear predominantly solid after complete collapse of the cyst. This appearance may range from an echogenic slit surrounded by a hypoechoic halo to a large, solid mass. These masses tend to be very vascular and show lowimpedance flow.

Hemorrhagic ovarian cysts can present as a variety of sonographic findings, depending on the size and organization of internal clot. Because of the presence of hemorrhage, the complicated functional cyst can have an appearance suggestive of that of a malignant tumor.[18] Although fibrinolyzed clot is typically hypoechoic, acute hemorrhage frequently appears as an irregular echogenic area, and may mimic a solid mass. As the clot begins to hemolyze, a reticular network of lowamplitude net-like strands is often demonstrated. Color Doppler can help support the diagnosis of hemorrhage by demonstrating absence of vascularity within solid portions consisting of organized clot.

It is important to point out that 53–89% of all functional cysts will undergo spontaneous regression; therefore, unless it is clinically unwise to delay surgical exploration (e.g. the presence of a very large mass[19]), a follow-up scan after 4–6 weeks is recommended.

Hydrosalpinx/Tubo-ovarian Complex or Abscess

Hydrosalpinges occur as a result of an inflammatory process, which produces adhesions of the fimbriated end of the tube, trapping intraluminal secretions. The secreted fluid distends the tube, resulting in a fusiform anechoic adnexal mass (Fig. 47.3). The

tapered fusiform shape and lack of peristalsis of a hydrosalpinx usually allows it to be differentiated from fluid-filled small bowel loops. In addition, the typical configuration of a hydrosalpinx (tapering as it enters the uterus and enlarging distally) is helpful in its sonographic recognition.

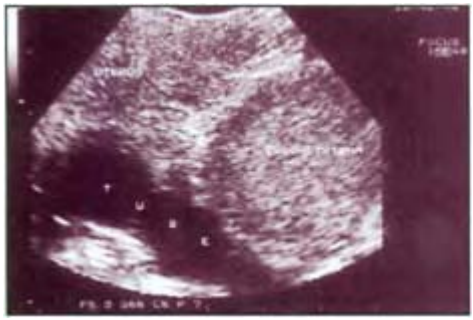

Figure 47.3: Transvaginal sonogram of sausage-like dilated tube with a small intraluminal projections (at upper part) that represents an endosalpingeal folds within a hydrosalpinx

A tubo-ovarian complex may arise if the inflammatory process involves the ovary, almost always secondary to salpingitis caused by pelvic inflammatory disease of bacterial origin.[20] It usually appears as a unilateral inflammatory conglomerate within which the ovary and tube are still recognizable. This may or may not progress to a tubo-ovarian abscess, in which there is a total breakdown of the adnexal structures on one or both sides.[21] With resolution, the only sequelae may be tubo-ovarian fibrous adhesions, but a healed abscess occasionally becomes a tuboovarian cyst, which may ultrasonographically resemble a cystic ovarian neoplasm.

The typical symptoms are abdominal or pelvic pain and, less consistently, fever, vaginal discharge or bleeding, and urinary symptoms. A history of pelvic inflammatory disease is present in only onethird to one-half of patients, suggesting common subclinical infections.

Sonographic markers for tubal inflammatory disease have been described by Timor-Tritsch et al.[21] The following findings were considered helpful:

- Thickening of the tube wall of=5 mm (100% of acute and 3% of chronic cases).
- "Cogwheel" sign,22 defined as a sonolucent cogwheel-shaped structure visible in crosssection of a tube with thick walls (86% of acute and 3% of chronic cases).
- Incomplete septa, correlating with folds or kinks in the dilated tube, which may be sonolucent or contain low-level echoes. These were seen in 92% of all cases; however, they were not discriminatory between acute and chronic cases.

- "Beads-on-a-string" sign, defined as hyperechoic mural nodules, measuring about 2 to 3 mm and seen on the cross-section of a fluidfilled distended structure. This is considred to represent flattened and fibrotic endosalpingeal folds (0% of acute, 57% of chronic cases).
- Tubo-ovarian complex, defined in the setting of pelvic inflammatory disease in which the ovaries and tubes are recognized but the ovary cannot be separated from the tube by pushing with the vaginal probe (36% of acute and 2% of chronic cases).
- Tubo-ovarian abscess, in which an acutely ill patient with marked tenderness at the touch of the ultrasonic probe demonstrates a total breakdown of the normal architecture of one or both adnexa, with formation of a conglomerate mass or fluid collection.
- Cul-de-sac fluid (50% of acute and 10% of chronic cases).

Although the true sensitivity and specificity of transvaginal sonography findings are not known, demonstration of sonographic markers as outlined previously, in the appropriate clinical setting, can assist in establishing the correct diagnosis. This will lower the frequency of more invasive diagnostic procedures. In the absence of a clinical history or findings in keeping with pelvic inflammatory disease, differentiation of a tubo-ovarian complex or tubo-ovarian abscess from a neoplastic process may be difficult sonographically.

Endometriosis

Endometriosis is defined as the presence of endometrial tissue outside of the endometrium and myometrium. It can involve a wide variety of locations, most commonly ovaries, uterine ligaments, rectovaginal septum, cul-de-sac, and pelvic peritoneum.[20] The true prevalence of endometriosis is unknown because most cases are asymptomatic. Estimates for the prevalence of the disease in women of reproductive age (80% of patients) range up to 15%.[20] Endometriosis has been documented in 15% of infertile women.[23] Typical symptoms attributed to pelvic endometriosis are acquired dysmenorrhea, lower abdominal, pelvic, and back pain, dyspareunia, irregular bleeding, and infertility.[20] The recurrent cyclic menstrual, inflammatory, and fibrotic changes within endometriotic lesions are likely responsible for most of the symptoms, although there is often no direct relationship between the extent of the disease and severity of symptoms.

Endometriotic foci may appear as punctate spots or patches of variable color, with a slightly raised or puckered surface, forming nodules, cysts, or both. In one-third to one-half of cases, ovarian endometriotic cysts are bilateral. They can partially or almost completely replace the normal tissue. The cysts rarely exceed 15 cm in diameter. They are commonly covered by dense fibrous adhesions, which may result in fixation to adjacent structures. The cyst walls are usually thick and fibrotic, with a smooth or shaggy, brown- to yellow-colored lining. The cyst content is typically altered, semifluid, or inspissated, chocolate-colored material.[20]

Transvaginal sonography does not detect endometriotic implants.[24,25] Endometriomas have a variety of appearances, ranging from an anechoic cyst to a cyst containing diffuse low-level echoes (Fig. 47.4) with or without solid components to a solid-appearing mass. Kupfer et al[25] described a typical sonographic pattern of a "cystic pelvic mass with homogeneous hypoechoic lowlevel echoes" in 82% of 38 surgically proven

endometriomas. Further studies confirmed these findings and showed that transvaginal sonography had a sensitivity of 82.4% to 88.9%, with a specificity of 89% to 97.7%.[26–30] False-positive diagnoses were mostly hemorrhagic cysts.[26,27]

Although the ultrasonographic findings are sometimes nonspecific, generally, differentiation from functional hemorrhage cysts or other echogenic cysts is possible by demonstrating multi- ple thick walls, homogeneity of the echogenic content, and multiplicity of the lesions.[18] In addition, unlike endometriomas, hemorrhagic cysts will usually demonstrate regression over subsequent cycles. Also, the presence of punctate or linear bright echogenic foci in the wall of the cyst favors the diagnosis of an endometrioma.

The use of color velocity imaging, pulsed Doppler,[26] or tumor markers (CA 125, CA 19–9)[29] do not improve the diagnostic accuracy of transvaginal sonography.

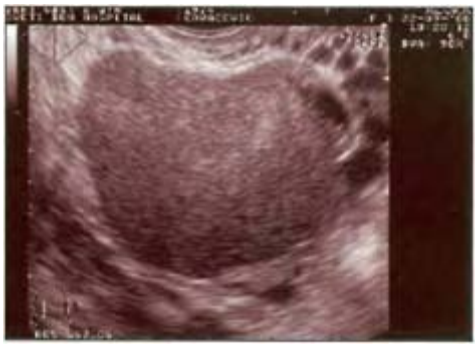

Figure 47.4: "Ground glass" appearance of an endometrioma. This well-defined mass is partly echogenic and demonstrates attenuation. Notice that the degree of echogenicity is less than that associated with dermoids

Paraovarian Cysts

Adnexal cystic masses that do not arise directly from the ovaries include paraovarian cyst, peritoneal inclusion cyst, and cyst of Morgagni, which arises from the fimbriated end of the tube. The most common type is the paraovarian cyst, which arises from Wolffian duct remnants in the mesovarium. It usually measures 3–5 cm, but can be as large as a pelvoabdominal cystadenoma. Occasionally, these cyts contain hemorrhage, and rarely they can contain internal septations.[31,32] Paraovarian cysts and tumors can usually be distinguished from the ovarian ones by their location. As in ovarian tumors,

paraovarian ones that contain solid areas or septation should be considered as potentially malignant.[33]

Complex Masses

Complex masses contain both fluid and solid areas. They can be predominantly cystic, or predominantly solid. Ovarian tumors that contain solid components or irregular septations, e.g. dermoid cysts, and most common surface epithelialstromal ovarian tumors of a serous, mucinous, and endometrioid subtype, are usually classified into this complex mass category.

Ovarian Dermoid Cysts

Mature cystic teratomas of the ovary, or dermoid cysts, are the most common benign germ cell tumor, and the most common ovarian neoplasm,[34] constituting 5–25% of all ovarian neoplasms. They occur most commonly during the reproductive years. Unlike other germ cell tumors of the ovary, however, they have a wider age distribution and may be encountered from infancy to old age.[20] A dermoid cyst is composed of well-differentiated derivates of the three germ layers: ectoderm, mesoderm, and endoderm, with ectodermal elements predominating. In its pure form it is benign, but a malignant transformation in one of its elements can occur in approximately 2% of the cases.

In 8–15% of the cases, the ovarian dermoid cysts are bilateral, with the possibility of several tumors being present in the same ovary. Grossly, the tumors vary in size from 0.5 cm to more than 40 cm. Approximately 60% measure 5–10 cm in diameter, and more than 90% measure less than 15 cm in diameter. The cut surface of the tumor reveals a cavity filled with fatty material, similar to normal sebum, and hair surrounded by a firm capsule of varying thickness. It is usually unilocular, but may also be multilocular.[20]

Usually a single, but possibly a multiple protuberance (Rokitansky protuberance) arises from the cyst wall and projects into the lumen. The protuberance is most commonly solid (although it can be partly cystic) and consists of a variety of different tissues. The hair present in the tumor arises from this protuberance, and bone or teeth,

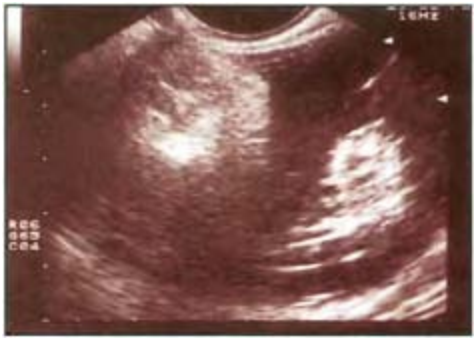

Figure 47.5: Complex predominantly cystic adnexal masses of ovarian

dermoid. Regional diffuse bright echoes are evident. Multiple hyperechoic lines and dots on the right side of the picture characteristic of a dermoid cyst

when present, tend to be located within this area. Dermoid cysts are often discovered as an incidental finding. When symptomatic, they usually present with abdominal pain, abdominal mass or swelling, and abnormal uterine bleeding.

Sonographic features ascribed to dermoid masses include the presence of regional diffuse bright echoes with or without posterior acoustic shadowing (Fig. 47.5), hyperechoic lines and dots, shadowing echodensity, and a fluid-fluid level.[18,35]

The feature that most commonly defines an ovarian mass as a cystic teratoma is regional diffuse hyperechoic solid components that attenuate the acoustic beam. Two types of tissue can produce this finding: clumps of hair in a cystic cavity or fat in a Rokitansky protuberance.[36] Hyperechoic lines and dots in a dermoid mass are attributed to the presence of hair.[37,38] Regional diffuse bright echoes and hyperechoic lines and dots are highly specific features of ovarian dermoids. Calcified structures, such as bone or teeth, result in shadowing echodensity, which is nonspecific. Fluid-fluid levels are presumably a result of sebum layered on serous fluid.[39]

In an evaluation of 252 adnexal masses, 74 of which were cystic teratomas, the positive predictive value for individual sonographic features associated with dermoid masses was 80% for shadowing echodensity, 75% for regionally bright echoes, 50% for hyperechoic lines and dots, and 20% for a fluid-fluid level. Fifty-five (74%) of the dermoids had two or more dermoid features, whereas none of the nondermoid masses had more than one feature, giving a positive predictive value for two or more ultrasonic dermoid features of 100%.[35]

Kurjak et al,[40] using a morphologic scoring system for dermoid cysts, achieved a sensitivity and specificity of 93.1% and 99.4%, respectively, in a study of 887 adnexal masses. When the presence of vascularity was assessed using color Doppler, 72% of cystic teratomas were mostly avascular, which, when combined with the scoring system, produced a sensitivity and specificity of 99.02% and 99.75%, respectively.

Ovarian Tumors Originating from the Surface Epithelium

Surface epithelial-stromal ovarian tumors account for about 60% of all ovarian neoplasms, and 80–90% of primary ovarian malignancies. Three broad epithelial categories, on the basis of epithelial differentiation, predominantly occur in this group: serous, mucinous, and endometroid, with frequencies of 46%, 36.5%, and 7.5%, respectively.

The spectrum of proliferative change these tumors exhibit is divided arbitrarily into three categories: benign, atypically proliferating (“of low malignant potential”, “borderline”), and malignant. The intermediate group of atypically proliferating tumors is defined as exhibiting greater cellular proliferation than that encountered in the benign

form of the same type of tumor but showing no destructive invasion of the stromal component.[20]

The mean age of patients with benign epithelial tumors is 45 years, and 50 years for those with atypically proliferating neoplasms. Invasive epithelial tumors are uncommon before 40 years of age. These tumors do not produce specific symptoms (Table 47.1).

Serous tumors Benign serous tumors are common, accounting for about one-quarter of all benign ovarian neoplasms, and 50–70% of all ovarian serous tumors. Although reported at all ages, they show a peak incidence in the fourth and fifth decade of life.[20]

Between 10% and 15% of ovarian serous tumors are categorized as atypically proliferating serous tumors. Their peak incidence is between 45 and 50 years of age.[20]

Malignant serous tumors account for approximately 40–50% of malignant ovarian neoplasms. They occur most frequently between 45 and 65 years of age, and in 80–85% of the cases they are widely disseminated at diagnosis.[20]

Between 12% and 20% of the benign serous tumors are bilateral (more often in the elderly women), while about 66% of malignant serous tumors are bilateral.[20]

Variations in gross appearances of benign serous tumors are due to the relative prominence in a given lesion between the three growth patterns: cystic, papillary, and adenofibromatous. Most cystic tumors are unilocular, but multilocular forms occur and vary in size up to 30 cm diameter. The cysts are usually filled with serous fluid. The linings of the cysts are either entirely flat or have focal, grossly visible, coarse papillary projections. Such papillary excrescences rarely cover the entire inner surface of the benign serous cysts. The third (adenofibromatous) variant is a solid neoplasm.[20]

Atypically proliferating serous tumors have gross features similar to those of benign serous tumors, but tend to have finer, more friable and exuberant papillary projections.[20]

Well-differentiated carcinomas are mostly cystic, multilocular tumors with soft, friable papillae, partly or mostly filling the cavities, and containing usually turbid or bloody fluid. External surfaces may be smooth or bosselated, and sometimes include surface papillae. Tumor adhesions to surrounding organs are common.[20]

Psammomatous calcifications are present in 15% of benign tumors and 60% of malignant

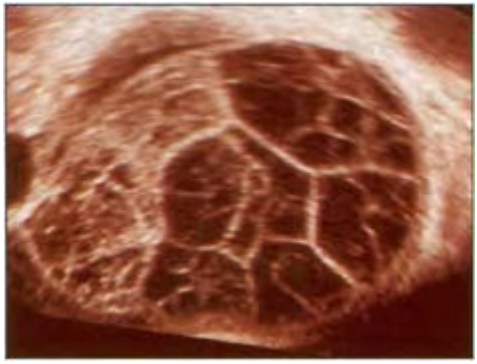

Figure 47.6: Transvaginal sonogram of “borderline”

serous cystadenoma. Note many internal thin-walled septations within the complex ovarian tumor

tumors, and may occasionally be very prominent, producing macroscopic calcification.[20]

Sonographically, benign serous cystadenomas appear as sharply marginated, anechoic masses that may be large and are usually unilocular. Internal thin-walled septations (Fig. 47.6) and, occasionally, papillary projections may be seen, the later often more florid in borderline tumors.[20]

Serous cystadenocarcinomas are usually multilocular, containing multiple papillary projections and septations; echogenic material is occasionally present within loculi.

Cystadenofibroma tends to have a solid component and is the most likely to mimic a malignant lesion. Ascites is common in serous cystadenocarcinomas but quite uncommon in cystadenomas.[41]

Mucinous tumors Benign mucinous cysts and cystadenomas comprise 20–25% of all benign ovarian neoplasms, and 75–85% of all ovarian mucinous tumors. They occur most often during the third to fifth decade of life, and are bilateral in only about 2% to 3% of the cases.[20]

Atypically proliferating mucinous tumors comprise 14% of all mucinous tumors. They have peak prevalence in women in the 30s, and are bilateral in 6–8% of tumors with intestinal-type epithelium, and 40% of tumors with endocervicallike epithelium.[20]

Malignant mucinous tumors comprise 5–10% of malignant primary ovarian neoplasms and a similar percentage of all ovarian mucinous tumors. They occur most commonly between the fourth and the seventh decade of life. Although in 15–20% of the cases they are bilateral, only 5% show extension beyond the ovaries at the time of laparotomy.[20]

Grossly, benign mucinous tumors and atypical proliferating mucinous tumors are typically multiloculated, cystic tumors measuring up to 50 cm in diameter. The serosal surface of the usually thick outer wall is smooth and opaque. The cysts contain a thick, tenacious mucinous material, occasionally somewhat more watery in consistency. Loculi are usually small and multiple, but tumors may be parvilocular or even a large simple cyst. The frank mucinous carcinomas tend to be cystic, multiloculated neoplasms, usually measuring 15 to 30 cm in diameter.

Sonographically, mucinous cystadenomas have thicker and more numerous septations and frequently contain fine, gravity-dependent echoes produced by the thick contents (Fig. 47.7).[42] The presence of debris may cause them to mimic solid components; however, gentle tapping on the cyst wall with the probe may result in movement, confirming the diagnosis of a pseudomass.

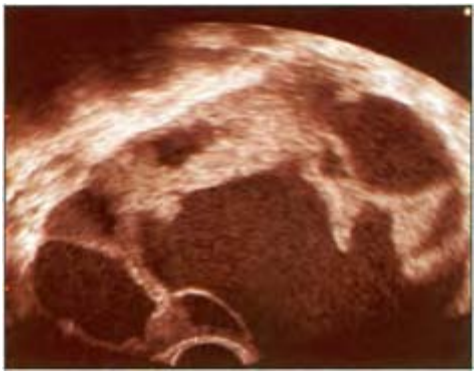

Figure 47.7:
Multiloculated appearance of an ovarian mucinous cystadenocarcinoma. Solid parts and thick, irregular septa are clearly visible. Note fine, homogenous echo of a thick, mucinous contents

Mucinous cystadenocarcinomas usually appear as large multiloculated cystic lesions containing echogenic material and papillary excrescences. They have papillary projections less frequently than the serous type.[41]

Endometrioid tumors Approximately 80% of ovarian endometrioid tumors are malignant. Endometrioid carcinomas are the second most frequently encountered malignant ovarian epithelial tumor, accounting for 20–25% of all ovarian carcinomas. They are bilateral in 28% of cases, and occur most frequently in the fifth and sixth decade of life. About 20–25% of these carcinomas are associated with a histologically similar lesion of the endometrium. Endometrioid carcinoma accounts for 70% of the tumors arising from endometriosis. Direct origin of endometrioid carcinoma from endometriotic tissue has been reported in up to 24% of the cases in some series.[20]

Grossly, endometrioid carcinomas are primarily cystic, most measuring 12–20 cm in diameter. On section, cysts contain friable, soft masses or papillae, as well as bloodstained fluid. Less commonly, neoplasms are solid, with widespread necrosis and hemorrhage.[20]

Ovarian endometrioid tumors are defined by "the presence of epithelial elements, stromal elements, or a combination of the two, that resemble closely the components of typical tumors of the endometrium".[20] Endometrioid ovarian carcinomas generally are regarded as having an overall better prognosis than either serous or mucinous carcinomas.[20]

Sonographically, endometrioid tumors usually present as a cystic mass containing papillary projections, although in some dases they are a predominantly solid mass.[43,44]

Solid Masses

Sex cord-stromal ovarian tumors (i.e. fibromas, thecomas, granulosa cell, and Sertoli-Leydig cell tumors) account for approximately 8% of all ovarian tumors. They are mostly solid; fibromas account for approximately one-half of cases, thus representing the most common ovarian lesion to appear on transvaginal sonography as a solid mass.

Fibroma

Fibromas account for 4% of all ovarian tumors. They occur at all ages but are most frequent in middle aged women (mean, 48 years).[20] Ovarian fibromas may also be part of basal cell nevus syndrome, a hereditary disease, when they are typically bilateral, multinodular, and calcified.

Meigs' syndrome (ascites and pleural effusion accompanying a fibrous ovarian tumor, usually a fibroma, and disappearing after the removal of the tumor) complicates about 1% of ovarian fibromas. Ascites alone is present 10–15% of ovarian fibromas larger than 10 cm in diameter.[20]

Fibromas range in size from microscopic to very large. Sectioning typically reveals hard, flat, chalky-white surfaces that have a whorled appearance. Focal or diffuse calcification and bilaterallity are each observed in fewer than 10% of the cases. Microscopy reveals intersecting bundles of spindle cells producing collagen. The absence of fat differentiates a fibroma from a thecoma. Differentiation from a fibrosed thecoma, however, is not always possible.[20]

Sonographically, two typical appearances have been described. The first has features similar to that of a uterine fibroid, with variable attenuation and multiple-edge shadows, occurring because of the whorl gross appearance of these tumors. This type of fibroma may be difficult to differentiate from a pedunculated fibroid if it completely replaces normal ovarian tissue and reaches large dimensions.[18] The second appearance is that of a hypoechoic mass with substantial attenuation.[18,45] Atypically, fibromas may be hyperechoic or may demonstrate a mixed heterogeneous pattern. Calcification may be identified.[46]

EVALUATION OF AN OVARIAN MASS

Morphologic Assessment

Transvaginal sonography plays an important role in the assessment of adnexal masses; however, the significant number of false-positive results produced limits the accuracy of the technique. Ultrasonic signs of malignant ovarian tumors include multilocular or multiple cysts, thick or irregular septa or walls, poorly defined borders, papillary projections, solid components, and echogenic elements.[47,48] In an attempt to improve specificity, different morphologic criteria, many of which are given a numeric value to produce a summated score, have been examined.[49–52] Depending on the value of the score, investigators hope to distinguish between benign and malignant masses using a cut-off value.

In a prospective comparison of four previously published morphologic scoring systems and a new "multicenter score", Ferrazzi et al[53] demonstrated a significant

improvement in diagnostic accuracy with the multicenter system. This was accounted for mainly by the introduction of two criteria that allowed correction for typical dermoids and endohemorrhagic corpora lutea. Even so, although the scores were sensitive, they were not specific, with the best diagnostic accuracy of 72% obtained with a sensitivity of 87% and specificity of 67%. By lowering the cut-off score by 1 point from 9 to 8, a sensitivity of 93% was achieved; the specificity fell to 56%.

Several investigators examined adnexal masses with three-dimensional ultrasound (3D US) and found the simultaneous, multiplanar display of perpendicular planes advantageous for examining the structure of masses or cystic collections and for assessing papillary projections or irregularities in the walls (Fig. 47.8) of otherwise benign appearing cysts. Bonilla-Musoles et al[54] reported on 76 women with ovarian masses studied with both 2D US and 3D US and found that 3D US was superior in (1) evaluating for papillary projections, (2) showing characteristics of cystic walls, (3) identifying the extent of capsular infiltration of tumors, and (4) calculating ovarian volume. In one patient, papillary projections were identified on 3D US that were not seen on 2D US. In a series of 45 patients with ovarian tumors, Merz et al[55] found that it was the multiplanar capability that was the most advantageous in examining these tumors. It was particularly helpful in grading the tumors that were cystic.

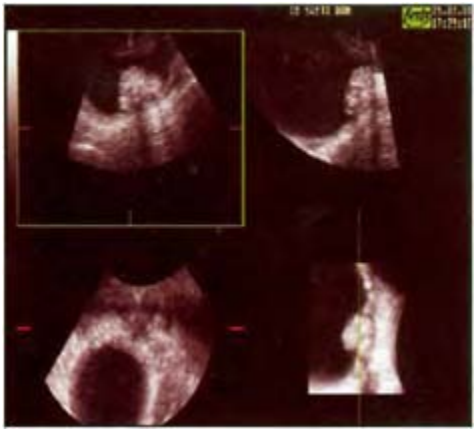

Figure 47.8: 3D US examining of a small papillary projection located on the internal cystic wall by simultaneous, multiplanar display of perpendicular planes.

Doppler Parameters

Transvaginal color Doppler sonography has been shown to be a clinically useful adjunct to grayscale sonography for the evaluation of patients with pelvic masses.[56,57] Color Doppler evaluation of the presence or absence of flow, the distribution of flow and the flow velocity waveforms seems to be helpful in distinguishing benign from malignant ovarian lesions. This topic is covered in detail in Chapter 49.

PERSISTENT VS REGRESSING MASSES

In the pre- or perimenopausal women, a followup examination may be indicated 6 to 8 weeks after the initial sonographic finding, in those masses thought to be benign, even though some may persist up to 2–3 months. About 70% of cysts in premenopausal women will demonstrate regression in 2 to 3 months.[58] If regression does not take place, one should consider other etiologies. Acute enlargement can result from intraluminal hemorrhage and/or torsion.

In postmenopausal women there is an increased risk of a pelvic mass malignancy. However, one study showed that up to 15% of asymptomatic postmenopausal women had cystic masses up to 3 cm in size.[59] If followed for 6 months, over half regress and approximately one-fourth enlarge, and one-fourth stay the same in size.[60] Clinical judgement in these cases is needed to determine which patients may benefit from surgery, aspiration and cytology, or observation. Serum CA 125 has only a limited role because of its poor sensitivity and specificity. Signs indicating the possibility of malignancy are enlargement, development of irregular solid areas, and ascites.

TRANSVAGINAL SONOGRAPHY IN OVARIAN CANCER SCREENING

In developed countries more women die annually from ovarian cancer than from all other gynecologic malignancies combined. For example, in the United States approximately 24,000 new cases are diagnosed each year, and 14,000 of these women will die of the disease.[61] Symptoms usually do not become apparent until the tumor compresses or invades adjacent structures, ascites develops, or metastases become clinically evident. As a result, around 65% of women with ovarian cancer have advanced disease (stage III/IV) at diagnosis with 5-year survival rate of only 20–30%, compared with the 5-year survival of over 90% in patients with stage IA ovarian cancer, when disease is confined to the ovary.[62] Given the burden of suffering associated with the development of ovarian cancer and the clear survival gradient related to the stage of disease at diagnosis,[63] there is much enthusiasm for the development of effective screening methods/assays for the early detection of epithelial ovarian cancer.

During the last decade, large prospective studies of screening for ovarian cancer have been performed.[64] Two distinct strategies have emerged, one based on ultrasound as the primary test, and the other involving the serum tumor marker CA for primary screening with ultrasound as the secondary test (multimodal screening). Table 47.3 summarizes the prospective ovarian cancer screening studies in the general population.[65–69] If we exclude those which used transabdominal ultrasound, an abandoned screening strategy due to

unacceptably high rate of false-positive results, several important lessons can be learned for forthcoming trials.

As seen on the Table 47.3, the data suggests that sequential multimodal screening has greater specificity and positive predictive value compared to strategies based on transvaginal ultrasound alone. For each case of ovarian cancer detected, four women underwent surgery in the multimodal studies compared to 17 women in the studies using ultrasound alone. However, transvaginal ultrasound as a first line test may offer higher sensitivity for early stage disease given that 21/32 (67.7%) cancers detected using ultrasound alone were stage I, compared to 7/17 (41.2%) cancers detected by the multimodal strategy. An ultrasoundbased strategy may have a greater impact on ovarian cancer mortality, albeit at a higher price in terms of surgical intervention for false-positive results.

Recently published studies indicate that 3D power Doppler imaging can improve the ability to differentiate benign from malignant ovarian masses, increasing significantly specificity and positive predictive value in ovarian cancer detection.[70,71] The problem of low positive predictive in ultrasound-only strategies may be solved by the introduction of new 3D ultrasound technologies, used together in a secondary screening process. The possible role of 3D ultrasound, 3D power Doppler and contrast-enhanced 3D power Doppler in early and accurate detection of ovarian cancer is currently under evaluation through the Zagreb Ovarian Cancer Screening Trial.[72]

Here we present an illustrative case of successfully detected stage IA ovarian cancer in an asymptomatic, 57-year-old postmenopausal patient included in our new screening trial. She was well educated and concerned about family history of cancer, because her mother and

Table 47.3 Most important prospective ovarian cancer screening studies in the general population using ultrasound as a screening tool

Study	*Inclusion criteria*	*Screening strategy*	*No. screened*	*No. of invasive epithelial ovarian cancers detected*[a]	*No. of positives screens*	*No. of positive screens/cancer detected*[b]
ULTRASOUND (US) APPROACH						
Gray scale US (level 1 screen), than repeat gray scale US (level 2 screen)						
van Nagell *et al*[65]	Age >50 years and postmenopausal or >30 with positive family history	TVS Annual screens Mean 4 screens/women	14469	11(6) 5 stage I	180	16.4
Gray scale US and CDI (level 1 screen)						

Kurjak *et al*[66]	Aged 40–71 years	TVS and CDI	5013	4 4 stage I	38	9.5
Gray scale US (level 1 screen) and other tests (level 2 screen)						
Sato *et al*[67]	Age >30 years	TVS then tumor markers if TVS +, CT and MRI if all previous +	51550	16(6) 12 stage I	324	20.3
Total				31(12) 21 stage I	542	17.5
MULTIMODAL APPROACH						
CA 125 (level 1 screen), then gray scale US (level 2 screen)						
Jacobs *et al*[68]	Age >45 years Postmenopausal	RCT Serum CA 125 TAS/TVS, if CA 125↑ 3 annual screens	10958	6 3 stage I	29	4.8
Jacobs *et at*[69]	Age >45 years Postmenopausal	Serum CA 125 TAS, if CA 125↑	22000	11 4 stage I	41	3.7
Total				17 7 stage I	70	4.1

TVS: transvaginal ultrasound; CDI: Color Doppler imaging; RCT: randomized controlled trial.
[a]The borderline/granulosa tumors detected are shown in parenthesis.
[b]Only invasive epithelial ovarian cancers included.

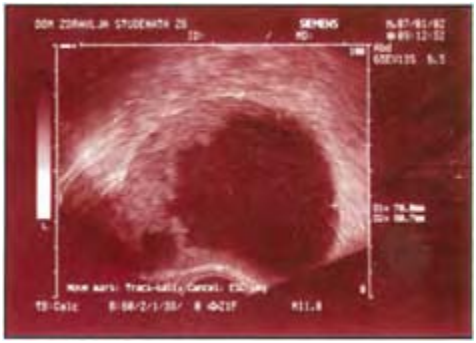

Figure 47.9: Multimodal ultrasound imaging of a complex ovarian tumor in a 57-year-old postmenopausal patient, detected at our screening

trial (Figures 47.9 to 47.12). B-mode showed noticeable solid component protruding into the cystic cavity, measuring 8 cm in larger diameter. Note thick, irregular septum on the basis of the lesion

mother's sister had breast cancer. Besides regular mammography and gynecological chek-ups, patient decided to perform gynecological ultrasound in an outpatient clinic, for the first time in her life.

Transvaginal gray scale sonography, performed by her primary care gynecologist, revealed a complex cystic-solid tumor of the right ovary, measuring 8 cm in diameter, with detectable papillas and thick, irregular septum (Fig. 47.9).

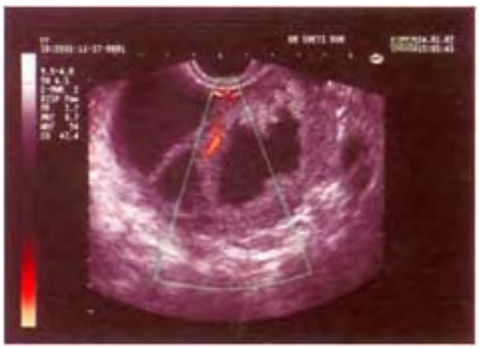

Figure 47.10: Thick septa, solid components, and gross papillary projection on the basis of the lesion were obtained more clearly by B-mode in different section. Also, 2D power Doppler was switched on, showing highly vascularized septum

Regarding ovarian morphology indicative for malignancy, she was immediately directed to our department for further ultrasound evaluation.

We confirmed previous TV US finding, and 2D power Doppler imaging showed highly vascularized zone within the septum (Fig. 47.10). Another step represented transvaginal color Doppler analysis of tumoral blood flow which revealed RI of 0.40 as the lowest value (Fig. 47.11). According to our color Doppler criterias, this finding was indicative for a malignant ovarian lesion.

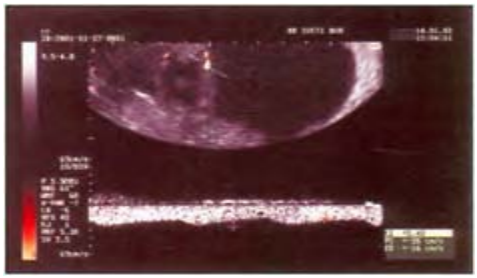

Figure 47.11: Further analysis of tumoral blood flow by transvaginal color Doppler within the vascularized septum (shown in Figure 47.2) revealed RI of 0.40 as the lowest value. According to our 2D color Doppler criterias, this finding was indicative for ovarian malignancy

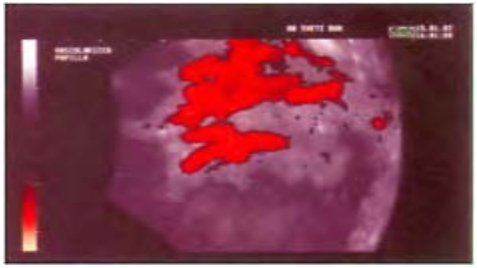

Figure 47.12: 3D power Doppler analysis revealed malignant neovascularization within

the papillary projection (shown in Figure 47.2.), characterized by irregular course of the tumoral vessels and complicated branching. Histopathologic finding was stage IA ovarian endometrioid adenocarcinoma

The vascular pattern obtained by further analysis with 3D power Doppler imaging clearly depicted disorganized, randomly dispersed vessels with irregular branching in the tumor papilla (Fig. 47.12), strongly associated with ovarian malignancy.

As a result, 3D power Doppler data on tumor vessels architecture enabled us to make more accurately preoperative sonographic diagnosis of an early stage ovarian cancer. On the other hand, CA-125 serum level of 16.3 U/ml was in normal ranges, giving us a false negative impression of a benign ovarian tumor.

Standard oncological surgical procedure was performed, and histopathology reported stage IA endometrioid adenocarcinoma of the ovary.

From the case described above, we will try to emphasize several details important for forthcoming ovarian cancer screening studies:

1. 3D power Doppler qualitative analysis of tumor angiogenesis allows accurate detection of the earliest appearance of ovarian malignancy, i.e. stage IA ovarian cancer;
2. At the present time, higher equipment costs and more sophisticated operator skills make 3D ultrasound technology ideally available in clinical and university hospital settings as a secondary screening tool;
3. As published by Holbert,73 and noted in the case above, routine screeningfor ovarian cancer by standard 2D ultrasound modalities, in terms of primary screening, is a valuable addition to the yearly examination in outpatient clinics and private gynecology office settings.

REFERENCES

1. Fleischer A, James AE Jr, Millis J et al. Differential diagnosis of pelvic masses by gray-scale sonography. Am J Roentgenol 1978; 131:469–74.
2. Mendelson EB, Bohm-Velez M, Joseph N et al. Gynecologic imaging: Comparison of transabdominal and transvaginal sonography. Radiology 1988; 166:321–24.
3. Leibman AJ, Kruse B, McSweeney MB. Transvaginal sonography: Comparison with transabdominal sono graphy in the diagnosis of pelvic masses. Am J Roentgenol 1988; 151:89.
4. Tessler FN, Schiller VL, Perrella RR et al. Transabdominal versus endovaginal pelvic sonography: Prospective study. Radiology 1989;170:553.
5. Moyle J, Rochester D, Sider L et al. Sonography of ovarian tumors: Predictability of tumor type. Am J Roentgenol 1983; 141:985–91.
6. Warner M, Fleischer A, Edell S et al. Uterine adnexal torsion: Sonographic findings. Radiology 1985; 154:773–75.

7. Fleischer A, Daniell J, Rodier J et al. Sonographic monitoring of ovarian follicular development. J Clin Ultrasound 1981; 9:275–80.
8. Bluth E, Ferrarri B, Sullivan M. Real-time ultrasonography of the pelvis as an adjunct to the digital examination. Radiology 1984; 153:789–91.
9. Granberg S, Wikland M. A comparison between ultrasound and gynecologic examination for detection of enlarged ovaries in a group of women at risk for ovarian carcinoma. J Ultrasound Med 1988; 7:59–64.
10. Lande IM, Hill MC, Cosco FE et al. Adnexal and culde-sac abnormalities: Transvaginal sonography. Radiology 1988; 166:325–32.
11. Vilaro MM, Rifkin MD, Pennell RG et al. Endovaginal ultrasound: A technique for evaluation of nonfollicular pelvic masses. J Ultrasound Med 1987; 6:697–701.
12. Callen P, DeMartins W, Filly R. The central uterine cavity echo: A useful anatomic sign in ultrasonographic evaluation of the female pelvis. Radiology 1979; 131:187–90.
13. Fleischer A, Entman S, Gordon A. TV and TA US of pelvic masses. J Ultrasound Med Biol 1989; 15:529–33.
14. Meire J, Ferant P, Guha T. Distinction of benign from malignant ovarian cysts by ultrasound. Br J Obstet Gynaecol 1978; 85:893–99.
15. Hall D, Hann L, Ferrucc J et al. Sonographic morphology of the normal menstrual cycle. Radiology 1979; 133:185–88.
16. Baltarowich OH, Kurtz AB, Pasto ME et al. The spectrum of sonographic findings in hemorrhagic ovarian cysts. Am J Roentgenol 1987; 148:901–05.
17. Reynolds T, Hill MC, Glassman LM. Sonography of hemorrhagic ovarian cysts. J Clin Ultrasound 1986; 14:449–53.
18. Atri M, Nazarnia S, Bret P et al. Endovaginal sonographic appearance of benign ovarian masses. Radiographics 1994; 14:747.
19. Osmers R. Sonographic evaluation of ovarian masses and its therapeutical implications. Ultrasound Obstet Gynecology 1996; 8:217.
20. Kurman RJ (Ed). Blaustein's Pathology of the Female Genital Tract (4th ed). New York, Springer-Verlag.
21. Timor-Tritsch IE, Lerner JR Montegaudo A et al. Transvaginal sonographic markers of tubal inflammatory disease. Ultrasound Obstet Gynecology 1998; 12:56.
22. Bellah RD, Rosenberg HK. Transvaginal ultrasound in a children's hospital: Is it worthwhile? Pediatr Radiol 1991; 21:570.
23. Strathy JH, Molgoard CA, Coulam CB et al. Endometriosis and infertility: A laparoscopic study of endometriosis among fertile and infertile women. Fertil Steril 1982; 38:667.
24. Friedman H, Vogelzang RL, Mendelson EB et al. Endometriosis detection by US with laparoscopic correlation. Radiology 1985; 157:217.
25. Kupfer MC, Schwimmer SR, Lebovic J. Transvaginal sonographic appearance of endometriomata: Spectrum of findings. J Ultrasound Med 1992; 11:129.
26. Alcazar JL, Laparte C, Jurado M et al. The role of transvaginal ultrasonography combined with color velocity imaging and pulsed Doppler in the diagnosis of endometrioma. Fertil Steril 1997; 67:487.
27. Mais V, Guerriero S, Ajossa S et al. The efficiency of transvaginal ultrasonography in the diagnosis of endometrioma. Fertil Steril 1993; 60:776.
28. Volpi E, De Grandis T, Zuccaro G et al. Role of transvaginal sonography in the detection of endometriomata. J Clin Ultrasound 1995; 23:163.
29. Guerriero S, Ajossa S, Paoletti AM et al. Tumor markers and transvaginal ultrasonography in the diagnosis of endometrioma. Obstet Gynecol 1996; 88:403.
30. Guerriero S, Mais V, Paoletti AM et al. The role of endovaginal ultrasound in differentiating endometriomas from other ovarian cysts. Clin Exp Obstet Gynecol 1995; 22:20.
31. Alpern M, Sandier M, Madrazo B. Sonographic features of paraovarian cysts and their complications. Am J Roentgenol 1984; 143:157–60.

32. Athey P, Cooper N. Sonographic features of paraovarian cysts. Am J Roentgenol 1985; 144:83–86.
33. Korbin CD, Brown DL, Welch WR. Paraovarian cystadenomas and cystadenofibromas: Sonographic characteristics in 14 cases. Radiology 1998; 208:459–62.
34. Koonings PP, Campbell K, Mishell DJ et al. Relative frequency of primary ovarian neoplasms: A 10-year review. Obstet Gynecol 1989; 74:921.
35. Patel MD, Feldstein VA, Lipson SD et al. Cystic teratomas of the ovary: Diagnostic value of 626 sonography. Am J Roentgenol 1998; 171:1061.
36. Quinn SF, Erickson S, Black WC. Cystic ovarian teratomas: The sonographic appearance of the dermoid plug. Radiology 1985; 155:477.
37. Malde HM, Kedar RR Chadha D et al. Dermoid mesh: A sonographic sign of ovarian teratoma. Am J Roentgenol 1992; 159:1349.
38. Bronshtein M, Yoffe N, Brandes JM et al. Hair as a sonographic marker of ovarian teratomas: Improved identification using transvaginal sonography and simulation model. J Clin Ultrasound 1991; 9:351.
39. Sheth S, Fishman EK, Buck JL et al. The variable sonographic appearances of ovarian teratomas: Correlation with CT. Am J Roentgenol 1988; 151:331.
40. Kurjak A, Kupesic S, Babic MM et al. Preoperative evaluation of cystic teratoma: What does color Doppler add? J Clin Ultrasound 1997; 25:309.
41. Sutton CL, McKinney CD, Jones JE et al. Ovarian masses revisited: Radiologic and pathologic correlation. Radiographics 1992; 12:853.
42. Fried AM, Kenney CM, Stigers KB et al. Benign pelvic masses: Sonographic spectrum. Radiographics 1996;16:321.
43. Williams AG, Mettler FA, Wicks JD. Cystic and solidovarian neoplasms. Semin Ultrasound 1983; 4:166.
44. Wagner BJ, Buck JL, Seidman JD et al. Ovarian epithelial neoplasms: Radiologic-pathologic correlation. Radiographics 1994; 14:1351.
45. Stephenson WM, Laing FC. Sonography of ovarian fibromas. Am J Roentgenol 1985; 144:1239.
46. Athey PA, Malone RS. Sonography of ovarian fibromas/thecomas. J Ultrasound Med 1987; 6:431.
47. Granberg S, Norstrom A, Wikland M. Tumors in the lower pelvis as imaged by vaginal sonography. Gynecol Oncol 1990; 37:224–29.
48. Rottem S, Levit N, Thaler I et al. Classification of ovarian lesions by high-frequency transvaginal sonography. J Clin Ultrasound 1990; 18:359.
49. Sassone AM, Timor-Tritsch IE, Artner A et al. Transvaginal sonographic characterization of ovarian disease: evaluation of a new scoring system to predict ovarian malignancy. Obstet Gynecol 1991; 78:70–76.
50. De Priest PD, Shenson D, Fried A et al. A morphology index based on sonographic findings in ovarian cancer. Gynecol Oncol 1993; 51:7.
51. Lerner JP, Timor-Tritsch IE, Federman A et al. Transvaginal sonographic characterization of ovarian masses using an improved, weighted scoring system. Am J Obstet Gynecol 1994; 170:81–85.
52. Bromley B, Goodman H, Benacerraf BB. Comparison between sonographic morphology and Doppler waveform for the diagnosis of ovarian malignancy. Obstet Gynecol 1994; 83:434.
53. Ferrazzi E, Zanetta G, Dordoni D et al. Transvaginal ultrasonographic characterization of ovarian masses: Comparison of five scoring systems in a multicenter study. Ultrasound Obstet Gynecol 1997; 10:192.
54. Bonilla Musoles F, Raga F, Osborne NG. Three-dimensional ultrasound evaluation of ovarian masses. Gynecol Oncol 1995; 59:129–35.

55. Merz E, Weber G, Bahlmann F et al. Sonographic assessment of ovarian tumors: Comparison of transvaginal three-dimensional ultrasound and standard two-dimensional vaginosonography. Ultraschall Med 1997;18:26.
56. Fleischer AC, Rodgers WH, Kepple DM et al. Color Doppler sonography of benign and malignant ovarian masses. Radiographics 1992; 12:879–85.
57. Kurjak A, Shalan H, Kupesic S et al. Transvaginal color Doppler sonography in the assessment of pelvic tumor vascularity. Ultrasound Obstet Gynecol 1993; 3:137–54.
58. Pinatti J. Interval from diagnosis to involution of cystic masses. Int J Gynecol Obstet 1988; 26:109–12.
59. Wolf S, Gosink B, Feldesman R et al. Prevalence of simple adnexal cysts in postmenopausal women. Radiology 1991; 180:5–9.
60. Levine D, Gosink B, Wolf S. Simple adnexal cysts: The natural history in post-menopausal women. Radiology 1992; 184:653.
61. Greenlee RT, Murray T, Bolden S et al. Cancer statistics, 2000. Cancer J Clin 2000; 50:7–33.
62. Heintz APM, Odicino F, Maisonneuve P et al. Carcinoma of the ovary. In: 24th Volume of the FIGO Annual Report on the Results of Treatment in Gynecological Cancer. J Epidemiol Biostat 2001; 6(1):107–38.
63. Kirwan JMJ, Tincello DG, Herod JJO et al. Effect of delays in primary care referral on survival of women with epithelial ovarian cancer: retrospective audit. BMJ 2002; 324:148–51.
64. Bell R, Petticrew M, Sheldon T. The performance of screening tests for ovarian cancer: results of a systematic review. Br J Obstet Gynecol 1998; 105: 1136–47.
65. van Nagell JR, DePriest PD, Reedy MB et al. The efficacy of transvaginal sonographic screening in asymptomatic women at risk for ovarian cancer. Gynecol Oncol 2000; 77:350–56.
66. Kurjak A, Shalan H, Kupesic S et al. An attempt to screen asymptomatic women for ovarian and endometrial cancer with transvaginal color and pulsed Doppler sonography. J Ultrasound Med 1994; 13:295–301.
67. Sato S, Yokoyama Y, Sakamoto T et al. Usefulness of mass screening for ovarian carcinoma using transvaginal ultrasonography. Cancer 2000; 89:582–88.
68. Jacobs IJ, Skates SJ, Macdonald N et al. Screening for ovarian cancer: a pilot randomised controlled trial. Lancet 1999; 353:1207–10.
69. Jacobs IJ, Skates SJ, Davies AP et al. Risk of diagnosis of ovarian cancer after raised serum CA 125 concentration: a prospective cohort study. BMJ 1996; 313:1355–58.
70. Kurjak A, Kupesic S, Anic T, Kosuta D. Three-dimensional ultrasound and power Doppler improve the diagnosis of ovarian lesions. Gynecol Oncol 2000; 76:28–32.
71. Cohen LS, Escobar PF, Scharm C et al. Three-dimensional power Doppler ultrasound improves the diagnostic accuracy for ovarian cancer prediction. Gynecol Oncol 2001; 82:40–48.
72. Kurjak A, Prka M. New developments in ovarian cancer screening. Ultrasound Rev Obstet Gynecol 2002; 2:167–77.
73. Holbert TR. Screening transvaginal ultrasonography of postmenopausal women in a private office setting. Am J Obstet Gynecol 1994; 170:1699–704.

Chapter 48
Fallopian Tube

Asim Kurjak, Sanja Kupesic, Drazena Bjelos

The Fallopian tubes are derived from the Müllerian ducts and arise from the cornual end of the uterus. They are a paired organ and their task is to serve as a conveyer for the oocytes and the sperm for their meeting for conception. The Fallopian tubes are about 9–11 cm long and are covered by peritoneum, which duplicates to form one of its loose attachments (mesosalpinx), to the broad ligament.

The arterial blood supply to the oviducts is derived from the terminal branches of the uterine and the ovarian arteries. The branches of the uterine arteries supply the medial two-thirds of each tube. The ovarian arteries supply the lateral one-third of the tube. The venous drainage parallels the arterial supply.

The ultrasonic scanning and evaluation of the Fallopian tube present a true challenge to even the best sonographers. The normal Fallopian tube can be imaged only if fluid surrounds it and creates a sonic interface to outline its boundaries.[1] The most proximal part of it can also be imaged in the normal state, since it is held steady by the uterus, which in this case serves as a landmark for finding the proximal part of the tube.

In certain instances some fluid is present in the pelvis. This, usually sonolucent fluid acts as a contrast medium to highlight the normal Fallopian tube.

1. At times, a certain amount of pelvic fluid is present and this may be enough to highlight portions of the Fallopian tube.
2. At midcycle, after the release of follicular fluid, at the time of ovulation or immediately after it, parts of the tube may be detectable.
3. Blood may be present in the pelvis for various reasons such as rupture of the corpus luteum, or rupture of an ectopic pregnancy. Such larger amounts of fluid in the pelvis may increase the chance to detect one or both Fallopian tubes.
4. Ascites present in the pelvis arising from ovarian hyperstimulation or other conditions, may serve as an excellent contrast medium around the Fallopian tube and the fimbriae in order to highlight them.
5. Fluid originating from infectious processes may also enable us to outline the Fallopian tubes.

If there is fluid in the pelvis, placing the patient into an anti-Trendelenburg position may increase the pooling of even small amounts of fluid and therefore, create the acoustic interface for imaging the tube.[2,3]

PELVIC INFLAMMATORY DISEASE

Pelvic inflammatory disease (PID) is defined as "the acute clinical syndrome associated with ascending spread of microorganisms (unrelated to pregnancy or surgery) from the vagina or cervix to the endometrium, Fallopian tubes, and/or contiguous structures".[4] Very rarely, PID can develop as a result of surgical intervention. PID causes more morbidity than necessary for three major reasons: women are not hospitalized when they should be, many women receive inadequate or inappropriate antibiotic therapy, and the male sex partner is not treated or is treated inadequately.

PID is mostly considered ascending and polymicrobial. Rarely, the infection is hematogenous or spreads directly from another abdominal organ (diverticulitis and appendicitis). Among the sexually transmitted pathogens, *N. gonorrhoeae* and *Chlamydia trachomatis* are most commonly identified.

Over half of women suffering from PID develop tubal damage without any symptoms of the disease, Chlamydia being the most frequent cause of this infection. Because of this observation, PID was classified into four major groups:

1. Silent (asymptomatic) PID (tubal scarring occurs without patient's knowledge),
2. Atypical PID (patients have only minimal symptoms),
3. Acute PID (this form is most commonly seen in patients presenting to emergency rooms), and
4. PID residual syndrome (patients suffer from chronic pelvic pain, infertility and scar tissue formation).5

Chronologically, PID can be divided into acute PID with formation of pyosalpinx and tuboovarian abscess and PID-residual syndrome with hydrosalpinx and scar tissue formation.

ULTRASOUND FINDINGS

Fallopian tube pathology is discerned by evaluating the wall of the tube, the luminal content, and the tubal motility, as well as its relation with the surrounding pelvic structures.

Early in the course of the acute inflammation, pelvic sonography may be entirely normal, as the process of inflammation precedes the tubes become thick-walled and irregular (Fig. 48.1). The associated pelvic exudate allows better delineation of the gynecologic structures. The inflamed tubes are represented by one of the following pictures:[6]

1. A dilated tubular structure.
2. Echogenic tubal wall which reflects the inflammatory process of the mucosal lining.

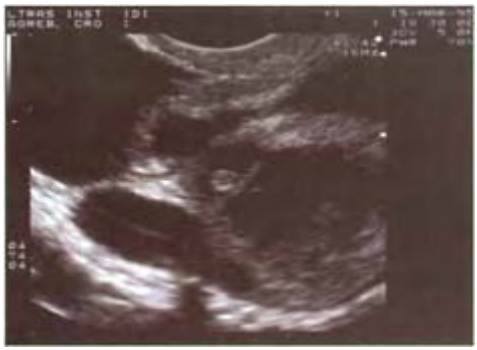

Figure 48.1: Complex adnexal mass occupying the pouch of Douglas in a patient with acute pelvic inflammation. Tubal diameter is increased, tubal mucosa is thickened and echogenic fluid fills the tubal lumen

3. The presence of internal echoes within the dilated tubes indicates pyosalpinx. Sonographicguided aspiration of the pus could be helpful for diagnostic purposes and for determining the optimal antibiotic therapy.
4. A complex adnexal mass with thickening of the ovarian capsule and loculated fluid collections in the adnexal cul-de-sac represents the tuboovarian abscess.

Sonographic appearance of hydrosalpinx differs depending on the stage of the disease. During the acute phase, the tubal wall is thick and tender to the probe touch, while in the chronic phase, hydrosalpinx shows a typically thin wall, which is not tender. Chronic hydrosalpinx is usually discovered accidentally, on a routine transvaginal scan or during an infertility procedure. The patients are often unaware of their pelvic pathology, but can recall an episode of pelvic pain or even overt pelvic inflammation.

Transvaginal sonography seems to be accurate in identification of Fallopian tube pathology by evaluating the structure of the tubal wall and luminal contents. However, it is difficult to differentiate tubal from ovarian pathology when complex masses are found. During the acute stage of pelvic inflammatory disease, the tortuous and dilated fluid-filled tube “embraces” the adjacent ovary. This ovary, therefore, can not be well delineated, although visualization of the ovarian follicles enables localization of the ovarian component of the mass. During the chronic stage of PID the thin-walled hydrosalpinx is the main sonographic hallmark. Hydrosalpinx produces the typical image of a homogeneous, elongated fluidfilled mass adjacent and medial to the ovary. Incomplete and thin tubal septa are clearly distinguished from the distended tubal wall. However, when hydrosalpinx is presented as a complex lesion with thick walls, septa,

suspicious papillary projections and mixed echogenic structures, incorrect diagnosis of an ovarian malignancy could be drawn.

COLOR DOPPLER FINDINGS

An improvement of transvaginal B-mode sonography was made after introduction of the color Doppler imaging. Color Doppler can depict the blood flow within the various tissues and tell us more about the vessel quality in a particular organ or structure. Color Doppler can also depict moving of the liquid component such as the case in hydrosalpinx, which moves when compressed by vaginal probe or sliding over bowels during peristalsis. Furthermore, color Doppler is very useful in making a differential diagnosis between hydrosalpinx and pelvic congestion syndrome. When color is turned on, pelvic congestion syndrome strikes the clinician with the amount of color on the screen, while hydrosalpinx remains black and white, the amount of color only depending on peristalsis or deliberate probe movements.

Kupesic et al[7] evaluated 102 women with laparoscopically proven PID. Seventy-two had acute symptoms, 11 presented with chronic pelvic pain, and 19 were infertility cases suspected of tubal etiology. The mean resistance index in patients with acute symptoms was 0.53±0.09. It significantly differed from those obtained in patients with chronic stage (RI=0.71±0.07), and infertility cases (RI=0.73±0.09). Therefore, the bizarre morphology during both the chronic and acute stages of PID if evaluated by color and pulsed Doppler should not cause an overlap with adnexal malignancy, since vascular resistance demonstrates significantly higher values.

Many studies have been undertaken to assess blood flow-related functional changes in the ovaries since our team first introduced the technique.[8] Significant changes have been demonstrated during the menstrual cycle in the active ovary, and most of them were attributed to angiogenesis in the follicle and, subsequently, the corpus luteum.[9,10] Transvaginal color Doppler proved to be useful in infertility evaluation and management, as well as in the assessment of adnexal masses and early detection of ovarian cancer.[11–14]

Kupesic and associates[7] assumed that an inflammatory process within the pelvis might affect ovarian blood flow. The ovary is in close proximity to the tube, which is the primary focus of infection, and it shares a significant part of its blood supply with the ipsilateral tube. Therefore, it can be expected that the ovarian blood flow is altered according to the changes in inflammatory process. Our study[7] demonstrated the correlation of intraovarian blood flow changes with pathophysiological ones. Findings obtained in the acute stage demonstrated rapidly changing patterns. The ongoing vasodilatation mediated by the local products of inflammation causes the decrease in RI (Fig. 48.2), while the subsequent edema of the

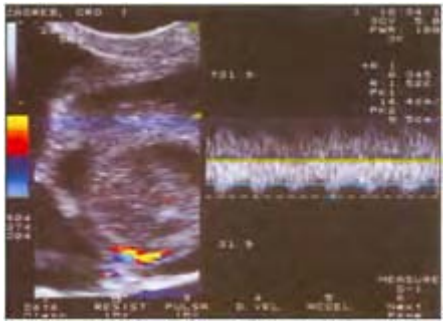

Figure 48.2: The same patient as in Figure 48.1. Note low impedance signals (RI=0.35) obtained from tiny tubal arteries

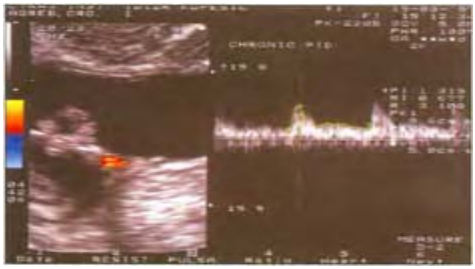

Figure 48.3: Complex adnexal mass containing fluid filled distended tube and pseudopapillomatous vascularized structure protruding into the tubal lumen. Moderate-to-high resistance blood flow signals (RI=0.68) are obtained from a pseudopapillomatous lesion. This finding suggests chronic PID

ovarian parenchyma causes the increase in the RI. As the ovarian capsule may vary in its rigidity, the intraovarian pressure differs from case to case. It affects the intensity of the intraovarian blood flow, which is reflected by variable values of RI. Furthermore, fluid collection within the tubes may influence the blood flow characteristics by compressing the vessels' wall. As the process advances, the proliferation of the fibroblasts and scarring tissue formation leads toward reduction of the local blood flow, which is demonstrated by the progressive increase in RI (Fig. 48.3). Very similar results were obtained by other authors, but on small series of patients.[5,15] We concluded that transvaginal color Doppler imaging might be used as an additional tool in evaluating the patients with suspected PID. Furthermore, we noticed that flow indices returned to normal values after treatment in 36 (48.65%) patients.

The same method was useful in differentiating pyosalpinx from hematosalpinx in ectopic pregnancy cases. Ectopic pregnancies are characterized with high velocity and low impedance (RI <0.42) blood flow signals[10,16] that indicate peritrophoblastic flow.

Transvaginal color and pulsed Doppler can also be helpful in differentiation between viable and non-viable ectopic pregnancy, which is characterized with significantly higher vascular resistance due to accumulation of the intraluminal blood and formation of hematosalpinx.

As the inflammation may mimic a wide variety of findings, and sometimes even suggest malignancy, serial assessment by color Doppler ultrasound is recommended, always with respect to the patient's age and the phase of the menstrual cycle. Serial examination may demonstrate morphological changes as well as variations in blood flow intensity according to the stage of the disease. Doppler studies are particularly useful in the chronic stage of PID, when pseudopapillomatous structures protruding into the cystic counterpart may morphologically suggest malignancy (Fig. 48.4). Absence of blood flow, typical for this stage, helps differentiating it from adnexal malignancy. In the acute stage, low resistance to blood flow, suggestive of malignancy may be demonstrated. In those patients, it is useful to do some additional tests (sedimentation rate, blood cells counts, CA125, etc.) that may help in reaching the final diagnosis. Serial ultrasound examination in these cases reveals the changes that correlate with the pathophysiological stage of the process. However, it should be concluded that there is no single para-

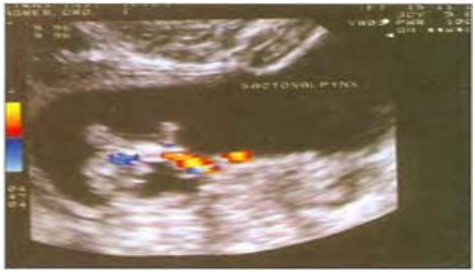

Figure 48.4: The same patient as in Figure 48.3. "Cogwheel" sign produced by

hyperechogenic knots and pseudopapillomatous structures is typical of chronic phase of PID. Color Doppler helps to differentiate suspicious morphology

meter that is sufficiently reliable for the adnexal mass characterization.[17]

In patients with tubo-ovarian abscess, abscess drainage under transvaginal sonographic guidance can hasten the recovery process and improve the efficacy of the antibiotic therapy.[18] Addition of the color Doppler facilities enables visualization of the large pelvic vessels and thereby may reduce the complication rate of the interventional procedure. However, a careful clinical examination, transvaginal ultrasound evaluation and blood tests are required before performing the procedure to avoid infection propagation.

THREE-DIMENSIONAL ULTRASOUND

Three-dimensional ultrasound helps in spatial delineation of the inflammatory conglomerates. Any scanned volume can be rotated in all dimensions and thus it is possible to observe borders of tissues and organs. By conventional B-mode ultrasound hydrosalpinx can sometimes by mistaken for a multilocular cyst, but when 3D is applied the true, spatial position and shape of hydrosalpinx is clearly visible. By using threedimensional volume sections it is possible to visualize the tortuous structure and contiguous spread of hydrosalpinx (Fig. 48.5). 3D ultrasound enables accurate visualization of three perpendicular planes simultaneously and by moving the

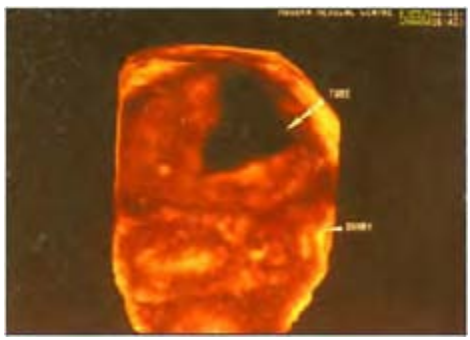

Figure 48.5: Three-dimensional image of chronic PID. Using this modality one can differentiate hydrosalpinx

from the surrounding ovary

cursor, sonographer “sees through” the slices of the hydrosalpinx. Another useful mode in this clinical situation is the so-called “niche” mode that enables the “cut-into” view of a certain tissue. With the use of this mode we can show the spatial spreading of hydrosalpinx, and at the same time, visualize the lumen. Furthermore, pseudopapillomatous structures within the tubal lumen can be better assessed. The surface of such papillary protrusions can be thoroughly scanned by surface mode, and its subtype “X-ray mode”. When applying this mode, the spaces that appeared anechoic on the conventional ultrasound scan are even darker, while the echoic tissues are shown lighter allowing better sharpness and contrast of the entire image.

Various inflammatory conglomerates sometimes pose a problem to the ultrasonographer. They may form a part of tubo-ovarian abscess or stay encapsulated by two sheets of peritoneum in the retrouterine space. Because of echogenicity and low vascular resistance, such structures can be mistaken for malignant tumors. Various forms of 3D ultrasound can define more clearly the spatial relations of such a structure and its connection to surrounding structures.

The vascularity of the Fallopian tube can be assessed by superimposing 3D power Doppler. By the use of this modality it is possible to visualize vascular pattern and to study the branching and shape of the vascular structures. The interesting future possibility for the use of 3D power Doppler stems from work on 3D color Doppler histograms and vascularity index (VI) measurements counting on the number of color voxels in the cube of the tissue, which represent the evolved vessels. Flow index (FI), a mean color value of all blood flow or induced flow intensities, represents the intensity of flow at the time of the three-dimensional sweep. With these indices it might be easier to quantify the flow and conclude on the phase of the inflammatory process. The changes caused by vasodilatation or those caused by scar tissue formation could be better understood.

Senoh et al[19] reported on a laparoscopy-assisted intrapelvic sonography with a high-frequency, realtime miniature transducer in the assessment of the Fallopian tubes. They developed a special 20 MHz flexible catheter-based high-resolution, real-time miniature (2.4 mm outer diameter) ultrasound transducer and tested it in the population of infertile patients. A total of 21 women (20 infertile, one with unilateral hydrosalpinx, and one tubal pregnancy) were studied with pelvic saline effusion under laparoscopy. The presented technique seems to be useful in the assessment of tubal texture and functional evaluation in tubal disorders, possibly in infertility practice.

BENIGN TUMORS OF THE FALLOPIAN TUBE

Although the muscles of the Fallopian tube and the uterus are of the same embryological origin (Müllerian ducts), leiomyoma of the Fallopian tube are exceptionally rare. Leiomyomas of the Fallopian tube are commonly incidental findings, as they are asymptomatic and small. However, there are reported cases of large tubal myomas associated with acute abdomen consequent to its torsion.[20]

Tubal pregnancy associated with tubal leiomyomas, in which the tubal myoma was the obstructing factor, have also been reported.[1,20,21] Kobayashi et al[22] reported on a case of a 28-yearold woman presented with secondary infertility in which pelvic ultrasound

showed a multicystic septated mass extending to the umbilicus. At laparotomy, a 25×14×4 cm mass originating from the left Fallopian tube and the tube was excised. Pathologic examination confirmed an angiomyofibroblastoma of the Fallopian tube. Although, angiomyofibroblastoma is a rare tumor that occurs most commonly in the vulva and vagina, this case shows that can occur in the Fallopian tube and should be differentiated from more aggressive angiomyxoma.

Conventional B-mode sonography reveals little of the nature of a benign tubal tumor. A smaller papilla can resemble a chronic PID remnant while a bigger mass in the oviduct can be mistaken for an inflammatory conglomerate. Because of its limited imaging possibilities, 2D ultrasound cannot always define the borders of the lesion and delineate it from the surrounding tissue.

Color Doppler can be used for the assessment of vascularity. As any other benign tissues, the oviduct leiomyomas would have a moderate-tohigh resistance index. If they undergo necrosis of inflammation, they can present a true complication in the diagnostic process, caused by a significant reduction of the vascular indices.

3D ultrasound can help in diagnosis of benign ovarian lesions by its possibility to precisely delineate and spatially define a certain tumor. With the use of 3D power Doppler it is possible to visualize regular branching of benign intratubal structures, and distinguish them from uterine and ovarian vascular network.

MALIGNANT TUMORS OF THE FALLOPIAN TUBE

Although rare, tubal malignancy must be considered in the differential diagnosis of an adnexal mass. Of all gynecological cancers, malignancy of the Fallopian tube is the most rare. The triad of pain, bleeding and leucorrhea is considered pathognomonic of tubal carcinoma. Sedlis[23] defined parameters for better differentiation between ovarian and tubal malignancies. He postulated that the tumor is of Fallopian origin if:

1. It derives from the Fallopian tube,
2. Has the same histological structure as oviduct mucosa,
3. There is a clear transition zone between benign and malignant epithelium, and
4. There is no endometrial or ovarian carcinoma.

Ultrasound Findings

The sonographic findings in all reported cases of Fallopian tube carcinoma were complex, predominantly cystic adnexal masses and/or sausageshaped structures apparently separated from the

Table 48.1: Review of literature on B-mode diagnosis of primary Fallopian tube carcinoma

Reference	*No. of cases*	*Histopathology*
Subramayon et al[30]	3	papillary cystadenocarcinoma
Meyer et al[31]	1	adenocarcinoma
Kol et al[47]	1	adenocarcinoma
Ajjimakorn et al[32]	4	papillary cystadenocarcinoma
Granberg and Jansson[33]	1	adenocarcinoma
Chang et al[28]	1	mixed Muellerian tumor
Chiou et al[27]	1	mixed Muellerian tumor
Slanetz et al[34]	9	adenocarcinoma and mixed Muellerian tumor
Ong[35]	1	adenocarcinoma

uterus.[24–37] Table 48.1 reviews data from the literature on B-mode diagnosis of primary Fallopian tube carcinoma.

In a remarkable review of 376 cases of tubal carcinoma, McGoldrick and colleagues found only one diagnosed preoperatively.[38] More recently, Eddy and colleagues analyzed the data of 74 patients regarding tubal malignancies and only two cases of tubal carcinoma were correctly diagnosed before surgery.[39]

Ayhan and colleagues reported a study of eight cases of primary Fallopian tube carcinoma.[24] Dava and colleagues described six adenocarcinomas of the Fallopian tube that resembled the female adnexal tumor of probable wolffian origin.[31] Microscopically, the tumors were characterized by a predominant pattern of small, closely packed cells punctured by numerous glandular spaces, which were typically small but occasionally were cystically dilated. Soundara and associates published a review of Fallopian tube carcinoma over 20 years.[26] Nine cases of tubal carcinoma were found among approximately 9000 gynecological malignancies.

Based on the data from the literature[26,38,39] more than 80% of patients have had pelvic mass detected before surgery. However, cervical cytology, X-ray of the pelvis, computed tomography or hysterosalpingography are usually no more specific than the pelvic examination. Conventional transvaginal sonography is one of the most important tools in preoperative diagnosis, but the efficacy of morphologic scoring systems alone is hampered by the degree of overlap between benign and malignant appearing adnexal masses.[35,41,42]

COLOR DOPPLER FINDINGS

Our group was first to publish a case of primary adenocarcinoma of the Fallopian tube (stage I FIGO) preoperatively diagnosed by color and pulsed Doppler ultrasound.[43] Podobnik and coworkers published the case of 69-year-old woman with a history of right-sided lower abdominal pain accompanied by profuse watery vaginal discharge for

the past 3 months.[44] Six years after the initial report Kurjak et al[45] reported on the series of eight cases of preoperatively diagnosed Fallopian tube malignancy. Probably the most illustrative case of successful preoperative diagnosis of the primary Fallopian tube carcinoma is a 45-year-old woman treated at our Department because of infertility problems. During the routine transvaginal ultrasound examination a pendular myoma and a complex bilateral adnexal mass were discovered. In the left adnexal region a sausage-shaped cystic structure 3.4×4.8×3.4 cm in size was present. In the upper part of the cyst, a solid papillary protrusion less than 1 cm, richly perfused with the lowest resistance index of 0.38 was detected (Fig. 48.6). In the right adnexal region a hydrosalpinx 3.0×1.6 cm was delineated from the ovary. Moderate vascular resistance (RI=0.55) was obtained from the Fallopian tube with chronic

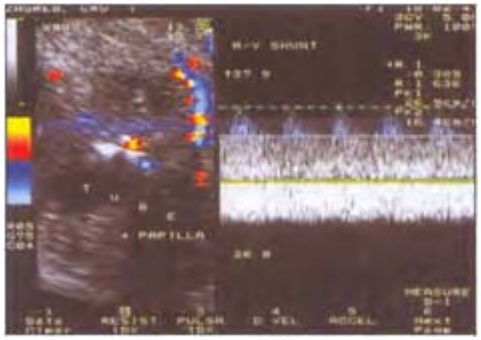

Figure 48.6: Fallopian tube carcinoma as seen by color Doppler ultrasound. Note vascularized papillomatous projection protruding into the distended tube in a postmenopausal patient. Low vascular resistance (RI=0.38) and arteriovenous shunt indicate tubal malignancy, which was confirmed by histopathology

inflammatory changes. According to the visualization of the area of neovascularization and low vascular impedance (RI=0.38) the authors suspected tubal carcinoma of the left side. Frozen section pathological examination at surgery, reported papillary Fallopian tube carcinoma. Table 48.2 reviews data from the literature on color Doppler diagnosis of primary Fallopian tube carcinoma.

THREE-DIMENSIONAL ULTRASOUND

A new progress in diagnostic procedures was made when 3D and power Doppler ultrasound was introduced. Transvaginal 3D ultrasound enables the clinician to perceive the true, spatial relations and thus easily distinguish the origin of an adnexal

Table 48.2: Review of literature on transvaginal color Doppler diagnosis of primary Fallopian tube carcinoma

Reference	*No. of cases*	*RI*	*Histopathology*
Shalan et al[43]	1	0.35	adenocarcinoma
Kurjak et al[45]	8	0.29–0.40	adenocarcinoma and papillary cystadenocarcinoma
Podobnik et al[44]	1	0.34	clear-cell carcinoma

mass, while 3D power Doppler allows detailed analysis of the neovascularization. Kurjak et al[46] were the first to report on preoperative diagnosis of the primary Fallopian tube carcinoma by 3D power Doppler ultrasound. Three-dimensional ultrasound was used to evaluate 520 adnexal masses prior to elective surgery during a 2-years' period. These lesions were originally detected with conventional transvaginal sonography and/or transvaginal color Doppler. Patients with suspicious morphology and/or Doppler findings underwent a second assessment at the referral center by the investigator performing 3D ultrasound that was unaware of the previous ultrasound examinations. Three-dimensional transvaginal ultrasound was performed using either 5 or 7.5 MHz transvaginal transducers (Voluson 530, Kretztechnik, Austria). Once the region of the interest was identified, a volume box was superimposed to scan the image. The patient was asked to lie still on the examination bed, while the ultrasound probe was kept steady in the vagina. Depending on the size of the volume box the scanning procedure lasted between 5 and 13 seconds. The ability to store 3D ultrasound data on a hard disk drive allowed the investigator to keep the examination time short (between 2 and 4 minutes). Detailed analysis of the adnexal tumor was performed after the patient had gone, and lasted between 10 and 20 minutes. Rotation and translation of the stored volumes allowed evaluation of different tumor sections in many planes. The "niche mode" enabled meticulous study through selected sections of the adnexal tumor and was found especially useful in evaluation of the sausage shaped complex masses. The "surface reconstruction" allowed plastic image of the inner and outer wall of the tumor (Fig. 48.7). Demonstration of the complex adnexal mass and/ or sausage shaped cystic lesions with papillary projections was the morphological criteria for detection of the tubal malignancy.

After B-mode analysis, power Doppler imaging was switched on together with the volume mode.

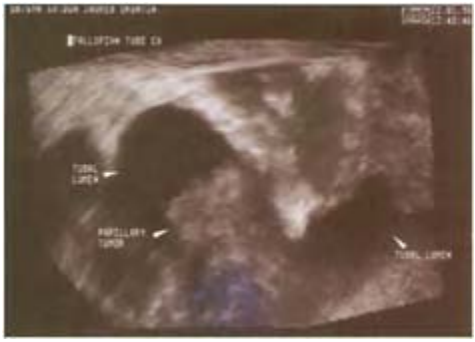

Figure 48.7: Three-dimensional ultrasound image of primary Fallopian tube carcinoma. Papillary protrusions suggestive of Fallopian tube malignancy are clearly seen within the distended tubal wall

In order to reduce the acquisition time the volume of the color box and sweep angle were reduced. The color frame rate was adjusted as follows: both color density and color quality were as low as necessary to obtain a good color image, while pulse repetition frequency was as high as possible in order to enable the display of targeted flow velocity. The spatial peak temporal average (SPTA) intensity was approximately 80 mW/cm^2. Wall filters (50 Hz) were used to eliminate low-frequency signals. The patient examination time by 3D power Doppler was 3 minutes. Using the fast line density, the average acquisition time was 48s (range 25–88 s). At the end of each examination combined color and gray rendering mode was used, allowing simultaneous analysis of the morphology, texture and vascularization. The subsequent analysis of the power Doppler reformatted sections lasted between 5 and 10 minutes. Demonstration of the chaotic, randomly dispersed vessels with irregular branching within the papillary protrusions and/or solid parts was suggestive of tubal malignancy. Other structural abnormalities of the malignant tumor vessels were demonstration of the microaneurysms, arteriovenous shunts, tumoral lakes, disproportional calibration, coiling and dichotomous branching (Fig. 48.8). Using the above-mentioned criteria five cases of Fallopian tube carcinoma were

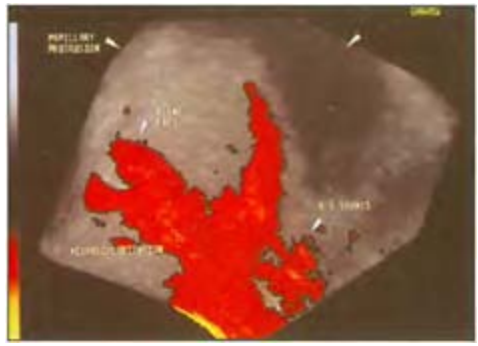

Figure 48.8: Three-dimensional power Doppler imaging enables evaluation of vascular geometry of the newly formed vessels in a case of Fallopian tube carcinoma. Note irregular branching of the vessels, blind-ended lakes and disproportional calibration all indicative for tumoral neovascularization

successfully identified prior to surgery. They all presented non-pathognomonic appearance by B-mode ultrasound: the image was usually similar to that of pyosalpinx or a fluid-filled tube with a significant solid component adjacent to the tube. Three-dimensional transvaginal ultrasound allowed more precise distinction of the tubal mass from that of the ovary, cervix and uterus. Furthermore, the change in shape and size of the mass and passage of free fluid from tubal mass through the uterine cavity can be documented dynamically. The three perpendicular planes displayed simultaneously on the screen provided the opportunity to obtain multiple sections of the tortuous adnexal lesion by the capacity of rotation and translation in any planes. The ability to reconstruct 3D plastic images improved the recognition of the adnexal lesion anatomy, characterization of the surface features and determination of the extent of tumor infiltration through the capsule.

The “niche” aspect of 3D ultrasound revealed intratumoral structures in selected sections, which was mandatory for evaluation of the tubal pathology. Multiple sections of the tumor, rotation, translation and reconstruction allowed prediction of the tumor spread to the uterus and/or the ovary, or other surrounding structures. Shortened scan-ning time and detailed analysis of the stored data by trained and experienced ultrasonographer were additional advantages of 3D over 2D sonography.

Tubal malignancy displays angiogenesis which can be detected by color and pulsed Doppler.[46–48] Reports from the literature demonstrate the potential of transvaginal color Doppler to depict tumor neovascularization and low resistance indices (below 0.42) typical of tubal malignancy. Malignant tumor vessels that are usually randomly dispersed within the central and peripheral parts demonstrate irregular course, complicated branching and disproportional calibration, features that can be recognized using three-dimensional power Doppler technology. Improved detection and classification of tumor architecture might contribute to better preoperative diagnostic for Fallopian tube carcinoma.

CONCLUSION

Transvaginal ultrasound with color Doppler facilities is useful not only for accurate assessment of the regional blood flow, but also for differentiating benign adnexal conditions from malignant. Based on color Doppler assessment one can distinguish acute pelvic inflammatory disease from the chronic one. The introduction of 3D ultrasound enables spatial delineation of examined structures giving the information whether the pathologic structure is of ovarian or tubal origin. It is expected that wide application of this novel technique will enable early detection of Fallopian tube tumors, which will enable introduction of adequate management and therapy, resulting in increase of the survival rate.

REFERENCES

1. Timor-Tritsch IE, Rottem S. Transvaginal ultrasonographic study of the Fallopian tube. Obstet Gynecol 1987; 70:424–28.
2. Timor-Tritsch IE, Bar-Yam Y, Elgali S, Rottem S. The technique of transvaginal sonography with use of a 6.5 MHz probe. Am J Obstet Gynecol 1988; 158:1019.
3. Timor-Tritsch IE, Rottem S, Lewit N. The Fallopian tubes. In: Timor-Tritsch IE, Rottem S (Eds). Transvaginal Sonography (2nd ed), New York: Elsevier 1991; 131–44.
4. Westroem L, Wolner-Hanssen R Pathogenesis of pelvic inflammatory disease. Genitourinary Medicine. 1993; 69:9–17.
5. Toth M, Chervenak FA. Color Doppler ultrasound in the diagnosis of pelvic inflammatory disease. In: Kurjak A (Ed). An Atlas of Transvaginal Color Doppler, Parthenon Publishing Group 1994; 215–21.
6. Patten RM, Vincent LM, Wolner-Hanssen P, Thorpe E Jr. Pelvic inflammatory disease: endovaginal sonography with laparoscopic correlation. J Ultrasound Med 1990; 9:681–89.
7. Kupesic S, Kurjak A, Pasalic L, Benic S, Ilijas M. The value of transvaginal color Doppler in the assessment of pelvic inflammatory disease. Ultrasound Med Biol 1995; 21:733–38.
8. Kurjak A, Zalud I, Jurkovic D, Alfirevic Z, Miljan M. Transvaginal color Doppler for the assessment of the pelvic circulation. Acta Obstet Gynecol Scand 1989; 68:131–34.
9. Collins W, Jurkovic D, Kurjak A, Campbell S. Ovarian morphology, endocrine function and intrafollicular blood flow during the periovulatory period. Hum Reprod 1991; 6:319–29.
10. Kurjak A, Kupesic S, Schulman H, Zalud I. Transvaginal color Doppler in the assessment of the ovarian and uterine blood flow in infertile women. Fertil Steril 1991; 56:870–73.
11. Bourne T. Transvaginal colour Doppler in gynaecology. Ultrasound Obstet Gynecol 1992; 80:359–73.
12. Kurjak A, Zalud I, Alfirevic Z. Evaluation of adnexal masses with transvaginal color ultrasound. J Ultrasound Med 1991; 10:295–99.

13. Kurjak A, Zalud I, Schulman H. Ectopic pregnancy: Transvaginal color Doppler study of trophoblastic flow in questionable adnexa. J Ultrasound Med 1991; 10:685–89.
14. Kurjak A, Predanic M, Kupesic S, Jukic S. Transvaginal color Doppler for the assessment of adnexal tumor vascularity. Gynecol Oncol 1993; 50:3–9.
15. Tinkannen H, Kujansuu E. Doppler ultrasound findings in tubo-ovarian infectious complex. J Clin Ultrasound 1993; 21:175–78.
16. Jurkovic D, Bourne TH, Jauniaux E, Campbell JS, Collins WP. Transvaginal color Doppler study of blood flow in ectopic pregnancies. Fertil Steril 1992; 57:68–73.
17. Kurjak A, Predanic M. New scoring system for prediction of ovarian malignancy based on transvaginal color Doppler sonography. J Ultrasound Med 1992; 11:631–38.
18. Teisala K, Heinonen PK, Punnonen JR. Transvaginal ultrasound in the diagnosis and treatment of tuboovarian abscess. Br J Obstet Gynaecol 1990; 97:178–80.
19. Senoh D, Yanagihara T, Akiyama M, Ohnishi Y, Yamashiro C, Tanaka H, Hayashi K, Hata T. Laparoscopy-assisted intrapelvic sonography with a high-frequency, real-time miniature transducer for assessment of the Fallopian tube: a preliminary report. Hum Reprod 1999; 14(3):704–06.
20. Woodruff JD, Pauerstein CJ. The Fallopian tube. (Baltimore: Williams and Wilkins) 1969.
21. Mroueh J, Margono F, Feinkind L. Tubal pregnancy associated with ampullary tubal leiomyoma. Obstet Gynecol 1993;81:880–82.
22. Kobayashi T, Suzuki K, Arai T, Sugimura H. Angiomyofibroblastoma arising from the Fallopian tube. Obstet Gynecol 1999; 94(5 Part 2 Suppl S):833–34.
23. Sedlis A. Carcinoma of the Fallopian tube. Surg Clinic N Am 1978; 58:121.
24. Ayhan A, Deren D, Yuce K, Tuncer Z, Mecan G. Primary carcinoma of the Fallopian tube: A study of 8 cases. Eur J Gynecol Oncol 1994; 15:147–51.
25. Dava D, Young RH, Scully RE. Endometrioid carcinoma of the Fallopian tube resembling an adnexal tumor of probable Wolffian origin: A report of six cases. Int J Gynecol Pathol 1992; 11:122–30.
26. Soundara RS, Ramdas CR Reddi RR Oumachigni A, Rajaram P, Reddy KS. A review of Fallopian tube carcinoma over 20 years (1971–90) in Pondicherry. Indian J Cancer 1991; 28:188–95.
27. Chiou YK, Su IJ, Chen CA, Hsieh CY Malignant mixed Muellerian tumor of the Fallopian tube. J Formos Med Associ 1991; 90(8):793–95.
28. Chang HC, Hsueh S, Soong YK. Malignant mixed Muellerian tumor of the Fallopian tube. Case report and review of literature. Chang Keng I Hsueh 1991; 14(4):259–63.
29. Tokunaga T, Miyazaki K, Okamura H. Pathology of the Fallopian tube. Curr Opin Obstet Gynecol 1991; 3(4):574–79.
30. Subramayon BR, Raghavendra BN, Whalen CA, Ye J. Ultrasonic features of Fallopian tube carcinoma. J Ultrasound Med 1984; 391–93.
31. Meyer JS, Kim CS, Price HM, Cooke JK. Ultrasound presentation of primary carcinoma of the Fallopian tube. J Clin Ultrasound 1987; 15:132–34.
32. Ajimakorn S, Bhamarapravati Y. Transvaginal ultrasound and the diagnosis of Fallopian tubal carcinoma. J Clin Ultrasound 1991; 19:116–19.
33. Granberg S, Jansson I. Early detection of primary carcinoma of the Fallopian tube by endovaginal ultrasound. Acta Obstet Gynecol Scand 1990; 69:667–68.
34. Slanetz PJ, Whitman GJ, Halpern EF, Hall DA, McCarthy KA, Simeone JF. Imaging of the Fallopian tube tumors. Am J Roentgenol 1997; 169:1321–24.
35. Ong CL. Fallopian tube carcinoma with multiple tumor nodules seen on transvaginal sonography. J Ultrasound Med 1998; 17:71–73.
36. Hinton A, Bea C, Winfield AC, Entman SS. Carcinoma of the Fallopian tube. Krol Radiol 1988; 10:113–15.

37. Ekici E, Vicdan K, Danisman N, Soysal ME, Cobanoglu O, Gokmen O. Ultrasonographic Appearance of Fallopian-Tube Carcinoma. International Journal of Gynecology and Obstetrics. 1992; 49:325–29.
38. McGoldrick JL, Strauss H, Rao J. Primary carcinoma of the Fallopian tube. Am J Surg 1943; 59:559–63.
39. Eddy GL, Schlaerth JB, Nalick RH, Gadis OJ, Nakamuira RM, Morrow CP Fallopian tube carcinoma. Obstet Gynecol 1984; 64:546–51.
40. Lerner JP, Timor-Tritsch IE, Federmann A, Abramovich G. Transvaginal ultrasonographic characterization of ovarian masses with an improved weighted scoring system. Am J Obstet Gynecol 1994; 170:81–85.
41. Bourne TH, Campbell S, Steer C, Whitehead MI, Collins WP Transvaginal color flow imaging a possible new screening technique for ovarian cancer. Br Med J 1994; 299:1367–71.
42. Kawai M, Kano T, Kikkawa F, Maeda O, Oguchi H, Tomoda Y. Transvaginal Doppler ultrasound with color flow imaging in the diagnosis of ovarian cancer. Obstet Gynecol, 1992; 79:463–66.
43. Shalan H, Sosic A, Kurjak A. Fallopian tube carcinoma: recent diagnostic approach by color Doppler imaging. Ultrasound Obstet Gynecol 1992; 2;297–99.
44. Podobnik M, Singer Z, Ciglar S, Bulic M. Preoperative diagnosis of primary Fallopian tube carcinoma by transvaginal ultrasound, cytological finding and CA125. Ultrasound Med Biol 1993; 19:587–91.
45. Kurjak A, Kupesic S, Ilijas M, Sparac V, Kosuta D. Preoperative diagnosis of primary Fallopian tube carcinoma. Gynecol Oncol 1998; 68:29–34.
46. Kurjak A, Kupesic S, Jacobs I. Preoperative diagnosis of the primary Fallopian tube carcinoma by threedimensional static and power Doppler sonography. Ultrasound Obstet Gynecol (submitted), 1999.
47. Kol S, Gal D, Friedman M, Paldi E. Preoperative diagnosis of primary Fallopian tube carcinoma by transvaginal sonography and CA 125. Gynecol Oncol 1990; 37:129–37.
48. Kurjak A, Kupesic S, Breyer B, Sparac V, Jukic S. The assessment of ovarian tumor angiogenesis: what does three-dimensional power Doppler add? Ultrasound Obstet Gynecol 1998; 12:136–46.

Chapter 49
Color Doppler in Adnexal Masses

Asim Kurjak, Ivanka Bekavac, Sanja Kupesic

INTRODUCTION

Evaluation of adnexal lesions is of particular importance in gynecological practice. Two main problems need answers: discrimination of benign and malignant adnexal masses and choice of the appropriate surgical treatment if necessary. It is now well established that ultrasonography is accepted as the gold standard in the evaluation of adnexal masses. Because ultrasound depicts the mass, characterization of the mass is typically performed during the same examination. Thus, de facto, ultrasound becomes the main triage method prior treatment. A majority of adnexal masses are nonneoplastic cysts. However, twenty-five percent of ovarian neoplasms are malignant.[1] For this reason, surgical removal of a suspected ovarian neoplasm is the standard procedure. In most institutions, the type of surgery performed (laparoscopy vs. laparotomy) depends on the probability of malignancy. The optimal ultrasound technique and diagnostic criteria to use when characterising a suspected adnexal neoplasm remains controversial. Papillary formations on the inside of the cyst wall and masses with a non-hyperechoic solid component are the most statistically significant predictors of a malignant ovarian mass. Ultrasound and morphologic parameters have a sensitivity of 80% and a specificity of 93%, that make this exam the gold standard for adnexal masses diagnosis.[2] Scoring system help differentiate benign from malignant masses (sensitivity 90%) (Table 49.1).[2] Doppler flow measurement and assessment of tumor

Table 49.1: Two-dimensional sonographic and color Doppler criteria for the diagnosis of adnexal malignancy proposed by our team

Volume	<10 cm^3	0
	>10 cm^3	2
Cyst wall	smooth <3 mm	0
thickness/structure	smooth >3 mm	1
	papillarities <3 mm	1

	papillarities >3 mm	2
Septa	no septa	0
	thin septa <3 mm	1
	thick septa >3 mm	2
Solid parts	solid area <1 cm	1
	solid area >1 cm	2
Echogenicity	sonolucency/low level echo	0
	mixed/high level echo	2
Tumoral blood flow	RI>0.42	0
	RI<0.42	2

Total score=sum of individual scores. Cut-off score greater or equal of 4 for morphology index and greater or equal to 6 for combined (morphology and vascular) index was associated with high risk of adnexal malignancy

vascularity by Doppler energy increase the confidence with which a correct diagnosis is made.[2] Color and pulsed Doppler sonography depicts the vascularity of the pelvic organs and can be used for assessment of angiogenesis in tumor masses, producing insights in tumor histology and metabolism. It has a primary role in vascular detection and establishment of blood flow features of malignant pelvic lesions (Fig. 49.1).

Recent technological advances such as three-dimensional volume acquisition and three-dimensional power Doppler may have clinical utility in the identification of abnormal ovarian architec ture, as well as vascularity. The addition of three-dimensional power Doppler provides a new tool for measuring the quality of tumoral vascularity, and its clinical value is not still validated.

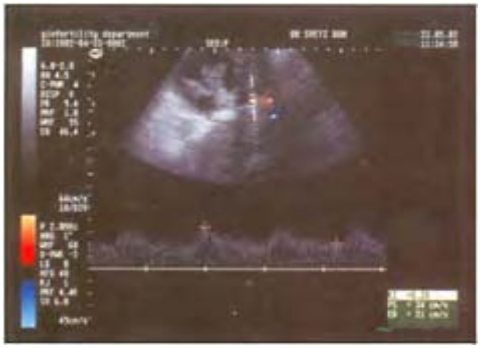

Figure 49.1: A transvaginal color Doppler sonogram of a multilocular ovarian

tumor. Blood-flow signals obtained from periphery of a lesion demonstrate low resistance to blood flow. Malignant ovarian tumor was proved by histopathology

THE MAIN BASIS OF ANGIOGENESIS

All organs of human body have a physiological duty to form certain compounds and molecules while disintegrating others, with the aim of maintaining the frail molecular equilibrium. In order to perform their task, all the organs and body parts must be connected by a single vascular network. As with other live tissue, vascular endothelium has the ability to regenerate and to spread through other tissues in order to perfuse them. The formation of new blood vessels is called angiogenesis and it results in neovascularization. It has been over 100 years since it was first observed that tumors angiogenesis differs from vascularity compared to normal tissues.[3] It was long believed that simple dilatation of existing host blood vessels accounted for tumor hyperemia.[4] Vasodilatation was generally thought to be a side effect of tumor metabolites released from necrotic parts of the tumor. However, some authors suggested that tumor hyperemia might be related to new blood vessel growth, i.e. neovascularization, rather than to dilatation. A report published in 1945 revealed that new vessels in the neighbourhood of a tumor implant arose from host vessels and not from the tumor itself.[5] Further experiments during 1960s with isolated perfused organs brought the new and exciting concept-that tumor growth is restricted in the absence of a vascular response.[6,7] In the following decades, scientists showed that tumors implanted into animals consistently induced the growth of new capillaries. Viable tumor cells were found to release diffusible angiogenic factors that stimulated new capillary growth and endothelial mitosis.[8,9] On the basis of these observations, Judah Folkman proposed a hypothesis that, once a tumor had occurred, every further increase in the tumor cell population had to be preceded by an increase in new capillaries, which sprouted towards the early growth of the tumor.[10] Since Folkman's hypothesis, for over 25 years it has been clear that the development of new blood vessels—called angiogenesis—is crucial for sustaining tumor growth, as it allows oxygenation and nutrient perfusion of the tumor and removal of waste products.[11,12] Moreover, increased angiogenesis coincides with increased tumor cell entry into the circulation, and thus facilitates metastasis.[13,14] Cancer cells activate quiescent vasculature to produce new blood vessels via an "angiogenetic switch", often during the premalignant stages of tumor development.

The density of the capillary network seems to be one of the factors determining the malignancy of a tumor. Metastases of highly vascularized tumors appear earlier than those of poorly vascularized tumors.[15,16] The reason for this is not just the capillary permeability that enables shedding of tumor cells into the blood stream, but also a current hypothesis that both the primary tumor and the distant metastases are involved in complex regulation by angiogenic and antiangiogenic factors.[17] The first indication of its

importance in tumor angiogenesis came from observations in the early 1980s that tumors secreted soluble factors that could stimulate vascular endothelial growth.[18] The basic and acidic fibre-blast growth factors were among the first to be identified and were soon followed by many others such as vascular endothelial growth factor/vascular permeability factor (VEGF/VPF) and transforming growth factors (TGF-alpha- and beta), to mention some of the most important.[19] Investigation of these factors, powerful molecules that control the formation of new blood vessels, are still in a progress.[20,21] Recent study reported on the expression of VEGF in ovarian epithelial tumors (OETs) in both epithelial and stromal compartments.[22] Furthermore they showed that VEGF is significantly increased in malignant OETs compared to benign and borderline tumors, and concluded that this factor may play a role in the development of ovarian cancer. Cooper et al analyzed the clinical relevance of serum VEGF levels in distinguishing patient with ovarian cancer from those with benign adnexal masses.[23] VEGF levels were significantly higher in patienrs with stage I ovarian cancer compared with those with benign disease or low malignant potential (LMP) tumors. Among patients with ovarian cancer, there were no significant differences in VEGF levels based on age, stage, grade, or level of cytoreduction. Furthermore preoperative VEGF levels >380 pg/ml are an independent risk factor for death because of the disease.[23] Except hemangiogenesis, pathways for lymphangiogenesis have been proposed (Fig. 49.2).[13] Electron microscopy, *in vitro* cultures and experiments on animal models have enabled us to understand the visible part of the angiogenic process—tumor vasculature.

TUMOR NEOVASCULARIZATION—CURRENT CONCEPTS

In general, tumor vasculature consists of the vessels recruited from the pre-existing network of the host vasculature, and the vessels grown from the host vessels under the influence of the angiogenic factors of cancer cells.[24,26] Although the tumor vasculature originates from the host vasculature, its organization may be completely different, depending upon the tumor type, its growth rate and its location. Macroscopically, tumor vasculature can be studied in terms of two ideal categories: peripheral and central. In tumors with peripheral vascularization, the centers are usually poorly perfused. In those with central vascularization, the opposite is expected. However, a tumor may consist of many territories, each exhibiting one or the other type of the ideal vascular pattern (Fig. 49.3). Microscopically, tumor vasculature is highly heterogeneous and does not conform to the standard normal vascular organization. Tumor neovascularity can be differentiated from normal vascular beds by the several main characteristics:[27]

1. A single branch, varied in caliber, formed from narrow and dilated segments;
2. Elongation and coiling;
3. Non-hierarchical vascular network, vascular rings and sinusoids;
4. No normal precapillary architecture with dichotomous branching, and no decrease in diameter of the higher-order branches;
5. Incomplete vascular wall: various gaps in the endothelium, discontinuity of the basal membrane and no muscular layer except in pre-existing vessels encased by the tumor.

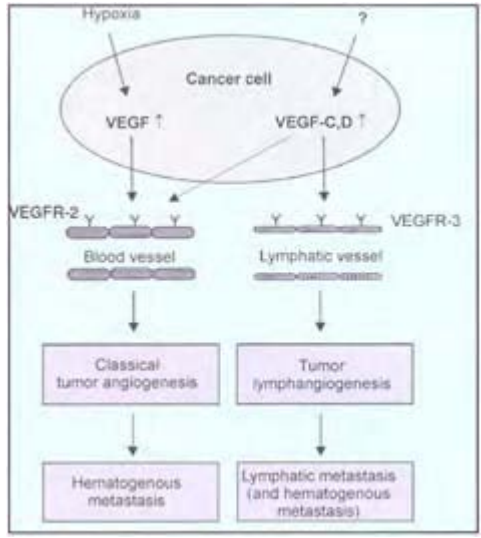

Figure 49.2: Dissecting tumor angiogenesis. Hypoxic tumor cells produce VEGF, which binds to and activates VEGFR-2 on vascular endothelial cells, leading to classical tumor angiogenesis. Tumor that secrete VEGF-C or VEGF-D may induce lymphangiogenesis by activating VEGFR-3 on lymphatic vessels, a process known as tumor lymphangiogenesis. Classical tumor angiogenesis has been shown to correlate with hematogenous metastasis. In the animal models, induction of lymphangiogenesis by

VEGF-C or VEGF-D led to an increase in tumor metastasis via the lymphatic system

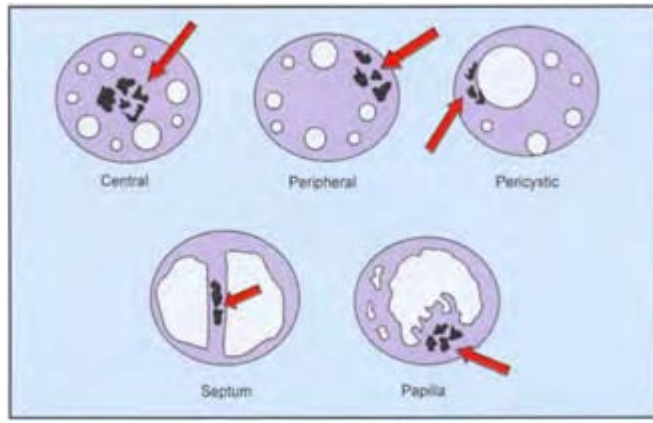

Figure 49.3: Schematic presentation of different types of vascularization within abnormal ovarian tissue

A key difference between normal and tumor vessels is that the latter are dilated, saccular and tortuous, and may contain tumor cells within the endothelial lining of the vessel wall.[28] In addition, unlike normal tissue with a relatively fixed route between the arterial and venous circulation, a tumor may have blood flowing from one venule to another via a series of vessels or directly via an arteriovenous shunt.

However, the morphologic appearance of the tumor vascular bed may not necessarily allow direct assessment of function of the tumor microcirculation. This is because only 20–80% of tumor vessels are perfused within any given tumor at a Particular time. Within a particular tumor, one investigator has noted variations in flow that can be as high as tenfold.[29] Another important aspect to consider is that the microvascular permeability of vessels within tumors is very heterogeneous, and tumors have been shown to be up to eightfold more permeable than normal tissues. Vascular endothelial growth factor (VEGF) has been shown to increase vascular permeability.[17] Some of the main characteristics of the tumor interstitial space are an expansion of its volume by three to five times compared to most host tissues. These results in a high interstitial fluid pressure of up to 50 mm Hg, when compared to normal tissues, in which the interstitial pressures are slightly subatmospheric. The major pathophysiologic mechanisms attributed to interstitial hypertension are absence of functioning lymphatic vessels, the high permeability of the vascular wall, and the rapid proliferation of tumor cells in

confined spaces.[26] High interstitial pressure leads to compression of vessels inside the tumor, and this may even lead to local stasis.

The relative perfusion of tumors resulting from these factors varies according to their growth. Initially, tumors have a hyperemic periphery with a relatively well perfused rim of tissue and later a relatively ischemic area centrally. As the tumor enlarges, areas of central necrosis develop. According to this, as regards perfusion rates, four regions can be recognized in a tumor: an avascular (necrotic) region; a seminecrotic (ischemic) region; a stabilized microcirculation; and an advancing front as a region of tumor hyperemia.[24,30] Depiction of these areas by imaging may be important in that the spatial distribution of chemotherapeutic agents varies according to the degree of tumor vascularity within different tumor regions. The multitude of data suggesting that the control of angiogenesis is separate from the control of cancer cell proliferation raise the possibility that drugs inhibiting angiogenesis could offer a treatment complementary to traditional chemotherapy, which directly targets tumor cells.[9,12,31] This exciting possibility has stimulated research on tumor angiogenesis and introduction of new three-dimensional power Doppler evaluation of tumor vessels architecture.[32–36]

ULTRASOUND MODALITIES IN IMAGING OF ADNEXAL TUMOR ANGIOGENESIS

Although the histological microvessel density technique is the current gold standard to characterize tumor angiogenesis, it may not be the ideal tool for clinical purposes because it needs to be performed on biopsy material and does not assess the functional pathways involved in the angiogenic activity of tumors. Non-invasive assessment of tumor vascularity is possible *in vivo* by means of Doppler sonography (Fig. 49.4). Before using any diagnostic technique involved in sonographic depiction of ovarian vascularity and flow, it is important that the investigator distinguishes the concepts of “tumor vascularity” and “tumor blood flow”. Tumor vascularity refers to the number of vessels per unit volume, whereas tumor blood flow is a measure of the number of flowing blood elements over a certain period of time in a selected area of interest.[27]

The role of color Doppler in evaluation of the adnexal mass was initiated in the early 1990s using spectral display that reflects flow toward and away

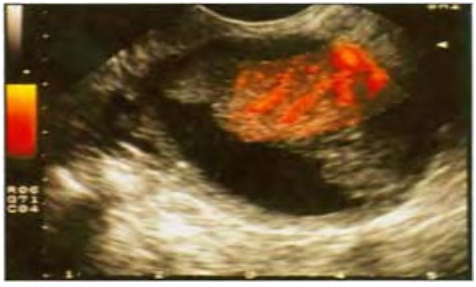

Figure 49.4: Tumoral vessels observed by color Doppler in central and

peripheral parts of the solid counterpart

from the transducer, which is angle dependent. Results were then calculated using impedance indices, resistance index (RI) and pulsatility index (PI), or velocity measurement such as timed average maximum velocity (TAMXV). The advantages of color Doppler technique were demonstrated and used in gynecology for the first time by groups in Zagreb and London.[37,38] The Zagreb group has studied pelvic masses, and observed low impedance intratumoral blood flow (RI <0.41) in malignant ovarian lesions. Both groups agreed that this technique can detect ovarian cancer as early as FIGO stage I a, and can be used as a screening technique for the disease. From those days on, nothing has essentially changed. A lot of research has been done to prove or dispute the use of color Doppler, but the final verdict was never reached. It is a fact that a difference in vascularity exists, and blood vessels in malignant adnexal lesions show lower resistance to blood flow than to those in benign adnexal masses (Figs 49.5 and 49.6). Tumor blood vessels have a paucity or lack of a muscular media of normal vessels and are more distensible. This combined with arteriovenous shunts seen in the tumor vascular network results in low impedance flow. However, because of focal areas of narrowing and dilatation within tumor vessels, focal areas of high systolic velocity can also be found.[39]

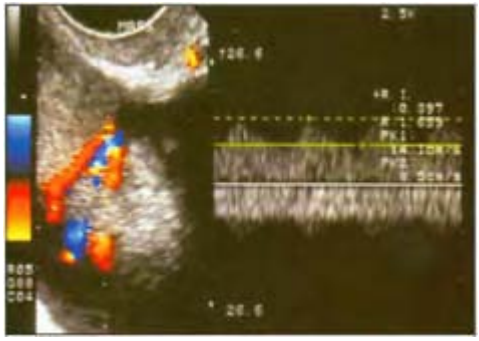

Figure 49.5: A malignant ovarian tumor with its characteristic image created by a solid counterpart. Pulsed Doppler waveform analysis shows lowresistance to blood flow

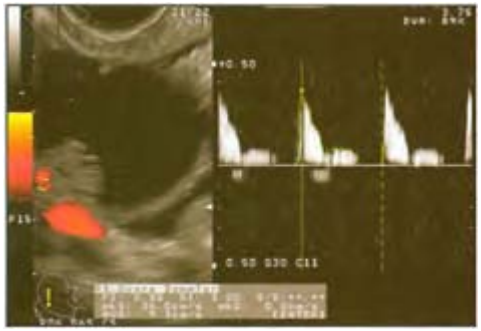

Figure 49.6: A transvaginal sonogram of an ovarian tumor with small echogenic formation (papilla) protruding into the lumen. Pulsed Doppler imaging demonstrates high resistance to blood flow. Benign ovarian tumor was confirmed by histopathology

Another factor that confounds this is the fact that most tumors have areas of variable perfusion. Our study reported on preexisting vessels with normal wall structure in 60% of malignant ovarian tumors.[40] This contributes to uneven tumor blood flow that makes it difficult to generalize a "characteristic" flow of ovarian tumors.[41] In a retrospective study, the histological sections of the ovarian tumors with known preoperative RI values were reviewed and the pattern of vascularization was studied.[42] The retrospective histological sections were evaluated for quantity of arterioles and venules. The arterioral fraction (defined as the number of arterioles divided by the same sum of the arterioles plus venules) and the density of vessels (defined as the number of arterioles and venules per microscopic field) were calculated in each histological section and correlated with preoperative RI values. Resistance index values showed a strong positive correlation ($r=+0.85$, $p<0.0005$) with the arteriolar fraction, and negative and weaker correlation ($r=-0.69$, $p<0.001$) with the density of vessels.

Diagnostic accuracy of values of flow indices in differentiating benign from malignant lesions has varied considerably, from over 96% to less than 40%.[43,44] More than 15 years of experience in multiple centers has shown that overlap in the specific impedance values obtained from vessels surrounding the ovary by frequency-based transvaginal color Doppler imaging precludes differentiation of benign versus malignant ovarian masses on the basis of impedance values alone.[45] Other limiting factors for this type of imaging represent slow flow and vessels of small diameter which are barely detectable.[46] Also, part of the problem with this technique is that only those vessels that are depicted can be

adequately studied. More specifically, it seems more important to provide information involving the vascular network rather than particular vessels.[47]

A solution to this problem has been offered by the introduction of amplitude-based transvaginal color Doppler imaging.[48] This imaging modality, known also as power Doppler ultrasound or Color Doppler Angio® takes into account the area under the curve of a spectral waveform and is related to the number of blood elements flowing over time. Power Doppler sonography has been found to be superior to frequency-based color Doppler sonography, especially in situations of low blood flow (low velocities), with the potential to detect alterations in blood flow.[49] Power Doppler ultrasound has the advantage that it is more sensitive, less angle-dependent and not susceptible to aliasing.[50,51] In this technique, the hue and brightness of the color signal represent the total energy of the Doppler signal. It displays the total flow in a confined area, giving an impression similar to that of angiography. The sensitivity of Power Doppler imaging is 14 dB greater than the standard Doppler imaging.[52] Because of this greater sensitivity in displaying smaller vessels, the vascularity is shown more completely.

Guerriero et al compared the diagnostic accuracy of conventional color Doppler (CCD) and power Doppler (PD) imaging in the diagnosis of ovarian cancer.[53] Six hundred fifty-six consecutive women with adnexal masses scheduled for surgery in two European university departments of obstetrics and gynecology underwent preoperative transvaginal ultrasound. Using both modalities of color Doppler, malignancy was suspected when arterial flow visualized in an echogenic portion defined as malignant by B-mode. They reported that the false-positive rates of B-mode imaging was similar in the two institutions (17 vs. 18%), while the false-positive rates of CCD and PD imaging were 4.6 and 7.4%, respectively. Although the overall diagnostic accuracy of two techniques seems comparable, a significantly lower sensitivity in differentiation of benign from malignant ovarian lesions was found using CCD (87 vs. 100%).

Several studies demonstrated the correlation of tumor vascularity as depicted on power Doppler imaging to an estimation of vascularity seen histologically. Good correlation (r=0.82) of vessels greater than 50 ^im in size but poor correlation with the actual microvessel count, which typically includes vessels less than 15 jum.[54,55] Power Doppler imaging has serious limitations in assessing temporal changes in flow and vessel size due to blooming of the color signal. This imaging modality permits the depiction of even smaller vessels, but, paradoxically, small intraparenchymal arterioles in benign and normal tissues may show a low impedance and a low-velocity blood flow pattern, giving rise to false-positive results.

It is clear that there is need for further improvement in the ultrasonic assessment of pelvic tumor angiogenesis and, to this end, there has been a growing interest in three-dimensional power Doppler ultrasound.

RECENT DATA ON CLINICAL APPLICATION OF COLOR AND PULSED DOPPLER IN ADNEXAL MASSES

It has already been pointed out, that since the introduction of color and pulsed Doppler for the assessment of ovarian vascularity, attitudes concerning its usefulness in the detection of adnexal malignancies have been equally divided (Table 49.2).[56–63] AH these

studies have concentrated on differences of velocimetric parameters (pulsatility index, resistance index, systolic and diastolic peak velocity, mean velocity) to blood flow between benign and malignant adnexal masses. Pulsed Doppler and vascular resistance to blood flow had been and still is one of the major features in the assessment of tumor vascular characteristics (Fig. 49.7). It is a fact that difference in vascularity exists and blood vessels in malignant adnexal lesions show lower resistance to blood flows than in benign adnexal masses (Table 49.3). Although different authors suggest different cut-off values, we have found that levels of 0.40 and 1.00 for resistance index and pulsatility index respectively are the best discriminatory value for differentiation between benign and malignant adnexal tumors (Fig. 49.10). We believe that major problem in observed overlap is due variation of RI and PI results within the same tumor because of different areas of vascularization (preexisting and newly formed vessels) inside of the tumor. The Doppler pitfalls and artifacts must be known before someone apply this technique to patients in the clinical situation. Although the conflicting data have already been extensively analyzed,[64] few recent studies considering clinical application of this technique will be presented. There is no doubt that complete ultrasonographic estimation of adnexal neoplasms should include Doppler analysis of vasculature parameters. This statement is supported by a recent multicenter European study performed as a collaborative work at 3 European university departments of obstetrics and

Table 49.2: General attitude towards transvaginal color Doppler sonography since 1989

Author	*Year*	*Department*	*No. of cases*	*Attitude towards Doppler*
Hata et al[91]	1989	Gynecology	21	In favor
Fleischer et al[92]	1991	Radiology	43	In favor
Kurjak et al[57]	1991	Gynecology	680	In favor
Weiner et al[58]	1992	Gynecology	53	In favor
Kawai et al[93]	1992	Gynecology	24	In favor
Tekay et al[94]	1992	Gynecology	72	Against
Hata et al[95]	1992	Gynecology	64	Against
Kurjak et al[96]	1992	Gynecology	83	In favor
Hamper et al[97]	1993	Radiology	31	Limited
Schneider et al[98]	1993	Gynecology	55	In favor
Timor-Tritsch et al[99]	1993	Gynecology	115	In favor
Jain et al[100]	1994	Radiology	50	Limited
Weiner et al[101]	1994	Gynecology	18	In favor
Levine et al[102]	1994	Radiology	35	Against
Brown et al[103]	1994	Radiology	44	Limited

Valentin et al[104]	1994	Gynecology	149	Against
Bromley et al[105]	1994	Gynecology	33	Limited
Carter et al[106]	1994	Gynecology	30	Limited
Prompeler et al[107]	1994	Gynecology	83	Limited
Chou et al[108]	1994	Gyneccology	108	In favor
Wu et al[109]	1994	Gynecology	410	In favor
Zaneta et al[110]	1994	Gynecology	76	In favor
Salem et al[111]	1994	Radiology	102	Against
Sawicki et al[112]	1994	Gynecology	65	In favor
Sengoku et al[113]	1994	Gynecology	28	In favor
Franchi et al[114]	1995	Gynecology	129	Limited
Maly et al[115]	1995	Gynecology	102	In favor
Stein et al[116]	1995	Radiology	169	Against
Carter et al[117]	1995	Gynecology	89	Limited
Fleischer et al[118]	1995	Radiology	126	In favor
Buy et al[119]	1996	Gynecology	132	Limited
Rehn et al[120]	1996	Gynecology	259	Limited
Predanic et al[121]	1996	Gynecology	106	In favor
Tailor et al[122]	1996	Gynecology	79	Limited
Alcazar[123]	1996	Gynecology	51	Limited
Wheeler et al[124]	1997	Gynecology	34	Limited
Reles et al[125]	1997	Gynecology	98	In favor
Emoto et al[126]	1997	Gynecology	106	In favor
Valentin et al[127]	1997	Gynecology	151	In favor
Takac et al[128]	1998	Gynecology	120	Limited
Guerriero et al[129]	1998	Gynecology	192	Limited
Leeners et al[130]	1998	Gynecology	265	In favor
Angeid-Beckman et al[131]	1998	Radiology	189	Against
Brown et al[132]	1998	Gynecology	211	Limited
Buckshee et al[133]	1998	Gynecology	34	In favor
Alcazar et al[134]	1999	Gynecology	94	In favor
Valentin et al[135]	1999	Gynecology	173	Limited

Gramellini et al[64]	2001	Gynecology	124	In favor
Sawicki et al[65]	2001	Gynecology	324	In favor
Pascual et al[66]	2002	Gynecology	24	In favor
Guerriero et al[63]	2002	Gynecology	826	In favor

Table 49.3: Doppler findings of benign anc maliqnant adnexal masses

Benign ovarian tumors
Regular distribution of blood vessels
Blood vessels are equally calibrated
Blood vessels have muscle fibers with moderate-to-high resistance index values (RI=0.42)
Malignant ovarian tumors
Irregular distribution of blood vessels
Blood vessels have irregular diameter
Low resistance index values (RI<0.42)
Display of tumoral lakes and arterio-venous shunts

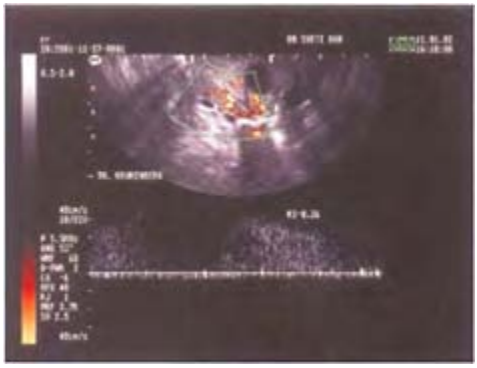

Figure 49.7: Transvaginal color Doppler sonogram of the multilocular cyst with septal blood flow

gynecology.[65] A total of 826 complex pelvic masses on which transvaginal sonography and evaluation of cancer antigen (CA) 125 plasma concentrations were performed before surgical exploration were included in the study. An adnexal mass was first studied in gray scale sonography, and a probable histologic type was predicted. Second, solid excrescences or solid portions of the tumor were evaluated for vascular

flow with color Doppler sonography (conventional or power). A mass was graded malignant if flow was shown within the excrescences or solid areas and benign if there was no flow. Color Doppler evaluation was more accurate in the diagnosis of adnexal malignancies in comparison with gray scale sonography (kappa =0.82 and 0.65, respectively) because of significantly higher specificity (0.94 versus 0.84; P<.001). The evaluation of the CA 125 plasma concentration did not seem to increase the accuracy of either method.

Similar results regarding clinical application of color Doppler were obtained by a prospective study carried out in 125 selected patients who presented an adnexal mass.[66] Out of 127 pelvic masses examined, histological analysis showed that 19 were malignant and 108 benign. The central importance of vascularization was useful for the diagnosis of a malignant neoplasm, with a diagnostic accuracy of 82.95%. Furthermore, in addition to color Doppler, pulsed Doppler study of a number of velocimetric parameters (pulsatility index, index of resistance, systolic and diastolic peak velocity, mean velocity) was performed. Unfortunately, no indicator obtained using pulsed Doppler was useful for diagnostic purposes.

On the other hand Sawicki et al contended that complete Doppler ultrasonographic estimation of ovarian neoplasms should include besides estimation and location of angiogenesis, qualification of resistance of flow.[67] Study was undertaken on 329 women with malignant and benign adnexal masses who underwent ultrasonographic and color Doppler examination 1–5 days before surgery (laparotomy, laparoscopy) thus allowing histological verification of diagnosis. Postoperatively 255 (77.5%) benign and 74 (22.5%) malignant tumors were seen. Doppler flow within the tumor was 74.5% in benign and 98.6% in malignant masses (p<0.0001). In benign lesions homogenous superficial or peripheral vasculature was visualized, and in the majority of cases (82.7%) it was of medium intensification. However in malignant central, peripheral or mixed vascularization of intensified character was found. Average value of the resistance index in all benign masses amounted to 0.77+/–0.14, however in malignant it was 0.39+/–0.07 (p<0.0001).

Furthermore, the study performed to determine the value of gray scale and color Doppler sonography in distinguishing borderline cystic tumors (BCTs) from benign cysts and malignant tumors of the ovary, obtained results in favour for the analysis of velocimetric parameters.[68] Borderline cystic tumors showed blood flow in 24 cases (89%) and lower pulsatility and resistance indices (RI) compared with benign lesions (p<0.001 for both). Multivariate analysis revealed intracystic papillae as the only independent predictor of BCTs (p<0.001). They concluded that when a cystic mass has papillae, this is the only abnormal finding detected by gray scale transvaginal sonography, and color Doppler imaging shows low RI values within the mass, a BCT should be suspected.

A novel mater of investigation has been the usefulness of color Doppler venous flow in the differential diagnosis of adnexal masses. Alcazar et al analyzed for arterial signals the resistance index and peak systolic velocity, and for veins the maximum venous flow velocity. According to their previous study using arterial Doppler, a tumor was considered malignant when flow was detected and the lowest index was <or=0.45. Using venous Doppler a mass was considered as malignant when flow was detected and the venous flow velocity was>or=the best cut-off found on the receiver operator characteristic curve. Definitive histopathological diagnosis was obtained in all cases. The

results obtained showed that evaluation by venous flow assessment of adnexal mass may be usefull to discriminate between malignant and benign tumors. Venous flow velocity was significantly higher in malignant masses (18.1 cm/s vs. 8.9 cm/s, P= 0.0006). Sensitivity, specificity, positive and negative predictive value for the combination of both arterial and venous Doppler were 88%, 91%, 79%, and 95% respectively.[69]

FALSE-POSITIVE RESULTS

Although significant difference in vascular characteristics between benign and malignant adnexal lesions exist, an overlap in findings is also observed and is, sometimes, imminent. The adequate knowledge about ultrasound physics and vascular changes through the menstrual cycle, as well as acknowledging morphological characteristics of certain adnexal tumor can reduce this overlap in results. Furthermore, the sonographer should be aware that an overlap is characteristic of any biological system. However, even an experienced ultrasonographer using sensitive equipment will not ecsape the occasional misinterpretation of the ultrasound and Doppler information in equivocal cases. False-positive results also can be caused by increased vascularity in some physiological conditions. An increased blood flow and decreased impedance to blood flow distal to the point of sampling can be seen in preovulatory follicles, and corpus luteum, suggesting that vascular information derived from the premenopausal ovary must always be related to the phase of the cycle. A ring of angiogenesis around the dominant follicle is most prominent at the moment of presumed ovulation. The velocity of the perifollicular blood flow tends to increase, while the resistance to blood flow decreases.[70] With the rupture of the follicle and the formation of the corpus luteum, angiogenesis continues and further dilatation of the stromal vessels occurs. The physiological corpus luteum and its variant are frequent false-positive conditions in distinguishing ovarian malignancy, because of abundant and prominent flow. Luteal vascularity, described as “a ring of fire”, is probably a consequence of marked dilatation of stromal ovarian blood vessels or “vascular luteal conversion” due to increased local levels of E2 prostaglandins which are known to be potent vasodilatators. Additional confusion to accurate assessment and recognition of luteal blood flow adds its appearance—a cystic structure with irregular walls with various types of intracystic echoes. Therefore, irregular cystic structure with echogenic fluid within the cavity, increased blood flow velocity and decreased resistance to blood flow may lead the sonographer to a wrong interpretation. Accordingly, physiological ovarian angiogenic activity should be excluded by carrying out the examination during the early proliferate phase of the menstrual cycle. However, it seems not to be completely true, because some corpus luteal activity and consequently increased ovarian

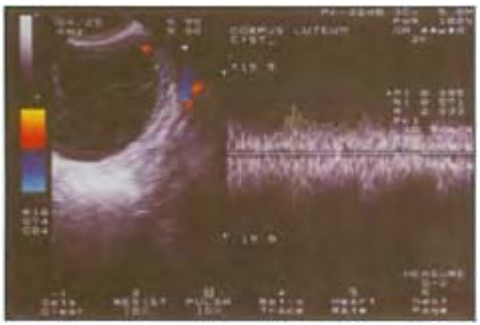

Figure 49.8: A transvaginal color Doppler sonogram of a corpus luteum cyst. Blood flow signals from the pericystic area demonstrate moderate vascular resistance (RI=0.57), typical of benign lesion

vascularity can be observed in first five days of the menstrual cycle. Therefore, corpus luteum and its blood flow can be treated as the true imitator of malignancy (Fig. 49.8). Ovarian lesions are a cause of great concern, because of the limited ability to distinguish accurately between benign and malignant neoplasms prior to surgery. This is particularly true for bizarre structures such as cystadenomas, corpus luteum cysts, ovarian fibromas, dermoid cysts and endometriomas (Figs 49.9 to 49.11).

Benign adnexal lesions which may cause falsepositive results are tubo-ovarian masses and endometriomas, both entities in which rich

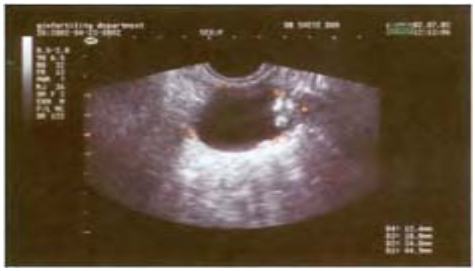

Figure 49.9: Two-dimensional view of the solid-cystic lesion

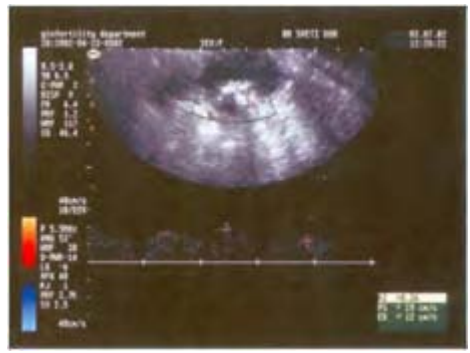

Figure 49.10: The same patient as in Figure 49.9. Pulsed Doppler revealed low resistance to blood flow, highly suspicious of malignant lesion. Histopathology revealed dermoid cyst

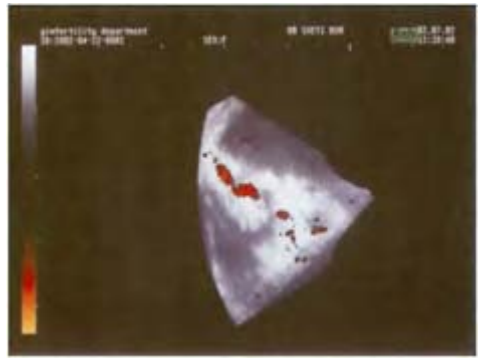

Figure 49.11: Three-dimensional power Doppler revealed regularly separated vessel in the solid counterpart

vascularity is usually triggered by inflammation. In addition, hormonal imbalances in overweight patients can produce blood flow patterns with low resistance index.

THREE-DIMENSIONAL ULTRASOUND AND POWER DOPPLER IMAGING OF BENIGN AND MALIGNANT ADNEXAL MASSES

Three-dimensional ultrasound (3D US) is a new, emerging technology that provides additional information to the evaluation of adnexal masses.[71]

Multiplanar and volume rendering display methods combined with the ability to rotate volume data into standard orientations are essential components of 3D US's current and future success.[72] Multiple sections of the tumor, rotation, translation, and reconstruction of 3D plastic images allow more precise evaluation of the tumor without increasing scanning time and patient discomfort.[73,74] Obvious advantages of three-dimensional ultrasound are improved recognition of the ovarian lesion anatomy, accurate characterization of the surface features, determination of the extent of tumor infiltration through the capsule, and clear depiction of the size and volume of the mass.[35,75] The surface mode is used in the assessment of superficial structures. If a cystic ovarian mass is found, three-dimensional surface-rendered image offers new possibilities for evaluation and the differentiation between benign and malignant disease.[76] Application of "transparent maximum/minimum" mode enables visualization of the intratumoral calcification or identification of the bone structures in dermoid tumors.[77] The "niche" aspect of three-dimensional ultrasound reveals intratumoral structures in selected sections which is mandatory for evaluation of the tubal pathology. As already mentioned new tool for study of angiogenesis is 3D power Doppler.[78,79] This three-dimensional modality allows the clinician to visualize the many overlapping vessels easily and quickly, and to assess their relationship to other vessels or surrounding tissues. The implementation of the 3D display permits the physician to view structures in three dimensions interactively, rather than having to assemble the sectional images mentally (Fig. 49.12).

The 3D power Doppler system may thus improve the information available on tumor vascularity and speed up the entire patient management process.[80] While 2D color Doppler is useful in detecting vascularized structures, 3D power Doppler is excellent in the study of vascular morphology. Morphological analysis of the blood vessel system represents another approach to tumor diagnosis which, so far, has not been

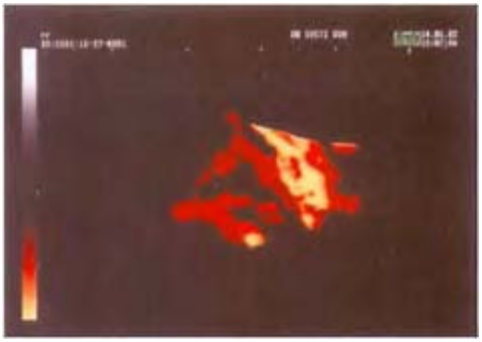

Figure 49.12: Three-dimensional power Doppler scan of a

malignant tumor
neovascularization.

extensively evaluated. There is a distinct impression that the distribution and branching pattern of blood vessels that supply a fast-growing tumor differ from those of a normal blood supply to normal organs. This means that blood vessel distribution seems to carry additional information that is missed in the present diagnostic approaches.[81,82]

FURHTER POSSIBILITIES AND CHALLENGES IN THE EVALUATION OF TUMOR ANGIOGENESIS

Our group made efforts in describing branching structures of tumor microvasculature like the blood vessel tree which is a mathematically complicated task that calls for the most recent mathematical apparatus. The branching pattern is the result of some principle (mathematical law) that acts repeatedly upon the blood vessels, so that they branch out in similar ways at different scale factors. Such objects that are self-similar at different scales are called fractals. The process is, presumably, similar to processes that govern the branching in an actual tree. If the underlying rule changes, the branching pattern must change too. We postulate that blood vessel trees are an example of fractal geometry.[83] The normal blood vessel trees (arteries and veins) form branched structures with eversmaller branches and diameters. The underlying proposition of our hypothesis is that there is a change in fractal dimension when the branching becomes unregulated by normal processes, i.e. when the ordered growth is replaced by disordered growth.[65]

Currently, the application of 3D power Doppler in the evaluation of neoplasm's is mainly qualitative or semiqantitative, for example in detecting whether the vascularity is present or not. Further development of the technology and the introduction of 3D quantification of blood flow, called the 3D color histogram, may improve our ability to differentiate between benign and malignant tumors and predict tumor prognosis.[84,85] The 3D color histogram measures the color percentage and flow amplitudes in the volume of interest. The histogram enables the vascularization and blood flow within a tissue block to be quantified, in contrast to 2D color histograms in which only single planes can be investigated.

Pairleitner et al recently reported on the use of cube method for measurement of blood flow and vascularization in 3D perspective.[86] The vascularization index (VI) represents the vessels in the tissue and is important for situation of both high and low vascularization. The flow index (FI), a mean color value, is important for characterizing high flow intensities (presumably tumors). The vascularization flow index (VFI) is a combination of VI and FI, and identifies the extremes between low vascularization and low blood flow on one side, and high vascularization and high blood flow, on the other. Although both VI and FI showed excellent reproducibility, VFI did not achieve accurate estimation between two observations, which may lead to unreliable measurement. It is expected that VI and FI may become good predictors for tumoral neovascularization, that can replace qualitative or semi-quantitative 3D power Doppler evaluation.[74]

Intravenous contrast agents for ultrasound studies have recently become commercially available.[87,88] With the utilization of ultrasound contrast agents perfusion imaging of the tumors has become more clear and provides meaningful physiological and pathological information for clinical decision making. They are of particular importance in cases of

"slow flow, low flow and no flow". Use of sonographic contrast agent facilitates imaging of tumor vessels. Orden et al showed that the number of vessels in power Doppler sonograms, both before and after contrast enhancement, was significantly higher in malignant than in benign adnexal lesions, as also was the increase in number of recognizable vessels after contrast agent administration.[89] Further more contrast agent uptake time was significantly shorter in malignant than in benign tumors. No significant differences were found in the power Doppler signal intensities or their changes between benign and malignant tumors.

One of the most exciting areas is the potential for using 3D power Doppler with contrast agents in tumoral microcirculation which enhance the ability to visualize vessel continuity more completely (in three orthogonal projections) and to demonstrate vessel branching (3D vascular reconstruction) more clearly. The higher detection rate of small vessels after injection of contrast agents may allow application of the mathematical models assessing three-dimensional vascular chaos and fractals.[65]

More recently, our group reported on the use of contrast-enhanced 3D power Doppler sonography for the differentiation of adnexal lesions.[90] We found that contrast enhanced, 3D power Doppler sonography provided better visualization of tumor vascularity in suspicious adnexal lesions than that obtained with non-contrast enhanced, 3D power Doppler sonography, and this led to a more exact differential diagnosis. With respect to differential diagnosis between malignant and benign ovarian lesions, contrast enhanced, 3D power Doppler sonography reached diagnostic sensitivity and specificity of 100% and 93.9%, respectively. The positive and negative predictive value of this method were 85.7% and 100%, respectively. Therefore, the diagnostic efficiency was improved with the use of sonographic contrast agent from 86.7% to 95.6%. Furthermore, our results show that the pattern of irregularly branching penetrating vessels in suspicious adnexal lesions demonstrated on 3D power Doppler ultrasound with or without contrast enhancement is an important feature that should be considered with other sonographic criteria to predict the likelihood of malignancy. If used together with 3D morphologic ultrasound assessment, enhanced 3D power Doppler imaging might precisely discriminate benign from malignant adnexal lesions (Table 49.4).

Table 49.4: Sensitivity, specificity, positive (PPV), and negative predictive values (NPV) of different color Doppler techniques in detection of adnexal malignancy obtained by Kurjak and co-workers[81]

Technique	*Sensitivity*	*Specificity*	*PPV*	*NPV*
2DUS/TVCD	0.89	0.98	0.86	0.99
3DUS/3DPD	0.97	0.99	0.97	0.99
Enhanced 3DPD	100	0.99	0.93	100

CONCLUSION

Color and pulsed Doppler sonography demonstates the vascularity of an adnexal mass, revealing the tumor histology and metabolism. Therefore, blood flow data should be considered to indicate the angiogenic intensity of a tumor, rather than indicating malignancy itself. It is a fact that, outside the qualification of structural details, ultrasonographic estimation of adnexal masses should include color Doppler analysis (presence of vascularization), but there is still no concensus wheather to use any of pulsed Doppler parameters, and which are the cut-off values between benign and malignant adnexal masses.

Furtermore, the results reported in recent literature on three-dimensional color Doppler are indeed provocative and, not surprisingly, raise many new questions about the regulation of tumor angiogenesis, the density of tumor vessels and the difference between vessel arhitecture in benign and malignant growths. Three-dimensional Doppler depiction of tumor angiogenesis has many clinical implications among which most important early detection of ovarian and endometrial cancers. Improved detection and classification of tumor arhitecture contributes to better diagnostic accuracy and consequently reduction of false positive findings and invasive procedures. Undoubtedly, further technological development and introduction of real-time 3D ultrasound imaging will contribute to more objective evaluation of adnexal tumor morphology and vascularity, which might lead to a significant reduction of morbidity and mortality, especially from ovarian cancer.

REFERENCES

1. Koonings PP, Campbell K, Mishell DR Jr, Grimes DA. Relative frequency of primary ovarian neoplasms: a ten year review. Obstet Gynecol 1989; 74:921–26.
2. Marret H. Doppler ultrasonography in the diagnosis of ovarian cysts: indications, pertinence and diagnostic criteria. J Gynecol Obstet Biol Reprod 2001; 30:20–33.
3. Warren BA. The vascular morphology of tumors. In: Peterson HI (Ed). Tumor Blood Circulation: angiogenesis, vascular morphology and blood flow of experimental human tumors. Boca Raton, FL: CRC Press, 1979; 1–47.
4. Coman DR, Sheldon WF. The significance of hyperemia around tumor implants. Am J Pathol 1946; 22:821–26.
5. Algire GH, Chalkley HW, Lagallais FY, Park HD. Vascular reactions of mice to wounds and to normal and neoplastic transplants. J Natl Cancer Inst 1945; 6:73–85.
6. Folkman J, Long D, Becker F. Growth and metastasis of tumor in organ culture. Tumor Res 1963; 16:453–67.
7. Folkman J, Cole P, Zimmerman S. Tumor behaviour in isolated perfused organs: in vitro growth and metastasis of biopsy material in rabbit thyroid and canine intestinal segment. Ann Surg 1966; 164:491–502.
8. Folkman J, Merler E, Abernathy C, Williams G. Isolation of a tumor factor responsible for angiogenesis. J Exp Med 1971; 133:275–88.
9. Klagsbrun M, D'Amore PA. Regulators of angiogenesis. Annu Rev Physiol 1991; 53:217.
10. Folkman J. What is the evidence that tumors are angiogenesis dependent? J Natl Cancer Inst 1989; 82:4–6.
11. Auerbach R. Angiogenesis-inducing factors: a review. In: Pick E (Ed). Limphokines, London: Academic Press, 1981; 4:69–88.
12. Rak JW, St Croix DB, Kerbel RS. Consequences of angiogenesis for tumor progression, metastasis and cancer therapy. Anti-Cancer Drugs 1995;6:3–18.
13. Plate KH. From angiogenesis to lymphangiogenesis. Nature Medicine 2001; 7(2):151–52.

14. Skobe M, Rockwell R Vosseler S, Fusenig NE. Halting angiogenesis suppresses carcinoma cell invasion. Nature Med 1997; 3:1222–27.
15. Gasparini G, Weidner N, Maluta S et al. Intratumoral microvessel density and p53 correlation with metastasis in head-and-neck squamous-cell carcinoma. Int J Cancer 1993; 55:739–44.
16. Gasparini G, Weidner N, Bevilacqua P et al. Tumor microvessel density, p53 expression, tumor size, and peritumoral lymphatic vessel invasion are relevant prognostic markers in node-negative breast carcinoma. J Clin Oncol 1994; 12:454–66.
17. Weidner N. Tumor angiogenesis: review of current applications in tumor prognostication. Semin Diagn Pathol 1993; 10:302–13.
18. Folkman J, Klagsburn M. Angiogenic factors. Science 1987; 2345:442–47.
19. Dvorak HF, Brown LF, Detmar M, Dvorak AM. Vascular permeability factor/vascular endothelial growth factor, microvascular hyperpermeability, and angiogenesis. Am J Pathol 1995; 146:1029–39.
20. Plate KH, Breier G, Weich HA, Rissau W. Vascular endothelial growth factor is a potential tumor angiogenesis factor in human gliomas in vivo. Nature 1992; 359:845–48.
21. Kim KJ. Inhibition of vascular endothelial growth factor-induced angiogenesis suppresses tumor growth in vivo. Nature 1993; 362:841–44.
22. Lu JJ, Stanczyk FZ, Zeng W. Expression of VEGF in ovarian epithelial tumors. J Soc Gynecol Investig 2001; 8(1)(Suppl):766.
23. Cooper BC, Ritchie JM, Broghammer CL, Coffin J, Sorosky JI, Buller RE, Hendrix MJ, Sood AK. Preoperative serum vascular endothelial factor levels: significance in ovarian cancer. Clin Cancer Res 2002; 8(10):3193–97.
24. Folkman J. Growth and metastasis of tumor in organ culture. Cancer 1963; 16:453–57.
25. Guilino PM. Extracellular compartments of solid tumors. In Becker J (Ed). Cancer. New York: Plenum Press, 1975; 327.
26. Jain RK. Determination of tumor blood flow: a review. Cancer Res 1988; 48:2641–46.
27. Kurjak A, Kupesic S, Breyer B. The assessment of ovarian tumor angiogenesis by three-dimensional power Doppler. In: Kurjak A (Ed). Three-Dimensional Power Doppler in Obstetrics & Gynecology. The Parhenon Publishing Group, 2000.
28. Jain RK, Ward-Harley K. Tumor blood flow characterization, modifications and role in hyperthermia. Trans Sonics Ultrasonics 1984; 31:504–09.
29. Vaupel P, Kallinowski F, Okunieff P. Blood flow oxygen and nutrient supply, and metabolic microenvironment of human tumors: A review. Cancer Res 1989; 49:6449.
30. Fleischer AC. Sonographic depiction of tumor vascularity and flow: from in vivo models to clinical applications. J Ultrasound Med 2000; 19:55–61.
31. Hanahan D, Folkman J. Parameters and emerging mechanisms of the angiogenetic switch during tumorigenesis. Cell 1996; 86:353–54.
32. Kurjak A, Kupesic S, Ilijas M, Sparac V, Kosuta D. Preoperative diagnosis of primary fallopian tube carcinoma. Gynecol Oncol 1998; 68:29–34.
33. Kurjak A, Jukic S, Kupesic S, Babic D. A combined Doppler and morphopathological study of ovarian tumors. Eur J Obstet Gynecol Reprod Biol 1997; 71:147–50.
34. Emoto M, Iwasaki H, Mimura K, Kawarabayashi T, Kikuchi M. Differences in the angiogenesis of benign and malignant ovarian tumors, demonstrated by analyses of color Doppler ultrasound, immunohistochemistry, and microvessel density. Cancer 1997; 80:899–907.
35. Suren A, Osmers R, Kuhn W. 3D Color Power Angio TM imaging: a new method to assess intracervical vascularization in benign and pathological conditions. Ultrasound Obstet Gynecol 1998; 2:133–38.
36. Kurjak A, Kupesic S. Three dimensional ultrasound and Power Doppler in assessment of uterine and ovarian angiogenesis: a prospective study. Croat Med J 1999; 40:413–20.
37. Kurjak A, Zalud I, Jurkovic D, Alfirevic Z, Miljan M. Transvaginal color Doppler for the assessment of pelvic circulation. Acta Obstet Gynecol Scand 1989; 68:131–37.

38. Bourne T, Campbell S, Steer C, Whitehead MI, Collins WP. Transvaginal color flow imaging: a possible new screening technique for ovarian cancer. Br Med J 1989; 299:1367–70.
39. Hata K, Kata T, Kitao M. Intratumoral peak systolic velocity as a new possible predictor for detection of adnexal malignancy. Am J Obstet Gynecol 1995; 172:1496–1500.
40. Kurjak A, Jukic S, Kupesic S, Babic D. A combined Doppler and morphopathological study of ovarian tumors. Eur J Obstet Gynecol Reprod Biol 1997; 71:147–50.
41. Levine D, Feldstein VA, Babcook CJ, Filly RA. Sonography of ovarian masses: poor sensitivity of resistive index for identifying malignant lesions. Am J Roentgenol 1994; 162:1355–59.
42. Kidron D, Bernheim J, Aviram R, Cohen I, Fishman A, Beyth Y, Tepper R. Resistance index to blood flow in ovarian tumors: correlation between resistance index and histological pattern of vascularization, Ultrasound Obstet Gynecol 1999; 13:425–30.
43. Kurjak A, Kupesic S. Transvaginal color Doppler and pelvic tumor angiogenesis: lessons learned and future challenges. Ultrasound Obstet Gynecol 1995; 6:145–59.
44. Kurjak A, Shalan H, Kupesic S, Predanic M, Zalud I, Breyer B, Jukic S. Transvaginal color Doppler sonography in the assessment of pelvic tumor vascularity. Ultrasound Obstet Gynecol 1993; 3:137–54.
45. Brown D, Frates M, Laing F et al. Ovarian masses: can benign and malignant lesions be differentiated with color and pulsed Doppler US? Radiology 1994; 190:333–36.
46. Stein SM, Laifer-Narin S, Johnson MB, Roman LD, Muderspach LI, Tyszka JM, Rails PW. Differentiation of benign and malignant adnexal masses: relative value of gray-scale, color Doppler, and spectral Doppler sonography. Am J Roentgenol 1995; 164:381–86.
47. Fleischer AC, Cullinan JA, Peery CV et al. Early detection of ovarian carcinoma with transvaginal color Doppler ultrasonography. Am J Obstet Gynecol 1996; 174:101–06.
48. Rubin JM, Bude RO, Carson PL, Bree Rl, Adler RS. Power Doppler US: a potentially useful alternative to mean frequency-based color Doppler US. Radiology 1994; 190:853–56.
49. Rubin JM, Adler RS, Fowlkes JB, Spratt S, Pallister JE, Chen JF, Carson PL. Fractional moving blood volume: estimation with power Doppler US. Radiology 1995; 197:183–90.
50. Winsberg F. Power Doppler sonography. J Ultrasound Med 1996; 15:164.
51. Papadimitriou A, Kalogirou D, Antonio G, Petridis N, Kalogirou O. Power Doppler ultrasound: a potential useful alternative in diagnosing pelvic pathological conditions. Clin Exp Obstet Gynecol 1996; 23:229–32.
52. Burns PN. Harmonic imaging with ultrasound contrast agents. Clin Radiol 1996;51:50–5.
53. Guerriero S, Alcazar JL, Ajossa S, Lai MP, Errasti T, Mallarini G, Melis GB. Comparison of conventional color Doppler imaging and power Doppler imaging for the diagnosis of ovarian cancer:results of a 654 European study. Gynecol Oncol 2001;83:299–304.
54. Meyerovitz CB, Fleischer AC, Pickens DR et al. Quantification of tumor vascularity and flow with amplitude color Doppler sonography in an experimental mode: Preliminary results. J Ultrasound Med 1996; 15:827.
55. Fleischer A, Wojcicki W, Donnely E et al. Quantified color Doppler sonography of tumor vascularity in an animal model. J Ultrasound Med 1999; 18:547.
56. Bourne TH, Campbell S, Steers CV, Whitehead MI, Collins WP. Transvaginal colour flow imaging: a possible new screening technique for ovarian cancer. Br Med J 1989; 299:1367–70.
57. Kurjak A, Zalud I, Jurkovic D, Alfirevic Z, Miljan M. Transvaginal color Doppler of the assessment of pelvic circulation. 1989; 68:131–36.
58. FleisherAC, RodgersWH, RaoBJ, KepplerDM, Worrel JA, Williams L, Jones HW III. Assessment of ovarian tumor vascularity with transvaginal color Doppler sonography. J Ultrasound Med 1991; 10:563–68.
59. Kurjak A, Zalud I, Alfirevic Z. Evaluation of adnexal masses with transvaginal color ultrasound. J Ultrasound Med 1991; 10:295–97.
60. Weiner Z, Thaler I, Beck D, Rottem S, Deutsch M, Brandes JM. Differentiating malignant from benign ovarian tumors with transvaginal color flow imaging. Obstet Gynecol 1992; 79:159–62.

61. Kurjak A, Schulman H, Sosic A, Zalud I, Shalan H. Transvaginal ultrasound, color flow, and Doppler waveform of the postmenopausal adnexal mass. Obstet Gynecol 1992; 80:917–21.
62. Hamper UM, Sheth S, Abbas FM, Rosenshein BN, Aronson D, Kurman JR. Transvaginal color Doppler sonography of adnexal masses: differences in blood flow impedance in benign and malignant lesions. Am J Roentgenol 1993; 160:1225–28.
63. Carter J, Saltzman A, Hartenbach E, Fowler J, Carlson L, Twiggs LB. Flow characteristics in benign and malignant gynecologic tumors using transvaginal color flow Doppler. Obstet Gynecol 1994; 83:125–30.
64. Kurjak A, Kupesic S, Zodan T. Color Doppler assessment of malignant adnexal masses. In: Kurjak A, Kupesic S (Eds). An Atlas of transvaginal Color Doppler. The Parthenon Publishing Group, New York, London 2000; 203–19.
65. Guerriero S, Alcazar JL, Coccia ME, Ajossa S, Scarselli G, Boi M, Gerada M, Melis GB. Complex pelvic mass as a target of evaluation of vessel distribution by color Doppler sonography for the diagnosis of adnexal malignancies: results of a multicenter European study. Journal Ultrasound Med 2002; 21:1105–11.
66. Gramellini D, Rutolo S, Verrotti C, Piantelli G, Fieni S, Vadora E. Sonographic characterisation, Doppler ultrasonography and tumor markers in the diagnosis of malignancy of ovarian masses. Minerva Ginecol 2001; 53:1–11.
67. Sawicki W, Spiewankiewicz B, Cendrowski K, Stelmachow J. Preoperative discrimination between malignant and benign adnexal masses with transvaginal ultrasonography and colour blood flow imaging. Eur J Gynaecol Oncol 2001; 22(2):137–42.
68. Pascual MA, Tresserra F, Grases PJ, Labastida R, Dexeus S. Borderline cystic tumors of the ovary: gray scale and color Doppler sonographic findings: J Clin Ultrasound 2002; 30:76–82.
69. Alcazar JL, Lopez-Garcia G. Transvaginal color Doppler assessment of venous flow in adnexal masses. Ultrasound Obstet Gynecol 2001; 17:434–38.
70. Kurjak A, Kupesic S, Schulman H, Zalud I. Transvaginal color Doppler in the assessment of ovarian and uterine blood flow in infertile women. Fertil Steril 1991; 56:870–73.
71. Bonilla Musoles F, Raga F, Osborne NG. Threedimensional ultrasound evaluation of ovarian masses. Gynecol Oncol 1995; 59:129–35.
72. Merz E. Three-dimensional transvaginal ultrasound in gynecological diagnosis. Ultrasound Obstet Gynecol 1999; 14:81–86.
73. Chan L, Lin WM, Verpairojkit B, Hartman D, Reece EA. Evaluation of adnexal masses using three-dimensional ultrasonographic technology: preliminary report. J Ultrasound Med 1997; 16:349–54.
74. Weber G, Merz E, Bahlmann F, Macchiella D. Ultrasound assessment of ovarian tumors: comparison between transvaginal 3D technique and conventional 2 dimensional vaginal ultrasonography. Ultraschall Med 1997; 18(1):26–30.
75. Riccabona M, Nelson TR, Pretorius DH. Threedimensional ultrasound: accuracy of distance and volume measurements. Ultrasound Obstet Gynecol 1996; 7.429–34.
76. Weber G, Merz E, Bahlman F. Three-dimensional sonography of cystic ovarian tumors. In: Merz E (Ed). 3D Ultrasonography and Gynecology. Lippincott Williams & Wilkins, Philadelphia 1998.
77. Kurjak A, Kupesic S. Ovarian lesions assessed by three-dimensional ultrasound and power Doppler. In: Kurjak A, Kupesic S (Eds). Clinical application of 3D sonography. The Parthenon Publishing Group 2000.
78. Downey BD, Fenster A. Vascular imaging with a three dimensional power Doppler system. Am J Roentgenol 1995; 165:665–68.
79. Kurjak A, Kupesic S, Sparac V, Kosuta D. Threedimensional ultrasonographic and power Doppler characterization of ovarian lesions. Ultrasound Obstet Gynecol 2000; 16:365–71.
80. Kurjak A, Kupesic S, Breyer B, Sparac V, Jukic S. The assessment of ovarian tumor angiogenesis: what does three-dimensional power Doppler add? Ultrasound Obstet Gynecol 1998; 12:136–46.

81. Kurjak A, Kupesic S, Sparac V, Bekavac I. Preoperative evaluation of pelvic tumors by Doppler and three-dimensional sonography. J Ultrasound Med 2001; 20:829–40.
82. Kurjak A, Kupesic S, Anic T, Kosuta D. Threedimensional ultrasound and power Doppler improve the diagnosis of ovarian lesions. Gynecol Oncol 2000; 76:28–32.
83. Breyer B, Kurjak A. Tumor vascularization Doppler measurements and chaos: what to do? Ultrasound Obstet Gynecol 1995; 5:209–10.
84. Fleischer AC, Pairleitner H. Transvaginal Doppler assesses ovarian flow. Diagn Imag 1998; 9:47.
85. Fleischer AC, Pairleitner H. 3D transvaginal color Doppler sonography: current and potential applications. Med Imag Int 1999; 9:10–13.
86. Pairleitner H, Steiner H, Hasenoehrl G, Staudach A. Three-dimensional power Doppler sonography: Imaging and quantifying blood flow and vascularization. Ultrasound Obstet Gynecol 1999; 14:139–43.
87. Ophir J, Parker KJ. Contrast agents in diagnostic ultrasound. Ultrasound Med Biol 1989; 15:319–33.
88. Goldberg BB, Merton AD, Forsberg F, Liu J, Rawool N. Color amplitude imaging: preliminary results using vascular sonographic agents. J Ultrasound Med 1990; 15:127–34.
89. Orden MR, Gudmundsson S, Kirkinen P Contrastenhanced sonography in the examination of benign and malignant adnexal masses. J Ultrasound Med 2000; 19:738–48.
90. Kupesic S, Kurjak A. Contrast enhanced threedimensional power Doppler sonography for the differentiation of adnexal masses. Obstet Gynecol 2000; 96:452–58.
91. Hata T, Hata K, Senoh D, Makihara K, Aoki S, Takamiya O, Kitao M. Doppler ultrasound assessment of tumor vascularity in gynecologic disorders. J Ultrasound Med 1989; 8:309–14.
92. Fleischer AC, Rodgers WH, Rao BJ, Keppler DM, Worrell JA, Williams L, Jones III, HW. Assessment of ovarian tumor vascularity with transvaginal color Doppler sonography. J Ultrasound Med 1991; 10: 563–68.
93. Kawai M, Kano T, Kikkawa F, Maeda O, Oguchi H, Tomoda Y. Transvaginal Doppler ultrasound with color flow imaging in the diagnosis of ovarian cancer. Obstet Gynecol 1992; 79:163–67.
94. Tekay A, Jouppila P. Validity of pulsatility and resistance indices in classification of adnexal tumors with transvaginal color Doppler ultrasound. Ultrasound Obstet Gynecol 1992; 2:338–44.
95. Hata H, Hata T, Manabe A, Sugimura K, Kitao M. A critical evaluation of transvaginal Doppler studies, transvaginal sonography, magnetic resonance imaging, and CA 125 in detecting ovarian cancer. Obstet Gynecol 1992; 80:922–26.
96. Kurjak A, Schulman H, Sosic A, Zalud I, Shalan H. Transvaginal ultrasound, color flow, and Doppler waveform of the postmenopausal adnexal mass. Obstet Gynecol 1992; 80:917–21.
97. Hamper UM, Sheth S, Abbas FM, Rosenshein BN, Aronson D, Kurman JR. Transvaginal color Doppler sonography of adnexal masses: Differences in blood flow impedance in benign and malignant lesions. Am J Roent 1993; 160:1225–28.
98. Schneider VL, Schneider A, Reed KL, Hatch KD. Comparison of Doppler with two-dimensional sonography and CA 125 for prediction of malignancy of pelvic masses. Obstet Gynecol 1993; 81:983–88.
99. Timor-Tritsch IE, Lerner JP, Monteagudo A, Santos R. Transvaginal ultrasonographic characterization of masses by means of color flow-directed Doppler measurements and a morphologic scoring system. Am J Obstet Gynecol 1993; 168:909–13.
100. Jain KA. Prospective evaluation of adnexal masses with endovaginal gray-scale and dupler and color Doppler US: Correlation with pathologic findings. Radiology 1994; 191:63–67.
101. Weiner Z, Beck D, Brandes JM. Transvaginal sonography, color flow imaging, computed tomography scanning, and CA 125 as a routine follow-up examination in women with pelvic tumor: Detection of recurrent disease. J Ultrasound Med 1994; 13:37–41.
102. Levine D, Feldstein VA, Babcook CJ, Filly RA. Sonography of ovarian masses: Poor sensitivity of resistive index for identifying malignant lesions. Am J Roent 1994; 162:1355–59.

103. Brown DL, Frates MC, Laing FC, DiSalvo DN, Doubilet PM, Benson CB, Waitzkin ED, Muto MG. Ovarian masses: Can benign and malignant lesions be differentiated with color and pulsed Doppler US? Radiology 1994; 190:333–36.
104. Valentin L, Sladkevicius R Marsal K. Limited contribution of Doppler velocimetry to the differential diagnosis of extrauterine pelvic tumors. Obstet Gynecol 1994; 83:425–33.
105. Bromley B, Goodman H, Benacerraf BR. Comparison between sonographic morphology and Doppler waveform for the diagnosis of ovarian malignancy. Obstet Gynecol 1994; 83:434–37.
106. Carter J,Saltzman A, Hartenbach E, Fowler J, Carson L, Twiggs LB. Flow characteristics in benign and malignant gynecologic tumors using transvaginal color flow Doppler. Obstet Gynecol 1994; 83:125–30.
107. Prompeler HJ, Sauerbrei WM, Latternann U, Pfleiderer A. Quantitative flow measurements for classification of ovarian tumors by transvaginal color Doppler sonography in postmenopausal patients. Ultrasound Obstet Gynecol 1994; 4:406–13.
108. Chou CY, Chang CH, Yao BL, Kuo HC. Color Doppler ultrasonography and serum CA 125 in the differentiation of benign and malignant ovarian tumors. J Clin Ultrasound 1994; 22:491–96.
109. Wu CC, Lee CN, Chen TM, Lai JI, Hsieh CY, Hsieh FJ. Factors contributing to the accuracy in diagnosing ovarian malignancy by color Doppler ultrasound. Obstet Gynecol 1994; 84:605–08.
110. Zaneta G, Vergani P, Lissoni A. Color Doppler ultrasound in the preoperative assessment of adnexal masses. Acta Obstet Gynecol Scand 1994; 73:637–41.
111. Salem S, White LM, Lai J. Doppler sonography of adnexal masses: The predictive value of the Pulsatility index in benign and malignant disease. Am J Roent 1994; 163:1147–50.
112. Savicki E, Spiewankiewicz B, Cendrowski K, Stelmachow J. Transvaginal Doppler ultrasound with colour flow imaging in benign and malignant ovarian lesions. Clin Exp Obst Gyn 1994; 22:137–42.
113. Sengoku K, Saitoh S, Abe M, Ishikawa M. Evaluation of transvaginal color Doppler sonography, transvaginal sonography and CA 125 for prediction of ovarian malignancy. Int J Gynecol Obstet 1994; 46:39–43.
114. Franchi M, Beretta P, Ghezzi F, Zanaboni F, Goddi A, Salvator S. Diagnosis of pelvic masses with transabdominal color Doppler, CA 125 and ultrasonography. Acta Obstet Gynecol Scand 1995; 75 734–39.
115. Maly Z, Riss P, Deutinger J. Localization of blood vessels and qualitative assessment of blood flow in ovarian tumors. Obstet Gynecol 1995; 85:33–36.
116. Stein SM, Laifer-Narin S, Johnson MB, Roman LD, Muderspach LI, Tyszka JM, Rails PW. Differentiation of benign and malignant adnexal masses: Relative value of gray-scale, color Doppler, and spectral Doppler sonography. Am J Roent 1995; 164:381–86.
117. Carter JR, Lau M, Fowler JM, Carlson JW, Carson LF, Twiggs LB. Blood flow characteristics of ovarian tumors: Implications for ovarian cancer screening. Am J Obstet Gynecol 1995; 172:901–07.
118. Fleischer AC, Cullinan JA, Peery CV, Jones III HW. Early detection of ovarian carcinoma with transvaginal color Doppler ultrasonography. Am J Obstet Gynecol 1996; 174:101–06.
119. Buy JN, Ghossain MA, Hugol D, Hassen K, Sciot C, True JB, Poitout P, Vadrot D. Characterization of adnexal masses: Combination of color Doppler and conventional sonography compared with spectral Doppler analysis alone and conventional sonography alone. Am J Roent 1996; 166:385–93.
120. Rehn M, Lohmann K, Rempen A. Transvaginal ultrasonography of pelvic masses: Evaluation of Bmode technique and Doppler ultrasonography. Am J Obstet Gynecol 1996; 175:97–104.
121. Predanic M, Vlahos N, Pennisi J, Moukhtar M, Aleem FA. Color and pulsed Doppler sonography, gray-scale imaging, and serum CA 125 in the assessment of adnexal disease. Obstet Gynecol 1996; 88:283–88.

122. Tailor A, Jurkovic D, Bourne TH, Natucci M, Collins WR Campbell SA. Comparison of intratumoral indices of blood flow veloctiy and impedance for the diagnosis of ovarian cancer. Ultrasound Med Biol 1996; 22:837–43.
123. Alcazar JL, Ruiz-Perez ML, Errasti T. Transvaginal color Doppler sonography in adnexal masses: which parameter performs best? Ultrasound Obstet Gynecol 1996; 8:114–19.
124. Wheeler TC, Fleischer AC. Complex adnexal mass in pregnancy: predictive value of color Doppler sonography. J Ultrasound Med 1997; 16(6):425–28.
125. Reles A, Wein U, Licthenegger W. Transvaginal color Doppler sonography and conventional sonography in the preoperative assessment of adnexal masses. J Clin Ultrasound 1997; 25(5):217–25.
126. Emoto M, Iwasaki H, Mimura K, Kawarabayashi T, Kikuchi M. Differences in the angiogenesis of benign and malignant ovarian tumors, demonstrated by analyses of color Doppler ultrasound, immunohistochemistry, and microvessel density. Cancer 1997; 80(5):899–907.
127. Valentin L. Gray scale sonography, subjective evaluation of the color Doppler image and measurement of blood flow velocity for distinguishing benign and malignant tumors of suspected adnexal origin. Eur J Obstet Gynecol Reprod Biol 1997; 72(1): 63–72.
128. Takac I. Analysis of blood flow in adnexal tumors by using color Doppler imaging and pulsed spectral analysis. Ultrasound Med Biol 1998; 24(8):1137–41.
129. Guerriero S, Ajossa S, Risalvato A, Lai MP, Mais V, Angiolucci M, Melis GB. Diagnosis of adnexal malignancies by using color Doppler energy imaging as a secondary test in persistent masses. Ultrasound Obstet Gynecol 1998; 11:277–82.
130. Leeners B, Funk A, Schild RL, Jorn H, Kemp B, Minkenberg R, Rath W. Preoperative determination of the structure of pelvic tumors with color-coded Doppler ultrasound and conventional transvaginal ultrasound. Zentralbl Gynakol 1998;120(10): 503–10.
131. Angeid-Backman E, Coleman BG, Arher PH, Jacobs JE, Langer JE, Horii S. Comparison of resistive index versus pulsatility index in assessing the benign etiology of adnexal masses. Clin Imaging 1998; 22(4): 284–91.
132. Brown DL, Doubilet PM, Miller FH, Frates MC, Laing FC, DiSalvo DN, Benson CB, Lerner MH. Benign and malignant ovarian masses:selection of the most discriminating gray-scale and Dppler sonographic features. Radiology 1998; 208(1); 103–10.
133. Buckshee K, Temsu I, Bhatla N, Deka D. Pelvic examination, transvaginal ultrasound and transvaginal color Doppler sonography as predictors of ovarian cancer. Int J Gynaecol Obstet 1998; 61(1):51–57.
134. Alcazar JL, Errasti T, Zornoza A. Transvaginal color Doppler ultrasonography and CA 125 in suspicious adnexal masses. Int J Gynecol Obstet 1999;66:255–61.
135. Valentin L. Pattern recognition of pelvic masses by gray-scale ultrasound imaging: the contribution of Doppler ultrasound. Ultrasound Obstet Gynecol 1999; 14:338–47.

Chapter 50
Sonographic Imaging in Infertility

Sanja Kupesic, Asim Kurjak, Drazena Bjelos

INTRODUCTION

Infertility is defined as the failure to conceive a desired pregnancy after 12 months of unprotected intercourse, and affects 10% of married couples. With recent technological development and proper use of medically assisted reproduction techniques, one half of these patients will become pregnant. Approximately 40% of the time the cause is attributable to the female, 40% of the time to the male, and about 20% of the time to combined factors. Traditionally, the causes of infertility are divided into cervical, endometrial/uterine, tubal, peritoneal, ovulatory and male factors.

More than any other new method, ultrasound has made significant improvements in the modern management of female infertility. Transvaginal sonography provides the reproductive endocrinologist with a tool that cannot only evaluate normal and stimulated cycles but also assists in follicle aspiration and subsequent transfer of the embryo. The addition of color Doppler capabilities to transvaginal probes permits visualization of small intraovarian and endometrial vessels, allowing depiction of normal and abnormal physiological changes in the ovary and uterus. It may help in prediction of ovulation and detection of certain ovulatory disorders and the luteal phase defect. Doppler investigation of ovarian blood flow may improve the early diagnosis of ovarian hyperstimulation syndrome in patients with ovulation induction. Initial impressions concerning the usefulness of blood flow studies in infertile patients have been confirmed by numerous studies during the last decade. This chapter reviews on the assessment of ovarian, uterine and tubal causes of infertility and on the current and future role of color Doppler and three-dimensional ultrasound in the field of reproductive endocrinology.

UTERINE/ENDOMETRIAL FACTORS OF INFERTILITY

The uterus provides the site of implantation and growth for developing pregnancy. Anything that results in distortion of the uterine cavity or interferes with the blood supply may result in infertility or pregnancy loss. The normality of the mucosal lining, glandular secretion and vascularity are necessary to support implantation and placentation. Uterine anomalies, polyps, myomata, neoplasia, infections and intrauterine scar tissue can lead to poor reproductive performance.

ENDOMETRIUM

During each month of female reproductive life, the functional layer of the endometrium is shed during menstruation, leaving behind an intact basal layer. In the first half of the menstrual cycle, increasing estrogen levels stimulate proliferation of the mucosa. Sonographically, this proliferative phase manifests as a triple line caused by the two opposed layers of hypoechoic mucosa. After ovulation, progesterone secreted by the corpus luteum stimulates endometrial secretory activity. During this secretory phase, increasing stromal edema results in a thicker echogenic endometrium. The endometrial lining may not grow properly in the luteal phase if there is inadequate progesterone production. Luteal phase deficiency has been associated with infertility and early pregnancy loss. Traditional diagnosis consists of an endometrial biopsy performed 2 days before the expected menses. Because the endometrium has a distinctive sonographic appearance in the follicular and luteal phases, some authors have suggested use of ultrasound to diagnose inadequate luteal phase and to determine appropriate luteal response of the endometrium before embryo transfer during *in vitro* fertilization. Color Doppler has also been used for determination of the optimal uterine conditions for embryo implantation.

The question of a correlation between endometrial thickness and the likelihood of conception, in the context of assisted conception, remains a contentious issue. However, a very thin endometrium (below 7 mm) seems to be accepted as a reliable sign of sub-optimal implantation potential.

Recently, Freidler and colleagues[1] reviewed 2665 assisted conception cycles from 25 reports. Eight reports found that the difference in the mean endometrial thickness of conception and non-conception cycles was statistically significant, while 17 reports found no significant difference. They concluded that results from various trials are conflicting and that insufficient data exist describing a linear correlation between endometrial thickness and the probability of conception. The main advantage of measuring endometrial thickness lies in its high negative predictive value in cases with minimal endometrial thickness. Gonen and colleagues[2] reported absence of pregnancy in donor insemination cycles where the endometrium thickness did not reach at least 6 mm. Similarly, in a group of oocyte recipients, no pregnancy was reported in women who had an endometrial thickness of less than 5 mm, whereas several pregnancies occurred in patients with an endometrium thinner than 7.5 mm.[3] Finally, in *in vitro* fertilization (IVF) cycles, Khalifa and colleagues reported a minimal endometrial thickness of 7 mm to be compatible with pregnancy.[4]

Endometrial pattern is defined as the relative echogenicity of the endometrium and the adjacent myometrium as demonstrated on a longitudinal ultrasound scan.

In a prospective study, Serafini and colleagues[5] found the multilayered pattern to be more predictive of implantation than any other parameter measured (Fig. 50.1). Sher and colleagues[6] correlated a non-multilayered echo pattern with advanced age and the presence of uterine abnormalities. In the literature, of 13 studies, which examined the value of endometrial pattern in predicting pregnancy, only four failed to confirm its predictive value. The endometrial pattern does not appear to be influenced by the type of ovarian stimulation and it is of prognostic value in both fresh IVF, as well as frozen embryo transfer cycles. Zaidi et al[7] reported that if subendometrial blood flow is detectable, the endometrial morphology may be less important than previously described.

Absence of subendometrial blood flow seems to be more significant negative predictor than morphological assessment.

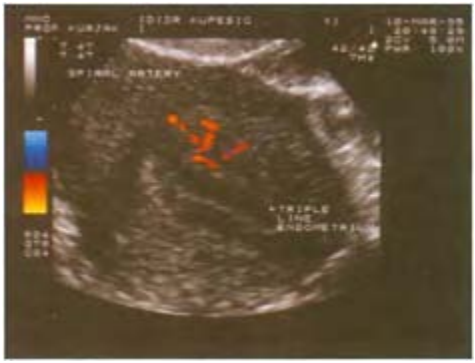

Figure 50.1: Color Doppler signals obtained from the spiral arteries at the periphery of the triple-line endometrium

The authors evaluated 96 women undergoing treatment on the day of human chorionic gonadotropin (hCG) administration. They asses- sed endometrial thickness, endometrial morphology, presence or absence of subendometrial or intraendometrial color flow, intraendometrial vascular penetration and subendometrial blood flow velocimetry on the day of hCG administration and related the results to pregnancy rates (Fig. 50.2). The overall pregnancy rate was 32.3% (31/ 96) and there was no significant difference between the pregnant and non-pregnant groups with regard to endometrial thickness, subendometrial peak systolic blood flow velocity (V_{max}) or subendometrial pulsatility index (PI). The pregnancy rates based on endometrial morphology were not significantly different, being 17.6% (3/ 17), 33.3% (2/6) and 35.6% (26/73) for types A (hyperechoic), B (isoechoic) and C (triple-line) endometria, respectively. In eight (8.3%) patients, subendometrial color flow and intraendometrial vascularization were not detected. Absence of blood flow was associated with failure of implantation ($p<0.05$). The pregnancy rates related to the zones of vascular penetration into the subendometrial and endometrial regions were: 26.7% (4/15) for Zone 1 (subendometrial zone), 36.4% (16/44) for Zone 2 (outer hyperechogenic zone) and 37.9% (11/29) for Zone 3 (inner hypoechogenic zone), and were not significantly different.

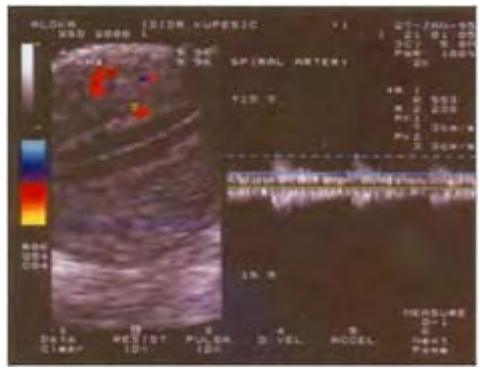

Figure 50.2: Blood flow velocity waveforms of the spiral arteries during the follicular phase. Note the triple-line endometrium (left) and the moderate resistance index (RI=0.55) (right) obtained from spiral arteries

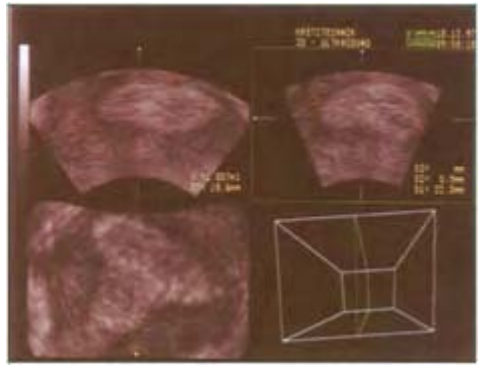

Figure 50.3: Three perpendicular planes of a uterus and endometrium. Note the clear separation of the endometrium. The computer software

enables endometrial volume calculation

Endometrial thickness obtained by two-dimensional sonography is considered the most important parameter of endometrial growth. However, this parameter does not include the total volume of the endometrium. For certain diagnostic information on endometrium, endometrial volume measurement might be important, since retarded endometrial development can be associated with primary infertility (Fig. 50.3). The ability to quantify the volume of the endometrium using 3D ultrasound may help to correlate cycle outcome with a quantitative parameter rather than endometrial thickness, which is prone to greater subjective variation in measurement.[8] By stepping through the volume in plane mode, the outer limits of endometrium are traced and volume calculations are performed immediately. The accurateness of this method has already been described.[9,10] To obtain the best results, stepping through the volume should be performed in small units. In each new plane the area tracing has to be corrected to its new extent. Low contrast in ultrasound data can increase the error of volume estimation. In general, the endometrium shows a good contrast to the surrounding myometrial tissue and therefore, in most cases volume estimation can be performed. Measurements could best be reproduced in longitudinal and transverse viewing planes. Other sources of measuring error may derive from the low contrast of the caudal end of the endometrium and the uterus. Endometrial fluid may also increase measuring error because the fluid volume may be too small to be measured accurately by 3D ultrasound.

Lee et al[11] were first to demonstrate volume estimation of the endometrium by 3D ultrasound. Using the same method Kyei-Mensah et al[12] assessed the reliability of 3D ultrasound in measuring endometrial volume on twenty patients undergoing ovarian stimulation. Endometrial volumes of these patients were obtained on the day of hCG administration. The intraobserver and inter-observer coefficient of variation were 8 and 11%, respectively. Repeatibility within and between investigators was also expressed as the Intra CC and Inter CC. The coefficients describe the proportion of variation in a measurement, which is caused by true biological subject differences. For a single measurement of endometrial volume, the Intra CC was 0.90 and Inter CC was 0.82. These results clearly demonstrate that 3D ultrasound volume measurements are highly reliable, with a small measurement error. However, one could expect higher interobserver differences in accurate delineation of the internal os and endometrial margins, which may explain the greater interobserver variability for endometrial volume than for ovarian volume. Since it is applied in the same manner as 2D vaginal ultrasound it does not cause additional discomfort.

Child et al[13] performed a prospective study that evaluated the usefulness of 3D ultrasound measurement of endometrial volume and thickness as a predictor of pituitary suppression and non-suppression following GnRH agonist administration for IVF. A total of 144 women undergoing 164 IVF cycles had transvaginal ultrasound measurement of the endometrial volume and thickness following 8–14 days of the buserelin acetate administration. Serum estradiol concentrations were measured on the same day. Receiver operating characteristic (ROC) curve analysis was used for statistics. A ROC curve was produced for each of four estradiol (E_2) thresholds commonly used by clinics to diagnose pituitary suppression (100, 150, 200, 250 pmol/l). From each curve, endometrial volume and thickness thresholds that best predicted pituitary suppression and, separately, non-

suppression were selected and the associated sensitivity, specificity, positive and negative predictive values were reported. The area under the curve (AUC) was consistently higher (better test) for 3D volume than thickness estimation for all four estradiol thresholds, although it was only significantly different when a threshold of 200 pmol/l was used. The AUC increased towards 1.0 (perfect test) for both volume and thickness measurement as the selected estradiol threshold increased. Their data suggested that different endometrial thickness or volume thresholds should be selected, depending on whether one wishes to screen for suppression or non-suppression.[13] For example, if suppression is considered as an estradiol concentration <150 pmol/l, then an endometrial thickness of <5.9 mm will identify (sensitivity) 91.7% of suppressed patients. However, only 41.9% of non-suppressed women will have an endometrial thickness of >5.9 mm and be identified as having failed pituitary suppression. For the same estradiol threshold of 150 pmol/l, an endometrial thickness of 3.7 mm will identify 80.6% of non-suppressed patients. If a higher sensitivity is preferred (higher likelihood of identifying non-suppressed women), then the endometrial threshold thickness may be reduced further. However, the positive predictive value will also reduce, meaning that more patients with an endometrium thicker than the threshold are in fact suppressed and will undergo a needless blood test. They concluded that 3D endometrial volume estimation provides a new tool, alongside endometrial thickness measurement, to diagnose pituitary suppression and non-suppression in patients undergoing IVF. Different endometrial thresholds must be selected depending upon whether the priority is to identify pituitary suppressed, or arguably more importantly, non-suppressed cycles.

It is expected that 3D endometrial volumetry studies will increase diagnostic potential and give additional information to 2D ultrasound. Furthermore, quantification of endometrial volume by 3D ultrasound in combination with blood flow studies may be the best way to predict pregnancy rates.

Kupesic et al[14] investigated the usefulness of transvaginal color Doppler and 3D power Doppler ultrasonography for the assessment of endometrial receptivity in patients undergoing *in vitro* fertilization procedures. The patients were evaluated for endometrial thickness and volume, endometrial morphology and subendometrial perfusion on the day of embryo transfer. Neither the volume nor the thickness of the endometrium on the day of embryo transfer had a predictive value for conception during IVF cycles. Patients who became pregnant were characterized by a significantly lower resistance index (RI=0.53+/−0.04 versus 0.64+/−0.04), obtained from subendometrial vessels by transvaginal color Doppler ultrasonography and a significantly higher flow index (FI=13.2+/−2.2 versus 11.9+/−2.4), as measured by a 3D power Doppler histogram. No difference was found in the predictive value of scoring systems analyzing endometrial thickness and volume, endometrial morphology and subendometrial perfusion by color Doppler and 3D power Doppler ultrasonography. High degree of endometrial perfusion shown by both techniques on the day of embryo transfer can indicate a more favorable endometrial milieu for successful *in vitro* fertilization.

UTERINE PERFUSION IN INFERTILE PATIENTS

Transvaginal color and pulsed Doppler sonography has been established as an additional tool in the management of infertile patients (Fig. 50.4). In anovulatory cycles, a continuous increase of the uterine artery RI has been detected (Fig. 50.5, Graph 50.1).[15,16] Moreover, in some infertile patients, an end-diastolic flow is absent.[17] The results of some research indicate that absent diastolic flow might be associated with infertility and poor reproductive performance.

Therefore, the uterine artery blood flow could be potentially used to predict a hostile uterine environment prior to embryo transfer. Steer and co-workers[18] calculated the probability of pregnancy by using pulsatility index (PI) values obtained from the uterine artery on the day of

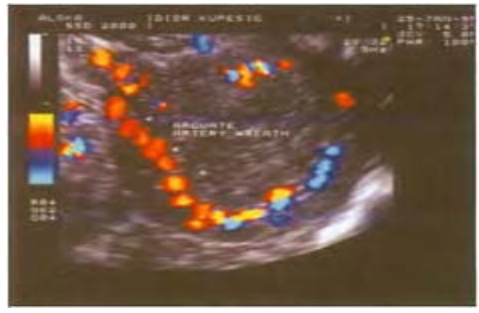

Figure 50.4: Transvaginal color Doppler scan of the uterus demonstrating an arcuate artery network encircling the uterus

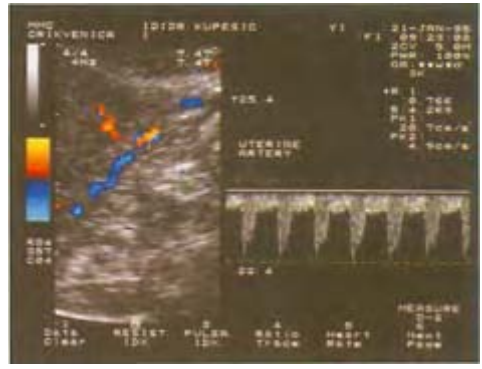

Figure 50.5: Uterine artery demonstrated laterally to the cervix at

the level of the cervicocorporeal junction (left). The blood flow velocity form the uterine artery in the secretory phase is characterized by increased end-diastolic velocity and decreased resistance index (RI=0.76)

Graph 50.1: Changes in the uterine artery blood flow in ovulatory and anovulatory cycles (From reference 15, with permission)

embryo transfer. With the use of these measurements, the highest probability of becoming pregnant was obtained in those patients with the medium values of PI for uterine arteries. A mean PI of more than 3.0 before the transfer can predict up to 35% of pregnancy failures (Fig. 50.6). Tsai and colleagues[19] evaluated the prognostic value of uterine perfusion on the day of hCG administration in patients who were undergoing intrauterine insemination. They calculated pulsatility index of the ascending branch of the uterine

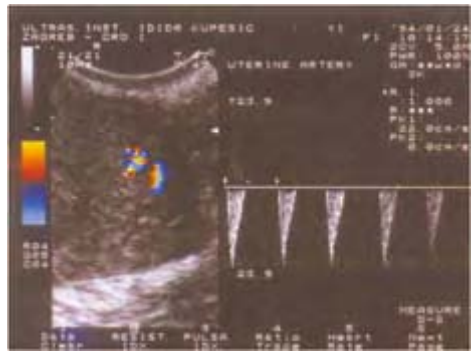

Figure 50.6: Absent diastolic flow of the uterine artery may be associated with infertility or poor reproductive performance

arteries on the day of administration of hCG, and compared the uterine artery vascular resistance to the outcome of intrauterine insemination. No pregnancy occurred when the PI of the ascending branch of the uterine arteries was more than 3. The fecundity rate was 18% when the pulsatility was less than 2 and was 19.8% when the pulsatility index was between 2 and 3. Their data suggest that the measurement of uterine perfusion on the day of hCG administration may have predictive value regarding fecundity in patients undergoing intrauterine insemination.

In infertile women uterine artery Pis measured in midluteal phase of the unstimulated cycles correlate inversely with endometrial thickness[20] suggesting a direct effect of uterine perfusion on endometrial growth (Table 50.1).[21] Furthermore, PI correlates directly with the age of the patients,[17] suggesting a detrimental effect of age on uterine perfusion. Cacciatore et al[22] did not find any correlation between uterine artery PI measured at the time of ET and endometrial thickness or the age of the patients. These findings could be explained also by the hormonal environment of the superovulated cycles, where the high E_2 levels achieved in almost all subjects are likely to reduce differences between individuals. A high prevalence

Table 50.1. Thickness of the endometrium and uterine perfusion in relation to serum estradiol levels in the proliferative phase of the cycle

Day of the cycle	*n*	*Thickness of the endometrium (mm)*	*Estradiol level (pmol/l)*	*Uterine artery RI*
1–5	25	4 (2–6)	140 (50–200)	0.89±0.04

6–7	12	5 (3–6)	170 (110–290)	0.88±0.06
8	10	7 (5–9)	250 (150–360)	0.90±0.04
9	14	9(5–11)	290 (210–450)	0.88±0.06
11	18	9.5 (7–12)	390 (270–650)	0.88±0.04
12	16	10 (7–13)	620 (250–1130)	0.87±0.04
13	22	11 (8–15)	870 (450–1500)	0.86±0.04
14	24	12 (10–16)	960 (350–1800)	0.85±0.04

Modified from reference 21, with permission

of increased uterine artery impedance among infertile patients with the diagnosis of endometriosis has been reported by Steer and co-workers.[20] In the present study women with a history of endometriosis have significantly higher PI and RI values than the others even after hormonal stimulation. These evidences, although gained in different settings, seem to suggest an adverse effect of endometriosis on the uterine perfusion. That could be another way endometriosis compromises a woman fertility potential. Whether this is due to mechanical effects on the pelvic vessels as a result of adhesions or is mediated by production of agents with vasoactive properties remains to be explained.

Cheung et al[23] evaluated still controversial problem whether the day of clomiphene citrate initiation has any impact on the pregnancy rate. This study aimed to compare the perifollicular vascularity and endometrial receptivity of ovulatory women who started clomiphene citrate on day 2 and day 5. They included in the study thirty-five women with regular ovulatory cycles. The patients were first monitored in a natural cycle and then randomized by computer-generated random numbers to receive 50 mg clomiphene citrate on days 2–6 or on days 5–9. The hormonal profile, the number of dominant follicles, the grading of perifollicular vascularity, endometrial thickness and Doppler flow indices of uterine/ subendometrial arteries were compared between both groups. All the above parameters were similar for both groups on the day of the LH surge and 7 days after the LH surge. Data in this study showed no differences in oocyte quality graded by the perifollicular vascularity and the endometrial receptivity assessed by endometrial thickness and Doppler flow indices of uterine and subendometrial vessels when clomiphene citrate was started in regularly ovulatory women on day 2 or on day 5.

Dada et al[24] performed a prospective longitudinal color Doppler study on utero-ovarian blood flow characteristics of pituitary desensitization. A total of 75 patients were recruited; 32 had IVF treatment, 20 frozen-thawed embryo transfer cycles and 23 patients were recipients of donated oocytes. All received early follicular-phase down-regulation and had color flow Doppler velocimetry of the utero-ovarian arteries three days before the start of menses and after 21 days of gonadotropin-releasing hormone (GnRH) analogue treatment. Ovarian volume, endometrial thickness, pituitary and ovarian hormone concentrations were recorded at each scan. The data showed that significant changes ($P<0.05$) were noted in these parameters and utero-ovarian vasculature during the down-regulation period, with good correlation between RI and E_2 estradiol estimations. Neither the type of GnRH analogue nor age influenced the changes in utero-ovarian blood flow. According to the data ovarian artery RI was the best Doppler predictor for pituitary suppression and a mean discriminatory cut-off value of

0.867±0.025 was found to have the highest specificity and positive predictive value. This study has defined cut-off values for satisfactory pituitary suppression with high positive predictive value and specificity in an early follicular phase of the long protocol of GnRH analogue down-regulation using color flow Doppler.

Recent clinically-controlled study from Pellizzari et al[25] was designed to investigate uterine and ovarian blood flow in patients with hypoestrogenic amenorrhea. Twelve women with hypoestrogenic amenorrhea and 13 eumenorrheic subjects (controls) were enrolled. Color and pulsed Doppler was used to visualize the uterine and ovarian arteries and blood vessels within the ovarian stroma in both groups. Four blood flow indices were calculated: the PI, the RI, the peak systolic velocity and the end-diastolic velocity. Peak systolic velocity underwent the most significant change in amenorrheicpatients, being significantly lower in comparison with that of controls, both in the uterine (P=0.0009) and ovarian (P= 0.001) arteries. Compared with controls, the end-diastolic velocity of the ovarian artery was significantly lower (P=0.039) in amenorrheic patients, and was also lower in the uterine artery (though not statistically significantly so). A reduction in blood flow was also evident in the ovarian stroma of the amenorrheic patients. Therefore, the authors concluded that the significant reduction in blood flow observed in hypoestrogenic amenorrhea suggested that estrogens play an important role in regulating both uterine and ovarian blood flow.

MULLERIAN ANOMALIES

Congenital uterine malformations are variable in frequency and are usually estimated to represent 3–4%, although less than half have clinical symptoms.[26–28] They are a result of defects in paired Mullerian duct development, fusion, or resorption and may be associated with renal anomalies. Any woman with an absent kidney or other renal contour abnormality should be carefully scanned for an uterine anomaly.

The respective frequency of symptomatic malformations is dominated by septate uterus.[28,29] During the first trimester of pregnancy, the risk of spontaneous abortion in this group is between 28% and 45%, while during the second trimester the frequency of late spontaneous abortions is approximately 5%.[28] Premature deliveries, abnormal fetal presentations, irregular uterine activity and dystocia at delivery are likely to prevail in cases of septate uterus.[30] Poor vascularization of the septum was proposed as a potential cause of miscarriages.[29] Electron microscopy study of Fedele et al[31] indicated a decrease in the sensitivity of the endometrium covering the septa of malformed uteri to preovulatory changes. This could play a role in the pathogenesis of primary infertility in patients with septate uterus.

It is clear that unfavorable obstetric prognosis can be transformed by surgical correction of the intrauterine septum. Hysteroscopic treatment was currently proposed as the procedure of choice for the management of these disorders. This simple and effective treatment has an obvious advantage that uterus is not weakened by a myometrial scar. Cararach et al[32] and Goldenberg et al[33] reported 75% and 88.7% pregnancy rates in patients after operative hysteroscopy was performed because of the septate uterus.

Clearly, simplicity and effectiveness of the hysteroscopy have faced the clinician with the need of an early and correct diagnosis of the uterine anomalies. When used as a screening test for detection of congenital uterine anomalies transvaginal ultrasound had a

sensitivity of almost 100%.[34,35] However, clear distinction between different types of abnormalities was impossible and operator dependent.[36,37]

X-ray hysterosalpingography (X-ray HSG) is an invasive test, which requires the use of contrast medium and exposure to radiation. Although HSG provides a good outline of the uterine cavity, the visualization of minor anomalies and clear distinction between different types of lateral fusion disorders is sometimes impossible. Fifteen years ago hysterosonography has been introduced.[38] This method implies transvaginal ultrasound after distension of the uterine cavity by instillation of a saline solution. This simple and minimally invasive approach allows anatomical images of the endometrium and myometrium, accurate depiction of the septate uterus and even the measurement of the thickness and height of the septum.[39]

Although some reports have indicated a high diagnostic accuracy of magnetic resonance imaging[40,41] in the diagnosis of congenital uterine anomalies, this technique is rarely routinely used for this indication. More recently, 3D ultrasound showed high diagnostic accuracy in detection of the septate uterus[42] suggesting that invasive procedures such as CO_2 diagnostic hysteroscopy are not needed in patients scheduled for corrective surgery.[43]

Kupesic and Kurjak attempted to evaluate the combined use of transvaginal ultrasound, transvaginal color and pulsed Doppler sonography, hysterosonography and 3D ultrasound in the preoperative diagnosis of septate uterus.[44]

A total of 420 infertile patients undergoing operative hysteroscopy were included in this study. With the use of B-mode transvaginal sonography, the morphology of the uterus was carefully explored with emphasis to the endometrial lining in both sagittal and transverse sections. The septum was visualized as an echogenic portion separating the uterine cavity into two parts (Fig. 50.7). Once experienced sonographer completed B-mode examination, another skilled operator who was unaware of the previous finding performed transvaginal color Doppler examination.

Color and pulsed Doppler was superimposed to visualize intraseptal and myometrial vascularity (Fig. 50.8). Flow velocity waveforms were obtained from all the interrogated vessels. For each recording, at least five waveform signals of good quality were obtained (Fig. 50.9). During each procedure the RI was automatically

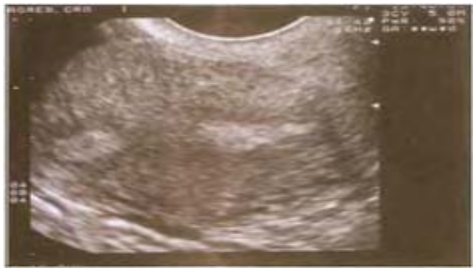

Figure 50.7: Transvaginal scan demonstrating a septate uterus. Note the two separate endometrial

echoes divided by a thick septum

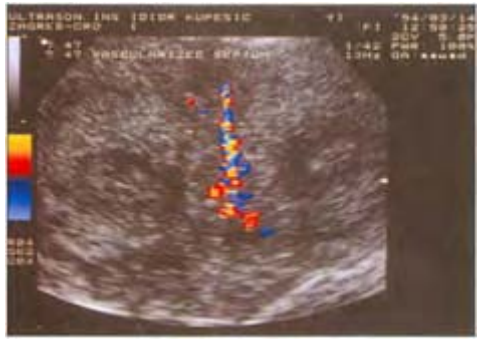

Figure 50.8: Septate uterus demonstrated by color Doppler imaging. Vascularity within the septal area is easily observed by this technique

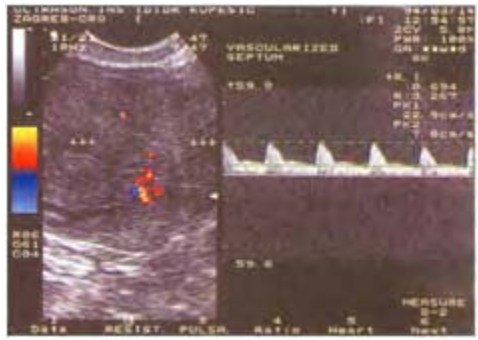

Figure 50.9: Pulsed Doppler waveform analysis (right) reveals moderate to high vascular resistance (RI=0.69) of the vessels involved in the septum

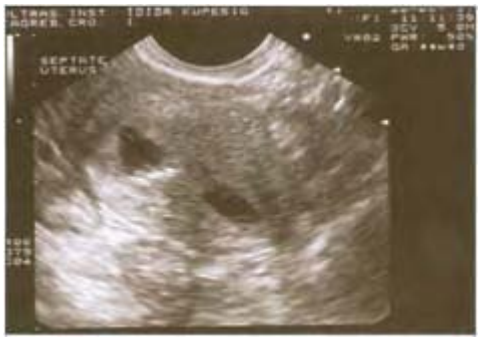

Figure 50.10: Septate uterus at hysterosonography. Note the two separate endometrial echoes divided by a thick septum

calculated from the maximum frequency envelope and was: peak systolic velocity minus end-diastolic velocity divided by peak systolic velocity. Instillation of isotonic saline (hysterosonography) was carried out on a gynecological examination table. Transverse and sagittal sections were carefully explored, and septum was visualized as an echogenic portion separating the uterine cavity into two parts (Fig. 50.10).

Eighty-six women undergoing hysteroscopy were examined by 3D ultrasound. When the patients were evaluated on 3D ultrasound, three perpendicular planes of the uterus were simultaneously displayed on the screen, allowing a detailed analysis of the uterine morphology (Fig. 50.3). Frontal reformatted sections were particularly useful for detection of the uterine abnormalities (Figs 50.11 and 50.12).

Table 50.2 summarizes the sensitivity, specificity, positive and negative predictive values of transvaginal sonography, transvaginal color and pulsed Doppler ultrasound, hysterosalpingography and 3D ultrasound for the diagnosis of the septate uterus. The sensitivity of transvaginal sonography in the diagnosis of septate uteri was 95.21%. Transvaginal color and pulsed Doppler enabled the diagnosis of septate uterus in 276 cases, reaching the sensitivity of 99.29%. In one patient with endometrial polyp and one with intrauterine

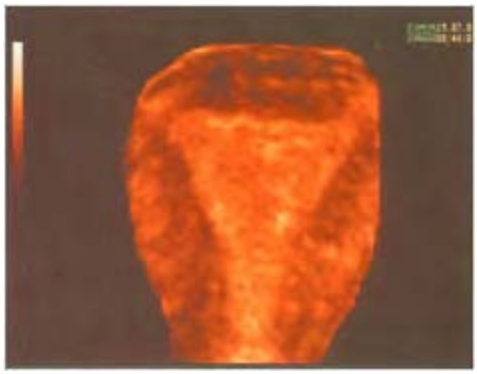

Figure 50.11: Planar section through a normal uterus, showing the convex shape of the uterine fundus and the straight upper border of the uterine cavity

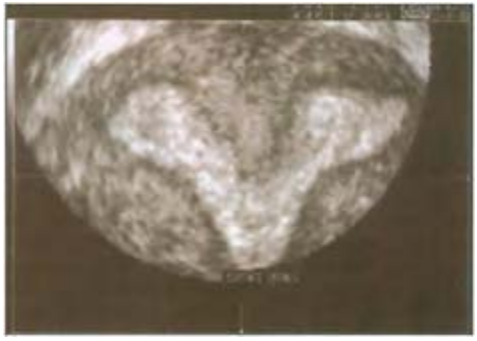

Figure 50.12: A case of a septate uterus. Note the thick septum that extends to the upper half of the uterine cavity

synechiae, septate uteri were not correctly diagnosed. Therefore, the reliability of color and pulsed Doppler examination was reduced if other intracavitary structures (such as endometrial polyp or submucous leiomyoma) were present.

Color and pulsed Doppler studies of the septal area revealed vascularity in 198 (71.22%) patients. The RI values obtained from the septum ranged from 0.68 to 1.0 (mean RI=0.84±0.16). Hysterosonography reached 100% specificity and positive

predictive value. In one patient with extensive intrauterine synechiae, hysterosonography did not detect an intrauterine septum.

Table 50.2. Sensitivity, specificity, positive (PPV) and negative predictive (NPV) values of various imaging modalities for the diagnosis of septate uterus in 420 patients with history of infertility and recurrent abortions

Imaging modality	*Sensitivity (%)*	*Specificity (%)*	*PPV (%)*	*NPV (%)*
Transvaginal sonography	95.21	92.21	95.86	91.03
Transvaginal color Doppler	99.29	97.93	98.03	98.61
Hysterosonography	98.18	100.00	100.00	95.45
Three dimensional ultrasound	98.38	100.00	100.00	96.00
From reference 44, with permission				

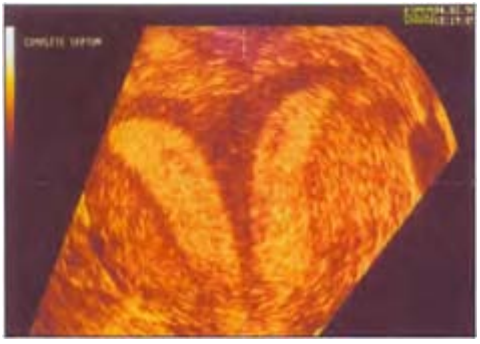

Figure 50.13: Frontal reformatted section of the septate uterus. Note the complete division of the uterine cavity and the concave shape of the uterine muscle. Since the fundal cleft is less than 1 cm this uterine anomaly is defined as a septate uterus. This was confirmed by a

hysterolaparoscopic procedure

The sensitivity and specificity of 3D ultrasonography were 98.38% and 100%, respectively. A false-negative result in one patient was caused by a fundal fibroid distorting the uterine cavity. Interestingly, in our study septate uterus was not mistaken for a bicornuate uterus (Fig. 50.13). However, in one patient with bicornuate uterus transvaginal ultrasonography misinterpreted septate uterus. One hundred eighty eight patients underwent X-ray HSG within 12 months prior to our examination. The sensitivity of X-ray HSG in the diagnosis of septate uteri was only 26.06%.

Fedele et al[31] recently indicated that intrauterine septum may be a cause of primary infertility. The ultrastructural morphological alterations of the septal area were indicative of irregular differentiation and estrogenic maturation of septal endometrial mucosa. Since the hormonal levels of the patients enrolled in this study were normal for the cycle phase, the most convincing hypothesis was that endometrial mucosa covering the septum was poorly responsive to estrogens probably due to scanty vascularization of the septal connective tissue.

Dabirashrafi et al[45] performed histologic study of the uterine septa from 16 patients undergoing abdominal metroplasty. Statistical analysis confirmed less connective tissue in the septum compared to the amount of muscle tissue, amount of muscle interlacing and vessels with a muscle wall, which was contradictory to the classic view about the histologic features of the uterine septum. Less connective tissue in the septum can be the reason for poor decidualization and placentation in the area of implantation.[35] Increased amounts of muscle tissue and muscle interlacing in the septum can cause an abortion by the higher and uncoordinated contractility of these muscles.

Recent study from our Department[44] found no correlation between septal height and thickness and occurrence of obstetrical complications ($p>0.05$). Pregnancy loss correlated significantly with septal vascularity. Patients with vascularized septa had significantly higher incidence of early pregnancy failure and late pregnancy complications than those with avascularized septa ($p<0.05$).

Three-dimensional ultrasound enables planar reformatted sections through the uterus which allow precise evaluation of the fundal indentation and the length of the septum (Fig. 50.12). Based on our experience, this technique may give a wrong impression of an arcuate uterus in patients with fundal location of the leiomyoma. In these cases uterine cavity has a concave shape, while fundal indentation is shallower. Furthermore, shadowing caused by the uterine fibroids, irregular endometrial lining and decreased volume of the uterine cavity (in cases of intrauterine adhesions) are obvious limitations of 3D ultrasound. More recently 3D power Doppler was used to detect vascularization of the uterine septa in a combined angio and gray rendering mode. This approach allows simultaneous analysis of the septal morphology, texture and vascularization.

Balen et al[46] described a technique of 3D reconstruction of the uterine cavity using a positive contrast medium (Echovist). The main problem that was encountered with Echovist was an acoustic shadowing artefact owing to its highly reflective properties. Despite this, Echovist proved to be superior to saline as an intrauterine contrast agent for 3D reconstruction while testing 10 patients with both methods.

Weinraub et al[47] applied 3D saline contrast hysterosonography to 32 volunteers 22–65 years of age, all in good health and with no evidence of active pelvic inflammatory disease.

It seems that contrast 3D hysterosonography offers a more comprehensive overview of the uterine cavity and surrounding myometrium, and gives access to planes unobtainable by conventional 2D ultrasound examination. Further research is required to document whether contrast instillation contributes to better diagnosis of uterine cavity pathology when compared to unenhanced frontal reformatted section.

Kupesic et al[48] studied the incidence of surgically correctable uterine abnormalities (congenital uterine anomalies, submucous leiomyoma, endometrial polyps and intrauterine synechiae) in the infertile population attending tertiary infertility clinic. All of the infertile patients enrolled in the study were evaluated by 3D ultrasound. Another objective was to assess pregnancy rates before and after operative hysteroscopy in patients affected by uterine causes of infertility. The authors found that the incidence of the uterine septum in general infertile population was 17.9%. Uterine septum was the most common uterine abnormality accounting for 77.1% of the intrauterine lesions. Out of 310 patients that were followed-up, 225 (72.6%) patients achieved pregnancy after hysteroscopic metroplasty for an intrauterine septum.

ENDOMETRIAL POLYP

Endometrial polyp is the anatomic defect that is implicated in the etiology of a recurrent pregnancy loss and infertility. Polyps appear as diffuse or focal thickening of the endometrium. Using hysterosonography an intracavitary polyp is seen surrounded by anechoic fluid, with the point of the attachment (Fig. 50.14). If the examination is performed in the follicular phase, use of the distending medium is not necessary to detect abnormal endometrial thickening. However, during the periovulatory and secretory phases, polyps are better visualized when outlined by fluid. By using transvaginal color and pulsed Doppler we can study minor arteries supplying the growth of the endometrial polyp. Three-dimensional ultrasound allows a detailed analysis of the uterine

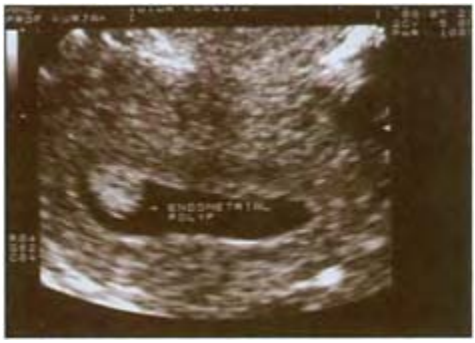

Figure 50.14:
Hysterosonography
outlines an intracavitary

polyp, which is seen as focal endometrial thickening

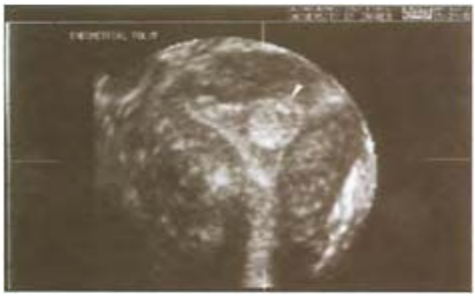

Figure 50.15: Frontal section through the uterus in a patient with an endometrial polyp in the left uterine horn

cavity in frontal reformatted sections, which enables clear demarcation of the polyps (Fig. 50.15).

SUBMUCOUS LEIOMYOMAS

Leiomyomas are benign growths of smooth muscle arising from the uterine wall. They are common in both fertile and infertile women, and their significance depends on their size and location. Large intracavitary myomas, which distort the shape of the uterine cavity and interfere with the endometrium are usually removed hysteroscopically (Fig. 50.16). Large intramural, noncavitary masses enlarge and distort the shape of the uterus

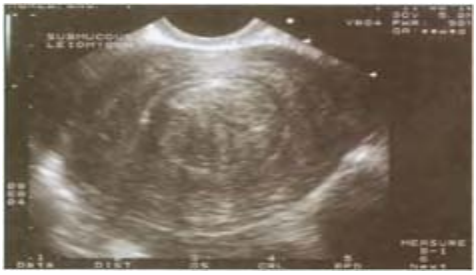

Figure 50.16: Transvaginal image of a submucous leiomyoma.

Note distortion of the uterine cavity since this leiomyoma interferes with the endometrium

and may interfere with uterine blood supply. These masses are usually removed by transabdominal or laparoscoplc myomectomy in women experiencing infertility. An intramural myoma, which is more subserosal and does not affect the cavity, might be left untreated. The diagnosis of a submucous leiomyoma is based on distortion of the uterine contour, uterine enlargement and textural changes. Since leiomyomas have a varying amount of smooth muscle and connective tissue, these benign tumors also have a variety of sonographic features. Sonographic texture ranges from hypoechoic to echogenic, depending on the amount of smooth muscle and connective tissue. Central ischemia, which is a consequence of tumor enlargement and inadequate blood supply, is usually followed by various stages of degeneration. The most common cause of calcification within the uterus is calcific degeneration within a leiomyoma. Other types of degeneration include cystic, myxomatous, and hyaline degeneration. Sometimes, because of the variety of appearances, submucous leiomyomas may be mistaken for endometrial polyps, endometrial carcinoma, blood or mucus. Patients with submucous leiomyomas have the uterine environment not conducive to nidation of a fertilized ovum and blood supply might be inadequate. Leiomyoma grows centripetally as proliferations of smooth muscle cells and fibrous connective tissue, creating pseudocapsule of compressed muscle fibers. Therefore, color Doppler demonstrates most of the myometrial blood vessels at its periphery (Fig. 50.17). Presence of blood vessels in the central portion of the leiomyomas is usually correlated with necrotic, degenerative and inflammatory changes. These vessels display lower RI values than peripherally located vessels, and sometimes can be misinterpreted for malignant neovascular pulsed Doppler signal.[49] Vascular impedance to blood flow in myometrial supplying vessels depends not only on size but location within the uterus. A significant difference was shown in blood flow characteristics for leiomyoma supplying vessels between entirely subserosal versus intramural

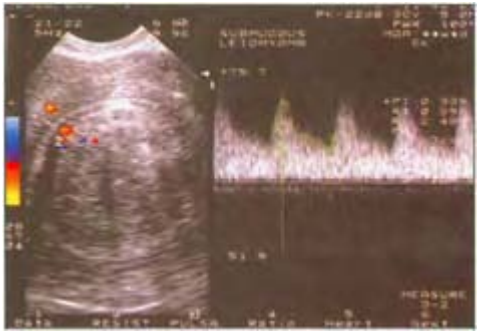

Figure 50.17: Color Doppler scan of the same patient as in Figure 50.16.

Peripheral leiomyoma vessels demonstrate moderate-to-high vascular resistance (RI=0.60)

and submucous leiomyomas. Lower impedance value for subserosal leiomyomas can be explained by the fact that these leiomyomas are supplied with blood vessels through a very small contact area. These blood vessels are surrounded with loose connective tissue and therefore dilated with very low vascular impedance to blood flow. In contrast, submucous leiomyomas and those located within the myometrium are supplied by blood vessels with higher vascular impedance. High basal tonus of myometrial tissue surrounding intramural or submucous leiomyomas could cause a difference in hemodynamic parameters. Three-dimensional ultrasound precisely estimates the relationship between submucous leiomyoma and the uterine cavity.

Kurjak et al[49] performed transvaginal color flow evaluation in 101 patients with palpable uterine fibroids and 60 healthy volunteers. The mean RI from the periphery of leiomyoma covered the value of 0.54, while mean PI value was 0.89. The pathohistological finding was a benign uterine tumor in all the cases, even when RI was very low. Lowered vascular resistance was present in cases with necrosis and secondary degenerative and inflammatory changes within the fibroid. Increased blood flow velocity and decreased RI (mean RI=0.74) in both uterine arteries occurred in patients with uterine leiomyomas.

There are several mechanisms by which leiomyomas may impair the normal reproductive function. It can be mechanical, by occlusion of the Fallopian tube and the cervix. Coutinho and Maia[50] have hypothesized that large leiomyomas may impair the rhythmic uterine contractions that facilitate sperm motility through the uterus. A large submucous leiomyoma may cause a mass effect within the uterine cavity that may impair the progression of pregnancy, cause premature rupture of the membranes, or cause preterm labor, both resulting in reduction of the uterine compliance. Exacoustos and Rosati[51] found a statistically significant increased incidence of threatened abortion, premature rupture of the membranes, abruptio placentae and pelvic pain was observed in patients with uterine leiomyomas ($p<0.001$). Abruptio placentae were particularly evident in women with leiomyoma volumes greater than 200 cm^3 of submucous location of superimposition of the placenta.[51]

Submucous leiomyoma may also influence the implantation of the embryo. Deligdish and Loewenthal[52] performed a histological study of the endometrium in women with a submucous leiomyoma. These investigators found that both the endometrium overlying a submucous leiomyoma and the endometrium opposite the leiomyoma was atrophic, possibly resulting from the hyperplastic, possibly due to increased vascularity, otherwise, at sites distant from the leiomyoma the biopsy results were normal.

Other investigators have documented venous dilatation in the endometrium overlying and adjacent to leiomyomas,[53] which was hypothesized to the result of vascular obstruction produced by one or more leiomyomas. Whereas reduced vascular flow may cause reduced hormone delivery and endometrium atrophy, changes in vascular flow may also alter delivery of cytokines and other serum factors that are involved in implantation

and normal immune response to the implanting fetus, reducing implantation and increasing pregnancy loss.

ADENOMYOSIS

Adenomyosis, characterized by ingrowing of the endometrium into the myometrium is usually asymptomatic, but may be presented by uterine bleeding, pain and infertility. A diffusely enlarged uterus without discrete fibroids, an intact endometrium and multiple small cysts in the myometrium have been reported as a suggestive appearance of adenomyosis.[54] Disordered echogenicity of the middle layer of the myometrium is present in some severe cases. Reported sensitivity and specificity of transvaginal ultrasound in detection of this benign entity is 86% and 50%, respectively.[54] Color Doppler may reveal increased vascularity mainly characterized with moderate vascular resistance.

ENDOMETRITIS

Chronic endometritis is characterized with increased echogenicity, thickness and vascularity of the endometrium. The most common cause of chronic endometrial infection is *Mycobacterium tuberculosis*. During the activation of the infection, pregnancy often terminates ectopically or as an abortion. Transvaginal sonographic findings may include calcified pelvic lymph nodes or smaller irregular calcifications in the adnexa, and deformity of the endometrial cavity suggestive of adhesions in the absence of a history of prior curettage or abortion. In the acute stage of the endometritis low to moderate impedance blood flow signals are easily obtained at the periphery of the endometrium. On the contrary, blood flow is usually absent in cases with irreversible tissue damage. Transvaginal sonography allows elucidation of the abnormal endometrial morphology, after which appropriate cultures should be taken and broad spectrum antibiotic therapy administered. In order to prevent the development of intrauterine adhesions (especially after D&C) administration of conjugated estrogen for one to two months is recommended. This therapy allows regeneration of the healthy endometrium, which is paralleled by sharp increase in end-diastolic velocities of the spiral arteries at the time of color flow and pulsed Doppler analysis.

ASHERMAN'S SYNDROME

Destruction of the endometrium may result in scarring and the development of bands of scar tissue, or synechiae within the uterine cavity. This destruction may occur as a result of a vigorous curettage of the uterus following an abortion or, more often, after curettage of an advanced pregnancy. Tuberculosis may also cause intrauterine synechiae, but only in rare cases. This may result in formation of the adhesive bands of different size with a subsequent partial or total obliteration of the endometrial cavity. Amenorrhea or hypomenorrhea characterizes menstrual pattern.

Patients with endometrial adhesions, such as Asherman's syndrome, may have a distorted endometrial pattern with areas where no endometrium can be imaged or mixed,

with areas that appear normal. Adhesions are observed as endometrial irregularities or hyperechoic bridges within the endometrial cavity.

Schlaff and Hurst[55] analyzed seven amenorrheic patients with severe Asherman's syndrome. Transvaginal sonography demonstrated a well-developed endometrial stripe in three of seven women, while three others had virtually no endometrium seen. All the patients with well-developed endometrium were found to have adhesions excluding the lower uterine segment and had resumption of normal menses and normalization of the cavity after hysteroscopy. The women with minimal endometrium had no cavity identified and derived no benefit from hysteroscopic surgery. The conclusion of that study was that endometrial pattern on transvaginal sonography is highly predictive of both surgical and clinical outcome in patients with severe Asherman's syndrome characterized by complete obstruction of the cavity at hysterosalpingogram. Intrauterine synechiae do not present increased vascularity on color Doppler examination. Three-dimensional ultrasound demonstrates a significant reduction of the endometrial cavity volume in all

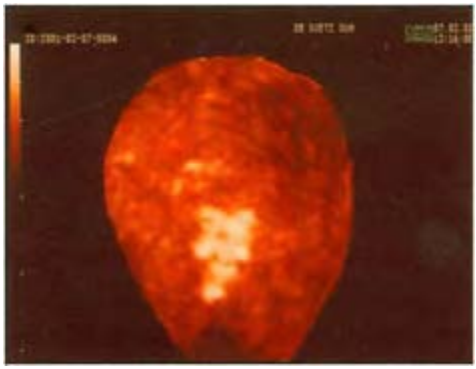

Figure 50.18: Irregular shape of the uterine cavity in a patient with severe intrauterine synechiae. Note the reduced endometrial volume in a coronal plane

reformatted sections (Fig. 50.18). They are better visualized during menstruation when intracavitary fluid outlines them or following the hysterosonography.

OVULATORY FACTORS OF INFERTILITY

Normal ovulation at midcycle is heralded by a slight rise in the basal body temperature, as well as a surge of luteinizing hormone (LH) in the urine. In some women, the results of tests to check for these parameters are equivocal, and it may be helpful to track ovarian follicular growth. Normally, the ovaries contain several follicles less than 5

mm in diameter. During the follicular phase of the cycle, usually one follicle is "recruited" by an unknown mechanism to grow in response to follicular stimulating hormone (FSH), and this is accompanied by a rise in serum estradiol. The follicle usually grows approximately 2 mm a day until midcycle, at which point it ruptures at an average diameter of 20 mm. After ovulation, the dominant cyst may get slightly larger, may get smaller, or may fill in with echoes. A small amount of fluid is often visible in the pelvis.

Transvaginal sonography is considered the most reliable method for monitoring the follicular growth. It enables accurate prediction of ovulation and detection of the ovulation abnormalities.

The success of IVF treatment is dependent on the ability of the ovary to respond to controlled stimulation by gonadotropins and to develop a reasonable number of mature follicles and oocytes simultaneously. Failure to respond is associated with cancellation of the cycle or poor outcome of the treatment. Prior prediction of the likelihood of optimal ovarian response is therefore essential in identifying patients who are most likely to benefit from IVF treatment.

Zaidi et al[56] were the first to show that there was a relation between ovarian stromal blood flow velocity and ovarian follicular response. They measured the ovarian stromal PSV in the early follicular phase and showed that poor responders had low ovarian blood flow PSV. Increased ovarian stromal blood flow velocity was detected in polycystic ovaries, in combination with relatively unchanged impedance to blood flow. This may reflect increased intraovarian perfusion and thus a greater delivery of gonadotropins to the granulosa-thecal cell complex resulting in production of the greater number of follicles. This mechanism may help to explain why patients with polycystic ovaries tend to respond excessively to the administration of gonadotropins,[54] and may possibly explain their increased risk of ovarian hyperstimulation syndrome.

Documentation of ovarian stromal vascularity at the initial baseline scan may be important and may provide useful information for assisted reproduction techniques. Furthermore, it seems that measurement of ovarian stromal blood flow in the early follicular phase is related to subsequent ovarian responsiveness in IVF treatment.[56] This is particularly useful since the ability to predict ovarian response to stimulation by exogenous gonadotropins is still central to success in any IVF program. Most units determine the dose of gonadotropins used for the first attempt based on the chronological age of the patient, with adjustments being made in subsequent attempts depending on their initial response. Unfortunately the ovarian age (capacity of the ovary to produce fertilizable oocytes) and chronological age are not always synchronous, leading to a degree of unpredictability of the number of developing follicles and collected oocytes. Certainly, if an inadequate dose of gonadotropins is used then there may be a relatively poor response, which reduces the number of oocytes retrieved, whereas if an excessive dose is used, there may be an increased risk of ovarian hyperstimulation syndrome.

Engmann et al[57] speculated that the ovarian stromal blood flow velocity after 2–3 weeks of pituitary suppression is a true representative of baseline ovarian blood flow because the ovaries are in a quiescent state. The primordial follicles in the ovary have no independent capillary network, lying simply among vessels of the stroma, and therefore depend on their proximity to the stromal vessels for the delivery of nutrients and hormones. The subsequent growth of primary follicles leads to the acquisition of a vascular sheath through the process of angiogenesis. The administration of a GnRH

agonist suppresses follicular activity and consequently the ovaries become inactive; ovarian stromal blood flow at this time might be at its lowest and may truly reflect the baseline ovarian blood flow.

Therefore, ovarian stromal blood flow velocity after pituitary suppression is predictive of ovarian responsiveness and the outcome of IVF treatment. One might speculate that by improving the ovarian stromal blood flow velocity, the delivery of gonadotropins to the follicles will be improved and as a result, the number and quality of mature oocytes produced and the implantation rate will improve.

The accuracy of diagnosis and monitoring of infertility treatments such as ovulation induction has increased greatly because of the availability of sophisticated ultrasound technology and equipment.[21] Accurate folliculometry is essential for safe and effective infertility treatment. In IVF-ET cycles, follicles with a mean follicular diameter of 12 to 24 mm are associated with optimal rates of oocyte recovery, fertilization, and cleavage.[58] This corresponds to follicular volumes of between 3 and 7 mL. In the hands of experienced operators, ultrasound alone suffices for cycle monitoring, with no necessity for additional hormonal estimations.[59–61]

The basic structural information provided by conventional scans in the longitudinal and transverse planes now can be augmented by new 3D ultrasound systems that provide an additional view of the coronal or C-plane, which is parallel to the transducer face.[21] The computer-generated scan is displayed in three perpendicular planes. Translation or rotation can be carried out in one plane, while maintaining the perpendicular orientation of all three, so that serial translation results in an ultrasound tomogram from which volumetric data can be captured.[62] Kyei-Mensah et al[21] evaluated the accuracy of 3D ultrasound measurement of follicular volume and compared it with current standard techniques. The volume of individual follicles was estimated by both methods and analyzed according to the volume of the follicular aspirates. The volume of follicular fluid aspirated was compared with the corresponding volume of the follicle measured by 3D ultrasound and with that of conventional 2D ultrasound volume measurement calculated using the formula $0.52\times(D_1\times D_2\times D_3)$. Limits of agreement and 95% confidence intervals were calculated and systematic bias between the methods was analyzed. The limits of agreement between the volume of follicular aspirate and follicular volume determined by ultrasound were +0.96 to −0.43 mL for 3D ultrasound measurements and +3.47 to −2.42 mL for 2D ultrasound measurements. The high accuracy of 3D measurement of follicular volume was clearly demonstrated in this study by the limits of agreement which are within 1 mL of the true volume. These limits encompass 95% of the volume measurements. On the other hand, the 2D ultrasound method produced limits of agreement that was up to 3.5 mL above or 2.5 mL below the true volume within the most important clinical range.

Therefore, the shape and number of the follicles influence the reliability of the standard 2D ultrasound technique of follicular volume measurement. There may be technical difficulty in measuring the diameters of a follicle when its shape is distorted because of compression by adjacent follicles. Penzias et al[63] showed that mean follicular diameter accurately predicted volume in round and polygonal follicles, but not in those that were ellipsoid. Rounded follicles were most prevalent in patients with few follicles. The patients selected for this study had produced fewer follicles than normal and represented the group in which the conventional technique was likely to be most accurate.

Kyei-Mensah et al[21] found that 3D ultrasound assessment of the follicular volume produced a more accurate reflection of the true volume. This is because the follicular shape does not affect 3D measurement since the changing contours are outlined serially to obtain the specific volume measurement. The disparity in accuracy between 3D ultrasound assessment of the follicular volume and the conventional approach is likely to increase significantly if there is a florid multifollicular ovarian response, because the conventional formula is less precise with ellipsoid follicles, which are likely to predominate in these cases. One limitation of 3D volume assessment is that follicles with a mean diameter of <10 mm cannot be assessed accurately because the limits of agreement are too wide in this range.

Feichtinger et al[64] found that 3D ultrasound may be useful for distinction of the ovarian cysts from the ovarian follicles. Since both the ovarian cysts and follicles demonstrate an elevation of the serum estradiol levels, it is difficult to distinguish between them by E2 assay alone. For the purpose of the prospective observational study the authors evaluated 50 IVF patients after ovulation induction. Three-dimensional ultrasound was used to search for the presence of cumuli in follicles greater than 15 mm. Only cumuli demonstrable in all three planes by multiplanar imaging predicted mature oocytes recovery. Follicles without visualization of the cumulus in all three planes were not likely to contain mature fertilizable oocytes.

Lass et al[65] tested the hypothesis that small ovaries measured on transvaginal sonography are associated with a poor response to ovulation induction by human menopausal gonadotropin (HMG) for IVF procedure. A total of 140 infertile patients with morphologically normal ovaries undergoing IVF were studied and represented. The mean ovarian volume of each patient was measured on transvaginal sonography before starting HMG. Subsequent routine IVF management was conducted without knowledge of the results of transvaginal sonography. The mean ovarian volume was 6.3 cm^3 (range 0.5–18.9, SD=3.1). Patients (n=17; group A) with small ovaries of $\leq$3 cm^3 represented group B. Both groups were of similar age (mean 35.8 versus 34.4 years). Early basal FSH concentrations were increased in group A (9.5 versus 7.0 mlU/ml, P=0.025). The cycle was abandoned before planned oocyte recovery in nine patients (52.8%) from group A and in 11 patients (8.9%) from group B because of poor response to ovulation induction.

Oyesanya et al[66] measured total ovarian volumes before the administration of HCG in 42 women undergoing treatment for infertility by *in vitro* fertilization and embryo transfer and considered to have an exaggerated response to stimulation (>20 follicles). Seven women who subsequently developed moderate or severe ovarian hyperstimulation syndrome (OHSS) (n=7; group 1) were compared with 35 matched controls (five matched controls per case; n=35; group 2) of similar age, number of follicles and duration of infertility who underwent follicular stimulation, oocyte recovery, IVF and embryo transfer during the same period, but did not develop moderate or severe OHSS (Fig. 50.19). The mean age, duration of infertility and total number of follicles were similar, but the mean total ovarian volume was significantly higher in the group of women who developed moderate or severe OHSS compared with controls (271.00± 87.00 versus 157.30±54.20 ml) (Fig. 50.20).

Kupesic and Kurjak[67] designed a study to evaluate whether ovarian antral follicle number, ovarian volume, stromal area and ovarian stromal blood flow are predictive of ovarian response and

Figure 50.19: Three-dimensional ultrasound scan of an ovary stimulated by human menopausal gonadotropin. Note two follicles and in one of them triangular structure presenting cumulus oophorus is clearly visualized

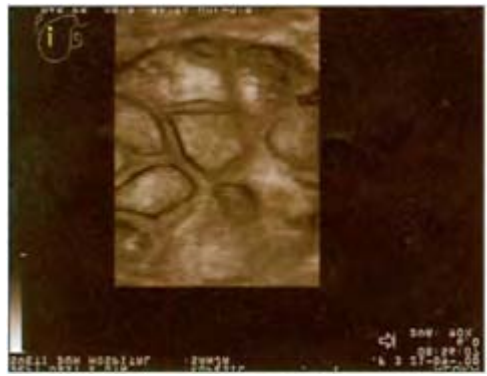

Figure 50.20: Three-dimensional ultrasound scan of a hyperstimulated ovary

in vitro fertilization (IVF) outcome. Total ovarian antral follicle number, total ovarian volume, total stromal area and mean flow index (FI) of the ovarian stromal blood flow

were determined by 3D and power Doppler ultrasound after pituitary suppression. Pre-treatment 3D ultrasound ovarian measurements were compared with subsequent ovulation induction parameters (peak estradiol on HCG administration day and number of oocytes) and cycle outcome (fertilization and pregnancy rates). The total number of antral follicles achieved the best predictive value for favorable IVF outcome, followed by ovarian stromal FI, total ovarian stromal area and total ovarian volume.

Recent study from Kupesic et al[68] evaluated whether ovarian antral follicle number, ovarian volume and ovarian stromal blood flow change with women age and if they are predictive of ovarian response and in *vitro* fertilization (IVF) outcome. Total ovarian antral follicle number, total ovarian volume and mean flow index (FI) of the ovarian stromal blood flow were determined by 3D and power Doppler ultrasound after pituitary suppression. Patients were separated into three groups based upon age and in each group median values of 3D ultrasound parameters (total ovarian antral follicle number, total ovarian volume and mean ovarian stromal vascularity) were measured and presented. Pre-treatment 3D ultrasound ovarian measurements were compared with subse¬ quent ovulation induction parameter (number of oocytes) and cycle outcome (fertilization and pregnancy rates). Increasing age is associated with poor ovarian response, smaller ovarian volume, lower antral follicle count and poor stromal vascularity.

Clearly, there is a place for 3D ultrasound studies in the assessment of the ovaries prior to ovulation induction and medically assisted reproduction, since it may be helpful in tailoring the dosage of stimulating drugs and prediction of the ovarian response.

POLYCYSTIC OVARIAN SYNDROME

Polycystic ovarian syndrome (PCOS) is one of the causes of anovulation and amenorrhea. In its classic form it is characterized by infertility, oligoand amenorrhea, hirsutism, acne or seborrhea, and obesity. Adams et al defined in 1986 the criteria for ultrasonographic diagnosis of polycystic ovaries: multiple (n>10), small (2–8 mm) peripheral cysts around a dense core of stroma in enlarged (≥8 ml) ovaries.69 However, ovaries which are normal in volume can be polycystic, as demonstrated by histological and biochemical studies. Anatomic structure of the ovaries cannot adequately be assessed with the transabdominal approach in about 42% of cases. Underlying causes are obesity, limited resolution of low-frequency transducers, a full bladder distorting pelvic anatomy, and bowel loops covering the adjacent ovary. More recently, the transvaginal approach for ultrasound scanning of the pelvic organs has been used. The high frequency of the transvaginal probe avoids the need for a full bladder and bypasses the problems of attenuation and artifacts associated with obesity. Furthermore, transvaginal ultrasonography has the advantage of improved resolution, better visualization of the pelvic organs, and greater acceptance among patients.

The number of follicles necessary to establish the diagnosis of polycystic ovaries by ultrasonography has been reported to vary between five and fifteen. However, in many reports the highest number of atretic follicles obtained in normal control patients was five per ovary, so it may conventionally be established that in polycystic ovaries the number of atretic follicles per ovary would be at least six. Matsunaga and colleagues identified two types of polycystic ovaries on the basis of ultrasonographic follicular distribution: the peripheral cystic pattern (PCP) and the general cystic pattern (GCP).70 In the PCR small

cysts are distributed in the subcapsular region of the ovary, whereas in the GCP they are scattered through the entire ovarian parenchyma. Recently, Takahashi and colleagues showed that these two different ovarian morphologies reflect histopathological differences, and that the PCP and GCP appearances reflect specific endocrine PCOS patterns.71

Another parameter considered in the diagnosis of polycystic ovaries is the ovarian volume. However, the wide volume overlap between normal and PCOS patients suggests that the discriminative capacity of ovarian volume alone is not sufficient for ultrasound diagnosis of PCOS.72 The role of a hyperechogenic ovarian stroma has been emphasized, but appraisal of the ovarian stroma echodensity,73 although comparable with computerized quantification,74 is absolutely subjective and may be differently interpreted by the operator.

Color Doppler studies showed that in patients with PCOS important changes in ovarian vascularization occur at the level of the intraovarian arteries. Although intraovarian arteries are usually not seen before day 8 to 10 of the 28-day cycle,71 Battaglia and colleagues detected distinct arteries with characteristic low vascular impedance as early as cycle day 3 to 5.76 In the studied population the results were associated with typical PCOS hormonal parameters and were inversely correlated with the LH/FSH ratio. Tonic hypersecretion of LH during the follicular phase of the menstrual cycle occurs in PCOS and is associated with theca cells and stromal hyperplasia with consequent androgen overproduction.76 Elevated LH levels may be responsible for increased stromal vascularization by different mechanisms that may act individually or in a cumulative way: neoangiogenesis, catecholaminergic stimulation, and leukocyte and cytokine activation (Fig. 50.21). In the same study the PCOS patients showed higher uterine pulsatility index (PI) values than non-hirsute normally menstruating women. This finding was correlated with androstenedione levels, confirming a possible direct androgen vasoconstrictive effect due to activation of specific receptors present in

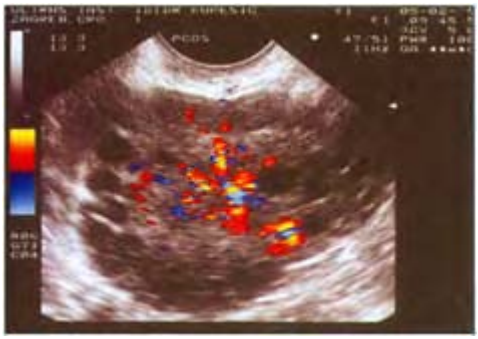

Figure 50.21: Transvaginal color Doppler scan of a polycystic ovary. Note peripheral distribution of

small follicles and
increased vascularity
within the ovarian stroma

the arterial vessel walls and collagen and elastin deposition in smooth muscle cells. The above condition, by reducing the uterine perfusion, has been supposed to be the cause that prevents blastocyst implantation, increasing the incidence of miscarriages in PCOS patients. Zaidi and colleagues[52] and Aleem and Predanic,[78] confirmed that Doppler analysis of the stromal arteries in PCOS may be useful to improve the diagnosis and to provide further information about the pathophysiology and evolution of the syndrome.

Doppler evaluation showed that PCP patients, in comparison with GCP patients, present significantly lower RI values at the level of the ovarian stromal arteries and that in 22% of GCP patients the intraovarian vessels are not recognized.[79] In addition, the GCP appearance of the ovary is more common in the early phase of the disease[70,71] during the peripubertal period. Thus, the ovarian morphology may evolve from a normal multicystic to polycystic PCP pattern, passing through an ovarian GCP aspect and untreated PCOS may be regarded as a progressive syndrome. Furthermore, by comparing oligo- vs. amenorrheic PCOS patients, it has recently been shown that amenorrheic patients are older and present higher PI values in uterine arteries and lower RI values in intraovarian vessels than oligomenorrheic patients.[80] This finding is associated with higher plasma LH and androstenedione levels and with a more elevated LH/FSH ratio. Furthermore, significantly higher ovarian volumes and subcapsular small-sized follicles are observed in amenorrheic PCOS patients. These data show that as the number of ovarian microcysts increases, ovarian volume enlarges and Doppler indices worsen, the clinical and endocrine abnormalities become more remarkable and the menstrual disturbances become more severe.[79]

Recently, it has been demonstrated that obese PCOS women show higher PI values within the uterine arteries than do lean patients.[81] This is associated with higher hematocrit values, hyperinsulinemia, higher triglyceride levels and lower high-density lipid (HDL) concentrations.

In overweight patients, hyperinsulinemia may be proposed as the uniting factor between increased vascular resistance, obesity, lipid abnormalities and cardiovascular disease.[81,82] Thus, assuming that PCOS patients are at increased risk for cardiovascular disease, it is possible to affirm that obesity may further increase the risk. Unopposed estrogen stimulation is an important contributing factor of endometrial carcinoma and helps to explain the increased risk in patients with obesity and chronic anovulation.

Recent advances in 3D ultrasound have made accurate non-invasive assessment of the irregularly shaped objects,[18,21] such as ovaries.

Wu et al[83] studied 44 women who presented with a history of irregular menstrual periods; the conditions of most of the women had been diagnosed as PCOS. The diagnosis of PCOS was based on the clinical symptoms (e.g. menstrual problems, obesity, acne, hirsutism), endocrinologic data (all with reversed serum LH/FSH ratio), and ultrasonographic features (increased ovarian stroma and volume, subcapsular cysts, and thickened capsule). Another 22 women with regular ovulatory cycles were recruited as normal controls. There was no statistically significant difference in age (range, 17–35 years) between the patient groups. Three-dimensional ultrasonography was performed to

store and document whole volumes of the ovaries for evaluation. Three perpendicular planes of bilateral ovaries were rotatable to obtain the largest dimensions, and the 3D volume was measured using the trapezoid formula. The ovaries of the patients with PCOS were larger in size, area, and volume than those of normal controls. The mean ovarian volumes (three dimensions; mean±SD) were 11.3±3.5 cm^3 in patients with PCOS and 5.5±1.4 cm^3 in the normal controls (P<0.0001). The volumes of the right ovary were 12.2±4.7 cm^3 and 5.3±2.0 cm^3 and the left ones were 10.5±3.6 cm^3 and 5.7±1.6 cm^3 in the PCOD and normal groups, respectively. The right ovary demonstrated a larger volume than the left ovary in women with PCOS (P<0.0001); however, the left ovary was significantly larger than the right one in the normal controls (P<0.0001).

The ovaries in PCOS were significantly increased in size, stroma, and volume (P<0.0001) compared with those of the normal controls. Cut-off values for ovarian area, stroma, and volume in PCOS were 5.2 cm^2 (sensitivity 93%, specificity 91%), 4.6 cm^2 (sensitivity 91%, specificity 86%), and 6.6 cm^3 (sensitivity 91%, specificity 91%), respectively. The stroma, total ovarian areas, and volume detected by careful rotation and outlining of the longitudinal ovarian cut were increased in 84% (37 of 44), 89% (39 of 44), and 80% (35 of 44) of the patients with PCOS, respectively, in comparison with normal controls. The total ovarian area was highly correlated with the stromal area (r^2=0.66).

Three maximal dimensions of the ovaries can be measured easily once the digital volume is documented from either transvaginal or transabdominal 3D ultrasonography, and superior volume determination can be obtained from 3D images. The volume measurement in 3D ultrasound is accurate and highly reproducible. The ability of reconstruction increases the diagnostic potential for PCOD. The ovaries in PCOS are usually enlarged bilaterally, but they may be about normal size (up to 20% in our study). The stroma areas in PCOS are hypertrophic, and provide yet another subjective ultrasonographic criterion that could differentiate PCOS from the multifollicular ovary. The multifollicular ovary demonstrates a normal or slightly increased size, but an increased number of follicles is noted without an increased amount of the stroma. However, the results are usually subjective and not quantitative. Using the computerized quantification measurement, an increased total ovarian area of >5.5 cm^2 highly correlates with increased ovarian stroma at a strict longitudinal ovarian section in the diagnosis of PCOS.[84]

The value of ovarian stroma can be obtained after subtracting the sum area of ovarian cysts from the total area. Using this method one can obtain more accurate volume data by outlining the contour of the ovary, which is better than traditional two-dimensional ultrasonographic scanning calculated by the ellipsoid formula (height×width×thickness×0.523).

In conclusion, 3D ultrasonography can complement two-dimensional ultrasonography for the diagnosis of PCOS. It allows excellent spatial evaluation of the ovaries with direct quantitative computations from the data.

Apart from morphological and volume measurements assessment of the ovarian and uterine vessels can be added to the traditional endocrinologic and ultrasonographic parameters clinically used for diagnosis of the PCOS.

Patients with PCOS undergoing ovulation induction for IVF are more likely to develop a greater number of follicles and generate more oocytes compared with women

with normal ovaries even though they require less gonadotrophin stimulation.[81] Furthermore, since they develop more follicles of all sizes and, in particular small and medium sized follicles, women with PCOS are at greater risk of OHSS.[86] This suggests that the PCOS is more sensitive to gonadotropin stimulation. The exact mechanism is unknown although it is possible that the increased ovarian stromal blood flow velocity, in combination with a relatively unchanged impedance to blood flow, may reflect increased intraovarian perfusion and thus a greater delivery of gonadotropins to the granulosa cells of the developing follicles. This theory may help to explain the greater likelihood of a multifollicular response. Women with PCOS have significantly greater stromal blood flow velocity as detected by transvaginal color Doppler ultrasound. This finding may help to explain the excessive response often seen in women with PCOS when they are administered gonadotropins. It seems that evaluation of the ovarian volume and stromal vascularity by 3D power Doppler ultrasound will further increase our knowledge on this enigmatic syndrome.

LUTEINIZED UNRUPTURED FOLLICLE SYNDROME

Luteinized unruptured follicle (LUF) syndrome is characterized with regular menses and presumptive ovulation as suggested by a cyclic hormonal profile, similar to that seen in normal ovulatory women but without release of the ovum. Although LUF syndrome was first diagnosed at laparoscopy by the absence of an ovulation stigma and the demonstration of lower concentrations of estradiol and progesterone in peritoneal fluid compared with normal ovulatory cycles, diagnosis is most commonly made on ultrasound examination, in which there is persistence of the ovarian follicle with progressive loss of its typical echo-free cystic appearance and accumulation of internal echogenicity. The precise etiology of LUF syndrome remains uncertain, but impairment of the midcycle LH surge, the absence of the pre-ovulatory progesterone rise, abnormalities of prostaglandin synthesis and a primary abnormality of the oocyte have all been suggested as possible causes. There is a possible association between LUF syndrome and unexplained infertility, chronic pelvic infection and endometriosis. The estimated frequency of this syndrome is between 6% and 47%.[83–85]

Kupesic and co-workers[87] tried to evaluate intraovarian RI in 47 healthy volunteers with ovulatory cycles and compare them to 28 patients with luteal phase defect (LPD), and four patients with LUF syndrome. Serial sonography allowed daily measurement of the mean follicular diameter and observation of the LUF syndrome development. The follicular collapse, demarcation of the hypoechoic structure with an irregular wall, formation of solid or complex structure representing the corpus luteum, and the extraovarian signs, such as the thickened endometrium and accumulation of the free fluid in the cul-de-sac were suggestive of ovulation. Doubtful cases (non-visualization of the corpus luteum and/or lack of the serial measurement) were excluded from the current study. LUF syndrome was documented by daily ultrasound observations and endocrinological measurement. During the period of expected ovulation the follicle remained the same size and maintained tense appearance. Luteinization of the unruptured follicle was seen as a progressive accumulation of the strong echoes located on its periphery.

In the group with regular ovulatory cycles, moderate to high RI (0.56+/−0.06) was obtained at the rim of the follicle. Significant decline of the RI occurred on the day of LH peak (RI 0.44+/ −0.04). The lowest RI values were obtained during the mid-luteal phase (RI 0.42+/−0.06), with a return to higher vascular resistance of 0.50+/ −0.04 during the late luteal phase. In 15 patients, endometrial biopsy was performed, and normal endometrial dating was detected. In the patients with LUF syndrome, no difference in terms of intraovarian RI was obtained after the LH peak. Similar RI values were obtained during the follicular and luteal phase (0.55+/−0.04 vs. 0.54+/ −0.06). Furthermore, there was no difference between the sides in terms of intraovarian vascular resistance. The mean progesterone value in this group was 14.1±6.2 ng/ml, and normal endometrial dating was obtained in all patients with LUF syndrome.

Merce and colleagues[88] who did not observe any drop in perifollicular intraovarian resistance after the LH peak reported similar results. Interestingly, the so called "luteal conversion" did not take place, indicating that the intraovarian and perifollicular neovascularization were either not produced, or were altered in LUF, probably because follicle failed to rupture.

Indeed, the rise in perifollicular blood flow during the periovulatory period appears to be primarily regulated by LH Zaidi et al[77] reported decreased blood flow velocity of the peripheral vessels in a patient with LUF syndrome after the LH surge to values comparable with those seen in the early follicular phase of the cycle. The reduction in peri-follicular blood flow velocity has also been reported in a patient with drug-associated LUF.[89]

Extensive Doppler measurements, biochemical research and 3D ultrasound studies still have to be done to fully clarify the causes and consequences of this syndrome.

LUTEAL PHASE DEFECT

The formation of corpus luteum is an important event in reproductive cycle and one of the crucial factors in early pregnancy support. After ovulation, blood vessels of the theca layer invade the cavity of the ruptured follicle starting the formation of the corpus luteum.

Small luteal cells produce more and more LH receptors and thus amplify the production of progesterone. This chain reaction goes till the so called mid-luteal phase which is characterized by peak values of blood LH, progesterone, and the lowest RI in corpus luteum blood vessels as proven by transvaginal color and pulsed Doppler by Kupesic et al.[90] Consequently, progesterone suppresses the secretion of gonadotropins, LH and progesterone levels decrease, and RI in the vessels of corpus luteum increases. Whether because of "intrinsic error of mechanism", or because of the interference with external factors (e.g. strenuous exercise, ovulation stimulating drugs), a condition called luteal phase defect (LPD) occurs. Various names have been assigned to the disorder: short luteal phase, luteal insufficiency, inadequate luteal phase, luteal defect and luteal phase deficiency. All these names describe the same condition: lack of progesterone, luteal phase of the cycle shorter than 11 days, and when related to endometrium, an out-of-phase endometrium by 2 or more days. The new method to detect corpus luteum abnormality is color Doppler ultrasonography. For a better visualization of the corpus luteum transvaginal approach is used. The research into the corpus luteum, LPD, early

pregnancy and early pregnancy failures has already taken a whole new direction. Until recently, research in this field was carried out mainly using B-mode and real time imaging. Glock et al[91] tried to determine whether the ultrasound appearance size, or change in size of the corpus luteum of early pregnancy correlated with serum progesterone, estradiol E2, or 17-hydroxyprogesterone or were even predictive of pregnancy outcome. Their hypothesis was: corpus luteum volumes of early human pregnancy would correlate with the serum concentration of steroids produced in the corpus luteum; appearance of the corpus luteum, based on the amount of cystic component, would correlate with serum hormone concentration or pregnancy outcome. The authors hypothesized that a decrease of the corpus luteum volume might be associated with pregnancy loss. Disappointingly, the acquired data showed a lack of correlation between corpus luteum size and steroid products and no correlation between changes in ovarian volume and steroid products levels in early human pregnancy. However, a decreasing corpus luteum volume before 8 weeks' gestation is associated with a higher probability of pregnancy loss. Color flow pulsed Doppler was used to determine dominant ovary with corpus luteum and the contralateral one. Dominant ovary showed low impedance waveform with RI 0.39–0.49, characteristic of the blood flow in early pregnancy. The contralateral ovary in each patient demonstrated a high impedance flow RI 0.69–1.0, characteristic of a nondominant ovary. One patient had an RI value of 0.74 in the ovary identified as having a corpus luteum, and RI of 0.79 in the opposite ovary; increased RI in both ovaries was associated with a nonviable pregnancy outcome. Kupesic et al[90] tried to evaluate intraovarian RI in 47 healthy fertile volunteers with ovulatory cycles and compare them to 28 patients with luteal phase defect (LPD) and four patients with LUF syndrome. Serial sonography allowed daily measurement of the mean follicular diameter, visualization of the follicular collapse and demarcation of the hypoechoic structure with an irregular wall, solid or complex structure representing the corpus luteum, as well as observation of the thickened endometrium, and presence of the free-fluid in the cul-de-sac (findings suggestive of ovulation). LPD was diagnosed by measuring the progesterone levels and performing the endometrial biopsy during the mid-luteal phase of the menstrual cycle. Sonographic and Doppler findings were correlated to hormonal and histopathological data.

In the group with regular ovulatory cycles (n=47) different ovarian RI values have been observed. During the stage of the follicular growth and development, moderate to high RI (mean 0.56 +0.06) was obtained at the rim of the follicle. Significant decline of the RI occurred for the day of LH peak (RI 0.44+0.04). The lowest RI values were obtained during the mid-luteal phase (RI 0.42+0.06), with a return to higher vascular resistance of 0.50+0.04 during the late luteal phase. In the LPD group (n=28) no difference was obtained in terms of intraovarian RI during the follicular phase. However, the mean RI throughout the luteal phase (RI 0.56+0.04) was significantly higher compared to the normals (Fig. 50.22). Furthermore, it did not show any difference between the early, middle and late luteal phase in LPD group (Graph 50.2).

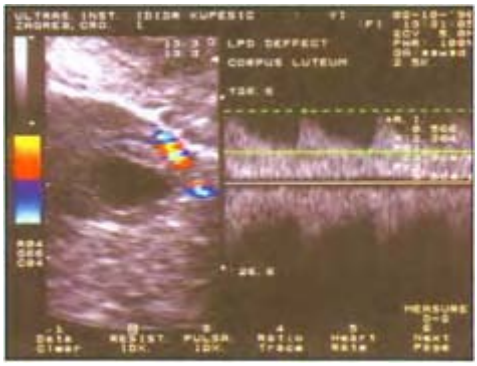

Figure 50.22: Transvaginal color Doppler scan of a corpus luteum in a patient with luteal phase defect. Note moderate-to-high resistance index (RI=0.57) obtained from intraovarian vessels

In the control group, both follicular and luteal RI was significantly lower on the dominant side. However, in the LPD group no difference occurred in terms of intraovarian RI between the sides.

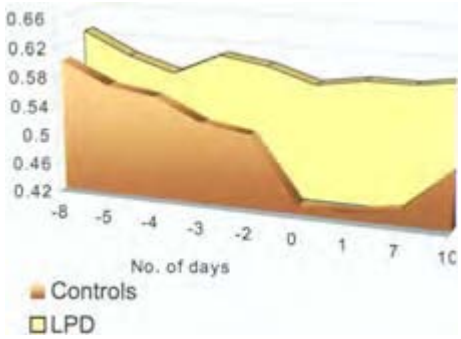

Graph 50.2: Intraovarian blood flow changes in patients with LPD and controls (Modified from

reference 90, with permission)

Mean progesterone levels were significantly lower in the LPD group (6.9+2.3 ng/ml) than in the controls (24.1+11.4 ng/ml), while histopathology revealed delayed endometrial pattern in all the patients with LPD. The correlation was observed between progesterone and RI during the midluteal phase.

Merce et al[88] elaborated on all aspects of transvaginal color and pulsed Doppler ultrasonography: its advantages, disadvantages, current possibilities and future directions. In their study of luteal ovarian blood flow they introduced the term "luteal conversion" to describe Doppler findings during the luteal phase: easily obtained Doppler signals, increase in intensity of frequency spectrum, increase in turbulence of the blood flow with extensive dispersion of the maximum frequencies and superposition of multiple waveforms presenting variable maximum systolic velocities and, finally, an increase in the surface and intensity of the intraovarian color signals. The authors observed that the RI of the dominant ovary drops during the luteal phase with respect to the follicular phase, as also occurs in normal cycles. They found no differences in this aspect when comparing with any phase of the normal cycle. No significant correlation was demonstrated between the index values and serum progesterone levels either.

Glock and Brumsted[92] correlated ovarian blood flow to values of progesterone throughout the cycle. Mean progesterone levels were significantly lower for LPD patients than for normal women throughout the luteal phase. Mean resistance index in LPD patients was significantly higher compared with normal women throughout the follicular and luteal phases. Although systolic and diastolic velocities were observed to be lower in LPD patients compared with normal women, these differences were not statistically different. High correlations were observed between progesterone and RI within each of the luteal time points, achieving its highest value during the mid-luteal phase. The mean RI in the dominant ovary was significantly lower than in the nondominant ovary throughout the cycle in normal women (0.50 versus 0.65), but not in those with LPD (0.60 versus 0.66, P=0.37). In the single anovulatory subject, RI values remained high (mean 0.76, range 0.70 to 0.82) in both ovaries.

This study[92] showed a clear correlation between the RI of corpus luteum blood flow and plasma progesterone in the natural cycle. The strongest correlation was seen in the mid-luteal phase, the period that corresponds to peak neovascularization of the corpus luteum. Consistent to this finding, the authors showed an increase in blood flow impedance in the late luteal phase, the period associated with the onset of corpus luteum regression. These findings suggest the possibility of using the RI of corpus luteum blood flow as an adjunct to plasma progesterone assay, as an index of luteal function.

Tinkanen,[93] on the other hand found no difference between the blood flow in the corpus luteum in controls with normal luteal phase and infertility patients with abnormal luteal phase. Short luteal phase, claims the author, is not due to premature vascular regression of the corpus luteum as evaluated by measurement of the vascular resistance.

Strigini et al[94] observed the change of impedance during the luteal phase of FSH-treated cycles. The uterine PI during stimulated cycles, both before and after ovulation, was significantly reduced compared with spontaneous cycles. That was explained by the increase of plasma E2. Furthermore, Strigini advocates administration of exogenous progesterone as a supplementation to FSH treated cycles, stating that uterine PI after

administration of progesterone drops even more than in spontaneous or only with FSH treated cycles.

Kupesic et al[90] correlated Doppler velocimetry, histological and hormonal markers. They presumed that when combined together, ultrasound results, measurement of hormone values and endometrial biopsy could explain more about pathophysiology of the LPD. They found out that mean progesterone levels were significantly lower in the group with LPD (10.2+4.3 ng/ml) than in controls (21+4.2 ng/ml). The FSH/LH ratio was significantly lower in the group with a delayed endometrial pattern compared to normal subjects during follicular and periovulatory phases (0.70 vs. 1.24; 0.58 vs. 0.75, respectively). There was a close correlation between E_2 estradiol levels and the mean diameter of the dominant follicle from days -5 to -1 relative to the days of sonographically observed ovulation. An increase in follicular diameter and endometrial thickness was noted for both normal and LPD groups.

Intraovarian blood flow resistance showed no difference between the groups during the proliferative phase. Patients in control group had a significantly lower RI in dominant than in nondominant ovary, whereas LPD patients had the almost same RI in both ovaries. The authors measured blood flow in spiral arteries as well. Spiral arteries in the control group demonstrated an RI of 0.53+0.04 during the periovulatory phase, and RI values of 0.50+0.02 and 0.51 +0.04 were obtained during the mid-luteal and late luteal phase, respectively. Higher impedance values during the periovulatory phase (RI=0.70 +0.06, $p<0.001$), mid-luteal phase (RI=0.72+ 0.06, $p<0.001$) and late luteal phase (RI=0.72 +0.04, $p<0.001$) were obtained from the spiral arteries in the LPD group. A close correlation has been found between plasma levels of E_2 and the mean diameter of the follicle. The study clearly demonstrated that patients with normal endometrial development show a similar trend of regression for uterine, radial and spiral artery impedance from the follicular to the luteal phase. In contrast, patients with a delayed endometrial pattern are characterized by increased uterine vascular resistance during the luteal phase. Since the most significant difference in terms of RI is obtained for spiral arteries, it might be expected that endometrial blood flow changes could be used to predict the development of the endometrium and likelihood of pregnancy.

Salim et al[95] correlated luteal blood in normal pregnancies to the flow in abnormal pregnancies. Their study proved the hypothesis that an absence of luteal flow cannot coexist with normal pregnancy. Impedance to intraovarian blood flow was significantly higher in patients with abnormal early pregnancy (missed, incomplete, and threatened abortion) than in women with normal pregnancy. However, this was not confirmed in patients with blighted ovum, molar, and ectopic pregnancy. The impedance to luteal blood flow was almost the same as in normal pregnancy. This difference among subgroups of abnormal early pregnancy may relate to a different natural history of the disease. Missed and incomplete abortions are manifested as failed early pregnancy with no prospects for further development. Threatened abortion is a potentially similar condition. Whether decreased corpus luteum blood flow is a potential cause or a consequence of the disease remains unclear. Anembryonic pregnancies, molar or ectopic pregnancies are somewhat different. These pathologic conditions usually are progressive and not self-limited. This can explain why is impedance to luteal blood flow in these women similar to that in women with normally progressing pregnancies.

Alcazar et al[96] agree only partially on the results Salim et al obtained.[95] Alcazar's group found out that mean RI in missed abortion was higher than in controls. This increased vascular resistance could be explained by the fact that missed abortion consists of a failure of early pregnancy to develop, in which the production of hCG is impaired, which in turn could have a negative effect on luteal function. On the other hand, they found no statistically significant difference in RI of the patients with threatened abortion.

TUBAL FACTOR OF INFERTILITY

The Fallopian tubes serve as the site of fertilization and early embryogenesis. The tubal mucosa responds to the hormonal changes during the menstrual cycle in order to facilitate the transport of sperm and fertilized ova in the process of fertilization. During the luteal phase, decreased tube secretion and more prominent ciliary activity propel the ovum into the uterine fundus. If conception does not occur, the secretory and ciliary cells are significantly reduced in number due to withdrawal of endocrine support.

The normal Fallopian tubes are narrow and usually not seen by transabdominal or transvaginal ultrasound unless they contain fluid within their lumina or area surrounded by fluid. The motility and transport function of the oviducts are impaired during all stages of pelvic inflammatory disease (PID). First, in the acute phase, the tube becomes thick and edematous and a large amount of purulent exudate fills the lumen. Later on, the inflammatory process may be organized to form tubo-ovarian abscess, which will, in most cases lead to scarring and occlusion of the tube. Chronic hydrosalpinx is the ultimate remnant of the PID: the tube is occluded, thin-walled and filled with fluid.

Infertility caused by tubal dysfunction is found in approximately 35% of patients. A history of PID, septic abortion, intrauterine contraceptive device, ruptured appendix, tubal surgery or ectopic pregnancy should alert the physician to the possibility of tubal damage. Amorphous acellular plugs have been identified as the probable cause of obstruction in the proximal tube in nearly 50% of women whose tubes did not opacify on hysterosalpingography (HSG). The improved pregnancy rate after uterotubal insufflation and hysterosalpingography suggests that their therapeutic effect may partially result from dislodgment of the Fallopian tube debris. Reversible spasm at the uterotubal junction is another cause of apparent obstruction on conventional HSG. In 100 patients with nonfilling on an initial hysterosalpingogram, Lang[97] found that only 39 had persistent occlusion after pharmacologic manipulation and selective tubal salpingography. In the remaining 61 patients the apparent cause of tubal nonfilling was spasm and debris in 49 patients, submucous fibroids in six, synechiae in three, salpingitis isthmica nodosa in two, and septated uterus in one.

Until a few years ago the assessment of the uterine cavity and the Fallopian tube lumen relied on complicated, painful and invasive procedures. The major problem was how to visualize the hollow space within these organs and how to describe the contours of the uterine and oviduct walls. The functions of the uterus and the Fallopian tubes depend on their cavities: a uterus filled with endometrial polyp or distorted by a myoma is an obstacle to implantation, while a tortuous and/ or narrow tube with the inflammatory changes does not permit oocytes to descend.

Hysterosalpingography, using radio-opaque dye for X-ray assessment of tubal and uterine anatomy, has been the standard form of investigation for several decades. The

disadvantage of this type of investigation is that ionizing radiation presents a risk to the oocyte: if the conception takes place in the investigation cycle, congenital fetal anomalies may occur. Furthermore, iodine-containing dyes used in X-ray hysterosalpingography can cause allergic reaction.

In the last two decades, laparoscopy has been the usual procedure for the assessment of tubal status. However, it requires general anesthesia and carries the risk of anesthetic and surgical complications, such as bowel or vascular injury, false pneumoperitoneum and postoperative discomfort.

Together with the development of ultrasound technique, a totally new concept of diagnostic procedures has been developed. We have already described in the chapter on hysterosonosalpingography benefits and limitations of the sonographic evaluation of the tubal patency.

PERITONEAL FACTOR

A peritoneal factor may be present in as many as 25% of couples in which no other infertility factor is discovered. Peritoneal factor of infertility is caused by endometriosis or pelvic adhesions. Endometriosis is caused by foci of secretory endometrium outside of the uterus. Because it undergoes cyclic bleeding, endometriosis is associated with pain, adhesions and some other poorly defined fertility problems. Laparoscopy is used for diagnosis as well as treatment of these lesions. No imaging test exists that can reliably detect pelvic adhesions or small endometriotic implants. If a peritoneal factor abnormality is visualized by sonography, the diagnosis can be confidently made.

CERVICAL FACTOR

Cervical factor indicates the ability of the cervical mucus to allow sperm survival and penetration, which is determined by assessing sperm motility in the cervical mucus 6 to 8 hours after intercourse (postcoital test).

CONCLUSION

Sonography can play a critical role in the diagnosis and treatment of fertility disorders. In addition, transvaginal color Doppler and 3D ultrasound with power Doppler facilities have made a significant improvement in the assessment of infertility. They may help in prediction of ovulation and detection of ovulatory disorders. Measurements of uterine perfusion have a predictive value regarding fecundity in patients undergoing different methods of medically assisted reproduction. Absent subendometrial and intraendometrial vascularization on the day of hCG administration appears to be a useful predictor of failure of implantation in IVF cycles, irrespective of the morphological appearance of the endometrium. Studies on spiral artery perfusion might produce a non-invasive assay of uterine receptivity, giving us more information on the pathophysiology of infertility, especially in the group of patients with unexplained causes.

Three-dimensional ultrasound offers the opportunity to assess gynecological structures of an infertile patient in three different volumes (uterus, left and right adnexa). The total examination time for the patient is tremendously reduced since patient can leave the

examination room once the volumes have been stored and all further investigations could be performed without the presence of the patient. This seems to be advantageous in patients scheduled for serial ovarian monitoring in whom planar reformatted sections allow more accurate and objective volumetric assessment of the leading follicles, which are not always spherical. Transvaginal ultrasound directed follicular aspiration and embryo transfer under 3D ultrasound guidance improves the operator's spatial evaluation and allows precise follicular and/or catheter tip location during the course of interventional procedures. The use of 3D transvaginal ultrasonography after injection of saline solution or/and echo enhancing contrast medium produces high diagnostic accuracy of the visualization of the uterine cavity especially its lateral portion close to the tubal ostia. Quantification of endometrial volume by 3D ultrasound in combination with blood flow studies contributes to the assessment of endometrial receptivity and has a potential to predict pregnancy rates in assisted reproductive techniques.

REFERENCES

1. Freidler S, Schenker JG, Herman A, Lewin A. The role of ultrasonography in the evaluation of endometrial receptivity following assisted reproductive treatments: a critical review. Hum Reprod (Update) 1996; 2:323–35.
2. Gonen Y, Calderon M, Direnfeld M, Abramovici H. The impact of sonographic assessment of the endometrium and meticulous hormonal monitoring during natural cycles in patients with failed donor artificial insemination. Ultrasound Obstet Gynecol 1991; 1:122–26.
3. Abdalla HI, Brooks AA, Johnson MR, Kirkland A, Thomas A, Studd JW. Endometrial thickness: a predictor of implantation in ovum recipients? Hum Reprod 1994; 9:363–65.
4. Khalifa E, Brzyski RG, Oehninger S, Acosta AA, Muasher SJ. Sonographic appearance of the endometrium: the predictive value for the outcome of in vitro fertilization in stimulated cycles. Hum Reprod 1992; 7:677–80.
5. Serafini P, Batzofin J, Nelson J, Olive D. Sonographic uterine predictors of pregnancy in women undergoing ovulation induction for assisted reproductive treatments. Fertil Steril 1994; 62:815–22.
6. Sher G, Herbert C, Maassarani G, Jacobs MH. Assessment of the late proliferative phase endometrium by ultrasonography in patients undergoing in vitro fertilization and embryo transfer (IVF/ET). Hum Reprod 1991; 6:232–37.
7. Zaidi J, Campbell S, Pitroff R, Tan SL. Endometrial thickness, morphology, vascular penetration and velocimetry in predicting implantation in an in vitro fertilization program. Ultrasound Obstet, 1995.
8. Kyei-Mensah A, Maconochie N, Zaidi J, Pittrof R, Campbell S, Tan SL. Transvaginal three-dimensional ultrasound: reproducibility of ovarian and endometrial volume measurements. Fertil Steril 1996; 66: 718–22.
9. Riccabona M, Nelson TR, Pretorius DH. Threedimensional ultrasound: accuracy of distance and volume measurements. Ultrasound Obstet Gynecol 1996; 4:29–34.
10. Gilja OH, Smievoll I, Thune N, Matre K, Hausken T, Odegaard S. In vivo comparison of 3D ultrasonography and magnetic resonance imaging in volume estimation of human kidney. Ultrasound Med Biol 1995; 21:25–32.
11. Lee A, Sator M, Kratochwil A, Deutinger J, VytiskaBinsdorfer E, Bernaschek G. Endometrial volume change during spontaneous menstrual cycles: volumetry by transvaginal three-dimensional ultrasound. Fertil Steril 1997; 68:831–35.
12. Kyei-Mensah A, Zaidi J, Pittrof R, Shaker A, Campbell S, Tan SL. Transvaginal three-dimensional ultrasound: accuracy of follicular volume measurements. Fertil Steril 1996; 65:371–76.

13. Child TJ, Sylvestre C, Tan SL. Endometrial volume and thickness measurements predict pituitary suppression and non-suppression during IVF. Hum Reprod 2002; 7(12):3110–13.
14. Kupesic S, Bekavac I, Bjelos D, Kurjak A. Assessment of endometrial receptivity by transvaginal color Doppler and three-dimensional power Doppler ultrasonography in patients undergoing in vitro fertilization procedures. J Ultrasound Med 2001; 20: 125–34.
15. Kurjak A, Kupesic-Urek S, Schulman H, Zalud I. Transvaginal color Doppler in the assessment of ovarian and uterine blood flow in infertile women. Fertil Steril 1991; 56:870.
16. Kurjak A, Kupesic-Urek S. Normal and abnormal uterine perfusion. In: Jaffe R, Warsof LS (Eds). Color Doppler Imaging in Obstetrics and Gynecology 1992; 255–63 (New York: McGraw Hill).
17. Goswamy RK, Silliams G, Steptoe PC. Decreased uterine perfusion a cause of infertility. Hum Reprod 1988; 3:955–58.
18. Steer CV, Mills CV, Campbell S. Vaginal color Doppler assessment on the day of embryo transfer (ET) accurately predicts patients in an in vitro fertilization programme with suboptimal uterine perfusion who fail to become pregnant. Ultrasound Obstet Gynaecol 1991; 1:79–82.
19. Tsai YC, Chang JC, Tai MJ, Kung FT, Yang LC, Chang SY. Relationship of uterine perfusion to outcome of intrauterine insemination. J Ultrasound Med 1996; 15:633–36.
20. Steer CV, Tan SL, Mason BA, Campbell S. Midluteal phase vaginal color Doppler assessment of uterine artery impedance in a subfertile population. Fertil Steril 1994; 61:53–58.
21. Kupesic S. The first three weeks assessed by transvaginal color Doppler. J Perinat Med 1996; 24: 301–17.
22. Cacciatore B, Simberg N, Fusaro P, Tiitinen A. Transvaginal Doppler study of uterine artery blood flow in in vitro fertilization—embryo transfer cycles. Fertil Steril 1996; 66(1):130–34.
23. Cheung W, Ng EH, Ho PC. A randomized double-blind comparison of perifollicular vascularity and endometrial receptivity in ovulatory women taking Clomiphene citrate at two different times. Hum Reprod 2002; 17(11):2881–84.
24. Dada T, Salha O, Allgar V, Sharma V. Utero-ovarian blood flow characteristics of pituitary desensitization. Hum Reprod 2001; 16(8):1663–70.
25. Pellizzari R Esposito C, Siliotti F, Marchiori S, Gangemi M. Colour Doppler analysis of ovrian and uterine arteries in women with hypoestrogenic amenorrhoea. Hum Reprod 2002; 17(12):3208–12.
26. Ashton D, Amin HK, Richart RM, Neuwirth RS. The incidence of asymptomatic uterine anomalies in women undergoing transcervical tubal sterilization. Obstet Gynecol 1988;72:28–30.
27. Sorensen S. Estimated prevalence of mulerian anomalies. Acta Obstet Gynecol Scand 1988; 67:441–45.
28. Gaucherand P, Awada A, Rudigoz RC, Dargent D. Obstetrical prognosis of septate uterus: a plea for treatment of the septum. Eur J Obstet Gynecol Reprod Biol 1994; 54:109–12.
29. Fedele L, Arcaini L, Parazzini F, Vercellini P, Nola GD. Metroplastic hysteroscopy and fertility. Fertil Steril 1993; 59:768–70.
30. Heinonen PK, Saarikoski S, Pystynen P. Reproductive performance of women with uterine anomalies. An evaluation of 182 cases. Acta Obstet Gynecol Scand 1982; 61:157–62.
31. Fedele L, Bianchi S, Marchini M, Franchi D, Tozzi L, Dorta M. Ultrastructural aspects of endometrium in infertile women with septate uterus. Fertil Steril 1996; 65:750–52.
32. Cararach M, Penella J, Ubeda J, labastida R. Hysteroscopic incision of the septate uterus: scissors versus resectoscope. Hum Reprod 1994; 9:87–89.
33. Goldenberg M, Sivan E, Sharabi Z. Reproductive outcome following hysteroscopic management of intrauterine septum and adhesions. Hum Reprod 1995; 10:2663–65.
34. Valdes C, Malini S, Malinak LR. Ultrasound evaluation of female genital tract anomalies: a review of 64 cases. Am J Obstet Gynecol 1984; 149:285–90.
35. Nicolini U, Bellotti B, Bonazzi D, Zamberleti G, Battista C. Can ultrasound be used to screen uterine malformation? Fertil Steril 1987; 47:89–93.

36. Reuter KL, Daly DC, Cohen SM. Septate versus bicornuate uteri: errors in imaging diagnosis. Radiology 1989; 172:749–52.
37. Randolph J, Ying Y, Maier D, Schmidt C, Riddick D. Comparison of real time ultrasonography, hysterosalpingography, and laparoscopy/hysteroscopy in the evaluation of uterine abnormalities and tubal patency. Fertil Steril 1986; 5:828–32.
38. Richman TS, Viscomi GN, Cherney AD, Polan A. Fallopian tubal patency assessment by ultrasound following fluid injection. Radiology 1984; 152:507–10.
39. Salle B, Sergeant P, Galcherand P, Guimont I, De Saint Hilaire P, Rudigoz RC. Transvaginal hysterosonographic evaluation of septate uteri: a preliminary report. Hum Reprod 1996; 11:1004–07.
40. Marshall C, Mintz DI, Thickman D, Gussman H, Kressel Y. MR evaluation of uterine anomalies. Radiology 1987; 148:287–89.
41. Carrington BM, Hricak M, Naruddin RN. Mullerian duct anomalies: MR evaluation. Radiology 1990; 170: 715–20.
42. Jurkovic D, Giepel A, Gurboeck K, Jauniaux E, Natucci M, Campbell S. Three dimensional ultrasound for the assessment of uterine anatomy and detection of congenital anomalies: a comparison with hysterosalpingography and two-dimensional sonography. Ultrasound Obstet Gynecol 1995; 5:233–37.
43. Taylor PJ, Gumming DC. Hysteroscopy in 100 patients. Fertil Steril 1979; 31:301–04.
44. Kupesic S, Kurjak A. Septate uterus: detection and prediction of obstetrical complications by different forms of ultrasonography. J Ultrasound Med 1998; 17:631–36.
45. Dabrashrafi H, Bahadori M, Mohammad K, Alavi M, Moghadami-Tabrizi N, Zandinejad R. Septate uterus: New idea on the histologic features of the septum in this abnormal uterus. Am J Obstet Gynecol 1995; 172:105–07.
46. Balen FG, Allen CM, Gardener JE, Siddle NC, Lees WR. 3-dimensional reconstruction of ultrasound images of the uterine cavity. The British Journal of Radiology 1993; 66:588–91.
47. Weinraub Z, Maymon R, Shulman A, Bukovsky J, Kratochwil A, Lee A, Herman A. Three-dimensional saline contrast rendering of uterine cavity pathology. Ultrasound Obstet Gynecol 1996; 277–82.
48. Kupesic S, Kurjak A, Skenderovic S, Bjelos D. Screening for uterine abnormalities by three-dimensional ultrasound improves perinatal outcome. J Perinat Med 2002; 30:9–17.
49. Kurjak A, Kupesic S, Miric D. The assessment of benign uterine tumor vascularization by transvaginal color Doppler. Ultrasound Med Biol 1992; 18:645–49.
50. Coutinho EM, Maia HS. The contractile response of the human uterus, Fallopian tubes, and ovary to prostaglandins in vivo. Fertil Steril 1971; 22:539–43.
51. Exacoustos C, Rosati P. Ultrasound diagnosis of uterine myomas and complications in pregnancy. Obstet Gynecol 1993; 82:97–101.
52. Delgdish L, Loewenthal M. Endometrial changes associated with myomata of the uterus. J Clin Pathol 1970; 23:676–79.
53. Farrer-Brown G, Beilby JO, Tarbit MH. Venous changes in the endometrium of myomatous uteri. Obstet Gynecol 1971; 38:743–46.
54. Brosens JJ, de Souza NM, Barker FG, Paraschos T, Winston RM. Endovaginal ultrasonography in the diagnosis of adenomyosis uteri: identifying the predictive characteristics. Br J Obstet Gynaecol 1995; 102(6):471.
55. Schlaff WD, Hurst BS. Preoperative sonographic measurement of endometrial pattern predicts outcome of surgical repair in patients with severe Asherman's syndrome. Fertil Steril 1995; 63:410–13.
56. Zaidi J, Barber J, Kyei-Mensah A, Pittrof R, Campbell S, Tan SL. Relationship of ovarian stromal blood flow at baseline ultrasound to subsequent follicular response in an in vitro fertilization program. Obstet Gynecol 1996; 88:779–84.

57. Engmann L, Sladkevicius P, Agrawal R, Bekir JS, Campbell S, Tan SL. Value of ovarian stromal blood flow velocity measurement after pituitary suppression in the prediction of ovarian responsiveness and outcome of in vitro fertilization treatment. Fertil Steril 1999; 71(1):22–29.
58. Wittmack FM, Kreger DO, Blasco L, Tureck RW, Mastroianni L Jr, Lessey BA. Effect of follicular size on oocyte retrieval, fertilization, cleavage, and embryo quality in in vitro fertilization cycles: a 6-year data collection. Fertil Steril 1994; 62:1205–10.
59. Golan A, Herman A, Soffer Y, Bukovsky I, Ron-El R. Ultrasonic control without hormone determination for ovulation induction in in-vitro fertilization/ embryo-transfer with gonadotrophin-releasing hormone analogue and human menopausal gonadotrophin. Hum Reprod 1994; 9:1631–33.
60. Shoham Z, DiCarlo C, Pater A, Conway GS, Jacobs HS. Is it possible to run a successful ovulation induction program based solely on ultrasound monitoring? The importance of endometrial measurements. Fertil Steril 1991; 56:836–41.
61. Tan SL. Simplification of IVF therapy. Curr Opin Obstet Gynecol 1994; 6:111–14.
62. Steiner H, Staudach A, Spitzer D, Schaffer H. Three-dimensional US in obstetrics and gynaecology: technique, possibilities and limitations. Hum Reprod 1994; 9:1773–78.
63. Penzias AS, Emmi AM, Dubey AK, Layman LC, DeCherney AH, Reindollar RH. Ultrasound prediction of follicle volume: is the mean diameter reflective? Fertil Steril 1994; 62:1274–76.
64. Feichtinger W. Transvaginal three-dimensional imaging for evaluation and treatment of infertility. In: Merz E (Ed). 3D Ultrasound in Obstetrics and Gynecology. Philadelphia: Lippincott Williams & Wilkins, 1998; 37–43.
65. Lass A, Skull J, McVeigh E, Margara R, Winston RM. Measurement of ovarian volume by transvaginal sonography before ovulation induction with human menopausal gonadotrophin for in-vitro fertilization can predict poor response. Hum Reprod 1997; 12: 294–97.
66. Oyesanya OA, Parsons JH, Collins WP, Campbell S. Total ovarian volume before human chorionic gonadotrophin administration for ovulation induction may predict the hyperstimulation syndrome. Hum Reprod 1995; 10:3211–12.
67. Kupesic S, Kurjak A. Predictors of in vitro fertilisation outcome by three-dimensional ultrasound. Hum Reprod 2002; 17(4):950–55.
68. Kupesic S, Kurjak A, Bjelos D, Vujisic S. Three-dimensional ultrasonographic ovarian measurements and in vitro fertilization outcome are related to age. Fertil Steril, in press, 2003.
69. Adams J, Franks S, Poison DW, Mason HD, Abdulwahid N, Tucker M, Morris DV, Price J, Jacobs HS. Multifollicular ovaries: clinical and endocrine features and response to pulsatile gonadotropinreleasing hormone. Lancet 1985; 2:1375–78.
70. Matsunaga I, Hata T, Kitao M. Ultrasonographic identification of polycystic ovary. Asia-Oceania J Obstet Gynecol 1985; 11:227–32.
71. Takahashi K, Ozaki T, Okada M, Uchida A, Kitao M. Relationship between ultrasonography and histopathological changes in polycystic ovarian syndrome. Hum Reprod 1994; 9:2255–58.
72. Battaglia C, Artini PG, D'Ambrogio G, Galli PA, Genazzani AR. Uterine and ovarian blood flow measurement. Does the full bladder modify the flow resistance? Acta Obstet Gynecol Scand 1994; 73:716–18.
73. Ardaens Y, Robert Y, Lemaitre L, Fossati P, Dewailly D. Polycystic ovarian disease: contribution of vaginal endosonography and reassessment of ultrasonic diagnosis. Fertil Steril 1991; 55:1062–68.
74. Robert Y, Dubrulle F, Gaillandre L, Ardaens Y, Thomas-Desrousseaux P, Lemaitre L, Dewailly D. Ultrasound assessment of ovarian stroma hypertrophy in hyperandrogenism and ovulation disorders: visual analysis versus computerized quantification. Fertil Steril 1995; 64:307–12.
75. Merce LT, Garces D, Barco MJ, De la Fuente P. Intraovarian Doppler velocimetry in ovulatory, dysovulatory and anovulatory cycles. Ultrasound Obstet Gynecol 1992; 2:197–202.
76. Battaglia C, Artini PG, D'Ambrogio G, Genazzani AD, Genazzani AR. The role of color Doppler imaging in the diagnosis of polycystic ovary syndrome. Am J Obstet Gynecol 1995; 172:108–13.

77. Zaidi J, Campbell S, Pirtrof R, Kyei-Mensah A, Shaker A, Jacobs HS, Tan SL. Ovarian stromal blood flow in women with polycystic ovaries—a possible new marker for diagnosis? Hum Reprod 1995; 10:1992–95.
78. Aleem FA, Predanic M. Transvaginal color Doppler determination of the ovarian and uterine blood flow characteristics in polycystic ovary disease. Fertil Steril 1996; 65:510–16.
79. Battaglia C, Artini PG, Salvatori M, Giulini S, Petraglia F, Maxia N, Volpe A. Ultrasonographic patterns of polycystic ovaries;color Doppler and hormonal correlations. Ultrasound Obstet Gynecol 1998; 11:332–36.
80. Battaglia C, Artini PG, Genazzani AD, Florio P, Salvatori M, Sgherzi MR, Giulini S, Lombardo M, Volpe A. Color Doppler analysis in oligo- and amenorrheic women with polycystic ovary syndrome. Gynecol Endocrinol 1997; 11:105–10.
81. Battaglia C, Artini PG, Genazzani AD, Sgherzi MR, Salvatori M, Giulini S, Volpe A. Color Doppler analysis in lean and obese women with polycystic ovary syndrome. Ultrasound Obstet Gynecol 1996; 7: 342–46.
82. Wild RA, Van Nort JJ, Grubb B, Bachman W, Hartz A, Bartholomew M. Clinical signs of androgen excess as risk factors for coronary artery disease. Fertil Steril 1990; 54:255–59.
83. Wu MH, Tang HH, Hsu CC, Wang ST, Huang KE. The role of three-dimensional ultrasonographic images in ovarian measurement. Fertil Steril 1998; 69:1152–55.
84. Robert Y, Dubrulle F, Gaillandre L, Ardaens Y, Thomas-Desrousseaux P, Lemaitre L. Ultrasound assessment of ovarian stroma hypertrophy in hyperandrogenism and ovulation disorders: visual analysis versus computerized quantification. Fertil Steril 1995; 64:307–12.
85. MacDougall MJ, Tan SL, Balen A, Jacobs HS. A controlled study comparing patients with and without polycystic ovaries undergoing in-vitro fertilization. Hum Reprod 1993; 8:233–37.
86. MacDougall MJ, Tan SL, Jacobs HS. In-vitro fertilization and the ovarian hyperstimulation syndrome. Hum Reprod 1992; 7:597–600.
87. Kupesic S, Kurjak A. The assessment of normal and abnormal luteal function by transvaginal color Doppler sonography. Eur J Obstet Gynecol Reprod Biol 1997; 72:83–87.
88. Merce LT, Garces D, De la Fuente F. Conversion lutea de la onda de velocidad de fluio ovarica: nuevo parametro ecografico de ovulacion y funcion lutea. Acta Obstet Gynecol Scand 1989; 2:113–14.
89. Bourne TH, Reynolds K, Waterstone J, Okokon E, Jurkovic D, Campbell S, Collins WP. Paracetamolassociated luteinized unruptured follicle syndrome: effect on intrafollicular blood flow. Ultrasound Obstet Gynecol 1991; 1:420–25.
90. Kupesic S, Kurjak A, Vujisic S, Petrovic Z. Luteal phase defect: comparison between Doppler velocimetry, histological and hormonal markers. Ultrasound Obstet Gynaecol 1997; 9:1–8.
91 Clock JL, Blackman JA, Badger GJ, Brumsted JR. Prognostic Significance of Morphologic Changes of the Corpus Luteum by Transvaginal Ultrasound in Early Pregnancy Monitoring. Obstet Gynecol 1995; 85:37–41.
92 Glock JL, Brumsted JR. Color flow pulsed Doppler ultrasound in diagnosing luteal phase defect. Fertil Steril 1995; 64:500–04.
93. Tinkanen H. The role of vascularization of the corpus luteum in the short luteal phase studied by Doppler ultrasound. Acta Obstet Gynecol Scand 1994; 73: 321–23.
94. Strigini FAL, Scida PAM, Parri C, Visconti A, Susini S, Genazzani AR. Modifications in uterine and intraovarian artery impedance in cycles of treatment with exogenous gonadotropins: effects of luteal phase support. Fertil Steril 1995; 64:76–80.
95. Salim A, Žalud I, Farmakides G, Schulmal H, Kurjak A, Latin V. Corpus luteum blood flow in normal and abnormal early pregnancy: Evaluation with transvaginal color and pulsed Doppler sonography. J Ultrasound Med 1994; 13:971–75.
96. Alcazar JL, Laparte C, Lopez-Garcia G. Corpus luteum blood flow in abnormal early pregnancy. J Ultrasound Med 1996; 15:645–49.

97. Lang EK. Organic vs. functional obstruction of the fallopian tubes: differentiation with prostaglandin antagonist-and B2-mediated hysterosalpingography and selective ostial salpingography. AJR 1991; 157: 77–80

Chapter 51
Ultrasound Markers of Implantation

Luis T Merce

INTRODUCTION

Implantation is the penetration of the embryo in the uterine endometrium. This process is characterized by exclusively taking place during a very specific time period called "implantation window". Between days 19 and 22 of the menstrual cycle a synchronization between the embryo development—in blastocyst stage—and endometrium receptivity occurs.

Current Assisted Reproduction Techniques (ART), especially *in vitro* fertilization (IVF), have made it possible to know the implantation process and the best conditions to get successful outcome. Today we know that the achievement of pregnancy after embryo transfer is closely related to the embryo quality, endometrium receptivity and the transfer technique.

Present it is firmly believed that the increase in pregnancy rates and the decrease of multiple gestations using ART requires a better knowledge of implantation markers. Ultrasonography and Doppler instrumentation offer the possibility to assess uterine and ovarian markers of implantation to use in clinical routine.[1] It is described below that endometrial sonographic and Doppler parameters give us information in reference to the endometrial receptivity and can be used as implantation markers.

ULTRASOUND IMPLANTATION MARKERS

Real time ultrasonography allows us to study mainly two implantation markers: endometrial thickness and endometrial morphological patterns. Ultrasound has also been used to evaluate the action of uterine contractions on the implantation process.[2] Pulsed, color and three-dimensional Doppler assessment are applied to study different variables of uterine and endometrial perfusion that also are used as receptivity factors.[2]

Endometrial Thickness

Endometrial thickness is defined as the maximal distance between the echogenic interfaces of the myometrium and the endometrium when measured on longitudinal plane of the uterus. Significant differences of this thickness have not been observed between

spontaneous and stimulated cycles even using different stimulation protocols.[3] This finding suggests that there is a maximal endometrial response induced by estrogen that is achieved during the natural ovulatory cycle.[4] A significant correlation between the endometrial thickness and endometrial histopathological dating has not been found either.[5]

In IVF stimulated cycles, the endometrium increases 1.9 mm between days 7 and 9 of the stimulation treatment, 0.9 mm between days 9 and 11 and 0.6 mm between the latter and the day of hCG administration.[6] The endometrial thickness grows 0.5 mm per day[7] or does not change until the embryo transfer day.[6] Significant differences have not been observed in the endometrial thickness between hCG day and the day of the embryo transfer,[8] which clearly has practical implications to decide timing to practice this measurement.

Table 51.1: Predictive values of ultra sonographic and Doppler parameters to achieve pregnancy with Assisted Reproduction Techniques

Parameters[1]	*Se*	*Sp*	*PPV*	*NPV*
Endometrial thickness[2]	95–100	3–22	26–45	87–100
Endornetdal pattern[3]	79–100	9–43	32–48	86–100
Uterine Doppler[4]	96400	13–35	44–56	88–100

[1]A11 the values are percentages;
[2]According to different authors, techniques and limits of endometrial thickness, between 6 and 10 mm;
[3]According to different authors and techniques;
[4]For a pulsatility index of uterine arteries between 3 and 3.3 according to different authors and techniques. Se: Sensitivity; Sp: Specificity; PPV: Positive predictive value; NPV: Negative predictive value.

There is not enough data to demonstrate if a linear relationship is established between the endometrial thickness and the probability of pregnancy after an ART.[9] The endometrial thickness ranges in an important number of studied cycles are similar in the cycles that conceived (n= 514; 8.6–11.8 mm) and the ones that did not (n=1110; 8.6–11.9 mm).[9] However in the conception cycles there is an accelerated growth in the endometrial thickness during the luteal phase, that reaches significant differences with regard to the endometrial thickness in non-conception cycles 14 days after the day of oocyte retrieval.[7,10]

As an implantation marker, endometrial thickness is characterized by its significant sensitivity (95%–100%), but also it shows a high number of false positives (78%–97%);[9] so its main advantage is a high negative predictive value (87%–100%) (Table 51.1). An endometrial thickness inferior to 7 mm on the day of hCG administration is considered an acceptable parameter for non-receptive endometrium. It has also been reported that implantation and pregnancy rates are negatively affected with an endometrial thickness of more than 14 mm.[11] On the other hand, a very thin (< 6 mm) or very thick (> 13 mm) endometrium has also been associated with an increase in early miscarriages.

Recently, on donor oocyte program with hormone replacement treatment it has been proven that pregnancy rates decrease as endometrial thickness decreases.[13] When endometrial thickness is equal to or greater than 9 mm a pregnancy rate of 68% is achieved, decreasing to 20% if endometrial thickness was less than 6 mm.[13] Although it is possible to achieve pregnancies with a thin endometrium,[14] this is always a very unfavorable predictive factor that requires further study of the endometrium.[13]

Other parameters have been assessed, such as the length and the width of the endometrium,[6] the endometrial area[15] and more recently the endometrial volume by three-dimensional ultrasound.[16–18] No advantage in using these parameters has been demonstrated over endometrial thickness, although pregnancy rate decreased significantly if endometrial volume is less than 2 ml (Fig. 51.1).[15]

ENDOMETRIAL PATTERN

The endometrial pattern is the relative echogenicity that the endometrium presents with respect to the adjacent myometrium. Its importance as an implantation marker resides in that it reflects the degree of histological development.[19]

During the proliferative phase of menstrual cycle the endometrium takes on “triple line” morphology (Fig. 51.2A) where the echogenic central line represents the uterine cavity, and the outer echogenic lines are caused by the basal layer of the endometrium or the interface between the endometrium and the myometrium. The

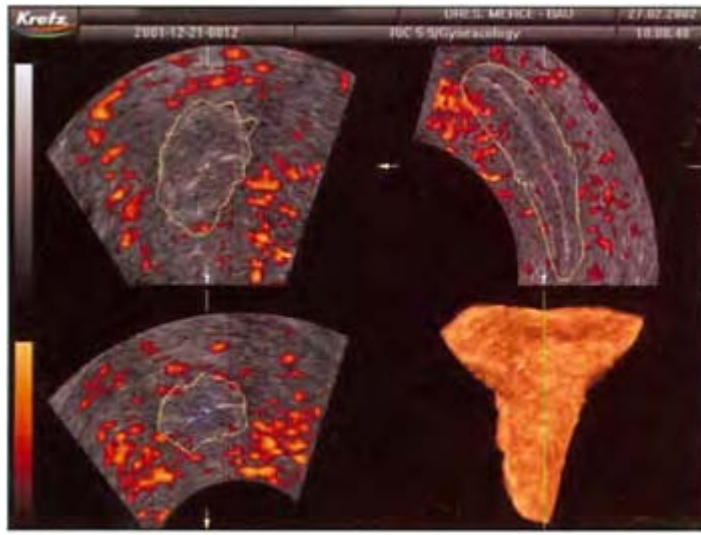

Figure 51.1: Rendering of endometrial volume with three-dimensional ultrasound. In the upper right figure the

endometrial thickness is viewed in a longitudinal plane

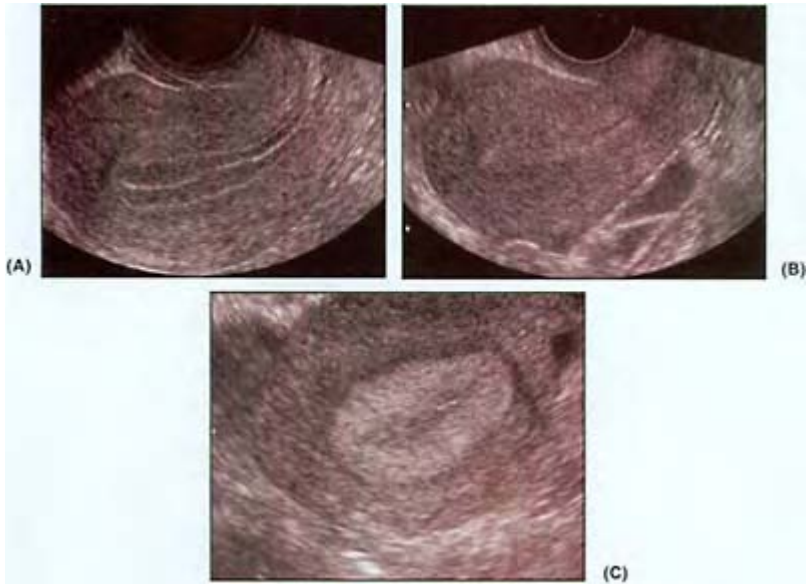

Figures 51.2A to C: Endometrial echogenicity patterns: (A) Multilayered proliferative endometrium or "triple line" pattern; (B) Endometrium non-multilayered and (C) Secretory endometrium

hypoechogenic zones between the outer and central line are the functional layer of the endometrium. This image is attributed to the glandular disposition, reduced secretion and scarce stromal edema.[20]

In the secretory phase of menstrual cycle, the endometrium acquires hyperechogenic morphology (Fig. 51.2C) that is due to stromal edema, spiralization of the endometrial glands and secretion caused by the action of progesterone.[2,6,10,21] However, since a correlation between echogenicity and progesterone has not been demonstrated,[8,22] other factors such as androgen and gonadotropin effect could explain these changes.[23,24]

The subendometrial halo or uterine junctional zone between the endometrium and the myometrium is a distinct compartment of the myometrium composed by comprising tightly packed muscle cells and an increased vascularity.[25]

Although initially four different endometrial echogenicity patterns were described[26] later it was reduced to three,[27] due to it results more predictive to consider a "triple line" pattern as only positive implantation marker (Fig. 51.2B).[28] The endometrial pattern does not appear to be influenced by the ovarian stimulation protocol and this pattern is also present when hormonal replacement for frozen embryo transfer is carried out.[4] Significant differences of the endometrial morphological pattern between hCG day and the transfer day have not been observed either.[8]

A "triple line" endometrium is the ultrasound marker that most precisely reflects endometrial receptivity, while the "non-triple line" pattern is frequently associated with non-conception cycles although the possibility of implantation must never be excluded.[9] Just as in thickness, the "triple line" endometrial pattern has high sensitivity (79–100%) but a high percentage of false positives (57–91%), subsequently its interest also lies in its high negative predictive value (75–100%) (Table 51.1). Although it is possible to achieve pregnancy with a"non-triple line" pattern, frequency is low.[4]

Because the increase in echogenicity during 694 the follicular phase is the endometrial parameter that best indicates low receptivity, an attempt has been made to evaluate this characteristic objectively by computerized analysis of endometrial morphology.[2,10,21,29] During the menstrual cycle, endometrial echogenicity increases significantly in both spontaneous and stimulated cycles,[10,29] but the most important fact is that implantation and pregnancy rates decrease progressively as endometrial echogenicity increases the day of hCG administration.[10,21] Therefore, there is an inverse relationship between the extent of endometrial echogenicity transformation and the possibility of pregnancy.

UTERINE DOPPLER

Doppler studies have demonstrated that uterine and endometrial artery resistance decreases significantly during the mesoluteal phase, i.e. in the period of embryo implantation.[30,36] It is very probable that these vascular changes directly participate during the implantation process because they are present in the embryo nidation from the first moment on. In rodents it has been tested that in 24 hours before establishes contact between the blastocyst and the endometrium an increase of the capillary permeability is produced by local mediation of prostaglandins where the invasion will take place.[37] Between the 6th and 12th post-ovulatory day the endometrium capillaries progressively dilate acquiring a sinusoidal appearance, while the syncytiotrophoblast penetrates the endometrium. Around the llth-12th day the uteroplacental circulation is completely established when maternal blood flows into syncytiotrophoblast lacunae.[38]

Goswany, Williams and Steptoe[39] demonstrated that the blood flow of the uterine arteries conditions IVF success and that uterine receptivity improved increasing perfusion by hormone replacement treatment. Despite many studies since published, there is no consensus on the importance of Doppler studies of these arteries in ART (Fig. 51.3). A substantial group of authors find significant differences in uterine artery

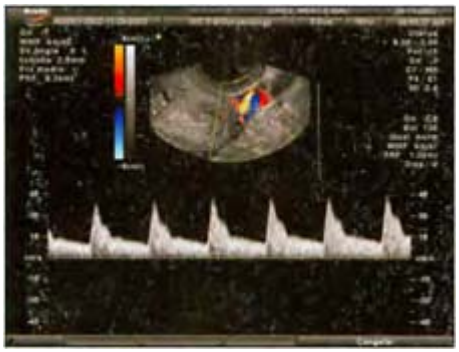

Figure 51.3: Flow velocity waveform of uterine artery on the day of hCG administration

resistance between cycles with or without pregnancy, yet another important group does not observe this difference.[40] These contradictory results are due to clear methodological differences such as the ovarian stimulation protocol used, the cycle day that the Doppler study was carried out or the sonographic examination route.[40]

Optimum uterine receptivity seems to occur when the mean pulsatility index of both arteries is between 2 and 3,[41–43] decreasing significantly the implantation and pregnancy rates when pulsatility is over 3 or 4[41,49] or when diastolic flow is not observed in the Doppler waveform.[48,49] These limits have been proposed as a clinical marker to indicate or not embryo transfer, so that the prediction of uterine receptivity presents high sensitivity (96–100%) and a high negative predictive value (88–100%) although ithas low specificity (13–35%) and positive predictive value (44–56%)[9] (Table 51.1). Inadequate blood flow would thus prevent implantation, although optimal uterine perfusion does not always mean pregnancy. In addition to this, high uterine resistance is observed in less than 10% of non-conception cycles, which suggests that this parameter is responsible for failure in implantation in very few cases.[50]

ENDOMETRIAL DOPPLER

Endometrial Doppler should reflect more appropriately the endometrial perfusion and uterine receptivity because the endometrium is the place where implantation occurs. Additionally, although uterine and endometrial blood flow perform in a similar way during the menstrual cycle, its correlation is weak when are evaluated by velocimetric indices.[51] During the luteal phase, vascular endothelial growth factor (VEGF) expression is increased in the endometrium[52,53] and there is greater angiogenic activity.[54] Recently, a close relationship between a strong VEGF expression in the endometrium and successful outcome of implantation has been demonstrated.[55]

Doppler study permits us to evaluate endometrial blood flow analyzing flow velocity waveforms of subendometrial and endometrial arteries[17,56–60] and color mapping by two-dimensional ultrasound57–59,61–63 or three-dimensional ultrasound.18,64

Vascular resistance of the endometrial spiral arteries or the subendometrial radial arteries (Fig. 51.4), also called intramyometrial subendometrial arteries35,40,58 is found to be decreased on the day of oocyte retrieval or the day of embryo transfer in patients who achieve pregnancy after embryo transfer,18,59 although not all authors can demonstrate this finding.17,57,60 We observed in an intrauterine insemination program58 that the peak systolic velocity of the dominant uterine artery was significantly higher in the mid-luteal phase in the cycles in which pregnancy was achieved. But, in addition to that, subendometrial radial arteries

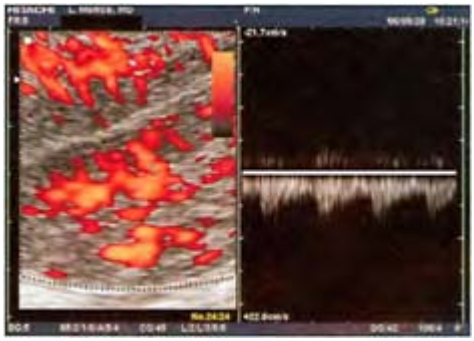

Figure 51.4: Flow velocity waveform of subendometrialendometrial arteries on hCG administration day

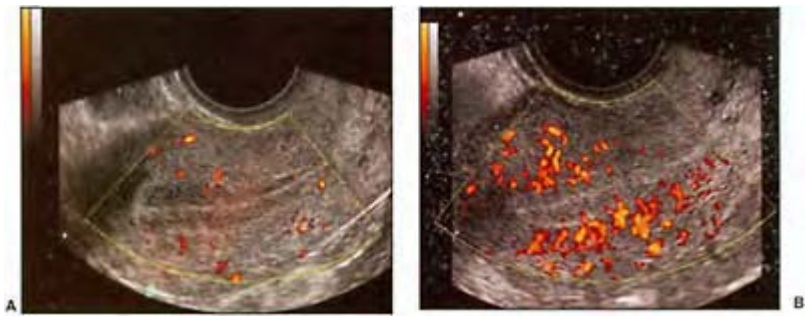

Figures 51.5A and B: Endometrial amplitude mapping Type 0 in which only myometrial vessels can be seen without reaching the

subendometrial halo (A) and endometrial amplitude mapping Type II when color signal reaches the endometrial cavity (B)

pulsatility was the only parameter that improved in those cycles where pregnancy was achieved after a first non-conception cycle, except when implantation failed and abortion or ectopic pregnancy was diagnosed.[40,58]

Color mapping of endometrial vascularity can be classified in various types according to the degree of penetration into the endometrial thickness, using conventional color[57,59,62] or with power Doppler.[61] In this way we can differentiate four types of endometrial blood flow: Type 0 or negative flow, when only surrounding myometrial vessels are seen without reaching the endometrium; Type I or peripheral flow, if the color signal reaches the hyperechogenic outer layer of the endometrium; Type II or intermediate when color mapping occupies the outer half of the endometrial hypoechogenic thickness; and Type III or central flow, if the vessels reach the endometrial cavity invading the entire endometrial thickness (Figs 51.5A and B). Recently, it has been proposed to consider the endometrial and subendometrial area as a whole when the uterine perfusion is assessed by color Doppler, since there is no difference between the endometrial and subendometrial blood flow with respect to the possibility of achieving pregnancy.[63] Nevertheless, color mapping is directly related to the sensitivity of the machine used and an adequate angle of insonation, so it is very important to always use the same characteristics, especially in the minimum velocity recorded. For this reason, power Doppler is more reliable because amplitude mapping can detect lower blood flow velocities and is unaffected by the angle of insonation. In general endometrial color mapping has been evaluated by a subjective way although the color area can also be quantified.[64]

The absence of color mapping at the endometrium and subendometrial myometrium means absolute implantation failure[57] or significant decrease[63] of the implantation rate, while the pregnancy rate increases when the vessels reach the subendometrial halo and endometrium.[57,63] The presence of vessels within the endometrium is associated with a thicker endometrium, which suggests a correlation between the endometrial perfusion and endometrial growth.[63] On the other hand, the absence of endometrial-subendometrial blood flow is accompanied by a high uterine artery resistance.[63] Women with a high endometrial surface flow in power Doppler study have more probability of pregnancy, while below 5 mm^2 it is difficult that implantation will take place even though there is adequate endometrial thickness.[64] We have not found significant differences of

Table 51.2: Uterine receptivity parameters on the day of hCG administration intrauterine insemination and IVF cycles[1]

Parameters	*IUI*		*p*	*IVF*		*p*
	Pregnant (n=10)	*Non-pregnant (n=40)*		*Pregnant (n=10)*	*Non-Pregnant (n=22)*	
ET	10.0±2.8	−10.3±23	ns	14.4±3.1	12.1±2.0	0.02
DPI	2.18±0.81	2.65±0.93	ns	2.18±0.49	2.21±0.44	ns
EF	14±0.9	L5±1.3	ns	3.1±1.2	2.2±1.4	ns
UMI	17±15	18±17	ns	46±18	29±17	0.01

[1] Values indicate mean ± SD; ET: Endometrial thickness in mm; UPI: Mean pulsatility index of both uterine arteries; EF: Endometrial blood flow evaluated by power Doppler mapping according to the following "scoring system": Absent, only miometrial (Type 0)=0; Peripheral (Type I)=1; Intermediate (Type II)=2; Central (Type III) =4; UMI: Uterine implantation index according to formula (ET×EF)+[EMP/UPI-notch], where ET is the endometrial thickness in mm, EF: endometrial flow according to the explained scoring system; EMP: endo-miometrial pattern, whose value is calculated by adding the endometrial pattern score (triple line=3; other types=0) and miometrial pattern (homogeneous=1; non-homogeneous=0); UPI value is the mean pulsatility index of both uterine arteries and uterine "notch" is pointed as present (0) o absent (1).

endometrial thickness, uterine and endometrial blood flow between conception and nonconception cycles after intrauterine insemination. On the contrary, all these parameters present higher values on the day of hCG administration in cycles that achieve pregnancy in an IVF program. Nevertheless only the endometrial thickness and the uterine implantation index—combining ultrasound and Doppler parameters—have significant differences (Table 51.2). When pregnancy is achieved with the absence of endometrial-subendometrial flow on the day of embryo transfer, more than half of these pregnancies end in spontaneous abortion,[63] which suggests that the development of endometrial vessel network should be important for the support of the first stages of pregnancy.

Three-dimensional ultrasound permits study of not only the endometrial volume but also the complete endometrial perfusion (Fig. 51.6).[18,65] Patients that achieve pregnancy have a high flow index on the day of embryo transfer[18] and low on the first day of stimulation.[65] Apparently decreased endometrial perfusion after treatment with agonists facilitates implantation success. In Table 51.3 our preliminary results using this technique are shown.

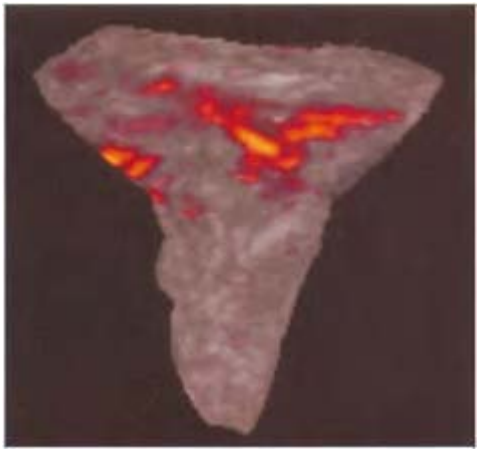

Figure 51.6: Three-dimensional power Doppler of endometrial vascularization on hCG administration day

REFERENCES

1. Mercé LT. Ultrasound markers of implantation. Ultrasound Rev Obstet Gynecol 2002; 2:110–23.
2. Fanchin R. Assessing uterine receptivity in 2001. Ultrasonographic glances at the new millennium. Ann N Y Acad Sci 2001; 943:185–202.
3. Imoedemhe DA, Shaw RW, Kirkland A, Chan R. Ultrasound measurement of endometrial thickness on different ovarian stimulation regimens during in vitro fertilization. Hum Reprod 1987; 2:545–47.

Table 51.3: Ultrasound, color and three-dimension al Doppler parameters in 10 IVF cycles on the day of hCG administration according to outcome[1]

Parameter	*Pregnancy (n=4)*	*Non-pregnancy (n=6)*	*p*
Endometrial thickness, mm	9.9±3.1	13.4±2.0	ns
Endometrial volume, ml	3.5±1.8	6.3±2.9	ns
Endometrial pattern[(2)]	3.01:0.0	2.5±1.2	ns
Endometrial blood flow[(3)]	2.0±1.4	2.0±1.1	ns
Vascularization Index[(4)]	46.20±11.56	38.56±9.19	ns
Flow index[(4)]	34.65±2.14	32.20±1.71	ns

Vaseularization-flow index[4]	15.92±3.44	12.48±3.42	ns

(1) Values indicate mean ±SD; (2) Endometrial pattern was quantified according to “triple line” pattern (3) or any other pattern (0); (3) Endometrial blood flow was evaluated by color mapping with power Doppler according to the next scoring system: absent, only miometrial (Type 0)=0; Peripheral (Type I)=1; Intermediate (Type II)=2; Central (Type III)=4; (4) All values are units

4. Tan SL, Biljan MM. Selection of candidates for in vitro fertilization based on color Doppler findings. In: Kupesic S, De Ziegler D (Eds). Ultrasound and Infertility. London: The Parthenon Publishing Group 2000; 155–68.
5. Li TC, Nuttall L, Klentzeris L, Cooke ID. How well does ultrasonographic measurement of endometrial thickness predict the results of histological dating?. Hum Reprod 1992; 7:1–5.
6. Bassil S. Changes in endometrial thickness, width, length and pattern in predicting pregnancy outcome during ovarian stimulation in in vitro fertilization. Ultrasound Obstet Gynecol 2001; 18:258–63.
7. Rabinowitz R, Laufer N, Lewin A, Navot D, Bar I, Margalioth EJ, Schenker JJ. The value of endometrial measurement in the prediction of pregnancy following in vitro fertilization. Fertil Steril 1986; 45:824–28.
8. Khalifa E, Brzyski RG, Oehninger S, Acosta AA, Muasher SJ. Sonographic appearance of the endometrium: the predictive value for the outcome of in vitro fertilization in stimulated cycles. Hum Reprod 1992; 7:677–80.
9. FriedlerS, Schenker JG, Herman A, Lewin A. The role of ultrasonography in the evaluation of endometrial receptivity following assisted reproduction treatments: a critical review. Hum Reprod Update 1996; 2:323–35.
10. Leibovitz Z, Grinin V, Rabia R, Degani S, Shapiro I, Tal J et al. Assessment of endometrial receptivity for gestation in patients undergoing in vitro fertilization, using endometrial thickness and the endometriummyometrium relative echogenicity coefficient. Ultrasound Obstet Gynecol 1999; 14:194–99.
11. Weissman A, Gotlieb L, Casper RE The detrimental *im* effect of increased endometrial thickness on implantation and pregnancy rates and outcome in an in vitro fertilization program. Fertil Steril 1999; 1:14749.
12. Dickey RP, Olar TT, Curole DN, Taylor SN, Rye PH. Endometrial pattern and thickness associated with pregnancy outcome after assisted reproduction technologies. Hum Reprod 1992; 7:418–21.
13. Noyes N, Hampton BS, Berkeley A, Licciardi F, Grifo J, Krey L. Factors useful in predicting the success of oocyte donation: a 3-year retrospective analysis. Fertil Steril 2001; 76:92–97.
14. Remohf J, Ardiles G, Garcia-Velasco, JA, Gaitan P, Simon C, Pellicer A. Endometrial thickness and serum oestradiol concentrations as predictors of outcome in oocyte donation. Hum Reprod 1997; 12:2271–76.
15. Turnbull LW, Rice CF, Horsman A, Robinson J, Killik SR. Magnetic resonance imaging and transvaginal ultrasound of the uterus prior to embryo transfer. Hum Reprod 1994; 9:2438–43.
16. Raga F, Bonilla-Musoles F, Casan EM, Klein O, Bonilla F. Assessment of endometrial volume by threedimensional ultrasound prior to embryo transfer: clues to endometrial receptivity. Hum Reprod 1999; 14: 2851–54.
17. Schild RL, Knobloch C, Dorn C, Fimmers R, van der Ven H, Hansmann M. Endometrial receptivity in an in vitro fertilization program as assessed by spiral artery blood flow, endometrial thickness, endometrial volume, and uterine artery blood flow. Fertil Steril 2001; 75:31–36.
18. Kupesic S, Bekavac I, Bjelos D, Kurjak A. Assessment of endometrial receptivity by transvaginal color Doppler and three-dimensional power Doppler ultrasonography in patients undergoing in vitro fertilization procedures. J Ultrasound Med 2001; 20:125–34.

19. Grunfeld L, Walker B, Bergh PA, Sandier B, Hofmann G, Navot D. High-resolution endovaginal ultrasonography of the endometrium: a non-invasive test for endometrial adequacy. Obstet Gynecol 1991; 78:200–04.
20. Parsons AK, Parada C, Parsons M, Mastry M. Ultrasound correlation with endometrial histology. Presented at the Society of Gynecologic Investigation, 38th Annual Meeting, San Antonio, Texas, March 20–23, 1991 Abstract 560; 378.
21. Fanchin R, Righini C, Ayoubi JM, Olivennes F, de Ziegler D, Frydman R. New look at endometrial echogenicity: objective computer-assisted measurements predict endometrial receptivity in in vitro fertilization-embryo transfer. Fertil Steril 2000; 74:274–81.
22. Bakos O, Lundvist O, Bergh T. Transvaginal sonographic evaluation of endometrial growth and texture in spontaneous ovulatory cycles—a descriptive study. Hum Reprod 1993; 8:799–806.
23. Tang B, Gurpide E. Direct effect of gonadotropins on decidualization of human endometrial stroma cells. J Steroid Biochem Mol Biol 1993; 47:115–21.
24. De Ziegler D, Fanchin R. Endometrial receptivity in controlled ovarian hyperstimulation (COH): the hormonal factor. In: Bulletti C, Gurpide E, Flagmini C (Eds). The Human Endometrium. Ann N Y Acad Sci 1994; 734:209–20.
25. Tetlow RL, Richmond I, Manton DJ, Greenman J, Turnbull LW, Killick SR: Histological analysis of the uterine junctional zone as seen by transvaginal Ultrasound. Ultrasound Obstet Gynecol 1999; 14:188–93.
26. Smith B, Porter R, Ahuja K, Craft I. Ultrasonic assessment of endometrial changes in stimulated cycles an in vitro fertilization and embryo transfer program. J In Vitro Fertil Embryo Transf 1984; 1:233–38.
27. Gonen Y, Casper RF. Prediction of implantation by the sonographic appearance of the endometrium during controlled ovarian stimulation for in vitro fertilization (IVF). J In Vitro Fertil Embryo Transf 1990; 7:146–52.
28. Sher G, Herbert C, Maassarani G, Jacobs MH. Assessment of the late proliferative phase endometrium by ultrasonography in patients undergoing in-vitro fertilization and embryo transfer (IVF/ET). Hum Reprod 1991; 6:232–37.
29. Leibovitz ZS, Degani R, Rabia R. Endometrium-tomyometrium relative echogenicity coefficient. A new sonographic approach for the quantitative assessment of endometrial echogenicity. Gynecol Obstet Invest 1998; 45:121–25.
30. Scholtes MCW, Wladimiroff JW, van Rijen HJM, Hop WCJ. Uterine and ovarian flow velocity waveforms in the normal menstrual cycle: a transvaginal study. Fertil Steril 1989; 52:981–85.
31. Sladkevicius P, Valentin L, Marsal K. Blood flow velocity in the uterine and ovarian arteries during the normal menstrual cycle. Ultrasound Obstet Gynecol 1993; 3:199–208.
32. TanSL, Zaidi J, Campbell S, Doyle P, Collins W. Blood flow changes in the ovarian and uterine arteries during the normal menstrual cycle. Am J Obstet Gynecol 1996; 175:625–31.
33. Bourne TH, Hagstrom HG, Granberg S, Josefsson B, Hahlin M, Hellberg P et al. Ultrasound studies of vascular and morphological changes in the human uterus after a positive self-test for the urinary luteinizing hormone surge. Hum Reprod 1996; 11:369–75.
34. Agrawal R, Conway GS, Sladkevicius P, Payne NN, Bekir J, Campbell S et al. Serum vascular endothelial growth factor (VEGF) in the normal menstrual cycle: association with changes in ovarian and uterine Doppler blood flow. Clin Endocrinol (Oxf) 1999; 50: 101–06.
35. Merce LT. Doppler de los cambios ovaricos y endometrialespreimplantatorios. In: KurjakA, Carrera JM (Eds). Ecografia en Medicina Materno-Fetal. Barcelona: Masson, 2000; 87–104.
36. Kupesic S, Merce LT, Zodan T, Kurjak A. Normal and abnormal corpus luteum function. In: Kupesic S, de Ziegler D (Eds). Ultrasound and Infertility. Lanes: The Parthenon Publishing Group, 2000; 67–76.
37. Psychoyos A, Martel D. Embryo-endometrial interactions at implantation. In: Edwards RG, Purdy JM, Steptoe PC (Eds). Implantation of the human embryo. London: Academic Press, 1985; 197–219.

38. Czyba JC, Montella A. Les deux premieres semaines du developpemnet embryonnaire. In: Czyba JC, Montella A (Eds). Biologie de la reproduction humaine. Montpellier: Sauramps medical, 1993; 217–28.
39. Goswany RK, Williams G, Steptoe PC. Decreased uterine perfusion-a cause of infertility. Hum Reprod 1988; 8:955–59.
40. Merce LT. Estudio Doppler de la implantacion y placentacion inicial. In: Kurjak A, Carrera JM (Eds). Ecografia en Medicina Materno-Fetal. Barcelona: Masson, 2000; 113–36.
41. Steer CV, Campbell S, Tan SL, Crayford T, Mills C, Mason BA, Collins WP The use of transvaginal color flow imaging after in vitro fertilization to identify optimum uterine conditions before embryo transfer. Fertil Steril 1992; 57:372–76.
42. Zaidi J, Pittrof R, Shaker A, Kyei-Mensah A, Campbell S, Tan SL. Assessment of uterine artery blood flow on the day of human chorionic gonadotropin administration by transvaginal color Doppler ultrasound in an in vitro fertilization program. Fertil Steril 1996; 65:37781.
43. Tsai Y-C, Chang J-C, Tai M-J, Kung F-T, Yang L-C, Chang S-Y. Relationship of uterine perfusion to outcome of intrauterine insemination. J Ultrasound Med 1996; 15:633–36.
44. Coulam CB, Bustillo M, Soenksen DM, Britten S. Ultrasonographic predictors of implantation after assisted reproduction. FertilSteril 1994; 62:1004–10.
45. Coulam CB, Stern JJ, Soenksen DM, Britten S, Bustillo M. Comparison of pulsatility indexes on the day of oocyte retrieval and embryo transfer. Hum Reprod 1995; 10:82–84.
46. Bustillo M, Krysa LW, Coulam CB. Uterine receptivity in an oocyte donation programme. Hum Reprod 1995; 10:442–45.
47. Havre R, Bettahar K, Grange G, Ohl J, Arbogast E, Moreau L, Dellenbach P. Predictive value of transvaginal uterine Doppler assessment in an in vitro fertilization program. Ultrasound Obstet Gynecol 1993; 3:350–53.
48. Tekay A, Martikainen H, Jouppila P The clinical value of transvaginal colour Doppler ultrasound in assisted reproductive technology procedures. Hum Reprod 1996; 11:1589–91.
49. Deichert U, Albrand-Thielman C, van de Sandt M. Doppler-sonographic pelvic blood flow measurements and their prognostic value in terms of luteal phase and implantation. Hum Reprod 1996; 11:1591–93.
50. Caccitore B, Simberg N, Fusaro P, Tiitinen A. Transvaginal Doppler study of uterine artery blood flow in in-vitro fertilization-embryo transfer cycles. Fertil Steril 1996; 66:130–34.
51. Dickey RP Doppler ultrasound investigation of uterine and ovarian blood flow in infertility and early pregnancy. Hum Reprod Update 1997; 3:467–503.
52. Torry DS, Holt VJ, Keenan JA, Harris G, Caudle MT, Torry RJ. Vascular endothelial growth factor expression in cycling human endometrium. Fertil Steril 1996; 66: 72–80.
53. Shifren JL, Tseng JF, Zaloudek CJ, Ryan IP, Meng IG, Ferrara N, Jaffe RB, Taylor RN. Ovarian steroid regulation of vascular endothelial growth factor in the human endometrium;implications for angiogenesis during the menstrual cycle and in the pathogenesis of endometriosis. J Clin Endocrinol Metab 1996; 81: 3112–18.
54. Rogers P, Abberton K, Susil B. Endothelial cell migra¬ tory signal produced by human endometrium during the menstrual cycle. Hum Reprod 1992; 7:1061–66.
55. Jinno M, Ozaki T, Iwashita M, Nakamura Y, Kudo A, Hirano H. Measurement of endometrial tissue blood flow: a novel way to assess uterine receptivity for implantation. Fertil Steril 2001; 76:1168–74.
56. Achiron R, Levran D, Sivan E, LipitzS, Dor J, Mashiach S. Endometrial blood flow response to hormone replacement therapy in women with premature ovarian failure: a transvaginal Doppler study. Fertil Steril 1995; 63:550–54.
57. Zaidi J, Campbell S, Pittrof R, Tan SL. Endometrial thickness, morphology, vascular penetration and velocimetry in predicting implantation in an in vitro fertilization program. Ultrasound Obstet Gynecol 1995; 6:191–98.

58. Merce LT, Moreno C, Bau S. Assessment of luteal and peri-implantation blood flow with color Doppler in A.I.H. In: Abstract Book of ESHRE Symposium on Reproductive Medicine. Valencia, 9–11 March, 1995; 12
59. Battaglia C, Artini PG, Giulini S, Salvatori M, Maxia N, Petraglia F et al. Colour Doppler changes and thromboxane production after ovarian stimulation with gonadotrophin-releasing hormone agonist. Hum Reprod 1997; 11:2477–82.
60. Yuval Y, Lipitz S, Dor J, Achiron R. The relationships between endometrial thickness, and blood flow and pregnancy rates in in-vitro fertilization. Hum Reprod 1999; 14:1967–71.
61. Merce LT. Aplicaciones del Doppler color en Reproduction. IV Curso Teorico-Practico sobre Doppler en Ginecologia, Obstetricia y Ecocardiograffa fetal. Barcelona, 2–4 de mayo, 2002.
62. Applebaum M. The Menstrual Cycle, Menopause, Ovulation Induction, an In Vitro fertilization. In: Copel JA, Reed KL (Eds). Doppler Ultrasound in Obstetrics and Gynecology. New York: Raven Press, 1995; 71–86.
63. Chien LW, Au HK, Chen PL, Xiao J, Tzeng CR. Assessment of uterine receptivity by the endometrialsubendometrial blood flow distribution pattern in women undergoing in vitro fertilization-embryo transfer. Fertil Steril 2002; 78:245–51.
64. Yang J-H, Wu M-Y, Chen C-D, Jiang M-C, Ho H-N, Yang Y-S. Association of endometrial blood flow as determined by a modified colour Doppler technique with subsequent outcome of in-vitro fertilization. Hum Reprod 1999; 14:1606–10.
65. Schild RL, Holthaus S, d'Alquen J, Fimmers R, Dorn C, van der Ven H, Hansmann M. Quantitative assessment of subendometrial blood flow by threedimensional-ultrasound is an important predictive factor of implantation in an in-vitro fertilization programme. Hum Reprod 2000; 15:89–94.

Chapter 52
Sonohysterography and Sonohysterosalpingography: A Text-atlas of Normal and Abnormal Findings

Sanja Kupesic, Asim Kurjak, Drazena Bjelos

Fallopian Tube

The number of cases of tubal sterility is increasing and tubal factors, such as tubal dysfunction or obstruction, account for approximately 35% of the causes of infertility.[1,2] A history of pelvic inflammatory disease (PID), septic abortion, intrauterine contraceptive device use, ruptured appendix, tubal surgery, or ectopic pregnancy should alter the physician to the possibility of tubal damage. One aspect of the infertility investigation, which has changed little over the last 20 years, is that of the assessment of Fallopian tube patency. Until now, the most frequently used procedures to demonstrate tubal patency have been X-ray hysterosalpingography (HSG) and chromopertubation during laparoscopy.[3]

Hysteroscopy is a technique, which complements hysterosalpingography. It can accurately differentiate between endometrial polyps and submucous leiomyomas and can be used for their treatment. The same method is useful in establishing the definitive diagnosis and treatment of intrauterine adhesions and some congenital anomalies of the uterus. Risk factors include perforation of the uterus, hemorrhage, infection and eventually anesthetic risk if anesthesia is required.

Hysteroscopy-directed falloposcopy can detect obstruction of the tubal ostium, and can be utilized to examine the entire length of the tubal lumen.[4] Treatment of the proximal tubal obstruction can immediately follow the diagnosis. Transcervical tubal cannulation or balloon tuboplasty performed by hysteroscopic approach are the methods of choice.[5]

Laparoscopy has been used as the gold standard for investigation of the luteal status in the last two decades, but it requires a general anesthesia and carries the risk of surgical complications, such as bowel or vascular injury, hemorrhage, infection, anesthetic risk, false pneumoperitoneum and postoperative discomfort. With a Jarcho-type of cannula placed in the uterine cavity, one can manipulate the uterus, and by instilling indigo-carmine saline, or other tinted saline, can test for tubal competence. Through laparoscopy one is equally able to visualize the total pelvic anatomy and the upper abdominal cavity.

It is also useful for evaluation of the ovarian disease, genital anomalies, tubal and adnexal competence and to differentiate between pelvic distortions. Furthermore, it is valuable to reach an accurate classification of endometriosis of the pelvis. Laparoscopy can be used as an adjunct in assessing possible causes of pelvic pain, the extent of pelvic neoplasia, as well as for a prognostic review of the previous infertility surgical procedure. It has also been helpful in obtaining peritoneal washings and cultures in patients with positive history of PID.

Ultrasound imaging of the pelvic organs has improved significantly with the use of highfrequency vaginal ultrasound probes where the need for bladder filling can be avoided. The normal Fallopian tube is usually not seen by vaginal sonography unless some fluid surrounds

Table 52.1: The accuracy of sonohysterosalpingography (sonoHSG) compared to X-ray HSG

Authors (year)	*Total number*	*Accuracy N (%)*	*Sensitivity (%)*	*Specificity (%)*
Richman et al (1984)[13]	36		100%	96%
Peters and Coulam (1991)[6]	27	19 (70.37)	–	–
Volpi et al (1991)[7]	21	19 (92.20)	–	–
Stem et al (1992)[8]	89	72 (80.90)		
Battaglia et at (1996)[31]	60	52 (86.66)		

it. The contrasting fluid may *be* one of the following: the normal serous fluid, follicular fluid during or after ovulation, blood, ascitic fluid, or products of an exudative or infectious process. If the Fallopian tube is not filled with fluid its lumen cannot be detected.

Sonohysterography (SHG) of the uterine cavity and sonohysterosalpingography (sonoHSG) of the tubes are informative variations of hysterosalpingography (HSG), a standard radiographic technique for studying the reproductive lumina outlined by transcervical infusion of the iodinated contrast under fluoroscopic observation. When sonographic evaluation of the uterine lumen with contrast is combined with evaluation of the tubes, this procedure can be termed sonohysterosalpingography, or sono-HSG. Sonohysterography has also been called hysterosonography and saline infusion Sonohysterography.

Benefits of sonohysterosalpingography (sonoHSG) are: avoidance of the ionization or idiosyncrasy to contrast media, method is easily repeatable, requires intraprocedural active participation of the patient (increases her knowledge of tubal status), is a dynamic procedure analyzing tubal motility, the procedure course may be stored, reviewed, analyzed and interpreted to the infertile couple using video-recorder, anesthesia is not required and also collaboration with the Radiology Department.

The accuracy of sonoHSG compared to X-ray HSG varies from 70.37% to 92.20% according Ttor to Peters et al[6] and Volpi et al[7] (Table 52.1). The

Table 52.2: The accuracy of sonoHSG compared to chromopertubation

Authors (year)	*Total number*	*Accuracy (%)*
Allahbadia et al (1993)[33]	27	25 (92.59)
Tdfekci et al (1992)[20]	38	37 (97.37)
Peters and Coulam (1991)[6]	58	50 (86.20)
Kupesic et al (1994)[9]	47	43 (91.48)
Stern et al (1992)[8]	121	99 (81.82)
Deichcrt et al (1992)[10]	16	16 (100.00)
Volpi et al (1996)[7]	29	24 (82.7)
Battaglia (1996)[31]	60	56 (93133)
Raga (1996)[36]*	42	39 (92)
Sladkevicius (200G)[39]*	67	
Jeanty (2000)[30]	115	91 (79.4)
Kiyokawa (2000)[42]*	25	

* three-dimensional hysterosonosalpingography

accuracy of sonoHSG compared to chromopertubation is from 81.82% according to Stern et al,[8] 91.48% Kupesic et al[9] to 100.00% according to Deichert et al (Table 52.2).[10]

HISTORICAL DEVELOPMENT OF THE ULTRASONIC ASSESSMENT OF THE FALLOPIAN TUBE

In 1954, Rubin[11] the first attempt by insufflating the Fallopian tubes.

Ultrasound visualization of the internal genital tract using exogenous contrast media was first described by Nanini et al, Richman et al and Randolph et al[12–14] who performed abdominal sonography after intracervical injection of the fluid.

Richman and colleagues[13] were the first to report on the transabdominal sonographic evaluation of tubal patency. In their studies they used a special intrauterine catheter, Harris uterine injector (Unimar, Canoga Park, CA). After injection of at least 20 ml of the ultrasonic contrast medium Hyskon (dextron in dextrose; Pharmacia Laboratories, Piscataway, NJ), the accumulation of the fluid in the cul-de-sac has been accepted as an indicator of tubal patency.

Randolph and co-workers[14] used transabdominal ultrasound for observation of the cul-de-sac after the injection of 200 ml isotonic saline through the Rubin cannula. The presence of retrouterine fluid was accepted as a criterion for patency of one or both tubes. Tubal patency was deduced indirectly from the presence of increasing fluid in the pouch of Douglas, without differentiation of the sides.

Following instillation of dextran or saline solution into the uterine cavity it was possible to visualize lesions such as submucous myomas and polyps by sonography and subsequently to confirm their presence by hysteroscopy. Although lesions of this type, which project into the uterine cavity, are clearly delineated by poorly echogenic or anechoic media, very small hollow cavities, such as the lumen of normal tubes, are rarely visualizable using these techniques.[13,15] Their demonstration requires visualization of the movement of a fluid, which in turn requires the use of a highly echogenic medium.[16–18]

A new transvaginal ultrasonographic technique was developed in 1989 by Deichert and colleagues.[19] They visualized the patent tube directly and hence showed tubal patency by transcervical injection of an echogenic and ultrasonic contrast fluid SHU 454 (Echovist; Schering, Berlin, Germany). The method has been called Hy-Co-Sy: transvaginal hysterosalpingocontrast-sonography. They used Rubin cannula or a bladder catheter no. 8.

Tiifekci and co-workers[20] have developed an easier technique in which the patient does not require hospitalization. By intrauterine injection of isotonic saline, they evaluated tubal patency directly and called this method transvaginal sonosalpingography.

Transvaginal sonosalpingography performed by using isotonic saline without anesthesia is physiological, easy to perform, safe, cost-effective, non-invasive and more convenient when compared with other conventional methods. Idiosyncrasy to the contrast agent cannot be expected.

ULTRASOUND CONTRAST AGENTS

All media having a different echogenicity from that of the human body can be used as contrast media. Contrast media are divided into two groups: hypoechogenic and hyperechogenic media.

Isotonic saline, Ringer or dextran solutions belong to the first group. Instillation of these media facilitates the detection of echogenic border surfaces. The main disadvantage is that it is not possible to visualize the phenomena of motion and flow.

Hyperechogenic contrast media enhances echo signals, allowing detection of the flow by both B-mode and Doppler ultrasound. Gramiak and Shah[21] and Meltzer and co-workers[22] found that small gas bubbles effectively reflect ultrasonic waves. Therefore, all the commercial echo contrast media contain microbubbles. Commercial products Echovist and Levovist (Schering AG, Berlin) represent suspension of microbubbles made of special galactose microparticles. Galactose microparticle granules are suspended either in galactose solution (Echovist) or in a sterile water (Levovist).[23]

Echovist (SHU 454) is an ultrasound contrast medium consisting of a suspension of only monosaccaride microparticles (50% galactose, diameter 2 mm), in a 20% aqueous solution of galactose (w/v). The echogenic suspension is reconstituted immediately before the use from granules and a vehicle solution (200 mg micro-particles in 1 ml of suspension).[24] This contrast medium has been licensed for gynecological applications on the market in 1995.

Levovist (SHU 508) microparticle granules contain in addition a very low concentration of physiological palmitic acid.

A few minutes before use, the granules have to be shaken vigorously for 5–10 seconds to be dissolved by an appropriate volume of aqueous galactose solution (Echovist) or

sterile water (Levovist). A milky suspension of galactose microparticles in a solution is created after disaggregation of the microparticle “snowball”. The suspension of Echovist is stable for about 5 minute after preparation. Due to its extended stability, Levovist may be administered up to 10 minute after the suspension procedure. Depending on the indication and the imaging modality (B-mode or Doppler), clinically adequate suspension of Echovist are with concentrations of 200 and 300 mg/ml. For Levovist, the maximum concentration is 400 mg/ml. The predominant limitation at concentrations lower than 200 mg/ml is the decreasing suspension stability. Concentrations exceeding 400 mg/ml are limited by a rapid increase of viscosity.

After intrauterine administration and emergence of Echovist from the fimbriae into the pelvis, the galactose microparticles dissolve. Warming to body temperature and dilution by the peritoneal fluid increases this progress. *In vitro*, a rise in temperature of the Echovist suspension to 37°C leads to complete dissolution within 30 minute. The dissolved galactose is subsequently absorbed and metabolized.

Numerous clinical studies in the field of echocardiography, venous vascular system analysis and HSG showed no evidence of serious side effects.

Absolute contraindication for instillation of these fluids is galactosemia (autosomal recessive disease in which, due to deficiency of galactose1-phosphate uridyltransferase, galactose cannot be metabolized into glucose).

In addition, ultrasound contrast agents are media which when administered via the vascular system or into body cavities, change the acoustic properties of the body region under investigation. The acoustic parameters, which contribute to tissue imaging by conventional sonographic units, are backscatter, attenuation and velocity of sound. Enhancement of backscatter is the most important contrast effect, since contrast agents introduce acoustic inhomogenities caused by microstructures (scatterers).

TECHNIQUE OF HY-CO-SY

Requirements

A case history must be obtained from a woman considered for examination using this technique, to rule out the possibility of the rare condition of galactosemia, which is the only absolute contraindication, apart from acute inflammatory disease of the genital organs. A gynecological and ultrasound examination prior to the procedure is necessary to define uterine position and anomalies if present, as well as both adnexal regions. Before any intervention, we perform a pregnancy test for legal reasons. The possibility of local or systemic infections is excluded by clinical examination (absence of elevated temperature), inspection of the genital tract and cervical smears. The procedure should not be performed on patients with active pelvic infections, and antibiotic prophylaxis (doxycycline and metronidazole) should be used in patients with a history of Hy-Co-Sy should be performed during the early follicular phase of the menstrual cycle, after complete cessation of menses. This avoids dispersion of menstrual debris into the peritoneal cavity. Procedures done in this period allow absorption of the media prior to ovulation, thus avoiding the presence of a foreign substance around the time of an imminent corpus luteum. This decreases any theoretic effect the media may have on tubal transport. Hysterosalpingography performed during the immediate premenstrual phase of

the cycle has been advocated in the evolution of possible cervical incompetence, as that is the point in the cycle at which there is the maximum uterine constriction. Therefore, in order to maximize the information obtained, the indication for the study has an influence on timing.

Patients are informed of the benefits and the possible risks of the procedure and the procedure itself is described to them in detail.

Anesthesia is generally not required for Hy-Co-Sy, and the patient can follow the results of the examination by herself on the monitor. If Hy-Co-Sy is performed without anesthesia, patients occasionally report discomfort, especially if the tubes are occluded. The degree of discomfort depends on the individual response of the patient. Premedication or sedation is routinely used: 5–10 mg of diazepam intravenously is beneficial, especially in anxious patients. Pain signifies the obstruction and potential intrayasation or tubal rupture, and should not be masked by anesthesia. However, tubal spasm may occur if Hy-Co-Sy is performed without or even with anesthesia. This could mimic a tubal occlusion. Pretreatment with atropine (0.5 mg) may prevent this complication. The parenteral administration of 1 mg glucagon may relieve the spasm and allow the flow of the contrast.

Procedure

The patient voids and is positioned supine on the gynecological table. With the patient's legs flexed, a speculum is inserted into the vagina and positioned such that the entire cervix is visualized and the os is easily accessible. The cervix and the vagina are then thoroughly scrubbed with Betadine solution. A tenaculum is placed on the anterior lip of the cervix, and the cannula is gently guided into the endocervical canal. Application of the contrast medium is performed via a small and very thin uterine catheter fitted with a balloon for stabilization and occlusion of the internal cervical os. The first observation to be made is of the uterine cavity, with verification of the catheter placement. After removal of the tenaculum, the transvaginal probe is gently introduced into the posterior fornix of the vagina. The contrast (sterile saline) is then injected slowly, under control of the ultrasound. Usually, no more than 5–10 ml of contrast is instilled into the uterine cavity. At this stage one can observe the morphology of the uterus and its endometrial lining and detect duplication anomalies of the uterus or existence of endometrial polyps or submucous fibroids that are protruding into the uterine cavity which is marked with anechoic contrast.

Benefits of sonoHSG include: reproducible and reliable assessment of tubal patency if used by a trained physician, avoids exposure to X-rays, allergic reactions and general anesthesia, it can be performed as outpatient procedure, is well tolerated, rapid and shows tubal patency to the patient in "real time". Limitations include: tubal spasm may lead to misdiagnosis of tubal occlusion (spasm also seen with other methods), tubal flow may give a false impression of tubal patency in hydrosalpinx, cannot visualize intrapelvic pathology and bowel, requires a degree of technical competence and 10–20 investigations are needed to acquire the new technique.

Benefits and limitations of hysterosonosalpingography are represented in Table 52.3.

GRAY SCALE HY-CO-SY (B-MODE)

Deichert and colleagues[10,25] evaluated transvaginal Hy-Co-Sy for the assessment of tubal patency with gray scale imaging (B-mode) and additional use of pulsed wave Doppler. During the last stages of the examination the ultrasound contrast medium, Echovist is prepared. The uterine cavity, which in most cases will still be dilated by the Ringer's solution instilled previously, is slowly filled with the echogenic ultrasound contrast medium. If the tube is patent, constant flow in a pattern resembling a point, spot or streak is seen. Further intermittent injections of volumes of 1–2 ml, given slowly and continuously, with further lateral sweeps of the US probe, allow visualization of intraluminal or intratubal flow under normal anatomical conditions via the pars intramuralis into the medial and distal segments of the tubes. For the diagnosis of tubal patency, two or three observation phases per tube are needed, with an

Table 52.3: Benefits and limitations of sonoHSG

Benefits	*Limitations*
• Reproducible and reliable assessment of tubal patettcy if usedby a trained physician	• Tubal spasm may lead to misdiagnosis of tubal occlusion (spasm also seen with other methods)
• Avoids exposure to X-rays	• In hydrosalpinx, tubal flow may give a false impression of tubal patency
• Avoids allergic reactions	
• Avoids general anesthesia	• Cannot visualise intrapelvic pathology and bowel
• Can be performed as outpatient procedure	
• Rapid	• Requires a degree of technical competence
• Well tolerated: little discomfort and few adverse events	• 10–20 investigations needed to acquire the new technique
• Shows tubal patency to the patient in "real time"	

observation period of continuous flow of about 10 seconds (while contrast medium is slowly injected). Although visualization of a longer segment of the tube beyond the pars intramuralis is convincing for tubal patency, one should carefully examine the adnexal regions for filling of the distal segments of the tube to exclude sactosalpinx. Examination of the pouch of Douglas for any increase in retrouterine fluid, compared with the picture at the start of the examination, completes the examination procedure.

PULSED DOPPLER ANALYSIS OF TUBAL PATENCY

Deichert and colleagues advise to confirm the findings using pulsed wave Doppler scanning, if the examination in B-mode reveals evidence suggesting tubal occlusion or if it is only possible to visualize a segment of tube of less than 2 cm in length.[10,25] After the Doppler gate has been positioned over the area to be examined, the gate width is reduced

to measure only the flow noise from the pertubation and not vascular or other noise. Brief injections (about 5 sec) of contrast medium are made again. The sounds heard, which are long, drawn-out and initially hissing, and the simultaneous visualization of a broad noise band on the monitor, the width of the band that slowly decreases after injection, indicate that the tube is patent. Thus unobstructed flow is characterized by a short filling phase with a rapid, steep increase foe in Doppler shift and a slow, uniform fall in Doppler shift along the time axis, indicating unobstructed free distal outflow. The absence of these acoustic signals or optical tracings indicates obstruction of tubal flow or tubal occlusion. In this case there is only a short, steep Doppler shift with no subsequent noise signals. This indicates an absence of outflow of contrast medium distal to the Doppler gate. A sonographic finding of unobstructed tubes on the basis of noise band in pulsed wave Doppler sonography is more impressive than that of a shorter segment of tube in standing B-mode.

Deichert and colleagues tried to determine whether the additional use of pulsed wave Doppler can improve the tubal diagnosis reached with gray scale imaging in doubtful cases.[10] They studied 17 patients with diagnosed sterility problems. Hysterosalpingo-contrast sonography by gray scale and by pulsed wave Doppler and follow-up chromolaparoscopy (n = 16) or HSG (n = 1) were performed. The diagnostic efficacies of gray-scale and pulsed wave Doppler were compared with each other and with a conventional control procedure (chromolaparoscopy or HSG). The gray scale findings were confirmed by pulsed wave Doppler in five cases on one side; confirmed by pulsed wave Doppler in seven cases on both sides; corrected by pulsed wave Doppler in one case on one side and confirmed on the other side by pulsed wave Doppler. In all 17 cases, the tubal findings after pulsed wave Doppler were confirmed by chromolaparoscopy or HSG. The additional use of pulsed wave Doppler in Hy-Co-Sy is recommended as a supplement to gray scale

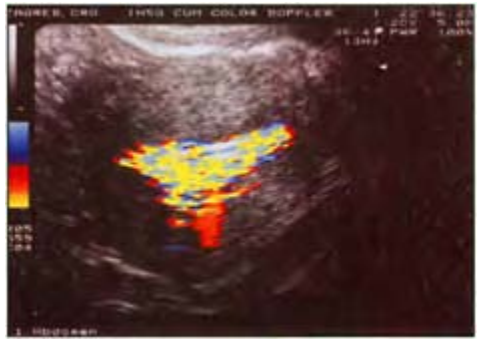

Figure 52.1: Transvaginal color Doppler scan of the uterus after injection of the isotonic saline solution. The triangular uterine cavity is clearly

outlined by color flow imaging

imaging in cases of suspected tubal occlusion and in the event of intratubal flow demonstrable only over a short distance.

Deichert assessed tubal patency, using Hy-Co-Sy, conventional HSG or laparoscopy with dye, in 76 women and visualized 152 Fallopian tubes.[25] In this study, Hy-Co-Sy showed 87.5% concordance with other techniques, predicted 100% of tubal occlusions and detected 86% of patent tubes.

According to Ayida and colleagues,[26] saline contrast sonohysterography as a screening test for any cavity abnormality, had 87.5% sensitivity, 100% specificity, 100% positive predictive value and 91.6% negative predictive value.

COLOR DOPPLER HYSTEROSALPINGOGRAPHY

Transvaginal color Doppler hysterosalpingography is a safe and efficacious method for evaluation of Fallopian tube patency without exposure to radiation or contrast dyes. The cost of the procedure is significantly lower than for X-ray HSG and it gives immediate results. It is advisable that all the scans are recorded on vide-recorder and/ or Polaroid films.

Further advantages of transvaginal sonosalpingography include the possibility of performing the procedure on an outpatient basis. This has significantly altered the need for inpatient facilities at some infertility departments. Similar to X-ray HSG bleeding, pregnancy and presence of adnexal masses on pelvic or ultrasound examination are contraindications for color Doppler HSG.

Equipment needed to perform color Doppler HSG includes an ultrasound unit with color Doppler capability and an intrauterine catheter. The intrauterine cannula is placed into the uterus. One balloon is placed on the level of the internal cervical os, while another one is fixed in the external cervical os. A tiny tubal catheter with a metal end is introduced after exploration of the uterine cavity. Approximately two to five ml of sterile saline is instilled into the uterine cavity (Fig. 52.1). After the observation of the morphology of the uterus end endometrial lining, the color Doppler is directed at the cornual region where the tubal catheter with a metal end should be located. The exact placement of the catheter is sonographically controlled. Color signals passing through the Fallopian tube indicate its patency, while the absence of such signals is interpreted as tubal occlusion.[6,27] Accumulation of the fluid in the cul-de-sac on the side of injection controlled by transvaginal color and pulsed Doppler is an accurate indicator of the ipsilateral tubal patency. Selective tubal injection increases the accuracy of the procedure and appropriateness of the interpretation. The procedure is repeated for the contralateral side (Fig. 52.2).

Difficulty in making the diagnosis of tubal occlusion arises in those patients with dilated hydrosalpinges because flow through the dilated Fallopian tube may stimulate spillage on the Doppler ultrasonography screen. To avoid this error, we should perform careful observation of both adnexa before the procedure. Since the tubal architecture is not demonstrated with color Doppler HSG. This method is not useful in preoperative salpingoplasty procedures.[28]

Using our modified technique, we compared the findings of color Doppler HSG from 47 patients with those of chromopertubation at the

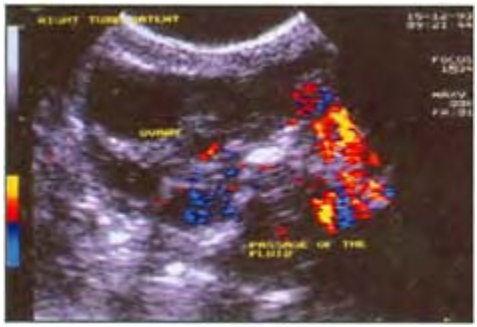

Figure 52.2: Transvaginal color Doppler hystero¬ salpingography demonstrates regular tubal patency. Note color flow signals passing through the right tube and simultaneous accumulation of the anechoic fluid in the cul-de-sac

time of laparoscopy.[9] Forty-three out of 47 (91.48%) color Doppler HSG findings agreed with observations at chromopertubation. In only one patient, in whom no patency was seen in both tubes under color Doppler evaluation, indirect diagnosis of tubal patency was performed observing accumulation of free fluid in the culde-sac. The increased incidence of conception during the three months after the procedure (in our study, two patients) may be an effect of a mechanical lavage of the uterus by dislodging the mucous plugs, breakdown of the peritoneal adhesions, or a stimulatory effect on the tubal cilia. No serious side effects were observed during and after the transvaginal color Doppler HSG procedure. Eighteen patients complained of pain that continued for 2 10 minutes after the procedure. No medication was required for these cases. The shortest time taken for the transvaginal color Doppler hysterosalpingography was 5 minutes, while the longest time was 14 minutes. After removing the instruments, the cervix is inspected for hemostasis and pressure is applied to the tenaculum site whenever necessary.

REVIEW OF THE LITERATURE

To assess the accuracy of the diagnosis of tubal occlusion with the use of color Doppler flow ultrasonography and HSG, Peters and Coulam[6] studied 129 infertile women. When results of ultrasonography-HSG were compared with those of X-ray HSG and/or chromopertubation, 69 of 85 (81%) studies showed agreement, and 50 out of 58 (86%) ultrasound hysterosalpingography findings agreed with observations at chromopertubation. The frequency of comparable findings between X-ray HSG and chromopertubation was 75%.

Richman and colleagues[13] evaluated tubal patency in 36 infertile women. They compared ultrasound findings with conventional hysterosalpingograms, which had been obtained simultaneously. Ultrasound demonstrated bilateral occlusion with a sensitivity of 100%, and showed tubal patency with a specificity of 96%.

Tufekci and colleagues[20] studied 38 women with infertility complaints. The results obtained from transvaginal sonosalpingography and laparoscopies were completely consistent for 29 cases (76.32%), and partially consistent for eight cases (21.05%). Only one case showed inconsistent result. Complete consistence means that the passage through both Fallopian tubes is identical by both methods. Partial consistence indicated identical results for only either the left or the right tube. Transvaginal sonosalpingography correctly indicated tubal patency or non-patency in 37 of 38 cases.

Heikkinen and co-workers[29] evaluated the advantages and accuracy of transvaginal sonosalpingography in the assessment of tubal patency with regards to laparoscopic chromopertubation. Sixty-one Fallopian tubes were examined by both techniques, resulting in concordance of 85%. By transvaginal sonosalpingography, 45 tubes were found to be patent and 16 occluded. In chromopertubation, 50 tubes were patent and 11 were occluded. Bilateral tubal patency was found by transvaginal sonosalpingography in 17 cases and by laparoscopy in 22 cases. Bilateral occlusion was found in three cases using either technique. Transvaginal sonosalpingography with the combination of air and saline is a low-cost, reliable, safe and comfortable examination method and it can be used for the primary investigation of infertility on an outpatient basis.

Jeanty et al[30] assessed the use of air as a sonographic contrast agent in the investigation of tubal patency by sono-hysterography. They examined 115 women assessed for infertility. After saline sonohysterography, small amounts of air were insufflating and the tubal passage of bubbles was monitored. Air-sonohysterography and laparoscopy with chromopertubation show agreement in 79.4%. In 17.2% of patients, the tubes were considered no visualized by air-sonohysterography when they were patent. The sensitivity was 85.7% and specificity 77.2%. In conclusion, air sonohysterography is a comfortable, simple, and inexpensive first line of tubal patency investigations yielding high accuracy.

Battaglia and co-workers[31] found that correlation between color Doppler HSG and roentgenogram HSG with chromolaparoscopy occurred in 86% versus 93% of all women studied.

Boudghene et al[32] compared the efficiency of air-filled albumin microspheres (Infoson) with saline solution in determining Fallopian tube patency during Hy-Co-Sy. Hy-Co-Sy was performed with a 7-MHz transvaginal probe using both B-mode and color Doppler and tubal patency was demonstrated by the appearance of contrast agent in the peritoneal cavity near the ovaries. Infoson enhanced Hy-Co-Sy provided a significantly

larger number of correct diagnoses (20/22 Fallopian tubes) than did saline Hy-Co-Sy (12/24 Fallopian tubes) and the same number as that achieved by HSG. A positive ultrasound contrast agent appears to be more efficient than saline solution at determining Fallopian tube patency in infertile women by means of Hy-Co-Sy and as efficient as an iodinated contrast agent in the same population explored by HSG.

Stern and colleagues[8] administered saline transcervically during transvaginal color Doppler sonography in 238 women. Traditional X-ray HSG was performed in 89 women. Laparoscopy with chromopertubation was performed in 121 women. Forty-nine women had all three procedures performed. Correlation between color Doppler HSG and X-ray findings with chromopertubation occurred in 81% versus 60% (p—0.0008) of all women studied. In forty-nine women who had all three procedures performed, color Doppler HSG results correlated with chromopertubation more often than X-ray HSG (82% versus 57%, p= 0.0152). In their previous report,[6] discrepancies between color ultrasound hysterosalpingography and chromopertubation findings involved a diagnosis of unilateral patency. They recommend repeating color ultrasound HSG before making a diagnosis of unilateral occlusion.

Allahbadia[33] reported a 92.6% agreement between color Doppler HSG compared with X-ray HSG and laparoscopy. The same author described the so-called *Sion* procedure or hydrogynecography. This procedure takes about 15 minutes as compared to the 5–6 minutes for sonosalpingography. After accomplishing sonosalpingography, sterile normal saline is injected until approximately 350 ml have flooded the pelvis. With the adnexa and uterus submerged in a fluid medium, the rescanning of the pelvis is repeated. If there is a bilateral tubal block and reflux of the saline is seen in the stem of the Foley's catheter, filling up the pelvis by alternative means is applied. The saline fills up the pelvis and delineates all sorts of adhesions. All the patients undergoing this procedure are given prophylactic antibiotics.

Contrary to optimistic results of different ultrasound techniques for evaluation of tubal patency, Balen and colleagues[34] found ultrasound contrast HSG using both sterile saline and Echovist contrast media insufficiently accurate and inferior to conventional X-ray HSG. False-positive rates in the range of 9% and false-negative rates in the range of 20% have been reported in the diagnosis of tubal obstruction by color Doppler HSG.[8] *Therefore, all abnormal hysterosalpingograms studies deserve laparoscopic or hysteroscopic follow-up.*

Normal X-ray or color Doppler HSG does not rule out the need for diagnostic laparoscopy. While X-ray HSG is *the* most accurate method of diagnosing intramural or intraluminal abnormalities of the Fallopian tube, color Doppler HSG is the only available non-invasive method for analyzing the tubal motility.

To obtain maximum information, a well-trained physician who is familiar with the color Doppler investigation and who is capable of manipulating the instruments, the patient's reproductive tract and the rate of injection should perform the procedure.

In the recent study from Sueoka et al[35] the authors developed the linear everting (LE) catheter to safely guide a Falloposcope into the entire length of Fallopian tube in order to observe the tubal lumen. This catheter may also be useful therapeutically for the recanalization of occluded tubes. On the basis of tubes attempted, the LE catheter successfully accessed 85.3% (87/102). A follow-up hysterosalpingogram was completed 1–3 months following the Falloposcopic tuboplasty (FT) procedure, which revealed an

overall patency rate of 79.4% (81/102). In their study, FT has been established as a highly useful, less invasive and novel treatment for tubal infertility.

THREE-DIMENSIONAL HYSTEROSONOSALPINGOGRAPHY

Recently, large technological efforts have been invested in promoting the capability to demonstrate the third dimension, although there is no doubt about the diagnostic value of two-dimensional ultrasound in obstetrics and gynecology. The three-dimensional (3D) ultrasound image is generated by superimposing the programmed volume box over the two-dimensional ultrasound scan image of the uterus.[36] The volumetric rotor is set into operation. The vaginal transducer then performs a sweep of transversal sections that are to be stored in the computer. The computer integrates the images and enables the sonographer to view three planes simultaneously. Once the perpendicular plane to the transducer is obtained, the calculated 3D image with the complete volume scan is stored in a removable computer disk. This scanning procedure lasts between 2 and 10 seconds. The examination of the patient is complete, while later sonographer can analyze selected sections. Three-dimensional images are generated only when the three planes are integrated and displayed on the screen. It is possible to rotate and translate any plane of the volume stored. To generate a final 3D image of the uterine cavity, a threshold has to be defined up to which echogenicity should be taken for reconstruction of the uterine cavity.[36] Depending on the structure to be studied, different 3D modes can be elaborated. The surface reconstruction mode allows study of the outer contour or profile of the uterus. The transparent maximum/minimum mode reveals objects with high echogenicity in the interior of a uterus. The basic structural information provided by conventional scans in the longitudinal and transverse planes now can be augmented by new 3D ultrasound that provides an additional view of the coronal or "c" plane, which is parallel to the transducer face (Fig. 52.3).[37] The computer generated scan is displayed in three perpendicular planes. The presentation of three perpendicular planes on one screen allows free scrolling of an endless amount of frames

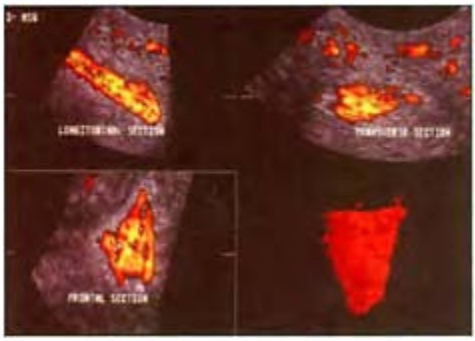

Figure 52.3: Multiplanar image of the uterus after injection of echogenic

contrast medium as obtained by power Doppler ultrasound. This modality facilitates visualization of normal uterine cavity in three orthogonal projections, while triangular shape of the uterine cavity is best imaged in frontal section

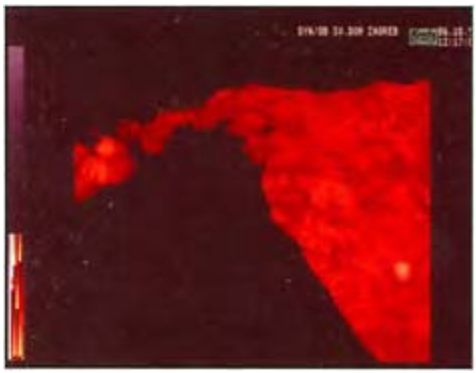

Figure 52.4: Three-dimensional power Doppler hysterosalpingography enables detailed analysis of the uterine cavity shape and continuity between the endometrial cavity and uterine angles

through the volume of interest. The coronal or "c" plane view allows more detailed analysis of the uterus and, for the first time, the endometrial cavity between the uterine angles can be visualized (Fig. 52.4). Translation or rotation can be carried out in one plane while maintaining the perpendicular orientation of all three. The images produced by transvaginal ultrasound are superior to those produced by transabdominal ultrasound because vaginal transducers are in closer proximity to the tissues.[37] Because of that, higher frequencies are used and artifactual echoes caused by multiple reflections from intervening tissues are minimized.

Demonstration of the coronal plane is mandatory for the diagnosis of uterine pathology, such as septate, arcuate or bicornuate uteri and also provides the most exact measurement of the endometrial width when transected in a midperpendicular manner. During 3D hysterosonography the typical triangulated uterine cavity appears in its full shape (Fig. 52.3).[38] Surface rendering, maximal/minimal or X-ray renderings provide even more information on uterine findings, such as anatomy of the uterine cavity and its content. There are two techniques to accomplish this goal: "native" approach, and the use of echogenic contrast medium that is especially useful for demonstrating the uterine cavity shape. Uterus is due to its dual consistency of endometrium and myometrium, an excellent ultrasonic medium. Those two media have different acoustic impedance that permits visualization of the size and shape of the uterus and its cavity. In addition, contrast medium is mandatory in cases where a thin endometrium or pathologic content of the uterine cavity precludes its visualization.

The negative contrast medium, normal saline, is used for demonstration of the entire uterine cavity, its shape, pathology, and the frame of the myometrial mantel, whereas for demonstrating the permeability of the Fallopian tubes a positive contrast medium (Echovist) is used.

Weinraub and Herman[38] were first to evaluate the findings of different pathology of uterus anatomy and pathological content of uterine cavity on 3D hysterosonography. Using three perpendicular planes on one screen, where the left upper plane is coronal and is termed "a", the right upper plane is sagittal and is termed "b", and the left lower plane is transverse and is termed "c" one can detect numerous causes of infertility. Looking at the fundal region in "a" it is very important not to overlook a small indentation, if it is present, in the case of septate uterus. The maximal endometrial width could be easily measured in sagittal plane. If the transverse section shows separated uterine cornua, finding is typical for arcuate uterus. Clear concavity in the middle of the uterine fundus dividing the uterine cavity creates a bicornuate uterus.

Hydrosonography is very useful in demonstration of intracavitary pathologies, such as: adhesions, myomas, endometrial polyps, endometrial carcinoma, or location of intrauterine devices (lUDs). Using 3D surface rendering in the cases of intrauterine adhesions and myomas, it is possible to present the spatial orientation and the correlation of the adhesions with the surrounding uterine walls, also round and smooth surface of the myomas giving the feeling of depth inside the uterine cavity.[38]

Hydrosonography, as well as 3D rendering is especially important for diagnosis of an endo- metrial polyp. Despite the fact that the cut in the coronal plane goes through the endometrial polyp it is not demonstrated on "a" plane and could be easily missed. When hydrosonography is used, the polyp or any other intracavitary lesion is easily examined in all three planes throughout the volume.[38]

Fallopian tubes can be demonstrated on ultrasound only when they contain fluid (hydrosalpinx, pyosalpinx, bleeding ectopic pregnancy, or a contrast medium). In the case of hydrosalpinx, the fluid-filled Fallopian tube is demonstrated in "a", "b" and "c" sections, in each plane resembling different shape due to its tortuosity. In "d" section, 3D rendering is shown. There are a number of difficulties in tubal visualization by 2D Hy-Co-Sy.[37] Due to its tortuosity, the tube can rarely be seen completely in a single scanning plane and the echo-contrast medium is, therefore, observed in small sections. The position of the tube is very variable and distended bowel may prevent the visualization of

the distal parts of the tubes. Therefore, usually only the tubal ostia and proximal parts of the tubes are visualized by gray scale 2D ultrasound imaging. Free spread of the dye is

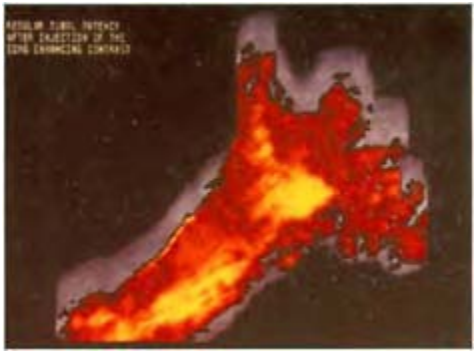

Figure 52.5: Three-dimensional power Doppler image of the entire tubal length and spillage of the contrast medium through the fimbrial end as demonstrated by echo-enhanced 3D PD hysterosalpingography

frequently difficult to visualize because the surrounding bowel can also produce strongly echogenic signals. Instead of visualizing the echo contrast with grayscale ultrasound, Sladkevicius and colleagues[39] used 3D power Doppler technology which is sensitive to slow flow. If the tube is patent, Doppler signals should be obtained from flow along the tube and free spill from the fimbrial end should be identified (Fig. 52.5). The aim of their study was to evaluate the feasibility of three-dimensional power Doppler imaging (3D-PDI) in the assessment of the patency of the Fallopian tubes during Hy-Co-Sy. Hysterosalpingo-contrast sonography using contrast medium Echovist was performed on 67 women. Findings on the 2D gray scale scanning and 3D PDI were compared. The first technique visualizes positive contrast in the Fallopian tube; the second demonstrates flow of medium through the tube. Contrast medium Echovist produced prominent signals on the 3D-PDI image. Free spill from the fimbrial end of the Fallopian tubes was demonstrated in 114 (91%) tubes using the 3D-PDI technique and in 58 (46%) of tubes using conventional Hy-Co-Sy. The mean duration of the imaging procedure was less with 3D-PDI, but the operator time, which included postprocedure analysis of the stored information, was similar. A significantly lower volume of contrast medium (5.9+/−0.6 mL) was used for 3D-PDI in comparison with that (11.2+/−1.9 mL) used for conventional 2D Hy-Co-Sy. The authors concluded that color coded 3D-PDI with surface rendering allowed visualization of the flow of contrast through the entire tubal length and

free spill of contrast was clearly identified in the majority of cases. The 3D-PDI method appeared to have advantages over the conventional Hy-Co-Sy technique, especially in terms of visualization of spill from the distal end of the tube, which was achieved twice as often with the 3D ultrasound technique. Although the design of the investigation did not allow the side effects of the two techniques to be compared, the shorter duration of the imaging and lower volume of the contrast medium used suggested that the 3D-PDI technique might have a better side effect profile. The 3D-PDI technique allowed better storage of the information for re-analysis and archiving than conventional Hy-Co-Sy.

Similarly, our group found that power Doppler visualization of echo-contrast flow is better than conventional imaging of the contrast media.

Ayida and colleagues[40] compared conventional 2- and 3D ultrasound scanning of the uterine cavity with and without saline contrast medium. The 2D scanning suggested cavity abnormalities in 4 of 10 women (fibroids, 3; hyperechoic thick endometrium, 1). The 3D scanning confirmed these and revealed one additional abnormality suggestive of a uterine septum. The 2D scanning with saline injection diagnosed abnormalities in 5 of 10 (uterine septum, 1; fibroids, 3; endometrial polyp, 1). The 3D contrast scanning with saline did not add any further information to 2D contrast scanning with saline. In this pilot study, 3D scanning to assess the uterine cavity appeared to offer no advantages over conventional 2D contrast sonography.

Weinraub and colleagues[41] have demonstrated the feasibility of combined 3D ultrasound and saline contrast hysterosonography. Since volume sampling has a short pick-up time of a few seconds, the examination is over almost immediately after the uterus is reasonably distended. In this uncomfortable examination such an advantage should not be underestimated. Evaluation of the uterine cavity at a later time allows the operator to manipulate the data at leisure and scrutinize findings in desired planes, which were not available during the initial examination. Simultaneous display of the three perpendicular planes offers a more comprehensive overview of the examined area and gives access to planes unobtainable by conventional 2D examination. Surface rendering may confirm the presence of pathological findings in equivocal cases, and characterize their appearance, size, volume and relationship to the surrounding structures. Surface rendering of the polypoid structures shows echogenic masses on a pedicle protruding into the uterine cavity. Submucous fibroids appear as mixed echogenic sites bulging into the cavity. Intrauterine synechiae appear as bands of varying thickness traversing the uterine cavity. This can be useful when deciding on treatment options, such as conservative management vs surgery, and can be a valuable tool in surgical procedures carried out under ultrasonographic guidance.

Kiyokava et al[42] evaluated 25 unselected infertile patients for tubal patency and uterine cavity by 3D Hy-Co-Sy with saline as a contrast medium. The efficacy of the procedure was compared with X-ray HSG as reference. The positive predictive value, negative predictive value, sensitivity, and specificity of predicting tubal patency by 3D Hy-Co-Sy were 100, 33.3, 84.4, and 100%, respectively. The full contour of the uterine cavity was depicted in 96% of cases by 3D Hy-Co-Sy and 64% by X-ray HSG ($P < 0.005$). The uterine cavity area measured on 3D Hy-Co-Sy correlated well with the volume of contrast medium required on HSG. Three-dimensional Hy-Co-Sy provided advantages of better assessment of uterine cavity over HSG. Compared with conventional HSG, the efficacy of 3D Hy-Co-Sy to assess tubal patency was acceptable. In addition,

the procedure of 3D Hy-Co-Sy appears to be better tolerated, requiring no sedation or anesthesia and a reduced examination time. Thus, 3D Hy-Co-Sy with saline as a contrast medium is feasible and could comprise a routine outpatient procedure in the initial evaluation of infertile women.

Unterweger et al[43] introduced a new method, three-dimensional dynamic magnetic resonance—hysterosalpingography (3D dMR-HSG) for imaging of the uterine cavity and Fallopian tube patency. The authors evaluated whether, by using a higher viscosity contrast solution, 20 ml of gandolium-polyvidone, direct visualization of the Fallopian tubes may be achieved. Three-dimensional dynamic magnetic-resonance—hysterosalpingography represents a new and promising imaging approach to female infertility causing less pain and avoiding exposure of the ovaries to ionizing radiation. By using a higher viscosity MR-contrast agent it allows not only visualization of the uterine cavity and Fallopian tube patency but also direct visualization of the Fallopian tubes.

CONCLUSION

Color Doppler and 3D hysterosalpingography are safe and efficacious methods for evaluation of Fallopian tube patency without exposure to contrast dyes or radiation. These procedures allow the physician to know the results immediately and are carried out on outpatient clinic basis.

Three-dimensional technique offers the possibility of simultaneous presentation of the uterine cavity and corresponding tube, shortening the procedure and the discomfort of the patient. Transvaginal 3D ultrasound examination time is not less than that needed for 2D sonography, but some parts of the examination, like measurements, reconstruction of the planes of interest and surface rendering can be performed off-line. The acquired volumes of the most appropriate planes of interest can be stored on removable hard disk for additional reevaluations and documentation. Ultrasonic tomography can be performed using one panel control, producing parallel sections in increments of less than 1 mm. The ability of 3D ultrasound systems to produce serial scans that can be stored for subsequent analysis, 3D reconstruction, accurate assessment of volume, and coronal plane with more detailed analysis of the uterus and endometrial cavity between uterine angles is superior to conventional 2D ultrasound.

REFERENCES

1. Hill ML. Infertility and reproductive assistance. In: Neiberg DA, Hill LM, Bohm-Velez M, Mendelson EB (Eds). Transvaginal Ultrasound 1992; 43–46 (St. Louis: Mosby Year Book).
2. Arronet GM, Aduljie SY, O'Brien IR. A 9 year survey of Fallopian tube dysfunction in human infertility: diagnosis and therapy. Fertil Steril 1969; 20:903–18.
3. Page H. Estimation of the prevalence and incidence of infertility in a population: a pilot study. Fertil Steril 1989;71:571–74.
4. Kerin JF, Williams DB, San Roman GA, Pearistone AC, Grundfest WS, Sucrey ES. Falloposcopic classification and treatment of Fallopian tube disease. Fertil Steril 1992; 57:731–35.
5. Thurmond AS, Rosch J. Non-surgical Fallopian tube recanalization for treatment of infertility. Radiology 1990; 174:371–74.
6. Peters JA, Coulam CB. Hysterosalpingography with color Doppler ultrasonography. Am J Obstet Gynecol 1991; 164:1530–32.

7. Volpi E, Zuccaro A, Patriarca S, Rustichelli, Sismondi, P. Transvaginal sonographic tubal patency testing air and saline solution as contrast media in a routine infertility clinic setting. Ultrasound Obstet Gynecol 1996; 7:43–48.
8. Stern J, Peters AJ, Coulam CB. Color Doppler ultrasonography assessment of tubal patency: a comparison study with traditional technique. Fertil Steril 1992; 58:897–900.
9. Kupesic S, Kurjak A. Gynecological vaginal sonographic interventional procedures—what does color add? Gynecol Perinatol 1994; 3:57–60.
10. Deichert U, Schlief R, van de Sandt M, Daume E. Transvaginal hysterosalpingo-contrast sonography for the assessment of tubal patency with gray scale imaging and the additional use of pulsed wave Doppler. Fertil Steril 1992; 57:62–67.
11. Rubin I. Differences between the uterus and tubes as a cause of oscillations recorded during uterotubal insufflation. Fertil Steril 1954; 5:147–53.
12. Nannini R, Chelo E, Branconi F, Tantini C, Scarselli GF Dynamic Echohysteroscopy. A New Diagnostic Technique in the Study of Female Infertility. Acta Europ Fertil 1981; 12:165–71.
13. Richman TS, Viscomi GN, deCherney A, Polan ML, Alcebo LO. Fallopian Tubal Patency Assessed by Ultrasound Fluid Injection. Radiology 1984; 152:507–10.
14. Randolph JR, YingYK, MaierDB, Schmidt CL, Riddick CH. Comparison of real-time ultrasonography, hysterosalpingography and laparoscopy/hysteroscopy. Fertil Steril 1986; 46:828–32.
15. Davison GB, Leeton J. A case of female infertility investigated by contrast-enhanced echogynecography. J Clin Ultrasound 1988; 16:44–47.
16. Allahbadia GN. Fallopian tubes and ultrasonography. The Sion experience. Fertil Steril 1992; 58:901–07.
17. Broer KH, Turanli R. Uberprufung des Tubenfaktors mitels Vaginalsonographie. Ultraschall Klin Prax 1992; 7:50–53.
18. Bonilla-Musoles F, Simon C, Sampaio M, Pellicer A. An assessment of Hysterosalpingosonography (HSSG) as a Diagnostic Tool for Uterine Cavity Defects and Tubal Patency. J Clin Ultrasound 1992; 20:175–81.
19. Deichert U, Schlief R, van de Sandt M, Junke I. Transvaginal hysterosalpingo-contrast sonography (Hy-Co-Sy) compared with conventional tubal diagnostics. Hum Reprod 1989; 4:418–22.
20. Tufekci EC, Girit S, Bayirli MD, Durmusoglu F, Yalti S. Evaluation of tubal patency by transvaginal sonosalpingography. FertilSteril 1992; 57:336–40.
21. Gramiak R, Shah PM. Echocardiography of the aortic root. Invest Radiol 1968; 3:356–66.
22. Meltzer RS, Tickner G, Sahines TP, Popp RL. The source of ultrasound contrast effect. J Clin Ultrasound 1980; 8:121.
23. Suren A, Puchta J, Osmers R. Fluid instillation into the uterine cavity. In: Osmers R, Kurjak A (Eds). Ultrasound and the Uterus 1995; 45–51 (Carnforth, UK: Parthenon Publishing).
24. Schlief R. Ultrasound contrast agents. Radiology 1991; 3:198–207.
25. Deichert U, van de Sandt M. Transvaginal hysterosalpingo-contrast sonography (Hy-Co-Sy). The assessment of tubal patency and uterine abnormalities by contrast enhanced sonography. Advances in Echo-Contrast 1993; 2:55–58.
26. Ayida G, Chamberlain P, Barlow D, Kennedy S. Uterine cavity assessment prior to in vitro fertilization: comparison of transvaginal scanning, saline contrast hysterosonography and hysteroscopy. Ultrasound Obstet Gynecol 1997; 10:59–62.
27. Peters JA, Stern JJ, Coulam CB. Color Doppler hysterosalpingography. In: Jaffe R, Warsof SL (Eds). Color Doppler in Obstetrics and Gynecology 1992; 283 (New York: McGraw Hill).
28. Groff TR, Edelstein JA, Schenken RS. Hysterosalpingography in the preoperative evaluation of tubal anastomosis candidates. Fertil Steril 1990; 53:417–20.
29. Heikkinen H, Tekay A, Volpi E, Martikainen H, Jouppila P Transvaginal salpingosonography for the assessment of tubal patency in infertile women: methodological and clinical experiences. Fertil Steril 1995; 64:293–98.

30. Jeanty P, Besnard S, Arnold A, Turner C, Crum P. Aircontrast sonohysterography as a first step assessment of tubal patency. J Ultrasound Med 2000; 19(8):519–27.
31. Battaglia C, Artini PG, D'Ambrogio G, Genazzani AD, Genazzani AR, Volpe A. Color Doppler hysterosalpingography in the diagnosis of tubal patency. Fertil Steril 1996; 65:317–22.
32. Boudghene FP, Bazot M, Robert Y, Perrot N, Rocourt N, Antoine JM, Morris H, Leroy JL, Uzan S, Bigot JM. Assessment of Fallopian tube patency by Hy-Co-Sy: comparison of a positive contrast agent with saline solution. Ultrasound Obstet Gynecol 2001; 18(5):525–30.
33. Allahbadia GN. Fallopian tube patency using color Doppler. Int J Gynecol Obstet 1993;40:241–44.
34. Balen FG, Allen CM, Siddle NC, Lees WR. Ultrasound contrast hysterosalpingography—evaluation as an outpatient procedure. Br J Radiol 1993;66:592–99.
35. Sueoka Asada H, Tsuchiya S, Kobayashi N, Kuroshima M, Yoshimura Y. Falloposcopic tuboplasty for bilateral tubal occlusion. A novel infertility treatment as an alternative for in-vitro fertilization? Hum Reprod 1998; 13:71–74.
36. Raga F, Bonilla-Musoles F, Blanes J, Osborne NG. Congenital Mullerian anomalies: diagnostic accuracy of three-dimensional ultrasound. FertilSteril 1996; 65: 523–28.
37. Kyei-Mensah A, Zaidi J, Pittrof R, Shaker A, Campbell S, Tan SL. Transvaginal three-dimensional ultrasound: accuracy of follicular volume measurements. Fertil Steril 1996; 65:371–76.
38. Weinraub Z, Herman A. Three-dimensional hysterosalpingography. In: Merz E (Ed). 3D Ultrasonography in Obstetrics and Gynecology 1998; 57–64 (Lippincott Williams & Wilkins, Philadelphia).
39. Sladkevicius R Ojha K, Campbell S, Nargund G. Threedimensional power Doppler imaging in the assessment of Fallopian tube patency. Ultrasound Obstet Gynecol 2000; 16(7):644–47.
40. Ayida G, Kennedy S, Barlow D, Chamberlain R Conventional sonography for uterine cavity assessment: a comparison of conventional two-dimensional with three-dimensional transvaginal ultrasound; a pilot study. Fertil Steril 1996; 66:848–50.
41. Weinraub Z, Maymon R, Shulman A, Bukovsky J, Kratochwil A, Lee A, Herman A. Three-dimensional saline contrast hysterosonography and surface rendering of uterine cavity pathology. Ultrasound Obstet Gynecol 1996; 277–82.
42. Kiyokawa K, Masuda H, Fuyuki T, Koseki M, Uchida N, Fukuda T, Amemiya K, Shouka K, Suzuki K. Three-dimensional hysterosalpingo-contrast sonography (3D-HyCoSy) as an outpatient procedure to assess infertile women: a pilot study. Ultrasound Obstet Gynecol 2000; 16(7):648–54.
43. Unterweger M, DeGeyter C, Frohlich JM, Bongartz G, Wiesner W. Three-dimensional dynamic MR-hysterosalpingography; a new, low invasive, radiation-free and less painful radiologic approach to female infertility. Hum Reprod 2002; 17(12):3138–41.

Chapter 53
Guided Procedures using Transvaginal Sonography

Sanja Kupesic, Asim Kurjak, Drazena Bjelos

With the recent advances in transvaginal ultrasonographic equipment settings and technique, guided procedures using transvaginal sonography, which in the past have been mostly performed abdominally, have replaced abdominally guided puncture in many cases.

The first who have used ultrasound-guided puncture procedures to achieve both diagnostic and therapeutic goals were Smith and Bartrum[1] who performed percutaneous aspiration of intraabdominal abscesses in 1974 and Gerzof et al who used an abdominal catheter placed sonographically to drain purulent collections.[2,3] The advantages of these procedures over surgery are: easier performation, accurate needle placement, rare injury to adjacent organs, low cost, shorter time of the procedure, speed of administration, portability and patient comfort. Possible rare complications include: bleeding, infection, and unintentional puncture of organs and in the case of multifetal reductions, miscarriage. Puncture procedures occur in three dimensions. This third dimension, due to ultrasound properties, is thinnest at the focal range of the probe and is inversely proportional to the operating frequency of the transducer crystal. This is called “slice thickness artifact” and means that the operator must take into account the third dimension of the image. Therefore, when the tip of the needle used for puncture procedures appears to be within the structure, in reality it is in front of or behind the structure imaged. When puncture procedures are performed abdominally, one of two techniques are employed: needle guide or free hand. When puncture procedures are performed transvaginally, there is limited mobility of the probe and the needle making the free hand approach difficult. A fixed needle guide attached to the probe shaft allows easier visualization of the entire length of the needle within the scanning plane and better control for exact needle placement. Recently developed automated puncture device when mated to the shaft of the vaginal probe, provides extreme accuracy and precision, while its high-velocity release makes the procedure virtually painless; no anesthesia or analgesia is required. This technique was first used for ovum pick-up in assisted reproductive technology programs, but it was quickly abandoned secondary to the need for reloading and reshooting for each new follicle aspirated. The automated puncture device is crucial where extreme accuracy is needed for any needle placement controlled and guided by the transvaginal probe. Manual needle introduction is less accurate and more painful because of the slower forward motion of the needle displacing mobile targets rather than penetrating them.

The punctures are usually performed with the guidance of 5.0 to 7.5 MHz vaginal transducer probes through a needle guide that is attached to the shaft of the probe. A software-generated fixed "biopsy guide" line is displayed on the ultrasound monitor screen, which marks the path of the entering needle. Needle ranging from 14 G to 21 G is employed, depending on the nature of the procedure itself; the narrowest possible needle able to perform the desired task should be used. For better imaging, the "zoom" feature of the equipment should be used as frequently as possible. After the initial withdrawal the needle, the pelvic structures and cul-de-sac must be observed sonographically for approximately 10 minutes and rescanned after a 2 to 3 hours observation period to check for internal bleeding or previously undetected complications.

TRANSVAGINAL PUNCTURE PROCEDURES

More commonly performed transvaginally directed punctures that are going to be described in this chapter are following:

1. Transvaginal oocyte retrieval
2. Ovarian cyst aspiration
3. Drainage of pelvic abscesses
4. Multiembryo reduction
5. Culdocentesis
6. Obstetrical implications
7. Treatment of ectopic pregnancy

TRANSVAGINAL OOCYTE RETRIEVAL

Experience has shown that the transvaginal technique using a needle guided transvaginal probe is superior to all other ultrasound-guided techniques.[4]

The proximity of the transducer to the pelvic organs makes possible the use of high frequency probes, thereby enhancing the resolution and clinical efficiency. The elastic vault of vagina allows approximation of the ovaries by increased pressure of the tip of the probe. Since there is no need for full urinary bladder, pelvic anatomy is undistorted and ovaries are kept beyond the focal zone of the transducer. Obesity or adhesions do not significantly inhibit the visualization of the follicles and are not contraindications for this technique.

Standardized programmed stimulation is monitored by transvaginal sonography.[5] Additional information may be obtained by hormonal estimation and color Doppler studies[6–8] of the ovarian and uterine circulation.

The entire treatment is carried out on an outpatient setting. The patient is placed on a gynecological table in lithotomy position. Although anesthesia or any sedative analgesia has been abandoned in about 50% of IVF programs,[9] sedative medication (consisting of Flunitrazepam, Droperidol and Pentazocine) may be used. Since the mean duration of the oocyte retrieval is 10 minutes, most of the patients easily tolerate the procedure. However, the operator should be aware of possible hypotonic reactions and discomfort experienced by some patients. Before inserting the probe into the cover, operator should apply the ultrasonic coupling gel. The cover (sterile condom, surgical rubber glove or

specially produced rubber cover) is stretched over the gel to expel the air from the tip of the probe. This can prevent the artifacts during the procedure. The gel or lubricant should not be used while inserting the probe because of spermicidal action and reported embryotoxicity.[10] Instead, one can use a physiologic saline or culture medium. Sterile needle guides are used for transvaginal puncture of the follicles. The keyboard of the ultrasound machine is covered with a sterile cover, which enables the operator to make any readjustment under sterile conditions. The patient's legs and perigenital area are then covered using the sterile drapes. After cleaning the vagina with isotonic saline or cultured medium the vaginal probe in inserted into the vagina.

To prevent potential risks of the puncture procedures automatic puncturing device has been developed. This device contains a mobile metal tube, the needle carrier into which the aspiration needle is inserted and locked by a twisting movement.[4] Before inserting the probe with a puncture device into the vagina, the device should be loaded and secured. After insertion, a detailed ultrasound examination is performed to locate the uterus and the ovaries. The probe is directed allowing the biopsy vector to be placed to the central part of the nearest follicle indicating the direction of the needle (Fig. 53.1). The operator counts the distance on the biopsy vector on the

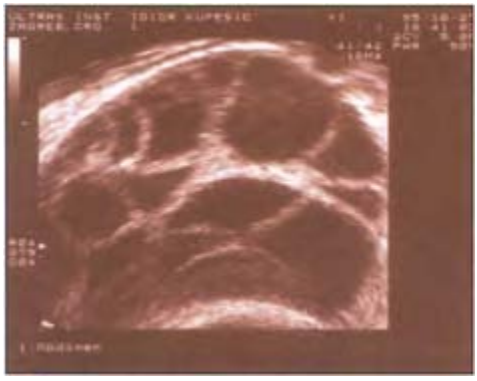

Figure 53.1: Transvaginal scan of a hyperstimulated ovary just before ultrasound guided aspiration of the oocytes. Note the biopsy vector placed in the mean diagonal section of the ovary

screen and "shoots" the follicle either automatically (using depth limiting screw on "shooting equipment") or manually. After the needle is rapidly advanced into the follicle, the operator begins the suction through the tubing connected with the suction pump. As the follicular fluid is aspirated one can see the follicle collapsing, while follicular fluid is

pulled into the collecting chamber.[4] Flushing procedure may be used to improve the satisfactory rate of the aspirated oocytes. Flushing medium that contains heparin is injected through the tubing or using an automated flushing system. All the follicles along the same line are aspirated without withdrawing the needle. Feichtinger et al[11] reported low incidence of complications while using transvaginal technique for oocyte recovery. Iliac veins were confused for a follicle and were mistakenly punctured in 2.4 percent. Bleeding into the pouch of Douglas was detected on the ultrasound screen and stopped spontaneously in all cases. An observation was made that filling the bladder may exert pressure on the site and, therefore, stop the bleeding. Color Doppler can easily prevent such a complication, since iliac vessels are easily obtainable using this technique (Fig. 53.2).

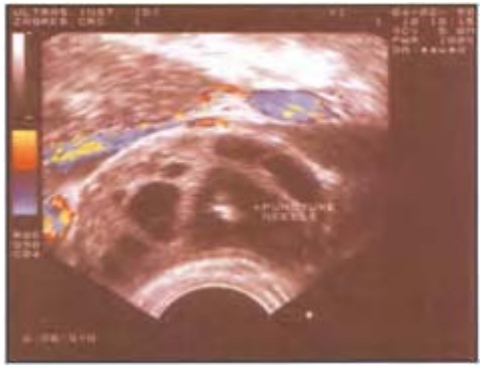

Figure 53.2: Transvaginal color Doppler scan of the ovary during aspiration procedure. The tip of the needle is advanced into the proximal follicle. Iliac vessels are clearly displayed using color Doppler facility

The bleeding from the vaginal vault is easily detectable and can be stopped by compression. Pelvic inflammatory disease (PID) is a rare complication of transvaginal follicle aspiration reported in 0.14% of the patients.[9] The infections were mostly caused by infected semen, and occurred in patients with positive history of PID.

Damario[12] reported a case of 26-year-old patient with Miillerian agenesis who underwent controlled ovarian hyperstimulation, transabdominal-transperitoneal ultrasound-guided oocyte retrieval and embryo transfer of 2 cleavage-stage embryos to the gestational carrier (her 44-yearold mother) resulting in twin pregnancy. For various reasons, patients with Miillerian agenesis may not be candidates for standard transvaginal ultrasound-guided oocyte retrieval. Although, laparoscopic oocyte retrieval has been

frequently used in this setting, the approach of transabdominal-transperitoneal ultrasound-guided oocyte retrieval may offer further advantages in selected cases.

Feichtinger[13] evaluated the possibility of performing follicle puncturing procedures under three-dimensional ultrasound control in close to real time using a new commercially available system. He has done a transvaginal needle-guided aspiration of 10 follicles using a newly developed ultrasound machine with a built-in rapid and powerful calculation software program for three-dimensional interactive volume and flow translation during operation. Interactive three-dimensional imaging was carried out during the aspiration of each follicle. Oocyte recovery was successful for all the follicles. There was a men delay of 5.00+/−1.22 seconds form coasting to resuming real-time ultrasound scanning during interactive volume calculation and the search for the needle tip in the three-dimensional mode. This did not delay the procedure remarkably but enabled the precise localization of both the needle and its tip after each penetration. The integration of flow signals allowed an impressive color-coded demonstration of the needle within the tissue, but the delay was significantly longer for color-coded volume acquisition (18.40+/−4.56 seconds). This technique seems to be potentially useful in fetal medicine, oncology and surgery.

Intrauterine transfer of fertilized oocytes cannot strictly be considered a sonographically guided procedure, but transvaginal sonography is occasionally used for directing embryo transfers. A new technique of embryo transfer based on ultrasound-guided transmyometrial puncture has been performed in 104 cases and described by Kato et al.[14] The use of this technique is proposed to overcome problems of difficult transfers because of cervical abnormalities. Thirty-eight patients conceived for a clinical pregnancy rate of 36.5% per attempt. No serious complications were observed. Tubal catheterization is a diagnostic and therapeutic technique of diagnosing tubal patency via injecting and observing fluid passage into the pelvis. The Fallopian tubes can be reached using a transvaginally guided catheter introduced into the cervix. In the same way, fertilized ova may be carried into ampullary portion of the tube.

OVARIAN CYST ASPIRATION

Transvaginal guidance permits direct visualization and aspiration of persistent follicular cysts.[11] Such cysts may impair folliculogenesis due to elaboration of hormones, or as a result of decreased perfusion by parenchymal compression. In the puncture of an ovarian or paraovarian cyst the center of the cyst is targeted and the needle is inserted. Such a procedure is highly debated in the literature. The concern of cell spillage from potentially malignant ovarian cyst into the abdominal cavity prevents many from using it more frequently. Although the aspirated fluid is necessarily submitted for cytologic evaluation, a negative cytologic examination may sometimes represent a false-negative result. High sensitivity and specificity of transvaginal color Doppler in differentiation between benign and malignant adnexal lesions seems to increase the reliability in decision making which cysts should be aspirated (Fig. 53.3).

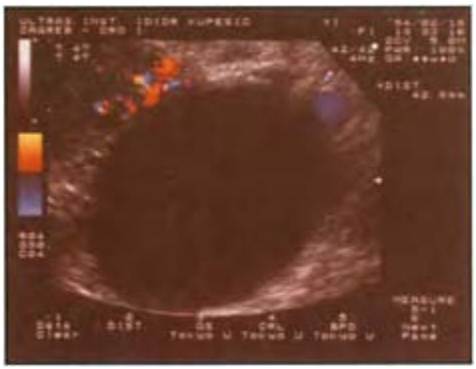

Figure 53.3: Simple ovarian cyst as seen by color Doppler ultrasound. Note smooth surface of the cyst and extraovarian vessels, while no vascularity is detected within the cystic wall. Color Doppler may help to avoid penetration of the surrounding vessels

Bret et al[15,16] published two papers describing their experience using transvaginal sonography in the aspiration of the ovarian cysts. They reported a 48% recurrence rate after cyst aspiration in premenopausal patients, and an 80% recurrence rate in postmenopausal women. This group attempted to prevent cyst recurrence by injecting alcohol immediately after cyst aspiration, but this procedure was successful in only 4 of 7 patients.[16]

The aspiration of endometriomata is considered to be relatively contraindicated. Aboulghar et al[17] studied 21 patients in which transvaginal ultrasonically guided aspiration of pelvic and endometriotic cysts was performed. Reaccumulation occurred in only 6 cases during a 12-month follow-up. Certainly, the aspiration of endometriotic cysts is technically simple; however, its overall benefit and safety are still inconclusive due to the lack of experience obtained by evaluating larger series.[18]

In infertility program Vaegemaekers et al[19] aspirated 32 unilocular anechoic cysts with an average diameter of 45 mm transvaginally. The authors concluded that ovarian cysts puncture in the early follicular phase could diminish the cancellation rate of *in vitro* fertilization cycles.

DRAINAGE OF PELVIC ABSCESSES

Infertility is attributed to tubal obstruction or dysfunction in 30 40% of patients. It is well known that tubal occlusion is a common sequelae of pelvic inflammatory disease (PID). Since recurrent episodes of PID are frequent, one should expect high incidence of this entity in infertile population. In patients with a tubo-ovarian abscess, abscess drainage with sonographic guidance can hasten the recovery process and improve the efficacy of antibiotic therapy. Once the needle is placed into the abscess cavity, the fluid can be aspirated as completely as possible and the needle withdrawn, or an indwelling drainage catheter can be placed.[11] Teisala et al[20] used transvaginal ultrasound guided aspiration to drain 10 tubo-ovarian abscesses receiving antimicrobial treatment. Only light sedation was required, and the procedure was well tolerated by the patients. This technique is accepted as an alternative to open laparoscopy for treating the tubo-ovarian abscess.

MULTIEMBRYO REDUCTION

During the past 15 years, the increased use of ovulation inducing drugs as well as the increased number of medically assisted reproduction procedures, resulted in a large number of multiple gestations. Multiple pregnancies are associated with high mortality and morbidity rates and the probability of achieving a term pregnancy with healthy neonates is inversely proportional to the number of the fetuses. Therefore, multiembryo reduction seeks to reduce the number of embryos to improve survival for the remaining ones.[21] Women with four or more embryos may be offered selective reduction, with the number of embryos usually reduced to two.[11] The procedure is normally delayed until after 8 weeks, when the spontaneous loss is relatively low. The transabdominal ultrasound guided technique was first presented by French group[22] and adopted by others.[23,24] With the developing use of transvaginal sonography this approach was attempted and successfully applied in multifetal reduction, as well. Advantages of this technique are: shorter puncture route and a more precise needle placement that reduces the risk of inadvertent injury to adjacent gestational sacs or other pelvic structures. Color Doppler may aid in monitoring fetal heart action during the interventional procedure (Fig. 53.4). The brief explanation of techniques for transvaginal multiembryo reduction is as following: baseline mapping procedure of the chorionic sacs, detailed evaluation of the heartbeats of the

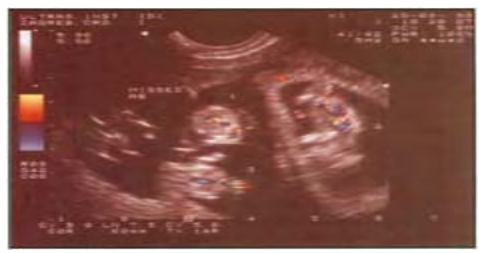

Figure 53.4: Transvaginal color Doppler scan of

quadriplet pregnancy. Color Doppler enables visualization and monitoring of heart activity during the procedure of multiembryo reduction

targeted fetus and placement of the needle with 0.5–1 ml of 2 mEq/ml KC1 solution. The heartbeat of each injected fetus is observed for 5–10 minutes to confirm cessation. The patients should be rescanned 3 hours after the procedure and then after 1 week for follow-up. The disadvantage of transvaginal fetal reduction is that at an early gestational age the final number of fetuses is not yet established.[18]

Coffler et al[25] reported on their experience with 90 women who underwent early (mean 7.5 weeks gestation, range 7.0–8.0 weeks) transvaginal selective embryo aspiration with KCl injected in the vicinity of the fetal heart. The procedure is associated with a total pregnancy loss rate of 11.7%. Early transvaginal embryo aspiration is a simple and relatively safe method for multiple pregnancy reduction. The overall pregnancy loss rate associated with early embryo aspiration is similar to that of procedures performed at later gestational age, but is significantly lower when the initial number of embryos is four or greater. Iberico et al[26] reported on early transvaginal intracardiac embryo puncture until asystolia is verified without the injection of any substances as an effective and safe technique. The baby take-home rate was 89.5% for twins and 80.0% for singletons.

DIAGNOSTIC CULDOCENTESIS

The introduction of transvaginal sonography has limited the need for diagnostic culdocentesis. The presence or absence of fluid in the pelvic cavity is easily established by the vaginal approach, but it may be necessary to differentiate between different biological fluids (clear fluid, blood or pus). The wide availability of transvaginal color Doppler sonography to distinguish the dominant pelvic pathology in the presence of pelvic fluid on the basis of different vascularity patterns, is very helpful in routine investigations. Sometimes, in conjunction with clinical signs, subjective symptoms, transvaginal color Doppler findings and the rapid β-human chorionic gonadotropin (β-hCG) test, the clinician still requires the information provided by culdocentesis. Inserting a needle in the cul-de-sac is a simple technique that can be performed safely and accurately with transvaginal ultrasound guidance.[27] High quality B-mode transvaginal sonography with superimposed color Doppler flow allows accurate simultaneous identification of the main pelvic vessels, physiological angiogenesis (corpus luteum) and ectopic peritrophoblastic blood flow. Color will help in accurate needle placement and in diminishing the risk of injury to adjacent vessels, especially in women who have had previous inflammatory disease of the pelvis with an obliterated cul-de-sac.

OBSTETRICAL PROCEDURES

The high frequency transvaginal probe enables detailed analysis of embryonic, extraembryonic and early fetal structures. By this method, screening for structural anomalies can be initiated during the first and early second trimester. Recent advances in tissue culture technology have established chorionic villous sampling and early amniocentesis as early invasive diagnostic modalities. Color Doppler imaging has added important information on the functional integrity of the maternal-fetal circulation. The main advantages of the application of color Doppler imaging in invasive transvaginal diagnostic techniques are as follows:

Chorionic Villous Sampling

The diagnostic accuracy and safety of chorionic villous sampling are nearly the same as those of amniocentesis. Chorionic villous sampling is generally performed with transabdominal ultrasound guidance, with either a catheter placed through the cervix or a needle placed percutaneously through the abdominal wall. The transvaginal route, in which the needle is placed through the vaginal and uterine wall, is usually performed at a gestational age of 8–12 weeks. Ultrasound-guided transmural puncturing promises to be most accurate, least traumatizing and less painful. The small depth of penetration under high-resolution ultrasound guidance is the most striking advantage of this method. Color Doppler allows precise sonographic imaging of the placental site by visualization of the umbilical cord and its insertion.

Early Amniocentesis

Using a transvaginal approach and directed needle it is possible to aspirate the amniotic fluid as early as 9 weeks of gestation. The advantages of early amniocentesis are clear images, patient acceptance and availability of chromosome analysis and amniotic α-fetoprotein[28] measurement. The main complications during this invasive procedure include fetal demise, rupture of the membranes, bleeding and infection. It seems that color Doppler could decrease the fetal loss rate by more precise identification of the placental localization and visualization of the umbilical cord.

CONSERVATIVE MANAGEMENT OF ECTOPIC PREGNANCY

In the past, the diagnosis of ectopic pregnancy was made at the time of laparotomy, and very often in the presence of a hemodynamically unstable patient. The physician was often left with little choice but to perform a salpingectomy, salpingo-oophorectomy or segmental resection of the Fallopian tube. At that time the physician's concern was to save the patient's life and usually not to preserve the potential of the affected Fallopian tube. More recently, using sensitive pregnancy tests and transvaginal and/or abdominal ultrasonography, it has become possible to diagnose ectopic pregnancy at such an early stage that less radical surgical and medical therapies are being used as the preferred treatment.

The use of a needle, which is inserted into a tubal pregnancy under transvaginal ultrasound guidance, can save a patient from a more invasive procedure. Feichtinger was

the first to describe the use of transvaginally guided needle puncture to treat the ectopic tubal gestation.[29] Since then, several centers have used this modality as an additional tool in treatment of patients with ectopic pregnancy.[28,30–33] One complication that may occur is concurrent or delayed hemorrhage, fortunately, this is a very uncommon event, and generally occurs during the first one or two days in approximately 15% of patients.[28] The other complication is the persistence of trophoblastic tissue within the Fallopian tube and a persistent elevation of the hCG levels following the procedure. Many of these cases can be treated in a non-surgical fashion, using the systemic administration of methotrexate.[34] Systemic use of methotrexate has been documented to be safe, effective and well tolerated.[34–35] Preliminary evidence suggests that fertility potential after such a treatment is comparable to that following the conservative surgery.[34–36]

Since the introduction of transvaginal sonography with color flow imaging within a high frequency probe, a more accurate and faster diagnosis of ectopic pregnancy is feasible. Color Doppler appears to be useful for the positive diagnosis of ectopic pregnancy with ultrasonography when no adnexal gestational sac is observed.[37] Peritrophoblastic flow is prominent, randomly dispersed inside the solid part of an adnexal mass, and clearly separated from ovarian tissue. A low impedance signal, and a resistance index usually less than 0.45 extracted from the color-coded area indicate invasive trophoblast. A clinical impression of probable tubal abortion is gained in patients with no color flow, or increased vascular resistance of the peritrophoblastic flow and a β-hCG level less than 1000 IU/ml. Using Doppler it is possible to identify the vitality and invasiveness of the trophoblast; these are the most important characteristics to consider when planning the management of ectopic pregnancy.

Eleven patients with unruptured ectopic pregnancy less than 3 cm in diameter were treated locally with methotrexate at our Department. After slight sedation, the tubal pathology (“tubal ring” containing the ectopic embryo or solid part of the complex adnexal mass) was imaged. Color flow was superimposed on the anatomical structure and pulsed Doppler waveform analysis showed low impedance (resistance index cut-off value of 0.45 or less) and high velocity. Using the equipment’s software-generated puncture path line, the needle was introduced in the area of the maximal color signal. We administered methotrexate, 1 mg/kg of body weight, into the area of active trophoblastic flow. Determination of serum β-hCG levels and transvaginal sonography were performed every second day, until the β-hCG levels reached non-pregnant levels. Color flow imaging, with its great potential for tissue characterization, was used for serial determinations of blood flow from questionable adnexa. In patients with successful salpingocentesis, serially analyzed serum levels of β-hCG returned to non-pregnant levels (n=9), while pulsed Doppler waveform analysis showed increasing values of impedance to flow. Changes in the vascularity could be correlated with the effect of medication on the vitality and invasiveness of ectopic active trophoblastic tissue.

Based on our own experience, transvaginal color Doppler incorporates both diagnostic and therapeutic potential with regard to ectopic pregnancy. By this method it is possible to follow patients under conservative treatment safely, comparing color Doppler findings to the decline in β-hCG. Serial β-hCG determinations showed that in patients who underwent successful salpingocentesis, the serum levels of β-hCG returned to non-pregnant levels after 10–22 days. Using color flow imaging, it becomes possible to avoid puncturing through a highly vascularized area: bleeding during or immediately following

the procedure is significantly reduced. In cases suspicious of tubal pregnancy in which color flow within the tubal pregnancy was absent and β-hCG levels were less than 1000 mIU/ml, local administration of methotrexate could not be advised.

There is still much to be learned about ectopic pregnancy, its diagnosis and management. Transvaginal color Doppler represents an important addition in the proper selection of patients for conservative treatment, as well as in defining the individual therapeutic strategy.

Monteagudo et al[38] reported on a successful transvaginal ultrasound-guided puncture and injection of a cervical pregnancy in a patient with simultaneous intrauterine pregnancy and a history of a previous cervical pregnancy. They treated a cervical pregnancy by selective reduction using an injection of potassium chloride guided by transvaginal sonography. The intrauterine gestation was delivered at a gestation of 34 weeks by Cesarean section. Timor-Tritsch et al[39] described a proposed transvaginal ultrasound-guided puncture route applied to cornual ectopic pregnancy, leading the needle into the cornual ectopic pregnancy, first traversing the myometrium and approaching the gestational sac from the medial aspect. The probe was rotated into a position that enable the software-generated directional puncture lines to “transect” the thick uterine myometrium before reaching the gestational sac. This line approaches the ectopic cornual pregnancy form the medial aspect and avoids the puncture of a stretched out thin myometrium. Only cornual pregnancies with positive heartbeats were considered for puncture. A 21 gauge needle was then introduced into the chorionic sac and the embryo, with the use of an automated puncture device. There was no need for analgesia, since this automated spring-loaded puncture device advances the needle with high speed, thus making it virtually a painless procedure. The embryo is injected with methotrexate (25 or 50 mg in 1 or 2 ml solvent, respectively) or, in the case of a live heterotopic pregnancy, with potassium chloride. Half of the amount is injected into the embryo to stop the heartbeats and, if possible, the balance into the placental site when the needle is extracted. After completing the procedure the puncture area is observed for about 5–10 minutes to detect any moderate post-procedure bleeding, if it occurs. Puncture injection of cornual pregnancies is a relatively new treatment modality, which seems promising, since it may avoid the risks of surgery, no uterine scar is left, the patients may not need a Cesarean section and cornual rupture during a desired future pregnancy is avoided. Approaching the cornual pregnancy with its chorionic sac, embryo and placenta form the medial aspect and traversing the thicker myometrium creates a significant and protective safety layer, through which rupture or bleeding are less likely to occur.

OTHER APPLICATIONS

Zanetta et al[40] reported on transvaginal ultrasound-guided fine needle sampling of deep cancer recurrences in the pelvis. For aspirates and biopsies, sensitivity was respectively 76 and 91, while accuracy was 83 and 91. This technique is a safe procedure with limited invasiveness and extremely high specificity even when performed on small targets (median diameter in the study was 30 mm). Whenever possible, biopsies should be preferred. A negative fine needle biopsies obtained from a clinically suspicious lesion requires a repeat sampling.

CONCLUSION

Although ultrasound guided procedures are most commonly used in the field of reproductive assistance, it is clear that similar technique can be applied in other clinical situations as well. The extreme accuracy and high patient tolerance have initiated the widespread use of transvaginally performed puncture procedures. With the increasing number of the reproductive technologies, there is an evident increase in the number of ectopic pregnancies. More about the diagnostic and treatment algorithm for ectopic pregnancy will be discussed separately. Hysterosalpingo-contrast sonography is a convenient alternative for evaluation of tubal patency and is presented in a separate chapter.

REFERENCES

1. Smith EH, Bartrum RJ Jr. Ultrasonically guided percutaneous aspiration of abscesses. AJR 1974; 122: 308–12.
2. Gerzof SG, Johnson WC, Robbins AH. Expanded criteria for percutaneous abscess drainage. Arch Surg 1985;120:227–32.
3. Gerzof SG, Johnson WC. Radiologic aspects of diagnosis and treatment of abdominal abscesses. Surg Clin North Am 1984;64:53–65.
4. Feichtinger W. Transvaginal oocyte retrieval. In: Chervenak FA, Isaacson GC, Campbell S (Eds). Ultrasound in Obstetrics and Gynecology 1993; 1397–406 (London: Little, Brown and Company).
5. Kemeter P, Feichtinger W. Experience with a new fixed-stimulation protocol without hormone determinations for programmed oocyte retrieval for in-vitro fertilization. Hum Reprod 1989;4(suppl):53–54.
6. Kurjak A, Kupesic S, Schulman H, Zalud I. Transvaginal color Doppler in the assessment of ovarian and uterine blood flow in infertile women. Fertil Steril 1991;56:870–73.
7. Kupesic S, Kurjak A. Uterine and ovarian perfusion during the periovulatory phase assessed by transvaginal color Doppler. Fertil Steril 1993;60:439–43.
8. Kurjak A, Kupesic S. Ovarian senescence and its significance on uterine and ovarian perfusion. Fertil Steril 1995;64:532–37.
9. Feichtinger W, Putz M, Kemeter P. New aspects of vaginal ultrasound in an in vitro fertilization program. Ann N Y Acad Sci 1988;541:125–30.
10. Schwimer SR, Rothman CM, Lebovic J an Oye, DM. The effect of ultrasound coupling gels on sperm motility in vitro. Fertil Steril 1984;42:946–50.
11. Hill ML, Nyberg DA. Transvaginal sonography guided procedures. In: Nyberg DA, Hill LM, Bohm-Velez M, Mendelson EB (Eds). Transvaginal Ultrasound 1992; 319–29 (St. Louis: Mosby Year Book).
12. Damario MA. Transabdominal-transperitoneal ultrasound-guided oocyte retrieval in a patient with Müllerian agenesis. Fertil Steril 2002;78(1):189–91.
13. Feichtinger W. Follicle aspiration with interactive three-dimensional digital imaging (Voluson): a step toward real-time puncturing under three-dimensional ultrasound control. Fertil Steril 1998;70(2):374–77.
14. Kato O, Takatsuka R, Asch RH. Transvaginal-transmyometrial embryo transfer: the Towako method; experiences of 104 cases. Fertil Steril 1993; 59(1l):51–53.
15. Bret PM, Guibaud L, Atri M. Transvaginal US-guided aspiration of ovarian cysts and solid pelvic masses. Radiology 1992;185:377.
16. Bret PM, Atri M, Guibaud L. Ovarian cysts in postmenopausal women: preliminary results with transvaginal alcohol sclerosis. Radiology 1992; 184: 661.

17. Aboulghar MA, Mansour RT, Serour GI, Rizk B. Ultrasonic transvaginal aspiration of endometriotic cysts: an optional line of treatment in selected cases of endometriosis. Hum Reprod 1991; 6:1408–10.
18. Lerner JP, Monteagudo A. Vaginal sonographic puncture procedures. In: Goldstein SR, Timor-Tritsch IE (Eds.) Ultrasound in Gynecology 1995; 223–38 (New York: Churchill Livingstone).
19. Waegemaekers CT, Berg-Helder A, Blankhart A, Naaktgeboren N. Transvaginal ovarian cyst puncture in the early follicular phase of an IVF cycle, indications and results. Hum Reprod 1988; 3(suppl 1): 80.
20. Teisala K, Heinonen PK, Punnonen R. Transvaginal ultrasound in the diagnosis and treatment of tuboovarian abscess. Br J Obstet Gynaecol 1990; 97: 178–80.
21. Berkowitz RI, Lynch L. Selective reduction: an unfortunate misnomer. Obstet Gynecol 1990; 75:873–74.
22. Dumez Y, Oury JF. Method for first trimester selective abortion in multiple pregnancy. Contrib Gynecol Obstet 1986; 15:50–53.
23. Birnholz JC, Dmowski WP, Binor Z, Radwanska E. Selective continuation in gonadotropin-induced multiple pregnancy. Fertil Steril 1987; 48:873.
24. Brandes JM, Itskovitz J, Timor-Tritsch IE. Reduction of the number of embryos in multiple pregnancy. Fertil Steril 1987; 48:326–27.
25. Coffler MS, Kol S, Drugan A, Itskovitz-Eldor J. Early transvaginal embryo aspiration: a safe method for selective reduction in high order multiple gestations. Hum Reprod 1999; 14(7):1875–78.
26. Iberico G, Navarro J, Blasco L, Simon C, Pellicer A, Remohi J. Embryo reduction of Multifetal pregnancies following assisted reproduction treatment: a modification of the transvaginal ultrasound-guided technique. Hum Reprod 2000; 15(10):2228–33.
27. Fleischer AC, Pennel RG, McKee MS, Worell JA, Keefe B, Herbert CM, Hill GA. Ectopic pregnancy: features and transvaginal sonography. Radiology 1990; 174:375–79.
28. Timor-Tritsch IE, Peisner DB, Monteagudo A. Vaginal sonographic puncture procedures. In: Timor-Tritsch IE, Rottem S (Eds). Transvaginal Sonography. New York: Elsevier, 1991; 427.
29. Feichtinger W, Kemeter P. Conservative treatment of ectopic pregnancy by transvaginal aspiration under sonographic control and methotrexate injection. Lancet 1987; 14, 1(8529):381–82.
30. Menard A, Crequat J, Mandelbroat L, Hanny JP, Mandelanat P. Treatment of unruptured tubal pregnancy by local injection of methotrexate under transvaginal sonographic control. Fertil Steril 1990; 54:47–48.
31. Egarter C. Methotrexate treatment of ectopic gestation and reproductive outcome. Am J Obstet Gynecol 1990; 62:406–09.
32. Brown DL, Felker RE, Stowall TG, Emerson DS, Ling FV. Serial endovaginal sonography of ectopic pregnancies treated by methotrexate. Obstet Gynecol 1991; 77:406–08.
33. Mottla GL, Rulin MC, Guzick DS. Lack of resolution of ectopic pregnancy by intratubal injection of methotrexate. Fertil Steril 1992; 57:685.
34. Stowall TG, Ling FW, Gray LA. Single dose methotrexate for treatment of ectopic pregnancy. Obstet Gynecol 1991; 77:754–57.
35. Fernandez H, Baton C, Lelaidier C, Frydman R. Conservative management of ectopic pregnancy: prospective randomized clinical trial of methotrexate versus prostaglandin sulphostrone by combined transvaginal and systemic administration. Fertil Steril 1991; 55:746.
36. Ory SL. Chemotherapy for ectopic pregnancy. Obstet Gynecol Clin N Am 1991; 18:123–24.
37. Kurjak A, Zalud I, Schulman H. Ectopic pregnancy: transvaginal color Doppler of trophoblastic flow in questionable adnexa. J Ultrasound Med 1991; 10:685–87.
38. Monteagudo A, Tarricone NJ, Timor-Tritsch IE, Lerner JP Successful transvaginal ultrasound-guided puncture and injection of a cervical pregnancy in a patient with simultaneous intrauterine pregnancy and a history of a previous cervical pregnancy. Ultrasound Obstet Gynecol 1996; 8(6):381–86.

39. Timor-Tritsch IE, Monteagudo A, Lerner JP. A “potentially safer” route for puncture and injection of cornual ectopic pregnancies. Ultrasound Obstet Gynecol 1996; 7(5):353–55.
40. Zanetta G, Brenna A, Pittelli M, Lissoni A, Trio D, Riotta S. Transvaginal ultrasound-guided fine needle sampling of deep cancer recurrences in the pelvis: usefulness and limitations. Gynecol Oncol 1994; 54(1):59–63.

Chapter 54
Ultrasound in the Postmenopause

Boris Ujevic, Biserka Funduk-Kurjak, Asim Kurjak

INTRODUCTION

The menopause occurs because the ovary has no longer any follicles to respond to hypothalamic/ pituitary stimulation. At menarche, there are some 250,000–300,000 oocytes present, which are gradually used up in the succession of menstrual cycle from that time until around 50 years age, which is the average age for the menopause in Europe and the United States.[1]

Climacteric defines a more prolonged period of estrogen withdrawal, starting with the first decrease in frequency of ovulation, and ending in atrophy of secondary sex characteristics. A single point in that curve, when insufficient follicle maturity results in inadequate estrogen and no menses, is the menopause.[1] The postmenopausal period begins with the last menstrual bleeding (LMB).

Prior the menopause, the remaining follicles begin to perform less well. Release of the hypothalamus and the pituitary gland from inhibition results in raised gonadotropins levels characteristic of the menopause and well above those seen in the menstrual cycle at times other than the LH surge. Eventually there is a 10–20-fold increase in FSH and approximately a 3-fold increase in LH, reaching a maximal level 1–3 years after menopause, after which there is a gradual, but slight, decline in both gonadotropins.[1]

Estrogen production by the ovaries does not continue beyond the menopause, however, estrogen levels in postmenopausal women can be significant, principally due to the extraglandular conversion of androstenedion and testosterone, produced by the adrenal gland and the postmenopausal ovary, respectively. The clinical impact of this estrogen will vary from one postmenopausal woman to another, depending upon the degree of extraglandular production, modified by variety of factors, such as body weight, age and stress.[1]

According to that degree wide ranges of clinical diversity and symptomatology can be seen in practice.

The genital organs undergo general atrophic changes. The ovaries become shrunken and fibrous. The uterus and tubes shrink and, in the case of the uterus, the body shrinks to a greater extent than the cervix so that the ratio of the body to cervix becomes 1:1 or even 1:2. The vaginal epithelium shrinks markedly, glycogen disappears from the cells, lactic acid is no longer produced and the environment of the vagina becomes alkaline.[1]

A series of menopausal symptoms arise in many patients. Some concerned directly with hormone deficiency, some possibly concerned with ageing, and some emotionally related. Those directly concerned with estrogen lack are vasomotor symptoms, and urogenital atrophic changes, which can lead to dyspareunia and incontinence. Demineralization of bone leads to postmenopausal osteoporosis. Cardiovascular changes are evident too. Premenopausal women appear to have some immunity from coronary thrombosis and anginal attacks, which may be related to their different lipid background when compared with men. After the menopause, all lipid levels rise and there is an increase in LDL cholesterol with little change in HDL cholesterol.[1]

CHALLENGES OF THE POSTMENOPAUSE

For a female life expectancy in the developed world approaching 80 years a woman may, on average, expect to spend some 30 years—or 40% of her active life—in the postmenopausal era.[1]

It is probably true, that women today have greater expectations of higher quality of life, than previous generations. Therefore, it seems likely that climacteric and postmenopausal women will continue to place increasing demands on health care resources for many years to come. The gynecological care of the fertile female population has already been well established in most countries. In the not too distant future, postmenopausal women will constitute the major proportion of the gynecological patient population. Preventive medicine and care for elderly will be an essential part of the general gynecological practice. In parallel with the demands “climacteric and postmenopausal clinics” are being established worldwide with the active participation of gynecologists, cardiologists, rheumatologists, etc.

With better nutrition, health care and living conditions more women are living long enough to develop ovarian and endometrial cancers, which are known to be more common after the menopause. Undoubtedly the care of postmenopausal population must include the early detection of ovarian and endometrial cancers, just as the access to the benefits of hormone replacement therapy.

Estimating the potential individual benefits and monitoring the hormonal replacement therapy are further challenges in the medical care of the postmenopausal women.

Vaginosonographic examination has become an examination technique that is accepted by postmenopausal women in particular and which gives the less experienced examiner an overall view of the internal genital tract in the female.

Recent advantages of transvaginal color Doppler and three-dimensional ultrasound enables the more experienced examiner to visualize even the smallest vessels and investigate blood flow characteristics in the poorly perfused small pelvis in the postmenopause, what helps him to differentiate between the normal, suspicious and pathologic variations of the structures or detect and follow the effects the hormone replacement therapy on the perfusion of genital tract. In this chapter we will discuss the details of the mostly unexplored and extensively investigated role of ultrasound in the management of the postmenopausal women.

INSTRUMENTATION

There are a variety of configuration of transvaginal probes including also the great number of overall size and shape. Examining a woman in the postmenopause the ovaries and the endometrium must be special field of interest. In general the curved linear multielement transducers afford the best density and overall field-of-view for imaging.[2]

In elderly women the stenosis of the upper part of the vagina or adhesions of the vaginal walls can occur in addition to the atrophic changes of the epithelia. One must take special care when introducing the probe into the vagina of a woman in the senescence. Transvaginal sonography can induce unnecessary bleeding and pain. The same caution applies to women who have vaginal adhesions secondary to previous surgery for whom the vaginal examination may be painful.

Using thinner transducers and lubricant gels could help to avoid the unnecessary injuries. The angled shaped transvaginal transducers (Aloka, Toshiba, General Electric) require narrower movements in the vagina when imaging the lateral structures of the female pelvis thus decreasing the discomfort.

It is advisable to have an additional medical person being present during any kind of vaginal procedure.

SCANNING IN THE POSTMENOPAUSE

The first and perhaps most important condition for transvaginal ultrasonography should be a thorough emptying of the urinary bladder. This is the condition, what makes the transvaginal ultrasonography more comfortable for the significant group of incontinent postmenopausal patients comparing to the transabdominal ultrasonography, which requires full bladder. On the other hand, some elderly patients who are unable to empty their bladder completely may need catheterization in order to the better visualization.

Once the probe covered with condom and some ultrasound coupling gel it is inserted into the introitus with slight downward pressure on the perineum while gently separating the labia majora with the fingers of the other hand. A small amount of coupling gel applied to the outside of the condom can act as lubricating interface. If the patient desires she can insert the probe herself.

Inserting the probe into the, midvagina the anteflexed uterus can be normally imaged in its sagittal (long-axis) plane. However, in the postmenopause with the lose of the strength of the uterine ligaments and the pelvic support, the uterus is frequently alter its position in the female pelvis. With the advanced ages it is usually situated in the midline in a straighten position and can be imaged only after inserting the probe into the fornix. Additionally, a descended, even a prolapsed uterus let the examiner to orientate only after the re-establish the about normal situation by pushing the uterus upwards manually and then holding there with the probe. There is less problem with the visualization of the retroverted, retroflexed uterus in this age. Trendelenburg position makes the examination easier, even if the cardiac status of the patient makes it impossible.

In the long axis, one can appreciate the different interfaces of the endometrium, beginning with the interface of the cervical canal. Because the echogen cervical mucus is very poor and the endometrium can be very thin and atrophic in the PostmenoPause,

visualization of the endometrium can be difficult, usually it appears in the form of a thin, echo-poor line in the midline of the sagittal plane of the uterus.

After adequate image in the long axes are obtained the probe can be moved 90° to image the uterus in a horizontal (semi-coronal, semi-axial) plane. The endometrium again have to be identified in the level of the tubal ostia.

Once the endometrium is adequately depicted in its long and short axes, the probe is withdrawn into the midvagina and images of the cervix can be obtained.

The ovaries usually located lateral to the uterus, above and medial to the hypogastric vessels, lying in the area called “Waldeyer’s fossa”. Their size, morphology and locations are altered by the age, previous diseases and surgeries and other factors in the postmenopause. During the reproductive year the follicles serve as sonographic “markers” of the ovaries. After the menopause it is hard to find them because these “markers” are not present, the ovaries themselves atrophy and there is less pelvic fluid to provide an acoustic interface. Their detection becomes more difficult with advancing of the age. Beside negative bimanual pelvic examination non-visualization of the ovaries can be accepted without serious concern about ovarian pathology. With the introduction of color coded Doppler flow imaging, by finding the color coded flow of the ovarian artery or vein one can better detect the otherwise sonographically “non detectable” ovaries. Using the other hand can be very useful for manipulating the ovaries into the “scanningsight” of the probe by pushing them slightly downward through the lower abdominal wall into the direction of the tip of the probe.[3]

Detecting some free fluid in the cul-de-sac doesn’t necessarily means pathological finding, but in the presence of that ovarian pathology must be searched with special care. The same goes for any palpated or visualized solid structure in the cul-de-sac. The vascularization of these gynecological findings must be examined intentionally also by color and pulsed Doppler.

When a large amount of fluid is present, such as in ascites, one of the first questions is whether the pathological condition arises from an ovarian tumor or is related to a non-gynecological disorder. Fluid is clearly outline the boundaries of the structures and ovarian pathology may be revealed. If the ovaries appear normal, one may consider other reasons leading to ascites.

Constipation is not rare in postmenopausal patients. Scibalas shouldn’t be confused with pelvic masses. Excluding the vascularization of a structure by the color Doppler helps in differentiating normal to abnormal.

Solid pelvic masses also must be differentiated from the intestines. In real-time mode the motion of the bowels help to distinguish the peristalting intestines from the fixed structures. In the postmenopause the peristalsis is frequently inert, which requires proper patience from the examiner. In case of a vascularized mass color and pulsed Doppler offers again a quick possibility.

From all of the above mentioned it follows, that the sonographer have to get know the finding of bimanual pelvic examination, which should, therefore, precede the transvaginal ultrasound examination. It strengthens the recommendation that the person, who performs the transvaginal ultrasound examination in a postmenopausal patient, should perform a bimanual pelvic examination before, thus orienteering the anatomical situation and obtaining previous information to decide, which is the adequate way for ultrasonography or is there any suspicious structure palpated. In case of uncertainty of the

origin of the palpated or visualized structure transrectal examination or enema might be also necessary.

THE POSTMENOPAUSAL OVARY

Visualization

In the reproductive years, the normal ovary is relatively easy to detect by transvaginal sonography. The characteristic small sonolucencies, representing follicles or corpus luteum are missing in the postmenopause. Ovarian volume and diameter decrease with age. The normal atretic ovaries become more difficult to image, but even in the senescence the small, but normal ovaries are sometimes imaged.[4]

The postmenopausal ovaries appears small, uniform hypoechoic ellipsoid structures with a smooth outline located above and medial to the hypogastric vessels.[5] A small amount of pelvic fluid, which is less frequent in the postmenopause than in the fertile period, may also help to delineate the ovaries. Larger amount of fluid (ascites) makes them easily outlined.

In significant number of patients, the ovaries may not be detected, even after considerable time spent searching for them.

Eventually, the ovary becomes an inert residue that consist of connective tissue, and it clings to the posterior leaf of the broad ligament. In the postmenopause loosing the strength of the ligaments and the support of the pelvic floor the uterus might descent, while the ovaries remain in their position fixed to the pelvic wall by the atrophic infundibulopelvic ligaments. In this situation their distance from the fornices increase, thus their transvaginal visualization becomes more difficult, sometimes impossible. This can be the reason, that Granberg and Wikland[6] found transvaginal sonography to be slightly less accurate (23%) than abdominal ultrasound (34%) in visualizing the postmenopausal ovary. The above mentioned use of the abdominal hand might help in directing them into the scanningsight of the transvaginal probe and distinguish them from the bowel.

Previous surgery or the presence of adhesions as the consequences of previous pelvic inflammatory diseases can also fix the ovaries in abnormal locations.

Hall et al[7] visualized both ovaries in two-thirds of postmenopausal patients and at least one ovary in three-fourth of patients. Campbell et al[8] identified both ovaries in 84% of postmenopausal patients by transabdominal sonography. Rodrigez et al[9] imaged 84% of the postmenopausal ovaries by transvaginal ultrasound. In a study of Fleischer et al[10] on postmenopausal patients at least one ovary was detected 80% of the time, and both ovaries were imaged 60% of the time also by transvaginal approach.

According to the published data the introduction of the transvaginal ultrasonography did not result in improvement in the visualization rate of the postmenopausal ovary. However, much clearer images can be obtained using the transvaginal approach when the ovaries are localized. When both the transvaginal and the transabdominal approach were used, the visualization rate came close to 100%.[6] Therefore, in case of any difficulty in detecting the postmenopausal ovary, the techniques of transabdominal and transvaginal ultrasound may be used to supplement each other.[11] In some cases the significantly

enlarged ovary can be situated out of the pelvis and out of the range of the transvaginal probe.

There is no consistent view as to whether the inability to visualize the postmenopausal ovary assures a lack of pathology. The general consensus seems to favor the view, that lack of visualization of postmenopausal ovaries and a negative bimanual examination suggests ovarian atrophy and lack of disease.[4] In a study Rodrigez et al[9] were not able to visualize 19 of 104 ovaries preoperatively and during the subsequent histological evaluation all were found to be atrophic without any sign of disease.

Inability to visualize the postmenopausal ovary, by our experience, can be accepted as normal finding.

Morphology and Biometry

The menopausal ovary tends to atrophy and shrink when the Graafian follicles and ova disappear. The tunica albuginea becomes dense and causes the surface of the ovary to become scarred and shrunken. The cortex is marked with increasing thinning as well as numerous corpora fibrosa and corpora albuginea, with areas of dense fibrosis and hyalinization.[12]

The ovarian weight decreases from an average of 14 gr in the fourth decade to approximately 5 gr in the postmenopausal state. Whereas the normal ovary measures 3.5×2.0×1.5 cm, after the menopause it shrinks to 2.0×1.5×0.5 cm, and some instances it may be even smaller. At this point it can be palpated very rarely.

Several ultrasound studies have attempted to define normal ovarian size, and the general conclusion is that it should not exceed 2×3× 4 cm.[4,10,13–17] According to the measurements of Fleischer[10] the mean size of the normal sonographically imaged postmenopausal ovary was 2.2×1.2×1.1 cm. Others measured postmenopausal ovarian volume rather than size* (*ovarian volume=d1×d2×d3×0.523 where d1, d2, d3 are the maximal transverse, anterioposterior and longitudinal parameters), the mean figure of this parameter was 4.33 cm^3 in the pioneer work of Campbell.[8] In the paper of Goswamy[14] the mean ovarian volume was reported to measure 3.6 ml after examining 2246 postmenopausal women by transabdominal ultrasound. Granberg et Wikland[6] found it less smaller (1.4+/−1.0 cm^3), though in a different age group. In the series of Hall et al[7] all the ovarian volumes were less or equal than 2.5 cm^3.

Despite the difference in the size reported for the normal ovary, there is a close correlation between the size of the left and the right ovaries. In the above mentioned work on a large population Goswamy et al[14] found 0.01 ml difference between the means of the volumes of the left and right ovaries. Difference in size is particularly important, since each serves to some extent as a normal control for its sister.[11] Campbell et al[8] recommends that an ovary twice than size of its pair should be regarded a suspicious finding.

Multiparous women have ovaries that are approximately 12% larger. There seems to be no additional effect of parity if the woman had more than two children compared with two. History of breast cancer was associated with an increase in mean ovarian volume of approximately 11%.[14] Hormone replacement therapy does not seem to influence neither the size nor the perfusion of the postmenopausal ovaries.[18,19]

Ovarian Malignancy in the Postmenopause

Although the ovary becomes too old to function, it is never too old to form a cancer.[12] Visualization and measurement of ovarian volume in the postmenopausal patient are sometimes difficult but potentially afford early detection cancer or neoplasm. Ovarian cancer is the fourth leading cause of cancer death in women both in the United States and the UK.[20] The incidence increases over the age of 40 and the peak age for the appearance of common epithelial ovarian cancer is age 77.[12] The importance of early detection of ovarian cancer is evidenced by the fact that 5 years survival rates for stage I disease are 50 to 70%, whereas these figures for stage III and IV disease are 13 and 4%, respectively. The 5-year survival rate for women with ovarian cancer has not changed significantly over the past 30 years.[20] The ovarian cancer is asymptomatic until it has reached an advanced stage and mostly it is not diagnosed until the advanced stage. Several attempts were made by different investigators to establish an ultrasound based safe and cost-effective screening system for ovarian malignancy, including morphological criteria, color and pulsed Doppler and scoring systems.

Despite of these efforts currently there are no fully accepted screening methods to detect ovarian cancer at an early stage. On the other hand ultrasonography offers the capability of detecting even small increases in ovarian size and at least the potential for early diagnosis of ovarian malignancy. It is the responsibility of the examiner to take a chance and search for the ovaries very thoroughly and measuring them precisely when examining a postmenopausal patient. In case of any suspicious finding, deviation from the normal ovarian morphology or enlargement of the ovarian diameters or volume, change in ovarian volume at repeat scan,[5] the patients must be immediately directed to the higher center and examined in details according to the established ovarian cancer screening protocols.

Postmenopausal Palpable Ovary Syndrome (PMPO)

Enlargement of the ovaries in elderly women was considered pathological by Barber et al, who called this the “post menopausal palpable ovary syndrome” (PMPO).[21] For years, surgical exploration and oophorectomy was recommended when PMPO was detected, i.e. the ovary continued to demonstrate the size and consistency of a premenopausal ovary.[22,23]

According to the approach of Barber, “in the postmenopausal palpable ovary syndrome, the finding what is interpreted as a normal-sized ovary in the premenopausal patient represents an ovarian tumor in the patient who is at least 5 years after the menopause. This statement doesn’t mean that anything that is palpated in the adnexa is abnormal. It only refers to the size and consistency of the ovary.”[12,24]

Thorough ultrasound examination might reveal small anechoic ovarian cysts in the background, which shouldn’t necessarily be considered abnormal (see below), but should be reevaluated in 6–8 weeks with another pelvic examination and sonogram. “If the findings are the same (and almost certainly will be), the patient doesn’t require an exploratory laparotomy with removal of the uterus, tubes and ovaries. However, she should be directed to return again for a repeat examination and sonogram. If the findings are again the same and the tumor markers have remained within the normal limits, the patient can be followed in 4–6 months.”[12,25] Following this, she can be followed

according to the judgment of the responsible gynecologists, but further close follow up (in every 6 months) is advisable.

However, the PMPO syndrome still keeps most of the clinicians in uncertainty even in the presence of a calming sonography finding.

Despite of the excellent resolution of the newest real-time equipment and the accepted follow-up algorithms, cautious examination of the ovaries by transvaginal color and pulsed Doppler is strongly recommended in PMPO syndrome to resolve the doubts.

Unilocular Ovarian Cysts in the Postmenopause

The spreading use of the transvaginal sonography and the improving resolution of the equipment led to the detection of more unilocular, simple ovarian cysts in postmenopausal women than earlier known. The question is what is the risk of a completely anechoic unilocular tumor being malignant and whether the risk of a simple cystic tumor being malignant increases with age and size?[26]

Occasionally, follicles can be found in a resting state in the advanced postmenopausal years. Generally, the advanced follicles identified in the postmenopausal ovaries are undergoing atretic changes, but they may contain small, cystic structures. Any observed corpus luteum is also undergoing atresia (corpora albicantia). Sometimes a small cyst may be present in the so called “burned out” corpus luteum or corpus albicans or in a follicle. However, either the follicle or the corpus luteum that may persist in patients in this age group will be in the resting state.[12]

Only the cysts without any septation and papillary formations can be regarded unilocular.[27] Many reports presented on unilocular and anechoic ovarian cysts in the postmenopause diagnosed by ultrasound.[26,28–34] The values in these studies indicate that anechoic unilocular ovarian cysts in postmenopausal women carry a low risk of malignancy.

Andolf et al reported[30] simple postmenopausal adnexal cysts (2–8 cm).[30] After the surgical treatment of 15 of them no malignancy was revealed. During the following of the another 15 by transvaginal ultrasound 6 disappeared after one months, altogether 12 disappeared after seven months. After two years, only two 2-cm cysts remained. In their next work 31 they confirmed on a larger number, that small anechoic lesions are seldom, if ever, malignant in elderly women. However, among their 33 patients having totally anechoic cysts >5 cm they found three malignancies.

Upon the histological examination of 28 unilocular postmenopausal cysts <5 cm Goldstein et al 32 reported also 0% incidence of malignancy. Another 14 patients were followed from 10–73 months without any change in size or character of the cyst.

Parker et al[33] reported 25 unilocular cysts (3–9 cm, mean 5 cm) diagnosed by transabdominal sonography in postmenopausal women, who later underwent cystectomy by laparoscopy or laparotomy. None of the cysts were malignant.

In their studies Granberg et al[27,29] examined 140 postmenopausal unilocular cysts, 60 of them were <5 cm in diameter, 51 measured 5–10 cm and 29 cysts were >10 cm. Only one malignant tumor was found among them, this measured 5 cm in diameter. The sensitivity and specificity for excluding malignancy in an ovarian cyst in postmenopausal women by transvaginal ultrasound was 100%.[26]

Valentin et al[34] followed 134 postmenopausal women found to have an adnexal cyst judged to be benign and not causing any symptoms. Transvaginal ultrasound examination

preformed at 3, 6 and 12 months, and then every 12 months. Median follow-up time was 3 years. In majority of women the cysts disappeared or remained unchanged. With advancing age chance for regression of cyst declining.

The cytological evaluation of the cyst content proved to be very limited value for identifying malignancy even after the irrigation of the cystic tumor, and the combination of it with transvaginal ultrasound did not increase the diagnostic accuracy as compared with ultrasound alone.[28]

Goldstein suggested that purely cystic masses <5 cm might be follow up with seriously ill patients.[32] Andolf and Jörgensen[30,31] suggested that postmenopausal women with unilocular adnexal tumors, anechoic or nearly anechoic, should be rescanned once a month. It is close agreement with the recommendations of Barber, as described above in connection with the PMPO syndrome.

Granberg et al also agree, though they emphasize, that however, in cases of nearly anechoic simple cyst, especially when diagnosed endovaginally, the tumor must be removed at surgery to obtain diagnosis.[26] If internal echoes or increase in size appears during the follow up surgical exploration would seem to be a wise precaution.[31] For simple, unilocular cysts ultrasound guided puncture was found a valuable alternative to laparoscopy or major surgery by Granberg et al.[26]

The malignant potential and time factor of unilocular anechoic ovarian cysts in postmenopausal women is not known. Granberg et al therefore recommend surgical removal of such a cyst if it persist for more than a year.[26]

With its widespread utilization in the near future transvaginal color Doppler will make it possible to increase the reality of ultrasound diagnosis of unilocular cystic ovarian lesions. In their paper of 18 stage I ovarian cancers Kurjak et al[35] reported that ovarian cancer stage I was also discovered in two simple unilocular ovarian cysts using transvaginal color Doppler as well as in two morphologically normal ovaries which would have been missed if the morphology alone was considered. This finding would have an important clinical implication as these simple cysts are not always innocent, and color Doppler is, therefore mandatory to rule out the malignant revascularization.

Our opinion (supported also by Ekerhovd[36]) is that simple unilocular and anechoic ovarian cysts without recordable blood flow, smaller (or equal) 5 cm in diameter can be considered benign. Cysts like that should be followed at 3, 6, 12, 18, 24 months, and then every 12 months. Any change in cyst morphology or increased cyst size or blood flow warranted removing of ovaries. Measurement of CA-125 is also recommended.

Color Doppler Velocimetry of the Postmenopausal Ovary

The ovarian blood flow is significantly affected by ageing and the postmenopausal ovary shows varying degree of avascularity.

The ovarian artery is a tributary of the upper aorta and reaches the lateral aspect of the ovary through the infundibulopelvic ligament. Color Doppler enables visualization of the ovarian artery at the lateral edge of the ovary. In some patients, especially in the postmenopausal, these vessels are not clearly visualized and the sample volume should be moved across the ligament and then through the ovary until the arterial signal is identified. Signals from the ovarian artery are characterized by low Doppler shifts of a small artery with low velocity.

The only published data from direct and non-invasive measurement of normal ovarian and uterine perfusion in the postmenopause are from Kurjak et al.[37] Unlike in the presence of unilateral folliculogenesis and corpus luteum formation during the normal menstrual periods, there is no differences in the vascular impedance between the left and right ovaries in the postmenopause.[38,39] Significantly increased ovarian blood flow impedance can be demonstrated already during the climacterium, when compared to that of the "dominant" ovary in a normal menstrual cycle. The mean RI increasing further in the next years of the postmenopause reaching the value of 1 after 10 years. The absence of the diastolic flow is common already in the early postmenopausal period and constantly found in patients with more than 11 years of postmenopause.

Even with the latest advanced equipment seems to be not possible to detect velocity waveform signals from the ovarian parenchyma in normal postmenopausal patients. This can be the result of the relative increase of the amount of the connective tissue. Therefore, any color flow obtained from a postmenopausal ovary should generate a high index of suspicion for abnormal revascularization and requires detailed pulsed waveform Doppler analysis.[37,40]

In a previous study Kurjak et al examined 1000 postmenopausal women with transvaginal color and pulsed Doppler sonography.[40] A total of 74% were asymptomatic; the others were referred or self referred for symptoms. There were 83 women with findings that resulted in surgery. Separation of the groups into benign and malignant cases did not reveal significant differences in age, duration of the menopause or symptomatology. A total of 29 tumors were malignant, a prevalence rate 36% in the group underwent surgery and 3% in the total postmenopausal group underwent examination. An ultrasound score was used to analyze the morphology of the tumors. The score was successful in separating benign from malignant tumors with all indices of normality >=90%. Color flow was identified in 27 of 29 malignant tumors and 35% of benign masses. A cut-off value in the Doppler resistance index 0.40, in the feeder vessels, had a sensitivity and specificity 96% and 95% for separating benign tumors from malignant tumors, respectively. Positive and negative predictive values were 96% and 95%.

In their next retrospective study on this topic already mentioned above, 18 patients with ovarian carcinoma stage I were studied to evaluate the efficiency of transvaginal color Doppler sonography.[35] Four of these patients were asymptomatic and self referred for their annual check-up. Another four asymptomatic women, two with morphologically normal ovaries and two with simple unilocular cysts, were picked up during the screening program. Ovarian carcinoma stage I was detected in two normal-sized ovaries from only color and pulsed color signals, which represented tumor angiogenesis, and low impedance to blood flow (RI<0.40).

Fleischer et al published data of nine stage I ovarian carcinomas where three of them had benign appearance but suspicious blood flow characteristics.[41]

Crade et al calculated, that a postmenopausal women with a mass greater than 5 cm and RI below 0.50 had a malignancy risk of 66%, while a mass having a RI value higher than 0.60 had only a risk of 2.4%.[42]

If further investigations by other laboratories also confirm these result, transvaginal color Doppler ultrasonography may provide a valuable tool for monitoring the ovarian

involution in the postmenopause and objective aid for choosing between the conservative, laparoscopic or radical management of pelvic masses found in postmenopausal patients.

THE POSTMENOPAUSAL UTERUS

Morphology

The uterus can be imaged in three major scanning planes with TVS. There is generally a homogenous echo pattern in the postmenopause, and the uterine cavity is frequently not imaged.[43] The uterine wall is smooth and clearly outlined against its surroundings. In the myometrium, towards its periphery and often protruding, can be found echoless vessels. In the postmenopause the arteries can calcify in this region. These calcifications appear as small, bright reflections, regularly spread in the uterine wall. They can evoke shadowing, which may impair the assessment of structures lying beyond, e.g. the endometrium.[44] Unlike in all phases of the menstrual cycles, undulatory motions, i.e. uterine contractions[45] cannot be observed in the postmenopause.

Biometry

As in the case of all genital organs in the female, the development, the maintenance of the fertile size and shape, and the postmenopausal physiologic involution of the uterus are highly dependent on the actual serum level of the estrogen.

Measurement of the uterus in the sagittal plane can be carried out either by determination of the portio-fundus distance or in postmenopause the separate measurement of the cervix and corpus uteri can be also used. It was already mentioned in the introduction, that the corpus-cervix ratio of the postmenopausal uterus shows remarkable changes in favor of the cervix, with advanced ages it can even fall below 1 and can reach the 1:2, like in childhood.

The sagittal measurement is supplemented by the determination of the largest anterio-posterior diameter of the corpus uteri, and of the largest transverse diameter of the corpus. The size of the corpus decreases markedly in the postmenopause, shrinking to average 4.5×1.5×2.5, with the cervix predominantly over the corpus in the sense of the elongation of the cervix.[43] The mean length of the postmenopausal uterus was shown to be 59+/−11 mm by Andolf et al.[46] The upper size limit of the postmenopausal uterus has been suggested to be 3 cm in the anterior-posterior diameter, with a cervical-fundal length of 8 cm. The patient who is only 1–3 years postmenopausal when still has significant endogenous estrogen production by the ovaries, or who has significant endogen estrogen production by fat from adrenal precursors will have larger uterus, than the patient who is over 10 years postmenopausal. Clinical judgment is needed in interpreting normality of uterine size in postmenopausal of uterine size in the postmenopausal patient.[11]

Uterine involution is a slow process. Myometrial thickness are changed as the years of the postmenopause progress. In their study Zalud et al[47] did not found significant changes in the myometrial thickness in women without HRT over the years after the menopause, though slow thinning can be observed. Myometrial thickness after the menopause

changes less than does endometrial thickness, which may suggest that these changes are more dynamic.

The Uterus under HRT

Comparing myometrial thickness between groups of postmenopausal with and without HRT, Zalud et al[47] did not demonstrated statistical difference, though slight difference were found in favor of women, who received HRT more than 5 years. These data are not surprising in the mirror of the findings of the same group, namely that the myometrial involution couldn't been statistically expressed over the years throughout the postmenopause, too. The involutional process of the myometrium is very slow and other factors, than estrogen can also influence, as the sizes of the uteruses of fertile women can show great variability, too.

Color Doppler Velocimetry in the Postmenopausal Uterus

The vascular supply of the uterus is provided by a complex network of arteries originating from the uterine artery, which is a branch of the hypogastric artery. The color Doppler signal from the main uterine vessels can be seen lateral to the cervix at the level of junction between the corpus and cervix.[48] Flow velocity waveforms from the radial arteries can be obtained within the myometrial fibers, while spiral arteries are visualized at the level of endometrial-myometrial junction.[38]

Visualization of both uterine artery by transvaginal color Doppler can be achieved even in the advanced years of the postmenopause. In contrary, visualization rate of the myometrial and endometrial vessels are highly dependent on the length of the postmenopausal period.

The ageing process affects the uterine perfusion. In general high impedance and high velocity is characteristic for the uterine arteries, though the uterine perfusion is largely dependent on age, phase of menstrual cycle, other conditions (e.g. pregnancy, tumor)[49] and there are complex relationships between the concentration of the ovarian hormones in the serum and uterine artery blood flow parameters.[50–52]

Additionally, there might be also a relationship between the serum gonadotropin levels and uterine perfusion. Examining normal postmenopausal patient and premenopausal patients treated with GnRH analogues Luzi et al found, that the pulsatility index of the uterine artery in spontaneous menopausal women is significantly higher than in artificial menopausal women. This phenomenon may be due to a different hormonal pattern which exists in the two groups, i.e. the gonadotropin levels increased in the former and decreased in the latter. The vascular compliance in artificially induced menopause is higher than that observed in spontaneous menopause, as shown by a higher diastolic flow and a less deep notch. The decrease of the vascular compliance in postmenopause can be caused by progressive sclerosis of the vessel walls.[53]

Resistance to blood flow increases in both the main uterine and the radial arteries as the years of postmenopause progress, though the increase of ovarian blood flow impedance is more pronounced. The fact, that uterine artery RI does not change significantly in the first years of menopause strongly support the thesis that ageing process initially affects the uterus less than the ovary.

The diastolic flow decreases in postmenopause and the systolic peak increases.[53] The RI in the main uterine arteries continuously increases with the number of the postmenopausal ages, but unlike in the case of the ovarian artery, doesn't reach the maximum in all women even at advanced ages.

Absent diastolic flow in uterine arteries was found in 15% of women with 1–5 years duration of menopause, while clear interruption of diastolic blood flow was observed in the uterine artery of one-third of the women in the next five years of the postmenopausal period. More than half of the women has this finding with 11–15 years lasting postmenopause and finally, 80% of women whom LMB occurred more than 16 years ago demonstrated absent diastolic blood flow signal indicative of high vascular impedance.

The changes in flow velocity patterns of the radial arteries in postmenopausal patients parallel the blood flow dynamics of the uterine arteries.

Visualization of clear Doppler signals from the spiral artery is possible only in less than one-third of postmenopausal women, in whom LMB occurred 1–5 years previously. The impedance is significantly increased in these vessels, too, when comparing to the premenopausal levels. In normal postmenopausal women already 6 years after the LMB no blood flow signals can be expected from the inner third of myometrium and the area of the myometrio-endometrial junction.[52]

Myomas and Malignant Potential after the Menopause

Uterine fibroids of 0.5 cm can be detected by TVS and their relationship to the endometrial cavity precisely defined (e.g. submucous, intramural, subserous). They appear with TVS as rounded, well defined, space occupying structures.[54]

Growth of myomas is known to be estrogen dependent. The management of the myoma around the menopause is highly conservative, since after the menopause they supposed to regress in the lack of the hormonal support. Myomas with good vascularization can be seen less frequently after the menopause. They show more hypoechogenic structure, compared to the normal uterine tissue, while homogenous, hyperechogenic myoma have often undergone regressive changes and have a large amount of connective tissue. Other regressive changes such as necrosis and caseous and cystic degeneration can be recognized by the presence of hypoechogenic regions or regions without echogenicity in the myoma. Such a necrotic myoma can be confounded with an ovarian cyst or a colliquated endometrial carcinoma depending on its localization. Hyalinization and calcifications of the myoma responsible for bright reflections can be seen frequently in the postmenopause.[43]

Transvaginal color Doppler can be used to assess leiomyoma vascularity, as well as the physiological and pathophysiological characteristics of uterine artery blood flow.[55,56] The vascularization of leiomyomas is supported by pre-existing myometrial vessels originating from terminal branches of uterine arteries. Since the leiomyoma grows centripetally as proliferation of smooth muscle cells and fibrous connective tissue, the color Doppler demonstrates most of the leiomyometrial blood vessels at its periphery. While their visualization rate high in the premenopausal period (58–70%),[57–59] it decreases after the menopause with the decreased blood supply of the uterus.[37]

The growing inclination of the myoma is in correlation with the increased blood flow in the uterine network, the latter is thought to be a result of large concentration of estrogen receptors and estrogens.[60–62] Whether the regression of the myoma after the

menopause is resulted directly by the fallen estrogen levels or it is only a secondary consequence of the decreased perfusion, still not known. Though Doppler studies on the perfusion of the uterine fibroids in the postmenopause are not available yet, it can be anticipated from the Doppler studies on myomas under treatment with GnRH analogues,[59,63] that with the decreasing estrogen levels the previously decreased impedance of the uterine artery and the supplying myometrial vessels are increasing to the level of a normal postmenopausal uterus leading to the involution of the myoma.

It must be emphasized, that in case of necrotic, degenerative changes in the myoma the presence of blood vessels in the central portion is usual and the impedance of them can be so low, that might be misinterpreted as malignant neovascularization.

One can use TVS as a means of monitoring the size and the ability for growth of the leiomyomas around and after the menopause. If there is evidence of rapid growth of a pre-described myoma in a postmenopausal women, and in ultrasound an increase of echoless areas as a sign of necrosis, laparotomy should be performed because of a suspected malignant transformation.

Though the sarcomas are account for only 1–3% of the malignant tumors of the uterus (including the endometrium), their early diagnosis can greatly depend on an occasional but accurate ultrasound examination, since there are scarcely any symptoms of an early process. It is expected to be more common, since the conservative treatment of uterine myomas is becoming more reliable alternative to the surgery.[64]

Nevertheless, there are, similar to macroscopic aspects, sonographic indications for the existence of sarcoma. Primary sarcomas in ultrasound examinations appear as poorly outlined masses, partly hyperechogenic, partly irregularly limited and hypoechogenic, or without echogenicity. Morphological differentiation from myoma can be facilitated by the absence of any systematic structure (onion-skin or whirlpool pattern). Differential diagnosis of inhomogenous, myometrial masses can be myomas undergoing carneous degeneration, with a pool of liquid or bleeding into the myoma.[43]

Application of the color and pulsed Doppler may confirm or preclude the *in vivo* diagnosis of uterine sarcoma. The presence of irregular, thin and randomly dispersed vessels in the peripheral and/or central area of tumor, with very low impedance shunts characterizes intratumoral neovascularization and is in favor of the malignant transformation. In benign uterine lesions, even if intratumoral vascularization can be detected, the resistance to blood flow was found significantly higher. Furthermore, in the case of the uterine sarcoma, both uterine arteries shows a low impedance in comparison with that of normal, even the postmenopausal or myomatous uterus.[65]

Unfortunately as the result of the wide range of the biological variations and the vascular characteristics of tumors an overlap exists between the blood flow patterns of benign and malignant uterine tumors. At the moment the realistic approach is to consider the above mentioned guidelines only in general, but one has to take the decreased intratumoral impedance and increased vascularity into serious consideration, especially it is accompanied with rapid growth of the tumor during the serial examination.

Leiomyomas under HRT

Leiomyomas are the most common pelvic tumors in women of the reproductive age; 20–25% of women have uterine myomas.[66] Higher concentrations of estrogens[60] and

estrogen receptors[61] within leiomyomas than in adjacent myometrium were taken as evidence of the hormone dependence of their growth.

Though they tend to regress after menopause with the decreasing serum level of the promoter estrogen, it is questionable, whether the introduction of the HRT promotes the growing process again. The data are confronting, in some papers myoma growing, in some there is no difference in size and in some there is even decreasing in size.[67–71] However, even if there are increasing in myoma size, this does not appear to cause clinical symptoms.

In practice, uterine and fibroid size can be closely monitored by ultrasound and HRT can be easily discontinued if the fibroid enlarge.

THE POSTMENOPAUSAL ENDOMETRIUM

Visualization and Morphology

After the menopause, decrease of ovarian estrogen production leads to atrophy of the endometrium. In consequence the endometrium of a postmenopausal women is typically thin when examined by TVS, which corresponds to the stratum basale adjacent to the myometrium.[72] Its sonographic feature is very similar to that of the endometrium in the early follicular phase.[73] The endometrial band is sonographically narrow and the echogenic line of the uterine cavity often cannot be visualized.[44] In the study of Andolf[46] the endometrium couldn't be localized in 7% of postmenopausal women without bleeding disorder. Granberg et al couldn't visualize 10% of the histologically atrophic postmenopausal endometrium.[74] In addition, shadowing arising from myomas or arteriosclerosis make visualization more difficult. Echotexture of the endometrium is usually more echogenic than the surrounding myometrium. In the above mentioned study of Andolf 85% of the assessable endometrium were less echogenic than the myometrium in asymptomatic postmenopausal women.

The poorly echogenic myometrial zone, the subendometrial halo round the endometrium is frequently absent in the postmenopause.[44] However, the interrupted subendometrial halo was reported as a common sign of the myometrial invasion of the endometrial carcinoma.[75]

The Postmenopausal Endometrial Thickness

Contrary to early methods of measurement of the thickness of the endometrium, today—according to general agreement—measurement should be carried out as follows: the uterus is viewed vaginosonographically in the longitudinal section and the total thickness of the endometrium is measured in the largest diameter (double layer). In the case of any kind of intrauterine fluid collection, the thickness of the fluid pool in the uterine cavity is subtracted from the total thickness.[73]

The postmenopausal endometrial thickness is 2–4 mm, with a considerable scatter range of 0–10 mm, and consequently there are different limiting values for the normal state in the literature. There is a correlation between the endometrial thickness and the body weight. Women with pure estrogen replacement therapy frequently have endometrial thickness exceeding that of postmenopausal women without it.[76]

Suspect Postmenopausal Endometrium

Endometrial carcinoma is the most common invasive gynecological malignancy in the United States and Europe today. The incidence of the disease increases considerably during the fifth decade of life and the average age at diagnosis is 59 years. In the more cosmopolitan, higher income population the rate has overcome the 40 cases per 100.000 related to increased longevity, increased cholesterol in diet, and exogenous estrogen supplementation or substances with an estrogen-like effect.[77,78] The five-year survival rate is related to myometrial invasion, ranging from 93.7%, when no invasion is present to 36.2% if the invasion is deep.[79] When the first clinical sign, vaginal bleeding occurs, the myometrial infiltration depth is already 10 mm on average.[72]

Of endometrial carcinomas 80–90% present with atypical bleeding demonstrating the ineffectiveness of exfoliative cervical cytology and the need for early recognition of this most frequent genital malignancy.[72,80] Until now curettage and histologic evaluation is the accepted method to assess the background of the atypical bleeding. However less than 10% of women with postmenopausal bleeding have endometrial cancer.[74,81] Therefore, a new non-invasive screening method must fulfill at least double requirements: it should be able to recognize the abnormal endometrial process at an earlier stage, than bleeding occurs and it should reduce the number of the "unnecessary" curettage, when postmenopausal bleeding occurs.

Several publications have reported that endosonographically measured endometrial thickness correlates closely with the presence or absence of endometrial cancer in asymptomatic postmenopausal women.[82,83] An endometrium, that measures greater than 8 mm from one myometrialendometrial interface to another in postmenopausal woman without HRT is highly likely to be associated with significant endometrium pathology. Approximately 10% of asymptomatic postmenopausal women have endometrium exceeding this cut-off level and 3.5% of them can be expected to have endometrial carcinoma.[84] There is, however, a significant false-positive rate. Using a cut off level of 8 mm we have a very high sensitivity, but a low specificity.[72] The only way to increase the specificity would be to adjust the cut-off value to a higher level, but in this case the sensitivity of the screening would decrease and more positive cases might be overlooked.

Another possible approach to reduce the number of false-positive findings could be the use of color Doppler.

The realistic approach is that endometrial thickness up to 5 mm can be regarded as completely normal finding in the postmenopause. Endometrial thickness 6–9 mm requires control examination in 3–6 months time, if the patient really asymptomatic. Endometrial thickness of 10 mm and above requires urgent histological examination.[73]

The most essential characteristic of a cancer screening method is not only detect the malignancy, but also improve the prognosis by early detection. Osmers et al[72] compared the myometrial invasion depth, the most prominent prognosis factor of asymptomatic endometrial cancers detected by TVS (cut-off value 8 mm) and symptomatic cancers (atypical bleeding). They concluded that early endometrial cancers detected by TVS will have better prognosis than symptomatic ones, since the average myometrial invasion was 4 mm and 10 mm, respectively.

Up to now, there are no sonomorphologic criteria to differentiate between benign and malignant endometrial neoplasm. Therefore we cannot detect endometrial cancer by TVS alone, but TVS is an excellent tool to define a risk group in postmenopausal women.[72]

Postmenopausal Bleeding and Transvaginal Sonography (transvaginal sonography versus dilatation and curettage)

In atypical bleeding in the postmenopause, besides clinical and cytological examination, careful sonographic assessment should be made of the ovaries and the cervix uteri.[73]

Transvaginal ultrasound has become an important tool for diagnosing endometrial pathology in women with postmenopausal bleeding, too. In patients with postmenopausal bleeding, the endometrium are considerably thicker, than in asymptomatic women.[85]

Several studies have been investigated the effectiveness of the endometrial thickness measurement in detecting malignancy in patients with postmenopausal bleeding, using different cut-off levels.[72,86–90] Summarizing the results of the published works in none of the case was endometrial carcinoma found below 5 cm.[73] According to the examinations of Osmers et al[72] with a chosen cut-off level of 8 mm, endometrial carcinoma could not be detected either in case of atypical bleeding. This cut-off levels applies not only to carcinoma, but also its preliminary stages, such as adenomatous hyperplasia with atypia. One might conclude at the first sight, that measuring an endometrium less than 5 mm is safe enough to exclude the possibility of endometrial carcinoma in case of postmenopausal bleeding. As far as we have very little knowledge about the origin and behavior of cancers, it is up to future studies to clarify how far, in patients with endometrial thickness below 5 mm and atypical bleeding, dilatation and curettage might be avoidable under certain circumstances with the help of sonographic follow-up.[73] While morphological criteria for the assessment of the endometrium have so far not gained acceptance, again transvaginal color Doppler can be proved to be a help of the clinician in the future.

Nevertheless, if this method is to be used for identifying those women who will not have a dilatation and curettage performed, based on the findings on the endometrium, training is needed to minimize the error. Karlsson et al found considerable differences, when compared the measurements of experienced and inexperienced examiners.[91]

Postmenopausal Intrauterine Fluid Collection

Occasionally, a small amount of intraluminal fluid may be detected in the postmenopausal uterus, the detection rate of it can reach the 16% in asymptomatic postmenopausal women.[73]

We can only speculate as to the pathophysiology of fluid accumulation in the uterine cavity. Senile cervical stenosis can prevent drainage of possibly minimal endometrial secretion leading to small intrauterine pools. This, however, speculative as some degree of cervical stenosis is ubiquitous in postmenopausal women, whereas intrauterine fluid is rare finding. Patients with ascites are more likely to have intrauterine fluid.[2] The possibility of the tubal cancer is rather theoretical, than practical, although one case one reported by Carlson.[92] Cancer of the cervix may obstruct the cervical canal and can cause intrauterine fluid accumulation. However, the main suspected reason must remain the endometrial malignancy.

Though the presence of intrauterine fluid has been considered ominous and related to malignancy by some authors,[93,94] the significance of this finding is still not clear,

especially in routine examinations. Management and clinical evaluation have also not determined.

In their recent series of twenty postmenopausal women with intrauterine fluid collection Pardo et al[95] revealed 3 cases of endometrial carcinoma, though it must be emphasized, that all of these positive cases the endometrial thickness was more than 4 mm.

Carlson et al reported also twenty cases of endometrial fluid collection in the postmenopause, of which five proved to be results of some kind of genital malignancy (two ovarian, one tubal, one endometrial, and one cervical).[92]

However, examining the fluid pools in the uterine cavity Osmers et al did not find association with pathological changes in narrow endometrium.[73]

The extensive use of sonography will lead to an eventual increase in the number of postmenopausal patients diagnosed with intrauterine fluid. In every case, careful scanning is recommended—to rule out ovarian and tubal pathology. Obviously, the endometrium must be submitted serious examination by transvaginal ultrasound. Polyploid growths and irregularity of the endometrial surface are particularly well seen when surrounded by intraluminal fluid.[2] Certainly, cytological evaluation of the cervix, with special regard to the cervical canal is essential. Additionally, both Pardo and Carlson recommend immediate endometrial sampling even in the cases of thin endometrium, until accumulated data permit dismissal of endometrial sampling in that cases.[92,95] According to Osmers et al indication for D&C is given only when there are pathological endometrial findings.[73] In the lack of any other suspicious finding and beside thin endometrium Fleischer also allows rescanning, but if it is present or even volume increase on repeat scans, this finding should be considered suspicious for an endometrial disorder.[2]

Undoubtedly, color Doppler offers an additional help in getting closer to the proper management, as it is able to assess the vascularization around this questionable ultrasound finding of postmenopausal intrauterine fluid collection.

Color Doppler Velocimetry and the Postmenopausal Endometrium

The visualization rate of the postmenopausal endometrial vessels are very low. The visualization rate of endometrial vessels is in accordance with decreasing endometrial thickness with the postmenopausal years.[52] As it was already mentioned, vascularization of the inner third of the myometrium and the endometrio-myometrial junction is possible only in about or less than one-third of those normal postmenopausal patient, who had the last menstrual bleeding not more than 5 years previously.[37] No flow can be detected in the normal, atrophic endometrium in the postmenopause.[75]

Although a thick endometrium may be a sign of pathological processes, no morphological features that are unique to malignant disease have been identified.[84] Transvaginal color and pulsed Doppler has shown that the presence of intratumoral vascularization with a low impedance to blood flow can be used as an end point in screening programs for some gynecological malignancies.[81–96,97]

Bourne et al reported the impedance to blood flow in the uterine arteries and the endometrial thickness in women with postmenopausal bleeding with or without cancer.[78] In the women with postmenopausal bleeding who did not have endometrial cancer and in those without postmenopausal bleeding were similar. Conversely, the highest PI in the

group with cancer (1.49) was below the lowest value in the group without cancer (1.95). Data from this study suggest that, in the presence of malignant tissue, the impedance to blood flow within the uterine artery is reduced significantly when compared to control groups. This observation was later confirmed by others.[98] If color Doppler is used to interrogate the endometrium in such cases, angiogenesis can be demonstrated as areas of color superimposed on the B-mode gray scale image and the sensitivity of the technique is enhanced.[81]

Hata et al found a feeder artery in patients of endometrial cancer, and in seven out of nine endometrial cancers even venous blood flow in the endometrium could be detected, while no flow was detected around and within the endometrium in noncancer patients.[99] These findings were confirmed by pelvic angiography.

In the work of Kurjak et al visualization rate of the abnormal blood flow within the endometrium was 100% in the cases of endometrial carcinoma.[75] Of the cases with detected endometrial carcinoma 90 had endometrial (tumoral) thickness >10 mm, which is already a suspect sonographic sign alone. However, 10% of these endometrial carcinomas with endometrial thickness 5–10 mm would have been missed without color Doppler.

It was also suggested in the same work, that color Doppler should help in distinguishing between cancerous and hyperplastic thickened endometrium. Flow could be detected only in 92% of cases of endometrial hyperplasia. Blood flow pattern was characterized with a low RI near or <0.40, which constituted statistically significant difference compared with that of endometrial hyperplasia, if any flow detected.[75]

By using color Doppler and measurement of the endometrium thickness together whilst maintaining the sensitivity, the false-positive rate of the ultrasound-based test is reduced.[78] If further data confirm, superimposing the color Doppler onto the endometrium at a questionable thickness (5–10 mm) and searching for vascularization in or around the endometrium might help to determine the further management of the patient and can lead a further reduction of the number of dilatation and curettage in the postmenopause.

The Endometrium under HRT

It is now well established that unopposed exogenous estrogen increases a woman's risk for endometrial hyperplasia and thus has an etiologic role in endometrial carcinoma[100,101] and that this effect is both dose- and duration dependent.[102] Stimulating normal menstrual cycles by the use of progestogens have been found to effectively reduce estrogen-induced breakthrough bleeding and lower the risk of endometrial hyperplasia and carcinoma.[85,102] Development of a hyperplasia can be prevented and a pre-existing glandular-cystic or adenomatous hyperplasia can be eliminated by regular administration of gestagens.[73]

Some of the most common adverse effects of postmenopausal estrogen treatment are bleeding disturbances, regardless of whether therapy is sequential or continuous estrogen/progestogen.[103] In those women, who receives exogenous hormones continuously, the delicate task of balancing appropriate dosages of estrogen and progestogen may lead to breakthrough bleeding even more often. Since utero-vaginal bleeding is the cardinal symptom of endometrial cancer, a disease which has been found to occur more frequently during unopposed estrogen therapy, it is not a surprise that

rising estrogen consumption resulted in a need for appropriate invasive examinations to be carried out more frequently. Jensen et al found that the frequency of D&C and endometrial biopsies in sequentially-treated women as compared with untreated women was 3.1 times higher in the 55–59 age group.[103]

Since transvaginal sonography has been progressively used as an alternative recourse of monitoring the endometrium both in the pre- and postmenopause detailed in the previous chapters, it is also suggested that it may be a useful method of monitoring the effects of HRT on the endometrium.[76,104,105] Vaginosonography as a screening method enables us to survey the postmenopausal endometrium, but sonographic assessment of endometrium is a completely different manner. It is therefore desirable to correlate hormone replacement regimens with the sonographic appearance of the endometrium. Establishment of the normal range of endometrial widths for each hormone regimen would help limit unnecessary invasive procedures for suspected endometrial hyperplasia.[76]

Woman which are receiving continuous hormone replacement are in favorable position. It is now well established that that kind of therapy is protective for endometrium. There are less cases of endometrial cancer in continuous regime group than in postmenopausal woman without any therapy.[106]

In women receiving sequential hormone replacement, endometrial thickness would be expected to vary throughout the cycle, depending on whether the endometrium was undergoing proliferative or secretory transformation due to estrogenic or progestational stimulation, respectively. For this purpose, the examiner should have knowledge of the type of hormonal replacement therapy and the day of the menstrual cycle, in order to distinguish pathological endometrial findings. It seems to be the best time of examination is in the early postmenstrual period.

Contrary, in woman receiving continuous hormone replacement endometrial thickness should be always the same (thin).

On the basis of the current literature and according to the recommendations of Osmers[73] and Lin[76] the following approach can be regarded as guidelines when examining the endometrium of an asymptomatic postmenopausal woman by vaginosonography.

1. A woman receiving sequential hormone replacement should be examined after completion of the progestational phase of the cycle (days 1–2).
2. All patients with hormonal replacement therapy are advised to undergo sonographic checks of the endometrium in 6 months time.
3.

a. Endometrial thickness up to 8 mm is regarded as normal finding,
b. Endometrial thickness between 8 and 15 mm is regarded suspicious. After administration of an oral gestagen, subsequent to the withdrawal bleeding, a second sonography is performed. If the endometrium still measures more than 8 mm, D&C is recommended. With endometrial thickness of less than 8 mm, control sonography in 3 months time is recommended. Women receiving unopposed estrogen or continuous estrogen and progestogen and having endometrial thickness between 8 and 15 mm need to undergo D&C.

c. Any patient with endometrial thickness of at least 15 mm should undergo histological diagnosis on grounds of the unusual thickness, regardless of symptoms or hormone status.

4. The endometrium of all postmenopausal women should be assessed vaginosonographically before the onset of HRT, whereas the guidelines for assessing the postmenopausal endometrium detailed in the previous chapter should be taken into consideration.

Above recommendations are only for woman on sequential therapy. Woman on continuous therapy should be regarded and followed as postmenopausal woman without therapy.

REFERENCES

1. Speroff L, Glass RH, Kase NG. Clinical Gynecologic Endocrinology and Infertility (4th ed). Baltimore: Williams & Wilkins 1989.
2. Fleischer AC, Kepple DM, Entman SS. Transvaginal sonography of uterine disorders. In: Timor-Tritsch IE, Rottem S (Eds). Transvaginal sonography (2nd ed). New York: Elsevier Science Publishing 1993; 109–30.
3. Zimmer EZ, Timor-Tritsch IE, Rottem S. The technique of transvaginal sonography. In: Timor-Tritsch IE, Rottem S (Eds). Transvaginal Sonography. New York: Elsevier Science Publishing 1993; 61–75.
4. Lerner JP, Timor-Tritsch IE. Morphological evaluation of the ovary using transvaginal Sonography. In: Kurjak A (Ed). Ultrasound and the Ovary. London, New-York: Parthenon Publishing 1994; 115–28
5. Campbell S, Royston P, Bhan V. Novel screening strategies for early ovarian cancer by transabdominal ultrasonography. Br J Obstet Gynaecol 1990; 96:304–11.
6. Granberg S, Wikland M. Comparison between endovaginal and transabdominal transducers for measuring ovarian volume. J Ultrasound Med 1987; 6:649–56.
7. Hall DA, McCarthy KA, Kopans DB: Sonographic visualization of the normal postmenopausal ovary. J Ultrasound Med 1986; 5:9–15.
8. Campbell S, Goswamy R, Goessens L, Whitehead M. Real-time ultrasonography for determination of ovarian morphology and volume: a possible early screening test for ovarian cancer? Lancet 1982; 1:425–29.
9. Rodrigez H, Platt L, Medearis A et al. The use of transvaginal sonography of evaluation of postmenopausal ovarian size and morphology. Am J Obstet Gynecol 1988; 159:810–14.
10. Fleischer A, McKee M, Gordon A et al. Transvaginal sonography of postmenopausal ovaries with pathological correlation. J Ultrasound Med 1990; 9:637–44.
11. Dodson MG. The Ovary. In: Dodson MG (Ed). Transvaginal ultrasound. New York: Churchill Livingstone 1995; 105–32.
12. Barber HRK. The postmenopausal ovary. In: Kurjak A (Ed). Ultrasound and the Ovary. London, New York: Parthenon Publishing 1994; 231–34.
13. Andolf E, Jorgensen C, Svelaneius E et al. Ultrasound measurement of ovarian volume. Acta Obstet Gynecol Scand 1987; 66:387–89.
14. Goswamy R, Campbell S, Royston J et al. Ovarian size in postmenopausal women. Br J Obstet Gynaecol 1988; 95:795–801.
15. Wehba S, Fernandes CE, Ferreira JA, Azevedo LH, Machado RB, Lunardelli JL, Lima SR, Iwamoto V. Transvaginal ultrasonography assessment of ovarian volumes in postmenopausal women. Rev Paulista de Med 1996; 114:1152–55.
16. Merz E, Miric-Tesanic D, Bahlmann, Weber G, Wellek S. Sonographic size of uterus and ovaries in pre- and perimenopausal women. Ultrasound Obstet Gynecol 1996; 7:38–42.

17. Tepper R, Zalel Y, Markov S, Cohen I, Beyth Y. Ovarian volume in postmenopausal women—suggestions to an ovarian size normogram for menopausal age. Acta Obstet Gynecol Scand 1995; 74:208–11.
18. Bakos O, Smith P, Heimer G, Ulmstein U. Transvaginal sonography of the internal genital organs in postmenopausal women on low-dose estrogen treatment. Ultrasound Obstet Gynecol 1994; 4: 326–29.
19. Bar-Hava I, Perri T, Zahavi Z, Brzezinski A, Dicker D, Ben-Rafael Z, Orvieto R. Influence of hormone replacement therapy on postmenopausal pelvic organs. Climacteric 2001; 4(2):160–65.
20. Davis AP, Oram D. Screening for ovarian cancer. In: Kurjak A (Ed). Ultrasound and the Ovary. London, New York: Parthenon Publishing 1994; 235–53.
21. Barber HRK, Graber EA. The PMPO syndrome. Obstet Gynecol 1971; 38:921–23.
22. Kase NG, Weingold AB. Principles and practice of clinical gynecology. New York: John Wiley and Sons, 1983; 579.
23. Barber HRK. Ovarian cancer: Diagnosis and management. Am J Obstet Gynecol 1984; 150:910–15.
24. Barber HRK. The postmenopausal palpable ovary syndrome. Compr Ther 1979; 5(9):58.
25. Barber HRK (Ed): A second look at the postmenopausal palpable ovary. Fern Patient 1988; 13: 13–14.
26. Granberg S, Wikland M. Endovaginal Ultrasound in the diagnosis of unilocular ovarian cysts in postmenopausal women. Ultrasound Quarterly 1992; 10:1–13.
27. Granberg S, Wikland M, Jansson I. Macroscopic characterization of ovarian cancer and relation to the histological diagnosis: criteria to be used for ultrasound evaluation. Gynecol Oncol 1989; 35:139–44.
28. Granberg S, Norstrom A, Wikland M. Endovaginal ultrasound and cytological evaluation of cystic ovarian tumors, a comparison. J Ultrasound Med 1991; 10:9–14.
29. Granberg S, Norström A, Wikland M. Tumours in lower pelvis imaged by vaginal ultrasound. Gynecol Oncol 1989; 37:224–29.
30. Andolf E, Jörgensen C. Simple adnexal cysts diagnosed by ultrasound in postmenopausal women. J Clin Ultrasound 1988; 16:301–03.
31. Andolf E, Jörgensen C. Cystic lesions in elderly women, diagnosed by ultrasound. Br J Obstet Gynaecol 1989; 96:1076–79.
32. Goldstein SR, Subramanyam B, Snyder JR, Beller U, Raghavendra N, Beckmann EM: The postmenopausal cystic adnexal mass: The potential role of ultrasound in conservative management. Obstet Gynecol 1989; 73:8–10.
33. Parker WH, Berek JS. Management of selected cystic adnexal masses in postmenopausal women by operative laparoscopy: a pilot study. Am J Obstet Gynecol 1990; 163:1574–77.
34. Valentin L, Akrawi D. The natural history of adnexal cysts incidentally detected at transvaginal ultrasound examination in postmenopausal women. Ultrasound Obstet Gynecol 2002; 20(2):174–80
35. Kurjak A, Shalan H, Matijevic R, Predanic M. Stage I ovarian cancer by transvaginal color Doppler sonography: a report of 18 cases. Ultrasound Obstet Gynecol 1993; 3:195–98.
36. Ekerhovd E, Wienerroith H, Staudach A, Granberg S. Preoperative assessment of unilocular adnexal cysts by transvaginal ultrasonography: a comparison between ultrasonographic morphologic imaging and histopathologic diagnosis. Am J Obstet Gynecol 2001; 184(2):48–54.
37. Kurjak A, Kupesic S. Ovarian senescence and its significance on uterine and ovarian perfusion. Fertil Steril 1995; 3:532–37.
38. Kurjak A, Kupesic-Urek S, Schulman H, Zalud I. Transvaginal color Doppler in the assessment of ovarian and uterine blood flow in infertile women. Fertil Steril 1992; 56:870–73.
39. Scholtes MCW, Wladimiroff J, Rijen HJM, Hop WCJ. Uterine and ovarian flow velocity waveforms in the normal menstrual cycle; a transvaginal color Doppler study. Fertil Steril 1989; 52:981–85.

40. Kurjak A, Schulman H, Sosic A, Zalud I, Shalan H. Transvaginal ultrasound, color flow, and Doppler waveform of the postmenopausal adnexal mass. Obstet Gynecol 1992; 80:917–21.
41. Fleischer AC, Rodgers WH, Kepple DM, Williams LL, Jones III HV. Color Doppler sonography of ovarian masses: a multiparameter analysis. J Ultrasound Med 1993; 12:41–48.
42. Grade M, Patel J, Yiu-Chiu V. Evaluation of 103 pelvic masses: correlation of surgical diagnosis with transvaginal ultrasound size, complexity scores and resistive index values. Ultrasound Obstet Gynecol 1993; 3(Suppl 1):23.
43. Kulenkampff D, Puchta J, Osmers R. Sonographic appearance of the myometrium. In: Osmers R, Kurjak A (Eds). Ultrasound and the Uterus. Carnforth, New York: Parthenon Publishing 1995; 53–59.
44. Rempen A. Normal sonographic features of the uterus. In: Osmers R, Kurjak A (Eds). Ultrasound and the uterus. Carnforth, New York: Parthenon Publishing 1995:1–12.
45. deVries K, Lyons KEA, Ballard G, Levi C, Lindsay DJ. Contractions of the inner third of the myometrium. Am J Obstet Gynecol 1990;162:679–82.
46. Andolf E, Dahlander K, Aspenberg P Ultrasonic thickness of the endometrium correlated to body weight in asymptomatic postmenopausal women. Obstet Gynecol 1993; 82:936–40.
47. Zalud I, Conway C, Schulman H, Trine D. Endometrial and myometrial thickness and uterine blood flow in postmenopausal women. J Ultrasound Med 1993; 12:737–41.
48. Kurjak A, Kupesic-Urek S. Normal and abnormal uterine perfusion. In: Jaffe R, Warsof LS (Eds). Color Doppler imaging on Obstetrics and Gynecology. New York: McGraw Hill 1992; 255–63.
49. Long MG, Boultbee JE, Hanson ME, Begent JHR. Doppler time velocity waveform studies of the uterine artery and the uterus. Br J Obstet Gynaecol 1989; 96:588–93.
50. Goswamy RK, Steptoe PC. Doppler ultrasound studies of the uterine artery in spontaneous ovarian cycles. Hum Reprod 1988; 3:721–23.
51. Goswamy RK, Williams G, Steptoe PC. Decreased uterine perfusion: A cause of infertility. Hum Reprod 1988; 3:955–58.
52. Kupesic S, Kurjak A. Uterine perfusion. In: Osmers R, Kurjak A (Eds). Ultrasound and the Uterus. Camforth, New York: Parthenon Publishing 1995; 87–90.
53. Luzi G, Coata G, Cucchia GC, Cosmi EV, Di Renzo GC. Doopler studies of uterine arteries in spontaneous and artificially induced menopausal women. Ultrasound Obstet Gynecol 1993; 3:354–56.
54. Lewit N, Thaler I, Rottem S. The uterus: a new look with transvaginal sonography. J Clin Ultrasound 1009; 18:331–36.
55. Kurjak A, Shalan H, Kupesic S, Predanic M, Zalud I, Breyer B, Jukic S. Transvaginal color Doppler assessment in the pelvic tumor vascularity. Ultrasound Obstet Gynecol 1993; 3:137–54.
56. Hata T, Hata K, Senoh D, Makihara K, Aoki S, Takimaya O, Kitao M. Doppler ultrasound assessment of tumor vascularity in gynecologic disorders. J Ultrasound Med 1989; 8:309–14.
57. Kurjak A, Zalud I. The characterization of uterine tumors by transvaginal color Doppler. Ultrasound Obstet Gynecol 1991; 1:50–52.
58. Kurjak A, Kupesic-Urek S, Miric D. The assessment of benign uterine tumor vascularisation by transvaginal color Doppler. Ultrasound Med Biol 1992; 18:645–49.
59. Matta WHM, Stabile I, Shaw RW, Campbell S. Doppler assessment of uterine blood flow changes in patients with fibroids receiving the gonadotropinreleasing hormone agonist Buserelin. Fertil Steril 1988; 49:1083–85.
60. Wilson EA, Yang F, Rees ED. Estradiol and progesterone binding in uterine leiomyomata and in normal uterine tissues. Obstet Gynecol 1980; 55:20–24.
61. Solues MR, McCarthy KS Jr. Leiomyomas: steroid receptor content. Variations within normal menstrual cycle. Am J Obstet Gynecol 1982; 143:6–11.

62. Filicori M, Hall DA, Loughlin JS, Rivier J, Vale W, Crowley WF Jr. A conservative approach to the management of uterine leiomyoma: pituitary desensitization by a luteining hormone-releasing analogue. Am J Obstet Gynecol 1983; 147:726–27.
63. Aleem F, Predania M. Uterine leiomyomata: transvaginal color Doppler studies and new aspects of management. In: Osmers R, Kurjak A (Eds). Uterus and Ultrasound. Carnforth: Parthenon Publishing 1995; 61–70.
64. Meyer WR, Meyer AR, Diamond MP Unsuspected leiomyosarcoma: treatment with gonadotropinreleasing hormone analogue. Obstet Gynecol 1990; 75:529–34.
65. Kurjak A, Kupesic S, Shalan H, Jukia S, Kosuta D, Ilijas M. Uterine sarcoma: A report of 10 cases studied by transvaginal color and pulsed Doppler sonography. Gynecol Oncol 1995; 59:342–46.
66. Vollenhoven BJ, Lawrence AS, Healy DL. Uterine fibroids: a clinical review. Br J Obstet Gynaecol 1990; 97:285–98.
67. Jirapinyo M, Theppisai U, Leelapatana P, Krasaesub S. Sonographic findings of uterus and ovaries in normal pre- and post-menopausal women. J Med Assoc Thai 1998; 81(7):527–31.
68. Fedele L, Bianchi S, Raffaelli R, Zanconato G A randomized study of the effects of tibolone and transdermal estrogen replacement therapy in postmenopausal women with uterine myomas. Eur J Obstet Gynecol Reprod Biol 2000; 88(1):91–94.
69. Colacurci N, De Franciscis P, Cobellis L, Nazzaro G, De Placido G. Effects of hormone replacement therapy on postmenopausal uterine myoma. Maturitas 2000; 35(2): 167–73.
70. Polatti F, Viazzo F, Colleoni R, Nappi RE. Uterine myoma in postmenopause: a comparison between two therapeutic schedules of HRT Maturitas 2000; 37(1):27–32.
71. Simsek T, Karakus C, Trak B. Impact of different hormone replacement therapy regimens on the size of myoma uteri in postmenopausal period. Tibolone versus transdermal hormonal replacement system. Maturitas 2002; 42(3):243.
72. Osmers R, Kuhn W. Endometrial cancer screening. Current Opinion Obstet Gynecol 1994;6:75–79.
73. Osmers R, Puchta J, Suren A. Pathological findings of the postmenopausal endometrium. In: Osmers R, Kurjak A (Eds). Ultrasound and the Uterus. Carnforth, New York: Parthenon Publishing 1995; 31–44.
74. Granberg S, Wikland M, Karlsson B, Nordstrom A, Friberg LG. Endometrial thickness as measured by endovaginal ultrasound for identifying endometrial abnormality. Am J Obstet Gynecol 1991; 164:47–52.
75. Kurjak A, Shalan H, Sosic A, Benic S, Zudenigo D, Kupesic S, Predanic M. Endometrial carcinoma in postmenopausal women: evaluation by transvaginal Color Doppler. Am J Obstet Gynecol 1993; 169:1597–603.
76. Lin MC, Gosin BB, Wolf SI, Feldsman M, Stuenkel CA, Braly PS, Pretorius DH. Endometrial thickness after the menopause: effect of the hormone replacement. Radiology 1991; 180:427–32.
77. Jones III HN. Endometrial carcinoma. In: Jones III HN, Wentz AC, Burnett LS (Eds). Novak's Textbook of Gynecology (11th ed). Baltimore: Williams & Wilkins 1988; 728–60.
78. Bourne TH, Campbell S, Whitehead MI, Steer CV, Collins WP. Detection of endometrial cancer in postmenopausal women by transvaginal ultrasonography and colour flow imaging. Br Med J 1990; 301:369.
79. Lehtovirta P, Cacciatore B, Wahlstrom T et al. Ultrasonic assessment of endometrial cancer invasion. J Clin Ultrasound 1987; 15:519–24.
80. Osmers R. Transvaginal sonography in endometrial cancer. Ultrasound Obstet Gynecol 1992; 2:2–3.
81. Bourne TH. Transvaginal color Doppler in Gynecology. Ultrasound Obstet Gynecol 1991; 1:359–73.
82. Osmers R, Volksen M, Rath W, Kuhn W. Vaginosonographic detection of endometrial cancer in postmenopausal women. Int J Gynecol Obstet 1990; 32:35–37.

83. Wikland M, Granberg S, Karlsson B. Assessment of the endometrium in the postmenopausal woman by vaginal sonography. Ultrasound Quarterly 1992; 10:15–27.
84. Osmers R, Volksen M, Schauer A. Vaginosonography for early detection of endometrial carcinoma. Lancet 1990; 1:1569–71.
85. Flowers CE, Wilborn WH, Hyde BM. Mechanisms of uterine bleeding in postmenopausal patients receiving estrogen alone or with a progestin. Obstet Gynecol 1983; 61:135–43.
86. Goldstein SR, Nachtigall M, Snyder JR, Nactigall L. Endometrial assessment by vaginal ultrasonography before endometrial sampling in patients with postmenopausal bleeding. Am J Obstet Gynecol 1990; 163:119–23.
87. Varner RE, Sparks JM, Cameron CD, Roberts LL; Soong SJ. Transvaginal sonography of the endometrium in postmenopausal women. Obstet Gynecol 1991; 78:195–99.
88. Botsis D, Kassanos D, Pyrgiotis E, Zourlas PA. Vaginal sonography of the endometrium in postmenopausal women. Clin Exp Obstet Gynecol 1992; 19:189–92.
89. Dorum A, Kristensen GB, Langebrekke A, Sornes T, Skaar O. Evaluation of endometrial thickness measured by endovaginal ultrasound in women with postmenopausal bleeding. Acta Obstet Gynecol Scand 1993; 72:116–19.
90. Bakos O, Smith P, Heimer G. Transvaginal ultrasonography for identifying endometrial pathology in postmenopausal women. Maturitas 1995; 20:181–89.
91. Karlsson B, Granberg S, Ridell B, Wikland M. Endometrial thickness as measured by transvaginal sonography: interobserver variation. Ultrasound Obstet Gynecol 1994; 4:320–25.
92. Carlson JA Jr. Arger P, Thompson S, Carlson EJ. Clinical and pathologic correlation of endometrial cavity fluid detected by ultrasound in the postmenopausal women. Obstet Gynecol 1991; 77:119–23.
93. Brechenridge JW, Kurtz AB, Ritchie WGM, Macht EL Jr. Postmenopausal uterine fluid collection: indicator 746 of carcinoma. Am J Radiol 1982; 139:529–34.
94. McCarthy KA, Hall DA, Kopans DB, Swann CA. Postmenopausal endometrial fluid collections: always of indicator of malignancy? J Ultrasound Med 1986; 5:647–49.
95. Pardo J, Kapan B, Nitke S, Ovaida J, Segal J, Neri A. Postmenopausal intrauterine fluid collection: correlation between ultrasound and hysteroscopy. Ultrasound Obstet Gynecol 1994; 4:224–26.
96. Kurjak A, Zalud I, Jurkovic D, Alfirevic Z, Miljan M. Transvaginal color flow Doppler for the assessment of pelvic circulation. Acte Obstet Gynecol Scand 1989; 68:131–35.
97. Kurjak A, Shalan H, Kupesic S, Kosuta D, Sosic A, Benic S, Ilijas M, Jukic S, Predanic M. An attempt to screen asymptomatic women for ovarian and endometrial cancer with transvaginal color and pulsed Doppler sonography. J Ultrasound Med 1994; 13:295–301.
98. Kupesic-Urek S, Shalan H, Kurjak A. Early detection of endometrial cancer by transvaginal color Doppler. Eur J Obstet Gynecol Reprod Biol 1993; 49:46–49.
99. Hata K, Hata T, Manabe A, Makihara K, Kitao M. New pelvic sonography for detection of endometrial carcinoma: a preliminary report. Gynecol Oncol 1992; 45:179–84.
100. Smith DC, Prentice R, Thompson DJ, Herrmann WL. Association of exogenous estrogen and endometrial carcinoma. N Engl J Med 1975; 293:1164–67.
101. Ziel HK, Finkle WD. Increased risk of endometrial carcinoma among users of conjugated estrogens. N Engl J Med 1975; 293:1167–70.
102. Whitehead MI, Townsend PT, Pryse-Davies J et al. Effects of various types and dosages of progestogens on the postmenopausal endometrium. J Reprod Med 1982; 27:539–48.
103. Jensen LC, Obel EB, Linhard E, Steendahl E, Fink B. Frequency of curettage in middle-aged women treated with sequential preparations versus untreated women. Maturitas 1992; 15:61–69.
104. Castelo-Branco C, Puerto B, Durán M, Gratacós E, Torné A, Fortuny A, Vanrell JA. Transvaginal sonography of the endometrium in postmenopausal women: monitoring the effect of hormone replacement therapy. Maturitas 1994; 19:59–65.
105. Meuwissen JHJM, van Langen H, Moret E, NavarroMorquecho I. Monitoring of oestrogen replacement therapy by vaginosonography of the endometrium. Maturitas 1992; 15:33–37.

106. Archer DF, Pickar JH. Hormone replacement therapy: effect of progestin dose and time since menopause on endometrial bleeding. Obstet Gynecol 2000; 96(6):899–905.

Chapter 55
Sonographic Evaluation of Acute Pelvic Pain

Sanja Kupesic, Alenka Aksamija, Asim Kurjak

Acute pelvic pain may be the manifestation of various gynecologic and non-gynecologic disorders from less alarming rupture of periovulatory follicle to more life-threatening conditions like rupture of ectopic pregnancy or perforation of inflamed appendix. Astute clinician should bear in mind all the possibilities when evaluating patient with presentation of the acute pelvic pain.[1,2] Locating the site of pain together with ultrasound examination of the affected area leads to prompt and accurate clinical diagnosis. Ultrasound has become a valuable aiding tool in the approach to the patient presented with acute pelvic pain that is gynecological or non-gynecological in origin such as appendicitis or urinary stones.[3] It would be advisable to offer some type of algorithm for differential diagnosis that could guide physicians through the management of such a problem (Table 55.1).

NON-GYNECOLOGIC ETIOLOGIES OF ACUTE PELVIC PAIN

Non-gynecological etiologies are divided into gastrointestinal and urinary causes.

Gastrointestinal Causes of Pelvic Pain

Appendicitis

Appendicitis is the most common surgical emergency. It affects all age groups, but is rare in very young and very old population. Appendicitis should always be considered in differential diagnosis if appendix has not been removed. Examination of the abdomen reveals tenderness in the right iliac fossa, with guarding due to the localized peritonitis. Rectal examination may reveal tenderness to the right. Moderate leucocytosis of 10,000–18,000 cells/mL is frequent but normal leukocyte count doesn’t exclude

Table 55.1: Etiology of acute pelvic pain

NON-GYNECOLOGIC ETIOLOGIES		*GYNECOLOGIC ETIOLOGIES*	
Gastrointestinal	*Urinary*	*Beta hCG−*	*Beta hCG+*
• Appendicitis	• Obstruction	• PID	• Normal intrauterine pregnancy
• Meckel's diverticulitis	• Infection	• Hemorrhagic ovarian cyst	
• Chron's disease			• Spontaneous abortion
• Yersinia infection		• Degenerating fibroids	• Ectopic pregnancy
• Mesenteric lymphadenitis		• Adnexal torsion	• Corpus luteum cyst
• Functional bowel disease		• Endometriosis	• Fibroids
		• Pelvic congestion syndrome	• Uterine dehiscence and rupture
		• Ovarian vein thrombosis	• Placental abruption

appendicitis. Sensitivity of ultrasound examination in diagnosis of appendicitis is approximately 90%, and specificity 95% when graded compression technique is applied. However, ultrasound is user dependent and requires considerable experience in order to perform it reliably.[4]

Meckel's Diverticulitis

This is the most frequent congenital abnormality of the gastrointestinal tract, affecting 2–3% of the population. The diverticulum projects from the wall of the ileum approximately 60 cm from the ileocaecal valve. It is usually symptomless, but 50% of them contain gastric mucosa that secrets hydrocloric acid. Peptic ulcers may bleed or perforate. Acute inflammation of the diverticulum may also occur and is clinically indistinguishable from the acute appendicitis.

Acute terminal ileitis due to Crohn's disease or Yersinia infection, non-specific mesenteric lymphadenitis and functional bowel disease-these conditions may be differentiated from other causes of acute lower abdominal pain by clinical presentation and diagnostic procedures like blood tests, stool cultures, radiology, ultrasound and CT scanning, colonoscopy and small bowel functional tests (e.g. a breath test for bacterial overgrowth).

Urinary Causes of Acute Pelvic Pain

Urinary Tract Obstruction

The urinary tract may be obstructed at any point between the kidney and urethral meatus. Loin pain may be dull or sharp, intermittent or constant, provoked by increase of urine volume that distends collecting system (fluid intake, diuretics, alcohol). Together with pain are encountered various disturbances of the urine flow from complete anuria to polyuria (due to impairment of renal tubular concentrating capacity). Routine blood and biochemical investigations (blood urea and serum creatinine, hyperkalemia, anemia of chronic disease and blood in urine) aid in diagnosis of urinary tract obstruction. Diagnosis of 748 urinary obstruction cannot be made based on these tests alone and further investigations must be performed (ultrasonography, radionuclide studies, excretion urography, anterograde pyelography and ureterography, retrograde ureterography, cystoscopy, urethroscopy, urethrography and pressure-flow studies).[4] Dilatation of renal pelvis and urether are typical signs of obstructive uropathy and may be detected by ultrasound easily. The thinning of renal parenchyma suggests long-term obstructive uropathy.

Urinary Tract Infection (UTI)

UTI is common in women, uncommon in men and of specific importance in children. Recurrent infection causes considerable morbidity-if complicated can cause severe renal disease including end-stage renal failure. It is also common source of Gramnegative septicemia. At least 50% of women will experience one episode of cystitis at some time of their lives. The most typical symptoms of UTI are frequency of micturition by day and night, painful voiding (dysuria), suprapubic pain and tenderness, hematuria and smelly urine. Loin pain and tenderness, with fever and systemic symptoms suggest extension of the infection to the pelvis or kidney, known as pyelitis or pylonephritis. However, localization of the site of the infection on the basis of symptoms alone is unreliable. UTI may also be present with minimal or no symptoms or may be associated with atypical symptoms such as abdominal pain, fever and hematuria without frequency or dysuria. The diagnosis is based on quantitative culture of a clean-catch mid-stream specimen of urine. In the evaluation of UTI it is advisable to bear in mind the possibility of interstitial cystitis. Chronic disorder of unknown etiology that affects lower urinary tract. It is characterized by bladder and pelvic pain that varies from moderate discomfort to severe, debilitating pain and related lower urinary tract symptoms including nocturia, diurnal urinary frequency and urgency: because the symptoms of interstitial cystitis resemble a urinary tract infection, it is often misdiagnosed and may remain so for months or even years.[5]

GYNECOLOGIC ETIOLOGIES OF ACUTE PELVIC PAIN

Ruptured ectopic pregnancy, salpingitis and hemorrhagic ovarian cysts are the three most commonly diagnosed gynecologic conditions presenting as an acute abdomen. Degenerating leiomyomas and adnexal torsion occur less frequently.[6] For

systematization, gynecologic causes of acute pelvic pain could be divided into conditions with negative pregnancy test, and conditions with positive pregnancy tests.

Acute Pelvic Pain with Negative Pregnancy Tests

Pelvic Inflammatory Disease (PID)

It is defined as the acute clinical syndrome associated with spread of micro-organisms (unrelated to pregnancy or surgery) from the vagina or cervix to the endometrium,7 Fallopian tubes and/or contiguous structures.8 This serious complication can lead to infertility, ectopic pregnancy and chronic pelvic pain.9,10 Sexually active adolescents are at the greatest risk for PID. Other risk factors include multiple sex partners, a high number of sex partners throughout the life, use of intrauterine device (IUD), untreated infected male sex partner(s), history of previous PID, presence oiNeisseria gonorrhoeae or C/i/amydfa trachomatis in reproductive tract and frequent vaginal douching.9 PID causes more morbidity than necessary for three reasons: women are not hospitalized when they should be, many women receive inadequate antibiotic therapy and male partner is not treated or is treated inappropriately.11 PID may present itself by various clinical manifestations: silent (asymptomatic), atypical, acute and chronic. Patient with acute PID complain mainly of low abdominal tenderness. Some of them may have increased body temperature, but it is not unusual to have patients with normal temperature. Laboratory findings show increased sedimentation rate and white blood cell count. Next step is to evaluate the pelvis ultrasonographically but it is advisable to have in mind that sonographic findings may be normal in the early course of the disease.[12] Pelvic inflammatory disease is usually presented with:

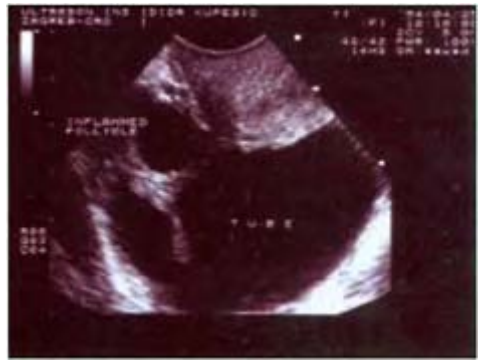

Figure 55.1: Transvaginal ultrasound scan of a chronic pelvic inflammatory disease. Note a tubular fluid-filled structure representing

dilated Fallopian tube and ovary containing inflamed follicles

1. Thickening of the tube wall of ≥5 mm,
2. "Cogwheel" sign defined as sonolucent cogwheel-shaped structure visible in crosssection of a tube with thick walls,
3. Incomplete septa correlate with mucosal folds in the dilated tube that is sonolucent or contain low-level echoes (Not discriminatory between acute and chronic cases) (Fig. 55.1),
4. "Beads-on-a-string" sign defines hyperechoic mural nodules measuring about 2 to 3 mm, visualized on the cross-section of a fluid filled distended tube,
5. Tubo-ovarian complex (ovary cannot be separated from the tube by pushing it with the vaginal probe),
6. Tubo-ovarian abscess (total breakdown of normal architecture of one or both adnexa with formation of the conglomerate mass or fluid collection) (Fig. 55.2),
7. Fluid in the cul-de-sac,
8. Low to moderate resistance index (RI=0.53 ±0.09) obtained from adnexal region.

Hemorrhagic Ovarian Cysts

Cyclic causes of pelvic pain include crampy abdominal pain due to normal menstruation and

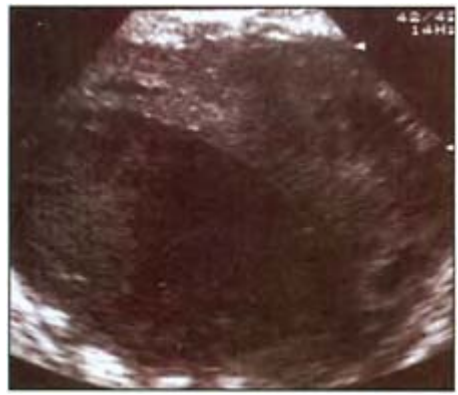

Figure 55.2: Transvaginal scan of a tubo-ovarian abscess. Note the thickened and irregular margins of the lesion filled with echogenic fluid

development of corpus luteum cyst. Corpus luteum cyst may be painful either due to the large size of the cyst, or due to the hemorrhage within the cyst (Fig. 55.3). Patients with hemorrhagic ovarian cyst may experience abrupt onset of low abdominal or pelvic pain. Cyst rupture with hemorrhage into the peritoneum is a rare cause of pelvic pain. Functional cysts other than corpus luteum can also be complicated by hemorrhage and rupture. Laboratory test will demonstrate low hematocrit. Hemorrhage is excellent evidence that an ovarian mass is benign. Of the hemorrhagic cysts reported in the

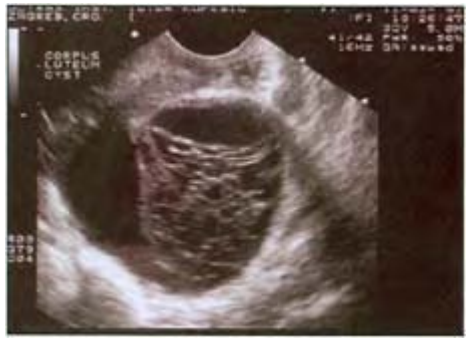

Figure 55.3: Transvaginal scan of a corpus luteum cyst. The internal appearance is created by the retracted clot and should not be mistaken with cystadenoma

sonographic literature 98% were non-neoplasmatic and the remaining 2% were benign tumors.[13,15] Ultrasonic appearance of the hemorrhagic cysts has different characteristics due to blood clots. They can look solid or have focal thickening of walls and fluid level often resembling an endometrioma. Some hemorrhagic ovarian cysts can mimic sonographic features of the solid ovarian masses, such as teratoma. In most of the cases, the degree of through transmission is greater than in truly solid masses, and the mass regresses in size over 2 to 3 weeks period. On sonography, the most common appearance is a complex mass with internal echoes, but with enhanced through transmission. Although fibrinolized clot is typically hypoechoic, acute intraparenchymal hemorrhage frequently appears as an irregular echogenic area. The cyst wall may be irregular in contour due to a clot that is adherent to it. Occasionally, mildly echogenic interface can be seen within a hemorrhagic cyst, most likely representing partially solid clot.[14,15] Hemorrhagic cysts show moderate to low vascular resistance (RI=0.50±0.08), usually detected at the periphery, while solid component representing blood clot remains avascular.

Degenerating Fibroids

Leiomyomas are the most common tumors of female pelvis and occur in 20–25% of women of reproductive age. Clinically, symptoms such as metrorrhagia, pelvic pain and infertility are usually present in patients with submucous leiomyomas, whereas subserous leiomyomas are mainly asymptomatic, but may cause lumbar pain and urinary or bowel symptoms due to compression.[16] Acute symptoms are seen if the leiomyomas undergoing torsion or necrosis (Fig. 55.4).[17] Ultrasound appearance of leiomyomas depends on size, site and age of the tumor. They are usually spherical in shape and sharply demarked from the myometrium, unlike adenomyosis. Sonographic texture of leiomyomas ranges from hypoechoic to echogenic, depending on the amount of smooth muscle and connective tissue. If present,

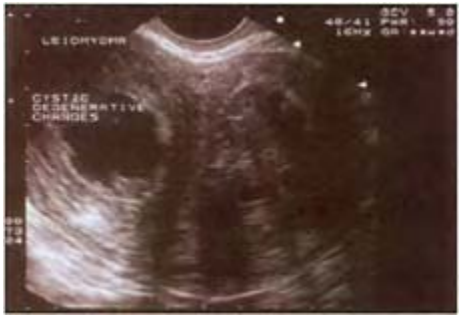

Figure 55.4: Transvaginal ultrasound scan of a leiomyoma with large necrotic area within the central part

secondary changes (necrosis, hemorrhage, degeneration or calcification) are represented by a wide spectrum of ultrasonic images. Leiomyoma undergoing cystic degeneration (hemorrhagic or proteolytic) present as an anechoic mass, which demonstrates far acoustic enhancement (Fig. 55.4). There might be highly echogenic portions and associated acoustic shadowing from areas of calcification, varying from small focal deposits to extensive calcifications, more usually seen in older women.[18] Color flow detects the myoma's feeder vessels that arise from the myometrial vasculature and form a regular ring of angiogenesis, and central vessels that develop as a response to the angiogenic activity of tumor cells, perhaps due to necrotic or inflammatory processes. Resistance index (RI) of the myometrial blood flow in the patients with leiomyoma is 0.54±0.12. Very low resistance indices are usually present in cases with secondary degenerative or inflammatory changes within leiomyoma. In these cases it is essential to differentiate this benign condition from uterine sarcoma that shows rapid increase in size and lower RI of the tumoral blood flow (RI=0.37 ±0.03) and RI of the uterine artery (RI=0.62 ±0.07, in comparison to RI of uterine artery in myomatous uterus that shows RI of 0.74±0.09).[19] Uterine arteries present lower impedance to blood flow in patients with fibroids (RI=0.74±0.09) comparing to normal patients (RI=0.84± 0.09).[20] The difference

in vascular signatures noted in this study may have predictive value in growth rate evaluation of these benign uterine masses.

Adnexal Torsion

Torsion of the ovary and the Fallopian tube is a gynecological emergency that manifests itself with acute pelvic pain.[21] It mostly occurs in patients with adnexal lesions between 4–8 cm in diameter. Masses smaller than this do not typically cause torsion, while larger masses are not mobile enough to cause torsion.[22] It has been reported in recent literature the occurrence of tubal torsion following tubal ligation and laparoscopic tubal cauteriza¬ tion.[23] Adnexal torsion is associated with massive edema and/or hemorrhage within the ovary. Doppler features relate to the grade and chronicity of the torsion.[24,26] In the initial stage of the torsion, venous blood flow is reduced while arterial signals demonstrate high-impedance blood flow signals (Fig. 55.5) indicating that venous and lymphatic occlusion occur first. It is useful to bear in mind that ovarian flow, both venous and arterial may be present in the setting of ovarian torsion. This is due either to partial torsion of the vascular pedicle or to the dual blood supply of the ovary (from the adnexal branch of the uterine artery and the ovarian artery). In extreme cases, reversed diastolic flow of the intraovarian arteries can be detected (Fig. 55.6).[27] At a late stage when

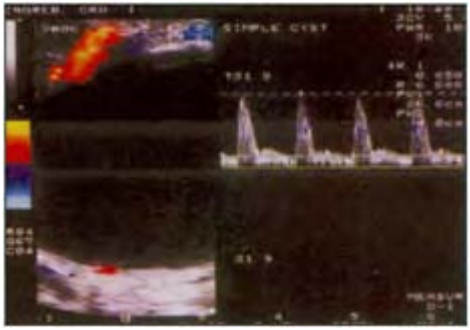

Figure 55.5: Transvaginal color Doppler scan of an unilocular cyst. During the initial stage of an ovarian torsion high vascular resistance signals (RI=0.85) are obtained at its periphery

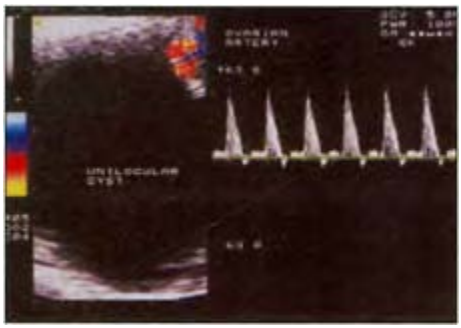

Figure 55.6: As torsion progresses one can detect reversed blood flow signals indicative of ischemic changes

occlusion is total and involves the arterial circulation, no adnexal blood flow is seen. Expeditious and early diagnosis of adnexal torsion is highly dependent on the operator's experience. Color Doppler allows prompt and early diagnosis of adnexal torsion before irreversible ischemic changes occur, leading to necrosis and gangrene of the involved organs. This may contribute to conservative surgery and may prevent surgical removal of the affected structures.[28]

Endometriosis

Endometriosis is defined as a condition resulting from ectopic location of the endometrial tissue outside the uterine cavity (peritoneal cavity, abdominal and pelvic organs and pelvic ligaments).[29] The precise etiology of this disease is still to be determined. Many theories, some of them more probable than the others have been proposed to explain the pathogenesis of endometriosis. The metastatic theory postulates the importance of the transportation of the viable endometrial cells regurgitated through the Fallopian tubes at the time of menstruation. The metaplasia theory explains the origin of endometriosis by metaplastic differentiation of the original celomic membrane with prolonged irritation and/or estrogen stimulation of endometrium-like tissue. It is proposed that adult cells undergo dedifferentiation back to their primitive origin and then transform into endometrial cells. The third, genetic theory, states that there may be a genetic component in the pathogenesis of endometriosis, since it has been shown that there is a statistically higher incidence of the endometriosis in the firstdegree relatives of patients with this disorder.[30] The classic symptom of endometriosis is chronic pain associated with menstruation and/or the immediate pre-menstrual phase, or persistent pain without the cyclicity.[31] Even though the classic symptom of endometriosis is chronic pain, in 21% of the cases it manifests itself with acute pelvic pain.[32] Other symptoms associated with this condition frequently noted are dysmenorrhea, dyspareunia, atypical bleeding, premenstrual spotting, menometrorrhagia, while rectal bleeding or hematuria although pathognomonic are rarely encountered. An endometrioma (so called "chocolate cyst")

has a variety of ultrasonographic appearances ranging from an anechoic cyst, cyst containing diffuse low-level echoes with or without solid components, to a solid-appearing mass. “Carpet-like” echoes can be found within 82% of endometriomas.[33] Sometimes it is difficult to differentiate an endometrioma from a hemorrhagic ovarian cyst or corpus luteum cyst but sonographer should always bear in mind typical morphological features of endometrioma: thick walls, homogenicity of the echogenic content and multiplicity of the lesions.[34] In order to facilitate recognition of endometriosis Kurjak and Kupesic[35] developed a new non-invasive scoring system using clinical symptoms, CA 125 level, sonographic findings and transvaginal color and pulsed Doppler parameters (Table 55.2) (Fig. 55.7).

Pelvic Congestion Syndrome

Pelvic congestion syndrome is a condition characterized with formation of pelvic varicosities with concomitant vascular stasis and congestion. There are three possible mechanisms of pelvic congestion. Varicose veins are thought to result from the effects of gravity and defective valves. The worsening of pelvic pain in erect position in women with pelvic pain syndrome and the improvement on lying down support this concept.

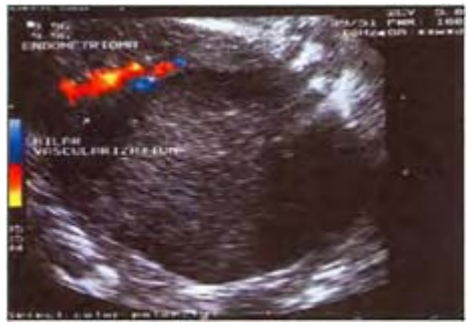

Figure 55.7: Transvaginal color Doppler scan of an ovarian endometrioma. Note echogenic fluid and peripheral vessels both indicative of ovarian endometriosis

The second possibility is that an abnormal increase in blood flow through a region with many arteriovenous connections could lead to a state of chronic pelvic venous dilatation. The third possibility is that pelvic varicosities may occur as a result of relaxation of the smooth muscle in the walls of the pelvic veins caused by some vasoactive substance as yet unidentified.[36] Pelvic congestion syndrome’s clinical manifestation is abdominal pain in the small pelvis. It is more common in the right iliac fossa, although some patients complain of left-sides pain and its moving from one side to the other is quite typical. Arterial type of congestion causes predominantly acute

symptoms, while venous congestion presents mainly with chronic pain.[37] Changes in position or abdominal pressure alter the symptomatology.[38] Syndrome tends to be accompanied by a polysymptomatic picture in which backache and headache together with leukorrhea, dysmenorrhea and functional bleeding like changes in frequency, amount and duration of bleeding or intermenstrual bleeding (result of minute hemorrhage from the excessively congested endometrium or endocervix which is not hormone conditioned). Leucorrhoeic discharge is characterized by clear mucus due to hypersecretion uncomplicated by infection. Many methods have been employed to diagnose this condition such as contrast-enhanced computed tomography and nuclear magnetic resonance,[39] angiography,[40] ultrasound and color Doppler sonography.[41,42] However, laparoscopy remains an essential part for investigating the pelvic pain.[43]

Table 55.2: Ing system for ovarian endometriosis[3]

Parameters	*Score*
Reproductive age	2
Chronic pain (premenstrual or menstrual)	1
Infertility	1
B-mode sonography	
Position	2
Multiplicity	1
Serial sonography positive	2
Thick wails	2
Homogeneous echogenicity	2
Clear demarcation from surrounding structures	1
Transvaginal color Doppler sonography	
Vascularization	2
Percystic/hilar location	2
Regularly separated vessels	2
Existence of notching	1
Resistance index <0.40 (menstrual phase)	2
Resistance index 0.40–0.60 (late follicular/corpus luteum phase)	2
CA 125 range 35–65 IU/ml	2

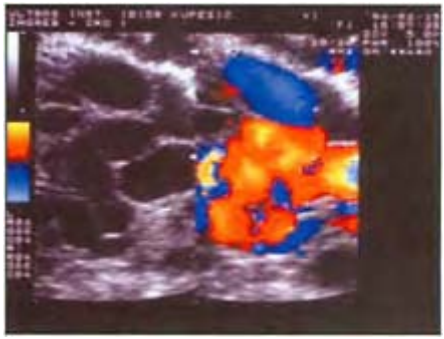

Figure 55.10: Transvaginal scan of a bizarre adnexal mass resembling a view of multilocular cyst. Color Doppler ultrasound reveals bright color signals typical of pelvic congestion syndrome

The sonographic finding of pelvic congestion syndrome includes multiple serpentine, anechoic structures within the pelvis (Figs 55.8 and 55.9).[41] Although real time sonography depicts this feature, the findings of multiple cystic lesions in the pelvis suggest the occurrence of other entities as well, including hydrosalpinx, multilocular ovarian cysts (Fig. 55.10), or fluid filled loops of bowel. Transvaginal color Doppler was shown as the safest and most definitive diagnostic technique within the gynecologist's reach. Its use has allowed a demonstration of the existence of vascular dilatation that affects not only the veins but also the arterial system.[37] The venous plexuses are more thick and in most of the cases observable

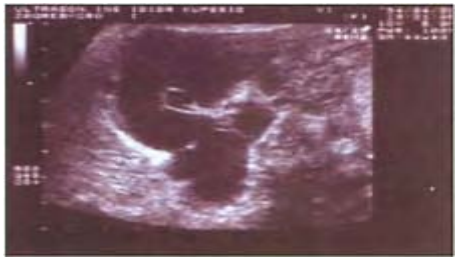

Figure 55.8: Transvaginal scan of anechoic sausage shape structure that can be

easily confused with a dilated tube on conventional sonography

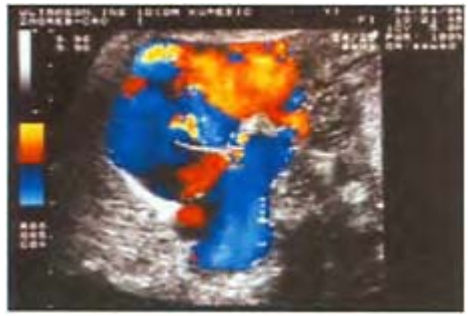

Figure 55.9: The same patient as in Figure 55.8. Color flow imagine facilitates visualization of greatly dilated veins

with vaginal sonography. This is not true for the arteries that are thinner and have a tendency to show their dilatation in intraparenchymatous locations usually visible only after switching color Doppler. Sometimes both systems are affected, with the vascular disturbance being more intense and more widespread because of the involvement of myometrial vessels as well. Therefore, crosssections of the dilated intramyometrial vessels may be misinterpreted as the "Swiss cheese" appearance of the myometrium as in the case of adenomyosis.

Ovarian Vein Thrombosis

This uncommon and potentially fatal disorder occurs most often postpartum, but it has been reported after surgical intervention in the pelvis, trauma of the pelvis or PID.[44] Pelvic vein thrombosis may occur in nonpuerperal patients with hypercoagulable blood and has significant sequelae.[45] Ovarian vein thrombosis affects right side in 80–90% of the cases even though it has been described on the left side and bilaterally.[46,48] Right-sided predominance is explained by dextrotorsion of the gravid uterus compressing the right ovarian vein and retrograde flow in the left ovarian vein.[49,50] Most cases occur during the first week after delivery, however, rare antepartum and delayed postpartum cases have been reported.[47]

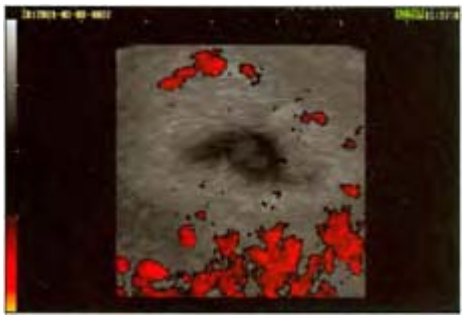

Figure 55.11: Three-dimensional power Doppler scan of an early pregnancy, which can sometimes cause acute pelvic pain. Power Doppler signals displayed from the periphery of the gestational sac represent intervillous and spiral artery blood flow

During a full-term pregnancy ovarian veins reach the three times their normal diameter. Immediate collapse of the dilated veins observed after deli¬ very results in low-pressure state when combined with hypercoagulability increases the risk of ovarian vein thrombosis.[51] Infection and stasis associated with the of hypercoagulable state in pregnancy have been cited as the etiologic factors,[46,51] as well as coexisting endometritis.[52] Whether thrombosis follows or precedes infection is unknown.

Acute Pelvic Pain with Positive Pregnancy Tests

Normal Intrauterine Pregnancy

Normal intrauterine pregnancy is probably the most common cause of pelvic pain in the first trimester. Grumpy pelvic pain is due to hormonal changes, rapid growth of uterus and increased blood flow. Besides clinical and laboratory signs (beta hCG) transvaginal ultrasound examination may give additional information on presence, location and development of pregnancy. The sonographic findings of normal intrauterine pregnancy depend on the gestational age:

4 weeks' gestation:

1. Decidual reaction-focal thickening of the endometrium without other signs of pregnancy.

2. Intradecidual sign-visualization of small sac (<5 mm) within one endometrial sheet.
3. Implantation hemorrhage-due to erosion of the endometrium during the implantation of an embryo. It is visualized as hypoechogenic area in the proximity of the gestational sac.

5 *weeks' gestation:*

1. Gestational sac-It is the only reliable sign of an intrauterine pregnancy; embryo and yolk sac are not yet visualized.
2. "Double ring" sign-It is important in differentiation of the intrauterine from ectopic pregnancy where there is a pseudogestational sac (Fig. 55.11).

5–6 weeks' gestation:

1. Visualization of the secondary yolk sac-The first detectable structure inside the gestational sac.
2. "Double bubble" sign-Two tiny sac repre¬ senting yolk sac and amnion.

6–7 weeks' gestation:

1. Visualization of an embryo (CRL=2–4 mm). Embryo is usually visualized 3–7 days after visualization of the yolk sac by transvaginal route.
2. Heart action-First shown adjacent to the yolk sac (in normal intrauterine pregnancy heart action must be visualized in embryo with CRL > 5 mm).

7–9 weeks' gestation:

1. Embryo is located within the amniotic cavity (CRL=12–14 mm).
2. Demonstration of the cavity within the embryo's head represents development of the central nervous system.
3. Clear visualization of the amniotic mem¬ brane.

Spontaneous Abortion

Threatened and spontaneous abortion are the most common complications of early pregnancy. Thirty to forty percent of pregnancies fail after 755 implantation, and only 10–15% manifest with clinical symptoms.[54–56] Patients with spontaneous abortion usually present in clinic during the 8–10 weeks from their last menstrual period with symptoms of vaginal bleeding and abdominal pain, with or without the expulsion of products of conception.[57] Decreased values of gestational sac diameter and/or its irregular shape, early growth retardation, registered on the basis of decreased crown-rump length (CRL) values are indicative enough for making the diagnosis of early pregnancy failure. Absence of clear visualization of the embryonic parts as well absence embryonic heart

activity is a clear sign of a nonviable gestation. There are two specific manifestations of early pregnancy failure, which is advisable to describe, blighted ovum and missed abortion. Blighted ovum or anembryonic pregnancy is a gestational sac in which an embryo either failed to develop or died at the stage too early to be visualized. The diagnosis of anembryonic pregnancy is based on the absence of embryonic echoes within the gestational sac large enough for the structures to be visible, independently of the clinical data or the menstrual cycle.[58] Gestational sac, in these patients, represents only an empty chorionic cavity. The studies of the intervillous circulation demonstrated lower PI values (0.54±0.04) of the artery-like signals in patients with blighted ovum when compared to those with normal pregnancies (0.80 ±0.04) and missed abortion (0.75±0.04).[59,60] Lower PI from the intervillous space of the anembryonic pregnancy group may reflect changes in the placental stroma, where the individual villi are prone to edema. The diagnosis of missed abortion is characterized by the identification of the fetus, which does not demonstrate any heart activity.[61] It is also determined as a type of spontaneous abortion where after a fetal demise spontaneous expulsion of conceptus outside of the uterus does not occur.[62] Ultrasound findings can be differentiated by the time that has passed from the incident that caused fetal demise and circulation break:

• *Gestational sac image* Recent-normal shape Later-collapsed, changed in shape and size

• *Embryo without heart action and dynamics* Recent-morphology preserved Later-smaller with altered morphology, completely amorphous or fragmented

• *Changes of trophoblast tissue*

Inhomogeneous, degeneratively changed (hydropic or calcified), presence of intrauterine hematomas, separation of membranes.

It is relatively easy to make this diagnosis by means of the transvaginal color Doppler facilities. The main parameter is the absence of the heart activity and the lack of color flow signals at expected position of the embryonic/fetal heart after the 6th gestational week.[63] However, one should be aware that the length of the time elapsing between arrest of embryonic development and clinical presentation will determine the sonographic image and should be considered in the interpretation.

Ectopic Pregnancy

Ectopic pregnancy occurs when fertilized ovum implants itself on the place other than the uterine cavity. Although ectopic is the most often localized in the Fallopian tube (95%), a zygote implantation may also occur in abdominal, ovarian, intraligamentous, cornual, intramural or cervical sites.[63,67] Ectopic pregnancy is the great masquerader. The clinical presentation can vary from vaginal spotting to vasomotor shock with hematoperitoneum. The classic triad of delayed menses, irregular vaginal bleeding and abdominal pain is most commonly not encountered. Patients presented with acute symptoms (frequently in emergency rooms) are usually at a more advanced gestational age compared to asymptomatic infertility patients who are closely followed because of their increased risk for ectopic pregnancy. Physical examination reveals abdominal tenderness or peritoneal irritation in the presence (or sometimes the absence) of a palpable adnexal mass. Dizziness and nausea may help in confirming the suspicion of an ectopic gestation. Astute clinicians should consider all presenting signs and symptoms as

the “rule-out an ectopic case” until an intrauterine pregnancy is diagnosed or ectopic pregnancy is found.[65] Diagnostic procedures are divided into two groups:

Non-invasive: History, general, clinical and gynecological examination, hormonal and other laboratory markers and ultrasound diagnostics.

Invasive: Culdocentesis,curettageandlaparoscopy.

Absolute value of beta hCG levels in circulation are much lower than the levels of the same hormone in normal intrauterine pregnancies of the same gestational age. Dynamics of the titer shows slower increase of circulating concentrations which prolongates the time for doubling its values.

The most important use of the quantitative beta hCG determination in conjunction with ultrasonography is that of understanding the value of the “discriminatory zone” of beta hCG. The discriminatory zone represents the level of beta hCG above which all normal intrauterine chorionic sacs will be detected by ultrasound. There is now almost a consensus in considering the discriminatory zone to be about 1000 mlU/ml with the use of transvaginal probe of at least 5 MHz.[68–71] Ultrasonography (but more precisely, transvaginal sonography), has become the “gold standard” laboratory modality for the effective and fast diagnosis of ectopic pregnancy.

Ultrasonographic criteria for ectopic pregnancy could be divided into uterine and extrauterine signs, barring in mind that all of them can be diagnostic or just suggestive.[72]

- Empty uterus, with or without increased endometrial thickness-the most common sign!
- Central hypoechoic area, or a sac like structure inside the cavity-the so called pseudogestational sac, and
- Concurrent intrauterine pregnancy-extremely rare.

Adnexal sonographic findings in women with ectopic pregnancy are variable:

- Gestational sac in adnexal region with clear embryonic echo and heart activity; directly proves ectopic pregnancy (seen in 15–28% of the cases),
- Visualization of the adnexal gestational sac with or without embryonic echo (without heart action); a tubal ring 1–3 cm in diameter, consisting of a concentric ring of 2–4 mm of echogenic tissue surrounding the hypoechoic center. Such a finding is detected in 46–71% of reported cases if tube is unruptured,
- Very often an unspecific adnexal tumor could be visualized,
- Free fluid in the cul-de-sac (40–83% of cases).

Corpus Luteum Cysts

Pelvic pain during pregnancy is usually attributed to the adnexal masses and most common cause is considered a corpus luteum cyst. Pain is typically lateralized and may be either due to the size of the cyst, hemorrhage within the cyst or torsion. Ultrasound characteristics of corpus luteum cyst are described above. Corpus luteum cyst usually resolves by the second trimester.

Leiomyoma

Because leiomyomas are hormonally responsive they usually grow and change echotexture during early pregnancy.[74] Their rapid growth with degeneration can lead to pelvic pain localized on the site of the fibroid. Leiomyomas have a variable sonographic appearance ranging from hypoechoic to hyperechoic and complex, depending on their

composition and the degree of degeneration. The size of leiomyoma increases with the gestational age, mainly due to pregnancy hormones. Leiomyomas also cause some blood flow changes in the uteroplacental circulation during pregnancy. Our study showed an increase of the flow velocity in radial arteries supplying uterine leiomyoma ($p<0.01$) from the 10th to 13th gestational week.[75] Probably this finding is a consequence of

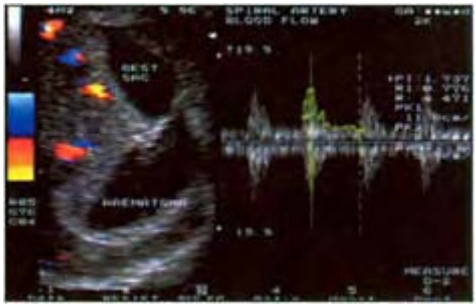

Figure 55.12: Intrauterine hematoma seen as echo-free area may lead to acute pelvic pain and may alterate regional blood flow in spiral arteries

the higher levels of estriol hormone that is metabolised in placenta. All these changes, however do not influence the blood flow in spiral and uterine arteries.[75]

Uterine Dehiscence and Rupture

Patients at high risk for uterine dehiscence and rupture have a history of prior surgical intervention on the uterine wall, which leads to thinning of the myometrium. Diagnosis of this life threatening condition is based upon extrusion of the uterine contents into the abdominopelvic cavity.

Placental Abruption

Placental abruption is a condition caused by acute separation of the placenta accompanied by vaginal bleeding, pain, uterine tenderness and hypovolemic shock. Placental abruption should always be considered if retroplacental hypoechoic complex (composed of uteroplacental vessels-predominantly veins) exceeds 1 to 2 cm in thickness. Uterine contraction may create focal thickening of this area. Differentiation from placental abruption may be made on the basis of a transient nature of the contraction and by switching on the color Doppler. Uterine leiomyomas can also be mistaken for the retroplacental hemorrhage, but are generally more rounded in shape and demonstrate greater vascularity on color Doppler.

Patient with conditions such as maternal hypertension, preeclampsia, abdominal trauma, cocaine abuse, cigarette smoking, advanced maternal age and male fetuses

(intriguing but unexplained phenomenon) are at increased risk of the complication.[76,77] Ultrasound presentation of placental hemorrhage depends on the gestational age, location, and patient's hematocrit. We can differentiate three types of abruptions considering location of separation:

1. Retroplacental hematoma is caused by hemorrhage from the spiral arteries, which leads to separation of the basal lamina from uterine the wall usually caused by hypertension or 758 overdose of the anticoagulable drugs.
2. Subchorionic (marginal) hematoma-is caused by hemorrhage from marginal veins, and leads to separation of the chorionic membrane from the decidua at the edge of placenta (Fig. 55.12).
3. Subamnionic hemorrhage is caused by hemorrhage from the fetal blood vessels at the fetal surface of the placenta.

CONCLUSION

Acute pelvic pain may be the manifestation of various gynecologic and non-gynecologic disorders from less alarming rupture of the follicular cyst to life threatening conditions such as rupture of ectopic pregnancy or perforation of inflamed appendix. In order to construct an algorithm for differential diagnosis we divide acute pelvic pain into gynecologic and non-gynecologic etiology, which is than subdivided into gastrointestinal and urinary causes.

Appendicitis is the most common surgical emergency and should always be considered in differential diagnosis if appendix has not been removed. Apart of clinical examination and laboratory tests, an ultrasound examination is sensitive up to 90% and specific up to 95% if graded compression technique is used. Still it is user-depended and requires considerable experience in order to perform it reliably. Meckel's diverticulitis, acute terminal ileitis, mesenteric lymphadenitis and functional bowel disease are conditions that should be differentiated from other causes of low abdominal pain by clinical presentation, laboratory and imaging tests. Dilatation of renal pelvis and urether are typical signs of obstructive uropathy and may be efficiently detected by ultrasound. Additional thinning of renal parenchyma suggests long-term obstructive uropathy.

Ruptured ectopic pregnancy, salpingitis and hemorrhagic ovarian cysts are three most commonly diagnosed gynecologic conditions presenting as an acute abdomen. Degenerating leiomyomas and adnexal torsion occur less frequently. For better systematization, gynecologic causes of acute pelvic pain could be divided into conditions with negative pregnancy test and conditions with positive pregnancy test.

Pelvic inflammatory disease may be ultrasonically presented with numerous signs such as thickening of the tubal wall, incomplete septa within the dilated tube, demonstration of hyperechoic mural nodules, free fluid in the "culde-sac" etc. Color Doppler ultrasound contributes to more accurate diagnosis of this entity since it enables differentiation between acute and chronic stages based on analysis of the vascular resistance. Hemorrhagic ovarian cysts may be presented by variety of ultrasound findings since intracystic echoes depend upon the quality and quantity of the blood clots. Color Doppler investigation demonstrates moderate to low vascular resistance typical of luteal flow. Leiomyomas undergoing degenerative changes are another cause of acute pelvic pain commonly present in patients of reproductive age. Color flow detects regularly

separated vessels at the periphery of the leiomyoma, which exhibit moderate vascular resistance. Although the classic symptom of endometriosis is chronic pelvic pain, in some patients acute pelvic pain does occur. Most of these patients demonstrate an endometrioma or “chocolate” cyst containing diffuse carpet-like echoes. Sometimes, solid components may indicate even ovarian malignancy, but if color Doppler ultrasound is applied it is less likely to obtain false-positive results. One should be aware that pericystic and/or hillar type of ovarian endometrioma vascularization facilitate correct recognition of this entity. Pelvic congestion syndrome is another condition that can cause an attack of acute pelvic pain. It is usually consequence of dilatation of venous plexuses, arteries or both systems. By switching color Doppler gynecologist can differentiate pelvic congestion syndrome from multilocular cysts, pelvic inflammatory disease or adenomyosis. Ovarian vein thrombosis is a potentially fatal disorder occurring most often in the early postpartal period. Hypercoagulability, infection and stasis are main etiologic factors, and transvaginal color Doppler ultrasound is an excellent diagnostic tool to diagnose it. Acute pelvic pain may occur even in normal intrauterine pregnancy. This may be explained by hormonal changes, rapid growth of the uterus and increased blood flow. Ultrasound is mandatory for distinguishing normal intrauterine pregnancy from threatened or spontaneous abortion, ectopic pregnancy and other complications that may occur in patients with positive pregnancy test. Incomplete abortion is visualized as thickened and irregular endometrial echo with certain amount of intracavitary fluid. If applied, color Doppler ultrasound reveals low vascular resistance signals in richly perfused intracavitary area. Transvaginal sonography has high sensitivity and specificity in visualization of uterine and adnexal signs of ectopic pregnancy. Color Doppler examination may aid in detection of the peritrophoblastic flow. Furthermore, it facilitates detection of ectopic living embryo, tubal ring or unspecific adnexal tumor. Corpus luteum cysts and leiomyomas are another cause of pelvic pain during pregnancy, which can be correctly diagnosed by ultrasound. Detection of uterine dehiscence and rupture in patients with history of prior surgical intervention on uterine wall relies exclusively on correct ultrasound diagnosis. In patients with placental abruption sonographer detects hypoechoic complex representing either retroplacental hematoma, subchorionc hematoma or subamniotic hemor-rhage. In closing, ultrasound has already become important and easily available tool, which can efficiently recognize patients with possibly threatening conditions of different origins.

REFERENCES

1. Baines PA, Allen GM. Pelvic pain and menstrual related illnesses. Emerg Med Clin North Am 2001; 19:763–80.
2. Hewitt GD, Brown RT. Acute and chronic pelvic pain in female adolescents. Med Clin North Am 2000; 84:1009–25.
3. Bau A, Atri M. Acute female pelvic pain: ultrasound evaluation. Semin Ultrasound CT MR 2000; 21:78–93.
4. Kumar R Clark M (Eds). Clinical Medicine: A Textbook for Medical Students and Doctors (3rd ed), London: WB Saunders Company Ltd, 1996.
5. Gray M, Albo M, Huffstutler S. Interstitial cystitis: a guide to recognition, evaluation, and management for nurse practitioners. J Wound Ostomy Continence Nurs 2002; 29:93–102.
6. Bennett GL, Slywotzky CM, Giovannello G. Gynecologic causes of acute pelvic pain. Radiographics 2002; 22:785–801.

7. Kupesic S, Kurjak A, Zodan T. Color Doppler ultrasound in the diagnosis of pelvic inflammatory disease. In: Kurjak A (Ed). An Atlas of Transvaginal Color Doppler. The London-New York: Parthenon Publishing Group, 2000; 127–35.
8. Westroem L, Wolner Hanssen P Pathogenesis of pelvic inflammatory disease. Genitourin Med 1993; 69:9–17.
9. Expert Committee on Pelvic Inflammatory Disease. Research directions for the 1990s. Sex Trans Dis 1991; 18:46–64.
10. Gales W, Wasserheit JN. Genital chlamydial infections: epidemiology and reproduction sequelae. Am J Obstet Gynecol 1991; 164:1771–81.
11. Toth M, Chervenak FA. Infection as the cause of infertility. In: Kupesic S, De Ziegler D (Eds). Ultrasound and Infertility. Carnforth, UK: Parthenon Publishing 2002:205–14.
12. Patten RM, Vincent LM, Wolner-Hanssen P Pelvic inflammatory disease: Endovaginal sonography with laparoscopic correlation. J Ultrasound Med 1990; 9:861–65.
13. Reynolds T, Hill MC, Classman LM. Sonography of hemorrhagic ovarian cyst. J Clin Ultrasound 1986; 14:449–53.
14. Baltrarowich OH, Kurtz AB, Pasto ME. The spectrum of sonographic findings in hemorrhagic ovarian cyst. Am J Roentgenol 1987; 148:901–05.
15. Bass IS, Haller JO, Freidman AP. The sonographic appearance of the hemorrhagic ovarian cyst in adolescents. J Ultrasound Med 1984; 3:509–14.
16. Kupesic S, Kurjak A. Color Doppler assessment of uterine leiomyoma and sarcoma. In: Kurjak A (Ed). An Atlas of Transvaginal Color Doppler. London-New York: The Parthenon Publishing Group 2000; 179–86.
17. Siskin GR Bonn J, Worthington-Kirsch RL. III. Uterine fibroid embolization:pain management. Tech Vase Interv Radiol 2002; 5:35–43.
18. Richengerg J, Cooperberg P Ultrasound of the Uterus. In: Callen P (Ed). Ultrasound in Obstetrics and Gynecology. Philadelphia: WB Saunders Company 2000; 814–46.
19. Kurjak A, Kupesic S, Shalan H, Jukic S, Kosuta D, Ilijas M. Uterine sarcoma: a case report of 10 cases studied by transvaginal color and pulsed Doppler sonography. Gynecol Oncol 1995; 59:342–46.
20. Kurjak A, Kupesic-UrekS, MiricD. The assessment of benign uterine tumor vascularization by transvaginal color Doppler. Ultrasound Med Biol 1992; 18:645–48.
21. Kupesic S, Kurjak A. Color Doppler assessment of patients with pelvic pain. In: Kurjak A (Ed). An Atlas of Transvaginal Color Doppler. London-New York: The Parthenon Publishing Group, 2000; 241–44.
22. Worthington-Kirsch RL, Raftopoulos V, Cohen IT. Sequential bilateral torsion of normal ovaries in a child. J Ultrasound Med 1986; 5:663–64.
23. Sozen I, Kadako R, Fleischman S, Arici A. Diagnosis and laparoscopic management of a Fallopian tube torsion following Irving tubal sterilization: a case report. Surg Endosc 2002; 16:217–21.
24. Fleischer A, Stein S, Cullinan J, Warner M. Color Doppler sonography of adnexal torsion. J Ultrasound Med 1995; 14:523–28.
25. Rosado WM, Trambert MA, Gosnik BB, Pretorius DH. Adnexal torsion: diagnosis by using Doppler sonography. Am J Roentgenol 1992; 159:1251–53.
26. Van Voorhis BJ, Schwaiger J, Syrop CH, Chapter FK. Early diagnosis of ovarian torsion by color Doppler ultrasonography. Fertil Steril 1992; 58:215–17.
27. Fleischer AC. Color Doppler sonography in pelvic pain. In: Kurjak A, Fleiscer AC (Eds). Doppler Ultrasound in Gynecology. Carnforth, UK: Pathenon Publishing, 1998; 9–88.
28. Lineberry TD, Rodriguez H. Isolated torsion of the fallopian tube in an adolescent: a case report. J Pediatr Adolesc Gynecol 2000; 13:135–37.
29. Kurjak A, Kupesic S. Benign ovarian lesions assessed by color and pulsed Doppler. In: Kurjak A (Ed). An Atlas of Transvaginal Color Doppler. London-New York: The Parthenon Publishing Group, 2000; 191–202.

30. Simpton JL, Elias S, Malinak LR, Buttram VC Jr. Heritable aspects of endometriosis I: genetic studies. Am J Obstet Gynecol 1980; 137:327–31.
31. Barlow D, Kennedy H. Endometriosis: clinical presentation and diagnosis. In: Shaw RW (Ed). Endometriosis. Carnforth, UK: Parthenon Publishing, 1989; 1–10.
32. Bai SW, Cho HJ, Kim JY, Jeong KA, Kim SK, Cho DJ, Song CH, Park KH. Endometriosis in an adolescent population: the severance hospital in Korean experience. Yonsei Med J 2002; 43:48–52.
33. Kupfer MC, Schwimer RS, Lebovic J. Transvaginal sonographic appearance of endometriomata: spectrum of findings. J Ultrasound Med 1992; 11:129–32.
34. Atri M, Nazarnia S, Bret P. Endovaginal sonographic appearance of benign ovarian masses. Radiographics 1996; 14:747–49.
35. Kurjak A, Kupesic S. Scoring system for prediction of ovarian endometriosis based on transvaginal color and pulsed Doppler sonography. Fertil Steril 1994; 62:81–88.
36. Beard RW, Highman JH, Pearce S, Reginald PW. Diagnosis of pelvic varicosities in women with chronic pelvic pain. Lancet 1985; 2:956–59.
37. Kurjak A, Kupesic S. Congestion syndrome of the uterus. In: Osmers R, Kurjak A (Eds). Ultrasound and the Uterus. Carnforth, UK: Parthenon Publishing, 1995; 115–18.
38. Bonilla-Musoles F, Ballesteros MJ. Transvaginal color Doppler in the diagnosis of pelvic congestion syndrome. In: Kurjak A (Ed). An Atlas of Transvaginal Color Doppler. Carnforth, UK: Parthenon Publishing, 1994; 207–15.
39. Fakhri A, Fisherman EK, Mitchel SE, Siegelman SS, White RI. The role of CT in the management of pelvic arteriovenous malformations. Cardiovasc Intervent Radiol 1987; 10:96–99.
40. Bottomley JR Whitehouse GH. Congenital arteriovenous malformations of the uterus demonstrated by angiography. Acta Radiol 1975; 16:43–48.
41. Diwan RV, Brennan JN, Selim MA. Sonographic diagnosis of arteriovenous malformations of the uterus and pelvis. J Clin Ultrasound 1983; 11:295–98.
42. Juhasz B, Kurjak A, Lampe LG. Pelvic varices simulating bilateral adnexal masses: differential diagnosis by vaginal color Doppler. J Clin Ultrasound 1992; 20:81–84.
43. Promecene PA. Laparoscopy in gynecologic emergencies. Semin Laparosc Surg 2002; 9:64–75.
44. Kurman RJ (Ed). Blaustein's Pathology of the Female Genital Tract (4th ed). New York: Springer-Verlag, 1994; 532–35.
45. Visaria SD, Davis JD. Pelvic vein thrombosis as a cause of acute pelvic pain. Obstet Gynecol 2002; 99:897–99.
46. Munisck RA, Gillanders LA: A review of the syndrome of puerperal ovarian vein thrombophlebitis. Obstet Gynecol Surv 1981; 36:57–61.
47. Simons GR, Piwnica Worms DR, Goldhaber SZ. Ovarian vein thrombosis. Am Heart J 1993; 136: 641–43.
48. Khurana BK, Rao J, Friedman SA. Computed tomographic features of puerperal ovarian vein thrombosis. Am J Obstet Gynecol 1998; 159:905–07.
49. Cranston PE, Hamrick-Turner J, Morano JU. Pseudothrombosis of the right ovarian vein: Pitfall of abdominal spiral CT. Clin Imaging 1995; 19:176–79.
50. Dure-Smith P Ovarian syndrome: Is it a myth? Urology 1995; 13:355–58.
51. Toland KC, Pelamder WM, Mohr SJ. Postpartum ovarian vein thrombosis presenting as urethral obstruction: A case report and review of literature. J Urol 1993; 149:1538–42.
52. Savader SJ, Otero RR, Savader BL. Puerperal ovarian vein thrombosis: Evaluation with CT, US and MR imaging. Radiology 1988; 167:637–39.
53. Kennedy A. Assessment of acute abdominal pain in the pregnant patient. Semin Ultrasound CT MR 2000; 21:64–77.
54. Hakim RB, Gray RH, Zacur H. Infertility and early pregnancy loss. Am J Obstet Gynecol 1995; 172: 1510–17.

55. Wilcox AJ, Weinbert C, O'Connor JF. Incidence of early loss in pregnancy. N Engl J Med 1988; 319: 159–64.
56. Alberman E. The epidemiology of repeated abortion. In: Beard RW, Bishop F (Eds). Early Pregnancy Loss: Mechanism and Treatment. New York: SpringerVerlag, 1988; 9–17.
57. Cetin A, Cetin M. Diagnostic and therapeutical decision-making with transvaginal sonography for first trimester spontaneous abortion, clinically thought to be complete or incomplete. Contraception 1998; 57: 393–97.
58. Kurjak A, Kupesic S. Blood flow studies in normal and abnormal pregnancy. In: Kurjak A, Kupesic S (Eds). An Atlas of Transvaginal Color Doppler. London-New York: Parthenon Publishing group 2000; 41–51.
59. Kurjak A, Kupesic S. Doppler assessment of intervillous blood flow in normal and abnormal early pregnancy. Obstet Gynecol 1997; 89:252–56.
60. Kurjak A, Kupesic S. Parallel Doppler assessment of yolk sac and intervillous circulation in normal pregnancy and missed abortion. Placenta 1998; 19:619–23.
61. Jaffe R, Warsof SL. Color Doppler imaging in the assessment of uteroplacental blood flow in abnormal first trimester intrauterine pregnancies: an attempt to define etiologic mechanism. J Ultrasound Med 1992; 11:41–44.
62. Kos M, Kupesic S, Latin V. Diagnostics of spontaneous abortion. In: Kurjak A (Ed). Ultrasound in Gynecology and Obstetrics. Zagreb: Art Studio Azinovic, 2000; 314–21.
63. Szulman AE. The natural history of early human spontaneous abortion. In: Barnea ER, Check JH, Grudzinkas JG, Marvo T (Eds). Implantation and Early Pregnancy in Humans. Carnforth UK: Parthenon Publishing 1993; 309–21.
64. Ectopic pregnancy. In: Speroff L, Glass RH, Kase NG (Eds). Clinical Gynecologic Endocrinology and Infertility. London: Williams and Wilkins 1999; 1149–67.
65. Timor-Tristch IE, Monteagudo A. Ectopic pregnancy. In: Kupesic S, de Ziegler D (Eds). Ultrasound and Infertility. London-New York: Parthenon Publishing group 2000; 215–39.
66. Kurjak A, Kupesic S. Ectopic pregnancy. In: Kurjak A (Ed). Ultrasound in Obstetrics and Gynecology. Boston: CRC Press 1990; 225–35.
67. Kupesic S, Kurjak A. Color Doppler assessment of ectopic pregnancy. In: Kurjak A, Kupesic S (Eds). An Atlas of Transvaginal Color Doppler. London-New York: Parthenon Publishing group 2000; 137–47.
68. Timor-Tristch IE, Rottem S, Thale I. Review of transvaginal ultrasonography: description with clinical application. Ultrasound Q 1988; 6:1–32.
69. Peisner DB, Timor-Tritsch IE. The discriminatory zone of beta hCG for vaginal probes. J Clin Ultrasound 18:280–85.
70. Possum GT, Dvajan V, Kletzky DA. Early detection of pregnancy with transvaginal ultrasound. Fertil Steril 1988; 49:788–91.
71. Bernascheck G, Euaelstorfer R, Csaicsich P. Vaginal sonography versus serum human chorionic gonadotropin in early detection of pregnancy. Am J Obstet 1988; 158:608–12.
72. Kurjak A, Zalud I, Volpe G. Conventional B-mode and transvaginal color Doppler on ultrasound assessment of ectopic pregnancy. Acta Med 1990; 44: 91–103.
73. Nyberg D. Ectopic pregnancy. In: Nyberg DA, Hill LM, Bohm-Velez M (Eds). Transvaginal Sonography. St. Luis: Mosby Year Book 1992; 105–21.
74. Rosati P, Bellatti U, Exacoustos C. Uterine myoma in pregnancy: ultrasound study. Int J Gynecol Obstet 1989; 28:109–17.
75. Kurjak A, Predanic M, Kupesic S, Zudenigo D, Matijevic R, Salihagic A. Transvaginal color Doppler in the study of early cornual pregnancies and pregnancies associated with fibroids. J Matern Fetal Invest 1992; 2:81–85.
76. Annath CV, Savitz DA, Luther ER. Maternal cigarette smoking as a risk factor for placental abruption, placenta previa and uterine bleeding in pregnancy. Am J Epidemiol 1996; 144:881–85.

77. Kramer M, Usher R, Pollack R. Etiologic determinants of abruptio placentae. Obstet Gynecol 1997; 89:21115.

Chapter 56
Gynecologic Ultrasound in Emergency Room

Vladimir Sparac, Asim Kurjak

INTRODUCTION

Ultrasound as non-invasive method is basically the first-line diagnostic procedure in emergency room after the information about the history and bimanual palpation. If we consider that sensitivity of bimanual palpation is in range of 40% up to 60% at most, significance of ultrasound examination is even more clear.

Transabdominal ultrasound examination in gynecology is today generally opsolent and replaced by vaginosonographic examination which provide superb image of pelvic organs. Capability of an ultrasound machines to demonstrate anatomy of the pelvic organs of interest has been additionally enhanced with color Doppler and pulsed Doppler modalities which introduced data about organ's vascularity and, therefore, indirect assessment of organ's normal and abnormal physiology. Vascular characteristics of gynecological organs in normal state, as well as in a state of functional disorders or developing benign or malignant lesions, showed to be supportive to a clinician in elucidating etiology and modifying a management of disease.

Although all known gynecological diseases can be the reason for examination in emergency room, in this chapter we will describe few lesions that are the most often cause to urgent visit to hospital.

UTERINE BLEEDING

Transvaginal ultrasonography is a highly sensitive method for detecting endometrial abnormalities.[1–3] Up to a third of women referred to a general gynecologic unit have abnormal uterine bleeding, and it remains the most frequent indication for gynecological surgical intervention. After the exclusion of pregnancy which is mandatory in all cases of abnormal uterine bleeding during the reproductive ages possible causes can be divided in genital diseases (polyps, hyperplasia, endometrial carcinoma, endometritis, submucous myomas, adenomyosis), systemic diseases and iatrogenic causes. If all of these have been excluded, diagnosis of dysfunctional bleeding can be established. Such diagnosis covers up to 60% of abnormal uterine bleeding, and indicate that there is no underlying organic pathology. TVCD is often used as a screening test to evaluate patients with abnormal bleeding for possible endometrial carcinoma and other types of intrauterine pathology.

Using conventional TVS, the thickness of the endometrium is generally measured in the sagittal plane to determine whether patients should go on to D and C. The thickness of the endometrium may have a varying thickness particularly if there is a focal thickening as seen in patients with endometrial polyps. Very often color Doppler demonstrate one feeding blood vessel that enters a structure of endometrial polyp. RI detected from those vessels is always higher than 0.42. The endometrial thickness of patients with cancer and those with endometrial hyperplasia sometimes overlap and these cases will need D and C procedure to cure the bleeding and diagnose possible neoplastic process. Generally, the finding of a regular endometrial echo with a thickness of less than 5 mm has been shown to have a high negative predictive value for the presence of any serious pathology.[4] Clinically it means that physician can try to stop bleeding with medicamentous hormonal treatment.

Leiomyomas are one of the most common tumors of the pelvic viscera in women of reproductive ages. Fibroids can remain intramural or can extend into the uterine lumen to become submucosal or outwards and become subserosal and pedunculated. Clinically the symptoms such as metrorrhagia or pelvic pain are most often connected with submucosal type. Besides the location the severity of symptoms is highly dependent on the number and size of leiomyomas. The ultrasound diagnosis of submucous leiomyomas is based on distorted endometrial contour, uterine enlargement and changes of its texture. Sonographic texture of fibroids ranges from hypoechoic to hyperechoic, depending on the amount of muscle tissue and connective tissue. Leiomyomas grow centripetally and create a pseudocapsule of compressed muscle fibers that is seen at ultrasound screen as a well demarcated edge which surrounds fibroid structure. Color Doppler analysis demonstrates the vascularization with moderate vascular resistance of 0.54+0.08 mainly located on the periphery of the fibroid.[5]

Another lesion that often result in abnormal vaginal bleeding is adenomyosis—presence of diffuse or focal endometrial tissue within the myometrium. Although definitive diagnosis has been established only after pathohistological analysis at extirpated uterus, sonographic characteristics are diffusely enlarged uterus with irregular hypoechoic zones within myometrium. Transvaginal ultrasound has a variable diagnostic rate with mean sensitivity and specificity of 80% and 74% respectively for diffuse adenomyosis.[6]

PELVIC INFLAMMATORY DISEASE (PID)

Pelvic inflammatory disease is defined as “the acute clinical syndrome associated with ascending spread of microorganisms from the vagina or cervix to the endometrium, Fallopian tubes and/ or contiguous structures”. The diagnosis of this entity sometimes can be difficult because of the wide variation of signs and symptoms.This is a reason why clinicians often delay diagnosing the condition what can result in acute formation of tubo-ovarian abscess or development of chronic pelvic pain, infertility and dyspareunia as a long term sequelae.

Procedure in emergency room should always combine and compare sonographic characteristics of adnexal masses with clinical status of patient (history, temperature, characteristics of pain, laboratory findings—complete blood count).

The majority of patients with acute salpingitis may exhibit at early phase normal gray scale ultrasound findings except the color Doppler parameters (RI, PI) which are lower due to inflammatory dilatation of affected blood vessels.[7] As the process of inflammation proceeds the tubes become thick-walled and irregular. Sonographic demarcation in this phase is easier owing to the process of pelvic exudation. The inflamed tubes may represent one of the following pictures:

1. A dilated tubular structure which is differentiated from pelvic veins by introduction of color Doppler—absence of blood flow.
2. Echogenic tubal wall which reflects the inflammatory process of the mucosal lining.
3. The presence of hypoechoic fluid within the dilated tubes indicates pyosalpinx.
4. A complex adnexal mass with the thickening of the ovarian capsule and loculated fluid collections in the adnexa and cul-de-sac represents the tubo-ovarian abscess.

Hydrosalpinx is often the final condition after the restoration of inflammatory process. Sonogra phic characteristics are tubular sausage-shaped, anechoic or hypoechoic structure with incomplete septa. Increased resistance index is obtained from the tubal walls and septa.

ECTOPIC PREGNANCY

Ectopic pregnancy is a gestation, which implants outside the uterine cavity. Any women with a positive pregnancy test and an empty uterus at the time of her scan required further investigation. The introduction of transvaginal ultrasound, laparoscopy and progress in process of qualitative and quantitative determination of human betachorionic gonadotrophin (bhCG) have revolutionized the management of early pregnancy complications. Although modern transvaginal probes with high resolution can visualize intrauterine gestational sac as early as a fifth week of amenorrhea and about 1000IU/L of bhCG ectopic pregnancy remains a big diagnostic challenge. One of the reasons is early visit of patients to the pregnancy unit what results with inconclusive finding and demands follow-up until the final determination of pregnancy site. Detection of intrauterine gestational sac virtually exclude ectopic pregnancy. The frequency of heterotopic pregnancy in spontaneous conceptions is estimated between 1:10000 and 1:50000, but is much higher (1:100) in assisted conceptions.[8]

As far as the location of ectopic pregnancies is concerned, more than 90% of ectopic pregnancies involve the fallopian tubes. The remaining ectopic sites are cornual region, cervix, ovary, and abdominal cavity. Patients very often have history of pelvic inflammatory disease.

Acute symptoms of the ectopic pregnancy are usually bleeding, pelvic pain and palpable adnexal mass. In cases where intraabdominal bleeding is present shoulder pain occurs and this is a one of pathognomonic marks of ruptured ectopic pregnancy.

The sonographic signs that may be encountered in cases of ectopic pregnancy are divided in two groups: “diagnostic” and “suggestive”.

Positive diagnostic signs mean very high possibility of extrauterine pregnancy and they are:

- Absence of intrauterine gestational sac
- Extrauterine/extraovarian adnexal mass
- Visualization of extrauterinely located embryo and positive heartbeats.

Positive suggestive signs are less convincing but indicative for ectopic nidation:

- Enlarged uterus with thick echogenic endometrium
- Free fluid (blood) or organized clot in cul-desac.

The corpus luteum is a useful guide when looking for an ectopic pregnancy, as it wil be on the ipsilateral side in over 85% of cases.[9] Typical (specificity 98.9%, sensitivity 84.4%) ectopic gestation forms a periovarian non-cystic adnexal mass.[10] Color Doppler findings can be determi¬ native for diagnosing ectopic pregnancy. Increased vascularity at the periphery of the gestational sac displays the same waveform like the luteal blood flow within the ovary, what means that the low resistance to blood flow must be detected out of the ovary in order to confirm the diagnosis of ectopic gestation.

TORSION OF ADNEXA

Adnexal torsion is another relatively frequent and urgent complication of adnexal tumors. Peduncule of torquated structure is formed from mesoovarium, infundibulopelvic and ovarian ligament. Symptoms have characteristics of sudden sharp pain in lower abdomen with combination of other acute abdomen symptoms.

Although all kind of adnexal tumors including pedunculated myomas can be torquated, mainly cystic tumors (functional cysts, cystadenomas, cystic teratomas and paraovarian cysts) are causing these symptoms.

Cystic teratomas are extremely mobile so they are the most frequent lesion that undergo torquation.

Sonographically torsions should be divided at incomplete and complete types. In incomplete types only partial occlusion happens and result is venous stasis with extravasation of blood in cystic tumor. Gray scale examination will detect this as hypoechoic or spider-web like structures inside of otherwise anechoic tumor. Color Doppler analysis will reveal slightly higher impedance in arterial pulsations 0.74–0.80, and undetectable venous flow. In complete type of torsion, gray scale examination will give very similar picture like the previous type, but during the color Doppler analysis no sign of blood flow will be detected pericystically. Treatment is operative and prompt detorquation with extirpation of cystic tumor can sometimes be enough so detorquated adnexa can be spared.

CONCLUSION

Transvaginal ultrasonography is a non-invasive, accurate and cost effective procedure, which has become irreplaceable diagnostic tool in modern emergency room. As bimanual pelvic examination is definitely insufficient and non-reliable for proper diagnosis, and often there is not much time for complex diagnostic procedures, ultrasound is the first-line method of choice. The ability to expand or reduce a differential diagnosis of a pelvic mass or of a patient’s symptomatology allows more precise and individualized care. After

the preliminary ultrasonographic triage of the patient it is much easier to decide what else from diagnostic procedures has to be done, or the patient has to be scheduled for emergency operative intervention.

REFERENCES

1. Fedele L, Bianchi S, Dorta M et al. Transvaginal hysteroscopy versus hysteroscopy in the diagnosis of the uterine submucosal myomas. Obstet Gynecol 1991; 77:745–48.
2. Kurjak A, Shalan H, Sosic A et al. Endometrial carcinoma in postmenopausal women: evaluation by transvaginal color Doppler ultrasonography. Am J Obstet Gynecol 1993; 169(6):1597–603.
3. Smith P, Bakos O, Heimer G et al. Transvaginal ultrasound for identifying endometrial abnormalities. Acta Obstet Gynecol Scand 1991; 70:591–94.
4. Granberg S, Wikland M, Karlsson B et al. Endometrial thickness as measured by endovaginal ultrasonography for identifying endometrial abnormality. Am J Obstet Gynecol 1991; 164:47–52.
5. Kurjak A, Kupesic S. Transvaginal color Doppler and pelvic tumor vascularity—lessons learned and future challenges. J Ultrasound Obstet Gynecol 1995; 6:145–49.
6. Fedele L, Bianchi S, Dorta M et al. Transvaginal ultrasonography in the diagnosis of diffuse adenomyosis. Fertil Steril 1992; 58:94–97.
7. Kupesic S, Kurjak A, Pasalic L, Benic S, Ilijas M. The value of transvaginal color Doppler in the assessment of pelvic inflammatory disease. Ultrasound Med Biol 1995; 21(6):733–38.
8. Ludwig M, Kaisi M, Bauer O et al. Heterotopic pregnancy in spontaneous cycle: do not forget about it! Eur J Obstet Gynecol Reprod Biol 1999; 87: 91–93.
9. Jurkovic D, Bourne TH, Campbell S et al. The diagnosis of ectopic pregnancy using transvaginal color flow imaging. Fertil Steril 1992; 57:68–73.
10. Brown DL, Doubilet PM. Transvaginal sonography for diagnosing ectopic pregnancy: positivity criteria and performance characteristics. J Ultrasound Med 1994; 13:259–66.

Chapter 57
Ultrasound in Gynecological Urology

Ivanka Bekavac, Renato Bauman, Radoslav Herman

In recent years, examination by ultrasound has taken important role in the diagnosis of female urinary tract, and is increasingly used as an alternative to radiological diagnosis. Together with history, clinical examinations and urodynamics, it improves the accuracy of the diagnosis of functional and morphological disorder.

Abdominal, perineal, rectal, ureteral and vaginal ultrasound have been applied to specific clinical problems with varying degrees of success. Transabdominal ultrasound was the first method to assess the angle between the urethra and the bladder. Due to the retropubic position of the target structures, bladder neck, urethra and the bladder wall, perineal (Fig. 57.1),[1–3] transrectal[4] and transvaginal[5] (Fig. 57.2) ultrasound are the ideal methods of visualizing. Introital ultrasound is a combination of transperineal and transvaginal approach in which transvaginal probe is applied on the perineum.[6] Color Doppler allows visualization of bladder and periurethral blood flow, as well as ureterovesical flow.

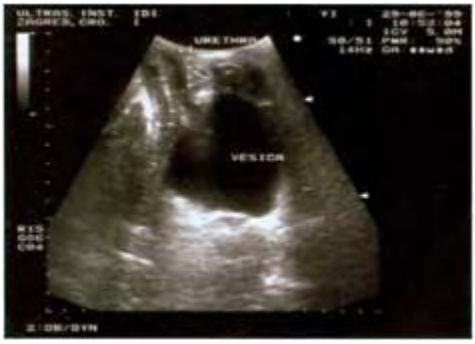

Figure 57.1: Transrectal scan showing bladder neck and urethra

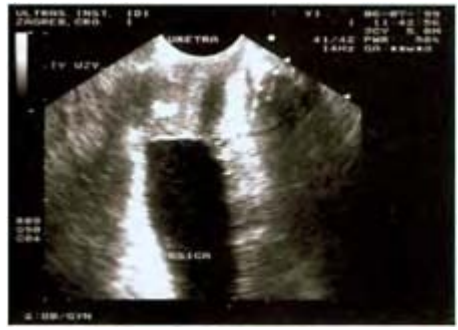

Figure 57.2: Transvaginal scan showing bladder neck and urethra

ULTRASOUND IMAGING OF THE LOWER URINARY TRACT

The role of ultrasound for imaging the female lower urinary tract is to demonstrate the anatomy of the lower urinary tract, the dynamic imaging of the urinary incontinence, and the results of the suprapubic surgery for "genuine stress incontinence" (GSI).

Urinary incontinence is a common complaint of many women of all ages. It becomes more frequent and more severe with advancing age. There are two main urodynamic diagnoses: genuine stress incontinence (GSI), where involuntary loss of urine occurs when the intravesical pressure exceeds the maximum urethral closure pressure in the absence of detrusor instability, and detrusor instability, where the detrusor is objectively shown to contract, either spontaneously or on provocation during bladder filling.[7]

Complete assessment of the incontinent patient includes history of disease, physical examination with full bladder, micturition diary, pad test, urodynamic evaluation including ultrasound examination in both recumbent and sitting positions.[8] Provocative maneuvers may permit assessment of the mobility and support of the bladder neck. Passive opening of the bladder neck and proximal urethra with urinary leakage concurrent with a cought or Valsalva's maneuver establishes diagnosis of GSI. Almost invariably there is descent of the bladder neck. The descent of more than 1 cm during straining of the bladder neck is considered diagnostic for hypermobility of the bladder neck. Therefore it is important to visualize and assess the changes of anatomic location of the bladder neck during straining or coughing; the normal bladder neck should always remain retropubic. In their study Leroy et al[9] reported that the descent or distortion of the bladder neck below the level of the symphisis was used as the endpoint to define urinary stress incontinence.

The transvaginal and perineal approach may be used to image urinary leakage into the proximal urethra. Some authors[10] recommend the use of transperineal ultrasound for imaging urethra and bladder neck, not only because of pressure applied to the urethra by the vaginal probe, but also because the probe moves on Valsalva's maneuver, making

measurements of bladder neck movement difficult, particulary in women with cystocele.[10]

In 1996 Schaer et al[1] reported on the fundamentals of perineal ultrasound examination for female incontinence. In four different investigations, each involving at least 30 patients, they investigated the influence of examination position, bladder filling volume and pressure of the ultrasound probe against the perineum on the position of the bladder neck, the size of the rectovesical angle and the occurrence of the funneling.

A comparison of the results obtained in the supine and upright position indicates that standing creates more pressure on the organs in the small pelvis, causing the meatus to lie lower, the angle to increase and funneling to occur more often. Pressure of the probe on the perineum can cause distorted measurements, changes in the position of the meatus internus and the angle. They found that different volumes of bladder filling did not affect the numerical measurements, but influenced the detection of bladder neck funnelling and the image quality.

Unfortunately, imaging of the bladder neck and detection of urinary leakage does not enable the observer to make a diagnosis of detrusor instability, as this requires pressure measurements to record uninhibited detrusor contractions. The assessment of bladder wall thickness allows an indirect measurements of the detrusor muscle thickness, and this provides a potential index of detrusor activity.

Kuhllar et al[11–12] were first to measure the bladder wall thickness and relate it to urodynamic changes. In their two studies they reported the increased thickness of the bladder wall associated with detrusor instability. It was probably due to an increase in the detrusor muscle secondary to detrusor overactivity. The increase in bladder wall thickness associated with age, in the normal and detrusor instability groups, is consistent with the development of detrusor hypertrophy, secondary to increased outflow obstruction possibly due to changes in urethral elastin and collagen. No increase with age was seen in the GSI group where there is minimal outflow obstruction. Clinical studies also suggests that ultrasound scanning should be performed to confirm the presence of paravaginal defects and that paravaginal defect repair may be added to Burch colposuspension for the treatment of genuine stress incontinence, as an operation to correct cystourethrocele and the posterior urethrovesical angle.[13]

COLOR DOPPLER IMAGING OF THE LOWER URINARY TRACT

Color Doppler allows the study of bladder and periurethral blood flow, has implications for the assessment of urethral function.

The trigone, bladder neck, and terminal part of the ureter are supplied by the inferior vesical artery. The fundus of the bladder is supplied by the superior vesical artery. Intramural blood flow is measured at the edge of the trigone where the ureters insert. Blood flow measurements within bladder wall are best visualized by transvaginal approach, and are reduced at residual urine volumes greater than 30 ml (most women empty their bladders to less than 10 ml),[14] thus making it important to ensure that the bladder is empty. Transvaginal sonography is used to assess bladder volume.[15] The determination of residual urine by sonography is noninvasive, easy and informative.

In the sagittal plane as the urethra enters the bladder, the bladder neck is seen at the junction of the urethra, and the urinary bladder. The sagittal plane of the pelvis is defined by the symphysis pubis, the urethra, and the urethrovesical junction. The symphysis pubis is a secondary cartilaginous joint with hyperechoic apperance. The urethra is identified as a hypoechoic area inferior to the symphysis pubis. After the bladder neck is seen, the probe must be rotated by 15° to visualize inferior vesical artery.

Blood flow in the lower urinary tract has been studied in normal women and women suffering urinary incontinence. Khullar et al[14] reported that at the menopause there appears to be a greater reduction in the velocity of flow through the inferior vesical artery. In their study based on thirty-eight women, they reported that the inferior vesical artery had a peak velocity of 12.4 cm/sec and a mean velocity of 5.4 cm/sec. There was a fall in the average peak and mean velocity of blood flow in the inferior vesical artery in women over the age 50 not taking hormone replacement therapy (3.1 and 1.8 cm/sec).

In their next study,[16] they reported about blood flow in the lower urinary tract in women suffering from genuine stress incontinence and detrusor instability. Women with genuine stress incontinence had lower peak (13.8 cm/sec), mean velocities (5.8 cm/sec), and pulsatility index (PI=1.43), than women with detrusor instability (peak velocity 16.7 cm/sec,mean velocity 7.1 cm/ sec, and PI 2.19). The reduced blood flow to the bladder neck in women with genuine stress incontinence is reduced further by increasing age. There was no significant change in intramural blood flow in normal asymptomatic women with genuine stress incontinence and detrusor instability, and no decrease was noted with age. Due to the reduction in the inferior vesical artery seen on the color Doppler, estrogen replacement therapy is used to treat genuine stress incontinence.

Fanti et al[17] applied meta-analysis to available data to evaluate the efficacy of estrogen therapy in the management of postmenopausal women with urinary incontinence. Meta-analysis found an overall significant effect of estrogen therapy on subjective improvement for all subject ($p<0.1$) and for subjects with genuine stress incontinence alone ($p<0.5$). The blood flow around the bladder neck in women can be measured by perineal color Doppler. Hormone replacement therapy increases the blood flow around the bladder neck in postmenopausal women with urinary stress incontinence. The clinical improvement of urinary stress incontinence can be seen with hormone replacement therapy after 3 months.[18]

The use of transvaginal color Doppler sonography to non-invasively evaluate the ureterovesical flow through the detection of the “ureteric jet effect” was first described by Dubbins et al in 1981.[19] The hyperechogenic stream created by the urine jet also produces a Doppler shift that can be detected by color Doppler examination.

Between 55% and 75%, operative ureteral injuries are sustained during gynecological rather than general surgery or urological procedures.[20] Gynecological ureteral iatrogenic trauma occurs most often during abdominal hysterectomy or excision of uterine adnexa.[21] If left unrecognized silent functional loss of affected kidney may ensure in the asymptomatic patient.

More recently Timor-Tritsch et al[22] evaluated the feasibility of the detection of ureteral jets into the bladder in obstetrics-gynecologic patients using transvaginal color Doppler. Fifty-two women were categorized in four groups; normal surgical, post-cesarean delivery, post-total abdominal hysterectomy and with only one functional kidney or ureter. Color Doppler was used to evaluate the time to detection of the first jet

and the number of jets in 5 minutes bilaterally. The results showed that urine jets could be detected bilaterally in all women except for those with one functional kidney. Time to detection of the first jet (98 sec) did not differ significantly in the non-surgical, cesarean or hysterectomy patients on either the left or right side. The total number of jets was similar in the non-surgical and cesarean patients but was lower in the hysterectomy group. This shows that TVCD is a simple accurate technique that can be used to evaluate ureteral jets into the bladder in women, and that it should be used when ureteral integrity is in question especially after surgery. The ureteral jets were visualized in the upper part of the bladder in an anteroposterior direction. Translabial color Doppler imaging of the lower urinary tract allows the documentation of fluid leakage from the bladder and it has the potential to become the new imaging standard for urogynecology.[23,24]

PATHOLOGY OF THE BLADDER AND THE URETHRA

Transvaginal sonography and color Doppler may detect malignancies of the bladder.

Granberg et al[25] reported on five bladder tumors in a prospective study of 400 women with postmenopausal bleeding. Gynecological symptoms sometimes can originate from the lower urinary tract and *vice versa*, and woman may sometimes mistake hematuria from vaginal bleeding. They recommend to examine the urinary bladder when doing endovaginal scanning of the pelvic organs to exclude tumors.

Vesical leiomyomata are rare, fewer than 200 cases have been reported in the literature. Approximately two-thirds of patients with these tumors are female.

Ortiz Ramiz et al[26] reported bladder leiomyoma to be found by transvaginal sonography.

Calculi may be visualized as echogenic structures freely movable.

Endometrioma can also be visualized, rising from the bladder wall.

CONCLUSION

The study of bladder and periurethral blood flow, as well as the ureterovesical flow has its diagnostic meaning, as well as evaluating the efficacy of treatment.

REFERENCES

1. Schaer GN, Koechli OR, Schuessler B, Haller U. Perineal ultrasound: determination of reliable examination procedures. Ultrasound Obstet Gynecol 1996; 7:347–52.
2. Khullar V, Abbot D, Cardozo LD, Kelleher CJ, Salvatore S, Bourne TH. Petrineal ultrasound measurement of the urethral sphincter in women with urinary incontinence: an aid to diagnosis? Br J Radiol 1994; 67:713–14.
3. Koebl H, Bernaschek G. A new method for sonographic uretrocystography and simultaneous pressure-flow measurements. Obstet Gynecol 1998; 74:417–22.
4. Richmond DH, Sutherst JR, Brown MC. Transrectal ultrasound scanning in urinary incontinence: the effect of the probe on urodynamic parameters. Br J Urology 1989; 43:582–85.
5. Quinn MJ, Beynon J, Mc Mortensen C, Smith PJB. Transvaginal endosonography: a new method to study the anatomy of the lower urinary tract in urinary stress incontinence. Br J Urol 1989; 62:414–18.

6. Kölbl H, Bernaschek G. Introitussonographie—eine neue Methode in der Blasenfunktionsonographie. Geburtsh.u.Frauenheilk. 1990; 50:295–98.
7. Abrams P, Blaivas JG, Stanton JT, Andersen JT. The standardisation of the terminology of lower urinary tract function. Br J Obstet Gynecol 1990; 6(Suppl): 1–16.
8. Gordon D, Groutz. Evaluation of female lower urinary tract symptoms: overview and update. Curr Opin Obstet Gynecol 2001; 13(5):521–27.
9. Leroy B, Jeny B. Contribution of vaginal echography in urinary incontinence. Arch Gynecol Obstet 1998; 244:530–37.
10. Wise BG, Burton G, Cutner, Cardozo LD. Effect of vaginal ultrasound probe on lower urinary tract function. Br J Urol 1992; 70:12–16.
11. Khullar V, Cardozo LD, Kelleher CJ, Abbot D, Bourne T. Transvaginal ultrasound measurements of bladder wall thickness in women. Ultrasound Obstet Gynecol 1993; (Suppl 2):107.
12. Khullar V, Salvatore S, Cardozo LD, Bourne T, Abbot D, Kelleher CJ. A novel technique for measuring bladder wall thickness in women using transvaginal ultrasound 1994; 4:220–24.
13. Martan A, Masata J, Halaska M, Otcenasek M, Svabik K. Ultrasound imaging of paravaginal defects in women with stress incontinence before and after paravaginal defect repair. Ultrasound Obstet Gynecol 2002; 19(5):496–500.
14. Khullar V, Cardozo LD, Kelleher CJ, Abbot D, Bourne T. Blood flow in lower urinary tract in normal women. Ultrasound Obststet Gynecol 1993; (Suppl 2):209.
15. Haylen B. Residual urine volumes in a normal female population: application of transvaginal ultrasound. Br J Urol 1989; 64:350–52.
16. Khullar V, Cardozo LD, Kelleher CJ, Abbot D, Bourne TH. Blood flow in the lower urinary tract in women with genuine stress incontinence and detrusor instability. Ultra Obstet Gynecol 1993; 3(Suppl 2): 105.
17. Fanti JA, Cardozo L, McClish DK. Estrogen therapy in the management of urinary incontinence in postmenopausal women: a meta-analysis. First report of the Hormones and Urogenithal Therapy Committee. Obstetrics & Gynecology 1994; 83:12–18.
18. Tsai E, Yang C, Chen H, Wu C, Lee J. Bladder neck circulation by Doppler ultrasonography in postmenopausal women with urinary stress incontinence. Obstet Gynecol 2001; 98(1):52–56.
19. Dubbins B, Kurtz AB, Darby J, Goldberg B. Ureteric jet effect: the echographic apperance of urine entering the bladder. Radiology 1998; 140:513–15.
20. Mann WJ, Arato M, Patsner B and Stone ML. Uretral injuries in an obstetrics and gynecology training program: etiology and management. Obstet Gynecol 1988; 72:82–85.
21. Grace PA, Murphy DM, Butler MR. Surgical injury to the urether: a report of 21 injuries in 19 patients. Int Med J 1983; 76:418–20.
22. Timor-Trisch IE, Haratz-Rubinstein N, Monteagudo A, Lerner JR Murphy KE. Transvaginal color Doppler sonography for ureteral jets, a method to detect ureteral patency. Obstetrics and Gynecology 1997; 89:113–17.
23. Dietz HP, McKnoutly L, Clarke B. Translabial color Doppler for imaging in urogynecology: a preliminary report. Ultrasound Obstet Gynecol 1999; 14(2): 144–47.
24. Dietz HP, Clarke B. Translabial color Doppler urodynamics. Int Urogynecol J Pelvic Floor Dysfunct 2001; 12(5):304–07.
25. Grandberg S, Wikland M, Norstrom A. Endovaginal ultrasound scanning to identify bladder tumors as the source of vaginal bleeding in postmenopausal women. Ultrasound Obstet Gynecol 1991; 1:63–66.
26. Ortiz Gamiz A, Poyato Galan JM, Sanchez E, Moyano Calvo JL, Arribas Gonzalez JM, Alvarez-Ossorio Fernandez JL, Molina Carranza A, Castineiras Fernandez J. Bladder leiomyoma: diagnosis by imaging. Arch Esp Urol 2002; 55(1):79–81.

Chapter 58
Ultrasound of the Breast

Boris Brkljacic, Ladislav Pavic

Ultrasound (US) has been been extensively used over the last twenty years for the diagnosis of breast changes. Recent rapid advances in US technology enable visualization of the breast and differentiation of its structures with high resolution and expand markedly the utilization of US for the diagnosis of breast diseases. Ultrasonic scanners are very numerous in developed, but also in developing countries. The examination is very convenient for the woman, there is no ionizing radiation exposure, no harmful effects on the breast, and the examination can be repeated whenever it is indicated. US enables also the realtime monitoring of the accurate placement of the needle within the breast lesion during the fineneedle aspiration and biopsy. Color and power Doppler are routinely used for the evaluation of the vascularization of the breast lesions. Also 3D US and contrast enhancers are being investigated extensively for evaluation of breast lesions.

In this chapter we will present the US equipment requirements for breast examination, the technique of the examination, normal sonographic anatomy of the breast, and US features of benign and malignant lesions of the breast. The utilization of color and power Doppler will be briefly presented, as well as US-guided aspirations/biopsies and US findings in postoperative breasts.

EQUIPMENT REQUIREMENTS FOR BREAST ULTRASOUND

Contemporary standards for breast ultrasound imaging require high-resolution real-time scanners, which most of the equipment producers meet.[1–4] Linear-array transducers with frequencies of 5 to 10 MHz are usually recommended, but our experience suggests minimum frequency of 7.5 MHz to be used. Higher frequencies can be used, when available (10 to 14 MHz). Higher frequencies generally improve resolution, but with increasing frequency soundbeam penetration decreases, which may present serious disadvantage in larger breasts. Transducer apertures should allow scanning width of 4.5 to 6.5 cm, and we find smaller width (3.5 cm and less) highfrequency probes suitable only for more detailed evaluation of superficially located lesions. Modern scanners have multifrequency or broadband frequencies transducers, and the selection of imaging frequencies for particular parts of the breasts and particular breast lesions should be tailored individually, according to the size of the breast and its structure.

Image quality in ultrasound is generally determined by resolution, image quality in the near field, and slice thickness. Resolution is defined as the smallest distance between two points that can be measured. Axial resolution (resolution along the direction of soundbeam), generally matches up two wavelengths of the ultrasound pulse, and the

minimum resolution is half of this value. Lateral resolution (resolution across the pulse width) is influenced by the size of transducer element or its aperture, by the frequency and the focus. Earlier transducers had fixed focus and are now obsolete. Most modern transducers have variable electronically controlled focus, allowing for the focusing of the soundbeam during both transmission (multiple transmit focusing) and reception (dynamic focusing). In this way sufficient lateral resolution can be maintained over a wide range of distances from the probe surface, but multiple transmit focusing can decrease the frame rate. If such multifocus capability is not desirable, the focus depth can be manipulated manually. Further focusing improvement can be achieved by electronically adjustment of the aperture, that is the area of the active piezoelectric array element.

Contrast resolution is determined by the sharpness of the lateral definition of the pulse and presents the system's ability to discern a weak echo next to a strong. Technically, contrast resolution depends both on the probe and the signal processing in the system. Tissue harmonic imaging, or just harmonic imaging, can further improve both spatial and contrast resolution. In harmonic imaging, harmonic echo frequencies are used to generate the image; while the original—fundamental tissue echo frequencies are suppressed by phase inversion between two consecutive transmit pulses. The potential benefit of this method in breast ultrasound examination is still under investigation.

The ultrasound signal can produce artifacts in the near field due to interference, hampering image quality in the near field. Modern systems can compensate for this effect by adjusting ultrasound beam profile electronically. In most older equipment the stand-off water or oil filled pads had to be used on top of the transducer to improve the near-field image quality of the breast. Air between the transducer and the pad had to be eliminated by gel or oil to allow soundbeam passage. And the repeated reflection of the soundbeam between the two can cause additional image artifacts—reverberation echoes or artifacts.

Slice thickness is a feature of technical design of the transducer, and a thin enough slice is a prerequisite to accurately discriminate between different closely located tissue areas of the breast. With thick slices echoes from a wide tissue slab are collected and presented averaged as a 2D image on the screen. In this way a cyst that should be presented as echo free will not be reliably presented due to the inclusion of adjacent solid tissue within the slab.

In order to assure the maximum operating quality of the system permanent equipment quality control should be maintained. This should include ongoing monitoring and evaluation, and also preventive maintenance. All actions in this respect should be documented.

EXAMINATION TECHNIQUE

The most important principle in breast ultrasound examination is to examine all of the breast tissue, so no area is missed.[1–4] According to this, examination technique can be slightly modified to meet the individual patient specifics and breast size. When examining outer quadrants, patient should be in contralateral posterior oblique position (elevated ipsilateral shoulder) with her arm extended over the head. This position flattens the breast tissue over the chest wall and decreases the thickness of the tissue section to be examined. For examination of medial quadrants, plane supine position is most useful. It

should be taken care that the breast parenchyma is followedthrough in every direction until it is substituted with peripheral fat tissue. After examining a breast, ipsilateral axilla should be scrutinized for possible enlarged lymph nodes.

There are two general examination techniques, the choice mostly depending on the individual preference of examiner.[2–5] Scanning can be performed in parallel parasagittal scanning planes, from top to the bottom, and with continuous transversal increments (from lateral to medial and back). Centripetal (radial) imaging in the radial and antiradial planes, centering at the nipple and stretching outwards, corresponds to the normal pattern of the ductal anatomy. The latter technique is specially advocated by the French authors. In our experience we find the radial technique more suited for examining large breasts and the parallel technique for smaller breasts. Whatever the technique, it is essentially important to visualize all breast areas, and especially the lesions, in at least two orthogonal planes. In order to avoid absorption and scattering artifacts, uniformly controlled tissue compression by the transducer and perpendicular insonation (characterized by strong reflectivity of the fascia pectoralis) is mandatory. Generally the first two focal zones are selected—ventral parenchyma border at a depth of 5–10 mm and the pectoralis muscle at a depth of 30–40 mm. Optimal imaging of the particular lesion, on the other hand, requires focusing of the soundbeam at the depth where the lesion is localized. This can be done by manually adjusting the focal zone or, sometimes with superficially located lesions, by a stand-off pad.

All lesions have to be dynamically examined regarding elasticity, mobility and delineation against the neighboring tissue, by applying various degrees of compression and varying the beam incidence and scanning planes. When scanning a palpable mass it can be helpful to pinpoint the lesion with a free hand under the probe to assure that the examined volume corresponds to the lesion.

There are two kinds of echoes that make up the sonographic image.[1–2] Specular echoes are strong echoes caused by reflection at interfaces with sufficient impedance difference between the neighboring tissues. These interfaces must also be sufficiently large, more than the soundbeam wavelength, and have a smooth surface. The angle of incidence equals the reflection angle, so the soundbeam striking a diagonal interface (Cooper’s ligaments) can be reflected away from the transducer causing acoustic shadowing. On the other hand, most echoes in glandular and fatty tissue, such as the breast, are scatter echoes. Scatter echoes occur at microscopic tissue interfaces with irregular surfaces. The size of these interfaces is similar or smaller than the soundbeam wavelength. In such circumstances, the soundwave is scattered in various directions, and the intensity of the echo that returns to the transducer is weak. During its travel through the tissue the soundbeam looses its energy, so in order to maintain the equalized brightness and intensity of the image at different depths, time-gain compensation is employed. Modern equipment automatically compensates for decreasing intensity of the beam at greater distances from the transducer. Usually the time-gain control requires only moderate individual adjustments, due to the variability in absorption patterns between different patients—lower absorption in fatty breasts and higher in dense breasts and some cases of mastopathy. The optimum main gain settings should be adjusted according to the echogenicity of the fatty tissue. It should not appear too dark in the image in order to allow distinguishing between hypoechoic lesions such as carcinoma and cysts.

All lesions and irregularities have to be documented, preferably in two orthogonal planes.[1–4] The diagnostic criteria, such as elasticity, fixation, and disruption of architecture, have to be established during the real-time examination, as they can't be analyzed retrospectively from the static images. These criteria always refer to the three-dimensional image impression of the entire examined tissue volume. Any changes in contour or absorption characteristics of a lesion, as caused by compression or decompression, should also be documented. All particular tissue characteristics, such as "echogenic border sign" for example, which may be obvious only during dynamic examination should be marked additionally, as well.

NORMAL BREAST ANATOMY AND SONOGRAPHIC ANATOMY

The mature female breast is composed of four structures: breast parenchyma (lobules); milk ducts; fat and connective tissue. On average there are 15–20 lobes in each breast, arranged centripetally around the nipple. The distribution of the lobes is not even. There is a preponderance of the glandular tissue in the upper outer portion of the breast, which is the site where approximately half of all breast cancers originate from. Each lobe organizes around a lactiferous duct, and lactiferous ducts converge into 6–10 larger collecting ducts that open in the nipple. Lactiferous ducts divide further into peripheral ducts, which divide into terminal ducts. Terminal ducts are first extralobular and then intralobular, as they branch and endup in ductules or acini. Each lobe comprises approximately 30 terminal branches (acini or ductules). Acini and terminal ducts present breast parenchyma, and are surrounded by loose mesenchyma. The lobule with its terminal branches, its short intralobular and longer extralobular duct form the "terminal duct-lobular unit" (TDLU). The breast fibrous tissue or mesenchyma comprises of interlobular and intralobular stroma. The intralobular stroma interconnects lobules within a single TDLU, while the interlobular stroma interconnects larger parenchymal divisions.

The breast parenchyma is imbedded in fatty tissue and supported by connective tissue, mainly Cooper ligaments. Cooper ligaments arise from the stromal tissue of the gland and insert into the prepectoral fascia and the skin.

Breast blood supply is very diverse. Upper lateral parts of the breast receive most of the blood supply from lateral thoracic artery, a branch of axillary artery. Further lateral portions of the breast are mostly supplied from intercostal arteries and also subscapular artery and dorsal thoracic artery. Central and medial portions receive blood supply by the perforating branches of internal mammary artery, where the prevalence of the blood supply of the breast comes from. In general the venous drainage of the breast is analogous to the arterial supply. The lymph vessels of the breast accompany the blood supply. Most of the lymph is drained along the lateral thoracic and thoracodorsal vessels into the axillary lymph nodes, which present the main drainage site. Lower inner quadrants mainly drain into internal mammary lymph node chain. Only smaller proportion of the breast lymph is drained into lymph vessels of the contralateral breast, internal mammary nodes and axilla.

Breasts begin developing in the embryo about 7 to 8 weeks after conception. They develop from an ectodermal invagination into chest wall mesenchyme along the primitive milk streak or "galactic band" which runs from the axilla to groin on the embryonic

trunk. Incomplete regression or dispersion of the galactic band leads to accessory mammary tissues found in 2–6% of adult women. Breast cancer can develop anywhere within the ductal epithelium, including the accessory mammary tissue, which should be carefully examined on ultrasonography. Most frequently seen are supernumerary nipples (polythelia) anywhere along the primitive milk line, though true accessory mammary glands are most frequently located in the axilla (polymastia). From weeks 12 to 16, the various subcomponents become more defined. Small groupings of cells begin to branch out laying the foundation for future ducts and milk producing glands. Other tissues develop into muscle cells which will form the nipple and areola. In the later stages of pregnancy, the mother's hormones, which cross the placenta into the fetus, cause breast cells to organize into branching tube-like structures thus forming the milk ducts. In the final 8 weeks lobules mature and actually begin to secrete colostrum. From infancy to just before puberty, there is no difference between the female and male breasts.

With the beginning of female puberty, the release of estrogen, at first alone, and then in combination with progesterone when the ovaries functionally mature, cause the breasts to undergo dramatic changes which culminate in the fully mature form. This process on average takes 3 to 4 years and is usually complete by age 16. Further maturation of the breast tissues occurs with lactation.

The adolescent female breast consists of lactiferous ducts with adventitial alveoli comprised mainly of connective tissue and small amounts of fatty tissue. During puberty, the ducts increase in length, and the terminal alveoli increase in number. Ductal growth activates mesenchymal metaplasia and formation of connective tissue.

The immature glandular tissue is initially hypoechoic, and cannot be always distinguished from the surrounding hypoechoic fatty tissue.[1–4] With the maturity the echogenicity of the glandular tissue increases, which doesn't always proceed uniformly over the whole tissue volume, producing alternating hypoechoic and hyperechoic areas.

In mature breast, under the influence of estrogen, progesterone, prolactine, STH, ACTH and corticoids, the ductal system becomes increasingly branched and glandular lobules develop. The growth and differentiation continue until about age 30. The majority of lobules are located peripherally from the nipple. In ultrasound the glandular tissue appears generally hyperechoic, although this might vary considerably.[14] Surrounding fatty tissue and interspersed fat lobules appear hypoechoic. Cooper ligaments appear as fine linear hyperechoic structures traversing the fatty tissue (Fig. 58.1). Due to their orientation, often parallel to the direction of the soundbeam penetration, they can sometimes reflect the soundbeam away from the probe producing acoustic shadows. The shadows can be eliminated by compression and changing the position of the transducer. The skin appears hyperechoic single or, with better-resolution probes, double-countour line, whose thickness does not exceed 3 mm. Since the retroareolar ducts run almost parallel to the direction of the soundbeam penetration, sound echoes are commonly reflected away from the probe so the acoustic shadow behind the nipple is produced. It can be augmented by the periductal fibrosis absorbing the soundbeam energy. The nipple shadow often impairs the visualization of the retroareolar region. The role of ultrasound is particularly important in glandular, mammographically "dense" breasts. In these breasts small cystic and solid lesions can be hidden on mammography by the surrounding dense parenchyma. However, on ultrasound these lesions can be visualized due to the different echogenicity between the lesions and surrounding parenchyma.

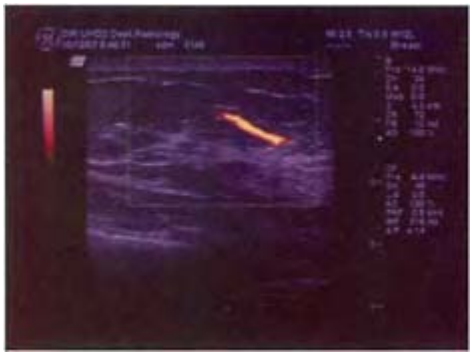

Figure 58.1: Normal breast with the power Doppler image of flow in the normal vessel. One can clearly visualize echogenic layer of skin, hypoechogenic fat tissue interspersed with tiny echogenic bands of Cooper ligaments, as well as posteriorly localized echogenic glandular parenchyma. Posterior to parenchyma one can visualize hypoechogenic retroglandular fat layer, and the pectoral muscle

With involution the breast parenchyma becomes atrophic and fatty and fibrous tissue become predominating. The involution starts in the medial portion of the breast and involves the retroareolar and lateral portions later. The fatty involuted breast appears hypoechoic, with only scarce moderately echogenic patches of parenchymal tissue.1–4 The connective tissue remains hyperechoic. With fatty involution the sensitivity of mammography increases and the role of ultrasound diminishes, as cancers and other lesions can be easily seen on mammography.

During pregnancy lobular hyperplasia, hyperemia and fluid retention in breast tissue occur. Milk production glandular cells begins in the second half of the pregnancy, and toward the end of the pregnancy the alveoli start to secrete and the parenchyma mostly displaces the stroma. Sonographically the echogenicity of the tissue decreases following

the increased water content.1– 4,6 The echo pattern appears generally homogenous and finely granular. In late pregnancy the distended lactiferous ducts can be recognized as tubular hypoechoic/anechoic structures.

Hormone replacement therapy (HRT) causes proliferation of the breast parenchyma. Estrogen instigates ductal proliferation and progesterone alveolar proliferation and it also increases water content in glandular cells. The HRT effects are therefore, more pronounced with estrogen-progesterone combinations than for estrogen alone. On mammography HRT causes breasts to appear more dense than normal.1,2,7,8 As the sensitivity of mammography decreases in dense breasts, sonography becomes an important adjunct in diagnosing focal findings detected on mammography, especially those that have developed or increased in size recently.1,2,7–9 The glandular tissue under HRT stimulation generally appears homogenous and hyperechoic, but variations such as those in breast dysplasia are possible. The knowledge of patterns of changes of breasts due to the hormonal impact is very important, because of the increasing proportion of menopausal women on HRT.

BREAST LESIONS AND ULTRASONOGRAPHY

The single most important breast lesion is breast cancer, and its early detection is of crucial importance.[9–11] In general, other breast lesions are important as far as they bare psychological strain on a woman, and as they should be differentiated from the breast cancer.

With regard to the location of origin, the breast lesions (benign and malignant) can be categorized as follows:[1,2,12,13]

Lesions in the main lactiferous ducts:

- ductectasia
- cystic dilatation of a main duct (large ductal cyst)
- main duct papilloma
- intraductal carcinoma

Lesions in the small and terminal ducts:

- hyperplasia
- peripheral duct papilloma
- ductal carcinoma

Lobular lesions:

- common cyst
- fibroadenoma
- adenosis
- tumor phyllodes
- lobular carcinoma

Stromal lesions:

• sarcoma

Unclassified lesions:

• radial scarring.

Sonographic Analysis of Focal Breast Lesions

The criteria for breast focal lesion sonographic evaluation should describe the lesion as accurately as possible, and precisely differentiate between a benign and malignant lesion.[2,4,5,9,13]

In evaluation of breast focal lesion following aspects should be scrutinized:

Margins

Demarcation of a lesion against the surrounding tissue has to be carefully assessed. Analysis of the margins has to define the margins proper and the contour of the lesion. In this respect, the margins can be sharp or indistinct, and contours are either smooth or uneven. All combinations are possible and bare diagnostic information. Sharp and smooth margins are generally inconsistent with malignancy, while indistinct and uneven margins signify malignancy with a necessary degree of confidence. The in-between combinations may be associated with both benign and malignant lesions. It should be always bared in mind, especially with small lesions, that sonographic appearance of margins depends not only on the lesion, but also on the resolution of the equipment used.

Echogenicity

Lesion is assessed in relation to the echogenicity of the adjacent tissue, and in reference to known structures such as fat and glandular tissue. *Anechoic* are lesions less echoic than fat, that contain no internal echoes, and this is a feature of cysts and malignant lesions. *Fat-equivalent* lesions have same echogenicity as fat; *hypoechoic*

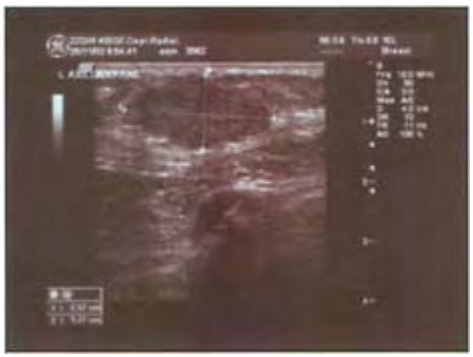

Figure 58.2: Solid, homogeneously hypoechogenic lesion

with very regular margins, localized in the axillary tail of the breast; size is 2.5×1.3 cm. Typical US features of fibroadenoma

lesions are less echogenic than glandular tissue; *isoechoic* approximate echogenicity of glandular tissue; and *hyperechoic* are more echogenic *(brighter)* than glandular tissue (Fig. 58.2) Hyperechoic lesions are usually benign. It should be always remembered that exceptions to these characteristics are not rare, so all have to be further diagnosed.

Internal Echo Pattern

It refers to the arrangement of echoes within the lesion. A nonhomogeneous echo pattern, consisting of scattered or more numerous internal echoes, is suspicious of malignancy. A homogeneous internal pattern, or absence of the internal echoes, is more consistent with benign lesions.

Posterior Acoustic Phenomena

Lesions can cause posterior shadowing, posterior enhancement, or no change in the posterior echogenicity. Posterior enhancement suggests a benign lesion. Posterior shadowing of different intensity, either central or unilateral, suggests malignancy (Figs 58.3A and B). Shadow width is not a diagnostic feature, and a true shadow must be present on two different scan planes. Nochange in posterior echogenicity bares no diagnostic information, as this pattern is seen in

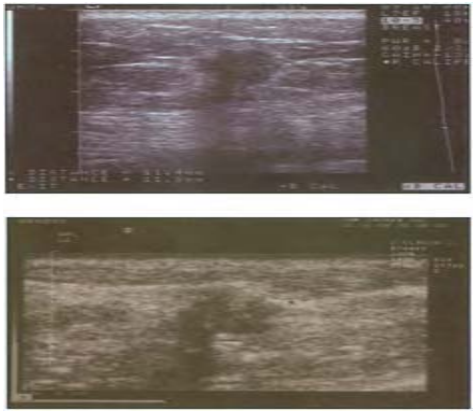

Figures 58.3A and B: Irregular solid lesions. (A) Small vertically oriented lesion, 12×11 mm in size,

with partial posterior acoustic shadowing and irregular margins. Invasive ductal carcinoma. (B) Predominantly hypoehogenic, heterogeneous small lesion (7×7 mm), with spiculated, irregular margins, and posterior acoustic shadowing. Invasive ductal carcinoma

both benign and malignant lesions. Areas of acoustic shadowing or enhancement that don't originate from local lesions, commonly appear in dense fibrous breasts, and yield no information regarding malignancy.

Effect of Compression on Shape and Internal Echo Pattern

Lesions that change in shape or internal echo pattern (become more homogenous) when compressed are almost certainly benign. The absence of shape or internal echo change under compression is, on the other hand, not a reliable sign of malignancy. Approximately 50% of benign breast lesions, do not change shape or echo pattern under compression.

Laterolateral to Anteroposterior Diameter Ratio (LL/AP-ratio, Width-to-height ratio)

Lesions with greater laterolateral than anteroposterior diameter (LL/AP-ratio>1) are more likely to be benign, and those with a greater anteroposterior diameter, or "taller-than-wide lesions" (LL/AP-ratio<1) are more likely to be malignant.

All these criteria have to be appreciated with due reserve, but their careful scrutiny can significantly help diagnosis, and guide future steps.

Benign Breast Lesions

Benign breast disorders present hormonally (estrogen, progesterone, prolactine, thyroxin, insulin) mediated, qualitative and quantitative tissue neoplasia before and during menopause.[1,2,12,14] The hormonal imbalance instigates two basic mechanisms. One is hormonally induced secretion coupled with retention of the secret and consecutive development of ectatic ducts and cysts. And the other is proliferation of ductal and lobular epithelium causing development of different patterns and degrees of epithelial hyperplasia—in the form of adenosis, epithelosis or atypical hyperplasia.

Hence, there are two basic groups of lesions—proliferative or hyperplastic changes and nonproliferative fibrocystic changes. The former are characterized by epithelial

(ductal or lobular) hyperplasia, and are significant for their malignant potential. Non-proliferative changes have no malignant potential, and their distinction from normal age-related breast changes is very vague, as is distinction between the individual types of this disorders.

Specifically, more common benign breast lesions are:

- macro and micro cysts
- sclerosing adenosis
- fibroadenoma
- mammary duct ectasia
- intraductal papilloma or papillomatosis
- epithelial hyperplasia involving the lobules
- epithelial hyperplasia involving the larger ducts.

Less common benign breast conditions are:

- lactational mastitis
- true lipomas
- fat necrosis
- foreign body granulomas secondary to paraffin or silicone
- sclerosing phlebitis (Mondor's Disease).

Cysts

Cysts tend to occur commonly and frequently around the fourth decade of life and in the perimenopausal period, and they often fluctuate with the menstrual cycle.[2,9,12,14,15] The breasts can form microcysts measuring 1–2 mm in diameter and macrocysts (simple or multiloculated), as well as multiple and solitary cysts. Cysts are thought to arise from dilatation or obstruction of collecting ducts. Cysts are round or oval, usually well demarcated from the surrounding tissue, smooth, firm, and mobile (Figs 58.4 to 58.6). If a cyst enlarges rapidly it can be tender. A cyst can present as a hard mass when the fluid is under tension and feel similar to a carcinoma on breast

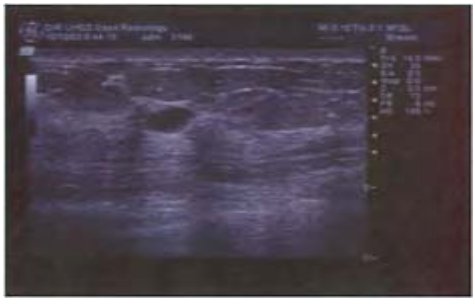

Figure 58.4: Breast cyst. Anechogenic lesion within the breast

parenchyma. Regular, smooth borders of the lesion, with pronounced posterior acoustic enhancement. Typical US image of the cyst

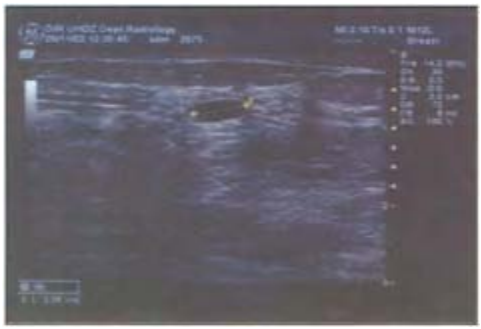

Figure 58.5: Breast cyst. A small cyst (length 6 mm) in the breast parenchyma with regular borders and posterior acoustic enhancement

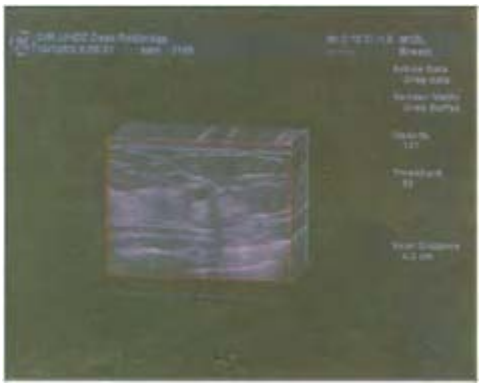

Figure 58.6: 3D image of the breast cyst

examination (palpation). It is not possible from the breast examination to distinguish a solid from a cystic mass. In postmenopausal women, who are not receiving hormone

replacement therapy, the finding of cystic lesions is uncommon, and if such lesions are detected further evaluation is necessary.

Cysts and fibrosis in breast are very common, and up to 50% of women in the age range between 30 and 40 have solitary or multiple breast cysts.[2,4,9,15] Macrocysts normally occur in 20–25% of women. For these reasons it is very difficult to make distinction between normal age-related

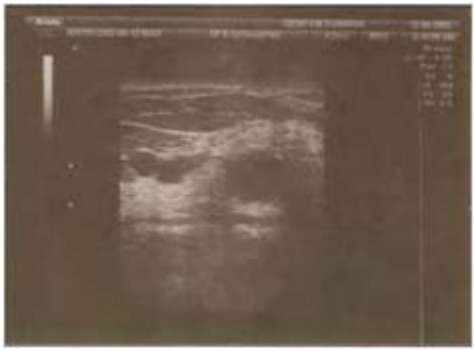

Figure 58.7: Multiple cysts of the breast within the echogenic breast parenchyma. Fibrocystic breast changes

breast changes and so called fibrocystic breast disease or dysplasia (Fig. 58.7). These descriptions should be discarded, and more specific histopathologic descriptions used.

Special kind of cysts is galactoceles and oil cysts. Galactoceles present focal or multiple retention cysts filled with breast milk, and they normally develop during pregnancy. Oil cysts are filled with oily, necrotic substance, and are usually related to some kind of trauma or breast surgery. They usually have typical appearance on mammography and sonography because of their peripheral *eggshell* calcifications (Figs 58.8 and 58.9).

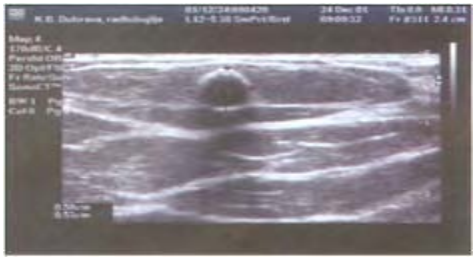

Figure 58.8: Oil-cyst. Partially calcified edge of

the cystic structure within the subcutaneous fat tissue. The diameter of the lesion is 6 mm

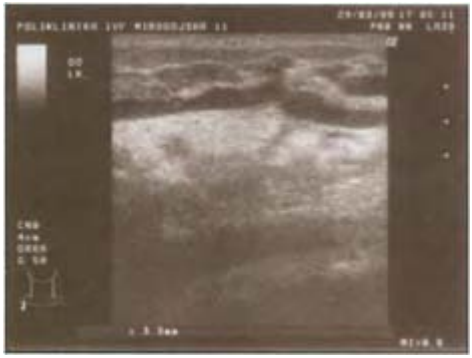

Figure 58.9: Dilated lactiferous ducts. Tubular anechogenic structures representing dilated ducts

Ultrasonographically simple cysts appear as round, oval or tabulated anechoic lesions with smooth walls and regular contours.[4,9,15–18] Because of their capsule-like borders they usually cast bilateral refraction shadows, and due to the highwater-proportion homogenous filling cause posterior acoustic enhancement. On high-resolution equipment even cysts as small as 2 mm in diameter can be reliably detected. The most important differentiating factors between cysts and solid lesions are anechoic center and capsule-like borders in cysts. As malignant solid lesions commonly present hypoechoic or anechoic central signal, optimal gain settings and state-of-art equipment must be used to reliably differentiate between such lesions and cysts.[4,9,13,15,16,18,19] Compressibility on dynamic examination is also a reliable sign of a benign lesion. Septations present common finding in cysts, and can usually be distinguished from intercystic vegetations (suspicious of malignancy) by dynamic scanning. In any doubtful finding further diagnostic measures (FNAC, FNAB, excision biopsy, etc.) are mandatory. If all sonographic criteria for simple cyst are present, no further evaluation is necessary, and diagnosis of simple cyst is very reliable.

Adenosis, *focal fibrosis* and *epithelial hyperplasia* are primarily histopathologic diagnoses.[2,9,12,14,15] Their ultrasonographic presentation is inconsistent, and can vary from local to generalized solid or cystic lesions, or vegetations within cystic lesions.[4,9,15,16,18] They vary in size and shape, and also margins and contours, which can diverge from very discrete and smooth to indistinct and uneven. Nevertheless, they usually have no respective malignant characteristics. They frequently present as homogenously hyperechoic areas of glandular tissue. Also, common findings are particularly regular hyperechoic structures, generally tubular in shape and following ductal system, extending

throughout the gland. Hypoechoic, isolated or multiple foci, which can be irregular or well circumscribed also appear, and are substantially suspicious of malignancy.

Adenosis presents nonneoplastic proliferation of terminal ductal segments, accompanied with a varying degree of stromal reaction.[12,14,15] There are several forms of adenosis, sclerosing adenosis being the most common. It refers to focal or generalized, nodular proliferation of the lobular epithelium and myoepithelium accompanied by desmoplasia. It is commonly associated with other kinds of breast lesions; such as fibroadenomas, ductal adenomas, papillomas, or atypical lobular hyperplasia and lobular carcinoma *in situ*, on the other hand. The relative risk of malignancy is increased by factor 1.5 2. Blunt duct adenosis present cystic expansion of secret containing ductules, lined with a flattened or slightly hyperplastic epithelium. Microglandular adenosis is a rare form, characterized by densely packed, isomorphic, small-diameter tubules growing into the surrounding fatty and connective tissue. Radial scar refers to focal tubular proliferation developing around a fibrous elastoid center that radiate outward. Due to its speculated form it resembles invasive carcinomatous growth, and is mammographically indistinct from carcinoma.[16,19,20] Areas of atypical hyperplasia, tubular, ductal, or lobular carcinoma can indeed develop within the radial scar.

Focal fibrosis refers to stromal proliferation associated with focal parenchymal atrophy. The foci are usually not larger than 1 3 mm in diameter.[12,14,15] Focal fibrosis occurs in younger women, age from 25 to 40. In sonography (similarly to diffuse fibrosis) it can produce hypoechoic focal lesions with acoustic shadowing, substantially suspicious of malignancy.[4,9,16,18] Other sonographic presentations, similar to those described with adenosis, are also possible.

Epithelial hyperplasia comprises three discrete forms[12,14,15] Ductal hyperplasia refers to intraductal epithelium proliferation of various presentations both regarding extent (diffuse or focal) and pattern. Lobular hyperplasia is characterized by simultaneous acinar and epithelial hyperplasia, causing enlargement of affected lobule. Atypical hyperplasia is further divided into ductal and lobular type. It is characterized by cellular atypia with disturbance of regular epithelial layering, with myoepithelial layer and basal membrane remaining intact. Hence, these lesions show some characteristics of carcinoma in situ lesions, and they increase the relative risk of malignancy by a factor of 4–5. Atypical ductal hyperplasia is primarily observed in postmenopausal women and corresponds, to same extent, with ductal carcinoma *in situ*. Atypical lobular hyperplasia, on the other hand, corresponds with lobular carcinoma in situ, but the lobule size is not enlarged.

Fibroadenoma

Fibroadenomas are the most common benign breast tumors, and among common breast lesions in general.[2,9,12,14,15] They occur in all age groups, with highest incidence between ages of 25 to 35. After age of 40 their incidence decreases, simultaneously as that of the malignant breast lesions increases. For this reason, all solid lesions in women over 40 years of age, regardless of sonographic appearance, should be suspected for malignancy. It is not uncommon for a breast carcinoma to present as a well-circumscribed, smoothly marginated, horizontally oriented lesion. Furthermore, in some 0.1 0.3% of fibroadenomas carcinomatous lesions can be found within.

Fibroadenomas are hormone-induced hyperplastic tumors of the lobular connective tissue.[2,12,14,15] Histologically they are fibroepithelial mixed lesions, surrounded by a

pseudocapsule. There are three general types of fibroadenoma. Adult fibroadenomas are usually found in young women under hormonal stimulation, and are characterized by edematous stroma, corresponding radiographically to “young” fibroadenomas. In older patients, during or after menopause, the stroma is focally or totally sclerotic, and these lesions radiographically correspond to “older” fibroadenomas. Juvenile fibroadenoma is another type of the lesion, and generally occurs under the age of 20. For commonly large size, it is sometimes called the giant fibroadenoma. It has a strong growth tendency and must be histologically differentiated from a phyllodes tumor. Despite the florid growth it has a good prognosis. The third and the less common type are adenomas, which are characterized by a dominant ductolobular component. In mammography and ultrasound adenomas are indistinguishable from fibroadenomas proper.[4,16,18]

Fibroadenomas are usually solitary lesions, measuring about 1–2 cm and seldom more than 4 cm in diameter. Multiple lesions are observed in less than 10% of patients. In close to 2/3 of patients fibroadenomas present with typical “benign” sonographic characteristics such as: round, oval, rarely lobulated contour; sharp borders with strong capsule echoes; homogenous hypoechoic internal pattern; bilateral refractive shadowing; posterior enhancement; horizontal orientation (LL/AP-ratio>1.5); and compressibility greater than 20% (Figs 58.10 to 58.12).[1,4,15,16,18] Sonographic characterization of fibroadenomas is straightforward in dense young breasts, but in older fatty-involuted breasts they may be more difficult to delineate from the surrounding tissue. Further on, in older patients with increasing fibrosis within the fibroadenoma, contour irregularities, heterogenous internal echoes, retrograde acoustic shadowing due to the

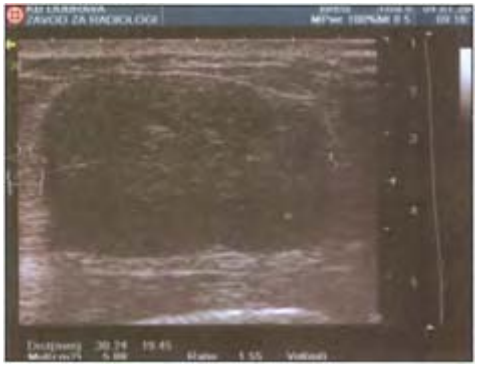

Figure 58.10: Large fibroadenoma of the breast. Hypoechogenic, solid lesion, with regular borders, 3× 2 cm in size, with no posterior acoustic phenomena

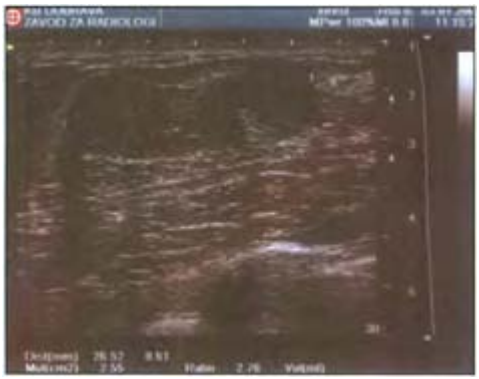

Figure 58.11:
Fibroadenoma. Large, spindle shaped fibroadenoma, 2.7×1 cm in size. The internal echostructure is slightly heterogeneous, borders are regular, there are no posterior acoustic phenomena

calcifications, and impaired compressibility may develop. Such lesions are difficult to differentiate from malignancies.

As findings resembling those of fibroadenoma do not exclude malignancies, following procedure in fibroadenoma evaluation is recommendable.[2,4,9,10,12,13] For sonographically typical fibroadenomas follow-up examinations at 6-month intervals are recommended, if there is no mammographic contraindication and if the patient is under age of 35. All newly discovered lesions; lesions in patients over age of 35; and all lesions

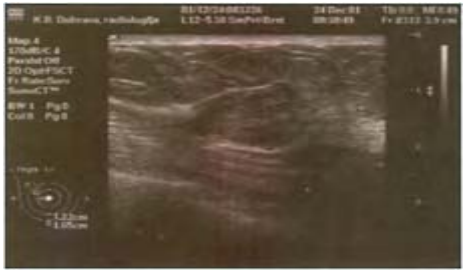

Figure 58.12:
Fibroadenoma. Markedly

irregular echostructure of the predominantly hyperechogenic mass. Very regular borders of the lesion. No posterior acoustic phenomena. FNAB finding: fibroadenoma

with findings deviating from typical presentation, should be further evaluated (FNAC, FNAB, excision biopsy, etc.).

Papilloma

Papillomas are rare, benign fibroepithelial breast tumors, which present some 1–1.5% of the breast tumors.[2,12,14,15] They are located intraductally and can cause watery or bloody discharge, duct distension, or cyst formation, where they are surrounded by a watery or bloody secretion. There are several types of papilloma (intraductal, small peripheral, papillary adenoma, juvenile papillomatosis) and some are associated with an increased risk of malignancy. They can be single or multiple spatially separate tumors, in contrast with papillomatosis that manifests as regional epithelial hyperplasia and is associated with even greater risk of malignancy.

Usually the first sign of papilloma is a discharge from the nipple, which occurs in some 80% of papillomas, and can be watery, yellowish, brownish, or bloody. Only seldom can papillomas be detected in sonography, and their presentation can vary significantly.[4,15,16,18] They can present as hypoechoic intracystic vegetations, which do not move with change of position, or they can present as solid, smooth, well-defined nodules. Rarely they may not present completely well circumscribed, or might have shadowing due to microcalcification. Reliable differentiation between papilloma and carcinoma is usually not possible on sonography, and yields further diagnostic evaluation (galactography, FNAC, FNAB, excision biopsy, etc.).

Hamartoma

Hamartomas present abnormal collection of tissues normally found in breast, such as parenchymal tissue, smooth muscle and fatty tissue.[2,12,14,15] They are surrounded by a pseudocapsule, and are not considered a premalignant lesion. Most hamartomas have characteristic mammographic presentation and are thus diagnosed.[1,17] Sonography is rarely needed, only when mammographic differentiation is obscured with neighboring dense tissue.[1,4,15,16,18] In sonography hamartomas appear as smoothly marginated, well-defined, horizontally oriented lesions. Pseudocapsule can readily be found as a hyperechoic marginal line. Hypoechoic fat islands, separated by hyperechoic septa, can be identified within the nodule. Further diagnostic evaluation is rarely necessary, and the exact histological diagnosis can be made only by excision biopsy.

Other Benign Breast Tumors

Other benign breast tumors are in general very rare; some of the more common are lipoma, leiomyoma, neurofibroma, chondroma, osteoma, angioma, epithelial and dermoid cysts, etc.[2,12,14,15] (Fig. 58.13). These tumors mostly present as smoothly outlined, oval and round structures, and it is difficult to distinguish them from fibroadenomas on the basis of imaging alone.[1,4,15,16,18] The specific diagnosis is therefore possible only histologically.

Inflammatory Lesions

In most developed countries the incidence of bacterial puerperal mastitis has significantly decreased over the last few decades, and that of subacute and chronic

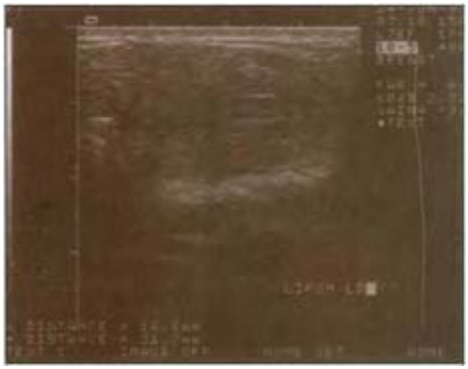

Figure 58.13: Lipoma of the breast. Large, superficial, homogeneous, markedly hypoechogenic lesion, with very regular borders and with the same echogenicity like fat. Typical appearance of lipoma

mastitis increased.[1,2,12,14,15] Chronic and subacute mastitis usually develop after inadequate therapy of the acute forms, and generally present with formation of abscesses and sometimes fistulas.

Sonographically mastitis presents with skin thickening; changes in echogenicity of the parenchyma and subcutaneous tissue; dilated ducts with hypoechoic content; acoustic shadowing with reactive fibrosis, etc.[1,2,16] Abscesses, on the other hand, usually present as irregularly circumscribed, hypoechoic or anechoic, lesions (purulent center) surrounded by a hyperechoic rim (demarcation zone and edema) (Figs 58.14A and B). Thus, they can cause difficulties in differentiating from malignant processes, so further

diagnostic evaluation (FNAC, FNAB) is sometimes necessary. Abscesses can be drained under sonographic guidance in real time.

Malignant Lesions of the Breast

Breast carcinoma is the most common malignant tumor in women in developed countries (Europe, America, Asia, Australia), and the leading cause of death in women aged 35 to 54 years.[7,9–11] The treatment and survival depend upon the stadium of the disease upon detection, therefore, the early diagnosis of cancer is of utmost importance.

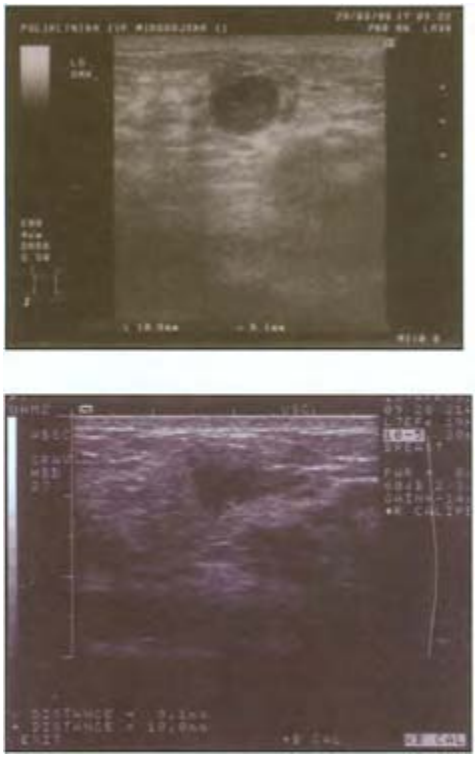

Figures 58.14A and B: Breast abscess. (A) Spherical lesion 11×9 mm in size with mixed internal echogenicity (anechoic and echoic content) and marked posterior acoustic enhancement. Clinically all signs of inflammation

were present. Breast abscess in the 25th week of gestation. (B) The same lesion two weeks after fine-needle aspiration of the pus: residual predominantly anechoic lesion. Pus aspiration was repeated

Carcinoma In situ

Carcinomas *in situ* are neoplasms, histologically corresponding to invasive carcinomas, but without penetration of the basement epithelial membrane.[1,2,12,14] They are not a required precursor of invasive processes, but rather mark an increased risk of development of a malignant disease. There are two types of carcinoma *in situ* lesions in breast—ductal carcinoma *in situ*, and lobular carcinoma in situ.

Ductal carcinoma *in situ* (DCIS) develops from lactiferous ductal epithelium, and in close to 1/ 3 of the cases is multifocal. It's incidence in screening population reaches 20–30%, and in patients with a palpable breast lesion 3–5%. Histologically there are five types, differing in cytological differentiation and malignant potential. Comedo DCIS is the less differentiated type and progresses into invasive carcinoma in close to 50% of cases. Better differentiated types alternate into invasive cancer in 20–30%.

Lobular carcinoma *in situ* (LCIS) arises in ductolobular units of breast parenchyma, but frequently involves extralobular ducts as well. In almost half of cases they are multicentric, and in 1/3 they are bilateral. They have much smaller malignant potential than DCIS, and are not considered a true carcinoma but rather a severe epithelial atypia.

Sonography does not substantially help in the detection, exclusion or differential diagnosis of carcinoma *in situ* lesions.[1,2,4,9,12] Most lesions cannot be sonographically distinguished from the normal breast parenchyma. Only rarely in case of DCIS, relatively strong echoes can be found, representing microcalcifications, or dilated hypoechoic ductal structures (Fig. 58.15). LCIS lesions are sonographically generally not recognizable.

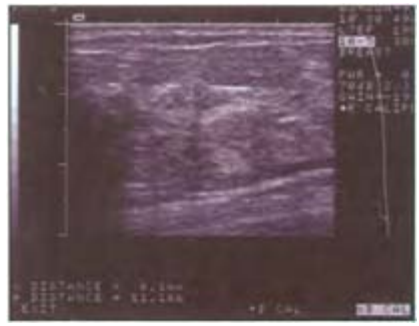

Figure 58.15: *In situ* ductal carcinoma. Echogenic, horizontally positioned lesion, 11×6 mm, with no distal acoustic phenomena. Internal echogenic foci correspond to microcalcifications on mammography

Invasive Carcinoma

Invasive carcinoma is the most frequent malignancy in women, and one of the leading causes of women death in the Western world.[1,2,12,14] Its lifetime prevalence is estimated to around 10%, differing on country, ethnicity, race, etc., and is still growing.

The goals of every diagnostic strategy for invasive breast carcinoma are: early detection in preferably asymptomatic patients, because the prognosis considerably worsens after the tumor exceeds 15 mm in diameter; evaluation, in clinically symptomatic patients and in patients with abnormal screening results, to help direct further procedure; and pre-interventional staging of the disease.[1,2,4,9,13,17,18] Early detection is nevertheless, the crucial factor of successful management of invasive breast carcinoma.

There are different types of invasive carcinoma—differing histologically and in prognosis.[1,2,12,14] Not otherwise specified (NOS) ductal carcinoma is the most frequent and makes 60–80% of invasive breast neoplasm. It is followed by invasive lobular carcinoma making 15% of invasive breast neoplasm, and other infrequent types of ductal carcinoma, such as medullary carcinoma (3–4%), mucinous (3%), tubular (2–3%) and papillary carcinoma (2%).

Ductal carcinomas develop from terminal ductolobular epithelium, and present in a variety of forms morphologically and histologically (Fig. 58.16). Lobular carcinoma arises from lobular epithelium and frequently exhibits diffuse growth. Contrary to ductal carcinoma, lobular carcinoma don't produce microcalcifications, which significantly hampers their early mammographic recognition (Fig. 58.17). This feature together with a

tendency to diffuse growth is responsible for their worse prognosis compared with invasive ductal carcinoma.

It is generally assumed that invasive breast carcinomas have characteristic sonographic features that allow relatively straightforward differentiation from benign lesions. However, this

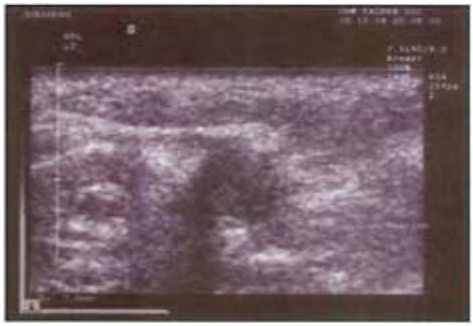

Figure 58.16: Small invasive ductal carcinoma. Lesion 8×7 mm in size, zoomed image. The lesion is solid, hypoechoic, with slightly irregular borders and slightly heterogeneous internal structure. Only partial acoustic shadowing is seen

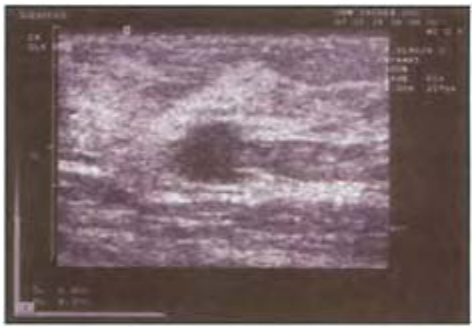

Figure 58.17: Small invasive lobular carcinoma. Size of the

lesion is 8×8 mm. The lesion is markedly hypoechogenic. There are no posterior acoustic phenomena, but the borders are markedly irregular

is often not true. Up to 25% of malignant lesions can present as well circumscribed nodular lesions mimicking fibroadenomas. Sensitivity of sonography is even more limited in detecting small, nonpalpable lesions as they may not present with typical malignant features. More than often small lesions are untypical isoechoic with normal glandular tissue, and when hypoechoic small carcinomas can be concealed with the surrounding fat tissue. For these reasons neither absence of *malignant* findings, nor the presence of *benign* features in sonography, can exclude positive finding in mammography or clinical examination.

Sonography is primarily used in further diagnostic evaluation of already detected lesions.[1,2,4,9,13,17,18] However, lesions invisible on mammography may be visualized on ultrasound, and even small, unpalpable carcinomas can be seen, especially in mammographically dense breasts. Sonography can often directly visualize the lesion in real-time examination. It also allows dynamic evaluation of the lesion, and evaluation of the surrounding regions (axial, supraclavicular region, liver, etc.), supplying thus, a number of additional data for directing further diagnostic evaluation.

Sonographically breast carcinoma characteristically presents as *hypoechoic* mass, with *irregular and uneven* margins, which may be *spiculated*, with the *rim* probably corresponding to the area of locally invasive malignant tissue projections, and strands of reactive fibrosis (Figs 58.18A and B). Some 10% of carcinomas are isoechoic with parenchyma, and the smaller hypoechoic lesions can easily be confused with the surrounding fat [1,13,16,18,19]

Vertical orientation (LL/AP-ratio<1) is another typical sonographic finding strongly suggestive of malignancy, but only some carcinomas present it. Horizontal orientation cannot exclude malignancy.

Posterior central or eccentric sound attenuation (shadowing) is also strongly suggestive of malignancies. Posterior attenuation is most likely a consequence of extensive fibrotic reaction, and the fibrotic tissue is believed to absorb the soundbeam energy. Only rare benign lesions, such as extensively fibrosed or calcified fibroadenomas can mimick this finding, but are usually reliably distinguished in mammography. Some carcinomas, on the other hand, present no significant posterior shadowing, and some (medullary and mucinous carcinomas) can even have posterior acoustic enhancement (Fig. 58.19). Many carcinomas present *heterogeneous internal echoes*, but this is even less specific feature. Due to the local

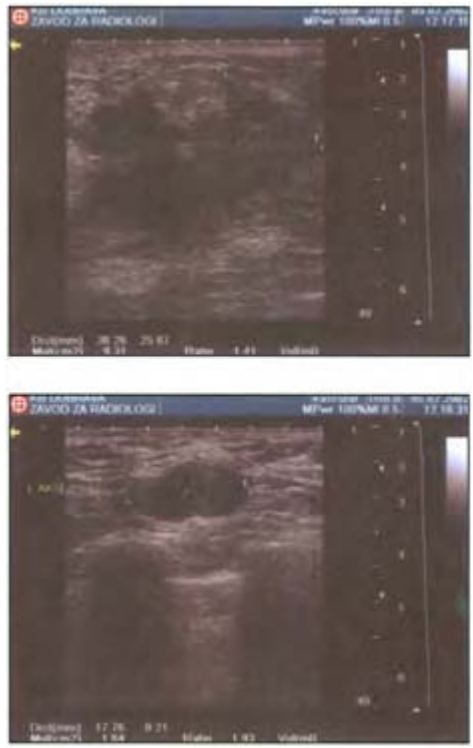

Figures 58.18A and B: Invasive ductal carcinoma. (A) B-mode image of the large irregular, spiculated, hypoehogenic breast cancer. Size 3.7×2.6 cm. (B) B-mode image of enlarged axillary lymph node that is diffusely hypoechoic, with no visible sinus. Metastatic axillary lymph node

invasion and extensive reactive fibrosis, most malignant lesions *distort normal breast tissue architecture*. This can sometimes be sonographically evident as interruption of parallel arrangement of breast parenchyma toward the transducer, as caused by a solid localized lesion. It can also present as interruption of subcutaneous fat layer by an isoechoic lesion; thickening and shortening of Cooper ligaments; and infiltration and

thickening of the skin, which presents as loss of interface between the hyperechoic skin and hypoechoic subcutaneous fat tissue, or the lesion itself. Distortion of the normal breast architecture

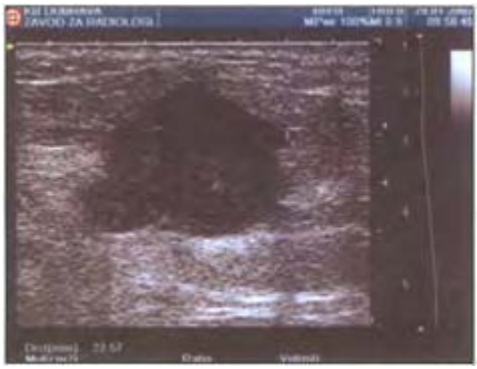

Figure 58.19: Medullary breast carcinoma. The lesion is hypoechogenic, only slightly heterogeneous. The margins are slightly irregular, but there are no distal acoustic shadowing or enhancement

is generally difficult to discriminate, due to the normal variability of breast echo patterns.

In dynamic sonographic evaluation many carcinomas exhibit *restricted mobility*. They are not so readily moved when manipulated either with a transducer or finger. Papillary intracystic carcinoma and secondary lesions can nevertheless, present regular mobility. Many carcinomas also present diminished compressibility in dynamic sonography, which is a reliable sign of malignancy. But good compressibility can also be found in some carcinomas, so it is not a specific feature as well.

High-resolution US is very helpful in assessing intraductal spread and multifocality of breast cancer, although it cannot compete with MRI.[1,21] US is useful for the detection of enlarged lymph nodes, particularly axillary lymph nodes. Addition of color Doppler is helpful to evaluate patterns of vascularization of lymph nodes, and thus to differentiate benign from metastatic lymph nodes.[22,23] Patients with US-detected metastases, confirmed by FNAC may be scheduled for axillary dissection.

Ultrasound Guided Fine-needle Aspiration Cytology and Fine-needle Core Biopsy

Fine-needle aspiration cytology (FNAC) and fine needle core biopsy (FNCB) are performed to improve specificity of breast examination and to avoid unnecessary interventions in benign breast lesions.[1,9,24–26]

Percutaneous punctures can be guided mammographically (stereotactic punctures) or sonographically.[9,24,25] Ultrasound-guided aspirations and biopsies are performed in the real time. Thus US allows direct visualization of the needle position within the lesion. Accordingly the puncture direction can be manipulated and adequately altered. Also the exact puncture location can be directly documented (Fig. 58.20).

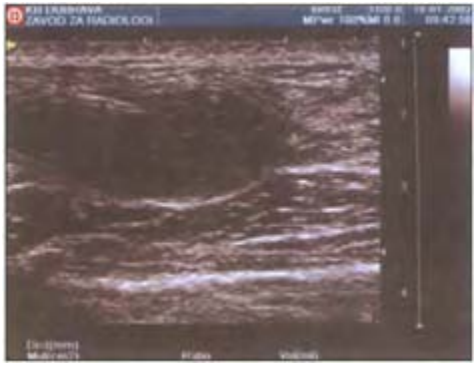

Figure 58.20: FNAC of the breast lesion. The needle is advanced into the lesion (fibroadenoma) in the realtime, under the US guidance. The shaft of the needle is clearly visible in the image, and the tip of the needle is visible within the lesion

The accuracy of the percutaneous aspiration/ biopsy depends on the size, location, and morphology of the lesion, as well as on the accuracy of targeting the lesion, needle diameter, and advance and the number of needle passes.[1,9,24–26] FNCB is generally done using a 14 gauge needle mounted on a spring-acting puncture device. Most literature proposes two or more passes with needle advancement of at least 15 mm, for adequate specimen retrieval. FNCB produces a small cylinder of target tissue and allows a complete histological diagnosis. Its sensitivity is around 92–98% and specificity up to 100%. It is, on the other hand, far more traumatizing procedure for a woman than FNAC. FNAC generally uses much finer needles (20 25 gauge in diameter), so the procedure is much less traumatizing even with a number of passing. The evaluation of the FNAC

acquired material is however, much more difficult, and the results more dependent on the skill of the examiner. Thus, FNAC has documented sensitivity of 53 98% and specificity of 89 100%. The negative result in FNAC cannot exclude a malignant lesion with suspicious sonographic, mammographic or clinical findings. In uncertain cases further investigation is mandatory (FNCB or surgical biopsy).

As both of these methods are highly examinerdependent, both regarding the puncture and cytology/histology, it is necessary that they be performed by skilled teams on regular basis. Only in these circumstances can reliable results be obtained.

Preoperative localization of lesions with wire is performed under US guidance, with the purpose of the safe location and surgical removal of impalpable or deeply positioned breast lesions.[1,2]

Doppler Imaging and 30-lmaging in Breast Evaluation

Modern transducers with color and power Doppler have high Doppler frequencies (7 MHz or more), that enable very good visualization of tumoral vessels and may help in the detection of small cancers. Vascular assessment has progressed enough to depict vessels in almost all breast tumors, and most fibroadenomas, while only few years ago vascularization could have been demonstrated only by injecting contrast media.

It is well documented that malignant processes in general have the typical vascular pattern[22–24] (Fig. 58.21). The pattern is described as hypervascular with vessels arising along the edge of the malignant process and extending into the center. Vessels in a malignant process are often branching and very irregular. In contrast with the malignant type vascularization, vessels in benign lesions are supposed to be smooth and aligned parallel with the surface of the lesion. Also blood flow in

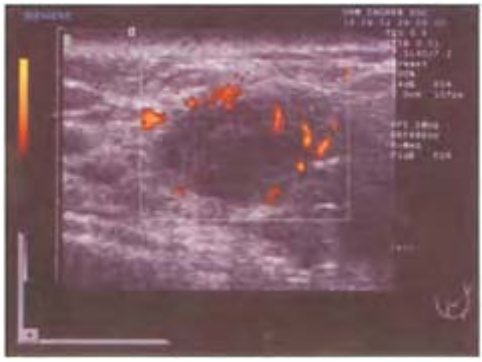

Figure 58.21: Power Doppler image of the large IDC, with peripheral irregular vessels. The lesion is heterogeneously hypoechogenic, with no

posterior acoustic phenomena

malignant vessels usually have very low resistance index. However, these general rules do not always apply in clinical circumstances. It was documented in some studies, and in our experience, that breast carcinoma exhibits similar or higher resistance index values in comparison to fibroadenomas.

Most modern ultrasound systems are equipped with color Doppler (GDI) and power Doppler (PDI) capabilities, which can reliably depict slow flow in breast vessels. Also some latest advances in ultrasound technology, such as 3D-imaging and contrast imaging, promise even greater sensibility in detecting slow flow patterns typical of malignant lesions (Figs 58.22A to D).[23,27,28]

Furthermore, ultrasound could be used for target-delivery of specific drugs conveyed by contrast agent to the specific lesion.[22–24] The complete perfusion with the drug-contrast is to be monitored in real time, and the agent activated with a high-mechanical-index pulse at the appropriate moment. Along with better visualization of vessel pattern, 3D-imaging is being reported to be superior in presentation of intraductal spread and multifocal lesions, as well as in surface rendering, compared with standard 2D-imaging.

These new data are highly promising, but they still await confirmation in sufficient number of controlled-design studies. In our experience in

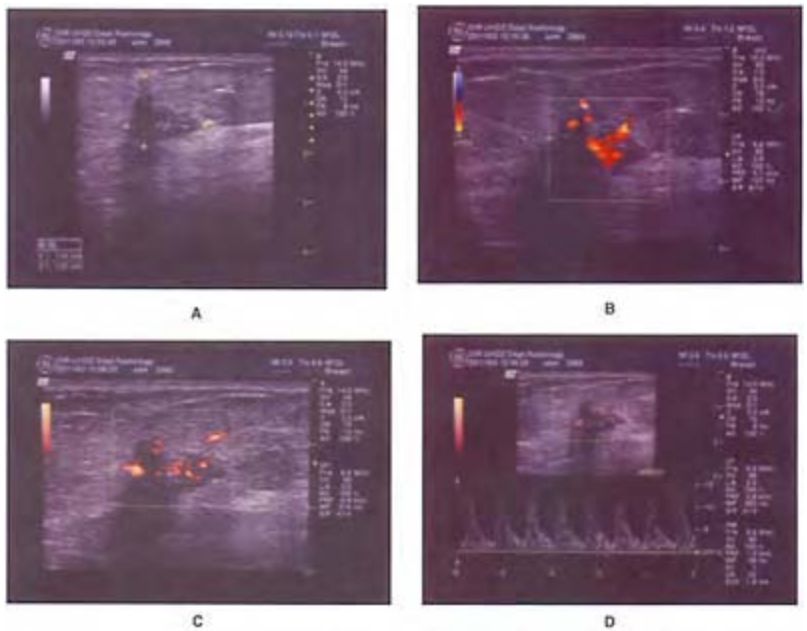

Figures 58.22A to D: Invasive ductal carcinoma. (A) Irregular

solid hypoechogenic lesion, 1.6×1.4 cm in size, with partial posterior attenuation of sound, and internal echogenic foci corresponding to microcalcifications on mammography. (B) Color Doppler image of the same lesion: abundant internal vascularization of the lesion, with irregular distribution of vessels depicted in color. (C) Power Doppler image of the same lesion: abundant internal vascularization and irregular distribution of vessels. (D) Spectral Doppler: Flow in the artery within the lesion—spectra indicate relatively high-resistant flow pattern

clinical practice today, Doppler imaging can be used for further investigation of benign-looking solid lesions. If suspicious vascular pattern or flow is found in otherwise benign-looking lesion, we believe that further investigation, such as FNAC or FNCB, is mandatory.

Breast Ultrasonography after Radiation Therapy and after Operative Procedures

Postoperative changes in breasts very often have similar imaging morphology like malignant lesions (Fig. 58.23).[1,2,29,32–34] These alterations are visible after biopsies, partial resection of breast, and mastectomy. Scars are visible after all surgical procedures, as well as architectural distorsion, edema, thickening of the skin, fluid collections, and dystrophic calcifications. Most of these changes regress spontaneously within the year following operation. Radiation therapy causes more pronounced breast changes, which tend to persist much longer, and are clearly visible on ultrasound and mammography.

Edema usually presents as a diffusely decreased echogenicity and loss of normal tissue

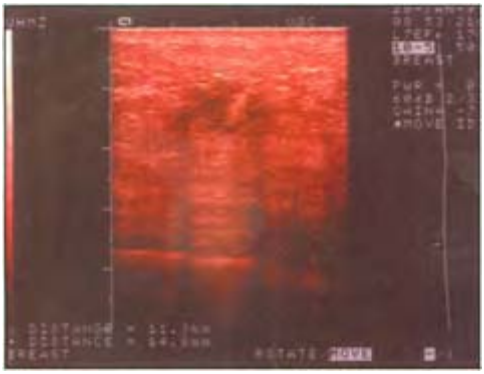

Figure 58.23:
Postoperative breast after quadrant resection of breast cancer. B-mode image of the postoperative scar that mimicks cancer. The lesion is heterogeneous, predominantly hypoechogenic, with irregular margins

differentiation. It is generally easily recognizable. Hematomas and seromas present as irregularly marginated hypoechoic lesions. With time they become more distinctly demarcated from the surroundings and can develop some internal echoes. Acute fat necrosis also generally appears as irregularly marginated hypoechoic lesions with varying degree of distal acoustic shadowing. These lesions are sonographically difficult to differentiate from malignant processes, which makes clinical examination and documentation crucially important.

Sonographically chronic scars usually present as ill-marginated and irregularly shaped, mostly multifocal hypoechoic lesions, sometimes casting posterior acoustic shadows, and accompanied with different degree of tissue architecture distortion. Skin thickening of different degree and dystrophic calcifications of different size are also commonly present, together with chronic fat necrosis (sonographically similar to the acute).

Even more than acute, chronic postoperative breast lesions are extremely difficult to distinguish from malignant lesions (primarily or recurrent). Meticulous clinical and sonographic regular-basis follow-up and documentation is therefore mandatory for adequate postoperative control.

Thoracic wall after mastectomy should be examined by ultrasound, and benign and malignant lesions can be differentiated in most of the cases. Tumor recurrence can be visualized, as well as infiltration of intercostal muscles, pectoral muscle or pleura. US enables evaluation of the depth of infiltration, and of the relation of the lesion to the

bones, pleura and blood vessels. Ultrasound is utilized also for the visualization of implants placed after subcutaneous mastectomy, and skin-flaps after the mastectomy. Fine-needle aspiration under US guidance prevents the damage of the implant during the procedure. Tumor recurrence visualization is impaired when implants are placed subcutaneously, and particularly meticulous US examination is indicated in these patients.

Radiation therapy induces fibrosis, with consequently mammographically “dense” breast appearance. Radiational fibrosis results in the increased echogenicity of the parenchyma and the whole breast, thickening of the skin, and distorsion of normal parenchymal architecture. Edema and skin thickening usually regress during two-year period. If the skin thickening is observed after previous regression, the tumor recurrence should be considered. Tumor recurrence after the conservative treatment may morphologically resemble the primary tumor, but it may also have very peculiar features. The diagnosis requires USguided aspiration or biopsy. Ultrasound is also very useful for the follow-up of hematoma, postoperative seroma, and for the detection of abscesses.

FDG-PET is useful for the evaluation of the therapy response in the selected group of patients, and clear advantage of PET is in its ability of fast examination of the whole body and of the detection of metastases that are clinically not suspected.[30,31]

Ultrasonography is extensively utilized for the follow-up of women after breast augmentation procedures, that are performed for the correction of congenital or acquired anisomasty or micromasty, or for the cosmetic reasons.[35] The silicon

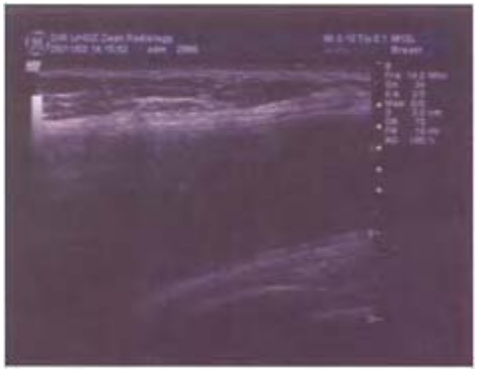

Figure 58.24: Breast implant. Saline breast implant positioned below the glandular parenchyma, anterior to the pectoral muscle. Normal implant borders, with anechogenic content of the implant

or saline implants are being used. Nowadays, subpectoral implant placement is much more common than subglandular, because of the risk of the development of fibrotic changes. Implants are being placed by laterocaudal or perimammilary approach. Mammographic imaging of implants required special projections. Unlike mammography, ultrasound can easily demonstrate all parts of the augmented breast (Fig. 58.24). US can be used for visualization of implant defects. However, MRI is the most accurate method for the evaluation of breast implants.

ULTRASOUND IN SCREENING ALGORITHM

The American Cancer Society and American College of Radiology recommend annual screening mammograms for women beginning at age 40 years.[9,36] For women younger than 40 years with a family history of breast cancer, annual screening mammograms should be first obtained 5 to 10 years before the age of the youngest affected relative. For women older than 75 years who are expected to live for 5 to 10 more years, clinical breast examination (CBE) and screening mammography should be performed annually. Whole breast ultrasonography has not yet been shown to be effective for routine screening because of the high false-positive rate and inability to detect microcalcifications consistently. However, in our experience, the high-resolution US, and utilization of high-frequency transducers, enable visualization of microcalcifications within lesions in high proportion of patients. Generally, US complements mammography in the evaluation of a palpable breast mass. It helps define shape, borders, and acoustic properties of the mass. The uses of ultrasonography are: assessment of the underlying cause of an abnormal finding on CBE, evaluation of a palpable breast mass in a young woman with dense breast tissue or a woman with breast implants, differentiation of poorly delineated masses as cystic or solid, and assessment of peripheral masses located outside the field of view of a mammogram.

In younger women mammography is less sensitive because of the increased breast density, resulting in a false-negative rate of up to 25%.[37] Because of that for women younger than 40 with a questionable or indeterminate CBE finding, ultrasonography is initial examination. Obtaining a diagnostic mammogram is the radiologist's decision. If findings are normal, a short-term interval follow-up is necessary (2–4 months). Additionally, ultrasonography can guide interventional procedures such as the fine-needle aspiration biopsy (FNAB) or fine-needle core biopsy (FNCB), as the needle can be visualized continuously within the mass, ensuring an adequate sample.

From our experience, we believe that the role of ultrasound in screening might soon be revised. Advances in US technology, and new techniques (3D, contrast studies, etc.) have enabled more precise detection and characterization of mammographically invisible lesions and with technical advances the screening sensitivity of ultrasound has markedly increased. We believe that the targeted US screening might be feasible in patients with dense, glandular breasts, and in high-risk patients. Accurate sonographic analysis may alter surgical approach to breast cancer.

REFERENCES

1. Heywang-Koebrunner SH, Dershaw DD, Schreer I. Diagnostic breast imaging. Stuttgart, Thieme, 2001.
2. Kopans DB. A systematic approach to breast imaging. In: Kopans DB (Ed). Breast Imaging, Lippincott Raven Publishers, Philadelphia 1998; 211–28.
3. Teubner J. Echomammography: Technique and results. In: Friedrich M, Sickles EA (Eds). Radiological diagnosis of breast diseases, Springer-Verlag, Berlin 2000; 181–220.
4. Kopans DB. Ultrasound and breast evaluation. In: Kopans DB (Ed). Breast Imaging, Lippincott Raven Publishers, Philadelphia 1998; 439–41.
5. ACR standard for performance of the breast ultrasound examination. 1998 standards. American College of Radiology, Reston, VA 1998; 317.
6. Kopans DB. The altered breast: Pregnancy, Lactation, Biopsy, Mastectomy, Radiation,. and Implants. In: Kopans DB (Ed). Breast Imaging (2nd ed). LippincottRaven, Philadelphia 1998; 445–69.
7. Jones C, Ingram D, Mattes E et al. The effect of hormone replacement therapy on prognostic indices in women with breast cancer. Med J Aust 1994; 161:106–10.
8. Roubidoux MA, Wilson TE, Orange RJ et al. Breast cancer in women who undergo screening mammography: relationship of hormone replacement therapy to stage and detection method. Radiology 1998; 208:725–28.
9. Pruthi S. Detection and evaluation of a palpable breast mass. Mayo Clin Proc 2001; 76:641–48.
10. Henderson IC. Risk factors for breast cancer development. Cancer 1993; 71:2127–40.
11. Stat Bite. Breast cancer incidence in the breast cancer prevention trial. J Natl Cancer Inst 1998; 90:648.
12. Kriger N, Hiatt RA. Risk of breast cancer after benign breast diseases: variation by histologic type, degree of atypia, age at biopsy, and length of follow-up. Am J Epidemiol 1992; 135:619–31.
13. Madjar H, Ladner HA, Sauerbrei W et al. Preoperative staging of breast cancer by palpation, mammography and high-resolution ultrasound. Ultrasound Obstet Gynecol 1993; 3:185–90.
14. Haagensen CD. Diseases of the Breast (2nd ed). Saunders, Philadelphia 1986.
15. Hughes LE, Mansel RE, Webster DJT. Benign disorders and diseases of the breast: concepts and clinical management. Bailliere Tindall, London, 1989.
16. Leucht D, Madjar H. Teaching Atlas of Breast Ultrasound. Thieme Medical Publishers, New York 1996; 176–81.
17. Pisano ED. The management of nonpalpable circumscribed breast masses. In: Friedrich M, Sickles EA (Eds). Radiological diagnosis of breast diseases, Springer, Berlin 2000; 149–66.
18. Stavros AT, Thickman D, Rapp CL et al. Solid breast nodules: use of sonography to distinguish between benign and malignant lesions. Radiology 1995; 196:123–34.
19. Adler DD. Imaging evaluation of spiculated masses. In: Friedrich M, Sickles EA (Eds). Radiological Diagnosis of Breast Diseases, Springer-Verlag, Berlin 2000; 137–48.
20. Kopans DB. Mammographic appearance of breast cancer. In: Kopans DB (Ed). Breast Imaging, Lippincott Raven Publishers, Philadelphia 1998; 375–408.
21. Siegmann KC, Muller-Schimple M, Schick F, Remy CT, Fersis N, Ruck P, Gorriz C, Claussen CD. MR imaging—detected breast lesions: histopathologic correlation of lesion characteristics and signal intensity data. Am J Roentgenolog 2002; 178(6):1403–09.
22. Cosgrove DO, Kedar RP, Bamber JC et al. Breast diseases: color Doppler US in differential diagnosis. Radiology 1993; 189:99–104.
23. Rizzatto G. Towards a more sophisticated use of breast ultrasound. Eur Radiol 2001; 11:2425–35.
24. Kopans DB. Imaging-guided needle placement for biopsy. In: Kopans DB (Ed). Breast Imaging (2nd ed). Lippincott Raven, Philadelphia 1998; 644–49.
25. Bauer M, Tontsch P, Schulz-Wendtland R. Fine-needle aspiration and core biopsy. In: Friedrich M, Sickles EA (Eds). Radiological Diagnosis of Breast Diseases, Springer, Berlin 2000;291–98.

26. Obenauer S, Fischer U, Baum F et al. Indications for percutaneous stereotactic vacuum core biopsy of the breast. Radiologe 2002; 42(1):11–18.
27. Kedar RP, Cosgrove D, McCready VR et al. Microbubble contrast agent for color Doppler US: effect on breast masses. Work in progress. Radiology 1996; 198:679–86.
28. Madjar H. Contrast ultrasound in breast tumor characterization: present situation and future tracks. Eur Radiol 2001; 11:41–46.
29. Mendelson EB, Tobin CE. Imaging the breast after radiation and surgery. In: Friedrich M, Sickles EA (Eds). Radiological Diagnosis of Breast Diseases, Springer, Berlin 2000; 299–318.
30. Khalkhali I, Itti E. Functional breast imaging using the single photon technique. Nucl Med Commun 2002; 23(7):609–11.
31. Rose C, Dose J, Avril S. Positron emission tomography for the diagnosis of breast cancer. Nucl Med Dommun 2002; 23(7):613–18.
32. Balu-Maestro C, Bruneton JN, Geoffary et al. Ultrasonographic posttreatment follow-up of breast cancer patients. J Ultrasound Med 1991; 10:1–7.
33. Scheer I. Radiodiagnostic aspects of conservative treatment of the malignant breast disease. Eur Radiol 1994; 4:95–101.
34. Dershaw DD, McCormick B, Cox L et al. Detection of local recurrence after conservative therapy for breast carcinoma. Cancer 1992; 46:186–90.
35. Ahn CY, DeBruhl ND, Gorczyca DP et al. Comparative silicone breast implant evaluation using mammography, sonography and magnetic resonance imaging: experience within 59 implants. Plast Reconstr Surg 1994; 94:620–27.
36. Barton MB, Harris R, Fletcher SW. Does this patient have breast cancer? The screening clinical breast examination: should it be done? how? JAMA 1999; 282:1270–80.
37. Morrow W, Wong S, Venta L. The evaluation of breast masses in women younger than forty years of age. Surgery 1998; 124:634–40.

Index

A
Abdominal diameters 230
Abdominal wall defects 291
Abnormal early pregnancy 143
  blighted ovum (anembryonic pregnancy) 147
  combined strategies for aneuploidy screening 160
  early pregnancy loss 151
    amnion evaluation 157
    crown-rump length 156
    embryonic heart rate 157
    gestational sac 152
    yolk sac 153
  ectopic pregnancy 151
  failure and vaginal bleeding 144
    incomplete and complete spontaneous abortion 145
    threatened abortion 144
  intrauterine hematomas 148
  missed abortion 146
  screening for chromosomopathies 157
    ductus venosus and heart failure 158
    heart analysis 160
    nasal bone 160
    nuchal translucency 157
    umbilical artery assessment 160
    umbilical cord diameter 160
Abnormalities associated 373
  fetal skin edema 374
  management 375
Absent nasal bone 139
Acute pelvic pain 747
  gynecologic etiologies 749
    negative pregnancy tests 749
    positive pregnancy tests 755
  non-gynecologic etiologies 747
    gastrointestinal causes 747
    urinary causes 748
Adenomyosis 598, 672
Adnexal masses 639
  challenges in the evaluation of tumor angiogenesis 650
  false-positive results 648
  main basis of angiogenesis 640
  recent data on clinical application of color and pulsed Doppler 645
  three-dimensional ultrasound and power Doppler imaging 649

tumor neovascularization 641
ultrasound modalities 643
Adnexal torsion 751, 765
Agenesis 392
ALARA principle 22
Alloimmune thrombocytopenia 384
Alloimmunized pregnancy
diagnosis 379
management 382, 383
non-invasive diagnosis 381
Amniocentesis 550, 722
complications 552
early 554
indications 551
technique 551
timing 551
Amnion 121
Amnionicity 351
Amniotic fluid volume 355
Anencephaly 387, 456
Angle independent parameters 422
Appendicitis 747
Artifacts in ultrasound 43
classification 44
enhancement 46
mirror artifacts 47
others artifacts 47
refraction (duplication) and side lobes 47
reverberation 44
shadowing 45
Doppler ultrasound artifacts
aliasing 48
angle of insonation 50
Doppler mirror artifact 50
range ambiguity 49
temporal ambiguity 49
mechanism 43
problem 43
Asherman's syndrome 672
Assessment of nephrouropathies 298

B
Biparietal diameter 226–228
Bladder and the urethra 770
Blighted ovum 147
Body stalk anomaly 292
Bowel disorders 293
Bowel obstruction 294
Brain 123
Brain sparing mechanism 397
Breast tumors 784

Breast ultrasound 772
Doppler imaging and 3D-imaging 789
equipment requirements 772
examination technique 773
fine-needle core biopsy 788
lesions 777
benign 779
inflammatory 784
malignant 784
screening algorithm 792
sonographic anatomy 774
ultrasound guided fine-needle aspiration cytology 788

C
Carcinoma 785
Cardiac activity 121
Caudal regression syndrome 393
Cephalic area 230
Cerclage 344
Cervical insufficiency 340, 344
diagnosis 340
etiologic factors 341
Cesarean section 445
Choledochal cysts 296
Choriocarcinoma 188
Chorionic villous sampling 721, 541
acceptance 547
complications 543
multiple pregnancy 545
placental confined mosaicism 546
technical aspects of the procedure 541
Chorionicity 352
Chromosomal abnormalities 389, 401
DiGeorge syndrome 391
monosomy X 391
triploidy 391
trisomy 13 389
trisomy 18 390
trisomy 21 390
Color Doppler hysterosalpingography 707
Conceptus 116
Congenital cystic adenomatoid malformation 274
Congenital heart defects 280
early fetal echocardiography 288
scanning 281
aortic and ductal arch view 285
four-chamber view 282
left ventricular outflow tract view 284
long axis view of the aortic arch 286
long axis view of the ductal arch 286
long axis view of the inferior and superior venae cavae 287

longitudinal views 281, 286
right ventricular outflow tract view 284
short axis view of the great vessels 285
three-vessels view 285
transverse and oblique views 281, 282
screening 281
Congenital uterine malformations 446
Conjoined twins 491
Cordocentesis 556
Corpus luteum 117
Corpus luteum cysts 757
Crown-rump length 227
Culdocentesis 721
Cysts 779

D

Decidual pseudosac 350
Development 224
Diaphragmatic defects 293
Diaphragmatic hernia 273
Doppler effect 11
Doppler examinations
accuracy 18
aliasing 19
artifacts 19
mirror image 20
precision 18
Doppler sampling sites in the fetus 96
descending aorta 98
ductus venosus 97
middle cerebral artery 97
umbilical artery 96
Doppler sonography in obstetrics 395
biophysical profile 403
Doppler flow velocity waveforms 396
indices 396
intrapartum studies 402
neuromotoric outcome 402
nomograms 397
prediction of fetal hemoglobin 407
safety 395
Doppler ultrasound
hazardous exposure to high temperature 23
methods of exposure time setting 23
thermal issues 24
two modes in the exposure 23
Double-decidual sign 119
Ductus venosus 410
Ductus venosus velocimetry 140
Duodenal atresia or stenosis 294

E
Echogenic bowel 295
Ectopic pregnancy 722, 756, 764
differential diagnosis 169
locations 168
risk factors 168
role of biochemical markers 169
role of ultrasound in the diagnosis 170
3D ultrasound 175
color Doppler facility 172
transabdominal 170
transvaginal 170
sites of implantation 176
cervical pregnancy 178
interstitial pregnancy 176
intra-abdominal pregnancy 179
ovarian pregnancy 179
Embryo 121
Embryogenesis 106
Embryonic period 114
Embryoscopy 558
transabdominal 559
transcervical 558
Embryoscopy-Fetoscopy
clinical application 557
Encephalocele 456
Endometrial carcinoma 600
Endometrial hyperplasia 598
Endometrial polyp 595, 669
Endometrial thickness 691
Endometrioid tumors 620
Endometriosis 615, 752
Endometritis 444, 672
Endometrium 115, 658
Esophageal atresia 293
Exencephaly (Acrania) 456
Exomphalos 138

F
Facial cleft 137
Fallopian tube 628
benign tumors 633
color Doppler findings 630
malignant tumors 633
color Doppler findings 634
three-dimensional ultrasound 635
ultrasound findings 633
pelvic inflammatory disease 628
three-dimensional ultrasound 632
ultrasound findings 629
Fallopian tube patency 701

gray scale Hy-Co-Sy 705
historical development of the ultrasonic assessment 702
pulsed Doppler analysis 706
technique of Hy-Co-Sy 704
procedure 705
requirements 704
Fertilization 103
Fetal arteries 423
Fetal behavior 500
abnormal behavioral patterns 513, 515
brain function impairment 514
eye movement patterns 501
circadian rhythm 503
ultradian rhythm 501
possible REM/NREM sleep 505
micturition 510
mouthing movement 507
penile tumescence 508
pupillary change 508
rapid eye movements and slow eye movements 505
Fetal blood sampling and tissue biopsy 556
Fetal central nervous system 250
acquired brain abnormalities *in utero* 266
intracranial hemorrhage 266
periventricular leukomalacia 268
porencephaly 267
assessment of enlarged ventricles 256
basic knowledge 250
congenital CNS anomalies 260
disorder of prosencephalic development 263
agenesis of the corpus callosum 264
holoprosencephaly 263
lissencephaly 265
neuroimaging of normal brain structure 253
posterior fossa anomalies
arachnoid cyst 265
cerebellar hypoplasia 265
choroid plexus cyst 266
Dandy-Walker complex 265
three-dimensional (3D) ultrasound technology 251
transvaginal approach to the fetal brain 250
Fetal descending aorta 403
Fetal diseases 434
Fetal distress 424
Fetal growth 136, 212
body parts 212
individual growth assessment 216
Fetal hydrops
diagnosis 372
Fetal learning 517
Fetal malformations 365
chromosomal anomalies 368

clinical use of the sonographic screening 369
number of scans and their timing 368
postnatal identification 368
inclusion or exclusion criteria 367
origin of the data/examiners' experience 367
prevention 365
sonographic screening 365
sonographic screening trials 369
Fetal nephropathy 531
Fetal organ measurements 216
Fetal organs biometry 232
Fetal puncture (fine needle aspiration) 526
exudation of renal status 530
technique generalization 526
Fetal structural malformations 137
Fetal therapy 559
Fetal thorax 272
Fetal tissue sampling 557
Fetal urinary aspiration 532
Fetal venous circulation 409
Fetal venous system 427
anatomy 428
classification 433
embryology 427
normal Doppler findings 429
physiology 428
structural anomalies 433
Fetopathology 386
Fetoscopy
transabdominal 557
Fetus acardius 491
Fibroadenoma 782
Fibroids 750
Fibroma 620
Fine needle core biopsy 788
Fine-needle aspiration cytology 788

G

Gastrointestinal system 123
Gastroschisis 291
Gastrulation 107
Genuine stress incontinence 767
Gestational age 103
ectoderm differentiation
primary 109
secondary 110
endoderm differentiation 110
implantation 106
bilaminar embryonic disc 107
lacunar or previllous stage 107
gastrulation 107

notochord 109
primitive streak 107
mesoderm differentiation 110
molecular basis of development 112
preimplantation period 103
cleavage and morula formation 105
early blastocyst 106
fertilization 103
vasculogenesis
developmentof heartprimordial 111
embryonic circulation 111
Gestational age assessment 127
choosing a due date 132
clinical methods 128
multiple pregnancies 131
Nägele's rule 127
ultrasound assessment
first trimester 128
second trimester 129
third trimester 129
ultrasound parameters 129
ultrasound pitfalls 133
using last menstrual period 127
Gestational sac 118
intradecidual 119
pseudogestational 119
Growth 224

H
Hamartoma 784
Head circumference 230
Heart rate 136
Hemorrhagic ovarian cysts 749
Hepatic masses 296
Holoprosencephaly 137, 458
Human embryo 103
Hydatidiform mole 185
invasive 187
partial 186
total 185
Hydrocephaly 458
Hydrosalpinx/tubo-ovarian complex 614
Hypoxemia 424
Hysteroscopy 701

I
Implantation 106, 691
ultrasound markers 691
endometrial Doppler 695
endometrial pattern 692
endometrial thickness 691

uterine Doppler 694
Implantation window 691
Infantile poly cystic disease 301
Inferior vena cava 410
Infertility 658
cervical factor 685
mullerian anomalies 665
adenomyosis 672
Asherman's syndrome 672
endometrial polyp 669
endometritis 672
submucous leiomyomas 670
ovulatory factors 673
luteal phase defect 681
luteinized unruptured follicle syndrome 680
polycystic ovarian syndrome 676
peritoneal factor 685
tubal factor 684
uterine/endometrial factors 658
uterine perfusion 662
Iniencephaly 389, 489
Inner cell mass 117
Instrumentation for Doppler measurements 14
2D color Doppler display 16
flow vs velocity 15
power Doppler ultrasound 17
Intracranial abnormalities 458
Intrauterine growth restriction 224, 398, 435
antenatal diagnosis 226
diagnosis of type 233
ultrasound diagnosis 227
ultrasound screening 226
classification 225
definitions 224
hemodynamic study of fetal deterioration 234
centralization of blood flow 238
decentralization of blood flow 241
reduction in umbilical blood flow 236
silent period of increase in resistance 235
incidence 224
obstetric management 242
Intrauterine hematomas 148
Intrauterine synechiae (adhesions) 597

L

Legal cases in obstetric ultrasound 80
failure to perform ultrasound 82
invented lesions 81
misreported cases 81
missed diagnosis 82
obstetrical procedures 82

wrongful birth 81
wrongful death 81
wrongful life 81
wrongful pregnancy 81
Leiomyoma 604, 737, 757
Leiomyosarcoma 605
Length of femur 231
Liver biopsy 529
complications 530
indications 530
technique 529
Lower urinary tract 767, 768
Luteal phase defect 681
Luteinized unruptured follicle syndrome 680

M
Magnetic resonance imaging
safety 569
indication and procedures for MRI during pregnancy 569
fetal anomalies 572
maternal tumors 571
pelvimetry 570
placenta 576
Maternal mortality and morbidity
causes 85
global overview 85
ultrasound features in early pregnancy 86
complete spontaneous abortion 88
ectopic pregnancy 88
incomplete spontaneous abortion 86
molar pregnancy 90
normal intrauterine gestation 86
Maturity 224
Meckel syndrome 389
Meckel's diverticulitis 748
Meconium peritonitis 294
Megacystis 139
Menstrual cycle 584
cervix 585
fallopian tubes 586
ovaries 585
uterus 584
menstrual phase 585
proliferative phase 584
secretory phase 584
Menstrual phase 114
Mesenteric and omental cyst 296
Micrognathia 137, 487
Middle cerebral artery 406
Monochorionic-diamniotic placentation 353
Mucinous tumors 619

Mullerian anomalies 665
Multicystic renal dysplasia 301
Multiembryo reduction 720
Multifetal gestations 349
  anomalies 360
  early assessment 349
  embryology and clinical characteristics 351
  ultrasonic evaluation 356
Multiple pregnancy
  incidence 562
  indications for prenatal diagnosis 563
  invasive procedures for prenatal diagnosis 564
  risk of aneuploidy 563
  the Greek experience 566
Muscle biopsy
  technique 537
Musculoskeletal system 122
Myomas 736

N

Nature of ultrasound 3
  beam from a piezoelectric transducer 6
  focusing 6
  practical aspects 8
    artifacts 10
    Doppler effect 11
    Doppler indices 13
    measurement 9
    puncture guiding 10
    resolution 9
    use of the probes 8
  probes 7
  scanner 4
  time gain compensation 6
  waves and interaction with tissues 3
Neural crest 110
Neural tube defect 387
Neurulation 109
Niche aspect 593
Nidation 106
Non-bowel cystic masses 296
Non-immune hydrops fetalis 434
Normal fetal anatomy 203
  abdomen 204, 208
  chest 204, 208
  gender 211
  head and brain 204
  limbs 204, 211
  spine 204, 206
Normal intrauterine pregnancy 755
Normal puerperium 439

Normal uterus 594
Notochord 109
Nuchal translucency 137, 488

O
Obstetric ultrasound 55
- “20 week” anomaly scan 61
- basics 55
- critique of radius trial 65
- diagnostic ability 67
- ethical dimensions 74
- first trimester ultrasonography 72
- guidelines for use 57
- meta-analyses of randomized controlled trials 66
- randomized controlled trials 59
- safety 56

Obstructive uropathies 303
- aspects related to renal function 316
  - acid-base balance 318
  - renal glomerule filtration 316
  - tubular dynamics of calcium 317
  - tubular dynamics of glucose 318
  - tubular dynamics of phosphate 317
  - tubular dynamics of potassium 317
  - tubular dynamics of sodium and chlorine 317
  - tubular dynamics of uric acid 317
  - urinary concentration capacity 318
- biochemical parameters 314
- biometric parameters 308
- calyceal dilatation 305
- comparative assessment 311
- dynamic parameters 309
- etiology 304
- intrauterine treatment 307
- ureter dilatation 305
- velocimetry patterns 312

Oligohydramnios 392
Omphalocele 292
Ontogenesis 501
Oocyte retrieval 717
Ovarian cancer screening 622
Ovarian cyst aspiration 719
Ovarian cysts 613
Ovarian dermoid cysts 617
Ovarian tumors 618
Ovarian vein thrombosis 754
Ovulation 115

P
Papilloma 783
Paraovarian cysts 616

Pelvic abscesses 720
Pelvic anatomy 581
  newborn and prepuberty 583
  postmenopausal state 583
Pelvic blood flow 586
  newborn and prepuberty 589
  postmenopausal state 589
  role of 3D ultrasound 589
Pelvic congestion syndrome 752
Pelvic inflammatory disease 606, 628, 749, 764
Pelvic masses 610
  differential diagnosis 613
    complex masses 617
    cystic masses 613
    Doppler parameters 621
    persistent vs regressing masses 621
    solid masses 620
  sonographic parameters 610
    associated lesions 612
    internal architecture 612
    origin and size 610
Perinatal mortality and morbidity 91
  causes 92
  prime causes in India 92
    antepartum fetal death 94
    congenital malformation 93
    fetoplacental circulation 96
    uteroplacental circulation 96
Persistent trophoblastic disease 190
Placenta
  abnormal lesions 332
    abscess 333
    tumors 332
  normal lesions 328
    intervillous thrombosis 329
    maternal blood lakes 329
    perivillous fibrin deposition 329
    placental calcifications 330
    placental infarcts 329
    subchorionic fibrin deposition 328
  placenta accreta 335
  placenta previa 334
  placental vessels 336
  retroplacental space 333
    placental abruption 333
    retroplacental hematomas 333
    subamniotic hematoma 334
  thickness, shape and volume 326
Placental abruption 758
Placental site trophoblastic tumor 190
Pleural effusions 277
Poly cystic ovarian syndrome 676

Polycystosis 302
Polyphemus 484
Postmenopausal palpable ovary syndrome 731
Postmenopause 726
  challenges 727
  instrumentation 727
  intrauterine fluid collection 740
    color Doppler velocimetry 741
    endometrium under HRT 741
  postmenopausal bleeding 739
  postmenopausal endometrium
    thickness 738
    visualization and morphology 738
  postmenopausal ovary 729
    color Doppler velocimetry 733
    malignancy 731
    morphology and biometry 730
    visualization 729
  postmenopausal uterus
    biometry 734
    color Doppler velocimetry 735
    leiomyomas under HRT 737
    morphology 734
    myomas and malignant potential 736
    uterus under HRT 735
  scanning 728
Postpartum period 439
Postpartum urinary retention 447
Preimplantation period 103
Primitive streak 107
Proboscis 484
Proliferative phase 115

R
REM/NREM sleep *in utero* 513
Renal agenesis 300
Retained placental tissue 442
Retrognathia 487

S
Screening 52
Sequestration of the lungs 275
Serous tumors 618
Skin biopsy 534
  complementary requirements 536
  complications 536
  indications 535
  technique 534
Slice thickness artifact 716
Somites 110
Spina bifida 387

Spontaneous abortion 755
Stuck twin 359
Submucous leiomyomas 670

T
Teratomas 490
Three-dimensional hysterosonosalpingography 710
Three-dimensional sonography 450
  early detection of fetal anomalies 456
  multiple pregnancy 454
  typical embryonic features during first trimester 451
  yolk sac 456
Three-dimensional ultrasonography 462
  assessment of fetal malformations 469
    fetal thorax and abdomen 472
    head and neck 469
    skeleton and extremities 474
  evaluation of normal fetal anatomy 464
    fetal thorax and abdomen 466
    head and face 464
    heart 466
    organ volume measurements 468
    skeleton and extremities 467
  main advantages in prenatal diagnosis 477
  modalities 463
  visualization of fetal malformations 480
    abdominal wall defects 492
    anomalies of the facies 484
    craniofacial malformations 482
    developmental anomalies 487
    ear malformations 486
    eye anomalies 487
    fetal head abnormalities 481
    kidney malformations 494
    limb abnormalities 494
    mandible defects 487
    medullary canal defects 490
    nasal bone defects 485
    neck anomalies 488
    paranasal facial masses 482
    positional anomalies and contractures 494
    umbilical cord anomalies 496
TORCH 394
Total intrauterine volume 232
Transvaginal puncture procedures 717
  diagnostic culdocentesis 721
  drainage of pelvic abscesses 720
  multiembryo reduction 720
  ovarian cyst aspiration 719
  transvaginal 717
Trap syndrome 491

Trophoblast 116
Trophoblastic diseases
  classification 185
  diagnosis 192
  symptoms 190
  therapy 197
Tumor neovascularization 641
Twin pregnancies 351
Twin-twin transfusion syndrome 358

U
3D ultrasound
  functions 27
  practical tips
    3D scanning 35
    electrical scalpel 38
    region of interest 36
    threshold 38
  technical aspects
    acquisition of 3D data 27
    construction of a 3D data set 28
    defocusing method 33
    real time ultrasonic beam tracing 32
    surface rendering 30
    volume rendering 31
    volume visualization 29
Ultrasound contrast agents 703
Ultrasound of the uterus 593
Umbilical arteries 397, 423
Umbilical artery pulsatility index 140
Umbilical cord
  area 320
  coiling 322
  diameter in the first trimester 321
  discordant arteries 322
  single umbilical artery 323
  tumors 324
Umbilical cord diameter 140
Umbilical vein 409
Unilocular ovarian cysts 732
Urinary tract infection 748
Urinary tract obstruction 748
Uterine bleeding 763
Uterine dehiscence 758
Uterine perfusion 662
Uteroplacental Doppler velocimetry 414
Uteroplacental perfusion 412

V
Vanishing twin 350
Vasculogenesis 111

VATER association 393
Ventriculocentesis 528
Volumetry 468

Y
Yolk sac 120